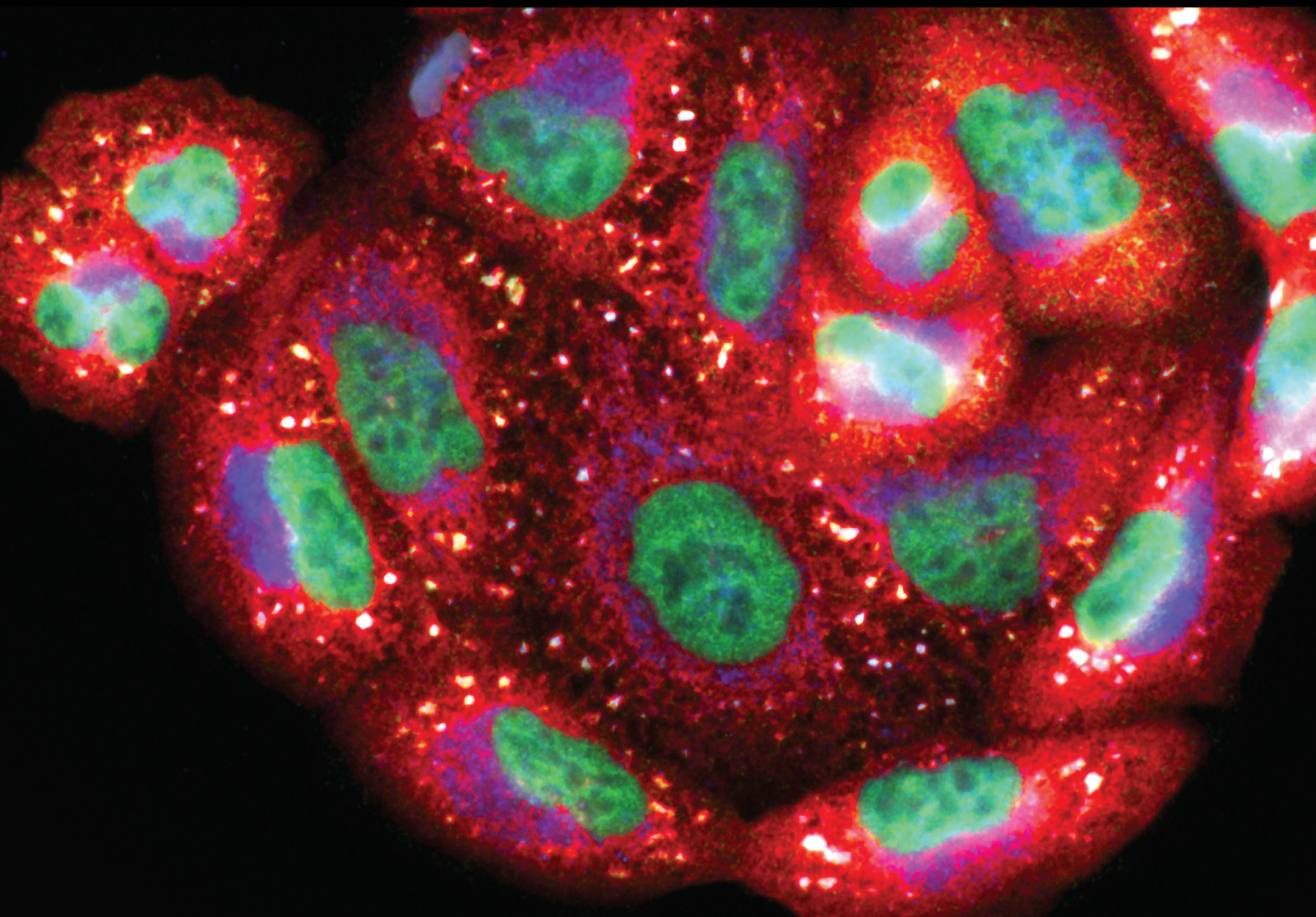# Plant Complexes and their Isolated Compounds for Oxidative Stress and Inflammation: from Basic Research to Clinical Evidence

Lead Guest Editor: Antonella Smeriglio
Guest Editors: Domenico Trombetta, Laura Cornara, Vincenzo De Feo, and Seyed M. Nabavi

Plant Complexes and their Isolated Compounds for Oxidative Stress and Inflammation: from Basic Research to Clinical Evidence
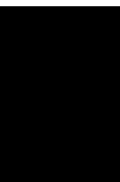
Plant Complexes and their Isolated Compounds for Oxidative Stress and Inflammation: from Basic Research to Clinical Evidence

Lead Guest Editor: Antonella Smeriglio
Guest Editors: Domenico Trombetta, Laura Cornara, Vincenzo De Feo, and Seyed M. Nabavi

Tim Hofer, Norway
John D. Horowitz, Australia
Silvana Hrelia, Italy
Dragan Hrncic, Serbia
Zebo Huang, China
Zhao Huang, China
Tarique Hussain, Pakistan
Stephan Immenschuh, Germany
Norsharina Ismail, Malaysia
Franco J. L, Brazil
Sedat Kacar, USA
Andleeb Khan, Saudi Arabia
Kum Kum Khanna, Australia
Neelam Khaper, Canada
Ramoji Kosuru, USA
Demetrios Kouretas, Greece
Andrey V. Kozlov, Austria
Chan-Yen Kuo, Taiwan
Gaocai Li, China
Guoping Li, USA
Jin-Long Li, China
Qiangqiang Li, China
Xin-Feng Li, China
Jialiang Liang, China
Adam Lightfoot, United Kingdom
Christopher Horst Lillig, Germany
Paloma B. Liton, USA
Ana Lloret, Spain
Lorenzo Loffredo, Italy
Camilo López-Alarcón, Chile
Daniel Lopez-Malo, Spain
Massimo Lucarini, Italy
Hai-Chun Ma, China
Nageswara Madamanchi, USA
Kenneth Maiese, USA
Marco Malaguti, Italy
Steven McAnulty, USA
Antonio Desmond McCarthy, Argentina
Sonia Medina-Escudero, Spain
Pedro Mena, Italy
Víctor M. Mendoza-Núñez, Mexico
Lidija Milkovic, Croatia
Alexandra Miller, USA
Sara Missaglia, Italy

Premysl Mladenka, Czech Republic
Sandra Moreno, Italy
Trevor A. Mori, Australia
Fabiana Morroni, Italy
Ange Mouithys-Mickalad, Belgium
Iordanis Mourouzis, Greece
Ryoji Nagai, Japan
Amit Kumar Nayak, India
Abderrahim Nemmar, United Arab
Emirates
Xing Niu, China
Cristina Nocella, Italy
Susana Novella, Spain
Hassan Obied, Australia
Pál Pacher, USA
Pasquale Pagliaro, Italy
Dilipkumar Pal, India
Valentina Pallottini, Italy
Swapnil Pandey, USA
Mayur Parmar, USA
Vassilis Paschalis, Greece
Keshav Raj Paudel, Australia
Ilaria Peluso, Italy
Tiziana Persichini, Italy
Shazib Pervaiz, Singapore
Abdul Rehman Phull, Republic of Korea
Vincent Pialoux, France
Alessandro Poggi, Italy
Zsolt Radak, Hungary
Dario C. Ramirez, Argentina
Erika Ramos-Tovar, Mexico
Sid D. Ray, USA
Muneeb Rehman, Saudi Arabia
Hamid Reza Rezvani, France
Alessandra Ricelli, Italy
Francisco J. Romero, Spain
Joan Roselló-Catafau, Spain
Subhadeep Roy, India
Josep V. Rubert, The Netherlands
Sumbal Saba, Brazil
Kunihiro Sakuma, Japan
Gabriele Saretzki, United Kingdom
Luciano Saso, Italy
Nadja Schroder, Brazil

Contents

Contents

Hindawi

Review Article

The Pharmacological Activities of *Crocus sativus* L.: A Review Based on the Mechanisms and Therapeutic Opportunities of its Phytoconstituents

Monica Butnariu [ID],[1] Cristina Quispe,[2] Jesús Herrera-Bravo [ID],[3,4] Javad Sharifi-Rad [ID],[5] Laxman Singh,[6] Nora M. Aborehab,[7] Abdelhakim Bouyahya [ID],[8] Alessandro Venditti [ID],[9] Surjit Sen,[10,11] Krishnendu Acharya,[10] Moein Bashiry,[12] Shahira M. Ezzat [ID],[13,14] William N. Setzer,[15] Miquel Martorell [ID],[16] Ksenija S. Mileski,[17] Iulia-Cristina Bagiu,[18,19] Anca Oana Docea,[20] Daniela Calina [ID],[21] and William C. Cho [ID][22]

[1]*Banat's University of Agricultural Sciences and Veterinary Medicine "King Michael I of Romania" from Timisoara, Timişoara, Romania*
[2]*Facultad de Ciencias de la Salud, Universidad Arturo Prat, Avda Arturo Prat 2120, Iquique 1110939, Chile*
[3]*Departamento de Ciencias Básicas, Facultad de Ciencias, Universidad Santo Tomas, Chile*
[4]*Center of Molecular Biology and Pharmacogenetics, Scientific and Technological Bioresource Nucleus, Universidad de La Frontera, Temuco 4811230, Chile*
[5]*Facultad de Medicina, Universidad del Azuay, Cuenca, Ecuador*
[6]*G.B. Pant National Institute of Himalayan Environment & Sustainable Development Kosi-Katarmal, Almora, Uttarakhand, India*
[7]*Biochemistry Department, Faculty of Pharmacy, October University for Modern Sciences and Arts (MSA), 6th of October 12566, Egypt*
[8]*Laboratory of Human Pathologies Biology, Department of Biology, Faculty of Sciences and Genomic Center of Human Pathologies, Faculty of Medicine and Pharmacy, Mohammed V University of Rabat, Morocco*
[9]*Dipartimento di Chimica, "Sapienza" Università di Roma, Piazzale Aldo Moro 5, 00185 Rome, Italy*
[10]*Molecular and Applied Mycology and Plant Pathology Laboratory, Department of Botany, University of Calcutta, Kolkata 700019, India*
[11]*Department of Botany, Fakir Chand College, Diamond Harbour, West Bengal 743331, India*
[12]*Department of Food Science and Technology, Nutrition and Food Sciences Faculty, Kermanshah University of Medical Sciences, Kermanshah, Iran*
[13]*Pharmacognosy Department, Faculty of Pharmacy, Cairo University, Kasr El-Ainy Street, Cairo 11562, Egypt*
[14]*Pharmacognosy Department, Faculty of Pharmacy, October University for Modern Sciences and Arts (MSA), 6th of October 12566, Egypt*
[15]*Department of Chemistry, University of Alabama in Huntsville, Huntsville, AL 35899, USA*
[16]*Department of Nutrition and Dietetics, Faculty of Pharmacy, University of Concepcion, Concepcion, Chile*
[17]*Department of Morphology and Systematic of Plants, Faculty of Biology, University of Belgrade, Studentski Trg 16, 11000 Belgrade, Serbia*
[18]*Victor Babes University of Medicine and Pharmacy of Timisoara Discipline of Microbiology, Timişoara, Romania*
[19]*Multidisciplinary Research Center on Antimicrobial Resistance, Timişoara, Romania*
[20]*Department of Toxicology, University of Medicine and Pharmacy of Craiova, 200349 Craiova, Romania*
[21]*Department of Clinical Pharmacy, University of Medicine and Pharmacy of Craiova, 200349 Craiova, Romania*
[22]*Department of Clinical Oncology, Queen Elizabeth Hospital, Kowloon, Hong Kong*

Correspondence should be addressed to Javad Sharifi-Rad; javad.sharifirad@gmail.com,
Miquel Martorell; martorellpons@gmail.com, Daniela Calina; calinadaniela@gmail.com, and William C. Cho; chocs@ha.org.hk

Crocus species are mainly distributed in North Africa, Southern and Central Europe, and Western Asia, used in gardens and parks as ornamental plants, while *Crocus sativus* L. (saffron) is the only species that is cultivated for edible purpose. The use of saffron is very ancient; besides the use as a spice, saffron has long been known also for its medical and coloring qualities. Due to its distinctive flavor and color, it is used as a spice, which imparts food preservative activity owing to its antimicrobial and antioxidant activity. This updated review discusses the biological properties of *Crocus sativus* L. and its phytoconstituents, their pharmacological activities, signaling pathways, and molecular targets, therefore highlighting it as a potential herbal medicine. Clinical studies regarding its pharmacologic potential in clinical therapeutics and toxicity studies were also reviewed. For this updated review, a search was performed in the PubMed, Science, and Google Scholar databases using keywords related to *Crocus sativus* L. and the biological properties of its phytoconstituents. From this search, only the relevant works were selected. The phytochemistry of the most important bioactive compounds in *Crocus sativus* L. such as crocin, crocetin, picrocrocin, and safranal and also dozens of other compounds was studied and identified by various physicochemical methods. Isolated compounds and various extracts have proven their pharmacological efficacy at the molecular level and signaling pathways both *in vitro* and *in vivo*. In addition, toxicity studies and clinical trials were analyzed. The research results highlighted the various pharmacological potentials such as antimicrobial, antioxidant, cytotoxic, cardioprotective, neuroprotective, antidepressant, hypolipidemic, and antihyperglycemic properties and protector of retinal lesions. Due to its antioxidant and antimicrobial properties, saffron has proven effective as a natural food preservative. Starting from the traditional uses for the treatment of several diseases, the bioactive compounds of *Crocus sativus* L. have proven their effectiveness in modern pharmacological research. However, pharmacological studies are needed in the future to identify new mechanisms of action, pharmacokinetic studies, new pharmaceutical formulations for target transport, and possible interaction with allopathic drugs.

1. Introduction

The genus *Crocus* is a member of the Iridaceae (subfamily Crocoideae) and consists of about 100 species that occur in the wild. These are mainly found in central-southern Europe (Balkan Peninsula), North Africa, and Western Asia [1]. Several species of this genus are currently used in gardens and parks as ornamental plants for their colorful flowers, while *Crocus sativus* L. (saffron) is the only species that is cultivated for the edible purpose [2]. The use of saffron is very ancient: its earliest representation appeared approximately 4000 years ago in some paintings and ceramics of the Minoan civilization in the region of Crete [3, 4]. The stigmas from flowers are traditionally handpicked at dawn to preserve all the aroma and organoleptic characteristics. Then the stigmas are dried in the shade and finally powdered [5]. Due to its distinctive flavor and yellow-orange color, it has an ancient use as spice in Arab, European, Indian, and Persian cuisine. It is also used in liquors, candies, food supplements [5, 6], and medical and coloring qualities [7–9].

Among the phytoconstituents, there have been described several compounds that are thought to be the chemical determinants of the bitterness, scent, and color of saffron [10]. These are formally terpenoids or thought to be derived from terpenoid precursors. In particular, these are the apocarotenoids such as *trans*-crocetin and its glycosylated forms (crocins), especially *trans*-crocetin di-($β$-D-gentiobiosyl) ester and *trans*-crocetin ($β$-D-gentiobiosyl)-($β$-D-glucosyl) ester, together with picrocrocin and safranal (Figure 1), formerly a monoterpene glycoside and a monoterpene, respectively, and believed to be degradation products of zeaxanthin. As minor components, which also contribute to the spice color and biological effects, there are a series of glycosidic derivatives of kaempferol (Figure 1) [11] and quercetin [12]. Other minor components that contribute to

the peculiar aroma of saffron are volatile compounds related to isophorone [13, 14].

Obviously, several of the medicinal and health-promoting properties attributed to saffron are due to the presence of these compounds. For example, safranal, in addition to its antioxidant and radical-scavenger properties, is useful as an anticonvulsant and antidepressant in preclinical models [15–18]. Due to the high added value of saffron as a spice and of its chemical constituents mainly related to the healthy properties, the studies on saffron and its plant source (C. sativus) are in the limelight, especially concerning the analytical methods used to evaluate the quality and to identify marker compounds related to the country of origin.

In this updated review, the following aspects of *Crocus* plants are considered: traditional uses, phytochemical composition, pharmacological properties with mechanisms evidenced from *in vitro* and *in vivo* studies, clinical studies, toxicological data, and upcoming clinical perspectives.

2. Methodology

An extensive search of the PubMed, Science, and Google Scholar databases was conducted to select the most important information for this updated review. The main search keywords were: "*Crocus* plant," "*Crocus sativus*," "ethnopharmacology," "phytoconstituents," "chemical compounds," "pharmacological activity," "pharmacological mechanisms," "human clinical studies," "toxicity," and "food preservatives."

Inclusion criteria are as follows: only extenso articles written in English that included data on *Crocus sativus* L. analyzed, chemical compounds isolated from each genus, pharmacological molecular research for each of the studied plants, types of *in vitro/in vivo* pharmacological studies, concentration and dose at which the chemical compounds
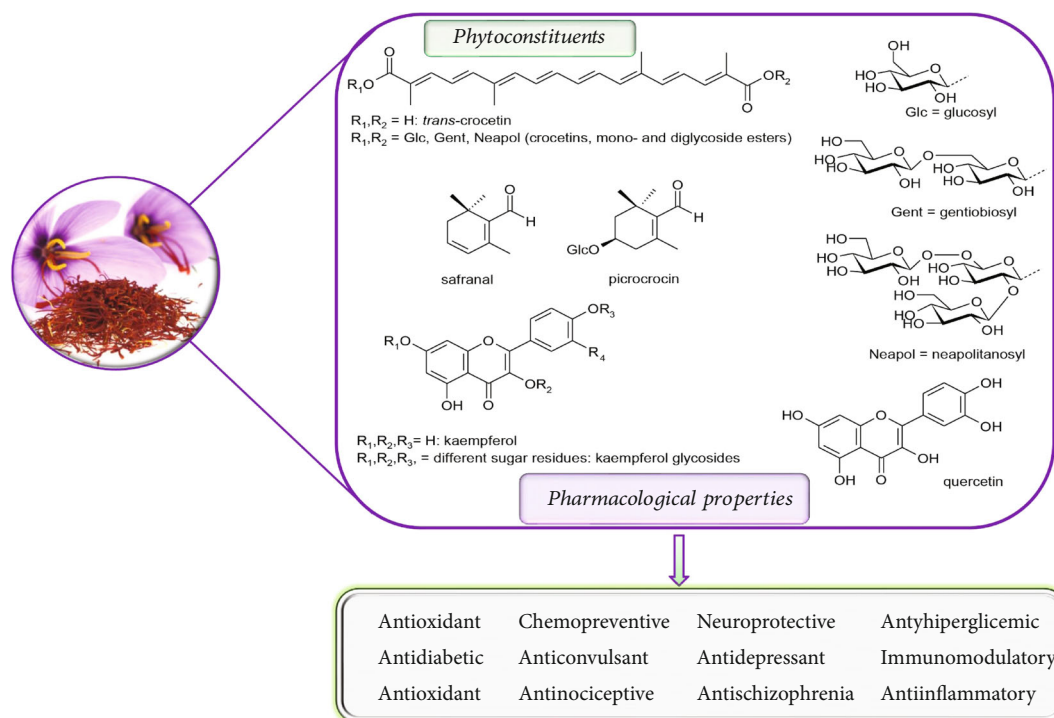
FIGURE 1: The main phytoconstituents of *Crocus sativus* L. and their pharmacological properties.

studied were pharmacologically active, clinical trials, and toxicological data. The chemical names were validated with PubChem and SciFinder, and the plant names were in accordance with The Plant List [19, 20]. The most important data have been summarized in the tables and figures presented in this article.

Exclusion criteria are as follows: abstracts, letters to the editor, papers in languages other than English, studies that did not have dose-effect correlations, studies that did not have proven pharmacological activity, and studies that included homeopathic preparations.

3. Traditional Medicine Use of *Crocus* Plants

The folklore knowledge and extensive traditional use of medicinal *Crocus sativus* L. have a long history worldwide [21, 22]. The cultivation of *Crocus* species for culinary and therapeutic purposes has been known from ancient times, first taking place in Greece and Iran. Later, the utilization of these plants was spread through the Mediterranean region to Eastern Europe and South Asia and China [1]. Although *C. sativus* was the most popular medicinal plant in European and Asian countries for ages, among medically significant herbs from this genus are also *Crocus caspius* Fisch. & C.A.Mey. ex Hohen, *Crocus heuffelianus* Herb., *Crocus hyemalis* Boiss. & Blanche, and *Crocus vernus* (L.) Hill. Their ethnobotanical importance is reflected through traditional use against various ailments and health disorders [23–27].

The traditional application of *C. sativus* is very diverse from diet and cosmetics to essential roles in medicine. It is a reputable plant owing to the specific aroma, flavor, and color of the stiles. As a valuable medicinal plant, it is a part

of many alternative therapies and folklore medicines [4, 22]. It is documented that saffron was applied for the treatment of about 90 health disorders by different cultures [28].

In some Asian countries, traditional knowledge on saffron healing effects dates from prehistoric periods [8, 29]. The first records about its medical application date from the 12th century BC [30]. Saffron was recognized by different nations in the Middle East and South Asia as a health-promoting drug and medicine to fight various diseases. It is believed that the people of ancient Persia were the first to cultivate this species for their traditional needs. In Persian traditional medicine, saffron was used as a tonic for the strength and meaning of the organism, especially the vascular and nervous system (NS). Additionally, it is an ingredient of recipes for the treatment of depression, insomnia, measles, and dysentery [8]. Concerning this, *C. sativus* remains one of the most important medicinal drugs in traditional Iranian medicine [4, 30].

It was an important curative herb in ancient Greece, Rome, and Egypt, South and Central Asia (Unani), Hindu (Ayurveda), and Chinese medicine [21, 31, 32]. Also, *C. sativus* has been utilized as a medicinal spice by the Moroccan people [30] and some locals in Jordan [23].

The ancient Romans added this plant to wines to prevent hangovers and intoxication. Also, it was used in ancient Egypt and Greece as a herbal remedy to fight ulcers on the skin or mucous membranes to reduce eye health problems such as pain, infection, or cataracts and to heal some urinary and menstrual disorders [30]. In Unani medicine, this spice is also recognized as a remedy for urinary and kidney infections, and it is used as a part of the mixtures against menstrual disorders. Besides, it is

considered stomachic, while in combination with honey, it is useful as a diuretic [31].

In Ayurveda medicine, saffron has many purposes as well. It is recommended against skin problems, asthma, arthritis, and kidney and digestive disorders. In powdered form, the herb is useful for external application on wounds, swellings, or major bleedings [30]. Powdered saffron is also advised for the treatment of poor vision, cataracts, and blindness [8]. This herb acts against diabetes when combined with ghee. Among its most famous roles in Ayurveda, the system is in the reduction of the enlargement of the spleen and the liver. [21, 28, 31].

In general, C. sativus is advised as a strengthening tonic that stimulates the immune defense, and it is a common ingredient of restorative preparations recommended for the general improvement of the physical and mental health of the body [30]. As an antiseptic and anti-inflammatory drug, it heals bacterial and fungal infections, inflammations, insect bites, and also apoplexy, alcoholism, arthritis, and diabetes [30].

Saffron's stigmas are extensively applied as an indigenous medicine across India. It serves as an antiseptic, analgesic, and expectorant agent as a nerve sedative and stimulator for immunity, blood flow, and menstruation. Also, it is effective against smallpox and a wide range of stomach problems. In lower doses, this spice can stimulate the contraction of the uterus in pregnancy, while in more significant amounts, it can cause general spasm and constriction [8]. It is a popular natural cosmetic in Iranian and Indian medicine for improvement of skin complexion, and as a part of folk phytopreparation, it brightens the skin of the body [33].

In the cosmetic practice, this spice showed to be effective against acne, erysipelas, skin, wounds, and similar skin diseases, while in China, it is recommended for purpura, eczema, and measles [8, 30].

The aqueous extract of saffron, in combination with other medicinal drugs, is useful for the treatment of painful and dislocated joints, sprains, or fractured bones [29, 34]. Some nations use saffron to treat migraines or mental disorders such as depression and dementia. For example, in Iran, insomnia, severe headaches, and obstructions in the area of the head and the neck are cured with boiled water preparation of saffron, while in India, it is applied against depression and similar mental disorders [1, 30]. Crocus sativus acts as an improving mood and calming anxiety agent [29]. The essential oil of saffron can be used as a sedative in combination with olive or sesame oil (as a medicine, the mixture of oils is left for five days with periodically stirring then filtered afterwards) [30]. The flowers of C. sativus are used as a part of alternative therapy for Alzheimer's disease [26].

Saffron is regarded as a stomachic and carminative drug, helpful for the liver, spleen, and stomach irregularities [29]. Also, it demonstrates emetic activity and can relieve problems with dyspepsia and to decrease appetite [30]. It helps with obesity-related metabolic disorders like hyperlipidemia and diabetes. Regarding this, the role of saffron in action against obesity was later confirmed [34]. Considering the cardiovascular system, C. sativus is used for many purposes. As cardiotonic, it affects the heart and speeds the circulation.

As a result of better blood flow, other medicaments reach the targeted organs more quickly. Saffron is used in England with the purpose to strengthen and stimulate the heart by better nutrition caused by faster blood flow. Besides these functions, the drug is applied in China against anemia and to prevent coagulation by breaking the blood clots [29, 34]. In both Western and Eastern parts of the world, it is used as a medicine for problems with the respiratory system [30]. The saffron essential oil quickens the lung's function, relaxes the breathing, and is recognized as an expectorant. It is known to combat coughs and colds, partly by its specific odor, as well as asthma, pleurisy, and diaphragmatic [32]. Additionally, the plant helps with urinary infections. Traditionally, it is used as a herbal antispasmodic remedy that prevents obstructed urination.

The diuretic combination of saffron and honey helps to release kidney stones [30]. Crocus sativus is a folk medicament advised for irregularities in the menstrual cycle, which expresses many beneficial roles in the female reproductive system. It alleviates dysmenorrhea and has an emmenagogue application. Saffron relieves the pain in the uterus when combined with other drugs. Also, it can be used against uterus ulcers when applied with wax or yolk and olive oil. Crocus sativus is an aphrodisiac drug recognized for treatment of impotence. It has a traditional role in sperm activation. As already mentioned, it demonstrates abortive activity in larger amounts which can cause the uterus spasm and abortion in the pregnancy. Also, it is popularly used as a postlabour antiseptic in cows [29, 30, 35].

According to literature data, other Crocus species are also utilized as natural phytotherapeutics. It is claimed in Iranian natural medicine that the endemic species C. caspius is medicinally effective against microbial infections [24]. The infusion of C. hyemalis aerial parts and stigma's filaments is recommended as an antitussive and antiasthmatic remedy and as a medicine for respiratory problems [23]. Furthermore, the significance of C. vernus in mountainous areas of Italy is expressed through the use of its flowers or entire flowering plant as an antiseptic, while the flower buds are advised externally against lice [27]. It was cited in traditional books that the mixture of C. sativus, Cyperus rotundus L., honey, and currant refreshes the memory and reduces forgetfulness and distraction [26].

Many beneficial properties of Crocus species are mainly related to a variety of carotenoids and their crocetin-type derivatives [1, 27]. The most important findings on the health-promoting effects of saffron are confirmed for cardiovascular ailments like blood pressure (BP), atherosclerosis, and coronary artery diseases. Furthermore, studies have confirmed that it impacts ocular blood flow, retinal function, and learning behavior, and it demonstrates anti-inflammatory, cytotoxic, and contraceptive activities [31].

4. Phytochemical Composition

Because of its wide range of pharmacological uses, saffron has undergone extensive biochemical and phytochemical studies (Supplementary material (available here), Tables 1 and 2), and several biologically active compounds have been

isolated. Each of these bioactive compounds has characteristic inherent properties (Figure 1).

Saffron showed antimicrobial effects and can protect foods from microbial attack. Saffron flower petals are rich in phenolic compounds showing antimicrobial and antioxidant activity. Crocin is the most powerful antibacterial agent in saffron, particularly against Gram-negative bacteria like *Escherichia coli*. The high antibacterial activity of crocin is attributed to the alcoholic groups (-OH) in its structure.

The peculiar quality and sensory properties in terms of aroma and taste have been attributed to three main bioactive compounds, crocin, picrocrocin, and safranal [36–38]. It also contains many nonvolatile components like lycopene, α- and β-carotene, and zeaxanthin [39].

The crocins, hydrophilic compounds, are considered the main active constituents that give saffron the golden yellow-orange color [40–42]. Picrocrocin is responsible for the bitter taste (the bitter glucoside) [43, 44]. Safranal, a monoterpene aldehyde, produces the characteristic odor and aroma. [45–47].

These bioactive compounds are the degradation products of carotenoids, i.e., derived from oxidative cleavage zeaxanthin carotenoid, and are known as apocarotenoids [48, 49]. Additional bioactive compounds that are present include carbohydrates, flavonoids, gum, minerals, proteins, sugars, and vitamins, which have been isolated and reported from the saffron stigma [47, 50, 51].

5. Pharmacological Activities

Traditional and alternative medicine has a significant impact on the current trends in preclinical and clinical research of medicinal plants [52–54]. Since saffron is a popular folk remedy in many countries, recent preclinical studies verified its wide application and the use of related *Crocus* species for medical purposes.

5.1. In Vitro studies

5.1.1. Cytotoxic Activity. Cancer is a term used to describe malignancies in which abnormal cells multiply in an uncontrolled and continuous manner and can invade the surrounding healthy tissues [53–55]. Abnormal cells come from any tissue in the human body and can occur anywhere in the body [56, 57]. The malignancies caused by this uncontrolled multiplication are numerous and difficult to control therapeutically [58, 59].

Antitumor effects of *Crocus* plant derivatives have been highlighted in a wide variety of isolated cell study models. The viability of healthy cells remained unaffected under treatment, while compared to malignant cells, including human cancer cells, saffron develops selective cytotoxic effects at micromolar doses.

Aqueous extract of saffron used in different concentrations (100, 200, 400, and 800 μg/mL) exhibited cytotoxic and proapoptotic effects when investigated on lung cancer cell line A549. It was found that saffron reduced the proliferation of the A549 cells in a dose-dependent manner. In addition, it induced morphological changes, reduced the number of viable cells, and induced apoptosis. The IC_{50} against A549 cells was 380 and 170 μg/mL after 48 and 72 hours, as reported by Samarghandian et al. [60].

Another study conducted by Vali et al. [61] on a breast cancer cell line (MCF-7), a synergistic effect was found between combinations of crocin with gamma radiation or paclitaxel in increasing apoptosis and decreasing survival rate of the cells. The MTT assay was used to determine the IC_{50} (3.5 mg/mL) of crocin after 48-hour treatment. Also, the treatment of MCF-7 with crocin at different time intervals increased apoptosis of the cells as detected by flow cytometry, where the combined therapy of crocin and paclitaxel increased apoptosis significantly over single therapy. On the other hand, the combined therapy caused an increase in the expression of caspase-7, caspase-9, P53, and poly (ADP-ribose) polymerase (PARP) [61].

Another approach was taken Mousavi et al. [62] on the MCF-7 cell line treated with aqueous saffron extract (100, 200, 400, and 800 μg/mL) using the trypan blue assay to investigate the morphological changes of cells under an inverted microscope as well as gene expression of matrix metalloproteinase (MMP). The treatment groups showed a significant reduction in MMP gene levels compared to the control group. Since MMPs regulate the signaling pathway that controls cell growth, inflammation, or angiogenesis, MMPs may be a target in cancer treatment and metastasis inhibition.

An earlier study was performed in which HeLa cells were treated with an ethanolic extract of saffron and its compounds. The IC_{50} for the ethanolic extract was 2.3 mg/mL, 3 mM for crocin and picrocrocin, separately, and 0.8 mM for safranal. Crocin, safranal, and picrocrocin showed a dose-dependent inhibition of cell growth, while crocetin did not show any effect on cell proliferation [63].

Sun et al. [64] examined the effect of crocin on human promyelocytic leukaemia cells and HL-60 cells *in vitro* where they found that crocin (0.625-10 mg/mL) significantly inhibited HL-60 cell proliferation dose-dependently and induced cell cycle arrest at G0-G1 phase in HL-60 by flow cytometry using propidium iodide staining.

Another study was performed by Tuberoso et al. [65] in which cytotoxicity of saffron juice was evaluated by MTT assay on Caco-2 colon cancer cell line; the cell viability was 30% at 48 h treatment with saffron juice (10 μL/mL), while at 24 h treatment, cell viability was 32% but only at a higher concentration (50 μL/mL).

5.1.2. Antimicrobial Activity. Bacterial infections can trigger various diseases such as pneumonia, otitis, diarrhea, and skin infections and are the result of severe infections with germs difficult to treat such as bacteria in the category of Gram-negative germs Enterobacteriaceae, Streptococci, *Escherichia coli*, or *Salmonella* [66, 67]. The main method of fighting bacterial infections is antibiotic treatment [68]. Although they are effective in most cases, their widespread use has led to antibiotic resistance. This phenomenon consists in the adaptation of bacteria and, consequently, to difficulties in treating infections. Due to the use of antibiotics, the saprophytic microbial flora is destroyed, the flora that

Table 1: *In vitro* biological activities of *Crocus* plants.

Extract/compound	Tested cell lines/methods of analysis	Effect/mechanisms	Ref.
Cytotoxic activity			
Saffron/aqueous extract	A549 lung cancer cells MTT Morphological change: inverted microscope Apoptosis: flow cytometry	$IC_{50} = 390\,\mu g/mL$ Inhibition and shrinkage of cancer cells ↑percentage of early and late apoptotic cells	[60]
Crocin/aqueous extract	MCF-7 breast cancer cells MTT Apoptosis: flow cytometry Caspase-7, caspase-9, P53, and PARP: western blot	$IC_{50} = 3.5\,mg/mL$ Crocin and paclitaxel: ↑apoptosis, ↑caspase-7, ↑caspase-9, ↑p53, and ↑PARP	[61]
Saffron and its derivatives/ethanolic extract	HeLa human cervical epithelioid carcinoma cells Cytotoxicity assay Morphological change: microscopy	$IC_{50} = 2.3\,mg/mL$ for saffron, $IC_{50} = 3\,mM$ for crocin, $IC_{50} = 0.8\,mM$ for safranal, and $IC_{50} = 3\,mM$ for picrocrocin ↑cytotoxicity	[63]
Saffron	HeLa human cervical epithelioid carcinoma cells colony formation inhibitory assay	↓tumor cell growth Trans-crocin 3: inhibitory effect	[90]
Crocin	HL-60 leukaemia cells Apoptosis: flow cytometry MTT	$IC_{50} = 0.625 - 10\,mg/mL$ ↓cell proliferation dose-dependently ↑cell cycle arrest at the G0-G1 phase	[64]
Saffron juice	Caco-2 colon cancer cells MTT	$IC_{50} = 50\,\mu L/m$ ↓cell viability	[65]
Saffron/aqueous extract	MCF-7 breast cancer cells gene expression level of MMP using RT PCR trypan blue test	↓MMP gene expression	[62]
Antimicrobial activity			
Crocus sativus/petroleum ether, methanolic extracts	Agar well diffusion	Petroleum ether extract: effective against *Proteus vulgaris*, *Bacillus subtilis*, *Pseudomonas aeruginosa* methanolic extract: ↓development of *S. aureus*, *E. coli*	[69]
Crocus sativus/two extracts one contained the aglycon part of flavonoids the other contained flavonoids glycosides	Agar well diffusion	The extract that contained the glycosidic part of flavonoids exhibited weak antimicrobial activity	[70]
Saffron/aqueous extract	Modified well plate test	↓growth inhibition zone tested pathogens: *E. coli*, *S. aureus*, and *S. faecalis*	[72]
Antioxidant activity			
Crocus chrysanthus (Herb.)/ethyl acetate, methanol, and water extracts	DPPH reductive potentials, metal chelating phosphomolybdenum method	The water extract showed the most powerful antioxidant activity	[81]
Crocin, saffron/ethanolic extract	Antihemolysis activity DPPH, lipid peroxidation Phosphomolybdenum method	The saffron extract exhibited 107 mg α-tocopherol/g DPPH radical-scavenging activity and 98.3, 90.8, and 33.1 mg α-tocopherol/g, respectively, for crocin-1, crocin-2, and crocin-3	[82]
Saffron/ethanolic, methanolic extract	DPPH ferric reducing antioxidant power	Methanolic extract 300 $\mu g/mL$: ↑↑antioxidant activity	[83]
Saffron/corms, tepals, and leaves	β-Carotene/linoleate model system, reducing power, DPPH, NO, radical scavenging, iron, and copper chelation	The best antioxidant activity: leaves and tepal extract, the least antioxidant activity: corms	[84]
Saffron/aqueous extract	Bronchial epithelial cells	↓NO, ↓iNOS, and ↓peroxynitrite ion generation ↓cytochrome c release	[86]
Antidiabetic			
Crocus chrysanthus (Herb.)/ethyl acetate, methanol, and aqueous extracts	α-Glucosidase inhibition α-Amylase inhibition	α-Glucosidase inhibition: 14.8-1.89 mmol acarbose equivalent/g according to different	[81]

Extract/compound	Tested cell lines/methods of analysis	Effect/mechanisms	Ref.
	extracts		
		α-Amylase inhibition: 0.8-0.15 mmol acarbose equivalent/g	

Abbreviations and symbols: ↑ increased, ↓ decreased, 2,2-diphenyl-1-picryl-hydrazyl-hydrate (DPPH), induced nitric oxide synthase (iNOS), nitric oxide (NO), and poly (ADP-ribose) polymerase (PARP).

facilitates digestion and supports the immune system. Thus, side effects such as gastrointestinal disorders, diarrhea, and allergic reactions occur. Therefore, alternative natural treatments with proven antibacterial effects are an important antimicrobial alternative.

Antimicrobial activity of *C. sativus* extracts (500, 750, and 1,000 μg/disc) was evaluated by the presence or absence of inhibition zone and zone diameter [69]. Maximum zone inhibition of the petroleum ether extract was shown against *Proteus vulgaris*, *Bacillus subtilis*, and *Pseudomonas aeruginosa*, whereas the methanolic extract showed maximum zone inhibition against *S. aureus* and *E. coli*, as demonstrated by Muzaffar et al. [69].

Kakouri et al. [70] investigated the antimicrobial activity of two extracts of *C. sativus* tepals. One extract contained the aglycon part of flavonoids and the other contained flavonoids glycosides. The antimicrobial activity of the extracts was evaluated against six bacterial species by well diffusion assay, where the extract that contained the glycosidic part of flavonoids exhibited weak antimicrobial activity. The best antimicrobial capacity was presented by tepal extract containing aglycons. Results from a study conducted by Hussein et al. [71] indicated strong antibacterial activity of the saffron extract against *E. coli* and *Staphylococcus aureus* at a concentration of 100 μg/mL. They claimed that the methanolic extract of crocin possesses the highest antibacterial activity against *E. coli* and *S. aureus* compared to other saffron pigments. They found that the antibacterial effect of crocin is approximately equal to chloramphenicol and ciprofloxacin (known as standard antibiotics) at 100 μg/mL concentration [71].

Another study was performed to assess the antimicrobial activity of aqueous extract of *C. sativus* collected from different areas in Iran using 3 different bacteria by a modified well plate test where different concentrations of extract were done and evaluated based on growth inhibition zone in which some of them had antimicrobial (*S. aureus* and *E. faecalis*) activity while others had no detectable activity (*E. coli*) [72].

5.1.3. Antioxidant Activity.
Oxidative stress is the term used for diseases caused by reactive oxygen species (ROS) called free radicals [73, 74] and is defined as the imbalance between oxidants and antioxidants, in favor of oxidants, with destructive and pathogenetic potential [75, 76]. Depending on the intensity, oxidative stress can occur intra- or extracellularly [77]. Intracellular oxidative stress can cause cell necrosis or more or less marked cell disorganization, with catastrophic effects in the case of a cell that cannot reproduce. Extracellular oxidative stress is also cytotoxic [78, 79]

(Figure 2). Among the saffron constituents, crocetin has stronger antioxidant activity (DPPH (2,2-diphenyl-1-picryl-hydrazyl-hydrate)) than safranal, and the potential of crocetin was equivalent to that of Trolox and butyl hydroxyl toluene (BHT) [80].

Crocin, ethanolic extract of saffron, and different extracts of *C. chrysanthus* were evaluated by different *in vitro* assays: antihemolysis, DPPH free radical-scavenging assay, *in vitro* lipid peroxidation, ferric reducing antioxidant power, phosphomolybdenum method, metal chelating, and reductive potentials [81–83]. The studied extracts and isolates from saffron exhibited significant antioxidant activity (Table 3); however, this activity is affected by the type of solvent used that is why they may be involved in the treatment of various diseases *via* free radical scavengers.

Another study was done to evaluate the antioxidant activity of corms, tepals, and leaves of saffron to increase the profitability of this crop in which the leaf extract showed the best antioxidant activity *via* total inhibition of the β-carotene oxidation at 10 μg/mL and a DPPH scavenger activity higher (up to 32 times) than those reported for traditional sources of antioxidants; a similar effect was shown with tepal extract, but in contrast, corm extract was a weak antioxidant [84].

Crocin had the stronger antioxidant capacity on rat pheochromocytoma (PC-12) cells than the standard antioxidant agent α-tocopherol so that it could reverse the results of the cell membrane damage and enhanced superoxide dismutase (SOD) level in oxidatively stressed neurons [85]. Bukhari et al. [86] investigated in stressed bronchial epithelial cells by cytokine combination the effects of *C. sativus*. Saffron treatment and its constituents (safranal and crocin) decreased nitric oxide of (NO), induced nitric oxide synthase (iNOS) levels, and peroxynitrite ion generation and prevented cytochrome c release.

Saffron constituents reduced lipid peroxidation [87] and prevented the increase of oxidative stress markers induced by diazinon through free radical-scavenging activity [88]. Moreover, a mitochondrial and lipid peroxidation protection against 3-nitropropionic acid toxin has also been reported in striatal synaptosomes isolated from rat brain [89].

A summarized scheme with the most representative antioxidant mechanisms of phytocompounds of *Crocus sativus* L. is shown in Figure 2.

5.2. In Vivo studies, cellular, and molecular pharmacology

5.2.1. Effects on Cardiovascular System

TABLE 2: *In vivo* evaluation of the pharmacological properties of *Crocus* plant.

Plant/compound/extract	Doses	Route	Model	Main pharmacological effect	Ref.
Crocetin	100 mg/kg	Oral	Rats stroke-prone spontaneously hypertensive rats high-oxidative stress model	Antioxidant ↓oxidative stress, ↓ROS in rats brain	[95]
Crocus sativus L./aqueous extract	10, 20, and 40 mg/kg	i.p.	Rats STZ-induced diabetes	Antihyperglycemic ↓blood glucose, ↓MDA, ↓NO, ↓lipids, ↓TG, ↓cholesterol, ↑glutathione level, ↑CAT, ↑SOD ↓inflammatory cytokines	[180]
Crocus sativus L./aqueous, ethanol extracts	500 mg/kg	i.v.	Rats, guinea pigs	Antihypertensive ↓blood pressure in a dose-dependent manner	[100]
Crocetin	20 mg/kg	Oral	Lung cancer-bearing mice benzo(a)pyrene- (B(a)p-) induced lung carcinoma	Antitumor ↑activities of enzymatic antioxidants ↑glutathione metabolizing enzymes	[203]
Crocetin	50 mg/kg	i.p.	Mice Benzopyrene-induced lung cancer model	Antitumor ↓proliferating cells	[204]
Zhejiang saffron	100 mg/kg	Oral	Mice Xenograft tumor	Antitumor ↓tumor size *via* caspase-3, caspase-8, caspase-9, and ↑apoptosis	[205]
Saffron/aqueous infusion	50-500 mg/kg	Oral	Mice DMBA-induced skin carcinogenesis	Antitumor ↓papilloma cells formation	[206]
Saffron/aqueous extract	100 mg/kg	Topical	Mice DMBA, croton oil-induced skin carcinogenesis, MCA-induced soft tissue sarcomas	Antitumor ↓tumor formation	[207]
Saffron	400, 800 mg/kg	Oral	Rats PTZ-induced seizures	Anticonvulsant ↓seizures frequency in a dose-dependent manner	[128]
Safranal	0.15, 0.35 mL/kg	i.p.	Mice PTZ-induced seizures	Anticonvulsant ↓seizures duration, delayed the onset of tonic convulsions	[16]
Safranal	72.75, 145.5, and 290 mg/kg	i.p.	Rats PTZ-induced seizures	Anticonvulsant ↓MCS, ↓GTCS	[17]
Crocin	200 mg/kg	i.p.	Mice PTZ-induced seizures	It did not show anticonvulsant activity	[16]
C. sativus L./hydroethanolic extract	50 mg/kg	Oral	Meriones shawi Pb-intoxicated (25 mg/kg bw, i.p.)	Neuroprotective ↑TH in SNC, VTA, LC, DS, and MFB ↑locomotor activity, ↓dysfunction in Pb-intoxicated meriones	[141]
Crocetin	25, 50, 75 μg/kg	i.p.	Rats 6-Hydroxydopamine (10 μg intrastriatal) Induced Parkinson's disease	Neuroprotective ↓dopamine utilization by tissues	[145]
Saffron	0.01% *w/v*	Oral	BALB-c mice MPTP-induced Parkinson's disease	Neuroprotective ↓ROS, ↑antioxidant effect → protect dopaminergic cells	[146]
C. sativus L./stigma extract	100 mg/kg	Oral	Rats Induction of cerebral ischemia MCAO	Neuroprotective ↓SOD, ↓CAT, ↓Na⁺, and K⁺-ATPase activities ↓glutamate, ↓aspartate induced by ischemia	[164]
Saffron/honey syrup	200, 500 mg/kg	Oral	Mice Aluminum chloride-induced neurotoxicity	Neuroprotective ↓neurotoxicity	[208]

Table 2: Continued.

Plant/compound/extract	Doses	Route	Model	Main pharmacological effect	Ref.
Saffron/aqueous extract	50, 100, 200 mg/kg	Oral	Rats Diazinon- (20 mg/kg) induced neurotoxicity	Neuroprotective ↓inflammation, ↓oxidative stress, and ↓neuronal damage	[88]
Crocin	30, 60, 120 mg/kg	Oral	Rats Ischemia/reperfusion injury model of stroke	Neuroprotective Crocin 60 mg/kg → ↓brain oedema	[158]
Crocetin	50 mg/kg	Oral	Rats Induced cerebral contusion	Neuroprotective ↑neurological function, ↓neuronal apoptosis ↑VEGFR-2, ↑SRF	[155]
Crocin	25, 50 mg/kg	i.p.	Rats Retinal damage induced by ↑intraocular pressure	Retinal damage protection ↑RGCs, ↓apoptosis, and ↑PI3K/AKT	[197]
Crocetin	100 mg/kg	Oral	Mice N-Methyl-d-aspartate in the murine retina	Retinal damage protection ↓NMDA, ↓GCL cell number, ↓TUNEL-positive cells, ↓b-wave amplitude, ↑caspase-3/7, and ↑caspase-3 in the GCL	[195]
Saffron/aqueous extract	50, 100, 150, and 250 mg/kg	i.p.	Rats	Effect on brain neurotransmitters ↑dopamine, ↑glutamate in a dose-dependent manner No effect on brain serotonin, norepinephrine	[209]
Saffron/aqueous, ethanolic extracts	80–320, 400–800 mg/kg	i.p.	Mice Naloxone-induced model	Effect on opioid system ↓morphine withdrawal signs ↓locomotor activity (open-field test)	[171]
Saffron/ethanolic extract safranal	10, 50, and 100 mg/kg 1, 5, and 10 mg/kg	i.p.	Mice	Effect on opioid system ↓acquisition, ↓expression of morphine conditioning place preference	[210]
Crocin	400, 600 mg/kg	i.p.	Mice	Effect on opioid system ↓acquisition, ↓reinstatement of morphine-induced conditioning place preference	[211]
Crocus sativus L./ethanolic extract from stigma	5, 10 μg/kg	Intra-accumbal	Rats	Effect on opioid system ↓time spent on the drug paired side, ↓expression of morphine conditioning place preference	[212]
Crocus sativus L./aqueous, ethanolic extracts from stigma safranal crocin	Extracts 0.2-0.8 g/kg Safranal 0.15-0.5 mL/kg Crocin 50-600 mg/kg	i.p.	Mice Forced open-field swimming test	Antidepressant Extracts, safranal, crocin: ↓immobility time, ↑stereotypic activities Safranal: ↑swimming time Safranal and crocin: ↑climbing time Crocin: ↑dopamine, ↑norepinephrine Safranal: ↑serotonin	[18]
Crocus sativus L./aqueous extract	30 mg/kg	ICV	Rats STZ-ICV Alzheimer's disease model	Anti-Alzheimer ↓cognitive deficits ↑learning, ↑memory via metabolism/enzyme mechanisms, no anatomical structural repair involved	[136]
Saffron	60 mg/kg	i.p.	BALB-c mice adult and aged	Cognitive enhancing effect ↑learning, ↑memory (passive avoidance behavior test) ↓AChE in adult mice No effect on AChE activity on aged mice	[213]
Crocin	30 mg/kg	ICV	Rats STZ-ICV Alzheimer's disease model	Anti-Alzheimer ↑memory (passive avoidance test) ↑spatial cognition (Y-maze task)	[137]

Table 2: Continued.

Plant/compound/extract	Doses	Route	Model	Main pharmacological effect	Ref.
				Hypolipidemic	
Crocin	25-100 mg/kg	Oral	Rats Diet-induced hyperlipidemia	↑faecal excretion of fat and cholesterol Not influence the elimination of bile acids ↓pancreatic lipase as a competitive inhibitor	[175]
Crocin safranal	25, 50, and 100 mg/kg 0.5, 1, and 2 mg/kg	i.p.l.	Rats Local inflammation induced by i.p.l. injection of carrageenan (100 μL, 2%)	Anti-inflammatory ↓oedema, ↓inflammatory pain responses ↓neutrophils	[214]
Crocus sativus L./ethanolic extract from stigma	20, 40, and 80 mg/kg	Oral	Rats Alloxan-induced diabetes	Antihyperglycemic 40 mg/kg: ↓blood glucose, ↑serum insulin	[182]
Safranal	0.2, 0.5, 0.75 mL/kg	Aerosol	Guinea pigs' citric acid aerosol for 10 min	Antitussive ↓cough count significantly as compared to the saline-treated group	[189]

Abbreviations and symbols: ↑ increase, ↓ decrease, body weight (bw), catalase (CAT), dimethylbenzene [a] anthracene (DMBA), dorsal striatum (DS), generalized tonic-clonic seizures (GTCS), intracerebroventricular (ICV), intraperitoneal (i.p.), intraplantar (i.p.l.), intravenously (i.v.), locus coeruleus (LC), 20-methylcholanthrene (MCA), 1-methyl-4-phenyl-1,2,3,6-tetrahydropyridine (MPTP), malondialdehyde (MDA), medial forebrain bundle (MFB), middle cerebral artery occlusion (MCAO), minimal clonic seizures (MCS), nitric oxide (NO), pentylenetetrazole (PTZ), phosphatidylinositol 3-kinase (*PI3K*)/ protein kinase B (*AKT*), reactive oxygen species (ROS), retinal ganglion cells (RGCs), serum response factor (SRF), substantia nigra compacta (SNc), superoxide dismutase (SOD), streptozotocin (STZ), triglycerides (TG), tyrosine hydroxylase (TH), ventral tegmental area (VTA), and vascular endothelial growth factor receptor-2 (VEGFR-2).
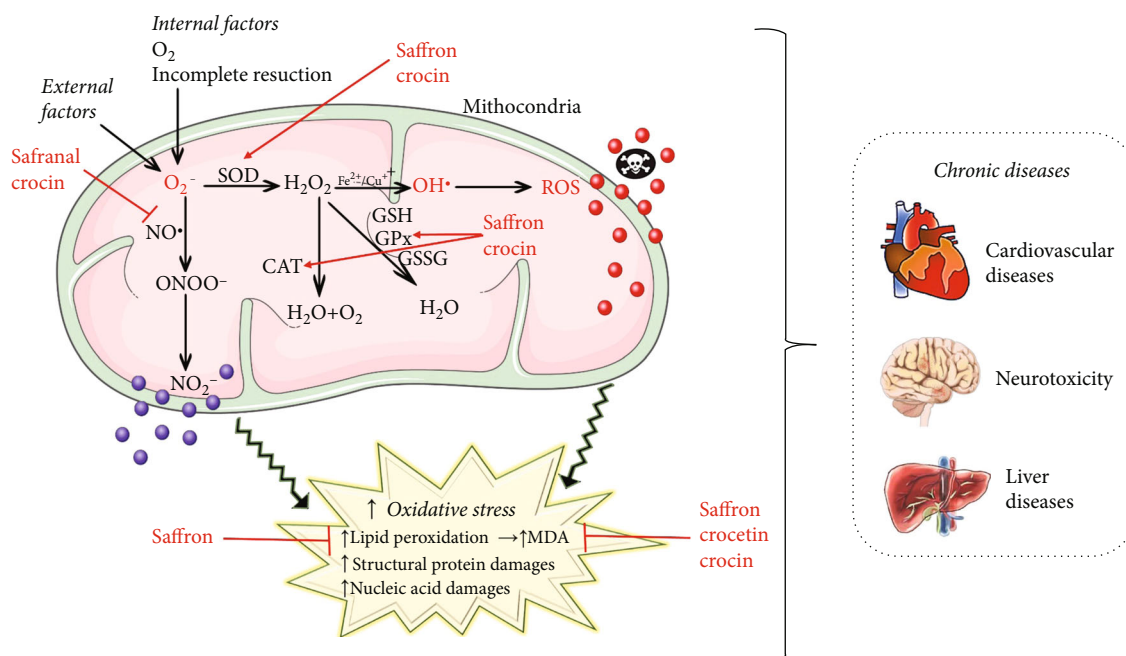
Figure 2: Illustrative scheme with different pathways of ROS formation and their impact on health. Bioactive compounds of *Crocus sativus* L. interfere with these mechanisms showing the beneficial effects for human health. Abbreviations and symbols: ↑ (increase, stimulate), ⊠ (decrease, inhibition), CAT (catalase), NO (nitric oxide), MDA (malondialdehyde), ROS (reactive oxidative species), glutathione peroxidase (GPx), GSSG (oxidized glutathione), GSH (reduced glutathione), O_2^- (superoxide), H_2O_2 (hydrogen peroxide), OH• (hydroxyl ions), and NO (nitric oxide).

(1) Antihypertensive Effect. High BP is a major cardiovascular risk factor with a growing incidence [75]. High BP can be controlled with medication, but natural remedies with proven antihypertensive effects are also used as adjuvant therapy [91].

Crocus sativus extract and safranal were reported to stimulate β2-adrenoreceptors [92, 93]. Also, safranal can act as a muscarinic receptor blocker, and *C. sativus* has an inhibitory or even antagonistic effect on histamine (H1) receptors [93].

Crocetin has been reported to lower the BP [94]. Yoshino et al. [95] observed the antioxidant potential of crocetin in stroke-prone spontaneously hypertensive rats and a significant inhibition of hydroxyl radical generation.

Crocin and safranal have BP-modulating features, but the mechanism of action is still under investigation [96].

TABLE 3: Clinical studies.

Type of extract	Type of study	Dose/period	Effect	References
Saffron extract	Randomized double-blind clinical trial	30 mg/day Six weeks	Saffron supplements statistically improved the mood of subjects compared to the placebo group based on the Hamilton depression rating scale (HAM-D)	[222]
Saffron extract	Randomized double-blind clinical trial	30 mg/day for six weeks	Treatment of mild to moderate depression ↓clinical signs	[215]
Hydroalcoholic extract of *Crocus sativus* L. coadministered with fluoxetine	Randomized double-blind clinical trial	(40 or 80 mg) (30 mg/day) Six weeks	*C. sativus* 80 mg plus fluoxetine was more effective in the treatment of mild to moderate depressive disorders	[223]
Crocin/aqueous extract	Clinical trial	15 mg twice daily	Well tolerated by schizophrenic patients with no severe side effects	[221]
Saffron extract (Affron®)	Randomized, double-blind, placebo-controlled study, youth aged 12–16 years	14 mg twice daily 8 weeks	Improved anxiety and depressive symptoms	[218]

Crocin and safranal showed a hypotensive effect in a dose-dependent manner, being safranal more potent [97].

In addition, the cardioprotective role of saffron and its constituents has been reported [98]. The aqueous extract of saffron stigmas was reported to have an antihypertensive and normalizing effect on the BP of normotensive and deso-xycorticosterone acetate (DOCA) salt-induced hypertensive rats [99]. Aqueous extract of saffron petals (500 mg/kg) reduced BP through its direct effect on the heart itself or the total peripheral resistance or both [100]. In rats' isolated vas deferens, contractile responses to electrical field stimulation were decreased by the petal extracts [100]; this effect was mediated by cotransmitter noradrenaline and ATP released from sympathetic nerves. Another study suggested that saffron exerted a significant cardioprotective effect by preserving hemodynamics and left ventricular functions [101].

(2) Antiarrhythmic effect. Saffron plays an important role in the electrophysiological remodeling of the atrioventricular (AV) node during atrial fibrillation [102]. Boskabady et al. [103] observed a potent inhibitory effect of saffron aqueous extract on the noradrenaline of the guinea pig's isolated heart. In patients with ischemic heart disease, crocin also can be utilized for the prevention or treatment of arrhythmias [104]. Crocin was tested against cardiac reperfusion-induced arrhythmia, where it showed a defensive role in cardiac reperfusion arrhythmias, through amplification of antioxidant systems [104].

Myocardial damage and arrhythmia are associated with increased malondialdehyde (MDA) level, decreased activity of antioxidant enzymes, accumulation of free radicals, and the effect on ion Ca^{2+} channels [105]. Inhibition of ADP

and collagen-induced platelet aggregation by crocetin *via* inhibition of Ca^{2+} elevation in stimulated platelets have also been reported in a dose-dependent manner [106]. The suggested cardioprotective effect of saffron mechanism is antioxidant activity, recovery, and upregulation of antioxidant enzymes [107], e.g., glutathione peroxidase (GPx), by inhibition of cardiac calcium channels.

(3) Effect on Myocardial Ischemia. In isoproterenol- (ISO-) induced myocardial infarction rat model, Goyal et al. [108] observed a dose-dependent preventive effect of saffron through histopathological and ultrastructural examinations. In addition, intravenous crocin reduced myocardial injury and lactate dehydrogenase (LDH) and creatine kinase (CK) level [109]. Orally administration did not show the same effects, possibly because of the inefficient absorption.

(4) Antiatherosclerotic Effect in Cardiovascular Diseases. In bovine aortic endothelial cells, crocin regulated redox status in a dose-dependent pattern and exhibits regression and inhibition of atherosclerosis *via* apoptosis by increasing Bcl 2/Bax ratio expression [109]. Antiatherosclerotic effects of saffron were observed mainly because of crocetin that decreased the level of cardiac markers, e.g., LDH, CK, and MDA, besides increasing the mitochondrial potential in noradrenaline-treated cardiac myocytes [110].

Crocetin administration significantly decreased total cholesterol (TC) deposits in aorta, atheroma, foam cells, and atherosclerotic lesions in the crocetin fed animals [110]. A possible mechanism involved is due to suppression of nuclear factor- (NF-) κB, which in turn decreases the vascular cell adhesion molecule-1 (VCAM-1) expression [111]. This antiatherosclerotic effect of crocetin has been also

attributed to its antioxidant activity that decreases ROS-induced MDA levels [101]. In another study, crocetin decreased the TC level in the blood and thus reduced the risk of atherosclerosis and heart attacks. This effect may be due to the reinforcement of blood circulation [112]. Hemmati et al. [113] compared the antiatherogenic effects of three medicinal plants *C. sativus*, *Beta vulgaris* L., and *Ziziphus jujuba* Mill. in diabetic rat models, where the three extracts possessed antiatherogenic activity, which is probably associated with the antioxidant capacities of the extracts.

5.2.2. Antiproliferative and Cytotoxic Activities.

Saffron and its carotenoid constituents are chemopreventive in the growth of human malignant cells and animal models. Chermahini et al. [114] reported that saffron and its constituents could inhibit the synthesis of cellular DNA and RNA with no effect on protein synthesis in tumor cells. The antitumor effect of saffron and its ingredients is due to the free radical-scavenging effect, together with the interaction with topoisomerase II [114, 115].

Saffron exerted a protective effect against the toxicity of cisplatin when applied with the cysteine and vitamin E [116, 117]. Saffron can potentiate the effect of other anticancer agents through the inhibition of colony formation and nucleic acid synthesis [116]. Saffron aqueous extract also reduced the dimethylnitrosamine- (DEN-) induced hepatic cancer through induction of apoptosis, inhibition of cell proliferation, oxidative stress, and inflammation [118]. Premkumar et al. [119] showed the antimutagenic and antioxidant potential of aqueous extract of saffron.

In mice, an aqueous extract of saffron has been found to prevent specific drugs (cisplatin, urethane, cyclophosphamide, and mitomycin C) that induced genotoxicity and oxidative stress besides increasing hepatic enzymes such as SOD, catalase (CAT), and nonenzymatic antioxidants [120]. The authors suggest that its chemopreventive role is observed because of its antioxidant activity and modulatory property during lipid peroxidation and detoxification.

5.2.3. Neuroprotective Effects

(1) Anticonvulsant Activity. In pentylenetetrazole- (PTZ-) and maximal electroshock seizure- (MES-) induced seizures in mice, Hosseinzadeh and Khosravan [121] indicated an anticonvulsant activity of aqueous and ethanolic extracts of *C. sativus*. Similar anticonvulsant activity was shown by safranal, contrary to that of crocin, which did not show any effect [16]. It is suggested that the anticonvulsant effect of safranal is mediated partly through GABA (A)-benzodiazepine receptor complex [122–126]. In addition, it is assumed that saffron's anticonvulsant and analgesic properties and its effects on morphine withdrawal might be due to an interaction between saffron, GABA, and opioid system [127]. Saffron did not significantly suppress PTZ-induced seizures at a dose of 200 mg/kg in rats [128].

(2) Neuroprotection in Neurodegenerative Diseases. Neurodegenerative diseases, such as Alzheimer's and Parkinson's diseases, are characterized by the presence of protein aggregates, inflammation, and oxidative stress in the central nervous system (CNS) [129]. A number of factors are involved in the onset of neurodegenerative diseases, which lead to the gradual deterioration of the health of the nervous system, with serious consequences on the quality of life of the patient with such a disease [130]. Although there are still no treatment solutions to restore nerve function in neurodegenerative diseases, more and more studies insist on several natural formulas that have been shown to have the effect of reducing symptoms and improving the quality of life of patients with neurodegenerative diseases. Alzheimer's disease is a neurodegenerative disease that causes disorders of memory, thinking, and behavior [131].

Saffron has been reported to inhibit the aggregation and deposition of amyloid β (Aβ) and thus prevent the short-term memory problems characteristic of mild to moderate Alzheimer's disease. Inhibition of Aβ fibrillogenesis by methanol and water extract of *C. sativus* stigmas is dose- and time-dependent [132–134]. Crocin was found more effective in preventing the toxic amyloid structures accumulation due to its amphiphilic properties [132]. On the other hand, *trans*-crocin 4 was more effective in Alzheimer's disease than dimethyl crocin in inhibiting Aβ fibrillogenesis through oxidation of the amyloid β-peptide fibrils [135]. Treatment with saffron extract could improve cognitive deficits induced by intracerebroventricular (ICV) injection of STZ in rats [136]. However, Khalili and Hamzeh [137] reported that the main component of saffron, crocin, is responsible for antagonizing the cognitive deficits caused by STZ-ICV in rats and can be used for treating the neurodegenerative diseases. Saffron had shown about 30% inhibitory effect on acetylcholinesterase (AChE) activity, which can be another mechanism for treating Alzheimer's disease [138, 139].

Parkinson's disease is related to dopamine deficiency due to genetic factors or Pb intoxication and is characterized by the degeneration of neurons in the substantia nigra [140]. The accumulation of lead (Pb) in the environment causes intoxication of the body, mainly affecting the CNS as it leads to structural and functional disruption of the CNS, and it may also develop Parkinson's disease. In a study performed by Tamegart et al. [141], the intraperitoneal injection of Pb caused a neurotoxic effect on the dopaminergic system and locomotor performance in Meriones shawi rats. The oral gavage of *C. sativus* (50 mg/kg body weight) prevented Pb-induced damages. Polyphenols such as quercetin and catechin have demonstrated Fe and Zn chelation activities. Thus, saffron may have a neuroprotective activity for neurodegenerative disorders, implying dopaminergic and noradrenergic injuries, especially heavy metal-induced Parkinson's disease.

Oxidative stress in the CNS is related with neurodegenerative diseases [142–144]. Crocetin could strengthen the antioxidant system and reduce thiobarbituric acid (TBARS), therefore inhibiting the effect of 6-hydroxydopamine, which is involved in inducing Parkinson's disease, and also decreased the utilization of dopamine [145]. In mice, saffron also showed effectiveness against MPTP- (1-methyl-4-

phenyl-1,2,3,6-tetrahydropyridine-) induced Parkinson's disease, as pretreatment with saffron protected the dopaminergic cells in the substantia nigra pars compacta and retina [146].

(3) Antidepressant Effect. Saffron and its components possess antidepressant and anxiolytic effects [132]. Crocin (50–600 mg/kg) reduced immobility time in rats in the forced swimming test, with the increase in climbing time [18]. Wang et al. [147] demonstrated that the petroleum ether and dichloromethane fractions *C. cerebral sativus* L. corms have an antidepressant effect.

The aqueous and ethanolic extracts of *C. sativus* petal and stigma [148], as well as safranal and crocin, had shown antidepressant activity in mice [18]. In addition, kaempferol, a constituent of *C. sativus* petals, also reduced immobility behaviors in mice at 100 and 200 mg/kg and rats at a dose of 50 mg/kg [149]. The reduced time of immobility in rats and mice is usually due to the selective serotonin reuptake inhibitors such as fluoxetine, and this may be the mechanism by which *C. sativus* exerts its antidepressant effects [150].

(4) The Effects on Neurotoxicity and Neuronal Oxidative Damages. Neurotoxicity refers to disturbances or damage to the CNS by toxic substances and toxins that affect the nervous system are called neurotoxins [52, 151].

Safranal has neuroprotective effects on oxidative damage markers in hippocampal tissue in ischemic rats [152] and in hippocampal tissue in rats treated with quinolinic acid [153]. Safranal decreases extracellular content of the excitatory amino acids, glutamate, and aspartate in the hippocampus of anaesthetized rats treated with kainic acid [154].

Crocetin can inhibit early stages of apoptosis and induce angiogenesis at the subacute stage as depicted by vascular endothelial growth factor receptor-2 (VEGFR-2) and serum response factor (SRF) expression levels, so it exerts *in vivo* neuroprotective effects the brain [155]. It has been demonstrated that crocetin could potentiate the antioxidant capacity in the brain and prevents 6-hydroxydopamine-induced neurotoxicity [145].

Crocin has a unique, protective effect on ethanol-induced impairment of learning and memory [134].

Sahraeil et al. [156] reported that saffron ethanolic extract and crocin are effective against chronic stress-induced Wistar rats, through interaction with hormonal, metabolic, and behavioral changes induced by electric shock stress in rats. Saffron extract and crocin also improved spatial cognitive abilities following chronic cerebral hypoperfusion, most probably due to their antioxidant potential [157].

Crocin also potentiated SOD and GPx activity and decreased MDA concentration in the cortex of the ischemic stroke rat model [158]. In an ischemic stroke rat model, crocin increased antioxidant enzyme activity of SOD, CAT, and GPx and reduced MDA levels and lipid peroxidation [89]. In cerebral ischemia, crocin inhibited oxidizing reactions in mice microvessels in addition to modulating the ultrastructure of cortical microvascular endothelial cells (CMEC) [159]. Crocin and crocetin can inhibit the activated microglia by the repression of the NF-κB transcriptional activity [160].

Both saffron extract and crocin may improve learning and memory [161, 162] as both can prevent oxidative stress in the hippocampus [138]. The enhancing effect of saffron on memory is mediated by its effect on the cholinergic system [162, 163].

Saffron and its derivatives act as curative agents in focal ischemia [164], autoimmune encephalomyelitis in C57BL/6 mice, cerebral ischemia [158], hippocampal ischemia [165], and renal ischemia/reperfusion [166]. In the whole brain and cerebellum, saffron extract reversed aluminum-induced changes in monoamine oxidase A and B activity and lipid peroxidation levels [167]. The antioxidant potential of saffron may be responsible for attenuation in cerebral ischemia-induced oxidative damage in the rat hippocampus [152]. Ghazavi et al. [123] investigated ethanolic extracts of saffron in mice and observed an increase of antioxidant potential, increased level of glutathione and its dependent enzyme, and a suppression of the increased levels of MDA, glutamate, and aspartate.

(5) Effect on Brain Receptors. Saffron was reported to have a similar effect to *N*-methyl-D-aspartate (NMDA) receptor antagonists on conditioning place preference induced by morphine [168]. Furthermore, saffron analgesic effect may be reduced by NMDA receptor antagonists, which suggested an interaction of saffron with the glutamatergic system [169].

Crocin (200 and 600 mg/kg) could inhibit the morphine withdrawal symptoms with no effect on the locomotor system [170, 171]. The saffron extract reduced morphine-induced memory impairment [125] and prevented morphine-induced inhibition of spatial learning and memory in rats [172].

5.2.4. Effects on Metabolisms

(1) Hypolipidemic Effect. Premkumar et al. [173] showed that saffron and its constituents decreased triglycerides (TGs), TC, alkaline phosphatase (ALP), aspartate transaminase (AST), alanine aminotransferase (ALT), MDA, and GPx, reduced glutathione (GSH) and oxidized glutathione (GSSG) levels in serum, and provoked an increasing effect on SOD, CAT, fluorescence recovery after photobleaching (FRAP), and GSH values in the liver tissue. Saffron was more effective than its constituents to quench free radicals and ameliorate the damages of hyperlipidemia [174].

In diet-induced hyperlipidemic rats, crocin showed hypolipidemic effect by reducing serum TG, TC, and low-density lipoprotein (LDL), and very-low-density lipoprotein (VLDL) levels [175]. Hypoglyceridemic and hypocholestero-lemic effects of crocin are also reported in quails kept on a hyperlipidemic diet [110, 176]. Crocin selectively inhibits pancreatic lipase through competitive inhibition and provokes lipid decrease [175].

In quails, the reduction of serum TC, LDL, and TG was also prominent in treatment with crocetin [110]. Cousins and Miller [177] reported that intraperitoneal injection of crocetin was more effective in showing hypolipidemic effect compared to that of the subcutaneous injection. In hypolipidemic rats, crocetin, along with crocin, showed an inhibitory effect on the increased serum TG, TC, and LDL levels [110, 176].

(2) Antihyperglycemic Effect. Diabetes is the most common disease of the endocrine system and is triggered when the amount of insulin secreted in the body is not optimal or when peripheral cells do not respond to its action (insulin is a hormone that lowers blood glucose) [178, 179].

Crocus sativus aqueous extract has also been reported to have an effect on streptozotocin- (STZ-) induced diabetic rats [180]. Diabetic rats treated with aqueous saffron extract showed reduced expression of inflammatory cytokines in the abdominal aorta. Thus, saffron can be useful also in treating diabetes mellitus and its vascular complications.

Saffron, crocin, and safranal have shown antihyperglycemic activity in the alloxan-diabetic rats through increasing blood insulin levels and caused the renewal of β-cells in alloxan-diabetic rats with neither liver nor kidney toxicities [181–183]. Crocetin was able to increase insulin sensitivity, improving impaired glucose tolerance, hypertension due to a high-fructose diet, and dexamethasone injection in rats [82, 175, 184]. Also, crocetin reduced the palmitate-induced insulin sensitivity in the rat adipocytes [185]. Crocetin could also prevent diabetes-related vascular complications [186, 187].

5.3. Other Pharmacological Activities. Saffron and safranal extract show preventive effects in lung pathology during lung inflammation of sensitized guinea pigs [188]. Safranal was shown to significantly reduce the cough count in citric acid aerosol-induced irritation in guinea pigs [189]. This effect may be due to competitive antagonistic activity to histamine H1 receptors [190]. Safranal was tested on the murine model of asthma, where it increased airway hyperresponsiveness and, in lungs, reduced iNOS production, bronchial epithelial cell apoptosis, and Th2-type cytokine production [86].

Saffron showed an important role as a curative agent in visual impairment due its antioxidant potential [191]. Saffron as a dietary supplement prevents the effects of continuous light exposure that may cause photoreceptor and retinal stress in albino rats, besides maintaining both morphology and function by acting as an apoptotic regulator [192, 193]. In ischemic retinopathy, crocin facilitates the recovery of retina functioning [194]. In murine retina, oral administration of crocetin prevents NMDA-induced retinal damage by inhibiting the caspase pathway [195], and *trans*-crocetin showed an antagonistic effect of *C. sativus* extract on NMDA receptors [196]. Crocin (50 mg/kg) inhibits retinal ganglion cell (RGC) apoptosis after retinal ischemia/reperfusion injury *via* phosphatidylinositol 3-kinase/AKT (PI3K/AKT) signaling pathway and increasing $Bcl-2/BAX$ ratio [197].

Crocin $(10 \mu M)$ could suppress tumor necrosis factor- (TNF-) α-induced expression of proapoptotic mRNA, which releases cytochrome c from mitochondria [198]. Moreover, crocetin can inhibit cell death of H_2O_2-induced RGC-5 and inhibit caspase-3 and caspase-9 activity [199].

Crocin analogues increased the blood flow in the retina and choroid and facilitated retinal function recovery [194].

Hosseinzadeh and Younesi [200] have shown that the ethanolic and aqueous extracts of saffron stigma could inhibit the acetic acid-induced writhing reflex *in vivo* and also had a curative effect on many complications such as the injury of the skeletal muscle of the lower limb [201] and reepithelialization of burn wounds [202].

The most relevant *in vivo* pharmacological studies with the major findings are shown in Table 2 and Figure 3.

6. Clinical Studies

Saffron extract (30 mg/kg for six weeks) had been reported to possess an antidepressant effect on patients similar to the effects of fluoxetine [215] and imipramine 100 mg/day [15] (Table 3). Saffron extract at this dose was equally effective to fluoxetine (40 mg/day) in improving depression symptoms in patients who were suffering from major depressive disorder (MDD) after undergoing percutaneous coronary intervention [216]. Basti et al. [217] also suggested its effectiveness in treating mild to moderate depression.

Lopresti et al. [218] designed a randomized, double-blind, placebo-controlled study for 8 weeks on patients with 12–16 years of age, with mild to moderate anxiety or depressive symptoms. Tablets containing saffron extract (Affron®, 14 mg b.i.d.) were used. The treatment improved anxiety and depressive symptoms in youth with mild to moderate symptoms, at least from the perspective of the adolescent. However, these beneficial effects were not corroborated by parents.

Administration of saffron, 30 mg/day, divided as 15 mg two times daily, in subjects of 55 years and more, was as effective as donepezil for the treatment of mild to moderate Alzheimer's disease [219]. The saffron extract had similar side effects to those of donepezil but with less vomiting [219]. Another study performed on 46 patients with mild to moderate Alzheimer's disease had shown that saffron improved the cognitive functions [220].

In another study, *C. sativus* extract administration for 3 months significantly increased white blood cell count in patients who had normal white blood cell count compared to crocin or placebo. No significant change was observed in hematologic factors during the study [221].

7. Safety and Toxicity Studies of *Crocus* Plants

The analysis of medicinal plants for toxicity is fundamental for their reliable and safe use among consumers [224]. Several investigations should be carried out to assure the safety of bioactive compounds. Indeed, preclinical studies based on animal toxicity are fundamental steps to determine the toxicity of drugs. In this step, studies focused on the determination of lethal dose (LD_{50}) and the toxicity against several
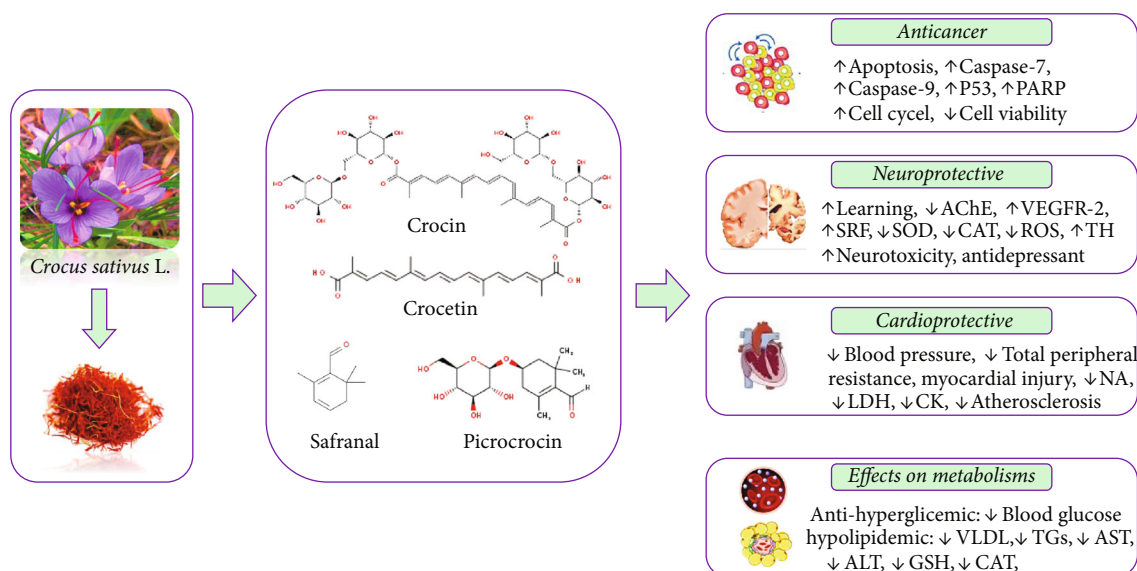
FIGURE 3: The role of *Crocus* plants' phytoconstituents in the pharmacotherapeutic management of various disorders and the possible molecular mechanisms of action. Abbreviations and symbols: ↑ increased, ↓ decreased, acetylcholinesterase (AChE), alkaline phosphatase (*ALP*), aspartate transaminase (*AST*), catalase (CAT), creatine kinase (CK), *glutathione* (*GSH*), lactate dehydrogenase (LDH), noradrenaline (NA), poly (ADP-ribose) polymerase (PARP), reactive oxygen species (ROS), serum response factor (SRF), superoxide dismutase (SOD), *tumor* protein *P53* (p53), tyrosine hydroxylase (TH), vascular endothelial growth factor receptor-2 (VEGFR-2), and very-low-density lipoprotein (VLDL).

organs (vital organs). Moreover, teratogenicity should also be evaluated in preclinical studies.

Preclinical toxicological studies of *C. sativus* and its bioactive cells were investigated by several studies in various animal models and different modes of administration.

Stigma and petal extracts of saffron exhibited moderated toxicological effects in mice using intraperitoneal administration. The LD_{50} values are 1.6 and 6 g/kg for stigma and petal extracts, respectively [225]. However, the oral administration in mice of total saffron showed an LD_{50} of 4120 mg/kg [225] (Table 4).

The ethanolic extract of saffron (stigma) showed significant effects using subacute doses in rats of the ethanolic extract (0.35, 0.7, and 1.05 g/kg i.p., for 2 weeks) that caused significant reductions in the hemoglobin (Hb) and hematocrit (HCT) levels and total red blood cell (RBC) count [226]. Moreover, the total white blood cell (WBC) count showed significant dose-dependent increases in extract-treated rats. The ethanolic extract has also exhibited necessary increases of AST, ALT, urea, uric acid, and creatinine levels, which were dose-dependent. It was also shown that an ethanolic extract increased the levels of some enzymes involved in liver injury, in particular, ALT and AST [226]. Moreover, the histopathological findings reported that ethanolic extract induced mild to severe hepatic and renal injuries, thus supporting the biochemical analysis [226].

In another study also carried out by Mohajeri et al. [227], a total extract of saffron administered in rats (0.35, 0.70, and 1.05 g/kg i.p., for 2 weeks) showed some toxicity in the given doses and caused major hepatic and renal tissue damages. The aqueous extract of saffron administered intraperitoneally at 25-100 mg/kg increased survival in rats so that no mortality was observed at a dose of 10 mg/kg [228]. In another subacute study carried out by Karimi et al. [229], the aqueous extract of the petal (1.2, 2.4, and 3.6 g/kg) and stigma (0.16, 0.32, and 0.48 g/kg) of saffron administered intraperitoneally showed a significant decrease of body weight in rats. The biochemical analysis revealed that both extracts reduced the levels of Hb, HCT, and RBC counts. Moreover, both extracts produced anemia [229]. In another study, Khayatnouri et al. [230] have evaluated the effect of saffron on the spermatogenesis index in rats. The authors showed that saffron administered at 200 mg/kg of saffron for 28 days exhibited significantly decreased spermatogenesis index, including such indicators as repopulation index, tubular differentiation index, and spermatogenesis index [230].

The subchronic toxicity of saffron was also evaluated in several additional studies [231–235]. Modaghegh et al. [232] have tested the subchronic toxicity of saffron tablets on rats at 200 and 400 mg per day for 1 week. The results showed that saffron might change some hematological and biochemical parameters. However, these adverse effects were within normal ranges because they had not altered clinical parameters [232]. Bahmani et al. [236] have tested the toxicity of the aqueous extract of saffron administered orally at 500, 1000, or 2000 mg/kg/day for three weeks to adult mice and neonates during lactation. The results did not show important toxicity ($LD_{50} = 4120$ mg/kg) in mice. In addition, the histological analysis indicated that the aqueous extract of saffron did not have any toxic effects. The administration of saffron to BALB-c mice at 4000 and 5000 mg/kg following five weeks exposure significantly decreased RBC and WBC counts and Hb level [231]. Moreover, saffron caused kidney dysfunction revealed by the increase of blood urea nitrogen (BUN) and creatinine levels treated in animals.

TABLE 4: Toxicological studies of *Crocus sativus* L.

Extract/ compound	Doses	*In vitro/ in vivo*	Route of administration	Model	Adverse effects	Ref.
Aqueous extract	1.2-2 g/bw	*In vivo*	Intraperitoneal	Mice	Nausea, vomiting, diarrhea, bleeding	[234]
Aqueous extract	4 g/bw daily	*In vivo*	Oral	Mice	Nontoxic	[235]
Aqueous extract	$IC_{50} = 50 - 400$ mg/mL	*In vitro* cytotoxic assay	—	CCD-18Lu Human normal lung cells	Noncytotoxic	[90]
Aqueous extract	500, 1000, and 2000 mg/kg daily saffron, three weeks	*In vivo*	Oral	Mice Neonates mice during lactation	$LD_{50} = 4120$ mg/kg ↑morphological changes in the kidney of neonates	[236]
Aqueous extract	50, 100, and 200 mg/kg	*In vivo*	Intraperitoneal	Rats Diazinon-induced toxicity	Prevented the toxicity induced by diazinon in rats	[238]
Ethanol extract stigmas	0.35, 0.70, 1.05 g/kg daily	*In vivo*	Intraperitoneal	Rats Subacute toxicity	↓Hb, ↓HCT, ↓RBC ↑AST, ↑ALT, ↑urea, ↑uric acid ↑creatinine ↑hepatic and renal tissue injuries, dose-dependent	[227]
Ethanol extract	2 mg/kg of cisplatin	*In vivo*	Oral	Mice Cisplatin-induced toxicity	↑life span of cisplatin-treated mice almost threefold	[250]
Aqueous extract	25-100 mg/kg	*In vivo*	Intraperitoneal	Rats Acute and subacute toxicity	↑survival No mortality at dose 10 mg/kg	[228]
Aqueous extract	Several doses	*In vivo*	Oral	Rats	21.42 mL/kg	
Aqueous extract	Several doses	*In vivo*	Intraperitoneal	Rats	1.48 mL/kg	[251]
Aqueous extract	Several doses	*In vivo*	Oral	Mice	5.53 mL/kg	
Aqueous extract	Several doses	*In vivo*	Intraperitoneal	Mice	3500 mg/kg	
Total extract	0.35, 0.70, and 1.05 g/kg	*In vivo*	Intraperitoneal	Rats	Hepatic, renal tissue damages anemia ↓Hb, ↓HCT, ↓RBC	[226]
Crocetin	10, 25, 50, 100, and 200 mM	*In vitro*	—	Frog (*Xenopus*) embryos	Crocetin is a teratogen, but less potent than ATRA	[252]
Safranal	0.1, 0.5, 1 mL/kg	*In vivo*	Intraperitoneal	Rats Immunotoxin effect	Showed important toxicity than other active constituents in saffron stigma	[247]
Safranal	1.2 mL/kg	*In vivo*	Intraperitoneal	Rats Acute, subacute toxicity	↓cytotoxicity	[228]
Safranal	1.2 mL/kg	*In vivo*	Intraperitoneal	Mice	$LD_{50} = 1.48$ mL/kg	
Safranal	1.2 mL/kg	*In vivo*	Intraperitoneal	Mice	$LD_{50} = 1.88$ mL/kg	
Safranal	1.2 mL/kg	*In vivo*	Intraperitoneal	Rats	$LD_{50} = 1.50$ mL/kg	[225]
Safranal	1.2 mL/kg	*In vivo*	Oral	Mice	$LD_{50} = 21.42$ mL/kg in	
Safranal	1.2 mL/kg	*In vivo*	Oral	Mice	$LD_{50} = 11.42$ mL/kg	
Safranal	1.2 mL/kg	*In vivo*	Oral	Rats	$LD_{50} = 5.53$ mL/kg	
Crocin	150-210 g	*In vivo*	Oral, intraperitoneal	Mice Rats	↑platelets, ↑creatinine ↓food intake	[242]

Abbreviations and symbols: ↑ increase, ↓ decrease, ALT (alanine aminotransferase), AST (aspartate transaminase), ATRA (all-trans retinoic acid), Hb (hemoglobin), HCT (hematocrit), and RBC (red blood cell).

Another study carried out by Amin et al. [237] showed that the aqueous saffron extract at lower doses (25, 50, and 100 mg/kg/day, administered intraperitoneally for 30 days) showed no toxicity on treated animals. Moreover, at these doses, this extract protects against ethylene glycol-induced calcium oxalate (CaOx) nephrolithiasis in rats [237]. These findings indicate that saffron extracts possess toxicity at higher doses, while they could present protective effects at lower doses.

In a recent study carried out by Hosseinzadeh et al. [233], an aqueous extract of saffron stigmas, administered intraperitoneally at 20 and 80 mg/kg, showed an important decrease of methyl methanesulfonate-induced DNA damage in mouse organs [233]. A study carried out by Hariri et al. [238] showed that aqueous extract administered intraperitoneally at 50, 100, and 200 mg/kg prevented toxicity induced by diazinon in rats.

The teratogenic effect of aqueous extracts of saffron was investigated in mice by Zeynali et al. [239]. The administration of this extract at 0.8, 0.4, and 0.2% significantly reduced the tail length, biparietal diameter, placental diameter, and weight of the fetus during the gestational period. Moreover, the mortality rate and the mean number of the resorbed fetus were significantly increased in a dose-dependent manner [239]. Edamula et al. [240] have evaluated the prenatal developmental toxicity of saffron in male Wistar rats. The administration of the saffron extract at 1000, 250, and 50 mg/kg had no effects on gravid uterine weight, early and late resorptions, corpora lutea and implantation counts, and food intake [240]. Moreover, skeletal examinations have confirmed the absence of any malformation and biochemical examinations did not show effects in biochemical parameters [240].

Crocin is a major compound of saffron extract that has shown important pharmacological properties. The toxicity evaluation of this component was reported in some studies [241–244]. The acute toxicity of crocin on rats and mice was tested by Hosseinzadeh et al. [242]. The results showed that oral and intraperitoneally administration of crocin at 3 g/kg over 2 days did not cause mortality. Moreover, biochemical, hematological, and pathological investigations revealed that crocin did not cause damage to any major organ in the body [242]. Indeed, at 180 mg/kg/day for 21 days, the intraperitoneal administration of crocin increased platelets and creatinine levels. Moreover, the same dose reduced weight, food intake, and alveolar size. Besides, at 90 mg/kg, crocin decreased the levels of albumin and ALP with a significant increase in LDL level [242].

On the other hand, it was previously reported by Wang et al. [241] that crocin induced important black pigmentation of the liver and acute hepatic damage associated with discoloration. These damages were observed only at a higher dosage (100 mg/kg for 2 weeks). However, crocin at 50 mg/kg/day (for 8 days) did not affect hepatic function [241]. Subacute toxicity of crocin on rats was examined in another study by Taheri et al. [243]. The results showed that the administration of crocin at 50, 100, and 200 mg/kg did not show negative effects on biochemical parameters such as ALT, AST, ALP, urea, uric acid, creatinine, MDA, and GSH. Moreover, no significant toxicity was observed using histopathological investigations [243].

On the other hand, the teratogenic effect of crocin was investigated by Moallem et al. [244] in mice. In this work, the intraperitoneal administration of crocin at 200 mg/kg and 600 mg/kg showed a disruption in skeletal formation. Moreover, at the same doses, crocin affected weight, length, growth, mandible, and calvaria of fetuses indicated by the examination of maternal and fetal factors [244].

The acute toxicity of safranal (main compound of saffron) was evaluated in male mice, female mice, and male Wistar rats. The intraperitoneal administration of safranal showed significant toxicity in male mice ($LD_{50} = 1.48$ mL/kg), female mice ($LD_{50} = 1.88$ mL/kg), and male Wistar rats ($LD_{50} = 1.50$ mL/kg). However, in oral administration of safranal, LD_{50} values were 21.42, 11.42, and 5.53 mL/kg in male mice, female mice, and male rats, respectively [225]. In this study, the authors suggested that the significant difference in LD_{50} values after intraperitoneal and oral administration is due to first-pass metabolism and lower absorption after oral exposure [225].

In another study, the subacute toxicity was evaluated in mice and rats. Safranal was administered orally at 0.1, 0.25, and 0.5 mL/kg/day over 21 days [245]. Safranal induced significant decreases in several hematological parameters such as RBC counts, HCT, Hb, and platelets. Moreover, safranal reduced some biochemical factors, including TC, TG, and ALP. Also, no noticeable heart, liver, or spleen lesions were observed after pathological examinations [246]. On the other hand, Riahi-Zanjani et al. [247] have tested the immunotoxic effect of safranal on cellular and humoral cells of the immune system in mice. The results of this work showed that the intraperitoneal administration of safranal at 0.1, 0.5, and 1 mL/kg within 3 weeks days (5 days/week) did not show any significant toxicity on immune system cells [247]. In other studies carried out by Moallem et al. [244], safranal administered at 0.075 and 0.225 mL/kg dysregulated skeletal formation and affected maternal and fetal factors such as weight, length, and growth [244].

The clinical investigations of saffron and its derivatives have also been reported [232, 248, 249]. The examination of saffron safety in healthy volunteers at 200 and 400 mg within 7 days by Modaghegh et al. [232] showed a decrease in arterial pressures, and standing systolic BPs were decreased in persons who received 400 mg [232]. Moreover, at the same concentrations (200 and 400 mg), saffron was found to be a safe drug on the coagulation system [248]. Mohamadpour et al. [249] also investigated the clinical toxicity of crocin in healthy volunteers. In this study, crocin was examined at 20 mg using a randomized, double-blind, placebo-controlled trial. Administrations of crocin tablets partially decreased thromboplastin time, amylase, and mixed WBC (monocytes, basophils, and eosinophils), which showed that crocin is a relatively safe product [249].

8. Discussion

Crocus plants have been traditionally used for several purposes (e.g., reduce bruises, promote blood circulation, anxiolytic, antitumor, antihyperglycemic, etc.) [147, 181, 253–256]. *Crocus sativus* is listed in the pharmacopoeias of

several realms such as Europe, the United Kingdom, Japan, and China [253, 257–259], as well as in other national or local standards.

Crocus plants have undergone comprehensive validation, including phytochemical profiling and determination of targeted biological activities. Saffron is a valuable plant whose main components include safranal, crocetin, crocin, and picrocrocin.

It has been shown in bioavailability tests that when administered orally, crocins are not resorbed as such, but only after an intestinal deglycosylation, after which they reach the bloodstream, being able to cross the blood-brain barrier. This is also the reason why a process for concentrating hydroalcoholic extracts has been developed, when a product with more than 90% crocin 1 is finally obtained, which, being subjected to an enzymatic transformation treatment with β-glucosidase, provides the active metabolite, trans-crocetin, with a concentration of 70% [260].

Both *in vivo* and *in vitro* studies have shown that much of the biological effectiveness of saffron can be attributed to its antioxidant potential resulting from the synergistic antioxidant capacity of its bioactive ingredients [261]. The antioxidant activity of *C. sativus* is mainly attributable to its antioxidant active constituents such as safranal, crocin, and crocetin [83].

The radical-scavenging activity of *Crocus* plant extracts is associated with its anti-inflammatory activity. Crocin and safranal showed anti-inflammatory and antinociceptive effects in the carrageenan model of inflammation with comparable effect to diclofenac [214]. The saffron extract was reported to possess a more significant radical-scavenging activity than carrot and tomato extracts [135]. Crocin and safranal mediate their antioxidant activities by modulating redox status in human plasma [87], mice [204], and primary hepatocytes of rats [262]. Saffron and crocin ameliorate the effects of *Vipera russelli* venom-induced oxidative stress and hematological alterations in adult mice [173, 263].

Crocetin, as a strong antioxidant compound, was demonstrated to inhibit lipid peroxidation, increase the activity of glutathione *S*-transferase (GST), GPx, CAT, and SOD, decrease damage marker enzymes such as aryl hydrocarbon hydroxylase (AHH), LDH, γ-glutamyl transferase (GGT), and adenosine deaminase (ADA) in rat liver tissues, inhibit proliferation of lung cancer cells [174, 264], reduce ROS-induced lipid peroxidation in primary hepatocytes of rats [262], and reduce the levels of oxidized LDL [111]. Crocetin decreased the expression of TNF-α, interleukin-1β, and induced iNOS in the liver of the hemorrhagic shock model [265]. Crocetin also decreased the indomethacin-induced rise in glutathione in nondiabetic and diabetic rats [266] and reduced ROS generated by BαP in mice [204] and angiotensin II-induced ROS [126].

Crocetin was found to be more effective than dimethyl crocetin and safranal as an anticancer and chemopreventive agent [264]. This may be due to the free hydroxyl moiety of the carboxylic group in crocetin that makes it potent for proton donor, thus more reactive to free radicals [203]. Saffron extracts administered orally or topically reduced the *in vivo* incidence of induced cancers, inhibiting tumor growth rate

and prolonging the life of test animals. Furthermore, the toxicity of cytostatic drugs (i.e., cisplatin) has been reduced in experimental models in animals.

The cardioprotective effect of crocetin against norepinephrine- (NE-) induced cardiac hypertrophy has been related with its modulation effects of endogenous antioxidant enzymatic activities [267]. However, the synergism between all these bioactive components significantly potentiates the antioxidant capacity of saffron [264].

Aqueous and ethanolic saffron extracts were tested, along with saffron and crocin, for antidepressant effects in mice using the forced swimming test. All proved to have antidepressant action, and the saffron and crocin content of the extracts administered is reflected in the recorded result. Crocin probably works by inhibiting dopamine and NE reuptake, while safranal inhibits serotonin reuptake at the synapse.

Saffron plays an important role in the food industry and home cooking, both as a preservative and a dye for foods and beverages [268].

The antibacterial activity of aqueous extracts of saffron stigmas was observed against *S. aureus*, *Enterococcus faecalis*, and *E. coli* by Cenci-Goga et al. [72]. It was concluded that stigmas of *C. sativus* have enough antimicrobial agents to exhibit preservative function in foods depending on its compatibility with the product [72]. Saffron, which contains carotenoids (mainly crocin), shows antiseptic activity as its alcoholic compounds can easily alter the cell protein nature and impair the permeability of the cell membranes [71]. In one more study, it was reported that the presence of antimicrobial agents in saffron stigma suppressed microbial growth. Cosano et al. [269], who considered several saffron products from different producing countries (Spain, Iran, Italy, Greece, and Morocco), showed saffron to be a safe additive having neither microbial load nor health risk to foods after addition when there are no other food-preservation methods [269]. A research carried out by Pintado et al. [270] introduced safranal and crocin as biologically active compounds responsible for bacterial growth inhibition. They reported that safranal and crocin could significantly preserve foods against *Salmonella*, *E. coli*, and *S. aureus* when added to foodstuff [270]. Abbasvali et al. [271] reported that an aqueous extract of saffron petals at a concentration of 5 mg/mL had strong antibacterial effects against *S. aureus*. They studied the preservation effects of petal extracts on the shelf life of shrimp and observed that aqueous petal extracts prolonged the shelf life of shrimp from 3 to 9 days. The influence of phenolic components on bacterial cell walls as well as chelation of metal ions necessary for microbial growth was deemed to be the main food-preservation factor. They concluded that aqueous saffron petal extracts contain significantly more phenolic compounds compared to either ethanolic or methanolic extracts and consequently showed stronger antimicrobial effects.

Another example of using saffron extract as a food preservative was reported by Aktypis et al. [272] in which saffron was added to ovine cheese. They found that saffron, as a natural additive, owed a mild reduction in bacterial growth over a month (30 days) after production weight *n*

is being kept at 4°C. Saffron not only made the food functional but also imparted a pleasant flavor to the product [272]. Phenolics, especially flavonoids, usually have strong antioxidant capacities, and thus, herbs rich in them are frequently used as antioxidant food supplements [138, 261]. Cosano et al. [269], who considered several saffron products from different producing countries (Spain, Iran, Italy, Greece, and Morocco), showed saffron to be a safe additive having neither microbial load nor health risk to foods after addition when there are no other food-preservation methods [269].

The limitations are represented by the toxicological evaluation of *Crocus* species which has not been widely studied, and the majority of toxicity tests have focused mainly on *C. sativus* and its major compounds. Toxicological investigations of saffron were carried out only in several studies [225, 227, 228, 232, 236, 238, 251]. The toxicological findings for saffron are not uniform and have some variability depending on plant parts used and experimental models.

To summarize, saffron is a valuable additive containing biologically active compounds which can add functional properties to food products. Saffron powder as well as extract can dramatically influence microbial growth when added to foods and served to preserve foods from spoilage. It should be noted that using saffron does have some limitations, such as an unacceptable flavor of food when used in large enough quantities to ensure high levels of preservation. Combination of saffron with other preservatives (e.g., salt and acid) or merging with other food-preservation methods (freezing, thermal processing) has been proposed to solve this limitation.

9. Overall Conclusions and Future Perspectives

Saffron has been used in several traditional medicinal systems against several diseases, including asthma, cardiovascular disease, depression, digestive ailments, and insomnia.

The *Crocus* plants, *C. sativus* being the most studied, comprise a matrix of phytochemicals promising for biotechnological and pharmaceutical purposes. The pharmaceutical and biotechnological industries are continuously searching for potential functional components in the plant kingdom, and there is excellent economic interest if it is determined to be more economical to obtain these compounds by extracting them from the plants as opposed to their chemical synthesis. In the case of saffron, the extraction of its phytocomponents may be limited by economic aspects. However, the study of the phytochemical profile of saffron and the study of the biological activities of these components may lead to the discovery of new mimetics of these compounds or improvements in the laboratory syntheses. Advances in plant research have been realized to develop saffron with better profiles for the food industry but not for pharmaceutical and biotechnological industries. Crocins, picrocrocin, and safranal are relevant in terms of aroma and taste, but as it has been exposed in this review, these components also possess interesting biological properties. A small number of clinical trials have been performed using saffron as a potential agent for anti-Alzheimer's, antidepressant, and anti-schizophrenia effects. Further efforts are needed to study the other biological effects shown in *in vitro* and *in vivo* studies in well-designed trials in humans.

Abbreviations

AChE: Acetylcholinesterase
ADA: Adenosine deaminase
AHH: Aryl hydrocarbon hydroxylase
ALP: Alkaline phosphatase
ALT: Alanine aminotransferase
AST: Aspartate transaminase
AV: Atrioventricular
Aβ: Amyloid β
BHT: Butyl hydroxyl toluene
BP: Blood pressure
BUN: Blood urea nitrogen
CaOx: Calcium oxalate
CAT: Catalase
CK: Creatine kinase
CMEC: Cortical microvascular endothelial cells
CNS: Central nervous system
DAD: Diode-array detection
DEN: Dimethylnitrosamine
DOCA: Desoxycorticosterone acetate
DPPH, 2: 2-Diphenyl-1-picryl-hydrazyl-hydrate
ESI: Electrospray ionization
FRAP: Fluorescence recovery after photobleaching
GC: Gas chromatography
GGT: γ-Glutamyl transferase
GPx: Glutathione peroxidase
GSH: Reduced glutathione
GSSG: Oxidized glutathione
GST: Glutathione S-transferase
Hb: Hemoglobin
HCT: Hematocrit
HPLC: Performance liquid chromatography
HPTLC: High-performance thin-layer chromatography
ICV: Intracerebroventricular
iNOS: Induced nitric oxide synthase
ISO: Isoproterenol
LC: Liquid chromatography
LDH: Lactate dehydrogenase
LDL: Low-density lipoprotein
MDA: Malondialdehyde
MDD: Major depressive disorder
MES: Maximal electroshock seizure
MMP: Matrix metalloproteinase
MPTP: 1-Methyl-4-phenyl-1,2,3,6-tetrahydropyridine
MS: Mass spectrometry
NE: Norepinephrine
NF-κB: Nuclear factor κB
NMDA: N-Methyl-D-aspartate
NMR: Nuclear magnetic resonance
NO: Nitric oxide production
NS: Nervous system
PARP: Poly (ADP-ribose) polymerase
PI3K/AKT: Phosphatidylinositol 3-kinase
PTZ: Pentylenetetrazole

RBC: Red blood cell
RGCs: Retinal ganglion cells
ROS: Reactive oxygen species
SOD: Superoxide dismutase
SRF: Serum response factor
TBARS: Thiobarbituric acid
TC: Total cholesterol
TG: Triglyceride
TLC: Thin-layer chromatography
TNF-α: Tumor necrosis factor-α
VCAM-1:   Vascular cell adhesion molecule-1
VEGFR-2:   Vascular endothelial growth factor receptor-2
VLDL: Very-low-density lipoprotein
WBC: White blood cells.

Data Availability

All the data used to support the findings of this study are included within the article.

Conflicts of Interest

The authors declare that the research was conducted in the absence of any commercial or financial relationships that could be construed as a potential conflict of interest.

Authors' Contributions

All authors made a significant contribution to the work reported, whether that is in the conception, study design, execution, acquisition of data, analysis, and interpretation, or in all these areas, that is revising or critically reviewing the article, giving final approval of the version to be published, agreeing on the journal to which the article has been submitted, and confirming to be accountable for all aspects of the work.

Supplementary Materials

Table S1: phytoconstituents of *Crocus* species detected by various techniques. Table S2: phytoconstituents of *Crocus* species detected by gas chromatography coupled to mass spectrometry (GC-MS). The Supplementary Material for this article can be found online. *(Supplementary Materials)*

References

[1] O. Ahrazem, A. Rubio-Moraga, S. G. Nebauer, R. V. Molina, and L. Gomez-Gomez, "Saffron: its phytochemistry, developmental processes, and biotechnological prospects," *Journal of Agricultural and Food Chemistry*, vol. 63, pp. 8751–8764, 2015.

[2] J. A. Fernández, O. Santana, J. L. Guardiola et al., "The world saffron and *Crocus* collection: strategies for establishment, management, characterisation and utilisation," *Genetic Resources and Crop Evolution*, vol. 58, pp. 125–137, 2011.

[3] R. Dewan, "Bronze age flower power: the Minoan use and social significance of saffron and *Crocus* flowers," *Chronica*, vol. 5, pp. 42–55, 2015.

[4] L. Mohtashami, M. S. Amiri, M. Ramezani, S. A. Emami, and J. Simal-Gandara, "The genus *Crocus* L.: A review of ethnobotanical uses, phytochemistry and pharmacology," *Industrial Crops and Products*, vol. 171, p. 113923, 2021.

[5] S. Z. Bathaie and S. Z. Mousavi, "New applications and mechanisms of action of saffron and its important ingredients," *Critical Reviews in Food Science and Nutrition*, vol. 50, pp. 761–786, 2010.

[6] Y. Deng, Z. G. Guo, Z. L. Zeng, and Z. Wang, "Studies on the pharmacological effects of saffron (*Crocus sativus* L.)–a review," *Zhongguo Zhong yao za zhi = Zhongguo zhongyao zazhi = China journal of Chinese materia medica*, vol. 27, no. 8, pp. 565–568, 2002.

[7] G. Betti and M. Schmidt, "Valorization of saffron (*Crocus sativus*)," *Acta horticulture*, vol. 739, pp. 397–403, 2013.

[8] B. K. Bhargava, "Medicinal uses and pharmacological properties of *Crocus sativus* Linn (saffron)," *International Journal of Pharmacy and Pharmaceutical Sciences*, vol. 3, pp. 22–26, 2011.

[9] M. Moghaddasi, "Saffron chemicals and medicine usage," *Journal of Medicinal Plant Research: Planta Medica*, vol. 4, no. 6, pp. 427–430, 2010.

[10] T. S. Cid-Pérez, G. V. Nevárez-Moorillón, C. E. Ochoa-Velasco, A. R. Navarro-Cruz, P. Hernández-Carranza, and R. Avila-Sosa, "The relation between drying conditions and the development of volatile compounds in saffron (*Crocus sativus*)," *Molecules*, vol. 26, no. 22, p. 6954, 2021.

[11] K. Zeka, K. C. Ruparelia, M. A. Continenza, D. Stagos, F. Veglio, and R. R. J. Arroo, "Petals of *Crocus sativus* L. as a potential source of the antioxidants crocin and kaempferol," *Fitoterapia*, vol. 107, pp. 128–134, 2015.

[12] A. Trapero, O. Ahrazem, A. Rubio-Moraga, M. L. Jimeno, M. D. Gomez, and L. Gomez-Gomez, "Characterization of a glucosyltransferase enzyme involved in the formation of kaempferol and quercetin sophorosides in *Crocus sativus*," *Plant Physiology*, vol. 159, pp. 1335–1354, 2012.

[13] F. N. Lamari, V. Papasotiropoulos, D. Tsiris et al., "Phytochemical and genetic characterization of styles of wild *Crocus* species from the island of Crete, Greece and comparison to those of cultivated *C. sativus*," *Fitoterapia*, vol. 130, pp. 225–233, 2018.

[14] O. Mykhailenko, I. Bezruk, L. Ivanauskas, and V. Georgiyants, "Comparative analysis of apocarotenoids and phenolic constituents of *Crocus sativus* stigmas from 11 countries: ecological impact," *Archiv der Pharmazie*, p. e2100468, 2022.

[15] S. Akhondzadeh, H. Fallah-Pour, K. Afkham, A. H. Jamshidi, and F. Khalighi-Cigaroudi, "Comparison of *Crocus sativus* L. and imipramine in the treatment of mild to moderate depression: a pilot double-blind randomized trial [ISRCTN45683816]," *BMC Complementary and Alternative Medicine*, vol. 4, no. 1, 2004.

[16] H. Hosseinzadeh and F. Talebzadeh, "Anticonvulsant evaluation of safranal and crocin from *Crocus sativus* in mice," *Fitoterapia*, vol. 76, pp. 722–724, 2005.

[17] H. Hosseinzadeh and H. R. Sadeghnia, "Protective effect of safranal on pentylenetetrazol-induced seizures in the rat: involvement of GABAergic and opioids systems," *Phytomedicine*, vol. 14, pp. 256–262, 2007.

[18] H. Hosseinzadeh, G. Karimi, and M. Niapoor, "Antidepressant effect of *Crocus sativus* L. stigma extracts and their constituents, crocin and safranal, in mice," *Acta Horticulturae*, vol. 650, pp. 435–445, 2004.

[19] "Plant List, T," http://www.theplantlist.org/.

[20] M. Heinrich, G. Appendino, T. Efferth et al., "Best practice in research – overcoming common challenges in phytopharmacological research," *Journal of Ethnopharmacology*, vol. 246, p. 112230, 2020.

[21] A. R. Krishnan, J. Mathew, S. A. Salam, V. Jiju, and A. Elessy, "A review on saffron as an alternative therapy in medicine and dermatology," *European Journal of Pharmaceutical and Medical Research*, vol. 4, pp. 283–286, 2017.

[22] M. Sheidai, M. Tabasi, M. Mehrabian, F. Koohdar, S. Ghasemzadeh-Baraki, and Z. Noormohammadi, "Species delimitation and relationship in *Crocus* L. (Iridaceae)," *Acta Botanica Croatica*, vol. 77, pp. 10–17, 2018.

[23] T. Aburjai, M. Hudaib, R. Tayyem, M. Yousef, and M. Qishawi, "Ethnopharmacological survey of medicinal herbs in Jordan, the Ajloun Heights region," *Journal of Ethnopharmacology*, vol. 110, pp. 294–304, 2007.

[24] M. Asadi, "Antioxidant and antimicrobial activities in the different extracts of Caspian saffron, *Crocus caspius* Fisch & C. A. Mey. ex Hohen," *Caspian Journal of Environmental Sciences*, vol. 14, pp. 331–338, 2016.

[25] Z. Demeter, G. Suranyi, V. A. Molnar et al., "Somatic embryogenesis and regeneration from shoot primordia of *Crocus heuffelianus*," *Plant Cell, Tissue and Organ Culture*, vol. 100, pp. 349–353, 2010.

[26] N. Jivad, N. Zare-Hassanabadi, and M. Azizi, "Effect of combination of honey, saffron (*Crocus sativus* L.) and sedge (*Cyperus rotundus* L.) on cognitive dysfunction in patients with Alzheimer's disease," *Advanced Herbal Medicine*, vol. 1, pp. 11–16, 2015.

[27] A. Pieroni, "Medicinal plants and food medicines in the folk traditions of the upper Lucca Province, Italy," *Journal of Ethnopharmacology*, vol. 70, no. 3, pp. 235–273, 2000.

[28] A. Bilal, A. H. Wani, A. Khan, R. Hamza, and F. A. Mohidin, "Saffron: a repository of medicinal properties," *Journal of Medicinal Plant Research*, vol. 5, pp. 2131–2135, 2011.

[29] Z. A. Shah, R. Mir, J. M. Matoo, M. A. Dar, and M. A. Beigh, "Medicinal importance of saffron: a review," *Journal of Pharmacognosy and Phytochemistry*, vol. 6, pp. 2475–2478, 2017.

[30] S. Z. Mousavi and S. Z. Bathaie, "Historical uses of saffron: identifying potential new avenues for modern research," *Avicenna Journal of Phytomedicine*, vol. 1, pp. 57–66, 2011.

[31] I. Hasan, A. H. Ansari, A. M. Sherwani, and M. Zulkifle, "The incredible health benefits of saffron: a review," *Journal of Pharmacy Research*, vol. 4, pp. 2156–2158, 2011.

[32] A. H. Rahmani, A. A. Khan, and Y. H. Aldebasi, "Saffron (*Crocus sativus*) and its active ingredients: role in the prevention and treatment of disease," *Pharmacognosy Journal*, vol. 9, pp. 873–879, 2017.

[33] A. A. D'Archivio and M. A. Maggi, "Geographical identification of saffron (*Crocus sativus* L.) by linear discriminant analysis applied to the UV–visible spectra of aqueous extracts," *Food Chemistry*, vol. 219, pp. 408–413, 2017.

[34] M. Mashmoul, A. Azlan, H. Khaza'i, B. N. Yusof, and S. M. Noor, "Saffron: a natural potent antioxidant as a promising anti-obesity drug," *Antioxidants*, vol. 2, pp. 293–308, 2013.

[35] M. A. Bonet and J. Valles, "Ethnobotany of Montseny biosphere reserve (Catalonia, Iberian Peninsula): plants used in veterinary medicine," *Journal of Ethnopharmacology*, vol. 110, pp. 130–147, 2007.

[36] L. Maggi, M. Carmona, S. D. Kelly, N. Marigheto, and G. L. Alonso, "Geographical origin differentiation of saffron spice (*Crocus sativus* L. stigmas) - preliminary investigation using chemical and multi-element (H, C, N) stable isotope analysis," *Food Chemistry*, vol. 128, pp. 543–548, 2011.

[37] M. Tsimidou and P. A. Tarantilis, "Special issue "Saffron (*Crocus sativus* L.): omics and other techniques in authenticity, quality, and Bioactivity Studies"," *Molecules*, vol. 22, 2016.

[38] R. Rocchi, M. Mascini, M. Sergi, D. Compagnone, D. Mastrocola, and P. Pittia, "Crocins pattern in saffron detected by UHPLC-MS/MS as marker of quality, process and traceability," *Food Chemistry*, vol. 264, pp. 241–249, 2018.

[39] S. Patel, M. Sarwat, and T. H. Khan, "Mechanism behind the anti-tumour potential of saffron (*Crocus sativus* L.): the molecular perspective," *Critical Reviews in Oncology/Hematology*, vol. 115, pp. 27–35, 2017.

[40] F. I. Abdullaev, "Cancer chemopreventive and tumoricidal properties of saffron (*Crocus sativus* L.)," *Experimental Biology and Medicine (Maywood, N.J.)*, vol. 227, no. 1, pp. 20–25, 2002.

[41] A. R. Gohari, S. Saeidnia, and M. K. Mahmoodabadi, "An overview on saffron, phytochemicals, and medicinal properties," *Pharmacognosy Reviews*, vol. 7, pp. 61–66, 2013.

[42] R. Srivastava, H. Ahmed, R. K. Dixit, Dharamveer, and S. A. Saraf, "*Crocus sativus* L.: a comprehensive review," *Pharmacognosy Reviews*, vol. 4, no. 8, pp. 200–208, 2010.

[43] A. M. Sánchez, M. Carmona, C. P. del Campo, and G. L. Alonso, "Solid-phase extraction for picrocrocin determination in the quality control of saffron spice (*Crocus sativus* L.)," *Food Chemistry*, vol. 116, pp. 792–798, 2009.

[44] M. V. Garcia-Rodriguez, J. Serrano-Diaz, P. A. Tarantilis, H. Lopez-Corcoles, M. Carmona, and G. L. Alonso, "Determination of saffron quality by high-performance liquid chromatography," *Journal of Agricultural and Food Chemistry*, vol. 62, pp. 8068–8074, 2014.

[45] P. Winterhalter and R. Rouseff, "Carotenoid-derived aroma compounds: an introduction," *ACS Symposium Series*, vol. 802, pp. 1–17, 2001.

[46] A. N. Assimopoulou, Z. Sinakos, and V. P. Papageorgiou, "Radical scavenging activity of *Crocus sativus* L. extract and its bioactive constituents," *Phytotherapy research: PTR*, vol. 19, pp. 997–1000, 2005.

[47] H. Caballero-Ortega, R. Pereda-Miranda, L. Riverón-Negrete et al., "Chemical composition of saffron (*Crocus sativus* L.) from four countries," *Acta Horticulturae*, no. 650, pp. 321–326, 2004.

[48] F. Bouvier, C. Suire, J. Mutterer, and B. Camara, "Oxidative remodeling of chromoplast carotenoids: identification of the carotenoid dioxygenase CsCCD and CsZCD genes involved in *Crocus* secondary metabolite biogenesis," *The Plant Cell*, vol. 15, pp. 47–62, 2003.

[49] A. R. Moraga, P. F. Nohales, J. A. Perez, and L. Gomez-Gomez, "Glucosylation of the saffron apocarotenoid crocetin by a glucosyltransferase isolated from *Crocus sativus* stigmas," *Planta*, vol. 219, no. 6, pp. 955–966, 2004.

[50] P. Winterhalter and M. Straubinger, "Saffron-renewed interest in an ancient spice," *Food Reviews International*, vol. 16, pp. 39–59, 2000.

[51] H. Rajabi, M. Ghorbani, S. M. Jafari, A. Sadeghi Mahoonak, and G. Rajabzadeh, "Retention of saffron bioactive components by spray drying encapsulation using maltodextrin,

gum Arabic and gelatin as wall materials," *Food Hydrocolloids*, vol. 51, pp. 327–337, 2015.

[52] B. Salehi, S. Sestito, S. Rapposelli et al., "Epibatidine: a promising natural alkaloid in health," *Biomolecules*, vol. 9, p. 10, 2019.

[53] A. Benkhaled, A. Senator, A. Boudjelal et al., "Oral acute toxicity and red blood cytotoxicity of the medicinal halophyte Limoniastrum guyonianum leaf extract," *Farmácia*, vol. 68, pp. 1136–1146, 2020.

[54] L. Pasayeva, E. Demirpolat, H. Fatullayev, and O. Tugay, "Cytotoxic and phytochemical investigation of Cousinia ermenekensis Hub.-MOR," *Farmácia*, vol. 68, pp. 521–525, 2020.

[55] S. S. Das, S. Alkhtani, P. Bharadwaj et al., "Molecular insights and novel approaches for targeting tumor metastasis," *International Journal of Pharmaceutics*, vol. 585, article 119556, 2020.

[56] D. Jain, P. Chaudhary, N. Varshney et al., "Tobacco smoking and liver cancer risk: potential avenues for carcinogenesis," *Journal of Oncology*, vol. 2021, 2021.

[57] J. Sharifi-Rad, C. Quispe, M. Butnariu et al., "Chitosan nanoparticles as a promising tool in nanomedicine with particular emphasis on oncological treatment," *Cancer Cell International*, vol. 21, pp. 318–318, 2021.

[58] B. K. Panigrahi and A. K. Nayak, "Carbon nanotubes: an emerging drug delivery carrier in cancer therapeutics," *Current Drug Delivery*, vol. 17, pp. 558–576, 2020.

[59] J. Sharifi-Rad, C. Quispe, J. K. Patra et al., "Paclitaxel: application in modern oncology and nanomedicine-based cancer therapy," *Oxidative Medicine and Cellular Longevity*, vol. 2021, Article ID 3687700, 24 pages, 2021.

[60] S. Samarghandian, A. Borji, S. K. Farahmand, R. Afshari, and S. Davoodi, "*Crocus sativus* L. (saffron) stigma aqueous extract induces apoptosis in alveolar human lung cancer cells through caspase-dependent pathways activation," *BioMed Research International*, vol. 2013, Article ID 417928, 12 pages, 2013.

[61] F. Vali, V. Changizi, and M. Safa, "Synergistic apoptotic effect of crocin and paclitaxel or crocin and radiation on MCF-7 cells, a type of breast cancer cell line," *International Journal of Breast Cancer*, vol. 2015, Article ID 139349, 7 pages, 2015.

[62] M. Mousavi, J. Baharara, and M. Asadi-Samani, "Anti-angiogenesis effect of *Crocous sativus* L. extract on matrix metalloproteinase gene activities in human breast carcinoma cells," *Journal of HerbMed Pharmacology*, vol. 3, pp. 101–105, 2014.

[63] J. Escribano, G. L. Alonso, M. Coca-Prados, and J. A. Fernandez, "Crocin, safranal and picrocrocin from saffron (*Crocus sativus* L.) inhibit the growth of human cancer cells in vitro," *Cancer Letters*, vol. 100, pp. 23–30, 1996.

[64] Y. Sun, H. J. Xu, Y. X. Zhao et al., "Crocin exhibits antitumor effects on human leukemia HL-60 cells in vitro and in vivo," *Evidence-based Complementary and Alternative Medicine: Ecam*, vol. 2013, article 690164, 7 pages, 2013.

[65] C. I. Tuberoso, A. Rosa, P. Montoro, M. A. Fenu, and C. Pizza, "Antioxidant activity, cytotoxic activity and metabolic profiling of juices obtained from saffron (*Crocus sativus* L.) floral by-products," *Food Chemistry*, vol. 199, pp. 18–27, 2016.

[66] O. Zlatian, A. T. Balasoiu, M. Balasoiu et al., "Antimicrobial resistance in bacterial pathogens among hospitalised patients with severe invasive infections," *Experimental and Therapeutic Medicine*, vol. 16, pp. 4499–4510, 2018.

[67] A. Ungureanu, O. Zlatian, G. Mitroi et al., "*Staphylococcus aureus* colonisation in patients from a primary regional hospital," *Molecular Medicine Reports*, vol. 16, pp. 8771–8780, 2017.

[68] Y. Taheri, N. Joković, J. Vitorović, O. Grundmann, A. Maroyi, and D. Calina, "The burden of the serious and difficult-to-treat infections and a new antibiotic available: cefiderocol," *Frontiers in Pharmacology*, vol. 11, 2021.

[69] S. Muzaffar, S. A. Rather, and K. Z. Khan, "In vitro bactericidal and fungicidal activities of various extracts of saffron (*Crocus sativus* L.) stigmas from Jammu & Kashmir, India," *Cogent Food & Agriculture*, vol. 2, p. 1158999, 2016.

[70] E. Kakouri, D. Daferera, S. Paramithiotis, K. Astraka, E. H. Drosinos, and M. G. Polissiou, "*Crocus sativus* L. tepals: the natural source of antioxidant and antimicrobial factors," *Journal of Applied Research on Medicinal and Aromatic Plants*, vol. 4, pp. 66–74, 2017.

[71] R. A. Hussein, N. A. Salih, and N. Eman Thabit, "Bioactivity of crocin pigment of saffron plant," *Plant Archives*, vol. 18, pp. 357–364, 2018.

[72] B. Cenci-Goga, R. Torricelli, Y. Hosseinzadeh Gonabad et al., "In vitro bactericidal activities of various extracts of saffron (*Crocus sativus* L.) stigmas from Torbat-e Heydarieh, Gonabad and Khorasan, Iran," *Microbiology Research*, vol. 9, no. 1, 2018.

[73] R. R. Mititelu, R. Padureanu, M. Bacanoiu et al., "Inflammatory and oxidative stress markers-mirror tools in rheumatoid arthritis," *Biomedicine*, vol. 8, p. 14, 2020.

[74] A. O. Docea, D. Calina, A. M. Buga et al., "The effect of silver nanoparticles on antioxidant/pro-oxidant balance in a murine model," *International Journal of Molecular Sciences*, vol. 21, p. 17, 2020.

[75] T. Docea, C. Tsarouhas, Z. Mitrut, S.-R. Kovatsi, S. Dardiotis, and D. Lazopoulos, "A mechanistic and pathophysiological approach for stroke associated with drugs of abuse," *Journal of Clinical Medicine*, vol. 8, 2019.

[76] R. Padureanu, C. V. Albu, R. R. Mititelu et al., "Oxidative stress and inflammation interdependence in multiple sclerosis," *Journal of Clinical Medicine*, vol. 8, 2019.

[77] B. Salehi, A. Rescigno, T. Dettori et al., "Avocado-soybean unsaponifiables: a panoply of potentialities to be exploited," *Biomolecules*, vol. 10, 2020.

[78] B. Salehi, M. S. Shetty, N. V. Anil Kumar et al., "Veronica plants-drifting from farm to traditional healing, food application, and phytopharmacology," *Molecules*, vol. 24, 2019.

[79] M. Sharifi-Rad, N. V. Anil Kumar, P. Zucca et al., "Lifestyle, oxidative stress, and antioxidants: back and forth in the pathophysiology of chronic diseases," *Frontiers in Physiology*, vol. 11, 2020.

[80] C. D. Kanakis, P. A. Tarantilis, H. A. Tajmir-Riahi, and M. G. Polissiou, "Crocetin, dimethylcrocetin, and safranal bind human serum albumin: stability and antioxidative properties," *Journal of Agricultural and Food Chemistry*, vol. 55, pp. 970–977, 2007.

[81] G. Zengin, M. Z. Aumeeruddy, A. Diuzheva et al., "A comprehensive appraisal on *Crocus chrysanthus* (Herb.) Herb. flower extracts with HPLC-MS/MS profiles, antioxidant and enzyme inhibitory properties," *Journal of Pharmaceutical and Biomedical Analysis*, vol. 164, pp. 581–589, 2019.

[82] Y. Chen, H. Zhang, X. Tian et al., "Antioxidant potential of crocins and ethanol extracts of Gardenia jasminoides ELLIS and *Crocus sativus* L.: a relationship investigation between

antioxidant activity and crocin contents," *Food Chemistry*, vol. 109, pp. 484–492, 2008.

[83] E. Karimi, E. Oskoueian, R. Hendra, and H. Z. Jaafar, "Evaluation of *Crocus sativus* L. stigma phenolic and flavonoid compounds and its antioxidant activity," *Molecules*, vol. 15, no. 9, pp. 6244–6256, 2010.

[84] R. Sánchez-Vioque, M. F. Rodríguez-Conde, J. V. Reina-Ureña, M. A. Escolano-Tercero, D. Herraiz-Peñalver, and O. Santana-Méridas, "In vitro antioxidant and metal chelating properties of corm, tepal and leaf from saffron (*Crocus sativus* L.)," *Industrial Crops and Products*, vol. 39, pp. 149–153, 2012.

[85] T. Ochiai, S. Ohno, S. Soeda, H. Tanaka, Y. Shoyama, and H. Shimeno, "Crocin prevents the death of rat pheochromyctoma (PC-12) cells by its antioxidant effects stronger than those of alpha-tocopherol," *Neuroscience Letters*, vol. 362, pp. 61–64, 2004.

[86] S. I. Bukhari, B. Pattnaik, S. Rayees, S. Kaul, and M. K. Dhar, "Safranal of *Crocus sativus* L. inhibits inducible nitric oxide synthase and attenuates asthma in a mouse model of asthma," *Phytotherapy research: PTR*, vol. 29, pp. 617–627, 2015.

[87] S. W. Jessie and T. P. Krishnakantha, "Inhibition of human platelet aggregation and membrane lipid peroxidation by food spice, saffron," *Molecular and Cellular Biochemistry*, vol. 278, pp. 59–63, 2005.

[88] S. A. Moallem, A. T. Hariri, M. Mahmoudi, and H. Hosseinzadeh, "Effect of aqueous extract of *Crocus sativus* L. (saffron) stigma against subacute effect of diazinon on specific biomarkers in rats," *Toxicology and Industrial Health*, vol. 30, pp. 141–146, 2014.

[89] E. C. Urrutia, L. Riverón-Negrete, F. Abdullaev et al., "Saffron extract ameliorates oxidative damage and mitochondrial dysfunction in the rat brain," *Acta Horticulturae*, vol. 739, no. 739, pp. 359–366, 2007.

[90] F. I. Abdullaev, L. Riveron-Negrete, H. Caballero-Ortega et al., "Use of in vitro assays to assess the potential antigenotoxic and cytotoxic effects of saffron (*Crocus sativus* L.)," *Toxicology In Vitro*, vol. 17, no. 5-6, pp. 731–736, 2003.

[91] J. Sharifi-Rad, C. F. Rodrigues, F. Sharopov et al., "Diet, lifestyle and cardiovascular diseases: linking pathophysiology to cardioprotective effects of natural bioactive compounds," *International Journal of Environmental Research and Public Health*, vol. 17, 2020.

[92] H. Nemati, M. H. Boskabady, and H. Ahmadzadef Vostakolaei, "Stimulatory effect of *Crocus sativus* (saffron) on beta2-adrenoceptors of guinea pig tracheal chains," *Phytomedicine*, vol. 15, pp. 1038–1045, 2008.

[93] M. H. Boskabady, M. Ghasemzadeh Rahbardar, H. Nemati, and M. Esmaeilzadeh, "Inhibitory effect of *Crocus sativus* (saffron) on histamine (H1) receptors of guinea pig tracheal chains," *Die Pharmazie*, vol. 65, pp. 300–305, 2010.

[94] U. H. Joshi, T. H. Ganatra, P. N. Bhalodiya, T. R. Desai, and P. R. Tirgar, "Comparative review on harmless herbs with allopathic remedies as anti-hypertensive," *Research Journal of Pharmaceutical, Biological and Chemical Sciences*, vol. 3, pp. 673–687, 2012.

[95] F. Yoshino, A. Yoshida, N. Umigai, K. Kubo, and M. C. Lee, "Crocetin reduces the oxidative stress induced reactive oxygen species in the stroke-prone spontaneously hypertensive rats (SHRSPs) brain," *Journal of Clinical Biochemistry and Nutrition*, vol. 49, pp. 182–187, 2011.

[96] A. Milajerdi, V. Bitarafan, and M. Mahmoudi, "A review on the effects of saffron extract and its constituents on factors related to neurologic," *Cardiovascular and Gastrointestinal Diseases*, vol. 3, pp. 9–28, 2015.

[97] B. M. Razavi and H. Hosseinzadeh, "Saffron: a promising natural medicine in the treatment of metabolic syndrome," *Journal of the Science of Food and Agriculture*, vol. 97, pp. 1679–1685, 2017.

[98] M. Imenshahidi, H. Hosseinzadeh, and Y. Javadpour, "Hypotensive effect of aqueous saffron extract (*Crocus sativus* L.) and its constituents, safranal and crocin, in normotensive and hypertensive rats," *Phytotherapy research: PTR*, vol. 24, pp. 990–994, 2010.

[99] M. Imenshahidi, B. M. Razavi, A. Faal, A. Gholampoor, S. M. Mousavi, and H. Hosseinzadeh, "The effect of chronic administration of saffron (*Crocus sativus*) stigma aqueous extract on systolic blood pressure in rats," *Jundishapur Journal of Natural Pharmaceutical Products*, vol. 8, pp. 175–179, 2013.

[100] M. Fatehi, T. Rashidabady, and Z. Fatehi-Hassanabad, "Effects of *Crocus sativus* petals' extract on rat blood pressure and on responses induced by electrical field stimulation in the rat isolated vas deferens and guinea-pig ileum," *Journal of Ethnopharmacology*, vol. 84, pp. 199–203, 2003.

[101] J. Sachdeva, V. Tanwar, M. Golechha et al., "*Crocus sativus* L. (saffron) attenuates isoproterenol-induced myocardial injury via preserving cardiac functions and strengthening antioxidant defense system," *Experimental and Toxicologic Pathology*, vol. 64, pp. 557–564, 2012.

[102] V. Khori, A. M. Alizadeh, H. Yazdi et al., "Frequency-dependent electrophysiological remodeling of the AV node by hydroalcohol extract of *Crocus sativus* L. (saffron) during experimental atrial fibrillation: the role of endogenous nitric oxide," *Phytotherapy research: PTR*, vol. 26, pp. 826–832, 2012.

[103] M. H. Boskabady, M. N. Shafei, A. Shakiba, and H. S. Sefidi, "Effect of aqueous-ethanol extract from *Crocus sativus* (saffron) on guinea-pig isolated heart," *Phytotherapy research: PTR*, vol. 22, pp. 330–334, 2008.

[104] Z. Jahanbakhsh, B. Rasoulian, M. Jafari et al., "Protective effect of crocin against reperfusion-induced cardiac arrhythmias in anaesthetized rats," *EXCLI Journal*, vol. 11, pp. 20–29, 2012.

[105] R. Mehdizadeh, M. R. Parizadeh, A. R. Khooei, S. Mehri, and H. Hosseinzadeh, "Cardioprotective effect of saffron extract and safranal in isoproterenol-induced myocardial infarction in Wistar rats," *Iranian Journal of Basic Medical Sciences*, vol. 16, pp. 56–63, 2013.

[106] L. Yang, Z. Qian, Y. Yang et al., "Involvement of Ca2+ in the inhibition by crocetin of platelet activity and thrombosis formation," *Journal of Agricultural and Food Chemistry*, vol. 56, pp. 9429–9433, 2008.

[107] S. Joukar, H. Najafipour, M. Khaksari et al., "The effect of saffron consumption on biochemical and histopathological heart indices of rats with myocardial infarction," *Cardiovascular Toxicology*, vol. 10, pp. 66–71, 2010.

[108] S. N. Goyal, S. Arora, A. K. Sharma et al., "Preventive effect of crocin of *Crocus sativus* on hemodynamic, biochemical, histopathological and ultrastuctural alterations in isoproterenol-induced cardiotoxicity in rats," *Phytomedicine*, vol. 17, pp. 227–232, 2010.

[109] G. Xu, Z. Gong, W. Yu, L. Gao, S. He, and Z. Qian, "Increased expression ratio of Bcl-2/Bax is associated with crocin-

mediated apoptosis in bovine aortic endothelial cells," *Basic & Clinical Pharmacology & Toxicology*, vol. 100, pp. 31–35, 2007.

[110] S. Y. He, Z. Y. Qian, N. Wen, F. T. Tang, G. L. Xu, and C. H. Zhou, "Influence of crocetin on experimental atherosclerosis in hyperlipidamic-diet quails," *European Journal of Pharmacology*, vol. 554, pp. 191–195, 2007.

[111] S. Zheng, Z. Qian, F. Tang, and L. Sheng, "Suppression of vascular cell adhesion molecule-1 expression by crocetin contributes to attenuation of atherosclerosis in hypercholesterolemic rabbits," *Biochemical Pharmacology*, vol. 70, pp. 1192–1199, 2005.

[112] M. Kamalipour and S. Akhondzadeh, "Cardiovascular effects of saffron: an evidence-based review," *The Journal of Tehran Heart Center*, vol. 6, no. 2, pp. 59–61, 2011.

[113] M. Hemmati, E. Zohoori, O. Mehrpour et al., "Anti-atherogenic potential of jujube, saffron and barberry: anti-diabetic and antioxidant actions," *EXCLI Journal*, vol. 14, pp. 908–915, 2015.

[114] S. Chermahini, F. Abd Majid, M. Sarmidi, E. Taghizadeh, and S. Salehnezhad, "Impact of saffron as an anti-cancer and anti-tumor herb," *African Journal of Pharmacy and Pharmacology*, vol. 4, pp. 834–840, 2010.

[115] F. I. Abdullaev, "Antitumor effect of saffron (*Crocus sativus* L.): overview and perspectives," *Acta Horticulturae*, no. 650, pp. 491–499, 2004.

[116] H. Mollaei, R. Safaralizadeh, E. Babaei, M. R. Abedini, and R. Hoshyar, "The anti-proliferative and apoptotic effects of crocin on chemosensive and chemoresistant cervical cancer cells," *Biomedicine & pharmacotherapy = Biomedecine & pharmacotherapie*, vol. 94, pp. 307–316, 2017.

[117] E. S. el Daly, "Protective effect of cysteine and vitamin E, *Crocus sativus* and *Nigella sativa* extracts on cisplatin-induced toxicity in rats," *Journal de Pharmacie de Belgique*, vol. 53, no. 2, 1998.

[118] A. Amin, A. A. Hamza, K. Bajbouj, S. S. Ashraf, and S. Daoud, "Saffron: a potential candidate for a novel anticancer drug against hepatocellular carcinoma," *Hepatology*, vol. 54, pp. 857–867, 2011.

[119] K. Premkumar, S. K. Abraham, S. T. Santhiya, and A. Ramesh, "Inhibitory effects of aqueous crude extract of Saffron (*Crocus sativus* L.) on chemical-induced genotoxicity in mice," *Asia Pacific Journal of Clinical Nutrition*, vol. 12, no. 4, pp. 474–476, 2003.

[120] S. A. Ordoudi, C. D. Befani, N. Nenadis, G. G. Koliakos, and M. Z. Tsimidou, "Further examination of antiradical properties of *Crocus sativus* stigmas extract rich in crocins," *Journal of Agricultural and Food Chemistry*, vol. 57, pp. 3080–3086, 2009.

[121] H. Hosseinzadeh and V. Khosravan, "Anticonvulsant effects of aqueous and ethanolic extracts of *Crocus sativus* L. stigmas in mice," *Archives of Iranian Medicine*, vol. 5, pp. 44–50, 2002.

[122] M. Sugiura, Y. Shoyama, H. Saito, and K. Abe, "Crocin (crocetin di-gentiobiose ester) prevents the inhibitory effect of ethanol on long-term potentiation in the dentate gyrus in vivo," *The Journal of Pharmacology and Experimental Therapeutics*, vol. 271, pp. 703–707, 1994.

[123] A. Ghazavi, G. Mosayebi, H. Salehi, and H. Abtahi, "Effect of ethanol extract of saffron (*Crocus sativus* L.) on the inhibition of experimental autoimmune encephalomyelitis in C57bl/6 mice," *Pakistan Journal of Biological Sciences: PJBS*, vol. 12, no. 9, pp. 690–695, 2009.

[124] H. R. Sadeghnia, M. A. Cortez, D. Liu, H. Hosseinzadeh, and O. C. Snead 3rd., "Antiabsence effects of safranal in acute experimental seizure models: EEG and autoradiography," *Journal of Pharmacy & Pharmaceutical Sciences*, vol. 11, pp. 1–14, 2008.

[125] S. M. Naghibi, M. Hosseini, F. Khani et al., "Effect of aqueous extract of *Crocus sativus* L. on morphine-induced memory impairment," *Advances in Pharmacological Sciences*, vol. 2012, Article ID 494367, 7 pages, 2012.

[126] S. Zheng, Z. Qian, N. Wen, and L. Xi, "Crocetin suppresses angiotensin II-induced vascular smooth-muscle cell proliferation through inhibition of ERK1/2 activation and cell-cycle progression," *Journal of Cardiovascular Pharmacology*, vol. 50, pp. 519–525, 2007.

[127] M. R. Khazdair, M. H. Boskabady, M. Hosseini, R. Rezaee, and A. M. Tsatsakis, "The effects of *Crocus sativus* (saffron) and its constituents on nervous system: a review," *Avicenna Journal of Phytomedicine*, vol. 5, pp. 376–391, 2015.

[128] B. P. V. Sunanda, B. Rammohan, K. Amitabh, and B. L. Kudagi, "The effective study of aqueous extract of *Crocus sativus* Linn. In chemical induced convulsants in rats," *World Journal of Pharmacy & Pharmaceutical Sciences*, vol. 3, pp. 1175–1182, 2014.

[129] D. Calina, A. M. Buga, M. Mitroi et al., "The treatment of cognitive, behavioural and motor impairments from brain injury and neurodegenerative diseases through cannabinoid system modulation-evidence from in vivo studies," *Journal of Clinical Medicine*, vol. 9, 2020.

[130] D. Tsoukalas, A. Buga, A. Docea et al., "Reversal of brain aging by targeting telomerase: a nutraceutical approach," *International Journal of Molecular Medicine*, vol. 48, 2021.

[131] B. Salehi, D. Calina, A. Docea et al., "Curcumin's nanomedicine formulations for therapeutic application in neurological diseases," *Journal of Clinical Medicine*, vol. 9, 2020.

[132] S. H. Alavizadeh and H. Hosseinzadeh, "Bioactivity assessment and toxicity of crocin: a comprehensive review," *Food and Chemical Toxicology*, vol. 64, pp. 65–80, 2014.

[133] M. B. Ebrahim-Habibi, M. Amininasab, A. Ebrahim-Habibi, M. Sabbaghian, and M. Nemat-Gorgani, "Fibrillation of alpha-lactalbumin: effect of crocin and safranal, two natural small molecules from *Crocus sativus*," *Biopolymers*, vol. 93, pp. 854–865, 2010.

[134] R. K. Singla and V. G. C. Bhat, "An overview. Indo Global Journal of Pharmaceutical Sciences," *Indo Global Journal of Pharmaceutical Sciences*, vol. 1, pp. 281–286, 2011.

[135] M. A. Papandreou, C. D. Kanakis, M. G. Polissiou et al., "Inhibitory activity on amyloid-beta aggregation and antioxidant properties of *Crocus sativus* stigmas extract and its crocin constituents," *Journal of Agricultural and Food Chemistry*, vol. 54, pp. 8762–8768, 2006.

[136] M. Khalili, Z. Kiasalari, B. Rahmati, and J. Narenjkar, "Behavioral and histological analysis of *Crocus sativus* effect in intracerebroventricular streptozotocin model of Alzheimer disease in rats," *Iranian Journal of Pathology*, vol. 5, pp. 27–33, 2010.

[137] M. Khalili and F. Hamzeh, "Effects of active constituents of *Crocus sativus* L., crocin on streptozocin-induced model of sporadic Alzheimer's disease in male rats," *Iranian Biomedical Journal*, vol. 14, pp. 59–65, 2010.

[138] B. Ghadrdoost, A. A. Vafaei, A. Rashidy-Pour et al., "Protective effects of saffron extract and its active constituent crocin

against oxidative stress and spatial learning and memory deficits induced by chronic stress in rats," *European Journal of Pharmacology*, vol. 667, pp. 222–229, 2011.

[139] G. D. Geromichalos, F. N. Lamari, M. A. Papandreou et al., "Saffron as a source of novel acetylcholinesterase inhibitors: molecular docking and in vitro enzymatic studies," *Journal of Agricultural and Food Chemistry*, vol. 60, pp. 6131–6138, 2012.

[140] M. Sharifi-Rad, C. Lankatillake, D. A. Dias et al., "Impact of natural compounds on neurodegenerative disorders: from preclinical to pharmacotherapeutics," *Journal of Clinical Medicine*, vol. 9, no. 4, p. 19, 2020.

[141] L. Tamegart, A. Abbaoui, R. Makbal et al., "*Crocus sativus* restores dopaminergic and noradrenergic damages induced by lead in Meriones shawi: a possible link with Parkinson's disease," *Acta Histochemica*, vol. 121, pp. 171–181, 2019.

[142] D. Tsoukalas, O. Zlatian, M. Mitroi et al., "A novel nutraceutical formulation can improve motor activity and decrease the stress level in a murine model of middle-age animals," *Journal of Clinical Medicine*, vol. 10, no. 4, p. 624, 2021.

[143] A. M. Aloizou, V. Siokas, G. Pateraki et al., "Thinking outside the ischemia box: advancements in the use of multiple sclerosis drugs in ischemic stroke," *Journal of Clinical Medicine*, vol. 10, no. 4, p. 19, 2021.

[144] J. Sharifi-Rad, C. Quispe, J. Herrera-Bravo et al., "A pharmacological perspective on plant-derived bioactive molecules for epilepsy," *Neurochemical Research*, vol. 46, no. 9, pp. 2205–2225, 2021.

[145] A. S. Ahmad, M. A. Ansari, M. Ahmad et al., "Neuroprotection by crocetin in a hemi-parkinsonian rat model," *Pharmacology, Biochemistry, and Behavior*, vol. 81, pp. 805–813, 2005.

[146] S. Purushothuman, C. Nandasena, C. L. Peoples et al., "Saffron pre-treatment offers neuroprotection to Nigral and retinal dopaminergic cells of MPTP-treated mice," *Journal of Parkinson's Disease*, vol. 3, pp. 77–83, 2013.

[147] Y. Wang, T. Han, Y. Zhu et al., "Antidepressant properties of bioactive fractions from the extract of *Crocus sativus* L," *Journal of Natural Medicines*, vol. 64, pp. 24–30, 2010.

[148] G. R. Karimi, H. Hosseinzadeh, and P. P. Khalegh, "Study of antidepressant effect of aqueous and ethanolic extract of *Crocus sativus* in mice," *Iranian Journal of Basic Medical Sciences*, vol. 4, pp. 11–15, 2001.

[149] H. Hosseinzadeh, V. Motamedshariaty, and F. Hadizadeh, "Antidepressant effect of kaempferol, a constituent of saffron (*Crocus sativus*) petal, in mice and rats," *Pharmacology*, vol. 2, pp. 367–370, 2007.

[150] J. F. Cryan and I. Lucki, "Antidepressant-like behavioral effects mediated by 5-Hydroxytryptamine(2C) receptors," *The Journal of Pharmacology and Experimental Therapeutics*, vol. 295, pp. 1120–1126, 2000.

[151] B. Salehi, J. Sharifi-Rad, F. Cappellini et al.et al., "The therapeutic potential of anthocyanins: current approaches based on their molecular mechanism of action," *Frontiers in Pharmacology*, vol. 11, p. 20, 2020.

[152] H. Hosseinzadeh and H. R. Sadeghnia, "Safranal, a constituent of *Crocus sativus* (saffron), attenuated cerebral ischemia induced oxidative damage in rat hippocampus," *Journal of Pharmacy & Pharmaceutical Sciences*, vol. 8, no. 3, pp. 394–399, 2005.

[153] H. R. Sadeghnia, M. Kamkar, E. Assadpour, M. T. Boroushaki, and A. Ghorbani, "Protective effect of safranal, a constituent of *Crocus sativus*, on Quinolinic acid-induced oxidative damage in rat hippocampus," *Iranian Journal of Basic Medical Sciences*, vol. 16, pp. 73–82, 2013.

[154] H. Hosseinzadeh, H. R. Sadeghnia, and A. Rahimi, "Effect of safranal on extracellular hippocampal levels of glutamate and aspartate during kainic acid treatment in anesthetized rats," *Planta Medica*, vol. 74, pp. 1441–1445, 2008.

[155] X. Bie, Y. Chen, X. Zheng, and H. Dai, "The role of crocetin in protection following cerebral contusion and in the enhancement of angiogenesis in rats," *Fitoterapia*, vol. 82, pp. 997–1002, 2011.

[156] H. Sahraeil, Z. Fatahi, A. H. Rohani, A. Eidi, Z. Hooshmandi, and S. A. Tavallaei, "Ethanolic extract of saffron and its constituent crocin diminish stress-induced metabolic signs and alterations of dopamine-related behaviours in rats," *International Research Journal of Pharmacy and Pharmacology*, vol. 2, pp. 165–173, 2012.

[157] H. Hosseinzadeh, H. R. Sadeghnia, F. A. Ghaeni, V. S. Motamedshariaty, and S. A. Mohajeri, "Effects of saffron (*Crocus sativus* L.) and its active constituent, crocin, on recognition and spatial memory after chronic cerebral hypoperfusion in rats," *Phytotherapy research: PTR*, vol. 26, pp. 381–386, 2012.

[158] A. Vakili, M. R. Einali, and A. R. Bandegi, "Protective effect of crocin against cerebral ischemia in a dose-dependent manner in a rat model of ischemic stroke," *Journal of Stroke and Cerebrovascular Diseases : The Official Journal of National Stroke Association*, vol. 23, pp. 106–113, 2014.

[159] Y. Q. Zheng, J. X. Liu, J. N. Wang, and L. Xu, "Effects of crocin on reperfusion-induced oxidative/nitrative injury to cerebral microvessels after global cerebral ischemia," *Brain Research*, vol. 1138, pp. 86–94, 2007.

[160] K. N. Nam, Y. M. Park, H. J. Jung et al., "Anti-inflammatory effects of crocin and crocetin in rat brain microglial cells," *European Journal of Pharmacology*, vol. 648, pp. 110–116, 2010.

[161] K. Abe and H. Saito, "Effects of saffron extract and its constituent crocin on learning behaviour and long-term potentiation," *Phytotherapy research: PTR*, vol. 14, pp. 149–152, 2000.

[162] N. Pitsikas and N. Sakellaridis, "*Crocus sativus* L. Extracts antagonize memory impairments in different behavioural tasks in the rat," *Behavioural Brain Research*, vol. 173, pp. 112–115, 2006.

[163] M. R. Ghadami and A. Pourmotabbed, "The effect of crocin on scopolamine induced spatial learning and memory deficits in rats," *Physiol-Pharmacol*, vol. 12, pp. 287–295, 2009.

[164] S. Saleem, M. Ahmad, A. S. Ahmad et al., "Effect of saffron (*Crocus sativus*) on neurobehavioral and neurochemical changes in cerebral ischemia in rats," *Journal of Medicinal Food*, vol. 9, pp. 246–253, 2006.

[165] K. M. Debatin, D. Poncet, and G. Kroemer, "Chemotherapy: targeting the mitochondrial cell death pathway," *Oncogene*, vol. 21, pp. 8786–8803, 2002.

[166] H. Hosseinzadeh, H. R. Sadeghnia, T. Ziaee, and A. Danaee, "Protective effect of aqueous saffron extract (*Crocus sativus* L.) and crocin, its active constituent, on renal ischemia/reperfusion-induced oxidative damage in rats," *Journal of Pharmacy & Pharmaceutical Sciences*, vol. 8, no. 3, pp. 387–393, 2005.

[167] Z. I. Linardaki, M. G. Orkoula, A. G. Kokkosis, F. N. Lamari, and M. Margarity, "Investigation of the neuroprotective action of saffron (Crocus sativus L.) in aluminum-exposed adult mice through behavioral and neurobiochemical assessment," Food and Chemical Toxicology, vol. 52, pp. 163–170, 2013.

[168] M. Lechtenberg, D. Schepmann, M. Niehues, N. Hellenbrand, B. Wunsch, and A. Hensel, "Quality and functionality of saffron: quality control, species assortment and affinity of extract and isolated saffron compounds to NMDA and sigma1 (sigma-1) receptors," Planta Medica, vol. 74, pp. 764–772, 2008.

[169] S. Nasri, S. Y. Hosseini, H. Sahraei, and H. Zardooz, "Inhibition of pain and inflamation induced by formalin in male mice by ethanolic extract of saffron (Crocus sativus) and its constituents crocin and safranal," Trauma Monthly, vol. 15, pp. 189–195, 2010.

[170] B. Amin and H. Hosseinzadeh, "Evaluation of aqueous and ethanolic extracts of saffron, Crocus sativus L., and its constituents, safranal and crocin in allodynia and hyperalgesia induced by chronic constriction injury model of neuropathic pain in rats," Fitoterapia, vol. 83, pp. 888–895, 2012.

[171] H. Hosseinzadeh and Z. Jahanian, "Effect of Crocus sativus L. (saffron) stigma and its constituents, crocin and safranal, on morphine withdrawal syndrome in mice," Phytotherapy research: PTR, vol. 24, pp. 726–730, 2010.

[172] H. Haghighizad, A. Pourmotabbed, H. Sahraei, M. R. Ghadami, S. Ghadami, and M. Kamalinejad, "Protective effect of saffron extract on morphine–induced inhibition of spatial learning and memory in rat," Physiol-Pharmacol, vol. 12, pp. 170–179, 2008.

[173] K. Premkumar, C. Thirunavukkarasu, S. K. Abraham, S. T. Santhiya, and A. Ramesh, "Protective effect of saffron (Crocus sativus L.) aqueous extract against genetic damage induced by anti-tumor agents in mice," Human & Experimental Toxicology, vol. 25, pp. 79–84, 2006.

[174] S. M. Asdaq and M. N. Inamdar, "Potential of Crocus sativus (saffron) and its constituent, crocin, as hypolipidemic and antioxidant in rats," Applied Biochemistry and Biotechnology, vol. 162, pp. 358–372, 2010.

[175] L. Sheng, Z. Qian, S. Zheng, and L. Xi, "Mechanism of hypolipidemic effect of crocin in rats: crocin inhibits pancreatic lipase," European Journal of Pharmacology, vol. 543, pp. 116–122, 2006.

[176] S. Y. He, Z. Y. Qian, F. T. Tang, N. Wen, G. L. Xu, and L. Sheng, "Effect of crocin on experimental atherosclerosis in quails and its mechanisms," Life Sciences, vol. 77, pp. 907–921, 2005.

[177] J. C. Cousins and T. L. Miller, "The effects of crocetin on plasma lipids in rats," The Ohio Journal of Science, vol. 85, pp. 97–101, 1985.

[178] S. Padhi, A. K. Nayak, and A. Behera, "Type II diabetes mellitus: a review on recent drug based therapeutics," Biomedicine & Pharmacotherapy, vol. 131, p. 110708, 2020.

[179] R. Nasimi Doost Azgomi, A. Karimi, M. M. Zarshenas, and A. Moini Jazani, "The mechanisms of saffron (Crocus sativus) on the inflammatory pathways of diabetes mellitus: a systematic review," Diabetes and Metabolic Syndrome: Clinical Research and Reviews, vol. 16, p. 102365, 2021.

[180] S. Samarghandian, M. Azimi-Nezhad, and T. Farkhondeh, "Immunomodulatory and antioxidant effects of saffron aqueous extract (Crocus sativus L.) on streptozotocin-induced diabetes in rats," Indian Heart Journal, vol. 69, pp. 151–159, 2017.

[181] S. Kianbakht and R. Hajiaghaee, "Anti-hyperglycemic effects of saffron and its active constituents, crocin and safranal, in alloxan-induced diabetic rats," Journal of Medicinal Plants, vol. 3, pp. 82–89, 2011.

[182] D. Mohajeri, G. Mousavi, and Y. Doustar, "Antihyperglycemic and pancreas-protective effects of Crocus sativus L. (saffron) stigma ethanolic extract on rats with alloxan-induced diabetes," Journal of Biological Sciences, vol. 9, pp. 302–310, 2009.

[183] A. Arasteh, A. Aliyev, S. Khamnei, A. Delazar, M. Mesgari, and Y. Mehmannavaz, "Effects of hydromethanolic extract of saffron (Crocus sativus) on serum glucose, insulin and cholesterol levels in healthy male rats," Journal of Medicinal Plant Research, vol. 4, pp. 397–402, 2010.

[184] L. Xi, Z. Qian, X. Shen, N. Wen, and Y. Zhang, "Crocetin prevents dexamethasone-induced insulin resistance in rats," Planta Medica, vol. 71, pp. 917–922, 2005.

[185] L. Xi, Z. Qian, G. Xu, C. Zhou, and S. Sun, "Crocetin attenuates palmitate-induced insulin insensitivity and disordered tumor necrosis factor-alpha and adiponectin expression in rat adipocytes," British Journal of Pharmacology, vol. 151, pp. 610–617, 2007.

[186] M. Xiang, Z. Y. Qian, C. H. Zhou, J. Liu, and W. N. Li, "Crocetin inhibits leukocyte adherence to vascular endothelial cells induced by AGEs," Journal of Ethnopharmacology, vol. 107, pp. 25–31, 2006.

[187] M. Xiang, M. Yang, C. Zhou, J. Liu, W. Li, and Z. Qian, "Crocetin prevents AGEs-induced vascular endothelial cell apoptosis," Pharmacological Research, vol. 54, pp. 268–274, 2006.

[188] M. H. Boskabady, A. Tabatabaee, and G. Byrami, "The effect of the extract of Crocus sativus and its constituent safranal, on lung pathology and lung inflammation of ovalbumin sensitized guinea-pigs," Phytomedicine, vol. 19, pp. 904–911, 2012.

[189] H. Hosseinzadeh and J. Ghenaati, "Evaluation of the antitussive effect of stigma and petals of saffron (Crocus sativus) and its components, safranal and crocin in guinea pigs," Fitoterapia, vol. 77, pp. 446–448, 2006.

[190] M. H. Boskabady, M. G. Rahbardar, and Z. Jafari, "The effect of safranal on histamine (H(1)) receptors of guinea pig tracheal chains," Fitoterapia, vol. 82, pp. 162–167, 2011.

[191] P. Shukurova and R. Babaev, "A study into the effectiveness of the application of saffron extract in ocular pathologies in experiment," Georgian Medical News, pp. 38–42, 2010.

[192] R. Maccarone, S. Di Marco, and S. Bisti, "Saffron supplement maintains morphology and function after exposure to damaging light in mammalian retina," Investigative Ophthalmology & Visual Science, vol. 49, pp. 1254–1261, 2008.

[193] S. Predieri, M. Magli, E. Gatti, F. Camilli, P. Vignolini, and A. Romani, "Chemical composition and sensory evaluation of saffron," Food, vol. 10, 2021.

[194] B. Xuan, Y. H. Zhou, N. Li, Z. D. Min, and G. C. Chiou, "Effects of crocin analogs on ocular blood flow and retinal function," Journal of Ocular Pharmacology and Therapeutics, vol. 15, pp. 143–152, 1999.

[195] Y. Ohno, T. Nakanishi, N. Umigai, K. Tsuruma, M. Shimazawa, and H. Hara, "Oral administration of crocetin prevents inner retinal damage induced by N-methyl-D-aspartate in mice," European Journal of Pharmacology, vol. 690, pp. 84–89, 2012.

[196] F. Berger, A. Hensel, and K. Nieber, "Saffron extract and trans-crocetin inhibit glutamatergic synaptic transmission in rat cortical brain slices," *Neuroscience*, vol. 180, pp. 238–247, 2011.

[197] Y. Qi, L. Chen, L. Zhang, W. B. Liu, X. Y. Chen, and X. G. Yang, "Crocin prevents retinal ischaemia/reperfusion injury-induced apoptosis in retinal ganglion cells through the PI3K/AKT signalling pathway," *Experimental Eye Research*, vol. 107, pp. 44–51, 2013.

[198] S. Soeda, T. Ochiai, L. Paopong, H. Tanaka, Y. Shoyama, and H. Shimeno, "Crocin suppresses tumor necrosis factor-alpha-induced cell death of neuronally differentiated PC-12 cells," *Life Sciences*, vol. 69, pp. 2887–2898, 2001.

[199] M. Yamauchi, K. Tsuruma, S. Imai et al., "Crocetin prevents retinal degeneration induced by oxidative and endoplasmic reticulum stresses via inhibition of caspase activity," *European Journal of Pharmacology*, vol. 650, pp. 110–119, 2011.

[200] H. Hosseinzadeh and H. M. Younesi, "Antinociceptive and anti-inflammatory effects of *Crocus sativus* L. stigma and petal extracts in mice," *BMC Pharmacology*, vol. 2, pp. 7–7, 2002.

[201] H. Hosseinzadeh, M. H. Modaghegh, and Z. Saffari, "*Crocus sativus* L. (Saffron) extract and its active constituents (crocin and safranal) on ischemia-reperfusion in rat skeletal muscle," *Evidence-based Complementary and Alternative Medicine: Ecam*, vol. 6, pp. 343–350, 2009.

[202] G. Khorasani, S. J. Hosseinimehr, P. Zamani, M. Ghasemi, and A. Ahmadi, "The effect of saffron (*Crocus sativus*) extract for healing of second-degree burn wounds in rats," *The Keio Journal of Medicine*, vol. 57, no. 4, pp. 190–195, 2008.

[203] V. Magesh, J. P. Singh, K. Selvendiran, G. Ekambaram, and D. Sakthisekaran, "Antitumour activity of crocetin in accordance to tumor incidence, antioxidant status, drug metabolizing enzymes and histopathological studies," *Molecular and Cellular Biochemistry*, vol. 287, pp. 127–135, 2006.

[204] V. Magesh, K. DurgaBhavani, P. Senthilnathan, P. Rajendran, and D. Sakthisekaran, "In vivo protective effect of crocetin on benzo(a)pyrene-induced lung cancer in Swiss albino mice," *Phytotherapy research: PTR*, vol. 23, pp. 533–539, 2009.

[205] D. D. Liu, Y. L. Ye, J. Zhang, J. N. Xu, X. D. Qian, and Q. Zhang, "Distinct pro-apoptotic properties of Zhejiang saffron against human lung cancer via a caspase-8-9-3 cascade," *Asian Pacific Journal of Cancer Prevention : APJCP*, vol. 15, pp. 6075–6080, 2014.

[206] I. Das, R. N. Chakrabarty, and S. Das, "Saffron can prevent chemically induced skin carcinogenesis in Swiss albino mice," *Asian Pacific Journal of Cancer Prevention : APJCP*, vol. 5, pp. 70–76, 2004.

[207] I. Das, S. Das, and T. Saha, "Saffron suppresses oxidative stress in DMBA-induced skin carcinoma: a histopathological study," *Acta Histochemica*, vol. 112, pp. 317–327, 2010.

[208] A. A. Shati, F. G. Elsaid, and E. E. Hafez, "Biochemical and molecular aspects of aluminium chloride-induced neurotoxicity in mice and the protective role of *Crocus sativus* L. extraction and honey syrup," *Neuroscience*, vol. 175, pp. 66–74, 2011.

[209] H. Ettehadi, N. M. Seyedeh, R. Mina et al., "Aqueous extract of saffron (*Crocus sativus*) increases brain dopamine and glutamate concentrations in rats," *Journal of Behavioral and Brain Science*, vol. 3, no. 3, pp. 315–319, 2013.

[210] H. Ghoshooni, M. Daryaafzoon, S. Sadeghi-Gharjehdagi et al., "Saffron (*Crocus sativus*) ethanolic extract and its constituent, safranal, inhibits morphine-induced place preference in mice," *Pakistan Journal of Biological Sciences: PJBS*, vol. 14, no. 20, pp. 939–944, 2011.

[211] F. Vahdati Hassani, M. Hashemzaei, E. Akbari, M. Imenshahidi, and H. Hosseinzadeh, "Effects of berberine on acquisition and reinstatement of morphine-induced conditioned place preference in mice," *Avicenna Journal of Phytomedicine*, vol. 6, pp. 198–204, 2016.

[212] A. Eidi, M. Kamalinejad, A. Khoshbaten et al., "Study of the effects of intra-nucleus accumbens shell injections of alcohlic extract of *Crocus sativus* on the acquisition and expression of morphine-induced conditioned place preference in rats," *Physiol-Pharmacol*, vol. 12, pp. 121–128, 2008.

[213] M. A. Papandreou, M. Tsachaki, S. Efthimiopoulos, P. Cordopatis, F. N. Lamari, and M. Margarity, "Memory enhancing effects of saffron in aged mice are correlated with antioxidant protection," *Behavioural Brain Research*, vol. 219, pp. 197–204, 2011.

[214] E. Tamaddonfard, A. A. Farshid, K. Eghdami, F. Samadi, and A. Erfanparast, "Comparison of the effects of crocin, safranal and diclofenac on local inflammation and inflammatory pain responses induced by carrageenan in rats," *Pharmacological Reports*, vol. 65, pp. 1272–1280, 2013.

[215] A. A. Noorbala, S. Akhondzadeh, N. Tahmacebi-Pour, and A. H. Jamshidi, "Hydro-alcoholic extract of *Crocus sativus* L. versus fluoxetine in the treatment of mild to moderate depression: a double-blind, randomized pilot trial," *Journal of Ethnopharmacology*, vol. 97, pp. 281–284, 2005.

[216] N. Shahmansouri, M. Farokhnia, S. H. Abbasi et al., "A randomized, double-blind, clinical trial comparing the efficacy and safety of *Crocus sativus* L. with fluoxetine for improving mild to moderate depression in post percutaneous coronary intervention patients," *Journal of Affective Disorders*, vol. 155, pp. 216–222, 2014.

[217] A. Akhondzadeh Basti, E. Moshiri, A. A. Noorbala, A. H. Jamshidi, S. H. Abbasi, and S. Akhondzadeh, "Comparison of petal of *Crocus sativus* L. and fluoxetine in the treatment of depressed outpatients: a pilot double-blind randomized trial," *Progress in Neuro-Psychopharmacology & Biological Psychiatry*, vol. 31, pp. 439–442, 2007.

[218] A. L. Lopresti, P. D. Drummond, A. M. Inarejos-Garcia, and M. Prodanov, "Affron®, a standardised extract from saffron (*Crocus sativus* L.) for the treatment of youth anxiety and depressive symptoms: a randomised, double-blind, placebo-controlled study," *Journal of Affective Disorders*, vol. 232, pp. 349–357, 2018.

[219] S. Akhondzadeh, M. S. Sabet, M. H. Harirchian et al., "Saffron in the treatment of patients with mild to moderate Alzheimer's disease: a 16-week, randomized and placebo-controlled trial," *Journal of Clinical Pharmacy and Therapeutics*, vol. 35, no. 5, pp. 581–588, 2010.

[220] S. Akhondzadeh, M. Shafiee Sabet, M. H. Harirchian et al., "A 22-week, multicenter, randomized, double-blind controlled trial of *Crocus sativus* in the treatment of mild-to-moderate Alzheimer's disease," *Psychopharmacology*, vol. 207, pp. 637–643, 2010.

[221] B. Mousavi, S. Z. Bathaie, F. Fadai et al., "Safety evaluation of saffron stigma (*Crocus sativus* L.) aqueous extract and crocin in patients with schizophrenia," *Avicenna Journal of Phytomedicine*, vol. 5, pp. 413–419, 2015.

[222] S. Akhondzadeh, N. Tahmacebi-Pour, A. A. Noorbala et al., "Crocus sativus L. in the treatment of mild to moderate depression: a double-blind, randomized and placebo-controlled trial," *Phytotherapy research: PTR*, vol. 19, pp. 148–151, 2005.

[223] S. Moosavi, M. Ahmadi, M. Amini, B. Vazirzadeh, and I. Sari, "The effects of 40 and 80 mg hydro-alcoholic extract of *Crocus sativus* in the treatment of mild to moderate depression," *Journal of Mazandaran University of Medical Sciences*, vol. 24, 2014.

[224] B. Salehi, A. Prakash Mishra, M. Nigam et al., "Ficus plants: state of the art from a phytochemical, pharmacological, and toxicological perspective," *Phytotherapy research: PTR*, vol. 35, no. 3, pp. 1187–1217, 2021.

[225] H. Hosseinzadeh, S. Sadeghi Shakib, A. Khadem Sameni, and E. Taghiabadi, "Acute and subacute toxicity of safranal, a constituent of saffron, in mice and rats," *Iranian Journal of Pharmaceutical Research : IJPR*, vol. 12, pp. 93–99, 2013.

[226] D. Mohajeri, M. Abbasi, A. Delazar, Y. Doustar, G. Mousavi, and B. Amouoghli Tabrizi, "Histopathological study of sub-acute toxicity of *Crocus sativus* L. (saffron) stigma total extract on liver and kidney tissues in the rat," *Pharmaceutical Sciences*, vol. 15, pp. 115–124, 2009.

[227] D. Mohajeri, G. Mousavi, and M. Mesgari, "Subacute toxicity of *Crocus sativus* L. saffron stigma ethanolic extract in rats," *American Journal of Pharmacology and Toxicology*, vol. 2, pp. 189–193, 2007.

[228] T. Ziaee, B. M. Razavi, and H. Hosseinzadeh, "Saffron reduced toxic effects of its constituent, safranal, in acute and subacute toxicities in rats," *Jundishapur Journal of Natural Pharmaceutical Products*, vol. 9, pp. 3–8, 2014.

[229] G. Karimi, N. Taiebi, H. Hosseinzadeh, and F. Shirzad, "Evaluation of subacute toxicity of aqueous extract of *Crocus sativus* L," *Stigma and Petal in Rats*, vol. 4, pp. 29–35, 2004.

[230] M. Khayatnouri, S. Safavi, S. Safarmashaei, D. Babazadeh, and B. Mikailpourardabili, "The effect of saffron orally administration on spermatogenesis index in rat," *Advances in Environmental Biology*, vol. 5, pp. 1514–1521, 2011.

[231] F. Muosa, K. AL-Rekabi, S. Askar, and E. Yousif, "Evaluation of the toxic effect of ethanolic extract of saffron in male mice after subchronic exposure. Donnish," *The Journal of Pharmacy and Pharmacology*, vol. 1, pp. 1–7, 2015.

[232] M. H. Modaghegh, M. Shahabian, H. A. Esmaeili, O. Rajbai, and H. Hosseinzadeh, "Safety evaluation of saffron (*Crocus sativus*) tablets in healthy volunteers," *Phytomedicine*, vol. 15, pp. 1032–1037, 2008.

[233] H. Hosseinzadeh, A. Abootorabi, and H. R. Sadeghnia, "Protective effect of *Crocus sativus* stigma extract and crocin (trans-crocin 4) on methyl methanesulfonate-induced DNA damage in mice organs," *DNA and Cell Biology*, vol. 27, pp. 657–664, 2008.

[234] M. Schmidt, G. Betti, and A. Hensel, "Saffron in phytotherapy: pharmacology and clinical uses," *Wiener Medizinische Wochenschrift*, vol. 2007, no. 157, pp. 315–319, 1946.

[235] J. P. Melnyk, S. Wang, and M. F. Marcone, "Chemical and biological properties of the world's most expensive spice: saffron," *Food Research International*, vol. 43, pp. 1981–1989, 2010.

[236] M. Bahmani, M. Rafieian, A. Baradaran, S. Rafieian, and M. Rafieian-Kopaei, "Nephrotoxicity and hepatotoxicity evaluation of *Crocus sativus* stigmas in neonates of nursing mice," *Journal of Nephropathology*, vol. 3, pp. 81–85, 2014.

[237] B. Amin, H. M. Feriz, A. T. Hariri, N. T. Meybodi, and H. Hosseinzadeh, "Protective effects of the aqueous extract of *Crocus sativus* against ethylene glycol induced nephrolithiasis in rats," *EXCLI Journal*, vol. 14, pp. 411–422, 2015.

[238] A. T. Hariri, S. A. Moallem, M. Mahmoudi, B. Memar, B. M. Razavi, and H. Hosseinzadeh, "Effect of *Crocus sativus* L. stigma (saffron) against subacute effect of diazinon: histopathological, hematological, biochemical and genotoxicity evaluations in rats," *Journal of Pharmacopuncture*, vol. 21, pp. 61–69, 2018.

[239] F. Zeynali, M. Dashti, M. Anvari, S. Hosseini, and S. Miresmaeili, "Studying teratogenic an abortificant effects of different doses of saffron (*Crocus sativus*) decoction in whole gestational period and the 3rd trimester of gestational period in mice," *International Journal of Reproductive BioMedicine*, vol. 7, 2009.

[240] R. Edamula, M. Deecaraman, D. S. Kumar, H. Krishnamurthy, and M. Latha, "Prenatal developmental toxicity of *Crocus sativus* (saffron) in wistar rats," *The International journal of pharmacology and toxicology*, vol. 2, pp. 46–49, 2014.

[241] C. J. Wang, L. S. Hwang, and J. K. Lin, "Reversible hepatic black pigmentation and enzyme alteration induced by prolonged feeding of high dose of crocin dyes in rats," *Proceedings of the National Science Council, Republic of China. Part B, Life Sciences*, vol. 8, pp. 246–253, 1984.

[242] H. Hosseinzadeh, M. Shariaty, A. Khadem-Sameni, M. Vahabzadeh, J. Ríos, and M. Recio, "Acute and subacute toxicity of crocin, a constituent of *Crocus sativus* L. (saffron), in mice and rats," *Pharmacology*, vol. 2, pp. 943–951, 2010.

[243] F. Taheri, S. Z. Bathaie, M. Ashrafi, and E. Ghasemi, "Assessment of crocin toxicity on the rat liver," *mdrsjrns*, vol. 17, pp. 67–79, 2014.

[244] S. A. Moallem, M. Afshar, L. Etemad, B. M. Razavi, and H. Hosseinzadeh, "Evaluation of teratogenic effects of crocin and safranal, active ingredients of saffron, in mice," *Toxicology and Industrial Health*, vol. 32, pp. 285–291, 2016.

[245] H. Hosseinzadeh, S. S. Shakib, A. K. Sameni, and E. Taghiabadi, "Acute and subacute toxicities of safranal, a constituent of saffron, in mice and rats," *Clinical Biochemistry*, vol. 44, no. 13, p. S122, 2011.

[246] R. Rezaee and H. Hosseinzadeh, "Safranal: from an aromatic natural product to a rewarding pharmacological agent," *Iranian Journal of Basic Medical Sciences*, vol. 16, pp. 12–26, 2013.

[247] B. Riahi-Zanjani, M. Balali-Mood, E. Mohammadi, H. Badie-Bostan, B. Memar, and G. Karimi, "Safranal as a safe compound to mice immune system," *Avicenna Journal of Phytomedicine*, vol. 5, pp. 441–449, 2015.

[248] H. Ayatollahi, A. O. Javan, M. Khajedaluee, M. Shahroodian, and H. Hosseinzadeh, "Effect of *Crocus sativus* L. (saffron) on coagulation and anticoagulation systems in healthy volunteers," *Phytotherapy research: PTR*, vol. 28, pp. 539–543, 2014.

[249] A. H. Mohamadpour, Z. Ayati, M. R. Parizadeh, O. Rajbai, and H. Hosseinzadeh, "Safety evaluation of crocin (a constituent of saffron) tablets in healthy volunteers," *Iranian Journal of Basic Medical Sciences*, vol. 16, pp. 39–46, 2013.

[250] S. C. Nair, M. J. Salomi, B. Panikkar, and K. R. Panikkar, "Modulatory effects of *Crocus sativus* and *Nigella sativa* extracts on cisplatin-induced toxicity in mice," *Journal of Ethnopharmacology*, vol. 31, no. 1, pp. 75–83, 1991.

[251] L. Kharchoufa, I. A. Merrouni, A. Yamani, and M. Elachouri, "Profile on medicinal plants used by the people of North Eastern Morocco: toxicity concerns," *Toxicon*, vol. 154, pp. 90–113, 2018.

[252] G. Martin, E. Goh, and A. W. Neff, "Evaluation of the developmental toxicity of crocetin on Xenopus," *Food and Chemical Toxicology*, vol. 40, pp. 959–964, 2002.

[253] Chinese Pharmacopoeia Commission, *Pharmacopoeia of the People's Republic of China*, The Medicine Science and Technology Press of China, Beijing, 2015.

[254] H. Hosseinzadeh and N. B. Noraei, "Anxiolytic and hypnotic effect of *Crocus sativus* aqueous extract and its constituents, crocin and safranal, in mice," *Phytotherapy research: PTR*, vol. 23, pp. 768–774, 2009.

[255] G. Georgiadou, V. Grivas, P. A. Tarantilis, and N. Pitsikas, "Crocins, the active constituents of *Crocus sativus* L., counteracted ketamine-induced behavioural deficits in rats," *Psychopharmacology*, vol. 231, pp. 717–726, 2014.

[256] K. Bajbouj, J. Schulze-Luehrmann, S. Diermeier, A. Amin, and R. Schneider-Stock, "The anticancer effect of saffron in two p53 isogenic colorectal cancer cell lines," *BMC Complementary and Alternative Medicine*, vol. 12, p. 69, 2012.

[257] European Directorate for the Quality of Medicines and Healthcare, *European Pharmacopoeia*, European Directorate for the Quality of Medicines and HealthCare, Strasbourg, 8th edition, 2014.

[258] Medicines & Healthcare Products Regulatory Agency, *British Pharmacopoeia*, The Stationery Office, London, 2013.

[259] The Editorial Committee of the Japanese Pharmacopoeia, *Japanese Pharmacopoeia*, Ministry of Welfare, Tokyo, 2011.

[260] N. Moratalla-López, M. J. Bagur, C. Lorenzo, M. E. M.-N. R. Salinas, and G. L. Alonso, "Bioactivity and bioavailability of the major metabolites of *Crocus sativus* L. flower," *Molecules*, vol. 24, p. 2827, 2019.

[261] M. Martinez-Tome, A. M. Jimenez, S. Ruggieri, N. Frega, R. Strabbioli, and M. A. Murcia, "Antioxidant properties of Mediterranean spices compared with common food additives," *Journal of Food Protection*, vol. 64, pp. 1412–1419, 2001.

[262] T. H. Tseng, C. Y. Chu, J. M. Huang, S. J. Shiow, and C. J. Wang, "Crocetin protects against oxidative damage in rat primary hepatocytes," *Cancer Letters*, vol. 97, pp. 61–67, 1995.

[263] M. Sebastin Santhosh, M. Hemshekhar, R. M. Thushara, S. Devaraja, K. Kemparaju, and K. S. Girish, "Vipera russelli venom-induced oxidative stress and hematological alterations: amelioration by crocin a dietary colorant," *Cell Biochemistry and Function*, vol. 31, pp. 41–50, 2013.

[264] F. I. Abdullaev and J. J. Espinosa-Aguirre, "Biomedical properties of saffron and its potential use in cancer therapy and chemoprevention trials," *Cancer Detection and Prevention*, vol. 28, pp. 426–432, 2004.

[265] R. Yang, X. Tan, A. M. Thomas et al., "Crocetin inhibits mRNA expression for tumor necrosis factor-alpha, interleukin-1beta, and inducible nitric oxide synthase in hemorrhagic shock," *JPEN Journal of Parenteral and Enteral Nutrition*, vol. 30, no. 4, pp. 297–301, 2006.

[266] S. Kianbakht and K. Mozaffari, "Effects of saffron and its active constituents, crocin and safranal, on prevention of indomethacin induced gastric ulcers in diabetic and nondiabetic rats," *Journal of Medicinal Plants Research*, vol. 8, pp. 30–38, 2009.

[267] X. C. Shen and Z. Y. Qian, "Effects of crocetin on antioxidant enzymatic activities in cardiac hypertrophy induced by norepinephrine in rats," *Die Pharmazie*, vol. 61, pp. 348–352, 2006.

[268] L. Ferrara, D. Naviglio, and M. Gallo, "Extraction of bioactive compounds of saffron (*Crocus sativus* L.) by ultrasound assisted extraction (UAE) and by rapid solid-liquid dynamic extraction (RSLDE)," *European Scientific Journal, ESJ*, vol. 10, 2014.

[269] I. Cosano, C. Pintado, A. Acevedo et al., "Microbiological quality of saffron from the main producer countries," *Journal of Food Protection*, vol. 72, pp. 2217–2220, 2009.

[270] C. Pintado, A. de Miguel, O. Acevedo, L. Nozal, J. L. Novella, and R. Rotger, "Bactericidal effect of saffron (*Crocus sativus* L.) on salmonella enterica during storage," *Food Control*, vol. 22, pp. 638–642, 2011.

[271] M. Abbasvali, A. Ranaei, S. S. Shekarforoush, and H. Moshtaghi, "The effects of aqueous and alcoholic saffron (*Crocus sativus*) tepal extracts on quality and shelf-life of Pacific white shrimp (Litopeneous vannamei) during iced storage," *Journal of Food Quality*, vol. 39, 742 pages, 2016.

[272] A. Aktypis, E. D. Christodoulou, E. Manolopoulou, A. Georgala, D. Daferera, and M. Polysiou, "Fresh ovine cheese supplemented with saffron (*Crocus sativus* L.): impact on microbiological, physicochemical, antioxidant, color and sensory characteristics during storage," *Small Ruminant Research*, vol. 167, pp. 32–38, 2018.

Review Article

Papaver Plants: Current Insights on Phytochemical and Nutritional Composition Along with Biotechnological Applications

Monica Butnariu [ID],[1] **Cristina Quispe** [ID],[2] **Jesús Herrera-Bravo** [ID],[3,4] **Marius Pentea** [ID],[1] **Ioan Sarac** [ID],[1] **Aylin Seylam Küşümler** [ID],[5] **Beraat Özçelik** [ID],[6,7] **Sakshi Painuli**,[8,9] **Prabhakar Semwal** [ID],[8,10] **Muhammad Imran**,[11] **Tanweer Aslam Gondal**,[12] **Simin Emamzadeh-Yazdi**,[13] **Natallia Lapava** [ID],[14] **Zubaida Yousaf**,[15] **Manoj Kumar** [ID],[16] **Ali Hussein Eid**,[17,18] **Yusra Al-Dhaheri**,[19] **Hafiz Ansar Rasul Suleria** [ID],[20] **María del Mar Contreras** [ID],[21] **Javad Sharifi-Rad** [ID],[22] **and William C. Cho** [ID][23]

[1]Banat's University of Agricultural Sciences and Veterinary Medicine "King Michael I of Romania" from Timisoara, Timisoara, Romania
[2]Facultad de Ciencias de la Salud, Universidad Arturo Prat, Avda. Arturo Prat 2120, Iquique 1110939, Chile
[3]Departamento de Ciencias Básicas, Facultad de Ciencias, Universidad Santo Tomas, Chile
[4]Center of Molecular Biology and Pharmacogenetics, Scientific and Technological Bioresource Nucleus, Universidad de La Frontera, Temuco 4811230, Chile
[5]İstanbul Okan University, Nutrition and Dietetics Department, Tuzla, İstanbul, Turkey
[6]Department Food Engineering, Faculty of Chemical and Metallurgical Engineering, Istanbul Technical University, Maslak, 34469 Istanbul, Turkey
[7]BIOACTIVE Research & Innovation Food Manufacturing Industry Trade LTD Co., Maslak, Istanbul 34469, Turkey
[8]Department of Biotechnology, Graphic Era University, 248001, Dehradun, Uttarakhand, India
[9]Himalayan Environmental Studies and Conservation Organization, Prem Nagar, Dehradun, 248001 Uttarakhand, India
[10]Department of Life Sciences, Graphic Era Deemed to be University, Dehradun-248002, Uttarakhand, India
[11]University Institute of Diet and Nutritional Sciences, Faculty of Allied Health Sciences, The University of Lahore-Lahore, Pakistan
[12]School of Exercise and Nutrition, Deakin University, Victoria 3125, Australia
[13]Department of Plant and Soil Sciences, University of Pretoria, Gauteng 0002, South Africa
[14]Medicine Standardization Department of Vitebsk State Medical University, Belarus
[15]Department of Botany, Jail Road, Lahore 54000, Pakistan
[16]Chemical and Biochemical Processing Division, ICAR-Central Institute for Research on Cotton Technology, 400019, Mumbai, India
[17]Department of Basic Medical Sciences, College of Medicine, QU Health, Qatar University, PO Box 2713, Doha, Qatar
[18]Biomedical and Pharmaceutical Research Unit, QU Health, Qatar University, PO Box 2713, Doha, Qatar
[19]Department of Biology, College of Science, United Arab Emirates University, UAE
[20]Department of Agriculture and Food Systems, The University of Melbourne, Melbourne 3010, Australia
[21]Department of Chemical, Environmental and Materials Engineering, Universidad de Jaén, Campus las Lagunillas, s/n, 23071 Jaén, Spain
[22]Facultad de Medicina, Universidad del Azuay, Cuenca, Ecuador
[23]Department of Clinical Oncology, Queen Elizabeth Hospital, Kowloon, Hong Kong

Correspondence should be addressed to Prabhakar Semwal; semwal.prabahakar@gmail.com,
María del Mar Contreras; mar.contreras.gamez@gmail.com, Javad Sharifi-Rad; javad.sharifirad@gmail.com,
and William C. Cho; chocs@ha.org.hk

The genus *Papaver* is highly esteemed in the pharmacy industry, in the culinary field, and as ornamental plants. These plants are also valued in traditional medicine. Among all *Papaver* species, *Papaver somniferum* L. (opium poppy) is the most important species in supplying phytochemicals for the formulation of drugs, mainly alkaloids like morphine, codeine, rhoeadine, thebaine, and papaverine. In addition, *Papaver* plants present other types of phytochemicals, which altogether are responsible for its biological activities. Therefore, this review covers the phytochemical composition of *Papaver* plants, including alkaloids, phenolic compounds, and essential oils. The traditional uses are reviewed along with their pharmacological activities. Moreover, safety aspects are reported to provide a deep overview of the pharmacology potential of this genus. An updated search was carried out in databases such as Google Scholar, ScienceDirect, and PubMed to retrieve the information. Overall, this genus is a rich source of alkaloids of different types and also contains interesting phenolic compounds, such as anthocyanins, flavonols, and the characteristic indole derivatives nudicaulins. Among other pharmacological properties, numerous preclinical studies have been published about the analgesic, anticancer, antimicrobial, antioxidant, and antidiabetic activities of *Papaver* plants. Although it highlights the significant impact of this genus for the treatment of a variety of diseases and conditions, as a future prospect, characterization works accompanying preclinical studies are required along with clinical and toxicology studies to establish a correlation between the scientific and traditional knowledge.

1. Introduction

Many plants are naturally rich sources of phytochemicals with valuable biological properties, which could have significant impact for the treatment of a variety of diseases and conditions and as potential alternative options for synthetic drugs. This is also the case of the genus *Papaver* (family Papaveraceae), which is known for its medicinal properties attributed to their phytochemical composition ([1]; [180].

This genus belongs to the family Papaveraceae, which is a cosmopolitan family growing from tropical to alpine ecosystems [1], mainly in the northern hemisphere [2]. The flowers have no style, but on the top of the ovary, a stigmatic tissue is arranged radially on a sessile stigmatic disc. Their similar characteristics in their flower shapes, colors, and fruits complicate the identification based only on morphological characteristics [2], and different number of species is given in literature. For example, it consists of ~80–100 species, including annual, biennial, and perennial herbs [1, 3]. As the family, the genus *Papaver* is widely natural distributed, especially in regions with Mediterranean climate [1, 4]. In the case of *Papaver somniferum* L. (opium poppy), the most important species and due to its narcotic properties, it is highly produced in countries such as Afghanistan, Myanmar, Mexico, and Lao PDR (or Laos) [5], but illegally [6]. Alternatively, Turkey is one of the main legal manufacturers of the poppy plant [7], along with Czechia, Spain, etc. Figure 1 shows the world production of poppy seeds in the last twenty years according to the data available from the Food and Agriculture Organization of the United Nations [8].

Other commonly cultivated species of the genus *Papaver* are *Papaver bracteatum* Lindl. (Iranian poppy), *Papaver rhoeas* L. (common poppy or corn poppy), *Papaver dubium* L., *Papaver pseudo-orientale* Medw., and *Papaver orientale* L. *P. bracteatum* that grow wild in high altitudes in north and northwest of Iran, in Russia and Caucasia regions [9]. *P. rhoeas* is an important competitive plant in winter cereals in southern Europe under Mediterranean climate [10] and thus called corn poppy. *P. dubium* is also called long-head

poppy. *P. dubium* is widespread throughout Europe and America and is an important weed in western Iran [11]. *P. orientale* and *P. pseudo-orientale* are distributed into the Caucasus area [12].

Concerning the natural product field, *P. somniferum* was the first source of natural drugs with the obtainment of analgesic morphine drugs [13], including codeine, morphine, and a variety of semisynthetic derivatives, mainly derived from thebaine, such as oxycodone and buprenorphine [14]. These compounds belong to the opiate family that has analgesic properties mainly by binding to the mu-opioid receptor within the central nervous system (CNS) and the peripheral nervous system. It leads to an overall reduction of the nociceptive transmission [15]. However, the latex of the opium poppy is not only used for the treatment of severe pain, but it is also subjected to opioid abuse and drug trafficking due to the narcotic properties of these compounds. Therefore, their production is regulated internationally.

P. bracteatum has high content of thebaine as the main alkaloid, which has been utilized in the production of codeine [16]. Besides these compounds, the nonnarcotic papaverine is another economically important alkaloid with vasodilator properties [1, 17].

Apart from the alkaloids, poppy plant is a rich source of phenolic compounds, such as anthocyanins, flavonols, and the characteristic indole derivatives nudicaulins, and essential oil volatiles, which altogether are responsible for its pharmacological activities.

Moreover, *Papaver* seeds are esteemed in the food sector, e.g., to be used in bakery and desserts and to produce oil. For example, *P. somniferum* seeds are used in some Central Eastern European countries (European Food Safety Authority, [18]). In this context, poppy can be classified into three main categories depending on the use: industrial poppy intended for alkaloid extraction from the capsule of the plant; culinary poppy when it is grown to obtain seeds and oil; both industrial and culinary poppy [19]. *P. rhoeas* is also used as garniture in salad in some regions [20], and the seeds of *P. bracteatum* are used in foods in Central Anatolia [21].
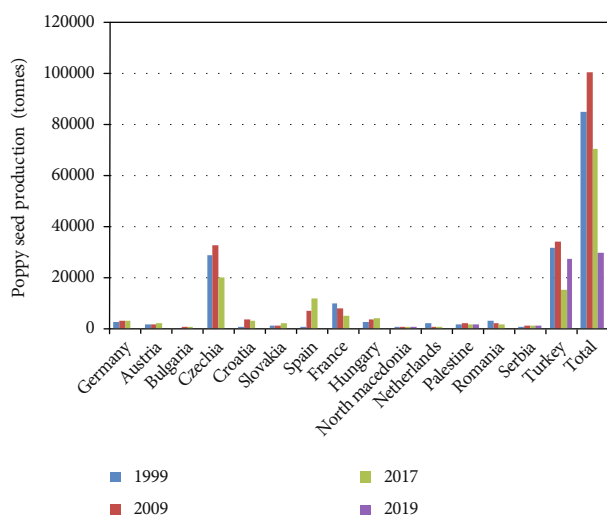
FIGURE 1: World production of poppy seeds in 1999, 2009, 2017, and 2019 according to FAOSTAT [8].

Other different use is as ornamental plants like *P. orientale* and *P. pseudo-orientale* [2].

Moreover, besides the aforementioned applications for the main important alkaloids, the bioactive properties of the genus *Papaver* are wide. Antioxidant, antimicrobial, anticancer, anti-inflammation, neuroprotection, and maintenance of fertility are some of the important bioactivities of the *Papaver* genus plant extracts, as depicted in the following. In this context, this review describes the traditional uses of *Papaver* species, their phytochemical composition, and bioactive properties, describing preclinical and clinical studies. Moreover, safety aspects are well discussed with important case studies. The overall components and pharmacological activities of the review are well illustrated in Figure S1.

2. Databases, e-Resources, and Keyword Search

Various search engines for the survey of the literature were used to compile the scientific information included in the current review. In particular, Google Scholar, ScienceDirect, PubMed, and SpringerLink were used. Literature was retrieved from the books and international journals of highly cited publishers, including Elsevier, Springer, Frontiers, Wiley, and Taylor and Francis. Very few information was derived from national journals with no information of the ranking on the basis of citations. The keywords "*Papaver*", "*Papaver somniferum*", "opium poppy", "opium", "traditional uses", "ethnopharmacology", "bioactivities", "biological activities", "phytochemical profile", and combinations of these words were used for deriving the particular information about the *Papaver* genus. Any article in the English language mentioning these keywords was included in the review article. The research articles, which were exclusively related to the agronomic traits of the *Papaver* genus, were excluded for compiling the information of the current review. Moreover, ChemBioDraw Ultra 12.0 (CambridgeSoft, Cambridge, MA, USA) was used to draw the chemical structures of the phytochemical compounds from the *Papaver* genus.

3. Ethnobotanical Uses of the *Papaver* Genus in Different Human Cultures

The traditional and medicinal properties of this genus have been documented since 3000 BC. The main analgesic compound "morphine" was isolated from *P. somniferum* L. by a German pharmacist "Sertüner" in 1905 [22]. The genus *Papaver* is not popular for traditional medicine due to narcotic and other side effects. Nevertheless, there are several uses such as anti-inflammatory, antidiabetic, analgesic, and remedy for cough and lung infection as described in traditional medicine and detailed in Table 1. This includes the use of the flowers, buds, seeds, fruits, and leaves or aerial parts of the most popular species of *Papaver* in different countries and cultures.

4. Phytoconstituents

The identification of the phytochemical composition of medicinal plants is highly important to provide a best known of the active compounds. It involves complex mixtures of natural compounds with different organic structures and varies depending on the plant source [48].

Papaver species contain alkaloids, phenolic compounds, and essential oil volatiles, among other components [49]. These classes found in different parts of the *Papaver* plants are discussed in the following subsections.

4.1. Alkaloids. As other phytochemicals, the production of alkaloids in poppy plants is induced by environmental stress conditions, but the details about regulatory processes are not well known and subjected of ongoing studies [50]. Moreover, the alkaloid composition varies even within the same species [51]. This makes that the *Papaver* genus yields more than 170 alkaloids [52, 53]. As an example, Figure 2 summarizes the type of alkaloids found in the genus *Papaver* with their chemical structures.

In particular, *P. somniferum* presents interesting benzylisoquinoline alkaloids, such as papaverine, and the morphinanes morphine, codeine, and thebaine (Table 2, Figure 2), as mentioned in Section 1. Since *P. somniferum* has been extensively utilized illegally, its cultivation is strictly regulated by the International Narcotics Control Board [54, 55]. The latex of the opium poppy, which surrounds the seed capsule [56], may contain up to 80 alkaloids, but the latter compounds, morphine, codeine, and thebaine, along with narcotine and narceine are generally the main alkaloids [17, 18].

P. bracteatum is also a source of the alkaloid thebaine, the precursor of the opiate analgesics codeine, buprenorphine, oxymorphone, and oxycodone [14, 57, 58]. The plant capsule of this species shows high concentrations of morphine and oripavine (another morphinan) as compared to the stem tissues. It seems that the origin and even the latitude affect the thebaine, morphine, and oripavine [59]. This makes that it has intraspecies variation. For example, another study found that the major alkaloids in this species were salutaridine (promorphinan) and thebaine [53].

TABLE 1: Traditional medical usage of *Papaver* species.

Papaver species	Country	Internal/external usage	References
P. argemone L.	Iran	Flower (headache, coughs)	Naghibi et al. [23]
P. bracteatum Lindl.	Iran	Flowers, leaves, seeds (hypnotic and sedative, respiratory tract infections, sore throat, food digestion, eyelid inflammation, spasm, rheumatism pains)	Farouji and Khodayari [24]
P. dubium L.	Turkey	Flower (colds, cough)	Altundaga and Ozturkb [25]; Çakılcıoğlu et al. [26]
P. lacerum Popov	Turkey	Buds (goiter)	Altundaga and Ozturkb [25]
P. lateritium K. Koch	Turkey	Flower (sedative, antitussive, bronchial, hypnotic)	Akbulut and Bayramoglu [27]
P. macrostomum Boiss. & A.Huet	Turkey	Flower (cough)	Altundaga and Ozturkb [25]
P. orientale L.	Turkey	Seed (laxative); leaf (asthma)	Altundaga & Ozturkb [25]
P. rhoeas L.	Turkey	Herb (sedative); fruit, seed (gastrointestinal diseases) External usage: aerial part (red spots on body); fruit (burns); seed (dermal diseases, wound)	Altundaga and Ozturkb [25]; Çakılcıoğlu et al. [26]; Polat and Satıl [28]; Ugulu [29]; Yipel et al. [30]
	Italy	Fruit, young shoot (sedative, hypnotic); young aerial part (depurative); leaf, flower (mental-nervous, hypnotic, mild sedative for child, cough)	González-Tejero et al. [31]; Mattalia et al. [32]; Naghibi et al. [23]; Pieroni, [33]; Pieroni and Quave [34]; Scherrer et al. [35]; Vitalin et al. [36];
	Algeria	Aerial part (respiratory diseases)	Gonzalez-Tejero et al. [31]
	Cyprus	Aerial part (nervous/mental conditions, digestive)	Gonzalez-Tejero et al. [31]
	Spain	Aerial part (respiratory diseases)	Gonzalez-Tejero et al. [31]
	Iran	Seed, capsule (antidiabetic); flower (addiction, sedative, hypnotic)	Bahmani et al. [37]; Nadaf et al. [38]
	Turkey	Fruit, seed (gastrointestinal, nervous and respiratory diseases)	Yipel et al. [30]
P. somniferum L.	Italy	Fruit, seed (tranquiliser, toothaches)	Pieroni and Quave [34]
	India	Seed (demulcent, spasmolytic, muscle catch, tonic); fruit (cough, diarrhea) External usage: leaf (swelling)	Jadnav [39]; Dar et al. [40]; Goyal [41]; Tayade and Patil [42]
	Pakistan	Herb (narcotic, stimulant, to increase performance, cough suppressant); fruit, leaf (analgesic, narcotics); seed (narcotic, analgesic, sedative, increases excitement and physical vigor)	Adnan et al., [43]; Alamgeer et al. [44]; Irfan et al. [45]; Ullah et al. [46]
	Korea	External usage: fruit, latex, stem (furuncle)	Kim and Song [47]

Concerning *P. rhoeas*, phytochemical composition has showed rhoeadine alkaloids as major compounds, including rhoeadine and rhoeagenine [60, 61]. Recent trends based on mass spectrometry (MS) analysis enabled the identification of a high number of phytochemicals from *Papaver* samples. For alkaloid profiling, electrospray ionization in the positive ionization modes generally leads to richer and complex chromatographic profiles with more intense signals for elucidation purposes [62]. Using this technique, for example, 55 alkaloids were characterized in the aerial parts of *P. rhoeas* and *P. somniferum*. This included benzophenanthridine, protoberberine, benzylisoquinoline, aporphine, and rhoeadine-type alkaloids (see examples, in Figure 2). The most characteristic feature was that rhoeadine alkaloids were observed only in *P. rhoeas* samples, and codeine and morphine were tentatively identified in *P. somniferum* [180] (Table 2).

In the latter work, different solvents were tested for extraction including ethyl ether with 10% ammonia, pure ethanol, and methanol, as well as aqueous-methanol 50% and 80%. Among them, ethanol can be applied to extract the aerial parts of *P. rhoeas* and *P. somniferum*, with advantages due to its high extraction efficiency [181] and as its low toxicity. Similarly, four *Papaver* species (*Papaver Lacerum* Popov, *Papaver syriacum* Boiss. & Blanche, *Papaver glaucum* Boiss. & Hausskn., and *P. rhoeas*) were collected from different sites in Turkey and the aerial parts were extracted using methanol. By using LC-tandem MS, two alkaloids, pronuciferine (proaporphine type) and roemerine (aporphine type), were determined in the selected species [63]. The latter compound was the major one in some *P. rhoeas* samples [64]. Recent studies showed that both alkaloids increase brain-derived neurotrophic factor (BDNF) protein expression in hippocampal SH-SY5Y cells demonstrating that besides the
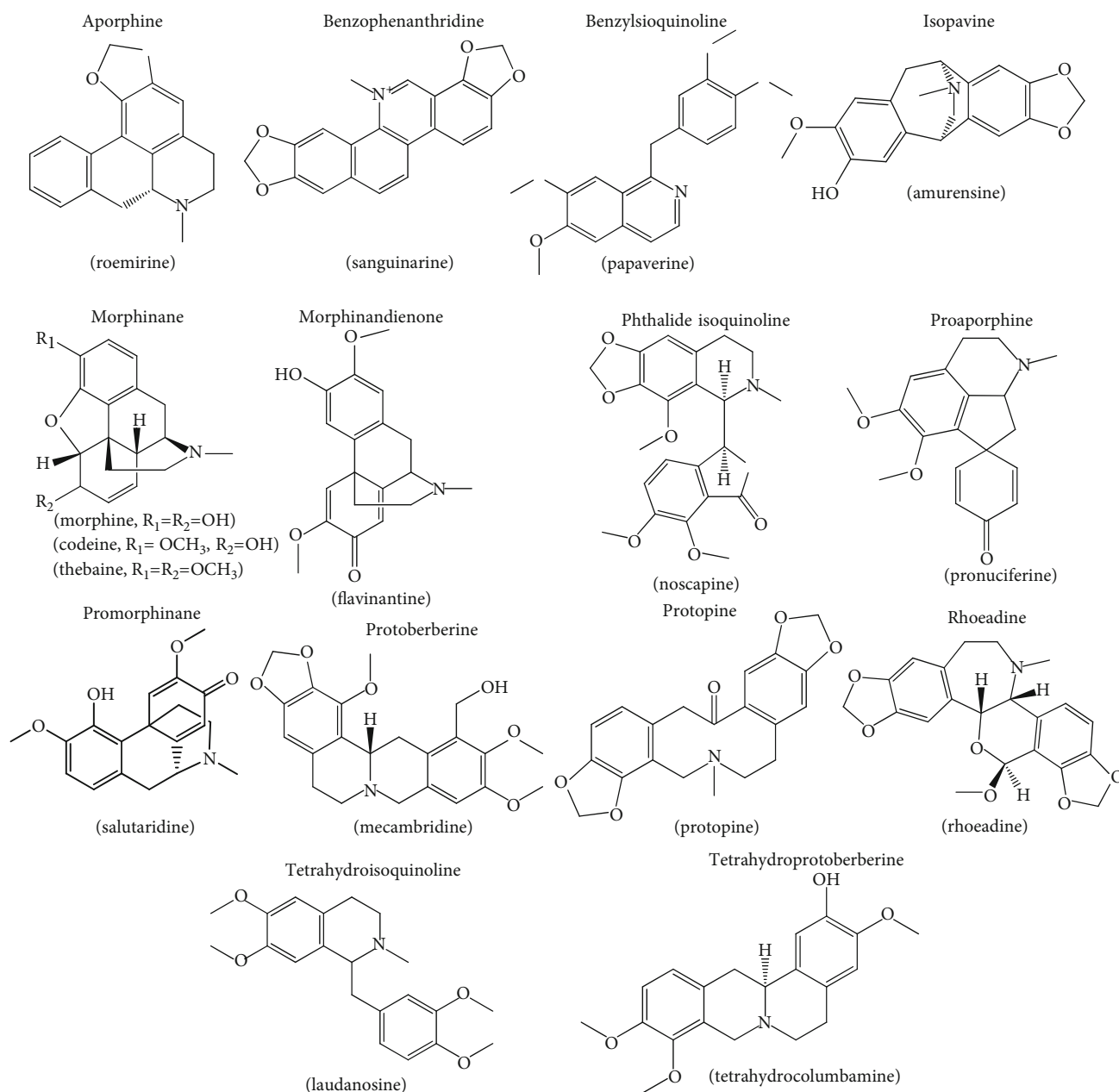
FIGURE 2: Selected alkaloids to exemplify the chemical structure of the different types found in the genus *Papaver*.

common poppy alkaloids, the former alkaloids could also be interesting [65]. Other compounds identified were salutaridine (promorphinan type), coulteropine (protopine type), and rhoeadine derivatives (epiglaucamine, glaudine, and rhoeagenine) [64]. Furthermore, using a combination of LC-MS and molecular networking, isoquinoline alkaloids in *Papaver nudicaule* L. and *P. rhoeas* aerial parts were clustered. 42 and 16 compounds were characterized, respectively, and a variation was observed depending on the color of the flowers [66].

P. macrostomum, which is widely distributed in Turkey, contains alkaloids such as protopine (protopine), benzylisoquinoline (macrostomine, dehydromacrostomine, sevanine), rhoeadine (rhoeadine, papaverrubine A-E), aporphine (iso-

corydine), isopavine (amurensine, amurensinine), protoberberine (cheilantifoline), proaporphine (mecambrine), and benzyl tetrahydroisoquinoline (laudanosine) types [67]. Moreover, the major alkaloids of *P. orientale* were oripavine (morphinan type) and mecambridine (protoberberine type) and of *P. pseudo-orientale* were also mecambridine and isothebaine (aporphine type) and orientalidine (protoberberine type). Main compounds of *Papaver duvium* L. are berberine and thalifendine, while roemerine is present in *P. lacerum*. The presence of isocorydine, stylopine (tetrahydroprotoberberine type) and tetrahydropseudocoptisine, roemerine, mecambrine, and allocryptopine depends on the subspecies [68]. The alkaloid composition of other less known *Papaver* species was described by Sariyar [53].

TABLE 2: Alkaloids characterized in *Papaver rhoeas* L. and *Papaver somniferum* L. by mass spectrometry in different locations. Adapted from [181].

Name	Formula	Mass (Da)	MS/MS fragments (*m/z*)	Alkaloid type	PR (R)	PR (SK)	PS
DL-Demethylcoclaurine*	$C_{16}H_{17}NO_3$	271.12	107.05, 255.10, 161.06, 143.05	Benzylsioquinoline	+	+	+
Coclaurine*	$C_{17}H_{19}NO_3$	285.14	107.05, 269.12, 175.07, 237.09	Benzylsioquinoline	+	+	+
Tetrahydropapaverine*	$C_{20}H_{25}NO_4$	343.18	192.10, 189.09, 151.08, 327.16	Benzylsioquinoline	-	-	+
Reticuline*	$C_{19}H_{23}NO_4$	329.16	192.10, 137.06, 143.05, 175.07	Benzylsioquinoline	+	+	+
Corytuberine*	$C_{19}H_{21}NO_4$	327.15	265.09, 237.09, 297.11, 205.06	Aporphine	+	+	+
Tetrahydrocolumbamine*	$C_{20}H_{23}NO_4$	341.16	178.09, 163.06, 176.07	Protoberberine (THPB)	-	-	+
Scoulerine*	$C_{19}H_{21}NO_4$	327.15	237.09, 207.04, 211.08, 239.07	Protoberberine (THPB)	-	-	+
L-Tetrahydropalmatine*	$C_{21}H_{25}NO_4$	355.18	192.10, 165.09, 176.07	Protoberberine (THPB)	+	-	+
Tetrahydroberberine (canadine)*	$C_{20}H_{21}NO_4$	339.15	176.07, 149.06, 174.05	Protoberberine (THPB)	+	-	+
Berberine*	$C_{20}H_{18}NO_4$	336.12	320.09, 292.10, 321.10, 306.08, 278.08	Protoberberine	+	+	+
Stylopine*	$C_{19}H_{17}NO_4$	323.12	176.07, 149.06	Protoberberine (THPB)	+	+	+
Dihydrosanguinarine*	$C_{20}H_{15}NO_4$	333.10	318.08, 319.08, 304.10, 276.10	Benzophenanthridine	+	+	+
Sanguinarine	$C_{20}H_{14}NO_4$	332.09	317.07, 274.09, 304.10	Benzophenanthridine	+	-	-
Protopine*	$C_{20}H_{19}NO_5$	353.13	188.07, 189.08, 149.06	Protopine	+	+	+
Allocryptopine*	$C_{21}H_{23}NO_5$	369.16	188.07, 189.08, 290.09	Protopine	+	-	-
Morphine	$C_{17}H_{19}NO_3$	285.14	201.09, 229.08, 185.06, 211.07	Morphinan	-	-	+
Mecambrine	$C_{18}H_{17}NO_3$	295.12	202.09, 171.07, 280.10	Proaporphine	-	-	+
Codeine	$C_{18}H_{21}NO_3$	299.15	215.11, 243.10, 225.09, 199.07	Morphinan	-	-	+
(S)-N-Methylcoclaurine	$C_{18}H_{21}NO_3$	299.15	269.12, 107.05, 271.13	Benzylisoquinoline	+	+	+
Armepavine	$C_{19}H_{23}NO_3$	313.17	107.05, 58.07, 269.12, 271.13, 298.11	Benzylisoquinoline	+	+	+
(S)-3′-Hydroxy-N-methylcoclaurine	$C_{18}H_{21}NO_4$	315.15	192.10, 123.04, 285.11, 300.12	Benzylisoquinoline	+	+	+
(S)-Cheilanthifoline	$C_{19}H_{19}NO_4$	325.13	178.09, 190.09, 163.06	Protoberberine	+	+	+
Papaverine	$C_{20}H_{21}NO_4$	339.15	202.09, 324.12, 296.13, 171.07	Benzylisoquinoline	-	-	+
Cryptopine	$C_{21}H_{23}NO_5$	369.16	352.12, 205.11, 165.09, 190.09	Protopine	+	+	+
Noscapine	$C_{22}H_{23}NO_7$	413.15	220.10, 353.10, 365.10, 179.07	Phthalide isoquinoline	+	-	+
Codeinone	$C_{18}H_{19}NO_3$	297.14	283.12, 282.11, 254.12, 266.12	Morphinan	+	-	-
Morphine N-oxide	$C_{17}H_{19}NO_4$	301.13	284.13, 241.09	Morphinan	-	-	+
Flavinantine	$C_{19}H_{21}NO_4$	327.15	178.09, 163.06	Morphinandienone	-	-	+
8,14-Dihydroflavinantine (or salutaridinol)	$C_{19}H_{23}NO_4$	329.16	285.11, 123.04, 58.07, 143.05	Morphinan	+	+	+
(S)-cis-N-Methylstylopine	$C_{20}H_{20}NO_4$	338.14	191.09, 190.09, 149.06	Protoberberine	+	+	-
Isocorydine	$C_{20}H_{23}NO_4$	341.16	297.11, 265.09, 237.09	Aporphine	+	+	+
Pseudoprotopine	$C_{20}H_{19}NO_5$	353.13	188.07, 189.08, 149.06	Protopine	+	+	-
Amurensinine N-oxide A (or amurensinine N-oxide B)	$C_{20}H_{21}NO_5$	355.14	190.06, 191.09, 277.09, 151.08	Isopavine	+	+	+
Rheagenine (or isorheagenine)	$C_{20}H_{19}NO_6$	369.12	352.12, 340.13, 324.12	Rhoeadine	+	+	-
Rhoeadine (or isorhoeadine)	$C_{21}H_{21}NO_6$	383.14	321.08, 303.06, 291.07, 366.13	Rhoeadine	+	+	-
Glaucamine (or isoglaucamine)	$C_{21}H_{23}NO_6$	385.15	368.15, 338.10	Rhoeadine	+	+	-
Coptisine	$C_{19}H_{14}NO_4$	320.09	292.10, 277.07, 290.08, 318.08, 262.09	Protoberberine	+	+	+

PR: *Papaver rhoeas*; PS: *Papaver somniferum*; THPB: tetrahydroprotoberberine; RS: Russia; SK: South Korea; *univocally identified through comparison with standards.

Rhoeadine is another group of alkaloids which is very common and widespread in the genus *Papaver* and contains at least 25 types. Particularly, alpinigenine, alpinine, and epialpinine were isolated from the *Papaver alpinum* L., whereas epiglaudine was isolated from the *P. glaucum*. Other rhoeadine-type alkaloids include glaucamine, glaudine, isorhoeadine, isorhoeagenine, isorhoeagenine-D-glucoside, *N*-methylporphyroxigenine, oreodine, oreogenine, papaverrubines A, B, C, D, E, F, G, H, rhoeadine, and rhoeagenine which are extracted from different species of *Papaver*. In general, all rhoeadines are characterized by a benzazepine system fused with six-membered acetal or hemiacetal moieties [69].

4.2. Phenolic Compounds.

Phenolic compounds are natural antioxidants and other interesting phytochemicals found in *Papaver* plants. For example, petals of *P. rhoeas* flowers present flavonoids, which are responsible for their color, including white, yellow orange, white, and red colors. Particularly, the red flowers of this species contain anthocyanins [70]. This agreed with the results obtained by Soulimani et al. [71], who showed that a lyophilized ethanolic aqueous extract of *P. rhoeas* petals has anthocyanins, whereas no alkaloids were detected. Anthocyanins such as pelargonidin glycosides have been detected in red and orange petals of the plant [72].

In *P. nudicaule* cultivars, the flavonoid-derived indole alkaloids, nudicaulins, along with pelargonidin glycosides (anthocyanin), and kaempferol and gossypetin glycosides (flavonols) have been reported in the apical petals (Figure 3) [73, 74]. Other flavonoids such as gossypetin glycosides are present in the basal spot of all cultivars whereas carotenoids are present in yellow-colored stamens [73]. Another study found nudicaulins, gossypetin 7-*O*-glucoside (gossypitrin), and seven kaempferol glycosides in yellow petals of this plant [75]. Moreover, *Papaver alpinum* L. also accommodates some of these compounds [74].

Among the solvents, water, ethanol, and aqueous ethanol can be applied to extract high amounts of phenolics, but among them, the water extract showed the highest phenolic content. It was found that the aqueous extract of *P. somniferum* stalk contains high amount of phenolics, including flavonoids. The methanol and aqueous extracts presented considerable amounts of the flavanol (−)-epicatechin and the benzoic acid syringic acid [76]. Moreover, the aerial parts of *P. macrostomum* had the flavone luteolin (Figure 3) [67].

4.3. Essential Oils and Other Components.

Dilek et al. [77] evaluated the essential oil composition of *P. somniferum* flowers after extraction by the hydrodistillation method. It mainly included *n*-nonadecane (9.0%), heneicosane (10.8%), *n*-pentacosane (7.9%), palmitic acid (7.3%), and 1-nonadecanol (16.3%) [77] (Figure 3). In another work, Krist et al. [78] identified the main volatile compounds in *P. somniferum* seed oil samples were 1-pentanol (3.3–4.9%), 1-hexanal (10.9–30.9%), 1-hexanol (5.3–33.7%), 2-pentylfuran (7.2–10.0%), and caproic acid (2.9–11.5%). It seems that the plant part could determine the composition of the volatile constituents, but little work has been done to investigate it.

The essential oil of the aerial parts of *P. rhoeas* that was gathered from the Elazig region in Turkey was obtained by hydrodistillation and analyzed using gas chromatography. Twenty-one constituents comprised the 98.6% of the total essential oil volatiles extracted from the plant. The major ones were phytol (52.8%), tricosane (7.8%), 2-pentadecanone (6%), and heneicosane (5.3%) (Figure 3); some of them are in common with *P. somniferum* [79]. Among them, the diterpene phytol is another interesting bioactive compound [80].

Moreover, the triglyceride composition of *P. somniferum* seed oil has been analyzed by matrix-assisted laser desorption/ionization-time-of-flight-MS and electrospray ionization ion trap-MS/MS. It enables the determination of the major triglyceride components, which were composed of linoleic, oleic, and palmitic acid, comprising approximately 70% of the oil [78]. The presence of high amount of unsaturated fatty acids makes the poppy seed oil suitable for its application in foods for maintaining the cardiovascular health.

4.4. Phytochemical Variation.

The type of phytochemical and its content mainly depend on the part used and solvent applied for the extraction, as it was discussed in the previous sections. Also, intraspecific variation occurs [51, 59], for example, due to different locations [59], growth stage, and conditions [181]. This is extremely important for standardization or to choose those plants with strong enough potency to be applied to obtain functional ingredients.

For example, in a relevant study, empty poppy capsules (poppy straw) of 15 cultivars of *P. somniferum* were studied for the phytochemical profile. The seeds were raised in randomised block design with 3 replications during three consecutive years in 2007, 2008, and 2009. The extracts from the poppy straw were prepared using 5% acetic acid under sonication and then analyzed using liquid chromatography-MS. The overall results showed that the ratio of the alkaloids, morphine, codeine, narcotine, papaverine, and thebaine was highly variable in the selected 15 poppy cultivars, more than the difference found between the years [81].

5. Biological Activities of the *Papaver* Genus

Papaver forms part of the traditional system of medicines that plays an important role in providing health care to large section of the world population. Therefore, in this section, we discuss the updated snapshot of the bioactivities and therapeutic applications of *Papaver* genus, some of them related to its traditional use (Table 1).

5.1. Analgesic Activities.

Few studies have already recognized that the treatment addressed to the immune system modulates the analgesic effect of the opiates isolated from poppy plant. It seems that during illness, the inhibition of morphine analgesia is due not only to the offsetting of analgesia by enhanced pain sensitivity but the action of endogenous antianalgesic mechanisms can be implied. The role of *N*-methyl-D-aspartate and central opioid receptors was established by Johnston

Phenolic compounds

Anthocyanin

(pelargonidin)

Benzoic acid

(syringic acid)

Flavanol

((-)-epicatechin)
((-)-epicatechin)

Flavone

(luteolin)

Flavonol

(kaempferol, R1=R2=H)
(gossypetin, R1=R2=OH)

Nudicaulin

(nudicaulin I, 3S,11S)
(nudicaulin II, 3R,11R)

Volatile compounds

Hydrocarbon

(n-nonadecane)

(n-heicosane)

(tricosane)

(n-pentacosane)

Fatty acid

(palmitic acid)

Alcohol

(1-nonadecanol)

Diterpenic alcohol

(phytol)

Ketone

(2-pentadecanone)

Figure 3: Phenolic compounds structures and main volatile compounds identified in *Papaver* plants.

and Westbrook [82], as well as the glial activation in the spinal cord. Other *Papaver* species have revealed some analgesia properties. Ibrar and group [83] reported the analgesic activity of the *Papaver pavoninum* C.A. Mey. extract. The study

was completed on a mouse model, and the results demonstrated that plant extract significantly reduced pain in mice at all the three doses (50, 100, and 150 mg/kg body weight), as indicated by reduction in number of writhes as 36.91,

57.01, and 68.39%, respectively. The reduction in pain was dose dependent; hence, the 150 mg/kg dose proved to be most effective than the standard analgesic drug. Similarly, the ethanolic extract from the aerial parts of *Papaver libanoticum* Boiss., an endemic plant to Lebanon, exhibited a potent dose-dependent analgesic activity, which involved activation of opioid receptors in the central nervous system. This activity could be attributed due to the presence of alkaloids, different to morphine or its derivatives, and phenolic compounds [178].

Alternatively, besides to have mild opioid activity [178], Shams et al. [84] tested the effect of the administration of a hydroalcoholic extract from *P. rhoeas* to mice to evaluate the analgesic tolerance induced by morphine (1–10 mg/kg) using the tail-flick method. The results indicated that the extract of *P. rhoeas* showed no effects on analgesia at 25–100 mg/kg. However, treated animals with different doses of the extract (25–100 mg/kg) before the administration of morphine were effective to decrease the analgesic tolerance promoted by morphine.

5.2. Cytotoxicity Studies and Anticancer Activity. Several studies have shown that *Papaver* genus, including *P. somniferum*, *P. rhoeas*, *Papaver lacerum* Popov, and *P. nudicaule*, can provide anticancer compounds, but most studies were performed *in vitro* or in silico ([85, 86]; [179]; [87–89]), as shown in Table 3. Their efficacy depends again on the part and solvent used [88]. Moreover, among the studied compounds, alkaloids have shown anticancer properties [86, 87]. Nonetheless, the most active alkaloids were berberine and macranthine; importantly, they demonstrated low toxicity against the Vero cell line, a noncancerous model. *P. somniferum*-based nanoparticles (PbO and Fe_2O_3) have shown cytotoxicity in HepG2 cell lines in order to treat hepatic carcinoma [87]. PbO-based nanoparticles demonstrated higher cytotoxicity (~79% inhibition) owing to more penetration due to its smaller size as compared to Fe_2O_3 nanoparticles (61% inhibition).

In another work, the chemical extracts from the petals of *P. rhoeas* have recently been tested for potential in the prevention of skin cancer. Sublethal UVB-mediated lesions at both DNA and RNA levels in human keratinocytes were observed, and thus, derived sunscreen based on the extracts of *Papaver* petals could be promising [90]. As commented before, petals can have phenolic compounds, other potential active compounds.

The lethality to brine shrimp can be applied as prescreen to existing cytotoxicity and antitumor assays [91]. In this context, other studies have tested *Papaver* extracts in brine shrimp eggs [91, 92]. It was established that the most active extract was obtained from *P. pavoninum* whole plant extracted with ethanol (lethal concentration 50% or LC_{50} = 2.54 μg/mL) compared to *P. rhoeas* seed extracts obtained with dichloromethane (LC_{50} = 24 μg/mL) and methanol (LC_{50} = 26 μg/mL) [83, 92]. Since the latter LC_{50} values were lower than 30 μg/mL, these extracts displayed significant cytotoxicity, according to Khalighi-Sigaroodi et al. [91], who tested extracts from other 23 plant species of the Leguminosae family.

Concerning *in vivo* studies, cytotoxicity has been mainly focused on concrete alkaloids and also the mechanisms of action studied in cancerous cell lines. Besides the aforementioned studies, the nonnarcotic alkaloids noscapine and papaverine have been found as potent anticancer agents against different human cancers such as breast, liver, bone, prostate, colorectal, and fibrosarcoma by inhibiting the cell proliferation, inducing apoptotic cell death, and causing cell cycle arrest [93].

Noscapine has been found to suppress the cell proliferation, migration, and invasion as well as also induce apoptosis. The supplementation of noscapine at the rate of 320 μM concentration to human skin cancer cell line (A-431) induced 80% cell death and induced the structural change in human serum albumin protein [94, 95]. Noscapine also presents strong anticancer potential against human epithelial ovarian and prostate cancers via inducing apoptosis in a receptor-dependent but radical oxygen species- (ROS-) independent manner [96]. Noscapine has anticancer activity against two LNCaP and PC-3 human prostate cancer cell lines, but it was combined with paclitaxel. This combination produced significantly lowering the mRNA expression of B-cell CLL/lymphoma (Bcl-2) and increasing the mRNA expression of Bcl-2-associated X protein (Bax), and Bax/Bcl-2 ratio, among other effects [97]. In this regard, the apoptosis of cancerous cells is regulated by the members of the Bcl-2 family (Bax, Bcl-2). Bcl-2 factors inhibit the apoptosis whereas Bax factors promote it; hence, the ratio of both the factors decides the fate of cancerous cells. Noscapine also improved its therapeutic anticancer potential in colon cancer SW480 cells through inducing apoptotic cell death by blocking the liver-intestine cadherin (CDH17) gene. It also shows a significant effect on the levels of proteins related to apoptosis (Cyt-c, Bax, Bcl-2, and Bcl-xL) [98]. In human SW480 colon cancer cells, noscapine markedly decreased the colony-forming ratio and cell viability, up-regulated the expression levels of cleaved-poly (ADP-ribose) polymerase and cleaved-caspase-3, inhibited cell proliferation, and promoted cell apoptosis [99]. Alternatively, another study proved that noscapine has been found effectively to inhibit proliferation and invasion of MG63 cell line by suppressing the phosphorylation of epidermal growth factor receptor (EGFR) gene and its downstream pathway [100].

There are also numerous studies on the anticancer effects of papaverine in cells. For example, papaverine exhibited anticancer activity on human glioblastoma (GBM) temozolomide (TMZ; as a first-line anticancer medicine)-sensitive U87MG and TMZ-resistant T98G cells via preventing tumor cell growth, suppressed cell migration, and significantly inhibited the cell proliferation. It was also reported that papaverine has a dose-dependent cytotoxic effect on human prostate cancer cells (PC-3) through inducing early and late apoptosis along with inducing sub-G1 cell cycle arrest, lowering the expression levels of Bcl-2 proteins, increasing the Bax protein levels, reducing the NF-κB levels, and downregulating the PI3K and phospho-Akt expression [101, 102]. This observation is in line with Antonarakis et al. [103] who also reported other mechanisms such as an enhancement in the expression levels of Bax protein, the release of

TABLE 3: Cytotoxicity of the *Papaver* genus.

Species/extract name	Design/model	Key effects	Countries	References
P. somniferum L. Lead and iron oxide nanoparticles	*In vitro* study HepG2 cell lines	(i) PbO NPs showed higher cytotoxicity (20.9%) as compared to Fe_2O_3 NPs (38.5%) (ii) The cytotoxicity of whole plant extract (57.6%) was lower than both NPs	Pakistan	[102]
P. Lacerum Popov	*In vitro* study HeLa cell line *In silico* study	(i) Two compounds, namely, tyrosol-1-O-β-xylopyranosyl-(1→6)-O-β-glucopyranoside) (I) and 5-O-(6-O-α-rhamnopyronosyl-β-glucopyronosyl) mevalonic acid (II), were isolated from this species (ii) Both compounds exhibited modest cytotoxic effect, $IC_{50} = 66.4\,\mu M$ and $54\,\mu M$, respectively (iii) *In silico* study showed that protein-tyrosine kinase Syk and aldo-keto reductase family-1 were the targets, respectively	Turkey	[85]
P. nudicaule L. (nudicaulin and derivatives) Methanol–water	*In vitro* study HeLa, HUVEC and K-562 cell lines	(i) Synthetic nudicaulin derivatives 6–11 showed high antiproliferative activity against HUVEC and K-562 cells (ii) Derivative compounds showed significant cytotoxic activity against HeLa cells	Germany	[86]
P. rhoeas L. Ethanol extract	*In vitro* study HCT116, MCF7, HaCaT, and NCM460 cell lines	(i) The compounds stylopine, canadine, sinactine, berberine, and epiberberine and the raw extract showed a dose-dependent inhibitory effect. The highest activity was found for compound berberine against all cell lines (HCT116: $IC_{50} = 90\,\mu M$; MCF7: $IC_{50} = 15\,\mu M$; HaCaT: $IC_{50} = 50\,\mu M$; NCM460: $IC_{50} \geq 200\,\mu M$)	Lebanon	[179]
Papaver alkaloids (amurine, armepavine, berberine, isocorydine, isothebaine, macranthine, mecambrine, mecambridine, narkotine, orientalidine, oripavine, salutaridine, and thebaine)	*In vitro* study HeLa, and Vero cell lines	(i) Berberine and macranthine were the most active alkaloids in all 13 compounds (ii) Dose-dependent studies were applied and revealed IC_{50} values of $12.08\,\mu g/mL$ (HeLa) and $71.14\,\mu g/mL$ (Vero) for berberine, and $24.16\,\mu g/mL$ (HeLa) and IC_{50} of $>300\,\mu g/mL$ (Vero) for macranthine	Turkey	[87]
P. somniferum L. Hexane, methanol, and ethyl acetate	*In vitro* study HT29, HeLa, C6 cells, and Vero cell lines	(i) The inhibitory effects of the leaf, root, stem, and capsule extracts were shown on cancer cell lines (ii) The extracts were able to destroy cellular membrane in tumor cell lines at high concentrations (iii) Stem ethyl acetate extract exhibited strong anticancer activity on all cell lines, with IC_{50} values ranged from 119 to $391\,\mu g/mL$), depending on the plant part and solvent	Turkey	[88]
P. rhoeas L. Methanol extract	*In vitro* study TK6 cell lines	(i) The highest inhibition of cell growth was observed at the concentrations of 5 mg/mL and 25 mg/mL after the treatment with plant extract	Slovakia	[89]
P. pavoninum Fisch & Mey. Ethanol extract	*In vitro* study Brine shrimp eggs	(i) The plant extract was found to produce outstanding dose-dependent cytotoxicity in terms of $LC_{50} = 2.54\,\mu g/mL$ (ii) The dose concentration of 100 and $1000\,\mu g/mL$ produced high cytotoxicity as 83.3% and 96.7% lethality, respectively	Pakistan	[83]

TABLE 3: Continued.

Species/extract name	Design/model	Key effects	Countries	References
P. rhoeas L. n-Hexane, dichloromethane, and methanol	In vitro study Brine shrimp eggs	(i) Dichloromethane and methanol extracts showed significant toxicity activity in brine shrimp lethality assay in terms of LC_{50} 24 and 26 μg/mL, respectively	United Kingdom	[92]

IC_{50}: 50% inhibitory concentration; LC_{50}: lethal concentration 50%; NPs: nanoparticles.

cytochrome C into the cytoplasm, reduction in the expression levels of X-linked inhibitor of apoptosis protein, and induction of apoptosis. Papaverine was also found effective against hepatic carcinoma by inhibiting the telomerase through downregulation of telomerase reverse transcriptase in humans in HepG-2 cells [104]. Likewise, noscapine and papaverine have an anticancer effect on human MCF-7 and MDA-MB-231 cell lines via enhancing apoptosis, causing cell cycle at G2/M phase, and arresting cell cycle at G_0/G_1 phase [105].

Moreover, papaverine in combination with low-frequency ultrasound improved the blood-brain barrier, which is involved in the maintenance of brain homeostasis and compromised in brain tumors [106, 107]. This combination was able to reduce the expression levels of zonula occluden-1, occludin, and claudin-5, enhancing the permeability of blood-tumor barrier. This can be a strategy for selective crossing this barrier by chemotherapeutic drugs [107]. Another in vivo study showed that papaverine also markedly delayed the tumor growth in a U87MG xenograft mouse model [108, 109].

Besides the latter compounds, sanguinarine is another promising anticancer compound effective against a variety of multidrug-resistant cancers and combined with chemotherapeutic agents to synergistically enhance their sensitivity [110]. Also, berberine has shown anticancer potential in cells ([87]; [179], among others, as Table 3 shows.

5.3. Antimicrobial Activity and Antiviral Activities. The antimicrobial activity of several extracts from Papaver plants is shown in Table 4. Among these studies, P. somniferum seed extracts, containing alkaloids and phenolic compounds, among other components, have shown the highest antimicrobial activity for the methanol extract against Staphylococcus aureus and Aspergillus species [111], whereas the aqueous and ethanolic extracts against root rot fungi at 5% [112]. In another work, AMA of P. somniferum in nanosystem was evaluated when it was used for the green synthesis of nanoparticles based on lead oxide (PbO) and iron oxide (Fe_2O_3). Both the nanoparticles resulted in effective antimicrobial activity against all the pathogenic microbial strains (Bacillus subtilis, Staphylococcus epidermidis, Klebsiella pneumoniae, Pseudomonas aeruginosa, Fusarium solani, Aspergillus flavus, Aspergillus fumigates, and Aspergillus niger) in a dose-dependent manner (4 to 10 mg/mL concentration) [102]. However, Papaver-based fabrication of PbO nanoparticles resulted in higher antibacterial property due to its small size than Fe_2O_3-based nanoparticles.

In a comparison study performed by Ünsal and coworkers [113], the antimicrobial extracts obtained with various solvents from the aerial parts of P. argemone, P. dubium, P. rhoeas, and Papaver clavatum Boiss. & Haussskn. ex Boiss. were recently investigated. Among the solvent tested, P. dubium extracted by petroleum ether and diethyl ether showed a higher effectiveness against S. aureus, with a minimum inhibitory concentration (MIC) of 9.76 and 19.52 μg/mL, respectively, compared to chloroform, ethanol, and acetone. Even, lower values have been reported for the tertiary alkaloids obtained from the aerial parts of P. rhoeas when it was tested against six bacterial species (S. aureus, S. epidermidis, Escherichia coli, K. pneumoniae, P. aeruginosa, and Proteus mirabilis), and three Candida strains (C. albicans, C. parapsilosis, and C. tropicalis) were studied using a microbroth dilution method. In this study, the plant samples were collected from 11 different sites, obtaining the best antimicrobial activity against S. aureus and C. albicans with an MIC value of 1.22 and 2.42 μg/mL in the site with the higher content of roemerine alkaloid [64]. Additionally, Table 4 displays the antimicrobial activity of other Papaver species. Among them, the results of Papaver pseudocanescens M. Pop extracts as an antiviral agent seem promising [114].

In a similar way, the antiviral activities of active compounds of P. rhoeas pollen against influenza H1N1, H3N2, and H5N1 viruses have been evidenced. Total, six flavonoids, including kaempferol derivatives and luteolin, and one alkaloid, chelianthifoline, were isolated and revealed neuraminidase inhibitory activities, reducing the ability of the virus to spread. The concentration required for 50% inhibition (IC_{50}) ranged from 10.7 to 100.5 μM for H1N1, 25.6 to 143.2 μM for H3N2, and 12.6 to 151.1 μM for H5N1. Among all tested compounds, luteolin was found to be the most active [115]. The antimicrobial activity of nudicaulin derivatives (synthesized in vitro and in vivo in P. nudicaule) has also been evaluated, but only one derivative (17-methyl-5,7,11,3′,4′-penta-O-methylnudicaulin) was slightly active [86].

5.4. Antioxidant Activity. The in vitro antioxidant activity of P. somniferum has been reported by using different methods, including the 2,2-diphenyl-1-picrylhydrazyl (DPPH), 2′-azinobis-(3-ethylbenzothiazoline-6-sulfonate) (ABTS), and chelating assays [119] (Table 5). Zhang and coworkers from China described the antioxidant activity of the powdered poppy capsule extractive by using DPPH assay and its relationship with quantitative fingerprinting. Morphine and codeine were among the components that have a positive influence in this bioactivity [120]. This agreed with the results obtained by other authors [121]. Moreover, a recent study evaluating different parts of the plant suggests that

TABLE 4: Antimicrobial activity of *Papaver* plants.

Species/extract name	Microbial strains	Key results	Assay	Country	References
P. somniferum L. Hexane, methanol, ethanol, and ethyl acetate extract	*Bacillus cereus* MTCC 430	0.14 mm ZOI	Disc-diffusion	India	[111]
	Staphylococcus aureus MTCC 3160	2.00 mm ZOI			
	Escherichia coli MTCC 40	0.10 mm ZOI			
	Salmonella typhi MTCC 3224	0.13 mm ZOI			
	Aspergillus niger MTCC 281	3.00 mm ZOI			
	Aspergillus oryzae MTCC 624	3.00 mm ZOI			
	Aspergillus flavus MTCC 227	1.50 mm ZOI			
	Penicillium chrysogenum MTCC 6795	2.00 mm ZOI			
P. pseudocanescens M. Pop Ethanol extract	Poliovirus type 1 (LSc-2ab)	21.4-49.7 μM IC$_{50}$	—	Bulgaria	[114]
	Human rhinovirus type 14 (HRV-14)	65-199 μM IC$_{50}$			
P. rhoeas L. Methanol, ethanol, water, and alcoholic-water extract	*Bacillus subtilis* ATCC 6633	—	Disc-diffusion	Serbia	[70]
	Staphylococcus aureus ATCC 6538	12-18 mm ZOI			
	Escherichia coli ATCC 8739	17-24 mm ZOI			
	Pseudomonas aeruginosa ATCC 9027	11-20 mm ZOI			
	Salmonella abony NCTC 6017	—			
	Aspergillus niger ATCC 16404	13-26 mm ZOI			
	Candida albicans ATCC 10231	—			
P. somniferum L. bee pollen Ethanol extract	*Penicillium citrininum*	4-5 mm ZOI	Disc-diffusion	Slovak	[116]
	Penicillium crustosum	4-9 mm ZOI			
	Penicillium expansum	1-4 mm ZOI			
	Penicillium brevicompactum	1-3 mm ZOI			
	Penicillium chrysogenium	—			
	Enterobacteriaceae	6-7 mm ZOI			
	Staphylococcus sp.	5-6 mm ZOI			
P. argemone L. subsp. davisii Petroleum ether, diethyl ether, chloroform, acetone, and ethanol extract	*Staphylococcus aureus* ATCC 65538	39-625 (μg/mL) MIC	Microbroth dilutions	Turkey	[113]
	Staphylococcus epidermidis ATCC 12228	312-1250 (μg/mL) MIC			
	Escherichia coli ATCC 25922	1250 (μg/mL) MIC			
	Klebsiella pneumonia ATCC 4352	1250 (μg/mL) MIC			
	Pseudomonas aeruginosa ATCC 27853	625-1250 (μg/mL) MIC			
	Proteus mirabilis ATCC 14153	1250 (μg/mL) MIC			
	Candida albicans ATCC 10231	312-625 (μg/mL) MIC			
P. clavatum Boiss. & Hausskn. ex Boiss Petroleum ether, diethyl ether, chloroform, acetone and ethanol extract	*Staphylococcus aureus* ATCC 65538	78-156 (μg/mL) MIC	Microbroth dilutions	Turkey	[113]
	Staphylococcus epidermidis ATCC 12228	312-625 (μg/mL) MIC			
	Escherichia coli ATCC 25922	312-625 (μg/mL) MIC			
	Klebsiella pneumonia ATCC 4352	—			
	Pseudomonas aeruginosa ATCC 27853	—			
	Proteus mirabilis ATCC 14153	625 (μg/mL) MIC			
	Candida albicans ATCC 10231	625 (μg/mL) MIC			

TABLE 4: Continued.

Species/extract name	Microbial strains	Key results	Assay	Country	References
P. dubium subsp. lecoqii var. lecoqii Petroleum ether, diethyl ether, chloroform, acetone, and ethanol extract	*Staphylococcus aureus* ATCC 65538	9-1250 (μg/mL) MIC	Microbroth dilutions	Turkey	[113]
	Staphylococcus epidermidis ATCC 12228	312-625 (μg/mL) MIC			
	Escherichia coli ATCC 25922	1250 (μg/mL) MIC			
	Klebsiella pneumonia ATCC 4352	625-1250 (μg/mL) MIC			
	Pseudomonas aeruginosa ATCC 27853	625-1250 (μg/mL) MIC			
	Proteus mirabilis ATCC 14153	625-1250 (μg/mL) MIC			
	Candida albicans ATCC 10231	625 (μg/mL) MIC			
P. rhoeas L. Petroleum ether, diethyl ether, chloroform, acetone and ethanol extract	Staphylococcus aureus ATCC 65538	39-156 (μg/mL) MIC	Microbroth dilutions	Turkey	[113]
	Staphylococcus epidermidis ATCC 12228	156-625 (μg/mL) MIC			
	Escherichia coli ATCC 25922	625-1250 (μg/mL) MIC			
	Klebsiella pneumonia ATCC 4352	—			
	Pseudomonas aeruginosa ATCC 27853	—			
	Proteus mirabilis ATCC 14153	625 (μg/mL) MIC			
	Candida albicans ATCC 10231	625 (μg/mL) MIC			
P. somniferum L. Aqueous and ethanol extract	*Fusarium solani*	13-20 mm ZOI	Paper disc	Pakistan	[112]
	Rhizoctonia solani	15-24 mm ZOI			
	Macrophomina phaseolina	15-22 mm ZOI			
	Fusarium solani	18-25 mm ZOI	Well method		
	Rhizoctonia solani	15-24 mm ZOI			
	Macrophomina phaseolina	21-29 mm ZOI			
P. macrostomum Boiss. & A.Huet Petroleum ether, diethyl ether, chloroform, acetone, and ethanol extract	*Staphylococcus aureus* ATCC 6538	1-14 mm ZOI	Disc-diffusion	Turkey	[67]
	Staphylococcus epidermidis ATCC 12228	5-32 mm ZOI			
	Escherichia coli ATCC 11229	1-7 mm ZOI			
	Pseudomonas aeruginosa ATCC 1539	2-9 mm ZOI			
	Proteus mirabilis ATCC 14153	1-16 mm ZOI			
	Klebsiella pneumoniae ATCC 4352	1-6 mm ZOI			
	Candida albicans ATCC 10231	3-6 mm ZOI			
	Candida glabrata ATCC 90030	5 mm ZOI			
	Candida guilliermondii KUEN 998	6 mm ZOI			
	Candida tropicalis KUEN 1021	2-4 mm ZOI			
	Candida pseudotropicalis KUEN 1012	5 mm ZOI			
	Candida krusei ATCC 6258	1-4 mm ZOI			
P. decaisnei Hochst. & Steud. ex Elkan Methanol extract	*Bacillus subtilis* ATCC 6633	Non-significant	Microbroth dilutions	Iran	[117]
	Candida albicans ATCC 10231	-			
	Escherichia coli ATCC 10536	Non-significant			
	Klebsiella pneumoniae ATCC 10031	-			
	Morganella morganii PTCC 1078	-			
	Pseudomonas aeruginosa ATCC 4027	Non-significant			
	Salmonella typhi PTCC 1185	-			
	Staphylococcus aureus ATCC 29737	-			
P. rhoeas L. Ethyl alcohol extract	*Bacillus subtilis* ATCC 6633	+	Microbroth dilutions	India	[118]
	Escherichia coli ATCC 10536	+			
	Saccharomyces cerevisiae ATCC 9763	+			

IC$_{50}$: inhibitory concentration at 50%; MIC: minimum inhibitory concentration; ZOI: zone of inhibition; -: not active; +: active.

the flower extract (rich in anthocyanins) and leaves showed the highest antioxidant activity depending on the antioxidant assay. Although it correlated with the phenolic content, the alkaloid extract showed the highest antioxidant values, with inhibitory concentration (IC$_{50}$) of 7.4 and 8.1 μg/mL in the DPPH and ABTS radical scavenging activity assays [122]. In another context, the antioxidant activity of PbO and Fe$_2$O$_3$ nanoparticles synthesized using *P. somniferum*

was evaluated. Using free radical scavenging assay (FRS), total reducing power assay (TRP), and total antioxidant capacity assay (TAC), it was observed that both the nanoparticles of *P. somniferum* exhibited concentration-dependent activity. PbO nanoparticles revealed the significant antioxidant activity in terms of FRS (54%), TRP (16.8 mg ascorbic acid equivalents/mg), and TAC (106.1 mg ascorbic acid equivalents/mg) while Fe_2O_3 nanoparticles showed 52% FRS activity, 16.8 mg ascorbic acid equivalents/mg TRP, and 131.1 ascorbic acid equivalents/mg TAC, respectively [102].

The antioxidant activity *in vivo* of *P. somniferum* has been also evaluated through the seed oil administered to rats, observing limited oxidative damage [123]. Concerning other species, the antioxidant activity of *P. rhoeas* has also been reported by three methods: DPPH, ABTS, and ferric reducing antioxidant power (FRAP) assays. The results clearly indicated that leaf extract demonstrated significant antioxidant activity with a half-maximal effective concentration (EC_{50}) 28.72 mg/100 g dry weight in DPPH, 185.29 mM Fe^{2+}/100 g DW in FRAP, and 12.07 mM Trolox equivalents (TE)/100 g dry weight in ABTS [124]. The water extract of this plant has also been evaluated for antioxidant potential using DPPH and superoxide anions assays. The IC_{50} value of *P. rhoeas* was 4.81 mg/mL for DPPH assay, and it was the highest antioxidant activity in the anti-ROS assay [125]. Moreover, the hydrophilic and lipophilic antioxidant activity of *P. rhoeas* was studied by using the TEAC assay. The leaves of wild *P. rhoeas* displayed the highest total antioxidant activity (1326 μmol TE/100 g fresh weight) among other assessed plant species, which correlated with their total phenolic and flavonoid content [126].

The antioxidant action of *Papaver* plants depends on the genotype as shown by Krošlák and coworkers. Their results suggested that there were differences in the antioxidant activity of *P. somniferum* seeds by using DPPH, ABTS, FRAP, and reducing power (RP) assays. The genotype major displayed the best antioxidant activity in all the assays, namely, DPPH (126.29), ABTS (31.05), FRAP (31.61), and RP (146.56) mg of TE. Alternatively, the genotype MS-423 showed the high inhibition against trypsin, thrombin, and collagenase enzymes [127]. Other important factor is the solvent used for extraction. The results by Selen Isbilir & Sagiroglu [20] indicated that water extract (WE) of *P. rhoeas* was the most effective compared to ethanol (EE), and acetone extracts (AE); total antioxidant activity of all the extracts was recorded to be 96.01% (WE), 94.98% (EE), and 89.07% (AE), respectively. The TRP of extracts was as follows: WE > EE > AE [20]. Other studies on antioxidant potential of *Papaver* genus are presented in Table 5, showing the selected solvent for extraction. Although it is difficult to compare all the solvents due to the use of different assays and units, it seems that the methanolic extract was higher in antioxidant activity compared to other solvents for the aerial parts of *P. bracteatum*.

From the aforementioned studies and Tables 4 and 5, it can be summarized that the bioactivity of the alkaloids derived from the *Papaver* genus depends on the extraction conditions, as the phytochemical composition. Extraction

condition may include the type of the solvent, extraction time, temperature, and other input factors. In addition, *Papaver* alkaloids or phytochemical extracts demonstrated more effective bioactivities in the nanoforms. Smaller nanoparticles penetrate more easily into the bacterial membrane and dissociate into respective ions causing oxidative stress, membrane leakage, and killing bacterial cells with more perfection. The use of well-established alkaloids for the treatment of various ailments in the human body may be utilized as nanoformulation to enhance the efficacy of the drug. There is further need to develop the field of nanotechnology with respect to *Papaver*-based drug formulations. In addition, testing other isolated compounds is required to assess the antimicrobial activity and antioxidant potential and their contribution in order to select most active plant extracts.

5.5. Antidiabetic Activity.

It is well known that α-amylase and α-glucosidase are key enzymes for the catabolism of complex carbohydrates into glucose and thus target to explore antidiabetic drugs. In this sense, the α-glucosidase inhibitory activity of *P. somniferum* seeds (aqueous and ethanol extracts) was also demonstrated. It was found that both the extracts showed less than 5% inhibitory activity [132]. Also, the α-amylase enzyme inhibition activity using *P. somniferum* pod-based PbO and Fe_2O_3 nanoparticles showed insignificant inhibition as 3% and 25%, respectively [102].

Apart from this, large number of researchers documented the antidiabetic potential of this genus in literature through traditional medicine knowledge [133–136]. Most of these studies referred to *P. rhoeas* and particularly to the seeds. For example, boiled seeds capsule of *P. rhoeas* were used by the communities with 22.85% frequency based on the information collected by 35 healers in Iran [37]. Alternatively, the antidiabetic effects of opium were low in experimental diabetic animals at an oral dose of 10 mg/kg body weight for 90 days, as reported by Ahmed and group. Although opium increased serum insulin and decreased serum glucose, the effect was not significant; this was due to metabolic disorders in diabetic animals. In addition, it is suggested that opium consumption in diabetic patient is not useful [137]. Similarly, Sadeghian et al. [138] reported the effects of available opium substance on glucose and lipid metabolism in streptozotocin-induced-diabetic rats by testing opium contained in the juice of the seed capsule of the *P. somnniferum*. The test rats were treated with normal opium (20 mg), starting on the fifth day after induction of diabetes for 30 days. The results demonstrated that glycaemia levels in the rats treated with opium (544.8 mg/dl) were similar to the levels determined in the control rats (524.6 mg/dL). In addition, the level of other parameters was similar: serum, total cholesterol, high-density lipoprotein, and triglyceride. Indeed, more studies are needed to clarify the role of *Papaver*, specifically, *P. rhoeas*, in the antidiabetic action and the active chemical components.

5.6. Properties in Fertility.

The role of *P. rhoeas* extract (dried petals macerated with 50% ethanol) on fertility has also been investigated in mouse oocytes [139]. The cumulus-oocyte complexes were cultured in a maturation

TABLE 5: Antioxidant activity of *Papaver* plants.

Species and type of extract	Assay	Key results	Countries	References
P. rhoeas L. Methanolic extract	DPPH	$IC_{50} = 1.4$ mg/mL	Slovakia	[89]
P. somniferum L. Ethanolic extract	Total reducing power	3592.56 mg/mL	Serbia	[116]
P. rhoeas L. Ethanolic extract	DPPH	81.47–89.71%	Serbia	[70]
P. rhoeas L. Methanolic extract	CUPRAC ABTS/persulfate FRAP	0.13 mmol TR/g 0.15 mmol TR/g 0.07 mmol TR/g	Turkey	[128]
P. somniferum L. Methanolic extract	Linoleic acid peroxidation	49.75 IC_{50} (μg/mL)	Iran	[129]
P. bracteatum Lindl Methanolic extract	Linoleic acid peroxidation	$IC_{50} = 3.51$ μg/mL	Iran	[130]
P. rhoeas L. Aqueous methanol extract	DPPH H_2O_2 Fe^{2+}	$EC_{50} = 63.01$ (μg/mL) 10.57–52.70% 86.85%	Turkey	[131]

ABTS: 2,2′-azino-bis(3-ethylbenzothiazoline-6-sulfonic acid; CUPRAC: cupric reducing antioxidant capacity; DPPH: 2,2-diphenyl-1-picrylhydrazyl; EC_{50}: half-maximal effective concentration; EC_{50}: half-maximal effective concentration; FRAP: ferric-reducing antioxidant power; TR: Trolox.

medium supplemented with different concentrations (low: 10-25 μg/mL; high: 50-200 μg/mL) of *P. rhoeas* extract. Low concentrations of extract showed moderate effects; however, higher concentration (100 μg/mL) significantly improved the rate of oocyte maturation and embryo development in mouse oocyte maturation medium [139]. In another study, similar findings were obtained while working on sheep oocytes [140]. The results demonstrated that plant extract displayed dose-dependent activity in a maturation medium. The concentration of 50 μg/mL was effective and improved the sheep oocyte maturation rate when the extract was supplemented in a maturation medium [140]. Flavonoids, including anthocyanins, have been associated with these effects, which can protect intracellular glutathione levels in oocytes [141].

5.7. Neurological/Mental Effects. Supplementation of *P. rhoeas* hydroalcoholic extract reduced depression and increased the neurotransmitters involved in depression, including dopamine, serotonin, and norepinephrine [142]. Depression is also linked with stress and increases glucocorticoid secretion into the blood. Nonetheless, the administration of a hydroalcoholic extract of *P. rhoeas* (15-60 mg/kg in male mice) enhanced the secretion of glucocorticoids, but it could reduce the side effects of stress [143]. In other work, *P. rhoeas* distillate decreased anorexia and improved learning ability, but it again increased the corticosterone levels [144]. These positive neurological/mental effects agreed with recent results that suggest that *P. rhoeas* hydroalcoholic extract has a reducing effect on depression in mice after short-term administration. In this sense, the antidepressant effect of *P. rhoeas* may not be due to the inhibition of the hypothalamic-pituitary-adrenal stress system, while it could be caused, at least in part, by the inhibition of glutamate or through antiopioid and anticholinergic effects [145].

Furthermore, sedative effects of *P. rhoeas* aqueous and alcoholic extracts have also been observed, being more marked when 10% ethanol was used as solvent for extraction [71].

5.8. Other Bioactivities. The antiulcerogenic activity of *P. rhoeas* root extract was assessed by using the ethanol-induced ulcerogenesis model in rats. The plant extract (670 mg/kg) exhibited statistically significant (95.6%) gastroprotective effects. In addition, histopathological studies confirmed the positive results of the extract *in vivo* [146]. The anti-inflammatory activity of extracts from *P. nudicaule* aerial parts and its mode of action in RAW264.7 macrophage cells have been also tested. Interestingly, in this work, the aerial parts were selected according to different colors (white, orange, yellow, scarlet, and pink) and under two different growth stages (after 60 and 90 days). All of the extracts of *P. nudicaule* displayed significant effects in reducing lipopolysaccharide- (LPS-) induced nitric oxide; the white flower extract-90 showed the best results. This extract also decreased the LPS-induced nitric oxide synthase 2 and cyclooxygenase 2. It inhibited the LPS-induced activation of nuclear factor-κB and signal transducer and the activator of transcription 3 signalling pathway [147]. As commented before, the phenolic composition depends on the color and the white ones have petals rich in kaempferol glycosides, but with a lack of pelargonidin glycosides and nudicaulins [73]. Moreover, *P. rhoeas* extracts prevented pain and inflammation due to their potential activity on opioid, glutamate, and nitric oxide systems, as well as elevated the plasma corticosterone concentration [148]. Furthermore, *P. somniferum* seeds have inhibitory activities against trypsin, thrombin, and collagenase, suggesting more vast pharmacological possibilities [127].

6. Safety and Adverse Effects

An undesired harmful effect resulting from a medication or other intervention such as surgery is known as an adverse effect. It may be termed a "side effect," when considered to be secondary to the therapeutic effect [149]. In contrast, dangerous, unintended reactions of medicines that occur at doses normally used for treatment are called adverse drug reactions (ADRs), even can lead to death in many countries [149]. In the case of morphine alkaloids, the pharmacologic properties of these compounds differ widely and their medicinal applications have some safety and adverse effects [150].

Various wanted and unwanted effects of opium consumption are discussed in the encyclopedia Canon of Medicine by Avicenna (980-1037 AD). Avicenna has mentioned on the mechanism of opioid-related respiratory depression, due to respiratory muscle spasm for respiratory failure. Similarly, it is mentioned in Canon of Medicine that opium can cause abnormal and difficult breathing, which can lead to death. A respiratory suppression side effect was observed with patients suffering from fever associated with tuberculosis due to the use of the topical opioid application on the chest. Constipation and painful bowel obstruction were other adverse effects of opium-based [177]. Avicenna has also mentioned poisoning, sluggishness, sedation, and abdominal contractions. Opium has highly addictive qualities and is reported to cause memory and reasoning dysfunction [177].

Remarkably, modern studies have confirmed the adverse effect of morphine alkaloids described by Avicenna [151–153]. Some of them are related to the binding to μ- and κ-opioid receptors, the accumulation of neuroexcitatory opioid metabolites, etc. One of the side effects of opioid-based pain relievers, including morphine and its derivatives, is severe constipation [154]. Kohberg et al. [155] and Rocker et al. [156] also reported constipation as the most frequent adverse effect. Moreover, other effects of morphine are on the CNS mediated by its high affinity to the μ-opioid receptor, such as nausea, vomiting, sedation, euphoria, miosis, respiratory depression, drowsiness, and obstipation [157]. Additional adverse effects are endocrinopathies and sleep disorders. Furthermore, long-term use of opioid can lead opioid tolerance (increased dose needed for analgesia) and hyperalgesia (paradoxical increase in pain with opioid administration) that involves μ-opioid receptor signalling pathways [158–160]. Wound healing can also be delayed by chronic morphine intake by inhibiting immune cell recruitment followed by wounding [161].

As codeine is a precursor of morphine, they share some pharmacological features with also direct activity at the opioid receptors, but the former has much lower potency. The most frequent side effects of codeine are constipation and nausea, and addition potential. Nevertheless, in some paediatric patients, the genotype predisposing to ultrarapid metabolism of codeine into morphine by the isoenzyme CYP2D6 can occur [157]. Codeine and morphine can be distributed into breast milk with complications for breastfed infants of mothers receiving codeine [162], even a case of severe neonatal toxicity in a breastfed infant has been reported [163]. In the case of noscapine, it is used as a centrally acting antitussive

compound and no toxicological properties have been characterized, but it can present headache and dizziness [157].

Poppy seeds from *P. somniferum* are commercially available in some countries and widely used as ingredients for various kinds of food, especially in Eastern Europe [164]. Poppy seeds for food uses are generally obtained from cultivars bred to accumulate lower amounts of opium alkaloids [56] and normally contain low levels (2-251 μg/g of morphine and 0.4-57 μg/g of codeine) [165]. The opioid concentrations come primarily from the alkaloid residue retained on the seeds [166]. Therefore, although the consumption of poppy seeds in foods is really in small amounts, EFSA set a general safe level of 10 μg per kilogram of body weight based on the morphine content of poppy seeds [157]. In this sense, only a rare case of death has been published consuming between 64 and 587 times the volume of poppy seeds (around 900 g). This extremely high ingest led to death due to complications of a bowel obstruction, but it did not cause lethal opiate toxicity [165].

Alternatively, extracts or infusions concentrated in opium alkaloids from poppy seeds can have adverse effects [56, 165], but there are few reports on this topic [166]. In any case, some authors have attempted the reduction of the content of opium alkaloids in the seeds using different treatments. For example, while the levels of opium alkaloids were not affected by baking or steam application, a high reduction of these compounds can be obtained by water washing or extended thermal treatment [56].

In another context, immunoglobulin E-mediated sensitization to poppy seeds is rare, but if it occurs, the clinical symptoms can be severe, e.g., due to cross-sensitizations events [167, 168].

Concerning other *Papaver* species, some case studies in humans suggest that unconscious ingestion of *P. rhoeas* can cause acute liver toxicity [169] and intoxication with different effects (nausea, restlessness, dyspnoea, contractions unconsciousness, numbness, etc.) [170]. Alternatively, an *in vivo* study performed by Soulimani and coworkers [71] suggests that extracts from *P. rhoeas* petals (without the presence of alkaloids) showed a lethal dose (LD$_{50}$) of 4000 mg/kg and thus very low toxicity. However, sedative effects were observed. A study *in vitro* showed that *P. rhoeas* leaf extract also showed promising antimutagen/anticlastogen activity [171] and thus suggesting low toxicity. Therefore, although *Papaver* extracts can have some beneficial effects, toxicity studies are further required to establish dosage and side effects. Nonetheless, the culinary use of some parts and *Papaver* plants indicates that the safety issues are controversial or the dosage is a prerequisite. This includes *P. somniferum* seeds, with the aforementioned exceptions [56, 165]; the shoots of *P. rhoeas*, the aerial parts of this species, and *Papaver strictum* Boiss. & Balansa are added to salads, minestra, etc. [32, 35, 172]. Additionally, in Turkey, poppy flowers are used as food colorant and for enhancing the flavour of herbal teas [64].

7. Clinical Trials

Besides the aforementioned case reports studies, there are a very limited number of clinical studies reporting the health

beneficial effects of *Papaver* plants, as far as we know. One of them tested the iodized poppy-seed oil as vehicle of the drug epirubicin against hepatocellular carcinoma [173, 174], but the anticancer effects of poppy have not been evidenced in humans. In the ClinicalTrials.gov database, there are two studies based on the administration of California poppy (*Eschscholzia californica Cham.*) (NCT03364101) but only one refers to the *Papaver* genus. In this work, ground poppy seeds were baked into a bran muffin and administered to evaluate the effect on postprandial blood glucose response, vascular, appetite, and sensory parameters (NCT01579656), but the results have still not been posted. Furthermore, a recent study on *P. rhoeas* combined with other herbs in syrup has improved sexual experience of men following consumption of this mixture with no drug-related serious adverse events. Therefore, the authors suggest that this aphrodisiac syrup can be applied alternatively to other chemical sexual drive enhancers with complicated side effects [175].

8. Conclusions and Future Perspectives

Besides the pharmacological interest of *P. somniferum*, the traditional use of different *Papaver* plants is widely established in different cultures and countries. This fact makes this genus attractive as a source of pharmacoactive extracts and compounds (alkaloids, phenolic compounds, and essential oil). These compounds are responsible for the multifaceted biological activities of the *Papaver* genus including anticancer, antioxidant, antimicrobial, and analgesic. The finding from different studies also demonstrated that these useful compounds are present throughout the plant including agro-residue generated from the *Papaver* plants. Nonetheless, pharmacological studies on extracts from these plants should be reinforced with characterization studies to know the active molecules, or if synergism exists that makes more interesting the use of the whole extracts. For that, bioassay-guided fractionation or even chemometrics with MS-based methodologies and HPLC with MS/MS can be applied to identify the overall profile of the *Papaver* plant extracts. This is especially important since the phytochemical composition and content as well as the bioactivity depend on several factors, including the genotype, the growth stage, and even the color of the flower. The phytochemical profile also depends on the method of extraction, input factors used for the extraction, and also on the style of preparation of the sample for analysis. Moreover, little is known about the bioactivity of the essential oil from these plants, even though some authors suggest the presence of phytol. This compound is valuable as a fragrance and exhibits a broad range of bioactivities [80].

Moreover, applications of this genus in nanotechnology seem promising, for example, to synthesize nanoparticles for different pharmacological purposes but further work is required, including more toxicity studies. In this sense, the use of plant extracts is increasing in green synthesis and the type of compounds present on these extracts can modulate the nanoparticle shape (Vijayaraghavan et al., [176]) and probably its functionality. Finally, although some preclinical results are promising, more clinical studies are needed to provide scientific evidence of the traditional use of *Papaver* plants before consumption and to avoid intoxication events. Overall, these studies along with a better known of the active molecules through comprehensive characterization and bioguided fractionation studies should be undertaken in future research.

Abbreviations

EFSA: European Food Safety Authority
IC_{50}: Inhibitory concentration at 50%
EC_{50}: Half-maximal effective concentration
LC_{50}: Lethal concentration 50%
MIC: Minimum inhibitory concentration
MS: Mass spectrometry
ZOI: Zone of inhibition.

Conflicts of Interest

The authors declare that they have no conflicts of interest.

Acknowledgments

References

[1] F. Labanca, J. Ovesnà, and L. Milella, "*Papaver somniferum* L. taxonomy, uses and new insight in poppy alkaloid pathways," *Phytochemistry Reviews*, vol. 17, pp. 853–871, 2018.

[2] J. Zhou, Y. Cui, X. Chen et al., "Complete chloroplast genomes of *Papaver rhoeas* and *Papaver orientale*: molecular structures, comparative analysis, and phylogenetic analysis," *Molecules*, vol. 23, no. 2, p. 437, 2018.

[3] D. J. Mabberley, *Mabberley's Plant-Book*, Cambridge University Press, Cambridge, 3th ed edition, 2008.

[4] S. Golmohammadzadeh, F. Zaefarian, and M. Rezvani, "Priming techniques, germination and seedling emergence in two *Papaver* species (*P. rhoeas* L. and *P. dubium* L., Papaveraceae)," *Brazilian Journal of Botany*, vol. 43, pp. 503–512, 2020.

[5] X. Liu, Y. Tian, C. Yuan, F. Zhang, and G. Yang, "Opium poppy detection using deep learning," *Remote Sensing*, vol. 10, p. 1886, 2018.

[6] United Nations, "Economic and Social Council," 2021, https://undocs.org/pdf?symbol=en/E/CN.7/2021/5.

[7] D. S. Kocabaş, M. Köle, and S. Yağcı, "Development and optimization of hemicellulose extraction bioprocess from poppy (*Papaver somniferum* L.) stalks assisted by instant controlled pressure drop (DIC) pretreatment," *Biocatalysis and Agricultural Biotechnology*, vol. 29, article 101793, 2020.

[8] FAOSTAT, 2021, https://www.fao.org/faostat/es/#data/QC.

[9] M. Hadipour, S. K. Kazemitabar, H. Yaghini, and S. Dayani, "Genetic diversity and species differentiation of medicinal plant Persian poppy (*Papaver bracteatum* L.) using AFLP and ISSR markers," *Ecological Genetics and Genomics*, vol. 16, article 100058, 2020.

[10] J. Torra and J. Recasens, "Demography of corn poppy (*Papaver rhoeas*) in relation to emergence time and crop competition," *Weed Science*, vol. 56, pp. 826–833, 2008.

[11] P. Razaghi and D. Zafari, "Characterization of fungi causing lesion blight on *Papaver dubium* in Iran," *Antonie Van Leeuwenhoek*, vol. 111, pp. 437–455, 2018.

[12] H. W. Lack, "The discovery and naming of Papaver orientale s.l. (Papaveraceae) with notes on its nomenclature and early cultivation," *Candollea*, vol. 74, no. 1, pp. 47–64, 2019.

[13] A. S. Choudhari, P. C. Mandave, M. Deshpande, P. Ranjekar, and O. Prakash, "Phytochemicals in cancer treatment: from preclinical studies to clinical practice," *Frontiers in Pharmacology*, vol. 10, p. 1614, 2020.

[14] T. T. Dang, A. Onoyovwi, S. C. Farrow, and P. J. Facchini, "Biochemical genomics for gene discovery in benzylisoquinoline alkaloid biosynthesis in opium poppy and related species," *Methods in enzymology*, vol. 515, pp. 231–266, 2012.

[15] P. B. Murphy, S. Bechmann, and M. J. Barrett, *Morphine*, StatPearls, 2021.

[16] N. Zare, R. Farjaminezhad, R. Asghari-Zakaria, and M. Farjaminezhad, "Enhanced thebaine production in *Papaver bracteatum* cell suspension culture by combination of elicitation and precursor feeding," *Natural Product Research*, vol. 28, pp. 711–717, 2014.

[17] United Nations, "Office on Drugs and Crime," 2020, https://www.unodc.org/unodc/en/data-and-analysis/bulletin/bulletin_1953-01-01_3_page005.html.

[18] EFSA, "EFSA, Opium alkaloids in poppy seeds:," 2019, https://www.efsa.europa.eu/en/press/news/180516.

[19] M. Singh, N. Chaturvedi, A. K. Shasany, and A. K. Shukla, "Impact of promising genotypes of *Papaver somniferum* L. developed for beneficial uses," *Acta Horticulturae*, vol. 1036, no. 1036, pp. 29–41, 2014.

[20] S. Selen Isbilir and A. Sagiroglu, "An assessment of In Vitro Antioxidant activities of different extracts from *Papaver rhoeas* L. leaves," *International Journal of Food Properties*, vol. 15, no. 6, pp. 1300–1308, 2012.

[21] U. Nyman and J. G. Bruhn, "*Papaver bracteatum*–a summary of current knowledge," *Planta Medica*, vol. 35, no. 2, pp. 97–117, 1979.

[22] J. B. Calixto, M. M. Campos, and A. R. S. Santos, "Botanical analgesic and anti-inflammatory drugs," in *Ethnopharmacology*, vol. II, Eolss Publishers, Oxford UK.

[23] F. Naghibi, S. Esmaeili, M. Malekmohammadi, A. Hassanpour, and M. Mosaddegh, "Ethnobotanical survey of medicinal plants used traditionally in two villages of Hamedan, Iran," *Research Journal of Pharmacognosy*, vol. 1, pp. 7–14, 2014.

[24] A. E. Farouji and H. Khodayari, "Ethnomedicinal plants of Farouj district, north khorasan province, Iran," *Journal of Herbal Drugs (An International Journal on Medicinal Herbs)*, vol. 1, pp. 31–36, 2016.

[25] E. Altundaga and M. Ozturkb, "Ethnomedicinal studies on the plant resources of east Anatolia, Turkey," *Procedia Social and Behavioral Sciences: The 2nd International Geography Symposium GEOMED2010*, vol. 19, 2011, pp. 756–777, East Anatolia; Turkey, 2011.

[26] U. Çakılcıoğlu, M. T. Şengün, and D. Türkoğlu, "An ethnobotanical survey of medicinal plants of Yazıkonak and Yurtbaşı districts of Elazığ province, Turkey," *Journal of Medicinal Plants Research*, vol. 4, pp. 567–572, 2010.

[27] S. Akbulut and M. M. Bayramoglu, "The trade and use of some medical and aromatic herbs in Turkey," *Studies on Ethno-Medicine*, vol. 7, pp. 67–77, 2013.

[28] R. Polat and F. Satıl, "An ethnobotanical survey of medicinal plants in Edremit gulf (Balıkesir–Turkey)," *Journal of Ethnopharmacology*, vol. 139, pp. 626–641, 2012.

[29] I. Ugulu, "Traditional ethnobotanical knowledge about medicinal plants used for external therapies in Alasehir, Turkey," *International Journal of Medicinal and Aromatic Plants*, vol. 1, pp. 101–106, 2011.

[30] M. Yipel, F. A. Yipel, I. O. Tekeli, and Y. Guzel, "Ethnoveterinary uses of medicinal plants in Mediterranean district, Turkey," *Revista de Chimie -Bucharest*, vol. 68, no. 2, pp. 411–416, 2017.

[31] M. R. González-Tejero, M. Casares-Porcel, C. P. Sánchez-Rojas et al., "Medicinal plants in the Mediterranean area: synthesis of the results of the project Rubia," *Journal of Ethnopharmacology*, vol. 116, no. 2, pp. 341–357, 2008.

[32] G. Mattalia, C. L. Quave, and A. Pieroni, "Traditional uses of wild food and medicinal plants among Brigasc, Kyé, and Provençal communities on the Western Italian Alps," *Genetic Resources and Crop Evolution*, vol. 60, pp. 587–603, 2013.

[33] A. Pieroni, "Medicinal plants and food medicines in the folk traditions of the upper Lucca Province, Italy," *Journal of Ethnopharmacology*, vol. 70, pp. 235–273, 2000.

[34] A. Pieroni and C. L. Quave, "Traditional pharmacopoeias and medicines among Albanians and Italians in southern Italy: a comparison," *Journal of Ethnopharmacology*, vol. 101, pp. 258–270, 2005.

[35] A. M. Scherrer, R. Motti, and C. S. Weckerle, "Traditional plant use in the areas of Monte Vesole and Ascea, Cilento National Park (Campania, southern Italy)," *Journal of Ethnopharmacology*, vol. 97, pp. 129–143, 2005.

[36] S. Vitalini, F. Tomè, and G. Fico, "Traditional uses of medicinal plants in Valvestino (Italy)," *Journal of Ethnopharmacology*, vol. 121, no. 1, pp. 106–116, 2009.

[37] M. Bahmani, A. Zargaran, M. Rafieian-Kopaei, and K. Saki, "Ethnobotanical study of medicinal plants used in the management of diabetes mellitus in the Urmia, Northwest Iran," *Asian Pacific Journal of Tropical Medicine*, vol. 7, pp. S348–S354, 2014.

[38] M. Nadaf, M. Joharchi, and M. S. Amari, "Ethnomedicinal uses of plants for the treatment of nervous disorders at the herbal markets of Bojnord, North Khorasan Province, Iran," *Avicenna journal of phytomedicine*, vol. 2, pp. 153–163, 2019.

[39] D. Jadnav, "Ethnomedical plants used by Bhil tribe of Bibdod, Madhya Pradesh," *Indian Journal of Traditional Knowledge*, vol. 5, pp. 263–267, 2006.

[40] P. A. Dar, N. Rashid, and A. Kalam, "Ethnomedicinal practices of Kashmir Valley: a review," *Journal of Pharmacognosy and Phytochemistry*, vol. 7, pp. 278–284, 2018.

[41] M. Goyal, "Use of ethnomedicinal plants for prophylaxis and management of postpartum complications among the Marwari community of Jodhpur District of Rajasthan," *Food Quality and Safety*, vol. 1, pp. 203–210, 2017.

[42] S. K. Tayade and D. A. Patil, "Ethnomedicinal applications of spices and condiments in Nandurbar District (Maharashtra)," *Journal of Ecobiotechnology*, vol. 2, pp. 8–10, 2010.

[43] M. Adnan, I. Ullah, A. Tariq et al., "Ethnomedicine use in the war affected region of northwest Pakistan," *Journal of Ethnobiology and Ethnomedicine*, vol. 10, no. 1, p. 16, 2014.

[44] T. A. Alamgeer, M. Rashid, M. N. Malik, and M. N. Mushtaq, "Ethnomedicinal survey of plants of Valley Alladand Dehri, Tehsil Batkhela, District Malakand, Pakistan," *International Journal of Basic Medical Sciences and Pharmacy*, vol. 3, pp. 2049–4963, 2013.

[45] M. Irfan, M. K. Nabeela, N. A. Khan et al., "Ethnomedicinal and traditional knowledge of phanerogames of Tehsil Munda, district Lower Dir, Khyber Pakhtunkhwa, Pakistan," *International Journal of Biosciences*, vol. 4, pp. 208–218, 2018.

[46] S. Ullah, M. Rashid Khan, N. Ali Shah, S. Afzal Shah, M. Majid, and M. Asad Farooq, "Ethnomedicinal plant use value in the Lakki Marwat District of Pakistan," *Journal of Ethnopharmacology*, vol. 158, p. 412, 2014.

[47] H. Kim and M. J. Song, "Analyss of ethnomedical practices for treating skin diseases in communities on Jeju Island (Korea)," *Indian Journal of Traditional Knowledge*, vol. 13, pp. 673–680, 2014.

[48] B. Salehi, S. Vlaisavljevic, C. O. Adetunji et al., "Plants of the genus Vitis: Phenolic compounds, anticancer properties and clinical relevance," *Trends in Food Science & Technology*, vol. 91, pp. 362–379, 2019.

[49] D. C. Hao, X.-J. Gu, and P. G. Xiao, "6- Phytochemical and biological research of *Papaver* pharmaceutical resources," *Medicinal Plants, Chemisty, Biology and Omics*, pp. 217–251, 2015.

[50] V. Jablonická, J. Ziegler, Z. Vatehová et al., "Inhibition of phospholipases influences the metabolism of wound-induced benzylisoquinoline alkaloids in Papaver somniferum L," *Journal of Plant Physiology*, vol. 223, pp. 1–8, 2018.

[51] S. Choe, S. Kim, C. Lee et al., "Species identification of Papaver by metabolite profiling," *Forensic Science International*, vol. 211, no. 1-3, pp. 51–60, 2011.

[52] O. Bayazeid and F. N. Yalçın, "Biological targets of 92 alkaloids isolated from *Papaver* genus: a perspective based on in silico predictions," *Medicinal Chemistry Research*, vol. 30, pp. 574–585, 2021.

[53] G. Sariyar, "Biodiversity in the alkaloids of Turkish Papaver species," *Pure and Applied Chemistry*, vol. 74, no. 4, pp. 557–574, 2002.

[54] S. Frick, R. Kramell, J. Schmidt, A. J. Fist, and T. M. Kutchan, "Comparative qualitative and quantitative determination of alkaloids in narcotic and condiment Papaver somniferum cultivars," *Journal of Natural Products*, vol. 68, pp. 666–673, 2005.

[55] A. Gümüşçü, N. Arslan, and E. O. Sarihan, "Evaluation of selected poppy (*Papaver somniferum* L.) lines by their morphine and other alkaloids contents," *European Food Research and Technology*, vol. 226, pp. 1213–1220, 2008.

[56] S. A. Shetge, M. P. Dzakovich, J. L. Cooperstone, D. Kleinmeier, and B. W. Redan, "Concentrations of the opium alkaloids morphine, codeine, and thebaine in poppy seeds are reduced after thermal and washing treatments but are not affected when incorporated in a model baked product," *Journal of Agricultural and Food Chemistry*, vol. 68, pp. 5241–5248, 2020.

[57] J. Carolan, I. Hook, J. Walsh, and T. Hodkinson, "Using AFLP markers for species differentiation and assessment of genetic variability of in vitro-cultured *Papaver bracteatum* (section Oxytona)," *In Vitro Cellular & Developmental Biology*, vol. 38, no. 3, pp. 300–307, 2002.

[58] T. Gürkök, E. Kaymak, G. Boztepe, M. Koyuncu, and I. Parmaksiz, "Molecular characterisation of the genus *Papaver* section Oxytona using ISSR markers," *Turkish Journal of Botany*, vol. 37, pp. 644–650, 2013.

[59] A. Qaderi, M. Omidi, A. Pour-Aboughadareh et al., "Molecular diversity and phytochemical variability in the Iranian poppy (_Papaver bracteatum_ Lindl.): A baseline for conservation and utilization in future breeding programmes," *Industrial Crops and Products*, vol. 130, pp. 237–247, 2019.

[60] Y. N. Kalav and G. Sariyar, "Alkaloids from Turkish *Papaver rhoeas*," *Planta Medica*, vol. 55, no. 5, p. 488, 1989.

[61] J.-P. Rey, J. Levesque, J.-L. Pousset, and F. Roblot, "Analytical studies of isorhoeadine and rhoeagenine in petal extracts of *Papaver rhoeas* L. using high-performance liquid chromatography," *Journal of Chromatography A*, vol. 596, pp. 276–280, 1992.

[62] M. Contreras, N. Bribi, A. M. Gómez-Caravaca, J. Gálvez, and A. Segura-Carretero, "Alkaloids Profiling of *Fumaria capreolata* by Analytical Platforms Based on the Hyphenation of Gas Chromatography and Liquid Chromatography with Quadrupole- Time-of-Flight Mass Spectrometry," *International Journal of Analytical Chemistry*, vol. 2017, Article ID 5178729, 16 pages, 2017.

[63] O. Bayazeid, C. C. Eylem, T. Reçber, F. N. Yalçın, S. Kır, and E. Nemutlu, "An LC-ESI-MS/MS method for the simultaneous determination of pronuciferine and roemerine in some *Papaver* species," *Journal of Chromatography B*, vol. 1096, pp. 223–227, 2018.

[64] I. Çoban, G. G. Toplan, B. Özbek, Ç. U. Gürer, and G. Sarıyar, "Variation of alkaloid contents and antimicrobial activities of *Papaver rhoeas* L. growing in Turkey and northern Cyprus," *Pharmaceutical Biology*, vol. 55, pp. 1894–1898, 2017.

[65] O. Bayazeid, *Department of Pharmacognosy Phytochemical and pharmacological studies on some Papaver species in Turkey*, Hacettepe University: Institute of Health Sciences, 2017.

[66] K. Song, J. H. Oh, S.-G. Lee, S. G. Lee, and I. J. Ha, "Molecular network-guided alkaloid profiling of aerial parts of *Papaver nudicaule* L. using LC-HRMS," *Molecules*, vol. 25, no. 11, p. 2636, 2020.

[67] Ç. Ünsal, G. Sarıyar, B. G. Akarsu, and A. Çevikbaş, "Antimicrobial activity and phytochemical studies on Turkish samples of *Papaver macrostomum*," *Pharmaceutical Biology*, vol. 45, no. 8, pp. 626–630, 2007.

[68] A. Mat, G. Sariyar, A. Deliorman, M. Atay, and N. Özhatay, "Alkaloids and bioactivity of *Papaver dubium* subsp. dubium and P. dubium subsp. laevigatum," *Natural Product Letters*, vol. 14, no. 3, pp. 205–210, 2000.

[69] HMDB, 2012, https://hmdb.ca/metabolites/HMDB0030169.

[70] D. A. Kostic, S. S. Mitic, M. N. Mitic et al., "Phenolic contents, antioxidant and antimicrobial activity of *Papaver rhoeas* L. extracts from Southeast Serbia," *Journal of Medicinal Plants Research*, vol. 4, no. 17, pp. 1727–1732, 2010.

[71] R. Soulimani, C. Younos, S. Jarmouni-Idrissi, D. Bousta, F. Khalouki, and A. Laila, "Behavioral and pharmaco-toxicological study of *Papaver rhoeas* L. in mice," *Journal of Ethnopharmacology*, vol. 74, no. 3, pp. 265–274, 2001.

[72] P. Hanelt, "Die Typisierung von *Papaver nudicaule* L. und die Einordnung von *P. nudicaule* hort. non L," *Die Kulturpflanze*, vol. 18, no. 1, pp. 73–88, 1970.

[73] B. Dudek, A.-C. Warskulat, and B. Schneider, "The occurrence of flavonoids and related compounds in flower sections of *Papaver nudicaule*," *Plants*, vol. 5, no. 2, p. 28, 2016.

[74] E. C. Tatsis, H. Böhm, and B. Schneider, "Occurrence of nudicaulin structural variants in flowers of papaveraceous species," *Phytochemistry*, vol. 92, pp. 105–112, 2013.

[75] W. Schliemann, B. Schneider, V. Wray et al., "Flavonols and an indole alkaloid skeleton bearing identical acylated glycosidic groups from yellow petals of *Papaver nudicaule*," *Phytochemistry*, vol. 67, pp. 191–201, 2006.

[76] B. Kirkan, M. S. Özer, C. Sarikurkcu, M. Copuroglu, M. Cengiz, and B. Tepe, "Can the stalks of *Papaver somniferum* L. be an alternative source of bioactive components?," *Industrial Crops and Products*, vol. 115, pp. 1–5, 2018.

[77] M. Dilek, A. Gültepe, and N. Öztaşan, "Determination of Essential Oil Composition and Investigation of, Antimicrobial Properties of Poppy (*Papaver Somniferum* L.) Flower," *AKU Journal of Science and Engineering*, vol. 18, no. 3, pp. 786–795, 2018.

[78] S. Krist, G. Stuebiger, H. Unterweger, F. Bandion, and G. Buchbauer, "Analysis of volatile compounds and triglycerides of seed oils extracted from different poppy varieties (*Papaver somniferum* L.)," *Journal of Agriculture and Food Chemistry*, vol. 53, no. 21, pp. 8310–8316, 2005.

[79] G. Dogan and E. Bagcı, "Essential oil composition of *Papaver rhoeas* L. (corn poppy) (Papaveraceae) from Turkey," *Hacettepe Journal of Biology and Chemistry*, vol. 42, no. 4, pp. 545–549, 2014.

[80] M. T. Islam, E. S. Ali, S. J. Uddin et al., "Phytol: a review of biomedical activities," *Food and Chemical Toxicology*, vol. 121, pp. 82–94, 2018.

[81] I. Stranska, M. Skalicky, J. Novak, E. Matyasova, and V. Hejnak, "Analysis of selected poppy (*Papaver somniferum* L.) cultivars: pharmaceutically important alkaloids," *Industrial Crops and Products*, vol. 41, pp. 120–126, 2013.

[82] I. N. Johnston and R. F. Westbrook, "Inhibition of morphine analgesia by LPS: role of opioid and NMDA receptors and spinal glia," *Behavioural Brain Research*, vol. 156, no. 1, pp. 75–83, 2005.

[83] M. Ibrar, M. Ehsan, U. Barkat, K. B. Marwat, and S. S. Mubarak, "Cytotoxic and of *Papaver pavoninum* Fisch & Mey," *Pakistan Journal of Botany*, vol. 47, no. 5, pp. 1895–1899, 2015.

[84] J. Shams, H. Sahraei, Z. Faghih-Monzavi et al., "Effects of *Papaver rhoeas* extract on the tolerance development to analgesic effects of morphine in mice," *Iranian Journal of Pharmaceutical Research*, vol. 7, pp. 141–147, 2008.

[85] O. Bayazeid, E. Bedir, and F. N. Yalcin, "Ligand-based virtual screening and molecular docking of two cytotoxic compounds isolated from *Papaver lacerum*," *Phytochemistry Letters*, vol. 30, pp. 26–30, 2019.

[86] B. Dudek, F. Schnurrer, H.-M. Dahse et al., "Formation of nudicaulins *in vivo* and *in vitro* and the biomimetic synthesis and bioactivity of o-methylated nudicaulin derivatives," *Molecules*, vol. 23, no. 12, p. 3357, 2018.

[87] R. Demirgan, A. Karagöz, M. Pekmez et al., "In vitro anticancer activity and cytotoxicity of some *papaver* alkaloids on cancer and normal cell lines," *African Journal of Traditional, Complementary and Alternative Medicines*, vol. 13, no. 3, pp. 22–26, 2016.

[88] D. A. Güler, A. Aydın, M. Koyuncu, İ. Parmaksız, and Ş. Tekin, "Anticancer activity of *Papaver somniferum*," *Journal of the Turkish Chemical Society, Section A: Chemistry*, vol. 3, no. 3, pp. 349–366, 2016.

[89] K. Hasplova, A. Hudecova, E. Miadokova et al., "Biological activity of plant extract isolated from *Papaver rhoeas* on human lymfoblastoid cell line," *Neoplasma*, vol. 58, no. 5, pp. 386–391, 2011.

[90] R. Ennamany, N. Leconte, J. Leclerc et al., "Sublethal UVB induces DNA lesions and pro-apoptotic gene transcription in human keratinocytes: attenuation by a mixture of plant extracts," *Journal of Preventive Medicine*, vol. 1, pp. 4–10, 2013.

[91] F. Khalighi-Sigaroodi, M. Ahvazi, A. Hadjiakhoondi et al., "Cytotoxicity and antioxidant activity of 23 plant species of Leguminosae family," *Iranian Journal of Pharmaceutical Research*, vol. 11, no. 1, pp. 295–302, 2012.

[92] P. Middleton, F. Stewart, S. Al-Qahtani et al., "Antioxidant, antibacterial activities and general toxicity of *Alnus glutinosa*, *Fraxinus excelsior* and *Papaver rhoeas*," *Iranian Journal of Pharmaceutical Research*, vol. 4, pp. 101–103, 2005.

[93] A. DeBono, B. Capuano, and P. J. Scammells, "Progress toward the development of noscapine and derivatives as anticancer agents," *Journal of Medicinal Chemistry*, vol. 58, pp. 5699–5727, 2015.

[94] M. A. Altinoz, G. Topcu, A. Hacimuftuoglu et al., "Noscapine, a non-addictive opioid and microtubule-inhibitor in potential treatment of glioblastoma," *Neurochemical Research*, vol. 44, no. 8, pp. 1796–1806, 2019.

[95] N. Maurya, J. K. Maurya, U. K. Singh et al., "In vitro cytotoxicity and interaction of noscapine with human serum albumin: effect on structure and esterase activity of HSA," *Molecular Pharmaceutics*, vol. 16, no. 3, pp. 952–966, 2019.

[96] L. T. P. Martin, M. W. Nachtigal, T. Selman et al., "Bitter taste receptors are expressed in human epithelial ovarian and prostate cancers cells and noscapine stimulation impacts cell survival," *Molecular and Cellular Biochemistry*, vol. 454, no. 1-2, pp. 203–214, 2019.

[97] A. Rabzia, M. Khazaei, Z. Rashidi, and M. R. Khazaei, "Synergistic anticancer effect of paclitaxel and noscapine on human prostate cancer cell lines," *Iran Journal of Pharmaceutical Research*, vol. 16, no. 4, pp. 1432–1442, 2017.

[98] X. Tian, M. Liu, Q. Zhu et al., "Down-regulation of liver-intestine cadherin enhances noscapine-induced apoptosis in human colon cancer cells," *Expert Review of Anticancer Therapy*, vol. 17, no. 9, pp. 857–863, 2017.

[99] Z. Han, X. Huang, M. Liu et al., "Knock-down of cadherin 17 inhibits proliferation and promote apoptosis in noscapine-resistant human SW480 colon cancer cells," *Xi Bao Yu Fen Zi Mian Yi Xue Za Zhi*, vol. 33, no. 5, pp. 606–610, 2017.

[100] M. He, L. Jiang, Z. Ren, G. Wang, and J. Wang, "Noscapine targets EGFR$^{P-Tyr1068}$ to suppress the proliferation and invasion of MG63 cells," *Scientific Reports*, vol. 6, no. 1, article 37062, 2016.

[101] H. Huang, L. J. Li, H. B. Zhang, and A. Y. Wei, "Papaverine selectively inhibits human prostate cancer cell (PC-3) growth by inducing mitochondrial mediated apoptosis, cell cycle arrest and downregulation of NF-κB/PI3K/Akt signalling pathway," *Official journal of the Balkan Union of Oncology*, vol. 22, no. 1, pp. 112–118, 2017.

[102] W. Muhammad, M. A. Khan, M. Nazir et al., "Papaver somniferum L. mediated novel bioinspired lead oxide (PbO) and iron oxide (Fe$_2$O$_3$) nanoparticles: In- vitro biological applications, biocompatibility and their potential towards HepG2 cell line," *Materials Science and Engineering: C*, vol. 103, article 109740, 2019.

[103] E. S. Antonarakis, M. A. Carducci, and M. A. Eisenberger, "Novel targeted therapeutics for metastatic castration-resistant prostate cancer," *Cancer Letters*, vol. 291, pp. 1–13, 2010.

[104] S. K. Noureini and M. Wink, "Antiproliferative effect of the isoquinoline alkaloid papaverine in hepatocarcinoma HepG-2 Cells — Inhibition of telomerase and induction of senescence," *Molecules*, vol. 19, no. 8, pp. 11846–11859, 2014.

[105] S. Sajadian, M. Vatankhah, M. Majdzadeh, S. M. Kouhsari, M. H. Ghahremani, and S. N. Ostad, "Cell cycle arrest and apoptogenic properties of opium alkaloids noscapine and papaverine on breast cancer stem cells," *Toxicology Mechanisms and Methods*, vol. 25, no. 5, pp. 388–395, 2015.

[106] C. D. Arvanitis, G. B. Ferraro, and R. K. Jain, "The blood–brain barrier and blood–tumour barrier in brain tumours and metastases," *Nature Reviews Cancer*, vol. 20, pp. 26–41, 2020.

[107] J. E. Wang, Y. H. Liu, L. B. Liu, C. Y. Xia, Z. Zhang, and Y. X. Xue, "Effects of combining low frequency ultrasound irradiation with papaverine on the permeability of the blood-tumor barrier," *Journal of Neurooncology*, vol. 102, no. 2, pp. 213–224, 2011.

[108] M. Benej, X. Hong, S. Vibhute et al., "Papaverine and its derivatives radiosensitize solid tumors by inhibiting mitochondrial metabolism," *Proceedings of National Academic Sciences*, vol. 115, no. 42, pp. 10756–10761, 2018.

[109] M. Inada, M. Shindo, K. Kobayashi et al., "Anticancer effects of a non-narcotic opium alkaloid medicine, papaverine, in human glioblastoma cells," *PLoS One*, vol. 14, no. 5, article e0216358, 2019.

[110] S. Galadari, A. Rahman, S. Pallichankandy, and F. Thayyullathil, "Molecular targets and anticancer potential of sanguinarine–a benzophenanthridine alkaloid," *Phytomedicine*, vol. 34, pp. 143–153, 2017.

[111] S. Kumaravel and K. Alagusundaram, "Antimicrobial activity and phytochemical analysis of selected Indian spices," *Journal of Pure and Applied Microbiology*, vol. 8, no. 5, pp. 4131–4136, 2014.

[112] S. Dawar, S. Abbas, M. Tariq, and M. Zaki, "In vitro fungicidal activity of spices against root infecting fungi," *Pakistan Journal of Botany*, vol. 40, no. 1, pp. 433–438, 2008.

[113] Ç. Ünsal, B. Özbek, G. Sarıyar, and A. Mat, "Antimicrobial activity of four annual *Papaver* species growing in Turkey," *Pharmaceutical Biology*, vol. 47, no. 1, pp. 4–6, 2009.

[114] R. Istatkova, L. Nikolaeva-Glomb, A. Galabov et al., "Chemical and antiviral study on alkaloids from *Papaver pseudocanescens* M. Pop," *Zeitschrift für Naturforschung C*, vol. 67, no. 1-2, pp. 22–28, 2012.

[115] I.-K. Lee, B. S. Hwang, D.-W. Kim et al., "Characterization of neuraminidase inhibitors in Korean *Papaver rhoeas* bee pollen contributing to anti-influenza activities in vitro," *Planta Medica*, vol. 82, no. 6, pp. 524–529, 2016.

[116] M. Kačániová, J. Nóžková, K. Fatrcová-Šramková, Z. Kropková, and J. Kubincová, "Antioxidant, antimicrobial actiyity and heavy metals content in pollen of *Papaver somniferum* L," *Ecological Chemistry and Engineering A*, vol. 17, no. 1, pp. 97–106, 2010.

[117] B. Bazzaz and G. Haririzadeh, "Screening of Iranian plants for antimicrobial activity," *Pharmaceutical Biology*, vol. 41, no. 8, pp. 573–583, 2003.

[118] M. de, A. Krishna de, and A. Banerjee, "Antimicrobial screening of some Indian spices," *Phytotherapy Research: An International Journal Devoted to Pharmacological and Toxicological Evaluation of Natural Product Derivatives*, vol. 13, no. 7, pp. 616–618, 1999.

[119] S. Ishtiaque, S. Naz, R. Siddiqi, S. Jabeen, and J. Ahmed, "Antioxidant activity and phenolic contents of ajwain, mustard, fenugreek and poppy seed," *Recent Innovations in Chemical Engineering*, vol. 7, no. 2, pp. 119–127, 2014.

[120] Y. Zhang, G. Sun, Z. Hou, B. Yan, and J. Zhang, "Evaluation of the quality consistency of powdered poppy capsule extractive by an averagely linear quantified fingerprint method in combination with antioxidant activities and two compounds analyses," *Journal of Separation Science*, vol. 40, pp. 4511–4520, 2017.

[121] S. Baros, M. Karsayová, K. Jomová, A. Gáspár, and M. Valko, "Free radical scavenging capacity of *Papaver somniferum* L. and determination of pharmacologically active alkaloids using capillary electrophoresis," *Journal of Microbiology, Biotechnology and Food Sciences*, vol. 1, p. 725, 2012.

[122] F. Sharopov, A. Valiev, I. Gulmurodov, M. Sobeh, P. Satyal, and M. Wink, "Alkaloid content, antioxidant and cytotoxic activities of various parts of *Papaver somniferum*," *Pharmaceutical Chemistry Journal*, vol. 52, pp. 459–463, 2018.

[123] L. Aksoy, "Oxidant/antioxidant equilibrium in rats supplemented with diesel fuel or with opium poppy (*Papaver somniferum* L.) seed oil biodiesel," *Revue de Médecine Vétérinaire*, vol. 164, no. 1, pp. 34–38, 2013.

[124] M. Kazazic, M. Djapo, and E. Ademovic, "Antioxidant activity of water extracts of some medicinal plants from Herzegovina region," *International Journal of Pure Applied and Biosciences*, vol. 4, no. 2, pp. 85–90, 2016.

[125] T. Todorova, M. Pesheva, F. Gregan, and S. Chankova, "Antioxidant, antimutagenic, and anticarcinogenic effects of *Papaver rhoeas* L. extract on *Saccharomyces cerevisiae*," *Journal of Medicinal Food*, vol. 18, no. 4, pp. 460–467, 2015.

[126] A. Montefusco, G. Semitaio, P. P. Marrese et al., "Antioxidants in varieties of chicory (*Cichorium intybus* L.) and wild poppy (*Papaver rhoeas* L.) of southern Italy," *Journal of Chemistry*, vol. 2015, Article ID 923142, 8 pages, 2015.

[127] E. Krošlák, T. Maliar, P. Nemeček et al., "Antioxidant and proteinase inhibitory activities of selected poppy (*Papaver somniferum* L.) genotypes," *Chemistry & Biodiversity*, vol. 14, no. 9, article e1700176, 2017.

[128] K. Alpinar, M. Özyürek, U. Kolak et al., "Antioxidant capacities of some food plants wildly grown in Ayvalik of Turkey," *Food Science and Technology Research*, vol. 15, no. 1, pp. 59–64, 2009.

[129] E. Souri, G. Amin, and H. Farsam, "Screening of antioxidant activity and phenolic content of 24 medicinal plant extracts," *DARU Journal of Pharmaceutical Sciences*, vol. 16, no. 2, pp. 83–87, 2008.

[130] E. Souri, G. Amin, A. Dehmobed-Sharifabadi, A. Nazifi, and H. Farsam, "Antioxidative activity of sixty plants from Iran," *Iranian Journal of Pharmaceutical Research*, vol. 3, pp. 55–59, 2004.

[131] S. Nehir El and S. Karakaya, "Radical scavenging and iron-chelating activities of some greens used as traditional dishes in Mediterranean diet," *International Journal of Food Sciences and Nutrition*, vol. 55, no. 1, pp. 67–74, 2004.

[132] K. Koga, H. Shibata, K. Yoshino, and K. Nomoto, "Effects of 50% ethanol extract from rosemary (*Rosmarinus officinalis*) on ?-Glucosidase inhibitory activity and the elevation of plasma glucose level in rats, and its active compound," *Journal of Food Science*, vol. 71, no. 7, pp. S507–S512, 2006.

[133] B. Baharvand-Ahmadi, M. Bahmani, P. Tajeddini, N. Naghdi, and M. Rafieian-Kopaei, "An ethno-medicinal study of medicinal plants used for the treatment of diabetes," *Journal of Nephropathology*, vol. 5, no. 1, p. 44, 2016.

[134] A. Dalar, "Plant taxa used in the treatment of diabetes in Van Province, Turkey," *International Journal of Secondary Metabolite*, vol. 5, no. 3, pp. 171–185, 2018.

[135] H. N. Mrabti, N. Jaradat, M. R. Kachmar et al., "Integrative herbal treatments of diabetes in Beni Mellal region of Morocco," *Journal of Integrative Medicine*, vol. 17, no. 2, pp. 93–99, 2019.

[136] S. Ö. Sarikaya, H. Harput, and Ü. Şebnem, "Medicinal plants used for the treatment of diabetes in Turkey," *Ankara Üniversitesi Eczacılık Fakültesi Dergisi*, vol. 39, no. 4, pp. 317–342, 2010.

[137] H. A. M. Ahmed, S. M. Ahmed, E. El Gawish, A. M. Alanwar, and M. Ibrahem, "Effects of opium addiction on some biochemical parameters in diabetic rats," *International Journal of Biochemistry Research & Review*, vol. 10, no. 3, pp. 1–6, 2016.

[138] S. Sadeghian, M. A. Boroumand, M. Sotoudeh-Anvari, S. Rabbani, M. Sheikhfathollahi, and A. Abbasi, "Effect of opium on glucose metabolism and lipid profiles in rats with streptozotocin-induced diabetes," *Endokrynologia Polska*, vol. 60, no. 4, pp. 258–262, 2009.

[139] A. Golkar-Narenji, H. Eimani, F. Samadi et al., "Effect of *Papaver rhoeas* extract on in vitro maturation and developmental competence of immature mouse oocytes," *Reproductive medicine and biology*, vol. 9, no. 4, pp. 211–215, 2010.

[140] R. Rajabi-Toustani, R. Motamedi-Mojdehi, M. Roostaei-Ali Mehr, and R. Motamedi-Mojdehi, "Effect of *Papaver rhoeas* L. extract on in vitro maturation of sheep oocytes," *Small Ruminant Research*, vol. 114, no. 1, pp. 146–151, 2013.

[141] G. T. Mbemya, L. A. Vieira, F. G. Canafistula, O. D. L. Pessoa, and A. P. R. Rodrigues, "Relatos sobre a contribuiçao in vivo e in vitro de plantas medicinais na melhora da fun çao reprodutiva feminina," *Reprodução & Climatério*, vol. 32, no. 2, pp. 109–119, 2017.

[142] T. A. Beck and B. A. Alford, *Depression: Causes and Treatment*, University of Pennsylvania Press, Pensilvania, USA, 2009.

[143] M. Ranjbaran, P. Mirzaei, F. Lotfi, S. Behzadi, and H. Sahraei, "Reduction of metabolic signs of acute stress in male mice by *Papaver rhoaes* hydro-alcoholic extract," *Pakistan Journal of Bological Sciences*, vol. 16, no. 19, pp. 1016–1021, 2013.

[144] P. Mirzaei, F. Lotfi Kashani, S. Behzadi, and H. Sahraei, "The effect of *Papaver rhoeas* distillate on learning, memory, corticosterone and anorexia in little laboratory mice under inescapable tension," *Medical Science Journal of Islamic Azad Univesity-Tehran Medical Branch*, vol. 23, pp. 21–29, 2013.

[145] N. Osanloo, A. Najafi-Abedi, F. Jafari et al., "Papaver rhoeas L. hydroalcoholic extract exacerbates forced swimming test-induced depression in mice," *Basic and Clinical Neuroscience*, vol. 7, no. 3, pp. 195–202, 2016.

[146] I. Gürbüz, O. Üstün, E. Yesilada, E. Sezik, and O. Kutsal, "Anti-ulcerogenic activity of some plants used as folk remedy in Turkey," *Journal of Ethnopharmacology*, vol. 88, no. 1, pp. 93–97, 2003.

[147] J.-H. Oh, M. Yun, D. Park et al., "Papaver nudicaule (Iceland poppy) alleviates lipopolysaccharide-induced inflammation through inactivating NF-κB and STAT3," *BMC Complementary and Alternative Medicine*, vol. 19, no. 1, p. 90, 2019.

[148] M. J. Millan, "The induction of pain: an integrative review," *Progress in Neurobiology*, vol. 57, pp. 1–164, 1999.

[149] WHO, 2019, https://link.springer.com/article/10.1007/s11060-010-0321-7.

[150] H. Pathan and J. Williams, "Basic opioid pharmacology: an update," *British Journal of Pain*, vol. 6, pp. 11–16, 2012.

[151] N. Bliesener, S. Albrecht, A. Schwager, K. Weckbecker, D. Lichtermann, and D. Klingmüller, "Plasma testosterone and sexual function in men receiving buprenorphine maintenance for opioid dependence," *The Journal of Clinical Endocrinology and Metabolism*, vol. 90, no. 1, pp. 203–206, 2005.

[152] S. Mercadante, "Pathophysiology and treatment of opioid-related myoclonus in cancer patients," *Pain*, vol. 74, no. 1, pp. 5–9, 1998.

[153] S. Takeda, L. I. Eriksson, Y. Yamamoto, H. Joensen, H. Onimaru, and S. G. E. Lindahl, "Opioid action on respiratory neuron activity of the isolated respiratory network in newborn rats," *Anesthesiology*, vol. 95, no. 3, pp. 740–749, 2001.

[154] A. Rumman, Z. R. Gallinger, and L. W. C. Liu, "Opioid induced constipation in cancer patients: pathophysiology, diagnosis and treatment," *Journal of Expert Review of Quality of Life in Cancer Care*, vol. 1, no. 1, pp. 25–35, 2016.

[155] C. Kohberg, C. U. Andersen, and E. Bendstrup, "Opioids: an unexplored option for treatment of dyspnea in IPF," *European Clinical Respiratory Journal*, vol. 3, article 30629, 2016.

[156] G. M. Rocker, A. C. Simpson, Joanne Young BHSc et al., "Opioid therapy for refractory dyspnea in patients with advanced chronic obstructive pulmonary disease: patients' experiences and outcomes," *CMAJ Open*, vol. 1, no. 1, pp. E27–E36, 2013.

[157] EFSA, 2018, https://www.efsa.europa.eu/en/press/news/180516.

[158] L. A. Colvin, F. Bull, and T. G. Hales, "Perioperative opioid analgesia–when is enough too much? A review of opioid-induced tolerance and hyperalgesia," *Postoperative pain Management and Opioids*, vol. 393, no. 10180, pp. 1558–1568, 2019.

[159] B. Gyawali, N. Hayashi, H. Tsukuura, K. Honda, T. Shimokata, and Y. Ando, "Opioid-induced constipation," *Scandinavian Journal of Gastroenterology*, vol. 50, pp. 1331–1338, 2015.

[160] T. Jitpakdee and S. Mandee, "Strategies for preventing side effects of systemic opioid in postoperative pediatric patients," *Pediatric Anesthesia*, vol. 24, pp. 561–568, 2014.

[161] J. L. Martin, L. Koodie, A. G. Krishnan, R. Charboneau, R. A. Barke, and S. Roy, "Chronic morphine administration delays wound healing by inhibiting immune cell recruitment to the wound site," *The American Journal of Pathology*, vol. 176, no. 2, pp. 786–799, 2010.

[162] P. O. Anderson, A. S. Manoguerra, and V. Valdes, "A review of adverse reactions in infants from medications in breast-milk," *Clinical Pediatrics*, vol. 55, pp. 236–244, 2016.

[163] P. Madadi, C. J. Ross, M. R. Hayden et al., "Pharmacogenetics of neonatal opioid toxicity following maternal use of codeine during breastfeeding: a case-control study," *Clinical Pharmacology and Therapeutics*, vol. 85, no. 1, pp. 31–35, 2009.

[164] J. Lainer, C. Dawid, A. Dunkel, P. Gläser, S. Wittl, and T. Hofmann, "Characterization of bitter-tasting oxylipins in poppy seeds (*Papaver somniferum* L.)," *Journal of Agricultural and Food Chemistry*, vol. 68, no. 38, pp. 10361–10373, 2020.

[165] L. M. Schuppener and R. F. Corliss, "Death due to complications of bowel obstruction following raw poppy seed ingestion," *Journal of Forensic Sciences*, vol. 63, no. 2, pp. 614–618, 2018.

[166] I. Haber, J. Pergolizzi Jr., and J. A. LeQuang, "Poppy seed tea: a short review and case study," *Pain and therapy*, vol. 8, no. 1, pp. 151–155, 2019.

[167] B. Frantzen, E. B. Bröcker, and A. Trautmann, "Immediate-type allergy caused by poppy seed," *Allergy*, vol. 55, no. 1, pp. 97-98, 2000.

[168] T. Oppel, P. Thomas, and A. Wollenberg, "Cross-sensitization between poppy seed and buckwheat in a food-allergic patient with poppy seed anaphylaxis," *International Archives of Allergy and Immunology*, vol. 140, no. 2, pp. 170–173, 2006.

[169] Y. K. Günaydın, Z. D. Dündar, B. Çekmen, N. B. Akıllı, R. Köylü, and B. Cander, "Intoxication due to *Papaver rhoeas* (corn poppy): five case reports," *Case Reports in Medicine*, vol. 2015, Article ID 321360, 3 pages, 2015.

[170] H. Gonullu, S. Karadas, A. C. Dulger, and S. Ebinc, "Hepatotoxicity associated with the ingestion of *Papaver rhoease*," *Journal of Pakistan Medical Association*, vol. 64, pp. 1189-1190, 2014.

[171] S. Gateva, G. Jovtchev, A. Stankov, and F. Gregan, "Antigenotoxic capacity of *Papaver rhoeas* L. extract," *International Journal of Pharmacy and Pharmaceutical Sciences*, vol. 6, no. 1, pp. 717–723, 2014.

[172] M. Kargıoğlu, S. Cenkci, A. Serteser, M. Konuk, and G. Vural, "Traditional uses of wild plants in the middle Aegean region of Turkey," *Human Ecology*, vol. 38, pp. 429–450, 2010.

[173] S. Higashi and T. Setoguchi, "Hepatic arterial injection chemotherapy for hepatocellular carcinoma with epirubicin aqueous solution as numerous vesicles in iodinated poppy-seed oil microdroplets: clinical application of water-in-oil-in-water emulsion prepared using a membrane emulsification technique," *Advanced Drug Delivery Reviews*, vol. 45, pp. 57–64, 2000.

[174] S. Higashi, M. Shimizu, T. Nakashima et al., "Arterial-injection chemotherapy for hepatocellular carcinoma using monodispersed poppy-seed oil microdroplets containing fine aqueous vesicles of Epirubicin initial medical application of a membrane-emulsification technique," *Cancer*, vol. 75, no. 6, pp. 1245–1254, 1995.

[175] N. Ebrahimpour, M. Khazaneha, M. Mehrbani, P. Rayegan, and M. Raeiszadeh, "Efficacy of herbal based syrup on male sexual experiences: a double-blind randomized clinical trial," *Journal of Traditional and Complementary Medicine*, vol. 11, pp. 103–108, 2021.

[176] K. Vijayaraghavan, S. P. K. Nalini, N. U. Prakash, and D. Madhankumar, "One step green synthesis of silver nano/ microparticles using extracts of *Trachyspermum ammi* and *Papaver somniferum*," *Colloids and Surfaces B: Biointerfaces*, vol. 94, pp. 114–117, 2012.

[177] M. Heydari, M. H. Hashempur, and A. Zargaran, "Medicinal aspects of opium as described in Avicenna's canon of medicine," *Acta Medico-Historica Adriatica*, vol. 11, no. 1, pp. 101–112, 2013.

[178] M. A. Hijazi, M. Aboul-Ela, K. Bouhadir et al., "Cytotoxic activity of alkaloids from *Papaver rhoeas* growing in Lebanon," *Records of Natural Products*, vol. 11, no. 2, p. 211, 2017.

[179] M. A. Hijazi, E. El-Mallah, M. Aboul-Ela, and A. Ellakany, "Evaluation of analgesic activity of *Papaver libanoticum* extract in mice: involvement of opioids receptors," *Evidence-based Complementary and Alternative Medicine*, vol. 2017, Article ID 8935085, 2017.

[180] J. Oh, Y. Shin, I. J. Ha et al., "Transcriptome profiling of two ornamental and medicinal *papaver* herbs," *International Journal of Molecular Sciences*, vol. 19, no. 10, p. 3192, 2018.

[181] J.-H. Oh, I.-J. Ha, M. Y. Lee et al., "Identification and metabolite profiling of alkaloids in aerial parts of *Papaver rhoeas* by liquid chromatography coupled with quadrupole time-of-flight tandem mass spectrometry," *Journal of Separation Science*, vol. 41, no. 12, pp. 2517–2527, 2018.

Review Article

The Role of Nutraceuticals in Osteoarthritis Prevention and Treatment: Focus on n-3 PUFAs

Francesca Oppedisano [iD],[1] Rosa Maria Bulotta,[2] Jessica Maiuolo,[1] Micaela Gliozzi,[1] Vincenzo Musolino,[1] Cristina Carresi,[1] Sara Ilari,[1] Maria Serra,[1] Carolina Muscoli [iD],[1] Santo Gratteri,[1] Ernesto Palma [iD],[1,2] and Vincenzo Mollace [iD][1,2,3]

[1]*Institute of Research for Food Safety & Health IRC-FSH, University Magna Graecia, 88100 Catanzaro, Italy*
[2]*Nutramed S.c.a.r.l., Complesso Ninì Barbieri, Roccelletta di Borgia, 88021 Catanzaro, Italy*
[3]*IRCCS San Raffaele Pisana, Via di Valcannuta, Rome, Italy*

Correspondence should be addressed to Francesca Oppedisano; oppedisanof@libero.it and Vincenzo Mollace; mollace@libero.it

Osteoarthritis (OA) is a disease caused by joint degeneration with massive cartilage loss, and obesity is among the risk factors for its onset, though the pathophysiological mechanisms underlying the disease and better therapeutic approach still remain to be assessed. In recent years, several nutraceutical interventions have been investigated in order to define better solutions for preventing and treating OA. Among them, polyunsaturated fatty acids (n-3 PUFAs) appear to represent potential candidates in counteracting OA and its consequences, due to their anti-inflammatory, antioxidant, and chondroinductive effects. PUFAs have been found to counteract the onset and progression of OA by reducing bone and cartilage destruction, inhibiting proinflammatory cytokine release, reactive oxygen species (ROS) generation, and the NF-κB pathway's activation. Moreover, a diet rich in n-3 PUFAs and their derivatives (maresins and resolvins) demonstrates beneficial effects on associated pain reduction. Finally, it has been shown that together with the anti-inflammatory and antioxidant properties of eicosapentaenoic (EPA) and docosahexaenoic (DHA) acids, their antiapoptotic and antiangiogenic effects contribute in reducing OA development. The present review is aimed at assessing evidence suggesting the potential benefit of nutraceutical supplementation with PUFAs in OA management according to their efficacy in targeting relevant pathophysiological mechanisms responsible for inflammation and joint destruction processes, and this may represent a novel and potentially useful approach in OA prevention and treatment. For that purpose, a PubMed literature survey was conducted with a focus on some in vitro and in vivo studies and clinical trials from 2015 to 2020.

1. Introduction

Osteoarthritis (OA) is a degenerative joint disease associated with massive cartilage loss [1–3], affecting approximately 15% of the total population, and 60% of the elderly population [4]. Normal articular cartilage is made up of connective tissue and covers the load-bearing surfaces at the ends of long bones [5]. The only cells in cartilage are chondrocytes, which constitute the cartilage extracellular matrix (ECM) through a balance between synthesis and degradation. The ECM is basically made up of collagen type II (COL2A1) and proteoglycans, such as aggrecan. This composition guar-antees structural integrity and the absence of friction during joint movement [5, 6]. Below the cartilage in the joint is a dense formation: the subchondral bone plate and trabecular bone in the epiphysis, the function of which is to support the loads applied to the joint. There are numerous vessels in the trabecular portion that provide nourishment to the cartilage. Bone formation is attributable to osteoblasts, while osteoclasts' function is bone resorption. In order to perform their functions, these cells need a continuous supply of adenosine triphosphate (ATP); therefore, they are metabolically very active. Articular joints also contain synovial tissue, which is subdivided into intima (the inner layer) and subintima.

The synovial intimal cells are fibroblast-like synoviocytes (FLS) and macrophage-like synoviocytes (MLS); the former is responsible for synovial fluid viscosity, while the latter is tissue-resident macrophages. Moreover, menisci, ligaments, tendons, and adipose depots are all responsible for biomechanical stability and joint function [5]. Hands, knees, and hips are particularly affected by OA, and more specifically, the articular bodies, capsules, bursae, cartilage menisci, ligaments, and muscles [1, 4, 7]. The osteochondral unit consists of cartilage, subchondral bone, and calcified cartilage. This unit, essential for load distribution and joint movement, is modified as OA progresses [1, 2, 4]. In the early stages of disease onset, the cortical plate and subchondral bone undergo rapid bone remodeling, with concomitant bone loss and increased porosity. Changes in calcified cartilage and tidemark destruction are related to the improper passage of substances and vessel generation. Modification of the osteochondral unit leads to unbalanced load distribution with consequent cartilage destruction, which, over time, determines OA onset and progression [1, 2]. Furthermore, alterations in subchondral bone are responsible for the different crosstalks between chondrocytes and bone cells, which contribute to cartilage destruction [1]. Chondrocytes, responsible for bone formation, are damaged by proinflammatory action of interleukins and metalloproteinases [1, 7]. Furthermore, chondrocytes express molecules such as VEGF (vascular endothelial growth factor), MMP-13 (matrix metallopeptidase 13), and RUNX2 (runt-related transcription factor 2), implicated in hypertrophy and differentiation [1, 2, 7]. Hypertrophy and the surrounding calcified extracellular matrix alter the tidemark on the osteochondral interface, causing microcracks and thinning of the cartilage [1, 2]. OA onset is characterized by greater bone remodeling, with simultaneous bone reduction under articular cartilage. Decreased remodeling and subchondral densification occur during disease progression, together with synovial inflammation and increased inflammatory and catabolic responses [1, 2, 8, 9]. In light of this, intervening on subchondral bone remodeling and maintaining osteochondral unit structural integrity could represent a therapeutic strategy in preventing the onset and progression of OA [1].

2. Role of Inflammation and Oxidative Stress in OA

The structural changes characterizing OA are determined by a series of factors, the most important of which is inflammation [10]. From a clinical point of view, joint inflammation in OA is characterized by joint swelling, warmth, and pain [2, 10]. In particular, inflammation of the synovial membrane, known as synovitis, occurs as a result of interaction between degraded cartilage fragments and the immune system, which generates a protective inflammatory response via synoviocytes [10]. The cartilage fragments are identified as foreign bodies, and therefore, trigger a response from both the innate and adaptive immune systems. Consequently, the inflammatory response is generated through the activation of inflammatory signaling pathways, such as the NF-κB (nuclear factor-κB) pathway [7, 10]. This change is closely

related to aging and also occurs in the absence of other conditions, such as obesity and metabolic syndrome [7]. The most studied inflammatory mediators of OA are cytokines that amplify low-grade inflammation, further compromising cartilage [10, 11]. However, obesity is one of the most important risk factors in the onset of OA [5]. It has been shown that the onset of posttraumatic OA is more linked to biomechanical factors, while metabolic OA arises following chronic inflammation and an unbalanced diet; conditions characteristic of obesity [5, 12]. In fact, chronic inflammation, characterized by the increased synthesis of proinflammatory cytokines, such as IL- (interleukin-) 1β and TNF- (tumor necrosis factor-) α, determines greater osteoclast activation, which is responsible for bone resorption [5]. Furthermore, hormones such as leptin and visfatin, which are associated with obesity, are also involved in OA onset and progression. It has been shown that knee osteoarthritis is the most common form among obese people and, in particular, among aging adults [12]. Therefore, damage to joints is not only determined by increased body weight but is also mainly due to a greater synthesis of matrix metalloproteinases (MMPs), such as MMP-1, −3, −9, and −13, disintegrin, and metalloproteinase with thrombospondin motifs (ADAMTS), such as ADAMTS-4 and −5, the presence of which is related to ECM degradation, synovitis, and cartilage and bone injuries [3, 5–7, 13]. IL-1β induces the upregulation of these enzymes in addition to other catabolic factors, including inflammatory mediators, nitric oxide (NO), prostaglandin E2 (PGE2), cyclooxygenase-2 (COX-2), and reactive oxygen species (ROS) [6, 14–16]. Additionally, oxidative stress can trigger joint inflammation and pain in response to cellular senescence or obesity-related systemic inflammation. In fact, ROS production is deeply involved in OA triggering the inflammation cycles and catabolism, leading to a reduction of glycosaminoglycans and collagen modifications, causing chondrocyte homeostasis alteration and irreversible cartilage matrix degradation with OA development [5–8]. Joint aging and dysfunction are also related to impaired autophagy, which results in chondrocytes losing the ability to maintain homeostasis and survive in pathological conditions. Indeed, in aged cartilage and in mouse joints with surgically induced OA, autophagic protein expression is downregulated [7, 17]. In OA inflammation, NO plays an important pathological role. NO is synthesized in chondrocytes by inducible NO synthase (iNOS), and its high production rate generates an inflammatory state that contributes to cartilage destruction and cell damage [7, 10]. Studies conducted in OA patients have shown greater NO concentration and iNOS expression in chondrocytes compared to the (still high) levels present at the synovial level. Therefore, NO produced at the cartilage level contributes to OA pathogenesis. In particular, a higher iNOS expression has been demonstrated in the superficial area of OA cartilage, which thus pinpoints the commencement of OA damage, i.e., the damaged cartilage is responsible for the greater NO production. The latter causes cartilage destruction, as it increases chondrocyte-mediated matrix degradation, increases MMPs activity and, at the same time, inhibits the synthesis of matrix components, such as COL2A1 and aggrecan. NO

contributes to OA pathogenesis by triggering the inflammatory response, along with increased synthesis of PGE2 and inflammatory cytokines [16]. Furthermore, NO can also be involved in mechanisms related to oxidative damage and chondrocyte death by apoptosis. Therefore, iNOS modulation represents a possible target for OA therapy; in fact, the chondroprotective effects of many molecules of plant origin, such as pomegranate extract, have been demonstrated [10].

3. Therapies in OA

OA is a disabling joint disease with a multifactorial mechanism, causing major impairment to quality of life, as well as pain, limitation of movement, and disability [2, 4, 10, 17]. To date, there are no effective therapies for OA; just therapies that confer symptomatic relief or a definitive treatment, such as joint arthroplasty [2, 10, 17]. Treatment such as joint arthroplasty still has a high postsurgical chronic pain incidence that ranges between 20% and 40% [18]. Osteoarthritis pain after prosthesis implantation is one of the most severe secondary syndromes, depending not only on surgery but also on organic changes before and after joints replacement [2, 10, 17]. Opioid employment could influence postsurgical pain and lead to tolerance or addiction. It is well known that the involvement in hypersensibility of the immune system, the nervous system, and the peptidergic ones is connected due to the opioid receptors on immune cells surface. Recently, it has been shown that the percentage of Mu-positive B cells is statistically lower in OA patients, and this data could be used as a biological marker for an objective diagnosis of chronic pain [19]. Therefore, in order to be effective, OA therapies must be applied either in a preventive manner, or in the initial stages of disease onset. Chronic joint pain is the main symptom of OA, and strategies to relieve it are necessary to improving the quality of life in patients with OA [14, 20]. In fact, the drugs used in OA patients are analgesic and/or nonsteroidal anti-inflammatories (NSAIDs), which only counteract symptoms without acting on OA progression and pathophysiology [7, 9, 21]. Additionally, in long-term therapy, NSAIDs have side effects at the gastrointestinal, renal, and cardiovascular levels; they also manifest liver toxicity, hemorrhaging, and negative effects on chondrocytes and cartilage matrix formation [7, 9, 22]. Consequently, in recent years, alternative solutions with fewer side effects have been sought by the scientific community, such as treatment with natural compounds. In fact, nutritional treatments for the prophylaxis and therapy of other diseases, including heart disease, hepatic steatosis, and metabolic syndrome, are all considered viable therapeutic alternatives [23–32]. Therefore, such compounds are believed to be important in the prevention and management of articular cartilage structural damage in OA [2, 3, 33]. The data obtained from *in vitro* and *in vivo* preclinical studies confirm the anti-inflammatory and antioxidant effects of the natural compounds used in counteracting both the progression and symptoms in OA [7]. Additionally, human clinical trials have demonstrated the effectiveness of natural compounds for the management and relief of OA pain; this

is likely attributable to their anti-inflammatory and antioxidant properties [20]. Thus, although nutraceutical supplementation with natural compounds has been widely used in the past decades to find better solutions to counteract OA development, the benefit of such an approach is not well defined and further studies are required to understand the potential for nutraceutical supplementation in OA treatment. Recently, evidence has been collected showing that polyunsaturated fatty acids (PUFAs) may represent right candidates for nutraceutical supplementation in treating OA, alongside with traditional pharmacological approach. In particular, it has been suggested that their selective anti-inflammatory and antioxidant properties may significantly produce chondroprotective thereby attenuating cartilage loss. In this review, we aim to summarize scientific data demonstrating the effectiveness of PUFAs in OA management and their potential role in nutraceutical supplementation in OA-related pathophysiological mechanisms. The interest in these nutraceuticals is linked to the fact that they represent important components of the Mediterranean diet.

4. Polyunsaturated Fatty Acids (PUFAs)

Polyunsaturated fatty acids (PUFAs), and all unsaturated fatty acids (FAs) in general, are lipids consisting of a long hydrocarbon chain with a carboxyl group (-COOH) at the polar hydrophilic end and a nonpolar hydrophobic methyl group (-CH3) at the opposite end [34]. Two classes of PUFAs, n-3 and n-6, are defined as "essential," as they must be taken in via the diet because humans do not have the $\Delta 12$- and $\Delta 15$-desaturases that catalyze double bond formation in positions n-3 and n-6 of the FA carbon chain. In particular, the n-3 PUFAs have their first double bond between the third and fourth carbon atoms, while n-6 PUFAs have it between the sixth and seventh carbon atoms, counting from the methyl end of the FAs [35]. Linoleic acid (LA, 18:2, omega-6) and α-linolenic acid (ALA, 18:3, omega-3) are essential PUFAs as they must be taken in via the diet [36]. The main products of LA metabolism are n-6 PUFA, γ-linolenic, and arachidonic acid, while n-3 PUFAs, such as eicosapentaenoic acid (EPA, 20:5 n-3) and docosahexaenoic acid (DHA, 22:6 n-3), derive from ALA [36, 37]. The vegetable dietary sources of LA are safflower, soy, and corn oils. ALA, on the other hand, is present in flax seeds, beans, nuts, and the leaves of some green plants. The levels of EPA and DHA obtained by the liver from α-linolenic acid are minimal, and most of their content in the body derives from the diet. In particular, EPA and DHA are abundant in the flesh of both lean and fatty marine fish, as well as in fish oil and algal-derived supplements, although they can also be found in lower quantities in many other foods of animal origin. Therefore, including them in our daily diet in the correct proportions is highly recommended [34–37].

4.1. Role of n-3 and n-6 PUFAs. Western diets (WD) usually have a higher content of n-6 PUFAs than n-3 PUFAs; the n-6/n-3 ratio is usually higher than 15 : 1. The recommended daily intake is around 4 : 15. This unbalanced ratio, in favor of n-6 PUFAs, favors proinflammatory eicosanoid synthesis,

causing the onset of inflammatory and autoimmune diseases [38]. EPA and DHA are incorporated into cellular phospholipid membranes, but are also precursors of immune-inflammatory signaling modulators. In particular, EPA and DHA generate prostaglandins, leukotrienes, and D- and E-series resolvins, which have potent anti-inflammatory effects through COX and lipoxygenase (LOX) activity [39, 40]. Conversely, n-6 PUFAs perform proinflammatory roles, regulating various inflammatory processes and genes. Furthermore, arachidonic acid is a precursor to proinflammatory mediating prostaglandins, thromboxanes, and leukotrienes, while linoleic acid causes more severe inflammatory responses [37]. Given the opposite effects of n-3 and n-6 PUFAs on the inflammatory response, their ratio is fundamental to the regulation of inflammatory signaling homeostasis [40]. Numerous epidemiological studies correlate n-3 PUFAs intake with long-term beneficial effects on human health. In fact, the efficacy of n-3 PUFAs in the prevention and treatment of various pathologies, such as cerebral ischemia, non-alcoholic fatty liver disease (NAFLD), cardiovascular diseases, and neurodegenerative diseases, is well known [26, 27, 41–44]. Importantly, several evidences have shown that PUFAs play an important role in OA.

4.2. PUFAs and OA

4.2.1. DHA, Bone Remodeling, and Angiogenesis.
To better investigate the role of the osteochondral unit in OA onset and progression, an *in vivo* study was conducted in an ACLT-induced rat model, and an *in vitro* one in RAW264.7 (mouse mononuclear macrophage leukemia cells) and HUVECs (human umbilical vein endothelial cells) [1]. In the *in vivo* model, DHA's effect on bone remodeling and vessel formation in the osteochondral unit was investigated. Microcomputed tomography (micro-CT) images of subchondral bone revealed DHA's positive effect on the bone surface to bone volume (BS/BV) and bone volume to tissue volume (BV/TV) ratios, indicating that DHA protects the microstructure of subchondral bone in the initial phase of OA. The reported study showed that DHA inhibits osteoclast differentiation, reducing areas of bone resorption and confirming osteoclasts' role in OA. DHA has been shown to inhibit mRNA and the protein expression of osteoclast markers TRAP (tartrate-resistant acid phosphatase) and CTSK (Cathepsin K), which are involved in bone turnover. Therefore, by inhibiting these protein expressions, DHA inhibits osteoclast differentiation and bone remodeling, along with bone mass preservation. RANKL (receptor activator of nuclear factor kappa-B ligand) is also involved in this process, as its expression is downregulated by the presence of DHA, both in ACLT rats and in cells, thus, preventing cartilage degradation. Furthermore, NFATc1 (nuclear factor of activated T-cells, cytoplasmic 1) is also involved in the terminal osteoclast differentiation process. It is known that NFATc1 and RANKL signaling pathways can perform their functions either in synergy or independently. The study's results for RAW264.7 cells treated with RANKL demonstrate that DHA presence reduces the levels of NFATc1 expression, influencing osteoclast differ-entiation. Similar results were recorded for the DHA regulation of MITF (microphthalmia-associated transcription factor) expression, a member of the MIT family that is involved in the differentiation process that regulates TRAP mRNA expression levels. In this way, DHA suppresses osteoclast differentiation. In addition, an increase in angiogenesis was found in OA development. It was also shown that DHA slows OA progression by reducing angiogenesis at the interface between subchondral bone and calcified cartilage, inhibiting the proliferation and migration of HUVECs. DHA blocks the VEGF–VEGFR2 signaling pathway, responsible for blood vessel formation, which is particularly active in OA models. Therefore, DHA slows down cartilage degeneration.

4.2.2. The n-6/n-3 PUFA Ratio and MMP-13 Expression.
Since MMP-13 expression increases in OA chondrocytes, the effects of different n-6/n-3 PUFAs ratios were studied both *in vitro* (in inflammatory human chondrocytes) and in Sprague-Dawley rats with arthritis induced by Freund's complete adjuvant, treated for six weeks [45]. In particular, the effects of LA/ALA ratios ranging from 1 : 1 to 10 : 1 were tested. The results obtained *in vitro* and *in vivo* studies showed no variation in cell proliferation, but an LA/ALA ratio of 1 : 1 is more effective in reducing mRNA and MMP-13 protein levels. In particular, the serum MMP-13 and IL-1 levels are lower when treated with LA/ALA ratios of 1 : 1 and 2 : 1. The same LA/ALA ratios reduced the paw swelling rate, and the histological analysis reported less cartilage damage. Therefore, this study demonstrates that an equal ratio of n-6 and n-3 PUFAs is the most effective in inhibiting MMP-13 expression and induced arthritis in rats, thus, representing a good approach for the treatment of OA symptoms. It is also known that MMP-13 is responsible for COL2A1 degradation and destruction, a condition that leads to OA onset and progression. COL2A1 synthesis is also inhibited by IL-1β, which is responsible for the upregulation of cartilage degradation mediated by MMPs.

4.2.3. DHA and MMP-13 Expression.
In light of these data and DHA's anti-inflammatory action, Wang et al. conducted a study on the effects of IL-1β on human chondrosarcoma SW1353 cells and on a rat model of adjuvant-induced arthritis (AIA), in order to test for DHA's possible protective effects on OA [46]. First, using flow cytometry and an MTT (3-(4,5-dimethylthiazol-2-yl)-2,5-diphenyltetrazolium bromide) assay, DHA concentrations <50 μg/mL were established as being safe for cell treatment. The mRNA and protein expressions were evaluated by RT-qPCR, ELISA, and Western blotting. Studies conducted on SW1353 cells treated with increasing DHA concentrations reported that DHA inhibits both MMP-13 mRNA expression and IL-1β-enhanced MMP-13 protein expression in a dose-dependent manner, with a maximal effect at a DHA concentration equal to 50 μg/mL. The mechanism underlying this inhibitory effect was also evaluated, concluding that DHA has no effect on JNK or ERK1/2 activation. On the contrary, DHA inhibits IL-1β-induced p38 activation, and particularly, p-38 phosphorylation. *In vivo* studies in an AIA rat model

confirmed the results obtained in cells pertaining to MMP-13 expression. In particular, histological and immunohistochemistry analyses have shown that the treatment of AIA rats with DHA increases the thickness of articular cartilage, reducing its destruction by inhibiting MMP-13 expression in the cartilage matrix. Many *in vitro* and *in vivo* studies have demonstrated the positive effects of n-3 PUFAs on cartilage repair, but these need to be confirmed by further clinical trials [47].

4.2.4. DHA, EPA, and Apoptosis. OA is also characterized by joint marginal osteophyte generation accompanied by synovitis. Therefore, OA was induced in the human chondrosarcoma cell line SW1353 by inflammatory factor IL-1β stimulation, and the effect of DHA on cell apoptosis was evaluated [48]. By determining B-cell lymphoma-2 (Bcl-2), Bcl-2-associated X protein (Bax), and cleaved caspase-3 expression, in addition to ERK, JNK, and p38 MAPK, in both the presence and absence of DHA, it was established that DHA has an inhibitory effect on IL-1β and reduces apoptosis by inhibiting the activation of the MAPK signaling pathway. In addition, EPA, injected intra-articularly into a mouse model of OA showed an antiapoptotic effect on chondrocytes in the presence of oxidative stress [7].

4.2.5. Controlled-Release EPA. A new therapeutic strategy for OA was investigated, in which patients could be treated with controlled-release EPA [49]. The study model was that of male mice exhibiting destabilization of the medial meniscus (DMM), treated with either a single injection of EPA (3 mg/mL) or with gelatin hydrogels containing EPA (3 mg/mL). Histological evaluation was carried out at 1 week and 8 weeks after DMM surgery. Gelatin hydrogels represent a safe drug delivery system through which a physiologically active substance, such as EPA, is gradually released in less than three weeks. Moreover, in this study, immunohistochemical analyses showed that EPA, incorporated into the gelatin hydrogel and released slowly over time, improved MMP-3-, MMP-13-, IL-1β-, and p-IKK α/β-positive cell ratios more effectively than a single injection of EPA, thereby grounding a more effective response to OA progression. This could represent an innovative and more efficient treatment for OA patients.

4.3. OA, Obesity, and PUFAs. Although obesity is considered one of the risk factors for knee OA given the increased load on bearing joints, it is also associated with OA in low-load-bearing joints, such as hand joints. Therefore, it has been shown that excess adipose tissue has not only a biomechanical action but also alters cartilage metabolism through the release of cytokines and adipokines. In this process, elevated leptin levels appear to play a particularly important role [50–52]. Furthermore, lipid-lowering drugs may modify the lipid profile and OA progression [50]. It is known, in fact, that in obesity, a diet richer in saturated fatty acids (SFA) and n-6 PUFAs determines an increase in systemic inflammation; while a higher n-3 PUFAs intake reduces joint degeneration with a strong anti-inflammatory and antioxidant effect [51, 53]. In particular, in a study conducted on

porcine cartilage explant and human articular chondrocytes (HACs), it was shown that a leptin concentration equal to 10 μg/mL, alone or in combination with IL-1β, determines cartilage destruction, with NF-κB, ERK, JNK, and p38 activation and consequent MMP3, MMP13, and ADAMTS4 secretion [52]. Treatment with EPA and DHA had protective effects; it inhibited cartilage damage following reduced ADAMTS4 secretion due to lower NF-κB and JNK activation.

4.3.1. PUFAs and Posttraumatic Osteoarthritis (PTOA). The fact that n-6 and n-3 PUFAs' contents in the diet influence OA onset in obesity has also been verified in posttraumatic osteoarthritis (PTOA) [54]. This is typically a disease that arises following trauma to the joints, and it presents obesity and metabolic syndrome as risk factors. Using the fat-1 transgenic mouse model, the n-6/n-3 PUFAs ratio was genetically altered through the n-3 fatty-acid desaturase enzyme, encoded by fat-1 gene, the function of which is dehydrogenating n-6 to n-3 PUFAs. In particular, male and female fat-1 and wild-type (WT) mice with PTOA induced by DMM surgery were fed a diet rich in n-6 PUFAs. The results obtained demonstrate that the increased serum content of n-3 PUFAs in obese fat-1 mice reduced OA and synovitis, despite their having a similar body weight to that of WT mice. Furthermore, this reduction is sex- and diet-dependent. In fat-1 mice, a reduction in systemic inflammation was also recorded; in fact, the greater presence of n-3 PUFAs in serum is related to a decrease in proinflammatory cytokines, such as interferon-γ (IFN-γ), TNF-α, and monocyte chemoattractant protein-1(MCP-1), and an increase in the anti-inflammatory response. Therefore, OA severity under obese conditions is more related to serum fatty acid levels and composition than to body weight. This study demonstrates that joint damage can be reduced in obese subjects given the greater presence of circulating n-3 PUFAs compared to n-6.

4.3.2. Lipid Profile and OA. A different balance between the FAs taken with the diet can alter the phospholipid layer that covers the cartilage surface [53]. This layer offers protection during joint loading, and therefore, protection against OA onset and severity. In order to evaluate the serum and synovial fluid lipid composition under OA conditions, a study was conducted on male mice fed for 24 weeks on a low-fat control diet and a high-fat diet (HFD) rich in SFA, n-3 PUFAs, or n-6 PUFAs. OA was induced following surgery for DMM. The results obtained show that mice fed a diet rich in n-3 PUFAs have a more stable lipid composition in the synovial fluid than mice fed a diet rich in SFAs and n-6 PUFAs. Furthermore, in serum, n-3 PUFAs negatively correlate with OA severity and positively correlate with adiponectin, which triggers an anti-inflammatory response. A contrary condition is associated with n-6 PUFAs, which also have a positive correlation with inflammatory adipokines. In addition, in serum, a high n-3/n-6 PUFA ratio corresponds to a less severe OA condition, with a lower presence of inflammatory adipokines. In contrast, the lipid profile in the synovial fluid of the joints was evaluated in a study

conducted on patients with end-stage knee OA and non-symptomatic controls [50]. Mass spectrometry was used to measure SFAs, monounsaturated fatty acids (MUFAs), and n-6 and n-3 PUFA concentrations; the n-6/n-3 ratio was also defined. In the synovial fluid of subjects with OA, the SFA concentrations, in particular tetracosadienoic acid, and the MUFA concentrations, in particular nervonic acid, were higher than in nonsymptomatic subjects. In contrast, the n-6 concentration, especially arachidonic acid, was lower in OA patient fluid than in the control, while the n-3 concentration was comparable. Therefore, the PUFA profiles in the two groups show a lower n-6/n-3 ratio in the OA group compared to the control. The results obtained in this study appear to contrast with other research, in which OA patients showed a higher content of n-6 PUFAs and a consequently higher n-6/n-3 ratio, explained by the proinflammatory properties of n-6 PUFAs and their derivatives. The contrast between the results of this study and those of previous ones can be attributed to the different OA phenotypes considered in this study, and the lower number of patients (only 29), whose lifestyle and pharmacological history were not known. Additionally, in this study, patients had end-stage knee OA with total knee replacement. In this condition, synovitis and inflammation may be replaced by a more pro-fibrotic phase, in accordance with a lower content of n-6 PUFAs, the concentration of which may be a little higher in the initial stages of OA. A 48-month study was conducted on 2092 subjects with knee OA [55]. The intake effects of total fat, SFAs, MUFAs, and PUFAs on knee OA progression were assessed annually. In particular, OA progression was monitored by evaluating over time the reduction in quantitative joint space width (JSW) between the medial femur and tibia of the knee, depending on the intake of the various types of fat. This study depends on the knowledge that a diet rich in fat, and the consequent overweight condition, determines variations in joint loading and changes in cartilage, highlighting a strong correlation between diet and OA pathogenesis. Therefore, it was established that total fat and SFAs are associated with a JSW loss, and thus, with greater knee OA structural progression. In contrast, subjects on a diet rich in MUFAs and PUFAs display lower JSW loss with slower knee OA progression. All this demonstrates that dietary fat is closely associated with knee OA structural progression.

4.3.3. n-3 PUFAs and GPR 120.

It is known that OA onset and progression in obesity are more related to lipid metabolism homeostasis and circulating adipokines than to adiposity and body weight. In obesity, oxidative stress determines adipocyte lipolysis, with the consequent release into circulation of free fatty acids, which can generate pro- or anti-inflammatory molecules [56]. For example, binding between n-3 PUFAs and G-protein coupled receptor 120 (GPR 120) leads to the synthesis of protectins and resolvins, thereby mediating anti-inflammatory effects in different cell types [5, 56]. In this regard, a study was conducted to define GPR120 involvement in OA [56]. GPR120 and its agonist DHA are already known to confer protection in obesity-associated type 2 diabetes. GPR120's involvement in carti-

lage degeneration during OA progression was confirmed by studies conducted in GPR120 knockout mice with OA surgically induced by ACLT. In the same study, the anti-inflammatory effect of GPR120 activation with DHA was reported *in vitro* in human chondrocytes. Furthermore, *in vivo* studies on OA have shown that n-3-GPR120 signaling inhibition leads to alterations in bone remodeling and osteophyte formation of the subchondral bone.

4.4. Pain in OA and PUFAs.

Furthermore, n-3 PUFA supplementation in humans also causes a reduction in pain and structural damage associated with increased function [57]. Some clinical studies have been performed on patients with active OA whose daily diet was supplemented with fish oil [38]. The trials ranged in duration from 12 to 104 weeks, and the number of patients enrolled ranged from 81 to 202. In these trials, WOMAC (Western Ontario and McMaster Universities Arthritis Index) scores were found to be lower, accompanied by a reduction in pain and a lower use of NSAID/analgesic. Importantly, none of these studies had any adverse effects related to the use of fish oil.

4.4.1. n-6:n-3 PUFA Ratio, Pain, and Psychosocial Distress.

Knee OA is known to be characterized not only by joint-specific inflammation but also by systemic inflammation [58]. Additionally, people with OA present chronic pain, functional limitations, and psychosocial suffering. Therefore, a study was conducted on 167 patients with knee OA in order to verify the possible effects of PUFAs on various OA aspects. In particular, a pilot study was conducted on the n-6:n-3 PUFA ratio in OA, taking into account the known anti-inflammatory, antinociceptive, and psychosocial distress ameliorative effects of n-3 PUFAs, compared to the opposite effects of n-6 PUFAs. To do this, the participants' plasma was collected, and the n-6:n-3 PUFAs ratio was measured. The data obtained were also evaluated on the basis of the clinical and functional importance of the n-6:n-3 PUFA ratio, the recommended value of which varies from 2 : 1 to 5 : 1. The group with a low n-6:n-3 ratio suffered less knee pain and had better physical functioning and less psychosocial distress.

4.4.2. EPA, L-Serine, and Pain.

Additionally, a randomized, double-blind, placebo-controlled, parallel group study was recently conducted to evaluate the effect of EPA and L-Serine on lower-back and knee pain [59]. The study was conducted on 120 adult participants with lower-back and knee pain for at least three months, divided into a placebo group and a group given 594 mg of L-Serine and 149 mg of EPA daily for eight weeks. In the following four weeks of observation, an improvement in lumbar and knee pain was recorded in subjects treated with the combination of L-Serine, which acts on nerve function, and EPA, which exerts an anti-inflammatory effect. The results obtained here will be further verified in future clinical studies.

4.5. Maresins and Resolvins in OA Treatment

4.5.1. Anti-Inflammatory Effect of Maresin-1.

In order to verify the possible anti-inflammatory therapeutic effect of

TABLE 1: Effects of PUFAs and derivatives in OA.

First author, year	References	Treatment	Properties	*In vitro/in vivo* models	Clinical trials
Xie et al., 2019	[1]	DHA	↓ bone mass loss ↓ osteoclast differentiation ↓expression of TRAP and CTSK ↓ osteoclasts differentiation and bone remodeling ↓ RANKL ↓ levels of NFATc1 and MITF ↓ angiogenesis ↓ VEGF–VEGFR2 signaling pathway	ACLT rat OA model; RAW264.7 cells; HUVECs cells	
Yu et al., 2015	[45]	LA/ALA	↓ MMP-13 and IL-1 ↓ paw swelling rate and cartilage damage	Inflammatory human chondrocytes; Sprague-Dawley rats with arthritis induced by Freund's complete adjuvant	
Wang et al., 2016	[46]	DHA	↓ MMP-13 ↓ IL-1β-induced p38 activation ↑ thickness of articular cartilage	Human chondrosarcoma SW1353 cells; rat model of AIA	
Xu et al., 2019	[48]	DHA	↓ apoptosis ↓ activation of the MAPK signaling pathway	Human chondrosarcoma SW1353 cells	
D'Adamo et al., 2020	[7]	EPA	↓ apoptosis in the presence of oxidative stress	Mouse model of OA	
Phitak et al., 2018	[52]	EPA and DHA	↓ cartilage damage ↓ ADAMTS4 secretion ↓ NF-κB and JNK activation	Porcine cartilage explant and HACs	
Kimmerling et al., 2020	[54]	n-6 PUFAs	↑ serum content of n-3 PUFAs ↓ OA and synovitis ↑ body weight ↓ IFN-γ, TNF-α, and MCP-1 ↑ anti-inflammatory response	Fat-1 transgenic mouse model with PTOA induced by DMM surgery	
Wu et al., 2017	[53]	HFD rich in SFA, n-3 PUFAs, or n-6 PUFAs.	↑ n-3 PUFAs, ↓ OA severity, ↑ anti-inflammatory response	Mouse model of OA induced by DMM surgery	
Lu et al., 2017	[55]	Diet rich in total fat, SFAs, MUFAs, and PUFAs	↑ total fat and SFAs ↓ JSW ↑ knee OA progression ↑ MUFAs and PUFAs ↑ JSW ↓ knee OA progression		Subjects with knee OA
Chen et al., 2018	[56]	DHA	↑ GPR120 activation ↑ anti-inflammatory effects	GPR120 knockout mice with OA induced by ACLT; human chondrocytes	OA patients
Akbar et al., 2017	[38]	Diet supplemented with fish oil	↓ WOMAC scores ↓ pain ↓ use of NSAIDs/analgesic		OA patients

TABLE 1: Continued.

First author, year	References	Treatment	Properties	*In vitro/in vivo* models	Clinical trials
Sasahara et al., 2020	[59]	L-serine and EPA	↓ lumbar and knee pain		Patients with lower-back and knee pain
Lu et al., 2020	[60]	Maresin-1	↑ COL2A1 ↓ MMP-13 ↑ PI3k/Akt signaling pathway activation ↓ NF-κB p65 signaling pathway	Rat model of OA induced by MIA; IL-1β -induced rat FLSs	
Benabdoune et al., 2016	[61]	RvD1	↓ COX-2, iNOS, MMP-13 ↓ p38/MAPK, JNK 1/2, and NF-κB p65 signaling pathways ↓ PGE2 and NO ↓ pain ↓ activation of caspase-3 and -9 ↓ LDH release ↑ Bcl2 and AKT ↑ GSH pool ↓ oxidative stress-induced apoptosis	Human OA chondrocytes treated with IL-1β or HNE	
Sun et al., 2019	[62]	RvD1	↑ macrophages' gene expression from a proinflammatory condition to an anti-inflammatory state ↓ cartilage degradation	Obese mice model with PTOA induced by DMM surgery	

↑ increase, ↓ decrease. DHA: docosahexaenoic acid; ACLT: anterior cruciate ligament transection; OA: osteoarthritis; RAW264.7: mouse mononuclear macrophage leukemia cells; HUVECs: human umbilical vein endothelial cells; TRAP: tartrate-resistant acid phosphatase; CTSK: cathepsin K; RANKL: receptor activator of nuclear factor kappa-*B* ligand; NFATc1: nuclear factor of activated T-cells, cytoplasmic 1; MITF: microphthalmia-associated transcription factor; VEGF: vascular endothelial growth factor; VEGFR2: VEGF receptor 2; LA: linoleic acid; ALA: α-linolenic acid; MMP-13: matrix metalloproteinase-13; IL-1β: interleukin-1β; AIA: adjuvant-induced arthritis; MAPK: mitogen activated protein kinase; EPA: eicosapentaenoic acid; ADAMTS4: disintegrin and metalloproteinase with thrombospondin motifs-4; NF-κB: nuclear factor-κB; JNK: c-Jun N-terminal kinases; HACs: human articular chondrocytes; n-6,-3 PUFAs: n-6,-3 polyunsaturated fatty acids; IFN-γ: interferon-γ; TNF-α: tumor necrosis factor-α; MCP-1: monocyte chemoattractant protein-1; PTOA: posttraumatic osteoarthritis; DMM: destabilization of the medial meniscus; HFD: high-fat diet; SFA: saturated fatty acids; MUFAs: monounsaturated fatty acids; JSW: joint space width; GPR120: G-protein coupled receptor 120; WOMAC: western Ontario and McMaster universities arthritis index; NSAIDs: nonsteroidal anti-inflammatory drugs; COL2A1: type II collagen; PI3K/Akt: phosphatidylinositol 3-kinase/protein kinase B; MIA: monosodium iodoacetate; FLSs: fibroblast-like synoviocytes; RvD1: resolvin D1; COX-2: cyclooxygenase-2; iNOS: inducible nitric oxide synthase; p38/MAPK: p38/mitogen activated protein kinase; NF-κB p65: nuclear factor-κB p65 subunit; PGE2: prostaglandin E2; NO: nitric oxide; HNE: 4-hydroxynonenal; LDH: lactate dehydrogenase; Bcl-2: B-cell lymphoma-2; GSH: glutathione.

maresin-1, a metabolite of DHA, a study was conducted in rats with OA, whereby endogenous maresin-1 was measured in the intra-articular lavage fluid (IALF) of rats in single-session treadmill experiments [60]. In another group of rats, OA was induced by monosodium iodoacetate (MIA) in the presence of exogenous maresin-1. Finally, the possible action mechanisms of maresin-1 were examined in IL-1β-induced rat FLSs. ELISA showed that 4 hours after exercise, the maresin-1 levels in IALF were higher, while in the MIA model of OA, there was an increase in COL2A1 in the cartilage and a reduction in MMP-13 in the synovium. *In vitro* experiments also recorded MMP-13 reductions, indicating PI3k/Akt (phosphatidylinositol 3-kinase/protein kinase B) signaling pathway activation

and NF-κB p65 signaling pathway inhibition as action mechanism of maresin-1.

4.5.2. Anti-Inflammatory, Antiapoptotic, and Antioxidant Role of RvD1.
D resolvins (RvD) are other DHA derivatives [61]. In particular, RvD1's anti-inflammatory, anticatabolic, and antiapoptotic properties were tested in human OA chondrocytes treated with IL-1β or HNE (4-hydroxynonenal). It is known from previous dog OA experiments that the level of RvD1 increases in the synovial fluids of dogs to resolve inflammatory conditions, but it has also been shown that RvD1 can regulate signaling pathways involved in oxidative stress and cell death. Research on OA chondrocytes has shown that RvD1 inhibits both mRNA transcription
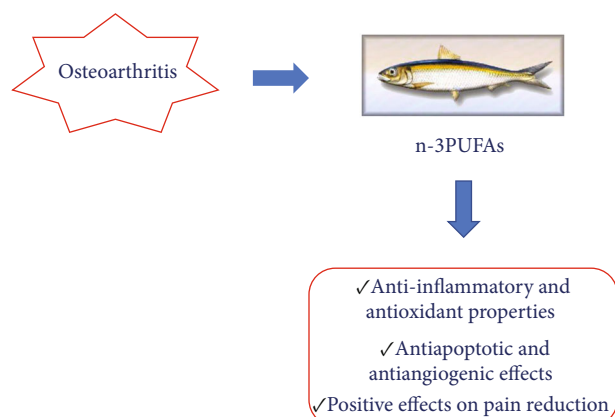
Figure 1: Main properties of n-3 PUFAs in OA treatment.

and COX-2, iNOS, and MMP-13 protein expression. It has been demonstrated that RvD1 deactivates the p38/MAPK, JNK 1/2, and NF-κB p65 signaling pathways, reducing IL-1β-induced inflammation in OA. Furthermore, the synthesis of PGE2 and NO is reduced, the accumulation of which is involved in OA progression and pain. In this experimental model, the involvement of apoptosis and oxidative stress in OA and RvD1's possible protective role was also investigated. Thus, apoptosis was induced by HNE treatment in OA chondrocytes pretreated with RvD1. The reported results confirm RvD1's antiapoptotic function, which would prevent damage to cartilage. In fact, RvD1 inhibited the HNE-induced activation of caspase-3 and -9, as well as LDH (lactate dehydrogenase) release, but it also increased antiapoptotic protein Bcl2 expression and reactivated Akt. The antioxidative role of RvD1 was demonstrated as the GSH (glutathione) pool was increased in OA chondrocytes. Therefore, supplementation with RvD1 can improve lesions and cartilage degradation, not only reducing the inflammatory state in OA but also preventing oxidative stress-induced apoptosis in OA chondrocytes, as RvD1 is able to restore redox status.

4.5.3. Association between Macrophages and RvD1. Additionally, in studying the relationship between OA, metabolic syndrome, and obesity, the roles of macrophage infiltration in the joint synovium and of RvD1 were investigated [62, 63]. The association between macrophages and RvD1 derives from the fact that, in inflamed tissues, resolvins mediate the transition of macrophages from a proinflammatory (M1) to an anti-inflammatory (M2) state; it also derives from the role that macrophage polarization plays in obesity-induced OA [62]. RvD1 could reduce this pathology by changing the macrophage proinflammatory condition. In order to verify this, C57Bl/6 mice were fed an HFD, and PTOA was induced by surgical destabilization of the meniscus. Under these conditions, it has been established that an HFD diet alone does not worsen cartilage degradation, whereas posttraumatic OA does. However, it has been found that an HFD worsens OA synovitis, resulting in greater macrophage infiltration, even in the absence of a posttraumatic event. Inflammation induced by obesity

under OA conditions is determined by both the migration and the local proliferation of synovial macrophages. Under these conditions, the role of macrophages has been confirmed by the intra-articular injection of clodronate liposomes, whose function is to analyze the effects of these cells. The resulting macrophage depletion improves synovitis and cartilage destruction in the obese mice model with PTOA. Once the role of macrophages in obesity-induced OA progression was verified, the effect of treatment with RvD1 was evaluated. RvD1's presence improves synovium thickening, as it changes the macrophages' gene expression from a proinflammatory condition to an anti-inflammatory state. Furthermore, under obese conditions, intra-articular RvD1 administration limits cartilage degradation by polarizing M2 macrophages. Moreover, randomized clinical trials have demonstrated a reduction in musculoskeletal pain in the presence of n-3 PUFAs, both in subjects with knee OA and in subjects with exercise-induced pain [64]. The effects of n-3 PUFAs on pain are attributable to cartilage degradation reduction and the increase in resolvins in synovial fluids.

5. Discussion and Conclusions

OA, considered by the Osteoarthritis Research Society International (OARSI) a disease characterized by molecular, anatomical, and physiological alterations, needs effective treatment with fewer side effects than current therapies [65]. Therefore, it has been shown that dietary interventions can yield positive results in preventing and slowing the disease. In this context, for example, polyphenols, thanks to their antioxidant and anti-inflammatory properties, are effective. In particular, Valsamidou et al. reported preclinical and clinical studies attesting the positive role of combined polyphenols in the OA treatment [65]. In this review, however, we wanted to focus on the latest research related to the treatment of OA with other components of the diet, PUFAs. *In vitro* and *in vivo* studies, as well as studies on patients, have shown that nutraceuticals such as n-3 PUFAs can prevent and counteract joint degeneration and cartilage loss in OA. Their efficacy is demonstrated at various molecular levels, but their anti-inflammatory and antioxidant properties seem to have a greater chondroprotective role. In addition, clinical trials have also reported their positive effect on the reduction of pain associated with OA, which is very important as it could improve patients' quality of life (Table 1) (Figure 1).

Conflicts of Interest

The authors declare no conflict of interest.

Authors' Contributions

V.M. (Vincenzo Mollace) and F.O. conceptualized and designed the review. F.O. and V.M. (Vincenzo Mollace) wrote the manuscript. F.O., R.M.B., J.M., M.G., V.M. (Vincenzo Musolino), C.C., S.I., M.S., C.M., S.G., E.P, and V.M (Vincenzo Mollace) participated in drafting the article and

References

[1] Y. Xie, W. Zhou, Z. Zhong, H. Yu, P. Zhang, and H. Shen, "Docosahexaenoic acid inhibits bone remodeling and vessel formation in the osteochondral unit in a rat model," *Biomedicine & Pharmacotherapy*, vol. 114, pp. 1–8, 2019.

[2] P. Castrogiovanni, F. M. Trovato, C. Loreto, H. Nsir, M. A. Szychlinska, and G. Musumeci, "Nutraceutical supplements in the management and prevention of osteoarthritis," *International Journal of Molecular Sciences*, vol. 17, pp. 1–14, 2016.

[3] G. J. Lee, I. A. Cho, K. R. Kang et al., "Biological effects of the herbal plant-derived phytoestrogen Bavachin in primary rat chondrocytes," *Biological & Pharmaceutical Bulletin*, vol. 38, no. 8, pp. 1199–1207, 2015.

[4] V. S. Simons, G. Lochnit, J. Wilhelm, B. Ishaque, M. Rickert, and J. Steinmeyer, "Comparative analysis of peptide composition and bioactivity of different collagen hydrolysate batches on human osteoarthritic synoviocytes," *Scientific Reports*, vol. 8, pp. 1–10, 2018.

[5] N. S. Harasymowicz, A. Dicks, C. L. Wu, and F. Guilak, "Physiologic and pathologic effects of dietary free fatty acids on cells of the joint," *Annals of the New York Academy of Sciences*, vol. 1440, no. 1, pp. 36–53, 2019.

[6] S. A. Lee, B. R. Park, S. M. Moon, J. H. Hong, D. K. Kim, and C. S. Kim, "Chondroprotective effect of cynaroside in IL-1β-induced primary rat chondrocytes and organ explants via NF-κB and MAPK signaling inhibition," *Oxidative Medicine and Cellular Longevity*, vol. 2020, 11 pages, 2020.

[7] S. D'Adamo, S. Cetrullo, V. Panichi, E. Mariani, F. Flamigni, and R. M. Borzì, "Nutraceutical activity in osteoarthritis biology: a focus on the nutrigenomic role," *Cell*, vol. 9, pp. 1–24, 2020.

[8] J. Abusarah, H. Benabdoune, Q. Shi et al., "Elucidating the role of protandim and 6-gingerol in protection against osteoarthritis," *Journal of Cellular Biochemistry*, vol. 118, no. 5, pp. 1003–1013, 2017.

[9] Z. Zhang, D. J. Leong, L. Xu et al., "Curcumin slows osteoarthritis progression and relieves osteoarthritis-associated pain symptoms in a post-traumatic osteoarthritis mouse model," *Arthritis Research & Therapy*, vol. 18, pp. 1–12, 2016.

[10] N. Ahmad, M. Y. Ansari, and T. M. Haqqi, "Role of iNOS in osteoarthritis: pathological and therapeutic aspects," *Journal of Cellular Physiology*, vol. 235, no. 10, pp. 6366–6376, 2020.

[11] H. Ishitobi, Y. Sanada, Y. Kato et al., "Carnosic acid attenuates cartilage degeneration through induction of heme oxygenase-1 in human articular chondrocytes," *European Journal of Pharmacology*, vol. 830, pp. 1–8, 2018.

[12] A. Basu, B. T. Kurien, H. Tran et al., "Strawberries decrease circulating levels of tumor necrosis factor and lipid peroxides in obese adults with knee osteoarthritis," *Food & Function*, vol. 9, no. 12, pp. 6218–6226, 2018.

[13] S. Schadow, V. S. Simons, G. Lochnit et al., "Metabolic response of human osteoarthritic cartilage to biochemically characterized collagen hydrolysates," *International Journal of Molecular Sciences*, vol. 18, pp. 1–20, 2017.

[14] M. H. Park, J. C. Jung, S. Hill et al., "FlexPro MD®, a combination of krill oil, astaxanthin and hyaluronic acid, reduces pain behavior and inhibits inflammatory response in monosodium iodoacetate-induced osteoarthritis in rats," *Nutrients*, vol. 12, pp. 1–15, 2020.

[15] S. Ravalli, M. A. Szychlinska, R. M. Leonardi, and G. Musumeci, "Recently highlighted nutraceuticals for preventive management of osteoarthritis," *World Journal of Orthopedics*, vol. 9, no. 11, pp. 255–261, 2018.

[16] S. Ilari, C. Dagostino, V. Malafoglia et al., "Protective effect of antioxidants in nitric oxide/COX-2 interaction during inflammatory pain: the role of nitration," *Antioxidants*, vol. 9, pp. 1–15, 2020.

[17] M. Y. Ansari, N. M. Khan, and T. M. Haqqi, "A standardized extract of _Butea monosperma (Lam.)_ flowers suppresses the IL-1 β-induced expression of IL-6 and matrix-metalloproteases by activating autophagy in human osteoarthritis chondrocytes," *Biomedicine & Pharmacotherapy*, vol. 96, pp. 198–207, 2017.

[18] V. Malafoglia, M. Celi, C. Muscoli et al., "Lymphocyte opioid receptors as innovative biomarkers of osteoarthritic pain, for the assessment and risk management of opioid tailored therapy, before hip surgery, to prevent chronic pain and opioid tolerance/addiction development: OpMarkArt (opioids-markers-arthroprosthesis) study protocol for a randomized controlled trial," *Trials*, vol. 18, pp. 1–8, 2017.

[19] W. Raffaeli, V. Malafoglia, A. Bonci et al., "Identification of MOR-positive B cell as possible innovative biomarker (Mu Lympho-Marker) for chronic pain diagnosis in patients with fibromyalgia and osteoarthritis diseases," *International Journal of Molecular Sciences*, vol. 21, pp. 1–15, 2020.

[20] A. Wang, D. J. Leong, L. Cardoso, and H. B. Sun, "Nutraceuticals and osteoarthritis pain," *Pharmacology & Therapeutics*, vol. 187, pp. 167–179, 2018.

[21] A. Mariano, A. Di Sotto, M. Leopizzi et al., "Antiarthritic effects of a root extract from Harpagophytum procumbens DC: novel insights into the molecular mechanisms and possible bioactive phytochemicals," *Nutrients*, vol. 12, pp. 1–16, 2020.

[22] S. E. Martinez, R. Lillico, T. M. Lakowski, S. A. Martinez, and N. M. Davies, "Pharmacokinetic analysis of an oral multicomponent joint dietary supplement (Phycox®) in dogs," *Pharmaceutics*, vol. 9, pp. 1–15, 2017.

[23] R. Ganguly, D. Hasanally, A. Stamenkovic et al., "Alpha linolenic acid decreases apoptosis and oxidized phospholipids in cardiomyocytes during ischemia/reperfusion," *Molecular and Cellular Biochemistry*, vol. 437, no. 1-2, pp. 163–175, 2018.

[24] F. Oppedisano, C. Muscoli, V. Musolino et al., "The protective effect of Cynara cardunculus extract in diet-induced NAFLD: involvement of OCTN1 and OCTN2 transporter subfamily," *Nutrients*, vol. 12, pp. 1–13, 2020.

[25] C. Carresi, M. Gliozzi, V. Musolino et al., "The effect of natural antioxidants in the development of metabolic syndrome: focus

on bergamot polyphenolic fraction," *Nutrients*, vol. 12, pp. 1–24, 2020.

[26] F. Oppedisano, J. Maiuolo, M. Gliozzi et al., "The potential for natural antioxidant supplementation in the early stages of neurodegenerative disorders," *International Journal of Molecular Sciences*, vol. 21, pp. 1–17, 2020.

[27] F. Oppedisano, R. Macrì, M. Gliozzi et al., "The anti-inflammatory and antioxidant properties of n-3 PUFAs: their role in cardiovascular protection," *Biomedicine*, vol. 8, pp. 1–18, 2020.

[28] F. Lauro, L. A. Giancotti, S. Ilari et al., "Inhibition of spinal oxidative stress by bergamot polyphenolic fraction attenuates the development of morphine induced tolerance and hyperalgesia in mice," *PLoS One*, vol. 11, pp. 1–12, 2016.

[29] S. Ilari, L. A. Giancotti, F. Lauro et al., "Antioxidant modulation of sirtuin 3 during acute inflammatory pain: the ROS control," *Pharmacological Research*, vol. 157, pp. 1–11, 2020.

[30] C. Muscoli, F. Lauro, C. Dagostino et al., "Olea Europea-derived phenolic products attenuate antinociceptive morphine tolerance: an innovative strategic approach to treat cancer pain," *Journal of Biological Regulators and Homeostatic Agents*, vol. 28, no. 1, pp. 105–116, 2014.

[31] J. Maiuolo, C. Muscoli, M. Gliozzi et al., "Endothelial dysfunction and extra-articular neurological manifestations in rheumatoid arthritis," *Biomolecules*, vol. 11, pp. 1–18, 2021.

[32] M. Gliozzi, J. Maiuolo, F. Oppedisano, and V. Mollace, "The effect of bergamot polyphenolic fraction in patients with non alcoholic liver steato-hepatitis and metabolic syndrome," *PharmaNutrition*, vol. 4S, pp. S27–S31, 2016.

[33] S. Cheleschi, A. Fioravanti, A. De Palma et al., "Methylsulfonylmethane and mobilee prevent negative effect of IL-1β in human chondrocyte cultures via NF-κB signaling pathway," *International Immunopharmacology*, vol. 65, pp. 129–139, 2018.

[34] H. Aarsetoey, H. Grundt, O. Nygaard, and D. W. Nilsen, "The role of long-chained marine N-3 polyunsaturated fatty acids in cardiovascular disease," *Cardiology Research and Practice*, vol. 2012, 15 pages, 2012.

[35] Y. Adkins and D. S. Kelley, "Mechanisms underlying the cardioprotective effects of omega-3 polyunsaturated fatty acids," *The Journal of Nutritional Biochemistry*, vol. 21, no. 9, pp. 781–792, 2010.

[36] A. Y. Landa-Juárez, M. I. Ortiz, G. Castañeda-Hernández, and A. E. Chávez-Piña, "Participation of potassium channels in the antinociceptive effect of docosahexaenoic acid in the rat formalin test," *European Journal of Pharmacology*, vol. 793, pp. 95–100, 2016.

[37] T. Behl and A. Kotwani, "Omega-3 fatty acids in prevention of diabetic retinopathy," *The Journal of Pharmacy and Pharmacology*, vol. 69, no. 8, pp. 946–954, 2017.

[38] U. Akbar, M. Yang, D. Kurian, and C. Mohan, "Omega-3 fatty acids in rheumatic diseases: a critical review," *Journal of Clinical Rheumatology*, vol. 23, no. 6, pp. 330–339, 2017.

[39] E. J. Baker, E. A. Miles, G. C. Burdge, P. Yaqoob, and P. C. Calder, "Metabolism and functional effects of plant-derived omega-3 fatty acids in humans," *Progress in Lipid Research*, vol. 64, pp. 30–56, 2016.

[40] E. Messamore, D. M. Almeida, R. J. Jandacek, and R. K. McNamara, "Polyunsaturated fatty acids and recurrent mood disorders: phenomenology, mechanisms, and clinical application," *Progress in Lipid Research*, vol. 66, pp. 1–13, 2017.

[41] M. I. Ayuso, R. Gonzalo-Gobernado, and J. Montaner, "Neuroprotective diets for stroke," *Neurochemistry International*, vol. 107, pp. 4–10, 2017.

[42] G. S. de Castro and P. C. Calder, "Non-alcoholic fatty liver disease and its treatment with n-3 polyunsaturated fatty acids," *Clinical Nutrition*, vol. 37, no. 1, pp. 37–55, 2018.

[43] D. B. Jump, K. A. Lytle, C. M. Depner, and S. Tripathy, "Omega-3 polyunsaturated fatty acids as a treatment strategy for nonalcoholic fatty liver disease," *Pharmacology & Therapeutics*, vol. 181, pp. 108–125, 2018.

[44] V. Mollace, M. Gliozzi, C. Carresi, V. Musolino, and F. Oppedisano, "Re-assessing the mechanism of action of _n − 3_ PUFAs," *International Journal of Cardiology*, vol. 170, no. 2, pp. S8–S11, 2013.

[45] H. Yu, Y. Li, L. Ma et al., "A low ratio of n-6/n-3 polyunsaturated fatty acids suppresses matrix metalloproteinase 13 expression and reduces adjuvant-induced arthritis in rats," *Nutrition Research*, vol. 35, no. 12, pp. 1113–1121, 2015.

[46] Z. Wang, A. Guo, L. Ma et al., "Docosahexaenoic acid treatment ameliorates cartilage degeneration via a p38 MAPK-dependent mechanism," *International Journal of Molecular Medicine*, vol. 37, no. 6, pp. 1542–1550, 2016.

[47] D. Apostu, O. Lucaciu, A. Mester et al., "Systemic drugs with impact on osteoarthritis," *Drug Metabolism Reviews*, vol. 51, no. 4, pp. 498–523, 2019.

[48] F. Xu, Y. Song, and A. Guo, "Anti-apoptotic effects of docosahexaenoic acid in IL-1β-induced human chondrosarcoma cell death through involvement of the MAPK signaling pathway," *Cytogenetic and Genome Research*, vol. 158, no. 1, pp. 17–24, 2019.

[49] M. Tsubosaka, S. Kihara, S. Hayashi et al., "Gelatin hydrogels with eicosapentaenoic acid can prevent osteoarthritis progression in vivo in a mouse model," *Journal of Orthopaedic Research*, vol. 38, no. 10, pp. 2157–2169, 2020.

[50] A. Van de Vyver, S. Clockaerts, C. H. A. van de Lest et al., "Synovial fluid fatty acid profiles differ between osteoarthritis and healthy patients," *Cartilage.*, vol. 11, no. 4, pp. 473–478, 2020.

[51] S. Thomas, H. Browne, A. Mobasheri, and M. P. Rayman, "What is the evidence for a role for diet and nutrition in osteoarthritis?," *Rheumatology (Oxford, England)*, vol. 57, suppl_4, p. iv61-iv74, 2018.

[52] T. Phitak, K. Boonmaleerat, P. Pothacharoen, D. Pruksakorn, and P. Kongtawelert, "Leptin alone and in combination with interleukin-1-beta induced cartilage degradation potentially inhibited by EPA and DHA," *Connective Tissue Research*, vol. 59, no. 4, pp. 316–331, 2018.

[53] C. L. Wu, K. A. Kimmerling, D. Little, and F. Guilak, "Serum and synovial fluid lipidomic profiles predict obesity-associated osteoarthritis, synovitis, and wound repair," *Scientific Reports*, vol. 7, pp. 1–11, 2017.

[54] K. A. Kimmerling, S. J. Oswald, J. L. Huebner et al., "Transgenic conversion of ω-6 to ω-3 polyunsaturated fatty acids via fat-1 reduces the severity of post-traumatic osteoarthritis," *Arthritis Research & Therapy*, vol. 22, pp. 1–10, 2020.

[55] B. Lu, J. B. Driban, C. Xu, K. L. Lapane, T. E. McAlindon, and C. B. Eaton, "Dietary fat intake and radiographic progression of knee osteoarthritis: data from the osteoarthritis initiative," *Arthritis Care Res. (Hoboken)*, vol. 69, no. 3, pp. 368–375, 2017.

[56] Y. Chen, D. Zhang, K. W. Ho et al., "GPR120 is an important inflammatory regulator in the development of osteoarthritis," *Arthritis Research & Therapy*, vol. 20, pp. 1–11, 2018.

[57] M. Loef, J. W. Schoones, M. Kloppenburg, and A. Ioan-Facsinay, "Fatty acids and osteoarthritis: different types, different effects," *Joint, Bone, Spine*, vol. 86, no. 4, pp. 451–458, 2019.

[58] K. T. Sibille, C. King, T. J. Garrett et al., "Omega-6: omega-3 PUFA ratio, pain, functioning, and distress in adults with knee pain," *The Clinical Journal of Pain*, vol. 34, no. 2, pp. 182–189, 2018.

[59] I. Sasahara, A. Yamamoto, M. Takeshita et al., "l-Serine and EPA relieve chronic low-Back and knee pain in adults: a randomeized, double-blind, placebo-controlled trial," *The Journal of nutrition*, vol. 150, no. 9, pp. 2278–2286, 2020.

[60] J. Lu, X. Feng, H. Zhang et al., "Maresin-1 suppresses IL-1β-induced MMP-13 secretion by activating the PI3K/AKT pathway and inhibiting the NF-κB pathway in synovioblasts of an osteoarthritis rat model with treadmill exercise," *Connective Tissue Research*, vol. 62, no. 5, pp. 508–518, 2021.

[61] H. Benabdoune, E. P. Rondon, Q. Shi et al., "The role of resolvin D1 in the regulation of inflammatory and catabolic mediators in osteoarthritis," *Inflammation Research*, vol. 65, no. 8, pp. 635–645, 2016.

[62] A. R. Sun, X. Wu, B. Liu et al., "Pro-resolving lipid mediator ameliorates obesity induced osteoarthritis by regulating synovial macrophage polarisation," *Scientific Reports*, vol. 9, pp. 1–13, 2019.

[63] B. M. Dickson, A. J. Roelofs, J. J. Rochford, H. M. Wilson, and C. De Bari, "The burden of metabolic syndrome on osteoarthritic joints," *Arthritis Research & Therapy*, vol. 21, pp. 1–10, 2019.

[64] C. R. Mendonça, M. Noll, M. C. R. Castro, and E. A. Silveira, "Effects of nutritional interventions in the control of musculoskeletal pain: an integrative review," *Nutrients*, vol. 12, pp. 1–17, 2020.

[65] E. Valsamidou, A. Gioxari, C. Amerikanou, P. Zoumpoulakis, G. Skarpas, and A. C. Kaliora, "Dietary interventions with polyphenols in osteoarthritis: a systematic review directed from the preclinical data to randomized clinical studies," *Nutrients*, vol. 13, pp. 1–18, 2021.

Research Article

Inflammatory Response and Oxidative Stress as Mechanism of Reducing Hyperuricemia of *Gardenia jasminoides-Poria cocos* with Network Pharmacology

Lijun Liu [1,2] **Shengjun Jiang** [2] **Xuqiang Liu** [2] **Qi Tang** [2,3,4] **Yan Chen** [2,3,4]
Jiaojiao Qu [2,3,4] **Li Wang** [2,3,4] **Qiang Wang** [5] **Yanli Wang** [5] **Jinmei Wang** [2]
Yan Zhang [6] **and Wenyi Kang** [2]

[1]*Huaihe Hospital, Henan University, Kaifeng 475004, China*
[2]*National R&D Center for Edible Fungus Processing Technology, Henan University, Kaifeng, 475004 Henan, China*
[3]*Joint International Research Laboratory of Food & Medicine Resource Function, Henan, Kaifeng 475004, China*
[4]*Functional Food Engineering Technology Research Center, Henan, Kaifeng 475004, China*
[5]*National Health Commission Key Laboratory of Birth Defect Prevention, Henan Institute of Reproductive Health Science and Technology, Zhengzhou 450002, China*
[6]*Hebei Food Inspection and Research Institute, Shijiazhuang 050091, China*

Correspondence should be addressed to Jinmei Wang; wangjinmeiscp@126.com, Yan Zhang; snowwinglv@126.com, and Wenyi Kang; kangweny@hotmail.com

Hyperuricemia (HUA) is a metabolic disease, closely related to oxidative stress and inflammatory responses, caused by reduced excretion or increased production of uric acid. However, the existing therapeutic drugs have many side effects. It is imperative to find a drug or an alternative medicine to effectively control HUA. It was reported that *Gardenia jasminoides* and *Poria cocos* could reduce the level of uric acid in hyperuricemic rats through the inhibition of xanthine oxidase (XOD) activity. But there were few studies on its mechanism. Therefore, the effective ingredients in *G. jasminoides* and *P. cocoa* extracts (GPE), the active target sites, and the further potential mechanisms were studied by LC-/MS/MS, molecular docking, and network pharmacology, combined with the validation of animal experiments. These results proved that GPE could significantly improve HUA induced by potassium oxazine with the characteristics of multicomponent, multitarget, and multichannel overall regulation. In general, GPE could reduce the level of uric acid and alleviate liver and kidney injury caused by inflammatory response and oxidative stress. The mechanism might be related to the TNF-α and IL-7 signaling pathway.

1. Introduction

Hyperuricemia (HUA) is the biochemical basis of gout, mainly caused by the decreased excretion or increased production of uric acid or both. In recent years, the number of patients with HUA has increased significantly, and it has shown a development trend of rejuvenation [1]. Uric acid is produced by xanthine oxidase (XOD), which could promote the activation of reduced coenzyme II (NAPDH) and

the release of reactive oxygen species (ROS), causing renal oxidative stress [2, 3]. Uric acid at normal concentrations exerts antioxidant effects *in vivo* but above normal physiological levels can act as a prooxidant to expand the body's oxidative stress damage [4–6]. While oxidative stress responses can activate inflammatory factors in kidney cells and induce innate immune responses *in vivo*, the activation of related proinflammatory factors induces the development of inflammation [7–9]. Hyperuricemia has been reported to

be closely related to oxidative stress and inflammatory responses [10]. At present, the drugs for the treatment of HUA in clinical practice including allopurinol, benzbromarone, and sodium bicarbonate can control the level of uric acid, but they have a series of toxic side effects such as liver and kidney function injury and hematopoietic dysfunction [11, 12]. Therefore, it is a hotspot to find the low-toxic and efficient antigout drugs from traditional Chinese medicine.

The fruit of *Gardenia jasminoides* is a traditional Chinese medicine which is commonly used to cure fever, red swelling, and pain [13]. *Poria cocos* could promote diuresis and dampness, strengthen the spleen, and calm the heart and is mainly used for the treatment of edema and diuretic detumescence medicine [14, 15]. *G. jasminoides* extracts can reduce uric acid levels in hyperuricemic mice by inhibiting XOD activity [16], but there are few studies on its mechanism.

Network pharmacology is a new method that integrates chemoinformatics, bioinformatics, traditional pharmacology, biological networks, and network analysis. Based on network pharmacology, the comprehensive network construction of medicinal components-active targets-disease targets of Chinese medicine can make the generalization of the pharmacological characteristics of Chinese medicine more comprehensive. In this study, the network pharmacology method combined with molecular docking was used, and the active ingredients in *G. jasminoides* and *P. cocoa* extracts (GPE) were used as the research objects to explore the efficacious ingredients, active targets, and potential mechanisms of GPE to reduce the high uric acid. Furthermore, animal experiments were carried out to verify the pharmacological effects of GPE.

2. Materials and Methods

2.1. Materials and Reagents

2.1.1. Instrument. Ultraperformance liquid chromatograph was purchased from Waters (Massachusetts, USA). High-resolution mass spectrometer (Q Exactive) was purchased from Thermo Fisher Scientific (Massachusetts, USA). Hypersil GOLD aQ column ($100 \text{ mm} \times 2.1 \text{ mm}$, $1.9 \mu\text{m}$) was purchased from Thermo Fisher Scientific (Massachusetts, USA). A low-temperature high-speed centrifuge (Centrifuge 5430) was purchased from Eppendorf (Hamburg, Germany). A vortex finder (QL-901) was purchased from Qilinbeier Instrument Manufacturing Co., Ltd. (Haimen, China). A pure water meter (Milli-Q) was purchased from Integral Millipore Corporation (Massachusetts, USA).

2.1.2. Reagent. d_3-Leucine, $^{13}C_9$-phenylalanine, d_5-tryptophan, and $^{13}C_3$-progesterone were used as internal standard. Methanol (A454-4) and acetonitrile (A996-4) were both chromatographic reagents, which were purchased from Thermo Fisher Scientific (Massachusetts, USA). Ammonium formate (17843–250 G) was obtained from Honeywell Fluka (New Jersey, USA). Formic acid (50144–50 mL) was obtained from DIMKA (Los Angeles, USA).

2.1.3. Materials. *Gardenia jasminoides* Ellis (1 kg) and *Poria cocos* (Schw.) Wolf (1 kg) were purchased from the Yuzhou Medicinal Material Market (Yuzhou, China) and identified as *Gardenia jasminoides* Ellis (Rubiaceae) and *Poria cocos* (Schw.) by Professor Changqin Li at Henan University (Kaifeng, China). The voucher specimen (20200718) was deposited in the National Research and Development Center of Edible Fungi Processing Technology, Henan University.

2.1.4. Preparation of Sample. The dried fruits of *G. jasminoides* and the dried sclerotia of *P. cocos* (1 : 1) were soaked in 15 L of water and decocted for 60 min and then filtered. The filter residues were decocted in 10 L of water for 30 min and filtered. The two filtrates were combined and freeze-dried to obtain GPE with a yield of 11%.

2.2. Chromatographic Methods

2.2.1. Chromatographic Conditions. Hypersil GOLD aQ column ($100 \text{ mm} \times 2.1 \text{ mm}$, $1.9 \mu\text{m}$) was used. The mobile phase was 0.1% formic acid-water (liquid A) and 0.1% formic acid-acetonitrile (liquid B) with the sequence as 0–2 min 5% B; 2–22 min 5–95% B; 22–27 min 95% B; 27.1–30 min 5% B. The flow rate was 0.3 mL/min, the column temperature was 40°C, and the injection volume was $5 \mu\text{L}$ [17].

2.2.2. Mass Spectrometry Conditions. The mass range was set at 150–1500 daltons, the MS resolution was 70000, the AGC was $1e^6$, and the maximum injection time was 100 ms. According to the strength of the MS ions, the top 3 peaks were selected for fragmentation. The MS^2 resolution was 35000, AGC is $2e^5$, the maximum injection time was 50 ms, and the fragmentation energy was set as 20, 40, and 60 eV. Ion source (ESI) parameter settings are as follows: sheath gas flow rate was 40 arb, aux gas flow rate was 10 arb, spray voltage of positive ion mode was 3.80 kV, spray voltage of negative ion mode was 3.20 kV, ion capillary temp was 320°C, and aux gas heater temp was 350°C [17].

2.2.3. Data Analysis. UPLC-MS/MS technology was used to systematically analyze the chemical constituents of GPE with positive and negative ion modes, respectively. The compounds were identified by comparing the retention time, accurate molecular weight, and MS^2 data with standard databases such as MZVault, MZCloud, and BGI Library (self-built standard Library by BGI Co., Ltd.).

2.3. Screening and Target Prediction of Active Compounds in GPE. The effective ingredients of GPE were screened by TCMSP database and LC-MS-MS identification results. The screening condition is oral bioavailability (OB) $\geq 30\%$. Drug likeness (DL) is greater than ≥ 0.18. At the same time, the target prediction of the Swiss target prediction platform is used. UniProt is used to standardize the names of the screened target proteins.

2.4. Acquisition of HUA Disease Targets. "High uric acid" as a keyword was used to search and screen databases such as GeneCards, Online Mendelian Inheritance in Man (OMIM),

PharmGkb, TTD, and DrugBank. Venny 2.1.0 was used to draw a Venn diagram to obtain HUA disease target.

2.5. Construction and Analysis of Protein Interaction Network.
Venny 2.1.0 was used to draw a Venn diagram and to obtain the intersection of GPE and the effective ingredients with the hyperuricemia target, which was the possible target of GPE in the treatment of hyperuricemia, and the intersection would be the target. A PPI protein interaction network was established in the database of the biomolecular functional annotation system STRING (https://string-db.org/), and the analysis was performed based on the results.

2.6. Topological Analysis of Protein Interaction Network (CytoNCA).
The PPI protein interaction files was imported and obtained from the STRING (https://string-db.org/) database into Bisogenet of Cytoscape to construct the PPI protein interaction network. CytoNCA in Cytoscape was used to perform topological analysis on the interaction network. The core network and key proteins for the treatment of HUA were obtained.

2.7. GO and KEGG Enrichment Analysis.
Gene Ontology (GO) was used to mainly analyze the gene and protein functions of various species from the three aspects: biological process (BP), cellular component (CC), and molecular function (MF). Kyoto Encyclopedia of Genes and Genomes (KEGG) pathway enrichment analysis is commonly used to clarify the role of target proteins in signaling pathways. In this study, the clusterProfiler program package in R language was used to perform GO enrichment analysis and KEGG (Kyoto Encyclopedia of Genes and Genomes) pathway analysis on shared targets. The corresponding target proteins in the GPE were directly mapped on the pathway where the drug target is enriched as the pathway for drug therapy, and a bubble chart is drawn for visualization.

2.8. Molecular Docking.
The 3D structure of the compound in GPE was obtained from PubChem (https://pubchem.ncbi.nlm.nih.gov/) and screened from the RCSB PDB (http://www.rcsb.org/) database. The water molecules and small ligand molecules of the core target protein from the crystal structure were removed, and the structure of the potential protein isolated. The genetic algorithm in the SYBYL-X software was used for semiflexible docking. The center coordinates and size of the box were set according to the position of the active site of the protein molecule and the area where it might have an effect on the small molecule of the ligand. The remaining parameters remained as default. The target protein was subjected to molecular docking analysis.

2.9. Animal Experiments

2.9.1. Materials and Reagents.
Potassium oxonate was purchased from Yuanye Biological Co., Ltd. (Shanghai, China). Benzbromarone was purchased from Heumann Pharma GmbH (Kunshan, China). CMC-Na was purchased from Shanghai Chemical Reagent Station Branch Factory (Shanghai, China). Uric acid (UA) content detection kit and XOD

activity detection kit were purchased from Solaibao Biotechnology Co., Ltd. (Beijing, China). Total superoxide dismutase (SOD), catalase (CAT), malondialdehyde (MDA), glutathione peroxidase (GSH-Px), total antioxidant capacity (T-AOC), blood urea nitrogen (BUN), creatinine (Cr), interleukin-1β (IL-1β), interleukin-6 (IL-6), interleukin (IL-2), interleukin-4 (IL-4), and tumor necrosis factor-α (TNF-α) detection kits were purchased from Nanjing Jiancheng Biotechnology Co., Ltd. (Nanjing, China). NADPH oxidase (NADPH-OX) kit, reactive oxygen species (ROS) kit, and β2 microglobulin (β2-MG) kit were purchased from Shanghai Jining Biotechnology Co., Ltd. (Shanghai, China).

2.9.2. Animals and Experimental Design

(1) Animals. Forty Specific Pathogen-Free (SPF) Sprague-Dawley (SD) male rats were provided by the Henan Laboratory Animal Center (laboratory animal license number: SCXK (Yu) 2017-0001). The rats were adapted for one week (temperature $25 \pm 2°C$, light circle 12 h/d, humidity 40 to 45%) before the experiment and fed with a standard diet with free access to water.

2.9.3. Experimental Grouping and Administration.
Thirty-six rats were randomly divided into six groups: blank control (BC) group, model control (MC) group, positive control (PC) group, GPE high-dose group (GPE-HD, 1000 mg/kg), medium-dose group (GPE-MD, 500 mg/kg), and low-dose group (GPE-LD, 250 mg/kg). The dosage of benzbromarone for the PC group was 8 mg/kg, and it was suspended with an appropriate amount of 0.5% CMC-Na. The BC group was administered with the same volume of 0.5% CMC-Na without benzbromarone.

2.9.4. Establishment of Hyperuricemic Rat Model.
Animal groups of GPE-HD, GPE-MD, and GPE-LD were administered for 15 d. Except for the blank group, the other groups were intraperitoneally injected with 300 mg/kg potassium oxonate 1 h before the last oral administration, and the blank group was injected with an equal volume of 0.5% CMC-Na. Two hours after the last administration, blood was collected from the abdominal aorta and centrifuged. The supernatant was collected by centrifugation at 3500 g for 10 min. The tissues of the liver and kidney were collected and frozen in a -80°C freezer.

2.9.5. Determination of Inflammatory Factors in Rat Plasma.
The contents of IL-2, IL-6, TNF-α, IL-4, and IL-1β in plasma were measured according to the ELISA kit instructions.

2.9.6. Determination of Antioxidative Stress Ability in Rats.
The liver tissues were collected to make tissue homogenates at the corresponding concentrations, and the activities of XOD, SOD, NADPH-OX, ROS, GSH-PX, T-AOC, CAT, and MDA in plasma and tissues were measured, respectively, according to the kit instructions.

2.9.7. Effects of Samples on Liver and Kidney Function Injury.
The contents of BUN, Cr, β_2-MG, and XOD in plasma were determined in strict accordance with the kit instructions.

TABLE 1: The compounds identified from GPE by LC-MS-MS in positive model.

RT (min)	Adducts	Formula	Measured value	Molecular weight	Name
0.871	$[M+H]^+$	$C_{10}H_{14}N_5O_7P$	347.06293	348.07007	Adenosine 5′-monophosphate
1.012	$[M+H]^+$	$C_6H_{14}O_6$	182.07906	183.08633	Galactitol
1.115	$[M+H]^+$	$C_9H_{11}NO_3$	181.07413	182.08142	L-tyrosine
1.12	$[M+H]^+$	$C_{10}H_{13}NO_4$	267.09656	268.1037	Adenosine
3.05	$[M+H]^+$	$C_{11}H_9NO_2$	187.06352	188.0708	Indole-3-acrylic acid
3.834	$[M+H]^+$	$C_{16}H_{26}O_8$	346.16224	347.17001	Jasminoside B
3.978	$[M+H]^+$	$C_{10}H_{12}N_2$	160.10024	161.10744	Tryptamine
4.18	$[M+H]^+$	$C_{10}H_{14}O$	150.1046	151.11189	Carvone
4.607	$[M+H]^+$	$C_{14}H_{14}N_2O_5$	290.09014	291.09741	Indole-3-acetyl-l-aspartic acid
5.912	$[M+H]^+$	$C_{15}H_{22}O_2$	234.16208	235.16927	Artemisinic acid
6.153	$[M+H]^+$	$C_{33}H_{40}O_{19}$	740.21617	741.22345	Mauritianin
6.216	$[M+H]^+$	$C_{10}H_{10}O_4$	194.05802	195.06546	Isoferulic acid
6.274	$[M+H]^+$	$C_{10}H_{16}O$	152.12026	153.12759	α-Pinene-2-oxide
6.295	$[M+H]^+$	$C_{27}H_{30}O_{16}$	610.15294	611.16016	Rutin
6.357	$[M+H]^+$	$C_{27}H_{30}O_{16}$	610.15294	611.15985	Rutin
6.514	$[M+H]^+$	$C_{10}H_{12}O_2$	164.08388	165.09126	4-Phenylbutyric acid
6.526	$[M+H]^+$	$C_{21}H_{20}O_{12}$	464.09551	465.10303	Isoquercitrin
6.531	$[M+H]^+$	$C_{15}H_{10}O_7$	302.04238	303.04974	Quercetin
6.84	$[M+H]^+$	$C_{27}H_{30}O_{15}$	594.1591	595.16565	Kaempferol-3-O-rutinoside
7.252	$[M+H]^+$	$C_9H_8O_3$	164.04749	165.05476	3-Hydroxycinnamic acid
7.407	$[M+H-H_2O]^+$	$C_{10}H_{10}O_4$	194.058	177.05469	Ferulic acid
10.436	$[M+H]^+$	$C_{12}H_{17}NO$	191.13118	192.13846	DEET
10.839	$[M+H]^+$	$C_{21}H_{32}O_2$	316.24007	317.24747	Pregnenolone
11.096	$[M+H]^+$	$C_{15}H_{18}O_2$	230.13068	231.13805	Dehydrocostus lactone
12.931	$[M+H]^+$	$C_{24}H_{30}O_6$	414.20437	415.21176	Bis(4-ethylbenzylidene)sorbitol
13.036	$[M+H]^+$	$C_{20}H_{34}O_2$	306.25575	307.26303	11(z),14(z),17(z)-Eicosatrienoic acid
14.969	$[M+H]^+$	$C_{18}H_{30}O_2$	278.22439	279.23169	A-Eleostearic acid
15.833	$[M+H]^+$	$C_{18}H_{30}O_3$	294.21933	295.22665	9-Oxo-10(e),12(e)-octadecadienoic acid
16.83	$[M+H]^+$	$C_{22}H_{32}O_2$	328.24016	329.24728	Docosahexaenoic acid
17.661	$[M+H]^+$	$C_{21}H_{38}O_4$	354.27686	355.28418	1-Linoleoyl glycerol
17.749	$[M+H]^+$	$C_{20}H_{34}O_2$	306.25572	307.26303	Γ-Linolenic acid ethyl ester
17.775	$[M+H-H_2O]^+$	$C_{33}H_{52}O_5$	528.3822	529.38953	Pachymic acid
18.518	$[M+H]^+$	$C_{16}H_{30}O_2$	254.2246	255.23183	Palmitoleic acid
18.577	$[M+H-H_2O]^+$	$C_{30}H_{48}O_3$	456.36039	457.36777	Ursolic acid
18.601	$[M+H]^+$	$C_{18}H_{37}NO_2$	299.28224	300.28952	Palmitoylethanolamide
18.962	$[M+H]^+$	$C_{21}H_{40}O_4$	356.29248	357.29977	Monoolein
19.038	$[M+H-H_2O]^+$	$C_{30}H_{46}O_3$	454.34482	455.35299	Dehydrotrametenolic acid
19.74	$[M+H]^+$	$C_{18}H_{35}NO$	281.27173	282.27899	Oleamide
20.128	$[M+H]^+$	$C_{16}H_{33}NO$	255.25618	256.26346	Hexadecanamide
20.812	$[M+H]^+$	$C_{20}H_{34}O_2$	306.25572	307.26303	Linolenic acid ethyl ester
22.464	$[M+H]^+$	$C_{18}H_{37}NO$	283.2874	284.29468	Stearamide
23.556	$[M+H]^+$	$C_{22}H_{43}NO$	337.3344	338.34174	Erucamide

TABLE 2: The compounds identified from GPE by LC-MS-MS in negative model.

RT (min)	Adducts	Formula	Measured value	Molecular weight	Name
0.769	[M-H]⁻	$C_{17}H_{27}N_3O_{17}P_2$	607.08107	606.07379	UDP-n-Acetylglucosamine
0.943	[M-H]⁻	$C_6H_{12}O_7$	196.05816	195.05075	Gluconic acid
0.945	[M-H]⁻	$C_{12}H_{22}O_{11}$	342.11583	341.10855	α,α-Trehalose
0.946	[M-H]⁻	$C_6H_{12}O_6$	180.06327	179.05606	L-Sorbose
0.999	[M-H]⁻	$C_4H_6O_5$	134.02147	133.01421	DL-Malic acid
1.113	[M-H]⁻	$C_6H_8O_7$	192.02686	191.01958	Citric acid
1.154	[M-H]⁻	$C_4H_6O_4$	118.02666	117.01942	Succinic acid
1.358	[M-H]⁻	$C_7H_6O_5$	170.02148	169.01421	Gallic acid
1.87	[2M-H]⁻	$C_{16}H_{24}O_{11}$	392.13228	391.12427	Shanzhiside
2.756	[M-H]⁻	$C_{16}H_{18}O_9$	354.0948	353.08759	Neochlorogenic acid
3.056	[M-H]⁻	$C_{16}H_{24}O_{10}$	376.13649	375.12929	Mussaenosidic acid
4.441	[M-H]⁻	$C_{16}H_{24}O_{10}$	376.13663	375.12943	Loganic acid
4.454	[M-H]⁻	$C_{16}H_{18}O_9$	354.0948	353.08762	Cryptochlorogenic acid
4.529	[M-H]⁻	$C_9H_6O_4$	178.02656	177.01924	Esculetin
4.554	[M+FA-H]⁻	$C_{23}H_{34}O_{15}$	550.18934	549.18079	Genipin 1-O-β-D-gentiobioside
4.663	[M-H]⁻	$C_9H_8O_4$	180.04225	179.03493	Caffeic acid
4.902	[M-H]⁻	$C_{16}H_{18}O_9$	354.0948	353.08762	Chlorogenic acid
5.028	[M+FA-H]⁻	$C_{17}H_{24}O_{10}$	388.13649	387.12878	Geniposide
5.69	[M-H]⁻	$C_7H_8O_2$	124.05246	123.04516	4-Hydroxybenzyl alcohol
5.734	[M-H]⁻	$C_9H_8O_3$	164.04736	163.04008	3-Coumaric acid
5.847	[M-H]⁻	$C_8H_{14}O_4$	174.08906	173.08179	Suberic acid
6.356	[M-H]⁻	$C_{11}H_{12}O_5$	224.06829	223.06102	Sinapic acid
6.384	[M-H]⁻	$C_{27}H_{30}O_{16}$	610.15473	609.14746	Rutin
6.556	[M-H]⁻	$C_{21}H_{20}O_{12}$	464.09505	643.08768	Isoquercitrin
6.729	[M-H]⁻	$C_{25}H_{24}O_{12}$	516.12591	515.11871	Isochlorogenic acid B
6.869	[M-H]⁻	$C_{27}H_{30}O_{15}$	594.1583	593.15118	Kaempferol-3-O-rutinoside
6.884	[M-H]⁻	$C_{25}H_{24}O_{12}$	516.12587	515.11884	3,5-Dicaffeoylquinic acid
7.057	[M-H]⁻	$C_{21}H_{20}O_{11}$	448.10017	447.0929	Astragalin
7.234	[M+cl]⁻	$C_{25}H_{24}O_{12}$	516.12591	551.0954	4,5-Dicaffeoylquinic
8.104	[M-H]⁻	$C_{15}H_{20}O_4$	264.13576	263.12848	(±)-Abscisic acid
8.451	[M-H]⁻	$C_{15}H_{10}O_7$	302.0424	301.03513	Morin
8.516	[M-H]⁻	$C_{15}H_{10}O_6$	286.04741	285.04013	Luteolin
10.273	[M-H]⁻	$C_{12}H_{14}O_4$	222.0889	221.08162	Monobutyl phthalate
11.813	[M-H]⁻	$C_{16}H_{12}O_5$	284.06801	283.06064	Acacetin
12.754	[M-H]⁻	$C_{18}H_{34}O_4$	314.24519	313.23782	(+/-)12(13)-Dihome
15.249	[M-H]⁻	$C_{31}H_{46}O_5$	498.33362	497.32639	Poricoic acid A
17.272	[M-H]⁻	$C_{32}H_{50}O_5$	514.36476	513.35754	3-O-Acetyl-1α-hydroxytrametenolic acid, pachymic acid
17.806	[M-H]⁻	$C_{33}H_{52}O_5$	528.38028	527.37286	Oleic acid alkyne
17.917	[M-H]⁻	$C_{18}H_{30}O_2$	278.2242	277.21689	Ursolic acid
18.595	[M-H]⁻	$C_{30}H_{48}O_3$	456.3596	455.35211	Ursolic acid

2.9.8. Pathological Changes of Liver and Kidney Tissues. Two hours after the last oral administration, the liver and kidney tissues were collected, washed with cold saline, fixed in 4% (wt/vol) paraformaldehyde solution for 24 h, rinsed in PBS for 6 h, dehydrated and embedded, then sliced into 5 μm sections by a microtome, stained with H&E, and observed and photographed under a microscope.

2.9.9. Detection of Uric Acid Levels in Rat Plasma. The content of UA in plasma was measured within 15-20 min in strict accordance with the kit instructions.

2.9.10. Statistical Processing. SPSS 19.0 software was used to process statistical data. Differences of data were analyzed by one-way ANOVA. Results were expressed as mean ±

TABLE 3: Effective ingredients in GPE.

MOL ID	Compound name	Source	Target no.
MOL000273	16α-Hydroxydehydrotrametenolic acid	*P. cocos*	2
MOL000275	Trametenolic acid	*P. cocos*	1
MOL000276	7,9(11)-Dehydropachymic acid	*P. cocos*	0
MOL000279	Cerevisterol	*P. cocos*	1
MOL000280	(2*R*)-2-[(3*S*,5*R*,10*S*,13*R*,14*R*,16*R*,17*R*)-3,16-Dihydroxy-4,4,10,13,14-pentamethyl-2,3,5,6,12,15,16,17-octahydro-1H-cyclopenta[a]phenanthren-17-yl]-5-isopropyl-hex-5-enoic acid	*P. cocos*	0
MOL000282	Ergosta-7,22E-dien-3beta-ol	*P. cocos*	1
MOL000283	Ergosterol peroxide	*P. cocos*	1
MOL000285	(2*R*)-2-[(5*R*,10*S*,13*R*,14*R*,16*R*,17*R*)-16-Hydroxy-3-keto-4,4,10,13,14-pentamethyl-1,2,5,6,12,15,16,17-octahydrocyclopenta[a]phenanthren-17-yl]-5-isopropyl-hex-5-enoic acid	*P. cocos*	0
MOL000287	Eburicoic acid	*P. cocos*	0
MOL000289	Poricoic acid	*P. cocos*	0
MOL000290	Poricoic acid A	*P. cocos*	0
MOL000291	Poricoic acid B	*P. cocos*	0
MOL000292	Poricoic acid C	*P. cocos*	0
MOL000296	Hederagenin	*P. cocos*	23
MOL000300	Dehydroeburicoic acid	*P. cocos*	0
MOL001406	Crocetin	*G. jasminoides*	14
MOL001663	3-Epioleanolic acid	*G. jasminoides*	0
MOL001941	Ammidin	*G. jasminoides*	8
MOL004561	Sudan III	*G. jasminoides*	13
MOL000098	Quercetin	*G. jasminoides*	153
MOL000358	Beta-sitosterol	*G. jasminoides*	37
MOL000422	Kaempferol	*G. jasminoides*	72
MOL000449	Stigmasterol	*G. jasminoides*	34
MOL001494	Mandenol	*G. jasminoides*	3
MOL001506	Supraene	*G. jasminoides*	0
MOL001942	Isoimperatorin	*G. jasminoides*	1
MOL002883	Ethyl oleate (NF)	*G. jasminoides*	1
MOL003095	5-Hydroxy-7-methoxy-2-(3,4,5-trimethoxyphenyl)chromone	*G. jasminoides*	26
MOL007245	3-Methylkempferol	*G. jasminoides*	11
MOL009038	GBGB	*G. jasminoides*	0
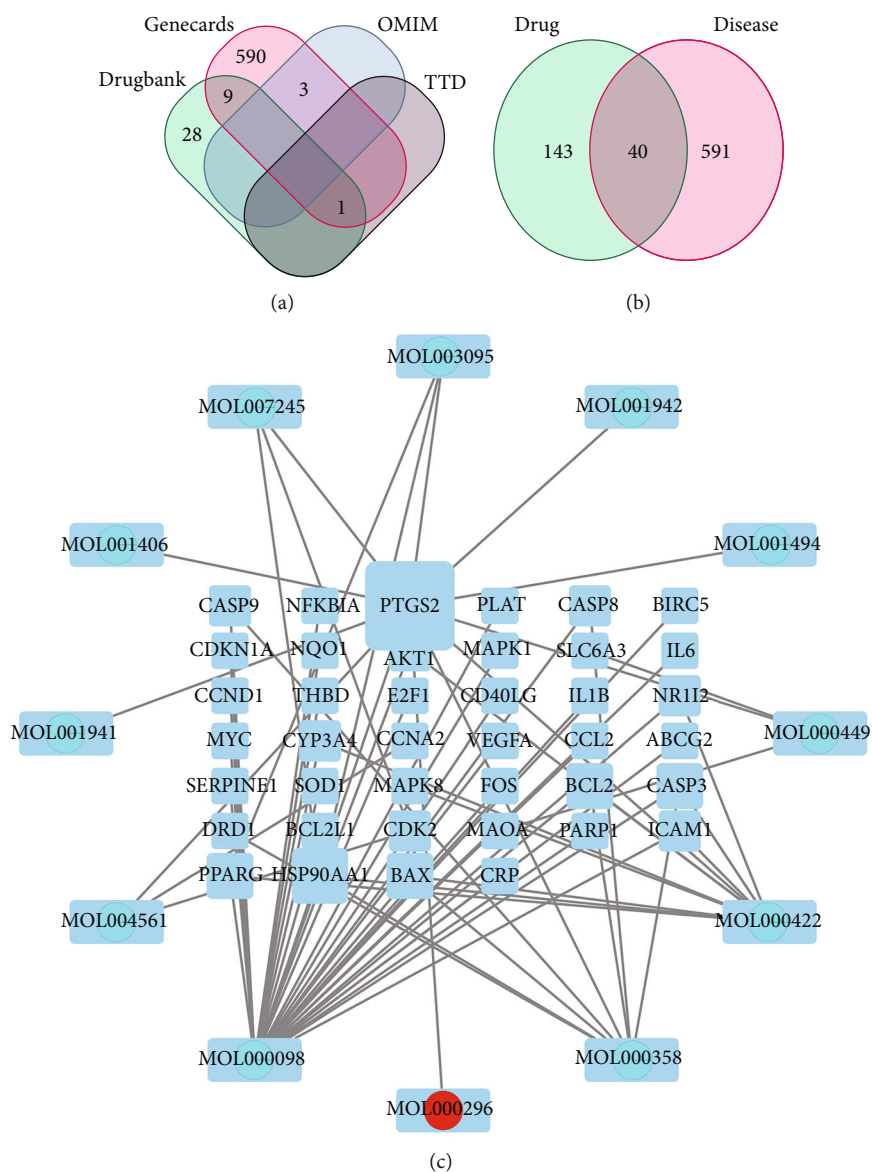
FIGURE 1: (a) HUA disease targets; (b) intersection of active component targets of GPE and hyperuricemic acid target; (c) regulation network of active components of GPE.

standard deviation (SD). $P < 0.05$ was considered significantly different.

3. Results and Analysis

3.1. Effective Ingredient Screening and Target Prediction in GPE.

Based on TCMSP database and LC-MS-MS identification results, the effective ingredients and target prediction data of GPE were selected (in Tables 1 and 2), and 30 effective compounds and corresponding gene targets of the GPE were obtained. The specific effective ingredients from GPE are illustrated in Table 3.

3.2. Intersection Analysis of the Effective Ingredient Targets of GPE and the Targets of HUA.

The 631 hyperuricemia-related targets were searched (Figure 1(a)) from GeneCards, Online Mendelian Inheritance in Man (OMIM), PharmGkb, TTD,

DrugBank, and other databases. There were 183 targets of GPE intersected with the disease targets, and 40 common targets of GPE and HUA were mapped as the Venn diagram (in Figure 1(b)).

3.3. GPE Effective Ingredient-Disease Target Regulatory Network.

Twelve effective ingredients and 40 related targets of GPE were introduced into Cytoscape 3.7.0 to obtain the "effective ingredient-target" regulatory network diagram (Figure 1(c)). In Figure 1(c), there were 52 nodes (12 ingredients, 40 targets) and 70 edges; round nodes represent active ingredients, square nodes represent corresponding targets, and black edges represent the relationship between active ingredients and HUA targets. The results showed that 58.3% (7) of the effective ingredients in GPE could act on multiple gene targets. Among them, quercetin, kaempferol, β-sitosterol, and hederagenin had

(a)

(b)

(c)
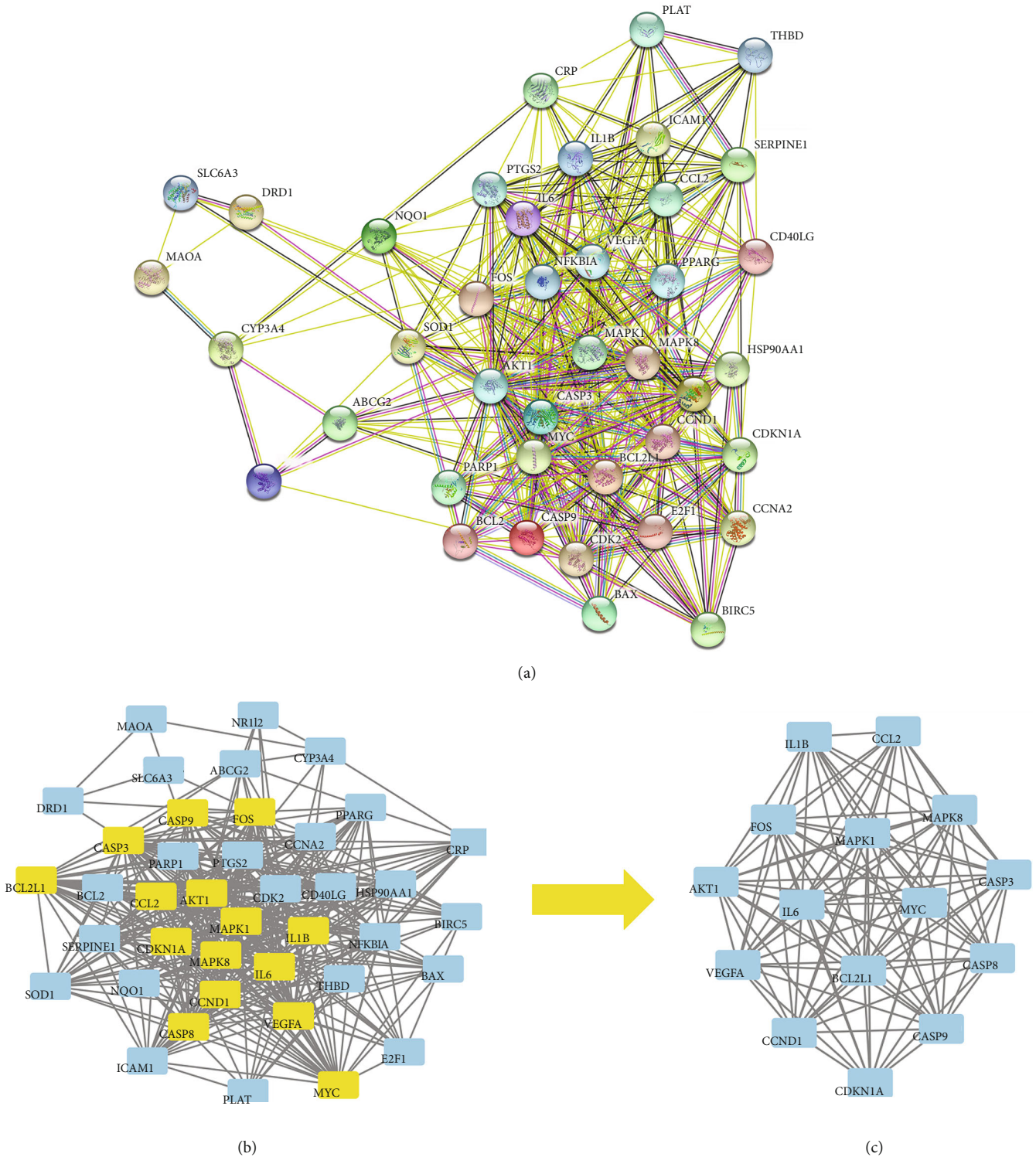
Figure 2: PPI protein interaction network of GPE in treatment of HUA targets (a) and CytoNCA Core Network Analysis (b, c).

many targets and played the important role in the regulation process. The same target could also be regulated by multiple effective ingredients. Thirteen targets (32.5%) were corresponding to more than two effective ingredients, indicating the complex and diverse action mechanism characteristics of GPE components.

3.4. Results of Core Target Screening and PPI Network Construction. The intersection target was imported into the STRING database, and the species was set as "Homo sapiens" to analyze protein interaction (Figure 2(a)). The relevant files were imported into the Cytoscape software to build a PPI network diagram; one node represented one

(a)

(b)
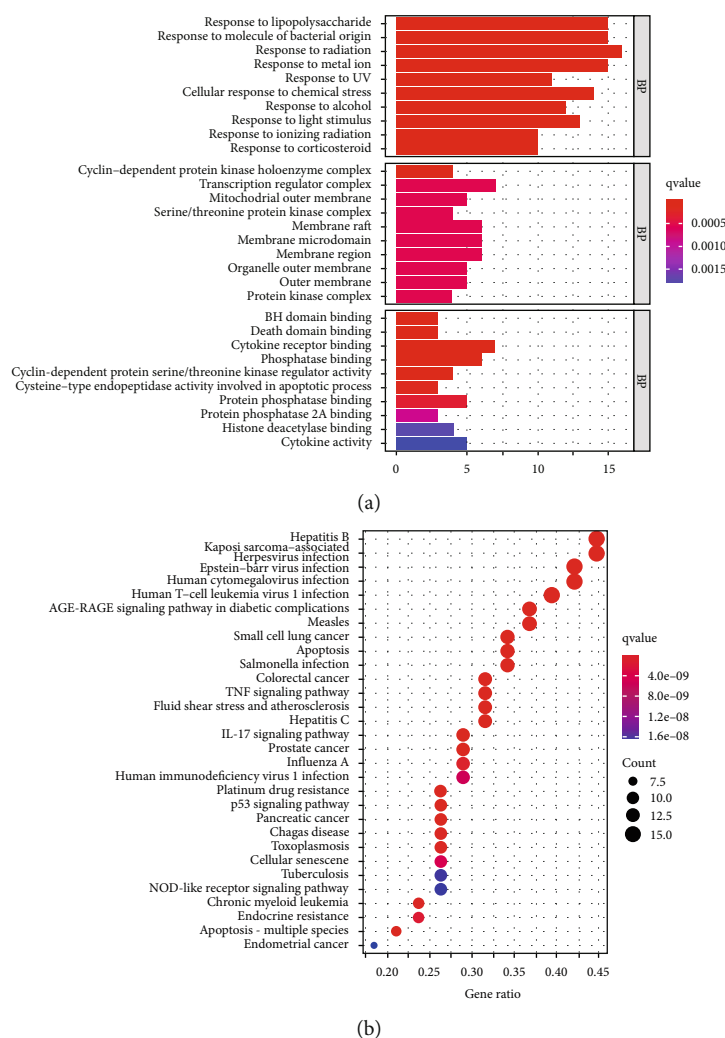
FIGURE 3: GO biological function enrichment bar chart (a) and KEGG pathway enrichment analysis bubble diagram (b).

target, and the TCMSP edge represented the target. We click on the interaction relationship and finally get the protein interaction network analysis diagram (Figure 2(a)). The network contained 15 key gene targets, i.e., IL-1B, IL-6, MAPK1, MAPK8, AKT1, MYC, VEGFA, CASP3, CASP8, CASP9, BCL2L1, FOS, CCND1, CDKN1A, and CCL2, which were the components of the core network (Figures 2(b) and 2(c)).

3.5. The Results of GO Function Enrichment Analysis.

GO describes the biological process (BP) of gene products (protein or RNA), molecular function (MF), and cellular component (CC) and organizes the functional concepts with different thicknesses into atlases for analysis and sorting according to P value (Figure 3(a)). In Figure 3(a), the abscissa represents the number of enriched genes and the color of the bar represents the size of the P value. When the color changed from blue to red, the P value changed to small. The process was mainly concentrated in the biological process, and there were 1591 enrichment results which were mainly involved in the reaction of oxidative stress, lipids,

TABLE 4: Binding energy of effective ingredients in GPE with potential HUA targets.

Compounds	Binding energy (kcal/mol)			
	AKT1	VEGFA	MAPK1	IL-6
Quercetin	-8.1	-6.9	-9.1	-9.4
Kaempferol	-8.1	-5.5	-7.5	-5.9
Hederagenin	-6.5	-7		

bacteria-derived molecules, and chemical substances. In molecular functions, there were 57 results which were related to cell death, cytokine receptors, and other enzyme activities. There were 27 enriched results for cell composition, which had the relationship with the cyclin-dependent protein kinase holoenzyme complex, transcription regulation complex, and mitochondrial outer membrane.

3.6. The Results of KEGG Pathway Enrichment Analysis.

The corresponding target protein of GPE was mapped to the

(a)

(b)

(c)

(d)

(e)

(f)
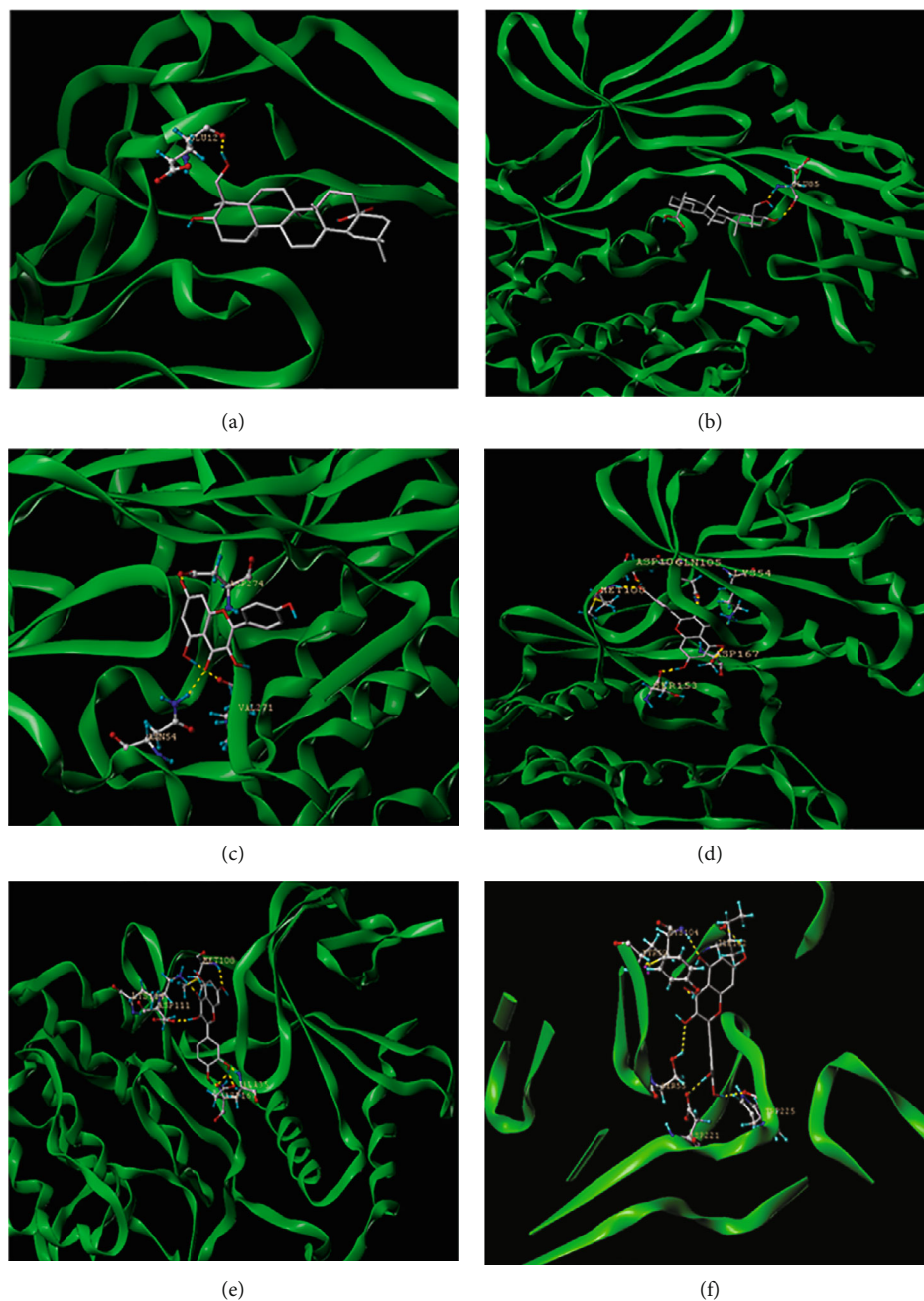
FIGURE 4: Molecular binding map of effective ingredients in GPE with HUA potential target: (a) hederagenin AKT1; (b) hederagenin VEGFA; (c) kaempferol AKT1; (d) kaempferol MAPK1; (e) quercetin IL-6; (f) quercetin MAPK1.

pathway by KEGG to analyze the activity, target, and pathway of drug. The signaling pathways mainly included the inflammatory signaling pathways of TNF and IL-7, apoptosis, tumors such as small cell lung cancer, and AGE-RAGE signaling pathway in diabetic complications. There were 139 pathways by the KEGG enrichment pathway analysis, and the top 20 pathways are shown in Figure 3(b).

3.7. Docking Prediction of Effective Ingredients and Core Target Molecules. The core targets of IL-6, AKT1, MYC, VEGFA, and MAPK1 protein with higher node degree

values and the best effective ingredients, quercetin, kaempferol, and hederagenin, in GPE were selected for molecular docking in the PPI protein interaction network (Table 4, Figure 4).

3.8. Verification of Animal Experiment

3.8.1. Effects on Plasma Uric Acid Levels of Hyperuricemic Rats. In Table 5 and Figure 5, the levels of uric acid in the model group were significantly increased compared with the blank group ($P < 0.001$), which indicated that the

TABLE 5: Effect of GPE on plasma uric acid levels in hyperuricemic rats (μg/mL, x̄ ± s) ($n = 6$).

Groups	UA
BC	3.37 ± 0.14
MC	5.56 ± 0.41[***]
PC	3.69 ± 0.06[###]
GPE-HD	4.64 ± 0.70[#]
GPE-MD	4.83 ± 0.25[#]
GPE-LD	3.70 ± 0.28[###]

Note: compared with BC, [*]$P < 0.05$, [**]$P < 0.01$, [***]$P < 0.001$; compared with MC, [#]$P < 0.05$, [##]$P < 0.01$, [###] $P < 0.001$.
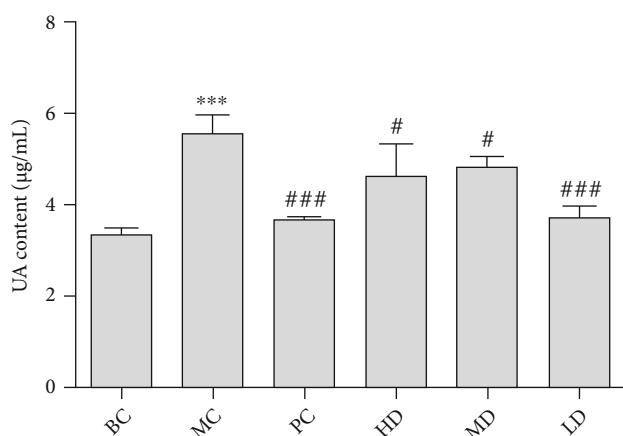
FIGURE 5: Effect of GPE on UA levels in hyperuricemic rats. Compared with BC, [*]$P < 0.05$, [**]$P < 0.01$, [***]$P < 0.001$; compared with MC, [#]$P < 0.05$, [##]$P < 0.01$, [###]$P < 0.001$.

hyperuricemic rat model was established. Compared with the MC, GPE-HD, GPE-MD, and GPE-LD could effectively reduce the levels of uric acid ($P < 0.05$). GPE-LD showed significant difference ($P < 0.001$), and there was no significant difference compared with the PC ($P > 0.05$).

3.8.2. Effect on Antioxidative Stress Ability of Hyperuricemic Rats. In Figures 6(b), 6(f), and 6(g), compared with BC, the contents of GSH-PX, T-AOC, and SOD in the plasma of MC were significantly decreased ($P < 0.001$), and the contents of CAT in the liver homogenate were significantly decreased ($P < 0.001$). In Figures 6(a), 6(c), 6(d), and 6(e), compared with BC, the contents of ROS, MDA, and NADPH in the plasma of MC were significantly increased ($P < 0.01$, $P < 0.001$, and $P < 0.01$, respectively); compared with MC, the levels of GSH-PX, T-AOC, and SOD in plasma of GPE-HD, GPE-MD, and GPE-LD were significantly increased ($P < 0.05$), and the contents of CAT in the liver homogenate of rats were significantly increased ($P < 0.05$). The contents of ROS, MDA, and NADPH in the plasma of GPE-HD, GPE-MD, and GPE-LD were significantly decreased ($P < 0.05$), indicating that GPE could improve oxidative stress produced by hyperuricemia.

3.8.3. Effect on Liver and Kidney Function in Hyperuricemic Rats. In Figure 7, compared with the BC, the contents of BUN, CRE, β2-MG, and XOD in the MC were significantly increased ($P < 0.05$); compared with the MC, the GPE-HD, GPE-MD, and GPE-LD could significantly reduce the BUN, CRE, β2-MG, and XOD in the plasma of rats ($P < 0.05$). Among them, the contents of β2-MG in the plasma of rats in the GPE-MD and GPE-HD were extremely significantly decreased ($P < 0.001$). It indicated that GPE could reduce uric acid in the plasma of hyperuricemic rats by reducing XOD activity and could improve liver and kidney damage produced by HUA.

3.8.4. Determination of Inflammatory Factors in Rat Plasma. In Figure 8, the expression levels of IL-1β, IL-2, IL-6, and TNF-α in the plasma in the MC were significantly increased compared with the BC ($P < 0.001$). The contents of IL-2, IL-6, and TNF-α in the plasma of the GPE-HD, GPE-MD, and GPE-LD were significantly decreased compared with those of the MC ($P < 0.05$), and the contents of IL-1β and IL-6 in the GPE-MD and GPE-HD were significantly decreased ($P < 0.001$). The contents of IL-4 in the plasma in the MC were significantly decreased compared with the those in the BC ($P < 0.001$). Compared with the MC, the IL-4 content in the plasma of the GPE-HD, GPE-MD, and GPE-LD was significantly increased ($P < 0.001$). The results showed that the GPE could improve the inflammatory level of hyperuricemia and also had an anti-inflammatory effect.

3.8.5. Pathological Changes of Renal Tissue in Rats. In Figure 9, the renal structure of BC was normal without inflammatory cell infiltration. In the MC group of rats, there were disorganized renal tubules, inflammatory factor infiltration in renal interstitial part, renal cortical edema, massive accumulation of lymphocytes, and inflammatory cell infiltration around glomeruli. The number of lymphocytes was relatively reduced in LD compared with MC, but there was still inflammatory cell infiltration, and tubular arrangement was scattered, which was not significant in GPE-MD compared with MC. The glomerular morphological structure of GPE-HD was basically normal with regular tubular arrangement.

3.8.6. Pathological Changes of Liver Tissue in Rats. In Figure 10, compared with BC, the hepatocytes of rats in MC were significantly swollen, tiny round fat vacuoles were observed in the cytoplasm, and the swelling of hepatocytes was alleviated to varying degrees in each group without other obvious abnormalities. The swelling of hepatocytes was most significantly alleviated in LD, indicating that GPE could protect the liver from damage.

4. Discussion

In recent years, the incidence of gout has increased exponentially. There are two main reasons for excessive uric acid in the body: (i) the excessive production of UA due to abnormal activity of XOD or excessive intake of exogenous purines and (ii) the accumulation of UA in the body due to the decrease of UA excretion [18]. Despite the current drugs that inhibit XOD having a good effect on reducing UA, there are severe adverse reactions such as renal injury
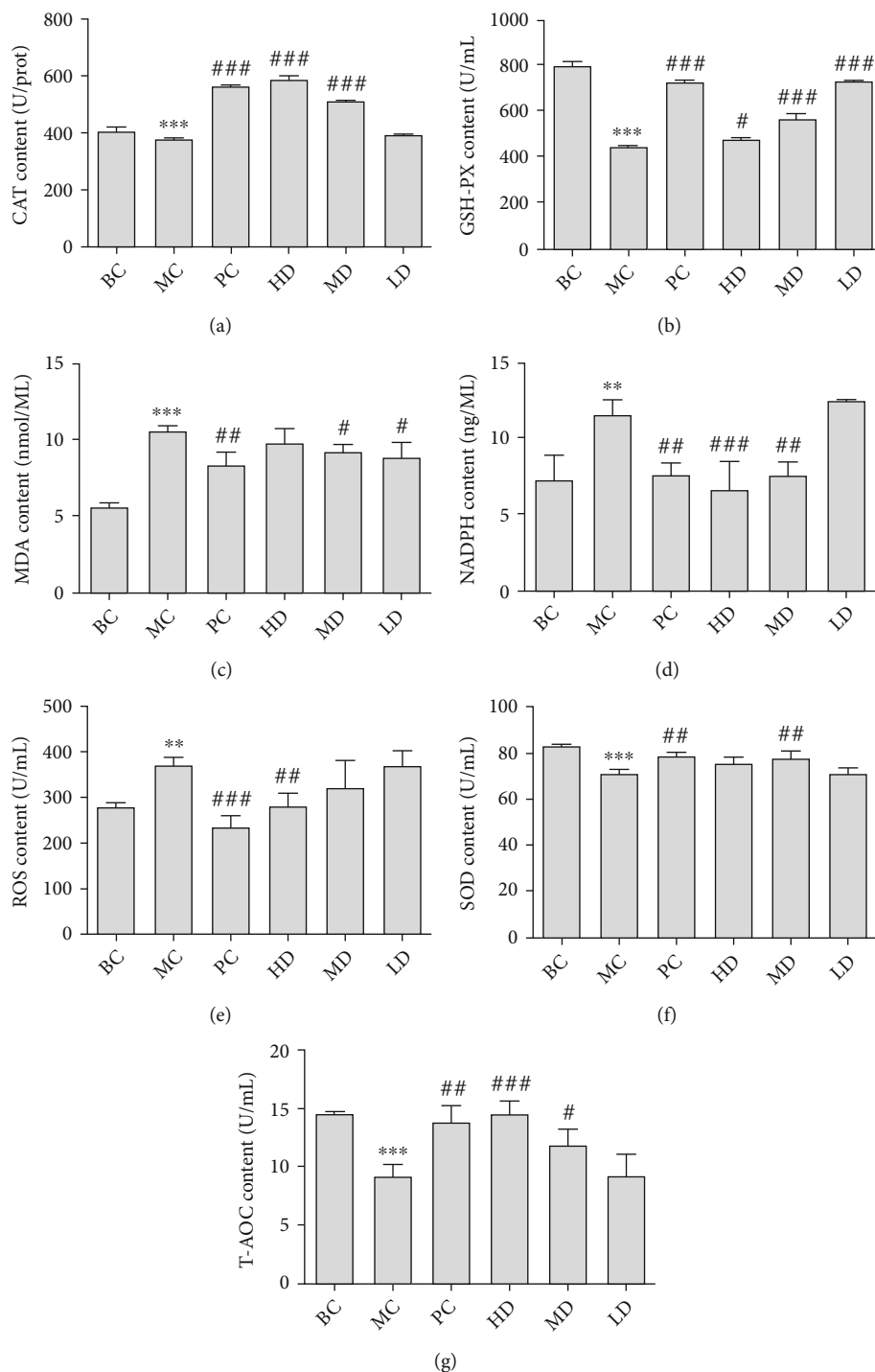
FIGURE 6: Effect of GPE on the levels of CAT (a), GSH-PX (b), MDA (c), NADPH (d), ROS (e), SOD (f), and T-AOC (g) in hyperuricemic rats. Compared with BC, $^*P < 0.05$, $^{**}P < 0.01$, $^{***}P < 0.001$; compared with MC, $^\#P < 0.05$, $^{\#\#}P < 0.01$, $^{\#\#\#}P < 0.001$.

and myelosuppression [19]. *Gardenia* has the effect of purging fire and removing annoyance, clearing heat and dampness, and cooling blood and detoxification. Besides, it is often used in diseases such as fever, swelling and pain, astringent pain of gonorrhea, and hematemesis. *Poria cocos* has the effects of promoting diuresis and dampness, invigorating the spleen, and calming the heart [20]. Thus, this

study discussed the potential mechanism of GPE in the treatment of HUA based on network pharmacology to understand the pharmacological mechanism of GPE.

Forty core targets of GPE in the treatment of HUA were screened in this study. Further analysis of the compound-disease-target regulatory network showed that quercetin, β-sitosterol, kaempferol, hederagenin, and other active
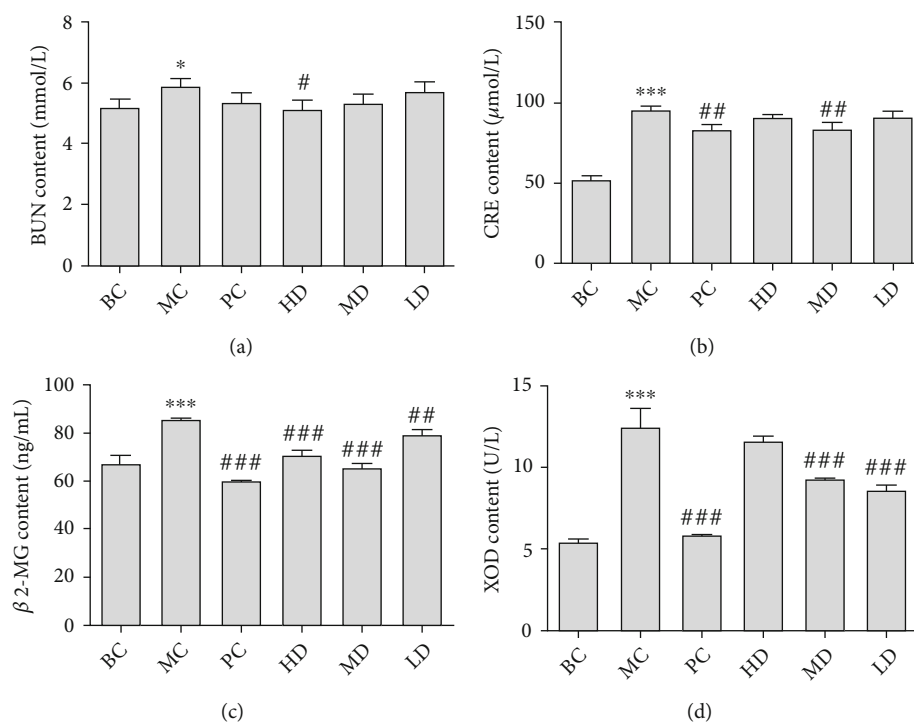
FIGURE 7: Effects of GPE on BUN (a), CRE (b), β2-MG (c), and XOD (d) levels in hyperuricemic rats. Compared with BC, $^{*}P < 0.05$, $^{**}P < 0.01$, $^{***}P < 0.001$; compared with MC, $^{\#}P < 0.05$, $^{\#\#}P < 0.01$, $^{\#\#\#}P < 0.001$.

ingredients could act on multiple targets in the network. Besides, the same target could also be regulated by multiple effective ingredients. Thirteen targets (32.5%) corresponded to more than two effective ingredients, indicating that there was the complex composition of GPE and the action mechanism of various targets. Quercetin can inhibit monosodium urate- (MSU-) induced mechanical hyperalgesia, leukocyte recruitment, the production of TNF-α and IL-1β, the production of superoxide anion, the activation of inflammatory reaction, the decrease of antioxidant level, the activation of NF-κB, and the expression of the inflammatory component mRNA [21]. β-Sitosterol can improve nephrotoxicity and kidney disease and adjust the activity of NRF-2 antioxidant enzymes to reduce nephrotoxic mouse creatinine and the expression of uric acid, urea, and iNOS to normal levels, and excessive peroxides and internal and external toxicants in the body are eliminated [22]. Hederagenin has antibacterial and anti-inflammatory pharmacological effects, and previous studies have shown that hederagenin can block the NF-κB signaling pathway to reduce the release of inflammatory factors such as IL-6, IFN-γ, TNF-α, and NO [23]. Some studies have shown that kaempferol may be a potential XOD inhibitor, because it can block the entry of the substrate by inserting the hydrophobic active site of XOD and inhibiting the activity of XOD by competing sites. Moreover, it can reduce the level of serum UA in hyperuricemia rat [24, 25]. PPI network also confirmed that there was a close relationship between GPE and HUA targets, and the results were reliable and of great reference value.

It is preliminarily predicted that GPE plays a role in the treatment of HUA through cell death, cytokine receptor and other enzyme activity pathways, TNF signal pathway, IL-7 signal pathway, and others through the GO functional enrichment analysis and KEGG pathway enrichment analysis of the core targets. During the pathological process of HUA, UA is an important endogenous antioxidant [26]. Under normal circumstances, the ROS generated are neutralized by the endogenous antioxidants, and there is an equilibrium between the ROS generated and the antioxidants present, but the continuous increase of the UA level will enhance the oxidative stress reaction *in vivo* [27]. The increase of the UA level in the blood can destroy the oxidation-reduction balance of the body through various ways, enabling the body to produce a mass of reactive oxygen species (ROS), damaging tissue cells, thus reducing the antioxidant capacity of the body and at last leading to the occurrence of oxidative stress damage [28–30]. NADPH oxidases (Nox) are one of many sources of ROS. Its catalytic product ROS participates in body defense and information transmission. The high level of ROS caused by excessive activation of NADPH will lead to tissue inflammation and further pathological damage of tissues and organs [31]. NADPH oxidase and its ROS products play a key role in the occurrence and development of acute kidney injury [32, 33]. The body scavenges reactive oxygen radicals through active enzymes such as superoxide dismutase (SOD), total antioxidant capacity (T-AOC), and peroxidase GSH-Px, thus reducing cell damage [34, 35]. Studies have shown that TNF-α can induce oxidative stress and inflammation. Besides, the increase of ROS production mainly comes from the intracellular NADPH oxidase pathway. TNF-α increases the level of oxidative stress mainly by

(a)

(b)

(c)

(d)

(e)
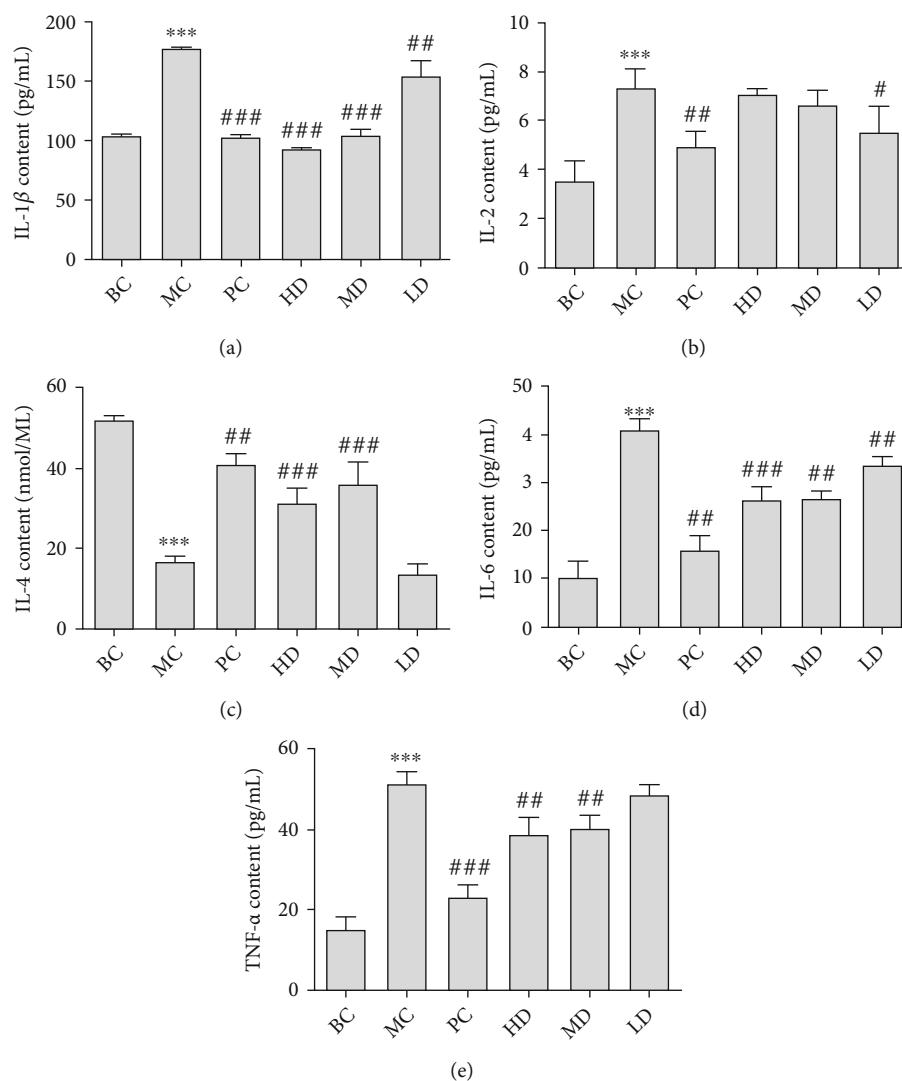
FIGURE 8: Effect of GPE on the contents of IL-1β (a), IL-2 (b), IL-4 (c), IL-6 (d), and TNF-α (e) levels in hyperuricemic rats. Compared with BC, $^{*}P < 0.05$, $^{**}P < 0.01$, $^{***}P < 0.001$; compared with MC, $^{\#}P < 0.05$, $^{\#\#}P < 0.01$, $^{\#\#\#}P < 0.001$.

upregulating the expression of NOX2 and its related subunits [36, 37]. IL-7 is a multifunctional cytokine, which can act on a variety of cells. The main function is to promote the development, antiapoptosis, and proliferation of immature B and T cells and to participate in the differentiation and maturation of thymocytes [38, 39]. The biological effect of IL-7 is mainly achieved through the binding of IL-7 to the IL-7 receptor (IL-7R). IL-7 activates the IL-7R signal pathway, upregulates the antiapoptotic protein, inhibits differentiated and activated T cell apoptosis, and downregulates the proapoptotic protein to prevent T cell apoptosis after binding to IL-7R. IL-7 has a strong immunomodulatory effect. As a consequence, IL-7 plays an important role in maintaining the homeostasis of immune function *in vivo* [40, 41].

High uric acid environment can cause oxidative stress, which is closely related to inflammation. Oxidative stress will promote the expression of inflammatory mediators such as TNF-α and IL-6 [42]. At the same time, inflammatory cells generate more reactive oxygen species after activation, resulting in an increase of oxidative stress level after inflammatory lesions. Another major cause of the creation of hyperuricemia is the reduction of uric acid excretion. Around 70% of uric acid in the body is excreted by the kidney. Uric acid is finally excreted with urine in the form of urate after glomerular filtration, renal tubular reabsorption, renal tubular secretion, and reabsorption after secretion [43]. β2-Microglobulin (β_2-MG) is a small molecule globulin produced by lymphocytes, platelets and polymorphonuclear leukocytes. The excretion of β_2-MG is extremely low under normal conditions, but its excretion increases when renal tubules are damaged or filtration function of glomerular decreases [44, 45]. Blood urea nitrogen (BUN) is one of the indicators of renal function, and it is the final product of human protein metabolism. When glomerular filtration ability decreased to a certain degree, BUN level tends to increase [46]. Serum creatinine (SCr) is an endogenous
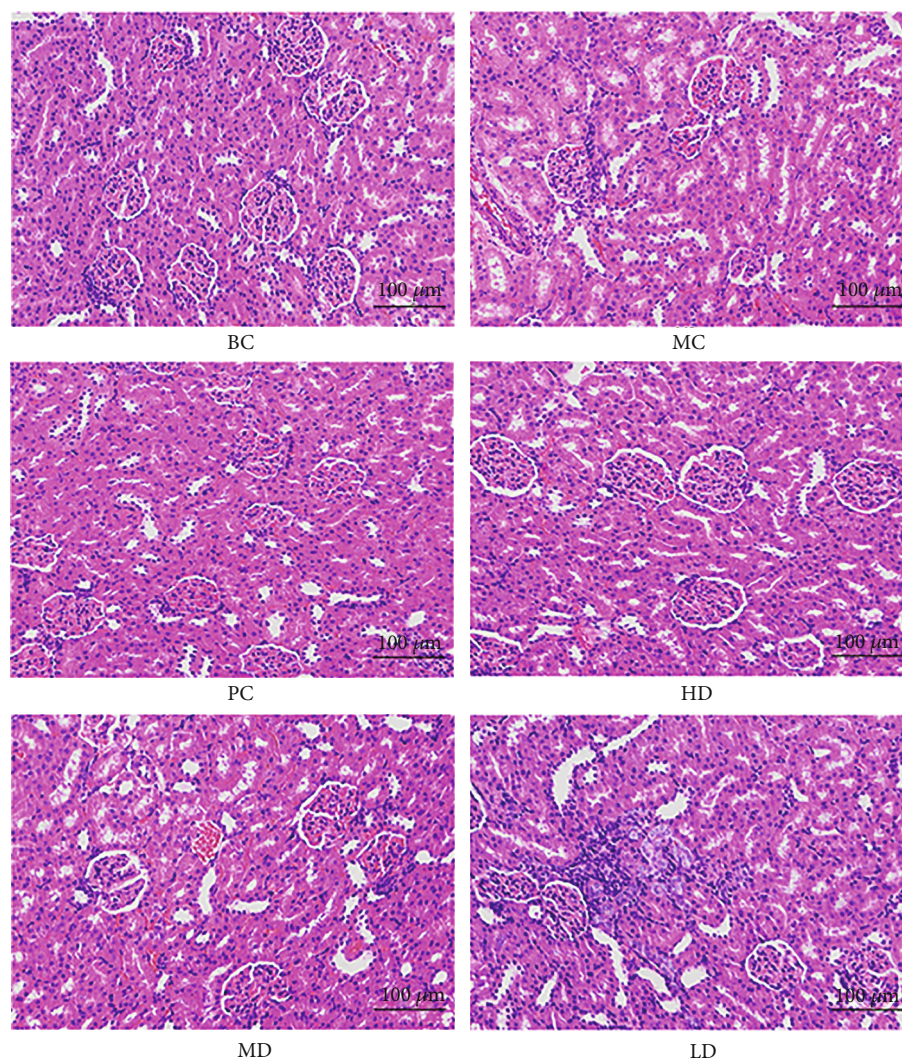
FIGURE 9: Pathological section of kidney tissue of hyperuricemic rats (200x).

creatinine filtered by glomerulus. Like BUN, the change of SCr content is also an important indicator of renal function [47]. When renal function is damaged, the level of SCr will increase [48]. In the clinic, the degree of renal function injury of patients is often judged by the detection of SCr index. Some studies have shown that hyperuricemia can damage rats' kidneys through inflammatory reaction and the oxidative stress pathway [49–51].

The model of hyperuricemia rats was established to demonstrate the results of network pharmacological analysis. The results showed that compared with the model group, the GPE group could significantly increase the activities of SOD, CAT, GSH-Px, and T-AOC in the plasma and liver tissue and decrease the levels of ROS, MDA, and NADPH in the plasma. It is suggested that GPE has the effect of antioxidant stress. The secretion of IL-4 was significantly increased after treatment with GPE. However, the contents of IL-6, IL-2, IL-1β, and TNF-α in the renal tissue of hyperuricemia rats were significantly decreased, indicating that GPE can enhance the secretion of IL-4 in hyperuricemia rats and

reduce the inflammatory level of hyperuricemia rats, which has a certain anti-inflammatory effect. Compared with the blank group, the levels of β2-MG, BUN, and SCr in the model group were significantly higher, indicating that the kidney of hyperuricemia rats was damaged. The sections of rat renal tissue in the model group showed that the renal tubules were messy, and the renal interstitium was infiltrated with inflammatory factors. It also indicated that the kidney in the model group was damaged, which led to the decline of renal function in hyperuricemia rats. These renal injuries can reduce the renal excretion of UA, thus increasing the level of uric acid in the body. Compared with the model group, the levels of β_2-MG, BUN, and Cr in the GPE group decreased significantly, indicating that the GPE can protect and improve renal function. It is speculated that GPE promotes the excretion of UA by improving the renal function damage caused by oxidative stress, thus reducing the level of UA. Besides, it can inhibit inflammatory reaction and antioxidant stress in order to achieve the purpose of treatment. Generally speaking, GPE has the characteristics of
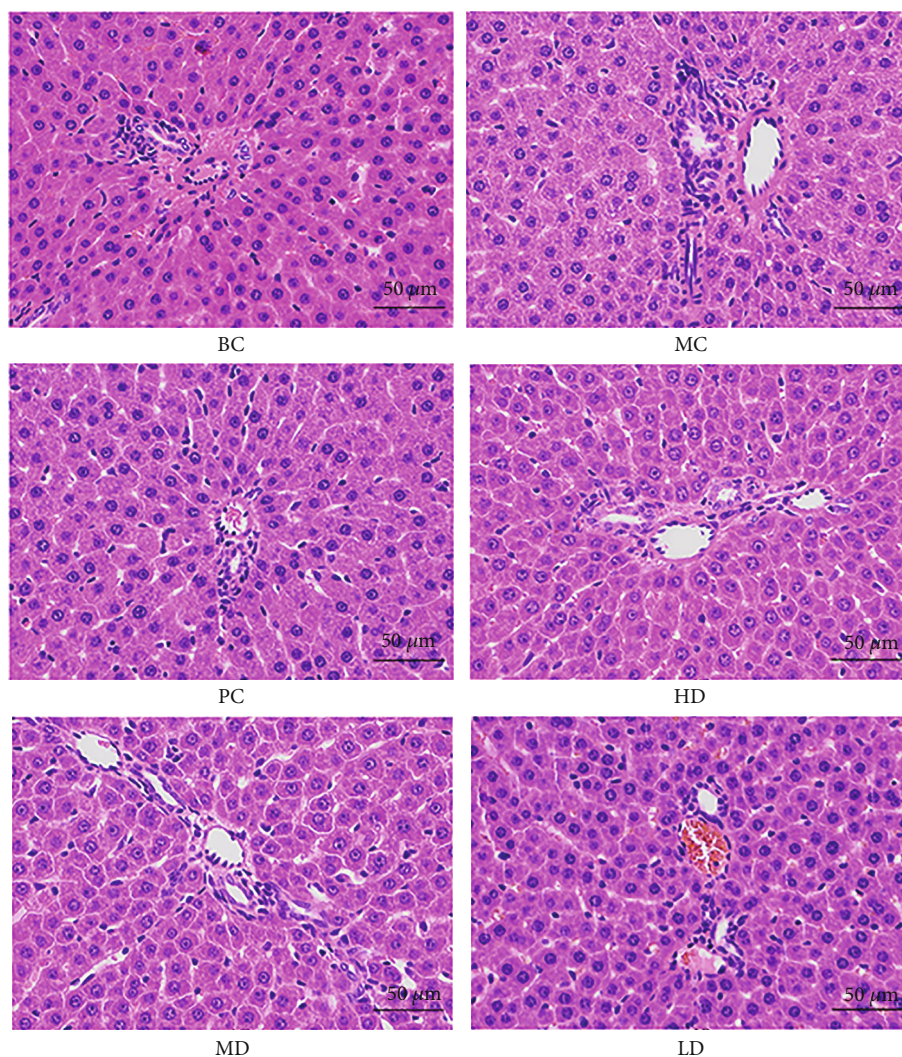
FIGURE 10: Histopathological section of liver tissue in hyperuricemic rats (400x).

multicomponents, multitargets, and multipathways in the treatment of HUA. It mainly plays a role in controlling the development of HUA through cell death, cytokine receptor, and other enzyme activity pathways, such as TNF α, IL-7, and other signaling pathways. Further animal experiments confirmed that GPE can reduce the level of oxidative stress in HUA model rats. In addition, regulating the expression of inflammatory factors such as TNF-α in renal tissue may be one of its mechanisms.

5. Conclusion

GPE has the characteristics of multicomponents, multitargets, and multipathways in the treatment of HUA. It mainly plays a role in controlling the development of HUA through cell death, cytokine receptor, and other enzyme activity pathways, such as TNF-α and IL-7 signaling pathways. Further animal experiments confirmed that GPE can reduce the level of oxidative stress in HUA model rats. In addition, regulating the expression of inflammatory factors such as TNF-α in renal tissue may be one of its mechanisms.

Data Availability

The [data type] data used to support the findings of this study are included within the article.

Ethical Approval

We confirm that all methods used in this study were carried out in accordance with relevant guidelines and regulations. Additionally, all experimental protocols were approved by Henan University.

Conflicts of Interest

The authors declare no conflicts of interest.

Authors' Contributions

Lijun Liu, Shengjun Jiang, Xuqiang, and Liu contributed equally to this work.

Acknowledgments

References

[1] Y. R. Yu, Q. P. Liu, H. C. Li, C. P. Wen, and Z. X. He, "Alterations of the gut microbiome associated with the treatment of hyperuricaemia in male rats," *Frontiers in Microbiology*, vol. 9, pp. 1–10, 2018.

[2] G. Y. Liang, Y. C. Nie, Y. B. Chang et al., "Protective effects of _Rhizoma smilacis glabrae_ extracts on potassium oxonate- and monosodium urate-induced hyperuricemia and gout in mice," *Phytomedicine*, vol. 59, p. 152772, 2019.

[3] A. Ota-Kontani, H. Hirata, M. Ogura, Y. Tsuchiya, and M. Harada-Shiba, "Comprehensive analysis of mechanism underlying hypouricemic effect of glucosyl hesperidin," *Biochemical and Biophysical Research Communications*, vol. 521, no. 4, pp. 861–867, 2020.

[4] C. Song and X. Zhao, "Uric acid promotes oxidative stress and enhances vascular endothelial cell apoptosis in rats with middle cerebral artery occlusion," *Bioscience Reports*, vol. 38, no. 3, pp. 1–9, 2018.

[5] M. Kurajoh, S. Fukumoto, S. Yoshida et al., "Uric acid shown to contribute to increased oxidative stress level independent of xanthine oxidoreductase activity in MedCity21 health examination registry," *Scientific Reports*, vol. 11, no. 1, p. 7378, 2021.

[6] C. Batandier, T. Poyot, N. Marissal-Arvy et al., "Acute emotional stress and high fat/high fructose diet modulate brain oxidative damage through NrF2 and uric acid in rats," *Nutrition Research*, vol. 79, no. 1, pp. 23–34, 2020.

[7] J. Zhang, Z. H. Yang, S. S. Zhang et al., "Investigation of endogenous malondialdehyde through fluorescent probe MDA-6 during oxidative stress," *Analytica Chimica Acta*, vol. 1116, pp. 9–15, 2020.

[8] J. Zhang, L. Zhou, L. Cui, Z. Liu, J. Wei, and W. Kang, "Antioxidant and _α_ -glucosidase inhibitiory activity of _Cercis chinensis_ flowers," *Food Science and Human Wellness*, vol. 9, no. 4, pp. 313–319, 2020.

[9] P. Mehnati, B. Baradaran, F. Vahidian, and S. Nadiriazam, "Functional response difference between diabetic/normal cancerous patients to inflammatory cytokines and oxidative stresses after radiotherapy," *Reports of Practical Oncology and Radiotherapy*, vol. 25, no. 5, pp. 730–737, 2020.

[10] D. Miricescu, A. Totan, C. Stefani et al., "Hyperuricemia, endothelial dysfunction and hypertension," *Romanian Journal of Medical Practice*, vol. 15, no. 2, pp. 178–182, 2020.

[11] Q. X. Yang, Q. L. Wang, W. W. Deng et al., "Anti-hyperuricemic and anti-gouty arthritis activities of polysaccharide purified from _Lonicera japonica_ in model rats," *International Journal of Biological Macromolecules*, vol. 123, pp. 801–809, 2019.

[12] K. Ogino, Y. Kinugasa, M. Kato, K. Yamamoto, T. Hamada, and I. Hisatome, "Uric-acid lowering treatment by a xanthine oxidase inhibitor improved the diastolic function in patients with hyperuricemia," *Journal of Cardiac Failure*, vol. 25, no. 8, p. S26, 2019.

[13] M. Q. Shan, T. J. Wang, Y. L. Jiang et al., "Comparative analysis of sixteen active compounds and antioxidant and anti-influenza properties of _Gardenia jasminoides_ fruits at different times and application to the determination of the appropriate harvest period with hierarchical cluster analysis," *Journal of Ethnopharmacology*, vol. 233, no. 233, pp. 169–178, 2019.

[14] Y. J. Wu, S. Li, H. X. Li et al., "Effect of a polysaccharide from _Poria cocos_ on humoral response in mice immunized by H1N1 influenza and HBsAg vaccines," *International Journal of Biological Macromolecules*, vol. 91, pp. 248–257, 2016.

[15] L. J. Deng, J. X. Yan, P. Wang, Y. Zhou, and X. A. Wu, "Effects of Pachman on the expression of renal tubular transporters rURAT1, rOAT1 and r OCT2 of the rats with hyperuricemia," *Western Journal of Traditional Chinese Medicine*, vol. 32, no. 6, pp. 10–14, 2019.

[16] J. X. Zhu, J. X. Zeng, G. M. Luo, Y. Y. Zhu, X. Y. Wang, and B. Wu, "Study on effective part of anti-hyperuricemia in Gardeniae fructus," *Chinese Journal of Experimental Traditional Medical Formulae*, vol. 18, no. 14, p. 159, 2012.

[17] F. Yang, H. L. Wang, G. Q. Feng, S. L. Zhang, J. M. Wang, and L. L. Cui, "Rapid identification of chemical constituents in Hericium erinaceus based on LC-MS/MS metabolomics," *Journal of Food Quality*, vol. 2021, Article ID 5560626, 10 pages, 2021.

[18] Q. Hong, L. Y. Wang, Z. Y. Huang et al., "High concentrations of uric acid and angiotensin II act additively to produce endothelial injury," *Mediators of Inflammation*, vol. 2020, Article ID 8387654, 11 pages, 2020.

[19] B. Era, G. L. Delogu, F. Pintus et al., "Looking for new xanthine oxidase inhibitors: 3-Phenylcoumarins _versus_ 2-phenylbenzofurans," *International Journal of Biological Macromolecules*, vol. 162, pp. 774–780, 2020.

[20] P. F. Yang, T. Hua, D. Wang, Z. W. Zhao, G. L. Xi, and Z. F. Chen, "Phytochemical and chemotaxonomic study of _Poria cocos_ (Schw.) Wolf," *Biochemical Systematics and Ecology*, vol. 83, pp. 54–56, 2019.

[21] K. W. Ruiz-Miyazawa, L. Staurengo-Ferrari, S. S. Mizokami et al., "Quercetin inhibits gout arthritis in mice: induction of an opioid-dependent regulation of inflammasome," *Inflammopharmacology*, vol. 25, no. 5, pp. 555–570, 2017.

[22] R. Sharmila, G. Sindhu, and P. M. Arockianathan, "Nephroprotective effect of β-sitosterol on N-diethylnitrosamine initiated and ferric nitrilotriacetate promoted acute nephrotoxicity in Wistar rats," *Journal of Basic and Clinical Physiology and Pharmacology*, vol. 27, no. 5, pp. 473–482, 2016.

[23] G. Wang, H. Tang, Y. Zhang, X. Xiao, Y. Xia, and L. Ai, "The intervention effects of _Lactobacillus casei_ LC2W on _Escherichia coli_ O157:H7 -induced mouse colitis," *Food Science and Human Wellness*, vol. 9, no. 3, pp. 289–294, 2020.

[24] S. H. Song, D. H. Park, M. S. Bae et al., "Ethanol extract of Cudrania tricuspidata leaf ameliorates hyperuricemia in mice via inhibition of hepatic and serum xanthine oxidase activity," *Evidence-based Complementary and Alternative Medicine*, vol. 2018, Article ID 8037925, 9 pages, 2018.

[25] Z. Li, Y. Xue, N. Wang et al., "High uric acid model in *Caenorhabditis elegans*," *Food Science and Human Wellness*, vol. 8, no. 1, pp. 63–66, 2019.

[26] I. Mirończuk-Chodakowska, A. M. Witkowska, and M. E. Zujko, "Endogenous non-enzymatic antioxidants in the human body," *Advances in Medical Sciences*, vol. 63, pp. 68–78, 2017.

[27] M. M. Abdel-Daim, S. M. M. Abuzead, and S. M. Halawa, "Protective role of Spirulina platensis against acute deltamethrin-induced toxicity in rats," *PLoS One*, vol. 8, no. 9, pp. 1–8, 2013.

[28] M. M. Abdel-Daim, "Synergistic protective role of ceftriaxone and ascorbic acid against subacute diazinon-induced nephrotoxicity in rats," *Cytotechnology*, vol. 68, no. 2, pp. 279–289, 2016.

[29] R. H. Abdou and M. M. Abdel-Daim, "Alpha-lipoic acid improves acute deltamethrin-induced toxicity in rats," *Canadian Journal of Physiology and Pharmacology*, vol. 92, no. 9, pp. 773–779, 2014.

[30] L. J. Yang, B. C. Chang, Y. L. Guo, X. P. Wu, and L. Liu, "The role of oxidative stress-mediated apoptosis in the pathogenesis of uric acid nephropathy," *Renal Failure*, vol. 41, no. 1, pp. 616–622, 2019.

[31] N. K. M. Abdelkhalek, E. W. Ghazy, and M. M. Abdel-Daim, "Pharmacodynamic interaction of Spirulina platensis and deltamethrin in freshwater fish Nile tilapia, Oreochromis niloticus: impact on lipid peroxidation and oxidative stress," *Environmental Science and Pollution Research International*, vol. 22, no. 4, pp. 3023–3031, 2015.

[32] S. Kovacevic, M. Ivanov, Z. Miloradovic et al., "Hyperbaric oxygen preconditioning and the role of NADPH oxidase inhibition in postischemic acute kidney injury induced in spontaneously hypertensive rats," *PLoS One*, vol. 15, no. 1, article e0226974, 2020.

[33] B. Y. Jeong, H. Y. Lee, C. G. Park et al., "Oxidative stress caused by activation of NADPH oxidase 4 promotes contrast-induced acute kidney injury," *PLoS One*, vol. 13, no. 1, pp. 1–22, 2018.

[34] X. Sun, Z. Xu, Y. Wang, and N. Liu, "Protective effects of blueberry anthocyanin extracts on hippocampal neuron damage induced by extremely low-frequency electromagnetic field," *Food Science and Human Wellness*, vol. 9, no. 3, pp. 264–271, 2020.

[35] X. Liu, C. Jiang, Y. Chen, F. Shi, C. Lai, and L. Shen, "Major royal jelly proteins accelerate onset of puberty and promote ovarian follicular development in immature female mice," *Food Science and Human Wellness*, vol. 9, no. 4, pp. 338–345, 2020.

[36] N. Maryam, M. Sina, B. Esmaeel et al., "Ameliorative effects of histidine on oxidative stress, tumor necrosis factor alpha (TNF-α), and renal histological alterations in streptozotocin/nicotinamide-induced type 2 diabetic rats," *Iranian Journal of Basic Medical Sciences*, vol. 6, no. 23, pp. 1–10, 2020.

[37] X. Li, F. L. Zhang, H. L. Zhou et al., "Interplay of TNF-α, soluble TNF receptors and oxidative stress in coronary chronic total occlusion of the oldest patients with coronary heart disease," *Cytokine*, vol. 125, p. 154836, 2020.

[38] C. Coppola, B. Hopkins, S. Huhn, Z. du, Z. Y. Huang, and W. J. Kelly, "Investigation of the impact from IL-2, IL-7, and IL-15 on the growth and signaling of activated CD4+ T cells," *International Journal of Molecular Sciences*, vol. 21, no. 21, pp. 7814–7823, 2020.

[39] M. S. Shin, D. Kim, K. Yim et al., "IL-7 receptor alpha defines heterogeneity and signature of human effector memory CD8^{+} T cells in high dimensional analysis," *Cellular Immunology*, vol. 355, pp. 104155–104159, 2020.

[40] Z. H. Zhao, Y. Li, W. Liu, and X. Li, "Engineered IL-7 receptor enhances the therapeutic effect of AXL-CAR-T cells on triple-negative breast cancer," *BioMed Research International*, vol. 2020, Article ID 4795171, 13 pages, 2020.

[41] C. Lundtoft, A. Afum-Adjei Awuah, J. Rimpler et al., "Aberrant plasma IL-7 and soluble IL-7 receptor levels indicate impaired T-cell response to IL-7 in human tuberculosis," *European Journal of Immunology*, vol. 13, no. 6, pp. 1–22, 2017.

[42] H. M. Al-Kuraishy, A. I. Al-Gareeb, and M. S. Al-Nami, "Vinpocetine improves oxidative stress and pro-inflammatory mediators in acute kidney injury," *International Journal of Preventive Medicine*, vol. 10, no. 1, pp. 142–142, 2019.

[43] X. Y. Xiong, L. Bai, S. J. Bai, Y. K. Wang, and T. Ji, "Uric acid induced epithelial–mesenchymal transition of renal tubular cells through PI3K/p-Akt signaling pathway," *Journal of Cellular Physiology*, vol. 234, no. 9, pp. 15563–15569, 2019.

[44] T. Fiseha, T. Mengesha, R. Girma, E. Kebede, and A. Gebreweld, "Estimation of renal function in adult outpatients with normal serum creatinine," *BioMed Central*, vol. 12, no. 1, pp. 462–467, 2019.

[45] R. Wang, H. T. Hu, S. Hu, H. He, and H. Shui, "β2-microglobulin is an independent indicator of acute kidney injury and outcomes in patients with intracerebral hemorrhage," *Medicine*, vol. 99, no. 8, article e19212, 2020.

[46] X. Yang, K. Zhao, W. Deng et al., "Apocynin attenuates acute kidney injury and inflammation in rats with acute hypertriglyceridemic pancreatitis," *Digestive Diseases and Sciences*, vol. 65, no. 6, pp. 1735–1747, 2020.

[47] M. Bian, J. Wang, Y. Wang et al., "Chicory ameliorates hyperuricemia via modulating gut microbiota and alleviating LPS/TLR4 axis in quail," *Biomedicine & Pharmacotherapy*, vol. 131, p. 110719, 2020.

[48] Y. Hatakeyama, T. Horino, K. Nagata et al., "Evaluation of the accuracy of estimated baseline serum creatinine for acute kidney injury diagnosis," *Clinical and Experimental Nephrology*, vol. 22, no. 2, pp. 405–412, 2018.

[49] X. W. Meng, C. X. He, X. Chen, X. S. Yang, and C. Liu, "The extract of _Gnaphalium affine_ D. Don protects against H_2O_2-induced apoptosis by targeting PI3K/AKT/GSK-3 β signaling pathway in cardiomyocytes," *Journal of Ethnopharmacology*, vol. 268, p. 113579, 2021.

[50] Y. Nakamura, H. Kobayashi, S. Tanaka, H. Yoshinari, F. Noboru, and A. Masanori, "Association between plasma aldosterone, and markers of tubular and glomerular damage in primary aldosteronism," *Clinical Endocrinology*, vol. 94, no. 6, pp. 920–926, 2021.

[51] S. Milanesi, D. Verzola, F. Cappadona et al., "Uric acid and angiotensin II additively promote inflammation and oxidative stress in human proximal tubule cells by activation of toll-like receptor 4," *Journal of Cellular Physiology*, vol. 234, no. 7, pp. 10868–10876, 2019.

Research Article

Preparation and Evaluation of Silymarin-Loaded Solid Eutectic for Enhanced Anti-Inflammatory, Hepatoprotective Effect: *In Vitro–In Vivo* Prospect

Abdulla Sherikar,[1] Mohd Usman Mohd Siddique [iD],[2] Mahesh More,[3] Sameer N. Goyal,[1] Milan Milivojevic,[4] Saad Alkahtani [iD],[5] Saud Alarifi [iD],[5] Md Saquib Hasnain [iD],[6] and Amit Kumar Nayak [iD][7]

[1]*Department of Pharmacology Shri Vile Parle Kelavani Mandal's Institute of Pharmacy, Dhule, Maharashtra 424001, India*
[2]*Department of Pharmaceutical Chemistry, Shri Vile Parle Kelavani Mandal's Institute of Pharmacy, Dhule, Maharashtra 424001, India*
[3]*Department of Pharmaceutics, Dr. Rajendra Gode College of Pharmacy, Dist Buldhana (M.S.), 443 101, Malkapur, India*
[4]*Department of Chemical Engineering, Faculty of Technology and Metallurgy, University of Belgrade, Belgrade 11000, Serbia*
[5]*Department of Zoology, College of Science, King Saud University, P.O. Box 2455, Riyadh, Saudi Arabia*
[6]*Department of Pharmacy, Palamau Institute of Pharmacy, Chianki, Daltonganj, 822102 Jharkhand, India*
[7]*Department of Pharmaceutics, Seemanta Institute of Pharmaceutical Sciences, Mayurbhanj, 757086 Odisha, India*

Correspondence should be addressed to Mohd Usman Mohd Siddique; palladiumsalt@gmail.com,
Md Saquib Hasnain; msaquibhasnain@gmail.com, and Amit Kumar Nayak; amitkrnayak@yahoo.co.in

Solubility of phytochemicals is a major concern for drug delivery, permeability, and their biological response. However, advancements in the novel formulation technologies have been helping to overcome these challenges. The applications of these newer technologies are easy for commercialization and high therapeutic outcomes compared to conventional formulations. Considering these facts, the present study is aimed to prepare a silymarin-loaded eutectic mixture with three different ratios of Polyvinylpyrrolidone K30 (PVP K30) and evaluating their anti-inflammatory, and hepatoprotective effects. The preliminary phytochemical and characterization of silymarin, physical mixture, and solid dispersions suggested and successfully confirmed the formation of solid dispersion of silymarin with PVP K30. It was found that the solubility of silymarin was increased by 5-fold compared to pure silymarin. Moreover, the *in vitro* dissolution displayed that 83% of silymarin released within 2 h with 2.8-fold increase in dissolution rate compared to pure silymarin. Also, the *in vivo* study suggested that the formulation significantly reduced the carbon tetrachloride- ($0.8620\pm0.05034^{**}$ for 1:3 ratio), paracetamol- ($0.7300\pm0.01517^{**}$ for 1:3 ratio), and ethanol- ($0.8100\pm0.04037^{**}$ for 1:3 ratio) induced hepatotoxicity in rats. Silymarin solid dispersion was prepared using homogenization methods that have prominent anti-inflammatory effect ($0.6520\pm0.008602^{**}$ with 8.33%) in carrageenan-induced rat paw model.

1. Introduction

Solid solution is an interchangeable solution state while solute interacting strongly in the form of eutectics. Solid dispersion method maximizes interaction with water and profoundly incorporates hydrogen bonds. Furthermore, it allows the intercalation of the lipophilic substance centrally giving the odor of hydrophilic monolayer polymer. Solid dispersion is widely used and a well-explored technique for the enhancement of solubility at both laboratory and commercial scale [1]. But macerates of plants or animal displayed the limited solubility in aqueous environment, and recent

literature showed that the organic extracts have better therapeutic potential as compared to the aqueous extracts. The possibility behind this is it may be due to the hydrophobic nature of most of the active constituents. These formulation challenges, mainly low solubility and poor bioavailability, limit the scope and commercial availability of phytochemicals [2, 3]. The formulation development of large number of phytoconstituents is also problematic. The different observations were noted while developing the formulation of phytoconstituents, mainly incompatibility with solvents, precipitation, phase separation, aggregation, etc. This creates an opportunity for the researchers to come up with different strategies for the enhancement of characterization of phytoconstituent extracts. For enhancing the bioavailability of phytoconstituents, novel solubility enhancement techniques like solid dispersion, complexation, nanocrystals, ultrasonication, and eutectic mixtures provide an alternative approach [4–8]. Silymarin (SL) is the active constituent of *Silybum marianum* L. Gaertn. (Family Asteraceae) traditionally used in the treatment of the liver, and it is regarded as a highly potent hepatoprotective agent [6, 9]. The major constituent of silymarin is silibinin (A and B), and it is found to be about 70–80% responsible for major therapeutic activity. The other flavanolignan components like silydianin, silycrystin, and isosilybin (A and B) also showed 10%, 20%, and 0.5% useful pharmacological activity, respectively. SL is an important class of phytopharmaceuticals having wide therapeutic applications as anticancer, antiviral, antifibrotic, etc. [10–12]. Despite this, it showed limited therapeutic outcome because of its poor solubility and limited bioavailability after oral administration. Furthermore, it undergoes first pass effect providing only 20–40% of therapeutic benefit. Orally administered silybin has not been detected in plasma due to poor solubility characteristics and oral absorption. Oral administration and first pass effect lead to very less bioavailability (approximately 0.95%) [13]. Various formulations of SL have been tried to enhance the solubility and bioavailability, but the significant results are still lacking. Overall, these factor forms the basis of present study, i.e., formulation of eutectic solid of silymarin. Many active pharmaceutical ingredients, including phytochemicals, have poor solubility and bioavailability. A group of researchers is actively working on the solubility enhancement techniques, including a new mechanism of solute–solvent or solute–solute interaction. In order to enhance the dissolution pattern of poorly soluble drug, the solid dispersion technique is widely employed [14, 15]. Moreover, this system is associated with formation of polymer conjugation of poorly soluble drugs through amorphization of drug in the presence of polymeric carrier [16, 17]. Polyvinylpyrrolidone K30(PVP K30), a derivatized longer chain, water-soluble, hydrophilic polymer, was used for making silymarin eutectic. Due to its nonirritant, nontoxic, biocompatible, and biodegradable characteristics of PVP K30, it is widely employed in drug delivery carrier. Furthermore, PVP K30 is a linear nonionic polymer which has wide range of pharmaceutical applications like solubility enhancement, protection of crystalline drug during processing, and delivery of drug [18, 19]. Also, Polyvinylpyrrolidone (PVP) not only forms complexes with the drug molecules, but also exhibits strong solute-solute interaction like hydrogen bonding, Van der Waals weak attraction, or London forces. For preparation of solid dispersion, the PVP is considered as a good candidate for enhancing solubility of drug that imparts protection to drug from loss due to external environment [19, 20]. The present study was aimed at enhancing the solubility and thereby bioavailability of SL by solid dispersion technique. The solid dispersion was prepared using appropriate proportions of PVP K30 and SL to be processed at optimum temperature. The silymarin solid dispersion (SDD) was conjugated with hydroxypropyl methylcellulose (HPMC) carrierto modulate long-term release. In the presence of PVP K30, solubility and dissolution characteristics of SL were set to be increased. *In vivo* pharmacokinetic study suggested that prepared silymarin solid dispersion has proven to have antioxidant and anti-inflammatory activity and hepatoprotective effect.

2. Experimental

2.1. Materials. Silymarin (SL) was received as a gift sample from BioXpert Innovations Pvt. Ltd., India. Polyvinylpyrrolidone K30 (PVP K30) and hydroxypropyl methylcellulose (HPMC) were made available from Loba Chemie Ltd., Mumbai, India. The remaining chemicals belong to analytical grade and are used as received unless it is specified.

2.2. Methods

2.2.1. Preparation of Silymarin-Encapsulated Solid Dispersion. The phytochemical has limited solubility and thereby, limits the therapeutic response. For enhancement of solubility, phytoconstituents are mixed with either surfactant or polymeric blend [21]. Variable ratios of SL and PVP K30 were taken for improving the solubility. In order to prepare the SL-based solid dispersion (SSD), the solvent evaporation technique was employed. Different concentrations of PVP K30 were used along with SL to verify the solubility characteristics. Methanol was used as common volatile solvent for the preparation containing SL and PVP K30. The concentration ratios (1 : 1, 1 : 2, and 1 : 3) were taken with respect to SL and PVP K30. For further experimentation, concentration ratios of SL to PVP K30 (1 : 1, 1 : 2, and 1 : 3) were used to notify as silymarin solid dispersion (SSD1, SSD2, and SSD3), respectively. PVP K30 and SL were dissolved in methanol (15 mL). The solution was ultrasonicated for 15 min to remove traces of aggregates. The methanolic solution containing PVP K30 and SL was added dropwise in 50 mL water containing PEG 4000 (0.2%). The whole mixture was homogenized (IKA Homogenizer T25) for 40 min at 10000 rpm. The methanol was evaporated in the Rota evaporator at a reduced temperature. The remaining aqueous solution was lyophilized at -40°C, and dry powder was collected for analysis.

2.3. Characterization. Preliminary characterization of SL, PVP K30, solid dispersion, and physical mixture was done

using sophisticated analytical instruments. The preliminary identification of SL was done using a UV-visible double-beam spectrophotometer (JASCO V630) and a Fourier transform infrared (FTIR) spectrophotometer with diffused reflectance assembly (JASCO 4100S) [22]. The stock solution containing SL was dissolved into 0.1 N HCl. The UV-visible spectra were recorded by scanning 200–400 nm. The maximum absorbance (λ_{max}) from the spectrum was identified and used in further evaluations like drug content or drug release. The preliminary identification of SL, PVP K30, physical mixture (SL+PVP K30), and SSD was evaluated using FTIR spectroscopy. The individual solid component was mixed with predried KBr in 1:100 ratio (solid:KBr) and analyzed using an FTIR spectrophotometer. The vibrational intensities of obtained spectra were compared with standards. Solubility analysis of pure SL and solid dispersion was performed using the shake flask method, and concentration was estimated after 48 h period of time using UV-visible spectrophotometric absorbance. The absorbance was correlated with calibration curve plotted in the respective solution state with linearity (R^2) 0.998.

2.4. In Vivo Pharmacological Study

2.4.1. Animals. The male albino Wistar rats weighing 180-200 g used were procured from the animal house, Laxmi Biofarm, Alephata, Pune. The different grouping of rats was done and kept in polyacrylic cages (38 cm × 23 cm × 10 cm) and maintained under standard laboratory conditions (temperature $(25 \pm 3)°C$) with dark and light cycle (12/12 h). The rats were allowed free access to a standard pellet diet and reversed osmosis water *ad libitum*. Before the initiation of the experiment, the period of one week was followed for the acclimatization of selected rats. *In vivo* pharmacological screening was conducted for pharmacological activity.

2.4.2. In Vivo Anti-Inflammatory Activity (Carrageenan-Induced Paw Edema in Rats). To induce acute inflammation in the paw of rats, 1% suspension of carrageenan in normal saline was prepared, and 0.1 mL subplantar injection was given to the right hind paw of rats. The digital plethysmometer (Orchid Scientific, Nashik) was used to measure paw volume to indicate acute inflammation at different time intervals like 0, 30, 60, 90, 120, and 180 min after carrageenan injection. The average foot swellings among the test and standard groups were regarded as a function of edema. The variations among the two readings were considered as the volume of edema. Moreover, the % inhibition of paw edema as a marker of anti-inflammatory activity by SSD was calculated by using.

$$\%\text{Edema} = \frac{C_0 - C_r}{C_0} \times 100, \quad (1)$$

where C_r is the average paw volume of the treated group and C_0 is the average paw volume of the control group. The animals were grouped as follows: Group 1: control group, Group 2: standard drug treated (containing 1.16% diclofenac sodium) [23], Group 3: administered with SSD (1:1)

100 mg/kg, p.o., Group 4: administered with SSD (1:2) 100 mg/kg, p.o., and Group 5: administered with SSD (1:3) 100 mg/kg, p.o.

2.4.3. In Vivo Hepatoprotective Activity. For hepatoprotective activity, 30 healthy albino Wistar rats of either sex were divided into 6 groups. Hepatoprotective activity was comparatively assessed using three different methods, such as carbon tetrachloride (CCl_4) method, ethanol method, and paracetamol method. During study, each group consists of 6 rats, and dosing was done frequently as mentioned in the individual model.

(1) Carbon Tetrachloride- (CCl_4-) Induced Hepatotoxicity in Rats. For the screening of *in vivo* hepatoprotective activity of SSD in CCl_4-induced hepatotoxicity in rats, the animals were grouped as follows.

Group 1: the rats were administered with sodium carboxymethylcellulose (NaCMC 0.5%, p.o.) as a vehicle for six days.
Group 2: the rats were administered with vehicle (NaCMC 0.5%, p.o.) for six days, and on day 7, they were treated with CCl_4, 1.5 mL/kg, p.o. [24].
Group 3: the rats were treated with standard drug, silymarin 100 mg/kg, p.o. [10], for six days, and on day 7, they were treated with CCl_4, 1.5 mL/kg, p.o.
Groups 4, 5, and 6: the rats were treated with SSD (1:1, 1:2, and 1:3) 100 mg/kg, p.o., for six days, and on day 7, these were treated with CCl_4, 1.5 mL/kg, p.o., respectively.

(2) Ethanol-Induced Hepatotoxicity in Rats. The animals were divided into different groups to screen in vivo hepatoprotective activity of SSD in ethanol-induced hepatotoxicity model.

Group 1: the rats were administered with 2% gum acacia (0.1 g/200 g b.w.) for 6 days.
Group 2: the rats were administered with vehicle and 2% gum acacia (0.1 g/200 g b.w.) for six days, and on day 7, they were treated with 3.76 g/kg b.w. ethanol (20%), p.o.
Group 3: the rats were treated with standard drug, silymarin 100 mg/kg b.w., p.o., respectively, for six days, and on day 7, they were treated with 3.76 g/kg b.w. ethanol (20%), p.o.
Groups 4, 5, and 6: the rats were treated with SSD (1:1, 1:2, and 1:3) 100 mg/kg, p.o., for six days, and on day 7, they were treated with 3.76 g/kg b.w. ethanol (20%), p.o., respectively [25].

(3) Paracetamol-Induced Hepatotoxicity in Rats. In the context of *in vivo* paracetamol-induced hepatotoxicity, the animals were divided into different groups.

Group 1: the rats were administered with 1% sodium-carboxymethylcellulose (NaCMC) 1 mL/kg b.w., p.o. for 6 days.
Group 2: the rats were administered with vehicle 1% NaCMC 1 mL/kg b.w., p.o., for six days, and on day 7, they were treated with 500 mg/kg b.w. paracetamol, p.o.

Group 3: the rats were treated with standard drug, sily-marin 100 mg/kg b.w., p.o., respectively, for six days, and on day 7, they were treated with 500 mg/kg paracetamol, p.o.

Groups 4, 5, and 6: the rats were treated with SSD (1:1, 1:2, and 1:3) 100 mg/kg, p.o., for six days, and on day 7, they were treated with 500 mg/kg paracetamol, p.o., respectively [23].

Hepatoprotective activity was biochemically evaluated for each model, such as alanine aminotransferase (ALT), aspartate aminotransferase (AST), alkaline phosphate (ALP), and total bilirubin.

After 48 h of administration of each hepatotoxic agent into a separate group of animals, blood samples were collected from the retro-orbital plexus. The blood was transferred into previously labelled centrifuge tube and allowed to clot for 30 min at room temperature. The tubes were centrifuged at 2500 rpm for 10 min, and serum was separated. The separated serum was analyzed using standard biochemical kits for the estimation of ALT, AST, ALP, and total bilirubin.

2.5. Statistical Analysis. The data were presented as the mean ± SEM. The data were analyzed by GraphPad Prism (version 5.0) using one-way ANOVA, followed by Dunnett's test.

3. Results and Discussion

3.1. Phytochemical Investigation. Phytochemical investigation suggested the presence of different types of primary phytoconstituents in the mixture like flavonoids, terpenoids, phenol, tannins, and reducing sugar. The generalized tested protocols cited in the text were used for superficial screening of SL extract. The phytochemical investigation suggested the presence of impurities and adulterants within an extract. In the present attempt, the phytochemical analysis is presented in Table 1, which shows supplied SL extract was pure and did not contain any impurities. The phytochemical investigation suggested the presence or absence of primary or secondary metabolites having prominent pharmacological activity. The chemical composition of SL was established by phytochemical investigation. The preliminary phytochemical investigation was in accordance with reported literature [26].

3.2. Fourier Transform Infrared Spectroscopy (FTIR). An FTIR spectrum was helpful for preliminary identification of SL and comparative evaluation of vibrational frequencies. The stretching and bending vibrational frequencies emerge from SL was depicted in Figure 1(a). Intermolecular interaction in physical mixture between solids was analyzed by vibrational changes during FTIR analysis. The frequencies can be served as probe for identification of surface functional groups and their interactions [29]. The broad intense peak that appeared at 3457 cm^{-1} was specifically due to oxygen-containing functionality of SL. The broad peak represented –OH stretching vibration mode. The distinct peaks observed at 2942 cm^{-1} and 2880 cm^{-1} were due to the presence of CH-CH stretching vibration.

The reactive flavonolignon ketone showed strong intense peak at 1639 cm^{-1}. A small intense peak at 1365 cm^{-1} and 1278 cm^{-1} was due to –OH bending and C-O-C stretching, respectively. Two conjugated peaks emerged at 1509 cm^{-1} and 1467 cm^{-1} representing aromatic ring stretching vibrations [21]. An intense peak appeared at 1731 cm^{-1} showed the presence of C-O stretch from aromatic ring structure. The in-plane vibration stretching of –C-H was observed at 1085 cm^{-1} corresponding to flavonolignans, while the peaks that appear at 996 cm^{-1} were due to benzopyran ring [30]. The SL primarily reveals the presence of polyphenolic moiety and confirms its structural vibrational frequencies from FTIR spectra [4].

FTIR spectra of PVP K30 are depicted in Figure 1(b). A broad spectrum at 3457 cm^{-1} and 1639 cm^{-1} was observed due to the presence of –OH stretching and carbonyl stretching vibrations, respectively, while two conjugative peaks at 2977 cm^{-1} and 2878 cm^{-1} are designated for CH-CH stretching from polymeric chain. A sharp peak at 1670 cm^{-1} was observed due to C=O stretching vibration mode [31]. Three conjugative sharp peaks around 1470–1437 cm^{-1} were due to the presence of C-H bending. A strong band at 1290 cm^{-1} was observed due to the in-plane OH bending vibration and interestingly involved in the interaction. The interaction may drop the crystallinity of phytoconstituent [32]. A small band at 1072 cm^{-1} emerges due to C-O stretching vibration. All the reported vibrational frequency confirmed the structural conformity of PVP K30 [33]. Physical interaction of SL and PVP K30 was analyzed using FTIR spectroscopy, and spectral elucidation is represented in Figure 1(c). Characteristic vibrational frequencies of both components were found to be superimposed in physical mixture that indicated no interaction between SL and PVP K30. Intensity of peaks increased or decreased simultaneously based on overlapping structure available. The physical mixture did not show any types of interaction between SL and PVP K30 [31]. The overlapping hydroxyl stretch was observed at 3624 cm^{-1} with decreasing CH-CH stretching at 2945 cm^{-1} and 2874 cm^{-1}. The C-O stretching at 1638 cm^{-1} was elongated, and a sharp peak was observed. A prominent peak was shown at 1274 cm^{-1} that represents C-N stretching. The decrease in peak intensity may be due to overlapping bands having similar functional groups [21]. FTIR spectrum of SSD3 is represented in Figure 1(d), which displayed distinct vibration intensity describing the successful formation of solid dispersion. The spectral intensity slightly increases, which may possibly be due to the weak Van der Waals interaction or hydrogen bonding between water molecule and PVP K30-encapsulating SL [31, 34]. A broad peak appeared at 3628 cm^{-1}, which showed strong interaction between SL and PVP K30 representing hydroxyl stretching. Two strong peaks observed at 2952 cm^{-1} and 2880 cm^{-1} showed CH$_2$-CH$_2$ stretching vibration; intensity slightly decreased after interaction. A strong peak observed at 1670 cm^{-1} was due to C=O stretching, which may be emerged from both SL and PVP K30. The small peak was observed at 1508 cm^{-1} represents N binding due to the presence of C-N in the structure of PVP K30 [34]. Two new peaks formed at 1423 cm^{-1} and 1374 cm^{-1} represent C-H bending were

TABLE 1: Phytochemical evaluation of silymarin extract.

Sr. no.	Phytochemical test	Observation	Inference
1	Mayer's test	No precipitate observed	Alkaloid absent
2	Dragendorff's test	Absence of orange color	Alkaloid absent
3	Wagner's test	Absence of reddish-brown precipitate	Alkaloid absent
4	Extract+aluminium chloride solution	Yellow-colored solution	Flavonoids present
5	Extract+Aq. NaOH	Yellow-orange color solution, disappears after addition of HCl	Flavonoid present
6	Extract+Conc. H_2SO_4	Orange-colored solution	Flavonoid present
7	Extract+Aq. ferric chloride (10%)	Deep blue-colored solution	Phenol present
8	Extract+ferric chloride (5%)	Green black-colored solution	Tannins presents
9	DW+extract+shake vigorously	Absence of foam layer	Saponins absent
10	Salkowski test	Reddish brown color at the interface	Terpenoids present
11	Extract+Conc. HCl	Yellow-colored precipitate not observed	Quinins absent
12	Extract+2 M NaOH	Blue green color not formed	Anthocyanin absent
13	Ninhydrin test	Purple color not observed in solution	Protein absent
14	Benedict's test	Red precipitate forms	Reducing sugar present
15	Iodine test	Purple color not formed after addition of iodine	Polysaccharide absent
16	Extract+2% HCl	No color change	Anthraquinones absent

**Note: the entire phytochemical test conducted as per protocol mentioned in [27, 28] without modification.
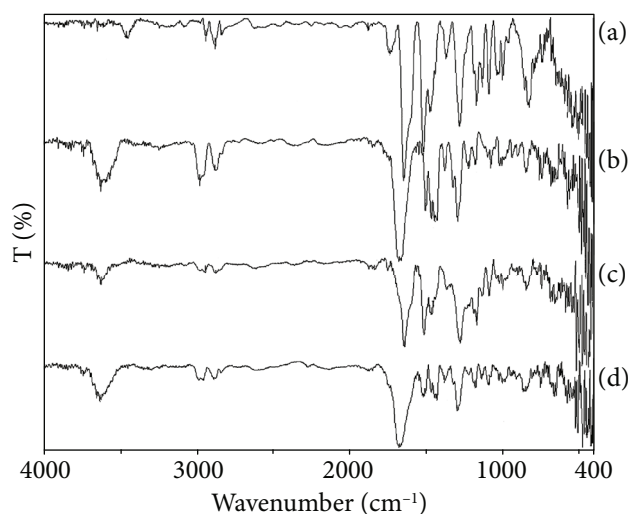
FIGURE 1: (a) FTIR spectra of silymarin, (b) PVP K30, (c) physical mixture, and (d) SSD3.

emerged due to physical interaction. A strong peak at 1290 cm^{-1} was emerged due to C-O bending vibration preserved from the PVP K30 [21, 31].

3.3. X-Ray Diffraction. Powdered XRD distinctively analyzes crystalline and amorphous transition in pharmaceutical products and processes. The X-ray diffraction spectrum of pure SL is depicted in Figure 2. Strong crystalline intense peaks were observed about 10.67°, 14.95°, 16.33°, 17.71°, 20.09°, 22.85°, 24.93°, 27.18°, and 29.73° at 2θ angle [21]. The intense peaks represented the complete crystalline structure of SL at following Miller indices, etc. Similarly, PVP K30 was amorphous in nature, but due to the hygroscopic nature of PVP, few intense peaks were observed

during analysis. The slight crystallinity was observed at 10.32°, 14.35°, 15.95°, 17.2°, 19.53°, 22.25°, 24.28°, 26.48°, and 28.95° at 2θ angle. The intense peaks assigned for respective miller indices confirm the crystalline nature [34]. The resultant solid dispersion formed by solvent evaporation methods can be able to successfully convert into amorphous form. The increased diffraction width in the diffraction angle suggested the decrease in crystallite size. In Figure 2 representing SSD, the crystalline bands at 11.25°, 20°, 27.43°, and 32.83° have broadened area which suggested that the small silymarin crystallites were encapsulated inside the polymeric structure [35]. In terms of solubility characteristics, the decrease in peak intensity or broadening of peak was preferably observed in amorphous forms and responsible for enhancement of solubility [21].

3.4. Solubility and Percentage Drug Content. Saturated solubility analysis of pure SL and prepared SSD is depicted in Figure 3. Aqueous solubility of SL was determined by shake flask method and observed to be $5 \pm 0.5 \, \mu$g/mL. The solubility of SL in aqueous media was found concentration dependent. Increase in concentration of PVP K30 leads to increase in solubility of SL. The SSD3 having a concentration ratio of $1:3$ showed more than 5-fold increase in solubility, while SSD1 and SSD2 had lower concentration that varied within 20–24 μg/mL, respectively. The solubility study described that SSD successfully enhanced in the presence of PVP K30 [21]. Figure 3 also represents percent of silymarin available in SSD1, SSD2, and SSD3. The percentage of drug was determined by UV-Vis spectrophotometric study and used for drug release as well as pharmacological evaluation. The percentage of SL loaded in solid dispersions was found to be 16.31, 19.3, and 28.3% with different batches, SSD1, SSD2, and SSD 3, respectively. SL loading efficiency was increased with increasing concentration of PVP K30 [35].
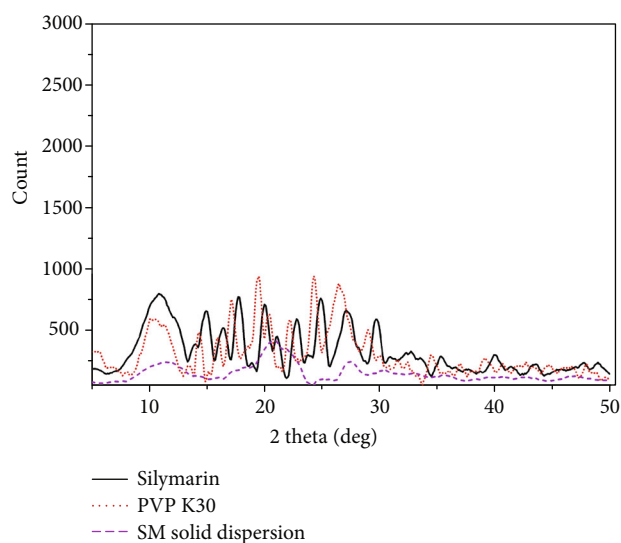
FIGURE 2: X-ray spectra of pure silymarin, PVP K30, and silymarin solid dispersion.
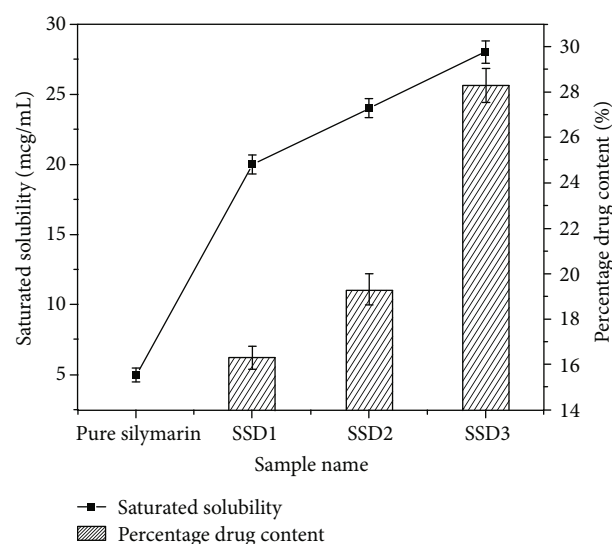
FIGURE 3: Saturated solubility and percentage drug content of pure silymarin and prepared SSD1, SSD2, and SSD3.

3.5. In Vitro Drug Release. Comparative drug release of pure SL and solid dispersion is depicted in Figure 4. Pure SL was released up to 24.86% within 2 h, while the solid dispersion with variable ratios released the maximum amount of SL into the dissolution medium. At 1 : 1 ratio (SSD1) release 44.1% of SL within 2 h enhanced the dissolution rate by 1.77-folds compared to pure SL. The interaction between PVP K30 and SL was stronger that led to increase in the saturation solubility almost by 5-folds as depicted in Figure 4. This helped to evaluate the dissolution rate of prepared SSD with increasing dissolution in the presence of PVP K30. The release of SL from the inner cores of PVP K30 was specifically by erosion as up to 25% of SL was released instantly within the first 15 min. Furthermore, increasing PVP K30 increased the dissolution and release of SL into
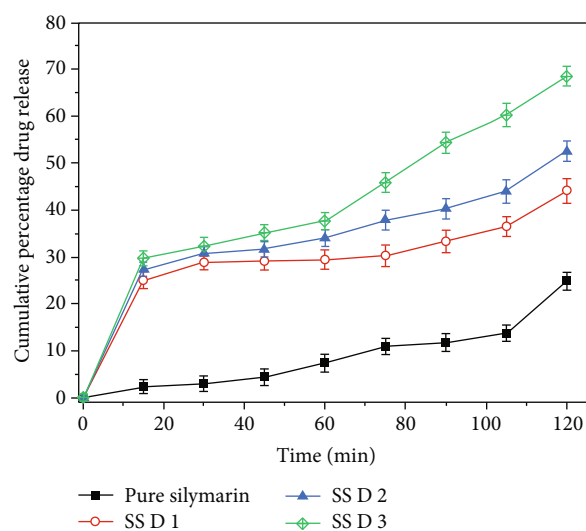
FIGURE 4: *In vitro* drug release study of pure silymarin in comparison with prepared SSD1, SSD2, and SSD3.

dissolution media as verified from Figure 4. SSD3 showed enhanced dissolution rate up to 2.8-fold increment compared to pure SL. SSD3 released more than 83% of SL within 2 h [36].

3.6. In Vivo Pharmacological Activity

3.6.1. Anti-Inflammatory Activity. The various stimuli like trauma, immunogenic reactions, and infection of microorganism initiate the inflammatory response as indication of physiological response among the individuals [25]. Fundamentally, the inflammatory response is characterized by enzymatic stimulation of arachidonic acid pathway and synthesis and release of eicosanoids like prostaglandins, thromboxanes, and leukotrienes by cyclooxygenase and 5-lipoxygenase enzymes [37]. Moreover, the drugs with central antipyretic and anti-inflammatory action cause downregulation of fever and inflammation, although the role of the antioxidant mechanism pathway in mediating the action of such agents has not yet been elucidated. Considerably, there are two phases of inflammation like early and delayed. The phase is associated with the synthesis of histamine, 5-hydroxytryptamin, bradykinin, and cyclooxygenase, whereas delayed phase is associated with infiltration of neutrophils and continuous production of metabolites of arachidonic acid [39].

(1) Carrageenan-Induced Rat Paw Edema. Figure 5 and Table 2 show carrageenan-induced rat paw edema anti-inflammatory response of prepared SSD in rats at variable interval of time. The SSD showed promising inhibition activity against carrageenan-induced rat paw edema. The solubility and dissolution were enhanced in the presence of PVP K30, which also provided permeability characteristics through the skin surface. After preparation of SSD in variable concentration ratios between SL and PVP K30, it significantly inhibited the edema produced by carrageenan. The
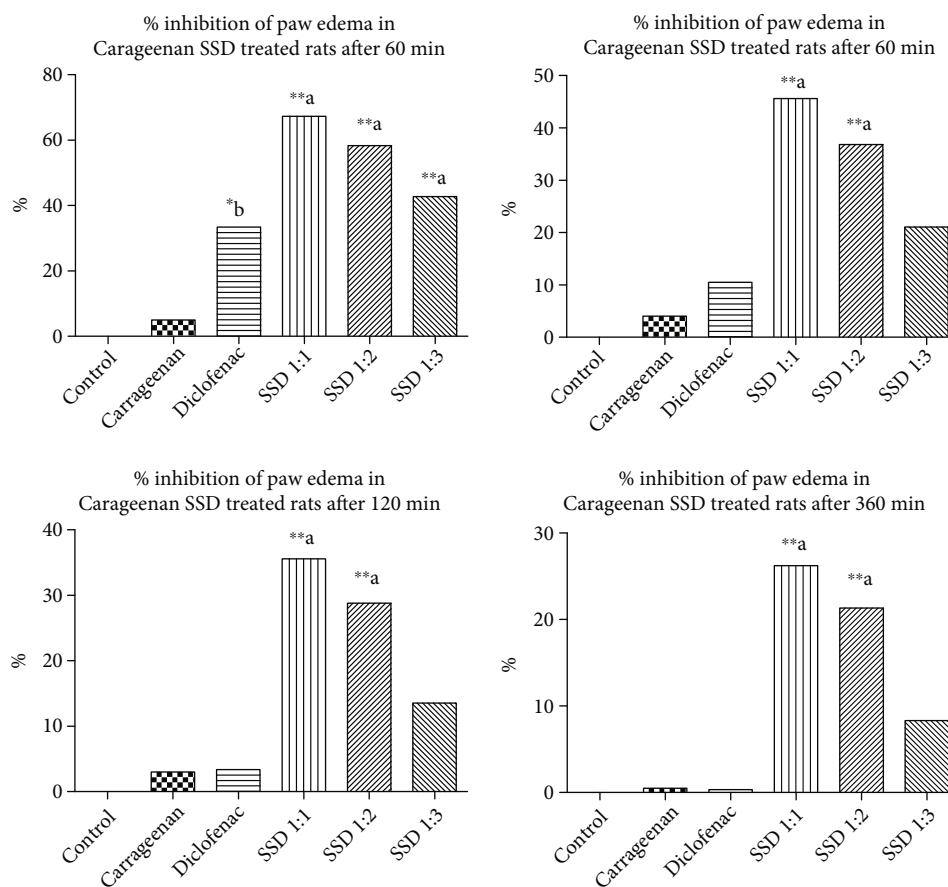
FIGURE 5: *In vivo* anti-inflammatory activity of silymarin solid dispersion. Carrageenan-induced animal model shows response measurement time points at 30 min, 60 min, 120 min, and 360 min, respectively. Statistical control: $^{*b}p < 0.05$ compared with control; ^{**a} $p < 0.001$ compared with control.

TABLE 2: *In vivo* anti-inflammatory activity of SSD in rats. *In vivo* carrageenan-induced paw edema in rats ($n = 6$).

Name of group	Edema value (mL) and % of inhibition			
	30	60	120	360
Control	0.8521 ± 0.006241	0.8754 ± 0.004578	0.8625 ± 0.005924	0.8425 ± 0.004231
Carrageenan treated	$0.5120 \pm 0.005831^{***\#}$	$0.5740 \pm 0.006782^{**\#}$	$0.5940 \pm 0.005099^{**\#}$	$0.6040 \pm 0.002449^{*\#}$
Std. diclofenac sodium (10 mg/kg)	$0.6860 \pm 0.005099^{*b}$ (33.46%)	0.6260 ± 0.005099 (10.52%)	0.6100 ± 0.003162 (3.38%)	0.6020 ± 0.003742 (0.33%)
SSD 1 : 1	$0.8600 \pm 0.07785^{**a}$ (67.31%)	$0.8280 \pm 0.07297^{**a}$ (45.61%)	$0.8060 \pm 0.06794^{**a}$ (35.59%)	$0.7760 \pm 0.06990^{**a}$ (26.22%)
SSD 1 : 2	$0.8140 \pm 0.01939^{**a}$ (58.36%)	$0.7820 \pm 0.01881^{**a}$ (36.84%)	$0.7600 \pm 0.01643^{**a}$ (28.81%)	$0.7360 \pm 0.01749^{*b}$ (21.31%)
SSD 1 : 3	$0.7340 \pm 0.008124^{**a}$ (42.80%)	0.6920 ± 0.007348 (21.05%)	0.6800 ± 0.009129 (13.55%)	$0.6520 \pm 0.008602^{**}$ (8.33%)

The data is presented as mean ± SEM. $^{*b}p < 0.05$ compared with control; $^{**a}p < 0.001$ compared with control.

wide variety of chemicals is successfully screened with the help of carrageenan-induced rat paw edema for their potential anti-inflammatory effects. The carrageenan-induced rat paw edema develops the biphasic response of inflammation [40]. The initial phase last for about 1 h and is thought to be mediated through release of various chemical mediators like histamine and serotonin. On the other hand, the later

phase is brought about by the release of substances like prostaglandins. Based on this, the second phase may be explained by an inhibition of cyclooxygenase or development of antioxidative properties [38, 39].

From Figure 5, statistical significance in comparison to standard SL, SSD has higher percentage. The different time

TABLE 3: *In vivo* hepatoprotective study by CCL_4 model in various biochemical parameters ($n = 6$).

Name of group	AST (IU/L)	ALT (IU/L)	ALP (IU/L)	Total bilirubin (mg/dL)
Normal group	54.92 ± 4.170	58.62 ± 4.284	142.9 ± 2.466	0.4740 ± 0.04501
CCl_4 group	151.2 ± 4.910***[#]	187.8 ± 3.545***[#]	267.0 ± 20.09***[#]	1.530 ± 0.03742***[#]
Silymarin treated	85.40 ± 3.103**[a]	99.59 ± 1.263**[a]	156.7 ± 4.358**[a]	0.6640 ± 0.03816**[a]
SSD (1 : 1)	138.1 ± 0.9782*[b]	174.6 ± 1.705*[b]	227.9 ± 4.450*[b]	1.222 ± 0.07915**[a]
SSD (1 : 2)	135.7 ± 2.565**[a]	161.0 ± 1.669**[a]	208.4 ± 2.632**[a]	1.064 ± 0.03415**[a]
SSD (1 : 3)	102.5 ± 1.176**[a]	118.2 ± 4.564**[a]	181.5 ± 4.432**[a]	0.8620 ± 0.05034**[a]

Values are expressed as mean $\pm$ SEM. ***[#]$p < 0.0001$ compared with control by the Student unpaired "t"-test; *[b]$p < 0.05$ compared with CCl_4; **[a]$p < 0.001$ compared with CCl_4.
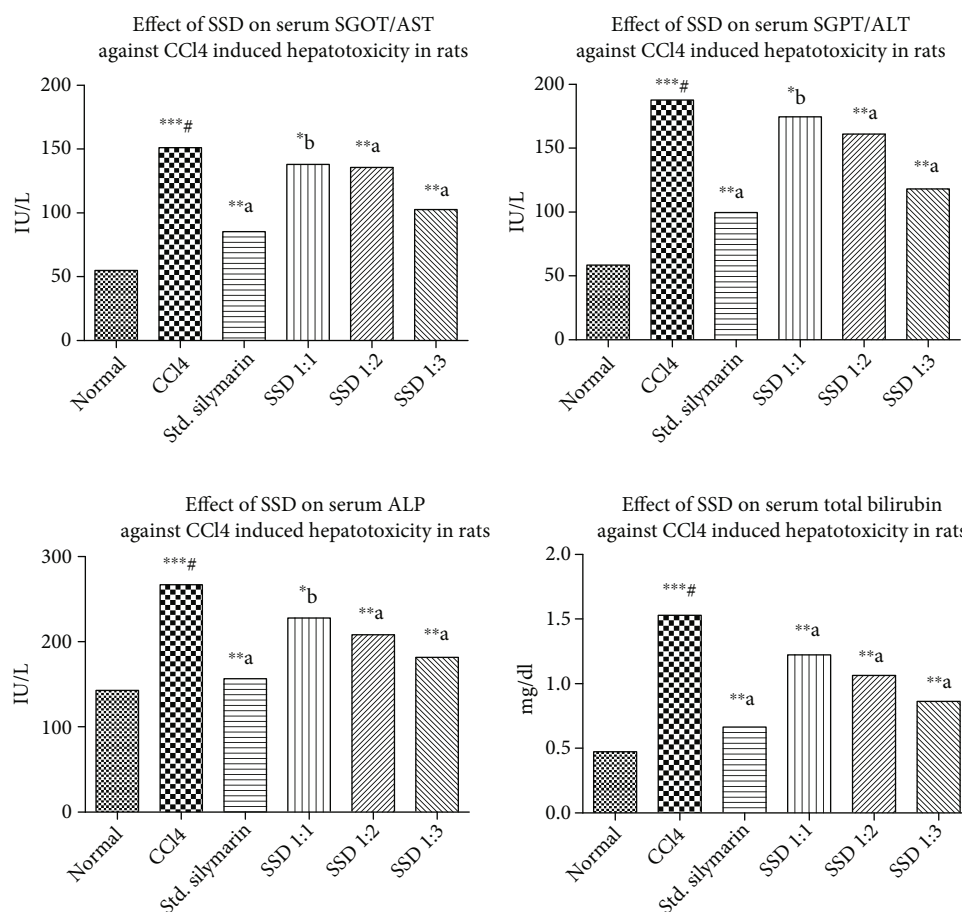
FIGURE 6: Carbon tetrachloride- (CCL_4-) induced hepatotoxicity assessment on silymarin and prepared SSD: effect on SGOT (AST), effect on SGPT (ALT), effect on ALP, and effect on total bilirubin against CCL_4. Statistical control: ***[#]$p < 0.0001$ compared with control by the Student unpaired "t"-test; *[b]$p < 0.05$ compared with CCL_4; **[a]$p < 0.001$ compared with CCL_4.

points recorded during experiment such as 30, 60, 120, and 360 min provide longer time effects. The positive control diclofenac showed the highest inhibition rate up to 0.33% after 360 min, while SSD (1 : 3) inhibited up to 8.33%. Initially, after 30 min of administration of SSD, % inhibition of edema was decreased from 67.31% (SSD1), 58.36% (SSD2), to 42.80% (SSD3) with respect to concentration of PVP K30 increased. At 360 min, the percent inhibition lowered to the values of 26.22% (SSD1), 21.31% (SSD2), and 8.33% (SSD3), respectively.

3.6.2. In Vivo Hepatoprotective Activity

(1) Carbon Tetrachloride Model. Despite its mild analgesic and antipyretic effect [40, 41], the oxymetabolite of carbon tetrachloride (CCl_4) has potential to cause liver toxicity through the depletion of GSH-Px level. Also, these metabolites cause lipid peroxidation and induce death of liver cells resulting in an elevation of serum enzyme AST, ALT, and ALP [24]. CCl_4 starts peroxidation in adipose tissue that results in loss of integrity of lipid membrane and starts
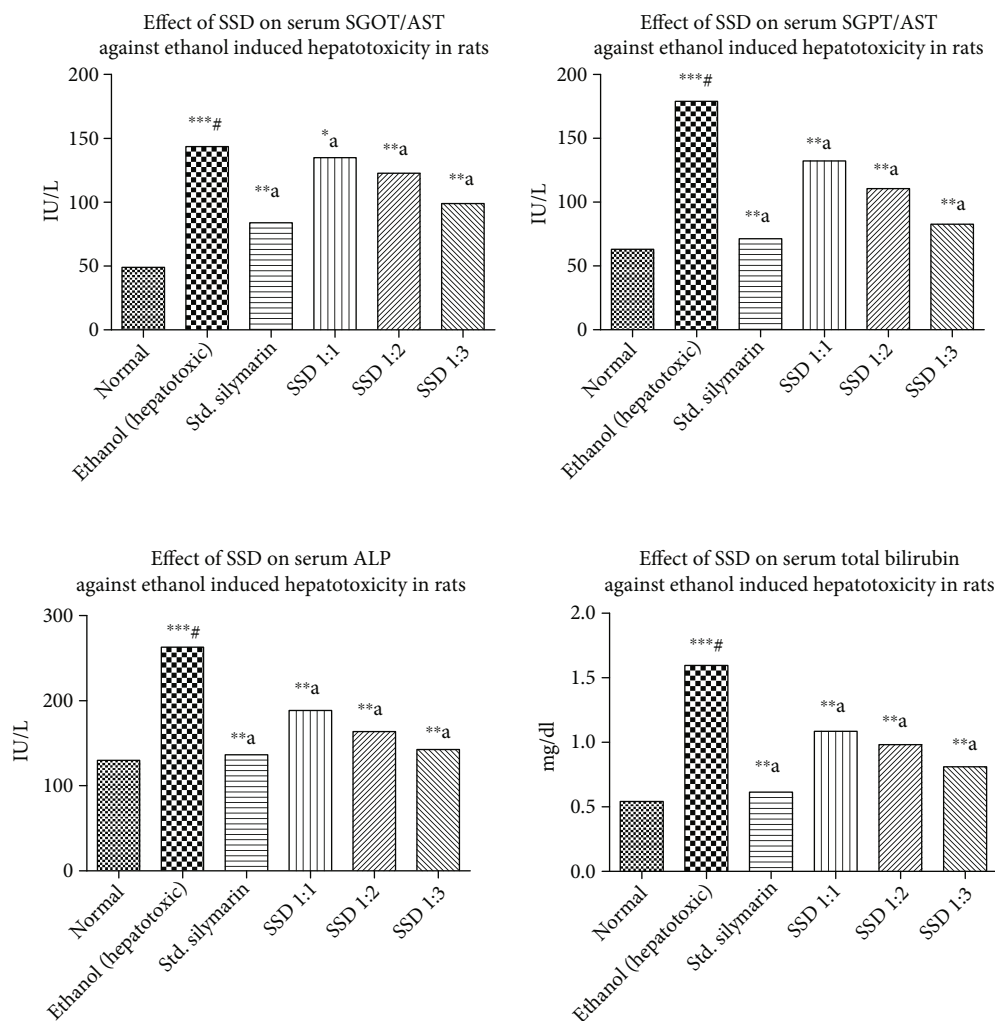
FIGURE 7: Ethanol-induced hepatotoxicity assessment of silymarin and prepared SSD: effect on SGOT/AST, effect on SGPT/ALT, effect on ALP, and effect on total bilirubin concentration, respectively. Statistical control: ****#$p < 0.0001$ compared with control by the Student unpaired "t"-test; **b$p < 0.05$ compared with ethanol; **a$p < 0.001$ compared with ethanol.

TABLE 4: In *vivo* hepatoprotective study by ethanol model on various biochemical parameters.

Name of group	AST (IU/L)	ALT (IU/L)	ALP (IU/L)	Total bilirubin (mg/dL)
Normal	49.04 ± 1.872	63.02 ± 1.286	130.0 ± 1.450	0.5420 ± 0.009165
Ethanol treated	143.5 ± 2.665****#	179.1 ± 2.207****#	262.8 ± 4.046****#	1.596 ± 0.02638****#
Silymarin-treated group	83.90 ± 1.672**a	71.34 ± 2.970**a	136.5 ± 2.970**a	0.6140 ± 0.02786**a
SSD (1:1)	134.9 ± 1.434*b	132.3 ± 6.644**a	188.6 ± 6.259**a	1.086 ± 0.05750**a
SSD (1:2)	122.7 ± 2.338**a	110.5 ± 2.478**a	163.9 ± 2.492**a	0.9820 ± 0.003742**a
SSD (1:3)	98.87 ± 0.9379**a	82.74 ± 3.654**a	142.5 ± 7.257**a	0.8100 ± 0.04037**a

Values are expressed as mean ± SEM. ****#$p < 0.0001$ compared with control by the Student unpaired "t"-test; *b$p < 0.05$ compared with ethanol; **a$p < 0.001$ compared with ethanol.

damaging hepatic tissue. The sequential liver damage was reflected by reduction in protein synthesis, metabolic enzyme inactivation, etc. Hepatocellular injury was measured by quantifying levels of bilirubin and other proteins and enzymes by biochemical test [42, 43], and the values are displayed in Table 3.

The mechanism of SL acts by maintaining the integrity of hepatocellular membrane and prevents permeation of toxins into the interior section of the liver to avoid further cellular damage. SL enhances ribosomal protein synthesis by activating nucleolar polymerase A (NPA). The NPA helps to start synthesis of hepatocytes and regenerating potential
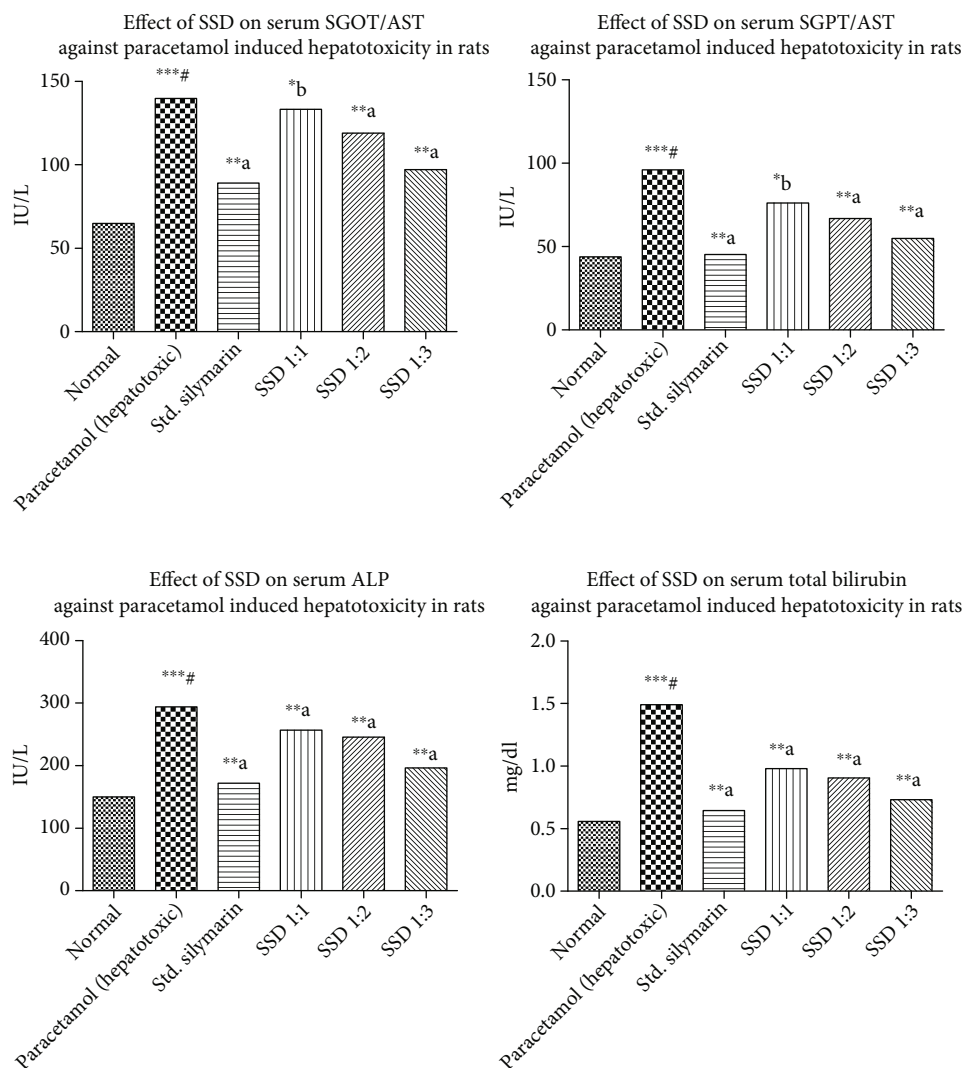
FIGURE 8: Paracetamol-induced hepatotoxicity assessment of silymarin and prepared SSD: effect on SGOT, effect on SGPT, effect on ALP, and effect on total bilirubin against paracetamol, respectively. Statistical control: ***#$p < 0.0001$ compared with control by the Student unpaired "t"-test; *b$p < 0.05$ compared with paracetamol; **a$p < 0.001$ compared with paracetamol.

TABLE 5: In vivo hepatoprotective study by paracetamol model on various biochemical parameters.

Name of group	AST (IU/L)	ALT (IU/L)	ALP (IU/L)	Total bilirubin (mg/dL)
Normal	64.90 ± 2.941	43.87 ± 2.496	150.3 ± 5.004	0.5580 ± 0.03441
Paracetamol-treated group	139.7 ± 1.732***#	95.93 ± 8.108***#	294.0 ± 13.55***#	1.490 ± 0.04012***#
Silymarin treated	89.01 ± 1.790**a	45.27 ± 4.737**a	171.8 ± 1.743**a	0.6440 ± 0.03092**a
SSD (1 : 1)	133.2 ± 1.132**b	76.01 ± 2.843*b	256.7 ± 3.839**a	0.9800 ± 0.005477**a
SSD (1 : 2)	119.1 ± 1.870**a	66.87 ± 3.418**a	245.7 ± 7.042**a	0.9060 ± 0.02839**a
SSD (1 : 3)	97.14 ± 0.8002**a	54.79 ± 3.859**a	196.6 ± 1.886**a	0.7300 ± 0.01517**a

Values are expressed as mean ± SEM. ***#$p < 0.0001$ compared with control by the Student unpaired "t"-test; *b$p < 0.05$ compared with paracetamol; **ap < 0.001 compared with paracetamol.

of the liver [44]. SSD has significantly reduced the levels of serum SGOT/AST, SGPT/ALT, ALP, and total bilirubin as represented in Figure 6. The enhanced solubility in the presence of PVP K30 at variable concentration significantly increased the bioavailability and permeability characteristics

compared to pure SL. The CCL$_4$ administration elevated the level of these biomarkers and started reducing efficiency of the liver. The SSD provided a stronger therapeutic potential by reducing the inflammatory response by preventing penetration of toxins like trichloromethyl and trichloromethylperoxy.

Comparatively, SSD (1:3) showed maximum reduction in the level of serum biomarkers. Protective ability of silymarin was enhanced after encapsulating with PVP K30.

(2) *Ethanol-Induced Hepatotoxicity in Rats.* Generally, the liver plays a vital role in carrying out enzyme-mediated different metabolic reactions in the body. According to extensive literature, it was observed that ingestion of ethanol causes damage of hepatic cells. The possible underlying mechanism involves the elevation of serum AST, ALT, ALP, and total bilirubin in rats and further structural and functional modulation of liver cells [45, 46]. Ethanol-based hepatotoxicity models were continuously evaluated due to multiple toxic reports available frequently in hospitals. The number of patients is increasing with liver toxicity due to higher consumption of alcohol. Phytomedicines are more effective in the management of liver toxicities. The recovery rate is higher comparative to chemotherapeutic agents. The effects of pretreatment with three SSD in the ratio of 1:1, 1:2, and 1:3 on the ethanol-induced elevation of serum AST, ALT, ALP, and total bilirubin are depicted in Figure 7. There was proportionate reduction in the elevated levels of serum AST, ALT, ALP, and total bilirubin with respect to PVP K30 concentration in the formulations. The SSD (1:3) showed higher reduction response due to the enhanced solubility of SL. The biomarker level proportionally decreased as solubility increased with composition ratio ranging from SSD 1:1 to 1:3. SSD with PVP in the ratio of 1:1 ($p < 0.05$), 1:2 ($p < 0.01$), and 1:3 ($p < 0.01$) significantly prevented the elevated level of serum AST, ALT, ALP, and total bilirubin. Our studies on the ethanol-induced hepatic damage were in accordance with previous reports [47]. This study demonstrated that pretreatment with three SSD in the ratio of 1:1, 1:2, and 1:3 had significantly reduced levels of serum AST, ALT, ALP, and total bilirubin, which were elevated by ethanol administration as shown in Figure 7 and Table 4.

(3) *Paracetamol-Induced Hepatotoxicity in Rats.* Paracetamol is one of the most important hepatotoxic agents reported in the treatment of pediatric patients. Many adverse events and dose dumping complications in the treatment of paracetamol were reported specifically related to toxicity. The biomarkers like SGPT, SGOT, ALT, and serum bilirubin were identified to assess the toxicity level of paracetamol in patients undergoing treatment. Generally, liver toxicity is induced by ingestion of paracetamol and it is routinely employed in the screening of wide range of chemicals for their hepatoprotective activity in rodents. The increased production of serum enzymes in blood stream was associated with central/submissive necrosis of the liver, which caused severe hepatic injury as shown in Figure 8 and Table 5.

4. Conclusion

SL is a natural lipophilic molecule, and it has an aqueous solubility of 5 μg/mL. Due to its low aqueous solubility, it has low oral bioavailability (23-47%), and after oral administration, it leads to poor therapeutic application. An attempt was tried to increase the solubility and bioavailability of silymarin by solid dispersion technique using PVP-K30. PVP K30 inhibited the crystallization of SL and produced amorphous solid eutectic mixture for therapeutic applications. The solubility was increased maximum up to 5-fold after encapsulation inside the PVP K30. A variable ratio pertaining to PVP K30 and SL was intact within the solution phase and forms a homogenous mixture. The stronger interactions were highly dissociated in the presence of dissolution medium and enhanced the release of SL from the inner compartment. The dissolution rate was increased by 2.8-fold compared to pure SL. The wettability characteristics and favourable interaction with the solvent molecules helped to dissociate silymarin instantly from the eutectic complex. In the presence of aqueous environment, thereby erosion of PVP K30 took place and released about 23% SL within the first 15 min. The drug release characteristics were increased with an enhanced bioavailability verified by anti-inflammatory and hepatoprotective activities. The local solubilisation effect was prominent and verified by anti-inflammatory response using carrageenan-induced inflammation in rats. All three hepatoprotective models showed reduction in the biomarker response that shows good bioavailability of silymarin in the presence of PVP K30.

Data Availability

All the data used to support the findings of this study are included within the article.

Conflicts of Interest

All the authors of this research article have declared that they have no competing financial or personal conflict of interest.

Acknowledgments

References

[1] S. R. Vippagunta, Z. Wang, S. Hornung, and S. L. Krill, "Factors affecting the formation of eutectic solid dispersions and their dissolution behavior," *Journal of Pharmaceutical Sciences*, vol. 96, no. 2, pp. 294–304, 2007.

[2] M. V. Eberhardt, K. Kobira, A. S. Keck, J. A. Juvik, and E. H. Jeffery, "Correlation analyses of phytochemical composition, chemical, and cellular measures of antioxidant activity of broccoli (Brassica oleraceaL. var. italica)," *Journal of Agricultural and Food Chemistry*, vol. 53, no. 19, pp. 7421–7431, 2005.

[3] Z. Marczynski, B. Skibska, S. Nowak, J. Jambor, and M. M. Zgoda, "Actual solubility (S|real.|), level of hydrophilic-lipophilic balance (HLBRequ., HLBD, HLBG) and partition coefficient (log P) of phytochemicals contained inExt. Camellia sinensisL.aqu. siccumin the light of general Hildebrand-

Scatchard-Fedors theory of solubility," *Herba Polonica*, vol. 64, no. 2, pp. 46–59, 2018.

[4] D. Sonali, S. Tejal, T. Vaishali, and G. Tejal, "Silymarin-solid dispersions: characterization and influence of preparation methods on dissolution," *Acta Pharmaceutica*, vol. 60, no. 4, pp. 427–443, 2010.

[5] J. Singh, M. Walia, and S. Harikumar, "Solubility enhancement by solid dispersion method: a review," *Journal of drug delivery and Therapeutics*, vol. 3, no. 5, pp. 148–155, 2013.

[6] G. Singh, L. Kaur, G. D. Gupta, and S. Sharma, "Enhancement of the solubility of poorly water soluble drugs through solid dispersion: a comprehensive review," *Indian Journal of Pharmaceutical Sciences*, vol. 79, no. 5, pp. 674–687, 2017.

[7] A. Hussain, A. Samad, M. Usman Mohd Siddique, and S. Beg, "Lipid microparticles for oral bioavailability enhancement," *Recent Patents on Nanomedicine*, vol. 5, no. 2, pp. 104–110, 2015.

[8] A. Hussain, M. Usman Mohd Siddique, S. Kumar Singh, A. Samad, S. Beg, and M. Wais, "Lipid-drug conjugates for oral bioavailability enhancement," *Recent Patents on Nanomedicine*, vol. 5, no. 2, pp. 87–95, 2015.

[9] W.-C. Hsu, L. T. Ng, T. H. Wu, L. T. Lin, F. L. Yen, and C. C. Lin, "Characteristics and antioxidant activities of silymarin nanoparticles," *Journal of Nanoscience and Nanotechnology*, vol. 12, no. 3, pp. 2022–2027, 2012.

[10] O. M. Abdel-Salam, A. A. Sleem, and F. A. Morsy, "Effects of biphenyldimethyl-dicarboxylate administration alone or combined with silymarin in the CCL4 model of liver fibrosis in rats," *The Scientific World JOURNAL*, vol. 7, 1255 pages, 2007.

[11] Z. Yang, L. Zhuang, Y. Lu, Q. Xu, and X. Chen, "Effects and tolerance of silymarin (milk thistle) in chronic hepatitis C virus infection patients: a meta-analysis of randomized controlled trials," *BioMed Research International*, vol. 2014, Article ID 941085, 9 pages, 2014.

[12] A. Alhusban, E. Alkhazaleh, and T. El-Elimat, "Silymarin Ameliorates Diabetes-Induced Proangiogenic Response in Brain Endothelial Cells through a GSK-3β Inhibition-Induced Reduction of VEGF Release," *Journal of Diabetes Research*, vol. 2017, Article ID 2537216, 9 pages, 2017.

[13] J.-W. Wu, L. C. Lin, S. C. Hung, C. W. Chi, and T. H. Tsai, "Analysis of silibinin in rat plasma and bile for hepatobiliary excretion and oral bioavailability application," *Journal of Pharmaceutical and Biomedical Analysis*, vol. 45, no. 4, pp. 635–641, 2007.

[14] F. Aqil, R. Munagala, J. Jeyabalan, and M. V. Vadhanam, "Bioavailability of phytochemicals and its enhancement by drug delivery systems," *Cancer Letters*, vol. 334, no. 1, pp. 133–141, 2013.

[15] J. Cao, J. Cao, H. Wang, L. Chen, F. Cao, and E. Su, "Solubility improvement of phytochemicals using (natural) deep eutectic solvents and their bioactivity evaluation," *Journal of Molecular Liquids*, vol. 318, p. 113997, 2020.

[16] K. Bobe, C. R. Subrahmanya, S. Suresh et al., "Formulation and evaluation of solid dispersion of atorvastatin with various carriers," *International journal of comprehensive pharmacy*, vol. 2, no. 1, pp. 1–6, 2011.

[17] S. K. Das, S. Roy, Y. Kalimuthu, J. Khanam, and A. Nanda, "Solid dispersions: an approach to enhance the bioavailability of poorly water-soluble drugs," *International journal of pharmacology and pharmaceutical technology*, vol. 1, no. 1, pp. 37–46, 2012.

[18] Y. Kubo, N. Yagi, and H. Sekikawa, "Stability of probucol-polyvinylpyrrolidone solid dispersion systems," *Yakugaku zasshi: Journal of the Pharmaceutical Society of Japan*, vol. 131, no. 4, pp. 629–634, 2011.

[19] B. V. Robinson, F. M. Sullivan, J. F. Borzelleca, and S. L. Schwartz, *PVP: a critical review of the kinetics and toxicology of polyvinylpyrrolidone (povidone)*, CRC Press, 2018.

[20] L.-F. Yin, S. J. Huang, C. L. Zhu et al., "In *vitro* and in *vivo* studies on a novel solid dispersion of repaglinide using polyvinylpyrrolidone as the carrier," *Drug Development and Industrial Pharmacy*, vol. 38, no. 11, pp. 1371–1380, 2012.

[21] A. M. Yousaf, U. R. Malik, Y. Shahzad, T. Mahmood, and T. Hussain, "Silymarin-laden PVP-PEG polymeric composite for enhanced aqueous solubility and dissolution rate: preparation and in vitro characterization," *Journal of pharmaceutical analysis*, vol. 9, no. 1, pp. 34–39, 2019.

[22] M. P. More, M. D. Patil, A. P. Pandey, P. O. Patil, and P. K. Deshmukh, "Fabrication and characterization of graphene-based hybrid nanocomposite: assessment of antibacterial potential and biomedical application," *Artificial cells, nanomedicine, and biotechnology*, vol. 45, no. 8, pp. 1496–1508, 2017.

[23] B. K. Singh, R. A. Pathan, K. K. Pillai, S. E. Haque, and K. Dubey, "Diclofenac sodium, a nonselective nonsteroidal anti-inflammatory drug aggravates doxorubicin-induced cardiomyopathy in rats," *Journal of Cardiovascular Pharmacology*, vol. 55, no. 2, pp. 139–144, 2010.

[24] L. W. Weber, M. Boll, and A. Stampfl, "Hepatotoxicity and mechanism of action of haloalkanes: carbon tetrachloride as a toxicological model," *Critical Reviews in Toxicology*, vol. 33, no. 2, pp. 105–136, 2003.

[25] K. L. Rock and H. Kono, "The inflammatory response to cell death," *Annual Review of Pathology: Mechanisms of Disease*, vol. 3, pp. 99–126, 2008.

[26] R. Eldalawy, W. M. Al-Ani, and W. A. Kareem, "Phenotypic, anatomical and phytochemical investigation of Iraqi Silybum marianum," in *Journal of Physics: Conference Series*, IOP Publishing., 2021.

[27] J. N. Amin, A. Murad, A. M. Motasem, S. R. Ibrahem, J. M. Ass' ad, and A. M. Ayed, "Phytochemical screening and in-vitro evaluation of antioxidant and antimicrobial activities of the entire Khella plant (Ammi visnaga. L.) a member of Palestinian flora," *International Journal of Pharmacognosy and Phytochemical Research*, vol. 7, pp. 137–143, 2015.

[28] S. M. M. Shah, F. A. Khan, S. M. H. Shah et al., "Evaluation of phytochemicals and antimicrobial activity of white and blue capitulum and whole plant of Silybum marianum," *World Applied Sciences Journal*, vol. 12, no. 8, pp. 1139–1144, 2011.

[29] M. P. More, R. V. Chitalkar, M. S. Bhadane et al., "Development of graphene-drug nanoparticle based supramolecular self assembled pH sensitive hydrogel as potential carrier for targeting MDR tuberculosis," *Materials Technology*, vol. 34, no. 6, pp. 324–335, 2019.

[30] A. E. El-Nahas, A. N. Allam, D. A. Abdelmonsif, and A. H. El-Kamel, "Silymarin-loaded eudragit nanoparticles: formulation, characterization, and hepatoprotective and toxicity evaluation," *AAPS PharmSciTech*, vol. 18, no. 8, pp. 3076–3086, 2017.

[31] D. Abedinoghli, M. Charkhpour, K. Osouli-Bostanabad et al., "Electrosprayed nanosystems of carbamazepine–PVP K30 for enhancing its pharmacologic effects," *Iranian journal of pharmaceutical research: IJPR*, vol. 17, no. 4, p. 1431, 2018.

[32] A. F. McDonagh and L. Tajber, "Crystallo-co-spray drying as a new approach to manufacturing of drug/excipient agglomerates: impact of processing on the properties of paracetamol

and lactose mixtures," *International Journal of Pharmaceutics*, vol. 577, p. 119051, 2020.

[33] W.-F. Zhu, L. Zhu, Z. Li et al., "The novel use of PVP K30 as templating agent in production of porous lactose," *Pharmaceutics*, vol. 13, no. 6, p. 814, 2021.

[34] B. B. Huang, D. X. Liu, D. K. Liu, and G. Wu, "Application of solid dispersion technique to improve solubility and sustain release of emamectin benzoate," *Molecules*, vol. 24, no. 23, p. 4315, 2019.

[35] R. Sun, C. Shen, S. Shafique et al., "Electrosprayed polymeric nanospheres for enhanced solubility, dissolution rate, oral bio-availability and antihyperlipidemic activity of Bezafibrate," *International Journal of Nanomedicine*, vol. Volume 15, pp. 705–715, 2020.

[36] A. A. Ramadan, A. M. Elbakry, H. A. Sarhan, and S. H. Ali, "Silymarin loaded floating polymer(s) microspheres:characterization, in-vitro/in-vivoevaluation," *Pharmaceutical Development and Technology*, vol. 25, no. 9, pp. 1081–1089, 2020.

[37] A. Heller, T. Koch, J. Schmeck, and K. van Ackern, "Lipid mediators in inflammatory disorders," *Drugs*, vol. 55, no. 4, pp. 487–496, 1998.

[38] N. Boughton-Smith, A. M. Deakin, R. L. Follenfant, B. J. R. Whittle, and L. G. Garland, "Role of oxygen radicals and arachidonic acid metabolites in the reverse passive Arthus reaction and carrageenin paw oedema in the rat," *British Journal of Pharmacology*, vol. 110, no. 2, pp. 896–902, 1993.

[39] D. Salvemini, Z. Q. Wang, P. S. Wyatt et al., "Nitric oxide: a key mediator in the early and late phase of carrageenan-induced rat paw inflammation," *British Journal of Pharmacology*, vol. 118, no. 4, pp. 829–838, 1996.

[40] R. O. Recknagel, "Carbon tetrachloride hepatotoxicity," *Pharmacological Reviews*, vol. 19, no. 2, pp. 145–208, 1967.

[41] R. O. Recknagel, E. A. Glende Jr., J. A. Dolak, and R. L. Waller, "Mechanisms of carbon tetrachloride toxicity," *Pharmacology & Therapeutics*, vol. 43, no. 1, pp. 139–154, 1989.

[42] G. Balata and H. Shamrool, "Spherical agglomeration versus solid dispersion as different trials to optimize dissolution and bioactivity of silymarin," *Journal of Drug Delivery Science and Technology*, vol. 24, no. 5, pp. 478–485, 2014.

[43] H. Najafzadeh, M. R. Jalali, H. Morovvati, and F. Taravati, "Comparison of the prophylactic effect of silymarin and deferoxamine on iron overload-induced hepatotoxicity in rat," *Journal of Medical Toxicology*, vol. 6, no. 1, pp. 22–26, 2010.

[44] S. Pradhan and C. Girish, "Hepatoprotective herbal drug, silymarin from experimental pharmacology to clinical medicine," *Indian Journal of Medical Research*, vol. 124, no. 5, pp. 491–504, 2006.

[45] H. Tsukamoto, Y. Takei, C. J. McClain et al., "How is the liver primed or sensitized for alcoholic liver disease?," *Alcoholism: Clinical and Experimental Research*, vol. 25, pp. 171S–181S, 2001.

[46] Z. Zhou, L. Wang, Z. Song, J. C. Lambert, C. J. McClain, and Y. J. Kang, "A critical involvement of oxidative stress in acute alcohol-induced hepatic TNF-α production," *The American Journal of Pathology*, vol. 163, no. 3, pp. 1137–1146, 2003.

[47] S. Ige, R. E. Akhigbe, O. Edeogho et al., "Hepatoprotective activities of Allium cepa in cadmium-treated rats," *International Journal of Pharmacy and Pharmaceutical Sciences*, vol. 3, no. 5, pp. 60–63, 2011.

Research Article

Anti-Inflammatory Activity and Chemical Analysis of Different Fractions from *Solidago chilensis* Inflorescence

Thais Morais de Brito [iD],[1] Fabio Coelho Amendoeira [iD],[1] Temistocles Barroso de Oliveira,[2] Laís Higino Doro,[1] Esdras Barbosa Garcia [iD],[1] Naína Monsores Felix da Silva,[1] Amanda da Silva Chaves [iD],[1] Flavia Fontenelle Muylaert [iD],[1] Tatiana Almeida Pádua [iD],[3] Elaine Cruz Rosas [iD],[3] Maria das Graças M. O. Henriques [iD],[3] Valber da Silva Frutuoso,[4] Simone Sacramento Valverde [iD],[2] and Fausto Klabund Ferraris [iD][1]

[1]*Laboratório de Farmacologia, Instituto Nacional de Controle de Qualidade em Saúde–FIOCRUZ, Rio de Janeiro, Brazil*
[2]*Laboratório de Química Medicinal de Produtos Bioativos, Instituto de Tecnologia em Fármacos–FIOCRUZ, Rio de Janeiro, Brazil*
[3]*Laboratório de Farmacologia Aplicada, Instituto de Tecnologia em Fármacos–FIOCRUZ, Rio de Janeiro, Brazil*
[4]*Laboratório de Imunofarmacologia, Instituto Oswaldo Cruz–FIOCRUZ, Rio de Janeiro, Brazil*

Correspondence should be addressed to Fausto Klabund Ferraris; fausto.ferraris@incqs.fiocruz.br

Solidago chilensis Meyen (Compositae) is a species native to South America (Brazil) popularly known as arnica. In Brazilian popular medicine, inflorescences and rhizomes of this plant have been used since the end of the 19th century to replace the exogenous and hepatotoxic *Arnica montana* L. in the treatment of edema and inflammatory pathologies. Although the anti-inflammatory activity of *S. chilensis* is evidenced in the literature, there is a lack of studies with enriched fractions or compounds isolated from it. The objective of the current study was to characterize phytochemically and to evaluate the pharmacological action *in vivo* and *in vitro* of the crude extract and the different fractions (hexane, dichloromethane, acetal, butanolic, and aqueous) isolated from the inflorescence of *S. chilensis*. The inflorescence crude extract (ScIE) and fractions were administered by intraperitoneal route to mice at different doses. In an LPS-induced pleurisy model, inhibition of leukocyte influx was observed for the ScIE and all fractions tested, as compared to controls. Dichloromethane (ScDicF), butanolic (ScButF), and aqueous (ScAquF) were selected for further analysis as they showed the best inhibitory effects in leukocyte migration and inflammatory cytokine and chemokine production: TNF-α, CXCL1/KC, CXCL2/MIP-2, and CCL11/eotaxin-1. In LPS-stimulated J774A.1 cell line, ScIE and the ScDicF exhibited an inhibitory effect on nitric oxide (NO) production and downmodulated the COX-2 expression; ScAquF failed to modulate NO production and COX-2 expression. In phytochemical analysis, HPLC-UV-DAD chromatograms of ScDicF and ScAquF showed the main peaks with UV spectrum characteristics of flavonoids; chlorogenic acid and isoquercetin were the most present phytochemicals identified in the ScAquF, and a high number of n-alkanes was found in ScHexF. Our study was the first to address biological effects and correlate them to phytochemically characterized fractions from inflorescences of *S. chilensis*.

1. Introduction

Solidago chilensis Meyen (= *Solidago microglossa*) is a member of the Compositae family widely used in Brazilian folk medicine, as well as in other South American countries such as Chile, Argentina, Bolivia, and Paraguay. *S.*

chilensis, popularly known as "Brazilian arnica," can exert multiple biological effects and is used as an antidepressant, gastroprotective, diuretic, burn treatment, skin diseases, anticancer, antiedematogenic, and anti-inflammatory [1–9].

In addition to the popular uses, some reports have emphasized the anti-inflammatory activity of *S. chilensis*,

where several types of extracts obtained, mainly from their rhizomes and leaves, were tested. In experimental models of inflammation, the modulation of these extracts in the inhibition of different inflammatory events, such as edema formation, mast cell degranulation, leukocyte recruitment, and inflammatory mediators' production (e.g., nitric oxide, interleukin-1β, and tumor necrosis factor-α), was observed [10–12]. These activities are related to the presence of flavonoid quercetrin, caffeoylquinic acid derivates, and flavonoid rutin [11, 12]; additionally, our recent investigation points to the presence of flavonoids derived from quercetin and kaempferol; and labdane diterpenes are partly responsible for these biological activities [13].

S. chilensis is part of the Brazilian National List of Medicinal Plants of Interest to Unified National Health System, and extracts obtained from rhizomes and inflorescences have been produced for anti-inflammatory use [13]. Although the activity of S. chilensis is evidenced in the literature, there are few studies with enriched/characterized fractions or isolated compounds, especially concerning extracts obtained from the inflorescences, relating them to the anti-inflammatory and antinociceptive activities already well described in this plant species [9, 14]. The generation of this knowledge can help in the identification of phytochemical markers that can be used in the future in the quality control of S. chilensis-based products.

In the present work, we evaluated, focusing on anti-inflammatory activity, the modulatory properties of different fractions obtained from the S. chilensis inflorescence crude extract. Based on the obtained results, we explored some mechanism of action of those fractions that presented greater biological activity and, in addition, we chemically characterized these fractions, in order to determine the main active compounds involved in the anti-inflammatory activity of S. chilensis.

2. Materials and Methods

2.1. Materials.
Alamar Blue cell viability reagent was purchased from Invitrogen (Massachusetts, USA). Dexamethasone, diclofenac sodium, dimethyl sulfoxide (DMSO), Dulbecco's Modified Eagle Medium (DMEM), ethylenediaminetetraacetic acid (EDTA), fetal bovine serum (FBS), Laemmli sample buffer, lipopolysaccharide (LPS), phosphate-buffered saline (PBS), and protease inhibitor cocktail were purchased from Sigma-Aldrich (St. Louis, MO, USA). Ether, ethanol, ethyl acetate, dichloromethane, methanol, n-butanol, and n-hexane were purchased from Tedia Way (Fairfield, OH, USA). Nitrocellulose membranes were purchased from Amersham Pharmacia Biotech (San Francisco, CA, USA). The chromatographic solvents (acetonitrile, acetic acid, and trifluoroacetic acid) were purchased from Merck (Darmstadt, Germany). Monoclonal antibodies anti-COX-2, anti-goat IgG biotin-conjugated antibody, and streptavidin-conjugated horseradish peroxidase were purchased from Santa Cruz Biotechnology (Texas, USA). The CXCL2/MIP-2, CXCL1/KC, CCL11/eotaxin-1, and TNF-α enzyme-linked immunosorbent assay (ELISA) kit were purchased from R&D Systems (Minneapolis, MN, USA). The

colorimetric kit used for the May-Grunwald-Giemsa method was purchased from Laborclin (Pinhais, PR, BR).

2.2. Plant Material.
Solidago chilensis Meyen was cultivated at Phytomedicine Agroecological Platform (PAF), FIO-CRUZ, Rio de Janeiro city, RJ, Brazil (22°93′52.74″S; 43°39′89.16″W). Their inflorescences were collected in the summer, between December and March, when they are produced due to increased sunlight. The central stems were collected from the same producers of inflorescence plants. The species identification was performed by Mariana Reis de Brito, Botany Herbarium of the Department of the Institute of Biology/UFRJ, and a voucher specimen was deposited under the code 32689/RFA. The study of the plant material was conducted under the register of Brazilian System for Management Genetic of Heritage and Associated Traditional Knowledge (SISGEN) (Process number AF96E16).

2.3. Ether-Ethanolic Crude Extract and Their Fraction Preparation.
The inflorescences of the plant material supplied were oven-dried 35-40°C and pulverized in a knife mil. 200 grams of material was weighed and submitted to dynamic maceration with ether : ethanol (1 : 1-3 L) for 6 hours [15]. After this period, the ether : ethanol extract was filtered, evaporated under reduced pressure (in a rotary evaporator Büchi R-124®), lyophilized, and weighed (200 g; 4.94% yield). The material was referred to as the Solidago chilensis inflorescence crude extract (ScIE) and was stored at room temperature until use.

A part of the ScIE was separated for the pharmacological assays, and another portion was used to successive liquid : liquid partition with solvents of increasing polarity (n-hexane, dichloromethane, ethyl acetate, and n-butanol) to obtain the fractions. The ScIE was resuspended with water : methanol (4 : 1v/v, 500 mL), and then, the organic phase was evaporated. The aqueous portion was added with 500 mL of n-hexane and separated in a glass separatory funnel. This process was carried out five times, totaling the use of 2.5 L of solvent. The organic phase was evaporated, and a 0.46% yield of the hexane fraction (ScHexF) was obtained. Likewise, the remaining aqueous portion was added with 500 mL of dichloromethane, four times, totaling the use of 2 L of solvent. The organic phase was evaporated, and 0.42% yield of the dichloromethane fraction (ScDicF) was obtained. Always adding 500 mL of solvent to the aqueous portion at a time, the partition was carried out with the solvents ethyl acetate (ten times, using 5 L of solvent in total) and n-butanol (once), obtaining a yield of 1.08% for the acetalic fraction (ScAceF) and 2.26% for the butanolic fraction (ScButF). The remaining aqueous fraction (ScAquF) showed 2.84% yield.

2.4. Characterization and Identification of Ether-Ethanolic Crude Extract and Their Fractions.
The high-performance liquid chromatography, coupled with ultraviolet spectroscopy, a diode-array detector (HPLC-UV-DAD) analysis, was carried out through two different methodologies, one developed to characterize flavonoids and phenolic compounds

in *S. canadensis* [16] and another developed to characterize labdane diterpenes, such as solidagenone, commonly found in *S. chilensis* [15]. The first one was used in ScIE, ScDicF, and ScAquF. E the second one was used only in ScDicF.

The characterization through a HPLC-UV-DAD for flavonoids and phenolic compounds was performed with LiChrospher 100 RP-18 column (Merck™) for analytical scale with 250 mm length, 4 mm in diameter, and 5 μm particle size, using C18 as stationary phase and DAD detector, type SPDM20A. A binary mixture was used as the eluent system, composed of acetic acid : water (1 : 40) and acetonitrile [16]. For the terpenes' investigation, a binary mixture with an isocratic eluent system, consisting of 0.05% trifluoroacetic acid and acetonitrile, was used [15]. Samples were diluted in the ratio of 10 mg/mL, and 10 μL aliquots were injected. An analysis was performed at 25°C with a flow rate of 1.0 mL·min^{-1}. The eluted compounds were analyzed for their absorption in UV at 310 nm for flavonoids and between 210 and 400 nm for terpenoids (solidagenone) [16, 17]. The analysis by HPLC-UV-DAD allowed the characterization of flavonoids and phenolic compounds through monitoring by internal normalization, coinjection of quercetin, and analysis of UV spectra, since all derivatives observed in the extract of *S. chilensis* have spectra in the UV characteristics of its aglycone (quercetin or kaempferol) in addition to chlorogenic acid, identified through its retention time in the methodology used, literature data, and UV spectrum, all also already rescribed for the genus *Solidago* [6, 16, 18–21]. The ScHexF was characterized through the Agilent 5973 GC-MS system (Agilent Technologies, USA). Helium was used as mobile phase and flow rate of 2 mL/min. The heating ramp followed the following schedule: 60°C (10 min); 60-120°C (60°C/min); 120-290°C (15°C/min); 290°C (17 min). The ionization voltage and temperature of injector and ion source were 70 eV and 260 and 300°C, respectively. The identification of organic compounds was performed using the MSD ChemStation E. 02.021431–Wiley 7N–1989-2011 software (Agilent Technologies, USA), which was used for data acquisition, library searching, and compound characterization.

2.5. Cell Culture. Murine macrophage cell line J774A.1 (ATCC TIB-67™) was maintained at Dulbecco's minimal essential medium (DMEM) with 10% FBS, and antibiotic mixture (penicillin, streptomycin, and ampicillin 100 units/mL), under predefined conditions of temperature at 37°C, 95% humidity, and 5% CO_2.

2.6. Cytotoxicity Assay. The J774.A1 cell line was plated in a 96-well microplate (1×10^5 cells/well, in quadruplicate) and cultured in the presence of ScIE and the five fractions at concentrations of 1, 10, 50, 100, and 200 μg/mL for 48 hours (in 5% CO_2, at 37°C). Cells cultured only with medium or culture medium containing 0.5% DMSO (extract diluent) were used as positive controls of cell viability. After 44 hours, 10% Alamar Blue was added to the wells. After 4 hours of incubation, the fluorescence signal was monitored in a microplate reader (Molecular Devices), Ex: 530-560 nm; Em: 590 nm [13].

2.7. Nitric Oxide Production. Macrophages J774.A1, incubated with ScIE and the five fractions or dexamethasone (20 pg/mL) for 1 hour, were plated in a 96-well microplate in a final concentration of 2.5×10^5 cells/well, in quadruplicate (in 5% CO_2 at 37°C). Macrophages were stimulated with LPS (1 μg/mL), and after 24 hours, nitrite levels were determined in supernatants with Griess' reagent. Absorbance was read at 540 nm using a microplate reader (Molecular Devices). The concentration of nitrite was calculated from a sodium nitrite standard curve (range 6.5–100 μM) [13].

2.8. Western Immunoblot Analysis. J774A.1 cells (1×10^6 cells), pretreated with ScIE, hexane, dichloromethane, and aqueous fraction (10 μg/mL) or dexamethasone (20 pg/mL) for 1 hour and stimulated with LPS (1 μg/mL), were lysed in buffer (50 mM Tris, 150 mM NaCl, pH 8.0, 1% NP-40) containing protease inhibitor cocktail (1 : 1000). After 15 min of incubation on ice, nuclear proteins were collected (supernatant after centrifugation at 14.000 × g for 10 min at 4°C). The total protein content in the nuclear extracts was determined by the Lowry method (Bio-Rad, San Diego, CA, USA). The cell lysates were denatured in Laemmli sample buffer (1% sodium dodecyl sulfate (SDS); 5% 2-mercaptoethanol; 10% glycerol and 0.001% bromophenol blue) and heated at 95°C for 3 min. The samples (10 μg of total protein) were resolved by 12% SDS-polyacrylamide gel electrophoresis (PAGE), and the proteins were transferred to nitrocellulose membranes. The membranes were blocked with Tween-PBS (0.5% Tween-20) containing 2% BSA and probed with the specific primary monoclonal antibodies anti-COX-2 (1 : 10000). After extensive washing in Tween-PBS, the nitrocellulose membranes were incubated with an anti-goat IgG biotin-conjugated antibody (1 : 20000) for 1 hour, followed by streptavidin-conjugated horseradish peroxidase (1 : 5000). Immunoreactive proteins were visualized by DAB staining. The bands were quantified by densitometry, using ImageJ (public domain) software programs [22–24].

2.9. Animals. Male Swiss Webster mice (20-25 g) were obtained from the Oswaldo Cruz Foundation Breeding Unit (Fiocruz, Rio de Janeiro, Brazil). Mice were kept in plastic cages with free access to food and fresh water in a room with controlled temperature (22 ± 2°C) and light (12 h/12 h light/-dark cycle) at the experimental animal facility until use. All experimental procedures were performed according to The Committee on Ethical Use of Laboratory Animals of Oswaldo Cruz Foundation, under license P17/13-5.

2.10. Pleurisy. For induction of pleurisy, the animals received intrathoracic (i.t.) administration of 100 μL of LPS (12.5 ng/animal) diluted in sterile PBS. Sensitized mice challenged with vehicle alone (saline) were used as the negative control group [25]. The animals were treated by intraperitoneal (i.p.) route, 1 hour before challenge with LPS, with ScIE at different doses (0.01, 0.1, 1, and 10 mg/kg), and in a second assay with ScIE and different fractions at a single dose of 10 mg/kg. In trials, the dexamethasone (5 mg/kg) and diclofenac sodium (50 mg/kg) groups were

(a)

(b)

(c)

(d)
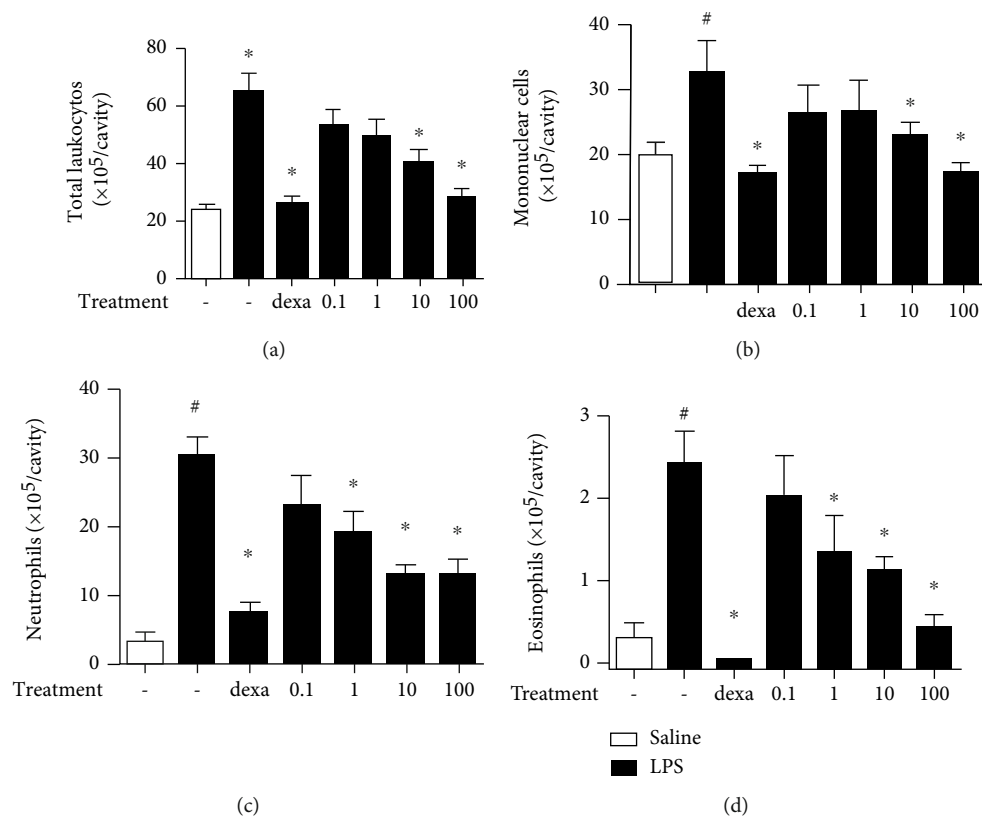
Figure 1: Effects of *S. chilensis* crude extract pretreatment (0.1, 1, 10, and 100 mg/kg) on pleural accumulation of total leukocytes (a), mononuclear cells (b), neutrophil (c), and eosinophil (d) populations in the pleural cavity of mice ($n = 6$) challenged with LPS (12.5 ng/animal). Dexamethasone was used as the reference drug. Mice were treated 1 hour before the challenge. Data represent mean ± standard error of the mean (SEM) ($n = 6$). Representative of two independent experiments performed. #$p < 0.05$ stimulated group (LPS) vs. nonstimulated group (saline); *$p < 0.05$ treated vs. untreated group.

used as a positive control, and the group was not treated as a negative control. All treatments were given in the final volume of 200 μL per animal by intraperitoneal (i.p.) route. For evaluation of pleurisy, the animals were euthanized 24 hours postchallenge and their chest cavities were washed with 1000 μL PBS containing EDTA (10 μM). The total leukocyte count was performed through a Neubauer chamber with dilution of the sample in Turk's dye, and differential leukocyte counting was performed using May-Grunwald-Giemsa-stained cytospins under brightfield microscopes (1000x magnification), and values are expressed as numbers of cells per cavity [22]. The washes were centrifuged (20,000 rpm-10 min), and the supernatant was collected and stored in a -70°C freezer for further analysis.

2.11. Determination of Proinflammatory Mediators. CXCL2/MIP-2, CXCL1/KC, CCL11/eotaxin-1, and TNF-α levels were measured in cell-free pleural washes recovered from mice 24 hours after LPS stimulation using a commercial ELISA kit purchased from R&D Systems (Minneapolis, MN, USA). The results are expressed as ng/mL based on a standard curve [22].

2.12. Statistical Analysis. Results are reported as the mean ± standard error of the mean (SEM) and were statistically analyzed by means of analysis of variance (ANOVA) followed by the Newman-Keuls-Student test or Student's *t*-test. Values of $p \leq 0.05$ were regarded as significant.

3. Results

3.1. Effect of S. chilensis Inflorescence Crude Extract on LPS-Induced Pleurisy. To verify the anti-inflammatory activity of the *S. chilensis* inflorescence crude extract (ScIE), mice were previously treated with dexamethasone (5 mg/kg, by intraperitoneal (i.p.) route) or with different doses of the ScIE (0.1, 1, 10, and 100 mg/kg, i.p.), and after 1 hour challenged with LPS (12.5 ng/cavity, i.t.). After 24 hours, the pleural inflammation induced by LPS is characterized by an intense leukocyte accumulation, with a marked increase in neutrophil and eosinophil numbers in the untreated group (LPS) when compared to the untreated and nonstimulated group (saline), as observed in Figure 1. Previous treatment with dexamethasone reduced basal levels of the leukocyte infiltrate including the polymorphonuclear cells (Figure 1). As for the ScIE, from the 10 mg/kg dose, a significant reduction in the total number of leukocytes was observed (Figure 1(a)). Mononuclear cell influx is inhibited by doses of 10 and 100 mg/kg of the extract (Figure 1(b)), and in the neutrophil and eosinophil populations, doses from 1 to 100 mg/kg of the extract were effective in reducing the
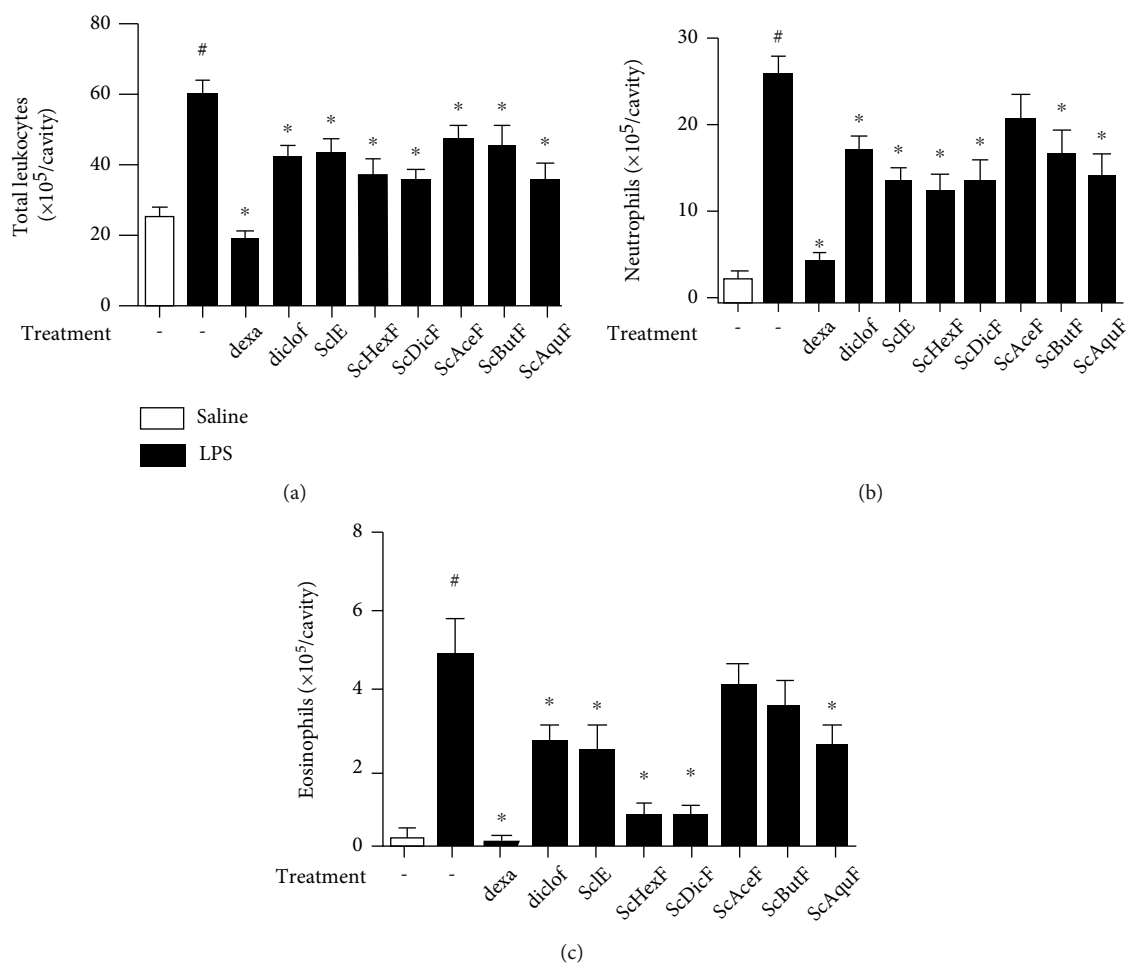
FIGURE 2: *In vivo* effect of the crude extract and different fractions of *S. chilensis* (10 mg/kg) on the recruitment of total leukocytes (a) and neutrophil (b) and eosinophil (c) populations in the pleural cavity of Swiss Webster mice stimulated (i.t.) with LPS (12.5 ng/per cavity). Dexamethasone (5 mg/kg, i.p.) and diclofenac sodium (10 mg/kg) were used as reference drugs. Mice were treated 1 hour before the challenge. Data represent mean ± standard error of the mean (SEM) ($n = 6$). Representative of three independent experiments performed. #$p < 0.05$ stimulated group (LPS) vs. nonstimulated group (saline); *$p < 0.05$ treated vs. untreated group.

migration, compared to the untreated group (Figures 1(c) and 1(d)). As the results between the 10 and 100 mg/kg doses of ScIE were not discrepant in all parameters, the 10 mg/kg dose was chosen for the assay with the *S. chilensis* fractions.

3.2. Effect of S. chilensis Fractions on LPS-Induced Pleurisy.
A second pleurisy trial was performed to determine whether there would be differentiated anti-inflammatory activity between the *S. chilensis* fractions at the predetermined dose of 10 mg/kg. Swiss Webster mice, previously treated with dexamethasone, diclofenac sodium, ScIE, and the different fractions obtained from *S. chilensis* (10 mg/kg), were stimulated with LPS (i.t.) after 1 h.

Similar to the reference drug-treated groups, both the ScIE and the fractions significantly reduced the influx of total leukocytes at the site of the induced inflammation (Figure 2(a)). By analyzing neutrophil recruitment, the reference drug, dexamethasone, reduced almost to baseline levels when compared to the untreated group (Figure 2(b)). Diclofenac sodium, as well as the *S. chilensis* butanolic fraction

(ScButF), presented approximately 19% reduction. The ScIE and the dichloromethane (ScDicF) and aqueous fractions (ScAquF) reduced the recruitment by around 24%, while the hexane fraction (ScHexF) presented better results with 28% inhibition (Figure 2(b)). There was no significant reduction for the group treated with the acetalic fraction (ScAceF) (Figure 2(b)).

The ScIE and ScAquF reduced by approximately 52% eosinophil accumulation, while the ScHexF and ScDicF showed a better inhibition profile with a 79% of reduction. On the other hand, ScAceF and ScButF, although presenting a tendency, did not obtain statistically significant differences from the LPS group (Figure 2(c)). Given the results, ScHexF, ScDicF, and ScAquF were selected to continue the studies.

3.3. Effect of S. chilensis Fractions on the Production of Chemotactic Inflammatory Mediators.
LPS stimulus induces the production of several inflammatory mediators, including cytokines and chemokines [25, 26]. To assess the difference in reducing the *in vivo* migration of leukocytes by the different *S. chilensis* fractions, we evaluated the production of
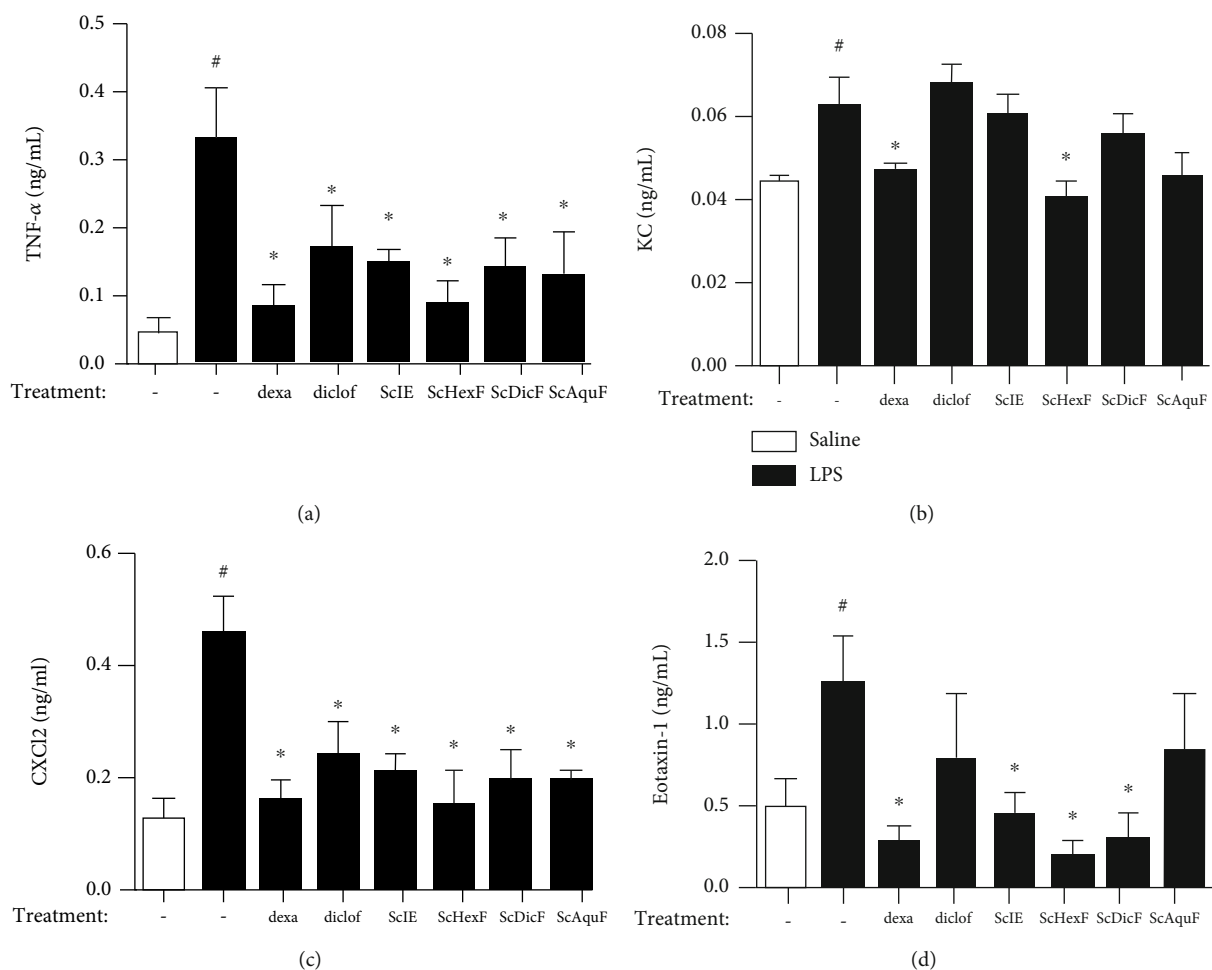
FIGURE 3: *In vivo* effect of crude extract and different fractions of *S. chilensis* (10 mg/kg) on the production of TNF-α (a), CXCL1/KC (b), CXCL2/MIP-2 (c), and CCL11/eotaxin-1 (d) mediators in the pleural lavage of Swiss Webster mice ($n = 6$) challenged with LPS (12.5 ng/animal, i.t.). Dexamethasone (5 mg/kg, i.p.) and diclofenac sodium (10 mg/kg, i.p.) were used as reference drugs. Data represent mean ± standard error of the mean (SEM) ($n = 6$). One representative ELISA from two independent experiments performed. $^{\#}p < 0.05$ stimulated group (LPS) vs. nonstimulated group (saline); $^{*}p < 0.05$ treated vs. untreated stimulated group (LPS).

TNF-α, CXCL1/KC, CXCL2/MIP-2, and CCL11/eotaxin-1 in pleural washes after the LPS (i.t.) challenge.

After 24 hours of LPS stimulation, a significant increase in the inflammatory mediator's production in the untreated was observed and stimulated with the LPS group when compared to the untreated and unstimulated group (saline) (Figure 3). In relation to the production of TNF-α mediator, a reduction was observed in all the treated groups when compared to the untreated LPS group. The dexamethasone and ScHexF groups had the best inhibition profiles, at approximately 89% and 86%, respectively (Figure 3(a)). When CXCL1/KC chemokine levels were determined, only dexamethasone and ScHexF were able to significantly attenuate this cytokine production (Figure 3(b)). CXCL2/MIP-2 level determination demonstrated that all treated groups showed inhibition of this chemokine release (Figure 3(c)). The inhibition of CXCL2/MIP-2 production is in line with the neutrophil recruitment reduction observed in Figure 2(b). As shown in Figure 3(d), there was a reduction of CCL11/eotaxin-1 pro-

duction in the dexamethasone-treated group. The ScIE and the ScDicF had a similar inhibitory profile, while the ScHexF showed a more pronounced reduction (91% of inhibition) (Figure 3(d)). These results corroborate with the inhibition of eosinophil recruitment observed in Figure 2(c). The groups treated with diclofenac or ScAquF did not inhibit CCL11/eotaxin-1 production (Figure 3d). It is noteworthy that the ScHexF was the only *S. chilensis* fraction that reduce all the cytokine/chemokine production analyzed by this study (Figure 3).

3.4. Cytotoxic Effect of the *S. chilensis* Crude Extract and Fractions in Cell Line J774A.1.

In order to verify whether the ScIE or their fractions have any cytotoxic effect that would impair the cell population used throughout the *in vitro* study, a cell viability analysis was performed with the J744A.1 murine macrophage cell line. As observed in the ScIE, most fractions were cytotoxic to almost 100% of the cell population at concentrations of 100 and 200 μg/mL (Table 1). The exception was for the ScAquF, which even

at the highest concentrations maintained around 80% of the viable cell population. The ScDicF and ScAceF at the concentrations of 50 μg/mL were cytotoxic to 37.5% and 70.4% of the population, respectively. Because of these results, the concentration of 10 μg/mL was chosen for the following experiments.

3.5. Evaluation of the Inhibitory Capacity of S. chilensis Fractions in the NO Production and COX-2 Expression In Vitro.

We previously demonstrated that the 10 μg/mL concentration of the ScIE significantly reduced nitric oxide (NO) production in the LPS-stimulated J774.A1 cell line [13]. Therefore, we indirectly quantify the NO production in LPS-stimulated J744A.1 cells previously treated with ScHexF, ScDicF, and ScAquF (10 μg/mL) (Figure 4(a)). After 24 hours of stimulation, there was a significant increase in the production of the stable metabolite of NO (nitrite) in the LPS-stimulated cells when compared to the untreated and unstimulated group (medium) (Figure 4(a)). Dexamethasone, ScIE, and ScHexF presented a percentage of approximately 30% of inhibition of the NO mediator production, while the SCDicF obtained the best reduction profile with 59% of inhibitory capacity. However, the ScAquF did not show any inhibitory activity in J744A.1 cell NO production (Figure 4(a)). In addition, ScIE and ScDicF inhibited the COX-2 expression in stimulated cells (Figures 4(b) and 4(c)). Differently, ScHexF and ScAquF failed to inhibit COX-2 expression.

3.6. Phytochemical Constituents of the S. chilensis Crude Extract and Fractions.

Based on the findings of biological activity presented by the fractions, we performed a phytoconstituent investigation in ScIE and their fractions (ScDicF, ScHexF, and ScAquF). Our group previously showed that ScIE contains 13.8% of flavonoids derived from quercetin and kaempferol, and 23.1% of diterpenes, probably furan labdanes [13].

The HPLC-UV-DAD chromatograms of ScDicF and ScAquF (Figure 5) showed the main peaks with UV spectrum characteristics of flavonoids. ScDicF contains afzelin (17%), quercetin (7.2%), chlorogenic acid (2.1%), isoquercetin (0.8%), quercitrin (0.4%), and an unknown flavonoid (10.4%) at 11.98 min retention time (Figure 5(a)). The ScAquF contains chlorogenic acid (58.2%), isoquercetin (4.1%), and an unknown flavonoid (25.1%) at 12.76 min retention time (Figure 5(b)). The flavonoid identification was carried out by comparison of the reference flavonoids, as quercetin coinjection, and by comparing retention time in the methodology used (UV spectrum) and literature data.

Through the HPLC-UV-DAD method, the presence of the labdanic diterpene solidagenone was not found in ScDicF, which has a retention time between 71 and 72 min (in the absorbance range of 254 nm). However, we observed a great diversity of signs suggestive of terpenes, as well as a great sign of a substance still not identified by us with 26% of the area, in the retention time of 53.71 min (Figure 6). This substance will be isolated for further identification.

The GC-MS chromatogram analysis showed a high number (35.4%) of n-alkanes (paraffins) in the ScHexF; in addition, the labdanic diterpene (solidagenone; 2.2%), ex bornyl acetate (0.5%), guaiene (0.42%), and Stigmasta-7,25-dien-3β-ol (0.58%) were also identified.

TABLE 1: Cytotoxic effect of crude extract and hexane, dichloromethane, acetalic, butanolic, and aqueous fractions from S. chilensis in murine macrophages J774A.1 (1×10^5 cells/well; $n = 4$, one representative assay of two independent experiments) expressed as a percentage of viable cells (%).

Sample	Dose (μg/mL)	Viability (%)
Control	—	100
DMSO	—	100
ScIE	1	100
	10	100
	50	90.7
	100	6.8
	200	0
ScHexF	1	100
	10	100
	50	88.9
	100	0.6
	200	0
ScDicF	1	82
	10	85.6
	50	37.5
	100	0
	200	0
ScAceF	1	83.9
	10	88.1
	50	70.4
	100	6.9
	200	0
ScButF	1	100
	10	100
	50	85.1
	100	0
	200	0
ScAquF	1	83.4
	10	83.6
	50	88.9
	100	81.6
	200	83.5

4. Discussion

Solidago chilensis is a plant species used in Brazilian popular medicine for the treatment, mainly of inflammatory pathologies, but there is little scientific evidence associating its therapeutic effect with the present metabolites [15, 27]. Although the literature has already described effective doses
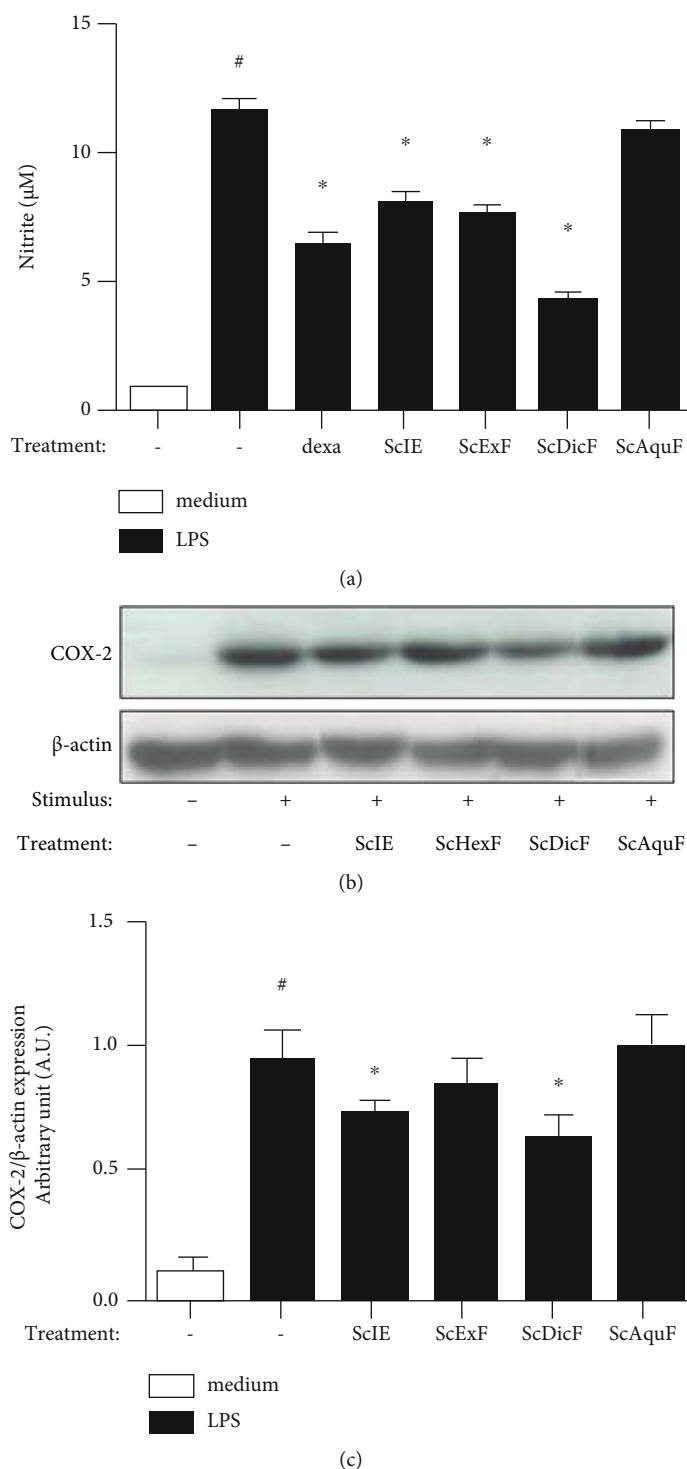
FIGURE 4: (a) The NO production was determined by the Griess reagent through the supernatant collected 24 h after the LPS simulation in treated cells with *S. chilensis* fractions (10 μg/mL). Dexamethasone (20 pg/mL) was used as the reference drug. (b, c) Effect of *S. chilensis* fractions in COX-2 expression in LPS-induced J774A.1 cells. Data represent mean $\pm$ standard error of the mean (SEM) ($n = 4$). Representative of two independent experiments performed. [#]$p < 0.05$ stimulated group (LPS) vs. nonstimulated group (medium); [*]$p < 0.05$ treated vs. untreated stimulated group (LPS).

for the anti-inflammatory activity of *S. chilensis* extracts in animal experimentation models, these studies were based on extractions made from rhizomes or aerial parts, or from the aqueous extract of inflorescences [10–12], which differs

from the proposal of this work, where only inflorescences were used in extraction with solvents of different polarities.

Among the doses tested in our study, the dose of 10 mg/kg was chosen because it was efficient in the proposed

model, corroborating the results found by Goulart et al. [10]. Although all fractions, as well as ScIE, modulated the total leukocyte infiltrate, the ScAceF and ScButF were not able to significantly inhibit the migration of polymorphonuclear cells. The fact that some fractions do not have the same pharmacological effect as ScIE can be explained by the fact that the phytocomponents responsible for the effects found in the ScIE were separated according to the affinity of secondary metabolites to from the solvents used (due to the polarity), or by the loss of the synergistic effect between these compounds during the liquid-liquid partition [28].

TNF-α is responsible for endothelial cell activation increasing the expression of adhesion molecules in the vascular endothelium, allowing leukocyte transmigration to the inflammation site. This cytokine is a potent neutrophil activator, mediating chemotaxis, adherence, degranulation, and respiratory burst, being produced not only by lymphocytes, macrophages, and active neutrophils but also by vascular endothelial, natural killer, and mast cells [29]. The data presented in this work show that the ScIE and the three tested fractions of S. chilensis significantly reduced the TNF-α values. It has already been seen that S. chilensis can modulate the levels of TNF-α, as well as the inhibition of the cytokine IL-1β in mouse experimentation models, with extracts from the rhizomes [10, 11]. It is suggested that the downmodulation of TNF-α and IL-1β attributes an antiinflammatory mechanism via inhibition of the activation of adhesion molecules, and blocking the release of specific cytokines in cell recruitment, such as chemokines of the C-X-C family [10, 11, 30].

Neutrophils are essential effector cells of the immune system and are considered the first line of defense against infections from fungi and bacteria. These cells, however, can contribute to tissue damage in diseases of acute processes, such as acute lung injury, and in the acute phase of chronic diseases such as rheumatoid arthritis. The destructive potential of neutrophils depends directly on the control of their recruitment to tissues [31]. The chemokines KC and MIP-2 are potent chemoattractants, and activators of neutrophils are known to have a crucial role in the migration of these cells from blood vessels to the sites of inflammation [32].

According to Filippo et al. [33], the KC and MIP-2 chemokines are produced by the activation of Toll-like receptors (TLRs), mainly in macrophages residing in the tissue. Both proteins are produced via MyD88, but MIP-2 is also synthesized via TRIF. In this work, a reduction of MIP-2 in ScIE and all tested fractions was observed, when compared to the group that did not receive treatment; however, the ScHexF was the only one that modulated KC production. The ScHexF may be the only one capable of interfering in the recruitment of neutrophils via the MyD88 pathway. Once maximum neutrophil infiltration occurs when both chemokines are concomitantly expressed, and inhibition of both at the same time prevents leukocyte recruitment [33]. Thus, the ScHexF would have the best antichemotactic effect of neutrophils, among all the fractions studied.

Eosinophils are leukocytes of multiple functionalities, acting in the pathogenesis of innumerable inflammatory processes, being more prominent in allergic processes and helminth infections [34]. Among the many molecules involved in the chemotaxis of this cell population, eotaxin-1, secreted mainly by cells of the bronchial epithelium, endothelial cells, and the eosinophil itself, acts as a potent chemoattractant, being just enough for local eosinophilic recruitment [35, 36]. The inhibition of eosinophilic populations in the washings of animals treated with some specific fractions (ScIE and ScHexF, ScDicF and ScAquF, the latter in lesser quantities) was an unprecedented fact of this study since the experimental models adopted in other studies involved the stimulation of the inflammatory process via carrageenan, a substance that generates inflammatory polymorphonuclear infiltrates with the majority presence of neutrophils [10–12]. Therefore, these groups were assessed for modulation of eotaxin-1 levels. Modulation of eotaxin-1 was possible in groups of mice previously treated with ScIE and the ScHexF and ScDicF, indicating that S. chilensis may have antiallergic activity, which has not been previously studied, but which is not uncommon in the Compositae family [27, 37]. Although the ScAquF was effective in modulating the migration of eosinophils, the levels of eotaxin-1 did not decrease significantly; therefore, it is necessary to investigate other modulation mediators and pathways, such as prostaglandins and leukotriene.

Our group evaluated the safety of this extract and fractions in vitro, and except for ScAquF, which maintained a cell viability profile greater than 80% in all concentrations tested, the other fractions, as well as the ScIE, showed high toxicity at doses of 100 and 200 μg/mL, with almost 100% of cell death. The ScDicF was the only one that at a concentration of 50 μg/mL made more than half of the cell population unviable. In order to use cells previously treated with the S. chilensis fractions, which maintained a cell viability profile equal to or greater than 70%, the concentration of 10 μg/mL was chosen as the maximum working concentration. The results obtained in this work can be associated with the findings of Barros et al. [2], where the concentration of 10 μg/mL of the methanolic extract of the leaves of S. chilensis did not show a cytotoxic effect in an L929 murine fibroblast strain [2].

NO is an important molecule in the defense system, acting as a vasodilator and cytotoxic agent mediated by macrophages in infectious processes [38, 39]. Although the literature has already described the ability of S. chilensis to modulate NO [10, 11], our group analyzed the modulation in vitro using a murine macrophage cell lineage treated with ScIE and different fractions obtained from inflorescences. Like the in vivo assay, a dose-response curve was constructed with ScIE. The data presented showed that only the ScAquF failed to inhibit the production of NO.

COX-2 is an enzyme produced by resident cells involved in the inflammatory process (macrophages, mast cells, and others) and is responsible for the synthesis of prostaglandins and thromboxanes, through stimulation with IL-1β, TNF-α, endotoxins, and others [40]. We observed for the first time that components present in the ScIE and dichloromethane fraction of S. chilensis have the property of significantly modulating the expression of COX-2. The reduction of

(a)

1– Chlorogenic acid
5– Isoquercetin

(b)
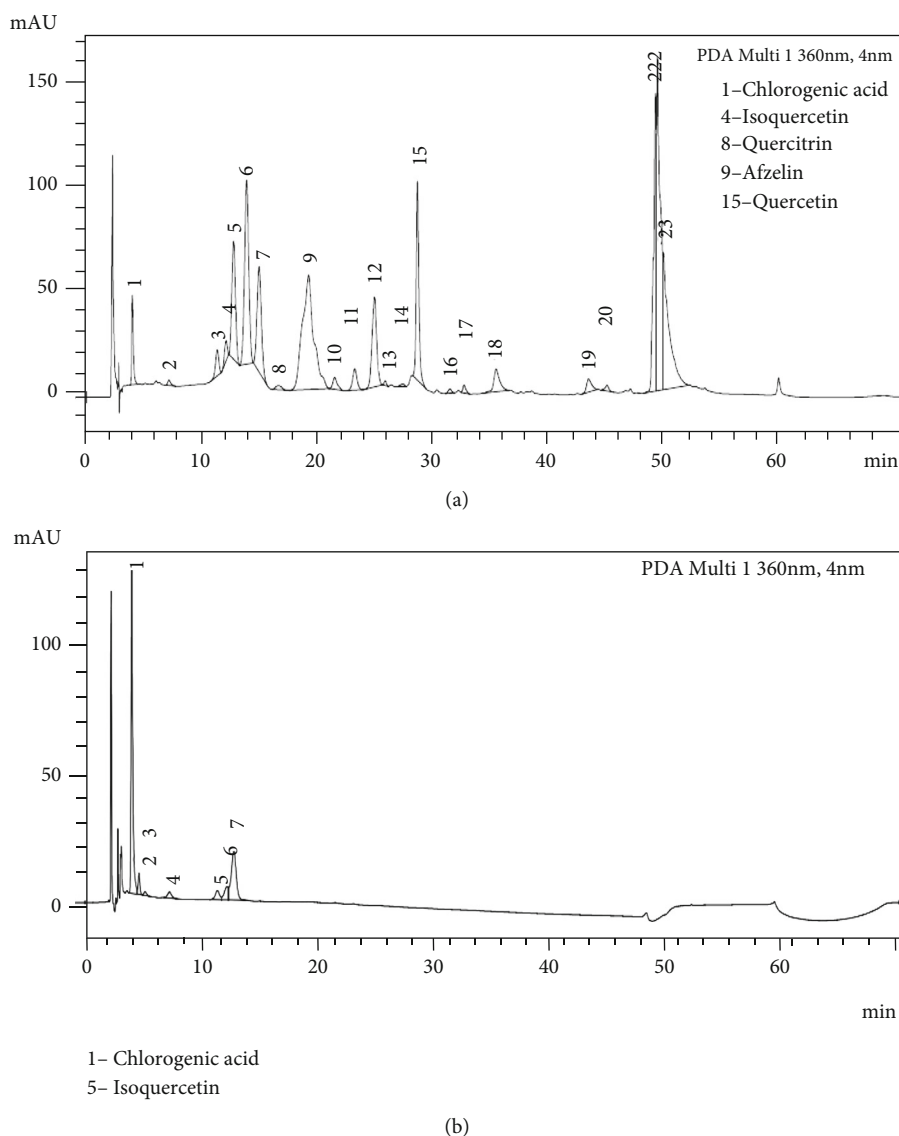
FIGURE 5: HPLC-UV-DAD of the ScDicF (a) and ScAquF (b) for flavonoid characterization. The chromatogram A showed the main peaks with UV spectrum characteristics of chlorogenic acid (1), isoquercetin (4), quercitrin (8), afzelin (1), and quercetin (15). And the chromatogram B showed the main peaks with UV spectrum characteristics of chlorogenic acid (1) and isoquercetin (5). Chromatographic conditions: temperature = 250°C; flow rate = 1.0 mL min^{-1}; λ = 360 nm; Inj.V. = 10 μL. Mobile phase: acetonitrile (eluent A) and acetic acid: water (1:40) (eluent B). In the first 15 min, 14% of the A eluent and 84% of the B eluent were used. 35% of the eluent A in the following 30 min and 100% of eluent A in the last 2 minutes.

COX-2 expression leads to the belief that there is some inhibitory activity via the gene pathway, where the protein is not being synthesized [41]. However, that does not rule out the fact that ScIE and fractions, even ScHexF or ScAquF that did not show an indication of reduced expression, cannot be inhibiting the functionality of the enzyme, as occurs in the case of nonsteroidal anti-inflammatory drugs, such as aspirin, or some selective for COX-2 such as celecoxib [40]. This evidence requires new tests to obtain more conclusive results, but given all the data presented, it can be suggested that a large part of the pharmacological activity is found in phytocomponents present in the dichloromethane fraction, with the main effect may be the inhibitory expression of COX-2 at the molecular level.

To identify the compounds that could be involved in the pharmacological effects found in this work, the ScIE, hexane, dichloromethane, and aqueous fractions were subjected to chromatographic analyses for the investigation of phytochemicals. The analysis by HPLC-UV-DAD showed that both the ScIE and the dichloromethane fraction are constituted by a large number of flavonoids derived from quercetin and kaempferol, between aglycone and glycosides, since the absorbance observed in UV is characteristic only of the aglycone. As for the aqueous fraction, in the same methodology, the presence of the isoquercitrin flavonoid and a large amount of chlorogenic acid were identified.

Although the majority of compounds have not been fully identified, most have quercetin as a flavonoid skeleton with
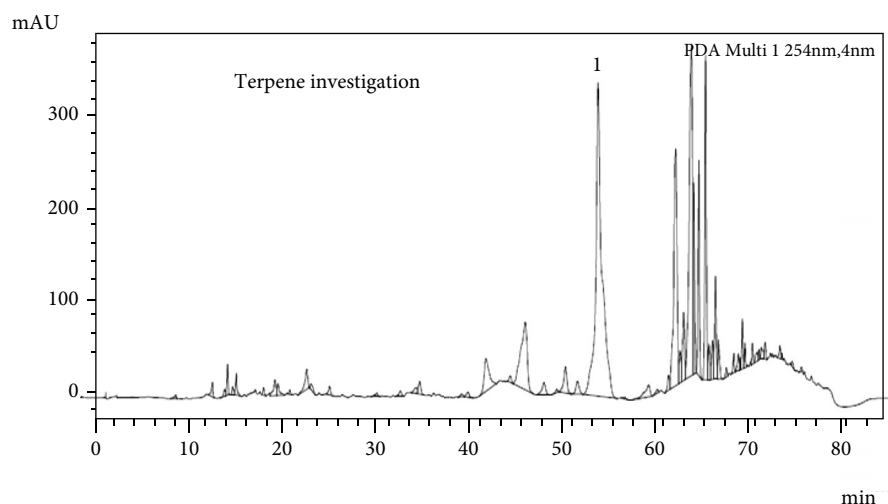
FIGURE 6: HPLC-UV-DAD of the ScDicF for the characterization of terpenes. The presence of the labdanic diterpene solidagenone was not found (retention time 71-72 min), but a great diversity of signs suggestive of terpenes can be observed, as well as a great sign (1) of a substance still not identified (26% of the area, retention time = 53.71 min). Chromatographic conditions: temperature = 300°C; flow rate = 1.0 mL min^{-1}; Λ = 254 nm; Inj.V. = 10 μL. Isocratic elution system; 0.05% trifluoroacetic acid (54.94 mL) and acetonitrile (27.06 mL).

strong antioxidant activity represented there, and already well described in the literature [42]. This antioxidant capacity of the flavonoids could explain the modulation of NO levels found in ScIE, and the ScDicF. Barros et al. [2] demonstrated the antioxidant potential of quercitrin and afzelin isolated from *S. chilensis* in a DPPH trial, as well as the ability of flavonoid quercitrin gallate (derived from quercetin) to modulate NO levels through inhibition of production, at the level of gene transcription, of the enzyme responsible for its synthesis (iNOS) in a lineage of RAW 264.7 macrophages [43].

Rao-Manjeet and Ghosh [44] demonstrated the potential of quercetin in modulating the levels of TNF-α in a lineage of RAW 264.7 macrophages, going according to the findings of this study in the ScIE and the dichloromethane fraction. Quercetin is already described for having anti-inflammatory activity through the reduction of leukotriene B4, prostaglandin E2 (PGE2), chemokines KC, MIP-2, RANTES, and CXCL8, all with chemoattractive properties of leukocytes [42, 45, 46]. Part of this activity is attributed to the ability of quercetin to inhibit the formation of the NF-κB transcription complex and to interrupt signaling between TLR4 and MyD88 [47]. Chlorogenic acid, found in large amounts in the aqueous fraction, also has anti-inflammatory activity attributed to the ability to suppress the production of NO, iNOS, and PGE2, also by blocking NF-κB [48, 49].

The labagenic diterpene solidagenone has been described as the main constituent of rhizomes of *S. chilensis*, and it has already been attributed some pharmacological effects such as antiulcer, gastroprotective, and immunomodulator [15, 50]. Using the methodology validated by Valverde et al. [15] for the identification, mainly, of ketone or lactonic groups through HPLC-UV-DAD, the presence of solidagenone in the ScIE and the ScDicF was investigated. Our results converge with those of the literature, where the ether-ethanolic extract of the inflorescences presented a considerable amount of solidagenone [15]. On the other hand, the ScDicF analysis was negative for the presence of solidagenone.

In the hexane fraction, in addition to a large amount of grease found, characteristics of the waxes found on the surfaces of flowers, the presence of solidagenone, exabornyl acetate, and guaiene were identified by GC-MS. The literature describes little about the pharmacological activities of these compounds. Bornyl acetate has been described as having analgesic and anti-inflammatory activity [51], but it is not guaranteed that the low percentage of this substance in the studied fraction is responsible for the pharmacological activity observed in this work. The same is true with solidagenone.

According to our analysis, quercetin and its derivatives would be excellent biomarkers of anti-inflammatory activity for extracts from the inflorescences of *Solidago chilensis*. It was found in the ScIE and the ScDicF in good proportions, and its anti-inflammatory and antioxidant properties are well described in the literature [42]. Although the ScHexF has shown good results in immunopharmacological tests, new analyses for the investigation of phytochemicals must be performed to improve the understanding of its effects. Solidagenone, despite being found in good proportions in the ScIE, needs further studies in more detail and in an isolated way about its pharmacological activities, as it is a metabolite little investigated in the literature, being a possible target of future studies.

5. Conclusion

The inflorescence crude extract and different fractions obtained from the ether-ethanolic extract of *S. chilensis* showed a differentiated anti-inflammatory effect in the proposed methodologies for evaluating *in vivo* and *in vitro* parameters. After phytochemical investigation, it is concluded

that quercetin (and its derivates) could be used as biomarkers for quality control of the anti-inflammatory activity of this species. More studies should be carried out to improve the understanding of the mechanism of action of the anti-inflammatory property of *S. chilensis*, as well as to confirm, and further explore, a possible antiallergic effect seen in this work, which had not been reported in the literature.

Data Availability

The datasets generated and/or analyzed during the present study are available from the corresponding authors upon reasonable request.

Conflicts of Interest

The authors declare no conflict of interest.

Authors' Contributions

T. M. de Brito performed experiments, analyzed data, and wrote the paper. T. B. de Oliveira, Laís Higino Doro, Amanda da Silva Chaves, Esdras Barbosa Garcia, Flavia Fontenelle Muylaert, and Tatiana Almeida Pádua performed the experiments. F. C. Amendoeira, M. G. M. O. Henriques, V. S. Frutuoso, S. S. Valverde, and F. K. Ferraris contributed to the design and improvement of the experiments. F. K. Ferraris, S. S. Valverde, and F. C. Amendoeira analyzed data and drafted the manuscript. All authors revised and approved the final manuscript.

Acknowledgments

References

[1] G. Locateli, B. de Oliveira Alves, D. Miorando et al., "Antidepressant-like effects of solidagenone on mice with bacterial lipopolysaccharide (LPS)-induced depression," *Behavioural Brain Research*, vol. 395, article 112863, 2020.

[2] M. de Barros, L. Mota da Silva, T. Boeing et al., "Pharmacological reports about gastroprotective effects of methanolic extract from leaves of Solidago chilensis (Brazilian arnica) and its components quercitrin and afzelin in rodents," *Naunyn Schmiedebergs Arch Pharmacology*, vol. 389, no. 4, pp. 403–417, 2016.

[3] M. Pio Corrêa, ""Dicionário de plantas úteis do Brasil e das exóticas cultivadas", Rio de Janeiro: Ministério da Agricultura," *IBDF*, vol. 6, p. 777, 1984.

[4] W. Mors, C. Rizzini, and N. Pereira, *Medicinal plants of Brazil*, Reference Publications, Algonac, 2000.

[5] M. Facury Neto, D. Fagundes, M. Beletti, N. Novo, Y. Juliano, and N. Penha-silva, "Systematic use of Solidago microglossa dc in the cicatrization of open cutaneous wounds in rats," *Brazilian Journal of Morphological Sciences*, vol. 21, no. 4, pp. 207–210, 2004.

[6] H. Lorenzi and F. Matos, *Plantas medicinais no brasil: nativas e exóticas cultivadas*, Instituto Plantarum, Nova Odessa, 2008.

[7] H. Catarino, N. de Godoy, N. Scharlack et al., "Ingap 670-nm laser therapy combined with a hydroalcoholic extract of Solidago chilensis meyen in burn injuries," *Lasers in Medical Science*, vol. 30, no. 3, pp. 1069–1079, 2015.

[8] E. Malpezzi-marinho, G. Molska, L. Freire et al., "Effects of hydroalcoholic extract of Solidago chilensis meyen on nociception and hypernociception in rodents," *BMC Complementary and Alternative Medicine*, vol. 19, no. 1, p. 72, 2019.

[9] S. Valverde, B. Santos, T. de Oliveira, G. Gonçalves, and O. de Sousa, "Solidagenone from Solidago chilensis meyen inhibits skin inflammation in experimental models," *Basic & Clinical Pharmacology & Toxicology*, vol. 128, no. 1, pp. 91–102, 2021.

[10] S. Goulart, M. I. G. Moritz, K. L. Lang, R. Liz, E. P. Schenkel, and T. S. Fröde, "Anti-inflammatory evaluation of _Solidago chilensis_ Meyen in a murine model of pleurisy," *Journal of Ethnopharmacology*, vol. 113, no. 2, pp. 346–353, 2007.

[11] R. Liz, S. Vigil, S. Goulart, M. Moritz, E. Schenkel, and T. Frode, "The anti-inflammatory modulatory role of Solidago chilensis meyen in the murine model of the air pouch," *Journal of Pharmacy and Pharmacology*, vol. 60, no. 4, pp. 515–521, 2008.

[12] E. Tamura, R. Jimenez, K. Waismam, and L. Gobbo-Neto, "Inhibitory effects of _Solidago chilensis_ Meyen hydroalcoholic extract on acute inflammation," *Journal of Ethnopharmacology*, vol. 122, no. 3, pp. 478–485, 2009.

[13] T. de Brito, F. Amendoeira, T. de Oliveira, V. Frutuoso, F. Ferraris, and S. Valverde, "Extract of Solidago chilensis meyen inflorescences: cytotoxicity and inhibitory activity on nitric oxide synthesis in activated macrophage cell line J774A.1," *Brazilian Journal of Pharmaceutical Sciences*, vol. 56, 2020.

[14] S. Valverde, S. Souza, T. de Oliveira et al., "Chemical composition and antinociceptive activity of volatile fractions of the aerial parts of Solidago chilensis (compositae)," *Rodriguésia*, vol. 71, pp. 1–9, 2020.

[15] S. Valverde, R. Azevedo, and T. Tomassini, "Utilização de clae como paradigma na obtenção e controle do diterpeno solidagenona a partir de inflorescências de Solidago chilensis meyen (arnica brasileira)," *Revista Brasileira de Farmacognosia*, vol. 90, no. 3, pp. 196–199, 2009.

[16] P. Apáti, K. Szentmihályi, A. Balázs et al., "HPLC analysis of the flavonoids in pharmaceutical preparations from Canadian goldenrod (Solidago canadensis)," *Chromatographia Supplement*, vol. 56, no. 1, pp. s65–s68, 2002.

[17] T. de Oliveira, B. Bastos, A. Kelly, S. Monteiro, and S. Valverde, "Flavonoids characterization using HPLC-UV-PDA in tincture produced from inflorescences of cultivated Solidago chilensis Meyen in Itaipava (RJ)," *Revista Fitos*, vol. 11, pp. 17–25, 2017.

[18] L. Torres, K. Akisue, and F. Roque, "Quercitrina em Solidago microglossa DC, A Arnica do Brasil," *Revista Farmácia e Bioquímica da USP*, vol. 23, pp. 33–40, 1987.

[19] R. Vila, M. Mundina, F. Tomi et al., "Composition and antifungal activity of the essential oil of Solidago chilensis," *Planta Medica*, vol. 68, no. 2, pp. 164–167, 2002.

[20] P. Apáti, *Antioxidant constituents in Solidago canadensis L. and its traditional phytopharmaceuticals [Ph.D. thesis]*, Hungarian Academy of Sciences, Chemical Research Centre, Institute of Chemistry, Budapest, 2003.

[21] T. Jiang, B. Huang, and P. Qin, "A survey of chemical and pharmacological studies on Solidago," *Journal of Chinese Integrative Medicine*, vol. 4, no. 4, pp. 430–435, 2006.

[22] F. Ferraris, K. Moret, A. Figueiredo, C. Penido, and M. Henriques, "Gedunin, a natural tetranortriterpenoid, modulates t lymphocyte responses and ameliorates allergic inflammation," *International Immunopharmacology*, vol. 14, no. 1, pp. 82–93, 2012.

[23] F. Conte, F. Ferraris, T. Costa et al., "Effect of gedunin on acute articular inflammation and hypernociception in mice," *Molecules*, vol. 20, pp. 2636–2657, 2015.

[24] T. Pádua, N. Torres, A. Candéa et al., "Therapeutic effect of lipoxin A4 in malaria-induced acute lung injury," *Journal of Leukocyte Biology*, vol. 103, no. 4, pp. 657–670, 2018.

[25] C. Penido, H. Castro-faria-neto, A. Vieira-de-abreu et al., "LPS induces eosinophil migration via CCR3 signaling through a mechanism independent of rantes and eotaxin," *American Journal of Respiratory Cell and Molecular Biology*, vol. 25, no. 6, pp. 707–716, 2001.

[26] C. Penido, A. Vieira-de-abreu, M. Bozza, H. Castro-faria-neto, and P. Bozza, "Role of monocyte chemotactic protein-1/CC chemokine ligand 2 on gamma delta T lymphocyte trafficking during inflammation induced by lipopolysaccharide or Mycobacterium bovis bacille Calmette-Guérin," *Journal of Immunology*, vol. 171, no. 12, pp. 6788–6794, 2003.

[27] T. de Oliveira, F. Silva, A. Kelly, and S. Valverde, "Solidago medicinais," *Revista Brasileira de Plantas Medicinais*, vol. 19, no. 2, pp. 304–310, 2017.

[28] S. Queiroz, C. Collins, and I. Jardim, "Métodos de extração e/ou concentração de compostos encontrados em fluidos biológicos para posterior determinação cromatográfica," *Química Nova*, vol. 24, no. 1, pp. 68–76, 2001.

[29] L. Borish and J. Stenki, "2\. Cytokines and chemokines," *The Journal of Allergy and Clinical Immunology*, vol. 111, no. 2, pp. s460–s475, 2003.

[30] J. Ruth, M. Amin, J. Woods et al., "Accelerated development of arthritis in mice lacking endothelial selectins," *Arthritis Research & Therapy*, vol. 7, no. 5, pp. r959–r970, 2005.

[31] C. Sadik, N. Kim, and A. Luster, "Neutrophils cascading their way to inflammation," *Trends in Immunology*, vol. 32, no. 10, pp. 452–460, 2011.

[32] R. Day and D. Link, "Regulation of neutrophil trafficking from the bone marrow," *cellular and Molecular Life Sciences*, vol. 69, no. 9, pp. 1415–1423, 2012.

[33] K. Filippo, R. Henderson, M. Laschinger, and N. Hogg, "Neutrophil chemokines KC and macrophage-inflammatory protein-2 are newly synthesized by tissue macrophages using distinct TLR signaling pathways," *The Journal of Immunology*, vol. 180, pp. 4308–4315, 2017.

[34] M. Rothenberg and S. Hogan, "The eosinophil," *Annual Review Immunology*, vol. 24, no. 1, pp. 147–174, 2006.

[35] D. Wu, J. Zhou, H. Bi et al., "CCL11 as a potential diagnostic marker for asthma?," *Journal of Asthma*, vol. 51, no. 8, pp. 847–854, 2014.

[36] D. Palomino and L. Marti, "Chemokines and immunity," *Einstein (são paulo)*, vol. 13, no. 3, pp. 469–473, 2015.

[37] V. Chandrashekhar, K. Halagali, R. Nidavani et al., "Anti-allergic activity of German chamomile (_Matricaria recutita_ L.) in mast cell mediated allergy model," *Journal of Ethnopharmacology*, vol. 137, no. 1, pp. 336–340, 2011.

[38] N. Cerqueira and W. Yoshida, "Óxido nítrico: revisão," *Acta Cirúrgica Brasileira*, vol. 17, no. 6, pp. 417–423, 2002.

[39] H. Jo, Y. Kim, S. Nam et al., "The inhibitory effect of quercitrin gallate on iNOS expression induced by lipopolysaccharide in balb/c mice," *Journal of Veterinary Science*, vol. 9, no. 3, pp. 267–272, 2008.

[40] W. Carvalho, R. Carvalho, and F. Santos, "Analgésicos inibidores específicos da ciclooxigenase-2: avanços terapêuticos," *Revista Brasileira de Anestesiologia*, vol. 54, no. 3, pp. 448–464, 2004.

[41] Y. Yo, X. Li, L. Qu et al., "DXXK exerts anti-inflammatory effects by inhibiting the lipopolysaccharide- induced NF-κB/COX-2 signalling pathway and the expression of inflammatory mediators," *Journal of Ethnopharmacology*, vol. 178, pp. 199–208, 2016.

[42] S. Kumar and A. Pandey, "Chemistry and biological activities of flavonoids: as overview," *The Scientific World Journal*, vol. 2013, Article ID 162750, 2013.

[43] H. Kim, M. Cho, and A. Reddy, "Down-regulatory effect of quercitrin gallate on nuclear factor-κB-dependent inducible nitric oxide synthase expression in lipopolysaccharide-stimulated macrophages RAW 264.7," *Biochemical Pharmacology*, vol. 69, no. 11, pp. 1577–1583, 2005.

[44] K. Rao-manjeet and B. Ghosh, "Quercetin inhibits LPS-induced nitric oxide and tumor necrosis factor-α production in murine macrophages," *International Journal of Immunopharmacology*, vol. 21, no. 7, pp. 435–443, 1999.

[45] K. Morikawa, M. Nonaka, M. Narahara et al., "Inhibitory effect of quercetin on carrageenan-induced inflammation in rats," *Life Sciences*, vol. 74, no. 6, pp. 709–721, 2003.

[46] F. Souto, A. Zarpelon, L. Staurengo-Ferrari et al., "Quercetin reduces neutrophil recruitment induced by CXCL8, LTB4, and FMLP: inhibition of actin polymerization," *Journal of Natural Products*, vol. 74, no. 2, pp. 113–118, 2011.

[47] M. Endale, S. Park, S. Kim et al., "Quercetin disrupts tyrosine-phosphorylated phosphatidylinositol 3-kinase and myeloid differentiation factor-88 association, and inhibits MAPK/AP-1 and IKK/NF-κB-induced inflammatory mediators production in RAW 264.7 cells," *Immunobiology*, vol. 218, no. 12, pp. 1452–1467, 2013.

[48] H. Su, Y. Kim, Y. Park, H. Lee, and K. Kim, "Anti-inflammatory effects of chlorogenic acid in lipopolysaccharide-stimulated RAW 264.7 cells," *Inflammation Research*, vol. 63, pp. 81–90, 2014.

[49] W. Chen and L. Wu, "Chlorogenic acid suppresses interleukin-1β-induced inflammatory mediators in human chondrocytes," *International Journal of Clinical and Experimental Pathology*, vol. 7, no. 12, pp. 8797–8801, 2014.

[50] J. Rodriguez, C. Theoduloz, M. Sánchez, I. Razmilic, and G. Schmeda-Hirschmann, "Gastroprotective and ulcer-healing effect of new solidagenone derivatives in human cell cultures," *Llife Sciences*, vol. 77, no. 17, pp. 2193–2205, 2005.

[51] X. Wu, X. Li, F. Xiao, Z. Zhang, Z. Xu, and H. Wang, "Studies on the analgesic and anti-inflammatory effect of bornyl acetate in volatile oil from Amomum villosum," *Journal of Chinese Medicinal Materials*, vol. 27, no. 6, pp. 438-439, 2004.

Research Article

The Antitriple Negative Breast cancer Efficacy of *Spatholobus suberectus* Dunn on ROS-Induced Noncanonical Inflammasome Pyroptotic Pathway

Feng Zhang,[1,2] **Qingqing Liu,**[1,2] **Kumar Ganesan,**[1,2] **Zeng Kewu,**[3] **Jiangang Shen,**[1] **Fang Gang,**[1,4] **Xiaohe Luo** [ID],[5,6] **and Jianping Chen** [ID][1,2]

[1]*School of Chinese Medicine, Li Ka Shing Faculty of Medicine, The University of Hong Kong, 10 Sassoon Road, Pokfulam, Hong Kong, China*
[2]*Shenzhen Institute of Research and Innovation, The University of Hong Kong, Shenzhen, China*
[3]*School of Pharmaceutical Sciences Peking University Health Science Center, Peking University, Peking, China*
[4]*Guangxi Key Laboratory of Applied Fundamental Research of Zhuang Medicine, Guangxi University of Chinese Medicine, Nanning, China*
[5]*The Center of Clinical Research of Endocrinology and Metabolic Diseases in Chongqing and Department of Endocrinology, Chongqing University Three Gorges Hospital, School of Medicine, Chongqing University, Chongqing, China*
[6]*Department of Laboratory Medicine, Chongqing University Three Gorges Hospital, School of Medicine, Chongqing University, Chongqing, China*

Correspondence should be addressed to Xiaohe Luo; xiaoheluo@163.com and Jianping Chen; abchen@hku.hk

Breast cancer (BCa) is the leading cause of women's death worldwide; among them, triple-negative breast cancer (TNBC) is one of the most troublesome subtypes with easy recurrence and great aggressive properties. *Spatholobus suberectus* Dunn has been used in the clinic of Chinese society for hundreds of years. Shreds of evidence showed that *Spatholobus suberectus* Dunn has a favorable outcome in the management of cancer. However, the anti-TNBC efficacy of *Spatholobus suberectus* Dunn percolation extract (SSP) and its underlying mechanisms have not been fully elucidated. Hence, the present study is aimed at evaluating the anti-TNBC potential of SSP both in vitro and in vivo, through the cell viability, morphological analysis of MDA-MB-231, LDH release assay, ROS assay, and the tests of GSH aborted pyroptotic noninflammasome signaling pathway. Survival analysis using the KM Plotter and TNM plot database exhibited the inhibition of transcription levels of caspase-4 and 9 related to low relapse-free survival in patients with BCa. Based on the findings, SSP possesses anti-TNBC efficacy that relies on ROS-induced noncanonical inflammasome pyroptosis in cancer cells. In this study, our preclinical evidence is complementary to the preceding clinic of Chinese society; studies on the active principles of SPP remain underway in our laboratory.

1. Introduction

There are seldom chemotherapeutic medications that can gain moderate success in triple-negative breast cancer (TNBC) management. Breast cancer (BCa) is the leading cause of women's death worldwide. Among them, TNBC accounts for almost 10-15% of all BCs, which refers to the absence of estrogen and progesterone receptors and overexpression of human epidermal growth receptor 2 [1, 2]. It is one of the most troublesome subtypes of BCa because of its easy recurrence and highly aggressive properties. Although some basic investigations related to immunotherapy and targeted therapy have shown great potential to inhibit the development of cancer [3, 4], they still seldom chemotherapeutic drugs, which can offer positive pathologic complete response for the management of TNBC in the clinic [5].

Spatholobus suberectus Dunn (SSD, Leguminosae), documented as a traditional Chinese medicine (TCM) named

"Ji Xue Teng," has been used in the clinic of Chinese society for hundreds of years in hematopoiesis and applied to treat rheumatism, anemia, and menoxenia [6]. SSD has widely been used in conventional medicines that possess various pharmacological activities, viz., antioxidant, antimutagenic, antiplatelet, immunomodulatory, antibacterial, antiviral, neuroprotection, and blood circulation improvement [7–12]. SSD comprises several bioactive compounds in which flavonoids are predominant, including $3',4',7$-trihydroxyflavone, $3'$-hydroxy-8-methoxyvestitol, butin, calycosin, dihydrokaempferol, dihydroquercetin, eriodictyol, liquiritigenin, plathymenin, and prunetin, and many of them exert anticancer properties [11, 13, 14]. Furthermore, numerous experimental pieces of evidence have been shown that crude extracts of SSD produce a favorable outcome in the management of cancer [15–17] and coronary heart diseases [18]. SSD has been used in the clinic of TCM as a potential drug to treat BCa patients and accounts for excellent response [19]. SSD has potent anticancer effects on BCa with the capacity of causing apoptosis and obstructing cell cycle, LDH, and BCa migration via the MAPK PI3K/AKT pathway [20, 21]. However, the anti-TNBC efficacy of SSP and its underlying mechanism has not been fully elucidated.

Earlier researchers paid great attention to investigating programmed cell death: apoptosis, which is believed not to trigger inflammation [22]. It is considered an essential component of several processes such as normal cell turnover, growth, the function of the immune system, embryonic development, and chemical-induced cell death [23]. Recently, pyroptosis is another kind of programmed cell death, which is varied in the mechanisms of apoptosis, and proved to be crucial for clearing dangerous infections [24, 25]. Pyroptosis is generally lytic cell demise accompanied by rapid cell membrane rupture [26], in which pores are initially formed in the membrane of the cell, causing water influx and cell swelling, causing cell-membrane damage. Hence, pyroptosis is believed to be more inflammatory and immunogenic than apoptosis [27]. Several pilot studies have also clarified that pyroptosis may trigger inflammation and recruit immune cells to the pyroptotic area [28, 29]. Currently, mounting research related to pyroptosis is extensively studied in cancer.

The relationship between ROS and tumor cell pyroptosis has been well established [30]. Low doses of ROS normally stimulate cell proliferation in a wide variety of cancer cell types [31, 32]. However, elevated ROS triggers tumor cell pyroptosis-dependent caspases [33]. Some chemotherapeutic drugs are addressed to induce tumor cell pyroptosis dependent on caspase-3 [34, 35]. Mechanistically, there are two different kinds of signaling pathways involved in pyroptosis. The first one is the caspase-1-dependent process, named "canonical" inflammasome activation, which is mediated by a dynamic mediator, gasdermin D (GSDMD) [36]. The dynamic caspases-1, -4, -5, and -11 generally cleave GSDMD within a linker between the domains of amino and carboxy-terminal. After the breakdown, the N-terminal generates pores in the cell wall to cause pyroptosis resulting in transmembrane ion flux, cytoplasmic swelling,

and osmotic lysis [37]. Secondly, a "noncanonical" inflammasome activation has been termed as a pathway that is ROS/caspases axis-dependent, which is also mediated by GSDMD or/and gasdermin E (GSDME) [38–41]. Nevertheless, there are seldom reports on TCM that can trigger pyroptosis in cancer management. Therefore, the present study is aimed at evaluating the anti-TNBC efficacy of SSP on TNBC cell lines by analyzing cellular characteristics including cell viability, cell morphology changes, LDH release assay, ROS assay, and glutathione (GSH) aborted pyroptotic noninflammasome signaling pathway.

2. Materials and Methods

2.1. Preparation of Spatholobus suberectus Percolation (SSP) Extract.
SSP extract was prepared in accordance with EMA guidelines as described previously with some modifications [42]. Briefly, dried SSD stems, which were provided by Guangdong Kangmei Pharmaceutical Co., Ltd. (Guangdong Province, China), were ground into coarse powder, and it was extracted using a percolating device with 10 times volume (v/w) of 60% ethanol. The filtrate was then concentrated under reduced pressure by a rotary evaporator (IKA RV 10, IKA- Werke GmbH & Co. KG, Darmstadt, Germany). The obtained percolation powder was then freeze-dried (percent yield 20%) and stored at 4°C for further use.

2.2. UHPLC Analysis.
The ultra high-pressure liquid chromatography (UHPLC) analysis was conducted with an Ultimate 3000 system (Thermo Scientific, MA, U.S.A.) equipped with a quaternary pump, a vacuum degasser, an auto-sampler, and a DAD UV-Vis detector. The gradient elution was composed of solvent A (water: 0.3% formic acid, v/v) and solvent B (acetonitrile). A reverse-phase packing C_{18} column (100 mm × 2.1 mm, 4 μm, ACE, UK) was used in this experiment. The mobile phase condition was performed as follows: 0 min, 2% (B); 2 min, 2% (B); 5 min, 10% (B); 12 min, 10% (B); 20 min, 20% (B); 25 min, 20% (B); 26 min, 25% (B); 32 min, 35% (B); and 37 min, 40% (B). The flow rate was 0.4 ml/min, and the injection volume was 5 μL. The experiment was operated at 30°C, and the detection wavelength was 280 nm. All solutions were prepared with 0.22 μm filtration (Sigma-Aldrich, St. Louis, MO, USA) for the samples. The mobile phase was purged before injection of UHPLC. Catechin (Sigma-Aldrich), procyanidin B2 (Sigma-Aldrich), epicatechin (Sigma-Aldrich), genistein (Sigma-Aldrich), formononetin (Sigma-Aldrich), and SSP were accurately weighed and then dissolved in methanol. Identification was achieved by comparing retention times (RT).

2.3. Cell Culture and Treatment.
MDA-MB-231, 4 T1, and BT 549 cells were obtained from American Type Culture Collection (ATCC, Manassas, VA, USA). All cells were maintained in Roswell Park Memorial Institute (RPMI) 1640 (Gibco, Grand Island, NY, USA.) or glucose-containing (4.5 g/L) Dulbecco's Modified Eagle Medium (DMEM, Gibco, Grand Island, NY, USA) according to the protocol of ATCC, which were supplemented with fetal

bovine serum (FBS, 10% v/v, Gibco, Grand Island, NY, USA), penicillin (Sigma-Aldrich, St. Louis, MO, USA, 100 U/ml), and streptomycin (Sigma-Aldrich, St. Louis, MO, USA, 100 μg/ml) in a humidified atmosphere of 5% CO_2 at 37°C. Cells were seeded onto 96-well plates at the density of $3 - 5 \times 10^3$/well. After undergoing serum starvation for 24 h, they were treated with different concentrations of SSP (200, 100, 50, 25, 12.5, 6.25, 3.13, 1.56 μg/ml) or docetaxel (Beijing Aosaikang Pharmaceutical Co., Ltd, Jiangsu, China; 500, 250, 125, 62.5, 31.25, 15.63, 7.81, 3.91 μg/ml). The tumor cell growth inhibitory effect of SSP or docetaxel on MDA-MB-231 and BT 549 was tested the cell viability and proliferation using CellTiter 96® AQueous Non-Radioactive Cell Proliferation Assay containing 3-(4,5-dimethylthiazol-2-yl)-5-(3-carboxymethoxyphenyl)-2-(4-sulfophenyl)-2H-tetrazolium) (MTS) kit (Promega, Wisconsin, U.S.A.) as per the manufacturer's protocol. The IC_{50} values of drugs for different cell lines were calculated by linear or nonlinear regression.

2.4. Determination of Intracellular ROS.

For the determination of intracellular ROS, a chloromethyl derivative of $2',7'$-dichlorofluorescein (CM-H2DCFDA, Cat# C6827, Sigma-Aldrich, St. Louis, MO, USA) and Dihydroethidium (Cat# D11347, Sigma-Aldrich, St. Louis, MO, USA) staining were used to determine hydroxyl, peroxyl, and other cellular ROS activities. $2',7'$-dichlorofluorescein and dihydroethidium were used to determine the generation of cell cytosolic hydrogen peroxide and superoxide, respectively, which were analyzed according to the manufacturer's protocol. Briefly, MDA-MB-231 cells (2×10^5 cells/ml) were treated with various concentrations of SSP (25, 50, 100 μg/ml) for 24 h, followed by staining with CM-H2DCFDA, and dihydroethidium (20 μM) was kept at room temperature for 45 minutes. Then, the cells were visualized under fluorescence microscopy.

2.5. Lactate Dehydrogenase Release Assay.

Lactate dehydrogenase (LDH) is a cytoplasmic enzyme that discharges into the culture medium during the cell getting rupture. The release of cytoplasmic enzymes is generally taking place due to inflammation (pyroptosis), recognized as an indicator of cell membrane damage. The leakage of the enzyme was determined in the culture medium using a CytoTox 96 Non-Radioactive Cytotoxicity Assay Kit (Promega, Wisconsin, U.S.A) as per the manufacturer's instructions. Absorbance at 490 nm was measured using a BioTek Synergy 2 microplate reader (BioTek, Winooski, VT, USA). The LDH release levels were calculated according to the formula:

$$\text{LDH release level} = 100\% \times \left(\frac{\text{Test OD} - \text{Blank OD}}{\text{Vehicle control OD} - \text{Blank OD}} \right) \tag{1}$$

2.6. Morphological Analysis by Scanning Electron Microscopy.

Morphological analysis was performed as described earlier [30]. Cells were treated with SSP (100 μg/ml) for 24 h and were fixed with 2.5% glutaralde-hyde (Sigma-Aldrich, St. Louis, MO, USA) overnight. The cells were rinsed thrice using phosphate buffer saline, and the critical point of the drying procedure was carried out. Samples were dehydrated through a graded series of ethanol (30, 50, 70, 95, and 100%) and dried in a Critical Point Dryer using liquid carbon dioxide. The dried specimens were mounted on specimen holders (aluminium stubs) for scanning electron microscopy (SEM), using double-sided adhesive tape, glue, colloidal silver, or colloidal carbon. Then, a thin layer (100-200 Å) of the metallic film was coated on the specimen surface for electrical conduction using either a sputter coater or a vacuum evaporator. Gold, gold-palladium, platinum, aluminium, or carbon was commonly used for the preparation of the thin conducting film. Image with a Hitachi S-3400 N scanning electron microscope was operated for the present study at 20 kV.

2.7. Animals.

Female (BALB/c) nude mice (6-7 weeks old) were purchased from Harlan Laboratories, Indianapolis, IN, USA, that were housed and maintained in Laboratory Animal Unit, the University of Hong Kong, a specific pathogen-free and climate-controlled room (22 ± 2°C, $50 \pm 10\%$ relative humidity) with a 12 h light/dark cycle and provided with diet and water ad libitum. The xenograft assay was performed as described before with some modifications [43, 44]. MDA-MB-231 cells (2×10^6/site) were implanted subcutaneously into the bilateral flank of each mouse. Palpable and measurable tumors were initially found 10 days after cell injection. Then, the animals were randomly assigned into four groups that were receiving the following treatments: the vehicle control group ($n = 5$) received Milli-Q water; the SSP-L group ($n = 5$) received SSP (0.4 g/kg/p.o, daily); the SSP-H ($n = 5$) group received SSP (0.8 g/kg/p.o, daily); the DTX group ($n = 5$) received docetaxel (5 mg/kg/i.p. week). The tumor size was calculated using the formula: $0.5 \times \text{length} \times \text{width}2$. All experiments were approved by the Institutional guidelines of Laboratory Animal Care and *Committee on the Use of Live Animals in Teaching and Research* (CULATR No.: 4484-17).

2.8. Acute Toxicity Study.

Acute toxicity studies were performed to determine the short-term adverse effects of a drug when administered in a single dose or multiple doses during 24 hours in two rodent species. The acute oral toxicity study was evaluated as per OECD guidelines. The studies were carried out in *BALB/c* mice (20–30 g) and Sprague-Dawley rats (150-180 g), respectively, using a single dose or multiple doses, which were treated orally. Thirty animals, divided into respective 5 groups, were designed for the study of acute toxicity via the oral route. Each group contains 6 animals (3 males and 3 females) receiving a single oral dose of 2, 4, 8, and 10 g/kg body weight of SSP extract, while the control group was administrated with distilled water. The general behavior of the animal and signs of toxicity were observed continuously for 1 h after the oral administration and then intermittently for 4 h and thereafter for 24 h. The animals were further observed once a day up to 14 days following treatment for behavioral changes and signs of toxicity and/or death and the latency of death. The LD_{50} value was
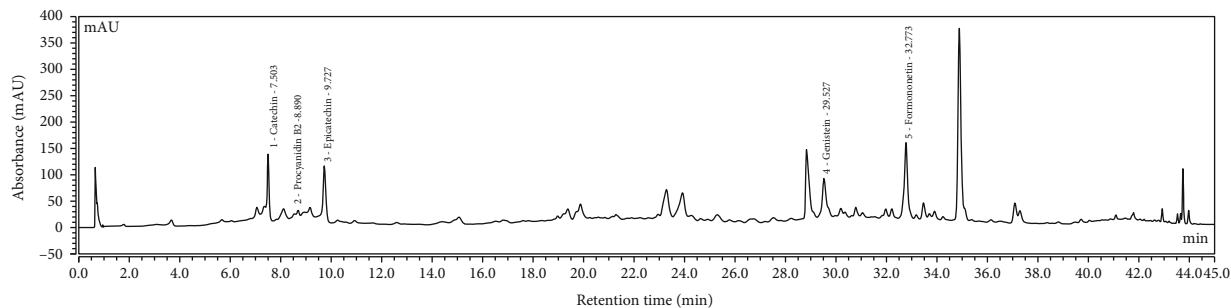
Figure 1: Identification of active constituents from SSP by UHPLC analysis.
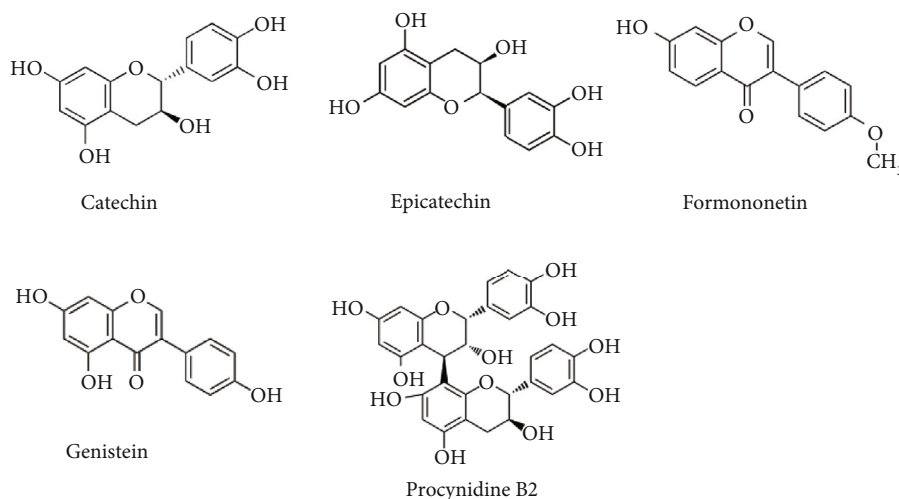
Figure 2: Structures of isolated compounds from SSP.

determined according to the method described by Kharch-oufa et al. [45].

2.9. Western Blot Analysis.

Western blot assay was conducted as previously described [17]. The proteins from the cell were lysed in RIPA buffer (pH = 7.4) comprised of protease inhibitors cocktail (10 μg/ml, Cat# 5872S, Cell Signaling Technology, MA, U.S.A.). The contents were centrifuged at 12,000 g at 4°C for 20 min, and the concentration of protein in the supernatants was determined using Bradford reagent (BioRad) with bovine serum albumin (BSA, Sigma Aldrich, St. Louis, MO, U.S.A.) as the standard. The protein samples were separated by electrophoresis on SDS-PAGE 10% or 12.5% gels. After blocked in 3% BSA, the membrane was incubated with primary antibodies, GAPDH (Cat# 2118 s, Cell Signaling Technology), caspase-1 (Cat# sc-56036, Santa Cruz Biotechnology, U.S.A.), GSDMD (Cat# 93709 s, Cell Signaling Technology), JNK1/2/3 (Cat# YT2440, Immunoway, TX, U.S.A.), caspase-3 (Cat# sc-7148, Santa Cruz Biotechnology), caspase-9 (Cat# 9502, CST), caspase-4 (Cat# ab238124, Abcam, Cambridge, United Kingdom), cleaved caspase-3 (Cat# 9661 s, Cell Signaling Technology), and GSDME (Cat# ab215191, Abcam) as needed. For secondary antibodies, antibodies to mouse (Cat# 7076, Cell Signaling Technol-

ogy) and rabbit (Cat# 7074, Cell Signaling Technology) were used. To visualize protein bands, a chemiluminescence (ECL) system (Cat# WBLUF0500, Millipore, MA, U.S.A.) was used.

2.10. Collection and Analysis of Biological Information.

The association between caspase-4, caspase-9, and overall survival was performed by the online tool KM plot (http://kmplot.com/) [46] with the Affymetrix ID: 213596_at and 237451_x_at, respectively. Differential gene expression analyses of the tumor, normal, and metastatic tissues were conducted by the online tool TNMplot (https://www.tnmplot.com/) with the genes' symbols based on RNA-Seq data offered by the database [47].

2.11. Statistical Analysis.

Nonlinear regression was operated with GraphPad Prism 7 (GraphPad Software, San Diego, CA, USA) choosing log(inhibitor) vs. response—variable slope (four parameters) as the equation. All data were expressed as mean ± standard deviation. Tukey's multiple comparison test was carried out on data from at least three independent experiments. The differences between the two groups were performed using two-tailed Student's t-test, and significance was established at $p \leq 0.05$.
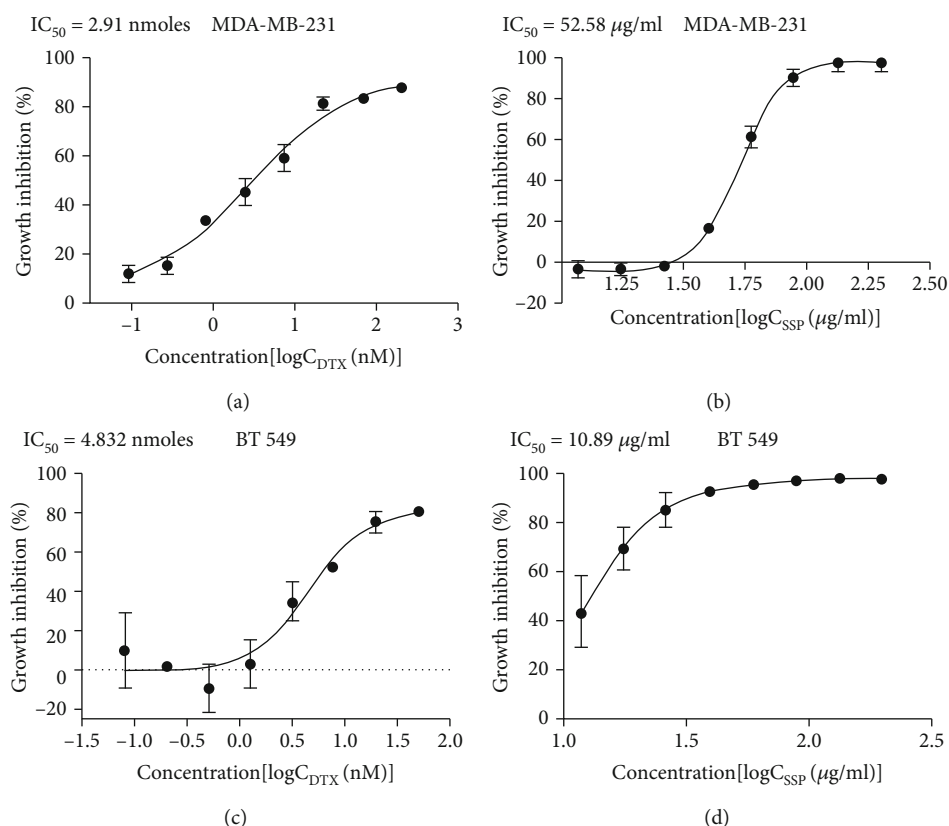
FIGURE 3: (a–d) Growth inhibitory efficacy of SSP and DTX on MDA-MB-231 and BT 549 cell lines.

3. Results

3.1. UHPLC Analysis of SSP.
A simple and speedy UHPLC method was used to determine the major constituents (catechin, procyanidin B2, epicatechin, genistein, and formononetin) that appeared in SSP. The constituents were separated on reverse-phase-C_{18} column developing a mobile phase comprised of formic acid (0.05%) in acetonitrile in the gradient elution mode. Under these conditions, flavonoids and isoflavones were separated in a 45 min run. The standard peaks 1-5 were identified as catechin (RT, 7.503 min), procyanidin B2 (RT, 8.690 min), epicatechin (RT, 9.727 min), genistein (RT, 29.527 min), and formononetin (RT, 32.773 min) (Figure 1) according to the retention time (RT) and UV-Vis spectra of the standards. The outcomes demonstrated that SSP contained five compounds (Figure 2). The analyses were repeated thrice and verified the constituents.

3.2. Growth Inhibitory Efficacy of SSP on Cancer Cell Lines.
The growth inhibitory efficacy (IC_{50}) of SSP was tested in the cell lines of MDA-MB-231 and BT 549 cells with the positive control (DTX) in vitro. The cells were treated with different concentrations of SSP (200, 100, 50, 25, 12.5, 6.25, 3.13, 1.56 μg/ml) or DTX (500, 250, 125, 62.5, 31.25, 15.63, 7.81, 3.91 nmoles), and growth inhibition curves were presented in Figures 3(a)–3(d). Through nonlinear regression, the IC_{50}(s) of SSP and DTX were prepared. For MDA-MB-231 cells, IC_{50} of DTX and SSP was 2.91 nmoles and

52.58 μg/ml, respectively. Similarly, for BT 549 cells, IC_{50} of DTX and SSP was 4.832 nmoles and 10.89 μg/ml, respectively. SSP and DTX exerted significant growth inhibition effects (IC_{50}) based on the increasing concentration exhibited in both cancer cell lines. The growth inhibition efficacy of SSP occurred significantly at lower concentrations in BT 549 and higher concentrations in MDA-MB-231. Moreover, DTX had growth inhibitory effects at minimum concentrations in MDA-MB-231 and maximum concentration in BT 549 (Figures 3(a)–3(d)).

3.3. Determination of Growth Inhibitory Efficacy of SSP in Xenograft Animals.
Subcutaneous injections of MDA-MB-231 (2×10^6 cells/0.1 ml) into the bilateral flank of each mouse were provided. Bodyweight, tumor growth, and tumor volume were monitored at 2 days intervals for 22 days. On day 22, the mice were sacrificed and measured their tumor volume at the endpoint (Figure 4(e)). There were significant body weight changes in the treated groups during the study period (Figure 4(b)). And treatment of SSP-L, SSP-H (0.4 and 0.8 g/kg/p.o, daily), and DTX (5 mg/kg/i.p. week) significantly inhibited the growth of tumors in the animals when compared to the vehicle group (Figures 4(c) and 4(e)). At the endpoint, tumor volume was significantly different ($^*p = 0.0151$) between the SSP-H-treated group and the vehicle group. In addition, DTX-treated animals were also significantly ($^*p = 0.0435$) reducing the growth of tumors (Figure 4(c)).

(a)

(b)

(c)

(d)

(e)
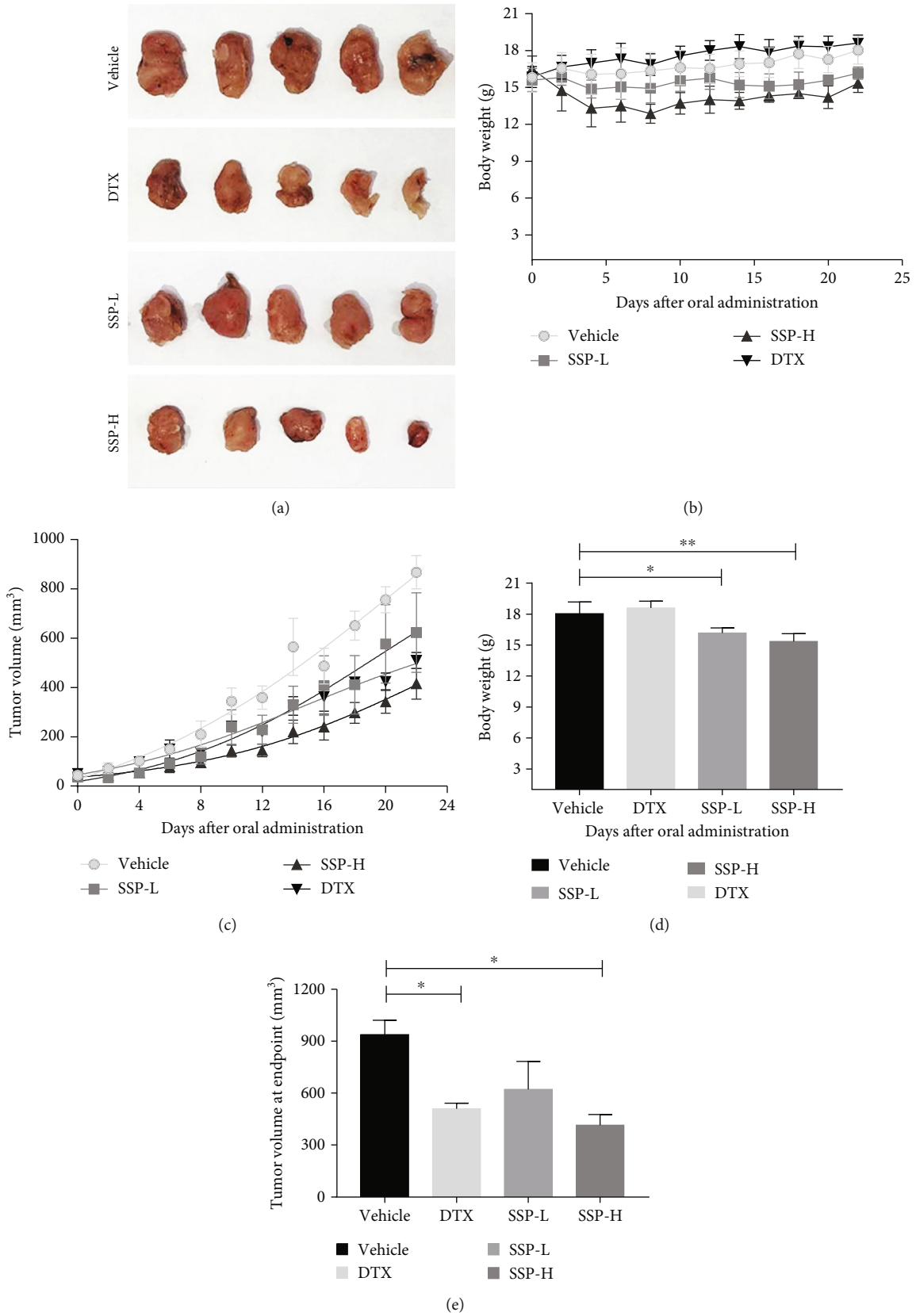
Figure 4: Effect of SSP on human TNBC cell line, MDA-MB-231, in the xenograft model. SSP played a positive role against MDA-MB-231. (a) Representative pictures of mice xenograft with different treatments for 22 days, (b) bodyweight curve, (c) tumor volume curve, and (d) analysis for the bodyweight of each group at an endpoint. Data were shown as mean ± SD ($n = 5$). (e) Analysis of tumor volume of each group at an endpoint. Data were shown as mean ± SE ($n = 5$). $^*p$ (vehicle vs.DTX) = 0.0435, $^*p$ (vehicle vs.SSP − H) = 0.0151.

TABLE 1: Mortality and clinical signs of acute toxicity of SSP.

Animals	Dose of SSP (g/kg b.w. p.o)	Mortality latency (h)	Toxic symptoms	LD$_{50}$ (g/kg b.w. p.o.)
	0	—	None	
	2.0	—	None	
BALB/c mice	4.0	—	None	10
	8.0	—	None	
	10.0	<1 h	Anorexia, hypoactivity	
	0	—	None	
	2.0	—	None	
Sprague-Dawley rats	4.0	—	None	>10
	8.0	—	None	
	10.0	—	None	

Animals were divided into respective 5 groups and 6 animals (3 males and 3 females) each. Each group receiving a single oral dose of 2, 4, 8, and 10 g/kg body weight of SSP extract, while the control group was administrated with distilled water. The general behavior, signs of toxicity and/or death, and the latency of death were observed continuously for 1 h after the oral administration and then intermittently for 4 h and thereafter for 24 h. The LD$_{50}$ value was determined according to the method described by Kharchoufa et al. [45].
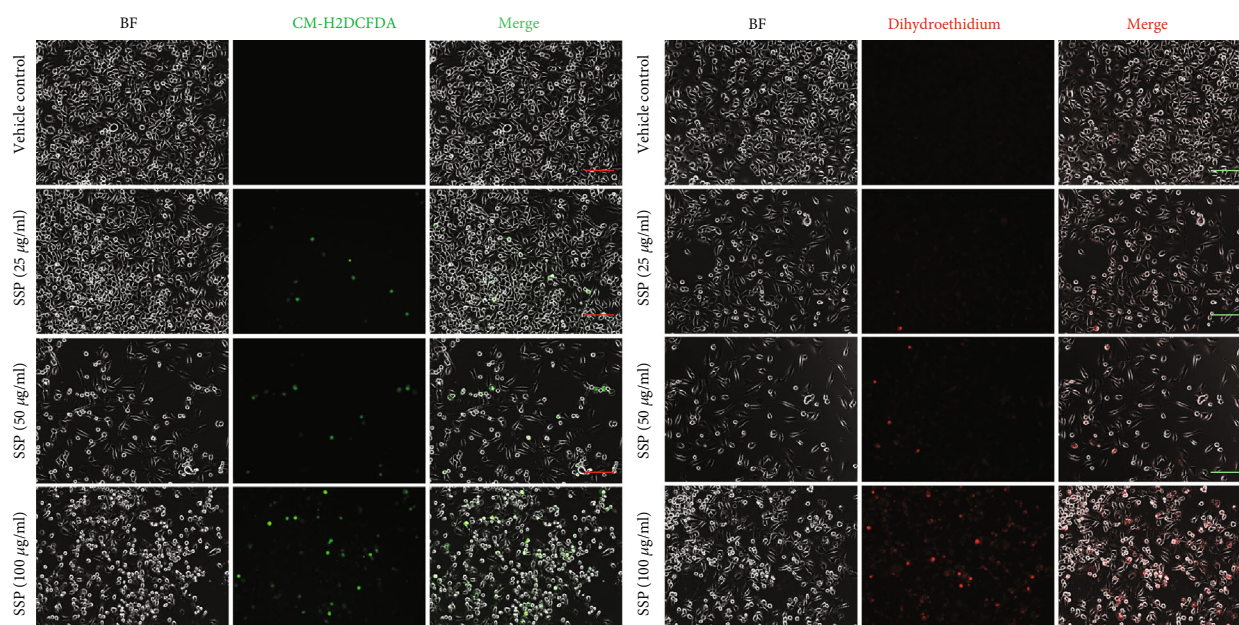
FIGURE 5: SSP upregulated ROS generation in MDA-MB-231 cells. The detection of intracellular ROS was based on CM-H2DCFDA and dihydroethidium staining of MDA-MB-231 cells after treatment with different doses of SSP (25, 50, and 100 μg/ml) for 24 h. Scale bar, 100 μm.

3.4. Evaluation of Acute Toxicity. The acute toxicity study was conducted to determine the harmful effects of SSP to the animals administered as a single or short-term exposure. This investigation assessed the changes in the behavior, sign, body weight, mortality, and other changes in the overall well-being of the animals. In the present study, the acute toxicity evaluation showed that the oral LD$_{50}$ value of SSP was 10 g/kg b.w. (Table 1).

3.5. Generation of Intracellular ROS by Treatment with SSP in MDA-MB-231 Cell Lines. To determine the effect of SSP on ROS generation, ROS was detected using CM-H2DCFDA for general oxygen species and dihydroethidium staining, which facilitated to show the expression levels of

superoxide and hydrogen peroxide. As shown in Figure 5, the Generation of ROS, specifically superoxide and hydrogen peroxide, were measured in a 24 h cultured plate containing MDA-MB-231 cells, which was shown in a dose-dependent manner of SSP (25, 50, and 100 μg/ml). The outcomes showed that SSP treatment upregulated ROS generation in which the number of cells was stained using CM-H2DCFDA and dihydroethidium in MDA-MB-231 cells.

3.6. SSP Triggers Pyroptotic Cell Death in TNBC Cells. The vehicle showed normal architecture of the MDA-MB-231 cells, which was observed under bright field by phase-contrast microscopy and SEM (Figures 6(a) and 6(c)). The treatment of SSP promoted pyroptotic cell death in 24 h

(a)

(b)

(c)

(d)

(e)

(f)
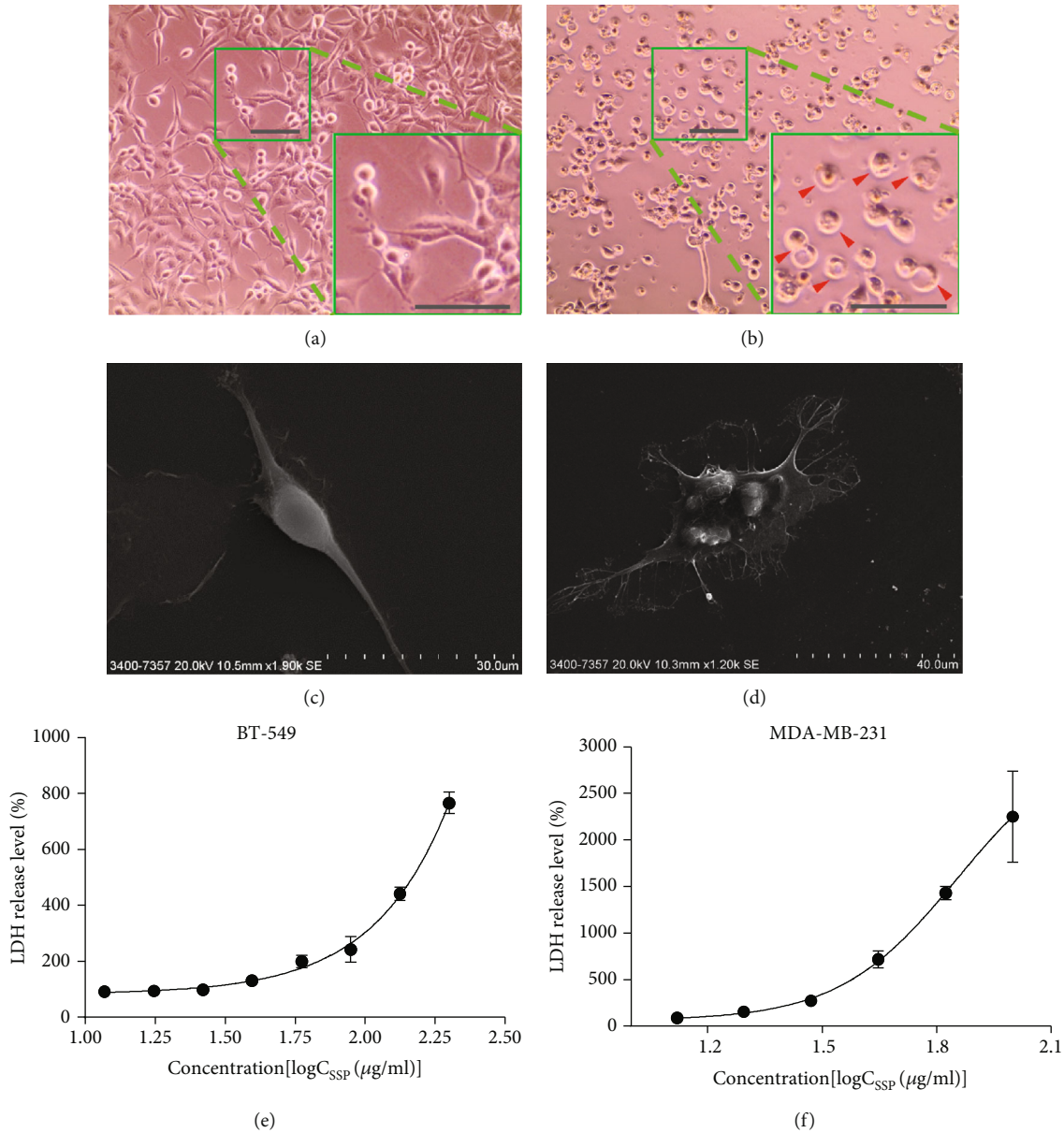
FIGURE 6: SSP promoted pyroptotic cell death in MDA-MB-231 cells. Bright field microscopic observation of (a, c) vehicle showed normal architecture of the cells. SEM observation (b, d) of SSP (100 μg/ml) in MDA-MB-231 cells exhibited flattened cells with the cabbage or fried egg-like the cell nucleus located in the center. Arrowhead indicated the bubbling of pyroptotic cells. Scale bar, 100 μm. (e, f) The release of LDH levels in BT-549 and MDA-MB-231 cell culture after 24 h treatment with SSP, respectively (100 μg/ml).

cultures of MDA-MB-231 cells, which showed flattened cells with the cabbage or fried egg-like morphology in which the cell nuclei located in the center or above the main plane of the cell body (Figures 6(b) and 6(d)). The observations were well documented in the SSP-treated groups with noticeable pyroptotic features in the cell. During the pyroptotic mechanism, the activation of caspases causes the loss of membrane integrity and release of cytosolic LDH, resulting in inflammatory cell death. LDH with other cellular contents was discharged during pyroptotic blebs of cellular demise. The leakage of the LDH was determined in the culture medium using a commercial assay kit. Figures 6(e) and 6(f) exhibit the release levels of LDH in BT-549 and MDA-

MB-231 cells after 24 h treatment with SSP (100 μg/ml). The western blot analysis of inflammasome protein showed caspase-4 cleaved GSDME that permeabilized into the cell membrane and might trigger pyroptosis, a form of inflammatory programmed cell death (Figure 7). The full-length GSDME (F-GSDME) degraded into an N-terminal fragment of GSDME (N-GSDME) by caspase-4 that transported into the cell membrane and lysed the cells (Noncanonical pathway). Moreover, caspase-1 did not involve in the cleaving of GSDMD in which there were no products of GSDMD-N and therefore, this mechanism of the inflammasome was a ROS-dependent noncanonical pathway (Figure 7).
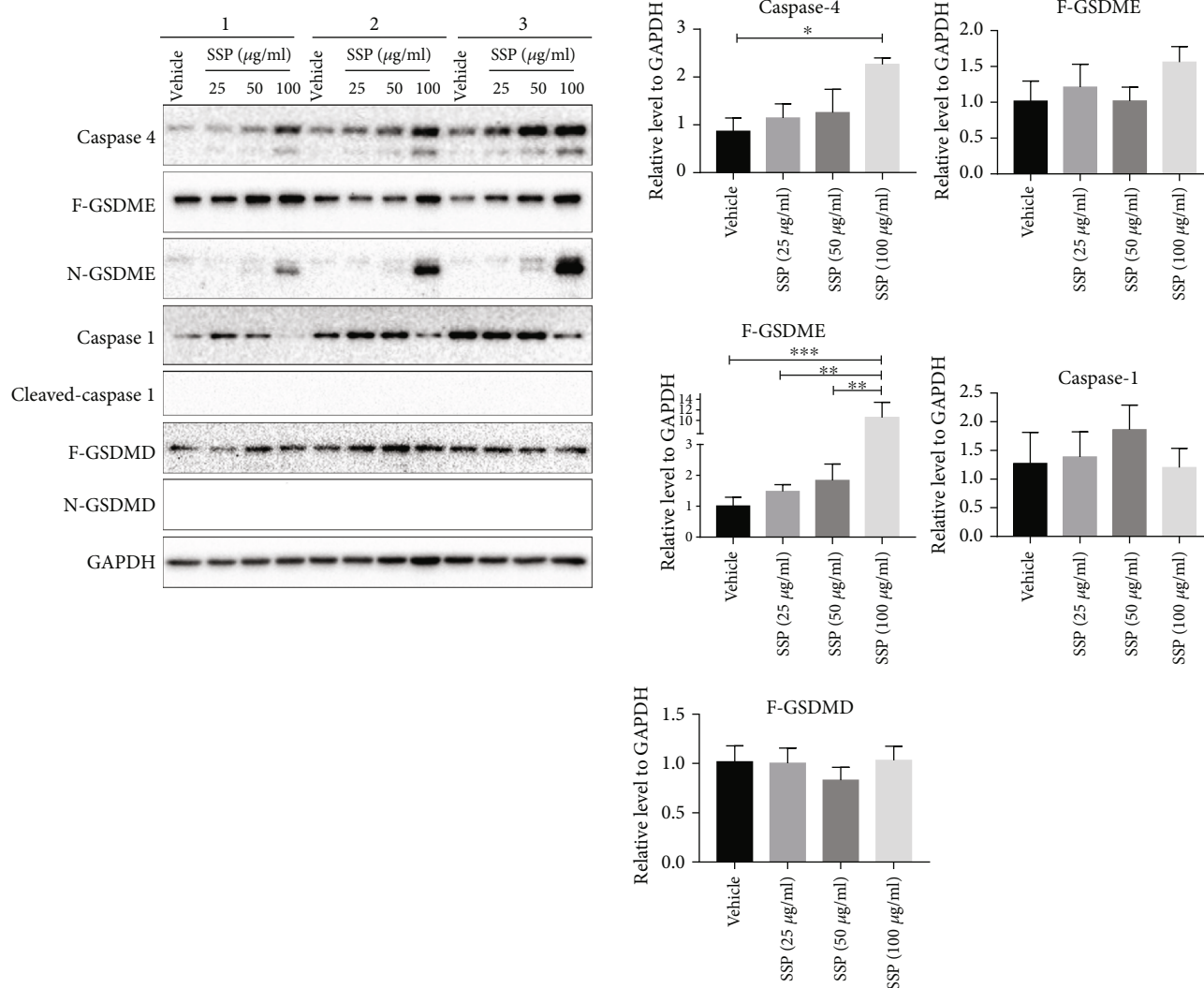
Figure 7: SSP triggered inflammatory cell death in MDA-MB-231 cells. Representative Western blot assay was involved in the pyroptotic signaling pathway in MDA-MB-231 cells that were connected with the treatment of SPP (25, 50, 100 μg/ml). The expression of caspase-4 cleaved GSDME that triggers pyroptosis. The full-length GSDME (GSDME-F) degraded into N-terminal fragment of GSDME (N-GSDME) that directly transferred to the plasma membrane and lysed the cells (noncanonical pathway). However, caspase-1 did not involve in the cleaving of GSDMD-F (canonical pathway) in which there were no products of GSDMD-N, and hence this inflammasome mechanism was a ROS-dependent noncanonical pathway. Data were shown as mean ± SD ($n = 3$). $^{**}p = 0.0031$, $^{***}p < 0.001$.

3.7. GSH Blocked SSP-Induced Pyroptosis in TNBC Cells. Glutathione (GSH) is an inhibitor of ROS, which markedly attenuates the SSP-induced ROS elevation in the cell and thus rescues pyroptotic cell death. BT-549 and MDA-MB-231 cells were pretreated with or without GSH (2 mmoles) for 2 h, followed by the treatment of SSP (100 μg/ml) or vehicle (Milli-Q water) for 24 h. The pretreatment of GSH improved the cell viability and demolished the LDH release in SSP-treated MDA-MB-231 and 4T1 cell lines due to its ROS scavenging potential (Figures 8(a) and 9(a)). Similarly, phase-contrast microscopic observation demonstrated that MDA-MB-231 and 4T1 cells treated with GSH followed by the administration of SSP showed less pyroptotic features, whereas SSP treatment showed flattened cells with fried egg-like morphology (Figures 8(b) and 9(b)). Western blot assay revealed GSH aborted pyroptotic signaling upon SSP

treatment. Cleaved caspase-3, caspase-4, and GSDME were involved in the inflammasome signaling pathway (Figures 8(c) and 9(c)).

3.8. The Relationship between Caspase-4/9 and Overall Survival of the Patients. Confirming prognostic or projecting candidate genes in suitably powered BCa cohorts is of greatest interest nowadays. Based on the online Kaplan-Meier plotter tool, we drew survival plots, which were used to assess the relevant expression levels of caspase-4 and caspase-9 genes on the clinical outcome of BCs individuals. Using the selected parameters, the analysis was operated on caspase-4 (Affy ID: 233596, 3951 patients) and caspase-9 (Affy ID: 237451_x, 1751 patients). Based on the median of participants, the relevant expression levels were demonstrated at the lower or higher risks of 1978
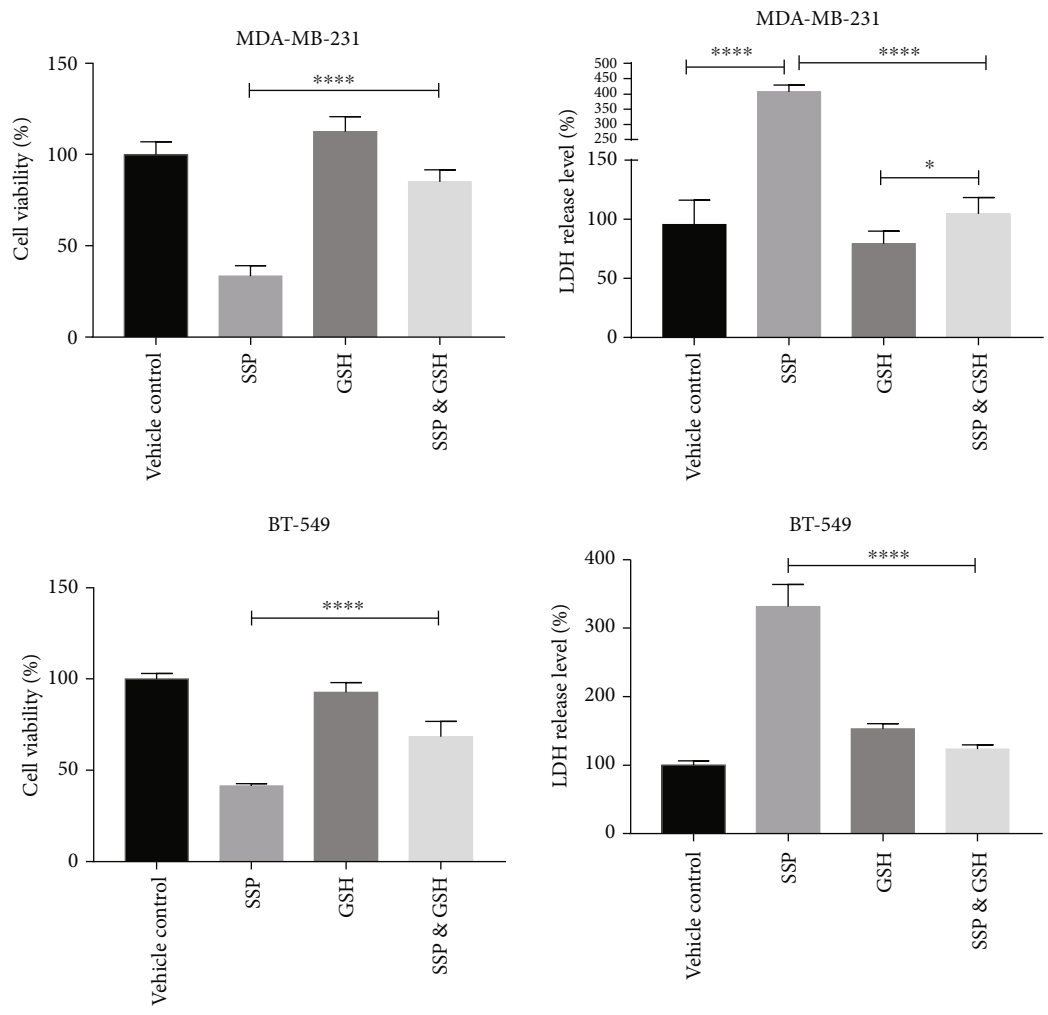
(a)
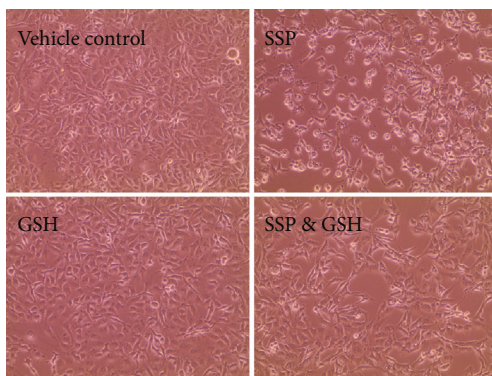
(b)

FIGURE 8: Continued.
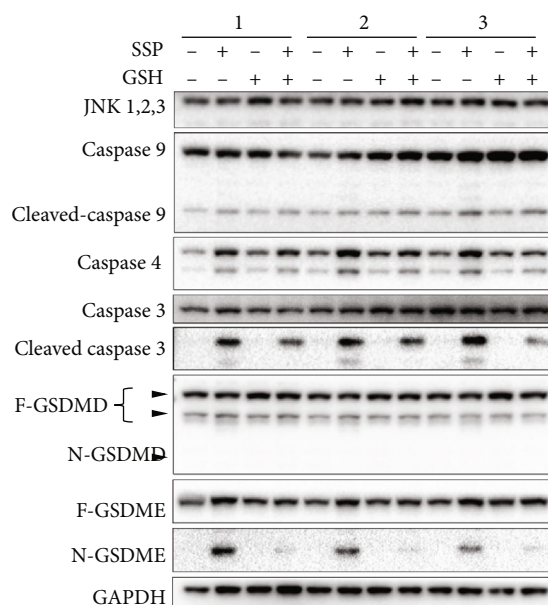
(c)

FIGURE 8: GSH blocked SSP-induced pyroptotic signaling pathways in TNBC cells. (a) Representative outcomes of the cell viability and LDH release assay in MDA-MB-231 and BT-549 cells upon the cotreatment of GSH and SSP. $****p < 0.0001$, $*p = 0.0493$. Data were shown as means ± SD ($n = 6$). (b) Representative phase-contrast microscopy of MDA-MB-231 cells upon the cotreatment of GSH and SSP. (c) Representative western blot assay for the detection of SSP induced pyroptotic inflammasome signaling pathways and GSH rescue experiment.

and 1973, respectively. The hazardous ratio of caspase-4 was 0.69 (p value 1.5e-15) with the median months' survival of the respective low and high expression cohorts of 38 and 68.75. Similarly, caspase-9 was exhibited at lower and higher risks of 896 and 868, respectively. The hazardous ratio of caspase-9 was 0.55 (p value 4.3e-14) with the median months' survival of the respective low and high expression cohorts of 25.2 and 57. The high levels of the caspase-4 and caspase-9 expression in BCa patients were associated with better survival (Figures 10(a) and 10(b)).

3.9. Differential Gene Expression Analysis of GSDME and Caspase-4 in Tumor, Normal, and Metastatic Tissues. Genes generally show differential expression in either tumor or metastatic tissues, which can be beneficial to envisage tumor formation and to facilitate cancer management as a biomarker. Using the TNM plot tool, based on an integrated dataset that was documented in the RNA sequencing data of normal ($n = 113$), tumor ($n = 1097$), and metastatic ($n = 07$) tissues, we compared the differential expression levels of selected genes in normal, tumor, and metastatic tissues. The expression of caspase-4 and GSDME was significantly inhibited in the tumor tissues. The fold changes of caspase-4 from tumor to normal and from metastasis to the tumor were about 0.76 and 1.41, respectively (Figure 10(c)). The analysis of GSDME exhibited fold changes from tumor to normal (0.61) and from metastasis to tumor (1.14) (Figure 10(d)).

4. Discussion

SSD is a traditional medicinal plant normally used in China for its hematopoietic and antiviral properties [48, 49]. Mounting research has been conducted in vitro and in vivo of SSD showing as a promising traditional medicinal drug in the management of various cancers [15, 17, 20, 21]. Presently, physicians from TCM have utilized *SSD* as a potential therapy for BCa patients and accomplished greater positive outcomes [19]. Studies have further suggested that SSD directly suppresses various molecular signaling pathways, upregulates apoptotic signaling, inhibiting LDH and arresting the cell cycle, and is thereby proved as a potential anticancer compound [19, 21, 50]. In addition, SSD protects against various effects of oxidative stress, cerebral ischemia, radiation, and diabetic complications [51–53]. However, the anticancer efficacy of SSP and its protective mechanism against the most fetal and invasive subtype of BCa, TNBC have not been completely revealed.

Earlier, several studies were reported that SSD comprised of various bioactive compounds, viz., (-)-sativan, formononetin, isoliquiritigenin, genistein, naringenin, medicarpin, prestegane, naringenin, blumenol A, protocatechuic acid, liquiritigenin, 7,4′-dihydroxy-8-methoxy-isoflavone, protocatechuic acid, glycyroside, and dulcisflavan that possesses cytotoxicity, anticancer, and antimutagenic properties [7, 8, 13, 14, 19]. The present study is also exhibited five distinguished bioactive compounds, viz., catechin, procyanidin B2, epicatechin, genistein, and formononetin, and all of them have greater antitumor, antimutagenic, and potential

(A)

(B)

(a)

(b)

(c)
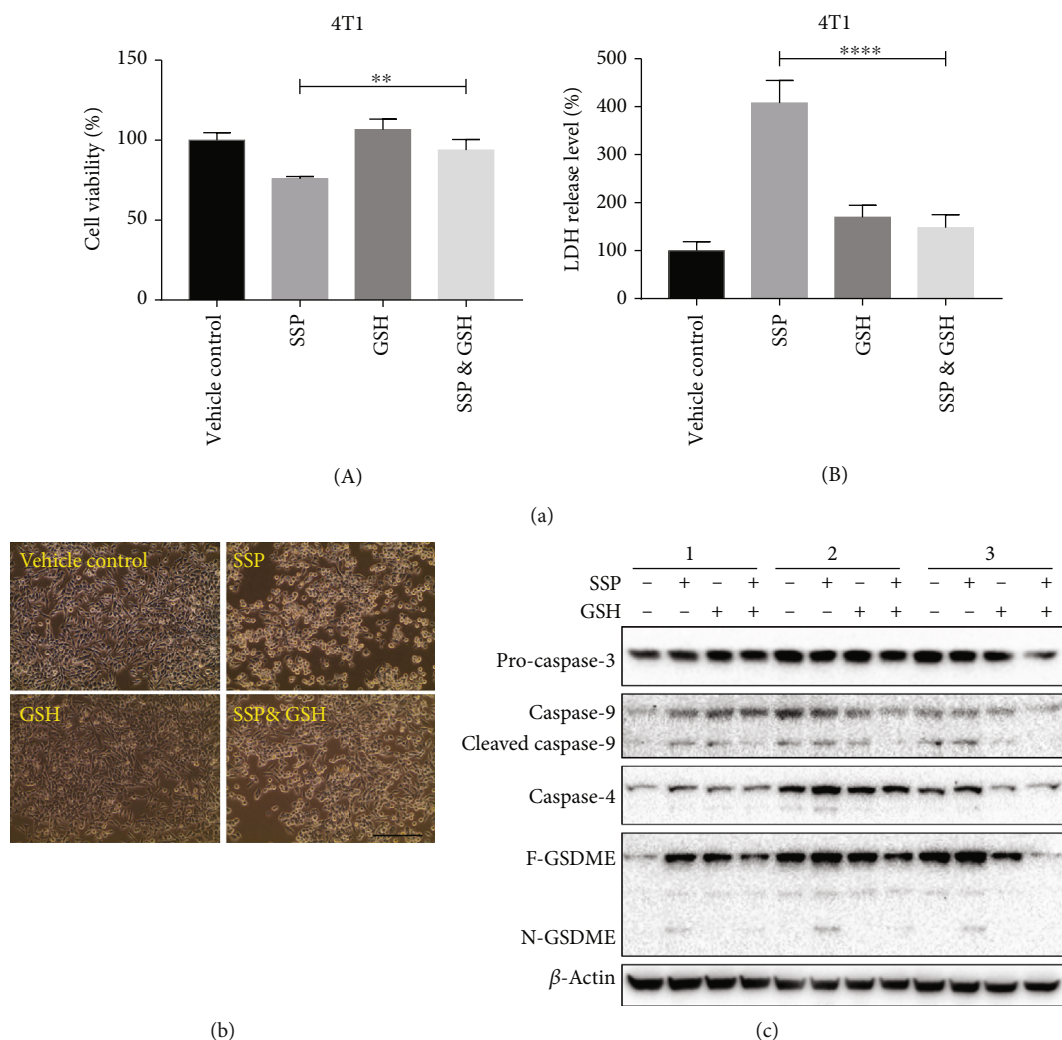
FIGURE 9: GSH blocked the efficacy of SSP and the pyroptotic signaling pathways in TNBC cells. (a) Representative result for cell viability detection of 4T1 cells after different treatments, $^{**}p < 0.01$. Data are shown as means $\pm$ SD ($n = 3$). (b) Representative result of LDH release assay in 4T1 cells after different treatments, $^{****}p < 0.0001$. Data are shown as means $\pm$ SD ($n = 3$). (b) Representative phase-contrast microscopy of 4T1 cells after different treatments. (c) Representative western blot assay for the detection of pyroptotic signaling pathways in GSH rescue experiment. BT-549 cells were pretreated with or without GSH (2 mM) for 2 h, followed by SSP (100 μg/ml) or vehicle treatment for 24 h, respectively, as specifically indicated.

genotoxic effects [31, 32, 54–59]. Some of these major compound(s) is/are responsible for the anti-TNBC efficacy of SSP, which is being studied in our laboratory. The outcome of acute toxicity indicated that the oral LD_{50} value of SSP was about 10 g/kg, and this extract is considered as low toxic to the animals. These findings offer preliminary data on the toxic profile of SSP. Hence, further studies (genotoxicity, subchronic toxicity, reproductive toxicity, etc.) are needed to validate the clinical studies of the plant.

In this study, SSP was investigated on three different TNBC cells: MDA-MB-231, 4T1, and BT 549 cell lines. SSP had significant cytotoxic and growth inhibitory effects on all cell lines in a dose-dependent manner. These effects can be mediated by the generation of ROS [60]. Previously, SSD treatment significantly increased cytotoxic effects through the generation of ROS in U266 and U937 cells [15]. ROS plays a critical role in multiple tumor chemother-

apy and involves cytotoxicity, autophagy, and apoptosis [61]. There were significant differences in the SSP-treated groups (bodyweight-15.35 g and tumor volume-415.4 mm³) and vehicle group (bodyweight-18.04 g and tumor volume-937.4 mm³), which showed about 55.69% tumor growth inhibition at the endpoint. Thus, SSP inhibits the growth of MDA-MB-231 human TNBC in a xenograft-bearing mouse model. This study was consistent with the earlier study upon the treatment of resveratrol inhibited the gaining of body weight and tumor growth in the animal models [62, 63].

In our study, we detected ROS generation upon SSP treatment, which was consistent with earlier investigations [15, 17]. The detection of intracellular ROS was based on the presence of CM-H2DCFDA and dihydroethidium staining of MDA-MB-231 cells upon the treatment of SSP (25, 50, and 100 μg/ml), and this ROS generation was
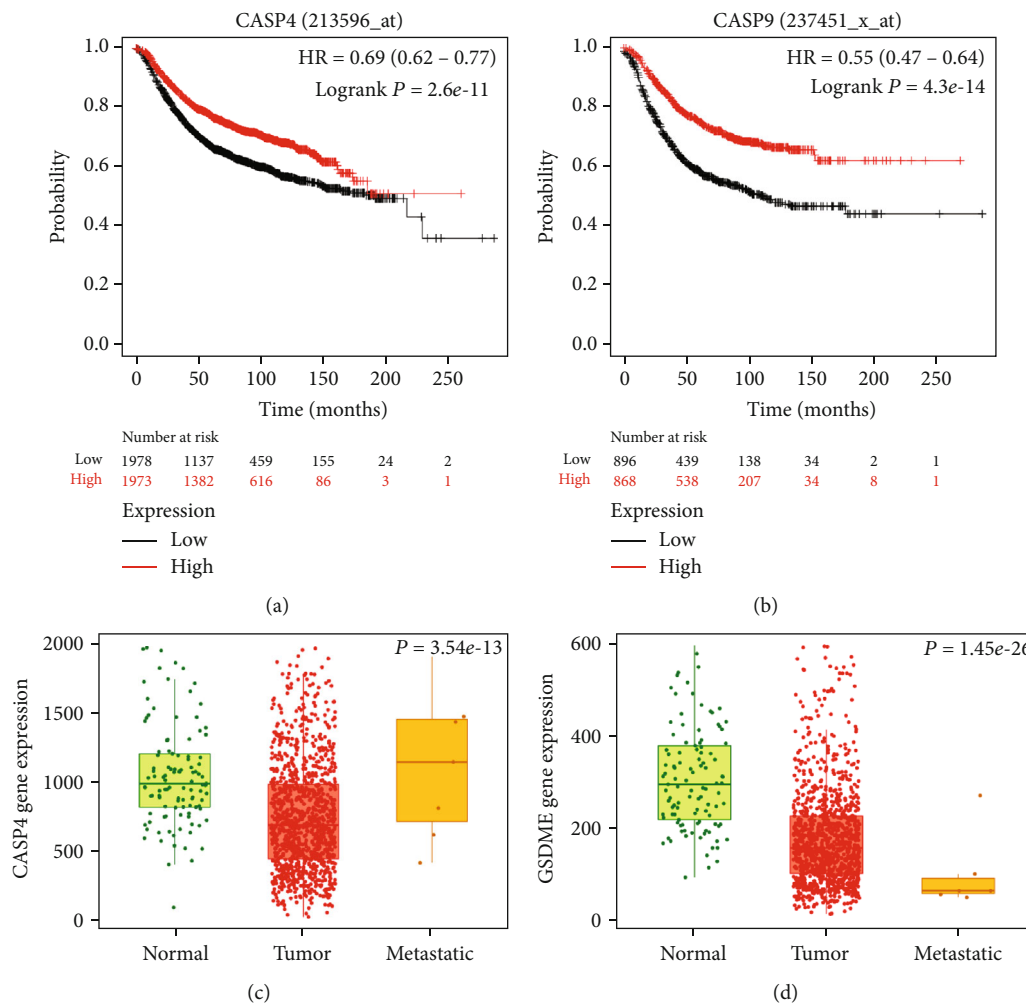
FIGURE 10: (a, b) The high expression of caspase-4/9 was connected with overall better survival of the BCa patients. (c, d) Analysis of GSDME and caspase-4 expression in normal, tumor, and metastatic states in BCa.

significantly greater in MDA-MB-231 cells when treated with the higher concentrations of SSP (100μg/ml). For TNBC management, to date, there is no promising medication. Hence, there is urgent to find novel anti-TNBC strategies or molecular targets. Natural compounds like SSP, in this setting, have many advantages, especially in the clinical practices of TCM or in preclinical research. In our study, SSP could inhibit the growth of TNBC both in vitro and in vivo, and this mechanism has been elucidated through noncanonical pyroptotic pathways. The expression of caspase-4, cleaved caspase-9, GSDME, and the N-fragment of GSDME was upregulated upon SSP administration in TNBC cells.

Earlier, researchers believed only SSD treatment could induce apoptosis [15, 17]. However, in the present study, SSP promotes pyroptotic cell death in TNBC cells. Pyroptosis is a process of programmed cell death, mediated by the key factors, GSDMD or GSDME, which can be activated by caspase-4 and/or caspase-3 [64–66]. Several caspases can cleave GSDMD or GSDME into the N and C-terminal domain of GSDMD or GSDME, in which the N-terminal fragments have the ability of pore-forming activity in the plasma membrane [37, 67]. The significant difference between apoptosis and pyroptosis is the microscopy and cellular osmotic features. The morphological analysis of SSP-treated TNBC cells is of pyroptotic features. The cells are exhibited flattened cells with the "cabbage" or "fried egg"-like, and the cell nucleus located in the center. The activation of GSDME causes a loss of membrane integrity and release-/discharge of cytosolic LDH, resulting in inflammatory cell death. LDH with other cellular contents is also discharged during the pyroptotic blebs of cellular demise [68]. Interestingly, SSP-treated TNBC cells have neither altered the expression of cleaved GSDMD nor cleaved caspase-1. This activation is performed through the activation of caspase-4 and caspase-3. The complex of N-GSDMEs inserts into the plasma membrane as pores resulting in cell lysis. In this process, canonical inflammasomes are not involved. Thus, the process was regarded as a noncanonical inflammasome pyroptotic signaling pathway.

The mechanisms underlying the events of the noncanonical inflammasome are still being described. Caspase-3, -8, -9, -7, -4, -5, and -11 trigger its activation, as they are recognized as molecular switches or effectors for pyroptotic cells

[34, 65, 69–72]. These activated caspases then generate GSDME and biologically active executioners, impacting pyroptotic cell death [64]. GSH is an inhibitor of ROS that attenuates SSP-induced ROS generation in the cell and hence rescues pyroptotic cell death. SSP treatment alone could cause pyroptosis through the activation of caspase-4 and caspase-9. These findings indicated that SSP-induced pyroptotic death is ROS-dependent. The present investigation validated that SSP promotes ROS generation in TNBC cells which triggers noncanonical pyroptosis and involves a novel anti-TNBC-based intervention strategy for the treatment of BCa.

Noncanonical inflammasome-associated pyroptosis has been reported to play in both pro-and anti-tumor development. The tumor microenvironment is shaped by a chronic inflammation in which polarized macrophages and stromal components promote tumor development [73–75]. Thus, non-canonical inflammasome activation and regulation have been vital especially in cancer and other disease management. Non-canonical pro-pyroptotic agents like SSP induce an acute inflammatory immune response that warrants further investigation in a clinical setting. Furthermore, our bioinformatic analysis of caspase -4, -9, and GSDME are well-established as cancer markers that are also involving in non-canonical pyroptotic mechanisms.

Bioinformatic tools are extensively used to evaluate gene expression levels and to explore their possible implications in the development of various cancers [76–78]. In the present study, survival analysis using the KM Plotter revealed that the low transcription levels of caspase-4 and 9 are related to low relapse-free survival in BCa. This study was consistent with earlier investigations in which researchers concluded that the caspase family is operated as new prognostic indicators in various cancers, including breast [79], gastric [80], ovary [81], and renal [82]. TNM plot analysis showed that the expression of caspase-4 and GSDME was significantly inhibited in clinical tissues in normal (113), tumor (1097), and metastatic (07) states, which was consistent with the earlier investigation [47]. Based on the study, the ROS-induced pyroptotic pathway which is associated with caspase-4/9 and GSDME that are potential targets of precision therapy for patients with TNBC.

5. Conclusions

TNBC is one of the most problematic classes of BCa with easy recurrence and considerably assertive type. SSD has been used in the clinic of TCM as a potential therapeutic agent to heal BCa individuals, which accounts for relatively positive responses. However, the anti-TNBC potential of SSP and its evidence-based in vitro and preclinical studies is still deficient. Hence, the present study was evaluated the anti-TNBC potential of SSP through various in vitro and in vivo studies. SSP showed significant growth inhibitory efficacy in both TNBC cell lines and xenograft animal models. Western blot analysis was also encouraged that SSP elevated inflammasome proteins such as caspase-4 and 9, which cleaved GSDME triggering pyroptosis and permeabilizing the cell membrane. Furthermore, cotreatment of

GSH and SSP markedly attenuates the SSP-induced ROS generation in the cell and validated the rescuing pyroptotic cell death. Survival analysis using the KM Plotter and TNM plot database exhibited the curved transcription levels of caspase-4 and 9 related to low relapse-free survival in patients with BCa. SSP is comprised of catechin, procyanidin B2, epicatechin, genistein, and formononetin that are recognized as anticancer agents. All findings strongly suggest that SSP possesses anti-TNBC efficacy and continues to be an inspiring and dynamic research niche in the upcoming days with evident antitumorigenesis effects and targets of eradicating BCa cells. However, well-controlled future clinical studies are quite required to advance an understanding of the pharmacological functions of SSP. Such information could be used to categorize effective preventive strategies targeting specific components of TNBC.

Abbreviations

AKT:	Serine/threonine-specific protein kinase
ATCC:	American Type Culture Collection
BCa:	Breast cancer
BSA:	Bovine serum albumin
CM-H2DCFDA:	Chloromethyl derivative of $2',7'$-dichlorofluorescein
CULATR:	Committee on the Use of Live Animals in Teaching and Research
DAD UV:	Vis detector diode array detector ultraviolet-visible detector
DMEM:	Dulbecco's Modified Eagle Medium
DTX:	Docetaxel
ER+:	Estrogen receptor
FBS:	Fetal bovine serum
F-GSDME:	Full-length GSDME
GAPDH:	Glyceraldehyde 3-phosphate dehydrogenase
GSDMD:	Gasdermin D
GSDME:	Gasdermin E
GSH:	Glutathione
H_2O_2:	Hydrogen peroxide
IC_{50}:	Half maximal inhibitory concentration
LDH:	Lactate dehydrogenase
MAPK:	Mitogen-activated protein kinase
N-GSDME:	N-Terminal fragment of GSDME
nmoles:	Nanomoles
mmoles:	Millimoles
PI3K:	Phosphatidylinositol 3-kinase
RIPA:	Radioimmunoprecipitation assay buffer
ROS:	Reactive oxygen species
RPMI:	Roswell Park Memorial Institute
SDS-PAGE:	Sodium dodecyl sulphate–polyacrylamide gel electrophoresis
SEM:	Scanning electron microscopy
SSD:	Spatholobus suberectus Dunn
SSP:	Spatholobus suberectus Dunn percolation extract
TNBC:	Triple-negative breast cancer
UHPLC:	Ultra high-pressure liquid chromatography.

Data Availability

The data used to support the findings of this study are available from the corresponding author upon request.

Ethical Approval

All experiments were approved by the Institutional guidelines of Laboratory Animal Care and *Committee on the Use of Live Animals in Teaching and Research* (CULATR No.: 4484-17).

Conflicts of Interest

The authors declare no conflicts of interest.

Authors' Contributions

Conceptualization, methodology, validation, and investigation were contributed by F.Z., Q.L., and K.G. Data curation was contributed by F. P, Z. K, F. G, and X.L. Original draft preparation, review, and editing were contributed by F.Z. and K.G. Supervision, resources, review and editing, project administration, and funding acquisition were contributed by J.S., X. L,and J.C. All authors have read and agreed to the published version of the manuscript.

Acknowledgments

References

[1] X. Li, J. Yang, L. Peng et al., "Triple-negative breast cancer has worse overall survival and cause-specific survival than non-triple-negative breast cancer," *Breast Cancer Research and Treatment*, vol. 161, no. 2, pp. 279–287, 2017.

[2] P. Kumar and R. Aggarwal, "An overview of triple-negative breast cancer," *Archives of Gynecology and Obstetrics*, vol. 293, no. 2, pp. 247–269, 2016.

[3] K. Oualla, H. M. el-Zawahry, B. Arun et al., "Novel therapeutic strategies in the treatment of triple-negative breast cancer," *Therapeutic Advances in Medical Oncology*, vol. 9, no. 7, pp. 493–511, 2017.

[4] K. Ganesan and B. Xu, "Deep frying cooking oils promote the high risk of metastases in the breast-A critical review," *Food and Chemical Toxicology*, vol. 144, article 111648, 2017.

[5] H. Zhu, J. You, Y. Wen et al., "Tumorigenic risk of Angelica sinensis on ER-positive breast cancer growth through ER-induced stemness in vitro and in vivo," *Journal of Ethnopharmacology*, vol. 280, 2021.

[6] S. Qin, L. Wu, K. Wei et al., "A draft genome for *Spatholobus suberectus*," *Science Data*, vol. 6, no. 1, p. 113, 2019.

[7] K. Inami, Y. Asada, T. Harada, Y. Okayama, N. Usui, and M. Mochizuki, "Antimutagenic components in Spatholobus suberectus Dunn against N-methyl-N-nitrosourea," *Genes Environment*, vol. 41, no. 1, 2019.

[8] H. L. Chen, J. Yang, Y. F. Fu, X. N. Meng, W. D. Zhao, and T. J. Hu, "Effect of total flavonoids of Spatholobus suberectus Dunn on PCV2 induced oxidative stress in RAW264.7 cells," *BMC Complementary and Alternative Medicine*, vol. 17, no. 1, p. 244, 2017.

[9] H. Cho, B. Chung, C. K. Kim, D. C. Oh, K. B. Oh, and J. Shin, "Spatholobus suberectus Dunn. constituents inhibit sortase A and Staphylococcus aureus cell clumping to fibrinogen," *Archives of Pharmacal Research*, vol. 40, no. 4, pp. 518–523, 2017.

[10] W. Park, C. H. Ahn, H. Cho, C. K. Kim, J. Shin, and K. B. Oh, "Inhibitory effects of flavonoids from Spatholobus suberectus on sortase A and sortase A-mediated aggregation of Streptococcus mutans," *Journal of Microbiology and Biotechnology*, vol. 27, no. 8, pp. 1457–1460, 2017.

[11] Y. F. Fu, L. H. Jiang, W. D. Zhao et al., "Immunomodulatory and antioxidant effects of total flavonoids of *Spatholobus suberectus* Dunn on PCV2 infected mice," *Scientific Reports*, vol. 7, no. 1, 2017.

[12] S. R. Chen, A. Q. Wang, L. G. Lin, H. C. Qiu, Y. T. Wang, and Y. Wang, "In vitro study on anti-hepatitis C virus activity of Spatholobus suberectus Dunn," *Molecules*, vol. 21, no. 10, 2017.

[13] F. Peng, H. Zhu, C. W. Meng, Y. R. Ren, O. Dai, and L. Xiong, "New isoflavanes from Spatholobus suberectus and their cytotoxicity against human breast cancer cell lines," *Molecules*, vol. 24, no. 18, 2017.

[14] R. N. Tang, X. B. Qu, S. H. Guan, P. P. Xu, Y. Y. Shi, and D. A. Guo, "Chemical constituents of *Spatholobus suberectus*," *Chinese Journal of Natural Medicines*, vol. 10, no. 1, pp. 32–35, 2012.

[15] H. J. Lim, M. N. Park, C. Kim et al., "MiR-657/ATF2 signaling pathway has a critical role in Spatholobus suberectus Dunn extract-induced apoptosis in U266 and U937 cells," *Cancers*, vol. 11, no. 2, p. 150, 2019.

[16] F. Peng, C. W. Meng, Q. M. Zhou, J. P. Chen, and L. Xiong, "Cytotoxic evaluation against breast Cancer cells of isoliquiritigenin analogues fromSpatholobus suberectusand their synthetic derivatives," *Journal of Natural Products*, vol. 79, no. 1, pp. 248–251, 2016.

[17] Z. Y. Wang, D. M. Wang, T. Y. Loo et al., "*Spatholobus suberectus* inhibits cancer cell growth by inducing apoptosis and arresting cell cycle at G2/M checkpoint," *Journal of Ethnopharmacology*, vol. 133, no. 2, pp. 751–758, 2011.

[18] Y. Fan, J. Liu, J. Miao et al., "Anti-inflammatory activity of the Tongmai Yangxin pill in the treatment of coronary heart disease is associated with estrogen receptor and NF-κB signaling pathway," *Journal of Ethnopharmacology*, vol. 276, 2021.

[19] F. Peng, L. Xiong, and C. Peng, "(-)-Sativan Inhibits Tumor Development and Regulates miR-200c/PD-L1 in Triple Negative Breast Cancer Cells," *Frontiers in Pharmacology*, vol. 11, p. 251, 2020.

[20] Z. Wang, D. Wang, S. Han et al., "Bioactivity-guided identification and cell signaling technology to delineate the lactate dehydrogenase A inhibition effects of Spatholobus suberectus on breast cancer," *PLoS One*, vol. 8, no. 2, article e56631, 2013.

[21] J.-Q. Sun, G.-L. Zhang, Y. Zhang et al., "Spatholobus suberectus Column Extract Inhibits Estrogen Receptor Positive Breast Cancer via Suppressing ER MAPK PI3K/AKT Pathway," *Evidence-Based Complementary and Alternative Medicine*, vol. 2016, Article ID 2934340, 13 pages, 2016.

[22] S. Elmore, "Apoptosis: a review of programmed cell death," *Toxicologic pathology*, vol. 35, no. 4, pp. 495–516, 2007.

[23] M. Umakoshi, S. Takahashi, G. Itoh et al., "Macrophage-mediated transfer of cancer-derived components to stromal cells contributes to establishment of a pro-tumor microenvironment," *Oncogene*, vol. 38, no. 12, pp. 2162–2176, 2019.

[24] J. Eitel, N. Suttorp, and B. Opitz, "Innate immune recognition and inflammasome activation in listeria monocytogenes infection," *Frontiers in Microbiology*, vol. 1, p. 149, 2019.

[25] E. A. Miao, I. A. Leaf, P. M. Treuting et al., "Caspase-1-induced pyroptosis is an innate immune effector mechanism against intracellular bacteria," *Nature Immunology*, vol. 11, no. 12, pp. 1136–1142, 2010.

[26] S. Nagata and M. Tanaka, "Programmed cell death and the immune system," *Nature Reviews Immunology*, vol. 17, no. 5, pp. 333–340, 2017.

[27] A. Malik and T. D. Kanneganti, "Inflammasome activation and assembly at a glance," *Journal of Cell Science*, vol. 130, no. 23, pp. 3955–3963, 2017.

[28] N. Gomez-Lopez, R. Romero, A. L. Tarca et al., "Gasdermin D: evidence of pyroptosis in spontaneous preterm labor with sterile intra-amniotic inflammation or intra-amniotic infection," *American Journal of Reproductive Immunology*, vol. 82, no. 6, article e13184, 2019.

[29] M. S. Swanson and A. B. Molofsky, "Autophagy and inflammatory cell death, partners of innate immunity," *Autophagy*, vol. 1, no. 3, pp. 174–176, 2005.

[30] B. Zhou, J. Y. Zhang, X. S. Liu et al., "Tom20 senses iron-activated ROS signaling to promote melanoma cell pyroptosis," *Cell Research*, vol. 28, no. 12, pp. 1171–1185, 2018.

[31] K. Ganesan and B. Xu, "Molecular targets of vitexin and isovitexin in cancer therapy: a critical review," *Annals of the New York Academy of Sciences*, vol. 1401, no. 1, pp. 102–113, 2017.

[32] K. Ganesan, K. Sukalingam, and B. Xu, "Impact of consumption of repeatedly heated cooking oils on the incidence of various cancers- A critical review," *Critical Reviews in Food Science and Nutrition*, vol. 59, no. 3, pp. 488–505, 2019.

[33] J. F. Teng, Q. B. Mei, X. G. Zhou et al., "Polyphyllin VI induces caspase-1-mediated pyroptosis via the induction of ROS/NF-κB/NLRP3/GSDMD signal axis in non-small cell lung cancer," *Cancers*, vol. 12, no. 1, p. 193, 2020.

[34] Y. Wang, W. Gao, X. Shi et al., "Chemotherapy drugs induce pyroptosis through caspase-3 cleavage of a gasdermin," *Nature*, vol. 547, no. 7661, pp. 99–103, 2017.

[35] C. Rogers, T. Fernandes-Alnemri, L. Mayes, D. Alnemri, G. Cingolani, and E. S. Alnemri, "Cleavage of DFNA5 by caspase-3 during apoptosis mediates progression to secondary necrotic/pyroptotic cell death," *Nature Communications*, vol. 8, no. 1, 2017.

[36] T. P. Monie, "The canonical inflammasome: a macromolecular complex driving inflammation," in *Macromolecular Protein Complexes*, J. Harris and J. Marles-Wright, Eds., vol. 83 of Subcellular Biochemistry, pp. 43–73, Springer, Cham, Switzerland, 2017.

[37] X. Liu, Z. Zhang, J. Ruan et al., "Inflammasome-activated gasdermin D causes pyroptosis by forming membrane pores," *Nature*, vol. 535, no. 7610, pp. 153–158, 2016.

[38] M. L. Elizagaray, M. T. R. Gomes, E. S. Guimaraes et al., "Canonical and non-canonical inflammasome activation by outer membrane vesicles derived from Bordetella pertussis," *Frontiers in Immunology*, vol. 11, 2020.

[39] Y. S. Yi, "Caspase-11 non-canonical inflammasome: a critical sensor of intracellular lipopolysaccharide in macrophage-mediated inflammatory responses," *Immunology*, vol. 152, no. 2, pp. 207–217, 2017.

[40] Y. S. Yi, "Regulatory roles of the caspase-11 non-canonical inflammasome in inflammatory diseases," *Immune Network*, vol. 18, no. 6, article e41, 2018.

[41] L. Vande Walle and M. Lamkanfi, "Pyroptosis," *Current Biology*, vol. 26, no. 13, pp. R568–R572, 2016.

[42] Y. Cheng, Y. Fu, Z. Wang, D. Yang, J. Chen, and D. Wang, "Determination on the contents of condensed tannins in Spatholobus suberectus Dunn. extracts and primary study on their anti-tumor activities," *Zhongshan Daxue Xuebao*, vol. 50, no. 2, p. 75, 2011.

[43] H. J. Kim, S. D. Cho, J. Kim et al., "Apoptotic effect of tolfenamic acid on MDA-MB-231 breast cancer cells and xenograft tumors," *Journal Of Clinical Biochemistry and Nutrition*, vol. 53, no. 1, pp. 21–26, 2013.

[44] M. K. You, M. S. Kim, K. S. Jeong, E. Kim, Y. J. Kim, and H. A. Kim, "Loquat (Eriobotrya japonica) leaf extract inhibits the growth of MDA-MB-231 tumors in nude mouse xenografts and invasion of MDA-MB-231 cells," *Nutrition Research and Practice*, vol. 10, no. 2, pp. 139–147, 2016.

[45] L. Kharchoufa, M. Bouhrim, N. Bencheikh et al., "Acute and subacute toxicity studies of the aqueous extract from Haloxylon scoparium Pomel (Hammada scoparia (Pomel)) by oral administration in rodents," *BioMed Research International*, vol. 2020, Article ID 4020647, 11 pages, 2020.

[46] B. Győrffy, A. Lanczky, A. C. Eklund et al., "An online survival analysis tool to rapidly assess the effect of 22,277 genes on breast cancer prognosis using microarray data of 1,809 patients," *Breast Cancer Research and Treatment*, vol. 123, no. 3, pp. 725–731, 2010.

[47] Á. Bartha and B. Győrffy, "TNMplot.com: a web tool for the comparison of gene expression in normal, tumor and metastatic tissues," *International journal of molecular sciences*, vol. 22, no. 5, article 2622, 2021.

[48] D. X. Wang, P. Liu, Y. H. Chen et al., "Stimulating effect of catechin, an active component of Spatholobus suberectus Dunn, on bioactivity of hematopoietic growth factor," *Chinese Medical Journal*, vol. 121, no. 8, pp. 752–755, 2008.

[49] J. Pang, J. P. Guo, M. Jin, Z. Q. Chen, X. W. Wang, and J. W. Li, "Antiviral effects of aqueous extract from Spatholobus suberectus Dunn. against coxsackievirus B3 in mice," *Chinese Journal of Integrative Medicine*, vol. 17, no. 10, pp. 764–769, 2011.

[50] H. Kim, S. S. Yi, H. K. Lee et al., "Antiproliferative Effect of Vine Stem Extract from Spatholobus Suberectus Dunn on Rat C6 Glioma Cells Through Regulation of ROS, Mitochondrial Depolarization, and P21 Protein Expression," *Nutrition and Cancer*, vol. 70, no. 4, pp. 605–619, 2018.

[51] R. Zhang, C. Liu, X. Liu, and Y. Guo, "Protective effect of *Spatholobus suberectus* on brain tissues in cerebral ischemia," *American Journal of Translational Research*, vol. 8, no. 9, pp. 3963–3969, 2016.

[52] P. Zhao, M. B. Alam, S. H. Lee et al., "Spatholobus suberectus exhibits antidiabetic activity in vitro and in vivo through activation of AKT-AMPK pathway," *Evidence-Based*

Complementary and Alternative Medicine, vol. 2017, Article ID 6091923, 12 pages, 2017.

[53] X. Z. Dong, Y. N. Wang, X. Tan, P. Liu, D. H. Guo, and C. Yan, "Protective effect of JXT ethanol extract on radiation-induced hematopoietic alteration and oxidative stress in the liver," *Oxidative Medicine and Cellular Longevity*, vol. 2018, Article ID 9017835, 12 pages, 2018.

[54] Y. Lee, "Cancer chemopreventive potential of procyanidin," *Toxicological Research*, vol. 33, no. 4, pp. 273–282, 2017.

[55] K. Ganesan and B. Xu, "Polyphenol-rich lentils and their health promoting effects," *International Journal of Molecular Sciences*, vol. 18, no. 11, p. 2390, 2017.

[56] K. Ganesan and B. Xu, "Polyphenol-rich dry common beans (*Phaseolus vulgaris* L.) and their health benefits," *International Journal of Molecular Sciences*, vol. 18, no. 11, p. 2331, 2017.

[57] K. Ganesan and B. Xu, "A critical review on polyphenols and health benefits of black soybeans," *Nutrients*, vol. 9, no. 5, p. 455, 2017.

[58] K. Ganesan, M. Jayachandran, and B. Xu, "Diet-derived phytochemicals targeting colon cancer stem cells and microbiota in colorectal cancer," *International Journal of Molecular Sciences*, vol. 21, no. 11, p. 3976, 2020.

[59] K. Ganesan and B. Xu, "Telomerase inhibitors from natural products and their anticancer potential," *International Journal of Molecular Sciences*, vol. 19, no. 1, p. 13, 2018.

[60] H. Hong, H. Wu, J. Chen et al., "Cytotoxicity induced by iodinated haloacetamides via ROS accumulation and apoptosis in HepG-2 cells," *Environmental Pollution*, vol. 242, Part A, pp. 191–197, 2018.

[61] D. F. Xue, S. T. Pan, G. Huang, and J. X. Qiu, "ROS enhances the cytotoxicity of cisplatin by inducing apoptosis and autophagy in tongue squamous cell carcinoma cells," *The International Journal of Biochemistry & Cell Biology*, vol. 122, article 105732, 2020.

[62] Y. Sun, Q.-M. Zhou, Y.-Y. Lu et al., "Resveratrol inhibits the migration and metastasis of MDA-MB-231 human breast cancer by reversing TGF-β1-induced epithelial-mesenchymal transition," *Molecules*, vol. 24, no. 6, article 1131, 2019.

[63] D. Sinha, N. Sarkar, J. Biswas, and A. Bishayee, "Resveratrol for breast cancer prevention and therapy: Preclinical evidence and molecular mechanisms," *Seminars in Cancer Biology*, vol. 40-41, pp. 209–232, 2016.

[64] J. Shi, Y. Zhao, K. Wang et al., "Cleavage of GSDMD by inflammatory caspases determines pyroptotic cell death," *Nature*, vol. 526, no. 7575, pp. 660–665, 2015.

[65] N. Kayagaki, I. B. Stowe, B. L. Lee et al., "Caspase-11 cleaves gasdermin D for non-canonical inflammasome signalling," *Nature*, vol. 526, no. 7575, pp. 666–671, 2015.

[66] W. T. He, H. Wan, L. Hu et al., "Gasdermin D is an executor of pyroptosis and required for interleukin-1β secretion," *Cell Research*, vol. 25, no. 12, pp. 1285–1298, 2015.

[67] J. Ding, K. Wang, W. Liu et al., "Pore-forming activity and structural autoinhibition of the gasdermin family," *Nature*, vol. 535, no. 7610, pp. 111–116, 2016.

[68] T. Yumnamcha, T. S. Devi, and L. P. Singh, "Auranofin mediates mitochondrial dysregulation and inflammatory cell death in human retinal pigment epithelial cells: implications of retinal neurodegenerative diseases," *Frontiers in Neuroscience*, vol. 13, article 1065, 2019.

[69] S. Matikainen, T. A. Nyman, and W. Cypryk, "Function and regulation of noncanonical caspase-4/5/11 inflammasome," *The Journal of Immunology*, vol. 204, no. 12, pp. 3063–3069, 2020.

[70] Y. H. Soung, E. G. Jeong, C. H. Ahn et al., "Mutational analysis of *caspase 1*, *4*, and *5* genes in common human cancers," *Human Pathology*, vol. 39, no. 6, pp. 895–900, 2008.

[71] R. A. Aglietti, A. Estevez, A. Gupta et al., "GsdmD p30 elicited by caspase-11 during pyroptosis forms pores in membranes," *Proceedings of the National Academy of Sciences of the United States*, vol. 113, no. 28, pp. 7858–7863, 2016.

[72] N. Kayagaki, S. Warming, M. Lamkanfi et al., "Non-canonical inflammasome activation targets caspase-11," *Nature*, vol. 479, no. 7371, pp. 117–121, 2011.

[73] J. Hou, R. Zhao, W. Xia et al., "PD-L1-mediated gasdermin C expression switches apoptosis to pyroptosis in cancer cells and facilitates tumour necrosis," *Nature Cell Biology*, vol. 22, no. 10, pp. 1264–1275, 2020.

[74] S. I. Grivennikov, F. R. Greten, and M. Karin, "Immunity, inflammation, and cancer," *Cell*, vol. 140, no. 6, pp. 883–899, 2010.

[75] J. Vakkila and M. T. Lotze, "Inflammation and necrosis promote tumour growth," *Nature Reviews Immunology*,, vol. 4, no. 8, pp. 641–648, 2004.

[76] C.-C. Sun, S.-J. Li, W. Hu et al., "Comprehensive analysis of the expression and prognosis for E2Fs in human breast cancer," *Molecular Therapy*, vol. 27, no. 6, pp. 1153–1165, 2019.

[77] A. Alshamsan, S. Khan, A. Imran, I. A. Aljuffali, and K. Alsaleh, "Prediction of *Chlamydia pneumoniae* protein localization in host mitochondria and cytoplasm and possible involvements in lung cancer etiology: a computational approach," *Saudi Pharmaceutical Journal*, vol. 25, no. 8, pp. 1151–1157, 2017.

[78] J. Zhou, X. Hui, Y. Mao, and L. Fan, "Identification of novel genes associated with a poor prognosis in pancreatic ductal adenocarcinoma via a bioinformatics analysis," *Bioscience Reports*, vol. 39, no. 8, 2019.

[79] J. Park, G. H. Kim, J. Lee et al., "MST2 silencing induces apoptosis and inhibits tumor growth for estrogen receptor alpha-positive MCF-7 breast cancer," *Toxicology and Applied Pharmacology*, vol. 408, article 115257, 2020.

[80] Z. Wang, F. Ni, F. Yu, Z. Cui, X. Zhu, and J. Chen, "Prognostic significance of mRNA expression of CASPs in gastric cancer," *Oncology Letters*, vol. 18, no. 5, pp. 4535–4554, 2019.

[81] J. Kumar, V. Murugaiah, G. Sotiriadis et al., "Surfactant protein D as a potential biomarker and therapeutic target in ovarian cancer," *Frontiers in Oncology*, vol. 9, p. 542, 2019.

[82] C. Zhao, Y. Zhou, Q. Ran et al., "MicroRNA-381-3p functions as a dual suppressor of apoptosis and Necroptosis and promotes proliferation of renal cancer cells," *Frontiers in Cell and Developmental Biology*, vol. 8, p. 290, 2020.

Research Article

Roles of *Suaeda vermiculata* Aqueous-Ethanolic Extract, Its Subsequent Fractions, and the Isolated Compounds in Hepatoprotection against Paracetamol-Induced Toxicity as Compared to Silymarin

Salman A. A. Mohammed [ORCID],[1] Hussein M. Ali,[1,2] Hamdoon A. Mohammed [ORCID],[3,4] Mohsen S. Al-Omar,[3,5] Suliman A. Almahmoud,[3] Mahmoud Z. El-Readi,[6,7] Ehab A. Ragab,[4] Ghassan M. Sulaiman [ORCID],[8] Mohamed S. A. Aly,[9] and Riaz A. Khan [ORCID][3]

[1]*Department of Pharmacology and Toxicology, College of Pharmacy, Qassim University, Qassim 51452, Saudi Arabia*
[2]*Department of Biochemistry, Faculty of Medicine, Al-Azhar University, Assiut 71524, Egypt*
[3]*Department of Medicinal Chemistry and Pharmacognosy, College of Pharmacy, Qassim University, Qassim 51452, Saudi Arabia*
[4]*Department of Pharmacognosy, Faculty of Pharmacy, Al-Azhar University, Cairo 11371, Egypt*
[5]*Department of Medicinal Chemistry and Pharmacognosy, Faculty of Pharmacy, JUST, Irbid 22110, Jordan*
[6]*Department of Clinical Biochemistry, Faculty of Medicine, Umm Al-Qura University, Makkah 21955, Saudi Arabia*
[7]*Department of Biochemistry, Faculty of Pharmacy, Al-Azhar University, Assiut 71524, Egypt*
[8]*Division of Biotechnology, Department of Applied Sciences, University of Technology, Baghdad 10066, Iraq*
[9]*Hospital of the Police Academy, Nasr City, Cairo 11765, Egypt*

Correspondence should be addressed to Hamdoon A. Mohammed; ham.mohammed@qu.edu.sa
and Riaz A. Khan; ri.khan@qu.edu.sa

Suaeda vermiculata, a halophyte consumed by livestock, is also used by Bedouins to manage liver disorders. The aqueous-ethanolic extract of *S. vermiculata*, its subsequent fractions, and pure compounds, *i.e.*, pheophytin-A (1), isorhamnetin-3-*O*-rutinoside (2), and quercetin (3), were evaluated for their hepatoprotective efficacy. The male mice were daily fed with either silymarin, plant aq.-ethanolic extract, fractions, pure isolated compounds, or carboxyl methylcellulose (CMC) for 7 days ($n = 6$/group, *p.o.*). On the day 7th of the administrations, all, except the intact animal groups, were induced with hepatotoxicity using paracetamol (PCM, 300 mg/kg). The anesthetized animals were euthanized after 24 h; blood and liver tissues were collected and analysed. The serum aspartate transaminase (AST) and alanine transaminase (ALT) levels decreased significantly for all the *S. vermiculata* aq.-ethanolic extract, fraction, and compound-treated groups when equated with the PCM group ($p < 0.0001$). The antioxidant, superoxide dismutase (SOD), increased significantly ($p < 0.05$) for the silymarin-, *n*-hexane-, and quercetin-fed groups. Similarly, the catalase (CAT) enzyme level significantly increased for all the groups, except for the compound 2-treated group as compared to the CMC group. Also, the glutathione reductase (GR) levels were significantly increased for the *n*-butanol treated group than for the PCM group. The oxidative stress biomarkers, lipid peroxide (LP) and nitric oxide (NO), the inflammatory markers, IL-6 and TNF-*α*, and the kidney's functional biomarker parameters remained unchanged and did not differ significantly for the treated groups in comparison to the PCM-induced toxicity bearing animals. All the treated groups demonstrated significant decreases in cholesterol levels as compared to the PCM group, indicating hepatoprotective and antioxidant effects. The quercetin-treated group demonstrated significant improvement in triglyceride level. The *S. vermiculata* aq.-ethanolic extract, fractions, and the isolated compounds demonstrated their hepatoprotective and antioxidant effects, confirming the claimed traditional use of the herb as a liver protectant.

1. Introduction

Liver disorders inflict people on a larger scale, and millions suffer worldwide. Various indigenous systems of medicine recommend a plethora of herbs and other botanical-based medicaments for treating various types of liver disorders. Several symptomatic and clinical indications are related to malfunctioning of the liver, which generally are grouped as nonalcoholic liver disorders. Primarily, oxidative stress, hepatic inflammation, and liver steatosis are considered prime causes [1]. Synthetic products, herbs, and herbal admixtures with strong antioxidant activity have been shown to reduce the sufferings and symptoms thereby exerting hepatoprotective activity [2]. However, clear-cut pieces of evidence for the hepatoprotection efficacy of the majority of the herbs are seldom and sparse.

Nonetheless, the liver protective-activity-established herbs and natural products including silymarin, glycyrrhizin, and other plant-based products have been effectively utilized as herbal concoctions and drinks [3]. The need for the bioactivity confirmation, dose, and administering frequency standardizations, together with investigations of any predictive and speculative side-effects owing to the herbs' quality, dose, administration frequency, and mechanism of action are imperative. Consequent to the exponential increments in the use of complementary and alternative medicines, especially the herbals, also among the patients with liver disorders [4], the bioactivity standardization and safety evaluation exercises of the frequently used formulations are needed to be accelerated and well-established. In this regard, animal model-based studies have shown anti-inflammatory and antioxidation-based positive effects on the liver [5] which contributes to the improvement in the liver's functioning. The investigations of liver biochemistry of the oxidative, antilipid-peroxidative, and inflammatory marker manifestations in the hepatic tissue have been widely used as a comparative standard for confirming proper/normal functioning of the liver [6]. The toxicity controls and prevention and the botanicals and other herbal-related liver toxicity generation products' investigational studies play an important part in finding safe uses of the plant-based products [7]. Objectively defined bioactivity testing endpoints defined by the standardized parametric levels of biomarkers and other biochemical, physiological, and histological observations for the standardized herbal extracts and isolated pure compounds are indispensable to verify the hepatoprotective actions of the traditional herbal medicament with ample confidence. Definitive histopathological evidence as liver's functional and biologic improvements is a step further towards activity levels and toxicological safety determinations of the products. Mechanistically, the stimulated uptake of glucose reduced serum triglycerides and hepatic cholesterol increased mitochondrial activity and ATP production, along with the reduced catabolic reactions, leading to cholesterol, bile acids, and plasma membrane's lipid level reductions, as well as the compromised immunomodulation, have been part of the primary indicators in hepatoprotective investigations milieu [8].

The halophytic herb, *Suaeda vermiculata* Forssk, a member of the plant family Amaranthaceae, grows in central Saudi Arabia and other Mediterranean regions. The plant belongs to the desert halophyte category and is used by nomads as a liver-protecting agent [9–11]. Antimicrobial, antioxidant, and cytotoxic activities of *S. vermiculata* extract, fractions, and their isolated compounds are reported. The major porphyrin-class product of the plant, pheophytin-A, has been isolated and evaluated for its antioxidant and cytotoxic effects [9, 12–14].

Recently, dose-dependent hepatoprotective action of *S. vermiculata* aqueous- (aq.-) ethanolic extract in the carbon tetrachloride- (CCl_4-) induced hepatotoxicity using rat models was demonstrated by us [14]. For the current study, the prophylactic action of the *S. vermiculata* aq.-ethanolic extract, its fractions, and isolated compounds on the paracetamol- (PCM-) induced liver toxicity in mice is investigated. The major constituents of the *n*-butanol (*n*-BuOH), ethyl acetate (EtOAc), and chloroform ($CHCl_3$) fractions were isolated-purified, characterized, and bioactivity evaluated. Paracetamol (PCM), also known as acetaminophen, a widely used nonprescription analgesic and antipyretic drug, that does not demonstrate liver toxicity at therapeutic doses but at elevated doses causes hepatic and renal toxicity in humans and experimental animals. PCM was used experimentally to induce liver toxicity in animal models during the current study [15]. The PCM toxicity is responsible for 50% of the acute liver failure cases in western countries [16]. A single (over) dose of PCM is known to rapidly induce hepatotoxicity [17–19] in mice, which is biomechanistically similar to the effects in humans, and is regarded clinically as a robust model [20]. Hence, mice were the preferred model compared to rats which were highly resistant to PCM-induced hepatotoxicity [18]. In this context, the current study sets out to confirm the traditionally claimed hepatoprotective activity of the plant-based tea, decoctions, and other crude formulations on the PCM-induced liver toxicity in the animal models. The current study also evaluated the safety of the plant materials' uses at usually the higher doses as practiced by the herbalists, including Bedouins and the locals. The plant, *S. vermiculata*, extract's effects on the kidneys, liver, blood sugar, and lipid levels in addition to the antioxidant and anti-inflammation actions in the PCM-induced toxicity-bearing animal models were investigated. During our previous study [14], only aq.-ethanolic extract's activity was evaluated in the CCl_4-induced hepatotoxic conditions using rat models, while the current study investigates the PCM-induced hepatotoxicity protection by the aq.-ethanolic and its subsequent fractions, *i.e.*, *n*-hexane, chloroform, ethyl acetate, and *n*-butanol, together with the compounds isolated from these fractions. The study demonstrated the hepatoprotective efficacy of these isolated compounds, *i.e.*, pheophytin-A, quercetin, and isorhamnetin-3-*O*-rutinoside, from $CHCl_3$, EtOAc, and *n*-BuOH fractions of the plant, respectively. In addition to the liver biomarkers, antioxidants, superoxide dismutase (SOD), catalase (CAT), and glutathione reductase (GR), as well as oxidative stress markers, *i.e.*, lipid peroxide (LP) and nitric oxide (NO), and inflammatory biomarkers (*i.e.*, IL6 and TNF-α levels), were also investigated in *in vivo* experimental conditions.

2. Materials and Methods

2.1. Chemicals and Reagents. All chemicals were of analytical grade. Methanol (HPLC grade) and formic acid were purchased from Sigma-Aldrich, USA. Pure paracetamol was obtained from Dr. Amin Dervish, Department of Pharmaceutics, College of Pharmacy, Qassim University, Kingdom of Saudi Arabia; locally available silymarin tablets (Micro Labs Limited, Mumbai, India) were used as obtained.

2.2. Plant Materials, Extraction, Fractionation, and Column Chromatographic Separations of the Major Constituents. The plants' whole herbs were collected in October 2019 from Buraydah, Qassim, KSA, and identified by Prof. Dr. Ahmed El-Oglah, Department of Biological Sciences, Yarmouk University, Irbid, Jordan. The plant material was compared to the authentic sample available in the herbarium of the College of Pharmacy, Qassim University, under the herbarium deposit # 78. The plant material (1.5 kg) was dried in shade and grinded to a coarse powder, which was exhaustively extracted three times with 70% aqueous-ethanol ($3 L \times 3$) using the cold maceration technique under stirring for 24 h for each cycle. The hydroalcoholic extract was filtered and evaporated to dryness under reduced pressure at a temperature < 40°C, yielding 86.3 g of the dried extract. Approximately, 50 g of the dried extract was suspended in 1 L of distilled water and fractionated between *n*-hexane, CHCl$_3$, EtOAc, and *n*-BuOH, in sequence, which resulted in 6.5 g, 4.5 g, 7 g, and 11 g of *n*-hexane, CHCl$_3$, EtOAc, and *n*-BuOH fractions, respectively. About 1.0 g of the CHCl$_3$ fraction was chromatographed over Sigel column chromatography (Sigel CC) eluted with *n*-hexane : ethyl acetate (100 : 0 to 70 : 30) to give five subfractions of A to E. Subfraction A (250 mg) was further purified on sephadex LH-20 using methanol as eluent to give compound 1 (120 mg). About 2.0 g of the *n*-BuOH fraction was subjected to Sigel CC using CHCl$_3$: MeOH (90 : 10 to 60 : 40) as eluent to give three major fractions A, B, and C. Fraction B (780 mg) was subjected to sephadex LH-20 gel filtration chromatography, followed by Sigel CC to give seven fractions (BA-BG). Fraction BD (300 mg) was subjected to RP-C$_{18}$ CC (Starta® C$_{18}$-E50g/150 ml, Giga, USA) eluted with 40-80% methanol, followed by preparative TLC (CHCl$_3$: MeOH : H$_2$O (80 : 20 : 2)) to yield compound 2 (170 mg) as a yellow amorphous powder. A part of the EtOAc fraction (2.0 g) was subjected to several Sigel CC and sephadex LH-20 filtration to yield compound 3 (135 mg) (Scheme 1, Supplementary file). The isolated compounds were subjected to ^{1}H and ^{13}C-NMR and HR-MS spectroscopic analyses to confirm their identities (Spectral data available in the Supplementary file).

2.3. Acute Toxicity Studies and Sample Size. Acute toxicity was performed according to the OECD guidelines [21, 22]. In brief, 12-weeks-old male mice ($n = 25$), weighing 20 ± 5 g and overnight fasted, were randomly given single 4 g/kg dose of either aq.-ethanol extract, or *n*-hexane, CHCl$_3$, EtOAc, and *n*-BuOH fractions ($n = 5$/group) through oral (*p.o.*) route. Mice were monitored for abnormal conduct and movements during the first three days while any deaths were

followed up to 2 weeks [22]. The experiments' required sample size was established by the mean ± SEM and AST values of the PCM-induced hepatotoxic and PCM-induced hepatotoxicity-treated animal groups, as reported earlier [23]. A two-tail option provided effect size *d* as 4.27 on G Power V.3.1.9.4 software [24], while to obtain the statistical power (1-β err prob) of 80% and a specific α error probability of 0.05, the least animal size per group was $n > 3$.

2.4. Experimental Animal Groups. The study was conducted as per the Animal Research: Reporting *In vivo* Experiments (ARRIVE) statement [25].

2.4.1. Hepatoprotective Effect of S. vermiculata Aqueous-Ethanolic Extract, Fractions, and Isolated Compounds in PCM-Induced Liver Toxicity. Male, 8-weeks-old, naïve C57BL/6 mice ($n = 66$), weighing 20 ± 5 g, were obtained from the animal house facility, College of Pharmacy, Qassim University, Saudi Arabia, with 3 mice/cage, one week before the beginning of the animal studies. The animals were maintained at 25°C with a relative humidity of ~65%. The institutional Research Ethics Committee approved the experimental procedure and the animal care (Approval ID 2019-CP-8), as per the Guidelines for the Care and Use of Laboratory Animals. Mice were distributed at random into nine groups ($n = 6$/group). The intact mice (group I) was not treated, while the other mouse groups received *p.o.* once daily with 0.5% carboxyl methylcellulose (CMC, negative control, group II), 100 mg/kg silymarin (positive control, group III), 100 mg/kg pheophytin-A (group IV), 100 mg/kg isorhamnetin-3-*O*-rutinoside (group V), 100 mg/kg quercetin (group VI), or 400 mg/kg aq.-ethanolic extract, 400 mg/kg *n*-butanol fraction, 400 mg/kg ethyl acetate fraction, 400 mg/kg chloroform fraction, and 400 mg/kg *n*-hexane fraction (groups VII-XI), for 7 days, followed by the induction of hepatotoxicity in the overnight fasted animals [26] using single intraperitoneal (*i.p.*) dose of the PCM (300 mg/kg) [17–19, 26] that was dissolved in warm normal saline (i). Twenty-four hours after PCM administration, blood [27] and tissue samples were collected from the sacrificed animals [17, 28].

Percentage hepatotoxic protection was determined using the formula below [29]:

$$\text{Hepatoprotection\%} = \left[\frac{a - b}{a - c}\right] \times 100, \quad (1)$$

where *a*, *b*, and *c* are the mean ± SEM of hepatotoxin, toxin treated with the tested sample, and control, respectively.

The liver tissues were homogenized, and the supernatant was obtained for measuring oxidant, antioxidant, and inflammatory markers.

2.5. Estimation of Serum Levels of AST, ALT, TP, and Creatinine. The concentration of ALT, AST, TP, and creatinine (Crescent Diagnostics, KSA; #CZ902L for ALT, #CZ904L for AST, and # 604 for creatinine) in plasma samples was estimated as described earlier [14].

2.6. Determination of Serum Levels of Glucose, Cholesterol, and Triglycerides. Glucose, cholesterol, and triglyceride levels

(Crescent Diagnostics Company; #605, #603, and #611) were measured according to the method described earlier [14].

2.7. Determination of Oxidants and Antioxidant Levels. The CAT enzymatic activity was assayed in serum by the colorimetric method wherein the catalase reacted with the known amount of excess hydrogen peroxide. The remaining hydrogen peroxide reacts with 3,5-dichloro-2-hydroxybenzene sulfonic acid and 4-aminophenazone forming a chromophore that gave color at 520 nm [30]. The SOD levels in the liver tissue were assayed also using a colorimetric method which depended upon the enzyme's potency in inhibiting the phenazine methosulfate-mediated reduction of the nitro blue tetrazolium dye. The absorbances were measured at 560 nm for 5 minutes for control and tissue samples [31]. The GR was assayed in liver-tissue samples by another colorimetric method based on reducing the dithio-bis-2-nitrobenzene acid with reduced glutathione, producing a yellow color that was checked at 405 nm [32]. Lipid peroxide (malondialdehyde) levels were determined in serum samples by the colorimetric method, where the reaction between the malondialdehyde and thiobarbituric acid under acidic conditions at 95°C for 30 minutes produced thiobarbituric acid-based pink products, which were assayed at 534 nm [33]. Serum NO was also measured by colorimetric determination that represented one of the final products of the NO *in vivo* conditions, in addition to the nitrate. The addition of Griess reagents converted nitrite into a deep purple azo compound that was measured at 540 nm [34]. All the oxidant and antioxidant reagents were provided by the Biodiagnostic Company, Cairo, Egypt.

2.8. Determination of Interleukin 6 (IL6) and Tumor Necrosis Factor-Alpha (TNF-α). IL6 and TNF-α were assayed in liver tissue homogenates by ELISA (enzyme-linked immunosorbent assay) kits (Cloud Clone Corp Company, USA). The microplate's measurements were at 450 nm (Microplate Reader, BioTek Instruments, Inc., Winooski, VT, USA).

2.9. Statistical Analysis. Data are represented as the mean ± standard error of the mean (SEM). Two-way ANOVA followed by a post hoc Tukey multigroup comparison assessed variations among the groups, and $p < 0.05$ was considered significant on GraphPad Prism 8.0.2. [35]. Normality of the data was obtained using the Kolmogorov–Smirnov test.

3. Results and Discussion

3.1. Isolation and Structure Elucidation of Major Constituents. The whole plant, *S. vermiculata*, was used for aq.-ethanolic extraction, followed by further fractionations of the aq.-ethanolic extract into different solvent-based fractions. The major constituents were isolated by repetitive column chromatographic (CC) purification techniques involving silica gel-based normal, and reverse-phase (RP) silica gel-based CCs, preparative TLC (Thin Layer Chromatography), and finally gel filtration (Sephadex LH-20) techniques. The compounds, pheophytin-A (1), isorhamnetin-3-O-rutinoside (2), and quercetin (3), isolated from various fractions, were fully characterized by their ^{1}H and ^{13}C NMR spectral data and the HR-

MS analyses and their comparison with the reported values. The isolation and characterization of compound 1, pheophytin-A, followed the previously reported method [9]. Compound 2 was isolated in a pure form as yellow amorphous powder from the *n*-BuOH fraction. The ^{1}H NMR spectrum of compound 2 showed the proton signal pattern for the C3-glycosylated flavonols by exhibiting two single protons at δ_H 6.21 and 6.41 assigned for the C6 and C8 protons of the flavonol structure, respectively. The ABX system of protons resonating at δ_H 7.95 (br s), δ_H 7.64 (d, J =8.5 Hz), and δ_H 6.94 (dd, J = 2.0 and 8.5 Hz) showed their presence at C2′, C5′, and C6′, respectively. The ^{1}H NMR spectrum also exhibited two proton doublets at δ_H 5.22 (J = 7.2 Hz) and δ_H 4.54 (J = 1.5 Hz), assigned to the glucose and rhamnose anomeric protons, respectively. The ^{13}C NMR spectrum of compound 2 resembled the carbon signal pattern of the glycosylated flavonol based upon comparison with literature data. In addition, HR-MS analyses of compound 2 showed a molecular ion peak (M$^{+·}$) as [M-H]$^-$ at *m/z* 623.16113 ($C_{28}H_{32}O_{16}$); therefore, the compound was identified as a flavonol glycoside; isorhamnetin-3-*O*-rutinoside (2) [36, 37]. Compound (3) was isolated from the EtOAc fraction as a yellowish powder. The ^{1}H and ^{13}C NMR spectral data were typically identical to the reported values for quercetin [38]. HR-MS analysis confirmed the compound's identity, which showed the molecular ion peak at *m/z* 303.04924 [M+H]$^+$, compatible with the molecular formula of quercetin. The presence of compounds 1-3 (Figure 1) has been confirmed by the previous LC-MS analysis of the *S. vermiculata* aq.-ethanolic extract. The relatively higher occurrences of these compounds (1, 2, and 3) as confirmed by the LC-MS in the aq.-ethanolic extract were at 23.69, 4.37, and 12.45%, respectively [14].

3.2. Acute Toxicity and Dose Selection. Among all the animal groups, 2 EtOAc and 1 *n*-hexane fraction-fed mice died on days 2 and 3 of the dose administrations, respectively, during oral drug administrations. The acute toxicity results conducted for 2 weeks were similar to the previously reported [14]. The results indicated safety at the administered dose. Corresponding to Hedge and Sterner scale, 10% (400 mg/kg) of the given dose was chosen for further experiments [39].

3.3. Hepatoprotective Activity of the S. vermiculata Aqueous-Ethanolic Extract, Fractions, and Isolated Compounds. For the hepatoprotective experiments, the AST and ALT biomarkers, the negative control group was significantly elevated ($p < 0.0001$) compared to the intact group (Table 1). The increased ALT and AST enzymatic levels were attributed to hepatic cell damage and necrosis due to the liver toxicity induced by the PCM, as also reported in previous studies. Also, the PCM toxicity led to reactive oxygen species (ROS) and LP releases causing oxidative stress [40, 41]. All the *S. vermiculata* aq.-ethanolic extract and fraction-fed groups showed a significant decrease in both the ALT and AST enzymatic activities as compared with the PCM alone group. Similarly, the isolated compounds; pheophytin-A, isorhamnetin-3-*O*-rutinoside, and quercetin fed-groups demonstrated significant reductions in ALT and AST levels than
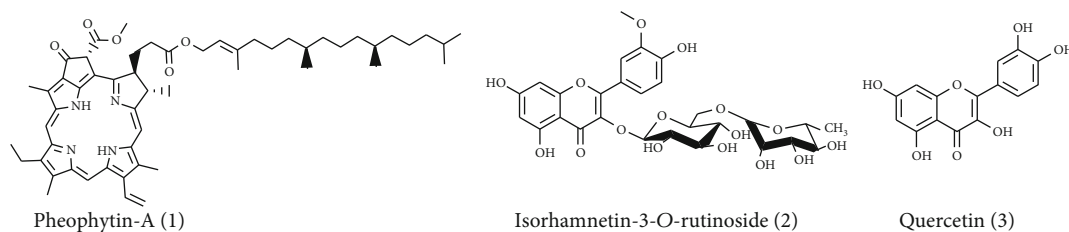
Figure 1: Chemical structures of the isolated compounds [1–3].

Table 1: Effects of S. vermiculata aq.-ethanolic extract, fractions, and isolated compounds on liver functions of the PCM-induced liver toxicity in the experimental mice*.

Animal groups	AST IU/L	ALT IU/L	TP g/dL
I. Intact control (no CMC, no extract/no fractions, no PCM)	64.11 ± 2.59^{C}	55.53 ± 11.82^{B}	5.07 ± 0.68^{A}
II. Negative control (vehicle CMC 0.5%)+PCM	293.05 ± 52.28^{A}	407.05 ± 105.06^{A}	4.96 ± 0.19^{A}
III. Silymarin 100 mg/kg+PCM	$108.26 \pm 10.40^{B,C}$	39.14 ± 7.44^{B}	5.08 ± 0.40^{A}
IV. Pheophytin-A 100 mg/kg+PCM	$133.28 \pm 7.66^{B,C}$	77.44 ± 15.73^{B}	4.99 ± 0.26^{A}
V. Isorhamnetin-3-O-rutinoside 100 mg/kg+PCM	112.54 ± 14.51^{BC}	40.75 ± 4.49^{B}	5.20 ± 0.35^{A}
VI. Quercetin 100 mg/kg+PCM	$129.44 \pm 4.15^{B,C}$	76.09 ± 13.41^{B}	5.70 ± 0.21^{A}
VII. Aqueous-ethanolic extract 400 mg/kg+PCM	$131.19 \pm 8.90^{B,C}$	49.61 ± 5.64^{B}	6.76 ± 1.18^{A}
VIII. n-Butanol fraction 400 mg/kg+PCM	138.27 ± 4.58^{C}	84.88 ± 3.59^{B}	5.00 ± 0.76^{A}
IX. Ethyl acetate fraction 400 mg/kg+PCM	$119.63 \pm 7.35^{B,C}$	60.10 ± 4.15^{B}	5.72 ± 0.60^{A}
X. Chloroform fraction 400 mg/kg+PCM	$107.50 \pm 13.56^{B,C}$	44.35 ± 2.71^{B}	4.93 ± 0.30^{A}
X1. n-Hexane fraction 400 mg/kg+PCM	164.52 ± 7.95^{B}	66.29 ± 10.96^{B}	4.30 ± 0.32^{A}

*Values denoted are the mean ± SEM. AST: aspartate transaminase; ALT: alanine transaminase; TP: total protein; CMC: carboxyl methylcellulose; PCM: paracetamol. Mean ± SEM not sharing the letters (A–C) in the respective column (AST, ALT, and TP) are significantly different ($p < 0.0001$). Raw data is available in the Supplementary file (Table S1).

the PCM-fed group demonstrated significant reductions in ALT and AST levels than the PCM-fed group. The administrations of these materials demonstrated hepatoprotective effects as indicated by the improvements in liver functions, and a significant decrease ($p < 0.05$) in liver-enzyme activities, as compared to the PCM-fed injury group, was observed. The protective effects of the aq.-ethanolic extract and fractions may be attributed to their antioxidative as well as anti-inflammatory effects. The renal biomarkers, i.e., urea, and creatinine levels remained unchanged. The TP (total proteins), creatinine, and glucose level values also remained nearly unchanged in S. vermiculata aq.-ethanolic extract and fraction-fed groups or the isolated compounds, i.e., pheophytin-A (1), isorhamnetin-3-O-rutinoside (2), and quercetin (3), in comparison to the negative group, as competitively maintained near the referral standard product, silymarin, a well-known liver-protecting natural product (Tables 1 and 2).

The PCM-fed group demonstrated significantly increased cholesterol and decreased triglyceride levels as compared with the intact group. The PCM toxicity caused oxidative stress and lipid peroxidation, leading to increased cholesterol levels. These results are in conformity with the previously reported study [42]. All the treated groups demonstrated decreased cholesterol levels than the PCM-induced toxic animal group, thereby indicating the hepatoprotective and antioxidative effects of the plant materials.

The quercetin-treated group demonstrated significant improvement in triglyceride level compared to the PCM-fed group. The silymarin, aq.-ethanolic extract, and the isorhamnetin-3-O-rutinoside groups also demonstrated improvements in triglyceride levels, but these were not significant. The improvements in lipid profile in the quercetin-treated group were attributed to its hepatoprotective and antioxidant effects, as also mentioned by a similar study reported earlier [43].

The total hepatoprotective percentage for the liver markers was also determined. The PCM-induced negative control animals' group (CMC (carboxyl methylcellulose)) was considered at 0% protection, while the intact group was considered to have 100% hepatoprotection. The hepatoprotection percentage was observed by measuring various biomarkers according to their maintained levels and compared with the controls (Figure 2). There is maintenance of the percent levels of the biomarkers in the aq.-ethanolic extract, fractions, and the isolated product-fed groups, as compared to the referral standard, silymarin. It confirmed the hepatoprotective properties of the aq.-ethanolic extract, fractions, and isolated products of the plant, S. vermiculata, which is in full consonant with the traditionally claimed hepatoprotective effects of the plant, including from the previous study that demonstrated the hepatoprotection using S. vermiculata ethanolic extract in CCl_4-induced liver injury models [14].

TABLE 2: Effects of *S. vermiculata* aq.-ethanolic extract, fractions, and isolated compounds on kidney functions, blood glucose, triglycerides, and cholesterol of the PCM-induced liver toxicity in mice*.

Animal groups	Creatinine mg/dL	Urea mg/dL	Glucose mg/dL	Cholesterol mg/dL	Triglycerides mg/dL
I. Intact control (no CMC, no extract/no fractions, no PCM)	0.62 ± 0.03^B	48.83 ± 2.47^{BC}	61.53 ± 5.25^B	106.30 ± 7.65^B	101.63 ± 19.62^A
II. Negative control (vehicle CMC 0.5%)+PCM	$0.67 \pm 0.03^{A,B}$	$55.01 \pm 2.31^{A,B,C}$	$67.26 \pm 4.55^{A,B}$	148.44 ± 13.23^A	$55.14 \pm 6.41^{B,C,D}$
III. Silymarin 100 mg/kg+PCM	$0.86 \pm 0.07^{A,B}$	$85.39 \pm 17.38^{A,B}$	$44.27 \pm 3.56^{A,B}$	$93.50 \pm 3.97^{B,C}$	$79.98 \pm 18.75^{A,B,C,D}$
IV. Pheophytin-A 100 mg/kg+PCM	$0.78 \pm 0.02^{A,B}$	92.73 ± 19.39^A	50.24 ± 5.29^B	$90.80 \pm 6.31^{B,C}$	$54.52 \pm 3.64^{B,C,D}$
V. Isorhamnetin-3-*O*-rutinoside 100 mg/kg+PCM	$0.86 \pm 0.03^{A,B}$	$52.46 \pm 1.56^{A,B,C}$	$62.56 \pm 7.10^{A,B}$	$88.35 \pm 3.30^{B,C}$	$94.01 \pm 11.75^{A,B,C}$
VI. Quercetin 100 mg/kg+PCM	$0.84 \pm 0.06^{A,B}$	$51.57 \pm 1.60^{A,B,C}$	$67.26 \pm 4.55^{A,B}$	148.90 ± 8.97^A	105.55 ± 5.54^B
VII. Aqueous-ethanolic extract 400 mg/kg+PCM	$0.67 \pm 0.19^{A,B}$	$59.44 \pm 4.50^{A,B,C}$	64.15 ± 4.59^B	$68.01 \pm 5.74^{C,D}$	$91.69 \pm 12.23^{A,B,C}$
VIII. *n*-Butanol fraction 400 mg/kg+PCM	0.90 ± 0.07^A	$47.87 \pm 1.95^{B,C}$	99.14 ± 13.23^A	50.03 ± 2.01^D	$50.09 \pm 1.21^{C,D}$
IX. Ethyl acetate fraction 400 mg/kg+PCM	1.03 ± 0.23^A	40.15 ± 2.33^C	$63.74 \pm 10.56^{A,B}$	$99.15 \pm 6.39^{B,C}$	$58.16 \pm 3.58^{A,B,C,D}$
X. Chloroform fraction 400 mg/kg+PCM	0.94 ± 0.06^A	$50.08 \pm 4.50^{B,C}$	54.27 ± 3.88^B	$96.82 \pm 11.47^{B,C}$	40.07 ± 2.08^D
X1. n-Hexane fraction 400 mg/kg+PCM	0.92 ± 0.04^A	$72.74 \pm 9.08^{A,B,C}$	$43.25 \pm 7.53^{A,B}$	$87.02 \pm 5.89^{B,C}$	40.76 ± 1.10^D

*Values denoted are the mean ± SEM. Mean ± SEM not sharing the letters (A–D) in the respective column are significantly different ($p < 0.05$). Raw data is available in the Supplementary file (Table S2).
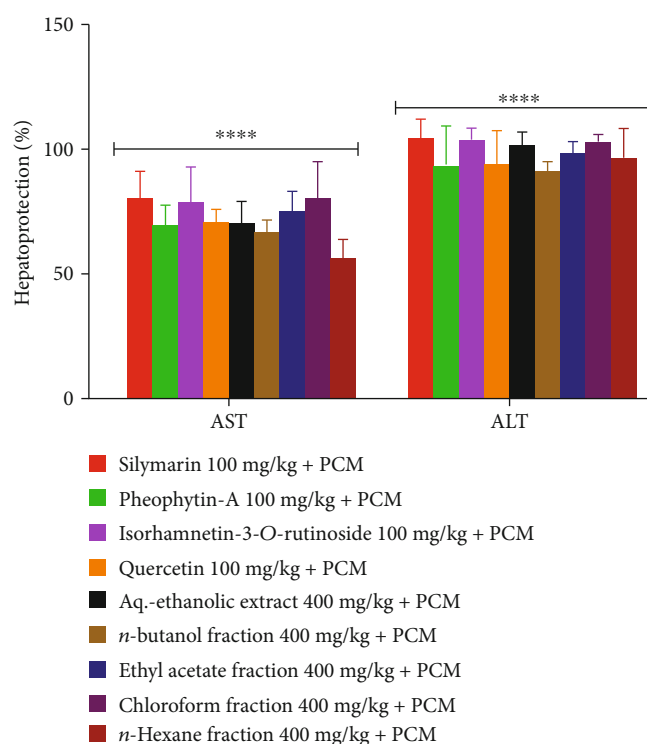
FIGURE 2: Percentage protection after PCM-induced elevations of AST and ALT enzyme levels in the negative and intact groups at 0 and 100% protection, respectively, and thus are not included in the above graph. Values denoted are the mean ± SEM and ****$P < 0.001$ for the groups when equated to the negative group.

3.4. Antioxidant Activity of S. vermiculata Aqueous-Ethanolic Extract, Fractions, and Isolated Compounds. Oxidative stress is considered to play significant roles in PCM-induced liver and renal damages in experimental animals [44, 45]. The oxidative stress is mitigated using endogenous antioxidants, or free radical scavengers, *e.g.*, plant extracts, and flavonoids [46]. As compared to the intact group, the PCM-administered group demonstrated significantly lowered antioxidant SOD and CAT enzymatic activity levels, which are crucial in ROS elimination. The significant decreases in the SOD and CAT activities demonstrated depleted antioxidant potentials in the PCM group which was attributed to the consumption of SOD and CAT during ROS detoxification [47]. The isolated compounds, quercetin (3) of *S. vermiculata*, silymarin, and *n*-hexane fraction, demonstrated significantly higher SOD values than the PCM group. Similarly, isolated compounds (1 and 3), aq.-ethanolic extract, all fractions, and silymarin-fed groups demonstrated significantly increased CAT enzymatic activity as compared to the PCM group. The quercetin's increased SOD and CAT enzymatic activity levels were in agreement with the previous study confirming its antioxidant role [47]. According to the previous study, the PCM-administered group demonstrated significantly reduced GR levels, as compared to the intact group [48]. The aq.-ethanolic extract and *n*-butanol fraction-treated groups demonstrated a significant increase in the GR levels, as compared to the PCM-fed group, while the remaining groups, including silymarin, did not improve the GR levels, as compared to the PCM-fed group. The NO is reported to demonstrate a peak value 24 hr after the PCM administration [45], and the current NO data is in conformity with the previous data demonstrating a significant increase in the PCM group when equated to the intact

TABLE 3: Effects of *S. vermiculata* aq.-ethanolic extract, fractions, and isolated compounds on antioxidant activity in PCM-induced liver toxicity in experimental mice[*].

Groups	CAT U/g	SOD U/g	GR mg/g	LP nmol/g	NO μmol/g
I. Intact control (no CMC, no extract/no fractions, no PCM)	$993.17 \pm 21.42^{A,B}$	210.60 ± 5.07^{A}	0.37 ± 0.02^{A}	6.85 ± 0.56^{A}	0.45 ± 0.05^{C}
II. Negative control (vehicle CMC 0.5%)+PCM	638.59 ± 13.89^{C}	$118.75 \pm 4.18^{C,D,E}$	$0.12 \pm 0.02^{C,D}$	5.82 ± 1.25^{A}	$0.95 \pm 0.05^{A,B}$
III. Silymarin 100 mg/kg+PCM	$862.72 \pm 12.51^{A,B}$	$190.40 \pm 13.39^{A,B}$	$0.07 \pm 0.02^{D,E}$	5.94 ± 0.35^{A}	N.D.
IV. Pheophytin-A 100 mg/kg+PCM	829.29 ± 26.27^{B}	$134.84 \pm 2.28^{C,D}$	0.03 ± 0.01^{E}	8.06 ± 0.21^{A}	1.31 ± 0.05^{A}
V. Isorhamnetin-3-*O*-rutinoside 100 mg/kg+PCM	449.34 ± 18.93^{D}	143.92 ± 10.04^{C}	0.04 ± 0.00^{E}	5.51 ± 0.95^{A}	1.30 ± 0.15^{A}
VI. Quercetin 100 mg/kg+PCM	$1020.50 \pm 17.92^{A,B}$	212.52 ± 3.12^{A}	0.03 ± 0.00^{E}	7.33 ± 0.31^{A}	N.D.
VII. Aqueous-ethanolic extract 400 mg/kg+PCM	$895.42 \pm 77.53^{A,B}$	$96.57 \pm 10.32^{D,E}$	$0.05 \pm 0.00^{D,E}$	7.97 ± 0.21^{A}	0.94 ± 0.05^{B}
VIII. *n*-Butanol fraction 400 mg/kg+PCM	$946.61 \pm 33.64^{A,B}$	$156.72 \pm 9.13^{B,C}$	0.26 ± 0.03^{B}	8.35 ± 0.16^{A}	N.D.
IX. Ethyl acetate fraction 400 mg/kg+PCM	$949.17 \pm 7.05^{A,B}$	$115.31 \pm 9.76^{C,D,E}$	0.16 ± 0.01^{C}	8.31 ± 1.02^{A}	N.D.
X. Chloroform fraction 400 mg/kg+PCM	$961.10 \pm 28.83^{A,B}$	87.67 ± 3.58^{E}	$0.05 \pm 0.01^{D,E}$	7.09 ± 0.73^{A}	N.D.
X1. *n*-Hexane fraction 400 mg/kg+PCM	$848.19 \pm 72.40^{A,B}$	206.39 ± 16.84^{A}	$0.06 \pm 0.01^{D,E}$	7.08 ± 0.46^{A}	N.D.

[*]Values denoted are the mean ± SEM. CMC: carboxyl methylcellulose; PCM: paracetamol; CAT: catalase; LP: lipid peroxide; SOD: superoxide dismutase; NO: nitric oxide; GR: glutathione reductase; N.D.: not determined. Mean ± SEM not sharing the letters (A–E) in the respective column (CAT, LP, SOD, NO, and GR) are significantly different ($p < 0.05$). Raw data is available in the Supplementary file (Table S3).

TABLE 4: Effects of *S. vermiculata* aq.-ethanolic extract, fractions, and isolated compounds on inflammatory markers in PCM-induced liver toxicity in experimental mice[*].

Groups	IL-6 pg/g	TNF-α pg/g
I. Intact control (no CMC, no extract/no fractions, no PCM)	6117.63 ± 33.57^{A}	7570.44 ± 34.82^{A}
II. Negative control (vehicle CMC 0.5%)+PCM	$5919.70 \pm 86.77^{A,B}$	7108.14 ± 32.36^{B}
III. Silymarin 100 mg/kg+PCM	$6031.83 \pm 33.25^{A,B}$	$7306.10 \pm 77.72^{A,B}$
IV. Pheophytin-A 100 mg/kg+PCM	5852.54 ± 71.40^{B}	7152.60 ± 21.56^{B}
V. Isorhamnetin-3-*O*-rutinoside 100 mg/kg+PCM	$5995.02 \pm 80.45^{A,B}$	$7304.19 \pm 43.91^{A,B}$
VI. Quercetin 100 mg/kg+PCM	$5956.74 \pm 54.92^{A,B}$	$7366.28 \pm 96.33^{A,B}$
VII. Aqueous-ethanolic extract 400 mg/kg+PCM	6167.27 ± 23.56^{A}	$7329.63 \pm 86.92^{A,B}$
VIII. *n*-Butanol fraction 400 mg/kg+PCM	5877.38 ± 18.22^{B}	7138.10 ± 45.15^{B}
IX. Ethyl acetate fraction 400 mg/kg+PCM	$5903.53 \pm 33.53^{A,B}$	7071.76 ± 24.95^{B}
X. Chloroform fraction 400 mg/kg+PCM	$6070.63 \pm 87.33^{A,B}$	$7344.04 \pm 101.51^{A,B}$
X1. *n*-Hexane fraction 400 mg/kg+PCM	$6015.82 \pm 28.20^{A,B}$	$7324.78 \pm 59.08^{A,B}$

[*]Values denoted are the mean ± SEM. CMC: carboxyl methylcellulose; PCM: paracetamol; IL6: interleukin-6; TNF-α: tumor necrosis factor-alpha. Mean ± SEM not sharing the letters (A–B) in the respective column (IL-6, TNF-α) are significantly different ($p < 0.05$). Raw data is available in the Supplementary file (Table S4).

group. All the tested and treated groups did not demonstrate any significant difference in NO as compared to PCM. The LP which triggers cellular injury through membrane enzyme and receptor deactivation, including protein cross-linking and fragmentation [49], was statistically not different among all the studied groups (Table 3). The previous study reported by us also showed the antioxidant effects of the *S. vermiculata* ethanolic extract through *in vitro* free radical scavenging parameter [14], while the current result demonstrated the *in vivo* antioxidant effects of the plant aq.-ethanolic extract, fractions, and the isolated compounds. The antioxidant effects of *S. vermiculata* were also previously reported [50], and the extracts' antioxidant effect was attributed to the high contents of flavonoids and related polyphenols [51]. Similarly, the antioxidant activity of quercetin was also detected in both the *in vivo*

and *in vitro* PCM-induced liver toxicity models [43]. Nonetheless, the elevated NO levels lead to deleterious reaction with superoxide anion (O_2^-) thereby generating peroxynitrite radical (ONOO−). The simultaneous production of NO and O_2^- is expected during the inflammation and other pathological conditions, while $ONOO^-$, being a potent oxidant, attacks multiple biological targets [52]. The NO scavenging effects on O_2^- are suggested to be a mechanism by which the host tissues are protected from the deleterious effects of O_2^- and O_2^--derived ROS [53].

3.5. *Effect of S. vermiculata on Inflammatory Markers.* The inflammatory cytokines, IL6 and TNF-α, respectively, are vital to the β-cell functional regulation. Their increased levels are associated with the elicitation of various diseases [54]. For the PCM-induced liver toxicity model, the levels of these

cytokines are reported to increase, indicating the advancement of liver damages [55]. During the current study, the TNF-α values decreased significantly in the PCM-fed group than in the intact group, while all the treated groups, including silymarin, demonstrated no change in its levels when compared to the PCM-fed group. The IL-6 did not demonstrate any significant difference among all the groups as compared to the PCM-fed group (Table 4). As observed earlier, the administration of ethanolic extract of *S. vermiculata* in a carrageenan-induced paw edema inflammation model decreased the inflammation [14, 56]. In contrast, in the current study, the inflammatory marker IL6 and TNF-α levels remained insignificant for the aq.-ethanolic extract as well as other fractions in addition to the 3 isolated compounds from the *S. vermiculata*.

Previous studies have demonstrated that one-week preadministration of the extract before the PCM-induced liver toxicity does not interfere with the P450 activity required for acetaminophen metabolism [57]. In our previous study, the effect of aq.-ethanolic extract after one-week administration on normal animals did not demonstrate any significant changes in the liver, kidney, and cardiac markers as compared to the intact animals [14]. There are no studies available that demonstrate hepatoprotection from PCM-induced liver toxicity using pheophytin-A and the flavonol glycoside, isorhamnetin-3-*O*-rutinoside in mice. This is the first report in this connection. However, quercetin has previously been demonstrated to improve liver markers, antioxidant activities, and reduction of LP and inflammatory markers in liver toxicity [47, 58, 59]. The current study also reiterates the quercetin role in liver protection.

4. Conclusion

The paracetamol (PCM) overdose induced liver injury and caused hepatic cell damage through elevations of AST and ALT enzymatic activities as compared to the intact group observed. The PCM group also increased the oxidative stress by elevating the nitric oxide (nitrite) levels and decreasing the antioxidant SOD, CAT, and GR levels as compared with the control. The TNF-α values also decreased significantly in the PCM-induced toxicity group when compared to the intact group. Thus, the current study demonstrated the hepatoprotective potency of the *S. vermiculata* aq.-ethanolic extract, fractions, and their major constituents, *i.e.*, pheophytin-A, a flavonol glycoside, isorhamnetin-3-*O*-rutinoside, and quercetin. The aq.-ethanolic extract, fraction, and the isolated compound, protective effects were confirmed by significant reductions in AST and ALT enzymatic activities as equated to the PCM-fed toxicity-bearing mice. The aq.-ethanolic extract, fraction, and the isolated compound treatments also decreased the oxidative stress induced by the PCM-generated toxicity through the elevation of antioxidant enzymatic activities of SOD and CAT. Also, the improvement of lipid profile with no adverse effects on the liver, kidney, and glucose markers was observed. The ongoing data on the potentials of the antioxidants, levels of biomarkers, and comparable liver-protective effects, equated to the referral standard, silymarin, confirmed the plant's role in hepatoprotection. The

safety of the extract and fractions, at higher doses, also confirmed the plant materials to be safe. Therefore, the plant materials' consumption by locals can be considered nontoxic within the tested dose level.

Data Availability

All the data were provided in the manuscript and supplementary file.

Conflicts of Interest

The authors declare no conflict of interest.

Supplementary Materials

Supplementary file includes four tables (Tables S1 to S4) that describe the raw data related to the demonstrated biological activities of S. vermiculata. The file also includes nine figures (Figures S1 to S9) that showed the NMR and mass spectra of the isolated compounds. Besides, one scheme that describes the extraction and chromatographic separation of isolated compounds is also provided in the Supplementary file. *(Supplementary Materials)*

References

[1] N. Chalasani, Z. Younossi, J. E. Lavine et al., "The diagnosis and management of non-alcoholic fatty liver disease: practice guideline by the American Association for the Study of Liver Diseases, American College of Gastroenterology, and the American Gastroenterological Association," *Hepatology*, vol. 55, no. 6, pp. 2005–2023, 2012.

[2] G. Musso, M. Cassader, and R. Gambino, "Non-alcoholic steatohepatitis: emerging molecular targets and therapeutic strategies," *Nature Reviews. Drug Discovery*, vol. 15, no. 4, pp. 249–274, 2016.

[3] D. Schuppan, J. Jia, B. Brinkhaus, and E. G. Hahn, "Herbal products for liver diseases: a therapeutic challenge for the new millennium," *Hepatology*, vol. 30, no. 4, pp. 1099–1104, 1999.

[4] J. B. Henson, C. L. Brown, S.-C. Chow, and A. J. Muir, "Complementary and alternative medicine use in United States adults with liver disease," *Journal of Clinical Gastroenterology*, vol. 51, no. 6, pp. 564–570, 2017.

[5] P. Lam, F. Cheung, H. Y. Tan, N. Wang, M. Yuen, and Y. Feng, "Hepatoprotective effects of Chinese medicinal herbs: a focus on anti-inflammatory and anti-oxidative activities," *International Journal of Molecular Sciences*, vol. 17, no. 4, p. 465, 2016.

[6] A. Ferramosca, M. Di Giacomo, and V. Zara, "Antioxidant dietary approach in treatment of fatty liver: new insights and updates," *World Journal of Gastroenterology*, vol. 23, no. 23, pp. 4146–4157, 2017.

[7] V. J. Navarro, I. Khan, E. Björnsson, L. B. Seeff, J. Serrano, and J. H. Hoofnagle, "Liver injury from herbal and dietary supplements," *Hepatology*, vol. 65, no. 1, pp. 363–373, 2017.

[8] F. Stickel and D. Schuppan, "Herbal medicine in the treatment of liver diseases," *Digestive and Liver Disease*, vol. 39, no. 4, pp. 293–304, 2007.

[9] H. A. Mohammed, M. S. al-Omar, M. Z. el-Readi, A. H. Alhowail, M. A. Aldubayan, and A. A. H. Abdellatif, "Formulation of ethyl cellulose microparticles incorporated pheophytin A isolated from *Suaeda vermiculata* for antioxidant and cytotoxic activities," *Molecules*, vol. 24, no. 8, p. 1501, 2019.

[10] H. A. Mohammed, M. S. Al-Omar, M. S. A. Aly, and M. M. Hegazy, "Essential oil constituents and biological activities of the halophytic Plants,Suaeda *VermiculataForssk andSalsola* CyclophyllaBakera growing in Saudi Arabia," *Journal of Essential Oil-Bearing Plants*, vol. 22, no. 1, pp. 82–93, 2019.

[11] H. A. Mohammed, "The valuable impacts of halophytic genus *Suaeda;* nutritional, chemical, and biological values," *Medicinal Chemistry*, vol. 16, no. 8, pp. 1044–1057, 2020.

[12] R. al-Tohamy, S. S. Ali, K. Saad-Allah et al., "Phytochemical analysis and assessment of antioxidant and antimicrobial activities of some medicinal plant species from Egyptian flora," *Journal of Applied Biomedicine*, vol. 16, no. 4, pp. 289–300, 2018.

[13] A. M. Mahasneh, J. A. Abbas, and A. A. El-Oqlah, "Antimicrobial activity of extracts of herbal plants used in the traditional medicine of Bahrain," *Phytotherapy Research*, vol. 10, no. 3, pp. 251–253, 1996.

[14] S. A. A. Mohammed, R. A. Khan, M. Z. el-Readi et al., "*Suaeda vermiculata* aqueous-ethanolic extract-based mitigation of CCl_4-induced hepatotoxicity in rats, and HepG-2 and HepG-2/ADR cell-lines-based cytotoxicity evaluations," *Plants*, vol. 9, no. 10, p. 1291, 2020.

[15] H. Forouzandeh, M. M. E. Azemi, I. Rashidi, M. Goudarzi, and H. Kalantari, "Study of the protective effect of Teucrium polium L. extract on acetaminophen-induced hepatotoxicity in mice," *Iran J Pharm Res*, vol. 12, no. 1, pp. 123–129, 2013.

[16] W. Lee, "Acute liver failure," *Seminars in Respiratory and Critical Care Medicine*, vol. 33, no. 1, pp. 36–45, 2012.

[17] M. R. McGill, C. D. Williams, Y. Xie, A. Ramachandran, and H. Jaeschke, "Acetaminophen-induced liver injury in rats and mice: comparison of protein adducts, mitochondrial dysfunction, and oxidative stress in the mechanism of toxicity," *Toxicology and Applied Pharmacology*, vol. 264, no. 3, pp. 387–394, 2012.

[18] Y. Lu, C. Zhang, Y.-H. Chen et al., "Immature mice are more susceptible than adult mice to acetaminophen-induced acute liver injury," *Scientific Reports*, vol. 7, no. 1, 2017.

[19] T. Kelava, I. Ćavar, and F. Čulo, "Influence of small doses of various drug vehicles on acetaminophen-induced liver injury," *Canadian Journal of Physiology and Pharmacology*, vol. 88, no. 10, pp. 960–967, 2010.

[20] H. Jaeschke, Y. Xie, and M. R. McGill, "Acetaminophen-induced liver injury: from animal models to humans," *Journal of Clinical and Translational Hepatology*, vol. 2, no. 3, pp. 153–161, 2014.

[21] OECD, *OECD Guidelines for Testing of Chemicals, Guideline 425: Acute Oral Toxicity-Up-and-Down Procedure*, OECD, Paris, 2006.

[22] E. A. H. Mohamed, C. P. Lim, O. S. Ebrika, M. Z. Asmawi, A. Sadikun, and M. F. Yam, "Toxicity evaluation of a standardised 50% ethanol extract of *Orthosiphon stamineus*," *Journal of Ethnopharmacology*, vol. 133, no. 2, pp. 358–363, 2011.

[23] E. M. Araya, B. A. Adamu, G. Periasamy, B. Sintayehu, and M. Gebrelibanos Hiben, "_In vivo_ hepatoprotective and _In vitro_ radical scavenging activities of _Cucumis ficifolius_ A. rich root extract," *Journal of Ethnopharmacology*, vol. 242, p. 112031, 2019.

[24] F. Faul, E. Erdfelder, A. G. Lang, and A. Buchner, "G∗Power 3: a flexible statistical power analysis program for the social, behavioral, and biomedical sciences," *Behavior Research Methods*, vol. 39, no. 2, pp. 175–191, 2007.

[25] C. Kilkenny, W. J. Browne, I. C. Cuthill, M. Emerson, and D. G. Altman, "Improving bioscience research reporting: the arrive guidelines for reporting animal research," *PLoS Biology*, vol. 8, no. 6, p. e1000412, 2010.

[26] M. R. McGill and H. Jaeschke, "Animal models of drug-induced liver injury," *Biochimica et Biophysica Acta (BBA) - Molecular Basis of Disease*, vol. 1865, no. 5, pp. 1031–1039, 2019.

[27] S. H. Bhat, R. Shrivastava, M. Y. Malla et al., "Hepatoprotective activity of *Argemone mexicana* Linn against toxic effects of carbon tetrachloride in rats," *World Journal of Pharmaceutical Research*, vol. 3, no. 3, pp. 4037–4048, 2014.

[28] J. C. Mossanen and F. Tacke, "Acetaminophen-induced acute liver injury in mice," *Laboratory Animals*, vol. 49, 1_suppl, pp. 30–36, 2015.

[29] B. G. Meharie, G. G. Amare, and Y. M. Belayneh, "<p>Evaluation of hepatoprotective activity of the crude extract and solvent fractions of Clutia abyssinica (Euphorbiaceae) leaf against CCl₄-induced hepatotoxicity in mice</p>," *Journal of Experimental Pharmacology*, vol. Volume 12, pp. 137–150, 2020.

[30] H. Aebi, "[13] Catalase *in vitro*," *Methods in Enzymology*, vol. 105, pp. 121–126, 1984.

[31] M. Nishikimi, N. Appaji Rao, and K. Yagi, "The occurrence of superoxide anion in the reaction of reduced phenazine methosulfate and molecular oxygen," *Biochemical and Biophysical Research Communications*, vol. 46, no. 2, pp. 849–854, 1972.

[32] E. Beutler, O. Duron, and B. Kelly, "Improved method for the determination of blood glutathione," *The Journal of Laboratory and Clinical Medicine*, vol. 61, pp. 882–888, 1963.

[33] S. Kei, "Serum lipid peroxide in cerebrovascular disorders determined by a new colorimetric method," *Clinica Chimica Acta*, vol. 90, no. 1, pp. 37–43, 1978.

[34] H. Montgomery and J. F. Dymock, "Determination of nitrite in water. Royal Soc Chemistry Thomas Graham House, Science Park, Milton Rd, Cambridge Cb4 0wf," *The Journal of medical laboratory technology*, vol. 22, pp. 111–118, 1961.

[35] B. R. Kirkwood and J. A. C. Sterne, *Essential Medical Statistics*, Wiley, Hoboken, New Jersey, 2010.

[36] M. Olszewska, "Flavonoids from prunus serotina ehrh," *Acta Poloniae Pharmaceutica*, vol. 62, no. 2, pp. 127–133, 2005.

[37] Z. Güvenalp, H. Özbek, T. Ünsalar, C. Kazaz, and D. Lö, "Iridoid, flavonoid, and phenylethanoid glycosides from *Wiedemannia orientalis*," *Turkish Journal of Chemistry*, vol. 30, pp. 391–400, 2006.

[38] T. J. Mabry, K. R. Markham, and M. B. Thomas, "The NMR spectra of flavonoids," in *The Systematic Identification of Flavonoids*, pp. 274–343, Springer, 1970.

[39] OECD, *Test No. 425: Acute Oral Toxicity: Up-and-Down Procedure*, OECD publishing, Paris, France, 2008.

[40] T. Kamiyama, C. Sato, J. Liu, Tajiri, Miyakawa, and Marumo, "Role of lipid peroxidation in acetaminophen-induced hepatotoxicity: comparison with carbon tetrachloride," *Toxicology Letters*, vol. 66, no. 1, pp. 7–12, 1993.

[41] S. D. Ray, V. R. Mumaw, R. R. Raje, and M. W. Fariss, "Protection of acetaminophen-induced hepatocellular apoptosis and necrosis by cholesteryl hemisuccinate," *Journal of Pharmacology and Experimental Therapeutics*, vol. 279, pp. 1470–1483, 1996.

[42] A. Elkomy, M. Aboubakr, A. Soliman, A. Abdeen, A. Abdelkader, and H. Hekal, "Paracetamol induced hepatic toxicity and amelioration by cinnamon in rats," *International Journal of Pharmacology and Toxicology*, vol. 4, no. 2, 2016.

[43] V. Tzankova, D. Aluani, M. Kondeva-Burdina et al., "Hepatoprotective and antioxidant activity of quercetin loaded chitosan/alginate particles _in vitro_ and _in vivo_ in a model of paracetamol-induced toxicity," *Biomedicine & Pharmacotherapy*, vol. 92, pp. 569–579, 2017.

[44] H. Jaeschke, T. R. Knight, and M. L. Bajt, "The role of oxidant stress and reactive nitrogen species in acetaminophen hepatotoxicity," *Toxicology Letters*, vol. 144, no. 3, pp. 279–288, 2003.

[45] J. Ghosh, J. Das, P. Manna, and P. C. Sil, "Acetaminophen induced renal injury via oxidative stress and TNF-α production: therapeutic potential of arjunolic acid," *Toxicology*, vol. 268, no. 1-2, pp. 8–18, 2010.

[46] S. R. Parmar, P. H. Vashrambhai, and K. Kalia, "Hepatoprotective activity of some plants extract against paracetamol-induced hepatotoxicity in Wistar rats," *Journal of Herbal Medicine and Toxicology*, vol. 4, pp. 101–106, 2010.

[47] M. I. Yousef, S. A. M. Omar, M. I. El-Guendi, and L. A. Abdelmegid, "Potential protective effects of quercetin and curcumin on paracetamol-induced histological changes, oxidative stress, impaired liver and kidney functions and haematotoxicity in rat," *Food and Chemical Toxicology*, vol. 48, no. 11, pp. 3246–3261, 2010.

[48] A. To, "Lophirones B and C attenuate acetaminophen-induced liver damage in mice: studies on hepatic, oxidative stress and inflammatory biomarkers," *Journal of Biochemical and Molecular Toxicology*, vol. 30, no. 10, pp. 497–505, 2016.

[49] S. Luqman and S. I. Rizvi, "Protection of lipid peroxidation and carbonyl formation in proteins by capsaicin in human erythrocytes subjected to oxidative stress," *Phytotherapy Research*, vol. 20, no. 4, pp. 303–306, 2006.

[50] T. A. Diab, T. Donia, and K. M. Saad-Allah, "Characterization, antioxidant, and cytotoxic effects of some Egyptian wild plant extracts," *Beni-Suef University Journal of Basic and Applied Sciences*, vol. 10, no. 1, 2021.

[51] R. A. Khan, M. R. Khan, S. Sahreen, and M. Ahmed, "Assessment of flavonoids contents and in vitro antioxidant activity of Launaea procumbens," *Chemistry Central Journal*, vol. 6, no. 1, 2012.

[52] A. O. Abdel-Zaher, R. H. Abdel-Hady, M. M. Mahmoud, and M. M. Y. Farrag, "The potential protective role of alpha-lipoic acid against acetaminophen- induced hepatic and renal damage," *Toxicology*, vol. 243, no. 3, pp. 261–270, 2008.

[53] J. S. Beckman, T. W. Beckman, J. Chen, P. A. Marshall, and B. A. Freeman, "Apparent hydroxyl radical production by peroxynitrite: implications for endothelial injury from nitric oxide and superoxide," *Proceedings of the National Academy of Sciences*, vol. 87, no. 4, pp. 1620–1624, 1990.

[54] P. Rieckmann, J. M. Tuscano, and J. H. Kehrl, "Tumor necrosis factor-α (TNF-α) and interleukin-6 (IL-6) in B-lymphocyte function," *Methods*, vol. 11, no. 1, pp. 128–132, 1997.

[55] M. K. Rasool, E. P. Sabina, S. R. Ramya et al., "Hepatoprotective and antioxidant effects of gallic acid in paracetamol-induced liver damage in mice," *The Journal of Pharmacy and Pharmacology*, vol. 62, no. 5, pp. 638–643, 2010.

[56] M. S. al-Omar, M. S. M. Sajid, N. S. Alnasyan et al., "The halophytic plant, *Suaeda vermiculata* Forssk extracts reduce the inflamed paw edema and exert potential antimicrobial activity," *Pakistan Journal of Botany*, vol. 53, no. 1, 2021.

[57] C. Pang, L. Shi, Y. Sheng et al., "Caffeic acid attenuated acetaminophen-induced hepatotoxicity by inhibiting ERK1/2-mediated early growth response-1 transcriptional activation," *Chemico-Biological Interactions*, vol. 260, pp. 186–195, 2016.

[58] C. Pang, Z. Zheng, L. Shi et al., "Caffeic acid prevents acetaminophen-induced liver injury by activating the Keap1-Nrf2 antioxidative defense system," *Free Radical Biology & Medicine*, vol. 91, pp. 236–246, 2016.

[59] C. Girish, B. C. Koner, S. Jayanthi, K. Ramachandra Rao, B. Rajesh, and S. C. Pradhan, "Hepatoprotective activity of picroliv, curcumin and ellagic acid compared to silymarin on paracetamol induced liver toxicity in mice," *Fundamental & Clinical Pharmacology*, vol. 23, no. 6, pp. 735–745, 2009.

Research Article

Neuroprotective Effects of Palmatine via the Enhancement of Antioxidant Defense and Small Heat Shock Protein Expression in Aβ-Transgenic *Caenorhabditis elegans*

Weizhang Jia [1], **Qina Su,**[1] **Qiong Cheng,**[1] **Qiong Peng,**[1] **Aimin Qiao,**[1] **Xiongming Luo,**[1] **Jing Zhang,**[1] **and Ying Wang** [1,2]

[1]*School of Biosciences & Biopharmaceutics, Guangdong Province Key Laboratory for Biotechnology Drug Candidates, Guangdong Pharmaceutical University, Guangzhou 510006, China*
[2]*Institutes for Life Sciences and School of Medicine, South China University of Technology, Guangzhou 510641, China*

Correspondence should be addressed to Ying Wang; wangying2@scut.edu.cn

Palmatine is a naturally occurring isoquinoline alkaloid that has been reported to display neuroprotective effects against amyloid-β- (Aβ-) induced neurotoxicity. However, the mechanisms underlying the neuroprotective activities of palmatine remain poorly characterized *in vivo*. We employed transgenic *Caenorhabditis elegans* models containing human Aβ_{1-42} to investigate the effects and possible mechanisms of palmatine-mediated neuroprotection. Treatment with palmatine significantly delayed the paralytic process and reduced the elevated reactive oxygen species levels in Aβ-transgenic *C. elegans*. In addition, it increased oxidative stress resistance without affecting the lifespan of wild-type *C. elegans*. Pathway analysis suggested that the differentially expressed genes were related mainly to aging, detoxification, and lipid metabolism. Real-time PCR indicated that resistance-related genes such as *sod-3* and *shsp* were significantly upregulated, while the lipid metabolism-related gene *fat-5* was downregulated. Further studies demonstrated that the inhibitory effects of palmatine on Aβ toxicity were attributable to the free radical-scavenging capacity and that the upregulated expression of resistance-related genes, especially *shsp*, whose expression was regulated by HSF-1, played crucial roles in protecting cells from Aβ-induced toxicity. The research showed that there were significantly fewer Aβ deposits in transgenic CL2006 nematodes treated with palmatine than in control nematodes. In addition, our study found that Aβ-induced toxicity was accompanied by dysregulation of lipid metabolism, leading to excessive fat accumulation in Aβ-transgenic CL4176 nematodes. The alleviation of lipid disorder by palmatine should be attributed not only to the reduction in fat synthesis but also to the inhibition of Aβ aggregation and toxicity, which jointly maintained metabolic homeostasis. This study provides new insights into the *in vivo* neuroprotective effects of palmatine against Aβ aggregation and toxicity and provides valuable targets for the prevention and treatment of AD.

1. Introduction

Once there is an imbalance between the production and clearance of amyloid-β peptide (Aβ), the accumulation of Aβ initiates self-assembly and the self-assembled Aβ then turns into toxic oligomers, large Aβ fibrils, and plaques associated with the onset and progression of Alzheimer's disease (AD) [1, 2]. Considerable research evidence suggests that oxidative stress is an early event in the development of AD, preceding the classic formation of fibrils that are even-

tually deposited as insoluble Aβ plaques and neurofibrillary tangles [3, 4]. Meanwhile, the aggregation and deposition of Aβ further increase oxidative stress and aggravate the inflammatory response, thereby causing progressive damage to neurons [5]. Therefore, the complex pathological mechanisms of AD include the aggregation of monomeric Aβ into oligomers or fibrils and Aβ-mediated oxidative stress. Prevention of these processes requires the regulation of signaling pathways to inhibit Aβ aggregation and excessive free radical release in order to maintain cellular homeostasis.

Heat shock factor 1 (HSF-1) is an essential regulator of both proteotoxicity and aging [6]. Small heat shock proteins (sHSP), which constitute one type of HSP regulated by HSF-1, act as the front line of defense for preventing or reversing abnormal protein aggregation [7, 8]. More importantly, some of them have been found to exert neuroprotective functions. Specifically, they interact with misfolded and damaging protein aggregates, such as Aβ, in AD to reduce the accumulation of misfolded proteins, block oxidative stress, and attenuate neuroinflammation and neuronal apoptosis; thus, they hold great potential as promising therapeutic agents in neurodegenerative diseases [9, 10]. Oxidative damage is a common and prominent feature of various neurodegenerative diseases and is implicated in the pathogenesis of AD [11]. Studies have shown that AD and other neurodegenerative diseases are associated with elevated levels of oxidative stress biomarkers and impaired antioxidant defense systems in the brain and peripheral tissues [12]. Active compounds with antioxidant properties exert neuroprotective effects by augmenting antioxidant defense and inhibiting Aβ-induced toxicity, which can normalize biomarkers related to oxidant/antioxidant imbalance [13–15].

Although organisms can respond to endogenous and exogenous stressors continuously and attempt to maintain homeostasis, they need externally supplied active substances, particularly when they are facing persistent and overwhelming stress, to adjust the molecular network in order to rebuild a steady state [16]. Otherwise, diseases can occur. Natural products, such as alkaloids, polyphenols, and saponins, have a variety of pharmacological activities [17, 18]. The neuroprotective activity of natural products that can inhibit Aβ aggregation and toxicity by inducing antioxidant and anti-inflammatory responses, regulating stress-related signaling, and modulating Aβ production and clearance has been extensively studied and used in the prevention and treatment of AD [19]. Alkaloids, which form a class of natural nitrogen-containing secondary metabolites, are important active components in Chinese Herbal Medicines. These compounds exert neuroprotective effects through suppression of oxidative stress, neuroinflammation, and apoptosis; reduction of Aβ aggregation; and enhancement of Aβ clearance. Through these effects, the compounds improve functional outcomes in AD [20–23]. Thus, they have great application value for the development of therapeutic agents for the treatment of AD. Although studies have confirmed that many alkaloids potentially exhibit anti-AD effects *in vitro* and *in vivo*, the molecular mechanisms responsible for these effects still need further study.

Palmatine, an isoquinoline alkaloid, has been reported to possess extensive biological functions, such as antioxidant, anti-inflammatory, neuroprotective, and blood lipid-regulating functions [21, 24]. In particular, studies have shown that palmatine might display anti-AD effects by inhibiting the activity of cholinesterase, decreasing Aβ aggregation, reducing the generation of high levels of reactive oxygen species (ROS), and attenuating oxidative damage [24–27]. Nevertheless, little is known about the inhibitory effects of palmatine on Aβ aggregation and toxicity *in vivo* and the signaling pathways that exert the neuroprotective

effects of palmatine are also not well understood. Due to advantageous features such as a short lifespan, rapid generation time, tractable genetic manipulation, and fully sequenced genome [28], the model species *Caenorhabditis elegans* has been widely used to study aging and aging-related neurodegenerative diseases and was therefore employed to investigate the action mechanisms of palmatine-mediated neuroprotective effects. The experiments indicated that palmatine inhibits Aβ aggregation and toxicity by enhancing antioxidant defense and sHSP expression to maintain homeostasis in *C. elegans*. This study provides insights into the neuroprotective effects of palmatine in vivo and provides valuable targets for the prevention and treatment of AD.

2. Materials and Methods

2.1. Chemical and Materials. The isopropyl-beta-d-thiogalactopyranoside (IPTG), $2',7'$-dichlorofluorescein diacetate (DCFH-DA), 5-fluoro-$2'$-deoxyuridine (FUDR), cholesterol, and $1,1'$-dimethyl-$4,4'$-bipyridinium dichloride (Paraquat or PQ) were purchased from Sigma Chemical Corp. (St. Louis, MO, USA). The detection assay kits of SOD and CAT enzyme activity and protein quantification (Bicinchoninic acid (BCA)) were acquired from Beyotime (Shanghai, China). The palmatine, Oil red O, Sudan black B, and Thioflavin S (ThS) were obtained from Aladdin (Shanghai, China). We bought the RNA extraction reagent (TRIzol) from Invitrogen (Carlsbad, CA, USA). The DNase I, restriction enzymes XbaI and KpnI, plasmid preparation, reverse transcription, and real-time PCR kits were provided by TaKaRa (Dalian, China). Other chemical reagents used in this study were supplied by Tianjin Damao Chemical Reagent Factory (Tianjin, China).

2.2. C. elegans and Culture. There are several worm strains involved in our work: the wild-type N2, the Aβ-transgenic CL2006 {dvIs2 [pCL12(unc-54/human Abeta(1-42) minigene) + rol-6(su1006)]} and CL4176 {dvIs27 [myo-3p::Abeta(1-42)::let-851 3 ′ UTR) + rol-6(su1006)]}, the transgenic CF1553 containing *sod-3p*::GFP {muIs84 [(pAD76) sod-3p::GFP + rol-6(su1006)]}, and CL2070 containing *hsp-16.2p*::GFP {dvIs70 [hsp-16.2p::GFP + rol-6(su1006)]}. This work was approved by the experimental animal ethics committee of Guangdong Pharmaceutical University with the approval number gdpulac2019015. *Escherichia coli*, such as OP50, NA22, and HT115 strains, were selected to feed worms based on different experimental conditions. All *C. elegans* were provided by the Caenorhabditis Genetics Center. The Aβ-transgenic CL2006 and CL4176 worms and the wild-type N2, CF1553, and CL2070 worms were cultured and maintained on nematode-growing medium (NGM) plates at 15°C and 20°C, respectively. The synchronous population was prepared by treatment of gravid adults with alkaline hypochlorite and hatched overnight.

2.3. Food Clearance and Body Length Assays. To select the suitable concentration range of palmatine, the wild-type nematodes were used to conduct food clearance and body length assays. In food clearance, $20 \mu L$ of S medium

TABLE 1: The primer sequences for real-time PCR and RNAi analyses.

Gene	Forward primer ($5'$ to $3'$)	Reverse primer ($5'$ to $3'$)	Application
β-Actin	CCACGAGACTTCTTACAACTCCATC	CTTCATGGTTGATGGGGCAAGAG	Real-time PCR
sod-3	GAGCTGATGGACACTATTAAGCG	GCACAGGTGGCGATCTTCAAG	Real-time PCR
hsp-16.11	CTCCATCTGAATCTTCTGAGATTG	CTTCGGGTAGAAGAATAACACGAG	Real-time PCR
hsp-16.2	CTCCATCTGAGTCTTCTGAGATTGT	CTCCTTGGATTGATAGCGTACGA	Real-time PCR
hsp-16.49	TCCGACAATATTGGAGAGATTG	GATCGTTTCGAGTATCCATGCT	Real-time PCR
fat-5	GTGCTGATGTTCCAGAGGAAGAAC	ATGTAGCGTGGAGGGTGAAGCA	Real-time PCR
Fat-7	CCAGAGAAAGCACTATTTCCCAC	CACCAAGTGGCGTGAAGTGT	Real-time PCR
hsf-1[a]	TGCTCTAGACTGTCCCAAGGTGGTCTAACTC	CGGGGTACCTCCCGAATAGTCTTGTTGC	RNAi

[a]Underlines indicate the restriction sites of XbaI (TCTAGA) and KpnI (GGTACC).

containing approximately 20 L1-stage worms was put into 80 μL of S medium including NA22 and palmatine with indicated concentration (0.05, 0.1, 0.2, and 0.4 mM) in a 96-well microplate and cultured at 20°C. Absorbance value (570 nm) was measured every 24 h and continued for six days. For the body length, L1-stage worms were placed on a NGM plate fed with OP50 containing different concentrations of palmatine (0.05, 0.1, 0.2, and 0.4 mM) and cultured at 20°C for two days. The worm images (approximately 100 per group) were acquired and analyzed using a Mshot MF52 inverted microscope (Mingmei, Guangzhou, China) with digital software.

2.4. Paralytic Assays. Using Aβ-transgenic CL2006 and CL4176 strains, we preliminarily detected the effect of palmatine for inhibiting Aβ-toxicity according to previously described [29]. The L1-stage CL2006 worms were fed on NGM solid plates including OP50 and different concentrations of palmatine (0.1 and 0.2 mM), which were placed at 15°C for 45 h and shifted to the new NGM solid plates (approximately 100 per group) containing OP50 with FUDR (75 μg/mL) and different concentrations of palmatine (0.1 and 0.2 mM) at 20°C for inducing Aβ peptide expression. Paralyzed worms were counted every day until all were palsied. For the CL4176 strain, the L1-stage worms were cultured at 15°C for 36 h on NGM plates containing different concentrations of palmatine (0.1 and 0.2 mM) and shifted to 23°C for inducing Aβ peptide expression. The amount of paralyzed worms was counted every 2 h until all palsied.

2.5. Measurement of the ROS Level. The ROS level in worms was evaluated through the DCFH-DA method as described previously [30]. L1-stage CL4176 worms were cultured at 15°C for 36 h on a NGM solid plate with or without palmatine (0.2 mM) and shifted to 23°C for another 36 h. Approximately 2000 worms in each group were lysed in PBST buffer (PBS containing 0.1% Tween 20) and used to collect the supernatant by centrifugation at 10000 g for 5 min. The protein content was determined by a BCA protein assay kit. A total volume of 50 μL DCFH-DA (100 mM) was placed into a black 96-well microplate containing 50 μL supernatant. The intensity of DCF was calculated with the Synergy H1 Microplate Reader (BioTek, Dallas, TX, USA) at 488 nm of excitation and 525 nm of emission.

2.6. Oxidative Survival and Lifespan Assays. Oxidative stress caused by paraquat was performed with the wild-type worms as reported previously [31]. L1-stage worms were incubated in S medium fed with NA22 at 20°C until the L4 stage and put into a 96-well microplate containing NA22, ampicillin (100 μg/mL), and FUDR (75 μg/mL). The worms were further cultured with or without palmatine (0.2 mM) for one day at 20°C and then exposed to paraquat (75 mM). The survival was counted every 12 h until all were dead (approximately 100 worms per group). For the lifespan assay, L4-stage wild-type worms were put into a 96-well microplate at the density of 15–20 individuals per well in 100 μL of culture medium (approximately 100 worms per group) and treated with or without palmatine (0.2 mM). The part of worms alive was counted every two days until all were dead.

2.7. Transcriptome Analysis and Real-Time PCR Verification. L1-stage wild-type worms were cultured on NGM plates fed OP50 with or without palmatine (0.2 mM) for two days at 20°C, and then, the worms were collected. Total RNA was prepared from the worms by using TRIzol, and further purified mRNA was used for Illumina sequencing at Shanghai Majorbio Bio-pharm Technology Co. Ltd. (China). A threshold false discovery rate (FDR) (≤ 0.05) and fold change (≥ 2.0) were used as criteria to screen differentially expressed genes (DEGs), which were categorized on the basis of Kyoto Encyclopedia of Genes and Genomes (KEGG) pathway analysis. At the same time, samples were prepared for real-time PCR detection as described above and the primer sequences are listed in Table 1.

2.8. Measurement of sod-3 and hsp-16.2 Expressions. Transgenic CF1553 and CL2070 worms containing sod-3p::GFP and hsp-16.2p::GFP reporters were used to determine the expression of the sod-3 and hsp-16.2 genes. Transgenic worms were cultured with or without palmatine (0.2 mM) on NGM plates at 20°C for two days and anesthetized on microscope slides for observation and determination of sod-3p::GFP and hsp-16.2p::GFP expression. Images were captured by using an Mshot MF52 inverted fluorescence microscope coupled with digital software, and the expression of the respective genes was ascertained by assessing the GFP signal using ImageJ software.

2.9. Detection of SOD and CAT Activity Levels. The wild-type strain was synchronized as described above, and L1-stage worms were cultured at 20°C for two days on NGM solid plates with or without palmatine (0.2 mM). Approximately 2000 worms were gathered and lysed in PBST buffer. The activity levels of SOD and CAT were detected with SOD and CAT assay kits, respectively, and a BCA protein assay kit was used to determine the protein concentration.

2.10. RNA Interference. In an RNAi-mediated gene knockdown experiment, *E. coli* HT115 was chosen as a food source for the worms as previously described with some changes [30]. An RNAi plasmid was built by partially cloning the *hsf-1* cDNA sequence into the *L4440* empty vector. The primer sequences with restriction sites for XbaI (TCTA GA) and KpnI (GGTACC) are displayed in Table 1. L1-stage CL2006 worms were cultured with or without palmatine at 15°C on NGM solid plates seeded with HT115 containing the *L4440* empty plasmid or the *hsf-1* recombinant plasmid for 45 h. The worms (approximately 100 per group) were then transferred to NGM plates and fed HT115 (containing the *L4440* empty plasmid or the *hsf-1* recombinant plasmid) in the presence of 5-FUdR (75 μg/mL) and palmatine (0.2 mM) at 20°C to induce Aβ peptide expression. Worm paralysis was observed, and the paralyzed worms were counted microscopically every day until all worms were palsied.

2.11. ThS Staining Assay. The wild-type and Aβ-transgenic CL2006 strains were used for the assay as described previously [32]. Here, wild-type worms were stained as negative control. L1-stage Aβ-transgenic CL2006 worms were cultured at 20°C for 90 h on NGM plates with or without palmatine (0.2 mM). In another group, CL2006 worms were continuously cultured at 15°C for 90 h and used for comparative analysis. All worms were collected and fixed at 4°C for one day in 4% paraformaldehyde (PFA). After PFA fixation, the worms were incubated at 37°C for one day in permeabilization solution including β-mercaptoethanol (5%), Triton X-100 (1%), and Tris–HCl (125 mM). The worms were washed and soaked in ThS solution (containing 0.125% ThS and 50% ethanol) at ambient temperature for 2 min and then decolorized with 50% ethanol until the staining agent in the solution completely disappeared. Images of the anterior pharyngeal bulb were acquired by using an Mshot MF52 inverted microscope.

2.12. Fat Staining. Fat staining was performed by using Oil Red O and Sudan black B as previously described [33, 34]. Briefly, L1-stage N2 and CL4176 strains were cultured on solid NGM plates seeded with OP50 with or without palmatine (0.2 mM). The N2 worms were cultured at 20°C for three days, while the CL4176 worms were cultured at 15°C for 36 h and shifted to 23°C for another 36 h. The worms used for Oil Red O staining were fixed at 4°C for 30 min in 4% PFA and subjected to three freeze-thaw cycles. The worms were dehydrated for 15 min in 60% isopropanol and stained for 6 h in an Oil Red O staining solution containing 40% water and 60% Oil Red O stock solution. For Sudan black B staining,

the worms were first fixed in 4% PFA, subjected to 3 freeze-thaw cycles, dehydrated in 25, 50, and 70% ethanol, and then dyed for 12 h in a 50% saturated Sudan Black B solution (70% ethanol). The images were obtained by using an Mshot MF52 inverted microscope, and ImageJ software was used for quantitative analysis.

2.13. Statistical Analysis. The data were analyzed by using GraphPad Prism version 7.0 for Windows (San Diego, California, USA). The *t*-test and one-way analysis of variance (ANOVA) were selected as the analytical methods. The survival and lifespan curves were created with the Kaplan-Meier method, and a log-rank test was selected to evaluate the statistical significance. The primers were designed by using Primer 3 version 0.4.0 software, and *β-actin* was used as the reference gene. All experiments were carried out at least three times, and a *p* value of <0.05 was considered to indicate statistical significance.

3. Results

3.1. Inhibition of Aβ Toxicity by Palmatine in Aβ-transgenic Nematodes. *C. elegans* is a powerful model organism with which to research the molecular mechanisms of neurodegenerative diseases and screen effective neuroprotective drugs [28]. In this work, we studied the neuroprotective effects of palmatine in the Aβ-transgenic *C. elegans* CL2006 and CL4176 strains (Figure 1(a)), which express human $A\beta_{1-42}$ in constitutive and inducible manners and show progressive and rapid paralytic phenotypes, respectively. The concentration of palmatine was confirmed through food clearance and body length assays, which indicated that a concentration of ≤0.2 mM was suitable in wild-type worms (Figures 1(b) and 1(c)). Therefore, according to the experimental design in Figure 1(d), we preliminarily tested the effects of palmatine against Aβ toxicity at concentrations of 0.1 and 0.2 mM. As shown in Figure 1(e), palmatine at 0.1 and 0.2 mM effectively protected against Aβ toxicity in progressively paralyzed CL2006 nematodes. A beneficial effect of palmatine was also observed in rapidly paralyzed CL4176 nematodes (Figure 1(f)). It is worth noting that palmatine at 0.2 mM showed a more effective protective effect against Aβ toxicity than palmatine at 0.1 mM and significantly delayed the paralytic process. In summary, these results suggest that palmatine exhibits neuroprotective activity against Aβ toxicity in Aβ-transgenic nematode models.

3.2. Alleviation of Oxidative Stress Rather Than Prolongation of Lifespan. There is considerable evidence to suggest that Aβ toxicity increases oxidative stress and free radical formation, which are closely associated with the progression of AD [11]. Since palmatine inhibited Aβ toxicity *in vivo*, as demonstrated above, we investigated the effects of palmatine on the oxidative status using transgenic CL4176 nematodes. As shown in Figure 2(a), the ROS level was significantly higher in the homogenate of Aβ-induced worms at 23°C than in the homogenate of the control worms at 15°C. However, the ROS level was significantly lower in the homogenate of worms

(a)

(b)

(c)

(d)

FIGURE 1: Continued.

(e)

(f)
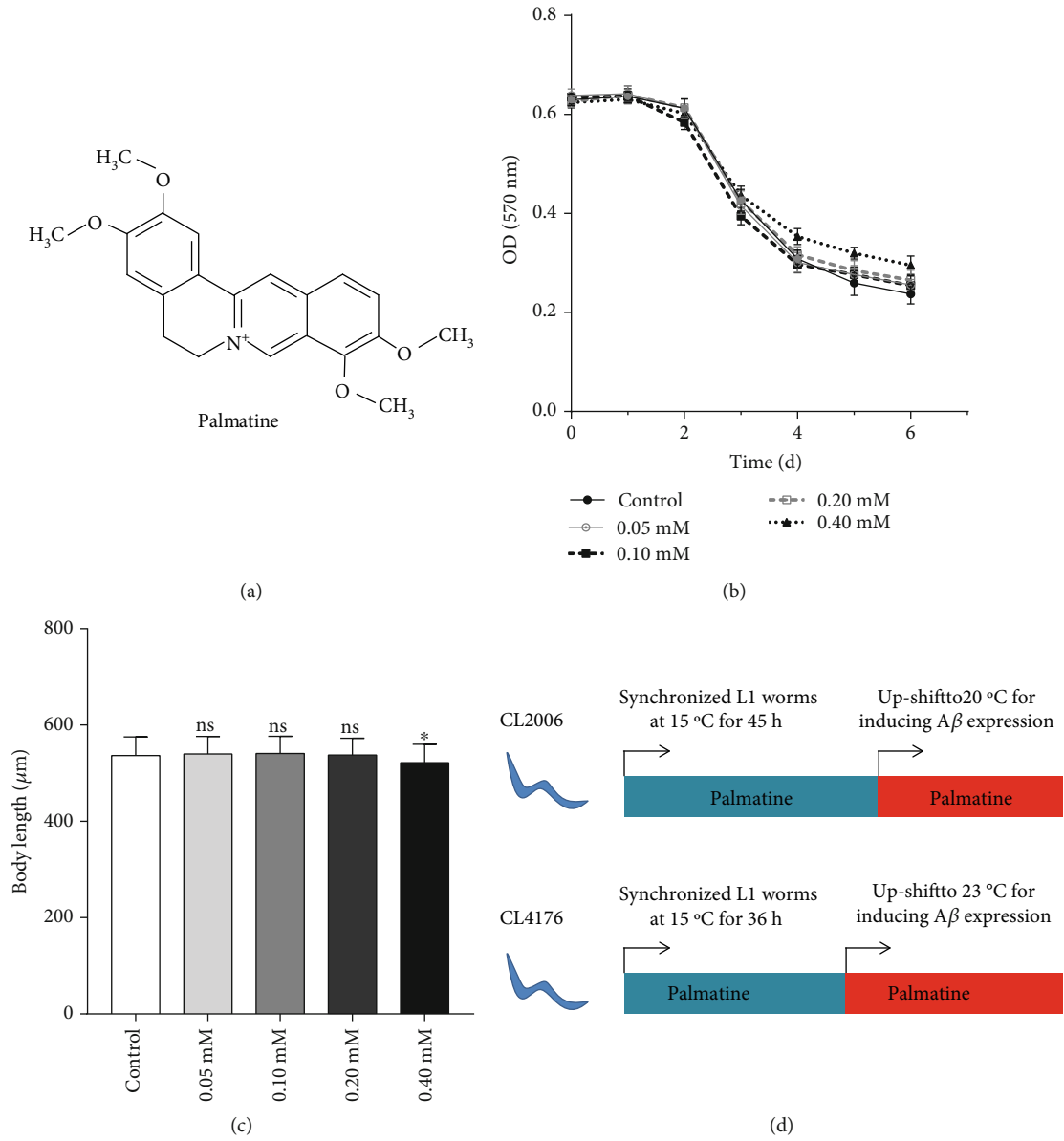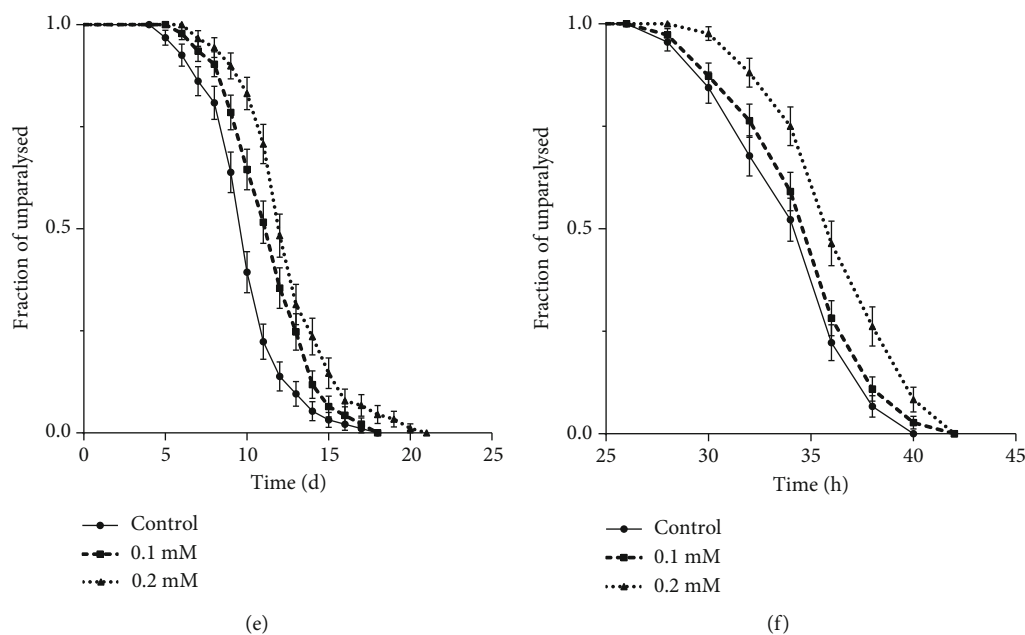
FIGURE 1: Inhibition of Aβ-toxicity of palmatine in transgenic *C. elegans*. (a) Chemical structure of palmatine. (b) Food clearance. Synchronized wild-type worms were cultured at 20°C in a 96-well plate with or without palmatine at different concentrations. The absorbance (at 570 nm) was detected daily for six days using a microplate reader. The results were displayed as mean ± SD from 5 parallel wells. (c) Body length. Synchronized wild-type worms were cultured at 20°C in NGM plates with or without palmatine at different concentrations for two days. The results were displayed as mean ± SD of approximately 100 worms. Statistical analysis was carried out with a one-way ANOVA. ns: no significant difference; $*p < 0.05$. (d) The experimental flowchart in Aβ-transgenic CL2006 and CL4176 nematodes. (e) The paralytic assay of CL2006 nematodes. Synchronized L1-stage worms were cultured with or without palmatine for 45 h at 15°C and upshifted to 20°C for inducing Aβ peptide expression. The fraction of paralytic worms was counted every day until all were palsied. (f) The paralytic assay of CL4176 nematodes. Synchronized L1-stage worms were cultured for 36 h at 15°C in NGM plates with or without palmatine and upshifted to 23°C for inducing Aβ peptide expression. The fraction of paralytic worms was counted every 2 h until all were palsied. The results were displayed as Kaplan-Meier survival curves and analyzed by using a log-rank test.

treated with palmatine at 23°C than in the homogenate of the untreated worms. These data suggest that palmatine plays a positive role in ROS scavenging and improves stress tolerance in Aβ-transgenic CL4176 worms. Next, we detected the protective effects of palmatine against oxidative stress through the assessment of paraquat-induced oxidative damage in wild-type nematodes. In Figure 2(b), the survival of the worms treated with palmatine prior to paraquat damage was significantly higher than that of the control worms, indicating the antioxidative stress activity of palmatine. However, as shown in Figure 2(c), palmatine did not significantly change the lifespan of the worms. Taken together, these findings show that the ROS-reducing capability of palmatine may contribute to its protection against Aβ toxicity.

3.3. Transcriptome-Based Discovery of Genes and Pathways Related to the Effects of Palmatine against Aβ Toxicity. Gene expression profiles can be used as signatures to search for the signaling pathways and downstream target genes of active compounds [35]. To understand the transcriptomic responses to palmatine, transcriptome sequencing was carried out on the Illumina MiSeq platform for wild-type nematodes treated with or without palmatine (0.2 mM) for 48 h. The raw RNA-Seq reads reported in this paper are found in the NCBI Sequence Read Archive (accession number PRJNA667515). Principal component analysis (PCA)

was used to assess the clustering of the samples, which manifested an obvious distinction between the control and palmatine-treated groups (Figure 3(a)). After treatment with palmatine, 602 DEGs were detected, including 522 upregulated genes and 80 downregulated genes. In Figure 3(b), the patterns of the changes in transcript abundance are shown in the heatmap of the DEGs, which were identified using an FDR cutoff of 0.05 and a fold change threshold of 2. To retrieve the functional information on the DEGs in the experimental group, coregulated genes were further classified into different categories, including lipid metabolism, biodegradation and detoxification, signal transduction, transport and catabolism, and aging of the endocrine system (Figure 3(c)). Furthermore, in pathway enrichment analysis (Figure 3(d)), the genes regulated by palmatine treatment were associated mainly with the aging regulation pathway, detoxification, and fatty acid degradation.

3.4. Validation of Gene Expression Levels by Real-time PCR. Among the RNA-sequencing data, we focused on the data for some signaling pathways related to stress resistance, such as aging, detoxification, and lipid metabolism pathways. To further validate the gene expression profiles, the gene expression levels of six representative candidate genes were analyzed via real-time PCR. The regulation patterns for the selected genes, including *sod-3*, *hsp-16.11*, *hsp-16.2*, *hsp-*

(a)

(b)

(c)
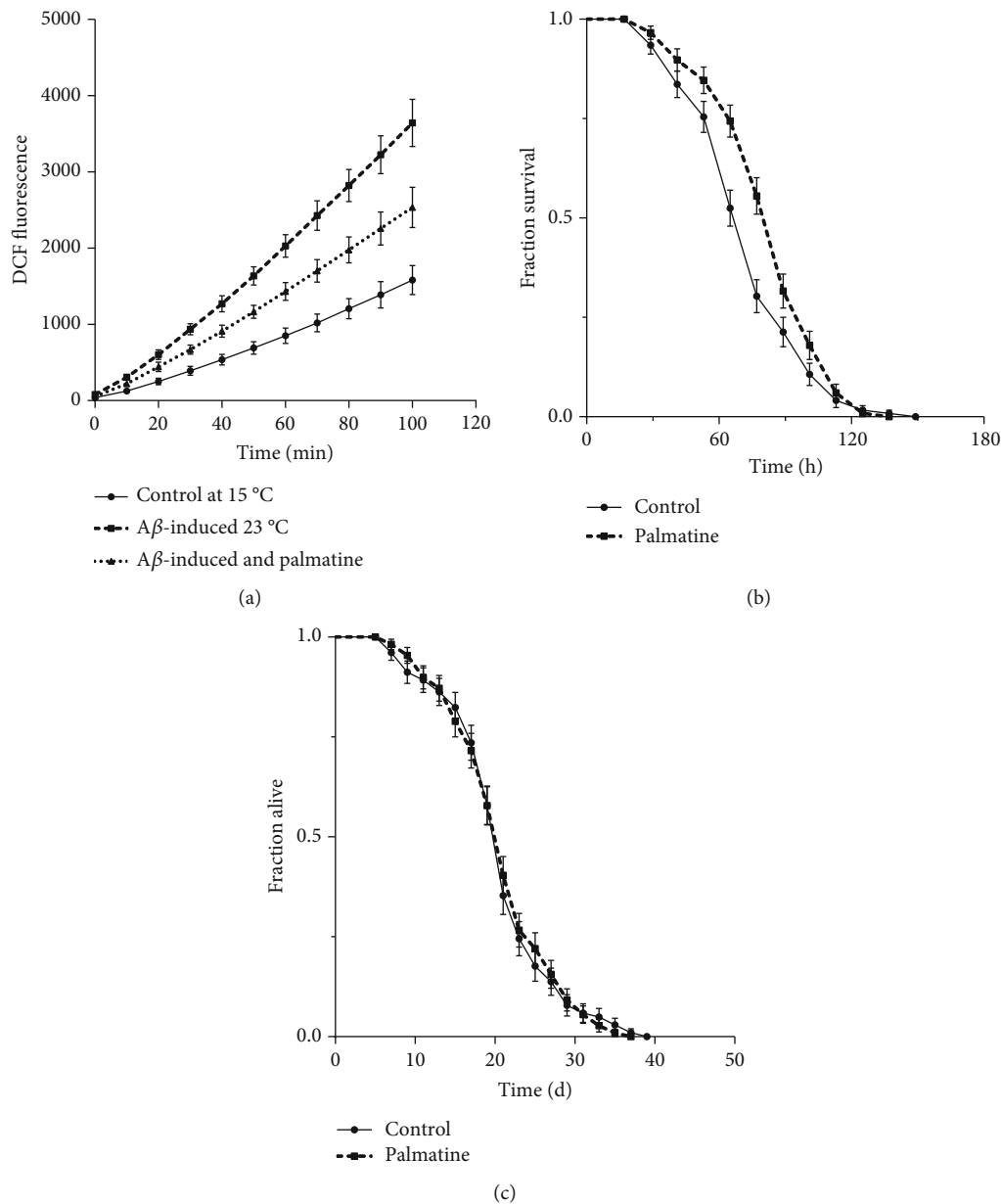
FIGURE 2: The effects of palmatine on the ROS level, oxidative stress, and lifespan. (a) The effects of palmatine on ROS in the AD model CL4176 strain. Synchronized *L1-stage* CL4176 worms were cultured with or without palmatine (0.2 mM) for 36 h at 15°C and then cultured at 23°C for another 36 h. These worms were collected and homogenized, and then, the lysate was used for detection of the ROS level. The curve is from a single experiment (values are means ± SD, $n = 3$). (b) Oxidative survival assay in wild-type nematodes. L4-stage wild-type nematodes (approximately 100 for each group) were pretreated with or without palmatine at 20°C for 24 h and then treated with 75 mM paraquat, and the fraction of survival was scored every 12 h until all dead. (c) Lifespan assay in wild-type nematodes. L4-stage wild-type worms were put into a 96-well plate at the density of 15–20 individuals/well in 100 μL of culture medium (≈100 worms/group) and administered with or without palmatine (0.2 mM). The fraction of alive worms was counted every two days until all deaths. The results were displayed as Kaplan-Meier survival curves and analyzed by using a log-rank test.

16.49, and *fat-5*, were consistent with the RNA-sequencing data; only marginal differences in the relative fold changes were observed. However, the *fat-7* gene did not show statistically significant differences among the control and palmatine-treated groups. As shown in Figure 4, special attention should be given to the *shsp* genes, which were significantly upregulated in the worms treated with palmatine compared with the normal control worms. Overall, the find-

ings show that palmatine treatment can activate resistance-related genes to inhibit Aβ toxicity.

3.5. Enhancement of sod-3p::GFP Expression and SOD and CAT Activity Levels. Since SOD is a key antioxidant enzyme for ROS scavenging, we employed the CF1553 strain containing a *sod-3p*::GFP transgenic reporter to explore the effects of palmatine on the transcriptional change of the

(a)

(b)

FIGURE 3: Continued.

(c)
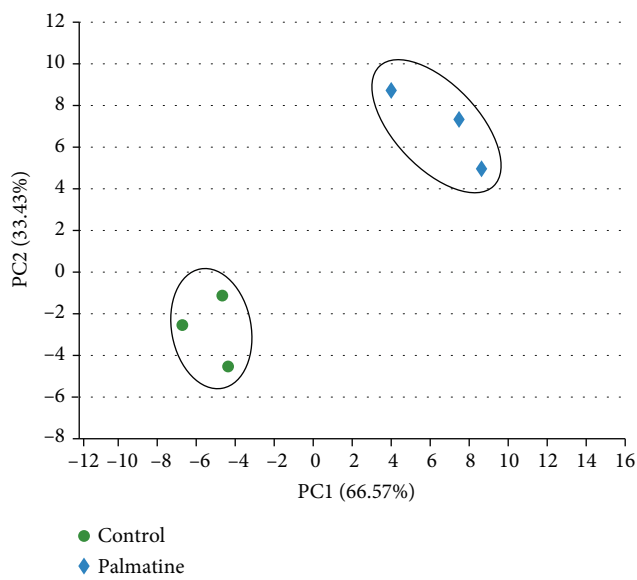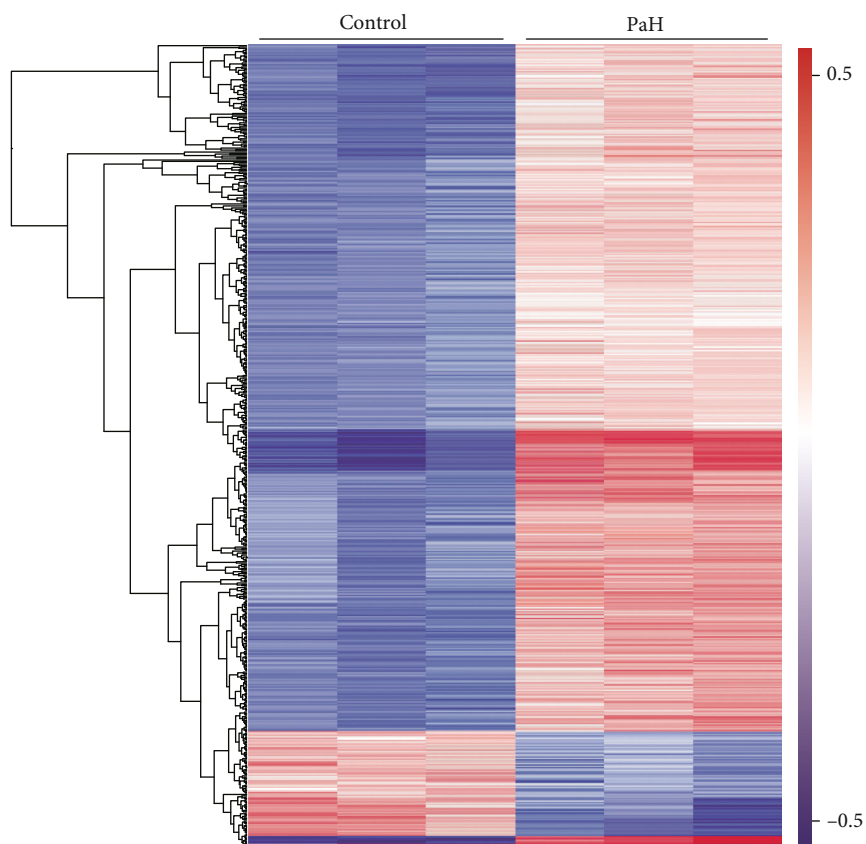
(d)

Figure 3: Transcriptome analysis of *C. elegans* treated with palmatine. (a) Principal component analysis (PCA) analysis. (b) The heatmap analysis of DEGs. (c) The annotation of DEGs in the palmatine-treated group classified on the basis of KEGG pathway analysis. (d) The significantly enriched DEG pathway. Synchronized L1-stage wild-type worms were cultured at 20 °C for two days with or without palmatine (0.2 mM) on NGM plates seeded with *OP50*, and three independent biological replicates for each group were collected for transcriptome sequencing.
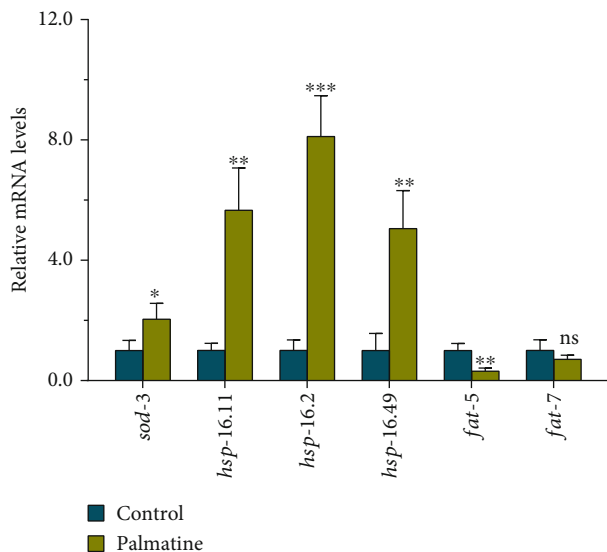
FIGURE 4: The verification of indicated target genes from RNA-Seq analysis by qPCR. L1-stage wild-type worms were cultured at 20°C for 48 h on NGM plates with or without palmatine (0.2 mM). Three independent biological replicates for each group were collected for real-time PCR. The result is presented as mean ± SD, and the statistical analysis was carried out with unpaired t-test. ns: no significant difference; $^*p < 0.05$; $^{**}p < 0.01$; $^{***}p < 0.001$.

sod-3 gene. When treated with palmatine for two days, the fluorescence level of sod-3p::GFP in the worms fed palmatine was markedly higher than that in the normal control worms, indicating that palmatine has the ability to enhance the expression of sod-3 in this nematode strain (Figures 5(a)–5(c)). In addition, we measured the enzyme activity of SOD in wild-type worms fed with or without palmatine (0.2 mM). As shown in Figure 5(d), the level of the SOD enzyme was significantly higher in the worms fed palmatine than in the normal control worms, further demonstrating that palmatine upregulated SOD expression. In addition, CAT is an essential antioxidant enzyme that can prevent cells from being poisoned by H_2O_2; we further examined the enzyme activity of CAT in wild-type worms fed palmatine (0.2 mM). As presented in Figure 5(e), the level of the CAT enzyme was significantly higher in the worms fed palmatine than in the normal control worms. In summary, these results indicate that palmatine has the ability to enhance antioxidant defense against oxidative stress caused by endogenous or exogenous stressors.

3.6. Involvement of the HSF-1 Transcription Factor in the Inhibition of Aβ Toxicity by Palmatine.

There is abundant evidence that the enhancement of protein folding and antiapoptotic capacity induced by elevations in HSP levels has the potential to improve therapeutic efficacy in neurodegenerative diseases [36, 37]. As shown by the transcriptome-based discovery of genes and pathways, the induced expression of sHSP may play the most important role in the inhibition of Aβ toxicity by palmatine. Therefore, we used the transgenic CL2070 strain expressing an hsp-16.2p::GFP transgenic reporter to explore the effects of palmatine on

the transcriptional change of the hsp-16.2 gene. After treatment with palmatine for two days, the fluorescence level of hsp-16.2p::GFP in the worms fed palmatine was significantly higher than that in the normal control worms, indicating that palmatine enhanced the expression of hsp-16.2 in this worm model (Figures 6(a)–6(c)). It is well known that the transcription factor HSF-1 coordinately activates the expression of shsp genes [36]. Thus, we further determined the protective effects of palmatine in C. elegans after hsf-1 RNAi to assess whether its inhibition of Aβ toxicity involved HSF-1. As presented in Figure 6(d), palmatine significantly alleviated the toxicity induced by Aβ when HT115 bacteria transformed with the empty vector L4440 were used, yet the alleviation of Aβ-induced toxicity disappeared when recombinant hsf-1 RNAi bacteria were used, indicating that the inhibition of Aβ toxicity by palmatine was mainly dependent on HSF-1. In summary, these results suggest that palmatine-mediated suppression of Aβ-induced toxicity relies on the regulator HSF-1 and subsequent upregulation of the expression of its target genes, such as hsp-12.11, hsp-16.2, and hsp-16.49.

3.7. Reductions in Aβ Deposits.

To investigate the inhibitory effects of palmatine on Aβ aggregation, ThS staining was performed in transgenic CL2006 nematodes to detect Aβ deposition, and then, the Aβ deposits in the worm head region were counted. Consistent with previous findings [32], the wild-type nematodes, used as negative controls, lacked ThS fluorescence because of the lack of Aβ deposition (Figure 7(a)). When Aβ-transgenic CL2006 worms were continuously cultured at 15°C, small amounts of Aβ deposits were formed due to the constitutive expression of the Aβ peptide in this strain (Figure 7(b)). After the worms were shifted to 20°C to induce Aβ peptide expression, the number of Aβ deposits per nematode was significantly increased compared to that in the worms incubated at 15°C, suggesting that elevated temperature can significantly enhance the expression of the Aβ peptide (Figure 7(c)). Compared to that in untreated CL2006 nematodes, Aβ deposition in nematodes treated with palmatine was obviously inhibited in the Aβ-transgenic worms (Figure 7(d)). The quantification of Aβ deposits also revealed significantly fewer deposits in palmatine-treated worms than in untreated worms (Figure 7(e)). Combined with the above experimental results indicating that palmatine can effectively delay the paralytic process of the CL2006 strain, these results indicate that palmatine can effectively inhibit Aβ aggregation and alleviate Aβ-induced toxicity.

3.8. Mitigation of the Aβ-mediated Lipid Metabolism Disorder.

Since transcriptome analysis suggested that lipid synthesis was obviously repressed by palmatine treatment, we used Oil Red O and Sudan Black B staining to detect the fat content in intestinal and hypodermal cells in wild-type and transgenic CL4176 nematodes (Figures 8(a)–8(d), staining with Oil Red O; Figure S1(a), S1(b), S1(c) and S1(d), staining with Sudan Black B) [33, 34]. Surprisingly, the content of lipid droplets was significantly increased after Aβ peptide expression was induced in transgenic
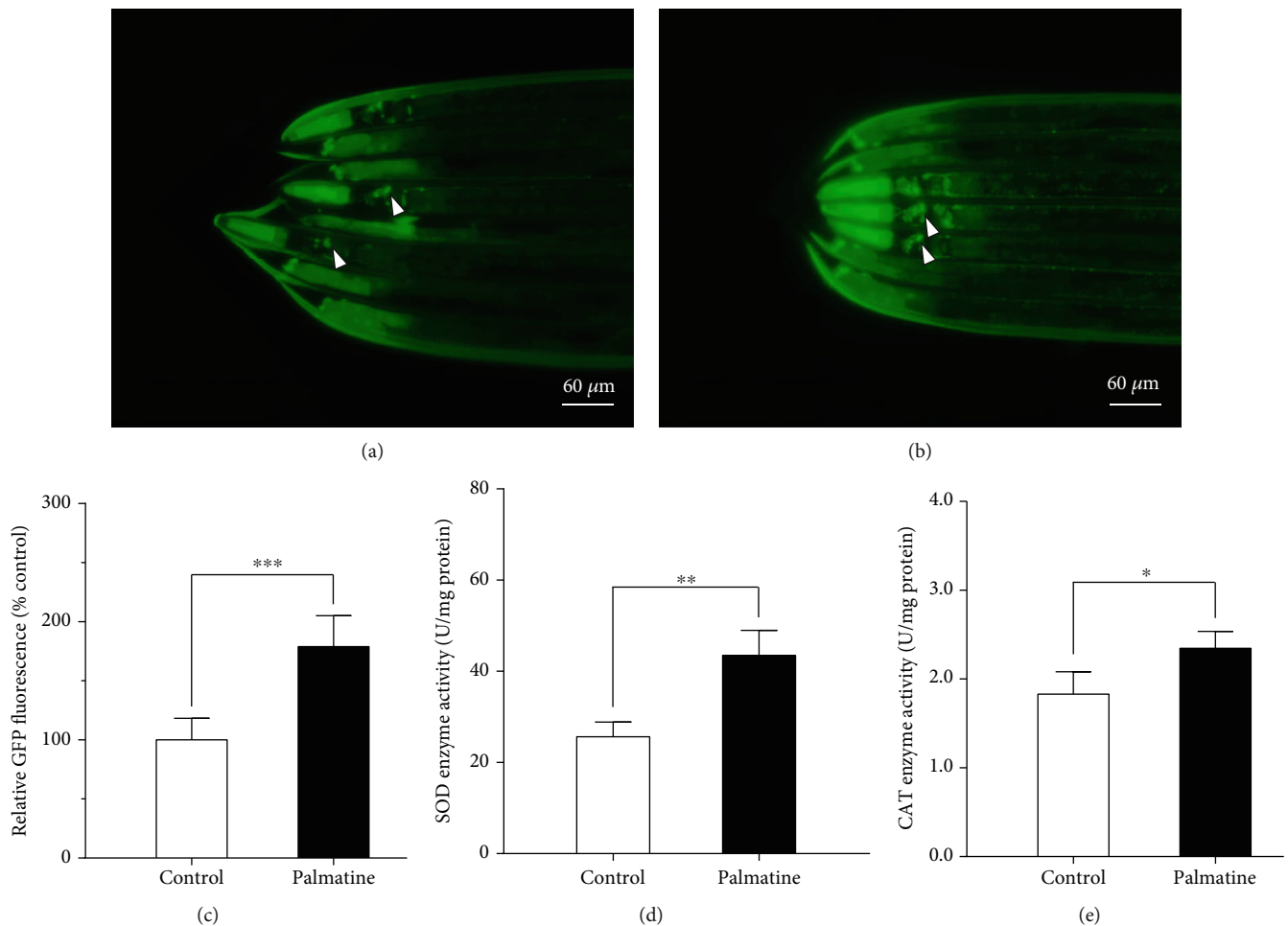
FIGURE 5: The effects of palmatine on *sod-3p*::GFP expression, SOD, and CAT activities. (a, b) The images of *sod-3p*::GFP treated with or without palmatine (0.2 mM). (c) Quantification of *sod-3p*::GFP fluorescence intensity. The transgenic CF1553 strain was cultured at 20°C for two days on NGM plates with or without palmatine (0.2 mM). The images were obtained by using a Mshot MF52 inverted fluorescence microscope. Quantified *sod-3p*::GFP intensity was done by ImageJ software. The result was displayed as mean ± SD ($n = 20$–25), and the statistical analysis was carried out with unpaired t-test. ***$p < 0.001$. (d) The effect of palmatine on the enzyme activity of SOD in wild-type worms. (e) The effect of palmatine on the enzyme activity of CAT in wild-type worms. Wild-type *worm*s were cultured from L1- to L4-stage at 20°C on NGM plates with or without palmatine (0.2 mM), and then, the worms were lysed to detect the enzyme activities of SOD and CAT. The result was displayed as mean ± SD, and the statistical analysis was done by unpaired t-test. *$p < 0.05$; **$p < 0.01$.

CL4176 worms compared with normal wild-type worms (Figure 8(e), staining with Oil Red O; Figure S1(e), staining with Sudan Black B), suggesting that Aβ aggregation and toxicity were accompanied by dysregulated lipid metabolism that caused excessive fat accumulation in Aβ-transgenic CL4176 nematodes. In addition, the effects of palmatine on fat accumulation in wild-type and transgenic CL4176 strains were evaluated. The palmatine-treated nematodes exhibited a lower lipid content than the wild-type nematodes (Figure 8(f), staining with Oil Red O; Figure S1(f), staining with Sudan Black B). Supplementation with palmatine in Aβ-transgenic CL4176 nematodes also significantly decreased the lipid content, as revealed by Oil Red O and Sudan Black B staining (Figure 8(g) and Figure S1(g)). These results indicate that palmatine reduces fat synthesis in wild-type nematodes and effectively inhibits lipid metabolism disorder induced by Aβ aggregation and toxicity in transgenic CL4176 nematodes.

4. Discussion

Although there is continuing debate about the Aβ hypothesis, the accumulated evidence supports the idea that steady-state imbalance between the production and clearance of Aβ is one of the important initiating events in the development of AD [38]. Elevated levels of Aβ oligomers have been found to drive the development of oxidative stress, neuroinflammation, synaptic loss, and nerve cell death [4]. Therefore, there is considerable interest in finding active compounds that can reduce Aβ aggregation and alleviate Aβ-induced toxicity [19, 21, 39]. Alkaloids are a large group of structurally complex natural products that exhibit a

(a)

(b)

(c)

(d)
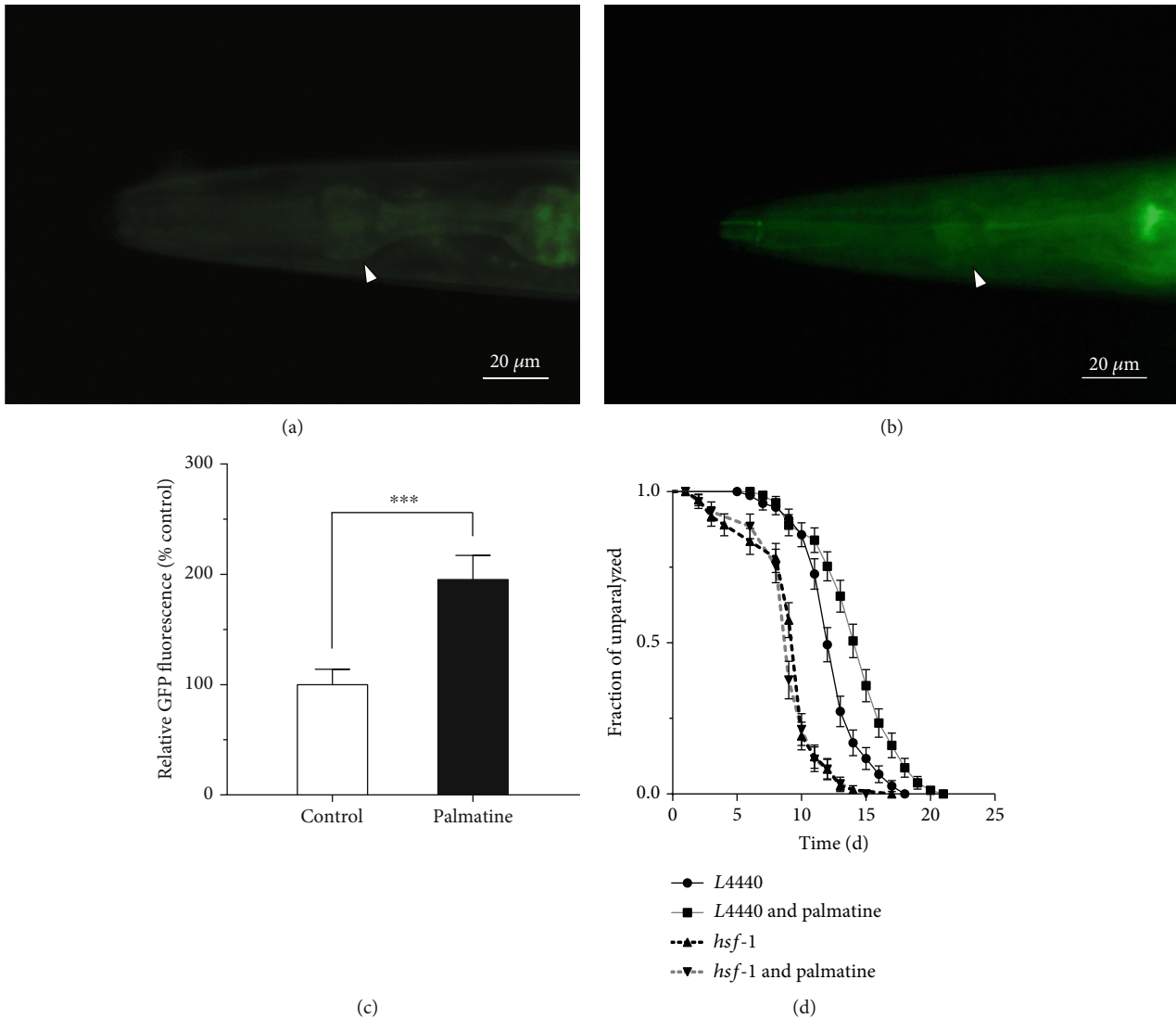
FIGURE 6: The effects of palmatine on *hsp-16.2p*::GFP expression and HSF-1 signaling pathway. (a, b) The images of *hsp-16.2p*::GFP in control and palmatine-treated groups. (c) Quantification of *hsp-16.2p*::GFP fluorescence intensity. The transgenic CL2070 strain was cultured at 20°C for two days on NGM plates with or without palmatine (0.2 mM). The images were obtained by using a Mshot MF52 inverted fluorescence microscope. Quantified *hsp-16.2p*::GFP intensity was done by ImageJ software. The result was displayed as mean ± SD ($n = 20$–25), and the statistical analysis was carried out with unpaired t-test. ***$p < 0.001$. (d) RNAi analysis of the change in inhibition of Aβ-toxicity by palmatine. L1-stage CL2006 strain was treated with or without palmatine (0.2 mM) at 15°C on NGM plates containing HT115 with *L4440* empty plasmid or *hsf-1* recombinant plasmid for 45 h and upshifted to 20°C for inducing Aβ peptide expression. The fraction of paralytic worm was counted every day until all were palsied. The result was displayed as the Kaplan-Meier survival curve and analyzed by using a log-rank test.

wide range of biological effects, including antioxidant and anti-inflammatory effects and Aβ production- and clearance-regulated effects [40–42]. In the present study, we confirmed that palmatine, a naturally occurring isoquinoline alkaloid, significantly suppressed Aβ-induced paralysis and displayed neuroprotective effects in the Aβ-transgenic CL2006 and CL4176 strains. The inhibition of the paralytic process was related to a reduction in Aβ oligomerization and alleviation of Aβ-induced toxicity [32]. Therefore, if there are similar mechanisms in humans and other species, the protective effects of palmatine against Aβ aggregation and toxicity may provide a rationale for its beneficial effects in humans.

The hallmarks of AD, such as Aβ oligomerization and neurofibrillary tangle formation, are intertwined with excessive ROS levels and elevated oxidative stress, which are considered to be the common effectors of the cascade of degenerative events [14, 43]. Previous research has shown that palmatine has the potential to inhibit oxidative stress by scavenging free radicals [27, 42]. In our study, palmatine reduced the elevated ROS levels derived from Aβ toxicity in the CL4176 strain. It is known that abiotic stresses, such as exposure to paraquat, often cause oxidative stress damage in organisms via overproduction of ROS [30, 31]. In the paraquat-induced oxidative damage model, we further

(a)

(b)

(c)

(d)

(e)
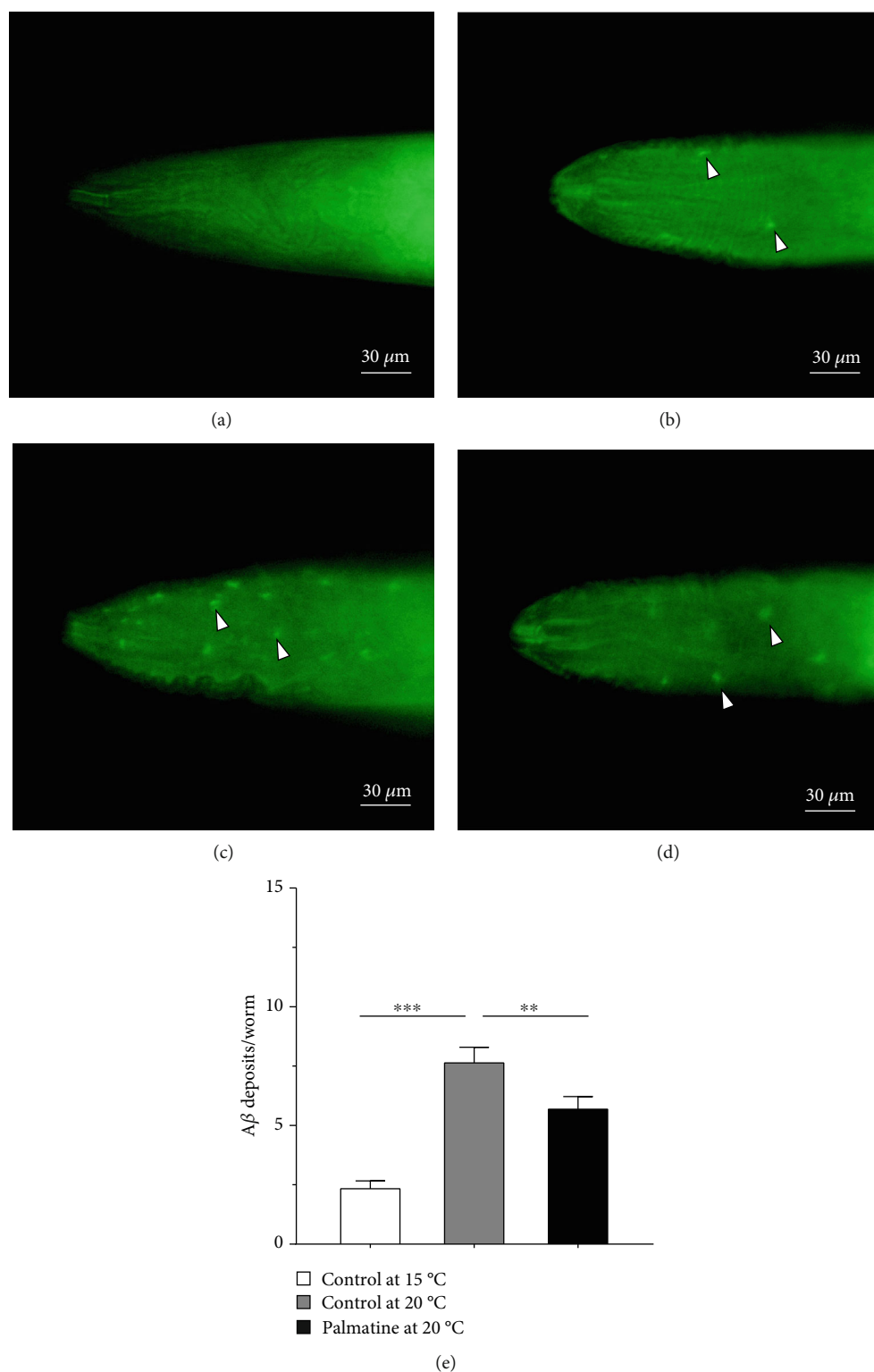
Figure 7: The effects of palmatine on Aβ deposits. (a) The image of wild-type nematodes. The worms were cultured at 20°C for 90 h and stained by ThS as negative control. (b) The images of Aβ-transgenic CL2006 nematodes at 15°C. The nematodes were continuously cultured at 15°C for 90 h and used for comparative analysis. (c, d) The images of Aβ-transgenic CL2006 nematodes treated with or without palmatine. The nematodes were incubated with or without palmatine (0.2 mM) at 20°C for 90 h. (d) Quantification of Aβ deposits. All the worms were collected and stained by ThS staining, and the fluorescence images were obtained by using a Mshot MF52 inverted fluorescence microscope. The depositions of Aβ were quantified after counting the ThS-positive deposits in the anterior pharyngeal bulb in each worm. The result was displayed as mean ± SD, and the statistical analysis was done by using a one-way ANOVA. $^{**}p < 0.05$; $^{***}p < 0.001$.
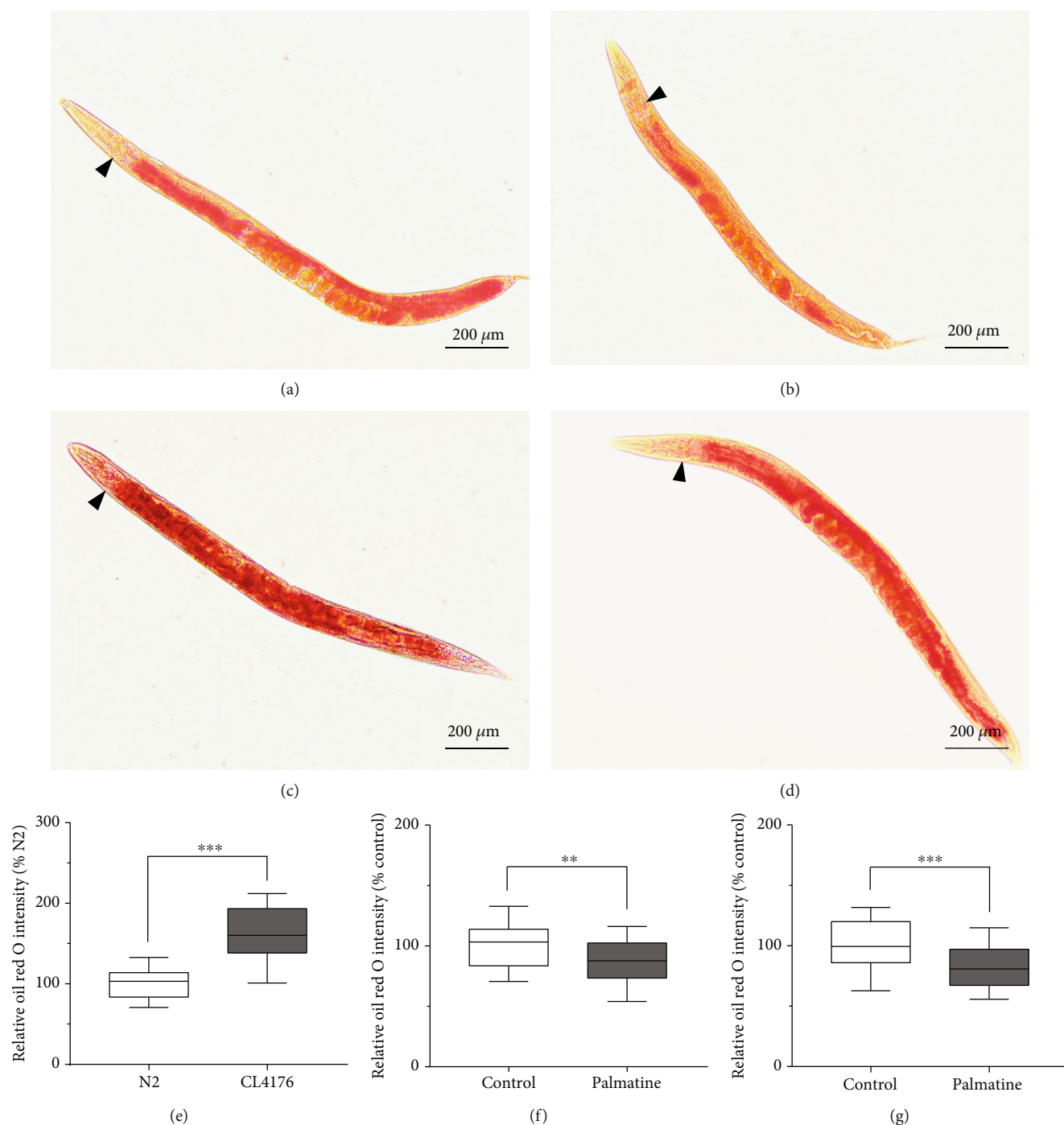
FIGURE 8: The effects of palmatine on fat accumulation. (a, b) The optical images upon Oil Red O staining in wild-type worms treated with or without palmatine (0.2 mM). (c, d) The optical images upon Oil Red O staining in CL4176 worms treated with or without palmatine (0.2 mM). (e) Comparative analysis of the Oil Red O intensity in wild-type and CL4176 worms treated with or without palmatine (0.2 mM). (f) Quantitative analysis of the Oil Red O intensity in wild-type worms treated with or without palmatine (0.2 mM). (g) Quantitative analysis of the Oil Red O intensity in CL4176 worms treated with or without palmatine (0.2 mM). L1-stage wild-type strain was cultured at 20°C for three days on NGM plates with or without palmatine (0.2 mM). Meanwhile, L1-stage CL4176 strain was cultured at 15°C for 36 h on NGM plates containing with or without palmatine (0.2 mM) and then placed at 23°C for another 36 h. The wild-type and CL4176 worms were collected and used for Oil Red O staining, respectively. The images were obtained by using a Mshot MF52 inverted fluorescence microscope. Quantified intensities were performed using ImageJ software. The results were displayed as mean ± SD ($n = 30$), and the statistical analyses were done by using an unpaired t-test. $^{*}p < 0.05$; $^{***}p < 0.001$.

demonstrated that palmatine treatment enhances resistance to oxidative stress. These results suggest that palmatine has an antioxidant effect against Aβ toxicity by reducing ROS production. However, palmatine did not affect the lifespan of wild-type nematodes, indicating that the protective mechanisms against oxidative stress may be distinct from mechanisms that delay senescence.

By transcriptome sequencing, we obtained candidate pathways and genes related to the effects of palmatine, including genes/pathways related to aging, detoxification, and lipid metabolism. In particular, the results highlighted that the expression of *shsp* was significantly upregulated by palmatine. These genes play important roles in modulating Aβ aggregation and toxicity [9, 10]. In addition, antioxidant-related genes, such as *sod-3*, were also activated, which may have enhanced antioxidant defense to protect cells from oxidative damage [44]. Palmatine has been shown to reduce the ROS level in the transgenic CL4176 strain and alleviate the oxidative damage caused by paraquat-induced oxidative stress. The elimination of excessive ROS is mediated by a range of antioxidant defense systems, which require the participation of antioxidant enzymes such as SOD and CAT [44, 45]. Our study confirmed that palmatine increases the fluorescence intensity of *sod-3p*::GFP in transgenic CF1553 nematodes and the activities of SOD and CAT in wild-type nematodes. These results agree with previous findings that alkaloids might activate the cellular antioxidant defense system against oxidative insults [20, 46, 47]. Together, these studies suggest that palmatine reduces the oxidative stress caused by Aβ toxicity by eliminating ROS and indicate a correlation between the enhancement of antioxidant defense and the alleviation of Aβ toxicity in transgenic nematodes.

Protein aggregation is one of the important characteristics of neurodegenerative diseases such as AD [43, 48]. HSP family members are the key cellular components that maintain protein homeostasis under unfavorable conditions, which might effectively block the formation of protein aggregates and prevent the occurrence and development of neurodegenerative diseases [10, 49]. Studies have indicated that a lack of sHSP aggravates the AD phenotype, whereas increased expression improves the symptoms of AD [50]. In the present study, palmatine upregulated the expression of *shsp* genes, including *hsp-16.11*, *hsp-16.2*, and *hsp-16.49*, in wild-type nematodes and enhanced the *hsp-16.2p*::GFP fluorescence intensity in transgenic CL2070 nematodes. As such, it is possible that the increased expression of sHSP suppressed protein aggregation and alleviated Aβ toxicity, suggesting that sHSP plays important roles in the neuroprotective effects of palmatine. It is known that the expression of sHSP is primarily determined by the transcription factor HSF-1, while decreased activity of HSF-1 has been shown to be a key part of the deleterious cascade in neurodegenerative disease [36, 37]. Our study showed that knockdown of *hsf-1* using RNAi not only significantly accelerated the process of paralysis but also completely abolished palmatine-induced inhibition of Aβ toxicity in transgenic CL2006 nematodes. These results are in accordance with previous studies showing that HSF-1 participates in the inhibition of Aβ tox-

icity [6, 37] and suggest that the increased resistance of worms treated with palmatine is closely related to HSF-1. Therefore, palmatine-mediated inhibition of Aβ toxicity involves the regulator HSF-1 and regulation of the expression of its target genes, such as *hsp-16.11*, *hsp-16.2*, and *hsp-16.49*.

Research has indicated that alkaloids have the potential to inhibit and prevent AD through both cholinesterase and Aβ pathways and through improvement of antioxidant capacity [20–23, 42]. It is worth noting that unlike the activation of antioxidant defense to alleviate Aβ-induced oxidative stress, the palmatine-induced upregulation of sHSP is associated with the inhibition of Aβ aggregation and breakdown of toxic oligomers [37, 51]. Research has shown the occurrence of a series of morphological transitions of aggregation, including the assembly of Aβ monomers into oligomers and fibrils and the eventual formation of extracellular Aβ plaque deposits [52]. Among the aggregates, Aβ oligomers have been identified as potent cytotoxins that initiate pathological events in AD [5]. Active substances, such as *Ginkgo biloba* extract EGb 761 and ginkgolide A, may convert toxic Aβ oligomers into nontoxic Aβ monomers to delay the paralysis of Aβ-transgenic nematodes [32]. It has been reported that palmatine chloride treatment *in vitro* can suppress the aggregation of tau and break down preformed tau aggregates [53]. In this work, palmatine delayed the process of paralysis and reduced Aβ deposition in transgenic CL2006 nematodes, suggesting that its neuroprotective effects *in vivo* may be achieved via effects on the early stages of the linear pathway, especially the formation of toxic Aβ oligomers.

Palmatine is reported to have the ability to regulate lipid metabolism and to exert anti-obesity effects [24, 27]. In this work, our study found that the aggregation of Aβ in transgenic CL4176 nematodes not only led to a paralytic phenotype but also accompanied excessive fat accumulation caused by Aβ toxicity-induced lipid metabolism disorder. Notably, palmatine markedly decreased the fat content both in the wild-type worms and in the Aβ-transgenic worms with high fat accumulation. A previous study has indicated that oleic acid is the substrate for the production of triacylglycerol and cholesteryl ester and that inhibiting the conversion of saturated stearic acid to oleic acid can contribute to reducing the fat content [54]. The current research showed that palmatine downregulated the expression of a stearoyl-CoA desaturase, *fat-5*, in wild-type worms, which is believed to play a critical role in the transformation of stearic acid into oleic acid [55]. However, overall, considering the modulation of antioxidant defense and sHSP expression, the alleviation of lipid disorder by palmatine is likely attributable not only to the reduction in fat synthesis but also to the inhibition of Aβ aggregation and toxicity, which jointly maintain metabolic homeostasis in transgenic CL4176 nematodes.

5. Conclusion

In the present study, palmatine suppressed Aβ-induced paralysis and reduced the elevated ROS levels in Aβ-transgenic nematodes, thus exhibiting neuroprotective effects

against Aβ toxicity. Based on DEG analysis, real-time PCR, and verification in transgenic CF1553 and CL2070 strains, our study demonstrated that the inhibition of Aβ toxicity by palmatine was attributable to the free radical-scavenging capacity and to the upregulation of the expression of resistance-related genes such as *sod-3* and *shsp*. In particular, the expression of *shsp*, which requires the involvement of the transcription factor HSF-1, played important roles in protecting cells from Aβ toxicity. In addition, we found that palmatine reduced Aβ deposition and mitigated excessive fat accumulation in the Aβ-transgenic CL2006 and CL4176 strains, respectively. In summary, these studies suggest that palmatine exerts neuroprotective effects through the modulation of antioxidant defense and sHSP expression to support homeostasis in Aβ-transgenic nematodes. The findings provide valuable targets for the prevention and treatment of AD.

Data Availability

The data that used to support the findings of this work are obtained from the corresponding author on reasonable request.

Conflicts of Interest

The authors have no competing interest.

Authors' Contributions

Weizhang Jia and Qina Su contributed equally to this work.

Acknowledgments

Supplementary Materials

Figure S1: the effects of palmatine on fat accumulation through Sudan black B staining in the wild-type and CL4176 *C. elegans*. (Supplementary Materials)

References

[1] J. M. Tarasoff-Conway, R. O. Carare, R. S. Osorio et al., "Clearance systems in the brain–implications for Alzheimer disease," *Nature Reviews Neurology*, vol. 11, no. 8, pp. 457–470, 2015.

[2] M. Ries and M. Sastre, "Mechanisms of Aβ clearance and degradation by glial cells," *Frontiers in Aging Neuroscience*, vol. 8, p. 160, 2016.

[3] D. G. Jo, T. V. Arumugam, H. N. Woo et al., "Evidence that γ-secretase mediates oxidative stress-induced β-secretase expression in Alzheimer's disease," *Neurobiology of Aging*, vol. 31, no. 6, pp. 917–925, 2010.

[4] A. Butterfield and D. Boyd-Kimball, "Oxidative stress, amyloid-β peptide, and altered key molecular pathways in the pathogenesis and progression of Alzheimer's disease," *Journal of Alzheimer's Disease*, vol. 62, no. 3, pp. 1345–1367, 2018.

[5] K. L. Viola and W. L. Klein, "Amyloid β oligomers in Alzheimer's disease pathogenesis, treatment, and diagnosis," *Acta Neuropathologica*, vol. 129, no. 2, pp. 183–206, 2015.

[6] K. A. Steinkraus, E. D. Smith, C. Davis et al., "Dietary restriction suppresses proteotoxicity and enhances longevity by an *hsf-1*-dependent mechanism in *Caenorhabditis elegans*," *Aging Cell*, vol. 7, no. 3, pp. 394–404, 2008.

[7] A. L. Hsu, C. T. Murphy, C. Kenyon et al., "Regulation of aging and age-related disease by DAF-16 and heat-shock factor," *Science*, vol. 300, no. 5622, pp. 1142–1145, 2003.

[8] M. Haslbeck, T. Franzmann, D. Weinfurtner, and J. Buchner, "Some like it hot: the structure and function of small heat-shock proteins," *Nature Structural & Molecular Biology*, vol. 12, no. 10, pp. 842–846, 2005.

[9] M. M. M. Wilhelmus, W. C. Boelens, I. Otte-Höller et al., "Small heat shock protein HspB8: its distribution in Alzheimer's disease brains and its inhibition of amyloid-β protein aggregation and cerebrovascular amyloid-β toxicity," *Acta Neuropathologica*, vol. 111, no. 2, pp. 139–149, 2006.

[10] Z. Zhu and G. Reiser, "The small heat shock proteins, especially HspB4 and HspB5 are promising protectants in neurodegenerative diseases," *Neurochemistry International*, vol. 115, pp. 69–79, 2018.

[11] G. Cenini, A. Lloret, and R. Cascella, "Oxidative stress in neurodegenerative diseases: from a mitochondrial point of view," *Oxidative Medicine and Cellular Longevity*, vol. 2019, Article ID 2105607, 18 pages, 2019.

[12] E. Niedzielska, I. Smaga, M. Gawlik et al., "Oxidative stress in neurodegenerative diseases," *Molecular Neurobiology*, vol. 53, no. 6, pp. 4094–4125, 2016.

[13] A. Smeriglio, A. Calderaro, M. Denaro, G. Laganà, and E. Bellocco, "Effects of isolated isoflavones intake on health," *Current Medicinal Chemistry*, vol. 26, no. 27, pp. 5094–5107, 2019.

[14] C. Y. Kim, C. Lee, G. H. Park, and J. H. Jang, "Neuroprotective effect of epigallocatechin-3-gallate against beta-amyloid-induced oxidative and nitrosative cell death via augmentation of antioxidant defense capacity," *Archives of Pharmacal Research*, vol. 32, no. 6, pp. 869–881, 2009.

[15] A. Smeriglio, S. Alloisio, F. M. Raimondo et al., "Essential oil of _Citrus lumia_ Risso: Phytochemical profile, antioxidant properties and activity on the central nervous system," *Food and Chemical Toxicology*, vol. 119, pp. 407–416, 2018.

[16] M. C. Barbalace, M. Malaguti, L. Giusti, A. Lucacchini, S. Hrelia, and C. Angeloni, "Anti-inflammatory activities of marine algae in neurodegenerative diseases," *International Journal of Molecular Sciences*, vol. 20, no. 12, p. 3061, 2019.

[17] A. Smeriglio, M. Denaro, V. D'Angelo, M. P. Germanò, and D. Trombetta, "Antioxidant, anti-inflammatory and anti-angiogenic properties of Citrus lumia juice," *Frontiers in Pharmacology*, vol. 11, p. 593506, 2020.

[18] L. Cornara, J. Xiao, and B. Burlando, "Therapeutic potential of temperate forage legumes: a review," *Critical Reviews in Food Science and Nutrition*, vol. 56, no. sup1, pp. S149–S161, 2016.

[19] C. Angeloni and D. Vauzour, "Natural products and neuroprotection," *International Journal of Molecular Sciences*, vol. 20, no. 22, p. 5570, 2019.

[20] M. Kolahdouzan and M. J. Hamadeh, "The neuroprotective effects of caffeine in neurodegenerative diseases," *CNS Neuroscience & Therapeutics*, vol. 23, no. 4, pp. 272–290, 2017.

[21] E. J. Seo, N. Fischer, and T. Efferth, "Phytochemicals as inhibitors of NF-κB for treatment of Alzheimer's disease," *Pharmacological Research*, vol. 129, pp. 262–273, 2018.

[22] C. Zhao, P. Su, C. Lv et al., "Berberine alleviates amyloid β-induced mitochondrial dysfunction and synaptic loss," *Oxidative Medicine and Cellular Longevity*, vol. 2019, Article ID 7593608, 11 pages, 2019.

[23] D. Janitschke, C. Nelke, A. A. Lauer et al., "Effect of caffeine and other methylxanthines on Aβ-homeostasis in SH-SY5Y cells," *Biomolecules*, vol. 9, no. 11, p. 689, 2019.

[24] J. Long, J. Song, L. Zhong, Y. Liao, L. Liu, and X. Li, "Palmatine: a review of its pharmacology, toxicity and pharmacokinetics," *Biochimie*, vol. 162, pp. 176–184, 2019.

[25] Y. Feng and X. Wang, "Antioxidant Therapies for Alzheimer's Disease," *Oxidative Medicine and Cellular Longevity*, vol. 2012, Article ID 472932, 17 pages, 2012.

[26] L. Wang, Y. Zhao, Y. Zhang et al., "Online screening of acetylcholinesterase inhibitors in natural products using monolith-based immobilized capillary enzyme reactors combined with liquid chromatography-mass spectrometry," *Journal of Chromatography A*, vol. 1563, pp. 135–143, 2018.

[27] D. Tarabasz and W. Kukula-Koch, "Palmatine: a review of pharmacological properties and pharmacokinetics," *Phytotherapy Research*, vol. 34, no. 1, pp. 33–50, 2020.

[28] L. Ma, Y. Zhao, Y. Chen, B. Cheng, A. Peng, K. Huang et al., "_Caenorhabditis elegans_ as a model system for target identification and drug screening against neurodegenerative diseases," *European Journal of Pharmacology*, vol. 819, pp. 169–180, 2018.

[29] P. F. Boasquívis, G. M. M. Silva, F. A. Paiva, R. M. Cavalcanti, C. V. Nunez, and R. de Paula Oliveira, "Guarana (*Paullinia cupana*) extract protects *Caenorhabditis elegans* models for Alzheimer disease and Huntington disease through activation of antioxidant and protein degradation pathways," *Oxidative Medicine and Cellular Longevity*, vol. 2018, Article ID 9241308, 16 pages, 2018.

[30] S. Zhao, Q. Cheng, Q. Peng et al., "Antioxidant peptides derived from the hydrolyzate of purple sea urchin (*Strongylocentrotus nudus*) gonad alleviate oxidative stress in _Caenorhabditis elegans_," *Journal of Functional Foods*, vol. 48, pp. 594–604, 2018.

[31] W. Jia, Q. Peng, L. Su et al., "Novel bioactive peptides from *Meretrix meretrix* protect Caenorhabditis elegans against free radical-induced oxidative stress through the stress response factor DAF-16/FOXO," *Marine Drugs*, vol. 16, no. 11, p. 444, 2018.

[32] Y. Wu, Z. Wu, P. Butko et al., "Amyloid- -Induced pathological behaviors are suppressed by Ginkgo biloba extract EGb 761 and ginkgolides in transgenic *Caenorhabditis elegans*," *Journal of Neuroscience*, vol. 26, no. 50, pp. 13102–13113, 2006.

[33] H. Peng, Z. Wei, H. Luo et al., "Inhibition of fat accumulation by Hesperidin in *Caenorhabditis elegans*," *Journal of Agricultural and Food Chemistry*, vol. 64, no. 25, pp. 5207–5214, 2016.

[34] X. Yu, Q. Su, T. Shen, Q. Chen, Y. Wang, and W. Jia, "Antioxidant peptides from *Sepia esculenta* hydrolyzate attenuate oxidative stress and fat accumulation in Caenorhabditis elegans," *Marine Drugs*, vol. 18, no. 10, p. 490, 2020.

[35] A. Subramanian, R. Narayan, S. M. Corsello et al., "A next generation connectivity map: L1000 platform and the first

[36] D. W. Neef, A. M. Jaeger, and D. J. Thiele, "Heat shock transcription factor 1 as a therapeutic target in neurodegenerative diseases," *Nature Reviews Drug Discovery*, vol. 10, no. 12, pp. 930–944, 2011.

[37] R. Gomez-Pastor, E. T. Burchfiel, and D. J. Thiele, "Regulation of heat shock transcription factors and their roles in physiology and disease," *Nature Reviews Molecular Cell Biology*, vol. 19, no. 1, pp. 4–19, 2018.

[38] C. Julien, C. Tomberlin, C. M. Roberts et al., "*In vivo* induction of membrane damage by β-amyloid peptide oligomers," *Acta Neuropathologica Communications*, vol. 6, no. 1, p. 131, 2018.

[39] C. Angeloni, M. C. Barbalace, and S. Hrelia, "Icariin and its metabolites as potential protective phytochemicals against Alzheimer's disease," *Frontiers in Pharmacology*, vol. 10, 2019.

[40] L. S. Li, Y. L. Lu, J. Nie et al., "Dendrobium nobileLindl alkaloid, a novel autophagy inducer, protects against axonal degeneration induced by Aβ25-35in hippocampus neurons *in vitro*," *CNS Neuroscience & Therapeutics*, vol. 23, no. 4, pp. 329–340, 2017.

[41] K. Macáková, R. Afonso, L. Saso, and P. Mladěnka, "The influence of alkaloids on oxidative stress and related signaling pathways," *Free Radical Biology and Medicine*, vol. 134, pp. 429–444, 2019.

[42] H. A. Jung, B. S. Min, T. Yokozawa, J. H. Lee, Y. S. Kim, and J. S. Choi, "Anti-Alzheimer and antioxidant activities of coptidis rhizoma alkaloids," *Biological and Pharmaceutical Bulletin*, vol. 32, no. 8, pp. 1433–1438, 2009.

[43] G. S. Bloom, "Amyloid-β and tau: the trigger and bullet in Alzheimer disease pathogenesis," *JAMA Neurology*, vol. 71, no. 4, pp. 505–508, 2014.

[44] N. Braidy, S. Selvaraju, M. M. Essa et al., "Neuroprotective effects of a variety of pomegranate juice extracts against MPTP-induced cytotoxicity and oxidative stress in human primary neurons," *Oxidative Medicine and Cellular Longevity*, vol. 2013, Article ID 685909, 12 pages, 2013.

[45] A. Smeriglio, D. Barreca, E. Bellocco, and D. Trombetta, "Chemistry, pharmacology and health benefits of anthocyanins," *Phytotherapy Research*, vol. 30, no. 8, pp. 1265–1286, 2016.

[46] K. Malczewska-Jaskóła, B. Jasiewicz, and L. Mrówczyńska, "Nicotine alkaloids as antioxidant and potential protective agents against _in vitro_ oxidative haemolysis," *Chemico-Biological Interactions*, vol. 243, pp. 62–71, 2016.

[47] B. C. Azevedo, M. Roxo, M. C. Borges et al., "Antioxidant activity of an aqueous leaf extract from *Uncaria tomentosa* and its major alkaloids mitraphylline and isomitraphylline in *Caenorhabditis elegans*," *Molecules*, vol. 24, no. 18, p. 3299, 2019.

[48] N. Sami, S. Rahman, V. Kumar et al., "Protein aggregation, misfolding and consequential human neurodegenerative diseases," *International Journal of Neuroscience*, vol. 127, no. 11, pp. 1047–1057, 2017.

[49] R. Bakthisaran, R. Tangirala, and C. M. Rao, "Small heat shock proteins: role in cellular functions and pathology," *Biochimica et Biophysica Acta*, vol. 1854, no. 4, pp. 291–319, 2015.

[50] L. Vendredy, E. Adriaenssens, and V. Timmerman, "Small heat shock proteins in neurodegenerative diseases," *Cell Stress & Chaperones*, vol. 25, no. 4, pp. 679–699, 2020.

[51] J. M. Webster, A. L. Darling, V. N. Uversky, and L. J. Blair, "Small heat shock proteins, big impact on protein aggregation

in neurodegenerative disease," *Frontiers in Pharmacology*, vol. 10, p. 1047, 2019.

[52] D. R. Thal, J. Walter, T. C. Saido, and M. Fändrich, "Neuropathology and biochemistry of Aβ and its aggregates in Alzheimer's disease," *Acta Neuropathologica*, vol. 129, no. 2, pp. 167–182, 2015.

[53] E. Haj, Y. Losev, V. Guru KrishnaKumar et al., "Integrating _in vitro_ and _in silico_ approaches to evaluate the "dual functionality" of palmatine chloride in inhibiting and disassembling Tau- derived VQIVYK peptide fibrils," *Biochimica et Biophysica Acta*, vol. 1862, no. 7, pp. 1565–1575, 2018.

[54] A. D. Barbosa, D. B. Savage, and S. Siniossoglou, "Lipid droplet-organelle interactions: emerging roles in lipid metabolism," *Current Opinion in Cell Biology*, vol. 35, pp. 91–97, 2015.

[55] S. M. Anderson, H. K. Cheesman, N. D. Peterson, J. E. Salisbury, A. A. Soukas, and R. Pukkila-Worley, "The fatty acid oleate is required for innate immune activation and pathogen defense in *Caenorhabditis elegans*," *PLoS Pathogens*, vol. 15, no. 6, article e1007893, 2019.

Review Article

The Beneficial Role of Natural Endocrine Disruptors: Phytoestrogens in Alzheimer's Disease

Anita Domańska [iD],[1,2] **Arkadiusz Orzechowski** [iD],[2†] **Anna Litwiniuk** [iD],[1] **Małgorzata Kalisz** [iD],[1] **Wojciech Bik** [iD],[1] and **Agnieszka Baranowska-Bik** [iD][3]

[1]*Department of Neuroendocrinology, Centre of Postgraduate Medical Education, Marymoncka 99/103, 01-813 Warsaw, Poland*
[2]*Department of Physiological Sciences, Institute of Veterinary Medicine, Warsaw University of Life Sciences-SGGW, Nowoursynowska 166, 02-787 Warsaw, Poland*
[3]*Department of Endocrinology, Centre of Postgraduate Medical Education, Cegłowska 80, 01-809 Warsaw, Poland*
[†]*Deceased*

Correspondence should be addressed to Anita Domańska; an_ita@wp.pl

Alzheimer's disease (AD) is the most common form of dementia with a growing incidence rate primarily among the elderly. It is a neurodegenerative, progressive disorder leading to significant cognitive loss. Despite numerous pieces of research, no cure for halting the disease has been discovered yet. Phytoestrogens are nonestradiol compounds classified as one of the endocrine-disrupting chemicals (EDCs), meaning that they can potentially disrupt hormonal balance and result in developmental and reproductive abnormalities. Importantly, phytoestrogens are structurally, chemically, and functionally akin to estrogens, which undoubtedly has the potential to be detrimental to the organism. What is intriguing, although classified as EDCs, phytoestrogens seem to have a beneficial influence on Alzheimer's disease symptoms and neuropathologies. They have been observed to act as antioxidants, improve visual-spatial memory, lower amyloid-beta production, and increase the growth, survival, and plasticity of brain cells. This review article is aimed at contributing to the collective understanding of the role of phytoestrogens in the prevention and treatment of Alzheimer's disease. Importantly, it underlines the fact that despite being EDCs, phytoestrogens and their use can be beneficial in the prevention of Alzheimer's disease.

1. Alzheimer's Disease

1.1. Introduction. Nowadays, dementia is estimated to affect over 45 million people worldwide and is believed to reach up to 115 million by 2050 [1]. Alzheimer's disease (AD) is a complex, neurodegenerative disorder of the central nervous system (CNS), which accounts for up to 70% of dementias [2]. Dementia can also be caused by other factors, such as brain injuries, vascular disorders, and numerous other diseases, e.g., Parkinson's disease (PD), Huntington's disease (HD), or Creutzfeldt-Jakob disease (CJD).

Alzheimer's disease was first identified more than a century ago by Alois Alzheimer, a German psychiatrist. In 1906, he described a case of dementia observed in a 50-year-old woman. He continued to track the progress of her disease until 1906 when she died [3]. He found at autopsy of her brain characteristic pathological microscopic changes, known today as visible gliosis around numerous senile plaques (SP) and abundant neurofibrillary tangles (NFT) [4]. Currently, about 35 million patients in the world are suffering from Alzheimer's disease.

The etiology and pathogenesis of Alzheimer's disease are complex and despite the efforts of researchers, the mechanisms are still not transparent. Much is yet to be discovered when it comes to precise biological processes. The major challenges include reasons why the disease progresses faster in some patients and slower in others, and finally, how to prevent, stop, or at least slow down the progression of AD [5]. The majority of AD patients (>95%) have sporadic onset, and less than 5% of the cases are related to dominant

gene mutations, including APP, PS1, or PS2 genes [3]. Notably, AD is a disease that begins much earlier before its symptoms arise, and according to Alzheimer's Association [5], it can be even up to 20 years earlier. Thus, early detection seems to be crucial for intervention in coping with the disease.

1.2. Symptoms and Stages of Alzheimer's Disease. Alzheimer's disease causes both cognitive and noncognitive symptoms and signs. Importantly, the symptoms and progress of AD vary among individuals. This heterogeneity is particularly challenging to patients, their families, and clinicians, considering the difficulty in forecast and recognition functional impairment and other upcoming symptoms [6]. Importantly, AD is characterized by neuronal degeneration in selective brain regions involved in cognition (hippocampus, entorhinal, and frontal cortices) and emotional behaviors (amygdala, prefrontal cortex, and hypothalamus). Current research identifies three stages of AD: preclinical Alzheimer's disease, mild cognitive impairment (MCI) due to Alzheimer's disease, and dementia due to Alzheimer's disease. Symptoms and signs of the disease are present in the last two stages, but importantly with a varying degree [7].

Preclinical AD is a stage in which patients have measurable and significant structural changes in the brain, composition of cerebrospinal fluid (CSF), and presence of blood biomarkers. On the other hand, symptoms such as memory loss are not developed at this point. Importantly, not all individuals with raised Alzheimer's biomarkers progress to develop dementia or mild cognitive decline, but most of them do [8]. Because of no perceptible symptoms, this stage of the disease is notably hard to detect.

MCI due to AD is a stage in which biomarkers such as elevated levels of beta-amyloid protein or neurofilament light chain (NFL) in CSF are raised. Moreover, an individual in this stage of the disease shows cognitive decline much greater than the one expected for her/his age. Importantly, the decline does not always impede patients' everyday activities.

Dementia due to AD is a stage in which prominent thinking, memory, and behavioral impairment affect an individual's daily life. Additionally, evidence of AD-related brain changes is also observed. Patients suffering from the mild stage of Alzheimer's dementia are frequently able to function autonomously in many areas, such as participating in their favorite activities, driving, and working. However, they should be assisted with some tasks to maximize their safety. In the next stage, the moderate stage of Alzheimer's dementia, individuals may find it hard to communicate and conduct their daily tasks, such as taking a shower, dressing up, or brushing their teeth. In this stage, visible changes in their behavior and personality are observed. For instance, they may get irritated easily, become anxious, fearful, or overly suspicious. The last stage of AD is the severe stage of Alzheimer's dementia. Patients suffering from this stage of the disease need help in every area of their lives and are likely to require around-the-clock care. Unambiguous AD diagnosis is classically made postmortem, once neuropathology has confirmed the specific senile plaque and fibrillary tangle deposition in an individual with clinical diagnostic symptoms observed during life.

1.3. Hypotheses of the Onset. There are numerous hypotheses when and how it comes to the induction and the beginning of AD. The ones which are considered to be crucial are the inflammation hypothesis, cholinergic hypothesis, tau hypothesis, amyloid β (Aβ) cascade hypothesis, and oxidative stress hypothesis.

1.3.1. Inflammation Hypothesis. The inflammation hypothesis suggests that reactive gliosis with coexisting neuroinflammation should be considered crucial in AD pathology. The theory assumes that reactive microglia and astrocytes which surround amyloid plaques secrete numerous proinflammatory cytokines. Thus, they are regarded as an early, prime mover in AD advancement [9].

1.3.2. Cholinergic Hypothesis. In turn, the cholinergic hypothesis is drawn from observations of noticeable cholinergic neuronal cell loss in AD postmortem brains [10]. Besides, neuroscientists confirm the significance of cholinergic neurotransmission in cognitive function, especially in attention and memory encoding [11]. Thus, this hypothesis procured the successful approval of cholinesterase inhibitors in clinical practice [12].

1.3.3. Tau Hypothesis. The tau hypothesis is related to a microtubule-associated protein, tau, which works as a reinforcement for a cytoskeleton in an axon. Under pathological conditions, such as Alzheimer's disease, tau proteins tend to aggregate forming intracellular NFT, thus weakening the cytoskeleton. As a result, not only the structure of the cell is deformed but also the intracellular transport of neurotransmitters encapsulated in vesicles is severely impaired. The aforementioned processes inevitably lead to neurodegeneration [13].

1.3.4. Amyloid β Hypothesis. Another important hypothesis concerns the Aβ protein as the main trigger of AD development. Amyloid-beta is produced by endoproteolysis of amyloid precursor protein (APP), encoded by the APP gene. Depending on enzymes that take part in the process, the processing of APP can be divided into two pathways, the nonamyloidogenic pathway and the amyloidogenic pathway [14]. The first pathway, also called the α pathway, is conducted by two main enzymes α-secretase and γ-secretase. As a result, soluble APP (sAPP) is produced, which is not harmful to the organism. The second pathway is called the β pathway. In this process, APP is hydrolyzed by β-secretase (BACE1) and then by γ-secretase, and in consequence, insoluble and toxic Aβ is created. Under normal conditions, Aβ protein is formatted in a very small quantity, since APP cleavage is mainly based on the α pathway. Importantly, a limited amount of APP is processed via the second pathway but the Aβ form is efficiently eliminated by the immune system. In unusual conditions, i.e., some mutations of *APP* gene, such as the Lys670Asn/Met671Leu (*Swedish mutation*), APP is prone to be processed by the β pathway, resulting in an excessive accumulation of insoluble Aβ and

eventually the development of senile plaques [15]. Importantly, Aβ has been the primary target for disease-modifying AD therapies for decades, but so far, Aβ-focused approaches have produced disappointing results in clinical experiments.

1.3.5. Oxidative Stress Hypothesis. Undoubtedly, oxidative stress plays an important role in the pathogenesis of AD. The brain exploits more oxygen than any other organ, and mitochondrial respiration is essential for neurons. Nevertheless, the high demand for oxygen increases the threat of reactive oxygen species (ROS) generation. Numerous researches support the concept that oxidative stress and nitrosative stress have a causative role in the pathogenesis of AD leading to the damage of fundamental cellular elements such as nucleic acids, lipids, and proteins [16]. Additionally, elevated levels of Aβ have been reported to be associated with increased concentrations of oxidation products formed from the aforementioned substances. By contrast, brain regions with low Aβ levels (e.g., cerebellum) did not show any increase in oxidative stress markers [17]. Oxidative stress (OS) refers to a circumstance in which ROS production overwhelms the cellular antioxidant defense systems that consist of antioxidant enzymes, such as superoxide dismutase (SOD), glutathione peroxidase (GPx), catalase, glutaredoxins, and thioredoxins, and also of nonenzymatic antioxidant factors [18]. Importantly, reduction or loss of function of the antioxidant enzymes, as denoted by decreased specific activity, has been reported in AD [19].

1.3.6. Mitochondria Hypothesis. When discussing the impact of OS on AD, it is worth mentioning the role of mitochondria and their dysfunction, through the production of ROS, as an important factor involved in the pathogenesis of AD. Growing evidence, such as documentation of disease staging generated by Alzheimer's Disease Neuroimaging Initiative, supports the notion that AD is not a linear downstream consequence of Aβ or SP deposition alone, but rather should be considered as a multifactorial disease [20, 21]. Some researchers insist that mitochondrial dysfunction is a dominant insult driving the most common, sporadic late-onset AD pathophysiology and refer to this pathology as a "mitochondrial cascade hypothesis" [22].

2. Alzheimer's-Like Diseases

Numerous important observations regarding AD and other related dementias have been made in animal studies. Although none of the existing models entirely exhibits the complete spectrum of this insidious human disease, critical aspects of AD pathology and disease process can be effortlessly outlined. Such diseases in animals are oftentimes called Alzheimer's-like diseases (ALD). Interestingly, there is only one group of animals, dogs, which has their own ALD named, and it is called canine cognitive dysfunction (CCD). What is worth highlighting, the vast majority of the transgenic animal models of ALD represent the familial form of Alzheimer's disease. Moreover, there are only a few studies regarding the sporadic form of AD in living ani-

mals other than companion animals. The reason for this is surprisingly simple as wild animals suffering from ALD are not able to be studied as neatly as domestic animals are.

Interestingly, many domestic animals exhibit several behavioral changes in their elderly years, e.g., they tend to display spatial disorientation, change relationships with their owners, change their day-night pattern, lose cognition, or simply exhibit inappropriate vocalization [14]. Importantly, except for behavioral symptoms, there are also numerous neuropathological manifestations found in animals that are similar or the same as in AD including Aβ oligomers, senile plaques, neuronal degradation and loss, AD biomarkers found in CSF, vascular amyloid, dysfunction in neurotransmitter systems, decreased neurogenesis, increased oxidative stress, and oxidative damage [23–27].

3. Endocrine Disruptors

Notably, scientists presume that AD is mostly caused by a combination of genetic, lifestyle, and environmental factors that affect the brain over time. Many studies point to environmental chemicals as an important component of neurological diseases' onset [28] Synthetic chemicals have become an inseparable part of people's lives, and some of these chemicals have been identified as endocrine disruptor chemicals (EDCs) or endocrine disruptors (EDs).

Endocrine disruptors are exogenous substances, mixtures of chemicals, or nonchemical exogenous factors that interfere with the human endocrine system, leading to adverse effects on hormonally controlled functions [29, 30]. Even though it is facile to automatically assume that EDCs are synthetic substances only, in fact, they are heterogeneous and vary from synthetic to natural chemicals. The best-known synthetic EDCs are polychlorinated biphenyls (PCB), plasticizers, pesticides, fungicides, and pharmaceutical agents. The most popular natural EDCs are phytoestrogens, predominantly found in food and drinks. There are also additional examples of natural EDCs, such as nicotine or, surprisingly, light [31]. Importantly, all of the aforementioned chemicals are widespread in the environment. EDCs interfere with hormone activities by mimicking hormones, promoting responses at improper times, or by halting hormone action, thus leading to alterations in the hormonal and homeostatic systems, and interfering with the ability of the body for communicating and responding to the environmental stimuli. EDCs tend to have a low binding affinity for hormone receptors, and their ability to activate or block hormone receptors may vary. Although it is generally difficult to define a *negative effect*, some researchers consider any biological response to an endocrine disruptor to be an adverse event [32].

Endocrine disruptors can be found in food, consumer products, water, soil, wildlife, and in people who were exposed to EDs through ingestion, inhalation, dermal contact, or injection. Endocrine disruptors can be divided into two large groups: chemicals and nonchemical exogenous factors. Subsequently, chemical EDs can be categorized into three primary groups: pesticides (e.g., glyphosate, dichlorodiphenyltrichloroethane (DDT)), chemicals in consumer products (e.g., parabens and heavy metals), and food contact

materials (e.g., bisphenol A (BPA) and phthalates) [33]. When it comes to nonchemical EDCs, a good example could be light [34].

Detrimental properties of EDs are well known to scientists, and importantly, there is a growing awareness regarding them in society. These substances are called *disruptors* not without a reason: exposure to EDs leads to increased incidence and prevalence of cancer; they are associated with the development of learning disabilities, deformations, impairing sexual development; and they can be highly teratogenic [35, 36]. Notably, endocrine disruptors have been linked to numerous diseases, e.g., attention-deficit hyperactivity disorder (ADHD), PD, diabetes mellitus, cardiovascular diseases, obesity, early puberty, infertility and other reproductive disorders, children and adult cancers, and AD [37]. Curiously, EDCs may lead to alterations in microbiota residing in the gut, which in turn may lead to neurobehavioral disorders like autism spectrum disorders [38].

A critical group of endocrine disruptors seems to be the dietary endocrine disruptors. Undeniably, food is essential for human life, and it plays a crucial role in determining the health and well-being of the consumer. Since food is the source of energy for humans, it is also one of the most significant sources of endocrine disruptors in our organisms. Importantly, dietary endocrine disruptors are not originated from food exclusively. Surely, there are numerous EDCs of animal or plant sources just like phytoestrogens, but it is worth mentioning that endocrine disruptors found in food are also pesticides (e.g., endosulfan or carbaryl), metals (e.g., aluminum or antimony), or plasticizers (e.g., bisphenol A or phthalates). When the term endocrine disruptors was used for the first time, scientists used it mainly to discuss the adverse effect of a certain substance on the endocrine system. Oral intake of EDCs was described to result in reduced fertility in men and women; breast, endometrial, and testicular cancer; birth defects of reproductive organs; and changes in the onset of puberty [39]. Nowadays, scientists are aware that the intake of dietary EDCs may lead to numerous diverse side effects. Polychlorinated biphenyls, for example, due to their lipophilic nature, remain global contaminants in the human body. They are proven to have neurotoxic, carcinogenic, immunotoxic, hepatotoxic, nephrotoxic, and cytotoxic effects in numerous experimental models and human studies [40]. Pesticides like carbaryl or endosulfan, in turn, have confirmed influence on developing obesity and metabolic disorders, deteriorating thyroid homeostasis and hypothalamo-pituitary axis, and causing hormone-sensitive cancers [41]. Plasticizers, which eagerly migrate from plastic packaging to food, are known to have serious neurotoxic effects, especially in children and pregnant women [42]. Similarly, the harmful impact has been denoted in the case of metals, which have a potential diabetogenic role and are denoted as EDCs inducing severe testicular damage [43].

Despite their bad fame, endocrine disruptors are increasingly described to have numerous positive side effects, and importantly, many of them are already confirmed by studies. Since AD is still a bit of a riddle for scientists, we decided to shed new light on some well-known EDs and EDCs and their presumed or confirmed roles in AD.

4. Phytoestrogens

Phytoestrogens are nonsteroidal, plant-derived compounds that may mimic or interact with estrogen hormones in mammals. They exhibit natural structural similarity to 17β-estradiol (E2), which is the most abundant circulating estrogen and the primary female sex hormone at the same time. Thus, phytoestrogens can easily interplay with estrogen receptors (ERs) and mediate estrogenic responses. Curiously, among two currently known forms of estrogen receptors (ERα and ERβ), phytoestrogens have a slightly higher relative binding affinity for ERβ [44]. Importantly, estrogen receptors' subtype distribution varies across tissues and cell types. Moreover, it changes over the lifespan and is sexually dimorphic [45]. When bound to estrogen receptors, phytoestrogens can commence either transcription or rapid, nongenomic actions via numerous mechanisms and pathways.

Transcription induced by phytoestrogens can be initiated through interactions with the estrogen response element or by binding early immediate genes, such as Jun and Fos [46]. When it comes to the nongenomic actions of phytoestrogens, it is believed that this kind of activity develops at the extracellular surface of the cell membrane, which means that a potential endocrine disruptor does not have to enter the cell in order to be active. The binding of phytoestrogens to ERs activates second messenger pathways, leading to such cellular responses as the rise of intracellular cAMP (cyclic adenosine monophosphate) or calcium levels, or promotion of nitric oxide release contributing to the stimulation of signal transduction pathways crucial, e.g., neuronal signaling or neuronal differentiation [47]. Importantly, a growing number of papers point out that phytoestrogens have an epigenetic activity being able to modify the action of DNA and histone methyltransferases, NAD-dependent histone deacetylases, and other modifiers of chromatin structure [48, 49]. Another molecular mechanism of phytoestrogen's activity is its ability to interfere with certain enzymes required for steroid biosynthesis and/or their degradation. For example, phytoestrogens can inhibit 11β-hydroxysteroid dehydrogenase type 1, an enzyme that takes a part in the synthesis of bioactive glucocorticoids from their inactive precursors [50]. Notably, phytoestrogens are also able to affect sex hormone-binding globulin synthesis in the liver and thus affecting sex hormones bioavailability. For example, soya containing a large amount of phytoestrogens is known to lower the risk of some cancers due to heightening sex hormone-binding globulin levels [50, 51].

Phytoestrogens can be divided into six main classes: flavonoids, pterocarpans, enterolignans, coumestans, mycotoxins, and stilbenes, depending on their chemical structure [52]. Importantly, flavonoids have numerous subclasses, e.g., flavones, flavanones, flavonols, isoflavones, and isoflavanes. The main phytoestrogens derived from the diet are genistein, daidzein, and glycitein, which belong to isoflavones [53]. You can find a graphical classification of phytoestrogens with a focus on phytoestrogens described in the article in Figure 1.
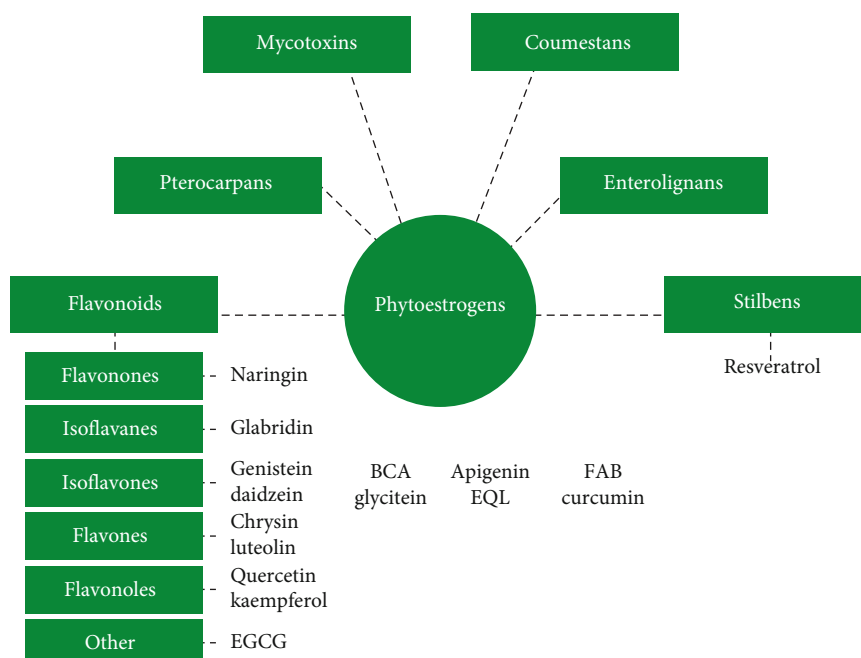
FIGURE 1: Classification of phytoestrogens with a focus on phytoestrogens described in the article.

Soy seems to be the richest source of plant estrogens. Interestingly, studies have shown great variability in isoflavone content and composition in soybeans, depending not only on the variety of soy but also on the environmental conditions [54]. Importantly, soybean is prevalently used in the food industry, including milk and meat substitutes, and has become increasingly widespread over the past 20 years. Even the pet-food industry uses heaps of soybeans and soybean-related products in their search. Back in 1998, Setchell suggested that the fertility problems of captive cheetahs could be related to the presence of soy isoflavone phytoestrogens in the standard animal diet [55].

Numerous studies indicate that phytoestrogens can exert adverse effects, especially on reproduction and fertility. Meena et al. performed a study in which pregnant rats received intraperitoneal injections of genistein at a dose level of 2, 20, or 100 mg/kg body weight for 7 days. The results indicated that male rats exposed to phytoestrogens in their mothers' wombs have impaired fertility and altered both spermatogenesis and steroidogenesis [56]. Consistent observations were made in humans in a population-based case-control study by Russo et al., who showed that high consumption of phytoestrogens was associated with a higher occurrence of prostate cancer [57]. Interestingly, even the widely known beneficial effects of soy intake for women with breast cancer are controversial, as *in vitro* studies showed that some phytoestrogens, namely, genistein and daidzein, even in the low concentrations were able to stimulate the proliferation of MCF-7 human estrogen-receptor alpha positive (ERα+) breast cancer cells. [58].

4.1. Cognitive Function. Importantly, phytoestrogens can also have an impact on the nervous system and behavior. Interestingly, in contrast to the aforementioned systems

and organs, the vast majority of the effects of phytoestrogens exerted on cognitive functioning turns out to be advantageous.

4.1.1. Cognitive Function: Human Studies. A meta-analysis of 10 placebo-controlled suitable randomized controlled trials conducted by Cheng et al. in 2015 revealed that supplementation with soy isoflavones indeed improves cognitive function and visual memory in postmenopausal women [59]. What is worth mentioning, researchers underline the importance of geographic features and treatment duration as important factors influencing the effect. A prominent study named SOPHIA was conducted on postmenopausal women [60]. Isoflavones were supplemented to women (110 mg/day), and after 12 weeks of daily supplementation, their cognitive function was assessed. It turned out that the treatment significantly improved performance in the recall of pictures and sustained attention and planning tasks [61].

Sekikawa et al., who proved that equol, a derivative of daidzein, is antiatherogenic and can improve arterial stiffness, stated that equol may help to prevent cognitive impairment or/and dementia [62].

Interestingly, very few studies included males and assessed their reaction to phytoestrogens supplementation. However, these studies provided truly captivating results. A case-control study by File et al. [63] indicated that dietary isoflavone supplementation improved cognitive function in men. Individuals received 100 mg of isoflavones per day for 10 weeks. The isoflavones varied depending on the meal served. Importantly, the diet contained a wide range of soya-containing foods, such as soya milk drinks or puddings, soya flour, or simply soya beans. Young, healthy adults exhibited a significant improvement in both short-term and long-term memory, and additionally, the mental

flexibility of studied subjects was improved. Li et al. [64], in turn, pointed out that a diet rich with phytoestrogens affected boys' brains more likely than girls'. In their study, they examined infants fed exclusively with soy formula from the first weeks of their life throughout the first year of life. The study also suggested that a soy-based diet may influence later life brain anatomy and function; however, the changes were modest, and therefore, the results cannot lead to any clinically relevant deficits or abnormal outcomes. Additionally, Thorp et al. [65] showed that oral isoflavone supplementation (capsules with 116 mg of isoflavone equivalents daily: 68 mg of daidzein, 12 mg of genistein, 36 mg of glycitin for six weeks) significantly enhanced spatial memory in men.

4.1.2. Cognitive Function: Animal Studies.
Unquestionably, the vast majority of studies regarding the impact of phytoestrogens on the cognitive system have been conducted on animals.

In 2020, Li et al. indicated that genistein has plenty of beneficial effects in diabetes mellitus-induced brain damage [66]. The authors revealed that this phytoestrogen not only improves brain insulin signaling but also increases neurotrophic support and alleviates AD-related pathologies, such as Aβ deposition and the level of hyperphosphorylated tau protein. As a result, cell growth and survival, synaptic plasticity, and cognitive function of such animals are significantly improved. Consistent results were reported by Park et al. [67]. They showed that genistein exerts a protective effect against neurodegeneration in mice [68].

Interestingly, as genistein has intrinsically low oral bioavailability, not only oral delivery of phytoestrogens has been investigated. Rassu et al. suggested that intranasal supplementation of genistein as nanoparticles may be considered to act as a potential preventive system against neurodegenerative disorders [69].

Due to the fact that phytoestrogens are widespread and commonly found in food and drinks, scientists have carried out studies regarding specific fares, dishes, and recipes. A study conducted on mice indicated that a Korean traditional fermented soybean paste named *Doenjang* alleviates neuroinflammation and neurodegeneration [70]. Another research showed that a diet containing high amounts of phytoestrogens not only reduces aggression in mice but also has a strong negative impact on the sociability of the animals [71].

Phytoestrogens, acting as estrogen agonists, can positively affect the synthesis of brain-derived neurotrophic factor (BDNF) and nerve growth factor (NGF). This hypothesis was confirmed back in 1999 by Pan et al., who showed the mRNA levels of BDNF in the frontal cortex were significantly higher in rats receiving soy isoflavones compared to those fed without any phytoestrogens [72]. NGF, in turn, increases the mRNA of choline acetyltransferase and increases its activities, thus promoting the release of acetylcholine. Importantly, NGF has an outcome principally on cholinergic neurons, which are the most prone to neurodegeneration in AD. Moreover, certain studies pointed out that NGF can be crucial in slowing the progression of AD since it impedes cholinergic basal forebrain atrophy. As a result, phytoestrogens, due to their ability to promote NGF and NGF receptor expression, are more and more often believed to be potential preventative treatment against AD [73].

4.2. Nervous System

4.2.1. In Vitro Neuroprotection.
Numerous studies have already indicated that phytoestrogens have neuroprotective effects against varied kinds of damage. This fact has been proven using a wide range of in vitro models.

Phytoestrogen isoflavones, principally biochanin A (BCA), significantly increase the expression of glutamate oxaloacetate transaminase (GOT), an enzyme that can metabolize neurotoxic glutamate, in mouse hippocampal HT4 neural cells [74]. A consistent result was confirmed by Tan et al., who indicated that BCA had strong neuroprotective effects against β-amyloid-induced neurotoxicity in PC12 cells [75]. This effect is exerted via a mitochondria-dependent intrinsic apoptotic pathway. Another widely known isoflavone, apigenin, was found to give an antiapoptotic effect in murine HT22 hippocampal neuronal cells as well as in human SH-SY5Y neuroblastoma cells [76, 77]. Additionally, apigenin can reduce glutamate-induced Ca^{2+} signaling in cultured murine cortical neurons [78]. Combined results indicate that this isoflavone possesses strong neuroprotective properties.

Equol (EQL), a metabolite of dietary daidzein (DAI), may mitigate the activation of BV-2 microglia. It also enhanced the neuroprotection of C6 astrocytes and N2a (Neuro2a) neuroblastoma cells [79]. One of the most recent studies regarding in vitro effects of EQL showed that this metabolite also had a neuroprotective effect against neurotoxins-induced toxicity in SH-SY5Y human neuroblastoma cells [80].

Quercetin is a well-known plant-derived antioxidant. It is one of the predominant flavonoids found in our daily diet. It has been revealed that quercetin decreased the maturation of APP, which in turn alters Aβ secretion and aggregation [81]. Additionally, quercetin glycosides have confirmed neuroprotective effects in such diseases as AD and PD. Magalingam et al. conducted an experiment, in which PC-12 cells pretreated with isoquercitrin and rutin were later exposed to 6-hydroxydopamine (6-OHDA), a synthetic, neurotoxic compound [82]. Cells exposed to glycosides markedly attenuated the expression of proapoptotic genes, such as *Casp1*, *Casp3*, and *Casp7*, when compared to the control cells.

Consistent research was carried out by Kim et al., in which quercetin and kaempferol demonstrated their neuroprotective effects by downregulating the expression of proapoptotic proteins in human SH-SY5Y cells [83]. Additionally, the aforementioned phytoestrogens significantly increased the viability of cells treated with Aβ.

Importantly, phytoestrogens showed a beneficial impact on cells not only in cellular models of AD. Abbruzzese et al. experimented with a startling outcome: genistein and BCA played dual roles in the regulation of autophagy [84]. Depending on whether autophagy is a neuroprotective and prosurvival mechanism or prodeath mechanism, they acted

either as autophagy initiation enhancers or as autophagy initiation inhibitors. The experiment was conducted on cortical neurons of Wistar rats in the model of ischemia that is a crucial process in many neurodegenerative diseases.

Flavonoid agathisflavone (FAB) is a phytoestrogen derived from the plant *Poincianella pyramidalis*. FAB significantly ameliorated neuroinflammation induced by LPS (lipopolysaccharide) and proinflammatory cytokines in cocultures of glia and neurons. This finding undoubtedly indicates that FAB has not only neuroprotective but also anti-inflammatory effects *in vitro*, which, in turn, may be considered as an ancillary for the treatment against numerous neurodegenerative diseases [85].

4.2.2. In Vivo Neuroprotection. Neuroprotective effects of phytoestrogens have been proven multiple times in *in vivo* models of AD. Ipriflavone (IPRI) is a nonhormonal isoflavone used in some countries as a treatment and prevention against osteoporosis caused by menopause. In a study by Hafez et al. on a rat model, IPRI turned out to play a great role in AChE inhibition, alleviated oxidative stress, reverted memory impairment, and, importantly, significantly increased the expression of two putative α-secretase enzymes: ADAM10 and ADAM17 [86]. Additionally, IPRI increased the expression of pERK1/22 (phosphorylated extracellular signal-regulated kinase 1, 2), a serine-threonine kinase that plays a crucial role in decreasing the BACE expression in the hippocampus. What is promising, IPRI significantly reduced tau and $A\beta$ pathologies.

Apigenin is a flavonoid widely spread among fruits and vegetables, such as parsley, oranges, or onions. It has anti-inflammatory, antioxygenic, antitumorigenic, and antimutagenic effects on numerous cell types [76, 87]. Importantly, apigenin plays also an important role in AD. Scientists have reported that apigenin inhibited oxidative stress in APP/PS1 double transgenic mice. Additionally, apigenin ameliorated AD-associated memory impairment in mice and reduced the spread of $A\beta$ plaques [88].

Quercetin is another phytoestrogen with strong anti-AD potential studied *in vivo*. In a study by Sabogal-Guaqueta et al., quercetin was administrated every 48 hours for three months on aged (21-24 months old), triple-transgenic AD model mice (3xTg-AD). Quercetin decreased not only extracellular β-amyloidosis but also microgliosis, astrogliosis, and tauopathy in the hippocampus and amygdala. Additionally, a visible reduction in β-amyloid 1-40 and β-amyloid 1-42 levels was observed. However, not only histological changes were observed but also quercetin had an enhancing effect on learning spatial memory tasks and improved risk-assessment behavior [89]. A similar conclusion was carried out by Shveta et al., who also confirmed the neuroprotective role of quercetin, but this time, the experiments were conducted on rats [90].

Numerous papers indicated that less-known phytoestrogens have also neuroprotective effects; however, these substances are still not studied sufficiently. A good example of this group could be naringin, a flavonoid found in citrus fruits, which weakens oxidative stress and neuroinflammation *in vivo* [91]. Some other phytoestrogens which have

confirmed neuroprotective impact *in vivo* and are not as widely known as aforementioned compounds are luteolin (LUT), commonly found in spices like parsley or thyme [92]; chrysin (CHR), a flavonoid that interacts with TTR protein (transthyretin) and thus TTR can play its role and take a part in $A\beta$ clearance [93; 94]; epigallocatechin gallate (EGCG), which is the major polyphenol component of green tea, has confirmed neuroprotective effect *in vivo* not only in AD but also in amyotrophic lateral sclerosis (ALS), multiple sclerosis (MS), and PD. EGCG, just like CHR, can bind to TTR and at the same time suppress β-amyloid fibril formation [93]. Neuroprotective effects *in vivo* were also observed with γ-mangostin (γ-M), originally isolated from *Garcinia mangostana* tree [94] and glabridin (GLA) isolated from the roots of *Glycyrrhiza glabra* L. [95–97].

Naturally, phytoestrogens have neuroprotective effects not only in AD models but also in a plethora of other neurodegenerative diseases. A study by Ohgomori et al. [98] showed that genistein alleviated the demyelination of mature mice oligodendrocytes induced by cuprizone (CPZ), and thus, phytoestrogens are considered to have therapeutic potential for treating patients with multiple sclerosis or those suffering from mental health disorders. Khanna et al. conducted an experiment on C57BL/6 mice, which were intraperitoneally injected with biochanin A for 4 weeks and afterward subjected to ischemic stroke injury [74]. It turned out that BCA treatment in mice induced GOT expression, attenuated stroke lesion volume, and improved sensorimotor functions. Furthermore, in the rat model of PD, BCA decreased the levels of proinflammatory cytokines such as IL-6, IL-1β, and TNFα and at the same time inhibited the generation of reactive oxygen species. In this study, male Sprague-Dawley rats were treated with BCA for 21 days [99]. Another study by Wang et al. [99] revealed that BCA attenuated behavioral deficits and dopamine depletion induced by the combined effect of iron and rotenone in Sprague-Dawley rats. Equol was confirmed to have neuroprotective possibilities against neurotoxicity induced by 1-methyl-4-phenylpyridinium (MPP+) using *in vivo* model of PD including *Caenorhabditis elegans* (*C. elegans*). Importantly, EQ prolonged the survival of *C. elegans* exposed to MPP+ from 72 to 108 hrs [80].

4.3. Cerebral Ischemia Injury. There is a growing number of data indicating the relationship between brain ischemia and Alzheimer's disease [100]. Besides, several studies revealed epidemiological and neuropathological factors linking ischemic brain neurodegeneration with the genotype and phenotype of Alzheimer's disease. Furthermore, Alzheimer's disease is a risk factor for stroke, and conversely, stroke enhances the risk of AD. Finally, dysregulation of Alzheimer's disease-associated genes including *amyloid protein precursor*, *α-secretase*, *β-secretase*, *presenilin 1*, *presenilin 2*, and *tau protein* occurs in a course of postischemic neurodegeneration [100]. Oxidative stress (OS) and neuroinflammation are crucial mechanisms in the progression of cerebral ischemia injury. Importantly, they both are components in the etiology of neurodegenerative diseases. Thus, maintaining physiological blood flow, halting OS, and limiting neuroinflammation are essential in the prevention of brain injuries [101].

Ever since it was denoted that men have a higher incidence of stroke compared with premenopausal women [102], estrogens are claimed to possess neuroprotective properties. This finding along with the widespread use of estrogens as hormone-replacement therapy (HRT) for amending postmenopausal syndromes caused a large number of reports insisting that estrogens may have neuroprotective effects on brain stroke. However, the results of numerous *in vivo* and *in vitro* studies are ambiguous as some confirm this hypothesis, whereas others claim that estrogens can be simply detrimental for postmenopausal women because of the potential deleterious side effects of hormone replacement therapy, such as increased cancer and stroke risk [103]. Thus, a lot of expectations are held concerning phytoestrogens, which seem to be the best and the safest alternative to estrogens.

Several phytoestrogens have been shown to strengthen endogenous antioxidant defenses. Some of them activate NRF2 (nuclear factor erythroid 2-related factor 2) and its gene targets, which are regulated by ARE (antioxidant response element) DNA sequence. Activation of the NRF-2/ARE pathway provokes the production of antioxidant enzymes, such as heme oxygenase-1 (HO-1) or NAD(P)H dehydrogenase (quinone 1) (NQO1). The examples of phytoestrogens that can activate the pathway in neurons are quercetin, curcumin, resveratrol, sulforaphane, epigallocatechin gallate, piceatannol, or brazilin [104, 105]. Some of the aforementioned phytoestrogens, like quercetin or curcumin, can additionally increase the expression of protein chaperones, involving heat-shock proteins and numerous growth factors such as BDNF, IGF (insulin-like growth factor), or FGF (fibroblast growth factor) [106]. Protein chaperones bind to other proteins, protect them, and mediate the unfolded protein response in the endoplasmic reticulum which ensues in neurons during ischemic stroke. Importantly, heat-shock protein response is a well-known and very important process of defense against ischemic stroke-induced stress conditions [107]. Heat shock proteins take a part in protein folding and protection and removal of aggregated proteins, and they could inhibit apoptotic cell death cascade [108].

5. Hormone Replacement Therapy

Some researches indicate that the risk of AD incidence and the severity of the disease differ indispensably between men and women. It is estimated that women suffer from the disease even twice as often as men. Although this discrepancy could be partially explained by differences in mean length of life, other mechanisms cannot be omitted. According to recent findings, a decrease in estrogen levels in the menopause period could be connected with AD-related brain changes [109]. Additionally, premature menopause also increases the risk of AD onset or development [110].

A question could be raised why estrogen depletion is so harmful to cognition processes. From the physiological point of view, estrogens act through a wide network of receptors. Two types of receptors could be distinguished, estrogen receptor alpha (ER-α) and estrogen receptor beta (ER-β).

ER-α acts as a neuroprotective element against AD by maintaining intracellular signaling cascades [111]. ER-β is a potent regulator of the innate immune response as well as is involved in the regulation of neuronal mitochondrial function [112]. Besides, reduced expression of ER-α has been found in hippocampal neurons of AD subjects. Furthermore, lower expression of ER-β was related to abnormal mitochondrial function and enhanced OS markers [111] A midlife change in neurohormonal activity in females is called the menopause transition. In this particular phase of women's life, there is a decline in the production and secretion of estrogens, mainly estradiol, from the ovaries. As an effect of the decrease of estrogen concentration, several changes in the brain are observed. Among them, there is a low estrogen-related metabolic dysfunction leading to the hypometabolic state [113].

Since data suggest that perimenopause increases a patient's vulnerability to developing not only AD but also other neurological diseases like PD, it may be a promising way to use hormonal replacement therapy for favorable effects on female cognitive function [114]. The coherent conclusion was also conferred by the group from Mayo Clinic. According to them, women who underwent bilateral or unilateral oophorectomy before the onset of natural menopause had a lifelong increased risk of cognitive impairment and dementia [115, 116].

Numerous research reviews, meta-analyses, and *in vivo* and *in vitro* experiments were conducted to examine the link between estrogen replacement therapy (HRT) and its effect on AD. In general, the results were promising. Imtiaz et al. [117] showed in their cohort study that long-term HRT was associated with a reduced risk of AD. The consistent result was presented by Song et al. in their meta-analysis [114]. These authors confirmed that estrogen replacement therapy decreases the risk of onset and/or development of not only AD but also PD. What is worth mentioning, recent reviews indicate that the positive outcome of HRT use in the case of AD may depend on such factors as the length of hormone administration, duration of treatment, and an individual's risk of developing cancer or/and stroke [118].

Of note, an interesting study was performed by Luoto et al., who assessed the impact of HRT on women's health and lifestyle. It turned out that 28% of HRT users had higher education, lived in the capital city's area, had a significantly higher healthy diet factor score, and were leaner than nonusers of HRT. Importantly, the use of HRT remained a significant determinant of body mass index, waist/hip ratio, and body fat percentage [119]. In addition, a recently published meta-analysis indicated that higher levels of education were connected with false negatives of the MMSE (the MiniMental State Examination), whereas lower levels of education were associated with false positives [120].

However, except for the optimistic results, some findings put in doubt the use of estrogens not only in the prevention of AD but also, if not primary, in hormone replacement therapy. Savolainen-Peltonen et al. [121] in their case-control study indicated that for women who initiated hormone replacement therapy before the age of 60, the use of HRT was associated with a 17% increase in the risk of AD.

TABLE 1: Summary of systems and processes influenced by phytoestrogens mentioned in the publication (with responding references).

Process/organ influenced by phytoestrogens	Specification	Reference number
Cognitive function	Human studies	[59–65]
	Animal studies	[66, 67, 68, 69, 70, 71, 72, 73]
Nervous system	*In vivo*	[74, 76, 80, 86–99, 130, 131]
	In vitro	[74–85]
Cerebral ischemia injury	—	[100–108]
Hormone replacement therapy	—	[73, 109–129, 132, 133]

The percentage was even higher in women who initiated HRT after the age of 60, and it reached up to 38%. Besides, not only an enhanced risk of AD and PD was observed in elderly women treated with estrogens but also increased mortality was indicated [119]. However, it should be highlighted that there is a critical period of effective estrogen treatment following menopause. The duration of this advantageous time depends on the depletion of estradiol receptors, the switch to a ketogenic metabolism by neuronal mitochondria, and a decrease of acetylcholine accompanying estradiol deficiency [122].

Interestingly, the side effects of HRT did not affect the nervous system only. For years, it was almost a dogma that any cardiovascular disease was prevented in women undergoing HRT. However, the Women's Health Initiative (WHI) trial of conjugated equine estrogens (CEE) and medroxyprogesterone acetate (MPA) showed in 2002 that HRT resulted in a significantly increased incidence of stroke and venous thromboembolism [123–125]. Because of the WHI results and other side effects of HRT, a lot of effort nowadays is put into finding a less harmful, but still efficient alternative to estrogens. Thus, phytoestrogens seem to be a very promising alternative. Importantly, phytoestrogens have an exceptional ability to act as estrogen agonists without any currently known detrimental effects. They could be the perfect solution and reconcilement between the positive impact of estrogens on AD and their harmful effects on health. The enthusiasm about the use of phytoestrogens emerged from epidemiologic studies indicating that PEs lower the risk of breast cancer and osteoporosis and mitigate the symptoms of menopause in women from countries with high phytoestrogens consumption [128, 129]. Additionally, some of the phytoestrogens own antioxidant properties *in vitro* through hydrogen/electron donation *via* hydroxyl groups; hence, they act as free radical scavengers and can suppress the progression of coronary heart disease and some types of cancer [126]. PEs are also able to upregulate the expression of manganese superoxide dismutase (MnSOD) and catalase, which enhances their antioxidant effect [125, 127]. In Table 1, you can find the summary of processes and organs affected by phytoestrogens and articles cited in the article regarding them.

There are two mechanisms by which phytoestrogens exert their impact: estrogen-mediated and nonestrogen-mediated. The nonestrogen-mediated mechanisms are inclusive of any reaction in which phytoestrogen plays a unique role. This means that phytoestrogens do not compete with estrogens but simply do their "own job." They protect neurons against OS and prevent the damage it causes [128]. The estrogen-mediated mechanisms, in turn, are inclusive of all reactions in which estrogen is a factor [73]. Substantially, in these mechanisms, phytoestrogens substitute estrogens when they are in low concentrations by simply binding to estrogen receptors. Examples of such mechanisms are reduction of tau protein phosphorylation, reduction of Aβ, promotion of Ca$^+$ outflow, or enhancing acetylcholine release [129].

5.1. Nonestrogen-Mediated Mechanisms

5.1.1. Antioxidant Properties and Effects on Neurons. Certain amyloid-beta peptides are known for having toxic properties. Phytoestrogens, in turn, often act as their functional antagonists [134].

Aβ is among the factors that stimulate lipid peroxidation in the neuronal cell membrane, the process that leads to the production of reactive oxygen species and respiratory burst. Subsequently, membrane proteins can be impaired and the homeostasis of ion distribution could be broken. As a consequence, the neuronal membrane depolarizes resulting in Ca^{2+} inflow via the *N-methyl-D-aspartate* (NMDA) receptor channels. As a result of such phenomena, the damage of lipids and DNA aggravates even more, eventually leading to neuronal death.

Auspiciously, numerous researches indicate that estradiol (and in turn phytoestrogens) is a natural antioxidant for membrane lipid peroxidation, and it mitigates Aβ toxicity against neurons [135–138]. Importantly, phytoestrogens significantly improve cerebral blood circulation and, therefore, increase oxygen and nutrient supply to the brain cells [139].

5.2. Estrogen-Mediated Mechanisms

5.2.1. Decrease in Aβ Production. What should be underlined once more is that not all APPs are detrimental to health. A large number of APPs is, in fact, advantageous. They are essential for synapses' formation, neuronal plasticity, or iron export. APPs may sustain cognitive functioning in patients with AD and ALD [73]. However, some APPs are precursors for neurotoxic Aβ.

Estrogens are known to regulate the metabolism of APP. They can promote the release of APPs in cortical neurons via
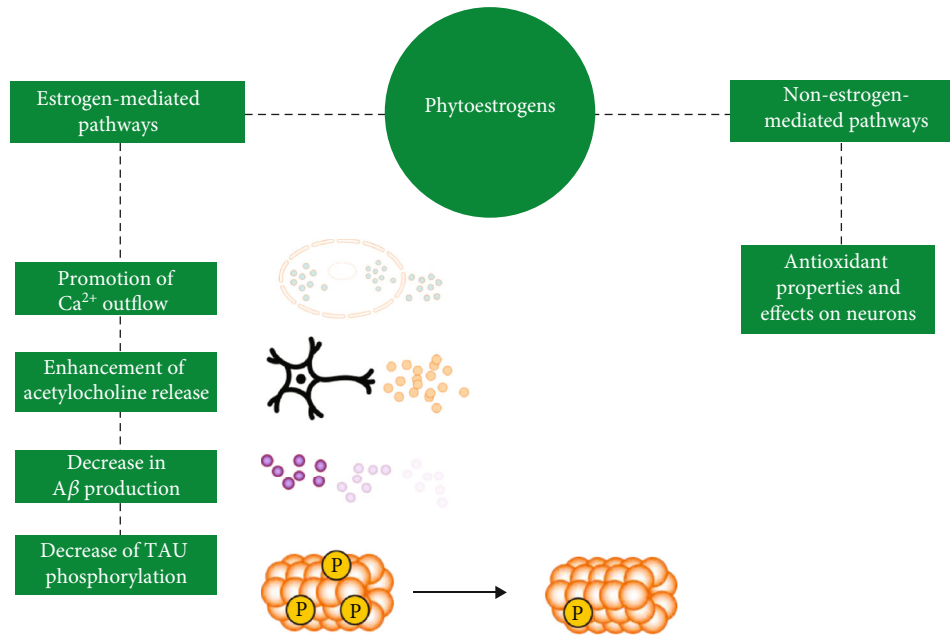
Figure 2: Estrogen- and nonestrogen-mediated mechanisms exerted by phytoestrogens on neurons.

the protein kinase C pathway. Phytoestrogens, in turn, may act as an alternative if the concentration of estrogens is not high enough, resulting in the same outcome. Regarding their ability to stimulate the excessive formation of APP in elderly individuals, phytoestrogens change the ratio between APP and $A\beta$ in favor of APPs. Eventually, the $A\beta$ production is reduced and serves antagonistic to the progression of AD [140, 141].

5.2.2. Decrease of Tau Protein Phosphorylation. Tau phosphorylation is one of the hallmarks of AD and ALDs. Once tau protein gets phosphorylated and converts to NFT, it destabilizes the structure of cell's cytoskeleton and impairs the functioning of a neuron and eventually leads to its death.

Estrogens are known for their anti-tau-phosphorylation features. So are phytoestrogens, exerting their effects by enhancing dephosphorylation in the proline-rich region of the tau molecule [142, 143]. It has been observed that phytoestrogens can significantly inhibit tau phosphorylation and fibrillation and the associated cytotoxicity [144]. Additionally, according to findings of numerous *in vivo* and *in vitro* studies, inhibition of tau phosphorylation prevents endoplasmic reticulum stress-mediated neurodegeneration [145–147].

5.2.3. Enhancing Acetylcholine Release. Since phytoestrogens act as estrogens' agonists, they similarly can affect processes that involve estrogens, such as promoting axon pruning, synaptic growth, or the expression of numerous factors, e.g., NGF. NGF plays an important role in the maintenance of cholinergic neuron integrity and function, both during development and adulthood. Importantly, NGF induces the expression and activity of acetylcholine esterase (AChE), a key enzyme to degrade acetylcholine in cholinergic synapses [148]. As a result, the release of acetylcholine is promoted. It

is important to note that cholinergic neurons are the target neurons for deterioration in AD and ALDs.

Many pieces of research showed that NGF plays an important role in delaying or even stopping the progression of AD as it fights cholinergic basal forebrain atrophy [149, 150]. Thus, more and more reports nowadays suggest that NGF, NGF receptor (NGF-R), and phytoestrogens promoting expression of NGF and NGF-R should be concerned as a potential preventative agent or, hopefully, even as a promising treatment against AD [151, 152].

5.2.4. Promotion of Ca^{2+} Outflow. Phytoestrogens like estrogens can inhibit the elevation of intracellular Ca^{2+} concentration and reverse the disequilibrium of calcium homeostasis often caused by $A\beta$. They achieve these results through the release of the intracellular Ca^{2+} via nongenomic signaling events, which are not influenced by extracellular Ca^{2+} concentration [73, 153, 154].

Appropriate calcium homeostasis is crucial among individuals suffering from AD. Curiously, it is prevalent among this group of patients since the imbalance of Ca^{2+} is caused by $A\beta$ peptides. When the homeostasis is unbalanced, numerous adverse effects can occur: calcium channels may be activated, there may be changes in the release of neurotransmitters, the neurilemma can be altered, and eventually, the apoptotic signaling cascade can be induced [71, 155].

Nowadays, phytoestrogens are widely studied in terms of their calcium-equilibrating properties, and the results are truly satisfactory. A lot of attention in these terms is attracted by genistein and other flavonoids, suggesting the importance of adequate nutrition for humans and animals [155, 156]. You can see estrogen- and nonestrogen-mediated mechanisms exerted by phytoestrogens on neurons in Figure 2.

6. Conclusions

AD is a progressive, irreversible neurodegenerative disease affecting a growing cohort of patients. Alzheimer's-like diseases (ALDs), in turn, are group of disorders, closely related to AD, from which our friends and life companions, animals, suffer frequently [14]. Even though numerous researches, regarding the diseases, are published daily and the knowledge about AD and ALDs is constantly growing, there is still no discovered nor invented drug, which would reverse or ultimately inhibit the development of the disease. Moreover, the medications that are already in use provide symptomatic treatment only. Besides, many of them tend to lower their effectiveness over time [157]. Furthermore, drugs that are broadly used nowadays, like rivastigmine, donepezil, or memantine, have multiple side effects impeding the everyday life and functioning of patients. Therefore, undoubtedly, a new approach should be concerned in terms of fighting against AD and ALDs.

Although phytoestrogens are commonly known as endocrine disruptors and by definition could have a negative impact on the endocrine system, they also have an enormous potential to influence cognition and brain functioning beneficially. Numerous *in vitro* and *in vivo* studies confirm that they do have neuroprotective and antioxidant effects and indeed mitigate the progression of AD in humans as well as ALDs in animals. Together with their widespread availability, multifariousness, and their positive impact on other disorders and ailments, phytoestrogens appear to be a promising medicament in the proximate future. Needless to say, more research is needed to provide indisputable confirmation of phytoestrogens' role not only in AD and ALDs but also in other aspects of well-being.

After all, an ancient proverb says "*The enemy of my enemy is my friend*". Hence, perhaps we should stop considering phytoestrogens as disruptors only, and focus on "our" evident, mutual opponents, such as Alzheimer's and Alzheimer's-like diseases.

Abbreviations

6-OHDA: 6-hydroxydopamine
AChE: Acetylcholinesterase
AD: Alzheimer's disease
ALD: Alzheimer's-like diseases
ALS: Amyotrophic lateral sclerosis
APP: Amyloid precursor protein
ARE: Antioxidant response element
Aβ: Amyloid β
BACE1: β-Secretase
BCA: Biochanin A
BDNF: Brain-derived neurotrophic factor
BPA: Bisphenol A
cAMP: Cyclic adenosine monophosphate
CCD: Canine cognitive dysfunction
CEE: Conjugated equine estrogens
CHR: Chrysin
CJD: Creutzfeldt-Jakob disease
CNS: Central nervous system
CPZ: Cuprizone
CSF: Cerebrospinal fluid
DAI: Daidzein
DDT: Dichlorodiphenyltrichloroethane
E2: 17β-estradiol
ED: Endocrine disruptor
EDC: Endocrine disruptor chemical
EGCG: Epigallocatechin gallate
EQL: Equol
ER: Estrogen receptors
ER-α: Estrogen receptor alpha
ER-β: Estrogen receptor beta
FAB: Flavonoid agathisflavone
FGF: Fibroblast growth factor
GLA: Glabridin
GOT: Glutamate oxaloacetate transaminase
GPx: Glutathione peroxidase
HD: Huntington's disease
HO-1: Heme oxygenase-1
HRT: Hormone-replacement therapy
IGF: Insulin-like growth factor
IPRI: Ipriflavone
LPS: Lipopolysaccharide
LUT: Luteolin
MCI: Mild cognitive impairment
MnSOD: Manganese superoxide dismutase
MPA: Medroxyprogesterone acetate
MPP+: 1-methyl-4-phenylpyridinium
MS: Multiple sclerosis
NFL: Neurofilament light chain
NFT: Neurofibrillary tangles
NGF: Nerve growth factor
NGF-R: NGF receptor
NMDA: N-methyl-D-aspartate
NQO1: NAD(P)H dehydrogenase
NRF2: Nuclear factor erythroid 2-related factor 2
OS: Oxidative stress
PCB: Polychlorinated biphenyls
PD: Parkinson's disease
ROS: Reactive oxygen species
sAPP: Soluble amyloid precursor protein
SOD: Superoxide dismutase
SP: Senile plaques
TPO: Thyroid peroxidase
TTR: Transthyretin
WHI: Women's Health Initiative
γ-M: γ-Mangostin.

Data Availability

Please contact with the main author of the work by email: adomanska@cmkp.edu.pl.

Conflicts of Interest

The authors declare no conflicts of interest.

Acknowledgments

References

[1] M. Rochoy, V. Rivas, E. Chazard et al., "Factors associated with Alzheimer's disease: an overview of reviews," *The Journal Of Prevention of Alzheimer's Disease*, vol. 6, no. 2, pp. 121–134, 2019.

[2] J. Garre-Olmo, "Epidemiología de la enfermedad de Alzheimer y otras demencias," *Revista de Neurología*, vol. 66, no. 11, pp. 377–386, 2018.

[3] P. P. Liu, Y. Xie, X. Y. Meng, and J. S. Kang, "History and progress of hypotheses and clinical trials for Alzheimer's disease," *Signal Transduction and Targeted Therapy*, vol. 4, no. 1, 2019.

[4] M. Zvěřová, "Clinical aspects of Alzheimer's disease," *Clinical Biochemistry*, vol. 72, pp. 3–6, 2019.

[5] Alzheimer's Association, "2021 Alzheimer's disease facts and figures," *Alzheimers Dement*, vol. 17, no. 3, pp. 327–406, 2021.

[6] R. T. Gottesman and Y. Stern, "Behavioral and psychiatric symptoms of dementia and rate of decline in Alzheimer's disease," *Frontiers in Pharmacology*, vol. 10, p. 1062, 2019.

[7] G. M. McKhann, D. S. Knopman, H. Chertkow et al., "The diagnosis of dementia due to Alzheimer's disease: recommendations from the National Institute on Aging-Alzheimer's Association workgroups on diagnostic guidelines for Alzheimer's disease," *Alzheimer's & Dementia*, vol. 7, no. 3, pp. 263–269, 2011.

[8] D. A. Bennett, J. A. Schneider, Z. Arvanitakis et al., "Neuropathology of older persons without cognitive impairment from two community-based studies," *Neurology*, vol. 66, no. 12, pp. 1837–1844, 2006.

[9] X. Du, X. Wang, and M. Geng, "Alzheimer's disease hypothesis and related therapies," *Translational Neurodegeneration*, vol. 7, no. 1, 2018.

[10] R. S. Convery, M. R. Neason, D. M. Cash et al., "Basal forebrain atrophy in frontotemporal dementia," *NeuroImage: Clinical*, vol. 26, p. 102210, 2020.

[11] M. E. Hasselmo and M. Sarter, "Modes and models of forebrain cholinergic neuromodulation of cognition," *Neuropsychopharmacology*, vol. 36, no. 1, pp. 52–73, 2011.

[12] F. Zemek, L. Drtinova, E. Nepovimova et al., "Outcomes of Alzheimer's disease therapy with acetylcholinesterase inhibitors and memantine," *Expert Opinion on Drug Safety*, vol. 13, no. 6, pp. 759–774, 2014.

[13] M. R. Brier, B. Gordon, K. Friedrichsen et al., "Tau and Aβ imaging, CSF measures, and cognition in Alzheimer's disease," *Science Translational Medicine*, vol. 8, no. 338, article 338ra66, 2016.

[14] A. Gołaszewska, W. Bik, T. Motyl, and A. Orzechowski, "Bridging the gap between Alzheimer's disease and Alzheimer's-like diseases in animals," *International Journal of Molecular Sciences*, vol. 20, no. 7, p. 1664, 2019.

[15] S. Liu, Y. P. Sun, X. L. Gao, and Y. Sui, "Knowledge domain and emerging trends in Alzheimer's disease: a scientometric review based on CiteSpace analysis," *Neural Regeneration Research*, vol. 14, no. 9, pp. 1643–1650, 2019.

[16] D. A. Butterfield, M. L. Bader Lange, and R. Sultana, "Involvements of the lipid peroxidation product, HNE, in the pathogenesis and progression of Alzheimer's disease," *Biochimica et Biophysica Acta (BBA) - Molecular and Cell Biology of Lipids*, vol. 1801, no. 8, pp. 924–929, 2010.

[17] C. Cheignon, M. Tomas, D. Bonnefont-Rousselot, P. Faller, C. Hureau, and F. Collin, "Oxidative stress and the amyloid beta peptide in Alzheimer's disease," *Redox Biology*, vol. 14, pp. 450–464, 2018.

[18] A. Tramutola, C. Lanzillotta, M. Perluigi, and D. A. Butterfield, "Oxidative stress, protein modification and Alzheimer disease," *Brain Research Bulletin*, vol. 133, pp. 88–96, 2017.

[19] T. S. Kim, C. U. Pae, S. J. Yoon et al., "Decreased plasma antioxidants in patients with Alzheimer's disease," *International Journal of Geriatric Psychiatry*, vol. 21, no. 4, pp. 344–348, 2006.

[20] D. P. Veitch, M. W. Weiner, P. S. Aisen et al., "Understanding disease progression and improving Alzheimer's disease clinical trials: recent highlights from the Alzheimer's Disease Neuroimaging Initiative," *Alzheimer's & Dementia*, vol. 15, no. 1, pp. 106–152, 2019.

[21] Y. Iturria-Medina, F. M. Carbonell, R. C. Sotero, F. Chouinard-Decorte, and A. C. Evans, "Alzheimer's Disease Neuroimaging Initiative. Multifactorial causal model of brain (dis)organization and therapeutic intervention: application to Alzheimer's disease," *NeuroImage*, vol. 152, pp. 60–77, 2017.

[22] J. M. Perez Ortiz and R. H. Swerdlow, "Mitochondrial dysfunction in Alzheimer's disease: role in pathogenesis and novel therapeutic opportunities," *British Journal of Pharmacology*, vol. 176, no. 18, pp. 3489–3507, 2019.

[23] J. K. Chambers, T. Tokuda, K. Uchida et al., "The domestic cat as a natural animal model of Alzheimer's disease," *Acta Neuropathologica Communications*, vol. 3, no. 1, 2015.

[24] E. Vallino Costassa, M. Fiorini, G. Zanusso et al., "Characterization of amyloid-β deposits in bovine brains," *Journal of Alzheimer's Disease*, vol. 51, no. 3, pp. 875–887, 2016.

[25] D. Gunn-Moore, O. Kaidanovich-Beilin, M. C. Gallego Iradi, F. Gunn-Moore, and S. Lovestone, "Alzheimer's disease in humans and other animals: a consequence of postreproductive life span and longevity rather than aging," *Alzheimer's & Dementia*, vol. 14, no. 2, pp. 195–204, 2018.

[26] S. E. Perez, C. C. Sherwood, M. R. Cranfield et al., "Early Alzheimer's disease-type pathology in the frontal cortex of wild mountain gorillas (_Gorilla beringei beringei_)," *Neurobiology of Aging*, vol. 39, pp. 195–201, 2016.

[27] D. Szabó, N. Gee, and Á. Miklósi, "Natural or pathologic? Discrepancies in the study of behavioral and cognitive signs in aging family dogs," *Journal of Veterinary Behaviorclinical Applications and Research*, vol. 11, pp. 86–98, 2016.

[28] E. Y. Yang, D. K. Lee, and J. H. Yang, "Environmental endocrine disruptors and neurological disorders," *Journal of the Korean Neurological Association*, vol. 36, no. 3, pp. 139–144, 2018.

[29] A. C. Gore, V. A. Chappell, S. E. Fenton et al., "EDC-2: The Endocrine Society's second scientific statement on endocrine-disrupting chemicals," *Endocrine Reviews*, vol. 36, no. 6, pp. E1–E150, 2015.

[30] R. T. Zoeller, T. R. Brown, L. L. Doan et al., "Endocrine-disrupting chemicals and public health protection: a statement

of principles from The Endocrine Society," *Endocrinology*, vol. 153, no. 9, pp. 4097–4110, 2012.

[31] K. L. G. Russart and R. J. Nelson, "Light at night as an environmental endocrine disruptor," *Physiology & Behavior*, vol. 190, pp. 82–89, 2018.

[32] L. N. Vandenberg, T. Colborn, T. B. Hayes et al., "Hormones and endocrine-disrupting chemicals: low-dose effects and nonmonotonic dose responses," *Endocrine Reviews*, vol. 33, no. 3, pp. 378–455, 2012.

[33] A. C. Gore, D. Crews, L. L. Doan, M. La Merrill, H. Patisaul, and A. Zota, "Introduction to endocrine disrupting chemicals (EDCs)," *A guide for public interest organizations and policy-makers*, pp. 21-22, 2014.

[34] N. E. De Long and A. C. Holloway, "Early-life chemical exposures and risk of metabolic syndrome," *Diabetes, Metabolic Syndrome and Obesity: Targets and Therapy*, vol. Volume 10, pp. 101–109, 2017.

[35] B. Eskenazi, J. Chevrier, S. A. Rauch et al., "In utero and childhood polybrominated diphenyl ether (PBDE) exposures and neurodevelopment in the CHAMACOS study," *Environmental Health Perspectives*, vol. 121, no. 2, pp. 257–262, 2013.

[36] T. B. Hayes, A. Collins, M. Lee et al., "Hermaphroditic, demasculinized frogs after exposure to the herbicide atrazine at low ecologically relevant doses," *Proceedings of the National Academy of Sciences*, vol. 99, no. 8, pp. 5476–5480, 2002.

[37] E. O. Adegoke, M. S. Rahman, Y. J. Park, Y. J. Kim, and M. G. Pang, "Endocrine-disrupting chemicals and infectious diseases: from endocrine disruption to immunosuppression," *International Journal of Molecular Sciences*, vol. 22, no. 8, p. 3939, 2021.

[38] C. S. Rosenfeld, "Microbiome disturbances and autism spectrum disorders," *Drug Metabolism and Disposition*, vol. 43, no. 10, pp. 1557–1571, 2015.

[39] S. Lymperi and A. Giwercman, "Endocrine disruptors and testicular function," *Metabolism*, vol. 86, pp. 79–90, 2018.

[40] I. N. Pessah, P. J. Lein, R. F. Seegal, and S. K. Sagiv, "Neurotoxicity of polychlorinated biphenyls and related organohalogens," *Acta Neuropathologica*, vol. 138, no. 3, pp. 363–387, 2019.

[41] D. Luo, Y. Pu, H. Tian et al., "Association of in utero exposure to organochlorine pesticides with thyroid hormone levels in cord blood of newborns," *Environmental Pollution*, vol. 231, Part 1, pp. 78–86, 2017.

[42] B. Yilmaz, H. Terekeci, S. Sandal, and F. Kelestimur, "Endocrine disrupting chemicals: exposure, effects on human health, mechanism of action, models for testing and strategies for prevention," *Reviews in Endocrine & Metabolic Disorders*, vol. 21, no. 1, pp. 127–147, 2020.

[43] L. De Toni, F. Tisato, R. Seraglia et al., "Phthalates and heavy metals as endocrine disruptors in food: a study on pre-packed coffee products," *Toxicology Reports*, vol. 4, pp. 234–239, 2017.

[44] H. B. Patisaul, "Endocrine disruption by dietary phyto-oestrogens: impact on dimorphic sexual systems and behaviours," *The Proceedings of the Nutrition Society*, vol. 76, no. 2, pp. 130–144, 2017.

[45] P. J. Kushner, D. A. Agard, G. L. Greene et al., "Estrogen receptor pathways to AP-1," *The Journal of Steroid Biochemistry and Molecular Biology*, vol. 74, no. 5, pp. 311–317, 2000.

[46] S. M. Belcher and A. Zsarnovszky, "Estrogenic actions in the brain: estrogen, phytoestrogens, and rapid intracellular signaling mechanisms," *The Journal of Pharmacology and Experimental Therapeutics*, vol. 299, no. 2, pp. 408–414, 2001.

[47] A. Nadal, E. Fuentes, C. Ripoll et al., "Extranuclear-initiated estrogenic actions of endocrine disrupting chemicals: is there toxicology beyond paracelsus?," *The Journal of Steroid Biochemistry and Molecular Biology*, vol. 176, pp. 16–22, 2018.

[48] E. K. Shanle and W. Xu, "Endocrine disrupting chemicals targeting estrogen receptor signaling: identification and mechanisms of action," *Chemical Research in Toxicology*, vol. 24, no. 1, pp. 6–19, 2011.

[49] N. Tagawa, S. Kubota, Y. Kobayashi, and I. Kato, "Genistein inhibits glucocorticoid amplification in adipose tissue by suppression of 11β-hydroxysteroid dehydrogenase type 1," *Steroids*, vol. 93, pp. 77–86, 2015.

[50] Y. L. Low, A. M. Dunning, M. Dowsett et al., "Implications of gene-environment interaction in studies of gene variants in breast cancer: an example of dietary isoflavones and the D356N polymorphism in the sex hormone-binding globulin gene," *Cancer Research*, vol. 66, no. 18, pp. 8980–8983, 2006.

[51] A. M. Mahmoud, W. Yang, and M. C. Bosland, "Soy isoflavones and prostate cancer: a review of molecular mechanisms," *The Journal of Steroid Biochemistry and Molecular Biology*, vol. 140, pp. 116–132, 2014.

[52] S. Lecomte, F. Demay, F. Ferrière, and F. Pakdel, "Phytochemicals Targeting Estrogen Receptors: Beneficial Rather Than Adverse Effects?," *International Journal of Molecular Sciences*, vol. 18, no. 7, p. 1381, 2017.

[53] D. S. Bar-El and R. Reifen, "Soy as an endocrine disruptor: cause for caution?," *Journal of Pediatric Endocrinology & Metabolism*, vol. 23, no. 9, pp. 855–861, 2010.

[54] H. Wang and P. A. Murphy, "Isoflavone composition of American and Japanese soybeans in Iowa: effects of variety, crop year, and location," *Journal of agricultural and food chemistry*, vol. 42, no. 8, pp. 1674–1677, 1994.

[55] K. D. Setchell, "Phytoestrogens: the biochemistry, physiology, and implications for human health of soy isoflavones," *The American Journal of Clinical Nutrition*, vol. 68, no. 6, pp. 1333S–1346S, 1998.

[56] R. Meena, C. Supriya, K. Pratap Reddy, and R. P. Sreenivasula, "Altered spermatogenesis, steroidogenesis and suppressed fertility in adult male rats exposed to genistein, a non-steroidal phytoestrogen during embryonic development," *Food and Chemical Toxicology*, vol. 99, pp. 70–77, 2017.

[57] G. I. Russo, M. Di Mauro, F. Regis et al., "Association between dietary phytoestrogens intakes and prostate cancer risk in Sicily," *The Aging Male*, vol. 21, no. 1, pp. 48–54, 2018.

[58] S. Poschner, A. Maier-Salamon, M. Zehl et al., "The impacts of genistein and daidzein on estrogen conjugations in human breast cancer cells: a targeted metabolomics approach," *Frontiers in Pharmacology*, vol. 8, p. 699, 2017.

[59] P. F. Cheng, J. J. Chen, X. Y. Zhou et al., "Do soy isoflavones improve cognitive function in postmenopausal women? A meta-analysis," *Menopause*, vol. 22, no. 2, pp. 198–206, 2015.

[60] D. Kritz-Silverstein, D. Von Mühlen, E. Barrett-Connor, and M. A. Bressel, "Isoflavones and cognitive function in older women: the SOy and Postmenopausal Health In Aging (SOPHIA) Study," *Menopause*, vol. 10, no. 3, pp. 196–202, 2003.

[61] C. E. Gleason, B. L. Fischer, N. M. Dowling et al., "Cognitive effects of soy isoflavones in patients with Alzheimer's disease," *Journal of Alzheimer's Disease*, vol. 47, no. 4, pp. 1009–1019, 2015.

[62] A. Sekikawa, M. Ihara, O. Lopez et al., "Effect of S-equol and soy isoflavones on heart and brain," *Current Cardiology Reviews*, vol. 15, no. 2, pp. 114–135, 2019.

[63] S. E. File, N. Jarrett, E. Fluck, R. Duffy, K. Casey, and H. Wiseman, "Eating soya improves human memory," *Psychopharmacology*, vol. 157, no. 4, pp. 430–436, 2001.

[64] T. Li, T. M. Badger, B. J. Bellando, S. T. Sorensen, X. Lou, and X. Ou, "Brain cortical structure and executive function in children may be influenced by parental choices of infant diets," *American Journal of Neuroradiology*, vol. 41, no. 7, pp. 1302–1308, 2020.

[65] A. A. Thorp, N. Sinn, J. D. Buckley, A. M. Coates, and P. R. Howe, "Soya isoflavone supplementation enhances spatial working memory in men," *The British Journal of Nutrition*, vol. 102, no. 9, pp. 1348–1354, 2009.

[66] R. Z. Li, X. W. Ding, T. Geetha, L. Al-Nakkash, T. L. Broderick, and J. R. Babu, "Beneficial effect of genistein on diabetes-induced brain damage in the ob/ob mouse model," *Drug Design, Development and Therapy*, vol. 14, pp. 3325–3336, 2020.

[67] Y. J. Park, J. W. Ko, S. Jeon, and Y. H. Kwon, "Protective effect of genistein against neuronal degeneration in ApoE-/- mice fed a high-fat diet," *Nutrients*, vol. 8, no. 11, p. 692, 2016.

[68] R. Langasco, S. Fancello, G. Rassu et al., "Increasing protective activity of genistein by loading into transfersomes: a new potential adjuvant in the oxidative stress-related neurodegenerative diseases?," *Phytomedicine*, vol. 52, pp. 23–31, 2019.

[69] G. Rassu, E. P. Porcu, S. Fancello et al., "Intranasal delivery of genistein-loaded nanoparticles as a potential preventive system against neurodegenerative disorders," *Pharmaceutics*, vol. 11, no. 1, p. 8, 2018.

[70] J. W. Ko, Y.-S. Chung, C. S. Kwak, and Y. H. Kwon, "Doenjang, A Korean Traditional Fermented Soybean Paste, Ameliorates Neuroinflammation and Neurodegeneration in Mice Fed a High-Fat Diet," *Nutrients*, vol. 11, no. 8, p. 1702, 2019.

[71] K. V. Sandhu, Y. E. Demiray, Y. Yanagawa, and O. Stork, "Dietary phytoestrogens modulate aggression and activity in social behavior circuits of male mice," *Hormones and Behavior*, vol. 119, p. 104637, 2020.

[72] Y. Pan, M. Anthony, and T. B. Clarkson, "Evidence for up-regulation of brain-derived neurotrophic factor mRNA by soy phytoestrogens in the frontal cortex of retired breeder female rats," *Neuroscience Letters*, vol. 261, no. 1-2, pp. 17–20, 1999.

[73] A. Hussain, E. S. Tabrez, A. Muhammad, and J. R. Peela, "The mechanisms of dietary phytoestrogen as a potential treatment and prevention agent against Alzheimer's disease," *Critical Reviews in Eukaryotic Gene Expression*, vol. 28, no. 4, pp. 321–327, 2018.

[74] S. Khanna, R. Stewart, S. Gnyawali et al., "Phytoestrogen isoflavone intervention to engage the neuroprotective effect of glutamate oxaloacetate transaminase against stroke," *The FASEB Journal*, vol. 31, no. 10, pp. 4533–4544, 2017.

[75] J. W. Tan and M. K. Kim, "Neuroprotective effects of biochanin A against β-amyloid-induced neurotoxicity in PC12 cells via a mitochondrial-dependent apoptosis pathway," *Molecules*, vol. 21, no. 5, p. 548, 2016.

[76] A. Y. Choi, J. H. Choi, J. Y. Lee et al., "Apigenin protects HT22 murine hippocampal neuronal cells against endoplasmic reticulum stress-induced apoptosis," *Neurochemistry International*, vol. 57, no. 2, pp. 143–152, 2010.

[77] S. S. Kang, J. Y. Lee, Y. K. Choi, G. S. Kim, and B. H. Han, "Neuroprotective effects of flavones on hydrogen peroxide-induced apoptosis in SH-SY5Y neuroblastoma cells," *Bioorganic & Medicinal Chemistry Letters*, vol. 14, no. 9, pp. 2261–2264, 2004.

[78] G. Losi, G. Puia, G. Garzon, M. C. de Vuono, and M. Baraldi, "Apigenin modulates GABAergic and glutamatergic transmission in cultured cortical neurons," *European Journal of Pharmacology*, vol. 502, no. 1-2, pp. 41–46, 2004.

[79] L. Subedi, E. Ji, D. Shin, J. Jin, J. H. Yeo, and S. Y. Kim, "Equol, a Dietary Daidzein Gut Metabolite Attenuates Microglial Activation and Potentiates Neuroprotection In Vitro," *Nutrients*, vol. 9, no. 3, p. 207, 2017.

[80] S. L. Johnson, H. Y. Park, D. A. Vattem, P. Grammas, H. Ma, and N. P. Seeram, "Equol, a blood-brain barrier permeable gut microbial metabolite of dietary isoflavone daidzein, exhibits neuroprotective effects against neurotoxins induced toxicity in human neuroblastoma SH-SY5Y cells and Caenorhabditis elegans," *Plant Foods for Human Nutrition*, vol. 75, no. 4, pp. 512–517, 2020.

[81] H. Khan, H. Ullah, M. Aschner, W. S. Cheang, and E. K. Akkol, "Neuroprotective effects of quercetin in Alzheimer's disease," *Biomolecules*, vol. 10, no. 1, p. 59, 2019.

[82] K. B. Magalingam, A. K. Radhakrishnan, and N. Haleagrahara, "Protective mechanisms of flavonoids in Parkinson's disease," *Oxidative Medicine and Cellular Longevity*, vol. 2015, Article ID 314560, 14 pages, 2015.

[83] J. H. Kim, S. Lee, E. J. Cho, and H. Y. Kim, "Neuroprotective effects of kaempferol, quercetin, and its glycosides by regulation of apoptosis," *Journal of the Korea Academia-Industrial cooperation Society*, vol. 20, no. 2, pp. 286–293, 2019.

[84] G. Abbruzzese, J. Morón-Oset, S. Díaz-Castroverde et al., "Neuroprotection by phytoestrogens in the model of deprivation and resupply of oxygen and glucose in vitro: the contribution of autophagy and related signaling mechanisms," *Antioxidants*, vol. 9, no. 6, p. 545, 2020.

[85] M. M. A. de Almeida, C. D. S. Souza, N. S. Dourado et al., "Phytoestrogen agathisflavone ameliorates neuroinflammation-induced by LPS and IL-1β and protects neurons in cocultures of glia/neurons," *Biomolecules*, vol. 10, no. 4, p. 562, 2020.

[86] H. S. Hafez, D. A. Ghareeb, S. R. Saleh et al., "Neuroprotective effect of ipriflavone against scopolamine-induced memory impairment in rats," *Psychopharmacology*, vol. 234, no. 20, pp. 3037–3053, 2017.

[87] R. Balez, N. Steiner, M. Engel et al., "Neuroprotective effects of apigenin against inflammation, neuronal excitability and apoptosis in an induced pluripotent stem cell model of Alzheimer's disease," *Scientific Reports*, vol. 6, no. 1, p. 31450, 2016.

[88] L. Zhao, J. L. Wang, R. Liu, X. X. Li, J. F. Li, and L. Zhang, "Neuroprotective, anti-amyloidogenic and neurotrophic effects of apigenin in an Alzheimer's disease mouse model," *Molecules*, vol. 18, no. 8, pp. 9949–9965, 2013.

[89] A. M. Sabogal-Guáqueta, J. I. Muñoz-Manco, J. R. Ramírez-Pineda, M. Lamprea-Rodriguez, E. Osorio, and G. P.

Cardona-Gómez, "The flavonoid quercetin ameliorates Alzheimer's disease pathology and protects cognitive and emotional function in aged triple transgenic Alzheimer's disease model mice," *Neuropharmacology*, vol. 93, pp. 134–145, 2015.

[90] N. Shveta, K. Rozy, and K. D. Devinder, "Neuroprotective role of quercetin against arsenic induced oxidative stress in rat brain," *Journal of Environmental & Analytical Toxicology*, vol. 6, p. 359, 2016.

[91] K. H. Jeong, U. J. Jung, and S. R. Kim, "Naringin attenuates autophagic stress and neuroinflammation in kainic acid-treated hippocampus in vivo," *Evidence-Based Complementary and Alternative Medicine*, vol. 2015, Article ID 354326, 9 pages, 2015.

[92] S. F. Nabavi, N. Braidy, O. Gortzi et al., "Luteolin as an anti-inflammatory and neuroprotective agent: a brief review," *Brain Research Bulletin*, vol. 119, no. Part A, pp. 1–11, 2015.

[93] T. Farkhondeh, H. S. Yazdi, and S. Samarghandian, "The protective effects of green tea catechins in the management of neurodegenerative diseases: a review," *Current Drug Discovery Technologies*, vol. 16, no. 1, pp. 57–65, 2019.

[94] S. J. Lee, E. Nam, H. J. Lee, M. G. Savelieff, and M. H. Lim, "Towards an understanding of amyloid-β oligomers: characterization, toxicity mechanisms, and inhibitors," *Chemical Society Reviews*, vol. 46, no. 2, pp. 310–323, 2017.

[95] L. Ciccone, N. Tonali, S. Nencetti, and E. Orlandini, "Natural compounds as inhibitors of transthyretin amyloidosis and neuroprotective agents: analysis of structural data for future drug design," *Journal of Enzyme Inhibition and Medicinal Chemistry*, vol. 35, no. 1, pp. 1145–1162, 2020.

[96] Y. Wu, J. Geng, X. Lei, Q. Wu, T. Chen, and L. Zhong, "Glabridin downregulates lipopolysaccharide-induced oxidative stress and neuroinflammation in BV-2 microglial cells via suppression of nuclear factor-κB signaling pathway," *Pharmacognosy Magazine*, vol. 16, no. 71, pp. 675–680, 2020.

[97] Y. Lee, S. Kim, Y. Oh, Y. M. Kim, Y. W. Chin, and J. Cho, "Inhibition of oxidative neurotoxicity and scopolamine-induced memory impairment by γ-mangostin: in vitro and in vivo evidence," *Oxidative Medicine and Cellular Longevity*, vol. 2019, Article ID 3640753, 14 pages, 2019.

[98] T. Ohgomori and S. Jinno, "Cuprizone-induced demyelination in the mouse hippocampus is alleviated by phytoestrogen genistein," *Toxicology and Applied Pharmacology*, vol. 363, pp. 98–110, 2019.

[99] J. Wang, W. Y. Wu, H. Huang, W. Z. Li, H. Q. Chen, and Y. Y. Yin, "Biochanin a protects against lipopolysaccharide-induced damage of dopaminergic neurons both in vivo and in vitro via inhibition of microglial activation," *Neurotoxicity Research*, vol. 30, no. 3, pp. 486–498, 2016.

[100] R. Pluta, S. Januszewski, and S. J. Czuczwar, "Brain ischemia as a prelude to Alzheimer's disease," *Frontiers in Aging Neuroscience*, vol. 13, p. 636653, 2021.

[101] Y. Wang, Y. Shi, and H. Wei, "Calcium dysregulation in Alzheimer's disease: a target for new drug development," *Journal of Alzheimer's Disease & Parkinsonism*, vol. 7, no. 5, p. 374, 2017.

[102] B. Stegmayr, K. Asplund, K. Kuulasmaa, A. M. Rajakangas, P. Thorvaldsen, and J. Tuomilehto, "Stroke incidence and mortality correlated to stroke risk factors in the WHO MONICA project. An ecological study of 18 populations," *Stroke*, vol. 28, no. 7, pp. 1367–1374, 1997.

[103] D. A. Schreihofer and L. Redmond, "Soy phytoestrogens are neuroprotective against stroke-like injury in vitro," *Neuroscience*, vol. 158, no. 2, pp. 602–609, 2009.

[104] V. Murugaiyah and M. P. Mattson, "Neurohormetic phytochemicals: an evolutionary-bioenergetic perspective," *Neurochemistry International*, vol. 89, pp. 271–280, 2015.

[105] J. Kim, D. Y. Fann, R. C. Seet, D. G. Jo, M. P. Mattson, and T. V. Arumugam, "Phytochemicals in ischemic stroke," *Neuromolecular Medicine*, vol. 18, no. 3, pp. 283–305, 2016.

[106] A. Murakami, "Modulation of protein quality control systems by food phytochemicals," *Journal of Clinical Biochemistry and Nutrition*, vol. 52, no. 3, pp. 215–227, 2013.

[107] F. R. Sharp, X. Zhan, and D. Z. Liu, "Heat shock proteins in the brain: role of Hsp70, Hsp 27, and HO-1 (Hsp32) and their therapeutic potential," *Translational Stroke Research*, vol. 4, no. 6, pp. 685–692, 2013.

[108] F. A. Wiegant, S. A. de Poot, V. E. Boers-Trilles, and A. M. Schreij, "Hormesis and cellular quality control: a possible explanation for the molecular mechanisms that underlie the benefits of mild stress," *Dose Response*, vol. 11, no. 3, pp. 413–430, 2012.

[109] A. Rahman, H. Jackson, H. Hristov et al., "Sex and gender driven modifiers of Alzheimer's: the role for estrogenic control across age, race, medical, and lifestyle risks," *Frontiers in Aging Neuroscience*, vol. 11, 2019.

[110] C. J. Pike, "Sex and the development of Alzheimer's disease," *Journal of Neuroscience Research*, vol. 95, no. 1-2, pp. 671–680, 2017.

[111] M. S. Uddin, M. M. Rahman, M. Jakaria et al., "Estrogen signaling in Alzheimer's disease: molecular insights and therapeutic targets for Alzheimer's dementia," *Molecular Neurobiology*, vol. 57, no. 6, pp. 2654–2670, 2020.

[112] M. McCarthy and A. P. Raval, "The peri-menopause in a woman's life: a systemic inflammatory phase that enables later neurodegenerative disease," *Journal of Neuroinflammation*, vol. 17, no. 1, p. 317, 2020.

[113] O. Scheyer, A. Rahman, H. Hristov et al., "Female sex and Alzheimer's risk: the menopause connection," *The Journal Of Prevention of Alzheimer's Disease*, vol. 5, no. 4, pp. 225–230, 2018.

[114] Y. J. Song, S. R. Li, X. W. Li et al., "The effect of estrogen replacement therapy on Alzheimer's disease and Parkinson's disease in postmenopausal women: a meta-analysis," *Frontiers in Neuroscience*, vol. 14, p. 157, 2020.

[115] H. Depypere, A. Vierin, S. Weyers, and A. Sieben, "Alzheimer's disease, apolipoprotein E and hormone replacement therapy," *Maturitas*, vol. 94, pp. 98–105, 2016.

[116] W. A. Rocca, J. H. Bower, D. M. Maraganore et al., "Increased risk of cognitive impairment or dementia in women who underwent oophorectomy before menopause," *Neurology*, vol. 69, no. 11, pp. 1074–1083, 2007.

[117] B. Imtiaz, M. Tuppurainen, T. Rikkonen et al., "Postmenopausal hormone therapy and Alzheimer disease: a prospective cohort study," *Neurology*, vol. 88, no. 11, pp. 1062–1068, 2017.

[118] C. Chávez-Pérez, A. Ceballos-Ramírez, and A. Suárez-Castro, "Efectos del uso del 17 β-estradiol y la genisteína en la enfermedad de Alzheimer en mujeres con menopausia [Effects of the use of 17 β-estradiol and genistein in Alzheimer's disease in women with menopause]," *Revista Española de Geriatría y Gerontología*, vol. 56, no. 4, pp. 236–240, 2021.

[119] H. Guo, M. Liu, L. Zhang et al., "The critical period for neuroprotection by estrogen replacement therapy and the potential underlying mechanisms," *Current Neuropharmacology*, vol. 18, no. 6, pp. 485–500, 2020.

[120] C. Zhou, Q. Wu, Z. Wang, Q. Wang, Y. Liang, and S. Liu, "The effect of hormone replacement therapy on cognitive function in female patients with Alzheimer's disease: a meta-analysis," *American Journal of Alzheimer's Disease and Other Dementias*, vol. 35, p. 1533317520938585, 2020.

[121] H. Savolainen-Peltonen, P. Rahkola-Soisalo, F. Hoti et al., "Use of postmenopausal hormone therapy and risk of Alzheimer's disease in Finland: nationwide case-control study," *BMJ*, vol. 364, p. l665, 2019.

[122] R. Luoto, S. Männistö, and E. Vartiainen, "Hormone replacement therapy and body size: how much does lifestyle explain?," *American Journal of Obstetrics and Gynecology*, vol. 178, 1 Part 1, pp. 66–73, 1998.

[123] C. Renoux, S. Dell'Aniello, and S. Suissa, "Hormone replacement therapy and the risk of venous thromboembolism: a population-based study," *Journal of Thrombosis and Haemostasis*, vol. 8, no. 5, pp. 979–986, 2010.

[124] J. C. Stevenson, "Hormone replacement therapy and cardiovascular disease revisited," *Menopause International*, vol. 15, no. 2, pp. 55–57, 2009.

[125] A. C. Moreira, A. M. Silva, M. S. Santos, and V. A. Sardão, "Phytoestrogens as alternative hormone replacement therapy in menopause: what is real, what is unknown," *The Journal of Steroid Biochemistry and Molecular Biology*, vol. 143, pp. 61–71, 2014.

[126] V. Coxam, "Phyto-oestrogens and bone health," *The Proceedings of the Nutrition Society*, vol. 67, no. 2, pp. 184–195, 2008.

[127] E. L. Robb and J. A. Stuart, "Multiple phytoestrogens inhibit cell growth and confer cytoprotection by inducing manganese superoxide dismutase expression," *Phytotherapy Research*, vol. 28, no. 1, pp. 120–131, 2014.

[128] C. Carreau, G. Flouriot, C. Bennetau-Pelissero, and M. Potier, "Enterodiol and enterolactone, two major diet-derived polyphenol metabolites have different impact on ERalpha transcriptional activation in human breast cancer cells," *The Journal of Steroid Biochemistry and Molecular Biology*, vol. 110, no. 1-2, pp. 176–185, 2008.

[129] S. Md, S. Y. Gan, Y. H. Haw, C. L. Ho, S. Wong, and H. Choudhury, "In vitro neuroprotective effects of naringenin nanoemulsion against β-amyloid toxicity through the regulation of amyloidogenesis and tau phosphorylation," *International Journal of Biological Macromolecules*, vol. 118, no. Part A, pp. 1211–1219, 2018.

[130] M. Alemi, S. C. Silva, I. Santana, and I. Cardoso, "Transthyretin stability is critical in assisting beta amyloid clearance-relevance of transthyretin stabilization in Alzheimer's disease," *CNS Neuroscience & Therapeutics*, vol. 23, no. 7, pp. 605–619, 2017.

[131] E. Y. Cotrina, A. Gimeno, J. Llop et al., "Calorimetric studies of binary and ternary molecular interactions between transthyretin, $A\beta$ peptides, and small-molecule chaperones toward an alternative strategy for Alzheimer's disease drug discovery," *10.1021/acs.jmedchem.9b01970*, vol. 63, no. 6, pp. 3205–3214, 2020.

[132] M. Messina, "Investigating the optimal soy protein and isoflavone intakes for women: a perspective," *Womens Health*, vol. 4, no. 4, pp. 337–356, 2008.

[133] G. Rizzo, "The antioxidant role of soy and soy foods in human health," *Antioxidants*, vol. 9, no. 7, p. 635, 2020.

[134] M. Yao, T. V. Nguyen, and C. J. Pike, "Estrogen regulates Bcl-w and Bim expression: role in protection against beta-amyloid peptide-induced neuronal death," *Journal of Neuroscience*, vol. 27, no. 6, pp. 1422–1433, 2007.

[135] P. Duarte-Guterman, S. E. Lieblich, C. Chow, and L. A. Galea, "Estradiol and GPER activation differentially affect cell proliferation but not GPER expression in the hippocampus of adult female rats," *PLoS One*, vol. 10, no. 6, article e0129880, 2015.

[136] T. W. Wu, J. M. Wang, S. Chen, and R. D. Brinton, "17Beta-estradiol induced Ca2+ influx via L-type calcium channels activates the Src/ERK/cyclic-AMP response element binding protein signal pathway and BCL-2 expression in rat hippocampal neurons: a potential initiation mechanism for estrogen-induced neuroprotection," *Neuroscience*, vol. 135, no. 1, pp. 59–72, 2005.

[137] H. Yi, X. Bao, X. Tang, X. Fan, and H. Xu, "Estrogen modulation of calretinin and BDNF expression in midbrain dopaminergic neurons of ovariectomised mice," *Journal of Chemical Neuroanatomy*, vol. 77, pp. 60–67, 2016.

[138] Y. Zhao, J. Zhao, X. Zhang et al., "Botanical drug puerarin promotes neuronal survival and neurite outgrowth against MPTP/MPP+-induced toxicity via progesterone receptor signaling," *Oxidative Medicine and Cellular Longevity*, vol. 2020, Article ID 7635291, 11 pages, 2020.

[139] I. M. C. M. Rietjens, J. Louisse, and K. Beekmann, "The potential health effects of dietary phytoestrogens," *British Journal of Pharmacology*, vol. 174, no. 11, pp. 1263–1280, 2017.

[140] S. Sahab-Negah, V. Hajali, H. R. Moradi, and A. Gorji, "The impact of estradiol on neurogenesis and cognitive functions in Alzheimer's disease," *Cellular and Molecular Neurobiology*, vol. 40, no. 3, pp. 283–299, 2020.

[141] K. Keyvani, Y. Münster, N. K. Kurapati et al., "Higher levels of kallikrein-8 in female brain may increase the risk for Alzheimer's disease," *Brain Pathology*, vol. 28, no. 6, pp. 947–964, 2018.

[142] M. Alvarez-de-la-Rosa, I. Silva, J. Nilsen et al., "Estradiol prevents neural tau hyperphosphorylation characteristic of Alzheimer's disease," *Annals of the New York Academy of Sciences*, vol. 1052, pp. 210–224, 2005.

[143] J. C. Means, A. A. Lopez, and P. Koulen, "Estrogen protects optic nerve head astrocytes against oxidative stress by preventing caspase-3 activation, tau dephosphorylation at Ser422 and the formation of tau protein aggregates," *Cellular and Molecular Neurobiology*, vol. 41, no. 3, pp. 449–458, 2021.

[144] Z. Zhenxia, L. Min, Y. Peikui et al., "Inhibition of tau aggregation and associated cytotoxicity on neuron-like cells by calycosin," *International Journal of Biological Macromolecules*, vol. 171, pp. 74–81, 2021.

[145] Y. J. Park, Y. M. Jang, and Y. H. Kwon, "Isoflavones prevent endoplasmic reticulum stress-mediated neuronal degeneration by inhibiting tau hyperphosphorylation in SH-SY5Y cells," *Journal of Medicinal Food*, vol. 12, no. 3, pp. 528–535, 2009.

[146] F. D. S. Petry, B. P. Coelho, M. M. Gaelzer et al., "Genistein protects against amyloid-beta-induced toxicity in SH-SY5Y cells by regulation of Akt and tau phosphorylation," *Phytotherapy Research*, vol. 34, no. 4, pp. 796–807, 2020.

[147] S. Ye, T. T. Wang, B. Cai et al., "Genistein protects hippocampal neurons against injury by regulating calcium/calmodulin dependent protein kinase IV protein levels in Alzheimer's disease model rats," *Neural Regeneration Research*, vol. 12, no. 9, pp. 1479–1484, 2017.

[148] E. Y. L. Liu, M. L. Xu, Y. Jin, Q. Wu, T. T. X. Dong, and K. W. K. Tsim, "Genistein, a phytoestrogen in soybean, induces the expression of acetylcholinesterase via G protein-coupled receptor 30 in PC12 cells," *Frontiers in Molecular Neuroscience*, vol. 11, 2018.

[149] A. Cattaneo and P. Calissano, "Nerve growth factor and Alzheimer's disease: new facts for an old hypothesis," *Molecular Neurobiology*, vol. 46, no. 3, pp. 588–604, 2012.

[150] S. Mitra, H. Behbahani, and M. Eriksdotter, "Innovative therapy for Alzheimer's disease-with focus on biodelivery of NGF," *Frontiers in Neuroscience*, vol. 13, 2019.

[151] A. C. Cuello, R. Pentz, and H. Hall, "The brain NGF metabolic pathway in health and in Alzheimer's pathology," *Frontiers in Neuroscience*, vol. 13, 2019.

[152] S. R. Wilkenfeld, C. Lin, and D. E. Frigo, "Communication between genomic and non-genomic signaling events coordinate steroid hormone actions," *Steroids*, vol. 133, pp. 2–7, 2018.

[153] P. Morley, J. F. Whitfield, B. C. Vanderhyden, B. K. Tsang, and J. L. Schwartz, "A new, nongenomic estrogen action: the rapid release of intracellular calcium," *Endocrinology*, vol. 131, no. 3, pp. 1305–1312, 1992.

[154] A. Demuro, I. Parker, and G. E. Stutzmann, "Calcium signaling and amyloid toxicity in Alzheimer disease," *Journal of Biological Chemistry*, vol. 285, no. 17, pp. 12463–12468, 2010.

[155] E. Hogervorst, S. Kassam, A. Kridawati et al., "Nutrition research in cognitive impairment/dementia, with a focus on soya and folate," *The Proceedings of the Nutrition Society*, vol. 76, no. 4, pp. 437–442, 2017.

[156] M. S. Uddin and M. T. Kabir, "Emerging signal regulating potential of genistein against Alzheimer's disease: a promising molecule of interest," *Frontiers in Cell and Developmental Biology*, vol. 7, 2019.

[157] D. Mohammad, P. Chan, J. Bradley, K. Lanctôt, and N. Herrmann, "Acetylcholinesterase inhibitors for treating dementia symptoms - a safety evaluation," *Expert Opinion on Drug Safety*, vol. 16, no. 9, pp. 1009–1019, 2017.

Research Article

Regulation of *Laminaria* Polysaccharides with Different Degrees of Sulfation during the Growth of Calcium Oxalate Crystals and their Protective Effects on Renal Epithelial Cells

Wei-Bo Huang,[1] Guo-Jun Zou,[1] Gu-Hua Tang,[1] Xin-Yuan Sun,[2] and Jian-Ming Ouyang [1]

[1]*Institute of Biomineralization and Lithiasis Research, Jinan University, Guangzhou 510632, China*
[2]*Department of Urology, Guangzhou Institute of Urology, Guangdong Key Laboratory of Urology, The First Affiliated Hospital of Guangzhou Medical University, Guangzhou Medical University, Guangzhou, Guangdong 510230, China*

Correspondence should be addressed to Jian-Ming Ouyang; toyjm@jnu.edu.cn

The original *Laminaria* polysaccharide (LP0) was sulfated using the sulfur trioxide-pyridine method, and four sulfated *Laminaria* polysaccharides (SLPs) were obtained, namely, SLP1, SLP2, SLP3, and SLP4. The sulfated ($-OSO_3^-$) contents were 8.58%, 15.1%, 22.8%, and 31.3%, respectively. The structures of the polysaccharides were characterized using a Fourier transform infrared (FT-IR) spectrometer and nuclear magnetic resonance (NMR) techniques. SLPs showed better antioxidant activity than LP0, increased the concentration of soluble Ca^{2+} in the solution, reduced the amount of CaOx precipitation and degree of CaOx crystal aggregation, induced COD crystal formation, and protected HK-2 cells from damage caused by nanometer calcium oxalate crystals. These effects can inhibit the formation of CaOx kidney stones. The biological activity of the polysaccharides increased with the content of $-OSO_3^-$, that is, the biological activities of the polysaccharides had the following order: LP0 < SLP1 < SLP2 < SLP3 < SLP4. These results reveal that SLPs with high $-OSO_3^-$ contents are potential drugs for effectively inhibiting the formation of CaOx stones.

1. Introduction

The prevalence and incidence of kidney stones are on the rise globally, and no effective drug to treat or prevent the disease is currently available [1]. Calcium oxalate (CaOx) is the main inorganic component of kidney stones, accounting for about 70%–80% [2]. CaOx in kidney stones mainly exists in the form of calcium oxalate monohydrate (COM) and calcium oxalate dihydrate (COD) [3]. COM is the most stable phase of thermodynamics and the most common form of stones. The incidence of stones caused by COM is twice that caused by COD [4]. Compared with COD, COM has a greater affinity for renal tubular cells [5] and is more difficult to be excreted in the urine. Therefore, COM in the body is more likely to induce kidney stone formation than COD crystals.

Oxidative stress-induced damage to renal tubular epithelial cells and decrease in inhibitor molecules in urine or in their activities are the important reasons for the formation of CaOx stones [6, 7]. Increasing the concentrations and/or activities of inhibitors in the urine, removing excess free radicals in the body, and protecting renal tubular epithelial cells from oxidative damage may inhibit the formation and recurrence of kidney stones.

The chemical structures of plant polysaccharides are very similar to the structure of CaOx crystal growth inhibitor glucosamine (GAGs), which is commonly found in urine. Plant polysaccharides contain a large number of anionic groups, such as sulfate groups ($-OSO_3^-$) and carboxyl groups ($-COO^-$), and can thus be used to inhibit the formation of CaOx kidney stones. Huang et al. [8] showed that plant polysaccharides can inhibit the growth and

aggregation of COM and induce the formation of COD. Gangu et al. [9] found that Gum Arabic (GA) can regulate the phase and morphology of CaOx, promote the formation of COD crystals, and inhibit the growth of COM crystals.

High concentrations of oxalic acid and CaOx or CaP crystals activate NADPH oxidase, produce excessive reactive oxygen species (ROS), and induce the inflammation and oxidative damage of renal epithelial cells, leading to the death of renal epithelial cells [10]. Tubular epithelial cell injury can induce the high expression of cell surface adhesion molecules, such as hyaluronic acid, osteopontin (OPN), and CD44, resulting in the accumulation of CaOx crystals in the kidney [11, 12]. Xi et al. [13] showed that high concentrations of calcium stimulate the attachment of CaOx crystals to rat renal tubular epithelial cells by inducing OPN expression, leading to the deposition of crystals in the kidney and the formation of CaOx stones. Plant polysaccharides can protect renal epithelial cells from oxidative damage by inhibiting the adhesion of CaOx crystals to cells. For example, Zhao et al. [14] found that tea polysaccharides can effectively protect HK-2 cells from COM damage, thus increasing cell viability, restoring cell morphology, increasing lysosome integrity, and reducing crystal adhesion. These features inhibit the production of kidney stones.

Plant polysaccharides not only effectively remove superoxide and various free radicals, such as hydroxyl, DPPH, and ABTS, but also reduce the level of lipid peroxidation, are less toxic, and have a lower number of side effects on the body. The biological activity of plant polysaccharides is not only related to its monosaccharide composition and molecular weight but also closely related to the content of active groups (such as $-OSO_3^-$ and $-COOH$) in polysaccharide molecules. These active groups reduce the rate of negative charge loss on cell surfaces and repair the charge barrier. Chen et al. [15] obtained three types of sulfated polysaccharides with a sulfated contents of 9.11%, 10.33%, and 21.44% from Ganoderma atrum. The scavenging ability of these components on DPPH free radicals is positively correlated with their $-OSO_3^-$ contents, that is, polysaccharides with high $-OSO_3^-$ contents are more resistant to oxidation. Chen et al. [16] modified Momordica charantia polysaccharide (MCP) by sulfation to obtain sulfated Momordica charantia polysaccharide (S-MCP) with a substitution degree of 0.45. S-MCP has a greater scavenging ability for superoxide anions than MCP. Lu et al. [17] modified chitooligosaccharides (COS) through sulfation to prepare COS-SI and COS-SII with substitution degrees of 0.8 and 1.9, respectively. Their protective effects on H_2O_2-induced MIN6 cell damage had the order COS-SII > COS-SI > COS, indicating that increasing the substitution degree of $-OSO_3^-$ in polysaccharides prevent H_2O_2-induced oxidative damage in MIN6 cells.

Laminaria is an important economic seaweed and is widely found in the seas of China, Japan, and Korea. It is also the favorite food of some Asians. In the past thousand years, the Chinese has used it as a traditional medicine to treat edema disease [18]. Laminaria polysaccharide (LP) is the main active component of Laminaria. The antioxidant activity of LP was positively correlated with the $-OSO_3^-$ content of polysaccharide. For example, Wang et al. [19] obtained

F1, F2, and F3 components with $-OSO_3^-$ contents of 23.3%, 36.41%, and 36.67% from Laminaria. The scavenging ability of the components on superoxide radicals had the following order: F3 > F2 > F1, which indicates that the strength of the antioxidant activity of the polysaccharides increases with $-OSO_3^-$ content. Wang et al. [20] extracted fucoidan (FPS) with a $-OSO_3^-$ content of 27.56% from Laminaria and sulfated FPS to obtain SO_3-FPS with a $-OSO_3^-$ content of 36.63%. The scavenging ability of SO_3-FPS on hydroxyl radicals was significantly stronger than that of FPS.

However, the $-OSO_3^-$ content of polysaccharide has a great relationship with its producing area and extraction method [21–23]. For example, Yoon et al. [21] extracted three polysaccharide components (S1, S2, and S3) from Laminaria cichorioides in the East Sea of Korea, and the $-OSO_3^-$ content in S1, S2, and S3 were 0.09%, 2.19%, and 1.38%, respectively. Cui et al. [22] extracted Laminaria japonica polysaccharide (LJPA-P) from Laminaria japonica collected from Qingdao, Shandong, China, by a joint extraction of hot water and citric acid, and the $-OSO_3^-$ content of LJPA-P was 4%. However, the polysaccharides isolated and purified by LJPA-P (LJPA-P1 and LJPA-P2) could not even detect the $-OSO_3^-$ content. Saha et al. [23] collected crude Laminaria angustata polysaccharide (WEP) from the Okha coast of Gujarat, India. The $-OSO_3^-$ content of WEP was 3% and purified Laminaria angustata polysaccharide (F2) with a $-OSO_3^-$ content of 4.2%. These polysaccharides with low $-OSO_3^-$ content need to be sulfated to enhance their biological activity.

In this study, LP0 was sulfated to different degrees, and four kinds of SLPs (SLP1–SLP4) with $-OSO_3^-$ contents of 8.58%, 15.1%, 22.8%, and 31.3% were obtained. The antioxidant activities, the ability to regulate CaOx crystals growth, and protective effects on renal epithelial cells of these SLPs were studied. The SLPs offer development prospects for drugs used in preventing and treating CaOx kidney stones.

2. Materials and Methods

2.1. Reagents and Apparatus. Reagents. Deuterium oxide (D_2O, 99.9%, sigma) was purchased from Macklin. Dimethyl sulfoxide (AR, >99%), formamide (ACS grade, ≥99.5%), potassium bromide (KBr, AR, 99.0%), and sulfur trioxide-pyridine complex (97%) were all purchased from Aladdin. Hydrogen peroxide 30% (H_2O_2), sodium oxalate (Na_2Ox), and calcium chloride dihydrate ($CaCl_2 \cdot 2H_2O$) were all purchased from Guangzhou Chemical Reagent Factory of China (Guangzhou, China). The experimental water is double-distilled water.

DMEM/F-12 culture medium and fetal bovine serum were purchased from Gibco company. Cell counting kit (CCK-8) was purchased from Dojindo Laboratory (Kumamoto, Japan). $2',7'$-dichlorodihydrofluorescein diacetate (DCFH-DA) was purchased from Shanghai Beyotime Bio-Tech Co., Ltd. (Shanghai, China). Human kidney proximal tubular epithelial (HK-2) cells were purchased from Shanghai Cell bank of Chinese Academy of Sciences.

Apparatus. Nuclear Magnetic Resonance Analyzer (Varian Bruker-600 MHz, Germany); Multifunctional Microplate

Reader (SafireZ, Tecan, Switzerland); Fourier Transform Infrared Absorption Spectrometer (EQUINOX55, Bruker, Germany); Constant temperature water bath (Ningbo Saifu Experimental Instrument Factory); D/max2400 X-ray powder diffractometer (Rigaku, Japan); X-L type environmental scanning electron microscope (ESEM, Philips, Eindhoven, Netherlands); OPTIMA-2000DV inductively coupled plasma emission spectrometer (ICP-AES, USA PE company); Nanoparticle sizer (Nano-ZS, Malvem, UK); Inverted fluorescence microscope (OLYMPUS, U-HGLGPS, Japan); Optical microscope (OLYMPUS, TH4-200, Japan); Gas chromatography-mass spectrometer (Agilent, USA).

2.2. Preparation of Laminaria Polysaccharide (LP0).

Samples of *Laminaria* were collected from the Guangdong of China from August to September 2019. The material was sorted, washed, and dried immediately by forced air circulation at 50–60°C. A hot water-extracted polysaccharide was obtained from the algal powder of Laminaria (diameter, 100-200 μm) with 90-fold volumes of distilled water for 5 h at 90°C. After centrifugation to remove residues (7000 rpm, 10 min), the supernatant was concentrated to one-third of the volume in a vacuum rotary evaporator. The concentrated solution was then precipitated with 3 volumes of the absolute ethanol overnight at 4°C. The precipitates were collected by centrifugation (3500 g, 10 min) and, then, resolved in warm water. Proteins were removed using the Sevag method. The supernatant of polysaccharides was dialyzed (Mw of cutoff 500 Da, Regenerated Cellulose) in distilled water for 72 h and vacuum freeze-dried.

2.3. Measurement of LP0 Average Molecular Weight and Monosaccharide Composition

2.3.1. LP0 Average Molecular Weight.

The molecular weight of LP0 was determined by the Ubbelohde viscosity method at 25 ± 0.2°C. After measuring the fall time of polysaccharide solution in the viscometer, specific (η_{sp}) and relative (η_r) viscosity was calculated according to the formulas $\eta_r = T_i/T_0$ and $\eta_{sp} = \eta_r - 1$, where T_i and T_0 were the falling time of LP0 solution and deionized water, respectively. Using the one-point method formula, the intrinsic viscosity $[\eta] = [2(\eta_{sp} - \ln \eta_r)]^{1/2}/c$ is obtained, where c is the concentration of the polysaccharide solution to be tested. The molecular weight of LP0 (M) was calculated through its $[\eta]$ value. Because the relationship between the intrinsic viscosity $[\eta]$ of the polymer solution and its molecular weight M can be expressed by the Mark-Houwink empirical equation, that is: $[\eta] = \kappa M^{\alpha}$, where κ and α are the two parameters of the empirical equation. For LP0: $\kappa = 8.21 \times 10^{-3}$, $\alpha = 0.782$. Take the average of 3 parallel experiments.

2.3.2. LP0 Monosaccharide Composition by GC-MS.

The monosaccharide component of LP0 was detected by GC-MS according to our previous study [24]. The details are as follows: 10 mg of LP0 polysaccharide was added to a 121°C sealed container containing 2.5 mol/L trifluoroacetic acid (TFA, 2 mL) for 90 min. The solution was concentrated to dryness under reduced pressure; then, the TFA was removed with MeOH to a neutral solution and concentrated to dryness under reduced pressure. The residue was dissolved in 2 mol/L NH_4OH (1 mL) and 1 mol/L fresh $NaBD_4$ (1 mL). The reaction was carried out at room temperature for 2.5 h and stirring at room temperature. Then, two drops of acetic acid were added to decompose excess $NaBD_4$ until no bubbles producing. The solution was concentrated to dryness under reduced pressure. The filtrate was added MeOH to remove boric acid and dried in vacuo. Add 1 mL acetic anhydride and acetylate at 100°C for 2.5 h.

The acetylated product was extracted with dichloromethane. The organic layer was washed with distilled water, dried, and analyzed by GC-MS. The HP-5MS capillary column (15 m × 250 μm × 0.25 μm) was programmed and the temperature was raised from 135°C to 180°C at 0.5°C/min, then to 190°C at 10°C/min and up to 310°C at 40°C/min. Helium acts as carrier gas, column flow rate 0.6 mL/min. The acetylated product was identified by debris ions in GC-MS and relative retention times in GC. The structure is identified by peaks and assessed by peak area. Standard monosaccharides (rhamnose, arabinose, fucose, sucrose, maltose, glucose, raffinose, fructose, and galactose) are used as references.

2.4. Sulfation and Characterization of LP0

2.4.1. Sulfation of LP0.

According to the reference [25, 26], the specific steps are as follows: accurately weigh 500 mg of LP0 into a 250 mL Erlenmeyer flask, add 30 mL of dimethyl sulfoxide, and stir at room temperature for 1 hour to completely dissolve the polysaccharide. Refer to Table 1 to add sulfur trioxide pyridine complex and 5 mL of formamide (sulfur trioxide-pyridine complex was dissolved in formamide in advance to make it transparent), and reacted for a certain period of time (0.5, 2, and 8 h) in a water bath. After the reaction, the sample was cooled to room temperature with ice water, neutralized to pH = 7.0 with 2.0 mol/L NaOH solution, and then transferred to a dialysis bag (Mw = 500 Da) for dialysis for 4 days, until the solution in the dialysis bag changed from light yellow to transparent. After dialysis, it is evaporated and concentrated to 3 mL at 50°C. The polysaccharide is precipitated with absolute ethanol. After standing overnight, it is centrifuged and dried to obtain sulfated polysaccharides SLP1, SLP2, SLP3, and SLP4 containing different $-OSO_3^-$ content.

2.4.2. Detection of $-OSO_3^-$ Content in Polysaccharides.

The $BaCl_2$-gelatin turbidimetric method was used to determine the $-OSO_3^-$ content of each SLPs [27], and K_2SO_4 was used as a standard to draw a standard working curve. The regression equation was as follows: $Y = 4.72803X + 0.01723$, $R^2 = 0.99498$, $n = 11$.

2.4.3. FT-IR Spectrum of SLPs.

Take 2.0 mg dried polysaccharide sample and 200 mg KBr, grind it to powder with an agate mortar, press the tablet, and scan in the wave number range of 4000-400 cm^{-1}.

2.4.4. ^1H NMR and ^{13}C NMR Spectra of SLPs.

According to the reference [28], weigh 20 mg dried polysaccharide sample,

TABLE 1: Sulfation conditions of five SLPs with different $-OSO_3^-$ content.

SLPs	Reaction time/h	Sulfation conditions Sulfur trioxide-pyridine complex/g	Reaction temperature/°C	$-OSO_3^-$ content/%
LP0	—	—	—	0.73
SLP1	0.5	1	40	8.58
SLP2	0.5	2	40	15.1
SLP3	2	5	60	22.8
SLP4	8	5	60	31.3

dissolve it in a nuclear magnetic tube containing 0.55 mL of deuterium oxide (D_2O). After being completely dissolved, it was placed in the magnetic field of a nuclear magnetic resonance spectrometer for detection.

2.5. The Regulation Effect of Different SLPs on the Growth of CaOx Crystals

(1) *CaOx Crystal Synthesis.* Add 20 mL $CaCl_2$ solution with a concentration of 22 mmol/L to a set of beakers, then add a certain amount of SLPs with different sulfation degrees, and add distilled water to make up to 24 mL. It is placed in a 37°C constant temperature water bath and magnetically stir for 5 minutes. Add 20 mL of 22 mmol/L Na_2Ox solution to make the final volume of the system 44 mL. At this time, $c(Ca^{2+}) = c(Ox^{2-}) = 10$ mmol/L in the solution, and the final polysaccharide concentration is 0.4 g/L, 0.8 g/L, 1.2 g/L, 1.6 g/L, and 2.4 g/L. The solution was stirred in a constant temperature water bath for 10 min, then transferred to a constant temperature water bath at 37°C and allowed to stand for 2 h, and centrifuged. The bottom CaOx precipitate obtained after centrifugation is dried in an oven. The soluble Ca^{2+} ions concentration in the supernatant of the solution is measured by the ICP method. The bottom CaOx precipitate is dried in a dryer and weighed. After weighing, XRD, FT-IR, Zeta potential, and SEM tests are performed

(2) *XRD Detection.* Take a certain amount of crystals and grind them into powder in a mortar for detection. The relative percentages of COM and COD in CaOx are calculated by the K value method according to the XRD spectrum

$$COD\% = \frac{I_{COD}}{I_{COM} + I_{COD}} \times 100. \quad (1)$$

In the formula, I_{COM} and I_{COD} are the intensities of the main diffraction peak ($\bar{1}01$) crystal plane ($d = 0.593$ nm) of COM and the main diffraction peak (200) crystal plane ($d = 0.618$ nm) of COD, respectively.

(3) *FT-IR Detection.* Take 2.0 mg sample and 200 mg KBr mixed, grind it to powder in an agate mortar, press the tablet, and scan in the wave number range of 4000~400 cm^{-1}

(4) *Observation by SEM.* Weigh 1.0 mg sample, ultrasonically disperse it in 5 mL absolute ethanol at low power, spot the sample on a 10 mm × 10 mm glass slide, and dry at room temperature. After spraying gold on the sample, observe the crystal morphology under SEM

(5) *Zeta Potential Measurement.* Weigh 1.0 mg sample, ultrasonically disperse it in 3 mL pure water, and measure with a nanoparticle sizer under a constant temperature of 25°C

2.6. Antioxidant Activity of Different SLPs.
The hydroxyl radical (•OH) scavenging and DPPH free radical scavenging capabilities of polysaccharides in vitro were detected by the H_2O_2/Fe^{2+} system method and DPPH reagent method, respectively. Parallel three times and take the average.

2.7. Cell Experiment

2.7.1. Cell Viability Detection.
Inoculate the cell suspension (density 1.0×10^5 cells/mL) in a 96-well plate, 100 μL per well, and incubate for 24 h in an incubator at 37°C, 5% CO_2, and saturated humidity to make the cells converge into a monolayer. The cells were divided into four groups: (a) cell-free culture medium group; (b) normal control group: only serum-free medium was added; (c) crystal damage group: 200 μg/mL COD crystals prepared with serum-free medium was added; (d) polysaccharide protection group: 20, 40, and 80 μg/mL *Laminaria* polysaccharide solution with $-OSO_3^-$ content of 0.73% (LP0), 8.58% (SLP1), 15.1% (SLP2), 22.8% (SLP3), and 31.3% (SLP4) was added to react with 200 μg/mL COD for 15 min; then, it was added to normal cells and incubated for 12 h. After reaching the action time, add 10 μL of CCK-8 reagent to each well, incubate for 2 h at 37°C, measure the absorbance (A) at 450 nm with a microplate reader, and measure the cells under each condition in parallel in 5 replicate wells. Calculate the average value of A to test the protective ability of polysaccharides.

The concentration of polysaccharide in cell experiment was controlled by the following methods: serum-free medium was used to prepare a polysaccharide solution with a higher concentration (500 μg/mL), and then, a certain volume of the above polysaccharide solution is taken according to the target concentration (such as 20, 40, or 80 μg/mL) of the experiment, combined with the amount of other reagents added in the experiment, and finally diluted to the same volume with serum-free medium.

2.7.2. Cytotoxicity Detection of Polysaccharides.
Inoculate the cell suspension (density 1.0×10^5 cells/mL) in a 96-well plate, 100 μL per well, and incubate for 24 h in an incubator at 37°C, 5% CO_2, and saturated humidity to make the cells converge into a monolayer. The cells were divided into two groups: (a) normal control group: only serum-free medium

was added; (b) polysaccharide group: 20, 40, and 80 μg/mL *Laminaria* polysaccharide solution were added to normal cells for 24 h. After 24 h of incubation, add 10 μL of CCK-8 reagent to each well, incubate at 37°C for 2 h, measure the absorbance (A) at 450 nm with a microplate reader, and measure the cells under each condition in parallel in 5 replicate wells. The average value of A is used to detect the toxicity of polysaccharides.

2.7.3. Detection of Reactive Oxygen Species (ROS) Levels.
Inoculate the cell suspension with a concentration of 1.0×10^5 cells/mL in a 6-well culture plate with a volume of 2 mL/well. After incubating for 24 h, aspirate the culture solution and wash the cells twice with PBS. The experimental model is divided into three groups: (a) normal control group: only serum-free medium was added; (b) crystal damage group: 200 μg/mL COD crystals prepared with serum-free medium was added; (c) polysaccharide protection group: 80 μg/mL *Laminaria* polysaccharide solution with -OSO_3^- content of 0.73% (LP0), 8.58% (SLP1), 15.1% (SLP2), 22.8% (SLP3), and 31.3% (SLP4) was added to react with 200 μg/mL COD for 15 min; then, it was added to normal cells and incubated for 12 h. After reaching the action time, aspirate the supernatant in the 6-well plate, add 500 μL DCFH-DA dilution to each well, incubate in a 37°C incubator for 30 min, wash the cells three times with PBS, and observe under a fluorescence microscope. The ImageJ software was used for semiquantitative analysis of ROS fluorescence.

2.7.4. Cell Morphology Observation.
Inoculate the cell suspension with a concentration of 1.0×10^5 cells/mL in a 6-well culture plate with a volume of 2 mL/well. After incubating for 24 h, aspirate the culture solution and wash the cells twice with PBS. The experimental model is divided into three groups: (a) normal control group: only serum-free medium was added; (b) crystal damage group: 200 μg/mL COD crystals prepared with serum-free medium was added; (c) polysaccharide protection group: 80 μg/mL *Laminaria* polysaccharide solution with -OSO_3^- content of 0.73% (LP0), 8.58% (SLP1), 15.1% (SLP2), 22.8% (SLP3), and 31.3% (SLP4) was added to react with 200 μg/mL COD for 15 min; then, it was added to normal cells and incubated for 12 h. After reaching the action time, observe the cell morphology under a microscope.

2.8. Statistical Analysis.
Experimental data were expressed by mean ± standard deviation $(\bar{x} \pm SD)$. The experimental results were statistically analyzed by the IBM SPSS Statistics 26 software, and the differences between the means of each experimental group and the control group were analyzed by Tukey. $P < 0.05$ indicates a significant difference; $P < 0.01$ indicates a very significant difference. $P > 0.05$ indicates no significant difference.

3. Results

3.1. Measurement of LP0 Average Molecular Weight and Monosaccharide Composition.
The average molecular weight of LP0 is determined to be 1788 ± 78 Da by the Ubbelohde viscosity method. Figures 1(a) and 1(b) present the GC-MS results of standard monosaccharides and LP0. The majority of LP0 is composed of maltose and glucose with traces of sucrose, fructose, and raffinose. The mass ratio of maltose to glucose to raffinose to fructose to sucrose is 12.49 : 1.42 : 0.09 : 0.08 : 0.03.

3.2. Sulfation and Characterization of LP0

3.2.1. Sulfation of LP0.
LP0 was sulfated using the sulfur trioxide-pyridine method [25, 26]. By controlling reaction time, the concentration of the reactant (sulfur trioxide pyridine) and temperature, four SLPs, namely, SLP1, SLP2, SLP3, and SLP4 with sulfate groups (-OSO_3^-) content of 8.58%, 15.1%, 22.8%, and 31.3%, respectively, were obtained (Table 1).

As shown in Table 1, the -OSO_3^- contents of the polysaccharides increase with reaction time, reactant concentration, and reaction temperature. However, SLP4 with an -OSO_3^- content of as high as 31.3% can be prepared only by comprehensively controlling the three reaction conditions.

3.2.2. FT-IR Spectrum Analysis of Different SLPs.
Figure 1(c) shows the FT-IR spectra of SLPs with different -OSO_3^- contents. The broad absorption peak around 3385 cm^{-1} is the stretching vibration of O–H. The peak at 2931 cm^{-1} is the –CH stretching vibration of the –CH$_3$ or –CH$_2$ group. The peak at 1640 cm^{-1} is the symmetric or asymmetric stretching vibration of C=O. The peak at 1024 cm^{-1} is the stretching vibration of C–O. The infrared characteristic absorption peaks of SLPs with different -OSO_3^- contents are shown in Table 2.

Compared with LP0, SLPs have two new peaks at 1259 and 820 cm^{-1}, which are the asymmetric stretching vibration of S=O and stretching vibration of C–O–S, respectively [29]. The intensities of the two peaks gradually increase with -OSO_3^- content in the polysaccharides (Figure 1(d)), that is, LP0 < SLP1 < SLP2 < SLP3 < SLP4. This result indicates successful sulfation modification.

3.2.3. ^{1}H NMR Spectrum Analysis.
Figures 1(e) and 1(f) are the ^{1}H NMR spectra of LP0 and SLP2, respectively. The D$_2$O solvent peak is around the chemical shift (δ) of 4.71 ppm. The signal peak of the ring proton (H2–H5) is 3.6–4.7 ppm, and the methyl proton H-6 is approximately 1.3 ppm [30].

In the ^{1}H NMR spectrum of LP0, δ 5.33, 4.90, 4.67, 3.68, 3.57, and 1.12 ppm are attributable to the chemical shift from H-1 to H-6 of $(1 \rightarrow 2,4)$-β-D-Malp; δ 5.30, 3.96, 3.58, 3.62, 3.20, and 1.10 ppm are attributable to the chemical shifts from H-1 to H-6 of $(1 \rightarrow 6)$-α-D-Malp; δ 5.15, 3.51, 3.78, 3.37, 4.11, and 3.82 ppm correspond to the chemical shifts from H-1 to H-6 of $(1 \rightarrow 4)$-α-D-Glcp; δ 4.59, 3.35, 3.70, 3.89, 3.91, and 3.87 ppm are attributable to the chemical shifts from H-1 to H-6 of $(1 \rightarrow 6)$-β-D-Glcp (Table 3) [31].

A new strong signal peak at δ 4.22 ppm was detected in the ^{1}H NMR spectrum of SLP2 after sulfation modification. The appearance of the peak is attributable to the change of chemical shift caused by the introduction of the -OSO_3^-

(a)

(b)

(c)

(d)

(e)

(f)

FIGURE 1: Continued.

(g)

(h)

(i)
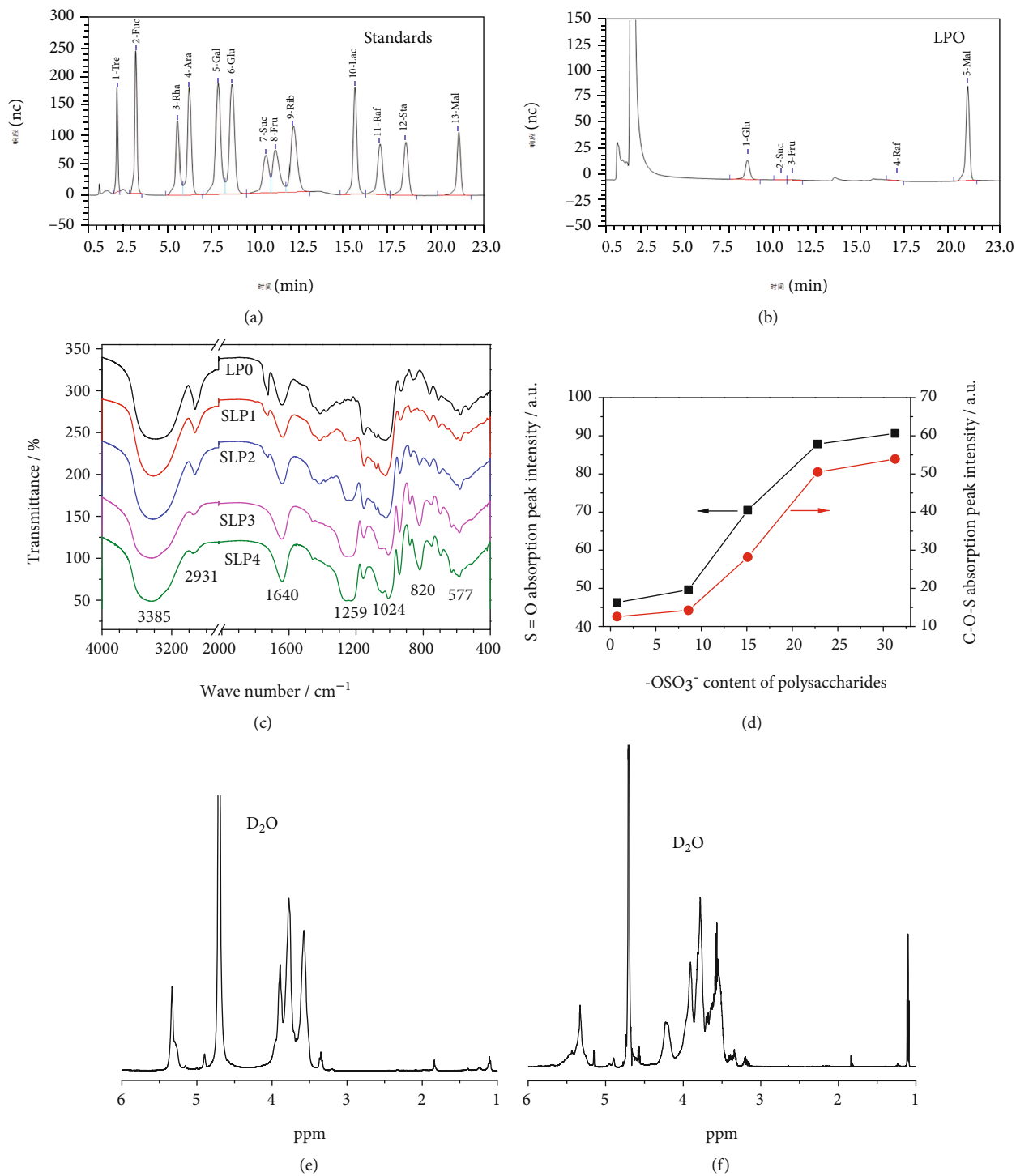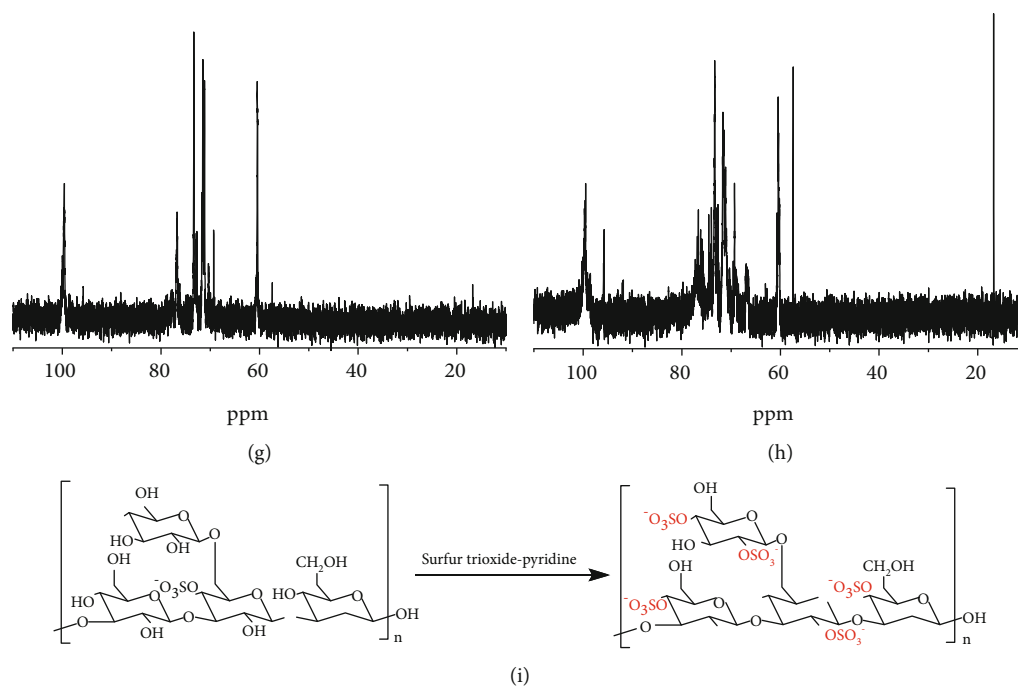
FIGURE 1: Characterization of SLPs with different -OSO$_3^-$ content. (a, b) GC-MS analysis. (c) FT-IR spectrum. (d) The absorption peak intensity of S=O asymmetric stretching vibration and C-O-S stretching vibration varies with the -OSO$_3^-$ content of polysaccharides. (e) ^{1}H NMR spectrum of LP0. (f) ^{1}H NMR spectrum of SLP2. (g) ^{13}C NMR spectrum of LP0. (h) ^{13}C NMR spectrum of SLP2. (i) LP0 sulfation reaction equation.

TABLE 2: FT-IR characteristic absorption peaks of SLPs with different –OSO$_3^-$ content.

| SLPs | –OSO$_3^-$content/% | Characteristic absorption peak/cm^{-1} | | | | | |
| | | O-H | -CH$_2$- | C=O | C-O | –OSO$_3^-$ | |
						S=O	C-O-S
LP0	0.73	3385	2931	1640	1024	/	/
SLP1	8.58	3416	2932	1636	1024	1252	817
SLP2	15.1	3418	2932	1640	1022	1254	820
SLP3	22.8	3424	2953	1642	1007	1258	821.5
SLP4	31.3	3424	2957	1640	1008	1259	822

group after sulfation [32]. The signal peak at δ 3.96 ppm shifts to δ 4.22 ppm, indicating that the hydroxyl group of SLP2 is sulfated. The signal peak of SLP2 at δ 1.10 ppm is significantly enhanced because of the substitution of the hydroxyl group by the –OSO$_3^-$ group after the sulfation of the polysaccharide.

3.2.4. ^{13}C NMR Spectrum Analysis. The ^{13}C NMR spectra of LP0 and SLP2 are shown in Figures 1(g) and 1(h). Multiple strong signal peaks were detected in the anomeric proton (δ 93–106 ppm) and high field (δ 16.5–18.5 ppm) regions [33]. The peaks at δ 99.99, 76.68, 80.45, 57.41, 69.30, and 16.77 ppm belong to the signal peaks from C-1 to C-6 of $(1\rightarrow2,4)$-β-D-Malp. The peaks at δ 99.60, 74.55, 70.36, 60.71, 62.67, and 16.65 ppm are attributable to the signal peaks from C-1 to C-6 of $(1\rightarrow6)$-α-D-Malp. The peaks at δ 95.75, 71.51, 72.69, 72.85, 71.71, and 60.45 ppm are, respectively, attributable to the signal peaks from C-1 to C-6 of $(1\rightarrow4)$-α-D-Glcp. The peaks at δ 100.27, 76.54, 78.70,

79.84, 73.33, and 71.17 ppm correspond to the signal peaks from C-1 to C-6 of $(1\rightarrow6)$-β-D-Glcp (Table 3) [31].

The ^{13}C NMR spectrum of SLP2 has the following changes relative to that of LP0:

(1) The high field signal peak of SLP2 at δ 71.46 ppm is weakened, and a new peak appears at δ 76.20 ppm. The reason is the movement of carbon directly attached to the electron-withdrawing group (–OSO$_3^-$ group) after sulfation to a lower field position [34]. This movement indicates that the hydroxyl group at C-2 is sulfated

(2) SLP2 shows signal peak splitting at δ 95–100 ppm. The functionalization of the –OH group on C-2 causes the signal peak of C-1 to split, and this split has a good correlation with the substitution degree of the C-2 atom [35], which further shows that the hydroxyl group on C-2 is sulfated

TABLE 3: Chemical shifts in ^{1}H NMR and ^{13}C NMR spectra of LP0 and SLP2 (δ).

| SLPs | Sugar residue | Chemical shift (ppm) | | | | | |
		H-1/C-1	H-2/C-2	H-3/C-3	H-4/C-4	H-5/C-5	H-6/C-6
LP0	$(1 \rightarrow 2,4)$-β-D-Malp	5.33/99.99	4.90/76.68	4.67/80.45	3.68/57.41	3.57/69.30	1.12/16.77
	$(1 \rightarrow 6)$-α-D-Malp	5.30/99.60	3.96/74.55	3.58/70.36	3.62/60.71	3.20/62.67	1.10/16.65
	$(1 \rightarrow 4)$-α-D-Glcp	5.15/95.75	3.51/71.51	3.78/72.69	3.37/72.85	4.11/71.71	3.82/60.45
	$(1 \rightarrow 6)$-β-D-Glcp	4.59/100.27	3.35/76.54	3.70/78.70	3.89/79.84	3.91/73.33	3.87/71.17
SLP2	$(1 \rightarrow 2,4)$-β-D-Malp	5.33/99.64	4.90/76.65	4.68/82.69	3.69/57.42	3.57/69.31	1.11/16.77
	$(1 \rightarrow 6)$-α-D- Malp	5.34/99.60	4.22/74.55	3.58/70.32	3.62/60.72	3.20/63.03	1.10/16.65
	$(1 \rightarrow 4)$-α-D-Glcp	5.15/95.75	3.56/71.46	3.78/72.67	3.36/72.85	4.11/71.65	3.82/60.46
	$(1 \rightarrow 6)$-β-D-Glcp	4.57/100.10	3.34/76.20	3.70/76.85	3.89/79.75	3.91/73.33	3.84/71.14

*Malp: maltose; Glcp: glucose.

(3) The signal peaks of SLP2 at δ 60.72 and 57.42 ppm are enhanced possibly because of the substitution of the hydroxyl group on C-4 by $-OSO_3^-$

(4) The new signal peak of SLP2 at δ 66.93 ppm is attributable to O-6 substituted carbon, indicating that O-6 is sulfated [36]. The peak of SLP2 at δ 16.77 ppm is significantly enhanced, indicating that the hydroxyl group at the C-6 position in the SLPs is replaced by $-OSO_3^-$

According to the above analysis and reference [37], the $-OH$ on C2, C4, and C6 of the original LP0 are replaced by $-OSO_3^-$ after the sulfation reaction (Figure 1(i)).

3.3. SLPs Regulate CaOx Crystallization

3.3.1. XRD Analysis of CaOx Crystal. Figures 2(a)–2(e) are the XRD spectra of CaOx crystals induced by LP0 and four SLPs with different sulfation degrees. The diffraction peaks at interplanar spacing (d) values of 0.591, 0.364, 0.296, and 0.235 nm are attributed to the ($\bar{1}$01), (020), ($\bar{2}$02), and (130) crystal planes of COM, respectively. The diffraction peaks at d values of 0.617, 0.441, 0.277, and 0.224 nm are attributed to the (200), (211), (411), and (213) crystal planes of COD, respectively.

(1) In LP0 and SLP1, no COD diffraction peak appears at all concentration ranges (0.40–2.40 g/L), indicating that they only form COM crystals

(2) In SLP2 and SLP3, when the concentration is low (0.4 g/L), only COM crystals form (Figures 2(c) and 2(d)). When the concentration of SLP2 increases to 1.6 g/L, COD crystals form. When the concentration of SLP3 increases to 0.8 g/L, COD crystals appear. As the concentration of polysaccharides continues to increase, the percentage of COD in the crystals gradually increases. When the concentration of SLP3 increases to 1.6 g/L, 100% COD crystals are induced (Figure 2(f)). In the SLP4 with the highest $-OSO_3^-$ content, 41.2% COD formation is induced at 0.4 g/L, and 100% COD formation is induced at 1.2 g/L

(3) At a concentration of 1.20 g/L, LP0, SLP1, SLP2, SLP3, and SLP4 induce 0, 0, 0, 81.0%, and 100% COD crystals, respectively. At a concentration of 2.40 g/L, the percentages of COD are 0, 0, 48.3%, 100%, and 100%, respectively

3.3.2. FT-IR Spectrum. Figure 3 shows the FT-IR spectra of CaOx crystals induced by SLPs at different concentrations. In LP0 and SLP1, the absorption peaks of induced crystals in all concentration ranges (0.4–1.6 g/L) are similar (Figures 3(a) and 3(b)), and five stretching vibration peaks at 3000–3600 cm^{-1} belong to the O–H bond of COM crystal water. The asymmetric stretching vibration $v_{as}(COO^-)$ and the symmetric stretching vibration $v_s(COO^-)$ of the carboxyl group are near 1619 and 1322 cm^{-1}, respectively (Table 4), indicating that only the COM crystal is formed [38, 39].

SLP2, SLP3, and SLP4 mainly induce the formation of COM at low concentrations and also induce COD crystal formation at high concentrations. The FT-IR spectrum of COD differs from that of COM. COD crystal has only one strong and broad absorption peak in the 3000–3600 cm^{-1} region, and $v_{as}(COO^-)$ and $v_s(COO^-)$ are at 1646 and 1330 cm^{-1}, respectively (Table 4) [38, 39].

Comprehensive XRD and FT-IR results show that the ability of SLPs to induce COD is positively correlated with the $-OSO_3^-$ content of polysaccharides. Increase in the $-OSO_3^-$ content or concentration of polysaccharides inhibits the formation of COM and induces the formation of COD.

3.3.3. SEM Observation of CaOx Crystal. Figure 4(a) shows the SEM images of each SLP that induces the formation of CaOx crystals at 1.6 g/L. The crystals formed in the blank group have a strong three-dimensional effect, and serious aggregation phenomena occur. Compared with the crystals in the blank group, the crystals regulated by LP0 and SLP1 gradually transform into lamellae, but the degree of aggregation is weakened. XRD results show that the crystals formed in the blank, LP0, and SLP1 groups are COM crystals.

COD crystals appear in SLP2-regulated crystals (approximately 27.7%, Figure 2(f)). Crystal size regulated by SLP3 and SLP4 is further reduced, the degree of aggregation between the crystals is further reduced, and the percentage of tetragonal bipyramid COD crystals is significantly
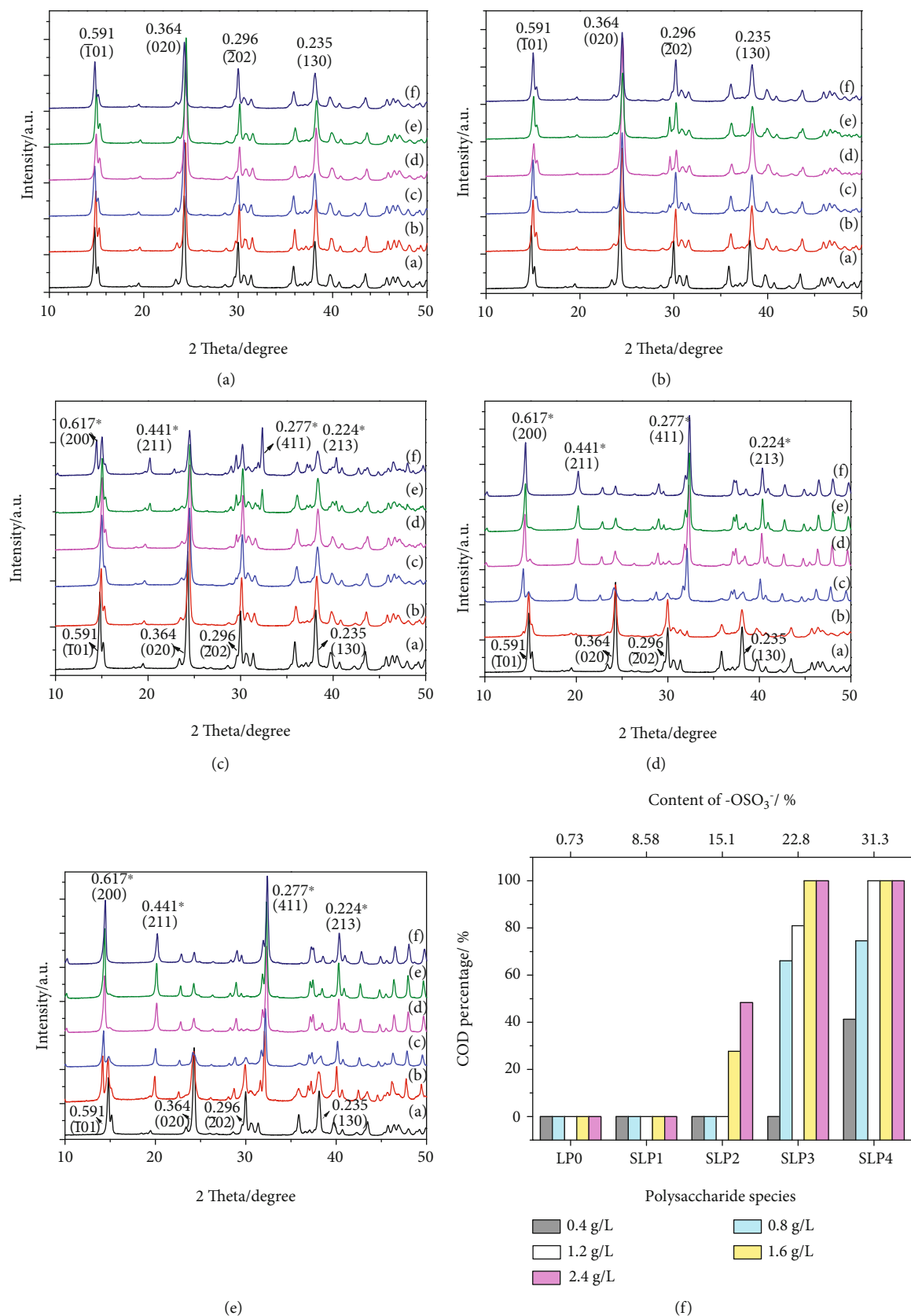
FIGURE 2: XRD spectra of CaOx crystals induced by SLPs at different concentrations. (a) LP0. (b) SLP1. (c) SLP2. (d) SLP3. (e) SLP4. (f) The percentage of COD in CaOx crystals formed in the presence of SLPs at various concentrations. Polysaccharide concentration in Figs.: (a) 0; (b) 0.4; (c) 0.8; (d) 1.2; (e) 1.6; (f) 2.4 g/L. Those marked with * are COD diffraction peaks, and those without * are COM diffraction peaks.
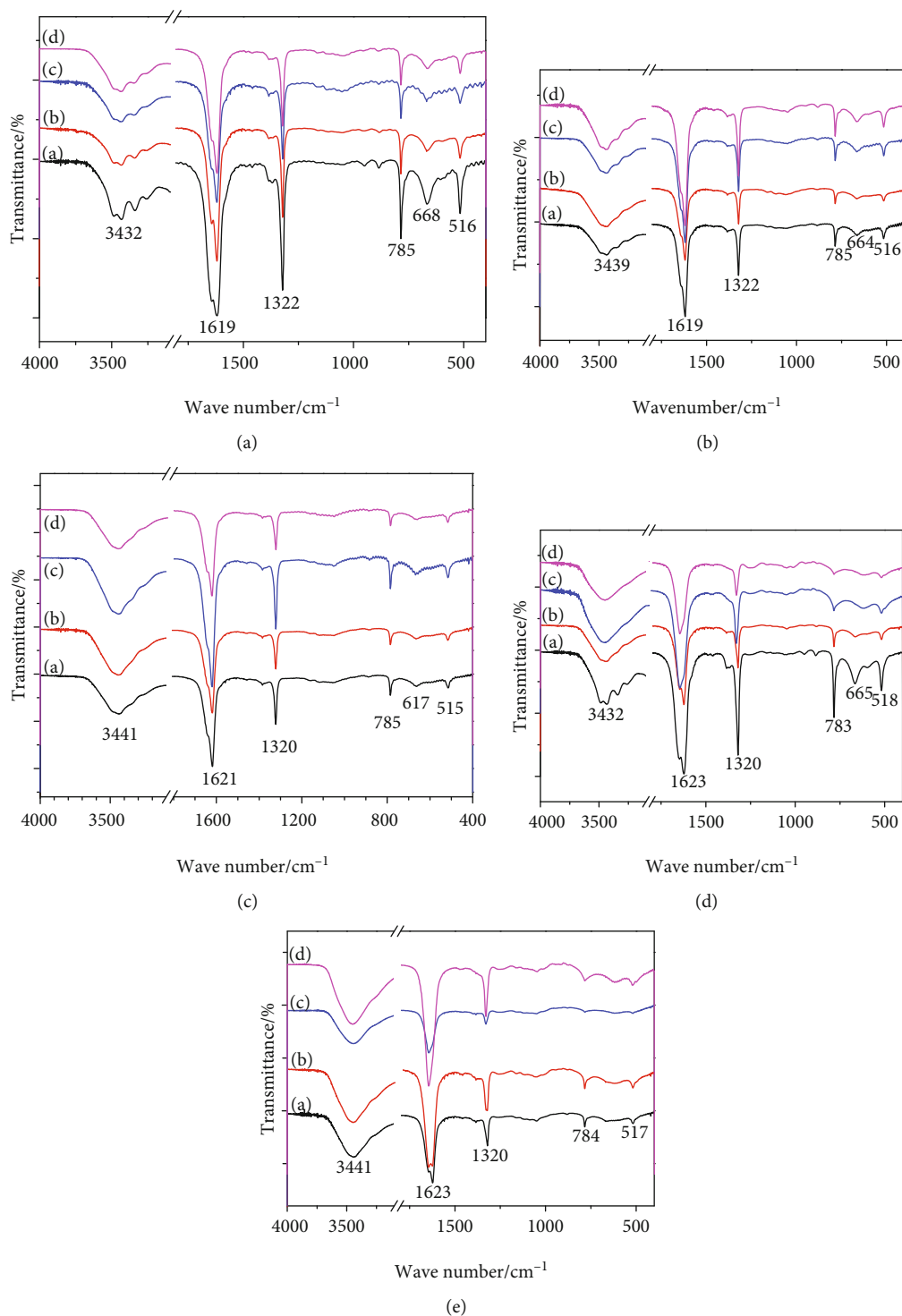
FIGURE 3: FT-IR spectra of CaOx crystals induced by SLPs at different concentrations. (a) LP0. (b) SLP1. (c) SLP2. (d) SLP3. (e) SLP4. In Figs. (a) 0.4; (b) 0.8; (c) 1.2; (d) 1.6 g/L.

increased. That is, an increase in $-OSO_3^-$ content of polysaccharide reduces the size and aggregation degree of CaOx crystals and induces the formation of COD crystals.

3.3.4. Detection of Soluble Ca^{2+} Ion Concentration and CaOx Precipitation in the System. The soluble Ca^{2+} ion concentration in each SLPs system at 1.6 g/L was detected by ICP, and

the mass of each CaOx crystal formed was weighed. As the $-OSO_3^-$ contents of the SLPs increase, the concentration of soluble Ca^{2+} ions in the supernatant gradually increases (Figure 4(b)), whereas the amount of CaOx precipitates gradually decreases (Figure 4(c)).

For example, the masses of CaOx precipitates induced by LP0 and SLP4 are 63.5 and 66.5 mg, respectively, and

TABLE 4: Infrared characteristic absorption peaks of CaOx crystals regulated by different concentrations of SLPs.

SLPs	c(SLPs)/g/L	COD/%	ν_{as}(COO⁻)/cm⁻¹	ν_{as}(COO⁻)/cm⁻¹	ν_s(COO⁻)/cm⁻¹	COM/cm⁻¹	COM/cm⁻¹	COM/cm⁻¹	COM/cm⁻¹	COD/cm⁻¹	COD/cm⁻¹
Blank	0	0		1619	1319	950	882	785	668		
LP0	0.4	0		1619	1319	950	882	785	668		
	0.8	0		1620	1319	950	882	785	668		
	1.2	0		1620	1319	951	882	785	668		
	1.6	0		1619	1319	951	883	785	663		
SLP1	0.4	0		1619	1319	952	882	785	664		
	0.8	0		1619	1320		881	785	664		
	1.2	0		1619	1320	948	881	785	667		
	1.6	0		1619	1320	950	882	785	668		
SLP2	0.4	0		1619	1320	951	883	785	662		
	0.8	0		1619	1320	952	881	785	665		
	1.2	0		1620	1320	951	883	785	668		
	1.6	27.7		1621	1321	952	882	785	660		
SLP3	0.4	0		1623	1320	950	882	784	665		
	0.8	66.1		1623	1323	948	881	784	664		617
	1.2	81.0	1645		1328			784		915	618
	1.6	100	1646		1329					917	619
SLP4	0.4	41.2		1625	1322		881	784	668		
	0.8	74.6	1645		1324			784		914	620
	1.2	100	1646		1330					913	621
	1.6	100	1646		1330					919	619

the corresponding substance amounts are 434.6 and 405.2 μmol. Soluble Ca^{2+} concentrations in the supernatant are 0.53 and 101.7 mg/L, and the substance amounts are 0.16 and 27.26 μmol, respectively. This is because COD has one more water molecule than COM, which increases its relative molecular mass, so the mass of the precipitate increases with the same amount of substance (Table 5).

3.3.5. Zeta Potential of CaOx Crystal.
Zeta potential can be used in measuring the amount of repulsive force between crystals. When the absolute value of the zeta potential increases, the strength of the repulsive force between crystals and the dispersion of crystals in a solution increases, and the aggregation of crystals is inhibited [40].

Figure 4(d) shows the absolute value of the Zeta potential of CaOx crystals produced by the regulation of five different SLPs with different –OSO₃⁻ contents. The absolute value of the zeta potential of the CaOx crystals produced by the regulation gradually increases. At the same concentration, as the –OSO₃⁻ content of polysaccharide increases, the absolute value of the crystal's Zeta potential gradually increases. For example, when the polysaccharide concentration is 2.4 g/L, the absolute values of the zeta potential of the CaOx crystals generated have the following order: LP0 (4.67 mV) < SLP1 (11.2 mV) < SLP2 (15.1 mV) < SLP3 (17.1 mV) < SLP4 (26.5 mV).

3.4. In Vitro Antioxidant Capacity of SLPs with Different –OSO₃⁻ Content.
On the basis of the tested ability of SLPs with different –OSO₃⁻ contents to scavenge hydroxyl (•OH) free radicals and DPPH free radicals, their in vitro antioxidant activities were compared. The –OSO₃⁻ group in SLPs can inhibit the generation of hydroxyl radicals by chelating Fe^{2+} [41]. In addition, when SLPs interact with DPPH, they transfer electrons or hydrogen atoms to DPPH, thereby neutralizing its free radicals [42].

Figures 5(a) and 5(b) shows the ability of SLPs with different –OSO₃⁻ content to scavenge •OH radicals and DPPH radicals and their concentration effects. As the concentration of polysaccharides increases, the ability to scavenge •OH free radicals and DPPH free radicals increases, that is, the antioxidant capacities of polysaccharides are concentration dependent. Notably, a polysaccharide concentration of 1.0 mg/mL is a turning point for improving the speed of scavenging free radicals. When the polysaccharide concentration is less than 1.0 mg/mL, the ability of polysaccharides to scavenge free radicals increases rapidly with polysaccharide concentration. When the polysaccharide concentration is greater than 1.0 mg/mL, the ability of polysaccharides to scavenge free radicals increases slowly with increasing polysaccharide concentration.

At the same concentration, as the –OSO₃⁻ contents of polysaccharides increase, the ability of the polysaccharides to scavenge free radicals increases, that is, the antioxidant capacities of SLPs are positively correlated with the content of –OSO₃⁻ in SLPs. In •OH free radicals, SLP3 and SLP4 have a significantly stronger free radical scavenging ability

(a)

(b)

(c)

(d)
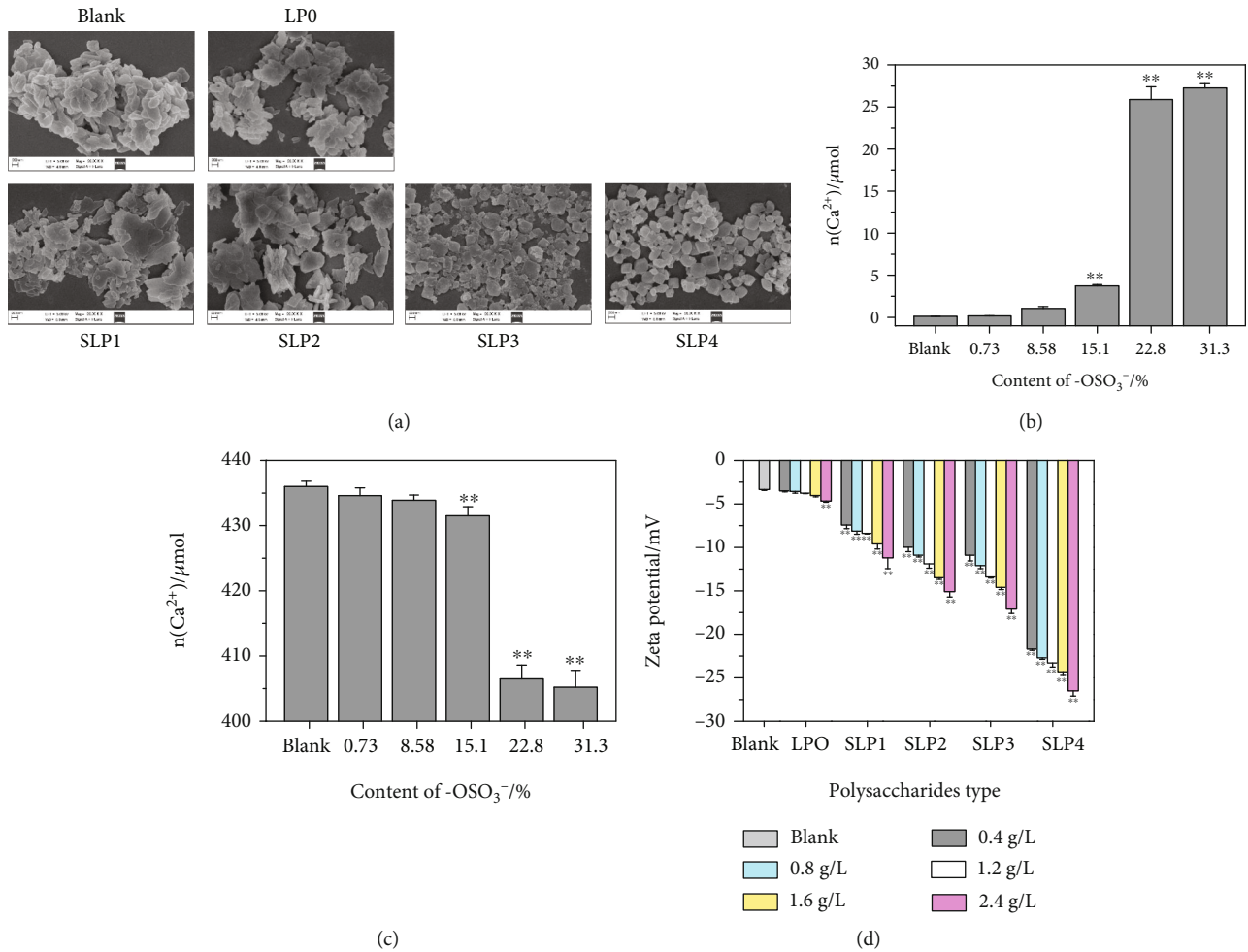
FIGURE 4: (a) SEM images of CaOx crystals, (b) soluble Ca^{2+} ions concentration in the supernatant, and (c) CaOx precipitate amount in the presence of SLPs at 1.6 g/L. (d) The influence of SLPs on the Zeta potential of CaOx crystals formed. Compared with the blank group, * $P < 0.05$; $^{**}P < 0.01$.

TABLE 5: The crystal phase of calcium oxalate crystals, the amount of precipitation and the concentration of soluble Ca^{2+} ions in the supernatant formed in the presence of 1.6 g/L SLPs.

SLPs	c(SLPs)/g/L	COD/%	c(Ca^{2+})/mg/L	n(Ca^{2+})/μmol	m(CaOx)/mg	n(CaOx)/μmol	n(total Ca^{2+})/μmol
Blank	—	0	0.35	0.11	63.7	436.0	436.1
LP0 (0.73%)	1.6	0	0.53	0.16	63.5	434.6	434.8
SLP1 (8.58%)	1.6	0	3.47	1.05	63.4	433.9	435.0
SLP2 (15.1%)	1.6	27.7	12.84	3.74	65.2	431.5	435.2
SLP3 (22.8%)	1.6	100	95.58	25.90	66.7	406.5	432.4
SLP4(31.3%)	1.6	100	101.7	27.26	66.5	405.2	432.5

than other polysaccharides. For DPPH free radicals, SLP4 with a high $-OSO_3^-$ content has a significantly stronger free radical scavenging ability than other polysaccharides.

3.5. Comparison of the Ability of SLPs with Different $-OSO_3^-$ Content to Protect HK-2 Cells from Oxidative Damage

3.5.1. Cell Viability. After HK-2 cells are damaged by 200 μg/mL nano-COD crystals for 12 h, cell viability

decreases from 100.00% ± 1.27% to 54.84% ± 0.85%, indicating that COD crystals have obvious damage to cells, and this damage was moderate, which was convenient to carry out the protection experiment of polysaccharide [14, 43]. The five polysaccharides used three concentrations of 20, 40, and 80 μg/mL to protect HK-2 cells. Cell viability test results show that cell viability increases compared with that in the nano-COD damage group because of the protection of HK-2 cells by the polysaccharides at each concentration,
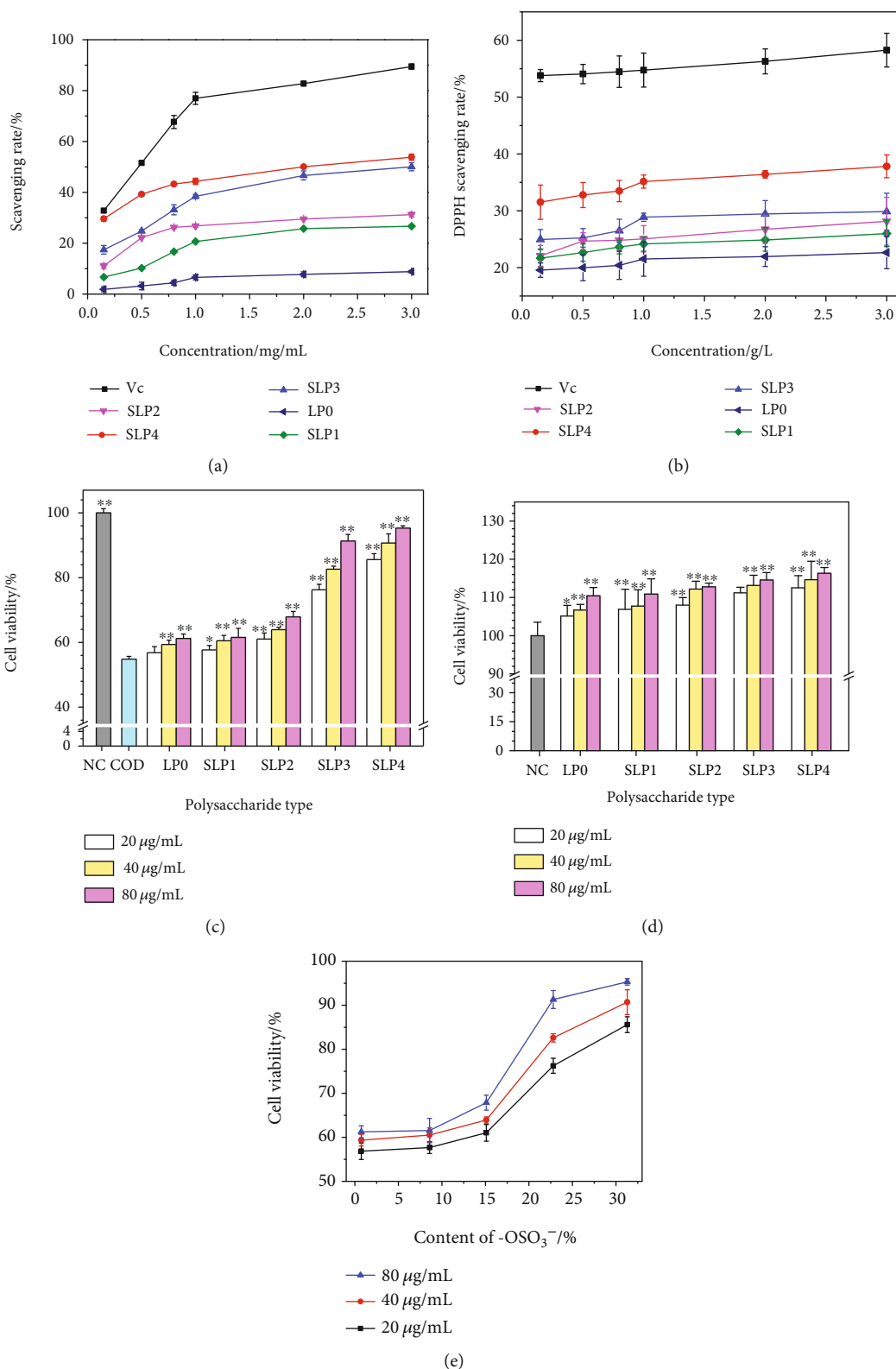
FIGURE 5: In vitro antioxidant capacity of SLPs. (a) Scavenging •OH free radicals; (b) Scavenging DPPH free radicals. Comparison of the ability of SLPs to protect HK-2 cells from oxidative damage. (c) Cell viability was detected by the CCK-8 method. Compared with the COD group, $^{*}P < 0.05$; $^{**}P < 0.01$. (d) Cell cytotoxicity was detected by the CCK-8 method. Compared with the NC group, $^{*}P < 0.05$; $^{**}P < 0.01$. (e) The relationship between cell viability and the $-OSO_3^-$ content of polysaccharide. NC: normal control; COD concentration: 200 μg/mL; damage time: 12 h; protection time: 12 h.

and each polysaccharide had the best protective effect at $80 \, \mu g/mL$.

The protective effect of each SLP on HK-2 cells was compared at the same concentration (Figure 5(c)), and the results show that the degree of protection against nano-COD crystal damage in the HK-2 cells increases with the polysaccharide $-OSO_3^-$ content. At the best protective concentration ($80 \, \mu g/mL$), the cell viability of the five polysaccharide protection groups is 61.24% (LP0), 61.54% (SLP1), 67.87% (SLP2), 91.30% (SLP3), and 95.31% (SLP4).

3.5.2. Cytotoxicity of Polysaccharides.
As shown in Figure 5(d), different concentrations of SLPs interact with cells for 24 h. Cell viability is greater than the normal group (100%), indicating that the polysaccharides are not toxic to cells at $20-80 \, \mu g/mL$ and can promote cell growth. SLP4 with the highest $-OSO_3^-$ content has the strongest effect on HK-2 cell proliferation.

3.5.3. Reactive Oxygen Species (ROS) Level.
A large amount of ROS is produced in damaged cells, resulting in abnormal cell function and even cell death [44]. Figure 6(a) shows the ROS fluorescence intensity of each group of cells. The intensities were detected using the DCFH-DA fluorescent probe method. The ROS fluorescence intensity in the normal group is the lowest. The ROS fluorescence intensity increases significantly after normal cells are damaged by 200 nm COD. After the addition of four kinds of polysaccharides, ROS fluorescence intensity decreases. As the $-OSO_3^-$ content of polysaccharide increases, the ROS fluorescence intensity gradually decreases. The highest degree decrease in ROS fluorescence intensity was observed after the addition of SLP4 (Figure 6(b)), owing to the protective effect of the polysaccharide. This result shows that SLPs can protect cells from damage caused by nano-COD crystals, and the protective ability of polysaccharides is positively correlated with the $-OSO_3^-$ contents of polysaccharides.

3.5.4. Cell Morphology.
As shown in Figure 6(c), the cell in the normal group is evenly distributed, the cell morphology is full, and the cells are tightly connected. After the normal cells are damaged by 200 nm COD, the number of cells is significantly reduced, cell shape shrinks, and the connections between cells are destroyed. After the addition of various polysaccharides, the degree of damage caused by COD on the cells is reduced, the number of cells in the protection groups is higher than that in the damage group, the connection between cells is gradually restored, and the cell morphology is significantly improved. The ability of the polysaccharides to protect HK-2 cells from COD damage increases with $-OSO_3^-$ content of polysaccharide. The cell morphology of SLP4 with the highest $-OSO_3^-$ content is closest to the normal group.

4. Discussion

4.1. Sulfation and Structural Analysis of SLPs.
Sulfation of polysaccharides can change the biological activity and function of natural products [45]. The sulfur trioxide-pyridine method is a common sulfation method. This paper uses this method to sulfate LP0 with an initial $-OSO_3^-$ content of 0.73%. By controlling the reaction time, reactant (sulfur trioxide-pyridine complex) concentration, and reaction temperature, four kinds of modified polysaccharides were obtained. The $-OSO_3^-$ contents are 8.58% (SLP1), 15.1% (SLP2), 22.8% (SLP3), and 31.3% (SLP4). The results of FT-IR, ^1H NMR, and ^{13}C NMR spectroscopy show that sulfation causes no change in the monosaccharide composition of polysaccharides. They are all composed of maltose and glucose with traces of sucrose, fructose and raffinose (Figures 1(a) and 1(b)). The main sugar residues are $(1 \rightarrow 2,4)$-β-D-Malp, $(1 \rightarrow 6)$-α-D-Malp, $(1 \rightarrow 4)$-α-D-Glcp, and $(1 \rightarrow 6)$-β-D-Glcp unit.

4.2. Enhanced Antioxidant Capacities of Sulfated SLPs.
Compared with LP0, sulfated SLPs have a better scavenging ability for •OH and DPPH radicals. The reason is that the introduction of $-OSO_3^-$ groups weakens the dissociation energy of O–H bonds in polysaccharide molecules [45] and improves the hydrogen supply capacities of polysaccharide derivatives. Hydrogen atoms provided by polysaccharides combine with free radicals to form stable free radicals and terminates free radical chain reaction, thereby increasing antioxidant activity [46, 47]. For example, after polysaccharides donate hydrogen atoms or single electrons to DPPH, nonradical compounds DPPH-H are generated [48]. Huang et al. [49] modified Mesona chinensis Benth polysaccharide through sulfation to obtain SMP. The scavenging rates of the two on DPPH free radicals are 75.11% and 86.95%, respectively, indicating that increase in the $-OSO_3^-$ contents of polysaccharides improve antioxidant activity. Hu et al. [50] modified Acanthopanax leucorrhizus polysaccharide (ALP) by sulfation to obtain S-ALP1 and S-ALP2 components with the substitution degrees of 0.48 and 0.73, respectively. The scavenging ability of the three on hydroxyl radicals is S-ALP2 > S-ALP1 > ALP, indicating that the antioxidant activity is positively correlated with the $-OSO_3^-$ content of polysaccharide, that is, the higher the $-OSO_3^-$ content of the polysaccharide, the stronger the antioxidant activity.

4.3. Sulfated SLPs Have a Stronger Ability to Regulate CaOx Crystallization.
Compared with the original LP0, the sulfated SLPs can better inhibit the formation of CaOx crystals (Figures 2–4), due to the following reasons.

First, the sulfated SLPs are rich in acidic $-OSO_3^-$ groups, which can better combine with the free Ca^{2+} ions in the solution to form soluble complexes, increase the soluble Ca^{2+} ion concentration in the system (Figure 4(b)), and reduce the amount of Ca^{2+} ions combined with Ox^{2-}, thereby reducing the amount of CaOx precipitation, which inhibit the formation of CaOx stones [51].

Second, SLPs form polyanions in the solution and are adsorbed on the surfaces of CaOx crystals, causing defects in crystal growth, preventing free particles from entering, and inhibiting the growth of CaOx crystals. Melo et al. [52] extracted four sulfated polysaccharide components from the marine alga Dictyopteris justii. Their $-OSO_3^-$ content was 3.9%, 4.3%, 6.8%, and 7.5%, respectively. Among

(a)

(b)

(c)
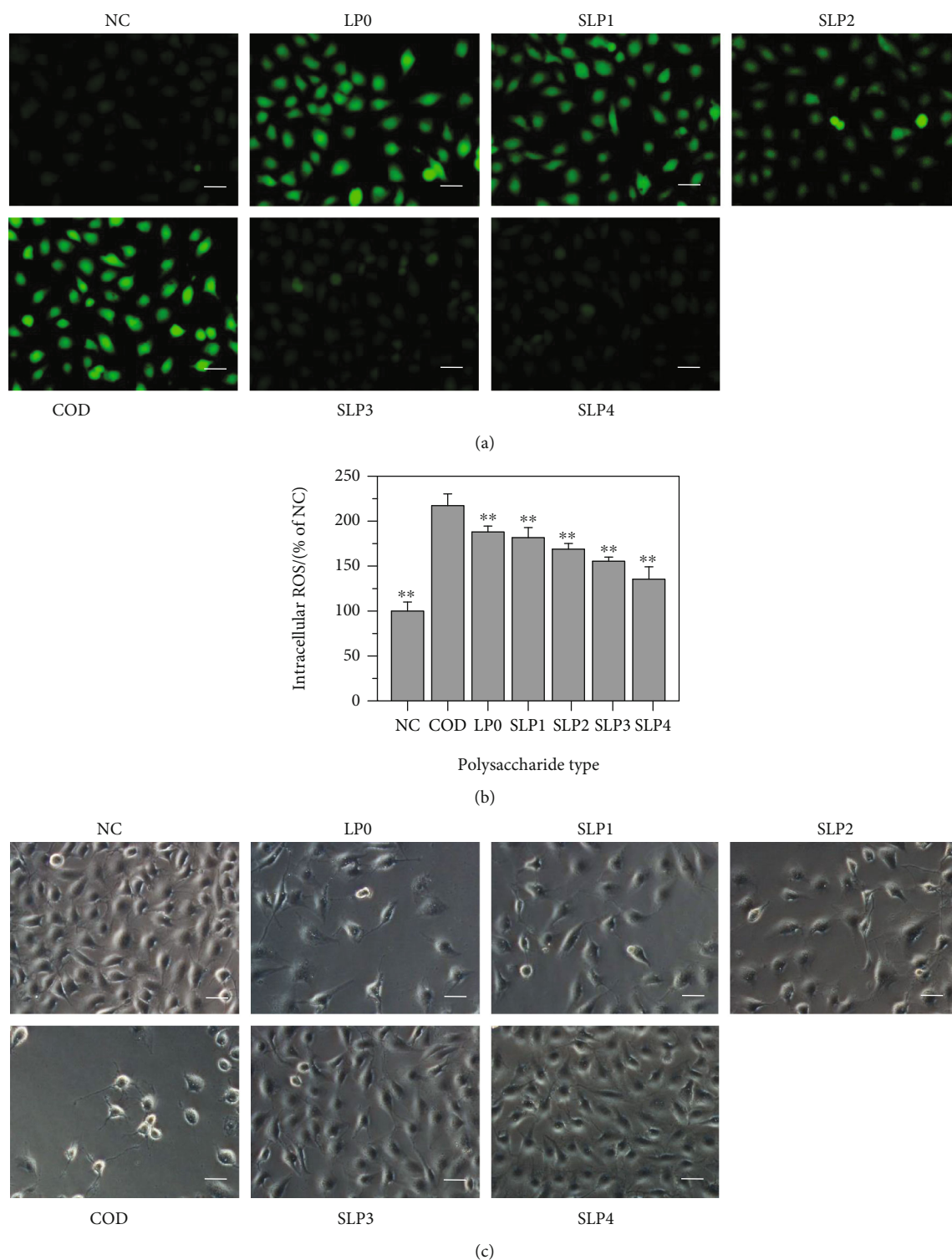
FIGURE 6: ROS level and cell morphology were detected before and after SLPs protect HK-2 cells. (a) ROS fluorescence microscope images. (b) Quantitative histogram of ROS fluorescence intensity. (c) Cell morphology. NC: normal control; polysaccharide concentration: 80 μg/mL; COD concentration: 200 μg/mL; damage time: 12 h; protection time: 12 h. Scale bars: 50 μm. Compared with the COD group, $^*P < 0.05$; $^{**}P < 0.01$.

them, the component with the highest $-OSO_3^-$ content has the best effect on inhibiting CaOx crystallization.

Third, SLPs with a high $-OSO_3^-$ content induce COD crystal formation. The reason is as follows: SLPs rich in acidic $-OSO_3^-$ groups can adsorb a large amount of Ca^{2+} ions through electrostatic attraction, enriching the Ca^{2+} ions on and near the polysaccharide surfaces and increasing $[Ca^{2+}]/[Ox^{2-}]$ molar ratio. Additionally, the energy
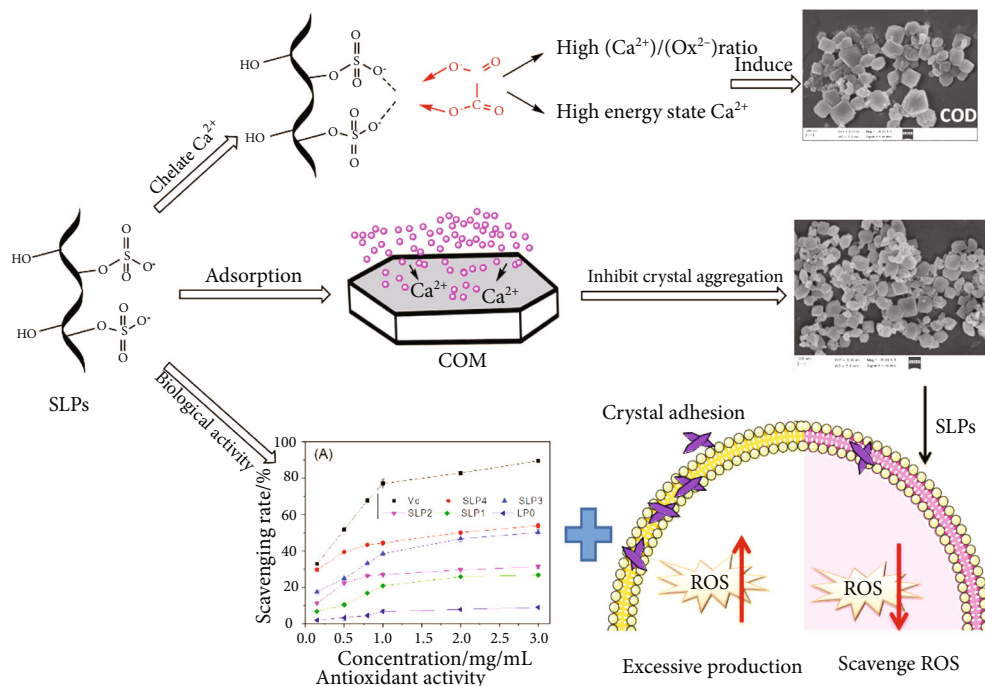
Figure 7: The mechanism diagram of SLPs inhibiting kidney stones formation.

interfaces of the polysaccharide molecule surfaces increase. The ratio of adsorbed Ca^{2+} ions leads to an increase in the energy state of free Ca^{2+} ions. The high-energy interface and high-energy state Ca^{2+} ions promote the formation of thermodynamic metastable COD [53]. Figure 7 shows the mechanism of SLPs inhibiting kidney stones formation.

Notably, SLP3 with $-OSO_3^-$ content of 22.8% is a turning point in the mutation of a polysaccharide effect, that is, the ability of SLP3 and SLP4 to regulate the formation of COD crystals and their antioxidant activity and ability to protect cells from COD crystals are significantly greater than those of LP0, SLP1, and SLP2.

Compared with COD, COM crystals are difficult to excrete from the body because of their stronger adhesion to damaged renal epithelial cells. Therefore, sulfated SLPs that induce COD crystals are more useful in inhibiting the formation of CaOx stones than the original LP0.

SLPs with high $-OSO_3^-$ contents can inhibit the aggregation of CaOx crystals (Figure 4(a)). Aggregated crystals are not only difficult to excrete from the body but also cause considerable damage to renal epithelial cells [54, 55], thereby increasing the risk of kidney stone formation. Figure 4(d) shows that the absolute value of the zeta potential of CaOx crystals generated by the regulation of sulfated SLPs is much higher than that of the original polysaccharide LP0. The surface charge density of a crystal and the amount of repulsive force between crystals increase with the absolute value of the zeta potential on the crystal surface, and the aggregation of crystals is inhibited [56].

4.4. Sulfated SLPs Have a Strong Ability to Protect HK-2 Cells from Crystal Damage. The biological activity of sulfated polysaccharides is closely related to their $-OSO_3^-$ content.

Compared with LP0, sulfated SLPs can better protect HK-2 cells from the damage of nano-COD crystals. The results of this paper show that the ability of SLPs to protect cells from crystals damage is positively correlated with their $-OSO_3^-$ content (Figure 5(e)). As the $-OSO_3^-$ content of SLPs increases, cell viability gradually increases (Figure 5(c)), ROS levels decrease (Figure 6(a)), and cell morphology gradually recovers (Figure 6(c)). The ability of SLP3 and SLP4 to protect cells from COD crystal damage is significantly greater than that of LP0, SLP1, and SLP2.

Jin et al. [57] found that sulfation modification can improve the antioxidant activity of polysaccharides and can better protect cells from oxidative damage and apoptosis induced by H_2O_2. Wang et al. [58] showed that compared with the original *Cyclocarya paliurus* polysaccharides, sulfated polysaccharides have a better protective effect on oxidative stress caused by H_2O_2. Moreover, Wang et al. [59] proved that sulfation modification can enhance the immune activity of *Lycium barbarum* polysaccharide.

5. Conclusions

In this study, the original LP0 was sulfated using the sulfur trioxide-pyridine method, and four kinds of sulfated polysaccharide SLPs with the $-OSO_3^-$ contents of 8.58%, 15.1%, 22.8%, and 31.3% were obtained. As the $-OSO_3^-$ content of polysaccharides increases, its regulating effect on the growth of CaOx crystals is enhanced. As a result, the concentration of soluble Ca^{2+} in the solution increases, the amount of CaOx crystal precipitation is reduced, the degree of CaOx crystal aggregation is significantly reduced, and the percentage of induced COD crystals increases. These effects can effectively inhibit the formation of CaOx kidney stones.

The in vitro antioxidant activity of SLPs is positively correlated with their $-OSO_3^-$ content. SLPs are not toxic to HK-2 cells. The level of their ability to protect cells from damage by nano-COD crystals increases with $-OSO_3^-$ content. Sulfation modification can improve the biological activities of polysaccharides, providing a good prospect for finding and developing effective drugs for treating kidney stones.

Data Availability

All the data supporting the results were shown in the paper and can be applicable from the corresponding author.

Conflicts of Interest

The authors declare that they have no competing interests.

Authors' Contributions

Wei-Bo Huang and Guo-Jun Zou contributed equally to this work.

Acknowledgments

References

[1] W. Y. Wang, J. Y. Fan, G. F. Huang et al., "Prevalence of kidney stones in mainland China: a systematic review," *Scientific Reports*, vol. 7, no. 1, 2017.

[2] S. Khamchun, K. Sueksakit, S. Chaiyarit, and V. Thongboonkerd, "Modulatory effects of fibronectin on calcium oxalate crystallization, growth, aggregation, adhesion on renal tubular cells, and invasion through extracellular matrix," *Journal of Biological Inorganic Chemistry*, vol. 24, no. 2, pp. 235–246, 2019.

[3] M. Mirković, A. Dosen, S. Erić, P. Vulić, B. Matović, and A. Rosić, "Phase and microstructural study of urinary stones," *Microchemical Journal*, vol. 152, 2020.

[4] L. S. Parvaneh, D. Donadio, and M. Sulpizi, "Molecular mechanism of crystal growth inhibition at the calcium oxalate/water interfaces," *The Journal of Physical Chemistry C*, vol. 120, no. 8, pp. 4410–4417, 2016.

[5] R. de Bellis, M. P. Piacentini, M. A. Meli et al., "In vitro effects on calcium oxalate crystallization kinetics and crystal morphology of an aqueous extract from ceterach officinarum: analysis of a potential antilithiatic mechanism," *PLoS One*, vol. 14, no. 6, article e0218734, 2019.

[6] J. Chung, I. Granja, M. G. Taylor, G. Mpourmpakis, J. R. Asplin, and J. D. Rimer, "Molecular modifiers reveal a mechanism of pathological crystal growth inhibition," *Nature*, vol. 536, no. 7617, pp. 446–450, 2016.

[7] R. Unno, T. Kawabata, K. Taguchi et al., "Deregulated MTOR (mechanistic target of rapamycin kinase) is responsible for autophagy defects exacerbating kidney stone development," *Autophagy*, vol. 16, no. 4, pp. 709–723, 2020.

[8] L. S. Huang, X. Y. Sun, Q. Gui, and J. M. Ouyang, "Effects of plant polysaccharides with different carboxyl group contents on calcium oxalate crystal growth," *CrystEngComm*, vol. 19, no. 32, pp. 4838–4847, 2017.

[9] K. K. Gangu, G. R. Tammineni, A. S. Dadhich, and S. B. Mukkamala, "Control of phase and morphology of calcium oxalate crystals by natural polysaccharide, gum Arabic," *Molecular Crystals and Liquid Crystals*, vol. 591, no. 1, pp. 114–122, 2014.

[10] S. R. Khan, "Reactive oxygen species, inflammation and calcium oxalate nephrolithiasis," *Translational andrology and urology*, vol. 3, no. 3, pp. 256–276, 2014.

[11] S. Y. Qi, Q. Wang, B. Xie, Y. Chen, Z. H. Zhang, and Y. Xu, "P 38 MAPK signaling pathway mediates COM crystal-induced crystal adhesion change in rat renal tubular epithelial cells," *Urolithiasis*, vol. 48, no. 1, pp. 9–18, 2020.

[12] W. Chen, W. R. Liu, J. B. Hou et al., "Metabolomic analysis reveals a protective effect of Fu-fang-Jin-Qian-Chao herbal granules on oxalate-induced kidney injury," *Bioscience Reports*, vol. 39, no. 2, 2019.

[13] Q. L. Xi, J. Ouyang, J. X. Pu, J. Q. Hou, and S. G. Wang, "High concentration of calcium stimulates calcium oxalate crystal attachment to rat tubular epithelial NRK cells through osteopontin," *Urology*, vol. 86, no. 4, pp. 844.e1–844.e5, 2015.

[14] Y. W. Zhao, L. Liu, C. Y. Li, H. Zhang, X. Y. Sun, and J. M. Ouyang, "Preprotection of tea polysaccharides with different molecular weights can reduce the adhesion between renal epithelial cells and nano-calcium oxalate crystals," *Oxidative Medicine and Cellular Longevity*, vol. 2020, Article ID 1817635, 13 pages, 2020.

[15] Y. Chen, H. Zhang, Y. X. Wang, S. P. Nie, C. Li, and M. Y. Xie, "Sulfated modification of the polysaccharides from Ganoderma atrum and their antioxidant and immunomodulating activities," *Food Chemistry*, vol. 186, pp. 231–238, 2015.

[16] F. Chen, G. L. Huang, Z. Y. Yang, and Y. P. Hou, "Antioxidant activity of Momordica charantia polysaccharide and its derivatives," *International Journal of Biological Macromolecules*, vol. 138, pp. 673–680, 2019.

[17] X. Y. Lu, H. Guo, and Y. L. Zhang, "Protective effects of sulfated chitooligosaccharides against hydrogen peroxide-induced damage in MIN6 cells," *International Journal of Biological Macromolecules*, vol. 50, no. 1, pp. 50–58, 2012.

[18] J. Wang, F. Wang, H. Yun, H. Zhang, and Q. B. Zhang, "Effect and mechanism of fucoidan derivatives from Laminaria japonica in experimental adenine-induced chronic kidney disease," *Journal of Ethnopharmacology*, vol. 139, no. 3, pp. 807–813, 2012.

[19] J. Wang, Q. B. Zhang, Z. S. Zhang, and A. E. Li, "Antioxidant activity of sulfated polysaccharide fractions extracted from Laminaria japonica," *International Journal of Biological Macromolecules*, vol. 42, no. 2, pp. 127–132, 2008.

[20] J. Wang, L. Liu, Q. B. Zhang, Z. S. Zhang, H. M. Qi, and P. C. Li, "Synthesized oversulphated, acetylated and benzoylated derivatives of fucoidan extracted from Laminaria japonica and their potential antioxidant activity in vitro," *Food Chemistry*, vol. 114, no. 4, pp. 1285–1290, 2009.

[21] S. J. Yoon, Y. R. Pyun, J. K. Hwang, and P. A. S. Mourão, "A sulfated fucan from the brown alga _Laminaria cichorioides_ has mainly heparin cofactor II-dependent anticoagulant activity," *Carbohydrate Research*, vol. 342, no. 15, pp. 2326–2330, 2007.

[22] C. Cui, J. H. Lu, D. X. Sun-Waterhouse et al., "Polysaccharides from Laminaria japonica: Structural characteristics and

antioxidant activity," *Lebensmittel-Wissenschaft & Technologie*, vol. 73, pp. 602–608, 2016.

[23] S. Saha, M. H. Navid, S. S. Bandyopadhyay, P. Schnitzler, and B. Ray, "Sulfated polysaccharides from Laminaria angustata: Structural features and in vitro antiviral activities," *Carbohydrate Polymers*, vol. 87, no. 1, pp. 123–130, 2012.

[24] J. M. Wang, X. Y. Sun, and J. M. Ouyang, "Structural characterization, antioxidant activity, and biomedical application of astragalus polysaccharide degradation products," *International Journal of Polymer Science*, vol. 2018, Article ID 5136185, 13 pages, 2018.

[25] E. Bedini, A. Laezza, M. Parrilli, and A. Iadonisi, "A review of chemical methods for the selective sulfation and desulfation of polysaccharides," *Carbohydrate Polymers*, vol. 174, pp. 1224–1239, 2017.

[26] S. Li and N. P. Shah, "Antioxidant and antibacterial activities of sulphated polysaccharides from Pleurotus eryngii and Streptococcus thermophilus ASCC 1275," *Food Chemistry*, vol. 165, pp. 262–270, 2014.

[27] R. Sakthivel and K. Pandima Devi, "Evaluation of physicochemical properties, proximate and nutritional composition of Gracilaria edulis collected from Palk Bay," *Food Chemistry*, vol. 174, pp. 68–74, 2015.

[28] P. Seedevi, M. Moovendhan, S. Viramani, and A. Shanmugam, "Bioactive potential and structural chracterization of sulfated polysaccharide from seaweed (Gracilaria corticata)," *Carbohydrate Polymers*, vol. 155, pp. 516–524, 2017.

[29] L. Chen and G. L. Huang, "Antioxidant activities of sulfated pumpkin polysaccharides," *International Journal of Biological Macromolecules*, vol. 126, pp. 743–746, 2019.

[30] Y. Kariya, B. Mulloy, K. Imai et al., "Isolation and partial characterization of fucan sulfates from the body wall of sea cucumber Stichopus japonicus and their ability to inhibit osteoclastogenesis," *Carbohydrate Research*, vol. 339, no. 7, pp. 1339–1346, 2004.

[31] X. Q. Zha, C. Q. Lu, S. H. Cui et al., "Structural identification and immunostimulating activity of a Laminaria japonica polysaccharide," *International Journal of Biological Macromolecules*, vol. 78, pp. 429–438, 2015.

[32] S. G. Chen, J. F. Wang, C. H. Xue et al., "Sulfation of a squid ink polysaccharide and its inhibitory effect on tumor cell metastasis," *Carbohydrate Polymers*, vol. 81, no. 3, pp. 560–566, 2010.

[33] J. Wang, Q. B. Zhang, Z. S. Zhang, H. Zhang, and X. Z. Niu, "Structural studies on a novel fucogalactan sulfate extracted from the brown seaweed Laminaria japonica," *International Journal of Biological Macromolecules*, vol. 47, no. 2, pp. 126–131, 2010.

[34] J. X. Li, Z. Chi, L. J. Yu, F. Jiang, and C. G. Liu, "Sulfated modification, characterization, and antioxidant and moisture absorption/retention activities of a soluble neutral polysaccharide from Enteromorpha prolifera," *International Journal of Biological Macromolecules*, vol. 105, no. Partt 2, pp. 1544–1553, 2017.

[35] J. L. Wang, H. Y. Guo, J. Zhang et al., "Sulfated modification, characterization and structure-antioxidant relationships of Artemisia sphaerocephala polysaccharides," *Carbohydrate Polymers*, vol. 81, no. 4, pp. 897–905, 2010.

[36] L. Liang, L. Ao, T. Ma et al., "Sulfated modification and anticoagulant activity of pumpkin (Cucurbita pepo, Lady Godiva) polysaccharide," *International Journal of Biological Macromolecules*, vol. 106, pp. 447–455, 2018.

[37] M. Zargarzadeh, A. J. R. Amaral, C. A. Custódio, and J. F. Mano, "Biomedical applications of laminarin," *Carbohydrate Polymers*, vol. 232, article 115774, 2020.

[38] B. Akın, M. Öner, Y. Bayram, and K. D. Demadis, "Effects of carboxylate-modified, "Green" inulin biopolymers on the crystal growth of calcium oxalate," *Crystal Growth & Design*, vol. 8, no. 6, pp. 1997–2005, 2008.

[39] E. Akyol and M. Öner, "Controlling of morphology and polymorph of calcium oxalate crystals by using polyelectrolytes," *Journal of Crystal Growth*, vol. 401, pp. 260–265, 2014.

[40] A. Inagawa, M. Fukuyama, A. Hibara, M. Harada, and T. Okada, "Zeta potential determination with a microchannel fabricated in solidified solvents," *Journal of Colloid and Interface Science*, vol. 532, pp. 231–235, 2018.

[41] D. F. Wei, T. Chen, M. F. Yan et al., "Synthesis, characterization, antioxidant activity and neuroprotective effects of selenium polysaccharide from Radix hedysari," *Carbohydrate Polymers*, vol. 125, pp. 161–168, 2015.

[42] S. Lajili, H. H. Ammar, Z. Mzoughi et al., "Characterization of sulfated polysaccharide from Laurencia obtusa and its apoptotic, gastroprotective and antioxidant activities," *International Journal of Biological Macromolecules*, vol. 126, pp. 326–336, 2019.

[43] H. Zhang, X. Y. Sun, X. W. Chen, and J. M. Ouyang, "Degraded Porphyra yezoensis polysaccharide protects HK-2 cells and reduces nano-COM crystal toxicity, adhesion and endocytosis," *Journal of Materials Chemistry B*, vol. 8, no. 32, pp. 7233–7252, 2020.

[44] S. R. Khan, "Reactive oxygen species as the molecular modulators of calcium oxalate kidney stone formation: evidence from clinical and experimental investigations," *Journal of Urology*, vol. 189, no. 3, pp. 803–811, 2013.

[45] J. H. Xie, Z. J. Wang, M. Y. Shen et al., "Sulfated modification, characterization and antioxidant activities of polysaccharide from Cyclocarya paliurus," *Food Hydrocolloids*, vol. 53, pp. 7–15, 2016.

[46] Y. Xu, Y. J. Wu, P. L. Sun, F. M. Zhang, R. J. Linhardt, and A. Q. Zhang, "Chemically modified polysaccharides: synthesis, characterization, structure activity relationships of action," *International Journal of Biological Macromolecules*, vol. 132, pp. 970–977, 2019.

[47] Z. J. Wang, J. H. Xie, M. Y. Shen, S. P. Nie, and M. Y. Xie, "Sulfated modification of polysaccharides: synthesis, characterization and bioactivities," *Trends in Food Science & Technology*, vol. 74, pp. 147–157, 2018.

[48] Y. Yuan and D. Macquarrie, "Microwave assisted extraction of sulfated polysaccharides (fucoidan) from Ascophyllum nodosum and its antioxidant activity," *Carbohydrate Polymers*, vol. 129, pp. 101–107, 2015.

[49] L. X. Huang, M. Huang, M. Y. Shen et al., "Sulfated modification enhanced the antioxidant activity of Mesona chinensis Benth polysaccharide and its protective effect on cellular oxidative stress," *International Journal of Biological Macromolecules*, vol. 136, pp. 1000–1006, 2019.

[50] H. B. Hu, H. M. Li, M. H. Han et al., "Chemical modification and antioxidant activity of the polysaccharide from Acanthopanax leucorrhizus," *Carbohydrate Research*, vol. 487, article 107890, 2020.

[51] M. Daudon, E. Letavernier, V. Frochot, J. P. Haymann, D. Bazin, and P. Jungers, "Respective influence of calcium and oxalate urine concentration on the formation of calcium

oxalate monohydrate or dihydrate crystals," *Comptes Rendus Chimie*, vol. 19, no. 11-12, pp. 1504–1513, 2016.

[52] K. Teodosio Melo, R. Gomes Camara, M. F. Queiroz et al., "Evaluation of sulfated polysaccharides from the brown seaweed Dictyopteris justii as antioxidant agents and as inhibitors of the formation of calcium oxalate crystals," *Molecules*, vol. 18, no. 12, pp. 14543–14563, 2013.

[53] C. Y. Zhang, W. H. Wu, J. Wang, and M. B. Lan, "Antioxidant properties of polysaccharide from the brown seaweed sargassum graminifolium (Turn.), and its effects on calcium oxalate crystallization," *Marine Drugs*, vol. 10, no. 12, pp. 119–130, 2012.

[54] D. M. G. Mosquera, Y. H. Ortega, P. C. Quero, R. S. Martínez, and L. Pieters, "Antiurolithiatic activity of Boldoa purpurascens aqueous extract: an in vitro and in vivo study," *Journal of Ethnopharmacology*, vol. 253, article 112691, 2020.

[55] L. C. B. P. Oliveira, M. F. Queiroz, G. P. Fidelis et al., "Antioxidant sulfated polysaccharide from edible red seaweed gracilaria birdiae is an inhibitor of calcium oxalate crystal formation," *Molecules*, vol. 25, no. 9, p. 2055, 2020.

[56] D. L. Gomes, K. R. T. Melo, M. F. Queiroz et al., "In vitro studies reveal antiurolithic effect of antioxidant sulfated polysaccharides from the green seaweed caulerpa cupressoides var flabellata," *Marine Drugs*, vol. 17, no. 6, p. 326, 2019.

[57] M. L. Jin, Y. M. Wang, M. Huang, Z. Q. Lu, and Y. Z. Wang, "Sulphation can enhance the antioxidant activity of polysaccharides produced by _Enterobacter cloacae_ Z0206," *Carbohydrate Polymers*, vol. 99, pp. 624–629, 2014.

[58] Z. J. Wang, J. H. Xie, L. J. Kan et al., "Sulfated polysaccharides from _Cyclocarya paliurus_ reduce H_2O_2-induced oxidative stress in RAW264.7 cells," *International Journal of Biological Macromolecules*, vol. 80, pp. 410–417, 2015.

[59] J. M. Wang, Y. L. Hu, D. Y. Wang et al., "Sulfated modification can enhance the immune-enhancing activity of lycium barbarum polysaccharides," *Cellular Immunology*, vol. 263, no. 2, pp. 219–223, 2010.

Research Article

Salidroside Suppresses the Proliferation and Migration of Human Lung Cancer Cells through AMPK-Dependent NLRP3 Inflammasome Regulation

Weidong Ma,[1] Ziyuan Wang,[1] Yan Zhao,[1] Qibin Wang,[2] Yonghong Zhang,[1] Pan Lei,[1,3] Wei Lu,[2] Shan Yan,[1] Jun Zhou,[1] Xiaojiao Li,[1] Wenjun Yu,[1] Yaoxin Zhong,[1] Li Chen,[1,2] and Tao Zheng ⓘ[1,2]

[1]*Institute of Wudang Traditional Chinese Medicine, Taihe Hospital, Hubei University of Medicine, Shiyan, Hubei, China*
[2]*Department of Pharmacy, Taihe Hospital, Hubei University of Medicine, Shiyan, Hubei, China*
[3]*Hubei Key Laboratory of Wudang Local Chinese Medicine Research, Hubei University of Medicine, Shiyan, Hubei, China*

Correspondence should be addressed to Tao Zheng; ztice@foxmail.com

Inflammatory reactions mediated by the NACHT, LRR, and PYD domain-containing protein 3 (NLRP3) inflammasome contributes to non-small-cell lung cancer (NSCLC) progression, particularly in patients with bacterial infections. Salidroside (SAL) has recently been shown to suppress lipopolysaccharide- (LPS-) induced NSCLC proliferation and migration, but its mechanism of action remains unclear. It has been shown that SAL improves metabolic inflammation in diabetic rodents through AMP-activated protein kinase- (AMPK-) dependent inhibition of the NLRP3 inflammasome. However, whether the NLRP3 inflammasome is regulated by SAL in NSCLC cells and how its underlying mechanism(s) can be determined require clarification. In this study, human lung alveolar basal carcinoma epithelial (A549) cells were treated with LPS, and the effects of SAL on cell proliferation, migration, AMPK activity, reactive oxygen species (ROS) production, and NLRP3 inflammasome activation were investigated. We found that LPS induction increases the proliferation and migration of A549 cells which was suppressed by SAL. Moreover, SAL protected A549 cells against LPS-induced AMPK inhibition, ROS production, and NLRP3 inflammasome activation. Blocking AMPK using Compound C almost completely suppressed the beneficial effects of SAL. In summary, these results indicate that SAL suppresses the proliferation and migration of human lung cancer cells through AMPK-dependent NLRP3 inflammasome regulation.

1. Introduction

Lung cancer is now the most fatal tumor globally, with estimates that by 2035, the disease will afflict more than 3 million individuals worldwide [1]. Approximately 85% of lung cancer cases are classified as non-small-cell lung cancer (NSCLC), including adenocarcinoma, squamous cell carcinoma, and large cell carcinoma [2]. Owing to the limitations in curative options, the current outcome of NSCLC is poor, with more advanced stages remaining incurable [3]. Thus, understanding the onset and development of NSCLC and finding more effective treatments are urgently needed.

Emerging evidence suggests that systemic inflammation contributes to tumorigenesis [4–6], including NSCLC [7].

In patients with lung cancer, concurrent bacterial infections enhance tumor progression [8] and increase mortality [9]. As the major pathogen in these cases, gram-negative bacteria negatively influence NSCLC through their effects on toll-like receptor- (TLR-) mediated inflammatory reactions, through the production of lipopolysaccharides (LPS) [8–10]. Moreover, the LPS-stimulated production of proinflammatory cytokines in NSCLC can predict the clinical outcome in metastatic NSCLC patients [11]. Accordingly, therapies that target LPS-induced inflammation can effectively ameliorate the adhesion and migration of NSCLC cells *in vivo* [10].

The NLRP3 inflammasome is the most well-characterized inflammatory mediator, and it is composed of NACHT, LRR, and PYD domain-containing protein 3 (NLRP3); apoptosis-
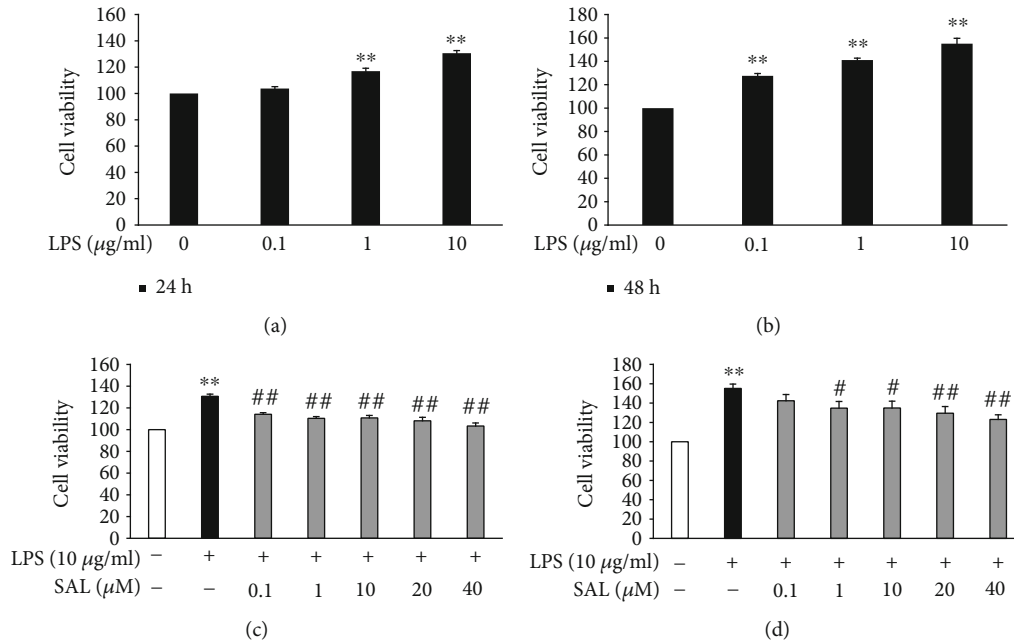
FIGURE 1: Effects of salidroside (SAL) on the proliferation of LPS-treated A549 cells. A549 cells were treated with the indicated concentrations of LPS (0.1, 1, and 10 μg/ml) for either 24 h (a) or 48 h (b). Cell viabilities were then measured using CCK-8 assays. A549 cells were treated with 10 μg/ml LPS in the presence or absence of SAL for either 24 h (c) or 48 h (d). Cell viabilities were then determined as described above. $^*p < 0.05$ and $^{**}p < 0.01$ vs. treatment without LPS; $^#p < 0.05$ and $^{##}p < 0.01$ vs. treatment with LPS alone. Values are means ± s.e.m. ($n = 4$).

associated speck-like protein containing a CARD; and caspase-1 [12]. The NLRP3 inflammasome is activated by pathogen-associated molecular patterns (PAMPs) or damage-associated molecular patterns (DAMPs), resulting in caspase-1 cleavage and the production of mature interleukin-1β (IL-1β) [6]. The NLRP3 inflammasome can also be activated by LPS under PAMPs which subsequently aggravates NSCLC [13]. Similarly, direct treatment of human lung alveolar basal carcinoma epithelial (A549) cells with IL-1β exhibits tumor-promoting effects *in vitro* [14].

Redox homeostasis plays an essential role in cellular functions and is also involved in the progress of cancer [15]. An imbalance in the production of reactive oxygen species (ROS) activates the NLRP3 inflammasome through either PAMPs or DAPMs. The overproduction of ROS causes the thioredoxin- (TRX-) interacting protein (TXNIP) to dissociate from TRX, inducing the NLRP3 inflammasome activation through TXNIP-NLRP3 interactions [16].

Natural products have historically made a major contribution to pharmacotherapy for cancer, and interest in natural products as drug leads provides a basis for making contributions to human health [17, 18]. Salidroside (SAL) is the main active ingredient of *Rhodiola rosea* and has been shown to exert therapeutic effects on diabetes and cardiovascular disease through its antioxidation and anti-inflammatory effects [19]. Studies suggest that SAL inhibits the growth of a range of human cancer cells including human mammary adenocarcinoma (MCF-7) [20], human mammary carcinoma (MDA-MB-231) [21], human hepatocellular carcinoma (HHCC), A549 [22], human malignant glioma (BT-325), and human gastric cancer (SGC-7901)

[23]. Wang et al. recently reported that SAL decreased proliferation and induced apoptosis in A549 cells through its ability to inhibit oxidative stress and p38 [24]. In our recent study, we found that SAL improves insulin resistance in high-glucose-incubated hepatocytes through AMP-activated protein kinase-(AMPK-) mediated inhibition of the NLRP3 inflammasome [25]. However, whether the NLRP3 inflammasome is regulated by SAL in NSCLC cells remains unclear.

In this study, we investigated the effects of SAL on the LPS-induced proliferation and migration of A549 cells. We further explored the effects of SAL on ROS production and NLRP3 inflammasome activation to define its mechanism(s) of action. We herein report the ability of SAL to suppress the proliferation and migration of human lung cancer cells through AMPK-dependent NLRP3 inflammasome regulation.

2. Materials and Methods

2.1. Cell Culture. A549 cells were obtained from the China Center for Type Culture Collection (Wuhan, China). Cells were cultured in high glucose DMEM containing 10% fetal bovine serum (#04-001-1ACS, Biological Industries, Kibbutz Beit Haemek, Israel), 100 IU/ml penicillin G, and 100 μg/ml streptomycin (#SV30010, HyClone, Logan, Utah, USA) at 37°C in a 5% CO_2 atmosphere. The medium was changed every two days. Cells were digested when confluency reached 80~90%. Cell monolayers were harvested in 0.25% trypsin-EDTA solution (#25200-056, Invitrogen, Grand Island, NY, USA).

2.2. Cell Treatment. After culturing in 96-well plates, 6-well plates, or 35 mm dishes for 24 h, A549 cells were treated with
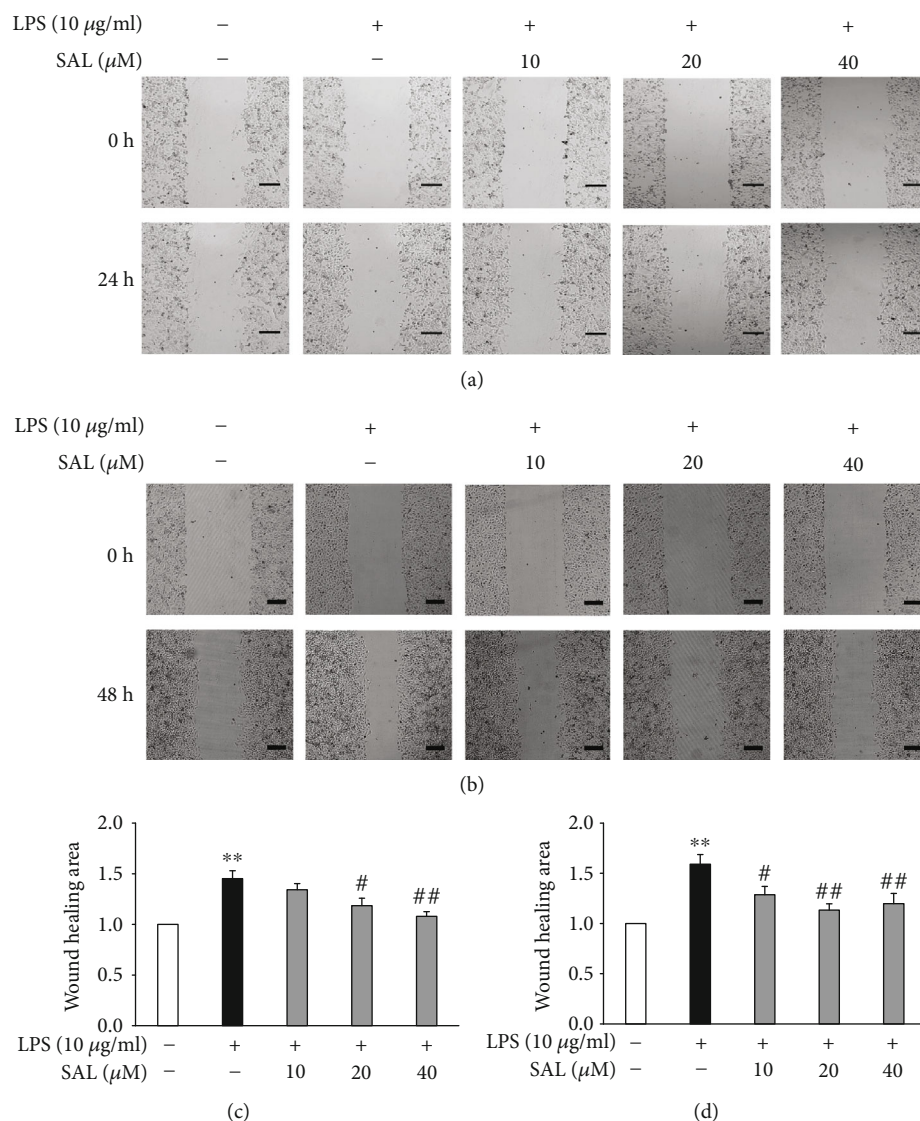
FIGURE 2: Effects of salidroside (SAL) on the migration of LPS-treated A549 cells. After exposure to $10\,\mu g/ml$ LPS and cotreatment with vehicle or SAL (10, 20, and $40\,\mu M$) for either 24 h (a, c) or 48 h (b, d), cell migration was determined through wound healing assays. Scale bar = $200\,\mu m$. $^{*}p < 0.05$ and $^{**}p < 0.01$ vs. treatment without LPS; $^{\#}p < 0.05$ and $^{\#\#}p < 0.01$ vs. treatment with LPS alone. Values are means ± s.e.m. ($n = 5$).

various concentrations of LPS (#L2880, Sigma-Aldrich, St. Louis, MO, USA) or SAL (#10338-51-9, purity > 98%, Tauto Biotech, Shanghai, China) for the indicated time periods. To inhibit AMPK activity, A549 cells were cotreated with $2\,\mu M$ Compound C (#S7306, Selleck Chemicals, Houston, TX, USA) following treatment with LPS or SAL. Recombinant human IL-1β was purchased from PeproTech (#200-01B, Cranbury, NJ, USA) and added to cells at a concentration of 15 ng/ml as previously described [14].

2.3. Cell Viability Assay.
For the assessment of cell viability, A549 cells were treated with the Cell Counting Kit-8 (CCK-8, #CK04, Dojindo Laboratories, Kumamoto, Japan) reagent according to the manufacturer's instructions.

2.4. Cell Migration Assay.
Cell migration was examined using scratch assays as previously described [13]. Briefly,

A549 cells were seeded to 100% confluence, and three scratches were introduced onto the cell layer using a sterile pipette tip. Cells were then washed in PBS three times and subsequently treated as indicated. Images were captured on a Leica DMi8 microscope (Leica Microsystems, Wetzlar, Germany) at the start of the experiment and at 24 or 48 h posttreatment. Wound healing areas were analyzed using ImageJ2x software (Wayne Rasband, National Institutes of Health, USA).

2.5. Oxidative Stress Measurement.
A549 cells in 96-well plates were treated as described, and intracellular ROS levels were assessed using DCFH-DA (#S0033, Beyotime Institute of Biotechnology, Shanghai, China) according to the manufacturer's instructions. After loading with the probes for 20 min, plates were washed 3 times by PBS, and medium containing DCFH-DA was readded for detection.
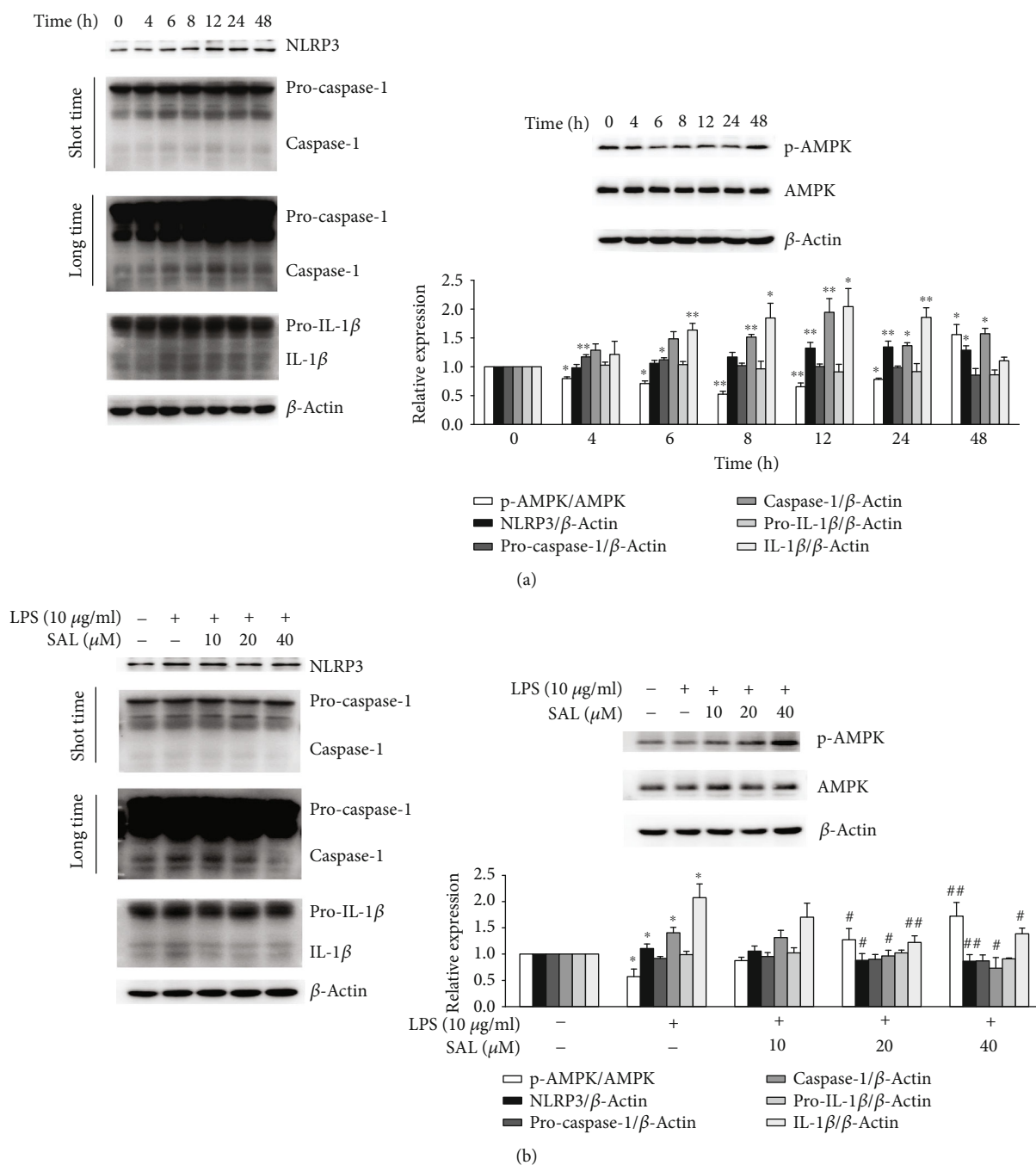
Figure 3: Effects of salidroside (SAL) on AMPK activity and NLRP3 inflammasome activation in A549 cells exposed to LPS. (a) A549 cells were treated with 10 μg/ml LPS for 4, 6, 8, 12, 24, and 48 h, and the levels of phosphorylated-AMPK, total-AMPK, NLRP3, caspase-1, and IL-1β in the cell lysates were determined by immunoblotting. (b) A549 cells were cotreated with 10 μg/ml LPS and various concentrations of SAL (10, 20, and 40 μM) for 12 h. The levels of phosphorylated-AMPK, total-AMPK, NLRP3, caspase-1, and IL-1β in the cell lysates were then determined by immunoblotting. $^*p < 0.05$ and $^{**}p < 0.01$ vs. treatment without LPS; $^{#}p < 0.05$ and $^{##}p < 0.01$ vs. treatment with LPS alone. Values are means ± s.e.m. ($n = 3$).

Fluorescent intensities were measured using a Tecan Infinite 200 PRO microplate reader (Tecan Group Ltd., Mannedorf, Switzerland) at excitation and emission wavelengths of 488 and 525 nm, respectively.

2.6. Protein Sample Preparation. Protein samples from A549 cells were extracted using a RIPA buffer (#P0013B,

Beyotime Institute of Biotechnology) according to the manufacturer's instructions. Briefly, A549 cells were washed in ice-cold PBS and lysed in a RIPA buffer supplemented with a protease inhibitor cocktail (#04693132001, Roche, Basel, Switzerland) and phosphatase inhibitor cocktail (#04906845001, Roche) for 15 min. Cell lysates were collected and centrifuged at 4°C at 14,000 rpm for

(a)

(b)

(c)
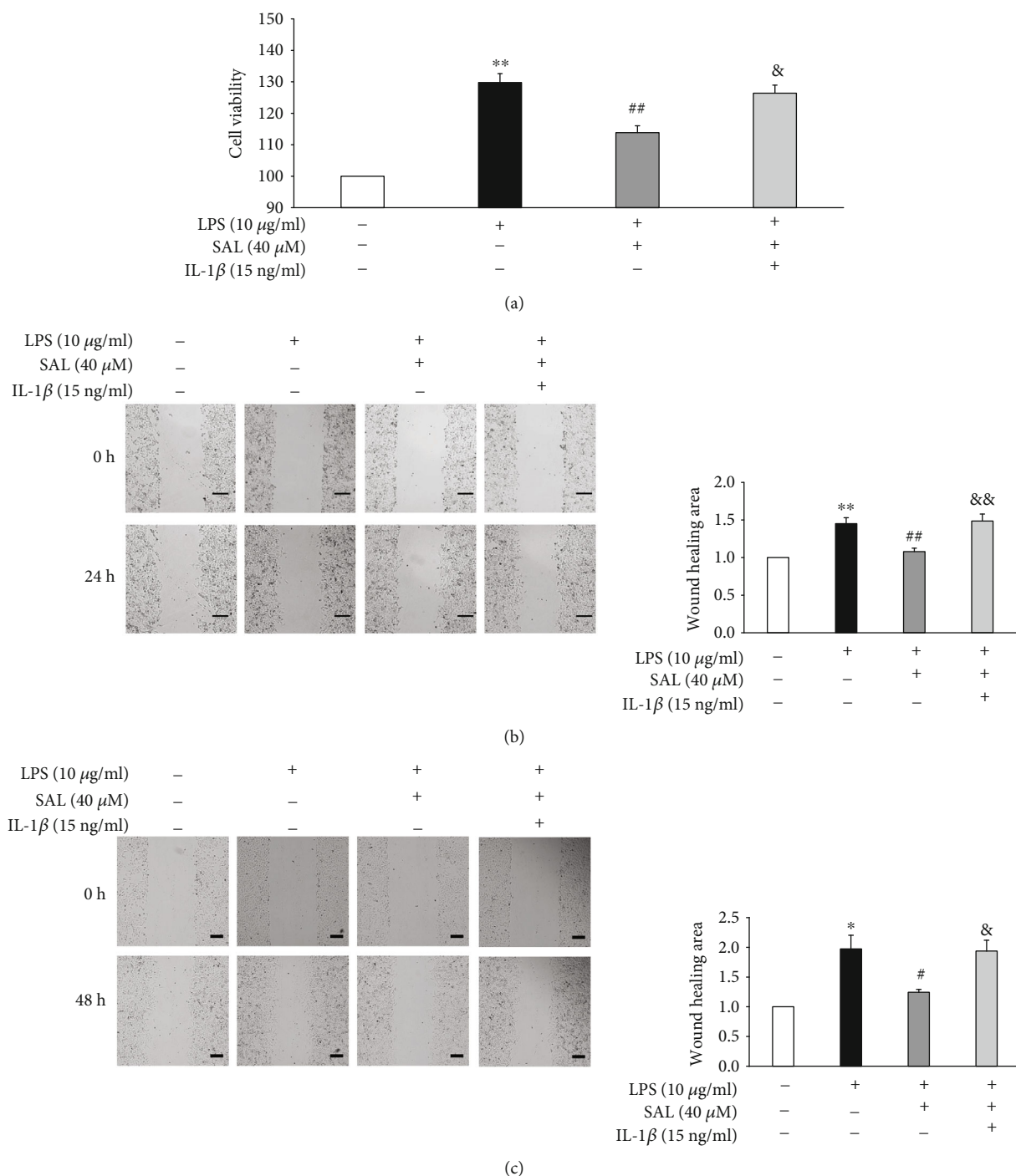
FIGURE 4: Coincubation with IL-1β abolishes the effects of salidroside (SAL) on cell proliferation and migration in LPS-exposed A549 cells. A549 cells were exposed to 10 μg/ml LPS in the presence of SAL (40 μM) and/or IL-1β (15 ng/ml) for 48 h. Cell viabilities were then measured using CCK-8 assays (a). After A549 cells were treated as described for 24 h (b) or 48 h (c), cell migration was determined through wound healing assays. Scale bar = 200 μm. $^{*}p < 0.05$ and $^{**}p < 0.01$ vs. no LPS treatment; $^{#}p < 0.05$ and $^{##}p < 0.01$ vs. cells treated with LPS alone; $^{&}p < 0.05$ and $^{&&}p < 0.01$ vs. cells treated with LPS plus SAL. Values are means ± s.e.m. ($n = 4$).

15 min. Protein concentrations of the collected supernatants were determined through BCA assays (#23225, Thermo Scientific, Rockford, IL, USA). Samples were denatured in a loading buffer, boiled for 5 min, and stored at -20°C for immunoblot analysis.

2.7. *Immunoblot Analysis.* Equal amounts of proteins (~40 μg) were separated on 9-11% SDS-PAGE gels and transferred to PVDF membranes. After blocking in 5% skimmed milk, membranes were probed overnight at 4°C with primary antibodies including anti-AMPK (#2532, Cell

(a)

(b)

(c)

(d)
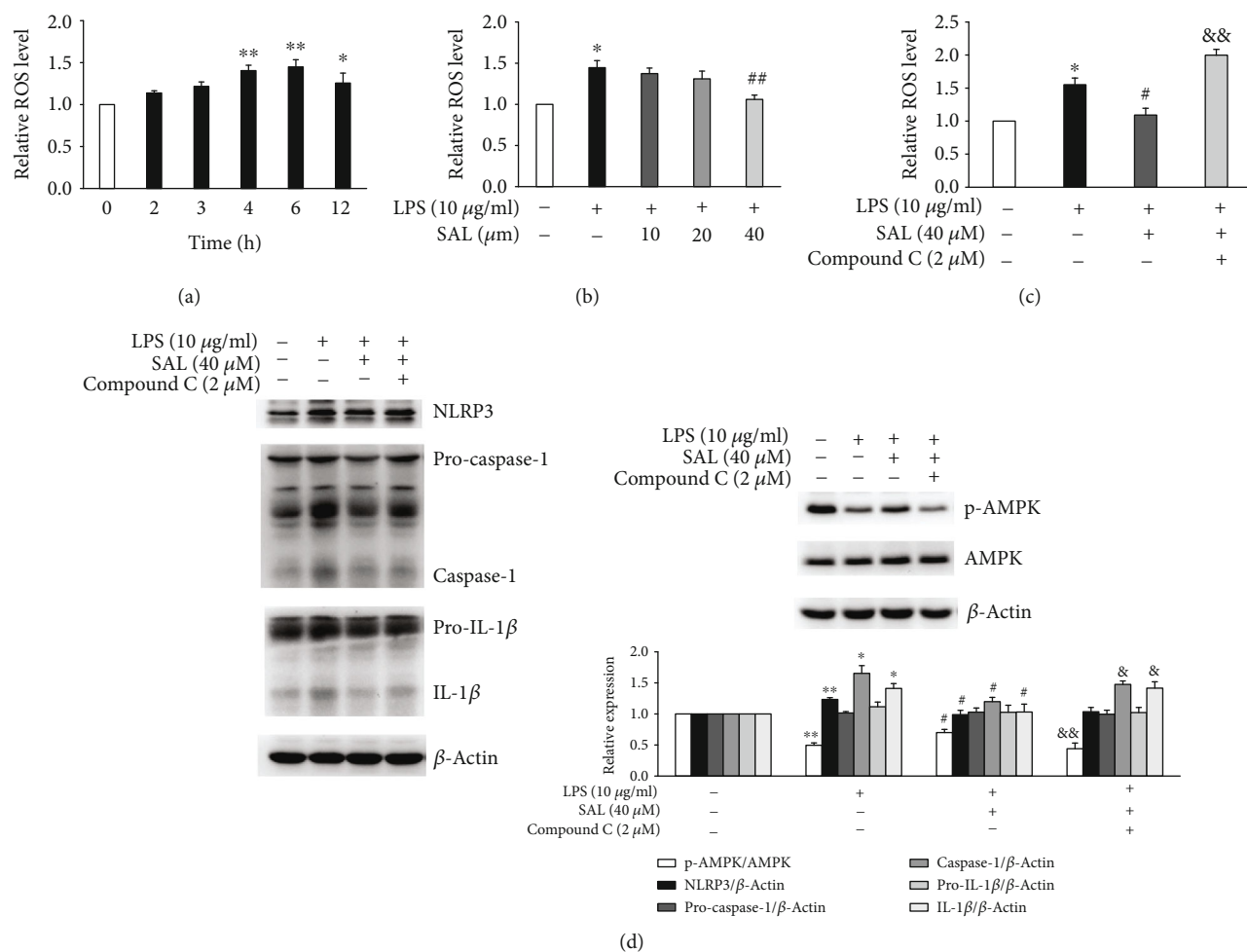
FIGURE 5: Effects of AMPK inhibition on ROS production and NLRP3 inflammasome activation in salidroside- (SAL-) treated A549 cells exposed to LPS. (a) In A549 cells exposed to $10\,\mu g/ml$ LPS for the indicated times, cellular ROS levels were determined using DCFH-DA. (b) In A549 cells exposed to $10\,\mu g/ml$ LPS in the presence of SAL at 10, 20, or $40\,\mu M$ for 6 h, ROS levels were measured as above. (c) In A549 cells exposed to $10\,\mu g/ml$ LPS in the presence of $40\,\mu M$ SAL or $2\,\mu M$ Compound C for 6 h, ROS levels were measured as described. (d) In A549 cells exposed to $10\,\mu g/ml$ LPS in the presence of $40\,\mu M$ SAL or $2\,\mu M$ Compound C for 12 h, the levels of phosphorylated-AMPK, total-AMPK, NLRP3, caspase-1, and IL-1β in the cell lysates were determined by immunoblotting. $^{*}p < 0.05$ and $^{**}p < 0.01$ vs. no LPS treatment; $^{\#}p < 0.05$ and $^{\#\#}p < 0.01$ vs. treatment with LPS alone; $^{\&}p < 0.05$ and $^{\&\&}p < 0.01$ vs. treatment with LPS plus SAL. Values are means ± s.e.m. ($n = 3$).

Signaling Technology, Beverly, MA, USA), anti-phospho-AMPK (#2535, Cell Signaling Technology), anti-NLRP3 (#15101, Cell Signaling Technology), anti-caspase-1 (#22915-1-AP, Proteintech, Chicago, IL, USA), anti-IL-1β (#sc-12742, Santa Cruz Biotechnology, Santa Cruz, CA, USA), and anti-β-actin (#A01010, Abbkine, Redlands, CA, USA). Membranes were washed 3 times in Tris-buffered saline with 0.1% Tween 20 and subsequently labeled with the HRP-conjugated goat anti-rabbit IgG (#A21020, Abbkine), goat anti-mouse IgG (#A21010, Abbkine), or mouse anti-Armenian hamster IgG (#sc-2789, Santa Cruz Biotechnology) at a dilution of 1 : 10000. Blots were imaged on a Tanon 5200 Chemiluminescent Imaging System (Tanon, Shanghai, China) and analyzed using ImageJ2x software.

2.8. Statistical Analysis. All data are expressed as the means ± SEM from at least three independent experiments.

SPSS 13.0 was used for all statistical analysis. An unpaired Student t-test was used to compare individual groups. Multiple-group comparisons were performed using a one-way ANOVA with post hoc testing. $p < 0.05$ were considered statistically significant.

3. Results

3.1. SAL Suppresses the LPS-Induced Proliferation of A549 Cells. The viability of A549 cells following their exposure to LPS (0.1, 1, and $10\,\mu g/ml$) was assessed. The results showed that LPS treatment for either 24 or 48 h increased cell viability compared to vehicle controls (Figures 1(a) and 1(b)). However, coincubation with SAL (0.1, 1, 10, 20, and $40\,\mu M$) for 24 and 48 h suppressed the LPS-induced increase in A549 cell proliferation in a concentration-dependent manner (Figures 1(c) and 1(d)).

(a)

(b)

(c)
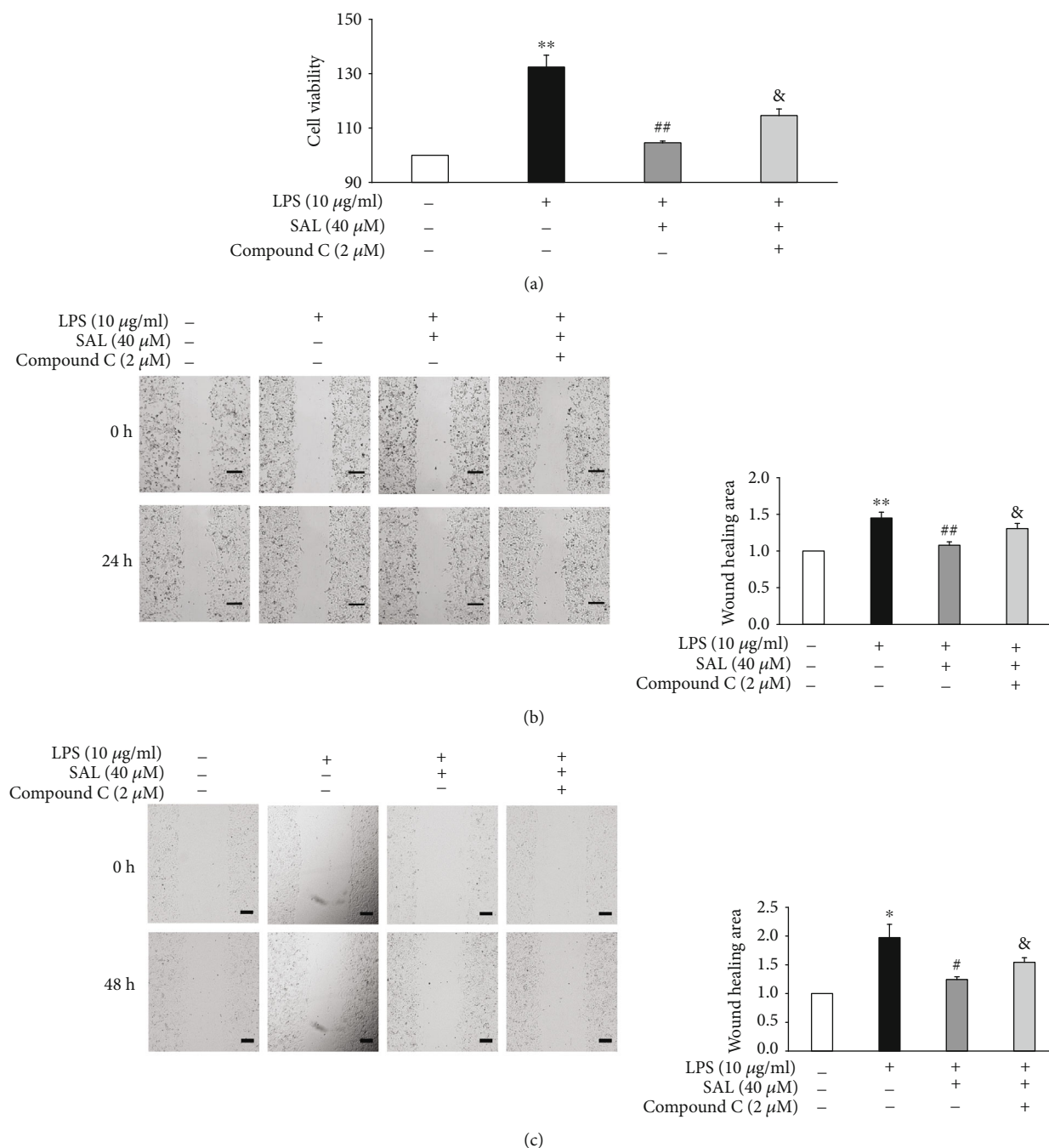
FIGURE 6: Influence of AMPK inhibition on the salidroside- (SAL-) mediated suppression of proliferation and migration in LPS-treated A549 cells. A549 cells were exposed to $10 \mu g/ml$ LPS in the presence of $40 \mu M$ SAL or $2 \mu M$ Compound C for 48 h. Cell viabilities were then measured using CCK-8 assays (a). After A549 cells were treated as described for 24 h (b) or 48 h (c), cell migration was determined through wound healing assays. Scale bar $= 200 \mu m$. $^*p < 0.05$ and $^{**}p < 0.01$ vs. treatment without LPS; $^{\#}p < 0.05$ and $^{\#\#}p < 0.01$ vs. treatment with LPS alone; $^{\&}p < 0.05$ and $^{\&\&}p < 0.01$ vs. treatment with LPS plus SAL. Values are means $\pm$ s.e.m. ($n = 3$).

3.2. SAL Inhibits the LPS-Induced Migration of A549 Cells. As shown in Figures 2(a) and 2(b), after exposure to $10 \mu g/ml$ LPS for 24 or 48 h, the migration of A549 cells was markedly enhanced. In contrast, A549 cells treated with SAL at concentrations of 10, 20, and $40 \mu M$ following LPS-induction showed lower levels of migration compared to cells exposed to LPS alone.

3.3. SAL Restores the LPS-Induced Decrease in AMPK Activity and Prevents Activation of the NLRP3 Inflammasome in A549 Cells. Since LPS-induced NLRP3 inflammasome activation plays a critical role in the tumorigenesis of NSCLC [10, 13], we investigated the effects of SAL on the NLRP3 inflammasome in LPS-treated A549 cells. As shown in Figure 3(a), compared to untreated cells, A549
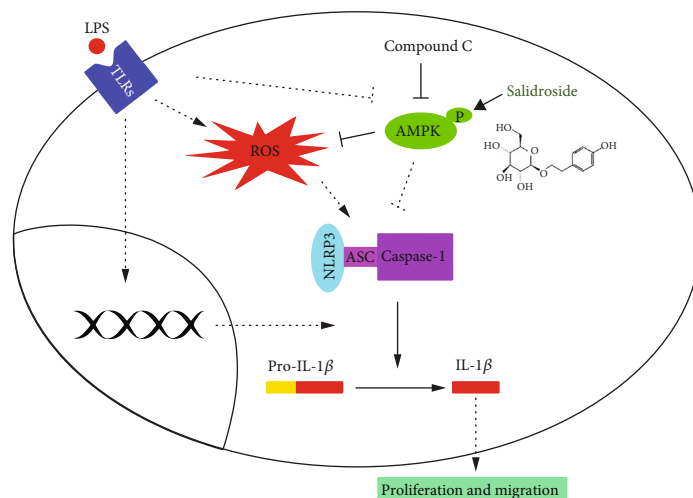
FIGURE 7: Schematic diagram highlighting the mechanism(s) of action of salidroside in NSCLC cells.

cells exposed to LPS for 4-24 h showed lower levels of AMPK phosphorylation and higher levels of NLRP3, caspase-1, and IL-1β. These results indicated that LPS-treated A549 cells exhibit impaired AMPK activity and enhanced NLRP3 inflammasome activation. In contrast, cells treated with SAL following LPS-induction showed higher levels of phosphorylated-AMPK. Moreover, cells treated with LPS+SAL showed significantly lower levels of NLRP3 inflammasome activation compared to those treated with LPS alone (Figure 3(b)).

3.4. SAL Mediates Its Effects on Cell Proliferation and Migration through the Inhibition of the NLRP3 Inflammasome.
We next investigated the role of the NLRP3 inflammasome activation in the proliferation and migration of A549 cells in response to SAL. In cells treated with either LPS or LPS+IL-1β, significantly higher levels of cell proliferation (Figure 4(a)) and migration (Figures 4(b) and 4(c)) were observed. These results confirmed that dysregulated NLRP3 inflammasome activation in A549 cells occurs following LPS stimulation, leading to abnormalities in cell proliferation and migration. However, the cotreatment of A549 cells with SAL suppressed the LPS-induced increase in A549 cell proliferation and migration (Figures 4(a)–4(c)). Conversely, cotreatment with IL-1β suppressed the effects of SAL on cell proliferation and migration in LPS-stimulated A549 cells. Taken together, these data suggest that the inhibitory effects of SAL on the NLRP3 inflammasome are necessary for its suppression on LPS-induced proliferation and migration of A549 cells.

3.5. SAL Decreases ROS Production and Suppresses the NLRP3 Inflammasome in an AMPK-Dependent Manner.
Excessive ROS production is a known cause of NLRP3 inflammasome activation [6, 16]. We therefore investigated the levels of cellular ROS in LPS-treated A549 cells using DCFH-DA. As shown in Figure 5(a), ROS production increased following 2-12 h of LPS exposure. However, cotreatment with SAL at a concentration of 40 μM significantly suppressed ROS generation (Figure 5(b)). SAL has

been shown to relieve oxidative stress through its effects on AMPK activation [19, 25, 26]. To investigate the role of AMPK, cells were treated with the AMPK inhibitor Compound C to confirm its requirement for the regulatory activity of SAL on ROS production and the NLRP3 inflammasome activation. The results showed that the inhibition of AMPK significantly increased ROS production compared to LPS and SAL cotreated A549 cells (Figure 5(c)). In addition, Compound C treatment in LPS and SAL cotreated cells decreased the phosphorylation of AMPK and increased the levels of NLRP3, pro-caspase-1, caspase-1, pro-IL-1β, and IL-1β (Figure 5(d)). These results suggest that SAL suppresses LPS-induced activation of the ROS/NLRP3 inflammasome axis in A549 cells through its effects on AMPK.

3.6. AMPK Inhibition Alleviates the Effects of SAL on LPS-Induced Proliferation and Migration.
We next investigated the effects of AMPK inhibition on the proliferation and migration of LPS- and SAL-treated A549 cells. The inhibition of AMPK by Compound C almost completely alleviated the beneficial effects of SAL, evidenced by the decrease in both cell proliferation and migration following exposure to LPS+SAL (Figures 6(a)–6(c)). Together, these data suggest that SAL activates AMPK to suppress LPS-induced A549 cell proliferation and migration.

4. Discussion

In this study, we show that the inhibitory effects of SAL on the proliferation and migration of LPS-treated A549 cells are mediated through its ability to activate AMPK and subsequently suppress the activation of the NLRP3 inflammasome. Details are summarized in Figure 7.

Inflammatory reaction contributes to tumor development and progression [27]. Accumulating evidence suggests that in NSCLC, patients with concurrent bacterial infections display more serious inflammatory reactions [9, 10]. Gram-negative bacteria are found in up to ~68% of NSCLC cases [9]. TLR4 signaling is activated by the LPS produced by

these bacteria leading to inflammatory responses. Chow et al. reported that TLR4 signaling is activated following the treatment of either murine or human NSCLC cells with heat-inactivated *E. coli*, a gram-negative bacteria, and these cells also showed enhanced adhesion and migratory phenotypes [10]. It has also been reported that in NSCLC patients with gram-negative bacterial infections, the excessive activation of the TLR4/IL-33 axis promotes tumor progression [8]. In patients with metastatic NSCLC, the *ex vivo* stimulation of blood cells with LPS increased the levels of IL-6 and IL-18, which correlated to the clinical outcome of the patients [11]. These findings suggest that inflammatory signaling represents a therapeutic target for the treatment of NSCLC.

The NRLP3 inflammasome mediates the LPS-elicited inflammatory reactions that occur in response to PAMPs. Wang et al. showed that in A549 cells treated with LPS +ATP, the enhanced activation of the NLRP3 inflammasome and increased cell proliferation and migration could be reversed with siRNA targeting NLRP3 or caspase-1 inhibition [13]. These results indicated that the deregulated activation of the NLRP3 inflammasome induced by PAMPs mediates the progression of NSCLC.

The NLRP3 inflammasome contributes to the progression of a range of human cancers. For example, the activation of the NLRP3 inflammasome in macrophages that surround colorectal cancer tissue can drive cancer cell metastasis to the liver [28]. A heterozygous NLRP3 (Q705K) mutation has also been shown to be associated with a poor outcome in patients with advanced colorectal cancer [29]. Moreover, inflammatory reactions caused by the NLRP3 inflammasome in fibroblasts leads to breast cancer progression and metastasis to both the liver and lung tissue [30, 31]. Furthermore, mycoplasma hyorhinis-induced activation of the NLRP3 inflammasome has been shown to promote gastric cancer metastasis [32].

Targeting the NLPR3 inflammasome is an effective approach for cancer treatment. Zou et al. reported that polydatin can suppress the proliferation and migration of A549 and H1299 cells through inhibition of the NLRP3 inflammasome [33]. Suppressing the activation of the NLRP3 inflammasome can also prevent the outgrowth and spontaneous metastasis of triple-negative breast cancer cells [34]. Interestingly, Dumont et al. found that 5-fluorouracil- (5-FU-) induced NLRP3 inflammasome activation is a critical factor limiting its anticancer efficacy. However, the suppression of the NLRP3 inflammasome decreased 5-FU-induced IL-1β secretion and caspase-1 activation, enhancing its curative effects [35]. Moreover, modulation of the tumor microenvironment through the inhibition of the NLRP3 inflammasome could suppress the migration and invasion of melanoma cells [36]. GL-V9, a small-molecule AMPK activator, could prevent colitis-associated cancer through the induction of mitophagy-mediated NLRP3 inflammasome inhibition [37] or through triggering autophagy-mediated NLRP3 inflammasome degradation [38].

Accumulating evidence suggests that SAL possesses anti-inflammatory effects through its ability to inhibit the NLRP3 inflammasome. In mice with acute liver injury induced by carbon tetrachloride, treatment with SAL effectively inhib-

ited the activation of the NLRP3 inflammasome and alleviated liver damage [39]. Similarly, SAL administration improved mechanical ventilation-induced lung injury in mice through the Sirt1-dependent inhibition of the NLRP3 inflammasome [40]. In dextran sulfate sodium-induced ulcerative colitis models, the protective effects of SAL were in part dependent on its inhibitory effects on the NLRP3 inflammasome [41]. Moreover, SAL has been shown to regulate the NLRP3 inflammasome through the TXNIP-NLRP3 pathway, providing protection against high glucose exposure, due to the accumulation of the extracellular matrix in glomerular mesangial cells [42] or through insulin resistance in hepatocytes [25]. Zhang et al. also demonstrated that SAL can alleviate Parkinson's disease through its ability to suppress pyroptosis in dopaminergic neurons, mediated by its inhibition of the NLRP3 inflammasome [43].

Wang et al. recently reported that SAL inhibits A549 cell proliferation, cell cycle progression, and metastasis and induces apoptosis through its regulatory effects on ROS generation and p38 MAPK signaling [24]. Additionally, SAL was shown to reduce the survival, migration, and invasion of A549 cells through the inhibition of Akt and MEK/ERK signaling through the upregulation of miR-195 expression [44]. In agreement with these findings, SAL could suppress the proliferation and migration of LPS-treated A549 cells. We further observed that in A549 cells treated with SAL, both the LPS-induced activation of the NLRP3 inflammasome and AMPK inhibition were effectively corrected. The inhibition of AMPK by its inhibitor Compound C almost completely alleviated the beneficial effects of SAL on A549 cell proliferation, migration, ROS production, and NLRP3 inflammasome activation. These results verify that the AMPK-signaling axis is key to the beneficial effects of SAL, not only during the pathological processes of insulin resistance and atherosclerosis [19, 45] but also during tumorigenesis. In a previous study, Wang et al. found that the expression level of epithelial-mesenchymal transition (EMT) marker snail remains unchanged in salidroside-treated A549 cells [24]. Lee et al. reported that farnesol inhibited the tumor growth of a xenograft mouse lung cancer model and abrogated the EMT process through regulating the Akt/mTOR pathway [46]. However, many previous findings have reported of entirely different actions of salidroside on Akt/mTOR signaling in human colorectal cancer cells [47] and human gastric cancer AGS cells [48]. Thus, whether EMT can be affected by salidroside and how its underlying mechanisms can be determined need to be further investigated.

Previous studies have shown that the abnormal activation of the NLRP3 inflammasome leads to an array of disease pathologies, including allergic airway disease, chronic obstructive pulmonary disease, and asbestosis [5, 49]. These findings highlight the NLRP3 inflammasome as a target for the prevention and/or treatment of lung disease. We speculate that the SAL-mediated regulation of the NLRP3 inflammasome may also improve these lung diseases, which now warrants further investigation in future studies.

In conclusion, we demonstrate that SAL suppresses the proliferation and migration of human NSCLC cells through

the AMPK-dependent regulation of the NLRP3 inflammasome. This highlights the therapeutic benefits of SAL for the treatment of NSCLC, particularly in cases that are accompanied by bacterial infections.

Abbreviations

AMPK: AMP-activated protein kinase
CCK-8: Cell Counting Kit-8
DAMPs: Damage-associated molecular patterns
EMT: Epithelial-mesenchymal transition
A549:   Human lung alveolar basal carcinoma epithelial
LPS: Lipopolysaccharides
NLRP3: NACHT, LRR, and PYD domain-containing protein 3
NSCLC: Non-small-cell lung cancer
PAMPs: Pathogen-associated molecular patterns
ROS: Reactive oxygen species
SAL: Salidroside
TLR: Toll-like receptor
TRX: Thioredoxin
TXNIP: TRX-interacting protein
5-FU: 5-Fluorouracil.

Data Availability

The data used to support the findings of this study are available from the corresponding author upon request.

Conflicts of Interest

The authors declare that they have no conflicts of interest.

Authors' Contributions

Tao Zheng and Li Chen conceived and designed the study. Weidong Ma, Ziyuan Wang, Yan Zhao, Yonghong Zhang, Pan Lei, Wei Lu, Shan Yan, and Jun Zhou performed the experiments. Weidong Ma, Qibin Wang, Tao Zheng, and Li Chen analyzed the research data and wrote the manuscript. Tao Zheng revised the manuscript.

Acknowledgments

References

[1] J. Didkowska, U. Wojciechowska, M. Mańczuk, and J. Łobaszewski, "Lung cancer epidemiology: contemporary and future challenges worldwide," *Annals of Translational Medicine*, vol. 4, no. 8, p. 150, 2016.

[2] R. L. Siegel, K. D. Miller, and A. Jemal, "Cancer statistics, 2016," *CA: a Cancer Journal for Clinicians*, vol. 66, no. 1, pp. 7–30, 2016.

[3] V. Petrilli, M. Bodnar, B. Guey, S. Hacot, and S. Lantuejoul, "Abstract 2038: a novel role for the NLRP3 inflammasome in lung cancer," *Cancer Research*, vol. 75, 15 Supplement, pp. 2038–2038, 2015.

[4] Q. Wei, K. Mu, T. Li et al., "Deregulation of the NLRP3 inflammasome in hepatic parenchymal cells during liver cancer progression," *Laboratory Investigation*, vol. 94, no. 1, pp. 52–62, 2014.

[5] M. Sayan and B. T. Mossman, "The NLRP3 inflammasome in pathogenic particle and fibre-associated lung inflammation and diseases," *Particle and Fibre Toxicology*, vol. 13, no. 1, p. 51, 2016.

[6] S. Hamarsheh and R. Zeiser, "NLRP3 inflammasome activation in cancer: a double-edged sword," *Frontiers in Immunology*, vol. 11, p. 1444, 2020.

[7] S. H. Jafri, R. Shi, and G. Mills, "Advance lung cancer inflammation index (ALI) at diagnosis is a prognostic marker in patients with metastatic non-small cell lung cancer (NSCLC): a retrospective review," *BMC Cancer*, vol. 13, no. 1, p. 158, 2013.

[8] M. Sun, Y. Bai, S. Zhao et al., "Gram-negative bacteria facilitate tumor progression through TLR4/IL-33 pathway in patients with non-small-cell lung cancer," *Oncotarget*, vol. 9, no. 17, pp. 13462–13473, 2018.

[9] T. Berghmans, J. P. Sculier, and J. Klastersky, "A prospective study of infections in lung cancer patients admitted to the hospital," *Chest*, vol. 124, no. 1, pp. 114–120, 2003.

[10] S. C. Chow, S. D. Gowing, J. J. Cools-Lartigue et al., "Gram negative bacteria increase non-small cell lung cancer metastasis via Toll-like receptor 4 activation and mitogen-activated protein kinase phosphorylation," *International Journal of Cancer*, vol. 136, no. 6, pp. 1341–1350, 2015.

[11] P. J. Vlachostergios, I. Gioulbasanis, S. Ghosh et al., "Predictive and prognostic value of LPS-stimulated cytokine secretion in metastatic non-small cell lung cancer," *Clinical & Translational Oncology*, vol. 15, no. 11, pp. 903–909, 2013.

[12] T. Zheng, Q. Wang, Y. Dong et al., "High glucose-aggravated hepatic insulin resistance: role of the NLRP3 inflammasome in Kupffer cells," *Obesity (Silver Spring)*, vol. 28, no. 7, pp. 1270–1282, 2020.

[13] Y. Wang, H. Kong, X. Zeng et al., "Activation of NLRP3 inflammasome enhances the proliferation and migration of A549 lung cancer cells," *Oncology Reports*, vol. 35, no. 4, pp. 2053–2064, 2016.

[14] L. Wang, L. F. Zhang, J. Wu et al., "IL-1β-mediated repression of microRNA-101 is crucial for inflammation-promoted lung tumorigenesis," *Cancer Research*, vol. 74, no. 17, pp. 4720–4730, 2014.

[15] A. Kirtonia, G. Sethi, and M. Garg, "The multifaceted role of reactive oxygen species in tumorigenesis," *Cellular and Molecular Life Sciences*, vol. 77, no. 22, pp. 4459–4483, 2020.

[16] R. Zhou, A. Tardivel, B. Thorens, I. Choi, and J. Tschopp, "Thioredoxin-interacting protein links oxidative stress to inflammasome activation," *Nature Immunology*, vol. 11, no. 2, pp. 136–140, 2010.

[17] the International Natural Product Sciences Taskforce, A. G. Atanasov, S. B. Zotchev, V. M. Dirsch, and C. T. Supuran, "Natural products in drug discovery: advances and

opportunities," *Nature Reviews. Drug Discovery*, vol. 20, no. 3, pp. 200–216, 2021.

[18] D. J. Newman and G. M. Cragg, "Natural products as sources of new drugs over the nearly four decades from 01/1981 to 09/2019," *Journal of Natural Products*, vol. 83, no. 3, pp. 770–803, 2020.

[19] T. Zheng, F. Bian, L. Chen, Q. Wang, and S. Jin, "Beneficial effects of *Rhodiola* and salidroside in diabetes: potential role of AMP-activated protein kinase," *Molecular Diagnosis & Therapy*, vol. 23, no. 4, pp. 489–498, 2019.

[20] G. Zhao, A. Shi, Z. Fan, and Y. E. du, "Salidroside inhibits the growth of human breast cancer in vitro and in vivo," *Oncology Reports*, vol. 33, no. 5, pp. 2553–2560, 2015.

[21] X. Hu, X. Zhang, S. Qiu, D. Yu, and S. Lin, "Salidroside induces cell-cycle arrest and apoptosis in human breast cancer cells," *Biochemical and Biophysical Research Communications*, vol. 398, no. 1, pp. 62–67, 2010.

[22] X. Zhu, D. Liu, Y. Wang, and M. Dong, "Salidroside suppresses nonsmall cell lung cancer cells proliferation and migration via microRNA-103-3p/Mzb1," *Anti-Cancer Drugs*, vol. 31, no. 7, pp. 663–671, 2020.

[23] X. Hu, S. Lin, D. Yu, S. Qiu, X. Zhang, and R. Mei, "A preliminary study: the anti-proliferation effect of salidroside on different human cancer cell lines," *Cell Biology and Toxicology*, vol. 26, no. 6, pp. 499–507, 2010.

[24] J. Wang, J. Z. Li, A. X. Lu, K. F. Zhang, and B. J. Li, "Anticancer effect of salidroside on A549 lung cancer cells through inhibition of oxidative stress and phospho-p38 expression," *Oncology Letters*, vol. 7, no. 4, pp. 1159–1164, 2014.

[25] T. Zheng, X. Yang, W. Li et al., "Salidroside attenuates high-fat diet-induced nonalcoholic fatty liver disease via AMPK-dependent TXNIP/NLRP3 pathway," *Oxidative Medicine and Cellular Longevity*, vol. 2018, Article ID 8597897, 17 pages, 2018.

[26] S. Xing, X. Yang, W. Li et al., "Salidroside stimulates mitochondrial biogenesis and protects against H_2O_2-induced endothelial dysfunction," *Oxidative Medicine and Cellular Longevity*, vol. 2014, Article ID 904834, 13 pages, 2014.

[27] I. C. Allen, E. M. E. TeKippe, R. M. Woodford et al., "The NLRP3 inflammasome functions as a negative regulator of tumorigenesis during colitis-associated cancer," *The Journal of Experimental Medicine*, vol. 207, no. 5, pp. 1045–1056, 2010.

[28] Q. Deng, Y. Geng, L. Zhao et al., "NLRP3 inflammasomes in macrophages drive colorectal cancer metastasis to the liver," *Cancer Letters*, vol. 442, pp. 21–30, 2019.

[29] J. Ungerbäck, D. Belenki, A. Jawad ul-Hassan et al., "Genetic variation and alterations of genes involved in NFκB/TNFAIP3- and NLRP3-inflammasome signaling affect susceptibility and outcome of colorectal cancer," *Carcinogenesis*, vol. 33, no. 11, pp. 2126–2134, 2012.

[30] N. Ershaid, Y. Sharon, H. Doron et al., "NLRP3 inflammasome in fibroblasts links tissue damage with inflammation in breast cancer progression and metastasis," *Nature Communications*, vol. 10, no. 1, p. 4375, 2019.

[31] Q. Hu, F. Zhao, F. Guo, C. Wang, and Z. Fu, "Polymeric nanoparticles induce NLRP3 inflammasome activation and promote breast cancer metastasis," *Macromolecular Bioscience*, vol. 17, no. 12, 2017.

[32] Y. Xu, H. Li, W. Chen et al., "Mycoplasma hyorhinis activates the NLRP3 inflammasome and promotes migration and inva-

sion of gastric cancer cells," *PLoS One*, vol. 8, no. 11, article e77955, 2013.

[33] J. Zou, Y. Yang, Y. Yang, and X. Liu, "Polydatin suppresses proliferation and metastasis of non-small cell lung cancer cells by inhibiting NLRP3 inflammasome activation via NF-κB pathway," *Biomedicine & Pharmacotherapy*, vol. 108, pp. 130–136, 2018.

[34] M. Yao, X. Fan, B. Yuan et al., "Berberine inhibits NLRP3 Inflammasome pathway in human triple-negative breast cancer MDA-MB-231 cell," *BMC Complementary and Alternative Medicine*, vol. 19, no. 1, p. 216, 2019.

[35] A. Dumont, C. de Rosny, T. L. Kieu et al., "Docosahexaenoic acid inhibits both NLRP3 inflammasome assembly and JNK-mediated mature IL-1β secretion in 5-fluorouracil-treated MDSC: implication in cancer treatment," *Cell Death & Disease*, vol. 10, no. 7, p. 485, 2019.

[36] H. E. Lee, J. Y. Lee, G. Yang et al., "Inhibition of NLRP3 inflammasome in tumor microenvironment leads to suppression of metastatic potential of cancer cells," *Scientific Reports*, vol. 9, no. 1, p. 12277, 2019.

[37] W. Guo, Y. Sun, W. Liu et al., "Small molecule-driven mitophagy-mediated NLRP3 inflammasome inhibition is responsible for the prevention of colitis-associated cancer," *Autophagy*, vol. 10, no. 6, pp. 972–985, 2014.

[38] Y. Zhao, Q. Guo, K. Zhao et al., "Small molecule GL-V9 protects against colitis-associated colorectal cancer by limiting NLRP3 inflammasome through autophagy," *Oncoimmunology*, vol. 7, no. 1, article e1375640, 2017.

[39] X. Zhang, G. Kuang, J. Wan et al., "Salidroside protects mice against CCl4-induced acute liver injury via down-regulating CYP2E1 expression and inhibiting NLRP3 inflammasome activation," *International Immunopharmacology*, vol. 85, p. 106662, 2020.

[40] Y. Wang, C. F. Xu, Y. J. Liu et al., "Salidroside attenuates ventilation induced lung injury via SIRT1-dependent inhibition of NLRP3 inflammasome," *Cellular Physiology and Biochemistry*, vol. 42, no. 1, pp. 34–43, 2017.

[41] J. Liu, J. Cai, P. Fan, N. Zhang, and Y. Cao, "The abilities of salidroside on ameliorating inflammation, skewing the imbalanced nucleotide oligomerization domain-like receptor family pyrin domain containing 3/autophagy, and maintaining intestinal barrier are profitable in colitis," *Frontiers in Pharmacology*, vol. 10, p. 1385, 2019.

[42] S. Wang, X. Zhao, S. Yang, B. Chen, and J. Shi, "Salidroside alleviates high glucose-induced oxidative stress and extracellular matrix accumulation in rat glomerular mesangial cells by the TXNIP-NLRP3 inflammasome pathway," *Chemico-Biological Interactions*, vol. 278, pp. 48–53, 2017.

[43] X. Zhang, Y. Zhang, R. Li, L. Zhu, B. Fu, and T. Yan, "Salidroside ameliorates Parkinson's disease by inhibiting NLRP3-dependent pyroptosis," *Aging (Albany NY)*, vol. 12, no. 10, pp. 9405–9426, 2020.

[44] M. Ren, W. Xu, and T. Xu, "Salidroside represses proliferation, migration and invasion of human lung cancer cells through AKT and MEK/ERK signal pathway," *Artificial Cells, Nanomedicine, and Biotechnology*, vol. 47, no. 1, pp. 1014–1021, 2019.

[45] T. Zheng, X. Yang, D. Wu et al., "Salidroside ameliorates insulin resistance through activation of a mitochondria-associated AMPK/PI3K/Akt/GSK3β pathway," *British Journal of Pharmacology*, vol. 172, no. 13, pp. 3284–3301, 2015.

[46] J. H. Lee, A. Chinnathambi, S. A. Alharbi, O. H. M. Shair, G. Sethi, and K. S. Ahn, "Farnesol abrogates epithelial to mesenchymal transition process through regulating Akt/mTOR pathway," *Pharmacological Research*, vol. 150, p. 104504, 2019.

[47] X. J. Fan, Y. Wang, L. Wang, and M. Zhu, "Salidroside induces apoptosis and autophagy in human colorectal cancer cells through inhibition of PI3K/Akt/mTOR pathway," *Oncology Reports*, vol. 36, no. 6, pp. 3559–3567, 2016.

[48] L. Rong, Z. Li, X. Leng et al., "Salidroside induces apoptosis and protective autophagy in human gastric cancer AGS cells through the PI3K/Akt/mTOR pathway," *Biomedicine & Pharmacotherapy*, vol. 122, p. 109726, 2020.

[49] F. Madouri, N. Guillou, L. Fauconnier et al., "Caspase-1 activation by NLRP3 inflammasome dampens IL-33-dependent house dust mite-induced allergic lung inflammation," *Journal of Molecular Cell Biology*, vol. 7, no. 4, pp. 351–365, 2015.

Research Article

Plant-Based Synthesis of Zinc Oxide Nanoparticles (ZnO-NPs) Using Aqueous Leaf Extract of *Aquilegia pubiflora*: Their Antiproliferative Activity against HepG2 Cells Inducing Reactive Oxygen Species and Other *In Vitro* Properties

Hasnain Jan ⓘ,[1] **Muzamil Shah,**[1] **Anisa Andleeb,**[1] **Shah Faisal,**[2] **Aishma Khattak,**[3] **Muhammad Rizwan,**[4] **Samantha Drouet,**[5] **Christophe Hano,**[5] **and Bilal Haider Abbasi** ⓘ[1]

[1]Department of Biotechnology, Quaid-i-Azam University, Islamabad 45320, Pakistan
[2]Institute of Biotechnology and Microbiology, Bacha Khan University, KPK, Pakistan
[3]Department of Bioinformatics, Shaheed Benazir University Peshawar, KPK, Pakistan
[4]Centre for Biotechnology and Microbiology, University of Swat, KPK, Pakistan
[5]Laboratoire de Biologie des Ligneux et des Grandes Cultures (LBLGC), INRA USC1328 Université d'Orléans, Cedex 2, France

Correspondence should be addressed to Hasnain Jan; hasnainjan@bs.qau.edu.pk and Bilal Haider Abbasi; bhabbasi@qau.edu.pk

The anti-cancer, anti-aging, anti-inflammatory, antioxidant, and anti-diabetic effects of zinc oxide nanoparticles (ZnO-NPs) produced from aqueous leaf extract of *Aquilegia pubiflora* were evaluated in this study. Several methods were used to characterize ZnO-NPs, including SEM, FTIR, XRD, DLS, PL, Raman, and HPLC. The nanoparticles that had a size of 34.23 nm as well as a strong aqueous dispersion potential were highly pure, spherical or elliptical in form, and had a mean size of 34.23 nm. According to FTIR and HPLC studies, the flavonoids and hydroxycinnamic acid derivatives were successfully capped. Synthesized ZnO-NPs in water have a zeta potential of -18.4 mV, showing that they are stable solutions. The ZnO-NPs proved to be highly toxic for the HepG2 cell line and showed a reduced cell viability of $23.68 \pm 2.1\%$ after 24 hours of ZnO-NP treatment. ZnO-NPs also showed excellent inhibitory potential against the enzymes acetylcholinesterase (IC$_{50}$: 102 μg/mL) and butyrylcholinesterase (IC$_{50}$: 125 μg/mL) which are involved in Alzheimer's disease. Overall, the enzymes involved in aging, diabetes, and inflammation showed a moderate inhibitory response to ZnO-NPs. Given these findings, these biosynthesized ZnO-NPs could be a good option for the cure of deadly diseases such as cancer, diabetes, Alzheimer's, and other inflammatory diseases due to their strong anticancer potential and efficient antioxidant properties.

1. Introduction

Nanotechnology is an interdisciplinary science that encompasses several disciplines, including electronics, biomaterials, and medicine. A number of techniques, including physical, chemical, and biological processes, can be used to create nanomaterials with useful characteristics as tiny as 10–100 nm in size [1, 2]. Because of their large surface area, small size, thermal conductivity, shape, surface morphology, charge, zeta potential, and crystal structure [3], nanoscale materials have piqued the interest of scientists, allowing them to be integrated

into biotechnological and biomedical sectors, particularly for the cure of deadly diseases, i.e., cancer and Alzheimer's [4, 5]. Traditional methods (chemical and physical) for producing nanoparticles have numerous limitations [6], including long-term processing, high prices, tedious procedures, hazardous by-products, and in particular the usage of poisonous chemicals [7]. However, due of its cost effectiveness, environmental friendliness, biocompatibility, convenience of use, and quick synthesis procedures, green synthesis is a favored technique for nanoparticle production [8, 9]. NPs can be biosynthesized by a variety of biological entities,

including cyanobacteria, fungus, actinomycetes, bacteria, algae, and plants. Green-synthesized nanoparticles offer a new perspective as a delivery vehicle, for specific and safer drug delivery, a promising alternative to cancer drugs. Several NPs have been synthesized by green synthesis, such as Ag, Cu, Au, ZnO, Se, and CuO, and many others that have unique biological activities [10–13].

Due to its multiple uses in several technical sectors, metal oxide NPs have been actively investigated during the last decade. ZnO-NPs are an interesting inorganic material with a varied series of uses in a variety of fields, including semiconductors, energy conservation, textiles, cosmetics, electronics, health care, catalysis, and chemical sensors [14–16]. ZnO-NPs are nontoxic, biocompatible, and cheap and have a wide range of biological uses, including targeted drug delivery, anti-inflammatory, wound healing, antimicrobial agents, anti-cancer, and bioimaging [17]. ZnO-NPs are also utilized in beauty care products and sunscreens due to their effective UV absorption capabilities [18]. The use of ZnO-NPs as additives in nutritional products was certified a few years ago to increase growth performance, improve antioxidant properties, and boost the quality of eggs and chickens [19].

Metal oxide (MNPs) may be produced in a variety of ways (chemical, physical, and biosynthetic) and have a diverse set of characteristics and uses. Green synthesis covers the synthesis from algae, fungus, plants, bacteria, and other microorganisms. They enable the large-scale manufacturing of ZnO-NPs devoid of contaminants [20]. Plant parts including the leaf, stem, root, fruit, and seed have been utilized to generate ZnO-NPs because of the specific phytochemicals they produce. Natural extracts of plant components offer a low-cost and environmentally beneficial alternative to using intermediary base groups [21]. Secondary plant compounds found in plant extracts function as both reducing agents and capping or stabilizing agents. Metal ions or metal oxides are reduced to zero valence metal NPs in bioreduction with the aid of plant-secreted phytochemicals such as polyphenolic compounds, alkaloids, polysaccharides, amino acids, vitamins, and terpenoids [20]. Plants of the *Lamiaceae* family such as *Vitex negundo*, *Plectranthus amboinicus*, and *Anisochilus carnosus* have been extensively researched, revealing NP production in a variety of sizes and forms, including rod-shaped, hexagonal, quasispherical, and spherical with agglomerates. The results clearly showed that the size of produced NPs reduces as the content of a plant extract increases. For the most part, the leaves of *A. indica* of the *Meliaceae* family have been utilized in the synthesis of ZnO-NPs. All tests revealed NPs with spherical and hexagonal disc shapes, as verified by XRD and TEM analyses. Alkane, amide, carbonate, alcohol, amine, and carboxylic acid were shown to be effective capping agents in these investigations. Furthermore, these synthesized NPs were also proved efficient in various biomedical applications like antimicrobial, anti-cancer, anti-diabetic, and antioxidants [20].

Aquilegia pubiflora is a medicinally valuable herb, which belongs to the *Ranunculaceae* family and is widespread in the Himalayas of India, northern Pakistan, and Afghanistan. This herbaceous plant is commonly called as hairy flowered columbine or Himalayan columbine but known locally as Thandi buti or Domba [22]. This species possesses many important pharmacological and medicinal properties including astringent, dyspepsia, cardiotonic, antiasthmatic, antipyretic, stimulant, and antijaundice. This plant's dried roots have been used to cure eye disorders, snakebites, homeopathy, inflammation, and toothaches and particularly for the nervous system [23]. A recent study found that the methanolic extract of *Aquilegia pubiflora* exhibits effective erythroid induction activity, indicating that this plant might be a source of fetal hemoglobin producing phytocompounds and could be utilized to treat β-thalassemia [24]. Moreover, *Aquilegia pubiflora* was mainly used for the treatment of influenza, skin burns, wound healing, jaundice, and gynecology, circulatory, and cardiovascular disease [25].

Here, we disclose the bio-assisted synthesis of ZnO-NPs through an ecofriendly approach using aqueous extracts of *Aquilegia pubiflora* as an efficient oxidizing/reducing and capping agent. The biosynthesis of ZnO-NPs has already been reported; however, their diverse biological properties including anti-Alzheimer's, antidiabetic, antiaging, and anti-cancer activities have been less exposed. The aim of the present study is therefore to investigate the biological effects of synthesized ZnO-NPs [7]. HPLC, FTIR, XRD, SEM, DLS, Raman, and PL were used to characterize the ZnO-NPs as we previously reported [26, 27]. The well-characterized ZnO-NPs were examined for their biological activities, including anti-inflammatory activity, anti-aging, anti-diabetic, and antioxidant activities. The anti-Alzheimer and anti-diabetic effects of ZnO-NPs were also screened, and the *in vitro* cytotoxic potential against cancer cell was examined for their possible application in the biomedical field.

2. Materials and Methods

2.1. Plant Identification and Extraction. The leaves of *Aquilegia pubiflora* were collected in the Swat area of Pakistan and determined to be disease-free and healthy. Plant identification and verification were carried out by Professor Mushtaq Ahmad of the Herbarium of the Department of Plant Sciences at Quaid-i-Azam University in Pakistan. The collected leaves were cut into tiny bits and properly washed with tap water to remove contaminants and dust spores. The cleaned leaves were stored in a closed room (at 25°C) for around 7 days to dry. In a sterile Willy mill, the dried leaves were crushed into a fine powder. To prepare the extract, 30 g of fine powder was mixed with 200 mL distilled water in a 500 mL flask, sonicated for 10 minutes, and maintained in a shaking incubator at 200 rpm and 37°C for two days. To get rid of any leftovers, the extract was filtered twice with nylon paper and then three times with Whatman No. 1 filter paper.

2.2. Biosynthesis of ZnO Nanoparticles. For the green synthesis of ZnO-NPs, the conventional process from Thema et al. was followed, with slight modifications to the extract and salt concentrations [28]. Before and after dissolving the aqueous extract with the precursor salt, UV and pH were monitored. 100 mL of extract was mixed with 6.0 g of zinc acetate dihydrate salt and swirled for 2 hours at 60°C on a magnetic stirrer. Only after reaction occurs, the temperature is lowered for

10 minutes at 25°C upon being centrifuged at 10,000 rpm (HERMLE Z326 K). The solution was separated, and the left-over pellet was rinsed multiple times with sterile water before being placed on a clean Petri plate and dried in the oven at 80°C. The dried materials were ground to a powdered form in a clean grinder and pulverized at 500°C for 2 hours to remove any impurities. For eventual physical characterization and biomedical uses, the annealed powder was put in a sealed sample vial, labeled, and stored.

2.3. Characterization of Biosynthesized ZnO-NPs.

As previously reported, the morphological, structural, and vibrational physiognomies of obtained ZnO-NPs were investigated utilizing a variety of characterization methods such as HPLC, FTIR, XRD, SEM, DLS, Raman, and PL [27]. HPLC and Fourier transform infrared spectroscopy (FTIR) (400–4000 cm^{-1}) were used to identify phytochemicals and associated functional groups on ZnO-NPs. XRD was used to verify the good crystallinity, phase recognition, and homogeneity of ZnO-NPs (Model-D8 Advance, Germany). To test the stability of ZnO-NPs after processing, the dispersal sustainability of the particles in purified water with various pH values was visually analyzed. SEM was used to investigate the morphological characteristics of particles. DLS was used to identify the optimum charge and stability of ZnO-NPs. Photoluminescence (PL) and Raman spectroscopy were used to identify oxygen vacancies and vibrational modes [27].

2.4. Antidiabetic Assays.

To explore the anti-diabetic ability of biosynthesized ZnO-NPs, both α-glucosidase inhibition and α-amylase bioassays were performed.

2.4.1. α-Amylase Inhibition Assay.

The α-amylase inhibiting action of ZnO-NPs was evaluated using the methodology of Zohra et al. with minor variations in NP concentrations [29]. For this test, a 96-well microplate was utilized, and 10 L of ZnO-NPs was added to each well, followed by 15 L of sodium phosphate buffer (pH 6.9), 25 mL of alpha-amylase, and 40 mL of starch solution. After 30 minutes of incubation at 50°C, the reaction was halted by adding 20 mL of 1 M HCl and 90 L of iodine solution. Like a control treatment, acarbose was utilized, while DMSO is being used as a negative control. A microplate reader was used to detect absorbance at 540 nm. The % inhibition of alpha-amylase by samples was determined using the following formula. The experiment was carried out in triplicate and twice.

$$\%\text{Enzyme inhibition} = \left(\frac{\text{Abs Sample} - \text{Abs negative control}}{\text{Abs blank} - \text{Abs negative control}} \right) \times 100. \quad (1)$$

2.4.2. α-Glucosidase Inhibition Assay.

The anti-diabetic potential of ZnO-NPs was additionally evaluated utilizing previously reported protocol by Saratale et al. with minor changes in sample concentration [30, 31]. At pH 6.8, 50 mL of phosphate buffer and p-nitrophenyl alpha-D-glucopyranoside substrate solution was produced, and 100 mg of BSA was added. 10 mL of ZnO-NPs was preincubated with 250 L α-glucosidase (0.15 units/mL) at 37°C

for 5 minutes. The master mixture was kept at 37°C for 15 minutes. After simply adding 2 mL of 200 mM Na$_2$CO$_3$ solution, the process was stopped. The absorbance of p-nitrophenol generated was measured at 400 nm using a UV-Vis spectrophotometer. Using the formula below, the % inhibition of α-glucosidase by samples was calculated. In the experiment, acarbose was used as a positive control and carried out in triplicate and repeated twice.

$$\%\text{Enzyme inhibition} = \left(\frac{\text{Abs Sample} - \text{Abs negative control}}{\text{Abs blank} - \text{Abs negative control}} \right) \times 100. \quad (2)$$

2.5. Antioxidant Assays

2.5.1. Total Antioxidant Capacity (TAC) Determination.

The TAC potential of ZnO-NPs was calculated by a previously described methodology by Shah et al., with slight modifications in applied concentration [31, 32]. Using a micropipette, 100 L of ZnO-NPs was added to the Eppendorf tubes. Thereafter, Eppendorf tubes comprising ZnO-NPs received 900 mL of TAC reagent (0.6 M sulfuric acid, 28 mM sodium phosphate, and 4 mM ammonium molybdate in 50 mL dH$_2$0). The solution was allowed to cool to room temperature after 2.5 hours in a water bath at 90°C. A spectrophotometer reader was used to quantify the reagent absorbance at 630 nm. The amount of ascorbic acid equivalent (AAE) per milligram of analyte was used to calculate TAC. The test was repeated three times in total.

2.5.2. Total Reducing Power (TRP) Determination.

The total reduction power of ZnO-NPs was tested using the approach outlined by Nazir et al. [32, 33]. 100 mL of ZnO-NPs was combined with 400 mL of C$_6$N$_6$FeK$_3$ and 0.2 molar phosphate buffer (pH 6.6) in Eppendorf tubes and maintained for 30 minutes at 55°C in a water bath. The solution was centrifuged for 8 minutes at 1200 rpm with 400 mL of C$_2$HCl$_3$O$_2$ added to each Eppendorf tube. The supernatant (140 mL) from each combination was poured into the wells of a 96-well plate containing 60 mL ferric cyanide solution. A spectrophotometer reader was used to quantify the reagent absorbance at 630 nm. The amount of ascorbic acid equivalent (AAE) per milligram of analyte was used to calculate TRP. The test was repeated three times in total.

2.5.3. Free Radical Scavenging Assay (FRSA).

The established protocol of Ahmed et al. evaluated the potential free radical scavenging capability of ZnO-NPs using a previously reported protocol [34, 35]. To assess the antioxidant capacity of test samples, DPPH reagents at concentrations ranging from 12.5 mL to 400 mL were employed. A 96-well plate was filled with 10 mL of ZnO-NPs, and 90 mL of DPPH reagent was applied to each well containing ZnO-NPs. The positive control was ascorbic acid, while the negative control was DMSO. A microplate detector was used to measure the absorbance of the reaction mixture at 515 nm.

2.5.4. ABTS Assay.

The ABTS test, commonly identified as the Trolox antioxidant assay, was performed using the

procedure of Faisal et al. with minor changes in applied concentrations [33, 36]. An ABTS solution for the reaction was made by combining 2.45 mM potassium per sulphate with 7 mM of ABTS chemical, subsequently 16 hours in the dark incubation. Upon mixing with test sample, the resulting tubes were incubated in the darkness for 15 minutes at 25°C. The absorbance of the test sample was measured at 734 nm using the Microplate Reader (BioTek ELX800). Negative and positive controls were employed, respectively, with DMSO and Trolox. The antioxidant potential of the samples was measured in TEAC, and the experiment was repeated three times.

2.6. Anti-Alzheimer's Activity.

Inhibiting the enzymes butyrylcholinesterase (BChE) and acetylcholinesterase (AChE) is a possible therapeutic target for Alzheimer's disease. The inhibitory ability of ZnO-NPs against AChE and BChE enzymes was evaluated using a slightly modified Elman's technique in terms of NP concentration and dosages, as previously published by Imran et al. [37, 38]. From the test sample, a concentration scale ranging from 12.5 μg/mL to 200 μg/mL was used. In brief, ZnO-NPs are distributed in a phosphate-buffered saline solution (PBS). The ultimate enzyme concentration for AChE was 0.03 U/mL, and for BChE, it was 0.01 U/mL. The reaction mixture was supplemented with DTNB (0.00022 M), acetylcholine iodide (ATchI; 0.0005 M), and butyrylcholine iodide (BTchI; 0.0005 M) produced in filtered water at 8°C. Galantamine hydrobromide (Sigma; GI660) produced in methanol was employed as a positive control in the experiment, and the reaction mixture stripped of the test sample was used as a negative control. The anticholinesterase activity is established on the splitting of ATchI into AChE and BTchI into BChE, which results in the production of the yellow-colored products. Using a spectrophotometer, the absorbance was eventually measured at 412 nm. Galantamine and ZnO-NPs have estimations for percent enzyme activity and percent enzyme inhibition with a temporal shift in the absorption rate. The following formulae were used to compute the percent enzyme inhibition.

$$V = \frac{\Delta Abs}{\Delta t},$$

$$\text{Inhibition } (\%) = 100 - \text{Enzyme activity } (\%), \quad (3)$$

$$\text{Enzyme activity } (\%) = \left(\frac{V}{V_{max}}\right) \times 100.$$

2.7. Anti-Inflammatory Activities

2.7.1. Against COX-1 and COX-2.

ZnO-NPs were evaluated for their ability to inhibit COX-1 (Ovine Kit 701050) and COX-2 (Human Kit 701050). As a positive control, ibuprofen 10 M was used, and arachidonic (1.1 mM) was used as a substrate. Both COX peroxidase components were measured in accordance with the kit's manufacturer's instructions. The test was carried out on a 96-well plate in triplicate and was repeated twice.

2.7.2. Against 15-LOX.

ZnO-NPs were tested for their ability to inhibit 15-LOX (760700 kit, Cayman France). 100 M NDGA was employed as a positive control, whereas 10 M $C_{20}H_{32}O_2$ was used as a substrate. Hydroperoxides are formed as a result of lipooxygenation, and their concentration was measured using a 15-lipooxygenase standard in 10 mM Tris-HCl buffer at 7.4 pH filter supplied with the kit. In a 96-well plate, ZnO-NPs and enzyme are mixed together and incubated for 5 minutes. The 5-minute incubation was followed by 15-minute incubation after the addition of the substrate and a 5-minute incubation period after the addition of the chromogen. Using a Synergy II reader, the absorbance was measured at 590 nm (BioTek Instruments, Colmar, France).

2.7.3. Against Secretory Phospholipase A2 (sPLA2).

An assay kit (10004883, Cayman Chem., France) was used to test the inhibitory ability of ZnO-NPs against sPLA2. 1.44 mM diheptanoyl thio-PC was used as a positive control, while 100 M thiotheramide-PC was used as a substrate. The cleavage of the diheptanoyl thio-PC ester produces free thiols, which were detected using DTNB at 420 nm in a 96-well microplate.

2.8. Antiaging Assay

2.8.1. Anti-AGE Formation Activity.

The previously reported protocol of Kaewseejan et al. was used to assess the inhibitory potential of vesperlysine AGEs and pentosidine AGE production [39]. 0.5 M glucose solution and 0.1 M PBS containing 0.02 percent (w/v) sodium azide were used to make BSA solution. ZnO-NPs were mixed with a 20 mg/mL BSA solution. The reaction mixture was kept at 37°C for five days in the dark. The fluorescence was estimated and quantified using a Versa Fluor fluorometer from Bio-Rad in France, with a 410 nm emission wavelength and a 330 nm excitation wavelength.

2.8.2. Tyrosinase Assay.

The tyrosinase test was performed using 5 mM L-DOPA, as previously described by Chai et al. [40]. L-DOPA diphenolase substrate was combined with 10 mL ZnO-NPs and sodium phosphate buffer (50 mM, pH 6.8). The final volume of the reaction mixture was raised to 200 mL by adding 0.2 mg/mL mushroom tyrosinase solution. As a control, extraction solvent in place of the tested ZnO-NPs was employed. At 475 nm, a microplate machine was used to track the reaction activities. The tyrosinase impact on ZnO-NPs was reported as % inhibition compared with matching control.

2.8.3. Elastase Assay.

Porcine pancreatic elastase was used in the elastase inhibition test (Sigma-Aldrich). The substrate used in the test was N(AAAVPN). The relative conversion of substrate into p-nitroaniline release at 410 nm was used to quantify the reaction traces using a microplate reader, following the approach of Wittenauer et al. [41].

2.8.4. Hyaluronidase Assay.

The potential of ZnO-NPs to inhibit hyaluronidase was tested using a technique established by Kolakul et al. [42]. A solution containing 0.03

percent (w/v) hyaluronic acid and 1.5 units of hyaluronidase was employed as a substrate. The undigested form of hyaluronic acid precipitated in an acid albumin solution (0.1 percent (w/v) BSA). The optical density (OD) at 600 nm was measured using a spectrophotometer. In contrast to the control, the antihyaluronidase potential was expressed as a percentage inhibition.

2.8.5. Collagenase Assay. The procedure from Wittenauer et al. was used, with a small change in applied concentration [41]. FALGPA obtained from Sigma-Aldrich functioned as a substrate. The reduction in FALGPA absorbance was measured at 335 nm using a microplate reader over a period of 20 minutes. The trial was conducted in triplicates, and anticollagenase activity was expressed as a percentage inhibition compared to the control.

2.9. Cytotoxicity against the HepG2 Cell Line. HepG2 cells (ATCC HB-8065) were grown in DME medium with 100 g/mL streptomycin, 10% FCS, 100 U/mL penicillin, and 2 mM L-glutamine and incubated at 37°C in a humidified CO_2 incubator with 5% humidity. 0.5 mM trypsin/EDTA was used to harvest the cells at 80-90 percent confluence. The cytotoxic potential of ZnO-NPs against HepG2 cells was determined using MTT tetrazolium dye. Preseeded HepG2 cells (>90% viability; 1×10^4 cells/well) were treated for 24 hours in a 96-well plate with 200 μg/mL test samples and incubated in a 5 percent humidified CO_2 incubator. After a 24 h incubation period, 10 mL of MTT dye (5 mg/mL) was added to each well and incubated for 3 h. After that, the insoluble formazan was dissolved in a 10% acidified SDS solution. The cells were then incubated overnight. The plates were examined at 570 nm using a microplate reader (Platos R 496, AMP). As a control, we utilized untreated HepG2 cells (NTC) and doxorubicin.

$$
\begin{aligned}
&\%\text{Viability} \\
&= \frac{\text{Absorbance of sample} - \text{Absorbance of sample control}}{\text{Absorbance of NTC} - \text{Absorbance of media}} \times 100.
\end{aligned}
\tag{4}
$$

Optical density of treated samples and NTC was measured at 570 nm.

3. Results and Discussion

3.1. Synthesis and HPLC Analysis of Green ZnO-NPs. Aquilegia pubiflora leaf extract has been employed as a reducing and stabilizing agent in the production of multifunctional ZnO-NPs in recent study. The genus *Aquilegia* is a member of the *Ranunculaceae* family, which comprises around 60 plant species used for a variety of medicinal purposes across the world, mostly in South Asia. Among the medicinally important phytochemicals identified in these plants are ferulic acid, β-sitosterol, apigenin, aquilegiolide, magnoflorine, berberine, caffeic acid, p-coumaric acid, genkwanin, glochidionolactone A, and resorcylic acid [27, 43]. These phytochemicals, such as phenolics and flavonoids, may have played an important role in the formation of stable nanopar-

ticles. HPLC was used to produce and quantify the fundamental phytochemicals responsible for the reduction and effective capping of synthesized NPs. Eight constituents were identified and measured, including four hydroxycinnamic acid derivatives (sinapic acid, ferulic acid, chlorogenic acid, and p-coumaric acid) and four flavonoids (orientin, vitexin, isoorientin, and isovitexin). Hydroxycinnamic acids and flavonoids are phenolics that are produced through the shikimic acid pathway and are involved in a range of biological processes in plants [27, 31]. Orientin and chlorogenic acid both protect plants against stresses and have a wide range of biological activities, including antifungal, anticancer, antidiabetic, antibacterial, antioxidant, anti-inflammatory, and hepatoprotective effects [44, 45]. According to the findings of earlier studies, flavonoids and hydroxycinnamic acid derivatives can be found on the surface of nanoparticles [27, 32, 46]. These plant active chemicals have a role in ZnO-NP capping. White ZnO-NP powder was produced after washing, drying, grinding, and calcination operations. The fine powder was collected and kept as ZnO-NPs in an airtight glass container before being employed for physicochemical and morphological evaluation, as well as biological applications [27].

3.2. Physicochemical and Morphological Characterization. The XRD pattern of synthesized ZnO-NPs showed the presence of pure and crystalline nanoparticles, with high diffraction peaks observed at various stages, i.e., 69.47°, 68.23°, 66.83°, 62.68°, 56.31°, 47.39°, 36.36°, 34.34°, and 36.36°, referring to different Miller indices, respectively (201), (212), (200), (103), (102), (101), (002), and (100) as shown in Figure 1S(A). The indexing of ZnO with a mean size of 19.58 nm supports the normal hexagonal wurtzite structure (JCPDF file no. 00-036-1451) [47, 48]. The FTIR spectra of the synthesized nanoparticles were estimated in the spectral range of 400–4000 cm^{-1} as shown in Figure 1S(B). The main absorption peaks were identified in the range of lower wavenumbers. The broad band observed at 3100 cm^{-1} corresponds to the O-H stretching mode of the hydroxyl group. The highest strength at 1459^{-1} in the protein amide connection indicated amine (-NH) vibration stretch. The prominent bands detected at 1028 cm^{-1} and 1384 cm^{-1} represented alcohols, phenolic compounds, and C-N stretching vibrations of aromatic amines in biomolecules. Zn-O refers to a distinct band that can be seen at 863 cm^{-1} [49–51]. The surface shape and particle size of green-synthesized ZnO-NPs are determined by scanning electron microscopy, as illustrated in Figures 2S(A) and 2S(B). The micrograph showed that, with some degree of aggregation, the particles exhibit a spherical structure. In previous research, such morphologies have also been identified. Furthermore, using the ImageJ program, the average particle size of the nanoparticles was 34.23 nm [52, 53]. The dispersion power of ZnO-NPs in deionized water at pH 2, pH 7, and pH 12 was investigated. It was noted that even after 24 h of sonication, ZnO-NPs demonstrated excellent dispersion at neutral pH. Moreover, at neutral pH, the dispersion effect was also enhanced by a highly negative zeta potential value [54]. The zeta potential and particle size

Table 1: α-Amylase and α-glycosidase potential at various concentrations.

Enzymes	Concentrations (μg/mL)					
	+ Control	12.5	25	50	100	200
α-Amylase	88.63 ± 3.79	$18.91 \pm 0.73^{***}$	$22.49 \pm 0.54^{**}$	$27.19 \pm 0.63^{**}$	$28.36 \pm 0.69^{**}$	$31 \pm 0.24^{*}$
α-Glucosidase	88.63 ± 3.79	$16.31 \pm 0.44^{***}$	$18.66 \pm 0.59^{**}$	$21.43 \pm 1.06^{*}$	$21.91 \pm 1.19^{*}$	$22.69 \pm 1.23^{*}$

distribution were investigated using the Malvern Zetasizer, as shown in Figures 3S(A) and 3S(B). The colloidal stability of particles is determined by the zeta potential $|\zeta|$, which is a common estimate of the surface load. Suspensions featuring $|\zeta|$ 15 mV are normally graded as stable colloids. The calculation also improves the stable dispersion potential of biogenic ZnO-NPs at pH 7 in distilled water. The negative surface charge on particles provides particle dispersion stability and prevents aggregation due to the high binding affinity of the extract compounds on metallic ions. In addition, calculations of the size distribution showed the average particle size to be 131 nm. The larger ZnO-NPs detected by DLS are due to the technique's bias against measuring larger particles (even aggregate) [54, 55]. Photoluminescence (PL) analysis of engineered nanomaterials is significant because it gives important information on the quality of the synthesized materials. Excitation wavelengths ranging from 500 nm to 900 nm were used to measure the PL. Characteristic peaks, referred to as trap state or deep state emission, were found at 510 nm, 552 nm, and 690 nm, as shown in Figure 4S(A). There are three possible charge states for oxygen vacancies in ZnO: neutral, single ionized, and double ionized. While the presence of oxygen is responsible for green oxygen emissions from ZnO-NPs, the rise in oxygen vacancies is linked to high PL emissions [56, 57]. Figure 4S(B) shows the Raman spectra of biosynthesized nanoparticles, which revealed typical peaks at 435 cm^{-1} and 572 cm^{-1} [27, 58].

3.3. Antidiabetic Activity.

Diabetes mellitus (DM) is a metabolic condition characterized by hyperglycemia that persists. It is caused by a lack of insulin synthesis or a lack of insulin sensitivity in the body's cells [59]. The International Diabetes Federation (IDF) study (2017) estimated that 425 million adults have diabetes, with that number expected to rise to 629 million by 2045 [60]. Lowering postprandial hyperglycemia is one of the important clinical approaches to diabetes care. This can be accomplished by inhibiting two essential digestive tract enzymes that hydrolyze carbohydrates, i.e., alpha-amylase and alpha-glucosidase [59]. Various doses of ZnO-NPs ranging from 12.5 μg/mL to 200 μg/mL were tested in the assay for α-amylase and α-glucosidase inhibition. Our findings suggest that ZnO-NPs have a mild inhibitory effect on α-amylase and α-glucosidase activity, which is consistent with previous research (Table 1) [61]. At the highest concentration of 200 μg/mL, the maximum inhibition of α-amylase was determined to be 310.24, whereas the maximum inhibition of α-glucosidase was calculated to be 22.691.23. Overall, both enzymes' % inhibition increased in a dose-dependent manner; however, α-amylase showed considerably greater inhibition as compared to α-glycosidase, while considering

the comparable inhibitory effect of both enzymes. Hence, ZnO-NPs synthesized from *Aquilegia pubiflora* have moderate antidiabetic properties; this could be due to the presence of some active compounds that inhibit diabetes-related enzymes.

***Highly significant, **slightly significant, and *nonsignificant difference from control at $P < 0.05$ by one-way ANOVA in the column. The values represent the mean ± SD of three replicates.

3.4. Antioxidant Activity.

A variety of test methods have been devised and employed due to the relevance of antioxidants in protecting natural and man-made materials. Methods based on inhibited autoxidation, oxygen consumption kinetics, or the formation of hydroperoxides and primary oxidation products are among them. Secondary oxidation products (e.g., carbonyl compounds) were also determined analytically [62]. However, most test methods do not involve substrate autoxidation. For this purpose, we have used four different antioxidant assays to gain a better understanding of test samples' antioxidant potential in terms of secondary oxidation products, primary oxidation products, and oxygen consumption kinetics [63]. Because the radical is stable and does not need to be generated as in other scavenging assays, the DPPH method is the most valid, easy, accurate, sensitive, and cost-effective method for evaluating the scavenging activity of antioxidants in fruits, vegetables, juices, extracts, and extract-mediated nanomaterials [62]. The results are very repeatable and comparable to ABTS, TAC, ORAC, and FRAC, as well as other scavenging methods. Another strategy, which considers the antioxidant concentration and reaction time to reach the scavenging reaction plateau, has been found to be superior to other methods (considering only antioxidant concentration) [63].

For these assays, five separate concentrations, i.e., 200, 100, 50, 25, and 12.5 μg/mL, were used and the results demonstrated that antioxidant potential of the ZnO-NPs was highly significantly upregulated shown in Table 2. Since aqueous extracts of *A. pubiflora* are available in this sample, it may be concluded that some of the phenolic compounds involved in capping of ZnO-NPs can quench the reactive oxygen species by acting as reducing/oxidizing agents. The test material's total antioxidant potential (TAC) is predicated on its conversion from Mo (VI) to Mo (V), and the greenish Mo (V)-phosphate complex had the fastest absorption at 695 nm. TAC assay reveals the quenching ability of the measured material compared to ROS species [64]. At a higher concentration of 200 μg/mL ZnO-NP concentration, moderate (71.66 ± 1.14) TAC activity was observed while at lower concentration of NPs (12.5 μg/mL) TAC activity was further decreased as 26.78 ± 1.22. The antioxidant potential of ZnO-

TABLE 2: Antioxidant potential of *A. pubiflora*-synthesized ZnO-NPs.

Conc. (μg/mL)	TAC (μg AAE/mg)	TRP (μg AAE/mg)	ABTS (TEAC)	DPPH (% FRSA)	Ascorbic acid
200	71.66 ± 1.14**	111.32 ± 1.24**	178.45 ± 2.64*	23.5 ± 1.38***	210.29 ± 4.72
100	53.71 ± 1.32**	86.71 ± 0.98**	124.32 ± 1.99*	18.11 ± 1.2***	186.31 ± 4.19
50	42.43 ± 0.84**	54.23 ± 0.92**	92.63 ± 2.25*	13.32 ± 1.74***	132.20 ± 4.03
25	31.72 ± 0.71**	32.87 ± 0.95**	68.54 ± 2.21*	7.0 ± 0.97***	119.18 ± 2.83
12.5	26.78 ± 1.22*	19.23 ± 1.13**	45.73 ± 1.91*	6.37 ± 1.82***	84.71 ± 2.51

NPs was further determined by engineered power reduction test (TRP). Redox-possessing agent can neutralize and absorb free radicals by transferring the ion from $Fe^{+}3$ to $Fe^{+}2$. ZnO-NPs with reducing strength are capable to reduce ferrous ions from ferric ions [65]. Reductants have the ability to reduce free radicals by splitting their chains and donating a hydrogen atom, and this reduction capacity is linked to antioxidant capacity [66].

TRP experiment indicated the maximum antioxidant potential ($111.32 \pm 1.24\,\mu$g AAE/mg) for the $200\,\mu$g/mL ZnO-NP tested concentration in terms of ascorbic acid equivalents in antioxidant activities. However, from overall antioxidant assays performed (TRP, TAC, DPPH, and ABTS) using different concentrations of ZnO-NPs, the highest antioxidant activity was noted for ABTS assay (178.45 ± 2.64) at $200\,\mu$g/mL ZnO-NP tested concentration. The reducing strength of the ZnO-NPs in the performed assays (TRP, TAC, DPPH, and ABTS) was shown to be gradually decreased with the decrease of tested concentrations of NPs. The highest reduction capacity for TRP assay was revealed at $200\,\mu$g/mL ZnO-NP concentration as $111.3 \pm 2.44\,\mu$g AAE/mg, and the least reduction potential was noted at $12.5\,\mu$g/mL as $19.11 \pm 2.6\,\mu$g AAE/mg. Both spectrophotometric approaches, DPPH free radical scavenging and ABTS assays, are based on the quenching of stable-colored DPPH and ABTS radicals, indicating the ability to scavenge of antioxidants [67]. At a concentration of $200\,\mu$g/mL ZnO-NPs, medium (23.5 ± 2.4) DPPH radical scavenging activity was observed while low radical scavenging potential (6.37 ± 1.82) was observed at $12.5\,\mu$g/mL. Similarly, the highest ABTS activity (178.45 ± 2.64) was recorded at $200\,\mu$g/mL ZnO-NP concentration and the lowest (45.73 ± 1.91) at $12.5\,\mu$g/mL. Some of the antioxidant chemicals involved in the reduction and stabilization of ZnO-NPs throughout the manufacturing process could also be responsible for imparting antioxidant capabilities to ZnO-NPs, according to the findings.

***Highly significant, **slightly significant, and *nonsignificant difference from control at $P < 0.05$ by one-way ANOVA in the column. Values are mean ± SD of triplicate.

3.5. In Vitro Anti-Alzheimer's Activity.
Alzheimer's disease (AD) is a chronic neurological disease that accounts for 60% to 80% of dementia cases worldwide. The condition is characterized by a gradual decline in cognitive functions such as memory, executive and visual spatial functioning, personality, and vocabulary. In the United States alone, one person develops Alzheimer's disease every 65 seconds, which is

alarming [68]. Cholinesterase inhibitors are new AD medicines accessible for people with any stage of the disease. For the successful inhibition of cholinesterase enzymes, a variety of synthetic and natural substances have been described. In tissue synapses or neuromuscular junctions, the enzymes catalyze the hydrolysis of acetyl choline (a neurotransmitter) into choline and acetic acid. Nanotechnology, a diverse field, is a potential hotspot for identifying various therapeutic strategies, including drug delivery across the blood-brain barrier in Alzheimer's disease. Efficient disintegration of mature fibrils and remarkable inhibition of the β-amyloid fibrillation mechanism have been suggested by *Terminalia arjuna*-dependent gold nanoparticles. In addition, gold nanoparticles have also been reported to be successful in inhibiting cholinesterase enzymes, suggesting that gold nanoparticles are neuroprotective [69]. Trehalose-functionalized gold nanoparticles disintegrate matured fibrils and inhibit protein aggregation [70]. *Bacopa monnieri*-based platinum nanoparticles commendably eradicate reactive oxygen species which tends to drop the ROS level in Parkinson disorder [71]. Selenium and other metal oxide nanoparticles are also used effectively for AD on *in vivo* and *in vitro* basis [72]. The decrease in acetyl choline levels leads to the development of Alzheimer's disease. The inhibitory reaction of two cholinesterase enzymes, butyrylcholinesterase (BChE) and acetylcholinesterase (AChE), was investigated using different biogenic ZnO-NP concentrations (AChE) [73]. The inhibitory response for both esterases was dose dependent, which was surprising. The most active concentration of ZnO-NPs was $200\,\mu$g/mL, which inhibited AChE by 64.76 ± 1.69 and BChE by 67.49 ± 0.60. At $12.5\,\mu$g/mL ZnO-NP concentration, the inhibitory response was 35.76 ± 1.01 for AChE and 27.51 ± 0.84 for BChE, respectively. Furthermore, no significant difference in percent inhibition was recorded against both enzymes at $25\,\mu$g/mL and $50\,\mu$g/mL concentrations of ZnO-NPs, with inhibition responses of 38.02 ± 1.03 at $25\,\mu$g/mL and 40.02 ± 0.09 at $50\,\mu$g/mL for AChE and 29.01 ± 0.94 at $25\,\mu$g/mL and 30.01 ± 0.08 at $50\,\mu$g/mL for BChE, respectively. Overall, ZnO-NPs were found to be highly active against both enzymes as indicated by their IC_{50} values of $102\,\mu$g/mL and $125\,\mu$g/mL for AChE and BChE. Overall results exhibited that biosynthesized ZnO-NPs have efficient anti-Alzheimer's activity and as shown by significant % inhibition at $200\,\mu$g/mL concentration, against both enzymes, respective to control as shown in Table 3. The results of the present study exhibited that *A. pubiflora*-mediated ZnO-NPs have effective anti-Alzheimer's activity when applied in high concentrations,

Table 3: Acetylcholinesterase (AChE) and butyrylcholinesterase (BChE) inhibition by ZnO-NPs at different concentrations.

Enzymes	Concentrations (μg/mL)				
	12.5	25	50	100	200
AChE	$35.76 \pm 1.01^{*}$	$37.54 \pm 0.54^{**}$	$40.89 \pm 0.63^{**}$	$52.44 \pm 0.69^{**}$	$64.76 \pm 1.69^{*}$
BChE	$27.51 \pm 0.84^{**}$	$27.69 \pm 0.59^{**}$	$36.81 \pm 1.06^{*}$	$49.73 \pm 1.19^{**}$	$67.49 \pm 0.60^{*}$
+ Control	52.41 ± 2.19	58.72 ± 2.11	62.79 ± 2.44	81.83 ± 2.68	86.20 ± 2.91

as shown by >65% inhibition against both enzymes. A previous study by Khalil et al. (2019) showed inhibition of several metallic NPs against AChE and BChE enzymes. Concentrations of biogenic metal oxide nanoparticles ranging from 1000 mg/mL to 62.5 mg/mL were examined. Surprisingly, both enzymes' responses to inhibition were found to be dose dependent. At 1000 mg/mL, biogenic lead oxide (PbO) nanoparticles were one of the most active samples, suppressing cholinesterases by 71% (AChE) and 67% (BChE). This was followed by cobalt oxide nanoparticles, which suppressed AChE and BChE by 70% and 68%, respectively. With IC_{50} values of 160.81 mg/mL and 261.67 mg/mL for AChE and BChE, respectively, biogenic iron oxide nanoparticles were the least effective [73].

***Highly significant, **slightly significant, and *nonsignificant difference from control at $P < 0.05$ by one-way ANOVA in the column. Values are mean $\pm$ SD of triplicate.

3.6. In Vitro Anti-Inflammatory Activity. Inflammation is an automated response exhibited by the body's immune system, against various bacteria, irritants, damaged cells, and adverse stimuli. Anti-inflammatory activities have been documented both *in vivo* and *in vitro* for different metallic NPs and for many secondary metabolites. ZnO-NP HPLC analysis shows good capping of flavonoids such as orientin, isoorientin, vitexin, and isovitexin. These flavonoids can exert anti-inflammatory stress in numerous ways, such as cyclooxygenase inhibition with often selective activity on COX-1 vs. COX-2, phospholipase A2, and lipoxygenases (enzymes developing eicosanoids), thus reducing the concentration of leukotrienes and prostanoids that plays a main role in developing inflammation [74]. In certain types of inflammatory disorders, existing therapies are currently ineffective to treat and mitigate the progression of the condition or even to eradicate the signs and symptoms of inflammation [75]. For example, we know that NPs have an exceptional capacity to penetrate the microbial membrane, so this issue can be solved by increasing drug penetration into the active site of microbial infection. The aim of recent science for developing NPs is to avoid and manage inflammatory and contaminated sites for identification [76–78]. So, to check the anti-inflammatory potential of *A. pubiflora*-mediated ZnO-NPs, various *in vitro* pathways such as COX-1, COX-2, sPLA2, and 15-LOX inhibitions were tested. All the pathways produced the most productive outcomes for the inhibitory activity of all experiments conducted. sPLA2 was found to have the highest inhibitory activity (32.90 ± 0.99%), followed by 15-LOX (24.57 ± 0.79%), COX-1 (18.41 ± 0.54%), and COX-2 (18.23 ± 0.57%), respectively, as shown in Figure 1(a). Overall results described that *A. pubiflora*-mediated ZnO-NPs

have showed efficient inhibition of two enzymes, sPLA2 and 15-LOX, of inflammatory processes.

3.7. In Vitro Antiaging Activity. This assay comprised a screening of *A. pubiflora*-mediated ZnO-NPs for anti-aging potential. A test sample (ZnO-NPs) at a fixed concentration of 200μg/mL was utilized to assess their in vitro potential to inhibit enzymes such as tyrosinase, elastase, collagenase, hyaluronidase, and AGEs. Collagenase, hyaluronidase, and elastase-like enzymes are responsible for the destruction of extracellular matrix components in enzymes. Deep wrinkles, skin tonus, and skin resilience losses are all caused by these enzymes [79–81]. Tyrosinase disorders are caused by the phenomenon of aging and are the main causative agents of malignant melanoma and freckles or melasma, such as pigment disorders [82]. Advanced glycation end products (AGEs) have been linked to aging and age-related disorders as a result of oxidative stress [83, 84]. Certain compounds that can deter these enzymatic processes or pathways are desirable and useful in cosmetic industries. According to several studies, SIRT-1 (a class III deacetylase) and radical aging theory have emerged as potent survival and oxidative stress management agents [85, 86]. In our recent study, ZnO-NPs produced with some phytochemicals have shown that these NPs are capable of being used as antiaging agents. Significant inhibitory activities of ZnO-NPs against pentosidine AGEs (up to 44.63 ± 1.26%) have been observed, followed by vesperlysine AGEs (up to 37.13 ± 1.99%). For collagenase (17.83 ± 0.81%) and tyrosinase (14.56 ± 0.89%), ZnO-NPs had intermediate inhibitory effect. The lowest observed pronounced inhibitory effects observed for elastase and hyaluronidase were 7.51 ± 0.31 and 8.73 ± 0.37, respectively, shown in Figure 1(b). It has been explained from the above findings that ZnO-NPs have a good inhibitory capacity against two enzymes, AGEs of pentosidine and vesperlysine. Previous research has shown that ZnO may absorb UV radiation and protect the skin from additional damage, making it a potential antiaging agent. When coupled with TiO_2, ZnO-NPs and green tea polyphenols show synergistic photoprotective effects on the skin, significantly reducing erythema [87]. ZnO is claimed to be an antiaging element in cosmetics and sunscreens since it is an active UVA/UVB-reflecting sunscreen ingredient that provides UVB protection of 75%. The anti-aging potential of ZnO-NPs and TiO_2-NPs in sunscreens is owing to their capacity to form complexes with proteins and cause the creation of free radicals, hence triggering ROS and inhibiting many proteins involved in aging [88].

3.8. Anticancer Activity against the HepG2 Cell Line. Plant-derived compounds are a promising treatment option for

(a)

(b)
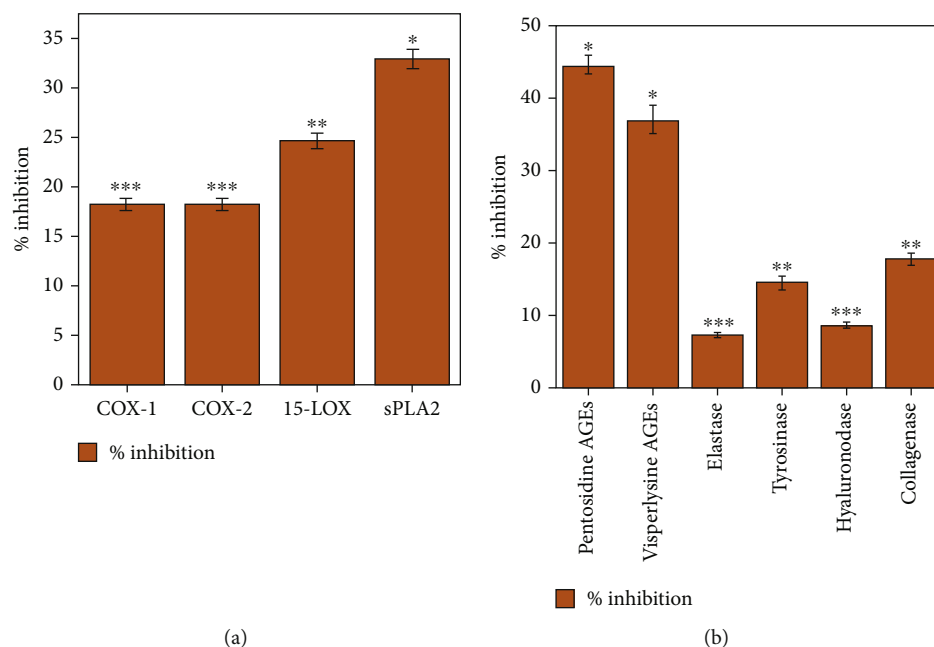
FIGURE 1: (a) Anti-inflammatory potential of synthesized ZnO-NPs with respect to their control value (68.39 ± 3.17). (b) Antiaging potential of ZnO-NPs with respect to their control value (74.83 ± 3.92). ***Highly significant, **slightly significant, and *nonsignificant difference from control at $P < 0.05$ by one-way ANOVA in the column. Values are mean ± SD of triplicate.

(a)

(b)
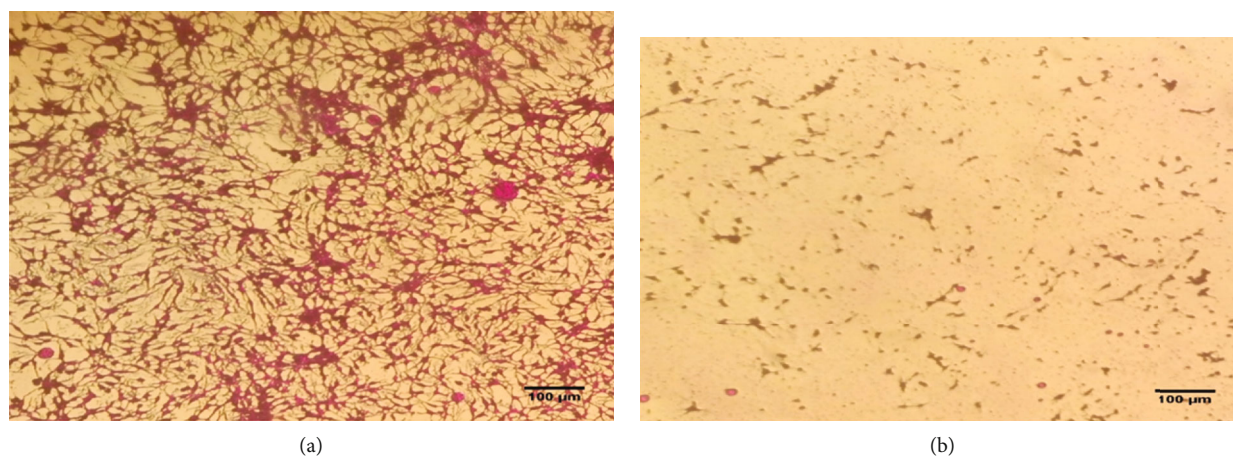
FIGURE 2: (a) Characteristic pictures of nontreated cells. (b) ZnO-NP-treated cells.

hepatocellular carcinoma [89]. In our research, FTIR and HPLC analyses reported the presence of alcohols, phenolic groups, and C-N stretching vibrations of aromatic amines of biomolecules, on the surface of synthesized ZnO-NPs; these groups are considered physiologically significant towards treatment of various pathogenic diseases including cancer [90]. A scientific hotspot for cancer therapy is provided by the toxic nature of NPs, having effective anti-cancer potential [55, 90]. In this study, the cytotoxicity of ZnO-NPs against human hepatocytes (HepG2 cell line) has been examined. HepG2 cells showed reduced cell viability of 23.68 ± 2.1% after 24 h ZnO-NP treatment, as compared to respective controls as shown in Figure 2. Moreover, the phase-contrast microscopic images of HepG2 cells treated with ZnO-NPs showed prominent apoptosis of cells after

for 24 h treatment. These results indicated the highly toxic effect of ZnO-NPs against human hepatocytes, as shown in Table 4. The three primary mechanisms responsible for the cytotoxic effect of ZnO-NPs include the breakdown of ZnO-NPs into Zn^{+2}, reactive oxygen species (ROS) formation, and DNA damage [91–93]. Moreover, physical properties such as size, surface chemistry, and dose dictate the overall uptake, elimination, and antitumor properties of the ZnO-NPs [93]. Various studies have showed the anticancer and antiproliferative effect of ZnO-NPs, via upregulating the tumor suppressor genes and apoptotic genes, downregulating the antiapoptotic genes, inducing DNA fragmentation, ROS production, and caspase-3 enzyme in HepG2 cells [94–96]. Our results are also consistent with these previously published studies regarding anticancer potential of

TABLE 4: Anticancer potential of ZnO-NPs and plant extract toward the HepG2 cell line.

Test sample	% inhibition	% viability
ZnO-NPs	76.32 ± 1.69	23.68 ± 2.1
NTC	100 ± 2.27	0.00
Doxorubicin	97.35 ± 2.84	2.65
Aquilegia pubiflora extract	24.52 ± 0.49	75.48 ± 1.81
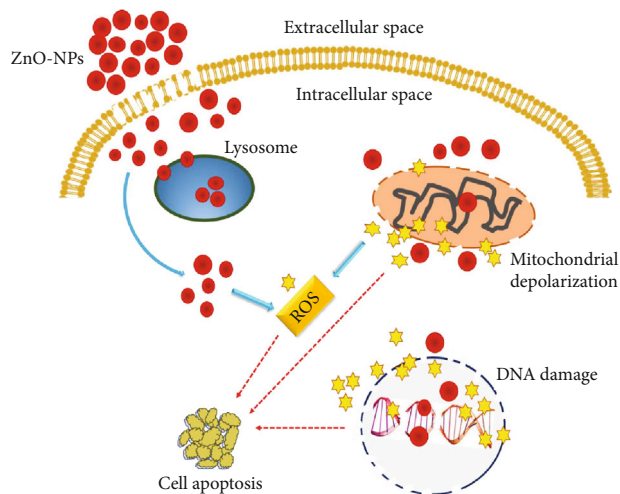
FIGURE 3: The proposed mechanism of ZnO-NP-mediated cytotoxicity in cancerous cell. NP accumulation and dissolution on the plasma membrane further lead toward lysosome and exert oxidative stress causing generation of ROS. Active ROS causes mitochondrial depolarization and DNA damages finally resulting in cell apoptosis.

Au-NPs against HepG2 cells. Plant-derived Au-NPs typically cause cellular death by causing reactive oxygen species (ROS). ROS disrupts signal transduction pathways while also increasing cellular death [97, 98]. The CeO_2-NP antiproliferative activities were also shown to successfully reduce the viability of the HepG2 cell line, with inhibition of 26.78%. The positive control doxorubicin and the negative control DMSO inhibited the HepG2 cells by 94.24% and 4.24%, respectively, as compared to the CeO_2-NPs [46]. Hence, the marked anti-tumor activity against HepG2 cells showed an exciting potential of biosynthesized ZnO-NPs as promising anti-cancer agents. Figure 3 shows the proposed mechanism of ZnO-NP-mediated cytotoxicity in cancerous cell; when ZnO-NPs get entry into the cancerous cell, they produced ROS species, disturbed mitochondrial membrane depolarization, and damaged DNA; all these events eventually leads to apoptosis or death of cancer cell.

Values are mean ± SD of triplicate.

4. Conclusion

This research work is the ongoing portion of the previously biosynthesized ZnO-NPs using aqueous extract of *Aquilegia pubiflora*, a well-known plant for its medicinal importance. The crystalline structure of the synthesized NPs has been confirmed by XRD analysis. The presence of phytochemicals in converting metallic ions to nanoparticles was investigated by FTIR and HPLC testing. SEM and Raman spectra determined morphology and vibrational modes, while apparent charge and steadiness were determined by DLS. The produced ZnO-NPs have shown good antioxidant and anti-Alzheimer capabilities. ZnO-NPs have also revealed a moderate inhibitory ability against alpha-amylase and alpha-glucosidase enzymes. Biosynthesized ZnO-NPs have shown an effective anti-Alzheimer's activity at a higher concentration and showed >65% inhibition against both AChE and BChE enzymes. It has been observed that biogenic ZnO-NPs are highly toxic to HepG2 cell lines as indicated by reduced cell viability of the HepG2 cell line after contact to ZnO-NPs. Moreover, ZnO-NPs have a good anti-aging property as demonstrated by their inhibitory capacity against two enzymes, AGEs of pentosidine and vesperlysine. Furthermore, *A. pubiflora*-mediated ZnO-NPs have showed efficient anti-inflammatory capacity as depicted by inhibition of sPLA2 and 15-LOX enzymes responsible for inducing inflammation. Our results concluded that the abovementioned ZnO-NPs could be considered for application in cosmetics, owing to their good anti-aging effect, and in treatment of various diseases including cancer, diabetes, Alzheimer's, and other inflammatory diseases, owing to their strong anti-cancer potential and efficient antioxidant properties. To explore its biomedical capabilities at both *in vitro* and *in vivo* levels, further research on ZnO-NPs is required.

Data Availability

The datasets used and analyzed during the current research work is available from the corresponding author on reasonable request.

Conflicts of Interest

All authors declare no competing interests.

Authors' Contributions

HJ conceptualized, designed, and performed the experiments. HJ wrote the manuscript. MS, AA, and SF provided reagents and analytical tools. AK, MR, and SD analyzed the data. CH and BHA supervised the research work. All authors read and approved the manuscript.

Supplementary Materials

We have provided supplementary material in a separate file. That file includes Figures 1S, 2S, 3S, and 4S as supplementary figures cited from our previous published article. *(Supplementary Materials)*

References

[1] C. Huang, A. Notten, and N. Rasters, "Nanoscience and technology publications and patents: a review of social science studies and search strategies," *The Journal of Technology Transfer*, vol. 36, no. 2, pp. 145–172, 2011.

[2] K. N. Thakkar, S. S. Mhatre, and R. Y. Parikh, "Biological synthesis of metallic nanoparticles," *Nanomedicine: Nanotechnology, Biology and Medicine*, vol. 6, no. 2, pp. 257–262, 2010.

[3] A. Fouda, G. Abdel-Maksoud, M. A. Abdel-Rahman, S. S. Salem, S. E. D. Hassan, and M. A. H. el-Sadany, "Eco-friendly approach utilizing green synthesized nanoparticles for paper conservation against microbes involved in biodeterioration of archaeological manuscript," *International Biodeterioration & Biodegradation*, vol. 142, pp. 160–169, 2019.

[4] S. M. Alsharif, S. S. Salem, M. A. Abdel-Rahman et al., "Multi-functional properties of spherical silver nanoparticles fabricated by different microbial taxa," *Heliyon*, vol. 6, no. 5, article e03943, 2020.

[5] M. S. Aref and S. S. Salem, "Bio-callus synthesis of silver nanoparticles, characterization, and antibacterial activities via _Cinnamomum camphora_ callus culture," *Biocatalysis and Agricultural Biotechnology*, vol. 27, article 101689, 2020.

[6] V. Kumar and S. K. Yadav, "Plant-mediated synthesis of silver and gold nanoparticles and their applications," *Journal of Chemical Technology & Biotechnology*, vol. 84, no. 2, pp. 151–157, 2009.

[7] S. Faisal, H. Jan, S. A. Shah et al., "Green synthesis of zinc oxide (ZnO) nanoparticles using aqueous fruit extracts ofMyristica fragrans: their characterizations and biological and environmental applications," *ACS Omega*, vol. 6, no. 14, pp. 9709–9722, 2021.

[8] M. Herlekar, S. Barve, and R. Kumar, "Plant-mediated green synthesis of iron nanoparticles," *Journal of Nanoparticles*, vol. 2014, 9 pages, 2014.

[9] F. Simonis and S. Schilthuizen, *Nanotechnology; Innovation Opportunities for Tomorrow's Defence*, Report TNO Science & Industry Future Technology Center, the Netherlands, 2006.

[10] S. S. Salem, E. F. el-Belely, G. Niedbała et al., "Bactericidal and in-vitro cytotoxic efficacy of silver nanoparticles (Ag-NPs) fabricated by endophytic actinomycetes and their use as coating for the textile fabrics," *Nanomaterials*, vol. 10, no. 10, p. 2082, 2020.

[11] A. Waris, M. Din, A. Ali et al., "A comprehensive review of green synthesis of copper oxide nanoparticles and their diverse biomedical applications," *Inorganic Chemistry Communications*, vol. 123, article 108369, 2021.

[12] H. Kumar, K. Bhardwaj, K. Kuča et al., "Flower-based green synthesis of metallic nanoparticles: applications beyond fragrance," *Nanomaterials*, vol. 10, no. 4, p. 766, 2020.

[13] G. M. F. Calixto, J. Bernegossi, L. de Freitas, C. Fontana, and M. Chorilli, "Nanotechnology-based drug delivery systems for photodynamic therapy of cancer: a review," *Molecules*, vol. 21, no. 3, p. 342, 2016.

[14] L. Al-Naamani, S. Dobretsov, and J. Dutta, "Chitosan-zinc oxide nanoparticle composite coating for active food packaging applications," *Innovative Food Science & Emerging Technologies*, vol. 38, pp. 231–237, 2016.

[15] B. R. Sankapal, H. B. Gajare, S. S. Karade, R. R. Salunkhe, and D. P. Dubal, "Zinc oxide encapsulated carbon nanotube thin films for energy storage applications," *Electrochimica Acta*, vol. 192, pp. 377–384, 2016.

[16] R. Kumar, O. al-Dossary, G. Kumar, and A. Umar, "Zinc oxide nanostructures for NO_2 gas–sensor applications: a review," *Nano-Micro Letters*, vol. 7, no. 2, pp. 97–120, 2015.

[17] P. K. Mishra, H. Mishra, A. Ekielski, S. Talegaonkar, and B. Vaidya, "Zinc oxide nanoparticles: a promising nanomaterial for biomedical applications," *Drug Discovery Today*, vol. 22, no. 12, pp. 1825–1834, 2017.

[18] M. D. Newman, M. Stotland, and J. I. Ellis, "The safety of nanosized particles in titanium dioxide- and zinc oxide-based sunscreens," *Journal of the American Academy of Dermatology*, vol. 61, no. 4, pp. 685–692, 2009.

[19] M. Abedini, F. Shariatmadari, M. A. Karimi Torshizi, and H. Ahmadi, "Effects of zinc oxide nanoparticles on the egg quality, immune response, zinc retention, and blood parameters of laying hens in the late phase of production," *Journal of Animal Physiology and Animal Nutrition*, vol. 102, no. 3, pp. 736–745, 2018.

[20] H. Agarwal, S. Venkat Kumar, and S. Rajeshkumar, "A review on green synthesis of zinc oxide nanoparticles - An eco-friendly approach," *Resource-Efficient Technologies*, vol. 3, no. 4, pp. 406–413, 2017.

[21] M. Heinlaan, A. Ivask, I. Blinova, H. C. Dubourguier, and A. Kahru, "Toxicity of nanosized and bulk ZnO, CuO and TiO_2 to bacteria _Vibrio fischeri and crustaceans Daphnia magna and Thamnocephalus platyurus_," *Chemosphere*, vol. 71, no. 7, pp. 1308–1316, 2008.

[22] U. Dhar and S. Samant, "Endemic plant diversity in the Indian Himalaya I. Ranunculaceae and Paeoniaceae," *Journal of Biogeography*, vol. 20, no. 6, pp. 659–668, 1993.

[23] A. Hazrat, M. O. Nisar, J. Shah, and S. H. Ahmad, "Ethnobotanical study of some elite plants belonging to Dir, Kohistan valley, Khyber Pukhtunkhwa, Pakistan," *Pakistan Journal of Botany*, vol. 43, no. 2, pp. 787–795, 2011.

[24] N. Aziz, M. N. Khan, F. Ul Haq et al., "Erythroid induction activity of_Aquilegia fragrans_and_Aquilegia pubiflora_and identification of compounds using liquid chromatography-tandem mass spectrometry," *Journal of King Saud University-Science*, vol. 33, no. 1, article 101227, 2021.

[25] H. Jan, H. Usman, M. Shah et al., "Phytochemical analysis and versatile In Vitro evaluation of antimicrobial, cytotoxic and enzyme inhibition potential of different extracts of traditionally used Aquilegia pubiflora Wall. Ex Royle," *BMC Complementary Medicine and Therapies*, vol. 21, no. 1, article 165, 2021.

[26] S. Faisal, Abdullah, H. Jan et al., "Bio-catalytic activity of novel Mentha arvensis intervened biocompatible magnesium oxide nanomaterials," *Catalysts*, vol. 11, no. 7, p. 780, 2021.

[27] H. Jan, M. Shah, H. Usman et al., "Biogenic synthesis and characterization of antimicrobial and anti-parasitic zinc oxide (ZnO) nanoparticles using aqueous extracts of the Himalayan columbine (Aquilegia pubiflora)," *Frontiers in Materials*, vol. 7, p. 249, 2020.

[28] F. Thema, E. Manikandan, M. S. Dhlamini, and M. Maaza, "Green synthesis of ZnO nanoparticles via Agathosma betulina natural extract," *Materials Letters*, vol. 161, pp. 124–127, 2015.

[29] T. Zohra, M. Ovais, A. T. Khalil, M. Qasim, M. Ayaz, and Z. K. Shinwari, "Extraction optimization, total phenolic, flavonoid contents, HPLC-DAD analysis and diverse pharmacological evaluations ofDysphania ambrosioides(L.) Mosyakin & Clemants," *Natural Product Research*, vol. 33, no. 1, pp. 136–142, 2019.

[30] R. G. Saratale, H. S. Shin, G. Kumar, G. Benelli, D. S. Kim, and G. D. Saratale, "Exploiting antidiabetic activity of silver nanoparticles synthesized usingPunica granatumleaves and anticancer potential against human liver cancer cells (HepG2),"

Artificial Cells, Nanomedicine, and Biotechnology, vol. 46, no. 1, pp. 211–222, 2018.

[31] H. Usman, M. A. Ullah, H. Jan et al., "Interactive effects of wide-spectrum monochromatic lights on phytochemical production, antioxidant and biological activities of Solanum xanthocarpum callus cultures," *Molecules*, vol. 25, no. 9, p. 2201, 2020.

[32] M. Shah, S. Nawaz, H. Jan et al., "Synthesis of bio-mediated silver nanoparticles from Silybum marianum and their biological and clinical activities," *Materials Science and Engineering: C*, vol. 112, article 110889, 2020.

[33] S. Nazir, H. Jan, D. Tungmunnithum et al., "Callus culture of Thai basil is an effective biological system for the production of antioxidants," *Molecules*, vol. 25, no. 20, p. 4859, 2020.

[34] M. Ahmed, M. Adil, I. U. Haq, M. K. Tipu, M. Qasim, and B. Gul, "RP-HPLC-based phytochemical analysis and diverse pharmacological evaluation ofQuercus floribundaLindl. ex A. Camus nuts extracts," *Natural Product Research*, vol. 35, no. 13, pp. 2257–2262, 2021.

[35] M. Shah, H. Jan, S. Drouet et al., "Chitosan elicitation impacts flavonolignan biosynthesis in Silybum marianum (L.) Gaertn cell suspension and enhances antioxidant and anti-inflammatory activities of cell extracts," *Molecules*, vol. 26, no. 4, p. 791, 2021.

[36] S. Faisal, M. A. Khan, H. Jan et al., "Edible mushroom (Flammulina velutipes) as biosource for silver nanoparticles: from synthesis to diverse biomedical and environmental applications," *Nanotechnology*, vol. 32, no. 6, article 065101, 2021.

[37] G. L. Ellman, K. D. Courtney, V. Andres jr., and R. M. Featherstone, "A new and rapid colorimetric determination of acetylcholinesterase activity," *Biochemical Pharmacology*, vol. 7, no. 2, pp. 88–95, 1961.

[38] M. Imran, H. Jan, S. Faisal et al., "In vitro examination of antiparasitic, anti-Alzheimer, insecticidal and cytotoxic potential of Ajuga bracteosa Wallich leaves extracts," *Saudi Journal of Biological Sciences*, vol. 28, no. 5, pp. 3031–3036, 2021.

[39] N. Kaewseejan and S. Siriamornpun, "Bioactive components and properties of ethanolic extract and its fractions from Gynura procumbens leaves," *Industrial Crops and Products*, vol. 74, pp. 271–278, 2015.

[40] W.-M. Chai, Q. Huang, M. Z. Lin et al., "Condensed tannins from longan bark as inhibitor of tyrosinase: structure, activity, and mechanism," *Journal of Agricultural and Food Chemistry*, vol. 66, no. 4, pp. 908–917, 2018.

[41] J. Wittenauer, S. Mäckle, D. Sußmann, U. Schweiggert-Weisz, and R. Carle, "Inhibitory effects of polyphenols from grape pomace extract on collagenase and elastase activity," *Fitoterapia*, vol. 101, pp. 179–187, 2015.

[42] P. Kolakul and B. Sripanidkulchai, "Phytochemicals and antiaging potentials of the extracts from Lagerstroemia speciosa and Lagerstroemia floribunda," *Industrial Crops and Products*, vol. 109, pp. 707–716, 2017.

[43] S. Mushtaq, M. A. Aga, P. H. Qazi et al., "Isolation, characterization and HPLC quantification of compounds from Aquilegia fragrans Benth: Their in vitro antibacterial activities against bovine mastitis pathogens," *Journal of Ethnopharmacology*, vol. 178, pp. 9–12, 2016.

[44] M. Naveed, V. Hejazi, M. Abbas et al., "Chlorogenic acid (CGA): a pharmacological review and call for further research," *Biomedicine & Pharmacotherapy*, vol. 97, pp. 67–74, 2018.

[45] K. Y. Lam, A. P. K. Ling, R. Y. Koh, Y. P. Wong, and Y. H. Say, "A review on medicinal properties of orientin," *Advances in Pharmacological Sciences*, vol. 2016, 9 pages, 2016.

[46] H. Jan, M. A. Khan, H. Usman et al., "TheAquilegia pubiflora(Himalayan columbine) mediated synthesis of nanoceria for diverse biomedical applications," *RSC Advances*, vol. 10, no. 33, pp. 19219–19231, 2020.

[47] N. Matinise, X. G. Fuku, K. Kaviyarasu, N. Mayedwa, and M. Maaza, "ZnO nanoparticles via Moringa oleifera green synthesis: Physical properties & mechanism of formation," *Applied Surface Science*, vol. 406, pp. 339–347, 2017.

[48] S. Vijayakumar, B. Vaseeharan, B. Malaikozhundan, and M. Shobiya, "Laurus nobilis leaf extract mediated green synthesis of ZnO nanoparticles: Characterization and biomedical applications," *Biomedicine & Pharmacotherapy*, vol. 84, pp. 1213–1222, 2016.

[49] G. Sangeetha, S. Rajeshwari, and R. Venckatesh, "Green synthesis of zinc oxide nanoparticles by aloe barbadensis miller leaf extract: Structure and optical properties," *Materials Research Bulletin*, vol. 46, no. 12, pp. 2560–2566, 2011.

[50] J. Huang, Q. Li, D. Sun et al., "Biosynthesis of silver and gold nanoparticles by novel sundried Cinnamomum camphora leaf," *Nanotechnology*, vol. 18, no. 10, article 105104, 2007.

[51] U. Vijayalakshmi, M. Chellappa, U. Anjaneyulu, G. Manivasagam, and S. Sethu, "Influence of coating parameter and sintering atmosphere on the corrosion resistance behavior of electrophoretically deposited composite coatings," *Materials and Manufacturing Processes*, vol. 31, no. 1, pp. 95–106, 2016.

[52] S. A. Khan, F. Noreen, S. Kanwal, A. Iqbal, and G. Hussain, "Green synthesis of ZnO and Cu-doped ZnO nanoparticles from leaf extracts of Abutilon indicum, Clerodendrum infortunatum, Clerodendrum inerme and investigation of their biological and photocatalytic activities," *Materials Science and Engineering: C*, vol. 82, pp. 46–59, 2018.

[53] D. Suresh, P. C. Nethravathi, Udayabhanu, H. Rajanaika, H. Nagabhushana, and S. C. Sharma, "Green synthesis of multifunctional zinc oxide (ZnO) nanoparticles using Cassia fistula plant extract and their photodegradative, antioxidant and antibacterial activities," *Materials Science in Semiconductor Processing*, vol. 31, pp. 446–454, 2015.

[54] R. H. Fang, A. V. Kroll, W. Gao, and L. Zhang, "Cell membrane coating nanotechnology," *Advanced Materials*, vol. 30, no. 23, article 1706759, 2018.

[55] K. Vimala, S. Sundarraj, M. Paulpandi, S. Vengatesan, and S. Kannan, "Green synthesized doxorubicin loaded zinc oxide nanoparticles regulates the Bax and Bcl-2 expression in breast and colon carcinoma," *Process Biochemistry*, vol. 49, no. 1, pp. 160–172, 2014.

[56] D. Raoufi, "Synthesis and microstructural properties of ZnO nanoparticles prepared by precipitation method," *Renewable Energy*, vol. 50, pp. 932–937, 2013.

[57] P. Uthirakumar and C.-H. Hong, "Effect of annealing temperature and pH on morphology and optical property of highly dispersible ZnO nanoparticles," *Materials Characterization*, vol. 60, no. 11, pp. 1305–1310, 2009.

[58] A. Diallo, B. D. Ngom, E. Park, and M. Maaza, "Green synthesis of ZnO nanoparticles by Aspalathus linearis: Structural & optical properties," *Journal of Alloys and Compounds*, vol. 646, pp. 425–430, 2015.

[59] S. S. Nair, V. Kavrekar, and A. Mishra, "In vitro studies on alpha amylase and alpha glucosidase inhibitory activities of

selected plant extracts," *European Journal of Experimental Biology*, vol. 3, no. 1, pp. 128–132, 2013.

[60] S. B. Aynalem and A. J. Zeleke, "Prevalence of diabetes mellitus and its risk factors among individuals aged 15 years and above in Mizan-Aman town, Southwest Ethiopia, 2016: a cross sectional study," *International Journal of Endocrinology*, vol. 2018, 7 pages, 2018.

[61] A. Ali, S. Ambreen, R. Javed, S. Tabassum, I. ul Haq, and M. Zia, "ZnO nanostructure fabrication in different solvents transforms physio- chemical, biological and photodegradable properties," *Materials Science and Engineering: C*, vol. 74, pp. 137–145, 2017.

[62] R. Amorati and L. Valgimigli, "Advantages and limitations of common testing methods for antioxidants," *Free Radical Research*, vol. 49, no. 5, pp. 633–649, 2015.

[63] S. Singh and R. Singh, "In VitroMethods of assay of antioxidants: an overview," *Food Reviews International*, vol. 24, no. 4, pp. 392–415, 2008.

[64] S. Saleem, L. Jafri, I. . Haq et al., "Plants Fagonia cretica L. and Hedera nepalensis K. Koch contain natural compounds with potent dipeptidyl peptidase-4 (DPP-4) inhibitory activity," *Journal of Ethnopharmacology*, vol. 156, pp. 26–32, 2014.

[65] M.-Y. Shon, T.-H. Kim, and N.-J. Sung, "Antioxidants and free radical scavenging activity of Phellinus baumii (Phellinus of Hymenochaetaceae) extracts," *Food Chemistry*, vol. 82, no. 4, pp. 593–597, 2003.

[66] L. Moreira, L. G. Dias, J. A. Pereira, and L. Estevinho, "Antioxidant properties, total phenols and pollen analysis of propolis samples from Portugal," *Food and Chemical Toxicology*, vol. 46, no. 11, pp. 3482–3485, 2008.

[67] M. Zia-Ul-Haq, S. A. Shahid, S. Ahmad, M. Qayum, and I. Khan, "Antioxidant potential of various parts of Ferula assafoetida L," *Journal of Medicinal Plants Research*, vol. 6, no. 16, pp. 3254–3258, 2012.

[68] J. Weller and A. Budson, "Current understanding of Alzheimer's disease diagnosis and treatment," *F1000Research*, vol. 7, article 1161, 2018.

[69] N. Suganthy, V. Sri Ramkumar, A. Pugazhendhi, G. Benelli, and G. Archunan, "Biogenic synthesis of gold nanoparticles from Terminalia arjuna bark extract: assessment of safety aspects and neuroprotective potential via antioxidant, anticholinesterase, and antiamyloidogenic effects," *Environmental Science and Pollution Research*, vol. 25, no. 11, pp. 10418–10433, 2018.

[70] S. Mandal, K. Debnath, N. R. Jana, and N. R. Jana, "Trehalose-functionalized gold nanoparticle for inhibiting intracellular protein aggregation," *Langmuir*, vol. 33, no. 49, pp. 13996–14003, 2017.

[71] J. Nellore, C. Pauline, and K. Amarnath, "Bacopa monnieri Phytochemicals Mediated Synthesis of Platinum Nanoparticles and Its Neurorescue Effect on 1-Methyl 4-Phenyl 1,2,3,6 Tetrahydropyridine-Induced Experimental Parkinsonism in Zebrafish," *Journal of Neurodegenerative Diseases*, vol. 2013, Article ID 972391, 8 pages, 2013.

[72] M. Nazıroğlu, S. Muhamad, and L. Pecze, "Nanoparticles as potential clinical therapeutic agents in Alzheimer's disease: focus on selenium nanoparticles," *Expert Review of Clinical Pharmacology*, vol. 10, no. 7, pp. 773–782, 2017.

[73] A. T. Khalil, M. Ayaz, M. Ovais et al., "In vitro cholinesterase enzymes inhibitory potential and in silico molecular docking studies of biogenic metal oxides nanoparticles," *Inorganic and Nano-Metal Chemistry*, vol. 48, no. 9, pp. 441–448, 2018.

[74] P. Rathee, H. Chaudhary, S. Rathee, D. Rathee, V. Kumar, and K. Kohli, "Mechanism of action of flavonoids as antiinflammatory agents: a review," *Inflammation & Allergy-Drug Targets*, vol. 8, no. 3, pp. 229–235, 2009.

[75] H. E. Gendelman, V. Anantharam, T. Bronich et al., "Nanoneuromedicines for degenerative, inflammatory, and infectious nervous system diseases," *Nanomedicine: Nanotechnology, Biology and Medicine*, vol. 11, no. 3, pp. 751–767, 2015.

[76] K. Blecher, A. Nasir, and A. Friedman, "The growing role of nanotechnology in combating infectious disease," *Virulence*, vol. 2, no. 5, pp. 395–401, 2011.

[77] V. Wagner, A. Dullaart, A. K. Bock, and A. Zweck, "The emerging nanomedicine landscape," *Nature Biotechnology*, vol. 24, no. 10, pp. 1211–1217, 2006.

[78] J. McMillan, E. Batrakova, and H. E. Gendelman, *Cell delivery of therapeutic nanoparticles, in Progress in molecular biology and translational science*, Elsevier, 2011.

[79] D. O. Coricovac, C. O. Soica, D. A. Muntean, R. A. Popovici, C. A. Dehelean, and E. L. Hogea, "Assessment of the effects induced by two triterpenoids on liver mitochondria respiratory function isolated from aged rats," *Revista de Chimie*, vol. 66, pp. 1707–1710, 2015.

[80] G. D. Liyanaarachchi, J. K. R. R. Samarasekera, K. R. R. Mahanama, and K. D. P. Hemalal, "Tyrosinase, elastase, hyaluronidase, inhibitory and antioxidant activity of Sri Lankan medicinal plants for novel cosmeceuticals," *Industrial Crops and Products*, vol. 111, pp. 597–605, 2018.

[81] R. Boran, "Investigations of anti-aging potential of Hypericum origanifolium Willd. for skincare formulations," *Industrial Crops and Products*, vol. 118, pp. 290–295, 2018.

[82] S. Briganti, E. Camera, and M. Picardo, "Chemical and instrumental approaches to treat hyperpigmentation," *Pigment Cell Research*, vol. 16, no. 2, pp. 101–110, 2003.

[83] T. Finkel and N. J. Holbrook, "Oxidants, oxidative stress and the biology of ageing," *Nature*, vol. 408, no. 6809, pp. 239–247, 2000.

[84] P. Gkogkolou and M. Böhm, "Advanced glycation end products: key players in skin aging?," *Dermato-Endocrinology*, vol. 4, no. 3, pp. 259–270, 2012.

[85] D. Harraan, "Aging: A Theory Based on Free Radical and Radiation Chemistry," *Journal of Gerontology*, vol. 11, no. 3, pp. 298–300, 1956.

[86] Y. S. Hori, A. Kuno, R. Hosoda, and Y. Horio, "Regulation of FOXOs and p53 by SIRT1 modulators under oxidative stress," *PLoS One*, vol. 8, no. 9, article e73875, 2013.

[87] S. Shanbhag, A. Nayak, R. Narayan, and U. Y. Nayak, "Anti-aging and sunscreens: paradigm shift in cosmetics," *Advanced Pharmaceutical Bulletin*, vol. 9, no. 3, pp. 348–359, 2019.

[88] H. G. Breunig, M. Weinigel, and K. König, "In vivo imaging of ZnO nanoparticles from sunscreen on human skin with a mobile multiphoton tomograph," *Bionanoscience*, vol. 5, no. 1, pp. 42–47, 2015.

[89] A. C. Janaki, E. Sailatha, and S. Gunasekaran, "Synthesis, characteristics and antimicrobial activity of ZnO nanoparticles," *Spectrochimica Acta Part A: Molecular and Biomolecular Spectroscopy*, vol. 144, pp. 17–22, 2015.

[90] M. M. Modena, B. Rühle, T. P. Burg, and S. Wuttke, "Nanoparticle characterization: what to measure?," *Advanced Materials*, vol. 31, article 1901556, 2019.

[91] S. Heim and F. Mitelman, *Cancer cytogenetics: chromosomal and molecular genetic aberrations of tumor cells*, John Wiley & Sons, 2015.

[92] M. Alaraby, B. Annangi, A. Hernández, A. Creus, and R. Marcos, "A comprehensive study of the harmful effects of ZnO nanoparticles using Drosophila melanogaster as an in vivo model," *Journal of Hazardous Materials*, vol. 296, pp. 166–174, 2015.

[93] P. Chen, H. Wang, M. He, B. Chen, B. Yang, and B. Hu, "Size-dependent cytotoxicity study of ZnO nanoparticles in HepG2 cells," *Ecotoxicology and Environmental Safety*, vol. 171, pp. 337–346, 2019.

[94] A. F. Ismail, M. M. Ali, and L. F. Ismail, "Photodynamic therapy mediated antiproliferative activity of some metal-doped ZnO nanoparticles in human liver adenocarcinoma HepG2 cells under UV irradiation," *Journal of Photochemistry and Photobiology B: Biology*, vol. 138, pp. 99–108, 2014.

[95] P. B. Ezhuthupurakkal, S. Ariraman, S. Arumugam et al., "Anticancer potential of ZnO nanoparticle-ferulic acid conjugate on Huh-7 and HepG2 cells and diethyl nitrosamine induced hepatocellular cancer on Wistar albino rat," *Nanomedicine: Nanotechnology, Biology and Medicine*, vol. 14, no. 2, pp. 415–428, 2018.

[96] A. Iswarya, B. Vaseeharan, M. Anjugam et al., "Multipurpose efficacy of ZnO nanoparticles coated by the crustacean immune molecule β-1, 3-glucan binding protein: toxicity on HepG2 liver cancer cells and bacterial pathogens," *Colloids and Surfaces B: Biointerfaces*, vol. 158, pp. 257–269, 2017.

[97] E. H. Ismail, A. Saqer, E. Assirey, A. Naqvi, and R. Okasha, "Successful green synthesis of gold nanoparticles using a Corchorus olitorius extract and their antiproliferative effect in cancer cells," *International Journal of Molecular Sciences*, vol. 19, no. 9, p. 2612, 2018.

[98] D. Nayak, S. Pradhan, S. Ashe, P. R. Rauta, and B. Nayak, "Biologically synthesised silver nanoparticles from three diverse family of plant extracts and their anticancer activity against epidermoid A431 carcinoma," *Journal of Colloid and Interface Science*, vol. 457, pp. 329–338, 2015.

Review Article

Pharmacological Properties and Health Benefits of Eugenol: A Comprehensive Review

Muhammad Farrukh Nisar [ID],[1,2] **Mahnoor Khadim**,[2] **Muhammad Rafiq** [ID],[2] **Jinyin Chen** [ID],[1,3] **Yali Yang** [ID],[4] **and Chunpeng Craig Wan** [ID][1]

[1]*Jiangxi Key Laboratory for Postharvest Technology and Nondestructive Testing of Fruits & Vegetables, College of Agronomy, Jiangxi Agricultural University, Nanchang 330045, China*
[2]*Department of Physiology and Biochemistry, Cholistan University of Veterinary and Animal Sciences (CUVAS), Bahawalpur 63100, Pakistan*
[3]*College of Materials and Chemical Engineering, Pingxiang University, Pingxiang 330075, China*
[4]*Department of Pathology, Affiliated Hospital of Yunnan University/Second People's Hospital of Yunnan Province, Kunming 650021, China*

Correspondence should be addressed to Yali Yang; appleyangyali@126.com and Chunpeng Craig Wan; chunpengwan@jxau.edu.cn

The biologically active phytochemicals are sourced from edible and medicinally important plants and are important molecules being used for the formulation of thousands of drugs. These phytochemicals have great benefits against many ailments particularly the inflammatory diseases or oxidative stress-mediated chronic diseases. Eugenol (EUG) is a versatile naturally occurring molecule as phenolic monoterpenoid and frequently found in essential oils in a wide range of plant species. EUG bears huge industrial applications particularly in pharmaceutics, dentistry, flavoring of foods, agriculture, and cosmeceutics. It is being focused recently due to its great potential in preventing several chronic conditions. The World Health Organization (WHO) has declared EUG as a nonmutant and generally recognized as safe (GRAS) molecule. The available literature about pharmacological activities of EUG shows remarkable anti-inflammatory, antioxidant, analgesic, and antimicrobial properties and has a significant effect on human health. The current manuscript summarizes the pharmacological characteristics of EUG and its potential health benefits.

1. Introduction

Eugenol (EUG) or 4-allyl-2-methoxyphenol is a phenylpropanoid having an allyl chain-substituted guaiacol (Figure 1). EUG, a naturally occurring compound, has been reported to be present in several plant families including Holy basil or tulsi leaves (Lamiaceae), *Eugenia caryophyllata* (clove), *Zingiber officinale* (ginger), bark and leaves of *Cinnamomum verum* (cinnamon), *Curcuma longa* (turmeric), and peppers (Solanaceae) [1], as well as various aromatic plants such as *Cinnamomum verum* (true cinnamon), *Ocimum basilicum* (basil), *Myristica fragrans* Houtt. (nutmeg), and *Cinnamomum loureirii* Nees. (Saigon cinnamon). The major

natural sources of EUG are *Eugenia caryophyllata* (syn *Syzygium aromaticum*) which comprises 45-90% [2], and cinnamon has 20-50% of EUG, but the commercial level extraction of EUG is quite expensive with longer cultivation times, while ginger, tulsi, and bay can be used instead of cinnamon and clove as cheaper source [1].

EUG can be prepared synthetically by guaiacol allylation with allyl chloride or produced through biotransformation process that involves microorganisms like *Escherichia coli*, *Corynebacterium* sp., and *Bacillus cereus* [3]. The pharmacological properties of EUG are numerous including antimicrobial, anti-inflammatory, analgesic, neuroprotective, antidiabetic, and antitumor activities that make it a
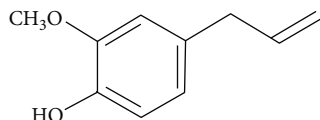
Figure 1: Structure of EUG.

versatile natural ingredient that helps in the prevention and cure of several disorders. The WHO declared EUG generally recognized as safe (GRAS) and a nonmutagenic substance. This naturally occurring molecule also has a large utilization in perfumery industry and food industry [4]. The antiseptic property made its use in mouthwashes as a disinfectant and also complexed with tooth fillers due to its pain relieving, antiseptic, and analgesic properties [5, 6]. In agricultural practices, EUG have extensively been used as an insect attractant and even in pesticide production. At commercial scale, EUG proven itself a versatile compound mainly due to its structure, complex formation, and an excellent substrate for carrying out biotranformations [7, 8].

Medicinally important plant species are a good source of active and potent drugs bearing extensive pharmacological properties. There is a huge list of pharmacological activities and bioactivities of EUG along with industrial utilization. In spite of its strong antioxidant properties, EUG protects neuron cells and recues the chances of the oxidative stress-oriented diseases as well as inflammatory diseases. Moreover, EUG is also used in local anesthesia to check the multiple pathological pains other than its wide utilization in dental clinics. Keeping in view the broad-spectrum utilization of EUG, the current review is aimed at highlighting and summarizing the recent advancements using EUG and exploring its pharmacological properties in a broader way. Moreover, this review will also discuss the roles of EUG in inflammatory and chronic diseases, in its antioxidant potential, and in neuroprotection.

2. Pharmacological Properties of EUG

The mechanism behind the therapeutic potential of EUG has been explained in huge literature. EUG is effective against a number of diseases such as reproductive disorders, nervous system disorders, blood glucose and cholesterol irregularities, microbial infections, tumorigenesis, hypertension, inflammations, and digestive complications [9]. Herein, the potential of EUG in combating severe illnesses and the mechanisms linked with health-promoting actions have been illustrated in detail [1].

2.1. Anticancer Activities. Cancer usually forms tumors by accumulation of cells and involves uncontrolled cell division. It is the second major cause of death worldwide, with a 6 million fatality rate annually [10, 11]. Cellular aggregation can be a consequence of inflammation because of inappropriate performance of signaling pathways [11]. Chemotherapy is mostly employed to destroy cancer cells, but in addition to targeting the diseased cells, it also causes division of normal cells of hair follicles, bone marrow, etc. Therefore, chemopreventive natural agents, like EUG, are preferred for tumor

therapy. These drugs, even at high dose, show no cytotoxic effect on healthy cells [12–14]. EUG has been declared non-mutagenic and noncarcinogenic by the US Food and Drug Administration (FDA) [15–17] (Figure 2).

Different studies on EUG demonstrated its strong potential in combating colon cancer, prostate cancer, skin tumors, and gastric cancers [11, 18–20]. Therapeutic drugs undergo apoptosis as a therapy for cancer and many other diseases. Apoptosis is programmed cell death which causes plasma membrane shrinkage, blebbing, fragmentation in chromosomal DNA, production of membrane-bound small apoptotic bodies which are phagocytozed by nearby surrounding cells, and chromatin condensation [10, 21]. Apoptosis is a vital function of the human body without which there is surely a great risk of many disorders like cancers, acquired immune deficiency syndrome (AIDS), etc. [10, 11, 22].

Drug combination therapies are mostly used in combating cancer [23]. EUG shows a synergistic effect when used with some chemoinhibitory drug leading to a great reduction in drug toxicity on healthy cells [24]. In an *in vitro* study, use of little quantity of EUG in combination with gemcitabine potentiates the effects of the drug with no side effects on healthy cells [1, 11, 25].

Breast cancer is ranked second among most common cancers in women, and it is classified as the fourth common cause of cancer-linked deaths worldwide [1]. Mammary epithelial cells in women are regulated by maintaining a balance among the process of their proliferation and apoptosis [26]. Disturbance in this balance leads to a rise in mammary epithelial cells finally causing breast cancer [26]. Vidhya and Devaraj [27] proved that breast cancer cells (MCF-7) experience strong antimutagenic activity of EUG. EUG is both time and dose dependent when suppressing proliferation of MCF-7 cells [17, 27]. Pisano and colleagues [28] also explained the antiproliferative action of EUG-associated biphenyl (S)-6,60-dibromo-dehydrodieugenol, by initiating apoptosis.

Melanoma or malignant melanoma develops from melanocytes and is a sort of skin cancer [29]. Among all skin cancers, melanoma accounts for 4% only. However, it has a high mortality rate with over 80% of death toll from skin cancer [30]. The antiproliferative effect of EUG against melanocytes was studied by Pisano and coworkers [28]. EUG seize cell cycle and promote apoptosis. This effect of EUG has also been studied in a B16 xenograft model by Miyazawa and Hisama [31]. EUG acts by synthesis of ROS [17] which causes inhibition of DNA synthesis thus delaying tumor growth. 40% reduction was reported in tumor size by the action of EUG [2, 32]. Another study was conducted by considering the anticancer activity of EUG on human melanoma cells (WM1205Lu). The results indicated apoptosis and cell cycle arrest at S-phase [2]. Ghosh and coworkers [33] examined EUG and isoeugenol for antimelanoma activity. They inferred that EUG, but not isoeugenol (isomer of EUG), showed anticancer activity against melanocytes [17].

Cervical cancer arises from the cervix. In 2002, cervical cancer resulted in 274,000 deaths [34]. More than 90% of cervical cancer cases are caused by human papillomavirus infection; most people who have had HPV infections, however, do not develop cervical cancer [35, 36]. Experiments
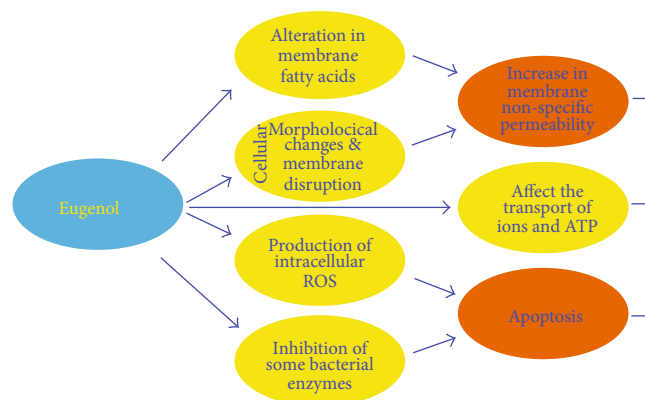
Figure 2: Cellular mechanism of EUG on cancer cells.

Figure 3: Prooxidant and antioxidant effects of EUG against cancer cells.

were conducted for studying the action of methyl EUG and cisplatin against cervical cancer cells (HeLa cells). The drugs were used separately and in combination. Methyl-EUG combined to cisplatin enhanced the anticancer effect by inducing apoptosis and destroying HeLa cells compared to the ample drug effects. Number of cells in G0/G1 phase, caspase-3 activity, and mitochondrial membrane potential loss were much enhanced in combination treatment in contrast to single drug exposure [23]. EUG showed a dose-dependent effect on HeLa cells [11].

2.2. Antioxidant Potential. Antioxidants protect body from the harms of free radicals by eliminating ROS or scavenging free radicals [37–39]. Unnecessary groups of free radicals are responsible for multiple human diseases like AIDS, cancer, and Parkinson's disease [1]. For a healthy body system, free radical production must be depressed [40]. Phenolic groups play a vital role in antioxidant action [41]. Availability of electrons for neutralizing free radicals is the basic principle of antioxidant action. Increasing the number of hydroxyl groups in phenol ring increases the capability to behave as hydrogen donor and prohibits oxidation [40]. Oxidative stress is an imbalance in antioxidant defense and ROS production [42, 43]. Due to the disturbance in equilibrium between prooxidants and antioxidants, ROS production enhances leading oxidative stress which is concerned with inhibition of normal body functions [40]. Moreover, EUG has been reported to pose both prooxidant and antioxidant effects when applied to the cancer cells in a concentration-dependent fashion [44] (Figure 3). It was shown by electron spin resonance that the scavenging effect of EUG is due to the allyl group in its structure [39, 45]. It hinders in lipid peroxidation leading to free radical destruction [46]. The EUG have great inhibitory effects on hexanal oxidation [47], copper-dependent LDL oxidation, iron-mediated lipid peroxidation [39], and nonenzymatic peroxidation in liver mitochondria [46] and hinder the onset of oxidative stress-mediated diseases. EUG has an extraordinary reducing ability [48] and donates phenolic hydroxyl groups that can react with free radicals, diminishing oxidative stress thus a desirous antioxidant. Moreover, the antioxidant behaviour of EUG is greater than most of the known or standard antioxidants such as Trolox [40].
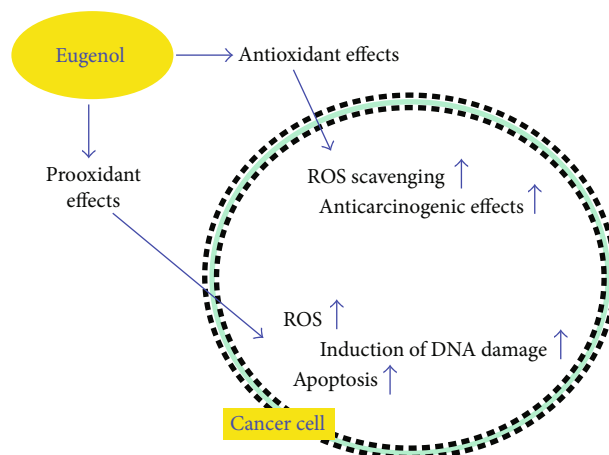
EUG shows dual properties, i.e., antioxidant as well as prooxidant actions, and later is the cause of cytotoxicity [49]. EUG behaves as an antioxidant at lower concentrations by minimizing ROS-mediated oxidative stress, but on the contrary, EUG at higher concentrations acts as a prooxidant to enhance the production of the ROS [16, 43, 50, 51]. Few studies showed that EUG eliminated free radicals through ABTS (2,2-azinobis (3-ethylbenzothiazoline-6-sulfonic acid) (76.9%) and DPPH (89.9%) in *L*-ascorbic acid [52]. Kaur and coworkers pretreated male Swiss albino mice with EUG and found a reduction in lipid peroxidation (LPO) and an inhibited depletion of antioxidant enzymes.

2.3. Cardiovascular Protection. Hyperlipidemia is the most common social issue in common people and causes cardiovascular diseases (CVDs) and lipid-related diseases [53]. CVDs and hyperlipidemic disorders are caused by less physical activity and high fatty acid intake [1]. High low-density lipoprotein cholesterol (LDL-c) leads to toxicity in vascular tissues and atherosclerosis/atherogenesis eventually causing diabetes; obesity; hypertension; inappropriate working of main body organs such as the kidneys, heart, and liver; and atherosclerosis [54].

CVD death and disease rate can be eradicated by less intake of lipids in the diet [55]. Reduced LDL-c concentrations also support in diminishing CVDs and improve atherosclerotic state [56, 57]. ROS causes an increase or imbalance in oxidative stress homeostasis which results in enhancing a number of chronic diseases like coronary heart disease (CHD). Increased ROS production causes oxidative damage due to the disturbance in cellular antioxidant status [58].

Dyslipidemia is another example which is linked with oxidative stress and causes disregulation in working of cellular antioxidant stress response system [59]. Rice bran is widely used since decades because of its cholesterol-lowering, free radical scavenging, and antiatherogenic actions [60].

However, it is preferable to use natural and safer drugs in as minimum quantities as possible. EUG has a great antihypercholesterolemic and antiatherogenic potential. Venkadeswaran et al. [61] reported hypolipidemic effects of EUG in

intraperitoneally injected Triton WR-1339 (300 mg/kg per B.W.) induced hyperlipidemic Wister male rats. EUG was more effective against high lipid and cholesterol content in comparison to a lipid-lowering drug (lovastatin). It caused a 55.88% reduction in total cholesterol; also, LDL-C (79.48%) and triglycerides (64.30%) were reduced.

EUG undergoes dose- and endothelium-dependent reversible vasodilator responses [20]. In hypersensitive rats, EUG showed a hyposensitive behaviour by inducing vascular relaxation [62]. The smooth muscle relaxant action of EUG is due to its blocking action on receptor-operated and voltage-sensitive channels. Vascular relaxation is done via endothelial-generated nitric oxide (NO) [63]. The hypocholesterolemic action of EUG was well explained by a recent study using a hyperlipidemic zebra fish model, where EUG caused a great reduction in triglyceride (80%) and cholesterol (68%) levels in serum samples [64].

Hypercholesterolemia also causes an imbalance in the serum concentration of malondialdehyde (MDA, increased) and superoxide dismutase (SOD, decreased). This effect was studied by Munisa et al. [65], by the application of EUG against MDA and SOD in rats with high cholesterol level. They concluded that EUG regressed the concentrations to their normal ranges. Eugenol exerted negative inotropic effects in guinea pig heart muscles [66]. According to Choudhary et al. [67] EUG hinders isoproterenol-induced cardiac hypertrophy. The study was conducted on male Wister rats against EUG. They concluded that apoptosis, isoproterenol-induced oxidative stress, and calcineurin action in serum were suppressed [20].

2.4. Antidiabetic Activity.
Hyperglycemia is a condition after which there is an outbreak of a degenerative disease called diabetes mellitus caused by abnormalities in glucose metabolism. Studies have shown that EUG is capable of curing several metabolic illnesses owing to its various pharmacological activities. EUG is a strong antidiabetic bioactive substance [1]. According to Anuj and Sanjay [39], EUG principally diminishes α-glucosidases after which it intercepts the development of advanced glycation end (AGE) products [68]. In the presence of inhibitory α-glycosidase compounds like EUG, dietetic complex carbohydrates do not undergo liberation of absorbable monosaccharides. The inhibitors prevent any drastic rise in meal-induced glucose level in blood by delaying the absorption of glucose into the bloodstream [69].

EUG enhances the activities of carbohydrate metabolism enzymes like glucose-6-phosphate dehydrogenase (31.05%) and instance hexokinase (62.25%). Studies show that a diminishing effect has also been observed by the application of EUG on creatine kinase (38.57%), glucose-6-phosphatase (24.45%), blood urea nitrogen (34.01%), and fructose-1,6-bisphosphatase [70].

Tahir et al. [68] demonstrated the antidiabetic potential of S. aromaticum and Cuminum cyminum (C. cyminum) following the α-amylase enzyme assay method. Starch is converted to simple sugars by α-amylase which is a human enzyme and is involved in causing diabetes. The rate at which glucose absorbs into the blood stream can be reduced by the application of inhibition of α-amylase enzyme. The enzyme retards the digestion of carbohydrates ultimately causing a decrease in blood glucose level. The antidiabetic activity is dose dependent. S. aromaticum depicted more antidiabetic potential than C. cyminum, as S. aromaticum is chiefly composed of EUG (18.7%) while the main constituent of C. cyminum is composed of á-pinene (18.8%) [68]; the antidiabetic potential of S. aromaticum was found to be 95.30% which is greater than 83.09% of C. cyminum. These results proved that EUG has a great antidiabetic potential compared with many related essential oils [68].

Srinivasan et al. experimented male diabetic rats by inducing streptozotocin drug (40 mg/kg per B.W.) in them. The activity of major enzymes taking part in the glucose metabolism was studied to examine efficacy of EUG. In contrast, only a 10 mg/kg per B.W. dosage of EUG greatly enhanced hepatic glycogen and insulin in plasma (46.15%) samples with a reduction in glycosylated haemoglobin (25.70%) and blood glucose (70%) [70].

2.5. Antiparasite Activity.
The majority of human parasites are a key cause of increased mortalities compared with rest of the issues excluding tuberculosis (TB) and AIDS [71]. Certain drastic effects of EUG have been reported on morphology and growth of various parasites like Trypanosoma cruzi, Giardia lamblia, and Leishmania donovani [72]. Schistosomiasis is a parasitic helminthic infection in about 78 different countries caused by parasitic flatworms or blood fluke schistosomes (S. haematobium, S. mansoni, S. japonicum, and S. mansoni) and also familiar as bilharzia or snail fever which is somewhat a neglected tropical disease [72–75]. Schistosomiasis gets settled in intestinal venules to affect the gut, urinary tract, and liver which results in retardation of growth, anemia, enlarged liver, and even liver fibrosis [72]. EUG can be used as an antiparasitic agent with least side effects than other chemotherapeutics in curing various parasitic diseases, and overdose of EUG shows antileishmanial, antimalarial, and antihelmintic potentials. In an in vivo study using mouse models, the drug-resistant parasite Schistosoma mansoni showed a great reduction (19.2%) following a synergistic effect of EUG in combination with conventional drugs [72]. Moreover, it is further noticed that EUG had no effect on egg development of worms owing to the fact that the oogram patterns of the treated group of mice and nontreated group of mice were similar, but the egg density in the walls of the intestines of mice was greatly reduced by the application of EUG [76]. Protozoans like Leishmania are the major cause of leishmaniasis in humans, and the pathogens are being transferred through the bite of infected phlebotomine female sandflies [77]. Leishmaniasis can be mucosal, visceral, or cutaneous and if it gets combined with human immunodeficiency virus may cause a serious condition [39]. Most of the pathogenic parasites have developed resistance with course of time against standard drugs; thus, use of natural phytochemicals like EUG is preferred [78]. Following a 60 min treatment of EUG in combination with essential oils showed absolute (100%) destruction of L. amazonensis parasites [79] primarily by the increased production of EUG-mediated nitric oxide (NO) which is an antileishmanial oxidant involved in triggering the killing of leishmania species [39, 79].

2.6. Antibacterial and Antiviral Activities. EUG have been well known for its antimicrobial potential and uses. Majority of food-borne diseases are attributed to the microorganisms and are an escalating health issue of global public. About one-third of the population in industrial countries are facing food-borne diseases issues. In the US, 31 notable pathogens give rise to approximately 9.4 million cases of food-borne diseases per annum [80]. EUG can be bactericidal (bacterial killing) or bacteriostatic (inhibiting bacterial growth) depending on the MIC (minimum inhibitory concentration) and MBC (minimum bactericidal concentration) [81] and have antivirus and antifungal effects at the same time. EUG shows dynamic antibacterial ability against a variety of strains of gram-negative (*Pseudomonas aeruginosa*, *Salmonella choleraesuis*, *Yersinia enterocolitica*, *Helicobacter pylori*, and *E. coli*) and gram-positive (*Streptococcus pneumonia*, *S. aureus*, *Enterococcus faecalis*, and *Streptococcus pyogenes*) bacterial strains. EUG has proven to be active against several bacterial enzymes like histidine, amylase, ATPase, and proteases [82, 83]. The presence of a free hydroxyl group in the EUG molecule is the main cause of its great antimicrobial activity [84]. EUG extracted from clove oil adversely disrupts the cell wall and cell membrane of bacteria, and this lysis leads to an enhanced fluidity and permeability of cell membrane [85, 86] followed by membrane expansion, leakage of intracellular fluids accompanied by proteins and lipids release, respiration inhibition, alteration of ion transport patterns of bacteria [81, 83], and disturbance of membrane-embedded proteins, consequently leading to the cell death [87]. Catherine et al. [88] tested the antibacterial potential of EUG in combating (MIC 0.15-0.25%) food-borne bacteria *E. coli*, *Yersinia enterocolitica*, *S. aureus*, and *Bacillus cereus* and proven that gram-negative bacteria are more resistant than its counterpart gram positive [88]. The combination therapy by making fusion of plants is quite effective for the treatment of critical bacterial infections [2, 89]. The antibacterial activity of EUG was amplified when combined with vancomycin, where the half of the bacterial membranes are damaged due to EUG and hence facilitate the vancomycin penetration into the membrane [2, 90]. The combined effect of EUG with gentamicin or ampicillin resulted in a much higher killing rate in an hour time than EUG applied alone [2, 91].

Herpes simplex virus (HSV) infects persons 50 years and is a frequent sexually transmitted infection [92]. The medicinal plants are a rich source of EUG that retards the replication of HSV by neutralizing and inactivating the viral infections [93, 94]. The mechanism behind antiviral actions of EUG is the upregulation of the expression of HSV-1-glycoprotein B that checks HSV replication [95], while some studies confirmed that EUG inhibits the replication of the HSV-1 and HSV-2 DNA molecules, as well as damages the outer envelope of newly synthesized virions [96–98]. The benefits of using combination chemotherapy includes enhanced antiviral activity, reduced dosage of toxic substances, and lessened development of drug resistance [99]. In in vivo study involving mouse models, *Eugenia caryophyllus* extracts rich in EUG which were applied in combination with acyclovir (ACV) showed an anti-HSV-1 potential in the brain and skins of mice [97, 100]. In this ACV-EUG therapy, ACV specifically targets DNA molecules and inhibits the replication process [101]. In HSV-1-infected mice, EUG therapy delayed the production of herpetic keratitis in the cornea [39] which shows a close association of EUG on the ocular herpetic infections [93]. EUG disintegrates the lipidic envelope of the HSV virus and also induces glutathione S-transferase (GST) expression in liver cells of rats, eventually blocking replication process.

2.7. Antifungal Activity. EUG has shown lethal effects on the growth of different strains of fungi such as *Fusarium graminearum*, *F. moniliforme*, *Tricophyton rubrum*, *Penicillium citrinum*, *Candida tropicalis*, *C. krusei*, and *Aspergillus ochraceus* . EUG either causes cell cycle arrest or affects fungal cell membrane integrity by disruption [102]. Owing to the lipophilic nature of the EUG, it gets accumulated in the phospholipid bilayer of fungal cells, altering the functions of vital membrane-bounded enzymes, affecting permeability, fluidity of membrane, and envelope morphogenesis [103, 104]. Another recent study claimed that by the addition of the methyl radical in the EUG, it may amplify its antifungal potent to many folds [105]. Combination therapies are often employed for better results. A synergistic interaction of EUG or isoeugenol with that of fluconazole (EUG/isoeugenol-fluconazole/amphotericin B) was applied against multidrug-resistant strain *C. albicans* and found extraordinary effectiveness [2]. Furthermore, EUG have been reported to affect the morphology of the fungal strains especially the hyphae of *B. cinerea* which showed much irregular structural features such as broken or shriveled hyphae, large vesicles, and leaked intracellular contents. In addition to morphological alterations, EUG induces the accumulation of ROS especially hydrogen peroxide (H_2O_2) in the fungal cells to generate oxidative stress which ultimately bursts the fungal hyphae [103].

2.8. Anti-Inflammatory Activity. Inflammation is called as the body's adaptive immunity response, triggered by noxious stimuli, tissue infection, and injury [106]. It can be chronic or acute [107], and anti-inflammatory drugs used nowadays have adverse effects [108]. EUG, with no side effects, has a tremendous anti-inflammatory potential (Figure 4). EUG can be used in the protection of damage resulting from oxidative stress [52]. The ROS-mediated oxidative stress results in cellular damage and LPO [109]. Saraiva et al. [108] showed that oxidative stress and inflammation are interlinked mechanisms. In a study, male Swiss albino mice when treated with EUG have undergone reduced LOP and in expression levels of inflammatory markers, viz., COX-2, iNOS, and cytokine tumor necrosis factor α (TNF-α), and antioxidant enzymes [19]. Generally, EUG pretreatment reduces inflammations (as a result of the action of LPS on lungs) in cells.

Biswas et al. [110] studied pulmonary inflammation in mouse and action of EUG as an antiagent. It was concluded that EUG causes significant reduction in the much higher levels of neutrophils and TNF-α and also maintained the proinflammatory mediators. Magalhães et al. [111] investigated anti-inflammatory properties of EUG in lipopolysaccharide-induced lung injury for 6 h *in vivo*. A decrease of
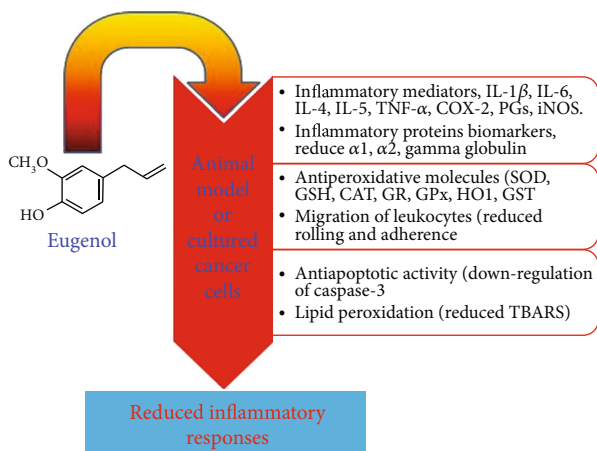
FIGURE 4: Effect of EUG on controlling the inflammations.

proinflammatory cytokines like TNF-α, NF-κB-mediated signalizing pathway, and macrophage infiltration were reported, eventually leading to an improvement in the function and structure of the lungs due to a decrease in inflammation [52]. EUG inhibits TNF-α and cyclooxygenase-2 (COX-2) expression [112]. Its anti-inflammatory action is attributed to macrophage chemotaxis and prostaglandin synthesis. In a study, it was revealed that EUG suppresses the activation of NF-κB-stimulating macrophages mainly due to TNF-α and COX-2 actions. COX-2 effect is enhanced by lipopolysaccharides (LPS) [113]. The expression of antioxidant enzymes like glutathione peroxidase (GPX) and superoxide dismutase (SOD) is significantly enhanced by EUG (Figure 4).

2.9. Antipyretic Activity. The antipyretic efficacy of EUG was examined by Feng and coworkers [114], where they found an antipyretic effect of EUG against a well-known antipyretic acetaminophen in rabbits made febrile by IL-1β. It shows a significant antifever action than acetaminophen when induced intragastrically, centrally, and intravenously. When given intragastrically, EUG in addition to treating fever, induces slight hypothermia unlike acetaminophen. Acetaminophen reduced fever by 68% at a dose of 1.3 mM/kg while EUG reduced 68% fever at a much less dosage. When given peripherally, it shows marked results in inhibiting fever. When given intravenously, respiration of rabbits and vasodilation in ears were increased. Increased respiration depicts that EUG have a positive action on the central nervous system (CNS). If prostaglandins and sodium archidonate mediate fever in the CNS, acetaminophen and EUG can inhibit fever by retardation of prostaglandin R and sodium archidonate synthesis. Both these drugs show the same antipyretic mechanism but EUG shows more potent behaviour as compared to acetaminophen [115].

2.10. Antinociceptive Activity (Analgesic). EUG is significantly efficient in relieving pain by reducing the responses that are linked with pain. It suppresses several responses to histamine, norepinephrine, and stimulation of periarterial sympathetic nerves [116] and inhibits prostaglandin synthesis [117]. It is mostly used as a dental analgesic and antiseptic

agent [118]. Its analgesic effect is linked to suppress Na$^+$, K$^+$, and Ca^{2+} voltage-dependent channels [119, 120]. The high-voltage-activated Ca^{2+} channel (HVACC) inhibition by EUG plays an important role in pain-relieving effect. It inhibited HVACC currents in both capsaicin-insensitive and capsaicin-sensitive dental primary afferent neurons [121]. TRPV-1 receptors are involved in pain stimulation. A study revealed that EUG inhibited TRPV-1 by suppressing voltage-activated Na$^+$ and Ca^{2+} channels [2, 122].

EUG is an antagonist towards NMDA (N-methyl-D-aspartate) and gamma-aminobutyric acid (GABA); both are involved in pain transmission [123, 124]. It inhibits Ca^{2+}-dependent release of neurotransmitters and also retards interleukin (IL-)1β and PGE2 synthesis [39]. Park et al. [125] studied the analgesic action of EUG in the orofacial part and reported its inhibitory action on VGSCs in trigeminal ganglion (TG) neurons.

Ferland et al. [126] performed experiments on a monoiodoacetate-induced rat model of osteoarthritis to find the effects of EUG. The affected limb showed marked improvement when administered with EUG for two days after osteoarthritis induction. Also, calcitonin gene-related peptide (CGRP) which is associated with spinal cord pain was reduced. The antinociceptive potential of EUG was investigated by Daniel et al. [127] in mice using acetic-acid-induced abdominal writhing process. EUG showed a significant result in decreasing the pain. The effect of EUG in several experimental pain models using mice was studied such as acetic acid-mediated abdominal constrictions, formalin-mediated hyperalgesia, and thermal pains, and 92.73%, 70.33%, and mild inhibitions in pain were found, respectively [128].

2.11. Effects on the Central Nervous System (CNS), Neuroprotection, and Antistress Activity. EUG in addition to acting on the periphery also performs actions in the central nervous system (Figure 5). The hydrophobic property of EUG makes it efficient in penetrating the blood-brain barrier for its entry into the brain and performs its action *in vivo* [129]. EUG guards neuronal cells against N-methyl-D-aspartate- (NDMA-) induced oxidative and excitotoxic injury [39]. EUG shows a neuroprotective potential on hippocampal tissues owing to its power reduce brain-derived neurotrophic factor (BDNF), and retardation of amyloid-β peptide (A-β) induced cell death through the abnormal blockage of Ca^{2+} (resulted from A-β) [130]. Its ability to restrict antioxidant and excitotoxicity effects also contributes in neuroprotection. In cell models, EUG improves actions of few glutathione-related proteins and shields essential neuronal cells from oxidative and excitotoxic effects [131]. The inhibitory action of EUG has been reported on 5-lipoxygenase, in addition to an improved action in response to excitotoxic and ROS-injured neuron cells [132].

Depression, a neurodegenerative disorder, causes common psychological disorders, and 10-20% of the general population suffer through it. EUG showed a marked effect as an antidepressant in force swimming test (FST) and tail suspension test (TST) comparable to an antistress drug imipramine [39]. The mechanism of action of these two
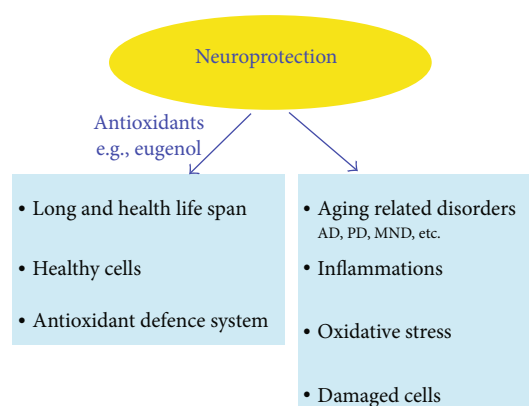
FIGURE 5: The role of EUG in neuroprotection and neurodegenerative diseases in the CNS involves various mechanisms including oxidative stress, damaged/unrepaired cells, and inflammations.

drugs is different. Real-time PCR (RT-PCR) showed that metallothionein-III (MT-III) was found to be linked with the antidepressive effect of EUG quite different from imipramine. This forms the basis of an alternative treatment if the patients develop resistance to typical drugs. EUG exhibits antiepileptic potential. It performs its action by blocking long-term potentiating and synaptic transmission in neurons [133]. Sen et al. [134] reported the antistress activity of EUG. EUG acts at a central level to pose neuroprotective effects against ischemia, excitotoxicity, and amyloid-β peptide. In experimental diabetes, EUG improves vascular and neuronal complications and suppresses the transmission of action potential in sciatic nerves [39]. It also elongates the kallikrein- and bradykinin-induced tranquilization [135]. EUG is a good medicine for Alzheimer's disease (AD) and depression. Moreover, the expression of the BDNF gene in the hippocampus is also controlled by EUG. It also retards monoamine oxidase A (MAO-A) and sometimes reverts back monoamines that are reduced in the brains of depressed patients [129]. EUG has been proved useful against stress-induced irritable bowel syndrome (IBS) [136].

Regulation of release of neurotransmitters by EUG eventually moderates different brain functions. Rats with 4 h restraint stress model were studied by Garabadu et al. [137], and antistress potential of EUG was observed. It was concluded that EUG administration enhanced ulcer index and corticosterone and norepinephrine levels. EUG also brought alteration in serotonin (5-HT) levels in almost all parts of the brain. This study elaborates the antistress actions of EUG that are ascribed with the modulation of hypothalamic pituitary adrenal (HPA) as well as brain monoaminergic systems (BMS). Under stress situations, sympathoadrenal (SA) and BMS and HPA regulate several physiological and psychological responses [137].

The neuroprotective efficacy of EUG and isoeugenol in response to acrylamide-mediated neuropathy in male albino rats was studied by Prasad [138], where it was found that both the drugs increase the behavioral index gait level and reduce the oxidative stress-linked markers like NO and ROS. Dopamine, acetylcholinesterase activity, and cytosolic

Ca^{2+} levels are also diminished in the brain. It is further demonstrated that EUG and isoeugenol potentially restrict acrylamide-mediated neuropathic condition in rats and due to this factor, they can be directly used through diet to soothe different neuropathic conditions in humans [138].

2.12. Neurodegenerative Disorders. Neurological disorders include a number of conditions whose inception results from subsequent degradation of normal function and morphology of neurons, mainly in the CNS [139]. Globally, 20 million people are suffering from only these three disorders [140]. Neural disorders have been ranked by the WHO as the second (12%) most reason of mortalities worldwide. Disorders linked with neurodegeneration include Parkinson's disease (PD), AD, prion diseases, ischemia, hydrocephalus, Huntington's disease, head and brain malformations, and spongiform encephalopathies [141]. Among the neurodegenerative diseases, AD, PD, and motor neuron disease (MND) are most common. Natural agents are frequently employed for the treatment of various neurological disorders (Figure 5). It was demonstrated by ancient Chinese researchers that a number of herbs used in treatment of AD consists of *Rhizoma acori graminei* extracts enriched with EUG [39].

The neurodegenerative disorder AD is described characterized by the loss of neurotransmitters and neurons and is accompanied by depression and PD [129]. Neuronal degeneration in the CNS involves various mechanisms including apoptosis, protein accumulation, ageing, and oxidative stress, which are contributing to neurodegenerative disorders (Figure 5). The most common among these is the aggregation of misfolded proteins, which display amyloid characteristic (formation of β-pleated sheets), calling this group of illness called as brain amyloidosis [140].

2.13. The Enhancement in Skin Permeation. The stratum corneum of the skin is composed in a way to control the passive movement of substances across the skin. A common way for enhancing drug permeation through the skin is the transdermal drug delivery. Use of small electric charge for the transport of a substance (drug) across the skin is called iontophoresis and is used to compensate for impermeability of the skin, in addition to chemical permeation enhancers like essential oils [142, 143]. Anuj and Sanjay [39] investigated the permeation enhancer ability of EUG in the absorption of tamoxifen. EUG increased the permeability of tamoxifen across porcine epidermis as compared to 50% ethanol. Furthermore, EUG and acetyl-eugenol were also seen for transdermal delivery of ibuprofen in rabbits and noted to enhance permeation with great 7.3 enhancement ratio [144].

2.14. Toxicity. EUG toxic behaviour has been studied in multiple *in vivo* studies. However, little or no information is available in humans [39]. EUG toxic behaviour depends mainly on its concentration; i.e., its effects are dose dependent [52]. The prooxidant effect of EUG leads to its toxicity [43], and Medeiros et al., [145] reported that toxicity of EUG is attributed to protein inactivation due to the binding of EUG at the lysine residues. Cytotoxicity of EUG is possibly

due to its metabolic reactions. The reactive metabolites then react further with DNA, forming adducts that can destroy nuclear genetic material. EUG has been proved as a contact allergen in dentistry [39] and makes its entry into the bloodstream by penetrating dental pulp tissue, causing chromosomal aberrations (CAs) in dental pulp cells in humans [146].

2.15. Wide Application of EUG in Dentistry. EUG, due to its antioxidant, anti-inflammatory, anesthetic, and analgesic potentials, is used extensively in dentistry at low dosage. In dental emergencies, it is used as an anodyne [147]. It is used as a cementing material in dentistry [118], and the first type of EUG cement was developed earlier back in 1933 which comprises of EUG liquid and ZnO powder, forming a paste. In tooth preparation, EUG owing to its sedative potential provides soothing action for assisting in pulp relaxation after contusion [148]. ZnO EUG cement is presently being used in dentistry in root canal sealing; temporary fillings and indirect pulp capping are the widespread uses of ZnO+EUG cement (ZOE) [147]. Park et al. [125] studied the action of EUG on pain behaviors in the orofacial region and the retardation of voltage-gated sodium channels (VGSCs) in trigeminal ganglion (TG) neuron cells.

2.16. Miscellaneous. At high concentrations, EUG has also been reported to provide anesthetic effects during a pharmacokinetic study using male Sprague-Dawley rats [149]. Tajuddin et al. [150] observed an improved sexual behaviour of male Swiss mice after EUG administration. It also shows antiulcerogenic effects. Furthermore, two ulcerogenic agents induced gastric ulcer which was diminished by treatment with EUG. The gravity of lesions was also decreased by EUG [151]. The antiulcer action of EUG is brought about by its free radical scavenging activity, less acid-pepsin secretion, inhibition of a great rise in NO level, and opening of ATP-sensitive potassium (KATP) channels [53]. *In vivo* examination finds that diarrhea caused by castor oil was reduced by EUG. Also, the intestinal aggregation of fluid induced by PGE2, the rate of intestinal transit, and the tone of isolated gut muscle and myometrium were also suppressed [152]. Karmakar et al. [153] reported an ovariectomised (OVX) model of rats induced with osteoporosis against EUG and its derivatives. The drug showed a marked effect on the efficiency of bone preservation.

3. Conclusion

The current review summarized the potential health benefits and effectiveness of EUG as a therapeutic agent which can be used in medicines and food for the treatment of inflammatory and oxidative stress-oriented disorders. The antioxidant, anti-inflammatory, antipyretic, analgesic, antiparasite, and antimicrobial properties of EUG are well described. It has a great role in neuroprotection, enhances skin permeability, relieves pains, and has a role in temporary dental filler formation (ZnO+EUG). EUG has no known toxicity in smaller quantities, but at higher concentrations, it behaves as prooxidant; hence, a strong anticancer activity is shown by this molecule. Furthermore, diverse applications of EUG such as its pharmacological importance in regulating blood cholesterol and lipid levels are also discussed. Future studies involving a specified dose range of EUG to cure different ailments are recommended to highlight this molecule for the development of drugs.

Abbreviations

5-HT:	5-Hydroxytryptamine (serotonin)
ABTS:	2,2-Azinobis (3-ethylbenzothiazoline-6-sulfonic acid)
ACV:	Acyclovir
AD:	Alzheimer's disease
AGE:	Advanced glycation end
AIDS:	Acquired immune deficiency syndrome
A-β:	Amyloid-β peptide
BDN:	Brain-derived neurotrophic factor
BMS:	Brain monoaminergic systems
CAs:	Chromosomal aberrations
CGRP:	Calcitonin gene-related peptide
CHD:	Coronary heart disease
CNS:	Central nervous system
COX-2:	Cyclooxygenase-2
CVD:	Cardiovascular diseases
DNA:	Deoxyribonucleic acid
DPPH:	2,2-Diphenyl-1-picrylhydrazyl
EUG:	Eugenol
FAO:	Food and Agricultural Organization (of United Nations)
FDA:	Food and Drug Administration
FST:	Force swimming test
GABA:	Gamma-aminobutyric acid
GPX:	Glutathione peroxidase
GRAS:	Generally recognized as safe
GST:	Glutathione S-transferase
H_2O_2:	Hydrogen peroxide
HPA:	Hypothalamic pituitary adrenal
HSV:	Herpes simplex virus
HVACC:	High-voltage-activated Ca^{2+} channel
IL-1β:	Interleukin-1β
IL-6:	Interleukin-6
iNOS:	Inducible nitric oxide synthase
KATP:	ATP-sensitive potassium channels
LDL:	Low-density lipoprotein
LDL-c:	Low-density lipoprotein cholesterol
LPO:	Lipid peroxidation
LPS:	Lipopolysaccharides
MAO-A:	Monoamine oxidase a
MBC:	Minimum bactericidal concentration
MCF-7:	Michigan Cancer Foundation-7
MDA:	Malondialdehyde
MIC:	Minimum inhibitory concentration
MND:	Motor neuron disease
MT-III:	Metallothionein-III
NF-κB:	Nuclear factor kappa light chain enhancer of activated beta cells
NO:	Nitric oxide
OVX:	Ovariectomised

PCR: Polymerase chain reaction
PD: Parkinson's disease
PGE2: Prostaglandin E_2
ROS: Reactive oxygen species
SA: Sympathoadrenal
SOD: Superoxide dismutase
TB: Tuberculosis
TG: Trigeminal ganglion
TNF-α: Tumor necrosis factor α
TRPV-1: Transient receptor potential vanilloid-1
TST: Tail suspension test
VGSCs: Voltage-gated sodium channels
WHO: World Health Organization
ZnO: Zinc oxide
ZOE: Zinc-oxide eugenol.

Data Availability

All of the data used to elaborate and explain the findings herein are already given within the draft.

Conflicts of Interest

None of the authors have declared the conflict of interest for the submission and publication of this article in this journal.

References

[1] A. A. Khalil, U. . Rahman, M. R. Khan, A. Sahar, T. Mehmood, and M. Khan, "Essential oil eugenol: sources, extraction techniques and nutraceutical perspectives," *RSC Advances*, vol. 7, no. 52, pp. 32669–32681, 2017.

[2] G. P. Kamatou, I. Vermaak, and A. M. Viljoen, "Eugenol—from the remote Maluku Islands to the international market place: a review of a remarkable and versatile molecule," *Molecules*, vol. 17, no. 6, pp. 6953–6981, 2012.

[3] M. R. Abrahão, G. Molina, and G. M. Pastore, "Endophytes: recent developments in biotechnology and the potential for flavor production," *Food Research International*, vol. 52, no. 1, pp. 367–372, 2013.

[4] A. Sartoratto, A. L. M. Machado, C. Delarmelina, G. M. Figueira, M. C. T. Duarte, and V. L. G. Rehder, "Composition and antimicrobial activity of essential oils from aromatic plants used in Brazil," *Brazilian Journal of Microbiology*, vol. 35, no. 4, pp. 275–280, 2004.

[5] B. K. Jadhav, K. R. Khandelwal, A. R. Ketkar, and S. S. Pisal, "Formulation and evaluation of mucoadhesive tablets containing eugenol for the treatment of periodontal diseases," *Drug Development and Industrial Pharmacy*, vol. 30, no. 2, pp. 195–203, 2004.

[6] N. Sarrami, M. N. Pemberton, M. H. Thornhill, and E. D. Theaker, "Adverse reactions associated with the use of eugenol in dentistry," *British Dental Journal*, vol. 193, no. 5, pp. 257–259, 2002.

[7] S. Ouk, S. Thiébaud, E. Borredon, and P. le Gars, "Dimethyl carbonate and phenols to alkyl aryl ethers via clean synthesis," *Green Chemistry*, vol. 4, no. 5, pp. 431–435, 2002.

[8] T. S. Kaufman, "The multiple faces of eugenol. A versatile starting material and building block for organic and bioorganic synthesis and a convenient precursor toward bio-based fine chemicals," *Journal of the Brazilian Chemical Society*, vol. 26, no. 6, pp. 1055–1085, 2015.

[9] F. M. Rauscher, R. A. Sanders, and J. B. Watkins III, "Effects of isoeugenol on oxidative stress pathways in normal and streptozotocin-induced diabetic rats," *Journal of Biochemical and Molecular Toxicology*, vol. 15, no. 3, pp. 159–164, 2001.

[10] R. Yu, S. Mandlekar, K. J. Harvey, D. S. Ucker, and A. N. Kong, "Chemopreventive isothiocyanates induce apoptosis and caspase-3-like protease activity," *Cancer Research*, vol. 58, no. 3, pp. 402–408, 1998.

[11] A. Hussain, K. Brahmbhatt, A. Priyani, M. Ahmed, T. A. Rizvi, and C. Sharma, "Eugenol enhances the chemotherapeutic potential of gemcitabine and induces anticarcinogenic and anti-inflammatory activity in human cervical cancer cells," *Cancer Biotherapy and Radiopharmaceuticals*, vol. 26, no. 5, pp. 519–527, 2011.

[12] B. B. Aggarwal and S. Shishodia, "Molecular targets of dietary agents for prevention and therapy of cancer," *Biochemical Pharmacology*, vol. 71, no. 10, pp. 1397–1421, 2006.

[13] S. Lev-Ari, A. Vexler, A. Starr et al., "Curcumin augments gemcitabine cytotoxic effect on pancreatic adenocarcinoma cell lines," *Cancer Investigation*, vol. 25, no. 6, pp. 411–418, 2007.

[14] J. Park, V. Ayyappan, E. K. Bae et al., "Curcumin in combination with bortezomib synergistically induced apoptosis in human multiple myeloma U266 cells," *Molecular Oncology*, vol. 2, no. 4, pp. 317–326, 2008.

[15] D. Opdyke, "Monographs on fragrance raw materials: hydroxycitronellal dimethylacetal," *Food and Cosmetics Toxicology*, vol. 13, no. 5, pp. 548-549, 1975.

[16] S. K. Jaganathan and E. Supriyanto, "Antiproliferative and molecular mechanism of eugenol-induced apoptosis in cancer cells," *Molecules*, vol. 17, no. 6, pp. 6290–6304, 2012.

[17] R. S. Bendre and J. Rajput, "Outlooks on medicinal properties of eugenol and its synthetic derivatives," *Natural Products Chemistry & Research*, vol. 4, no. 212, p. 2, 2016.

[18] K. B. Harikumar, A. B. Kunnumakkara, G. Sethi et al., "Resveratrol, a multitargeted agent, can enhance antitumor activity of gemcitabine in vitro and in orthotopic mouse model of human pancreatic cancer," *International Journal of Cancer*, vol. 127, no. 2, pp. 257–268, 2010.

[19] G. Kaur, M. Athar, and M. S. Alam, "Eugenol precludes cutaneous chemical carcinogenesis in mouse by preventing oxidative stress and inflammation and by inducing apoptosis," *Molecular Carcinogenesis: Published in cooperation with the University of Texas MD Anderson Cancer Center*, vol. 49, no. 3, pp. 290–301, 2010.

[20] K. Pramod, S. H. Ansari, and J. Ali, "Eugenol: a natural compound with versatile pharmacological actions," *Natural product communications*, vol. 5, no. 12, p. 1934578X1000501, 2010.

[21] A. Fleischer, A. Ghadiri, F. Dessauge et al., "Modulating apoptosis as a target for effective therapy," *Molecular Immunology*, vol. 43, no. 8, pp. 1065–1079, 2006.

[22] N. Okada, A. Hirata, Y. Murakami, M. Shoji, H. Sakagami, and S. Fujisawa, "Induction of cytotoxicity and apoptosis and inhibition of cyclooxygenase-2 gene expression by eugenol-related compounds," *Anticancer Research*, vol. 25, no. 5, pp. 3263–3269, 2005.

[23] J.-L. Yi, S. Shi, Y. L. Shen et al., "Myricetin and methyl eugenol combination enhances the anticancer activity, cell cycle

arrest and apoptosis induction of cis-platin against HeLa cervical cancer cell lines," *International Journal of Clinical and Experimental Pathology*, vol. 8, no. 2, pp. 1116–1127, 2015.

[24] A. Gemma, K. Takenaka, Y. Hosoya et al., "Altered expression of several genes in highly metastatic subpopulations of a human pulmonary adenocarcinoma cell line," *European Journal of Cancer*, vol. 37, no. 12, pp. 1554–1561, 2001.

[25] F. H. Sarkar and Y. Li, "Using chemopreventive agents to enhance the efficacy of cancer therapy," *Cancer Research*, vol. 66, no. 7, pp. 3347–3350, 2006.

[26] D. R. Youlden, S. M. Cramb, C. H. Yip, and P. D. Baade, "Incidence and mortality of female breast cancer in the Asia-Pacific region," *Cancer Biology & Medicine*, vol. 11, no. 2, pp. 101–115, 2014.

[27] N. Vidhya and S. N. Devaraj, "Induction of apoptosis by eugenol in human breast cancer cells," *Indian Journal of Experimental Biology*, vol. 49, no. 11, pp. 871–878, 2011.

[28] M. Pisano, G. Pagnan, M. Loi et al., "Antiproliferative and pro-apoptotic activity of eugenol-related biphenyls on malignant melanoma cells," *Molecular Cancer*, vol. 6, no. 1, p. 8, 2007.

[29] S. Kachhap, A. Pratap, and D. S. Toppo, "Abdominal malignant melanoma: rare case report," *International Journal of Scientific Research*, vol. 8, no. 9, 2019.

[30] A. J. Miller and M. C. Mihm Jr., "Melanoma," *New England Journal of Medicine*, vol. 355, no. 1, pp. 51–65, 2006.

[31] M. Miyazawa and M. Hisama, "Suppression of chemical mutagen-induced SOS response by alkylphenols from clove (Syzygium aromaticum) in the Salmonella typhimurium TA1535/pSK1002 umu test," *Journal of Agricultural and Food Chemistry*, vol. 49, no. 8, pp. 4019–4025, 2001.

[32] G. C. Kim, D. S. Choi, J. S. Lim et al., "Caspases-dependent apoptosis in human melanoma cell by eugenol," *The Korean Journal of Anatomy*, vol. 39, no. 3, pp. 245–253, 2006.

[33] R. Ghosh, N. Nadiminty, J. E. Fitzpatrick, W. L. Alworth, T. J. Slaga, and A. P. Kumar, "Eugenol Causes Melanoma Growth Suppression through Inhibition of E2F1 Transcriptional Activity," *Journal of Biological Chemistry*, vol. 280, no. 7, pp. 5812–5819, 2005.

[34] D. M. Parkin, F. Bray, J. Ferlay, and P. Pisani, "Global cancer statistics, 2002," *CA: a Cancer Journal for Clinicians*, vol. 55, no. 2, pp. 74–108, 2005.

[35] E. F. Dunne and I. U. Park, "HPV and HPV-associated diseases," *Infectious Disease Clinics*, vol. 27, no. 4, pp. 765–778, 2013.

[36] C. M. Tarney and J. Han, "Postcoital bleeding: a review on etiology, diagnosis, and management," *Obstetrics and Gynecology International*, vol. 2014, Article ID 192087, 8 pages, 2014.

[37] İ. Gülcin, "Antioxidant and antiradical activities of L-carnitine," *Life Sciences*, vol. 78, no. 8, pp. 803–811, 2006.

[38] I. Gülçin, E. Bursal, M. H. Şehitoğlu, M. Bilsel, and A. C. Gören, "Polyphenol contents and antioxidant activity of lyophilized aqueous extract of propolis from Erzurum, Turkey," *Food and Chemical Toxicology*, vol. 48, no. 8-9, pp. 2227–2238, 2010.

[39] G. Anuj and S. Sanjay, "Eugenol: a potential phytochemical with multifaceted therapeutic activities," *Pharmacology*, vol. 2, pp. 108–120, 2010.

[40] İ. Gülçin, "Antioxidant activity of eugenol: a structure–activity relationship study," *Journal of Medicinal Food*, vol. 14, no. 9, pp. 975–985, 2011.

[41] S.-W. Huang and E. N. Frankel, "Antioxidant activity of tea catechins in different lipid systems," *Journal of Agricultural and Food Chemistry*, vol. 45, no. 8, pp. 3033–3038, 1997.

[42] H. Sies, *Oxidative Stress: Oxidants and Antioxidants*, Academic Press, New York, 1991.

[43] T. Atsumi, S. Fujisawa, and K. Tonosaki, "A comparative study of the antioxidant/prooxidant activities of eugenol and isoeugenol with various concentrations and oxidation conditions," *Toxicology In Vitro*, vol. 19, no. 8, pp. 1025–1033, 2005.

[44] D. P. Bezerra, G. Militão, M. de Morais, and D. de Sousa, "The dual antioxidant/prooxidant effect of eugenol and its action in cancer development and treatment," *Nutrients*, vol. 9, no. 12, p. 1367, 2017.

[45] M. OGATA, M. HOSHI, S. URANO, and T. ENDO, "Antioxidant activity of eugenol and related monomeric and dimeric compounds," *Chemical and Pharmaceutical Bulletin*, vol. 48, no. 10, pp. 1467–1469, 2000.

[46] E. Nagababu and N. Lakshmaiah, "Inhibition of microsomal lipid peroxidation and monooxygenase activities by eugenol," *Free Radical Research*, vol. 20, no. 4, pp. 253–266, 1994.

[47] K.-G. Lee and T. Shibamoto, "Antioxidant property of aroma extract isolated from clove buds [Syzygium aromaticum (L.) Merr. et Perry]," *Food Chemistry*, vol. 74, no. 4, pp. 443–448, 2001.

[48] H. Nam and M.-M. Kim, "Eugenol with antioxidant activity inhibits MMP-9 related to metastasis in human fibrosarcoma cells," *Food and Chemical Toxicology*, vol. 55, pp. 106–112, 2013.

[49] S. Fujisawa, T. Atsumi, Y. Kadoma, and H. Sakagami, "Antioxidant and prooxidant action of eugenol-related compounds and their cytotoxicity," *Toxicology*, vol. 177, no. 1, pp. 39–54, 2002.

[50] J. Chogo and G. Crank, "Chemical composition and biological activity of the Tanzanian plant Ocimum suave," *Journal of Natural Products*, vol. 44, no. 3, pp. 308–311, 1981.

[51] M. Asha, D. Prashanth, B. Murali, R. Padmaja, and A. Amit, "Anthelmintic activity of essential oil of _Ocimum sanctum_ and eugenol," *Fitoterapia*, vol. 72, no. 6, pp. 669-670, 2001.

[52] J. N. Barboza, C. da Silva Maia Bezerra Filho, R. O. Silva, J. V. R. Medeiros, and D. P. de Sousa, "An overview on the anti-inflammatory potential and antioxidant profile of eugenol," *Oxidative Medicine and Cellular Longevity*, vol. 2018, Article ID 3957262, 9 pages, 2018.

[53] M. A. Morsy and A. A. Fouad, "Mechanisms of gastroprotective effect of eugenol in indomethacin-induced ulcer in rats," *Phytotherapy Research: An International Journal Devoted to Pharmacological and Toxicological Evaluation of Natural Product Derivatives*, vol. 22, no. 10, pp. 1361–1366, 2008.

[54] S. Jain, R. R. Kulkarni, and D. P. Jain, "Current drug targets for antihyperlipidemic therapy," *Mini Reviews in Medicinal Chemistry*, vol. 10, no. 3, pp. 232–262, 2010.

[55] Å. L. Amundsen, L. Ose, M. S. Nenseter, and F. Y. Ntanios, "Plant sterol ester–enriched spread lowers plasma total and LDL cholesterol in children with familial hypercholesterolemia," *The American Journal of Clinical Nutrition*, vol. 76, no. 2, pp. 338–344, 2002.

[56] T. Ichihashi, M. Izawa, K. Miyata, T. Mizui, K. Hirano, and Y. Takagishi, "Mechanism of hypocholesterolemic action of S-8921 in rats: S-8921 inhibits ileal bile acid absorption," *Journal of Pharmacology and Experimental Therapeutics*, vol. 284, no. 1, pp. 43–50, 1998.

[57] W. Shi, M. E. Haberland, M. L. Jien, D. M. Shih, and A. J. Lusis, "Endothelial responses to oxidized lipoproteins determine genetic susceptibility to atherosclerosis in mice," *Circulation*, vol. 102, no. 1, pp. 75–81, 2000.

[58] E. Hopps, D. Noto, G. Caimi, and M. R. Averna, "A novel component of the metabolic syndrome: the oxidative stress," *Nutrition, Metabolism and Cardiovascular Diseases*, vol. 20, no. 1, pp. 72–77, 2010.

[59] M. M. Duarte, J. B. T. Rocha, R. N. Moresco et al., "Association between ischemia-modified albumin, lipids and inflammation biomarkers in patients with hypercholesterolemia," *Clinical Biochemistry*, vol. 42, no. 7-8, pp. 666–671, 2009.

[60] K. Srinivasan, "Antioxidant potential of spices and their active constituents," *Critical Reviews in Food Science and Nutrition*, vol. 54, no. 3, pp. 352–372, 2014.

[61] K. Venkadeswaran, A. R. Muralidharan, T. Annadurai et al., "Antihypercholesterolemic and antioxidative potential of an extract of the plant, Piper betle, and its active constituent, eugenol, in triton WR-1339-induced hypercholesterolemia in experimental rats," *Evidence-based Complementary and Alternative Medicine*, vol. 2014, Article ID 478973, 11 pages, 2014.

[62] L. F. L. Interaminense, D. M. Jucá, P. J. C. Magalhães, J. H. Leal-Cardoso, G. P. Duarte, and S. Lahlou, "Pharmacological evidence of calcium-channel blockade by essential oil of Ocimum gratissimum and its main constituent, eugenol, in isolated aortic rings from DOCA-salt hypertensive rats," *Fundamental & Clinical Pharmacology*, vol. 21, no. 5, pp. 497–506, 2007.

[63] C. E. N. Damiani, L. V. Rossoni, and D. V. Vassallo, "Vasorelaxant effects of eugenol on rat thoracic aorta," *Vascular Pharmacology*, vol. 40, no. 1, pp. 59–66, 2003.

[64] S. Jin and K.-H. Cho, "Water extracts of cinnamon and clove exhibits potent inhibition of protein glycation and antiatherosclerotic activity in vitro and in vivo hypolipidemic activity in zebrafish," *Food and Chemical Toxicology*, vol. 49, no. 7, pp. 1521–1529, 2011.

[65] A. Munisa and J. D. Parangtambung, "The effect of clove leaf methanol extract on the profiles of superoxide dismutase and malondialdehyde in the liver of rabbits under hypercholesterolemia condition," *Translational Biomedicine*, vol. 6, no. 2, pp. 1–5, 2015.

[66] O. Sensch, W. Vierling, W. Brandt, and M. Reiter, "Effects of inhibition of calcium and potassium currents in guinea-pig cardiac contraction: comparison of β-caryophyllene oxide, eugenol, and nifedipine," *British Journal of Pharmacology*, vol. 131, no. 6, pp. 1089–1096, 2000.

[67] R. Choudhary, K. Mishra, and C. Subramanyam, "Prevention of isoproterenol-induced cardiac hypertrophy by eugenol, an antioxidant," *Indian Journal of Clinical Biochemistry*, vol. 21, no. 2, p. 107, 2006.

[68] H. U. Tahir, R. A. Sarfraz, A. Ashraf, and S. Adil, "Chemical composition and antidiabetic activity of essential oils obtained from two spices (Syzygium aromaticum and Cuminum cyminum)," *International Journal of Food Properties*, vol. 19, no. 10, pp. 2156–2164, 2016.

[69] H. Genç Bilgiçli, A. Kestane, P. Taslimi et al., "Novel eugenol bearing oxypropanolamines: synthesis, characterization, antibacterial, antidiabetic, and anticholinergic potentials," *Bioorganic Chemistry*, vol. 88, p. 102931, 2019.

[70] S. Srinivasan, G. Sathish, M. Jayanthi, J. Muthukumaran, U. Muruganathan, and V. Ramachandran, "Ameliorating effect of eugenol on hyperglycemia by attenuating the key enzymes of glucose metabolism in streptozotocin-induced diabetic rats," *Molecular and Cellular Biochemistry*, vol. 385, no. 1-2, pp. 159–168, 2014.

[71] S. Hirst and L. Stapley, "Parasitology: the dawn of a new millennium," *Parasitology Today*, vol. 16, no. 1, pp. 1–3, 2000.

[72] A. M. el-kady, A. A. Ahmad, T. M. Hassan, H. E. M. el-Deek, S. S. Fouad, and S. S. al-Thaqfan, "<p>Eugenol, a potential schistosomicidal agent with anti-inflammatory and antifibrotic effects against Schistosoma mansoni, induced liver pathology</p>," *Infection and drug resistance*, vol. -Volume 12, pp. 709–719, 2019.

[73] D. G. Colley, A. L. Bustinduy, W. E. Secor, and C. H. King, "Human schistosomiasis," *The Lancet*, vol. 383, no. 9936, pp. 2253–2264, 2014.

[74] E. Quansah, E. Sarpong, and T. K. Karikari, "Disregard of neurological impairments associated with neglected tropical diseases in Africa," *Eneurologicalsci*, vol. 3, pp. 11–14, 2016.

[75] T. Vos, A. D. Flaxman, M. Naghavi et al., "Years lived with disability (YLDs) for 1160 sequelae of 289 diseases and injuries 1990-2010: a systematic analysis for the Global Burden of Disease Study 2010," *The Lancet*, vol. 380, no. 9859, pp. 2163–2196, 2012.

[76] D. M. Metwally, E. M. al-Olayan, M. Alanazi, S. B. Alzahrany, and A. Semlali, "Antischistosomal and anti-inflammatory activity of garlic and allicin compared with that of praziquantel in vivo," *BMC Complementary and Alternative Medicine*, vol. 18, no. 1, p. 135, 2018.

[77] H. Kato, E. Gomez, A. Cáceres, H. Uezato, T. Mimori, and Y. Hashiguchi, "Molecular epidemiology for vector research on leishmaniasis," *International Journal of Environmental Research and Public Health*, vol. 7, no. 3, pp. 814–826, 2010.

[78] R. R. Mendonça-Filho, I. A. Rodrigues, D. S. Alviano et al., "Leishmanicidal activity of polyphenolic-rich extract from husk fiber of _Cocos nucifera_ Linn. (Palmae)," *Research in Microbiology*, vol. 155, no. 3, pp. 136–143, 2004.

[79] T. Ueda-Nakamura, R. R. Mendonça-Filho, J. A. Morgado-Díaz et al., "Antileishmanial activity of Eugenol-rich essential oil from _Ocimum gratissimum_," *Parasitology International*, vol. 55, no. 2, pp. 99–105, 2006.

[80] E. Scallan, P. M. Griffin, F. J. Angulo, R. V. Tauxe, and R. M. Hoekstra, "Foodborne illness acquired in the United States—unspecified agents," *Emerging Infectious Diseases*, vol. 17, no. 1, pp. 16–22, 2011.

[81] K. P. Devi, S. A. Nisha, R. Sakthivel, and S. K. Pandian, "Eugenol (an essential oil of clove) acts as an antibacterial agent against _Salmonella typhi_ by disrupting the cellular membrane," *Journal of Ethnopharmacology*, vol. 130, no. 1, pp. 107–115, 2010.

[82] M. Hyldgaard, T. Mygind, and R. L. Meyer, "Essential oils in food preservation: mode of action, synergies, and interactions with food matrix components," *Frontiers in Microbiology*, vol. 3, p. 12, 2012.

[83] A. Marchese, R. Barbieri, E. Coppo et al., "Antimicrobial activity of eugenol and essential oils containing eugenol: a mechanistic viewpoint," *Critical Reviews in Microbiology*, vol. 43, no. 6, pp. 668–689, 2017.

[84] F. Nazzaro, F. Fratianni, L. de Martino, R. Coppola, and V. de Feo, "Effect of essential oils on pathogenic bacteria," *Pharmaceuticals*, vol. 6, no. 12, pp. 1451–1474, 2013.

[85] A. Gill and R. Holley, "Disruption of Escherichia coli, Listeria monocytogenes and Lactobacillus sakei cellular membranes by plant oil aromatics," *International Journal of Food Microbiology*, vol. 108, no. 1, pp. 1–9, 2006.

[86] C. T. Filgueiras and M. C. D. Vanetti, "Effect of eugenol on growth and listeriolysin O production by Listeria monocytogenes," *Brazilian Archives of Biology and Technology*, vol. 49, no. 3, pp. 405–409, 2006.

[87] D. Trombetta, F. Castelli, M. G. Sarpietro et al., "Mechanisms of antibacterial action of three monoterpenes," *Antimicrobial Agents and Chemotherapy*, vol. 49, no. 6, pp. 2474–2478, 2005.

[88] A. A. Catherine, H. Deepika, and P. S. Negi, "Antibacterial activity of eugenol and peppermint oil in model food systems," *Journal of Essential Oil Research*, vol. 24, no. 5, pp. 481–486, 2012.

[89] M. M. Iwu, "African medicinal plants in the search for new drugs based on ethnobotanical leads," in *Ciba Foundation Symposium 185-Ethnobotany and the Search for New Drugs: Ethnobotany and the Search for New Drugs: Ciba Foundation Symposium 185*, John Wiley & Sons, Ltd, Chichester, UK, 2007.

[90] S. Hemaiswarya and M. Doble, "Synergistic interaction of eugenol with antibiotics against Gram negative bacteria," *Phytomedicine*, vol. 16, no. 11, pp. 997–1005, 2009.

[91] S.-E. Moon, H.-Y. Kim, and J.-D. Cha, "Synergistic effect between clove oil and its major compounds and antibiotics against oral bacteria," *Archives of Oral Biology*, vol. 56, no. 9, pp. 907–916, 2011.

[92] G. Straface, A. Selmin, V. Zanardo, M. de Santis, A. Ercoli, and G. Scambia, "Herpes simplex virus infection in pregnancy," *Infectious Diseases in Obstetrics and Gynecology*, vol. 2012, Article ID 385697, 6 pages, 2012.

[93] F. Benencia and M. Courreges, "In vitro and in vivo activity of eugenol on human herpesvirus," *Phytotherapy Research: An International Journal Devoted to Pharmacological and Toxicological Evaluation of Natural Product Derivatives*, vol. 14, no. 7, pp. 495–500, 2000.

[94] A. Astani, J. Reichling, and P. Schnitzler, "Screening for antiviral activities of isolated compounds from essential oils," *Evidence-based Complementary and Alternative Medicine*, vol. 2011, Article ID nep187, 8 pages, 2011.

[95] A. T. Palamara, C. F. Perno, M. R. Ciriolo et al., "Evidence for antiviral activity of glutathione: in vitro inhibition of herpes simplex virus type 1 replication," *Antiviral Research*, vol. 27, no. 3, pp. 237–253, 1995.

[96] J. Serkedjieva and N. Manolova, "Plant polyphenolic complex inhibits the reproduction of influenza and herpes simplex viruses," in *Plant Polyphenols*, pp. 705–715, Springer, 1992.

[97] Y. Tragoolpua and A. Jatisatienr, "Anti-herpes simplex virus activities of Eugenia caryophyllus (Spreng.) Bullock & SG Harrison and essential oil, eugenol," *Phytotherapy Research: An International Journal Devoted to Pharmacological and Toxicological Evaluation of Natural Product Derivatives*, vol. 21, no. 12, pp. 1153–1158, 2007.

[98] J. Serkedjieva and S. Ivancheva, "Antiherpes virus activity of extracts from the medicinal plant Geranium sanguineum L," *Journal of Ethnopharmacology*, vol. 64, no. 1, pp. 59–68, 1998.

[99] A. A. Barquero, L. E. Alché, and C. E. Coto, "Antiviral activity of meliacine on the replication of a thymidine kinase-deficient mutant of herpes simplex virus type 1 alone and in combination with acyclovir," *International Journal of Antimicrobial Agents*, vol. 9, no. 1, pp. 49–55, 1997.

[100] M. Kurokawa, K. Nagasaka, T. Hirabayashi et al., "Efficacy of traditional herbal medicines in combination with acyclovir against herpes simplex virus type 1 infection in vitro and in vivo," *Antiviral Research*, vol. 27, no. 1-2, pp. 19–37, 1995.

[101] M. N. Prichard and C. Shipman Jr., "A three-dimensional model to analyze drug-drug interactions," *Antiviral Research*, vol. 14, no. 4-5, pp. 181–205, 1990.

[102] G. B. Zore, A. D. Thakre, S. Jadhav, and S. M. Karuppayil, "Terpenoids inhibit _Candida albicans_ growth by affecting membrane integrity and arrest of cell cycle," *Phytomedicine*, vol. 18, no. 13, pp. 1181–1190, 2011.

[103] C. Wang, J. Zhang, H. Chen, Y. Fan, and Z. Shi, "Antifungal activity of eugenol against Botrytis cinerea," *Tropical Plant Pathology*, vol. 35, no. 3, pp. 137–143, 2010.

[104] J. Sikkema, J. A. de Bont, and B. Poolman, "Mechanisms of membrane toxicity of hydrocarbons," *Microbiological Reviews*, vol. 59, no. 2, pp. 201–222, 1995.

[105] A. Ahmad, A. Khan, L. A. Khan, and N. Manzoor, "In vitro synergy of eugenol and methyleugenol with fluconazole against clinical Candida isolates," *Journal of Medical Microbiology*, vol. 59, no. 10, pp. 1178–1184, 2010.

[106] R. Medzhitov, "Origin and physiological roles of inflammation," *Nature*, vol. 454, no. 7203, pp. 428–435, 2008.

[107] L. Ferrero-Miliani, O. H. Nielsen, P. S. Andersen, and S. E. Girardin, "Chronic inflammation: importance of NOD2 and NALP3 in interleukin-1beta generation," *Clinical & Experimental Immunology*, vol. 147, no. 2, pp. 227–235, 2007.

[108] R. A. Saraiva, M. K. A. Araruna, R. C. Oliveira et al., "Topical anti-inflammatory effect of _Caryocar coriaceum_ Wittm. (Caryocaraceae) fruit pulp fixed oil on mice ear edema induced by different irritant agents," *Journal of Ethnopharmacology*, vol. 136, no. 3, pp. 504–510, 2011.

[109] A. Ayala, M. F. Muñoz, and S. Argüelles, "Lipid peroxidation: production, metabolism, and signaling mechanisms of malondialdehyde and 4-hydroxy-2-nonenal," *Oxidative Medicine and Cellular Longevity*, vol. 2014, Article ID 360438, 31 pages, 2014.

[110] S. K. Biswas, J. B. Lopes, and D. Faria, "Which comes first: renal inflammation or oxidative stress in spontaneously hypertensive rats?," *Free Radical Research*, vol. 41, no. 2, pp. 216–224, 2007.

[111] C. B. Magalhães, D. R. Riva, L. J. DePaula et al., "In vivo anti-inflammatory action of eugenol on lipopolysaccharide-induced lung injury," *Journal of Applied Physiology*, vol. 108, no. 4, pp. 845–851, 2010.

[112] X. Huang, Y. Liu, Y. Lu, and C. Ma, "Anti-inflammatory effects of eugenol on lipopolysaccharide-induced inflammatory reaction in acute lung injury via regulating inflammation and redox status," *International Immunopharmacology*, vol. 26, no. 1, pp. 265–271, 2015.

[113] P. Patlevič, J. Vašková, P. Švorc Jr., L. Vaško, and P. Švorc, "Reactive oxygen species and antioxidant defense in human gastrointestinal diseases," *Integrative medicine research*, vol. 5, no. 4, pp. 250–258, 2016.

[114] J. Feng and J. Lipton, "Eugenol: antipyretic activity in rabbits," *Neuropharmacology*, vol. 26, no. 12, pp. 1775–1778, 1987.

[115] P. Brodin and A. Røed, "Effects of eugenol on rat phrenic nerve and phrenic nerve-diaphragm preparations," *Archives of Oral Biology*, vol. 29, no. 8, pp. 611–615, 1984.

[116] W. Hume, "Effect of eugenol on constrictor responses in blood vessels of the rabbit ear," *Journal of Dental Research*, vol. 62, no. 9, pp. 1013–1015, 1983.

[117] F. Dewhirst and J. Goodson, "Prostaglandin synthetase inhibition by eugenol, guaiacol and other dental medicaments," in *Journal of Dental Research*, vol. 53, p. 104, American Association for Dental Research, Alexandria, VA, USA, 1974.

[118] K. Markowitz, M. Moynihan, M. Liu, and S. Kim, "Biologic properties of eugenol and zinc oxide-eugenol: a clinically oriented review," *Oral Surgery, Oral Medicine, Oral Pathology*, vol. 73, no. 6, pp. 729–737, 1992.

[119] G. Chung, J. N. Rhee, S. J. Jung, J. S. Kim, and S. B. Oh, "Modulation of CaV2. 3 calcium channel currents by eugenol," *Journal of Dental Research*, vol. 87, no. 2, pp. 137–141, 2008.

[120] C.-K. Park, H. Y. Li, K. Y. Yeon et al., "Eugenol inhibits sodium currents in dental afferent neurons," *Journal of Dental Research*, vol. 85, no. 10, pp. 900–904, 2006.

[121] S.-J. Lee, J. I. Han, G. S. Lee et al., "Antifungal effect of eugenol and nerolidol against Microsporum gypseum in a guinea pig model," *Biological and Pharmaceutical Bulletin*, vol. 30, no. 1, pp. 184–188, 2007.

[122] M. Inoue, T. Fujita, M. Goto, and E. Kumamoto, "Presynaptic enhancement by eugenol of spontaneous excitatory transmission in rat spinal substantia gelatinosa neurons is mediated by transient receptor potential A1 channels," *Neuroscience*, vol. 210, pp. 403–415, 2012.

[123] H. Aoshima and K. Hamamoto, "Potentiation of GABAA receptors expressed in Xenopus oocytes by perfume and phytoncid," *Bioscience, Biotechnology, and Biochemistry*, vol. 63, no. 4, pp. 743–748, 1999.

[124] B. Yang, Z. G. Piao, Y. B. Kim et al., "Activation of vanilloid receptor 1 (VR1) by eugenol," *Journal of Dental Research*, vol. 82, no. 10, pp. 781–785, 2003.

[125] C.-K. Park, K. Kim, S. J. Jung et al., "Molecular mechanism for local anesthetic action of eugenol in the rat trigeminal system," *PAIN*, vol. 144, no. 1, pp. 84–94, 2009.

[126] C. E. Ferland, F. Beaudry, and P. Vachon, "Antinociceptive effects of eugenol evaluated in a monoiodoacetate-induced osteoarthritis rat model," *Phytotherapy Research*, vol. 26, no. 9, pp. 1278–1285, 2012.

[127] A. N. Daniel, S. M. Sartoretto, G. Schmidt, S. M. Caparroz-Assef, C. A. Bersani-Amado, and R. K. N. Cuman, "Anti-inflammatory and antinociceptive activities A of eugenol essential oil in experimental animal models," *Revista Brasileira de Farmacognosia*, vol. 19, no. 1B, pp. 212–217, 2009.

[128] S. L. Bodhankar, R. Kurian, D. K. Arulmozhi, and A. Veeranjaneyulu, "Effect of eugenol on animal models of nociception," *Indian Journal of Pharmacology*, vol. 38, no. 5, p. 341, 2006.

[129] Y. Irie, "Effects of eugenol on the central nervous system: its possible application to treatment of Alzheimer's disease, depression, and Parkinson's disease," *Current Bioactive Compounds*, vol. 2, no. 1, pp. 57–66, 2006.

[130] Y. Irie and W. M. Keung, "Rhizoma acori graminei and its active principles protect PC-12 cells from the toxic effect of amyloid-β peptide," *Brain Research*, vol. 963, no. 1-2, pp. 282–289, 2003.

[131] G. Bupesh, K. Meenakumari, J. Prabhu et al., "Molecular properties and insilico neuroprotective activity of eugenol against glutamate metabotrophic receptors," *International Journal of Pharmaceutical Sciences Review & Research*, vol. 40, no. 1, pp. 318–323, 2016.

[132] H. Kabuto, M. Tada, and M. Kohno, "Eugenol [2-methoxy-4-(2-propenyl) phenol] prevents 6-hydroxydopamine-induced dopamine depression and lipid peroxidation inductivity in mouse striatum," *Biological and Pharmaceutical Bulletin*, vol. 30, no. 3, pp. 423–427, 2007.

[133] M. Müller, H. C. Pape, E. J. Speckmann, and A. Gorji, "Effect of eugenol on spreading depression and epileptiform discharges in rat neocortical and hippocampal tissues," *Neuroscience*, vol. 140, no. 2, pp. 743–751, 2006.

[134] P. Sen, P. C. Maiti, S. Puri, A. Ray, N. A. Audulov, and A. V. Valdman, "Mechanism of anti-stress activity of Ocimum sanctum Linn, eugenol and Tinospora malabarica in experimental animals," *Indian Journal of Experimental Biology*, vol. 30, no. 7, pp. 592–596, 1992.

[135] K. Yazaki, "Study of behavioral pharmacology on rats. Tranquilizing effects induced by endogenous or exogenous bradykinin. Shika gakuho," *Dental Science Reports*, vol. 89, no. 10, pp. 1529–1548, 1989.

[136] D. Garabadu, A. Shah, A. Ahmad et al., "Eugenol as an anti-stress agent: modulation of hypothalamic–pituitary–adrenal axis and brain monoaminergic systems in a rat model of stress," *Stress*, vol. 14, no. 2, pp. 145–155, 2011.

[137] D. Garabadu, A. Shah, S. Singh, and S. Krishnamurthy, "Protective effect of eugenol against restraint stress-induced gastrointestinal dysfunction: potential use in irritable bowel syndrome," *Pharmaceutical Biology*, vol. 53, no. 7, pp. 968–974, 2015.

[138] S. N. Prasad, "Neuroprotective efficacy of eugenol and isoeugenol in acrylamide-induced neuropathy in rats: behavioral and biochemical evidence," *Neurochemical Research*, vol. 38, no. 2, pp. 330–345, 2013.

[139] P. Srivastava and R. S. Yadav, "Efficacy of natural compounds in neurodegenerative disorders," in *The Benefits of Natural Products for Neurodegenerative Diseases*, pp. 107–123, Springer, 2016.

[140] M. Wahid, A. Ali, F. Saqib et al., "Pharmacological exploration of traditional plants for the treatment of neurodegenerative disorders," *Phytotherapy research*, vol. 34, no. 12, pp. 3089–3112, 2020.

[141] D. C. Rubinsztein, "The roles of intracellular protein-degradation pathways in neurodegeneration," *Nature*, vol. 443, no. 7113, pp. 780–786, 2006.

[142] P. F. C. Lim, X. Y. Liu, L. Kang, P. C. L. Ho, Y. W. Chan, and S. Y. Chan, "Limonene GP1/PG organogel as a vehicle in transdermal delivery of haloperidol," *International Journal of Pharmaceutics*, vol. 311, no. 1-2, pp. 157–164, 2006.

[143] R. Jeevan, R. Venkat, M. A. Khan et al., "Effect of menthol and related terpenes on the percutaneous absorption of propranolol across excised hairless mouse skin," *Journal of Pharmaceutical Sciences*, vol. 86, no. 12, pp. 1369–1373, 1997.

[144] Q. Shen, W. Li, and W. Li, "The effect of clove oil on the transdermal delivery of ibuprofen in the rabbit by in vitro and in vivo methods," *Drug Development and Industrial Pharmacy*, vol. 33, no. 12, pp. 1369–1374, 2007.

[145] M. H. Medeiros, P. Dimascio, A. P. Pinto, R. R. Vargas, and E. J. H. Bechara, "Horseradish peroxidase-catalyzed

conjugation of eugenol with basic amino acids," *Free Radical Research*, vol. 25, no. 1, pp. 5–12, 1996.

[146] H. Someya, Y. Higo, M. Ohno, T. W. Tsutsui, and T. Tsutsui, "Clastogenic activity of seven endodontic medications used in dental practice in human dental pulp cells," *Mutation Research/Genetic Toxicology and Environmental Mutagenesis*, vol. 650, no. 1, pp. 39–47, 2008.

[147] R. Gerosa, M. Borin, G. Menegazzi, M. Puttini, and G. Cavalleri, "In vitro evaluation of the cytotoxicity of pure eugenol," *Journal of Endodontics*, vol. 22, no. 10, pp. 532–534, 1996.

[148] S. P. Brinker, "Provisional excellence with zinc-oxide non-eugenol temporary cement," *Provider*, vol. 501, p. 355110, 2014.

[149] S. A. GUENETTE, F. BEAUDRY, J. F. MARIER, and P. VACHON, "Pharmacokinetics and anesthetic activity of eugenol in male Sprague–Dawley rats," *Journal of Veterinary Pharmacology and Therapeutics*, vol. 29, no. 4, pp. 265–270, 2006.

[150] S. A. Tajuddin, A. Latif, and I. A. Qasmi, "Aphrodisiac activity of 50% ethanolic extracts of Myristica fragrans Houtt.(nutmeg) and Syzygium aromaticum (L) Merr. & Perry.(clove) in male mice: a comparative study," *BMC Complementary and Alternative Medicine*, vol. 3, p. 6, 2003.

[151] R. Capasso, L. Pinto, M. L. Vuotto, and G. di Carlo, "Preventive effect of eugenol on PAF and ethanol-induced gastric mucosal damage," *Fitoterapia*, vol. 71, pp. S131–S137, 2000.

[152] A. Bennett, I. F. Stamford, I. A. Tavares et al., "The biological activity of eugenol, a major constituent of nutmeg (Myristica fragrans): studies on prostaglandins, the intestine and other tissues," *Phytotherapy Research*, vol. 2, no. 3, pp. 124–130, 1988.

[153] S. Karmakar, M. Choudhury, A. S. Das, A. Maiti, S. Majumdar, and C. Mitra, "Clove (Syzygium aromaticum Linn) extract rich in eugenol and eugenol derivatives shows bone-preserving efficacy," *Natural Product Research*, vol. 26, no. 6, pp. 500–509, 2012.

Research Article

Protective Effect of Jiang Tang Xiao Ke Granules against Skeletal Muscle IR via Activation of the AMPK/SIRT1/PGC-1α Signaling Pathway

Ying Bai [1], **Jiacheng Zuo,**[1] **Xin Fang,**[2] **Rufeng Ma,**[1] **Tian Tian,**[1] **Fangfang Mo,**[1] **Qianqian Mu,**[3] **Yi Zhang,**[4] **Na Yu,**[5] **Xueli Bao,**[2] **Dongwei Zhang,**[1] **Sihua Gao** [1] [1] **and Dandan Zhao** [1] [1]

[1]*College of Traditional Chinese Medicine, Beijing University of Chinese Medicine, Beijing, China*
[2]*Beijing University of Chinese Medicine Affiliated Third Hospital, Beijing, China*
[3]*Dongzhimen Hospital of Beijing University of Chinese Medicine, Beijing, China*
[4]*School of City Management, Beijing Open University, Beijing, China*
[5]*Educational Office, Beijing Tiantan Hospital, Capital Medical University, Beijing, China*

Correspondence should be addressed to Sihua Gao; gaosihua1216@163.com and Dandan Zhao; bucmzhaodandan@163.com

The Jiang Tang Xiao Ke (JTXK) granule is a classic Chinese herbal formula that has been put into clinical use in the treatment of type 2 diabetes mellitus for decades. However, whether its ability to ameliorate skeletal muscle insulin resistance (IR) is through modulation of the AMPK/SIRT1/PGC-1α signaling pathway remains unknown. Therefore, we aimed to investigate the effects of JTXK granules on IR in skeletal muscle of high-fat diet-induced diabetic mice and C2C12 cells and analyze the underlying mechanisms. In the present study, we showed that JTXK granules attenuated body weight gain, reduced body fat mass, improved body lean mass, and enhanced muscle performance of diabetic mice. JTXK granules also improved glucose metabolism and skeletal muscle insulin sensitivity and partially reversed abnormal serum lipid levels, which might be related to the regulation of the AMPK/SIRT1/PGC-1α pathway, both in skeletal muscle tissue of diabetic mice and in C2C12 cells. Furthermore, drug-containing serum of JTXK granules was capable of enhancing glucose uptake and mitochondrial respiration in C2C12 cells, and AMPKα was proven to be closely involved in this process. Taken together, these results suggest that the JTXK granule ameliorates skeletal muscle IR through activation of the AMPK/SIRT1/PGC-1α signaling pathway, which offers a novel perspective of this formula to combat IR-related metabolic diseases.

1. Introduction

Insulin resistance (IR) is a heterogeneous metabolic defect that primarily refers to the abnormality of insulin-mediated glucose disposal [1]. IR is not only the main characteristic of obesity or type 2 diabetes mellitus (T2DM) but also the promoter of these metabolic diseases [2]. Skeletal muscle, accounting for the largest portion of insulin-mediated glucose uptake, utilization, and storage, is crucial in metabolic disorders [3, 4]. Enormous evidence

has shown that mitochondrial dysfunction in skeletal muscle tissue plays an essential role in impaired insulin signaling. A reduced rate of mitochondrial ATP synthesis was observed in skeletal muscle of obese patients, prediabetic patients, and offspring of diabetic patients [5, 6]. Long-term hyperglycemia and hyperlipidemia lead to mitochondrial impairment [7], and mitochondrial dysfunction in turn will aggravate glucolipid metabolic disorder [8]. Therefore, maintaining the functional integrity of skeletal muscle mitochondria is considered an important approach

to improve insulin sensitivity and glucolipid metabolism [9, 10].

Activation of adenosine monophosphate-activated protein kinase (AMPK) in response to insulin can boost the translocation of GLUT4 from the cytoplasm to the membrane and promote glucose uptake, transportation, and utilization [11]. Besides that, AMPK activation can also improve fatty acid oxidation, reduce ectopic lipid deposition in skeletal muscle cells, and thus increase insulin sensitivity [12]. In addition, AMPK promotes mitochondrial synthesis by directly phosphorylating peroxisome proliferator-activated receptor coactivator 1 α (PGC-1α). PGC-1α is known to increase gene expressions that are related to long-chain fatty acid oxidation, mitochondrial DNA replication, and cellular oxidative metabolism [13]. Meanwhile, sirtuin 1 (SIRT1) is an important energy metabolism monitor with NAD^+-dependent deacetylase activity, and it has been proven to interact with PGC-1α [14]. By activating the AMPK/-SIRT1/PGC-1α axis, mitochondrial synthesis and oxidative phosphorylation can be promoted, and high-fat diet-(HFD) induced obesity and IR thus can be retarded.

The Jiang Tang Xiao Ke (JTXK) granule, composed of *Rehmannia glutinosa* (Gaertn.) DC. (Dihuang), *Panax ginseng* C.A.Mey. (Renshen), *Coptis chinensis* Franch. (Huanglian), *Salvia miltiorrhiza* Bunge (Danshen), and so on, is a classic formula from traditional Chinese medicine. Our previous studies have shown that JTXK granules exhibited an overt therapeutic effect in the management of diabetes through the improvement of glucolipid metabolism, protection of islet ßeta-cells, and inhibition of oxidative stress and inflammatory reactions in various organs and tissues [15–18]. There are studies supporting that the main active ingredients from this herbal formula, for example, berberine and ginsenoside Rb1, are capable of activating AMPK signaling [19, 20]. However, whether and how JTXK granule ameliorates skeletal muscle IR is still not clear. Therefore, we attempted to investigate the role of JTXK granules in the control of skeletal muscle IR in HFD-induced diabetic mice and C2C12 cells, as well as their influence on the AMPK/-SIRT1/PGC-1α signaling pathway.

2. Materials and Methods

2.1. Reagents and Equipment.
JTXK granule was produced and quality-controlled as previously reported [17]. The fingerprint of this granule that illustrated the main ingredients is shown in Supplementary Figure 1 (S1). C2C12 cells were obtained from the National Infrastructure of Cell Line Resource (Beijing, China). The blood lipid kits were purchased from Nanjing Jiancheng Bioengineering Institute (Nanjing, China). Equipment used in the study includes the NMR animal body composition analyzer from Shanghai Newmai Electronic Technology Co., Ltd. (Shanghai, China), as well as the Hitachi 7080 automatic biochemical analyzer (Tokyo, Japan). Antibodies against AMPKα, SIRT1, PGC-1α, PPARα, and UCP3 (Cat #: ab32047, ab110304, ab54481, ab215270, and ab180643) were purchased from Abcam (Cambridge, UK); antibodies against CPT1 and Na,K-ATPase (ab12252; 3010S) were from Cell Signaling Technol-ogy (Danvers, USA); and antibodies against GLUT4 and Lamin B1 (66846-1-lg; 66095-1-lg) were from Proteintech (Rosemont, USA). All other materials are commercially available.

2.2. Animal Models and Experimental Design.
Male 8-week-old C57BL6/J mice were purchased from Beijing Sibeifu Animal Technology Co., Ltd. (Beijing, China). Mice were kept on an ad libitum basis and allowed free access to tap water and feed. All the mice were housed in the animal laboratory with a barrier environment in Beijing University of Chinese Medicine (certification number SCXK (Jing) 2016-0002) with a temperature of 25°C and humidity of 55 ± 5%. The protocols were approved by the Animal Care Committee of Beijing University of Chinese Medicine (Beijing, China).

After one week of adaptive feeding, mice were randomly divided into the normal group (NC group, $n = 8$) and HFD-fed group ($n = 32$). Mice in the normal group were fed the standard chow diet (AIN-96G feed from Sibeifu Bioscience Co., Ltd., Beijing, China), while their counterparts received HFD feeding, of which 45% of calories are from fat (MD12032, Jiangsu Hengrui Medicine Co., Ltd., Jiangsu, China) during the entire experiment. The diabetic model induction process lasted 12 weeks. After 12 weeks of feeding, mice whose body weight gain was 20% heavier than the average weight of the normal group with fasting blood glucose higher than 7.0 mmol/L were considered diabetic mice [21]. Then, the eligible diabetic mice were randomly divided into the model group (DM group), metformin group (Met group), and JTXK group with 8 mice in each. Mice in the metformin group were administrated with metformin (100 mg/kg) by gavage; mice in the JTXK group were given JTXK granules dissolved in sterilized water (1.75 g/kg); mice in the normal and DM groups received the same amount of sterile water. During the treatment, body weight and food intake were recorded once a week. After 8 weeks of intervention, the body composition of all mice was assessed by the NMR animal body composition analyzer. Then, all mice were sacrificed after anesthesia with 4% formaldehyde with their blood sample and skeletal muscle tissue collected for further analysis. The experimental design is shown in Figure 1(a).

2.3. Glucose and Insulin Tolerance Test.
The oral glucose tolerance test (OGTT) was performed after the mice were fasted for 8 h from 7:00 a.m. to 3:00 p.m. Blood glucose levels were assessed before and 30, 60, 90, and 120 min after intragastric administration of glucose (2 g/kg) to the mice. For the insulin tolerance test (ITT), mice were firstly fasted for 5 h from 8:00 a.m. to 1:00 p.m., then were injected intraperitoneally with insulin (0.5 U/kg). Blood glucose levels were measured before and 30, 60, 90, and 120 min after injection.

2.4. Treadmill Test.
A treadmill test was used to evaluate exercise capacity and endurance. Before the formal test, mice in each group received a 6-day treadmill adaption training, which was to set the speed to 10 m/min and the running platform to 5° and allow mice to run for 5 min. When the formal test was performed, set the treadmill to 5° and the speed to 20 m/min [20]. The exhaustion standard included the following:

(a)

(b)

(c)

(d)

(e)

(f)

Figure 1: Continued.

(g)

(h)

(i)
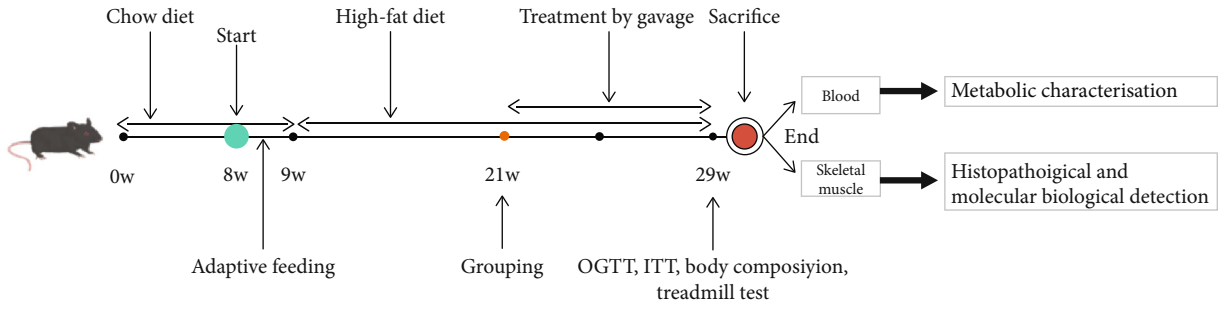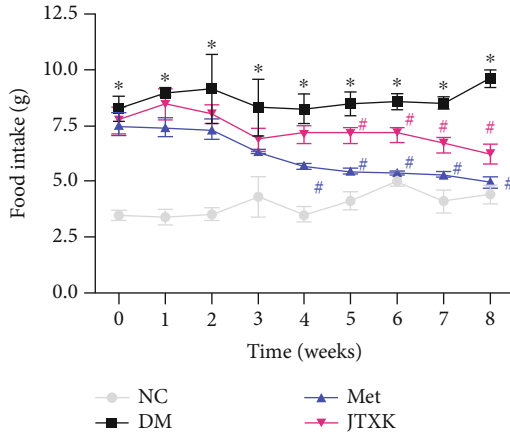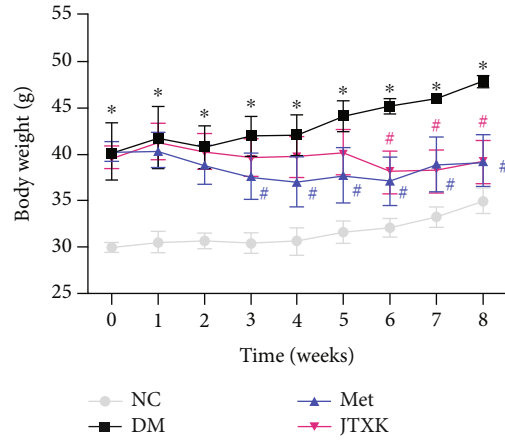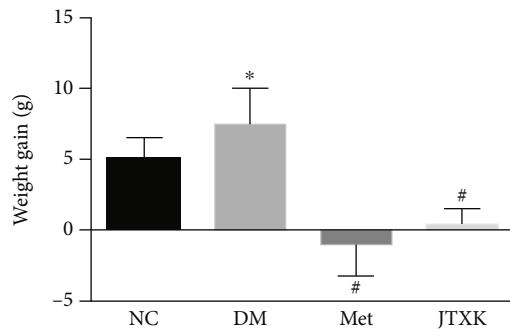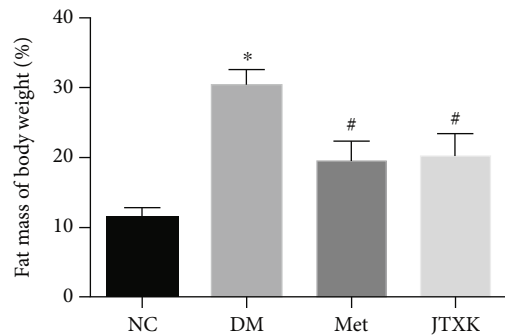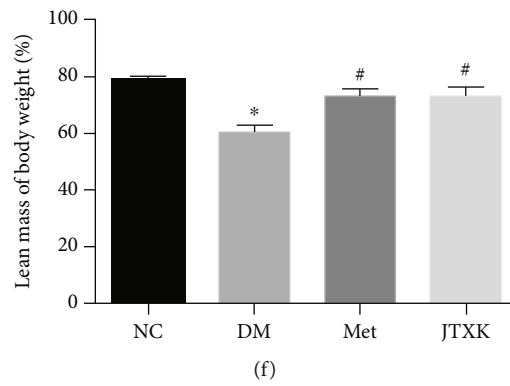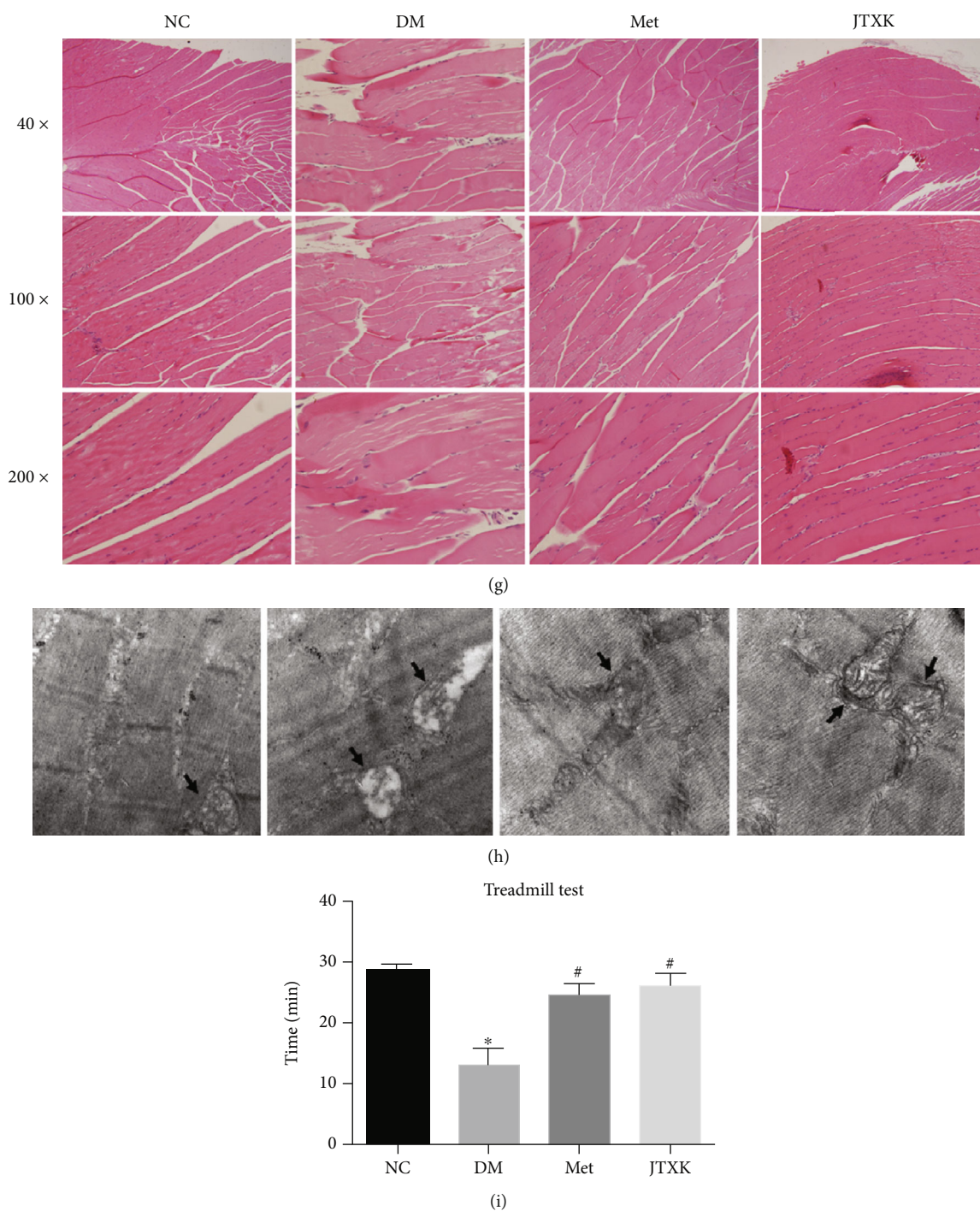
FIGURE 1: Effect of JTXK granules on HFD-fed diabetic mice. (a) Experimental design of the present study. (b) Food intake of mice in each group. (c, d) Body weight alteration. (e) Body fat rate and (f) body lean rate of mice after the intervention. (g) H&E staining and (h) electron microscopy of skeletal muscle tissue. (i) Treadmill test results of the mice in each group. NC, DM, Met, and JTXK mean the normal control, diabetes, metformin, and Jiang Tang Xiao Ke granule groups, respectively. Data were presented as mean ± SD. $n = 8$ in each group. $^{*}P < 0.05$, compared with the NC group. $^{#}P < 0.05$, compared with the DM group.

continuous drop into the powder grip with shock, resting in the abdomen position, being always in the last third of the runway, being short of breath, and unable to run on the treadmill for 10 s despite mechanical prodding. The exhaustion time of each mouse was recorded for analysis.

2.5. Biochemical Analysis. Serum triglyceride (TG), total cholesterol (TC), high-density lipoprotein (HDL), and low-density lipoprotein (LDL) were determined using the commercial assay kits from Nanjing Jiancheng Bioengineering Institute (Nanjing, China). All the assays were conducted in

accordance with the manufacturer's instructions. Absorbance values of these measurements were detected by the automatic biochemical analyzer.

2.6. Skeletal Muscle Tissue Hematoxylin and Eosin Staining. The skeletal muscles were exposed, and then the gastrocnemius muscles from the hind limb were collected. The skeletal muscle tissue was fixed in a 4% neutral formaldehyde buffer for 24 h and then embedded in paraffin. Next, the embedded paraffin blocks were cut into 4 μm sections and stained with hematoxylin and eosin according to the set routine. The optical microscope (Olympus, Japan) was used to observe the histopathological changes in muscular tissue.

2.7. Transmission Electron Microscopy (TEM). Skeletal tissue was immediately rinsed in PBS after removing from the mice. The tissue was diced into 2 mm cubes and fixed with 4% glutaraldehyde and 0.2% tannic acid in PBS overnight. Samples were washed with PBS and postfixed in 1% osmium tetroxide for 2 h. Samples were then dehydrated through a graded series of acetone and embedded in SPI-Pon 812 resin (SPI Co., USA) 24 h at 36°C, 48°C, and 60°C, respectively. Embedded tissue was cut into 70 nm sections and stained with uranyl acetate (30 min), followed by 0.2% lead citrate (30 min). Images were photographed under an electron microscope (Hitachi H-7650, Japan).

2.8. Cell Culture and Experimental Design. C2C12 cells were cultured in DMEM containing 10% fetal bovine serum (FBS). All the cells were cultured at 37°C with 95% humidity and 5% CO_2. Cells were passaged every 2-3 days. When cells grew to 80% confluence, the medium was replaced by high-glucose (25 mM) DMEM containing 2% horse serum to induce differentiation. Differentiation media were replenished every other day by removing 75% of the cell medium, followed by adding the fresh medium. Then, the differentiated C2C12 myotubes were treated with DMEM containing 0.4 mmol/L of palmitic acid and 1% FBS for 24 h to induce IR. For the treatment, the C2C12 myotube cells were incubated in the medium containing DCS of JTXK or control serum for 48 h.

2.9. Preparation of Drug-Containing Serum of JTXK. The drug-containing serum (DCS) of JTXK was obtained following our previous procedures [22]. Specifically, we administrated JTXK granules to rats (10.7 g/kg BW) by gavage for 3 consecutive days. And on the third day, rats were sacrificed and blood samples were taken and centrifuged for collecting the DCS. The control rats were given the same amount of water to provide control serum.

2.10. Construction of the AMPKα Knockdown Cell Line. Generation of the AMPKα knockdown cell line was accomplished by Genloci Biotechnologies, Inc. (Jiangsu, China). The sequence of the siRNA oligo specific for AMPKα (Gene ID: 105787) was GTTGGATTTCCGTAGTATTAT. Cells were suspended in a sterile tube, centrifuged at 1000 rpm for 4 min, and added with DPBS. And then, 30 μg of pEGFP-N1 plasmid with siRNA was added to the system and delivered to the cells by electroporation at 600 V (30

ms, 1 pulse). The transfected cells were cultured in DMEM for 48 h and then transferred into a medium containing 2 μg/mL Puro. Then, limiting dilution analysis was applied to screen out positive clones and RT-PCR was conducted to confirm the transfection rate.

2.11. Glucose Consumption Assay. The glucose oxidase method was used to examine the glucose levels in the culture medium of the C2C12 cells. According to the manufacturer's instructions, 5 μL of the supernatant or different concentrations of the glucose standard solution were added into a 195 μL working solution. The absorbance was determined at 570 nm after incubation for 20 min at 37°C. The glucose consumption was calculated by the glucose concentration of blank wells subtracted from that of cell-plated wells.

2.12. Mitochondrial Function Evaluation. Mitochondrial function was evaluated by measuring the oxygen consumption rate on the Seahorse XF Extracellular Flux Analyzer (Seahorse Bioscience, USA) according to the manufacturer's protocol. The C2C12 cells were treated with the JTXK drug-containing serum or control vehicle in XF24 analyzer microplates. 48 h later, the medium was changed to an XF basic medium supplemented with 11 mM glucose, 4 mM glutamine, and 2 mM pyruvate. Then, the cells were incubated with the sequential addition of 1 μM oligomycin, 5 μM carbonyl cyanide-(trifluoromethoxy)phenylhydrazone, and 0.5 μM rotenone/antimycin A. The mitochondrial respiratory parameters, such as basal respiration, ATP production, maximum respiration, and spare respiratory capacity, were calculated.

2.13. Western Blotting. Proteins were extracted from skeletal muscle tissue and C2C12 cells with a precool RIPA lysis buffer containing 1% PMSF. After centrifugation, the total protein was extracted and the concentration was measured according to the BCA kit. Equal amounts of total protein per sample were subjected via SDS-PAGE separation gel and concentration gel and transferred to polyvinylidene fluoride (PVDF) membranes using a wet blotting system (Bio-Rad Laboratories, Inc., USA). Membranes were blocked with 5% skim milk dissolved in Tris-buffered saline and incubated with diluted AMPKα, CPT1, PGC-1α, PPARα, SIRT1, UCP3, and GLUT4 (1 : 1000, 5% skim milk diluted) at 4°C overnight. On the following day, the membrane was incubated for 1.5 h with the horseradish peroxidase- (HRP-) conjugated secondary antibody (1 : 5000 diluted) at room temperature. Then, the membranes were incubated with high-sensitivity ECL luminous liquid (Proteintech Biotechnology, USA), and images were captured with Azure Biosystems, Inc., USA. Densitometry analyses of immunoblots were performed with the ImageJ software package.

2.14. Real-Time PCR (RT-PCR). Total RNA was isolated from skeletal muscle and C2C12 cells with the TRIzol reagent according to the manufacturer's instructions. cDNA was synthesized using a RevertAid First Strand cDNA Synthesis Kit (Thermo Fisher Scientific, USA). RT-PCR was performed on a StepOne™ RT-PCR System (Applied Biosystems, USA) using the SYBR Green Master Mix (Invitrogen,

TABLE 1: Sequences of RT-PCR primers.

Gene	Primer sequences (5′-3′)
AMPKα	F: AAACCCACAGAAATCCAAACAC
	R: CCTTCCATTCATAGTCCAACTG
PGC-1α	F: CCCTGCCATTGTTAAGACC
	R: TGCTGCTGTTCCTGCTCCT
SIRT1	F: TTGTGAAGCTGTTCGTGGAG
	R: GGCGTGGAGGTTTTTCAGTA
PPARα	F: AGGAAGCCGTTCTGTGACAT
	R: TTGAAGGAGCTTTGGGAAGA
CPT1	F: AGAACCACCAAAGCGGAAA
	R: TCCCACAGGAGACAGAAACC
UCP3	F: CCCTGACTCCTTCCTCCCTG
	R: GCACTGCAGCCTGTTTTGCTGA

USA). The amplification conditions were set as follows: pre-denaturation at 95°C for 10 min, followed by 40 cycles of amplification (95°C for 15 s, 60°C for 60 s). For each sample, PCR reactions were run in triplicate. And for each group, there were six samples. The gene-specific primers are shown in Table 1. Calculations were performed by a comparative method (such as $2^{-\Delta\Delta CT}$).

2.15. Statistical Analysis. All data were presented as mean ± standard deviation (SD). Datasets with more than two groups to be compared were analyzed using one-way analysis of variance (ANOVA) and Tukey's post hoc multiple comparison test. For statistical analyses of groups comparing two variables, two-way ANOVA was conducted, followed by Tukey's post hoc multiple comparison test. $P < 0.05$ was considered statistically significant. All the figures and statistical analyses were generated on GraphPad Prism 7 (GraphPad Software, USA).

3. Results

3.1. JTXK Granules Attenuated Body Weight Gain and Improved Skeletal Muscle Content and Performance. Twelve weeks of HFD feeding caused significant overeating of obese diabetic mice, while treatment with metformin or JTXK significantly reduced food intake (Figure 1(b)). As a consequence, mice in the metformin and JTXK groups exhibited significant weight loss compared with DM group mice after corresponding treatment (Figures 1(c) and 1(d)). The results of body composition showed that after 8 weeks of treatment, mice in the DM group showed a significantly higher body fat rate and less body lean mass than mice in the normal control group. Body fat rates of mice in the Met and JTXK groups, which were 19.50% and 20.29%, respectively, were significantly lower than that of DM mice (30.46%) (Figure 1(e), $P < 0.05$). Meanwhile, in comparison with DM mice, metformin and JTXK granules both improved the body lean mass of diabetic mice (Figure 1(f), $P < 0.05$). Moreover, according to results from the treadmill test, a higher body fat rate and less body lean mass accompanied impaired skeletal muscle performance, while treatment with metformin and JTXK

granules prevented this alteration (Figure 1(i), $P < 0.05$). Next, we performed H&E staining and electron microscopy of skeletal muscle tissue (Figures 1(g) and 1(h)). Skeletal muscle fibers of diabetic mice were arranged irregularly with inflammatory infiltration observed. There were lipid droplets and swelling mitochondria in the skeletal muscle tissue, while these pathological changes were ameliorated in Met and JTXK groups. Thus, we concluded from the above results that JTXK granules attenuated body weight gain, reduced body fat mass, improved body lean mass, and enhanced muscle performance of diabetic mice.

3.2. JTXK Granules Improved Glucose Tolerance and Insulin Sensitivity and Decreased Lipid Content of Diabetic Mice. To investigate the effect of JTXK granules on glucose tolerance and insulin sensitivity, OGTT and ITT were conducted after 8 weeks of treatment. Blood samples were collected for detection of serum glucose, insulin levels, and lipid contents. Compared with normal mice, mice in the DM group showed evidently impaired glucose tolerance with obvious hyperglycemia before and after oral administration of glucose (Figure 2(a), $P < 0.05$). The area under the curve (AUC) among groups was 14.28 ± 4.17 (NC), 27.57 ± 8.19 (DM), 14.57 ± 2.45 (Met), and 14.53 ± 3.96 (JTXK), which indicated that treatment with metformin and JTXK granules improved glucose tolerance significantly (Figure 2(b), $P < 0.05$). Consistent with OGTT, results from serum glucose also revealed that diabetic mice exhibited apparent hyperglycemia, while metformin and JTXK granules could improve glucose metabolism (Figure 2(c), $P < 0.05$). In addition, long-time HFD feeding also leads to reduced insulin sensitivity. The results of ITT showed that the blood glucose level of diabetic mice was still higher than that of the other mice 30, 60, 90, and 120 min after insulin injection intraperitoneally. And AUC of ITT in the DM group (700.90 ± 61.85) was evidently increased when compared with that in the NC group (403.50 ± 28.43). Notably, metformin and JTXK granule treatment decreased blood glucose levels at 30, 60, 90, and 120 min and decreased AUC of ITT significantly (Figures 2(d) and 2(e), $P < 0.05$). Moreover, treatment with metformin and JTXK granules also attenuated the HFD-induced hyperinsulinemia and abnormal HOMA-IR index markedly (Figures 2(f) and 2(g), $P < 0.05$). As for blood lipid profiles, long-time HFD feeding caused dyslipidemia in diabetic mice, represented by the ascended FFA, TC, TG, and LDL-C level and descended HDL-C level (Figures 2(h)–2(l), $P < 0.05$). Aside from HDL-C, metformin and JTXK granule treatment markedly attenuated these alterations (Figures 2(h)–2(k), $P < 0.05$). Compared with diabetic mice, JTXK mice also exhibited a higher level of serum HDL-C (Figure 2(l), $P < 0.05$). In brief, JTXK granule treatment improved glucose metabolism and insulin sensitivity and partly reversed abnormal serum lipid levels.

3.3. JTXK Granules Activated AMPK/SIRT1/PGC-1α Signaling in Skeletal Muscle of Diabetic Mice. To explore the underlying mechanism of JTXK granules in ameliorating skeletal muscle IR of diabetic mice, we analyzed the expression of important proteins and genes in the
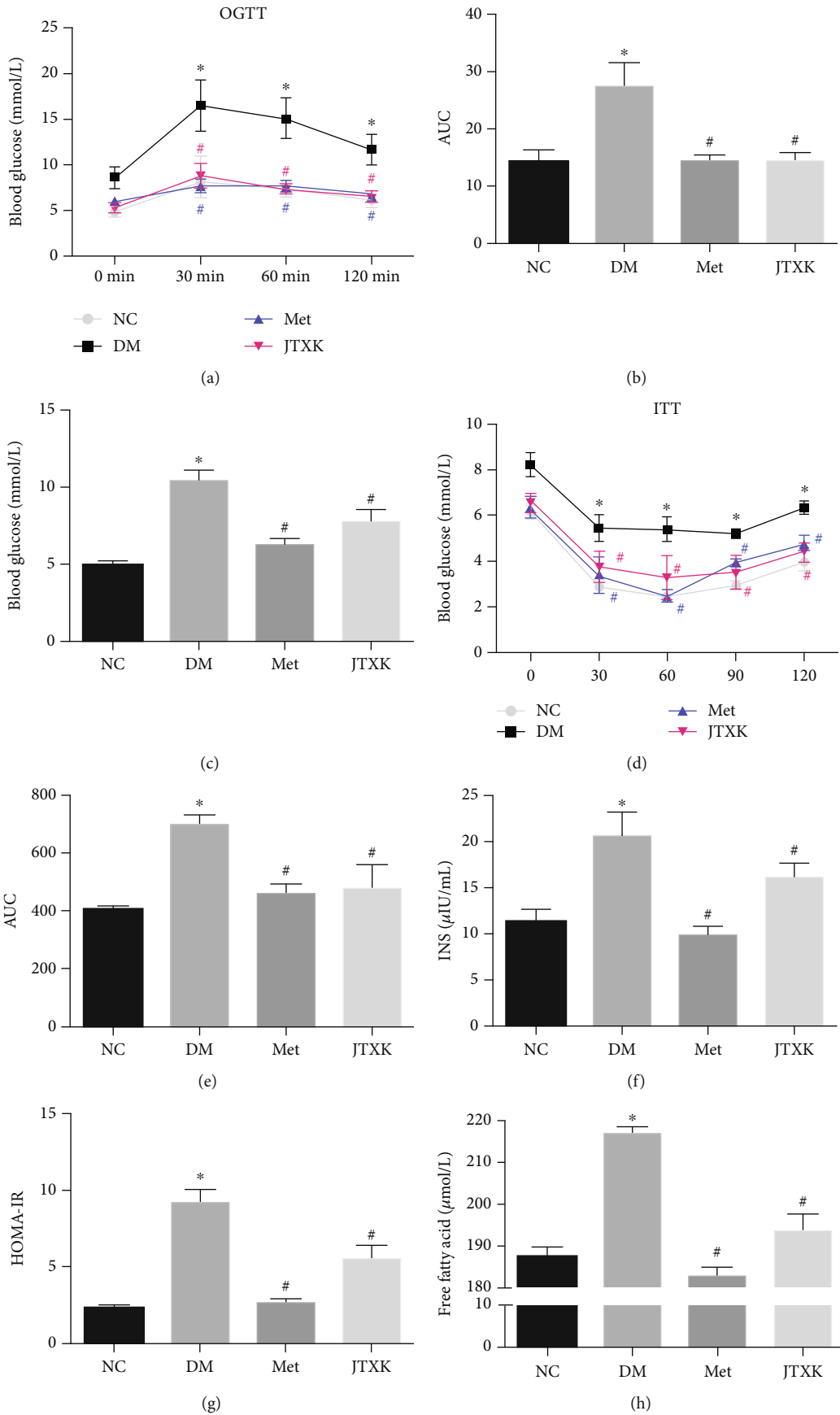
Figure 2: Continued.
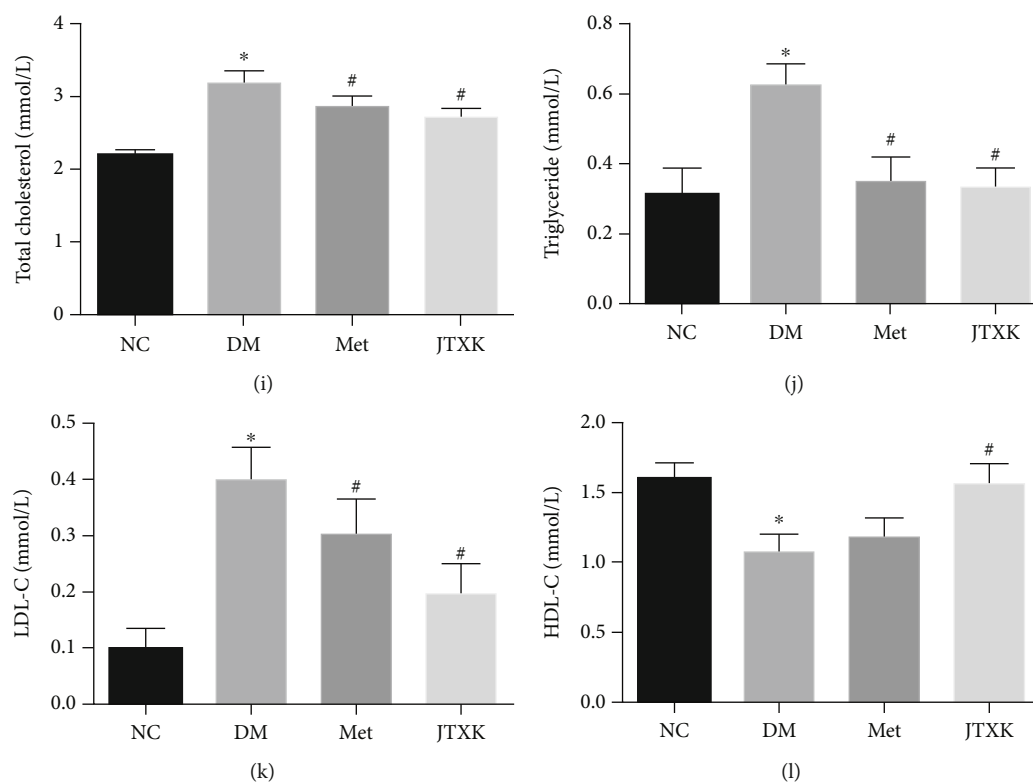
(i)

(j)

(k)

(l)

FIGURE 2: JTXK granules improved glucose tolerance, insulin sensitivity, and lipid profiles in diabetic mice. (a) OGTT test results and (b) area under the curve. (c) Fasting blood glucose. (d) ITT test and (e) area under the curve. (f) Fasting serum insulin level. (g) Homeostasis model assessment: insulin resistance in each group after treatment. Lipid profiles are represented by serum (h) free fatty acid, (i) total cholesterol, (j) triglyceride, (k) LDL-C, and (l) HDL-C contents. NC, DM, Met, and JTXK mean the normal control, diabetes, metformin, and Jiang Tang Xiao Ke granule groups, respectively. Data were presented as mean ± SD. $n = 8$ in each group. $^*P < 0.05$, compared with the NC group. $^#P < 0.05$, compared with the DM group.

AMPK/SIRT1/PGC-1α signaling pathway. As shown in Figures 3(a)–3(h), the protein expressions of AMPKα, SIRT1, PGC-1α, PPARα (both in cytosolic and in nuclear), CPT1, and UCP3 in skeletal muscle of diabetic mice were evidently lower than that of normal mice ($P < 0.05$). After 8 weeks of intervention with metformin or JTXK granules, expressions of those proteins in these two groups were significantly increased in comparison with that in diabetic mice ($P < 0.05$). Diabetic mice also exhibited reduction of GLUT4 membrane translocation, while treatment with metformin and JTXK granules increased GLUT4 translocation (Figure 3(i), $P < 0.05$). As shown in Figures 3(j)–3(o), the mRNA expressions of AMPKα, SIRT1, and UCP3 in skeletal muscle of diabetic mice were lower than that of normal mice ($P < 0.05$), while treatment with metformin or JTXK granules markedly increased these gene expressions by approximately 2-fold ($P < 0.05$). Compared with the DM group, metformin or JTXK granules also increased PGC-1α, PPARα, and SIRT1 expression significantly ($P < 0.05$). The above results indicated it is possible that JTXK granules ameliorated skeletal muscle IR through modulation of the AMPK/SIRT1/PGC-1α pathway.

3.4. JTXK Granules Improved Glucose Uptake and Mitochondrial Respiration in C2C12 Cells via Activation of AMPKα. To further verify the effect of JTXK granules

through in vitro experiment, we analyzed the glucose uptake ability and mitochondrial respiration in C2C12 cells after intervening with DCS of JTXK or metformin. As shown in Figures 4(a) and 4(b), for normal differentiated C2C12 cells, intervention with metformin or DCS did not affect their glucose uptake ability ($P > 0.05$). Next, we induced C2C12 cell insulin resistance by exposing them to 0.4 M palmitic acid for 24 h. According to the results, IR C2C12 cells exhibited impaired glucose uptake capacity, while treatment with metformin or DCS for 24 or 48 h significantly improved the glucose consumption of IR C2C12 cells (Figures 4(c) and 4(d), $P < 0.05$). In the in vivo experiment, obvious alteration in the AMPK/SIRT1/PGC-1α pathway was observed, so we assumed that JTXK probably acts through this signaling pathway. Therefore, we next analyzed the glucose uptake ability in the AMPKα knockdown C2C12 cell line (A-KD group in the figure). As shown in Figures 4(e) and 4(f), after 24 and 48 h of intervention with metformin or DCS, glucose consumption in these two groups was apparently enhanced ($P < 0.05$).

As AMPK is the pivot regulator in energy metabolism, we further investigated the effects of JTXK on mitochondrial energy metabolism (Figure 5(a)). Compared with the control group, DCS of JTXK granules increased the basal respiration (Figure 5(b)), ATP-linked respiration (Figure 5(c)), maximum respiration (Figure 5(d)), and spare respiratory

FIGURE 3: Continued.

(i)

(j)

(k)

(l)

(m)

(n)

(o)
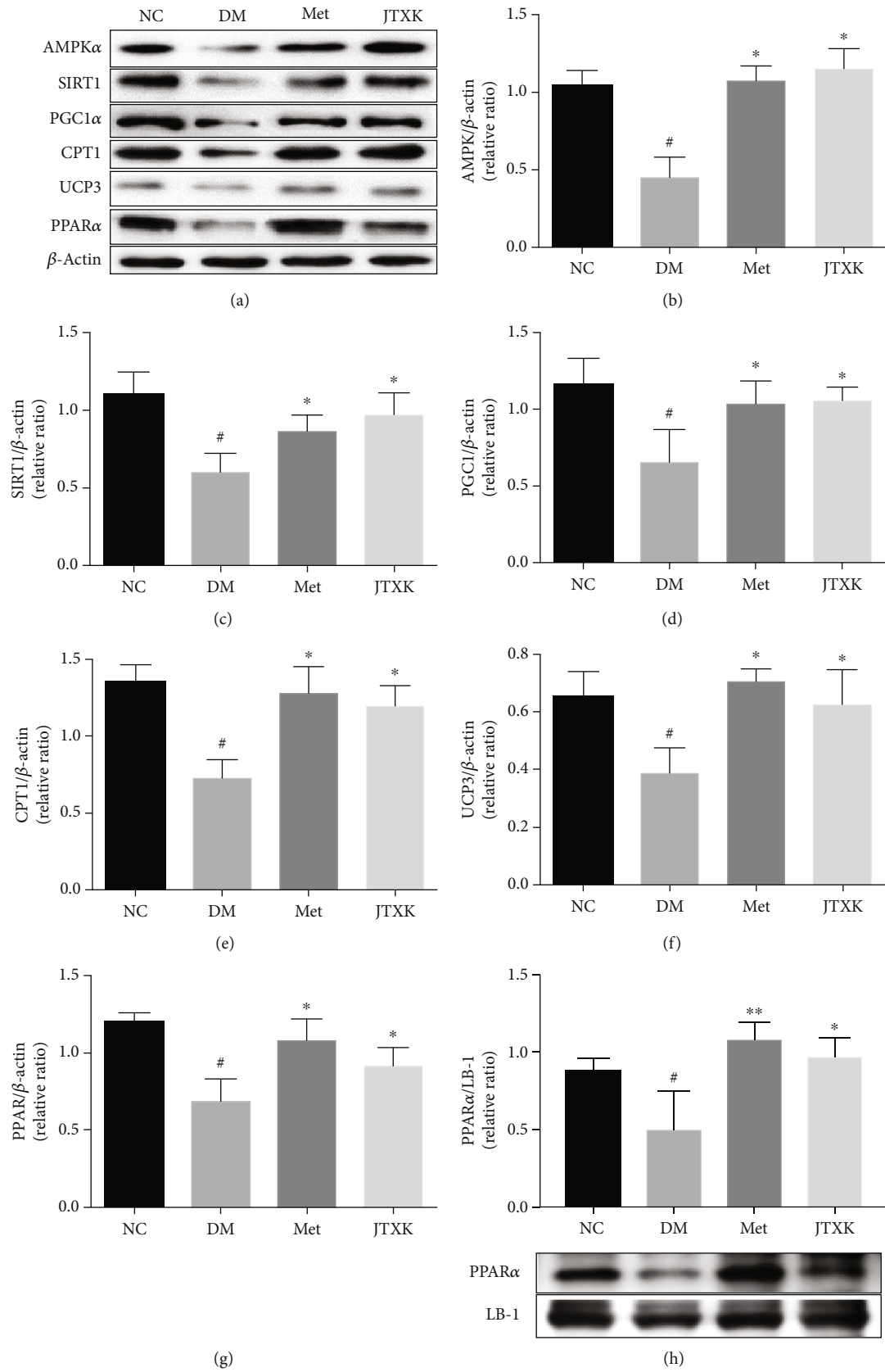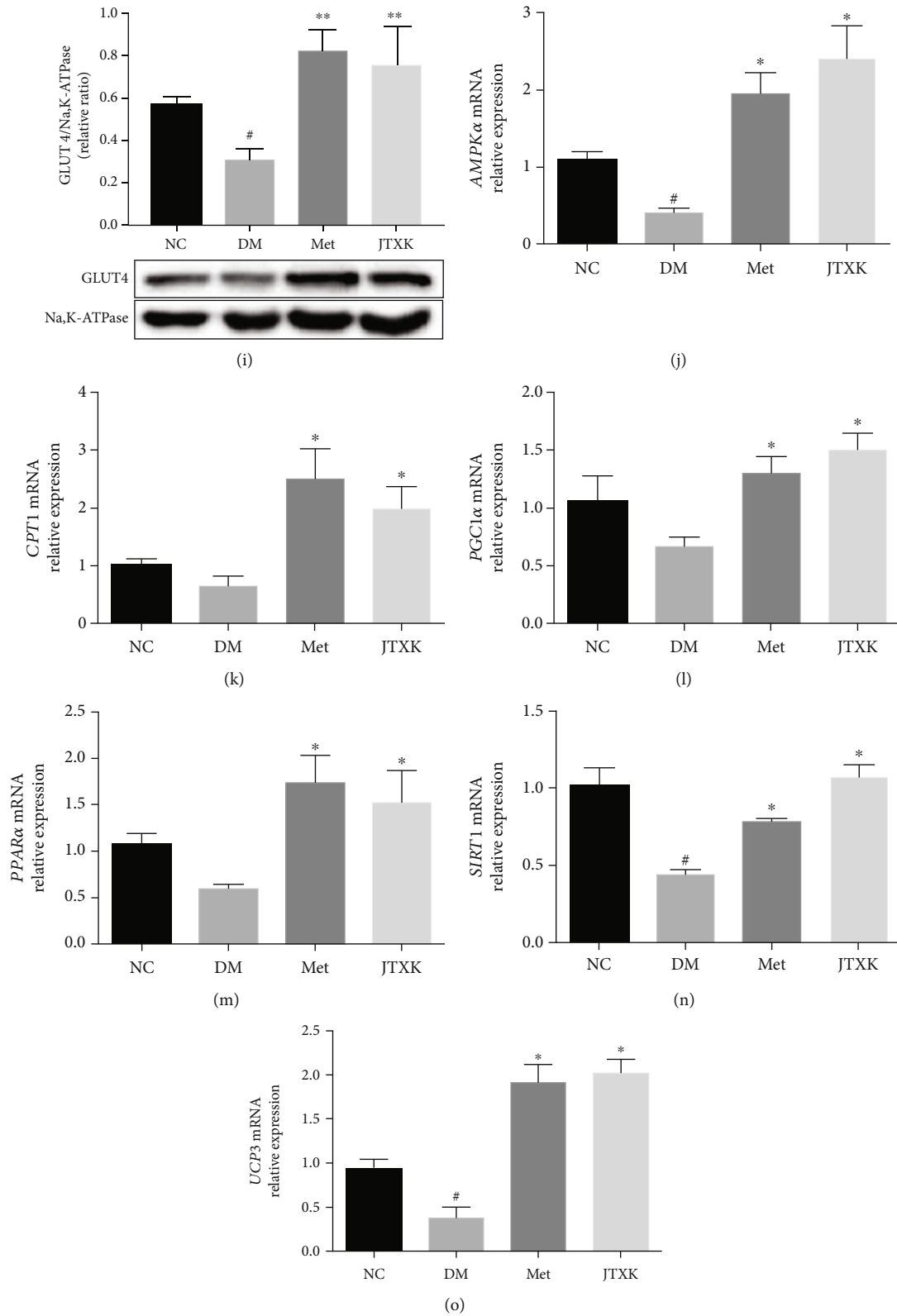
FIGURE 3: Effect of JTXK granules on AMPK/SIRT1/PGC-1α signaling in skeletal muscle of HFD-induced diabetic mice. The relative protein expression levels of AMPKα, SIRT1, PGC-1α, CPT1, UCP3, and PPARα (both in cytosolic and in nuclear) in the skeletal muscle (a–h) and GLUT4 membrane translocation (i) were determined by western blotting. Gene expressions of AMPKα, CPT1, PGC-1α, PPARα, SIRT1, and UCP3 (j–o) were determined by RT-PCR. NC, DM, Met, and JTXK refer to the normal control, diabetes, metformin, and Jiang Tang Xiao Ke granule groups, respectively. Data were presented as mean ± SD. $n = 6$ in each group. $^{*}P < 0.05$, compared with the NC group. $^{\#}P < 0.05$, compared with the DM group.
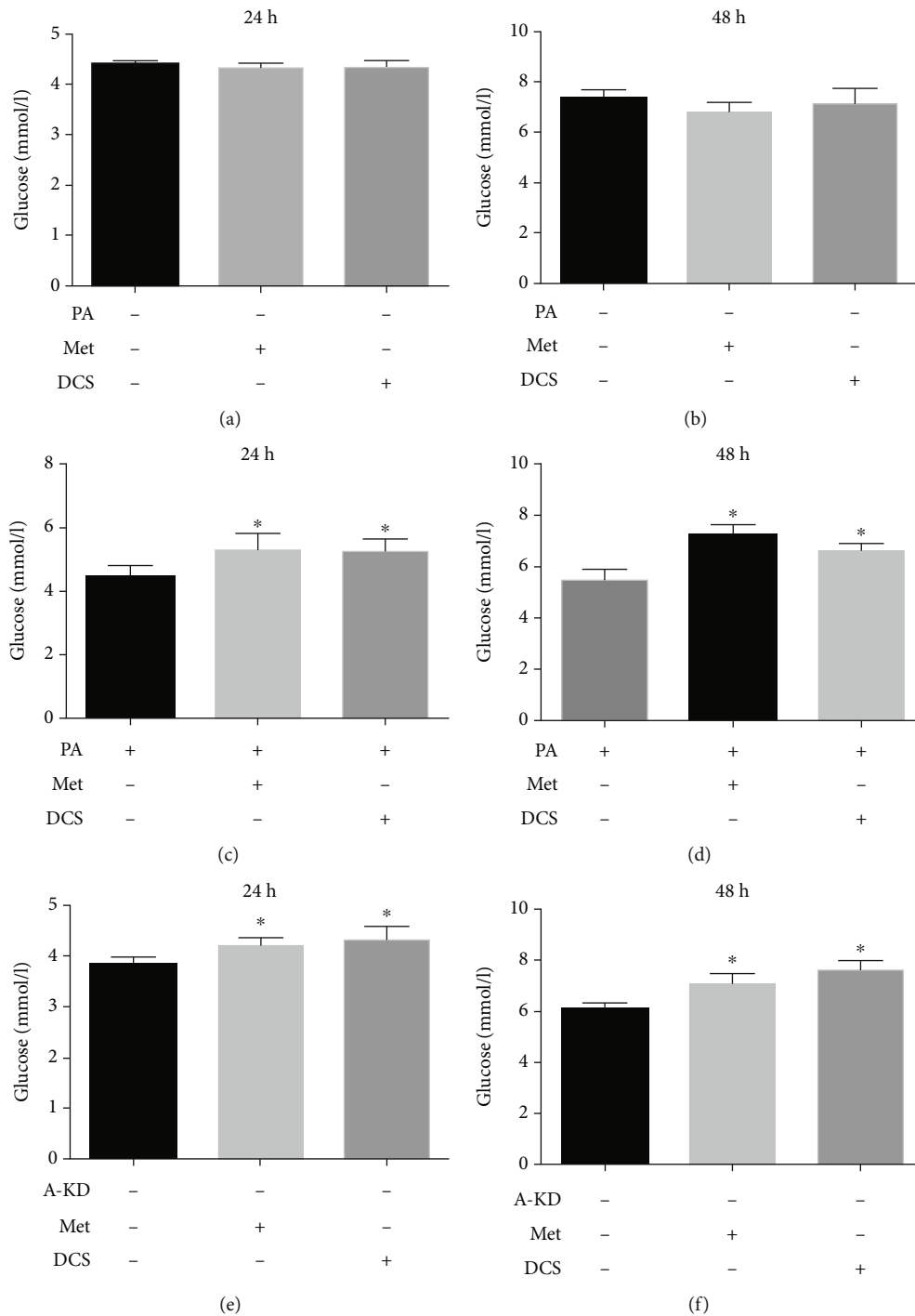
FIGURE 4: Effect of JTXK granule drug-containing serum on glucose uptake of C2C12 cells. Glucose uptake ability after intervention with drug-containing serum of JTXK granules in (a, b) normal C2C12 cells, (c, d) IR C2C12 cells, and (e, f) AMPKα knockdown C2C12 cells. A-KD indicates AMPKα knockdown. PA, Met, and DCS mean palmitic acid, metformin, and drug-containing serum of Jiang Tang Xiao Ke granules, respectively. Data were presented as mean ± SD. $^*P < 0.05$, compared with the blank control.

capacity (Figure 5(e)) of C2C12 cells with statistical significance ($P < 0.05$). For the AMPKα knockdown C2C12 cell line (A-KD group), compared with C2C12 cells, the basal respiration, ATP-linked respiration, maximum respiration, and spare respiratory capacity of C2C12 cells were significantly decreased ($P < 0.05$). As expected, the impaired mitochon-

drial respiration of AMPKα knockdown C2C12 cells was restored by intervention with DCS ($P < 0.05$). Furthermore, the effect of DCS on A-KD C2C12 cells was weaker than that on C2C12 cells, indicating that the effect of DCS on improving mitochondrial energy metabolism of C2C12 cells is closely related to the regulation of AMPKα. Thus, we

(a)

(b)

(c)

(d)

(e)
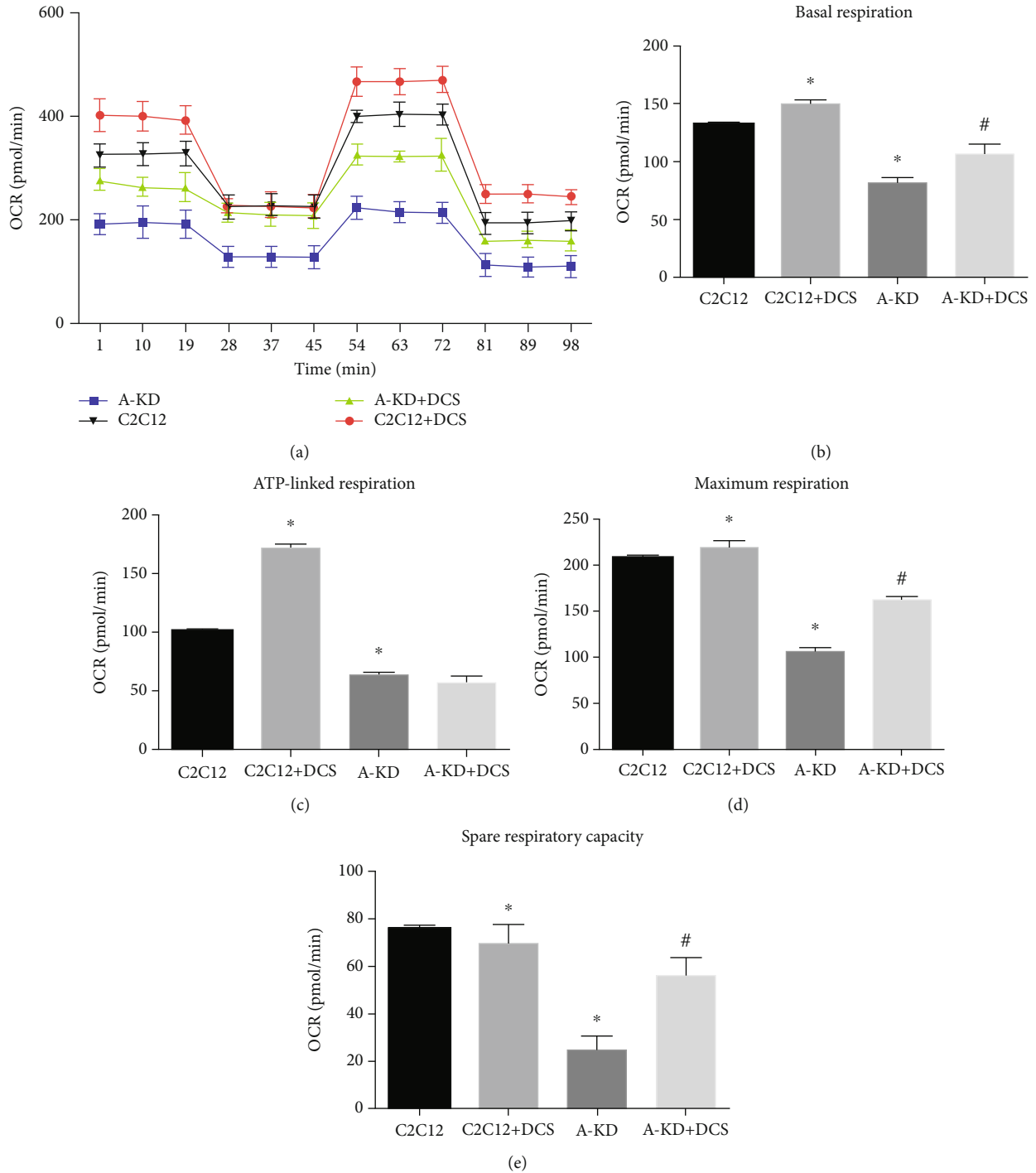
FIGURE 5: Effect of drug-containing serum of JTXK granules on mitochondrial respiration of C2C12 cells. (a) Oxygen consumption rate, (b) basal respiration, (c) ATP-linked respiration, (d) maximum respiration, and (e) spare respiratory capacity measured by Seahorse. A-KD and DCS indicate AMPKα knockdown and drug-containing serum of Jiang Tang Xiao Ke granules, respectively. Data were presented as mean ± SD. $^*P < 0.05$, compared with the C2C12 group. $^\#P < 0.05$, compared with the A-KD group.

concluded that AMPKα was closely involved in the effect of JTXK on enhancing glucose uptake and mitochondrial respiration in C2C12 cells.

3.5. JTXK Granules Promoted AMPK/SIRT1/PGC-1α Signaling in IR C2C12 Cells. Next, we further investigated

whether DCS of JTXK could affect AMPK/SIRT1/PGC-1α signaling in C2C12 cells. As shown in Figures 6(a)–6(g), DCS of JTXK markedly upregulated the protein expressions of AMPKα, SIRT1, PGC-1α, PPARα, UCP3, and CPT1 ($P < 0.05$). Consistent with results of western blotting, DCS of JTXK increased AMPKα, SIRT1, PGC-1α, PPARα,

(a)

(b)

(c)

(d)

(e)

(f)
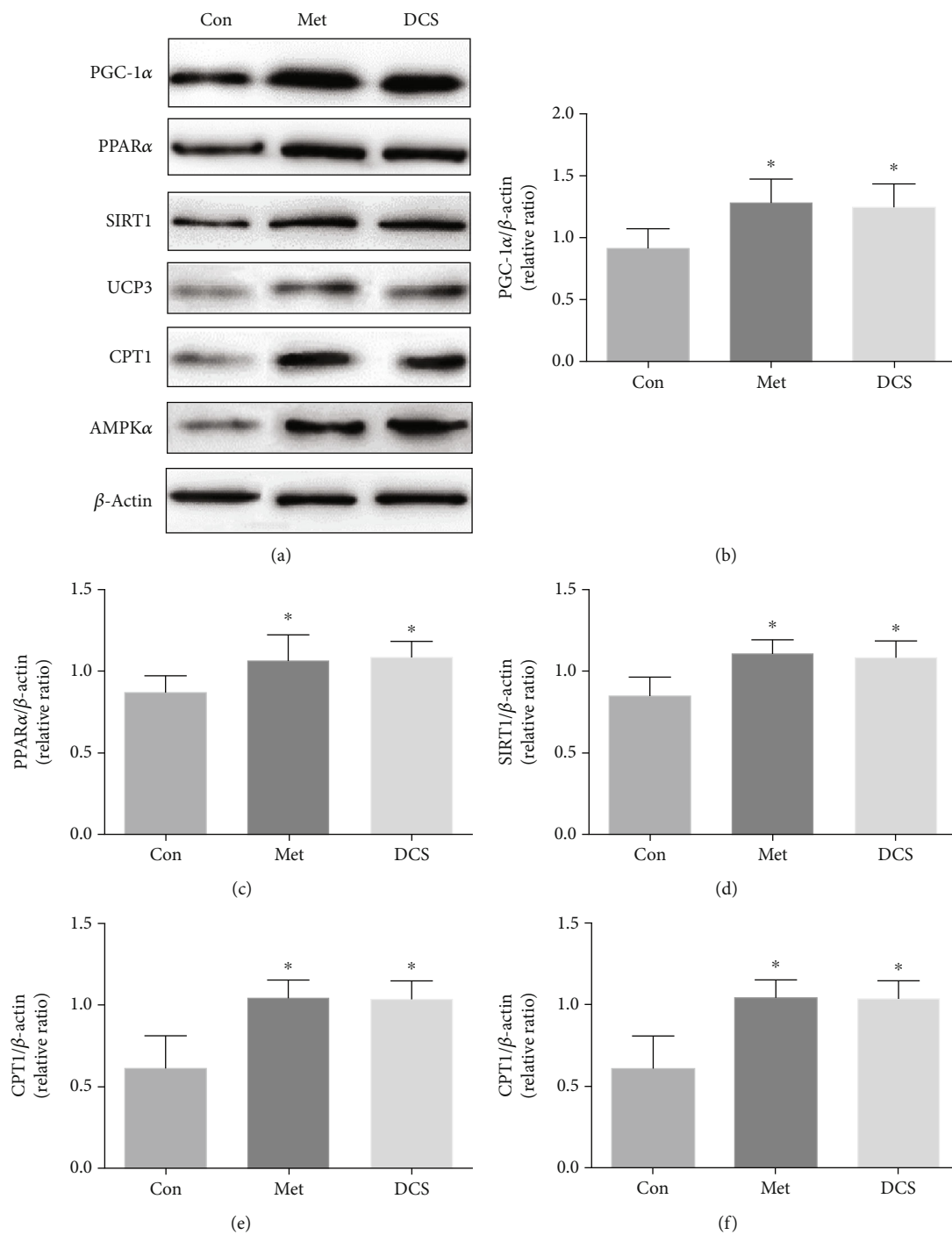
FIGURE 6: Continued.
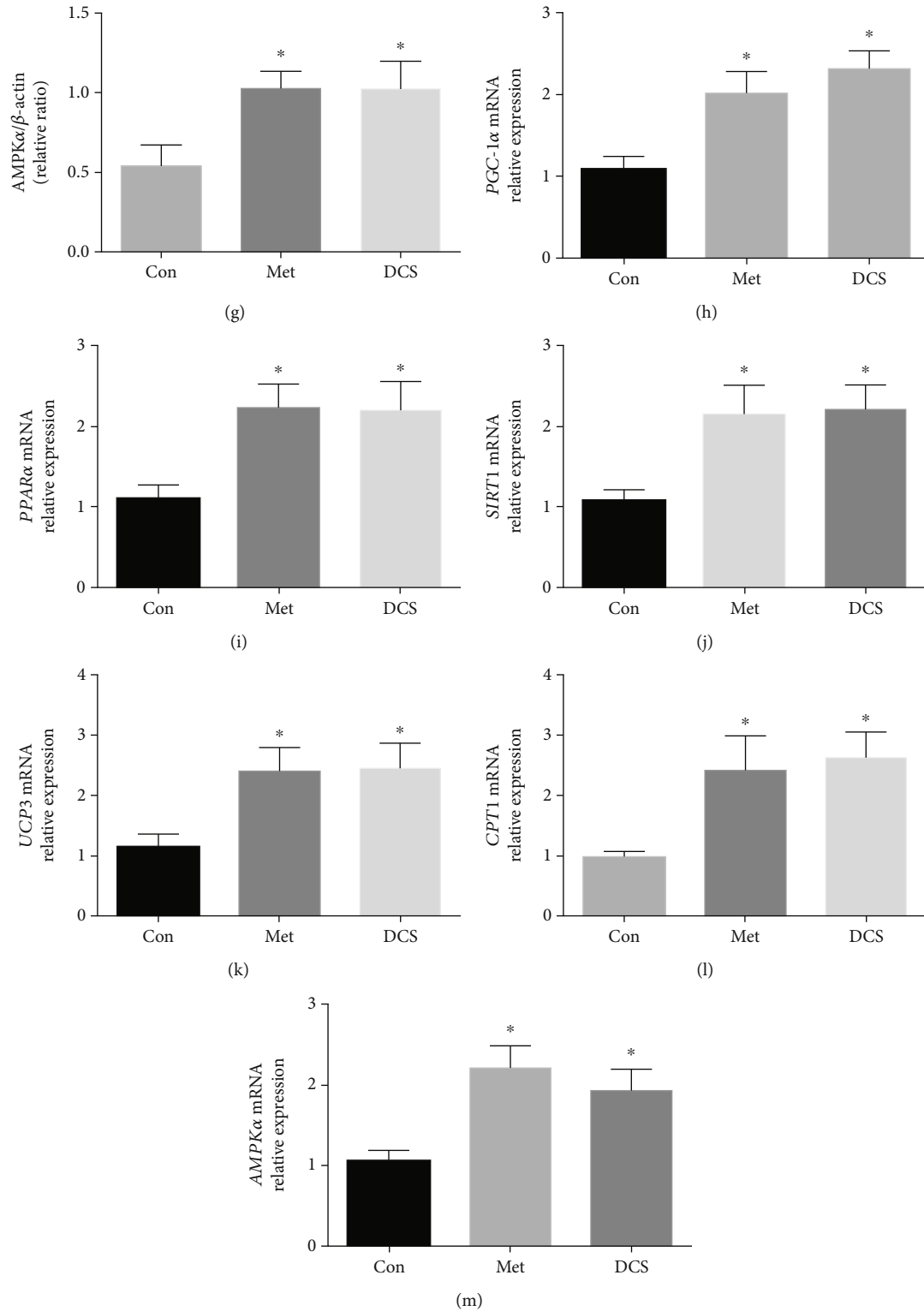
FIGURE 6: Effect of JTXK granule drug-containing serum on AMPK/SIRT1/PGC-1α signaling in IR C2C12 cells. (a–g) Protein expressions of AMPKα, SIRT1, PGC-1α, PPARα, UCP3, and CPT1 measured by western blotting. (h–m) Relative gene expressions of AMPKα, SIRT1, PGC-1α, PPARα, UCP3, and CPT1 measured by RT-PCR. Con, Met, and DCS mean the control, metformin, and drug-containing serum of Jiang Tang Xiao Ke granules, respectively. Data were presented as mean ± SD. *$P < 0.05$, compared with the Con group.

UCP3, and CPT1 mRNA expressions by 1.87-, 2.09-, 2.17-, 2.03-, 2.19-, and 2.62-fold ($P < 0.05$, Figures 6(h)–6(m)). Therefore, it is reasonable to postulate that JTXK granules could promote AMPK/SIRT1/PGC-1α signaling in IR C2C12 cells.

4. Discussion

The present study demonstrated the following. (1) JTXK granules attenuated body weight gain, reduced body fat mass, improved body lean mass, and enhanced muscle performance of diabetic mice. (2) JTXK granules improved glucose metabolism and insulin sensitivity and partly reversed abnormal serum lipid levels. (3) JTXK granules increased the gene as well as protein expression of important molecules in the AMPK/SIRT1/PGC-1α pathway, both in skeletal muscle tissue of HFD-fed mice and in C2C12 cells. (4) The JTXK granule was capable of enhancing glucose uptake and mitochondrial respiration in C2C12 cells, and AMPKα was proven to be closely involved in this process.

In the last decades, significant investigation breakthroughs have been witnessed in the study of traditional Chinese medicine. Among these, herbal medicine stands in a critical position in traditional Chinese medicine practice. The JTXK granule is an effective herbal formula derived from rich clinical practice and exhibits a satisfying therapeutic effect in the management of IR-related metabolic disorders, including obesity, prediabetes, and overt diabetes. This formula is composed of *Rehmannia glutinosa* (Gaertn.) DC. (Dihuang), *Panax ginseng* C.A.Mey. (Renshen), *Salvia miltiorrhiza* Bunge (Danshen), *Cornus officinalis* Siebold & Zucc. (Shanzhuyu), *Coptis chinensis* Franch. (Huanglian), *Pueraria montana* var. lobata (Gegen), and so on. To better understand the essential and substantial basis of this formula, the fingerprint technique was applied to illustrate the main ingredients (Fig S1). According to our previous studies, JTXK granules ameliorated IR in diabetic mice by regulating PI3K/Akt signaling in skeletal muscles [17]. Besides, we also found that ginsenoside Rb1, one of the ingredients recognized in JTXK granules, exerts a beneficial effect on increasing insulin sensitivity in skeletal muscle of obese mice. And the mechanism is through upregulating AMPKα expression and increasing AMPK phosphorylation [20]. Here, we proved a novel mechanism of JTXK granules in mitigation of skeletal muscle IR through activation and modulation of AMPK/SIRT1/PGC-1α signaling concerning mitochondrial respiration.

Western diet and sedentary lifestyle have made metabolic disorders such as diabetes, obesity, and metabolic syndrome become an important disease spectrum threatening human health. Among metabolic disorders, IR is a common phenomenon as well as the main pathological factor. Therefore, investigating effective drug candidates for IR has been a hot topic in this research field. In the present study, we chose metformin, the first-line drug for diabetes, as the positive control to compare the effect of JTXK granules on skeletal muscle IR. In line with our previous results, JTXK granules exhibited a favorable effect on attenuating body weight gain and reducing food intake. In addition, JTXK granules also helped to regulate body composition, ameliorate pathological changes in skeletal muscle, and enhance muscle performance. In the skeletal muscle of diabetic mice, we also observed lipid droplets and swelling mitochondria, and JTXK granule intervention obviously relieved these changes. Studies have shown that compared with insulin-sensitive individuals, the mitochondrial DNA copy number in leukocytes of obese people was 6.9-fold lower, and the number of mitochondria was positively correlated with glucose utilization and oxidation while negatively correlated with BMI and serum FFA levels [5, 23]. Moreover, overnutrition (e.g., HFD) results in an elevated lipid burden (e.g., FFA) as well as mitochondrial oxidative stress, which will lead to the accumulation of incomplete fatty acid oxidation and reactive oxygen species (ROS). Both incomplete fatty acid oxidation and ROS contribute to impairment in insulin action and are considered closely related to the development of IR [24].

Although the exact mechanism that leads to the development of IR in skeletal muscle is not yet fully understood, accumulation of glucose and FFA have been shown to play a primary role [25, 26]. In the current study, we observed impaired glucose tolerance and abnormal lipid profiles in diabetic mice. After 8 weeks of treatment with JTXK granules, fasting blood glucose and insulin levels were significantly decreased, along with improved glucose tolerance and insulin sensitivity. JTXK granule intervention also reduced serum FFA, TC, TG, and LDL-C contents and increased HDL-C content significantly. As mentioned before, elevated glucose and FFA levels were the main cause of glucolipotoxicity [27]. And the consequences of glucolipotoxicity involve mitochondrial dysfunction, ROS production, and endoplasmic reticulum stress, of which all contribute to the progression of metabolic disorders [28]. This raises the possibility that JTXK granules might act through the signaling pathway that is related to mitochondrial biogenesis or metabolism.

In the present study, we claimed that JTXK granules enhanced expression levels of proteins and genes related to mitochondrial energy metabolism, including AMPKα, PGC-1α, SIRT1, PPARα, UCP3, and CPT1. JTXK granules also enhanced GLUT4 membrane translocation, which is considered a primary mediator of glucose removal from the blood circulation as well as an essential regulator of whole-body glucose homeostasis [29]. PGC-1α emerged as a key transcriptional coactivator in understanding how nuclear regulatory signals are linked to the biogenesis of mitochondria, antioxidant defense, and inflammatory response in skeletal muscle [30]. Accumulating studies have shown that HFD induces downregulation of PGC-1α, while its overexpression prevents HFD-induced reduction of mitochondrial respiration in hepatocytes and promotes exercise-induced autophagy in skeletal muscle [31, 32]. As the most prominent and extensively studied member of sirtuins, SIRT1 plays a critical role in the regulation of PGC-1α by deacetylation [33]. Besides, SIRT1 and PPARs both trigger mitochondrial biogenesis, so activation of PGC-1α/PPARs might offer a novel strategy in the treatment of mitochondrial-related diseases [34]. AMPK and SIRT1 are both upstream regulatory factors of PGC-1α. There may be an internal relationship between

them, which plays a significant role in energy metabolism. After AMPK activation, it acts on the downstream SIRT1 by affecting the NAD^+ level, which enhances mitochondrial oxidative phosphorylation capacity and ATP production through the SIRT1/PGC-1α signaling pathway [35]. So it is clear that the AMPK/SIRT1/PGC-1α network is a critical energy-sensing signaling pathway and that AMPK activation will induce the concurrent deacetylation and phosphorylation of its downstream targets and relieve the susceptibility to IR-associated metabolic disorders [36]. It reveals that AMPK activation helps prevent diabetic disorders in many tissues and organs, including skeletal muscle, hepatic tissue, and renal podocytes, by suppressing apoptosis and reducing oxidative stress [37–39]. To the best of our expectation, AMPKα knockdown C2C12 cells exhibited apparent impaired mitochondrial respiration capacity, indicating the essential position of AMPKα in mitochondrial metabolism. JTXK granules restored mitochondrial respiration capacity in IR C2C12 cells but were less effective on A-KD C2C12 cells, which proved that AMPKα regulation was closely involved in the therapeutic mechanisms of JTXK granules. Taken together, our findings provide us a novel image that the JTXK granule ameliorates skeletal muscle IR through activation of AMPKα and modulation of the AMPK/-SIRT1/PGC-1α signaling network.

5. Conclusions

In sum, we demonstrate that JTXK granules could improve glucose and lipid metabolism and ameliorate skeletal muscle IR, which are associated with activation of the AMPK/-SIRT1/PGC-1α signaling pathway (Fig S2). Our results indicate that the JTXK granule is a promising formula to be promoted in clinical use for the treatment of obesity, T2DM, and other IR-related metabolic disorders. However, further strictly designed clinical trials for the clinical promotion of JTXK are still necessary. And caution must be taken when considering the study duration, intervention methods, dosage and drug forms, inclusion criteria, and so on, for every single element counts when evaluating the therapeutic effect of the Chinese herbal medicine formula.

Data Availability

The original data will be available upon request.

Additional Points

Highlights. JTXK granules attenuated body weight gain and improved glucolipid metabolism of diabetic mice. JTXK granules improved skeletal muscle insulin sensitivity of diabetic mice. JTXK granules improved glucose uptake and mitochondrial respiration via activation of AMPKα. JTXK granules ameliorated diabetes through activating AMPK/-SIRT1/PGC-1α signaling.

Conflicts of Interest

The authors declare no conflicts of interest.

Authors' Contributions

Acknowledgments

Supplementary Materials

Supplementary 1. Fig S1: fingerprint chromatogram of JTXK granules. (10) Puerarin. (16) Coptisine. (18) Salvia acid B. (19) Berberine. (22) Paeonol.

Supplementary 2. Fig S2: graphic abstract. JTXK granules improved glucolipid metabolism and ameliorated skeletal muscle IR through the regulation of the AMPK/-SIRT1/PGC-1α signaling pathway.

References

[1] S. P. Khadke, A. A. Kuvalekar, A. M. Harsulkar, and N. Mantri, "High energy intake induced overexpression of transcription factors and its regulatory genes involved in acceleration of hepatic lipogenesis: a rat model for type 2 diabetes," *Biomedicine*, vol. 7, no. 4, p. 76, 2019.

[2] R. J. Johnson, S. E. Perez-Pozo, Y. Y. Sautin et al., "Hypothesis: could excessive fructose intake and uric acid cause type 2 diabetes?," *Endocrine Reviews*, vol. 30, no. 1, pp. 96–116, 2009.

[3] R. A. DeFronzo, E. Jacot, E. Jequier, E. Maeder, J. Wahren, and J. P. Felber, "The effect of insulin on the disposal of intravenous glucose. Results from indirect calorimetry and hepatic and femoral venous catheterization," *Diabetes*, vol. 30, no. 12, pp. 1000–1007, 1981.

[4] R. A. DeFronzo and D. Tripathy, "Skeletal muscle insulin resistance is the primary defect in type 2 diabetes," *Diabetes Care*, vol. 32, supplement_2, pp. S157–S163, 2009.

[5] A. Franko, J. C. von Kleist-Retzow, M. Böse et al., "Complete failure of insulin-transmitted signaling, but not obesity-induced insulin resistance, impairs respiratory chain function in muscle," *Journal of Molecular Medicine*, vol. 90, no. 10, pp. 1145–1160, 2012.

[6] R. Putti, V. Migliaccio, R. Sica, and L. Lionetti, "Skeletal muscle mitochondrial bioenergetics and morphology in high fat diet induced obesity and insulin resistance: focus on dietary fat source," *Frontiers in Physiology*, vol. 6, p. 426, 2016.

[7] J. E. Vela-Guajardo, S. Garza-González, and N. García, "Glucolipotoxicity-induced oxidative stress is related to

mitochondrial dysfunction and apoptosis of pancreatic β-cell," *Current Diabetes Reviews*, vol. 17, no. 5, 2021.

[8] H. Y. Lee, J. S. Lee, T. Alves et al., "Mitochondrial-targeted catalase protects against high-fat diet-induced muscle insulin resistance by decreasing intramuscular lipid accumulation," *Diabetes*, vol. 66, no. 8, pp. 2072–2081, 2017.

[9] S. Di Meo, S. Iossa, and P. Venditti, "Skeletal muscle insulin resistance: role of mitochondria and other ROS sources," *The Journal of Endocrinology*, vol. 233, no. 1, pp. R15–r42, 2017.

[10] R. M. Morrow, M. Picard, O. Derbeneva et al., "Mitochondrial energy deficiency leads to hyperproliferation of skeletal muscle mitochondria and enhanced insulin sensitivity," *Proceedings of the National Academy of Sciences of the United States of America*, vol. 114, no. 10, pp. 2705–2710, 2017.

[11] A. Gruzman, G. Babai, and S. Sasson, "Adenosine monophosphate-activated protein kinase (AMPK) as a new target for antidiabetic drugs: a review on metabolic, pharmacological and chemical considerations," *The review of diabetic studies: RDS*, vol. 6, no. 1, pp. 13–36, 2009.

[12] V. T. Samuel, K. F. Petersen, and G. I. Shulman, "Lipid-induced insulin resistance: unravelling the mechanism," *The Lancet*, vol. 375, no. 9733, pp. 2267–2277, 2010.

[13] C. F. Cheng, H. C. Ku, and H. Lin, "PGC-1α as a pivotal factor in lipid and metabolic regulation," *International Journal of Molecular Sciences*, vol. 19, no. 11, p. 3447, 2018.

[14] J. G. Ryall, S. Dell'Orso, A. Derfoul et al., "The NAD$^+$-dependent SIRT1 deacetylase translates a metabolic switch into regulatory epigenetics in skeletal muscle stem cells," *Cell Stem Cell*, vol. 16, no. 2, pp. 171–183, 2015.

[15] Y. Bai, X. Bao, G. Jiang et al., "Jiang Tang Xiao Ke granule protects hepatic tissue of diabetic mice through modulation of insulin and Ras signaling - a bioinformatics analysis of microRNAs and mRNAs network," *Frontiers in Pharmacology*, vol. 11, p. 173, 2020.

[16] F. F. Mo, T. An, Z. J. Zhang et al., "Jiang Tang Xiao Ke granule play an anti-diabetic role in diabetic mice pancreatic tissue by regulating the mRNAs and microRNAs associated with PI3K-Akt signaling pathway," *Frontiers in Pharmacology*, vol. 8, p. 795, 2017.

[17] N. Yu, X. Fang, D. Zhao et al., "Anti-diabetic effects of Jiang Tang Xiao Ke granule via PI3K/Akt signalling pathway in type 2 diabetes KKAy mice," *PLoS One*, vol. 12, no. 1, article e0168980, 2017.

[18] D. D. Zhao, N. Yu, X. K. Li et al., "Antidiabetic and antioxidative effect of Jiang Tang Xiao Ke granule in high- fat diet and low-dose streptozotocin induced diabetic rats," *Evidence-Based Complementary and Alternative Medicine*, vol. 2014, Article ID 475192, 8 pages, 2014.

[19] S. Bansod, N. Doijad, and C. Godugu, "Berberine attenuates severity of chronic pancreatitis and fibrosis via AMPK- mediated inhibition of TGF-β1/Smad signaling and M2 polarization," *Toxicology and Applied Pharmacology*, vol. 403, article 115162, 2020.

[20] D. Zhao, Y. Bai, R. Wu et al., "Effects of ginsenoside Rb1 on skeletal muscle insulin resistance and adenosine monophosphate? Activated protein kinase signaling pathway in obese mice," *World Journal of Traditional Chinese Medicine*, vol. 5, pp. 42–49, 2019.

[21] A. Heydemann, "An overview of murine high fat diet as a model for type 2 diabetes mellitus," *Journal of Diabetes Research*, vol. 2016, Article ID 2902351, 14 pages, 2016.

[22] M. Fangfang, L. Haixia, H. Jing, Z. Dandan, T. Tian, and G. Sihua, "Effects of Jiang Tang Xiao Ke granule drug contained serum on FoxO1 expression in INS-1 cell," *World Journal of Traditional Chinese Medicine*, vol. 12, 2017.

[23] L. D. Zheng, L. E. Linarelli, L. Liu et al., "Insulin resistance is associated with epigenetic and genetic regulation of mitochondrial DNA in obese humans," *Clinical Epigenetics*, vol. 7, no. 1, 2015.

[24] H. B. Kwak, "Exercise and obesity-induced insulin resistance in skeletal muscle," *Integrative medicine research*, vol. 2, no. 4, pp. 131–138, 2013.

[25] M. A. Abdul-Ghani and R. A. DeFronzo, "Pathogenesis of insulin resistance in skeletal muscle," *Journal of Biomedicine & Biotechnology*, vol. 2010, Article ID 476279, 19 pages, 2010.

[26] D. J. Den Hartogh, F. Vlavcheski, A. Giacca, and E. Tsiani, "Attenuation of free fatty acid (FFA)-induced skeletal muscle cell insulin resistance by resveratrol is linked to activation of AMPK and inhibition of mTOR and p70 S6K," *International Journal of Molecular Sciences*, vol. 21, no. 14, 2020.

[27] M. Prentki, M. L. Peyot, P. Masiello, and S. R. M. Madiraju, "Nutrient-induced metabolic stress, adaptation, detoxification, and toxicity in the pancreatic β-cell," *Diabetes*, vol. 69, no. 3, pp. 279–290, 2020.

[28] W. el-Assaad, E. Joly, A. Barbeau et al., "Glucolipotoxicity alters lipid partitioning and causes mitochondrial dysfunction, cholesterol, and ceramide deposition and reactive oxygen species production in INS832/13 ss-cells," *Endocrinology*, vol. 151, no. 7, pp. 3061–3073, 2010.

[29] S. Huang and M. P. Czech, "The GLUT4 glucose transporter," *Cell Metabolism*, vol. 5, no. 4, pp. 237–252, 2007.

[30] C. Kang and L. Li Ji, "Role of PGC-1α signaling in skeletal muscle health and disease," *Annals of the New York Academy of Sciences*, vol. 1271, no. 1, pp. 110–117, 2012.

[31] J. F. Halling, S. Ringholm, M. M. Nielsen, P. Overby, and H. Pilegaard, "PGC-1α promotes exercise-induced autophagy in mouse skeletal muscle," *Physiological Reports*, vol. 4, no. 3, article e12698, 2016.

[32] E. M. Morris, M. R. Jackman, G. M. Meers et al., "Reduced hepatic mitochondrial respiration following acute high-fat diet is prevented by PGC-1α overexpression," *American Journal of Physiology-Gastrointestinal and Liver Physiology*, vol. 305, no. 11, pp. G868–G880, 2013.

[33] Z. Gerhart-Hines, J. T. Rodgers, O. Bare et al., "Metabolic control of muscle mitochondrial function and fatty acid oxidation through SIRT1/PGC-1alpha," *The EMBO Journal*, vol. 26, no. 7, pp. 1913–1923, 2007.

[34] T. Valero, "Mitochondrial biogenesis: pharmacological approaches," *Current Pharmaceutical Design*, vol. 20, no. 35, pp. 5507–5509, 2014.

[35] R. Cerutti, E. Pirinen, C. Lamperti et al., "NAD$^+$-dependent activation of Sirt1 corrects the phenotype in a mouse model of mitochondrial disease," *Cell Metabolism*, vol. 19, no. 6, pp. 1042–1049, 2014.

[36] S. Hou, T. Zhang, Y. Li, F. Guo, and X. Jin, "Glycyrrhizic acid prevents diabetic nephropathy by activating AMPK/SIRT1/PGC-1α signaling in db/db mice," *Journal of Diabetes Research*, vol. 2017, Article ID 2865912, 10 pages, 2017.

[37] A. A. Eid, B. M. Ford, K. Block et al., "AMP-activated protein kinase (AMPK) negatively regulates Nox4-dependent activation of p53 and epithelial cell apoptosis in diabetes∗," *The*

Journal of Biological Chemistry, vol. 285, no. 48, pp. 37503–37512, 2010.

[38] B. K. Min, C. J. Oh, S. Park et al., "Therapeutic effect of dichloroacetate against atherosclerosis via hepatic FGF21 induction mediated by acute AMPK activation," *Experimental & Molecular Medicine*, vol. 51, no. 10, pp. 1–12, 2019.

[39] Y. Nishida, A. Nawaz, T. Kado et al., "Astaxanthin stimulates mitochondrial biogenesis in insulin resistant muscle via activation of AMPK pathway," *Journal of Cachexia, Sarcopenia and Muscle*, vol. 11, no. 1, pp. 241–258, 2020.

Research Article

The Extracts of *Angelica sinensis* and *Cinnamomum cassia* from Oriental Medicinal Foods Regulate Inflammatory and Autophagic Pathways against Neural Injury after Ischemic Stroke

Cheng Luo,[1] Qi Chen,[2] Bowen Liu,[3] Shengpeng Wang,[3] Hualin Yu,[1] Xiaowei Guan,[4] Yonghua Zhao [ID],[3] and Yitao Wang [ID][3]

[1]*The Second Department of Neurosurgery, First Affiliated Hospital of Kunming Medical University, Kunming, China*
[2]*The Affiliated Hospital of Southwest Medical University, Luzhou, China*
[3]*State Key Laboratory of Quality Research in Chinese Medicine, Institute of Chinese Medical Sciences, University of Macau, Macao, China*
[4]*Department of Human Anatomy and Histoembryology, School of Medicine and Life Sciences, Nanjing University of Chinese Medicine, Nanjing, China*

Correspondence should be addressed to Yonghua Zhao; yonghuazhao@um.edu.mo and Yitao Wang; ytwang@um.edu.mo

The study indicates inflammation and autophagy are closely related to neural apoptosis in the pathology of ischemic stroke. In the study, we investigate the effects and mechanisms of the extracts of *Angelica sinensis* and *Cinnamomum cassia* (AC) from oriental medicinal foods on inflammatory and autophagic pathways in rat permanent middle cerebral artery occlusion model. Three doses of AC extract were, respectively, administered for 7 days. It suggests that AC extract treatment ameliorated scores of motor and sensory functions and ratio of glucose utilization in thalamic lesions in a dose-dependent manner. Expression of Iba1 was decreased and CD206 was increased by immunofluorescence staining, western blotting results showed expressions of TLR4, phosphorylated-IKKβ and IκBα, nuclear P65, NLRP3, ASC, and Caspase-1 were downregulated, and Beclin 1 and LC3 II were upregulated. Low concentrations of TNF-α, IL-1β, and IL-6 were presented by ELISA assay. Additionally, caspase 8 and cleaved caspase-3 expressions and the number of TUNEL positive cells in ipsilateral hemisphere were decreased, while the ratio of Bcl-2/Bax was increased. Simultaneously, in LPS-induced BV2 cells, it showed nuclear P65 translocation and secretion of proinflammatory cytokines were suppressed by AC extract-contained cerebrospinal fluid, and its intervened effects were similar to TLR4 siRNA treatment. Our study demonstrates that AC extract treatment attenuates inflammatory response and elevates autophagy against neural apoptosis, which contributes to the improvement of neurological function poststroke. Therefore, AC extract may be a novel neuroprotective agent by regulation of inflammatory and autophagic pathways for ischemic stroke treatment.

1. Introduction

Stroke has been a top-ranked cause of mortality and disability in both the 50–74-year and 75-years-and-older age groups, globally [1]. Prevalent data of stroke show that 84.4% of the total number belongs to ischemic stroke [2]. Numerous literatures have indicated that neuroinflammatory response plays an essential role in the propagation of brain damage after stroke [3]. Due to cerebral vascular occlu-

sion by thrombosis at the onset of ischemic stroke, regional cerebral blood flow (CBF) instantaneously decreases and stagnates, which induces shear stress on endothelial cells (ECs) and platelets resulting in excessive adhesion molecules secretion, contributing to circulating leukocytes recruitment and binding onto ECs. It exacerbates coagulation cascades and initiates the earliest inflammatory response [4]. Following the disruption of blood-brain barrier (BBB), circulating leukocytes are apt to infiltrate into brain parenchyma.

Leukocyte infiltration combined with danger-/damage-associated molecular patterns (DAMPs) from injured and dying neurons triggers a cerebral inflammatory cascade as a marker of activation of microglia and astrocytes [5]. DAMPs activate Toll-like receptors (TLRs) of subfamilies of pattern recognition receptors (PRRs) on microglia, astrocytes, and oligodendrocytes and activated TLRs, like TLR4, interacting with the myeloid differentiation primary-response protein 88 (MyD88) upregulates nuclear factor-kappa B (NF-κB) signaling [6, 7]. As another subfamilies of PRRs, Nod-Like receptors (NLRs) located in the cytoplasm primarily involved in the formation of NLR proteins (NLRPs) inflammasome which exerts important action in the neurovascular unit and has been a novel target on vascular diseases [8]. NLRP3 inflammasome, as the most featured member of the NLR family, participates in neuronal apoptosis after ischemic stroke [9]. Presently, NF-κB signaling has been demonstrated to involve in the activations of NLRP1 and NLRP3 inflammasomes, and inhibition of the pathway not only decreases interleukin- (IL-) 1β, IL-18, tumor necrosis factor- (TNF-) α, and IL-6 but also attenuates apoptotic cells in cerebral tissue after cerebral ischemia [10, 11]. Therefore, the inhibition of neuroinflammatory pathways is a crucial target for cerebral protection poststroke.

Recent research reports that moderate autophagy rescues injured cells by removing damaged tissues and proteins [12, 13]. Autophagy has closed interaction with apoptosis by multiple mechanistic overlaps. Evidence illustrates that mitochondria-dependent intrinsic apoptotic pathway activating caspase-3 not only arouses apoptotic cell death but also inhibits autophagy in ischemic stroke resulting from antiapoptotic protein Bcl-2 binding to Beclin-1 [13], so suppressed apoptosis and increased autophagy contributed to the recovery of hippocampus injury in cerebral ischemia/reperfusion rats [14]. Although mechanisms between autophagy and inflammation are not clear at present, it indicates that autophagy negatively regulates inflammasome activation against inflammation, whose efficacies mainly embody that the phagocytic actions of autophagy advance apoptotic corpse clearance as well as autophagy transports inflammasome components into lysosomes for degradation and sequesters IL-1β [15, 16]. It is necessary to develop innovative pharmacological agents targeting inflammatory and autophagic pathways in ischemic stroke.

Chinese herbs begin to systematically treat stroke before 1800 years and have accumulated abundant clinical experiences and effective prescriptions. Emerging studies suggest that compounds extracted from Chinese herbs exert significant neuroprotective effects via multiple approaches [17]. *Angelica sinensis* (Oliv.) Diels, root and rhizome, and *Cinnamomum cassia* (L.) J. Presl, stem bark, as oriental herbs from medicinal foods, their combination had been reported to be used to treat stroke in Chinese medicinal literature before 300 years [18]. They are widely used as either traditional medicines or functional foods in East and South-East Asia countries such as Korea, Japan, India, Thailand, Vietnam, and Indonesia [19, 20]. In the study, we investigate neuroprotective effects of the extracts of *Angelica sinensis* and *Cinnamomum cassia* (AC) on

cerebral tissue and hypothesize the mechanisms might be related to the regulation of inflammatory and autophagic pathways following cerebral ischemia.

2. Materials and Methods

2.1. The Extracted Method and Quality Control. The root and rhizome of *Angelica sinensis* (Oliv.) Diels and stem bark of *Cinnamomum cassia* (L.) J. Presl, were purchased from Guangzhou Zisun Pharmaceutical Co., Ltd., China, which are accordant with the standards of Chinese Pharmacopoeia (2015 edition) by confirmation of Professor Quan Zhu. We performed the method of steam distillation for the extracts of AC (1 : 1 of two herbal medicine weight ratio), and detailed procedures refer to our previous article [21]. The extracts (yield: 25%) were obtained by lyophilizing the concentrated sample with a Virtis Freeze Dryer (The Virtis Company, New York, USA). 5 mg of AC extract was dissolved in 5 ml of 30% methanol and filtered, which was directly subjected to ACQUITY UPLC system on PAD λe detector ($\lambda = 200 – 400$ nm), autosampler, in-line degasser, Waters ACQUITY-UPLC CLASS system (Waters Corp., Milford, USA) on an ACQUITY UPLC HSS T3 column (150 mm × 2.1 mm, 1.8 μm). Reference compounds are ferulic acid ($tR = 2.59$ min, purity HPLC > 98%), Senkyunolide I ($tR = 4.42$ min, purity HPLC > 98%), and Trans-Cinnamic acid ($tR = 6.32$ min, purity HPLC > 98%), which were purchased from Chengdu Chroma-Biotechnology Co., Ltd., China.

2.2. Middle Cerebral Artery Occlusion Model and Group Division. Male Sprague-Dawley (SD) rats weighing 220-250 g were provided by Kunming Medical University Laboratory Animal Services Center. All animal operations conformed to the NIH Guide for the Care and Use of Laboratory Animals (National Institutes of Health Publication No. 85–23, revised in 1985), and University of Macau ethical committee approved the experimental protocol. Permanent middle cerebral artery occlusion (MCAo) model was established according to our previous report [21]. Briefly, 2% pentobarbital sodium (4 mL/kg) was used to anesthetize SD rats by intraperitoneal injection, and subsequently, middle cerebral artery was occluded by inserting 4-0 surgical nylon suture coated with polylysine. Simultaneously, rats in the sham group were subject to the same administered procedure except for suture occlusion. All operated rats were put on animal heating pads to maintain their rectal temperature at 37°C, and only MCAo rats with a score of 2 assessed by 5-point scale neurological deficit score [22] were randomly divided into four groups after they recovered consciousness.

Treatment groups include low dosage of AC extract (Low) group, middle dosage of AC extract (Middle) group, and high dosage of AC extract (High) group, and 1.6 g/kg, 3.2 g/kg, and 6.4 g/kg of AC extract solved in distilled water were, respectively, administered to rats by gavage once daily for 3 days before operation and continuing to 7 days after MCAo surgery. Rats in MCAo and Sham groups were given the same volume of distilled water.

2.3. The Harvest of Cerebrospinal Fluid. At day 7, rats ($n = 6$) in sham, MCAo, and high dose of AC extract groups were intraperitoneally injected into 2% pentobarbital sodium (4 mL/kg) for deep anesthetization, and then 1 mL injector was slowly inserted into posterior atlantooccipital membrane avoiding arteria spinalis dorsalis to harvest $30 \mu L$ CSF from each rat. Collections of CSF in each group were, respectively, termed sham group's, MCAo group's, and high dose group's CSF.

2.4. MicroPET/CT Imaging and Neurological Functional Assessment. ^{18}F-FDG-PET/CT imaging was performed to evaluate glucose uptake of rats ($n = 5$) in ipsilateral hemisphere at days 1, 3, and 7. The detailed performance procedure was described in our previous article [23]. Briefly, rats in each group were anesthetized with isoflurane (3.0% in air) asphyxiation, then, intravenously administered with 37 MBq (~1 mCi) of ^{18}F-FDG. After 60 min later, microPET/CT images and CT images were, respectively, acquired for 30 min using a FLEX X-PET and X-O small animal imaging system (TriFoil) and with 256 projections over 2 min for attenuation correction and anatomy landmarks. Commercial software (Visage Imaging) with $72 \mu m$ isotropic CT spatial resolution and 2 mm for PET imaging was used for the coregistered images of PET and CT. For quantitative analysis, volume of interests (VOIs) were, respectively, drawn on six regions (Amygdala, Caudate Putamen, Cortex Motor, Cortex Somatosensory, Hypothalamus and Thalamus Whole) of contralateral and ipsilateral hemispheres. Percent-injected dose of ^{18}F-FDG per c.c. of brain tissue (%ID/cm^3) was obtained from each VOI. Metabolic ratio of each region was calculated with the following formula: ratio = %ID/c.c.of lesion region/%ID/c.c.of contralateral side.

Additionally, we invited a colleague who was unknown to the experimental group division to evaluate the amelioration of neurological function in rats poststroke. At day 7 after ischemia, assessment of motor recovery ($n = 6$) including spontaneous activity, symmetry in the movement of four limbs, forepaw outstretching, and climbing, and test of sensory recovery ($n = 6$) including body proprioception and response to vibrissae touch [24] were performed.

2.5. TLR4 siRNA Transfection in BV2 Microglial Cells. BV2 microglial cell lines purchased from China Center for Type Culture Collection were seeded at a density of 2.5×10^5 cells/ml into 6-well dishes and cultured with Dulbecco's modified Eagle's medium (Gibco; Thermo Fisher Scientific, Inc., USA) supplemented with 10% fetal bovine serum at 37°C with 5% CO_2. Cells were transfected with siRNA against TLR4, when they presented logarithmic growth to 70% confluent. According to manufacturer's protocol, BV2 microglial cells were transfected with TLR4 siRNA consisting of three target-specific 19-25 nt siRNAs to knock down gene expression using siRNA Transfection Reagent (CAT#: sc-40261, Santa Cruz Biotechnology, Inc.). Negative control of TLR4 siRNA transfection contained a scrambled sequence that did not cause specific degradation of any known cellular mRNA (CAT#: sc-37007, Santa Cruz Biotechnology, Inc.).

2.6. Lipopolysaccharide-Stimulated BV2 Microglial Cells Incubated with CSF. Before lipopolysaccharide- (LPS-) stim-ulated BV2, 15% high dose group's CSF was, respectively, added into BV2 and TLR4 siRNA-transfected BV2. Simultaneously, 15% MCAo group's CSF was, respectively, added into BV2, TLR4 siRNA, and negative TLR4 siRNA-transfected BV2. 15% Sham group's CSF added into BV2 was used to be as normal control. Subsequently, 100 ng/mL of LPS derived from *Escherichia coli* O111:B4 (Sigma-Aldrich, Inc. Cat#: L4391) was employed to stimulate these BV2 cells for 24 hours based on preliminary experiments and other reports [25], except BV2 in the normal group. Ultimately, LPS+ high dose group's CSF (High), LPS + TLR4 siRNA+High, LPS, LPS + TLR4 siRNA, and LPS + negative TLR4 siRNA groups were formed.

2.7. Western Blotting. At day 7, rats ($n = 3$) in five groups were sacrificed by excessive anesthesia and transcardially perfused with 4°C sterile saline. Total proteins were extracted from the ipsilateral hemisphere of each group as well as different processed BV2 in vitro, and nuclear/cytoplasmic proteins were isolated using NE-PER Nuclear and Cytoplasmic Extraction Kit (Thermo Scientific™ 78833, USA). Protein concentration was determined by a bicinchoninic acid protein assay kit (Beyotime Institute of Biotechnology, Shanghai, China). Equal amounts of proteins were separated on 10% sulfate-polyacrylamide gel electrophoresis and transferred to polyvinylidene fluoride membranes. Subsequently, membranes were blocked in 5% (w/v) skimmed dried milk for 1 h at room temperature and incubated with primary antibodies for anti-TLR4 (1 : 2000, Signalway Antibody), anti-IKKβ (1 : 2000, CST), anti-p-IKKβ (1 : 1500, CST), anti-IκBα (1 : 1500, CST), anti-p-IκBα (1 : 1500, CST), anti-P65 (1 : 2000, CST), anti-NLRP3(1 : 2000, Signalway Antibody), anti-ASC (1 : 2000, Signalway Antibody), anti-Caspase1(1 : 2000, CST), anti-cleaved Caspase 3,8 (1 : 2000, CST), anti-Bcl-2 (1 : 2000, CST), anti-Bax (1 : 2000, CST), anti-Beclin 1 (1 : 2000, SAB), anti-LC3 (1 : 2000, CST), β-actin (1 μg/mL, Abcam), and Lamin B1 (1 : 1000, sc-374015, Santa Cruz Biotechnology, Inc., USA) at 4°C overnight. The membranes were gently washed with TBST [50 mM Tris-HCl (pH 7.4; Acros Organics BVBA, Geel, Belgium), 150 mM NaCl, 0.05% Tween 20 (Acros Organics BVBA)] three times and incubated with goat anti-rabbit IgG (H &L) or goat anti-mouse IgG (H &L) secondary antibodies (1 : 5000; Thermo Fisher Scientific, USA) at room temperature for 1 h. Signals of reactive bands were visualized by fluorescence scanner (LI-COR, Lincoln, Nebraska, USA), and quantitative analysis of targeted proteins was by ratio of corresponding proteins to β-actin or Lamin B1 (nuclear internal control), and phosphorylated levels of IKKβ and IκBα were analyzed by total levels of corresponding proteins. Western blots were duplicated three independent times.

2.8. TUNEL Assay. Rats ($n = 3$) were sacrificed at day 7, and their brain tissues were fixed with fresh 4% paraformaldehyde solution. Fresh frozen coronal sections of $8 \mu m$ thickness were cut by a cryostat microtome (Shandon Cryotome FSE, Thermo Fisher Scientific, USA). Subsequently, slices were fixed again for half an hour in 4% paraformaldehyde. After washing with PBS for three times, slices were incubated
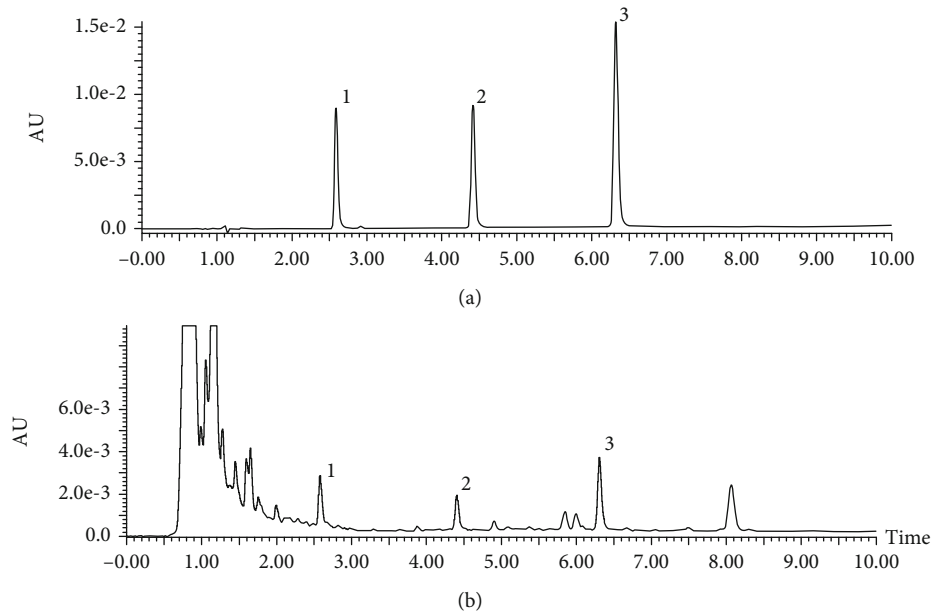
FIGURE 1: Quality control of AC extract by HPLC. Representative HPLC chromatogram of mixed standard solution (a) and AC extracts (b) with ferulic acid (1), Senkyunolide I (2), and Trans-Cinnamic acid (3); UV detection $\lambda = 203$ nm.

with 0.3% Triton X-100 at 4°C for 15 min. TUNEL assay (MA0224, MeiLunBio®, CHA) was performed according to the manufacturer's recommendations.

2.9. Immunofluorescence Staining. Every fifth slice of a total section was used to detect activations of microglia in ipsilateral hemisphere by incubation with primary antibody against Iba1 (1 : 200, Abcam, UK) and anti-CD206 (1 : 500, Abcam, UK) at 4°C for overnight. BV2 cells in six groups seeded on slides were fixed with 4% paraformaldehyde for 30 min at 4°C, permeabilized with 0.3% Triton X-100 for 15 min, and incubated with anti-P65 (1 : 500, CST) overnight. Both brain tissue and cell slides were washed with PBS and, respectively, incubated with the bs-0294D-FITC (1 : 200, Beijing Biosynthesis Biotechnology Co., Ltd., CHA) and Alexa Fluor® 488 goat anti-rabbit immunoglobulin (1 : 200, Life Technologies) secondary antibodies for 1 h at room temperature. Nuclei were stained with $4'$, 6-diamidino-2-phenylindole (DAPI; Sigma). The number of BV2 with positive signal of nuclear P65 was calculated in five randomly selected microscopic fields at 400× magnification. Fluorescent labeling of Iba1, CD206, and TUNEL were observed with the Leica TCS SP8 laser scanning confocal microscope (Leica Microsystems Inc., Buffalo Grove, USA), and five nonoverlapping fields of one slice in the penumbral cortex were measured. Image-Pro Plus software (Media Cybernetics, Rockville, MD, USA) was used for quantitative analysis.

2.10. ELISA Assay. TNF-α, IL-1β, and IL-6 in serum of peripheral blood, CSF, ipsilateral hemisphere, and conditional mediums from BV2 were measured using ELISA assay. At day 7, 5 ml blood was extracted from the abdominal aorta in deeply anesthetized rats ($n = 3$) after 2 hours of the last gavage and placed it in tubes at room temperature for 1 ~ 2 hours before it became condensation at 4°C. Finally, blood sample

was centrifuged at 4°C 2000 rpm for 20 min to separate the serum. Ipsilateral hemisphere was homogenized in PBS using a tissue homogenizer, followed by incubated with the addition of 200 μL of radioimmunoprecipitation assay buffer on ice for 10 min. Then, samples were centrifuged at $12500 \times$ g for 5 min at 4°C, and supernatant was obtained. Conditional mediums were collected at time point after BV2 incubated with different CSF for 24 hours. TNF-α (Cat No: RTA00), IL-1β (Cat No: RLB00), and IL-6 (Cat No: R6000B) ELISA kits (R&D Systems, USA) were performed according to manufacturer's instructions. Optical density (OD) was measured at a mean wavelength of 570 nm by using SpectraMax Paradigm Multi-Mode Microplate Reader (San Jose, CA, USA).

2.11. Statistical Analysis. Continuous variables were presented based on the average ± standard deviation, and GraphPad Prism 5.0 (GraphPad Software, Inc.) was applied to the statistical analysis. One-way ANOVA was used to compare two means from two independent groups followed by Tukey's multiple comparisons test. A value of $p < 0.05$ was considered statistical significance in all analyses.

3. Results

3.1. Quality Control Results of AC Extract. Quality control results by HPLC analysis indicated that the content of ferulic acid was 0.042 ± 0.001%, the content of Senkyunolide I was 0.021 ± 0.001%, the content of Trans-Cinnamic acid is 0.026% in AC extract, and the chromatographic peaks of ferulic acid, Senkyunolide I, and Trans-Cinnamic acid in AC extract, as well as the peak of reference solution were shown in Figure 1.

3.2. AC Extract Treatment Ameliorated Cerebral Glucose Utilization and Neurological Outcome. As shown in
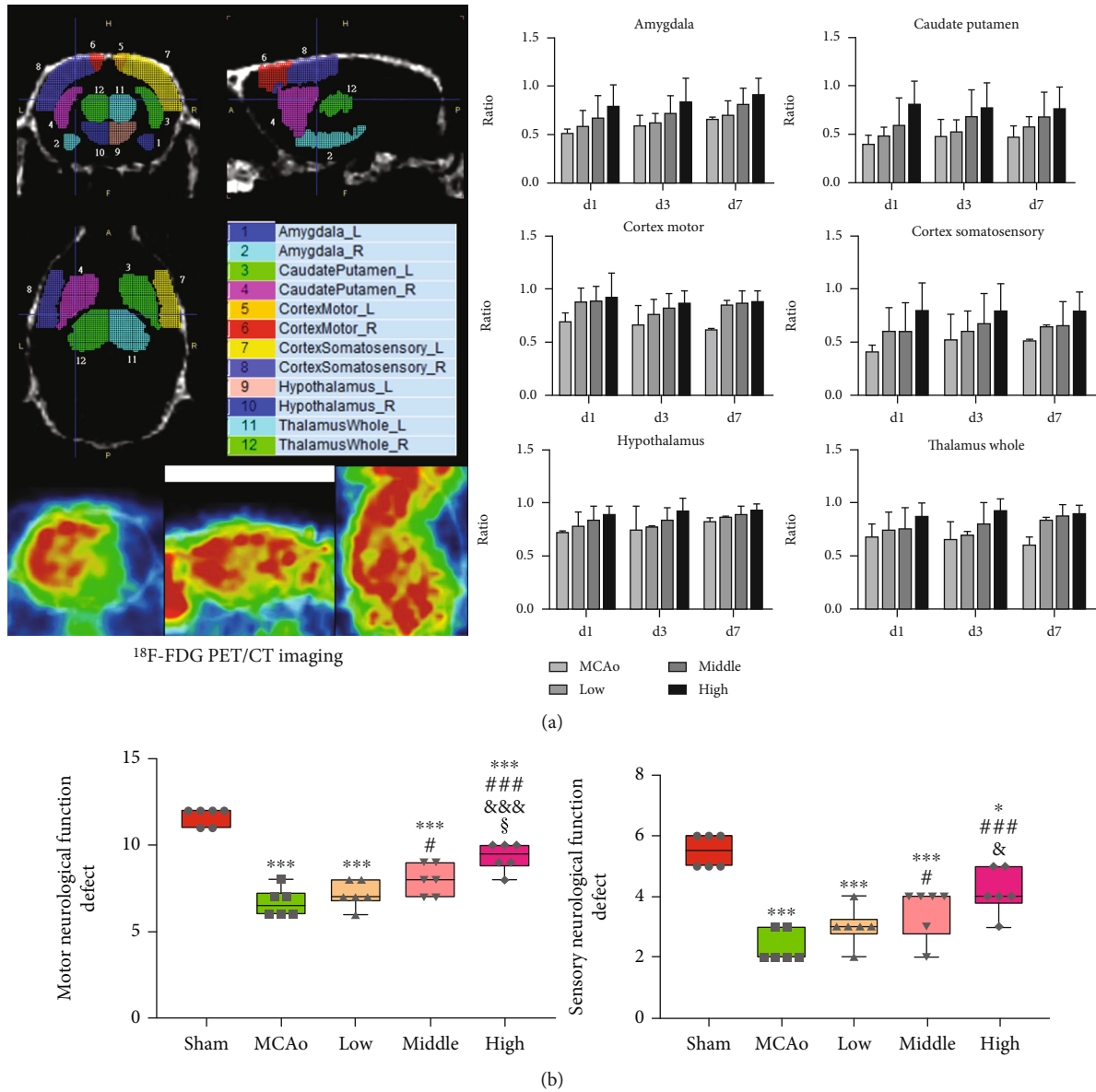
(a)

(b)

FIGURE 2: Cerebral glucose utilization and neurological function assessment. (a) Metabolic ratio of ^{18}F-FDG in 6 regions of brain was presented. (b) Evaluation of motor and sensory function scores. Data presented as mean ± standard deviation. $^*p < 0.05$, $^{***}p < 0.001$ vs. Sham; $^{\#}p < 0.05$, $^{\#\#\#}p < 0.001$ vs. MCAo; $^{\&}p < 0.05$, $^{\&\&\&}p < 0.001$ vs. low; $^{\$}p < 0.05$ vs. middle.

Figure 2(a), AC extract treatment improved glucose utilization in six ipsilateral lesion regions in a dose-dependent manner. Especially in Thalamus Whole region, the ratio in high dose group was obviously higher than that in MCAo group at day 3 ($p < 0.05$). Outcomes of neurobehaviors test at day 7 in Figure 2(b) suggested that motor function in high dose group was the most significant amelioration among three therapeutic groups ($p < 0.05$ vs. middle dose, $p < 0.001$ vs. low dose). Simultaneously, sensory functional outcome also suggested the same improved trend, and attenuated sensory deficiency in high dose group was more obvious than that in low dose group ($p < 0.05$).

3.3. AC Extract Treatment Suppressed Proinflammatory Microglial Phenotype.
As classic biomarkers of microglia,

increasing Iba1 expression represents microglial activation, and CD206 is regarded as an anti-inflammatory marker of microglia. As shown in Figure 3(a), the images of immunofluorescence staining showed that positive signals of Iba1 (red) and CD206 (green) widely distributed in ipsilateral hemisphere, and there existed sporadic overlapping signals (yellow). Quantitative analysis indicated that Iba1 expression in MCAo group was distinctly ascended ($p < 0.001$, vs. middle-high dose groups), while treatment with AC extract reversed the results in a dose-dependent manner at day 7 (Figure 3(b)). Simultaneously, expressions of CD206 in three dose groups suggested a significantly increasing trend compared with that in MCAo group ($p < 0.001$, Figure 3(c)). The results illustrated that AC extract treatment inhibited activated microglial cells and

(a)

(b)

(c)
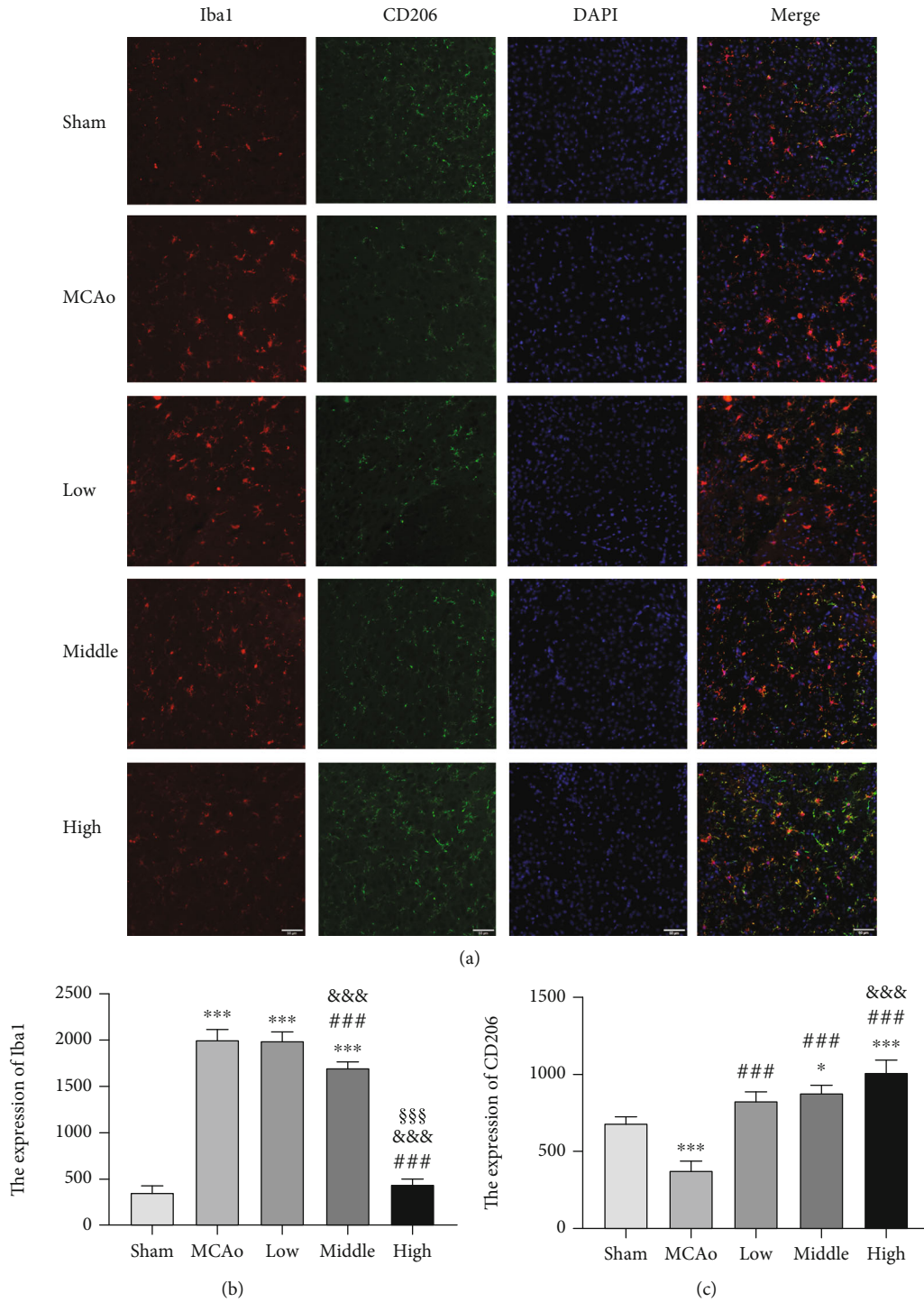
FIGURE 3: Microglial inflammatory phenotypes in ischemic boundary zone after stroke. (a) Immunofluorescence staining images of Iba1 (red) and CD206 (green) were presented (magnification, ×400). (b and c) Relative expressions of Iba1 and CD206 in ischemic cortex zone were analyzed. Scale bar 50 μm. Data presented as mean ± standard deviation. ***$p < 0.001$ vs. sham; ###$p < 0.001$ vs. MCAo; &&&$p < 0.001$ vs. low; §§§$p < 0.001$ vs. middle.

facilitated them to transform to anti-inflammatory phenotype after ischemic stroke.

3.4. AC Extract Treatment Inhibited TLR4/NF-κB Pathway, NLRP3 Inflammasome Assembly, and TNF-α, IL-1β, and IL-6 Secretion. Western blotting results showed that treatment with a high dose of AC extract not only notably suppressed TLR4 expression but also inhibited phosphorylation of IKKβ and IκBα compared with low-middle dose treatment ($p < 0.05$, Figures 4(a) and 4(b)). Nuclear P65 expressions in tree treatment groups indicated dose-dependent response to descend compared with that in

(a)

(b)

(c)

(d)

(e)

(f)
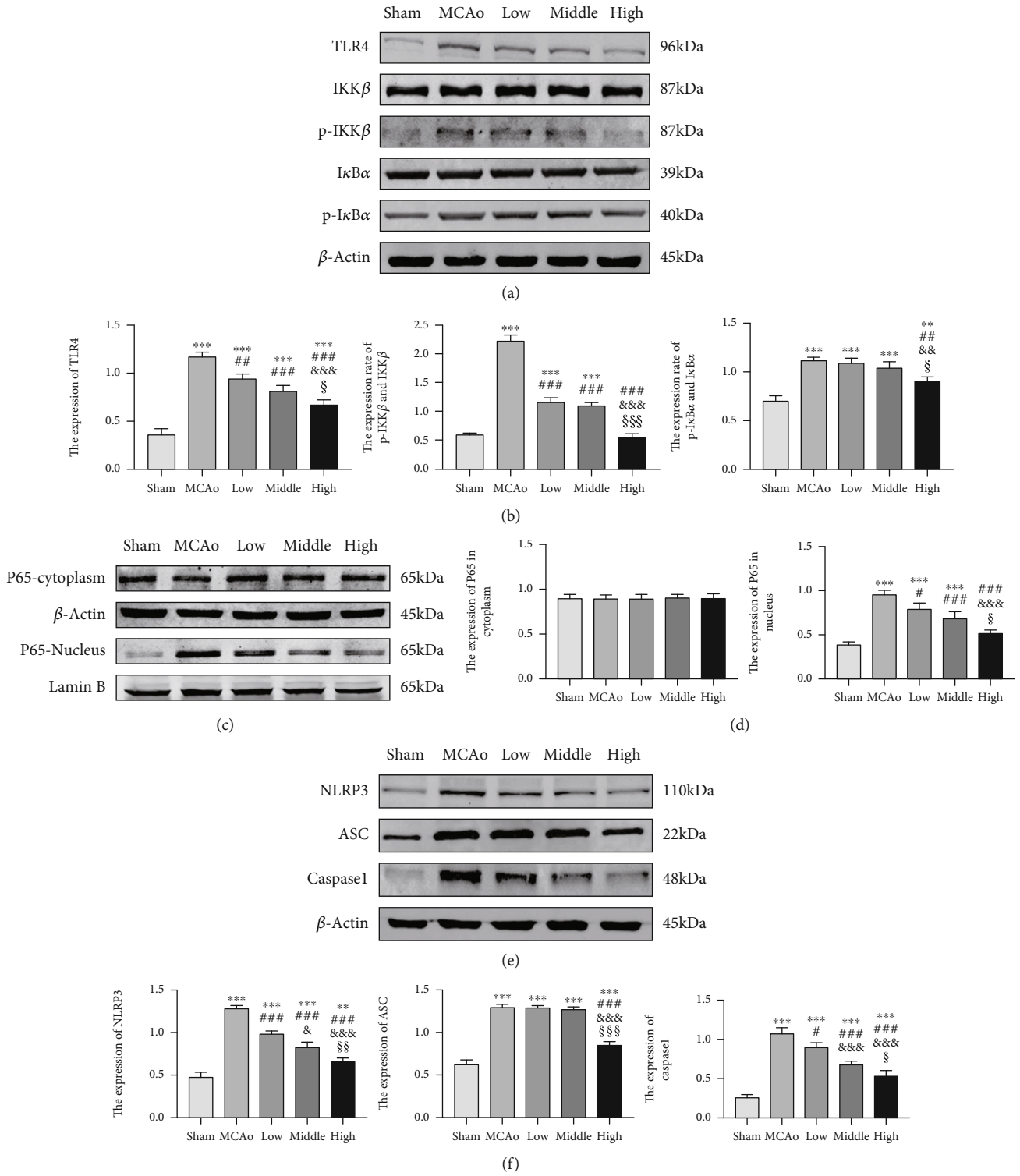
FIGURE 4: Continued.

(g)
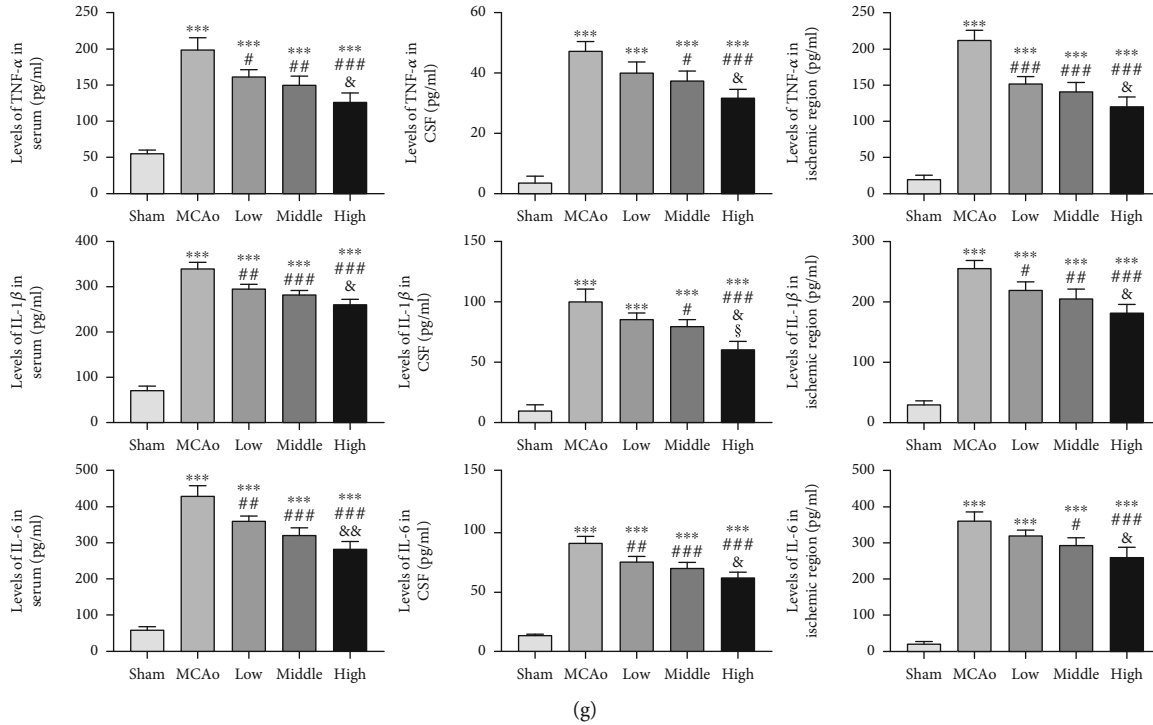
Figure 4: TLR4/NF-κB pathway, NLRP3 inflammasome, and inflammatory cytokines poststroke. (a, c, and e) Representative western blot belts for TLR4, phosphorylated IKKβ and IκBα, nuclear and cytoplasmic P65, NLRP3, ASC, and caspase-1 in each group's ipsilateral hemisphere. (b, d, and f) Quantitative analysis of TLR4/NF-κB pathway and NLRP3 inflammasome. (g) ELISA assay of TNF-α, IL-1β, and IL-6 in serum of peripheral blood, CSF, and ipsilateral hemisphere. Data presented as mean ± standard deviation. $^{**}p < 0.01$, $^{***}p < 0.001$ vs. sham; $^{\#}p < 0.05$, $^{\#\#}p < 0.01$, $^{\#\#\#}p < 0.001$ vs. MCAo; $^{\&}p < 0.05$, $^{\&\&}p < 0.01$, $^{\&\&\&}p < 0.001$ vs. low; $^{\S}p < 0.05$, $^{\S\S\S}p < 0.001$ vs. middle.

MCAo group ($p < 0.001$, Figures 4(c) and 4(d)), and the expression of P65 in cytoplasm had no obvious alteration among five groups. As shown in Figure 4(e), expressions of NLRP3, ASC, and cleaved caspase-1 obviously elevated in MCAo group at day 7, suggesting stroke stress-activated NLRP3 inflammasome assembly. Quantitative analysis showed that AC extract treatment prevented assembly of NLRP3 inflammasome by reducing NLRP3, ASC, and caspase-1 expressions, and high dose of AC extract presented the most predominantly inhibited action among three doses groups ($p < 0.05$, vs. low-middle dose group, Figure 4(f)).

Quantitative analysis suggested that the amount of TNF-α in CSF and supernatant of ipsilateral hemispheric homogenizer was more than 8 ∼ 10 folds in MCAo group as much as that in sham group, and its amount in serum of peripheral blood was 4 folds higher than that in the sham group. In the MCAo group, changed trends of IL-1β and IL-6 were parallel with that of TNF-α in CSF, brain parenchyma, and serum. The results showed that concentrations of TNF-α, IL-1β, and IL-6 in the brain were notably ascended compared with those in peripheral blood poststroke. High dose of AC extract group distinctly reduced TNF-α, IL-1β, and IL-6 concentrations whatever in CSF or brain parenchyma and serum of peripheral blood in comparison with low dose group ($p < 0.05$, Figure 4(g)).

3.5. AC Extract Treatment Decreased Nuclear P65 Translocation and TNF-α, IL-1β, and IL-6 Concentrations

via Targeting TLR4 in LPS-Stimulated Microglial Cells. It indicated that TLR4 expression and the number of BV2 with nuclear P65 positive signal in LPS + High group were obviously decreased compared with those in LPS and LPS + negative TLR4 siRNA groups ($p < 0.001$, Figures 5(a) and 5(b)). Furthermore, combination treatment of TLR4 siRNA and high dose group's CSF did not further reduce the number of BV2 with nuclear P65 positive signal, showing AC extract should target TLR4 against nuclear P65 translocation in LPS-stimulated microglial cells.

In vitro, quantitative analysis in Figure 5(c) indicated concentrations of TNF-α, IL-1β, and IL-6 were high in LPS and LPS + negative TLR4 siRNA groups, but this inflammatory cytokine production was inhibited in LPS + High and LPS + TLR4 siRNA groups. Simultaneously, TLR4 siRNA plus high dose group's CSF treatment failed to further downregulate concentrations of TNF-α, IL-1β, and IL-6, suggesting AC extract treatment decreased inflammatory cytokines secretion via antagonizing TLR4.

3.6. AC Extract Treatment Facilitated Autophagy in Ipsilateral Hemisphere. Evidence showed that cytosolic form of LC3 (LC3-I) is conjugated to phosphatidylethanolamine (PE) to become an LC3-PE conjugate (LC3-II), which is required for the formation of autophagosomal membranes, and Beclin 1 is important for the localization of autophagic proteins to a preautophagosomal structure [13, 26]. As shown in Figure 6, we found expressions of LC3-II and Beclin

(a)

(b)

(c)
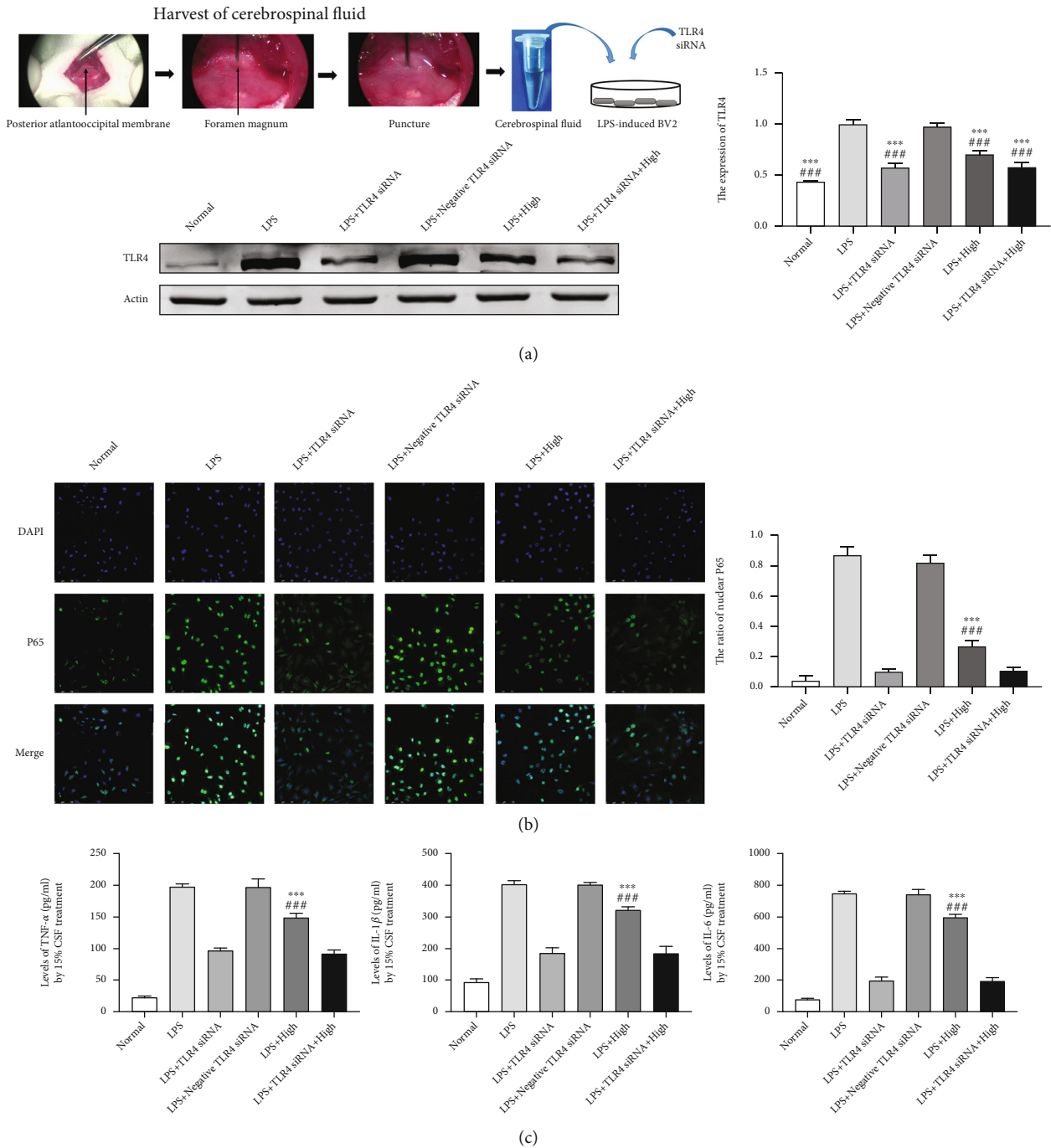
FIGURE 5: TLR4 and nuclear P65 expressions and inflammatory cytokines concentrations in LPS-stimulated BV2 microglial cells. (a) Schematic diagram of LPS-stimulated BV2 microglial cells incubated with CSF and transfected with TLR4 siRNA, as well as TLR4 expression by western blotting. (b) Immunofluorescence staining with nuclear p65 (green) was presented in LPS-induced BV2 microglial cells (magnification, ×400) and positive signal analysis. (c) ELISA assay of TNF-α, IL-1β, and IL-6 in conditional culture medium. Data presented as mean ± standard deviation. ***$p < 0.001$ vs. LPS; ###$p < 0.001$ vs. LPS + negative TLR4 siRNA. Scale bar 50 μm.

(a)

(b)
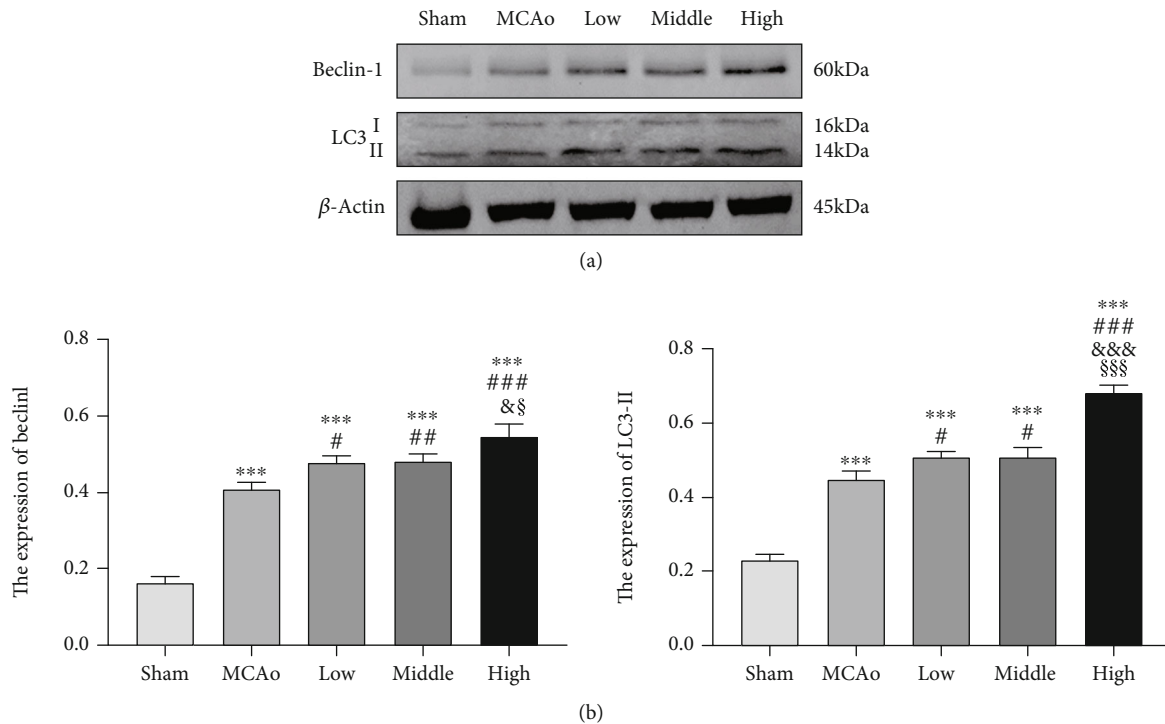
FIGURE 6: Upregulation of autophagy after ischemic stroke. (a) Representative western blotting belts for LC3-II and Beclin 1 and (b) quantitative analysis were presented. Data presented as mean ± standard deviation. $***p < 0.001$ vs. Sham; $^{#}p < 0.05$, $^{##}p < 0.01$, $^{###}p < 0.001$ vs. MCAo; $^{&}p < 0.05$, $^{&&&}p < 0.001$ vs. low; $^{§}p < 0.05$, $^{§§§}p < 0.001$ vs. middle.

1 obviously elevated in MCAo group compared with sham group ($p < 0.001$), showing stroke triggered autophagy. Three dose groups further enhanced expressions of LC3-II and Beclin 1, especially high dose group was the most significant ($p < 0.05$, vs. low-middle dose group), which indicated that AC extract treatment enhanced autophagy in a dose-dependent manner poststroke.

3.7. AC Extract Treatment Attenuated Apoptosis in Ipsilateral Hemisphere. As shown in Figure 7(a), cells with red TUNEL signal distributed in ischemic boundary zone, and quantitative analysis indicated that TUNEL expression was markedly ascended in MCAo group and yet three doses of AC extract groups dose-dependently attenuated TUNEL signals ($p < 0.05$). Moreover, western blotting results in Figures 6(b) and 6(c) indicated Bcl-2/Bax ratio gradually rose from low to high dose of AC extract groups compared with MCAo group ($p < 0.001$), and expressions of Caspase 8 and cleaved Caspase 3 in high dose group were lower than those in MCAo group ($p < 0.05$), which contributed to attenuation of apoptotic pathway.

4. Discussion

Evidence suggests that inflammation and autophagy are closely associated with cerebral ischemic injury [27]. Our study firstly demonstrates that combination treatment of *Angelica sinensis* and *Cinnamomum cassia* is able to suppress neuroinflammatory response via inhibiting TLR4/NF-κB pathway and NLRP3 inflammasome assembly and advance

autophagy by elevating LC3-II and Beclin 1 expressions, as well as attenuate apoptosis by increasing Bcl-2/Bax ratio and decreasing caspase 8 and cleaved caspase-3 expressions, which is beneficial to exerting neuroprotective effect flowing cerebral ischemia (Figure 8).

Due to CBF interruption after stroke, several DAMPs (e.g., high mobility group box 1, heat-shock proteins, and nucleic acids) are derived from injured and necrotic cells release, and simultaneously, BBB disruption is implicated in leukocyte infiltration into the brain parenchyma, both of which contribute to the initiation of postischemic inflammation [6, 25]. Following ischemic progression, microglia can switch from an early anti-inflammatory phenotype to a proinflammatory phenotype, especially LPS and inflammatory cytokines can facilitate microglial transformation into proinflammatory phenotype [28]. In the current study, AC extract treatment can notably decrease Iba1 positive signal and increase CD206 positive signal, suggesting its inhibited proinflammatory efficacy on microglial cells after ischemic stroke.

On the membrane of microglia, there exist TLRs activated not only by DAMPs but also by pathogen-associated molecular patterns, e.g., LPS [29]. It is reported that TLR2 and TLR4 involve in inflammatory injury and subsequent ischemic damage poststroke, and TLR4-deficient mice present distinctly decreased infarcted volume, positive microglial number, and NF-κB's p65 subunit after focal ischemic stroke [25, 29]. In the present study, we demonstrate that AC extract treatment notably reduces TLR4 expression whatever in ipsilateral hemisphere or in LPS-stimulated BV2 microglial cells
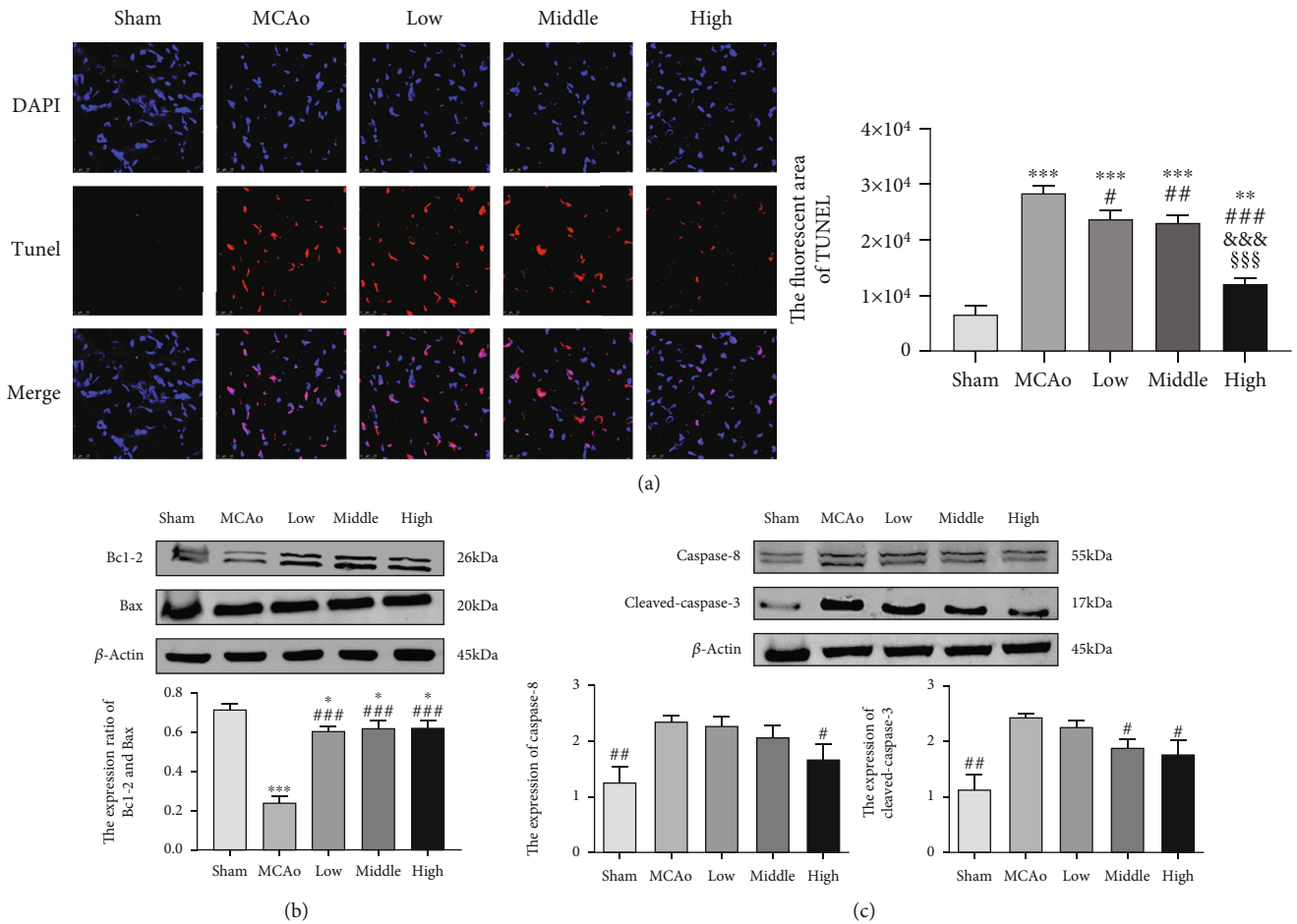
(a)

(b)

(c)

Figure 7: TUNEL staining and apoptotic pathway in ischemic penumbra. (a) Immunofluorescence staining with TUNEL (red) was presented (magnification, ×400) and quantitative analysis of TUNEL fluorescence. (b and c) Representative western blot belts for Bcl-2, Bax, Caspase-8, and cleaved-Caspase-3 and quantitative analysis. Data presented as mean ± standard deviation. $^*p < 0.05$, $^{**}p < 0.01$, $^{***}p < 0.001$ vs. Sham; $^{#}p < 0.05$, $^{##}p < 0.01$, $^{###}p < 0.001$ vs. MCAo; $^{\&\&\&}p < 0.001$ vs. low; $^{\S\S\S}p < 0.001$ vs. middle. Scale bar 25 μm.

by western blotting, and its efficacy on inhibition of TLR4 is similar to TLR4 siRNA's in vitro, showing AC extract can antagonize TLR4 activation.

The activated NF-κB transcriptional pathway not only plays a predominant role in inflammatory aspects but also is critical to the regulation of apoptosis [30]. TLRs, NLRs, proinflammatory cytokines, and chemokine family, and so on, as "molecular switch" function of NF-κB, phosphorylate IκBα by the IκB kinase (IKK) complex is composed of IKKα, IKKβ, and regulatory IKKγ. Moreover, in IKK complex, it is reported that IKKβ has higher capacities for IKK activation and NF-κB induction than IKKα [31, 32]. Phosphorylation of IκBα allows for NF-κB nuclear translocation and DNA binding. Amount of literature show that suppression of TLR4/NF-κB pathway attenuates brain edema and infarction volume and enhances antiapoptotic ability in MCAo model of rats [33]. In the present study, it suggests that treatment with AC extract obviously reduces phosphorylated IKKβ and IκBα, as well as nuclear P65 expression in a dose-dependent manner, contributing to inhibition of nuclear transcriptional activity of NF-κB. Interestingly, in vitro, the number of LPS-stimulated BV2 microglial cells with nuclear P65 positive signal was not further altered after combining

TLR4 siRNA with high dose group's CSF, suggesting AC extract mainly targets TLR4 instead of other targets in NF-κB pathway.

TLRs and NLRs exert stepwise effects on the production of IL-1β, which suggests that TLR signaling yields pro-IL-1β and subsequently caspase-1 activated by NLRPs inflammasome cleaves it into IL-1β [6]. Recent reports evidence that NLRP3 inflammasome plays important mediating roles in inflammation and innate immunity response in central nervous system diseases [34]. In animal models of stroke, high NLRP3-inflammasome assembly and IL-1β expression occur, while NLRP3 deficiency improves neurovascular damage [35]. In the present study, it shows that treatment with AC extract downregulates expressions of NLRP3, ASC, and caspase-1 in a dose-dependent manner poststroke, which contributes to directly reducing the level of IL-1β, as well as other proinflammatory cytokine concentrations.

The study has indicated that TNF-α, IL-1β, and IL-6 secreted by activated microglia involve in neuronal cell apoptosis at stroke onset [36]. Hotter and colleagues [37] found IL-6 was an inflammatory marker of cerebral parenchymal damage. By ELISA assay, we discover there exists an interesting phenomenon on TNF-α, IL-1β, and IL-6 concentrations
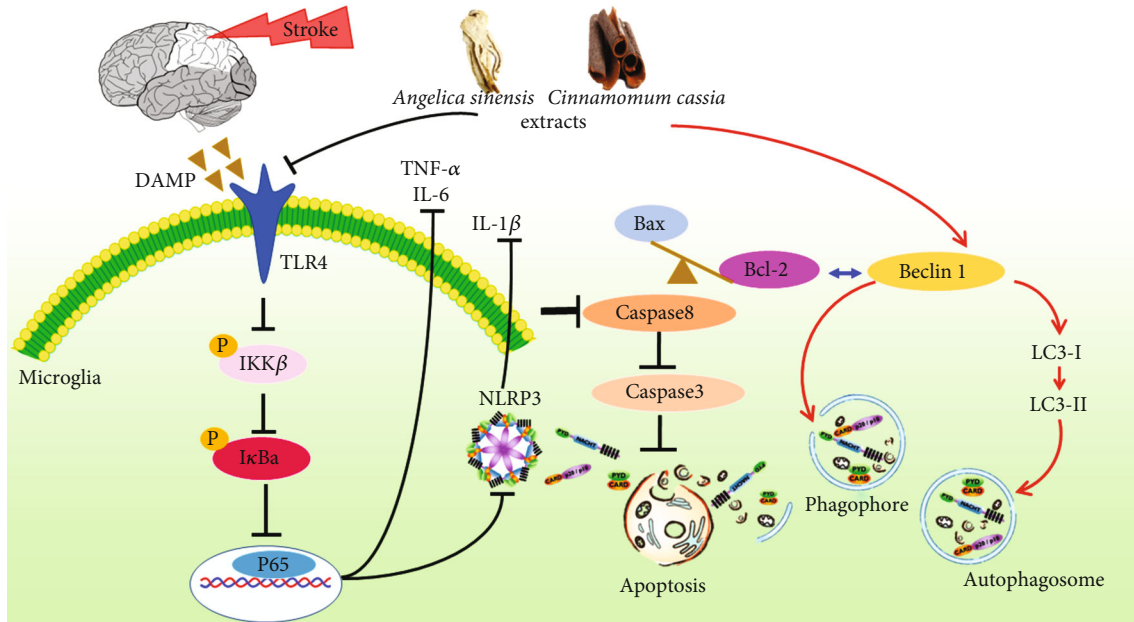
FIGURE 8: The schematic diagram of mechanisms of AC extract against neural injury by regulation of inflammatory and autophagic pathways after ischemic stroke.

between in peripheral blood and brain parenchyma. In CSF and supernatant of ipsilateral hemispheric homogenizer, concentration of these inflammatory cytokines is obviously higher than that in serum. It reported that inflammasome proteins quickly diffuse into CSF after traumatic brain injury, so the quantity of inflammasome proteins in CSF may be used as biomarkers to predict long-term outcome or guide therapeutic interventions with the goal of lowering inflammasome protein concentrations [6]. Similar to the result, we hypothesize that alterations of TNF-α, IL-1β, and IL-6 concentrations in CSF are more suitable to represent inflammatory response after ischemic stroke. In the current study, AC extract treatment notably decreases TNF-α, IL-1β, and IL-6 concentrations in CSF, ipsilateral hemisphere, and peripheral blood, suggesting the ability of attenuating inflammatory cytokines. Moreover, in vitro, we found that treatment of high dose group's CSF plus TLR4 siRNA reduced TNF-α, IL-1β, and IL-6 concentrations in LPS-stimulated BV2, while it failed to further aggravate the attenuation compared with therapy alone. It once again demonstrates that AC extract treatment acts on inhibition of TLR4 followed by deactivating its downstream pathways.

Evidence indicates that upregulations of LC3-II and Beclin-1 expressions, as activated autophagy-related signals, play important roles in the formation of autophagosomes [13]. Our western blot results indicated that LC3-II and Beclin-1 expressions significantly elevated after AC extract treatment, which should contribute to the initiation of autophagy. The study discovers Bcl-2 binding to Beclin-1 after the onset of apoptosis inhibits autophagy, while activated autophagy conduces to injured neuronal cells to survive against apoptosis in rat MCAo model [13, 38]. Therefore, we hypothesize that upregulation of autophagy by AC extract treatment might contribute to appropriate degrada-

tion and digestion of integral cellular components, as well as isolation between Bcl-2 and Beclin-1. As a primary apoptotic pathway, Bax binding competition with Bcl-2 and other members of the Bcl-2 family in mitochondria membrane triggers activation of mitochondrial pathway following focal ischemia, which also directly releases apoptosis-inducing factor into nucleus resulting in chromatin condensation and large scale DNA fragmentation [39]. Additionally, after cerebral ischemia, Fas-associated death domain protein binding to procaspase-8 triggers activation of caspase 8; subsequently, caspase-3 is activated and causes caspase 3-dependent cell death [40]. Our result show AC extract treatment obviously increases the Bcl-2/Bax ratio and decreases caspase8/3 expressions, which contributes to antiapoptosis.

Caspase-1 activity, IL-1β, TNF-α, and NLRP3 have been demonstrated to be associated with modulation of apoptosis after stroke [9, 41, 42], causing activation of caspase-dependent pathways of cell death. In MCAo/reperfusion model, activated autophagic pathway attenuates NLRP3 inflammasome might be related to phagocytic actions and transportation into lysosomes [15, 16, 43], and TLR4-modulated NF-κB pathway has a negative effect on autophagy regulation [27]. In the present study, elevated autophagy and suppressed TLR4-modulated NF-κB pathway by AC extract treatment contribute to decreasing caspase-1, IL-1β, TNF-α, and NLRP3 expressions, which might be beneficial to attenuation of caspase-dependent pathways of apoptosis and explanation of relationship among inflammation, autophagy, and apoptosis, embodying multiple therapeutic advantages of AC extract on ischemic stroke. Of course, precise mechanisms need to be explored in the next study. Whatever these therapeutic effects ameliorate neurological functional outcomes after ischemia. Literature suggest that neurons in the infarct area can release damage signal to distal

brain regions (e.g., thalamus) to trigger microglia-related secondary neurodegeneration [44]. Disruption of thalamic circuitry severely affects motor recovery [45]. Our results indicated that AC extract treatment significantly enhanced glucose utilization in thalamic lesion region, as well as elevated anti-inflammatory microglial phenotype, autophagy, and antiapoptosis, which contributes to the improvement of motor recovery due to integrity of thalamic circuitry poststroke.

Additionally, accumulating literature demonstrate active compounds extracted from *Angelica sinensis* and *Cinnamomum cassia* exert significant neuroprotective action by anti-inflammation or autophagy poststroke. Trans-cinnamaldehyde decreases iNOS, COX-2 expression, and NF-κB signaling pathway against neuroinflammation in ischemia/reperfusion model [46], and cinnamaldehyde inhibits expressions of TLR4, TNF-receptor-associated factor 6, and nuclear translocation of NF-κB in permanent MCAo model [47]. *Angelica sinensis* and its compounds have significant effects of anti-inflammation and antioxidative stress [48], and as a main active compound of *Angelica sinensis*, ferulic acid pretreatment exerted neuroprotective effects against apoptosis through activating 70 kDa heat shock protein (HSP70)/Bcl-2- and HSP70/autophagy-induced signaling pathways after focal cerebral ischemia [49]. In our study, we hypothesize these compounds from *Angelica sinensis* and *Cinnamomum cassia* play the main pharmacological role in neuroprotection. Precise pharmacodynamic research needs to be investigated in further study.

5. Conclusions

In summary, our study demonstrates that the extracts of *Angelica sinensis* and *Cinnamomum cassia* from oriental medicinal foods have significant capacities of inhibiting neuroinflammation, advancing autophagy, and antiapoptosis, which contributes to the improvement of neurological functional outcome. The mechanisms are associated with suppressing TLR4/NF-κB pathway and NLRP3 inflammasome and enhancing LC3-II and Beclin-1 expressions after ischemic stroke. Therefore, we think AC extract is a novel neuroprotective agent of regulation of inflammatory and autophagic pathways for stroke treatment.

Data Availability

Due to patent application and commercialization, the data used to support the findings of this study are available from the corresponding author upon request after publication of this article.

Conflicts of Interest

The authors declare that there is no conflict of interest regarding the publication of this paper.

Authors' Contributions

Cheng Luo and Qi Chen contributed equally to this work.

References

[1] GBD 2019 Diseases and Injuries Collaborators, "Global burden of 369 diseases and injuries in 204 countries and territories, 1990–2019: a systematic analysis for the Global Burden of Disease Study 2019," *Lancet*, vol. 396, no. 10258, pp. 1204–1222, 2020.

[2] C. O. Johnson, M. Nguyen, G. A. Roth et al., "Global, regional, and national burden of stroke, 1990-2016: a systematic analysis for the Global Burden of Disease Study 2016," *Lancet Neurology*, vol. 18, no. 5, pp. 439–458, 2019.

[3] S. Dabrowska, A. Andrzejewska, B. Lukomska, and M. Janowski, "Neuroinflammation as a target for treatment of stroke using mesenchymal stem cells and extracellular vesicles," *Journal of Neuroinflammation*, vol. 16, no. 1, article 1571, p. 178, 2019.

[4] J. Anrather and C. Iadecola, "Inflammation and stroke: an overview," *Neurotherapeutics*, vol. 13, no. 4, pp. 661–670, 2016.

[5] R. Macrez, C. Ali, O. Toutirais et al., "Stroke and the immune system: from pathophysiology to new therapeutic strategies," *Lancet Neurology*, vol. 10, no. 5, pp. 471–480, 2011.

[6] K. A. Kigerl, J. P. de Rivero Vaccari, W. D. Dietrich, P. G. Popovich, and R. W. Keane, "Pattern recognition receptors and central nervous system repair," *Experimental Neurology*, vol. 258, pp. 5–16, 2014.

[7] V. Kumar, "Toll-like receptors in the pathogenesis of neuroinflammation," *Journal of Neuroimmunology*, vol. 332, pp. 16–30, 2019.

[8] I. N. Mohamed, T. Ishrat, S. C. Fagan, and A. B. el-Remessy, "Role of inflammasome activation in the pathophysiology of vascular diseases of the neurovascular unit," *Antioxidants & Redox Signaling*, vol. 22, no. 13, pp. 1188–1206, 2015.

[9] X. Ye, T. Shen, J. Hu et al., "Purinergic 2X7 receptor/NLRP3 pathway triggers neuronal apoptosis after ischemic stroke in the mouse," *Experimental Neurology*, vol. 292, pp. 46–55, 2017.

[10] D. Y. Fann, Y. Lim, Y. Cheng et al., "Evidence that NF-κB and MAPK signaling promotes NLRP inflammasome activation in neurons following ischemic stroke," *Molecular Neurobiology*, vol. 55, no. 2, pp. 1082–1096, 2018.

[11] Z. Zheng and M. A. Yenari, "Post-ischemic inflammation: molecular mechanisms and therapeutic implications," *Neurological Research*, vol. 26, no. 8, pp. 884–892, 2004.

[12] Y. Sun, Y. Zhu, X. Zhong, X. Chen, J. Wang, and G. Ying, "Crosstalk between autophagy and cerebral ischemia," *Frontiers in Neuroscience*, vol. 12, p. 1022, 2019.

[13] P. Wang, B. Z. Shao, Z. Deng, S. Chen, Z. Yue, and C. Y. Miao, "Autophagy in ischemic stroke," *Progress in Neurobiology*, vol. 163-164, pp. 98–117, 2018.

[14] S. Zhou, B. Qiao, X. Chu, and Q. Kong, "Oxymatrine attenuates cognitive deficits through SIRT1-mediated autophagy in ischemic stroke," *Journal of Neuroimmunology*, vol. 323, pp. 136–142, 2018.

[15] B. Levine, N. Mizushima, and H. W. Virgin, "Autophagy in immunity and inflammation," *Nature*, vol. 469, no. 7330, pp. 323–335, 2011.

[16] J. Harris, T. Lang, J. P. W. Thomas, M. B. Sukkar, N. R. Nabar, and J. H. Kehrl, "Autophagy and inflammasomes," *Molecular Immunology*, vol. 86, pp. 10–15, 2017.

[17] H. Ting, C. Chang, K. Lu et al., "Targeting cellular stress mechanisms and metabolic homeostasis by Chinese herbal drugs for neuroprotection," *Molecules*, vol. 23, no. 2, p. 259, 2018.

[18] L. Zhang, *Medical Book of Lu Zhang*, China Press of Traditional Chinese Medicine, 1999.

[19] D. Champakaew, A. Junkum, U. Chaithong et al., "Assessment of Angelica sinensis (Oliv.) Diels as a repellent for personal protection against mosquitoes under laboratory and field conditions in northern Thailand," *Parasites & vectors*, vol. 9, no. 1, article 1650, p. 373, 2016.

[20] J. Liu, Q. Zhang, R. Li et al., "The traditional uses, phytochemistry, pharmacology and toxicology of Cinnamomi ramulus: a review," *Journal of Pharmacy and Pharmacology*, vol. 72, no. 3, pp. 319–342, 2019.

[21] B. Liu, C. Luo, Z. Zheng et al., "Shengui Sansheng San extraction is an angiogenic switch via regulations of AKT/mTOR, ERK1/2 and Notch1 signal pathways after ischemic stroke," *Phytomedicine*, vol. 44, pp. 20–31, 2018.

[22] J. B. Bederson, L. H. Pitts, M. Tsuji, M. C. Nishimura, R. L. Davis, and H. Bartkowski, "Rat middle cerebral artery occlusion: evaluation of the model and development of a neurologic examination," *Stroke*, vol. 17, no. 3, pp. 472–476, 1986.

[23] C. Luo, X. Bian, Q. Zhang et al., "Shengui Sansheng San ameliorates cerebral energy deficiency via citrate cycle after ischemic stroke," *Frontiers in Pharmacology*, vol. 10, p. 386, 2019.

[24] J. H. Garcia, S. Wagner, K. F. Liu, and X. J. Hu, "Neurological deficit and extent of neuronal necrosis attributable to middle cerebral artery occlusion in rats. Statistical validation," *Stroke*, vol. 26, no. 4, pp. 627–635, 1995.

[25] T. Shichita, R. Sakaguchi, M. Suzuki, and A. Yoshimura, "Postischemic inflammation in the brain," *Frontiers in Immunology*, vol. 3, p. 132, 2012.

[26] K. Saijo and C. K. Glass, "Microglial cell origin and phenotypes in health and disease," *Nature Reviews Immunology*, vol. 11, no. 11, pp. 775–787, 2011.

[27] Y. Mo, Y. Sun, and K. Liu, "Autophagy and inflammation in ischemic stroke," *Neural Regeneration Research*, vol. 15, no. 8, pp. 1388–1396, 2020.

[28] S. Zhang, "Microglial activation after ischaemic stroke," *Stroke and Vascular Neurology*, vol. 4, no. 2, pp. 71–74, 2019.

[29] K. Hyakkoku, J. Hamanaka, K. Tsuruma et al., "Toll-like receptor 4 (TLR4), but not TLR3 or TLR9, knock-out mice have neuroprotective effects against focal cerebral ischemia," *Neuroscience*, vol. 171, no. 1, pp. 258–267, 2010.

[30] A. Hoffmann and D. Baltimore, "Circuitry of nuclear factor kappaB signaling," *Immunological Reviews*, vol. 210, no. 1, pp. 171–186, 2006.

[31] Z. W. Li, W. Chu, Y. Hu et al., "The IKKβ subunit of IκB kinase (IKK) is essential for nuclear factor κB activation and prevention of apoptosis," *The Journal of Experimental Medicine*, vol. 189, no. 11, pp. 1839–1845, 1999.

[32] Y. S. Song, M. Kim, H. Kim et al., "Oxidative stress increases phosphorylation of IκB Kinase-α by enhancing NF-κB-Inducing kinase after transient focal cerebral ischemia," *Journal of Cerebral Blood Flow & Metabolism*, vol. 30, no. 7, pp. 1265–1274, 2010.

[33] O. A. Harari and J. K. Liao, "NF-κB and innate immunity in ischemic stroke," *Annals of the New York Academy of Sciences*, vol. 1207, no. 1, pp. 32–40, 2010.

[34] K. Zhou, L. Shi, Y. Wang, S. Chen, and J. Zhang, "Recent advances of the NLRP3 inflammasome in central nervous system disorders," *Journal of Immunology Research*, vol. 2016, Article ID 9238290, 9 pages, 2016.

[35] F. Yang, Z. Wang, X. Wei et al., "NLRP3 deficiency ameliorates neurovascular damage in experimental ischemic stroke," *Journal of Cerebral Blood Flow & Metabolism*, vol. 34, no. 4, pp. 660–667, 2014.

[36] K. L. Lambertsen, K. Biber, and B. Finsen, "Inflammatory cytokines in experimental and human stroke," *Journal of Cerebral Blood Flow & Metabolism*, vol. 32, no. 9, pp. 1677–1698, 2012.

[37] B. Hotter, S. Hoffmann, L. Ulm, C. Meisel, J. B. Fiebach, and A. Meisel, "IL-6 plasma levels correlate with cerebral perfusion deficits and infarct sizes in stroke patients without associated infections," *Frontiers in Neurology*, vol. 10, p. 83, 2019.

[38] B. Lv, F. Li, J. Han et al., "Hif-1α overexpression improves transplanted bone mesenchymal stem cells survival in rat MCAO stroke model," *Frontiers in Molecular Neuroscience*, vol. 10, p. 80, 2017.

[39] I. Ferrer and A. M. Planas, "Signaling of cell death and cell survival following focal cerebral ischemia: life and death struggle in the penumbra," *Journal of Neuropathology and Experimental Neurology*, vol. 62, no. 4, pp. 329–339, 2003.

[40] B. R. S. Broughton, D. C. Reutens, and C. G. Sobey, "Apoptotic mechanisms after cerebral ischemia," *Stroke*, vol. 40, no. 5, pp. e331–e339, 2009.

[41] D. Radak, N. Katsiki, I. Resanovic et al., "Apoptosis and acute brain ischemia in ischemic stroke," *Current Vascular Pharmacology*, vol. 15, no. 2, pp. 115–122, 2017.

[42] F. S. Silverstein, "Can inhibition of apoptosis rescue ischemic brain?," *The Journal of Clinical Investigation*, vol. 101, no. 9, pp. 1809-1810, 1998.

[43] Y. Wang, C. Meng, J. Zhang, J. Wu, and J. Zhao, "Inhibition of GSK-3β alleviates cerebral ischemia/reperfusion injury in rats by suppressing NLRP3 inflammasome activation through autophagy," *International Immunopharmacology*, vol. 68, pp. 234–241, 2019.

[44] F. Block, M. Dihné, and M. Loos, "Inflammation in areas of remote changes following focal brain lesion," *Progress in Neurobiology*, vol. 75, no. 5, pp. 342–365, 2005.

[45] J. E. Anttila, K. W. Whitaker, E. S. Wires, B. K. Harvey, and M. Airavaara, "Role of microglia in ischemic focal stroke and recovery: focus on toll-like receptors," *Progress in Neuropsychopharmacology & Biological Psychiatry*, vol. 79, no. Part A, pp. 3–14, 2017.

[46] Y. Chen, Y. Wang, W. Huang et al., "Trans-cinnamaldehyde, an essential oil in cinnamon powder, ameliorates cerebral ischemia-induced brain injury via inhibition of neuroinflammation through attenuation of iNOS, COX-2 expression and NFκ-B signaling pathway," *Neuromolecular Medicine*, vol. 18, no. 3, pp. 322–333, 2016.

[47] J. Zhao, X. Zhang, L. Dong et al., "Cinnamaldehyde inhibits inflammation and brain damage in a mouse model of permanent cerebral ischaemia," *British Journal of Pharmacology*, vol. 172, no. 20, pp. 5009–5023, 2015.

[48] C. L. L. Saw, Q. Wu, Z. Su et al., "Effects of natural phytochemicals in Angelica sinensis (Danggui) on Nrf2-mediated gene expression of phase II drug metabolizing enzymes and anti-inflammation," *Biopharmaceutics & Drug Disposition*, vol. 34, no. 6, pp. 303–311, 2013.

[49] C. Y. Cheng, S. T. Kao, and Y. C. Lee, "Ferulic acid exerts anti-apoptotic effects against ischemic injury by activating HSP70/Bcl-2- and HSP70/autophagy-mediated signaling after permanent focal cerebral ischemia in rats," *The American Journal of Chinese Medicine*, vol. 47, no. 1, pp. 39–61, 2019.

Research Article

Wogonin Strengthens the Therapeutic Effects of Mesenchymal Stem Cells in DSS-Induced Colitis via Promoting IL-10 Production

Qiongli Wu [iD],[1,2] Shujuan Xie [iD],[1] Yinhong Zhu,[1] Jingrou Chen,[1] Jiatong Tian,[3] Shiqiu Xiong,[4] Changyou Wu [iD],[2] Yujin Ye [iD],[5] and Yanwen Peng [iD][1]

[1]*The Biotherapy Center, The Third Affiliated Hospital, Sun Yat-sen University, Guangzhou 510630, China*
[2]*Department of Immunology, Zhongshan School of Medicine, Sun Yat-sen University, Guangzhou 510080, China*
[3]*Department of Physics, King's College London, London, UK WC2R 2LS*
[4]*Cell Biology Group, National Measurement Lab, LGC, Fordham, Cambridgeshire, UK CB7 5WW*
[5]*Department of Rheumatology, The First Affiliated Hospital, Sun Yat-sen University, Guangzhou 510080, China*

Correspondence should be addressed to Yujin Ye; graceyeyj@hotmail.com and Yanwen Peng; pengyw@mail.sysu.edu.cn

Qiongli Wu and Shujuan Xie contributed equally to this work.

Received 21 February 2021; Accepted 20 May 2021; Published 22 June 2021

Academic Editor: Domenico Trombetta

Inflammatory bowel diseases (IBD) are prevalent and debilitating diseases; their clinical remedy is desperately unmet. Mesenchymal stem cells (MSCs) are pluripotent stem cells with multiple immunomodulatory effects, which are attributed to their efficacy in the IBD rodent model. Optimization of MSC regimes in IBD is a crucial step for their further clinical application. Wogonin is a flavonoid-like compound, which showed extensive immunomodulatory and adjuvant effects. This research is aimed at investigating whether and how Wogonin boosted the therapeutic efficiency of MSCs on DSS-induced colitis. Our results showed that the MSC treatment with Wogonin significantly alleviated the intestinal inflammation in IBD mice by increased IL-10 expression. In vitro experiments, Wogonin obviously raised the IL-10 production and ROS levels of MSCs in a dose-dependent manner. Meanwhile, western blot data suggested Wogonin improves the IL-10 production by inducing transcript factor HIF-1α expression via AKT/GSK3β signal pathway. Finally, the favorable effects of Wogonin on MSCs were confirmed by IL-10 blockade experiment in vivo. Together, our results suggested that Wogonin significantly increased the IL-10 production and enhanced the therapeutic effects of MSCs in DSS-induced colitis. This work suggested Wogonin as a novel optimal strategy for MSC clinical application.

1. Introduction

Inflammatory bowel disease (IBD) is a chronic, relapsing-remitting, inflammatory gastrointestinal disease with a rising incidence worldwide in the past two decades [1]. However, current therapeutic options are far from satisfactory. Recently, cell therapies have been explored in IBD, including mesenchymal stem cells (MSCs) [2]. MSCs are pluripotent stem cells, possessing self-renew ability and multidifferentiation potential function [3]. MSCs showed therapeutic features including angiogenesis, tissue repair, and immunomodulation, among which IL-10 was an important effector molecule [4]. Several researches supported that IL-10 is highly relevant to IBD, and IL-10$^{-/-}$ mice would spontaneously develop colitis [5].

In humans, polymorphisms in IL-10 [6] have been found to be correlated with very early onset of colitis. Our previous studies on rodent models of IBD also showed that MSC administration could significantly improve intestinal inflammation via IL-10 [7, 8]. Consistently, some strategies have been proposed to improve the therapeutic efficiency of MSC, and engineering IL-10 overexpressing MSCs have achieved better therapeutic efficacy in immune relative diseases [9–11].

Accumulating researches indicated the extracts of herbal plants have diverse biological activities [12]. *Scutellaria baicalensis* is widely used as Chinese herbal medicine, and Wogonin is one of its major bioactive compounds [13]. Wogonin is a flavonoid-like compound which possesses anticancer and immunomodulatory effects [14]. Although

TABLE 1: The division animal groups and the histological scoring system.

Animal groups	Tissue inflammation	Extent	Regeneration	Crypt damage	Percentage involvement	Histological score
Control/	None	None	Complete regeneration or normal tissue	None	—	0
IBD/	Slight	Mucosa	Almost complete regeneration	Basal 1/3 damaged	1%–25%	1
MSCs/	Moderate	Mucosa and submucosa	Regeneration with crypt's depletion	Basal 2/3 damaged	26%–50%	2
Wogonin/	Severe	Transmural	Surface epithelium not intact	Only surface epithelium intact	51%–75%	3
Wogonin+MSCs	—	—	No tissue repair	Entire crypt and epithelium lost	76%–100%	4

there is evidence that both MSCs and Wogonin could alleviate IBD [15–20], it is still unclear whether combining MSCs with Wogonin be more superior to either therapy alone.

In this research, we demonstrated that Wogonin extended the therapeutic efficiency of MSCs on DSS-induced murine colitis in vivo. It was due to the increased IL-10 expression in the intestinal tissue and peritoneal cavity. Mechanistic studies suggested that Wogonin enhanced IL-10 production and ROS levels in MSCs via AKT/GSK3β signal pathway. Furthermore, in vivo, the data exhibited that neutralizing anti-IL-10 antibody can abrogate the therapeutic effects of a combination of MSCs and Wogonin on colitis.

2. Material and Methods

2.1. Animals.
Male C57BL/6 mice aged 8-12 weeks were purchased from the Nanjing Model Experimental Animal Center and housed in pathogen-free conditions at Sun Yat-sen University. The age- and weight-matched of mice were applied for all mouse-related experiments. All animal studies were approved by the Zhongshan School of Experimental Animal Ethics Committee, Sun Yat-sen University, Guangzhou, China, and in strict compliance with the corresponding guidelines.

2.2. Reagents and Antibodies.
Reactive Oxygen Species Detection Assay Kit was purchased from BioVision (San Francisco, CA, USA). Wogonin was purchased from MedChemExpress (Israel Shekel), and LPS was purchased from Sigma-Aldrich (St. Louis, MO, USA). The following antibodies were used for cell surface staining: CD34-PE, CD44-FITC, CD29-PE-Cy7, Sca-1-AF700, CD45-AF700, and CD49e-APC are all from BioLegend and Mouse IL-10 ELISA Set and Zombie Green™ Fixable Viability Kit were purchased from BD Biosciences. Mouse IL-10 MAb was purchased from R&D Systems.

2.3. Induction and Assessment of Colitis.
Dextran sulfate sodium salt (DSS) was purchased from MP Biomedicals (United States) which was used to induce acute colitis in mice. 3% (w/v) DSS was dissolved in sterile water and supplied to the mice in drink water for 7 days, followed by regu-

lar drinking water until day 8. Mice were randomly divided into five groups, and there were 6 mice in each group: the mice were fed regular water as the control group, were exposed to 3% DSS water as the IBD group, were administrated 1×10^6 MSCs via peritoneal injection as the MSC group, and were injected 10 mg/kg Wogonin via i.p. as the Wogonin group, and the combination of MSC and Wogonin group received both 1×10^6 MSCs and 10 mg/kg Wogonin. Meanwhile, body weights of animals were scaled and recorded daily. Eight days later, the animals were sacrificed, and the length of the colon from the cecocolic junction to the anal verge was measured. Severity of the disease was assessed by weight loss, colon length, and histopathology scores of the colon. Colon tissues were processed for histological analysis by hematoxylin and eosin (H&E) stain. Histology was used to evaluate the inflammation (I) (0, none; 1, slight; 2, moderate; 3, severe), extent (E) (0, none; 1, mucosa; 2, mucosa and submucosa; 3, transmural), regeneration (R) (4, no tissue repair; 3, surface epithelium not intact; 2, regeneration with crypt's depletion; 1, almost complete regeneration; 0, complete regeneration or normal tissue), crypt damage (C) (0, none; 1, basal 1/3 damaged; 2, basal 2/3 damaged; 3, only surface epithelium intact; 4, entire crypt and epithelium lost), and percentage involvement (P) (1, 1%–25%; 2, 26%–50%; 3, 51%–75%; 4, 76%–100%) according to previous reports [21]. The division animal groups and the histological scoring system are listed in Table 1.

2.4. HE Staining.
Colon tissue was removed and then immersed in 4% paraformaldehyde. After dewaxing with dehydrated alcohol gradient, the tissue was embedded in paraffin and stained with hematoxylin and eosin (H&E).

2.5. MSC Differentiation Assays.
MSCs were isolated from the bone marrow of 6-8 weeks C57BL/6 mice, according to the improved low-density culture method [22]. The StemPro™ Osteogenesis Differentiation Kit (Thermo Fisher Scientific) and StemPro™ Adipogenesis Differentiation Kit (Thermo Fisher Scientific) were used for osteogenic and adipogenic differentiation in vitro, according to the manufacturer's recommended procedures. All cells at 6-8 passage were used in this study.
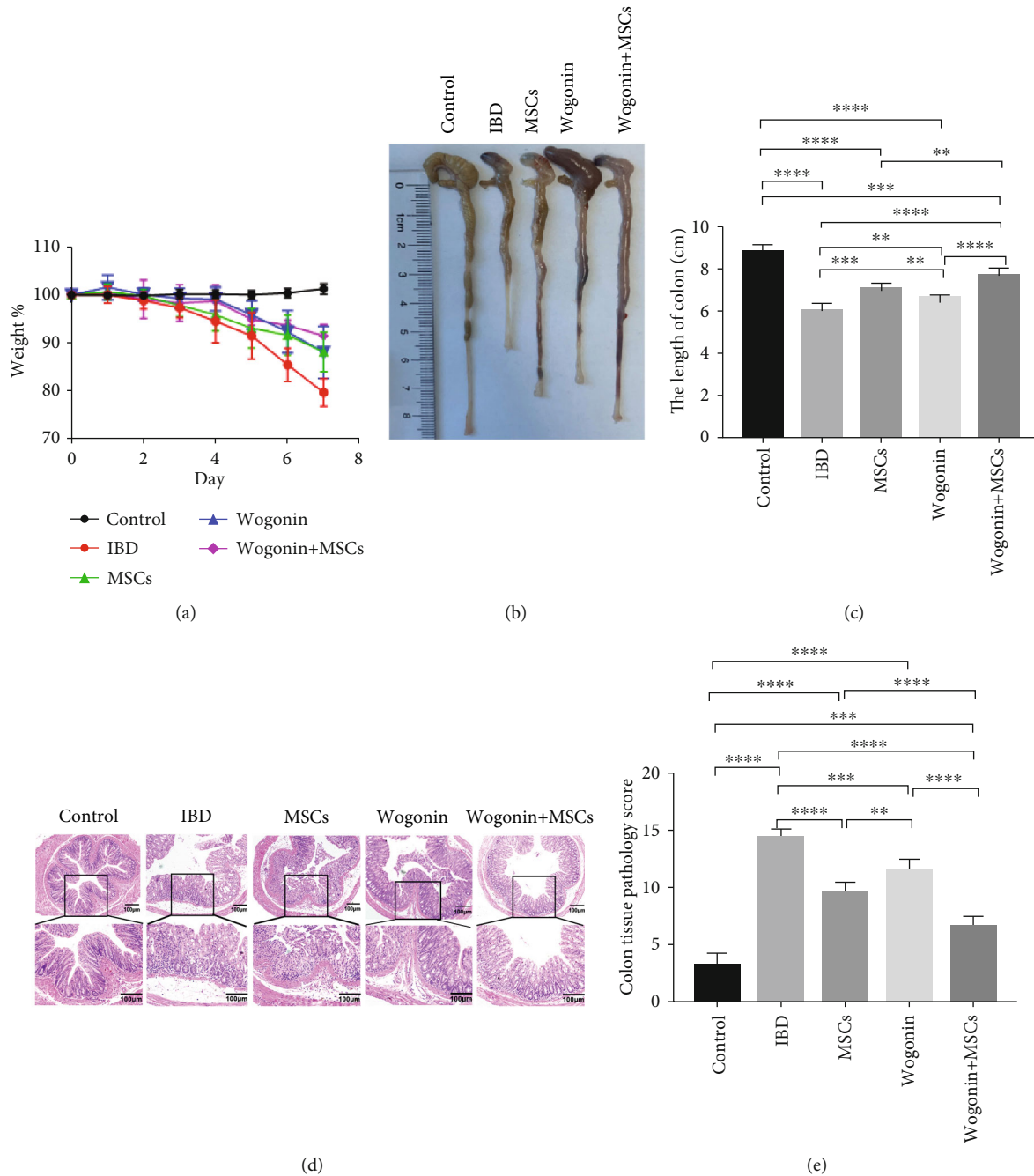
Figure 1: A combination of MSCs and Wogonin possessed optimal therapeutic effects on DSS-induced colitis. Mice were administered 3% DSS in drinking water for 7 days, followed by regular drinking water. On the 2nd day, mice received MSC treatment, Wogonin treatment, or a combined treatment, respectively. Then, mice were euthanized on day 8. (a) Body weights were monitored daily, and the values were expressed as percentage weight loss. (b, c) Colon length of five groups of mice was measured and recorded on day 8. (d) Representative H&E staining of the distal colon. Scale bar = 100 micros. Magnification, 40x and 100x. (e) Colonic histopathological scores of all mice were evaluated on day 8. Data represent mean values ± SEM. The statistical significance of difference between two means was calculated with an unpaired. A one-way ANOVA was performed, $^{**}P < 0.01$; $^{***}P < 0.001$; $^{****}P < 0.0001$. $n = 6$/group.

2.6. ELISA. Supernatants of cultured cells and mouse peritoneal lavage fluid samples were collected for detection of mouse IL-10 by enzyme-linked immunosorbent assay (ELISA Kit IL-10 from BD Biosciences, San Jose, CA, USA). The sensitivities of ELISA kits were 31.2 pg/ml for IL-10. ELISA assays were performed according to the manufacturer's instructions.

2.7. RNA-seq. After 24 h Wogonin treatment, RNA was extracted from both untreated MSCs and treated MSCs using Trizol (Invitrogen, Carlsbad, CA). RNA-seq data were normalized through the DESeq2 pipeline, and gene heat map was fulfilled with packages pheatmap under R 4.0.2. The gene ontology analysis was performed based on clusterProfiler written by Yu et al. [23].
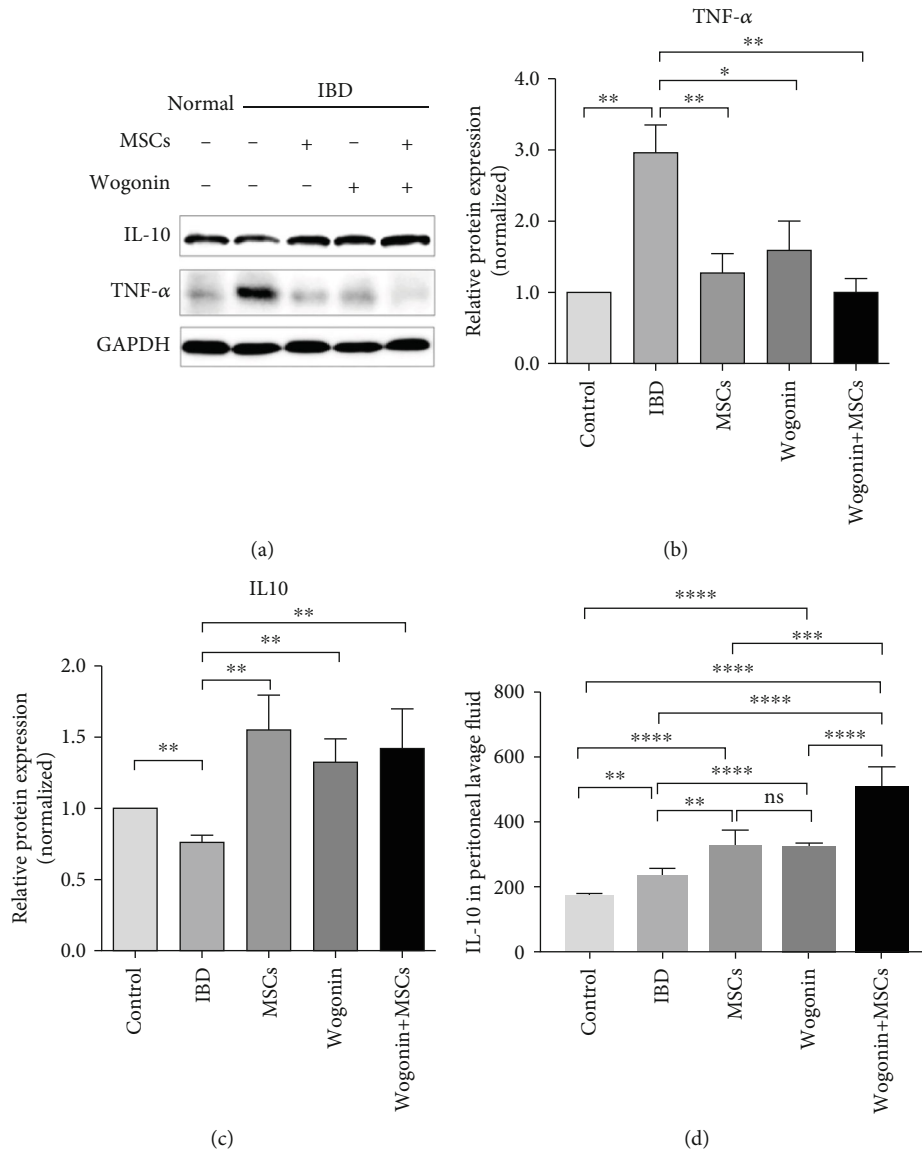
(a)

(b)

(c)

(d)

Figure 2: MSCs and Wogonin increased IL-10 levels in both colon tissue and peritoneal lavage fluid. Mice were administered 3% DSS in drinking water for 7 days, followed by regular drinking water. On the 2nd day, mice received MSCs, Wogonin, or a combined treatment, respectively. The colon tissue and peritoneal lavage fluid were collected on 8 d. (a) The expression of TNF-α and IL-10 in the colon was detected by western blot, and the results represented three independent experiments. (b) TNF-α and (c) IL-10 expressions were calculated separately. (d) The IL-10 levels of peritoneal lavage fluid were measured by ELISA. Data represent mean values ± SEM. The statistical significance of difference between two means was calculated with an unpaired. $n = 6$/group. A one-way ANOVA was performed, $^*P < 0.05$; $^{**}P < 0.01$; $^{***}P < 0.001$; $^{****}P < 0.0001$; ns: no significance.

2.8. Western Blot. Cells or homogenized tissue were lysed in ice-cold RIPA buffer (50 mM Tris-HCl pH 8.0, 150 mM sodium chloride, 1% NP-40, 0.5% sodium deoxycholate, 0.1% sodium dodecyl sulfate, 2 mM EDTA containing 1x protease inhibitor cocktail, and phosphatase inhibitor (Roche)). Equivalent total protein extracts were separated by SDS-polyacrylamide gel electrophoresis (PAGE) and transferred to nitrocellulose membrane (GE Healthcare Life Sciences, Germany). After that, membranes were blocked with 5% bovine serum albumin (BSA) for 1 h at room temperature. Primary antibodies were incubated, and a horseradish peroxidase-conjugated secondary antibody was followed.

The primary antibodies used were as follows: antibodies for TNF-α antibodies (#11948T), HIF-1α antibodies (#4914S), p-GSK3β (#9323T), GSK3β (#9315S), p-AKT (#4060S), AKT (#4691S), p-Stat3 (#9145S), Stat3 (#9404S), p-JNK (#4671), JNK (#9258), and GAPDH (#2118) were obtained from Cell Signaling Technology; all those antibodies were diluted with antibody solution and used at a dilution of 1 : 2000. IL-10 (sc-365858) was obtained from Santa Cruz and employed in a 1 : 500 dilution. The secondary antibodies were used at dilution 1 : 5000. All proteins were visualized by Chemiluminescent HRP Substrate (Millipore, WBKLS0500), and chemical luminescence of membranes was detected by
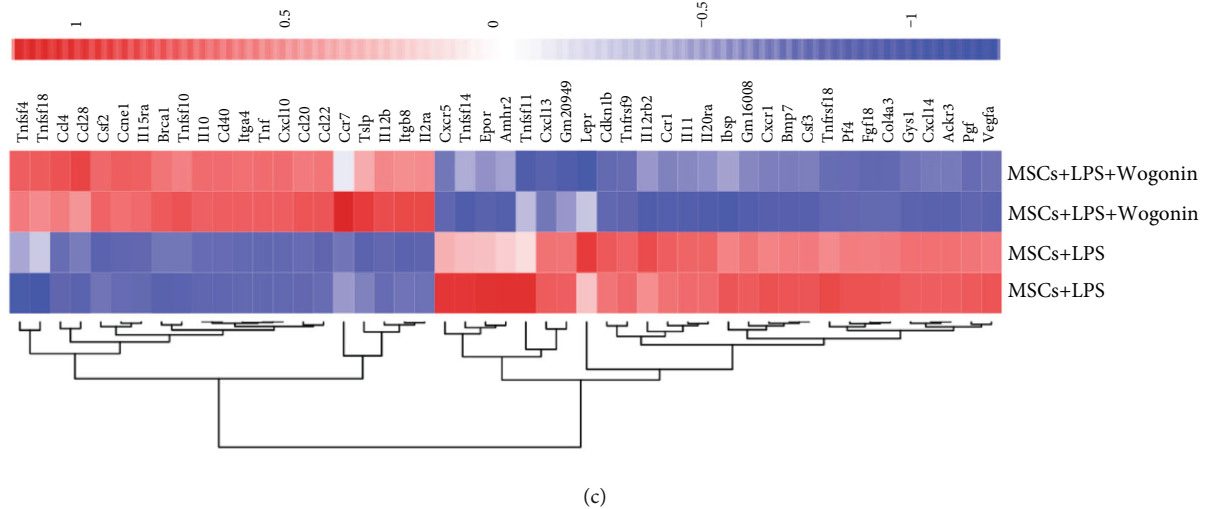
(a)

(b)

Figure 3: Continued.

(c)
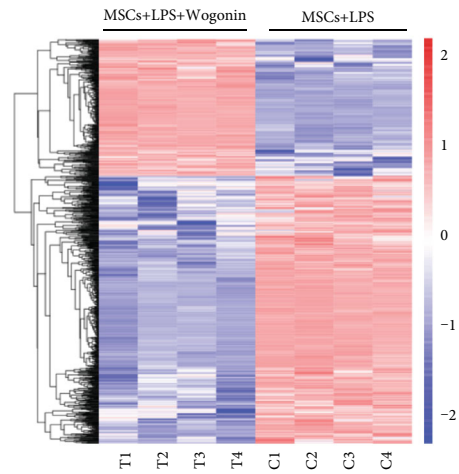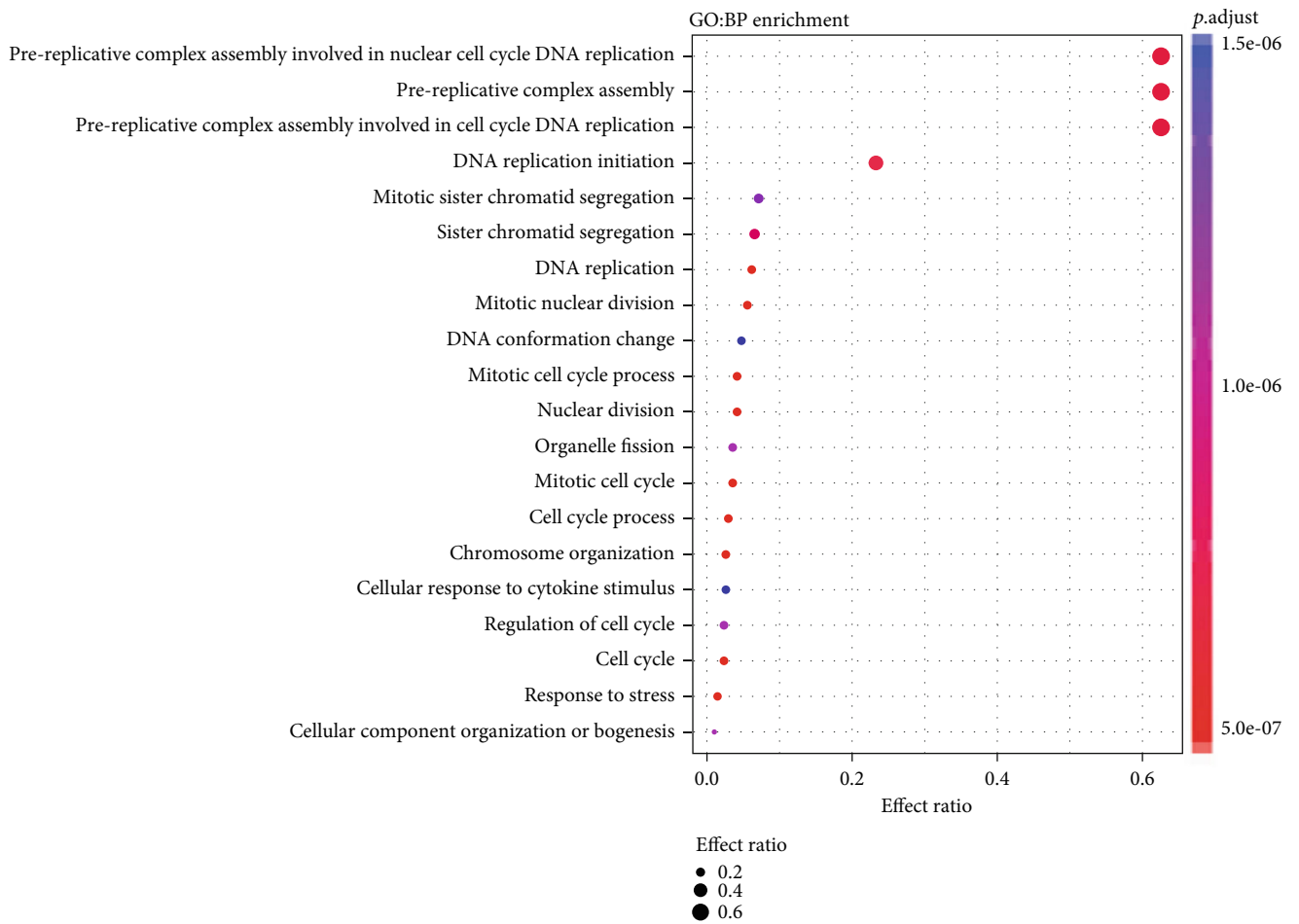
FIGURE 3: Transcriptome analysis of Wogonin-treated MSCs. (a) The heat map showed the transcriptome changes of Wogonin-treated MSCs and untreated MSCs. (b) Gene ontology analysis on two different groups. (c) Heat map gene expression of cytokine and chemokines in MSCs, each gene expression was scaled based on heat map packages.

the Bio-Rad luminescent imaging system. The gray value of each protein bands was quantified by Image J software.

2.9. *Flow Cytometry.* For cell surface marker staining, the cells were washed with PBS buffer containing 0.1% BSA and 0.05% sodium azide and labeled with surface markers and dead/live streaming antibodies for 30 min at 4°C in dark, then washed twice with PBS buffer containing 0.1% BSA and 0.05% sodium azide. All the above stained cells were assayed by FACS Aria II (Becton Dickinson, San Jose, USA), and the data were analyzed by FlowJo software (TreeStar, San Carlos, USA).

For ROS detection, CS&T beads (BD, 661414) were used for machine calibration and performance tracking. BD rainbow beads were for PMT voltage optimization (BD, 559123). MSCs were treated with Wogonin (0, 12.5, 25, and 50 μM) in the presence of LPS. After 24 h, cells were incubated with 20 μM DCF-DA at 37°C for 20 min, then detected by flow cytometry. Fluorescence minus one (FMO) was applied for positive cell gating. Anti-rat Igk negative control compensation particle set (BD, 552845) was used for fluorochrome compensation.

2.10. *IL-10 Blockade Experiment In Vivo.* Eight to twelve weeks C57BL/6 male mice were exposed to 3% DSS water for 7 days, then fed the regular water. On the 2nd day, all mice were peritoneal injected 1×10^6 MSCs and 10 mg/kg Wogonin. Three of them additionally received neutralizing anti-mouse IL-10 antibody (R&D Systems) at a dose of 100 μg/mouse via peritoneal injection. On day 8, the colonic length and pathological lesions of the colon were detected.

2.11. *Statistical Analysis.* All statistical tests were performed with GraphPad Prism 7 (GraphPad Software Inc., San Diego, USA). Significant differences between data sets were performed with either the unpaired Student's t test when comparing two groups, one-way ANOVA for more than two

groups, or two-way ANOVA for two variables (GraphPad Software Inc., San Diego, CA, USA). Data were represented as mean or mean ± SEM. $^{****}P < 0.0001$; $^{***}P < 0.001$; $^{**}P < 0.01$; $^{*}P < 0.05$; and $P > 0.05$, not significant, as stated in figure legends.

3. Results

3.1. *Wogonin Enhanced the Therapeutic Effects of MSCs on DSS-Induced Colitis via Increasing IL-10.* To explore the influence of Wogonin on the therapeutic effects of MSCs, we compared the effect of MSCs or Wogonin alone, and the effect when combined. From day 5, weight loss was observed in all mice except the control mice. As shown in Figure 1(a), the IBD mice lost most weight, but the combination of MSC and Wogonin group had the least weight loss. In this study, colon length was also recorded as an index of mouse colitis. On the 8th day, all colon tissues were collected and measured. The results indicated that the length of colon tissues from all mice exposed to DSS was shorter than those from the control groups. Interestingly, the colons from the combination group were significantly longer than those from the Wogonin or MSC groups (Figures 1(b) and 1(c)). This implied that a combination of Wogonin and MSCs possessed better therapeutic effects on murine colitis than using them separately. Meanwhile, colon histopathological examination consistently showed less intestinal inflammation in the combination group comparing to the other treatment groups (Figure 1(d)). The pathological score of the combination of MSCs and Wogonin-treated mice was the lowest in all treated mice (Figure 1(e)).

To investigate the possible therapeutic mechanisms, the expression of TNF-α and IL-10 in colon was determined by western blot. The data suggested that DSS administration significantly enhanced the expression of proinflammatory cytokine TNF-α and reduced the expression of anti-inflammatory cytokine IL-10 in the colon tissue. No matter

(a)

(b)

(c)

(d)
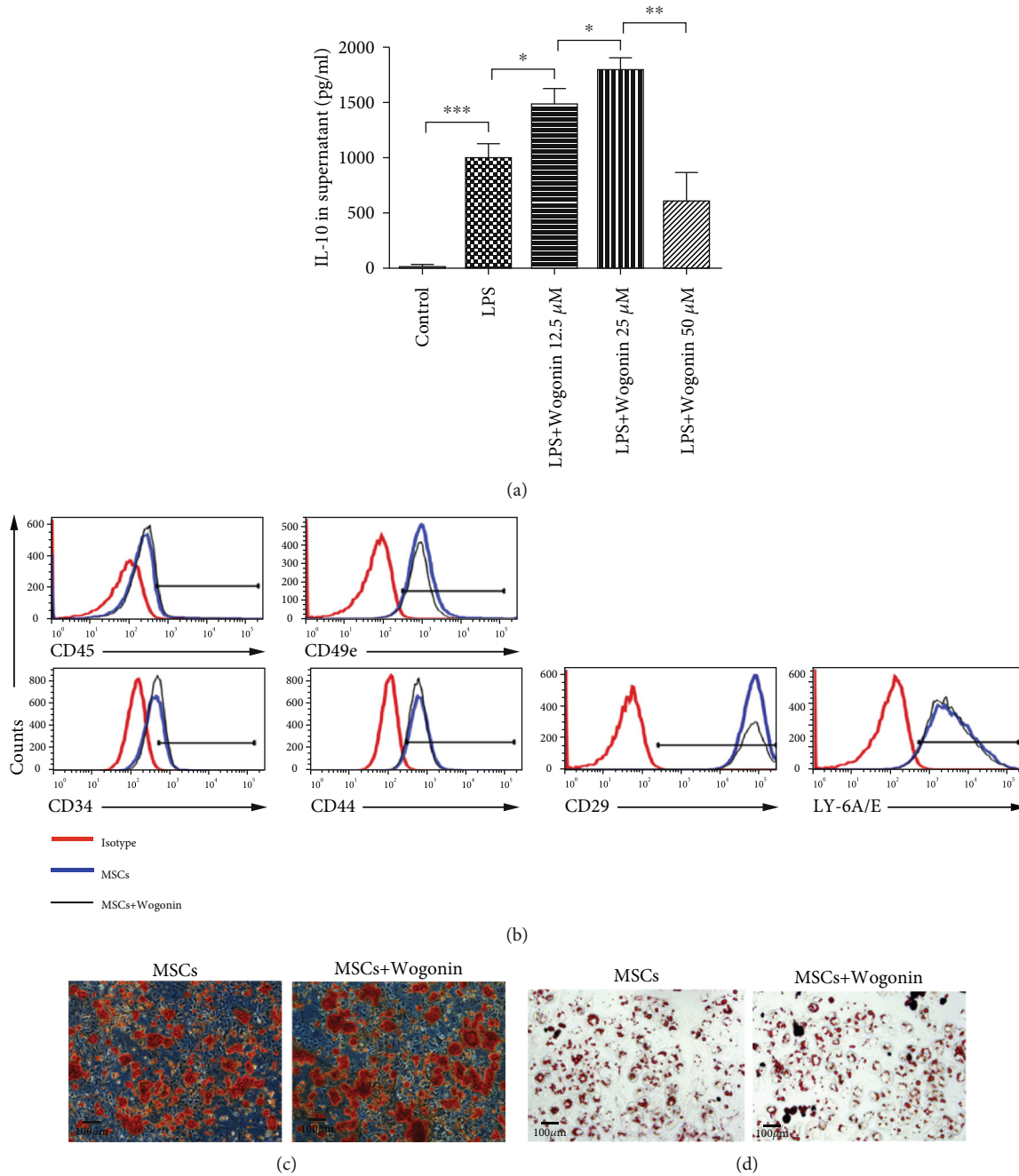
FIGURE 4: Wogonin increased the IL-10 production of MSCs. (a) MSCs were stimulated by Wogonin at a different dose (12.5, 25, and 50 μM) in the presence of LPS. 24 h later, the IL-10 level in supernatant was detected by ELISA. Data represent mean values $\pm$ SEM of three independent experiments. The statistical significance of difference between two means was calculated with an unpaired. A one-way ANOVA was performed, $^*P < 0.05$; $^{**}P < 0.01$; $^{***}P < 0.001$. (b) After 24 h stimulation of 25 μM Wogonin, the surface markers of both untreated MSCs and Wogonin-treated MSCs were analyzed by flow cytometry. (c) The osteogenic differentiation was showed by Alizarin red S staining. (d) The adipogenic differentiation was shown by Oil O staining.

whether MSCs and Wogonin are used together or alone, they could significantly reduce local TNF-α and increased local IL-10 (Figures 2(a)–2(c)). To further inspect the change of cytokines, the levels of TNF-α and IL-10 in peritoneal lavage fluids were detected by ELISA. However, the level of TNF-α was too low to be detected. In line with western blot data, IL-10 significantly increased in peritoneal lavage fluids from

the combination group comparing to the MSC or Wogonin groups. This result suggests that IL-10 may be the key factor for Wogonin strengthening the therapeutic effect of MSC (Figure 2(d)).

3.2. Wogonin Promoted IL-10 Production of MSCs. To understand how Wogonin strengthened the therapeutic effects of

(a)

(b)
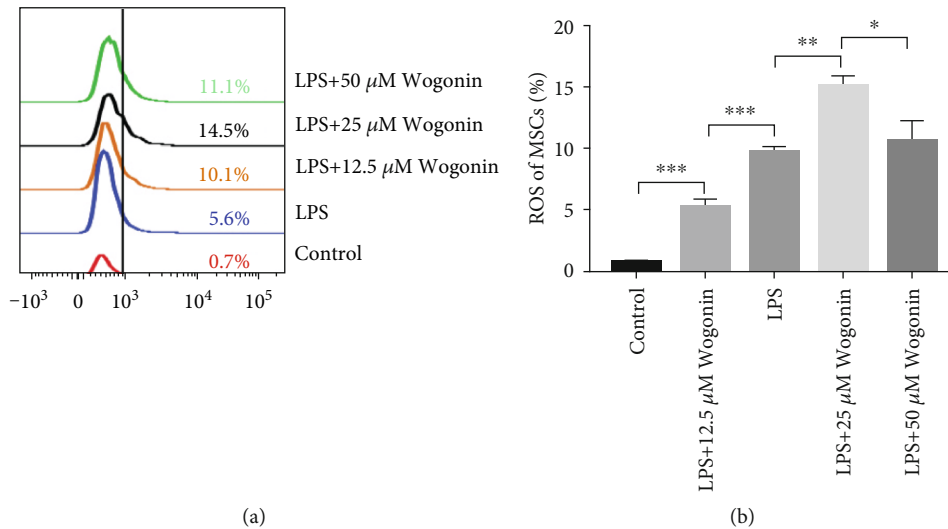
FIGURE 5: Wogonin upregulated ROS level of MSCs. MSCs were stimulated by Wogonin at a different dose (12.5, 25, and 50 μM) in the presence of LPS. 24 h later, the ROS level in MSCs was detected by flow cytometry. (a) Representative histogram of ROS levels of MSCs. (b) The results represented three independent experiments for quantification of ROS levels in MSCs. Values are means ± SEM. The statistical significance of difference between two means was calculated with an unpaired. A one-way ANOVA was performed, $^*P < 0.05$; $^{**}P < 0.01$; $^{***}P < 0.001$.

MSCs, we compared the difference of gene expression profiles between untreated MSCs and Wogonin-treated MSCs in the presence of LPS. After 24 h stimulation, untreated MSCs and Wogonin-treated MSCs were collected, and the transcriptome analysis was performed. The transcriptome analysis identified the upregulation of 1000 genes and downregulation of 2000 genes in Wogonin-treated MSCs (Figure 3(a)). GO analysis indicated that the upregulated genes were highly enriched in the cell cycle (Figure 3(b)).

Furthermore, RNA-seq analysis also revealed that Wogonin enhances the expression of various chemokines and IL-10 in MSCs (Figure 3(c)).

To further verify the influence of Wogonin on the IL-10 production of MSCs, we activated MSCs with different concentrations of Wogonin in the presence of LPS in vitro. After 24 h stimulation, the supernatant was collected, and the IL-10 level was detected by ELISA. As shown in Figure 4(a), the IL-10 secretion from MSCs gradually increased in a dose-dependent manner, reached the peak at 25 μM, then decreased when continuously increasing Wogonin dosage. It was illustrated that 25 μM was the optimal dose of Wogonin to increase the IL-10 production in MSCs.

To clarify whether Wogonin affects the characteristics of MSCs, we firstly analyzed surface markers of untreated MSCs and 25 μM Wogonin-treated MSCs. Comparing to untreated MSCs, MSCs expressed the same panel of surface markers after Wogonin treatment, including CD29, CD44, CD49e, and Sca-1, and did not express the hematopoietic stem cell markers CD34 or CD45 (Figure 4(b)). Additionally, osteogenic differentiation and adipogenic differentiation were tested. As confirmed by Alizarin red S staining and Oil O staining, respectively, Wogonin-treated MSCs showed no change in mesodermal differentiation capacity compared with untreated MSCs (Figures 4(c) and 4(d)).

3.3. Wogonin Increased ROS Level in MSCs. To investigate the effects of Wogonin on ROS level in MSCs, different doses of Wogonin were used to stimulate MSCs in vitro, and the ROS levels of MSCs were detected by DCFDA staining and analyzed by flow cytometry. The results showed that Wogonin treatment obviously increased the ROS level of MSCs in a dose-dependent manner, being greatest at 25 μM (Figures 5(a) and 5(b)). When Wogonin dose was increased to 50 μM, ROS level decreased instead, which was consistent with the IL-10 expression of MSCs (Figures 3(a) and 3(b)). These data implied that Wogonin treatment regulated the ROS level of MSCs.

3.4. Effect of Wogonin on the GSK3β/AKT Signaling Pathway of MSCs. To elucidate the potential signaling pathways of Wogonin increasing IL-10 production in MSCs after Wogonin treatment, we tested protein expression level IL-10 of MSCs that were cultured with LPS in the absence or presence of Wogonin at different dose firstly. A role for transcript factor HIF-1α involved in IL-10 expression was well established; therefore, the expression of HIF-1α was also detected. Consistent with IL-10 in MSC supernatant, we found that HIF-1α and IL-10 gently upregulated in the presence of Wogonin treatment, significantly on 25 μM dose, but decreased on 50 μM dose (Figures 6(a) and 6(b)). Next, signaling pathways involved in IL-10 production were assessed, and western blot analysis showed a remarkable increase of phosphorylation of glycogen synthase kinase 3β (GSK3β) and phosphorylation of AKT in the presence of Wogonin with 25 μM, while total GSK3β and AKT changed slightly (Figures 6(a), 6(c), and 6(d)). Phosphorylation of Stat3 signaling kept intact on Wogonin treatment (Figures 6(a) and 6(e)). These results suggested that Wogonin upregulates the IL-10 production involved in GSK3β/AKT signaling pathways.

(a)

(b)

(c)

FIGURE 6: Continued.

(d)

(e)
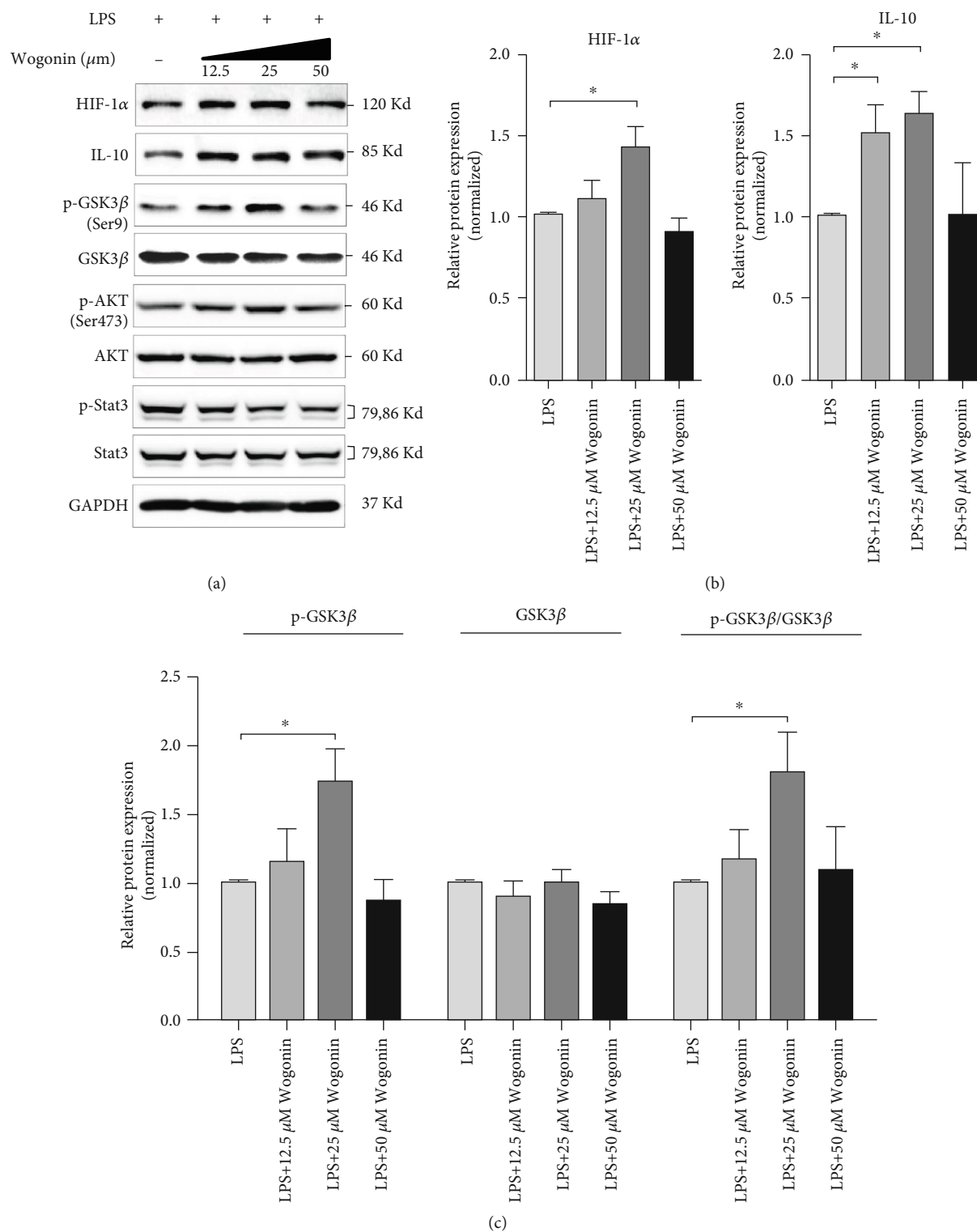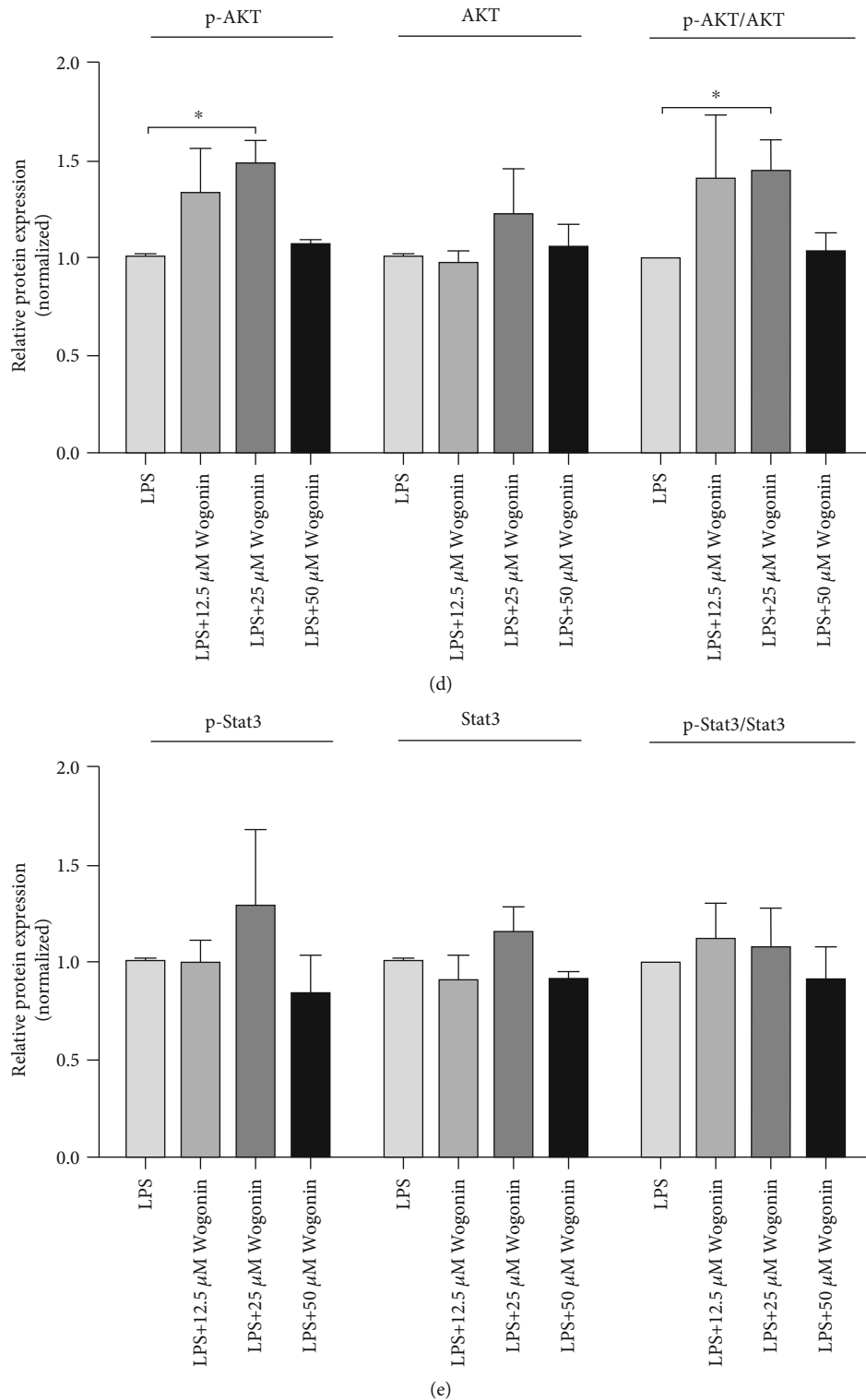
Figure 6: Wogonin improves the IL-10 production in MSCs via GSK3β/AKT pathway. MSCs were stimulated by Wogonin at a different dose (12.5, 25, and 50 μM) in the presence of LPS. After 24 h stimulation, western blot was performed. The cell extract probed with antibodies as indicated, and GAPDH as loading control. Relative protein expression was calculated, respectively. (a) The representatives of the protein expression of HIF-1α, IL-10 as well as GSK3β, AKT, and Stat3 and their phosphorylated forms (p-GSK3β, p-AKT, and p-Stat3). The effects of Wogonin on the expression of HIF-1α and IL-10. (b) The effects of Wogonin on GSK3β. (c) AKT (d) and Stat3 (e) signaling pathways. All the western blotting experiments were repeated three times. Values are means ± SEM. The statistical significance of difference between two means was calculated with two-way ANOVA followed by multiple comparisons with t test and Bonferroni correction, $^*P < 0.05$.

(a)

(b)
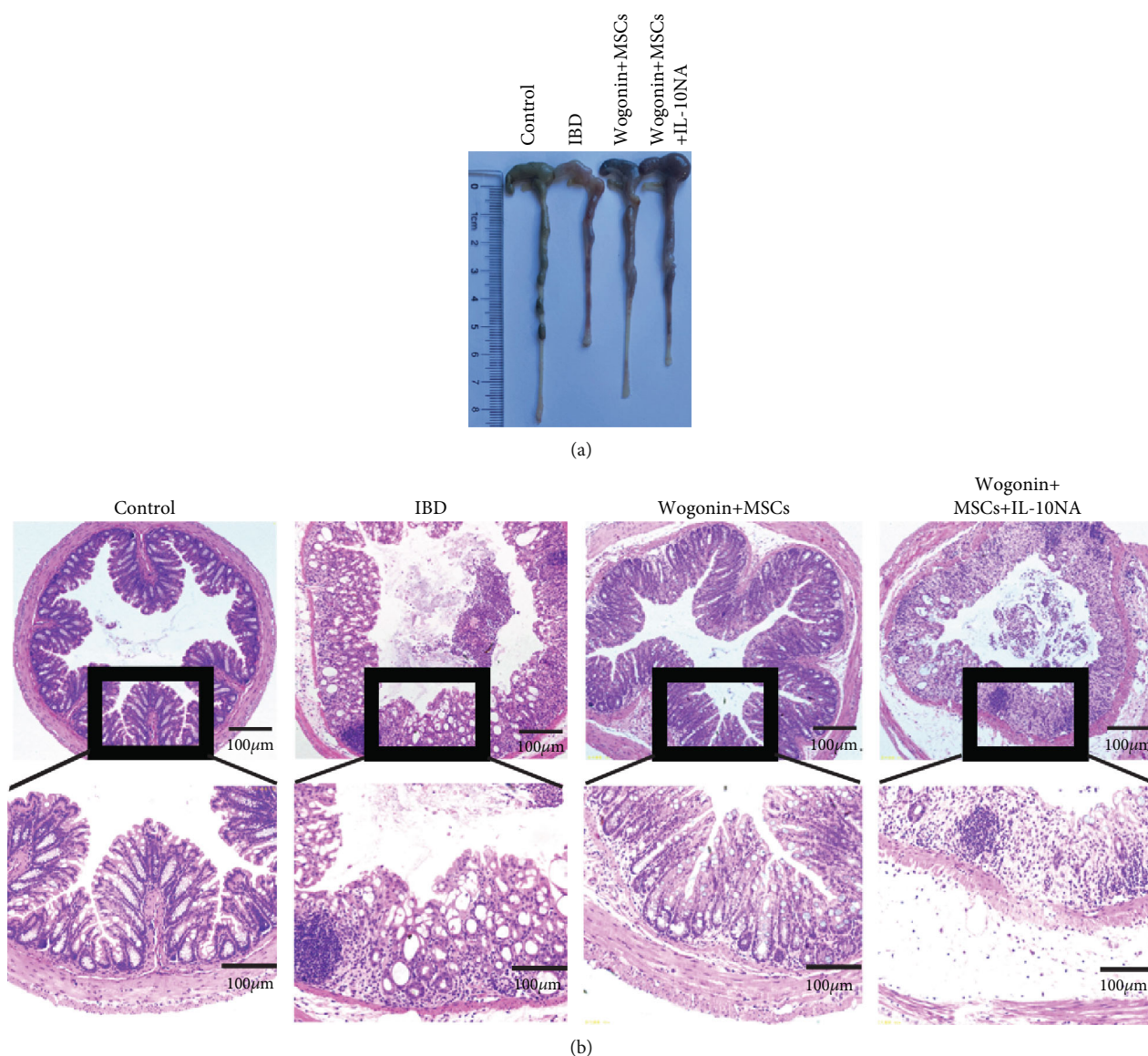
Figure 7: IL-10 blockade abrogated the therapeutic effects of a combination of MSCs and Wogonin on colitis. On day 2 after exposing to 3.0% DSS water, mice received a combination of MSCs and Wogonin or additionally add neutralizing anti-IL-10 antibody, respectively. The colon length and histological analysis were performed on day 8. (a) Representative of colon length from the different groups. (b) Representative images of H&E staining slides. Magnification, 40x and 100x. Three independent experiments showed similar results.

3.5. IL-10 Blockade Abrogated the Therapeutic Effects of a Combination of MSCs and Wogonin on Colitis. To confirm the crucial role of IL-10 on ameliorating mouse colitis, neutralizing IL-10 antibody was used for the combination of MSCs and Wogonin mice. As shown in Figure 7, IL-10 blockade abolished the improvement of the combination on murine intestinal inflammation. After IL-10 neutralization, the shorter colon length was observed, compared with the no neutralization mice (Figure 7(a)). HE staining data also suggested that more serious intestinal epithelial structure damage and more inflammatory cell infiltration were observed in the colon tissues from the IL-10 neutralization mice than those from no IL-10 neutralization mice (Figure 7(b)). These results further demonstrated that the increased production of IL-10 in MSCs is a key factor for

Wogonin to improve the therapeutic efficacy of MSC on DSS-induced colitis.

4. Discussion

Ulcerative colitis (UC), along with Crohn's disease (CD), is chronic and debilitating inflammatory bowel disease (IBD). IBD has been reported to have high prevalence with increasing trends in the rate of incidence [24]. The hygiene hypothesis is the most popular explanation for this growing incidence; meanwhile, the particular etiological factors were still enigma [25]. The impairment of colon mucus layer barrier and epithelium and change of luminal microbial diversity (dysbiosis) were commonly observed in the pathogenesis of UC. TNF-α and multitude of Th2-derived cytokines were

reported to be involved in this process [26]. The lack of a cure or effective long-term treatment options has resulted in substantial morbidity of IBD [27], which highlighted the urgent demand of investigation of a new therapeutic regime.

Mesenchymal stem cells (MSCs) are multipotent stromal cells which can differentiate into different cell types according to their residential niches. The cells sprinted into the clinic stage center due to their features of versatile development potential, self-renewal, allogenic compatibility, and immunomodulatory effects. MSCs are currently being widely tested as a cellular therapy in chronic intestinal diseases, including IBD, and showed promising clinical outcomes with unmet optimization and improvement [28–30], such as in vivo low level of MSC recruitment, and persistence decreased their therapeutic efficacy [31].

To overcome these hurdles, IFN-γ, TGF-β, IGF-1C, IL-1β, and PGE2 were applied to precondition MSCs before they were administered onto different experimental models, and pretreated MSCs showed an enhanced therapeutic effect, with different limitations [32–36]. All of these promising explorations encouraged us to search further alternatives.

Wogonin is a natural flavonoid component extracted from the dried root of Scutellaria baicalensis. Various studies showed its direct anti-inflammatory effects and immunoregulation on immune cells [37]. Interestingly, Wogonin was proved as a particular therapeutic adjuvant for anti-inflammation [14], which inspired our explorations of the potential role of Wogonin in MSC medication on IBD.

On our solid and highly repeatable DSS-induced mouse colitis model, MSCs and Wogonin showed an additive or synergetic effect on the mitigation of colitis. As expected, TNF-α amount in inflammatory colon tissue was decreased by MSCs, Wogonin alone, and their combinations. This was consistent with the alleviated intestinal inflammation by pathology score, which echoed by previous reports.

As another key player of inflammation, IL-10 is an anti-inflammatory factor, playing a critical role in the suppression of autoimmune reactivity and in termination of the inflammatory response. IL-10 from T cell have been established an anti-inflammatory effect in IBD [38], and IL-10 secreted from MSCs have been proved to attenuate inflammation in mice [9–11, 39, 40]. Our recent report showed Wogonin regulated IL-10 production [41]. Hence, it is interesting to study the effect of Wogonin on IL-10 production from MSC in our mouse model.

Strikingly, IL-10 amount in peritoneal lavage fluid was increased by Wogonin and MSCs additively, which did not show in intestinal tissues. Comparably, TNF-α amount in peritoneum was under detectable range. This indicated that Wogonin might directly alter peritoneal MSCs on-site.

To verify this hypothesis and examine the full profile of the effect of Wogonin on MSCs from a different level, LPS-activated MSCs cocultured with/without Wogonin in vitro.

Firstly, Wogonin enhanced abundant proliferation-associated gene expression in MSCs, but not those development-associated genes. This was consistent with no surface, and differentiation markers were changed by Wogonin culture. Meanwhile, both TNF-α and IL-10 mRNA amounts were augmented along with the activation of numerous chemokine genes. This echoed with the increased protein amount of peritoneal IL-10.

Secondly, there is a clear dose-effect of Wogonin enhancing IL-10 production from MSCs. 25 μM Wogonin showed optimal augment effect, and higher concentration suppressed further IL-10 secretion. Reactive oxygen species (ROS) generation by NADPH oxidase has been shown to interact with IL-10 production in macrophages [42, 43]. Hence, it is not surprising to repeat this on MSCs. All these results indicated the adjuvant feature of Wogonin on MSC activation.

To further investigate the molecular machinery of Wogonin on MSCs, TLR4 signaling pathways were explored. Strikingly, the TLR4/AKT/GSK3β pathway was triggered by Wogonin. It is still difficult to pinpoint the target receptor on MSCs due to the herb derivative, and their discovery of this machinery on MSCs suggested the new strategy in IBD therapy [44]. Our in vivo IL-10 neutralization data reinforced this concept.

To our knowledge, our study firstly showed Wogonin enhanced IL-10 production from MSCs directly, which restrained DSS-induced colitis. This implied new therapeutic strategy for IBD.

5. Conclusions

Although MSCs show promising therapeutic potential in treating inflammatory bowel disease (IBD), their efficacy is influenced by multiple factors. Wogonin, a bioactive compound from Scutellaria baicalensis, has diverse immunoregulatory effects. Our present study demonstrated that Wogonin extended the therapeutic efficiency of MSCs on DSS-induced murine colitis in vivo, which was due to the increased IL-10 expression in the intestinal tissue and peritoneal cavity. RNA sequencing analysis suggested Wogonin enhanced IL-10 expression, which was confirmed via in vitro experiments. Furthermore, western blot data implied that Wogonin upregulates transcript factor HIF-1α in MSCs via AKT/GSK3β signal pathway. Summarily, our study found that combining MSCs with Wogonin was superior to MSC therapy alone, which provides a novel strategy for MSC clinical application on IBD.

Data Availability

The data used to support the findings of this study are included within the article.

Conflicts of Interest

The authors declared no potential conflicts of interest with respect to the research, authorship, and/or publication of this article.

Authors' Contributions

Qiongli Wu, Shujuan Xie, and Yanwen Peng designed experiments, performed research, and interpreted data. Yinhong Zhu established a mouse IBD model. Yinhong Zhu, Jiatong Tian, and Jingrou Chen performed cell culture

and differentiation assays. Qiongli Wu contributed to flow cytometry analysis. Shujuan Xie performed western blot. Changyou Wu and Shiqiu Xiong substantively revised the manuscript. Yanwen Peng and Yujin Ye supervised research and interpreted data. Yanwen Peng, Qiongli Wu, Shujuan Xie, and Yujin Ye wrote the manuscript. Qiongli Wu and Shujuan Xie contributed equally to this work. All authors have read and approved the final manuscript.

Acknowledgments

References

[1] S. C. Ng, H. Y. Shi, N. Hamidi et al., "Worldwide incidence and prevalence of inflammatory bowel disease in the 21st century: a systematic review of population-based studies," *The Lancet*, vol. 390, no. 10114, pp. 2769–2778, 2018.

[2] C. Andrea, P. Francesco, and S. Sergio, "Cell therapy in inflammatory bowel disease," *Pharmacological Research*, vol. 163, article 105247, 2021.

[3] A. I. Caplan, "MSCs: the sentinel and safe-guards of injury," *Journal of Cellular Physiology*, vol. 231, no. 7, pp. 1413–1416, 2016.

[4] M. Barnhoorn, E. de Jonge-Muller, I. Molendijk et al., "Endoscopic administration of mesenchymal stromal cells reduces inflammation in experimental colitis," *Inflammatory Bowel Diseases*, vol. 24, no. 8, pp. 1755–1767, 2018.

[5] R. Kuhn, J. Lohler, D. Rennick, K. Rajewsky, and W. Muller, "Interleukin-10-deficient mice develop chronic enterocolitis," *Cell*, vol. 75, no. 2, pp. 263–274, 1993.

[6] H. Zhu, X. Lei, Q. Liu, and Y. Wang, "Interleukin-10-1082A/G polymorphism and inflammatory bowel disease susceptibility: a meta-analysis based on 17,585 subjects," *Cytokine*, vol. 61, no. 1, pp. 146–153, 2013.

[7] K. Chao, S. Zhang, Y. Qiu et al., "Human umbilical cord-derived mesenchymal stem cells protect against experimental colitis via CD5$^+$ B regulatory cells," *Stem Cell Research & Therapy*, vol. 7, no. 1, p. 109, 2016.

[8] X. Chen, C. Cai, D. Xu et al., "Human mesenchymal stem cell-treated regulatory CD23(+) CD43$^+$ B cells alleviate intestinal inflammation," *Theranostics*, vol. 9, no. 16, pp. 4633–4647, 2019.

[9] C. K. Min, B. G. Kim, G. Park, B. Cho, and I. H. Oh, "IL-10-transduced bone marrow mesenchymal stem cells can attenuate the severity of acute graft-versus-host disease after experimental allogeneic stem cell transplantation," *Bone Marrow Transplantation*, vol. 39, no. 10, pp. 637–645, 2007.

[10] W. Liao, V. Pham, L. Liu et al., "Mesenchymal stem cells engineered to express selectin ligands and IL-10 exert enhanced therapeutic efficacy in murine experimental autoimmune encephalomyelitis," *Biomaterials*, vol. 77, pp. 87–97, 2016.

[11] S. T. Peruzzaro, M. M. M. Andrews, A. Al-Gharaibeh et al., "Transplantation of mesenchymal stem cells genetically engineered to overexpress interleukin-10 promotes alternative inflammatory response in rat model of traumatic brain injury," *Journal of Neuroinflammation*, vol. 16, no. 1, p. 2, 2019.

[12] A. Triantafyllidi, T. Xanthos, A. Papalois, and J. K. Triantafillidis, "Herbal and plant therapy in patients with inflammatory bowel disease," *Annals of Gastroenterology*, vol. 28, no. 2, pp. 210–220, 2015.

[13] H. Liao, J. Ye, L. Gao, and Y. Liu, "The main bioactive compounds of Scutellaria baicalensis Georgi. for alleviation of inflammatory cytokines: a comprehensive review," *Biomedicine & Pharmacotherapy*, vol. 133, p. 110917, 2021.

[14] D. L. Huynh, T. H. Ngau, N. H. Nguyen, G. B. Tran, and C. T. Nguyen, "Potential therapeutic and pharmacological effects of Wogonin: an updated review," *Molecular Biology Reports*, vol. 47, no. 12, pp. 9779–9789, 2020.

[15] S. Soontararak, L. Chow, V. Johnson et al., "Mesenchymal stem cells (MSC) derived from induced pluripotent stem cells (iPSC) equivalent to adipose-derived MSC in promoting intestinal healing and microbiome normalization in mouse inflammatory bowel disease model," *Stem Cells Translational Medicine*, vol. 7, no. 6, pp. 456–467, 2018.

[16] Z. J. Ma, Y. H. Wang, Z. G. Li et al., "Immunosuppressive effect of exosomes from mesenchymal stromal cells in defined medium on experimental colitis," *International Journal of Stem Cells*, vol. 12, no. 3, pp. 440–448, 2019.

[17] M. R. Irhimeh and J. Cooney, "Management of inflammatory bowel disease using stem cell therapy," *Current Stem Cell Research & Therapy*, vol. 11, no. 1, pp. 72–77, 2016.

[18] W. Y. Jiang, G. S. Seo, Y. C. Kim, D. H. Sohn, and S. H. Lee, "PF2405, standardized fraction of Scutellaria baicalensis, ameliorates colitis in vitro and in vivo," *Archives of Pharmacal Research*, vol. 38, no. 6, pp. 1127–1137, 2015.

[19] G. Chen, Y. Yang, C. Hu et al., "Protective effects of Huangqin decoction against ulcerative colitis and associated cancer in mice," *Oncotarget*, vol. 7, no. 38, pp. 61643–61655, 2016.

[20] Y. Sun, Y. Zhao, J. Yao et al., "Wogonoside protects against dextran sulfate sodium-induced experimental colitis in mice by inhibiting NF-κB and NLRP3 inflammasome activation," *Biochemical Pharmacology*, vol. 94, no. 2, pp. 142–154, 2015.

[21] Y. Feng, X. He, S. Luo et al., "Chronic colitis induces meninges traffic of gut-derived T cells, unbalances M1 and M2 microglia/macrophage and increases ischemic brain injury in mice," *Brain Research*, vol. 1707, pp. 8–17, 2019.

[22] J. Lei, D. Hui, W. Huang et al., "Heterogeneity of the biological properties and gene expression profiles of murine bone marrow stromal cells," *The International Journal of Biochemistry & Cell Biology*, vol. 45, no. 11, pp. 2431–2443, 2013.

[23] G. Yu, L. G. Wang, Y. Han, and Q. Y. He, "clusterProfiler: an R package for comparing biological themes among gene clusters," *OMICS: A Journal of Integrative Biology*, vol. 16, no. 5, pp. 284–287, 2012.

[24] S. Alatab, S. G. Sepanlou, K. Ikuta et al., "The global, regional, and national burden of inflammatory bowel disease in 195 countries and territories, 1990-2017: a systematic analysis for the Global Burden of Disease Study 2017," *The Lancet Gastroenterology & Hepatology*, vol. 5, no. 1, pp. 17–30, 2020.

[25] D. P. Strachan, "Hay fever, hygiene, and household size," *BMJ*, vol. 299, no. 6710, pp. 1259-1260, 1989.

[26] F. Heller, P. Florian, C. Bojarski et al., "Interleukin-13 is the key effector Th2 cytokine in ulcerative colitis that affects epithelial tight junctions, apoptosis, and cell restitution," *Gastroenterology*, vol. 129, no. 2, pp. 550–564, 2005.

[27] A. Ferguson, D. M. Sedgwick, and J. Drummond, "Morbidity of juvenile onset inflammatory bowel disease: effects on education and employment in early adult life," *Gut*, vol. 35, no. 5, pp. 665–668, 1994.

[28] N. A. Manieri, M. R. Mack, M. D. Himmelrich et al., "Mucosally transplanted mesenchymal stem cells stimulate intestinal healing by promoting angiogenesis," *Journal of Clinical Investigation*, vol. 125, no. 9, pp. 3606–3618, 2015.

[29] C. Grim, R. Noble, G. Uribe et al., "Impairment of tissue resident mesenchymal stem cells in chronic ulcerative colitis and Crohn's disease," *Journal of Crohns & Colitis*, 2021.

[30] J. Z. Ko, S. Johnson, and M. Dave, "Efficacy and safety of mesenchymal stem/stromal cell therapy for inflammatory bowel diseases: an up-to-date systematic review," *Biomolecules*, vol. 11, no. 1, 2021.

[31] H. Tanaka, Y. Arimura, T. Yabana et al., "Myogenic lineage differentiated mesenchymal stem cells enhance recovery from dextran sulfate sodium-induced colitis in the rat," *Journal of Gastroenterology*, vol. 46, no. 2, pp. 143–152, 2011.

[32] L. Liu, Y. R. He, S. J. Liu et al., "Feline adipose tissue-derived mesenchymal stem cells pretreated with IFN-gamma enhance immunomodulatory effects through the PGE(2) pathway," *Journal of Veterinary Science*, vol. 22, no. 2, article e16, 2021.

[33] K. Lynch, O. Treacy, X. Chen et al., "TGF-beta1-licensed murine MSCs show superior therapeutic efficacy in modulating corneal allograft immune rejection in vivo," *Molecular Therapy*, vol. 28, no. 9, pp. 2023–2043, 2020.

[34] X. Cao, L. Duan, H. Hou et al., "IGF-1C hydrogel improves the therapeutic effects of MSCs on colitis in mice through PGE2-mediated M2 macrophage polarization," *Theranostics*, vol. 10, no. 17, pp. 7697–7709, 2020.

[35] L. Liu, Y. R. He, S. J. Liu et al., "Enhanced effect of IL-1beta-activated adipose-derived MSCs (ADMSCs) on repair of intestinal ischemia-reperfusion injury via COX-2-PGE2 signaling," *Stem Cells International*, vol. 2020, Article ID 2803747, 18 pages, 2020.

[36] F. Y. Yang, R. Chen, X. Zhang et al., "Preconditioning enhances the therapeutic effects of mesenchymal stem cells on colitis through PGE2-mediated T-cell modulation," *Cell Transplantation*, vol. 27, no. 9, pp. 1352–1367, 2018.

[37] J. Wang, K. Li, Y. Li, and Y. Wang, "Mediating macrophage immunity with wogonin in mice with vascular inflammation," *Molecular Medicine Reports*, vol. 16, no. 6, pp. 8434–8440, 2017.

[38] H. de Souza, C. Fiocchi, and D. Iliopoulos, "The IBD interactome: an integrated view of aetiology, pathogenesis and therapy," *Nature Reviews Gastroenterology & Hepatology*, vol. 14, no. 12, pp. 739–749, 2017.

[39] J. Wang, H. Ren, X. Yuan, H. Ma, X. Shi, and Y. Ding, "Interleukin-10 secreted by mesenchymal stem cells attenuates acute liver failure through inhibiting pyroptosis," *Hepatology Research*, vol. 48, no. 3, pp. E194–E202, 2018.

[40] J. J. Choi, S. A. Yoo, S. J. Park et al., "Mesenchymal stem cells overexpressing interleukin-10 attenuate collagen-induced arthritis in mice," *Clinical and Experimental Immunology*, vol. 153, no. 2, pp. 269–276, 2008.

[41] L. Fan, D. Qiu, G. Huang et al., "Wogonin suppresses IL-10 production in B cells via STAT3 and ERK signaling pathway," *Journal of Immunology Research*, vol. 2020, Article ID 3032425, 12 pages, 2020.

[42] S. Dokka, X. Shi, S. Leonard, L. Wang, V. Castranova, and Y. Rojanasakul, "Interleukin-10-mediated inhibition of free radical generation in macrophages," *American Journal of Physiology. Lung Cellular and Molecular Physiology*, vol. 280, no. 6, pp. L1196–L1202, 2001.

[43] J. Deng, X. Wang, F. Qian et al., "Protective role of reactive oxygen species in endotoxin-induced lung inflammation through modulation of IL-10 expression," *Journal of Immunology*, vol. 188, no. 11, pp. 5734–5740, 2012.

[44] N. Tokuhira, Y. Kitagishi, M. Suzuki et al., "PI3K/AKT/PTEN pathway as a target for Crohn's disease therapy (review)," *International Journal of Molecular Medicine*, vol. 35, no. 1, pp. 10–16, 2015.

Review Article

Neuroprotective Phytochemicals in Experimental Ischemic Stroke: Mechanisms and Potential Clinical Applications

Hui Xu [1,2] **Emily Wang,**[3] **Feng Chen,**[1] **Jianbo Xiao** [4] **and Mingfu Wang** [1,2]

[1]*Institute for Advanced Study, Shenzhen University, Shenzhen 508060, China*
[2]*School of Biological Sciences, The University of Hong Kong, Pokfulam Road, Hong Kong, China*
[3]*Rice University, Houston, Texas, USA*
[4]*International Research Center for Food Nutrition and Safety, Jiangsu University, Zhenjiang 212013, China*

Correspondence should be addressed to Jianbo Xiao; jianboxiao@yahoo.com and Mingfu Wang; mfwang@hku.hk

Ischemic stroke is a challenging disease with high mortality and disability rates, causing a great economic and social burden worldwide. During ischemic stroke, ionic imbalance and excitotoxicity, oxidative stress, and inflammation are developed in a relatively certain order, which then activate the cell death pathways directly or indirectly via the promotion of organelle dysfunction. Neuroprotection, a therapy that is aimed at inhibiting this damaging cascade, is therefore an important therapeutic strategy for ischemic stroke. Notably, phytochemicals showed great neuroprotective potential in preclinical research via various strategies including modulation of calcium levels and antiexcitotoxicity, antioxidation, anti-inflammation and BBB protection, mitochondrial protection and antiapoptosis, autophagy/mitophagy regulation, and regulation of neurotrophin release. In this review, we summarize the research works that report the neuroprotective activity of phytochemicals in the past 10 years and discuss the neuroprotective mechanisms and potential clinical applications of 148 phytochemicals that belong to the categories of flavonoids, stilbenoids, other phenols, terpenoids, and alkaloids. Among them, scutellarin, pinocembrin, puerarin, hydroxysafflor yellow A, salvianolic acids, rosmarinic acid, borneol, bilobalide, ginkgolides, ginsenoside Rd, and vinpocetine show great potential in clinical ischemic stroke treatment. This review will serve as a powerful reference for the screening of phytochemicals with potential clinical applications in ischemic stroke or the synthesis of new neuroprotective agents that take phytochemicals as leading compounds.

1. Introduction: Ischemic Stroke

Stroke occurs when the blood supply to the brain tissue is interrupted or reduced. Generally, stroke can be divided into two major categories: ischemic stroke and hemorrhagic stroke, according to how the blood flow is disrupted. Ischemic stroke is caused by the occlusion of cerebral arteries by thrombi or embolisms, blocking the blood flow to one part of the brain. Hemorrhagic stroke results from the ruptures of a weakened blood vessel, leading to the accumulation of blood in the surrounding brain tissue [1]. Of the two, ischemic stroke is the primary type, accounting for about 80% of all strokes [2]. Stroke ranks second in the cause of death worldwide, and about 5.5 million people die from stroke

each year (WHO health statistics). Besides, stroke has a high disability rate, resulting in permanent disability for around 50% of its survivors [3]. Many risk factors are associated with stroke, such as age, hypertension, obesity, hyperlipidemia, diabetes, smoking, and alcohol consumption. With the great increase in the aging population, the occurrence of stroke is predicted to continue rising, and the mortality of stroke may exceed 12% by 2030 [4]. Hence, stroke is a challenging disease that greatly increases the worldwide economic and social burden.

1.1. Pathophysiology of Ischemic Stroke. When ischemic stroke occurs, blood flow to the specific territory of the brain that is supplied by the occluded artery is reduced. Generally,

the ischemic area of the brain can be divided into the infarct core and the ischemic penumbra according to the severity of the blood flow reduction. The infarct core is characterized by a rapid decrease in ATP levels and energy stores and severe ionic disruption, which result in cell death within a few minutes. Surrounding the core area is the ischemic penumbra. In this area, blood flow reduction is less severe due to perfusion from collateral blood vessels. Hence, the insult to the ischemic penumbra is much milder than that to the infarct core. As a result, multiple milder cell death mechanisms occur in this area such as inflammation and apoptosis, providing promising therapeutic targets for ischemic stroke [5]. Notably, the ischemic penumbra is dynamic, in which the infarct core expands at the cost of the penumbra during cerebral ischemia. Hereby, early reperfusion is the most effective manner to reduce the cerebral infarction of ischemic stroke patients [6].

Ischemic stroke injuries include two parts: ischemic injury and reperfusion injury. The cell death mechanisms of the ischemic brain are redundant, and at least three dominant mechanisms are involved: ionic imbalance and excitotoxicity, oxidative/nitrosative stress, and inflammation. Notably, those mechanisms are developed in a relatively certain order and become the dominant events at different stages of ischemic stroke. Generally, ionic imbalance and excitotoxicity play a critical role in the ischemic phase, and oxidative/nitrosative stress peaks at the beginning phase of reperfusion, while inflammation lasts for several days or weeks after reperfusion. After activation, those mechanisms affect the function of cell membranes and organelles such as the mitochondria, endoplasmic reticulum (ER), lysosomes, and nuclei. Consequently, different cell death pathways are activated, including apoptosis and necrosis [5]. Autophagy/mitophagy is also activated in ischemic stroke, but whether it promotes or decreases the cerebral ischemia-reperfusion (I/R) injuries has not been agreed upon at present. Studies suggested that apoptosis and cytoprotective autophagy/mitophagy tended to be induced by moderate cerebral I/R injuries, while necrosis or destructive autophagy/mitophagy was activated during severe I/R damage [7]. The major mechanisms of cell death in ischemic stroke are illustrated in Figure 1.

1.2. Major Pharmacological Therapies for Ischemic Stroke. Major approaches to treat ischemic stroke can be divided into two types: recanalization and neuroprotection. Recanalization is aimed at restoring the blood flow with thrombolytic agents or accessory devices in the acute phase of ischemic stroke (from minutes to hours) or preventing the reoccurrence of stroke with antiplatelet and anticoagulant agents, while neuroprotection is aimed at protecting neurons from the different pathological factors of ischemic stroke [8]. Recently, researchers also pronounced the theory of promoting brain neurogenesis to achieve long-term recovery after ischemic stroke. Several compounds are found to enhance neurogenesis in experimental stroke models, such as epigallocatechin-3-gallate (EGCG), curcumin, and ginkgolide K [9–11]. Yet, no agents are clinically approved for this therapy at present.

1.2.1. Thrombolysis. Intravenous (IV) thrombolysis with recombination tissue plasminogen activator (r-tPA, alteplase) is the only US Food and Drug Administration-(FDA-) approved pharmacological treatment for acute ischemic stroke [12]. tPA promotes the conversion of plasminogen to plasmin, an active proteolytic enzyme that cleaves the cross-linkages between fibrin molecules of clots [13]. Notably, r-tPA has a very short therapeutic window and is best when administrated within 3 h after symptom onset. Patients can still benefit from r-tPA when it is administrated between 3 and 4.5 h after cerebral ischemia. However, r-tPA is not recommended for patients whose treatment cannot be initiated within 4.5 h because it will greatly increase the rate of intracranial hemorrhage and neuronal excitotoxicity [14]. Clinically, the short therapeutic window drastically limits the eligible patients and only about 15% of the hospitalized patients are treated with r-tPA [14].

1.2.2. Antiplatelets and Anticoagulants. Antiplatelet and anticoagulant therapies are aimed at preventing the reoccurrence of stroke via the prevention of clot formation. Antiplatelets inhibit platelet activation or aggregation, while anticoagulants suppress the functions of clot-forming factors such as factors II, VII, and X. The common antiplatelet agents include aspirin, clopidogrel, dipyridamole, tirofiban, and eptifibatide. Clinical studies show that the risk of early recurrent stroke is decreased by aspirin administration within 48 h of ischemic stroke onset [15]. As for anticoagulants such as heparin, warfarin, dabigatran, rivaroxaban, and apixaban, it is found that urgent therapeutic anticoagulation benefits high-risk cardioembolic stroke patients. Yet, the use of anticoagulants may lead to symptomatic intracranial hemorrhage in unselected ischemic stroke patients [13].

1.2.3. Neuroprotection. Neuroprotective agents could reduce ischemic brain injuries via the promotion of neuronal survival, neuroplasticity, synaptogenesis, and neurogenesis. Hence, neuroprotection therapy could be combined with thrombolytic agents to reduce the second injuries of reperfusion [16]. Over the past two decades, over 1000 potential neuroprotective agents were found in experimental ischemic stroke, with nearly 200 agents having undergone clinical trials [17]. Particularly, edaravone and Dl-3-n-butylphthalide show great efficacy in clinical treatment and have been approved for ischemic stroke treatment in Japan and China, respectively.

Edaravone, with the trade name Radicut/Radicava, is a medication developed by Mitsubishi Tanabe Pharma of Japan. Edaravone is a free radical scavenger that targets peroxyl radicals. It was approved for the treatment of ischemic stroke in 2001 and amyotrophic lateral sclerosis (ALS) in 2017 [18]. Edaravone is widely applied in Japan, China, and other Asian countries, and nearly half of ischemic stroke patients receive edaravone treatment in Japan [19]. Clinical studies show that the combination of edaravone and intravenous thrombolysis therapy improves the neurological outcome of ischemic stroke patients [19, 20]. Besides, edaravone is also found to reduce in-hospital mortality and
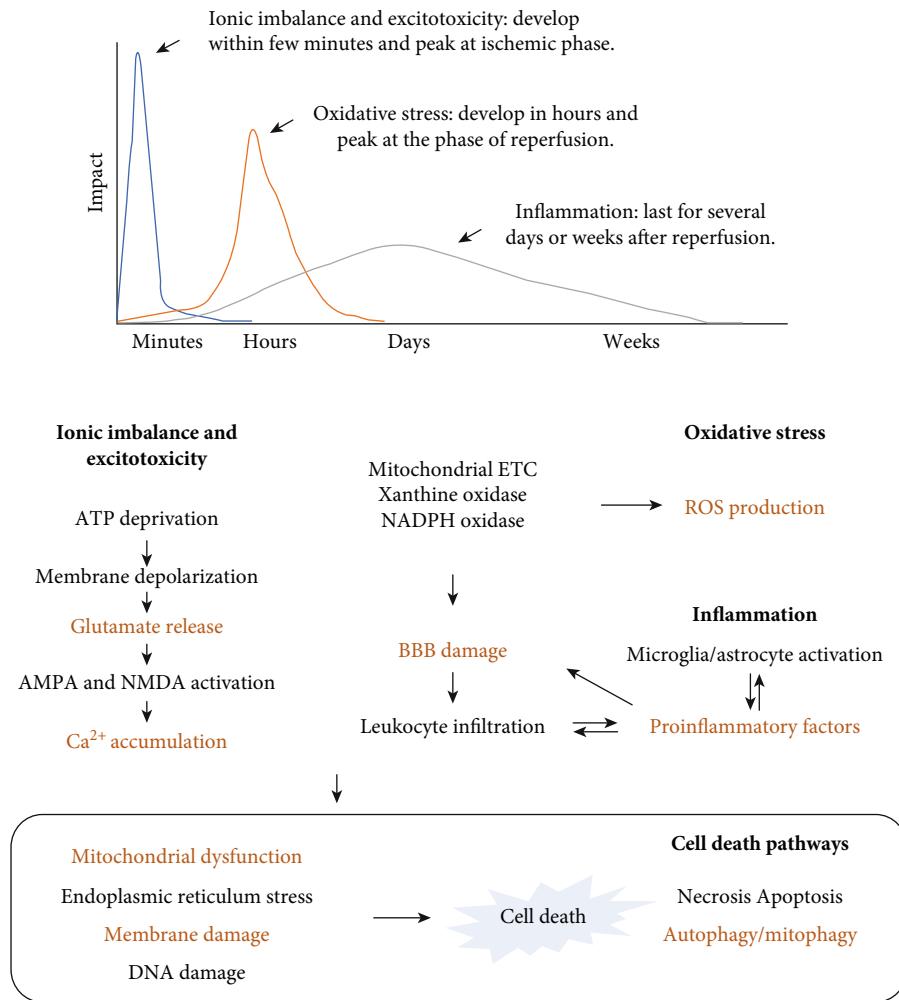
FIGURE 1: Dominant cell death mechanisms in ischemic stroke. Ionic imbalance and excitotoxicity, oxidative stress, and inflammation are major causes that lead to brain cell death in ischemic stroke. Ionic imbalance and excitotoxicity are developed within few minutes after ischemia and are the leading cause of cell death during the ischemic phase. Oxidative stress peaks at the beginning phase of reperfusion due to the sharply increased ROS production after oxygen restoration, while inflammation can last for several days or weeks after reperfusion contributing to the delayed cell death after ischemic stroke. Generally, these mechanisms can activate various cell death pathways such as necrosis, apoptosis, and autophagy/mitophagy directly or indirectly by promoting the dysfunction of organelles such as the mitochondria and endoplasmic reticulum.

intracranial hemorrhage when combined with endovascular thrombolysis therapy [21].

Dl-3-n-butylphthalide (NBP) is a neuroprotective drug developed by CSPC Pharmaceutical Group Limited. NBP is originally extracted from the seeds of *Apium graveolens*; synthesized NBP was later approved for ischemic stroke treatment in 2002. Clinically, NBP soft capsules and injections have been used to treat mild to moderate ischemic stroke patients in China. NBP is a multitargeted agent, exerting neuroprotection in ischemic stroke via antioxidation, anti-inflammation, antiapoptosis, and mitochondrial protection [22]. Clinical studies indicate that NBP improves neurological deficits such as waking, speaking, sense, thought, and memory impairments, promoting long-term recovery of ischemic stroke patients [23].

1.3. Common Models for Experimental Ischemic Stroke Research

1.3.1. Middle Cerebral Artery Occlusion Model. Most ischemic strokes occur in the middle cerebral artery (MCA) territory of the human brain, so animal models are developed to induce ischemia in this area to mimic the clinical situation. There are several ways to occlude the MCA in experimental ischemic stroke research, and the most commonly used one is the intraluminal suture MCA occlusion (MCAO) model. In this model, a monofilament is inserted into the internal carotid artery (ICA) and advanced to the origin of MCA to block the blood flow. The monofilament can be left in the blood vessel to mimic the permanent ischemia (pMCAO) or pulled out to achieve reperfusion as a model of transient focal cerebral ischemia (tMCAO/R). Normally, 60-120 min of ischemia is commonly used in rats to induce neuronal death and cerebral infarction. In addition, MCA can also be occluded directly by clipping, ligation, or hooks through the craniectomy [2]. Robinson et al. firstly report an approach that can achieve direct occlusion of the distal MCA

(dMCAO) through ligation in Sprague-Dawley rats. The dMCAO model is more reproducible than the suture MCAO model, but it may induce skull trauma, resulting in cortical inflammation and spreading depression [24, 25].

1.3.2. Photothrombotic Model. The photothrombotic stroke model is induced by the intravascular photooxidation of a photosensitive dye (e.g., Rose Bengal). For stroke induction, the photosensitive dye is intravenously or intraperitoneally injected, after which the targeted cerebral vessel is illuminated with a light beam of a specific wavelength through the intact skull to activate the dye. The activated dye then promotes endothelial injuries and platelet aggregation via the formation of superoxides. Notably, the application of stereotactic coordinates during illumination makes it possible to induce infarction at the desired cortical brain region. Due to its high reproducibility and low mortality, this model is often used to study the long-term functional outcomes after stroke. Yet, the photothrombotic model has fundamental discrepancies with the pathophysiology of human ischemic stroke because of the lack of the ischemic penumbra and collateral blood flow [25–27].

1.3.3. Thromboembolic Clot Model. The thromboembolic model involves the application of prepared blood clots to achieve focal cerebral vascular occlusion. The clots are usually formed spontaneously or induced by thrombin from autologous blood. Besides, injection of thrombin directly to the MCA or intracranial segment of ICA is also a common method to induce clots. This model has a high similarity to the mechanism of vascular occlusion in human ischemic stroke, so it is often used to study thrombolysis or mechanical reperfusion-related strategies [28]. For example, Ma et al. reported the effect of pinocembrin in extending the therapeutic window of r-tPA with this model [29]. However, the infarct location and size induced by the thromboembolic model are variable due to differences in the size and elasticity of clots. Hence, this model is less reproducible than the MCAO model [25].

1.3.4. Global Cerebral Ischemia Model. Global cerebral ischemia is aimed at blocking all the blood flow to the brain, causing neuronal injuries to the selectively vulnerable brain areas such as the CA1 pyramidal neurons of the hippocampus and neocortex. There are many ways to achieve global cerebral ischemia including decapitation, neck tourniquet, ventricular fibrillation, and occlusion of ICAs and vertebral vessels. Currently, the most used method is bilateral ICA occlusion, namely, the two-vessel occlusion (2-VO) model. Notably, the 2-VO model induces cerebral injuries in the vulnerable brain areas with a very short ischemia period. It is found that damage can be observed in the hippocampus of animals that only suffer from 2 min of bilateral ICA occlusion. Although the global cerebral ischemia model is not fully compliant with the pathogenesis of human ischemic stroke, it still has advantages in studying the poststroke cognitive and neurological outcomes due to its selective damage to the vulnerable hippocampus [30].

2. Neuroprotective Strategies of Phytochemicals in Experimental Ischemic Stroke

Dominant mechanisms that lead to cell death in ischemic stroke include ionic imbalance and excitotoxicity, oxidative stress, and inflammation. After initiation, these events then activate various cell death pathways, including necrosis, apoptosis, and autophagy/mitophagy, directly or indirectly by causing the dysfunction of organelles, such as mitochondria and ER. Theoretically, all the events in this damaging cascade could be modulated to achieve potential neuroprotection in ischemic stroke. Notably, several strategies have been proved to be effective in experimental ischemic stroke, and the major strategies that are modulated by phytochemicals are reviewed in this section.

2.1. Calcium Modulation and Antiexcitotoxicity. Glucose and oxygen deprivation disrupts the electron transport chain (ETC), limiting the production of ATP in mitochondria. ATP depletion then enhances the anaerobic metabolism, inducing disorder of Na^+/K^+-ATPase and Ca^{2+}/H^+-ATPase pumps. As a result, the intracellular H^+, Na^+, and Ca^{2+} levels are greatly elevated, causing neuronal cell membrane depolarization and acidosis [5]. Membrane depolarization markedly elevates the release of excitatory amino acids such as glutamate. Meanwhile, the reuptake of those excitatory amino acids is impaired due to energy failure. Hence, glutamate is excessively accumulated in the extracellular space, leading to the activation of two glutamate-dependent Ca^{2+} ion channels: NMDA (N-methyl-D-aspartate) and AMPA (α-amino-3-hydroxy-5-methyl-4-isoxazolepropionic acid) receptors [31]. Consequently, intracellular Ca^{2+} is dramatically elevated, activating many Ca^{2+}-dependent enzymes to promote necrotic and apoptotic cell death [32]. Accordingly, inhibition of intracellular Ca^{2+} accumulation or extracellular glutamate levels would reduce neuronal damage. In addition, ionic imbalance and excitotoxicity peak at the end of ischemia, so agents that target this strategy should be administrated as early as possible. Late administration could lead to ineffectiveness or even damage to brain tissues. Detailed strategies for calcium modulation and antiexcitotoxicity include enhancing the reuptake of glutamate, upregulating the inhibitory amino acid systems, modulating the activity of NMDA receptors, and regulating the non-glutamate-dependent calcium-permeable cation channels.

2.1.1. Enhancing the Reuptake of Glutamate. Reuptake of glutamate is mediated by the excitatory amino acid transporters (EAATs) in astrocytes and neurons. Three types of EAATs are found in the central nervous system (CNS) of rodents, including GLAST (glutamate/aspartate transporter), GLT-1 (glutamate transporter-1), and EAAC1. Under ischemia conditions, functions of EAATs are suppressed due to ionic imbalance and ATP depletion, enhancing the neurotoxicity of glutamate. Hence, upregulation of the expression or activity of EAATs helps to reduce excitotoxicity in ischemic stroke [33]. Notably, the effectiveness of EAAT modulation has been indicated by many *in vitro* and *in vivo* studies. Several

EAAT activators such as ginsenoside Rb1 and harmine have been found to possess neuroprotective activities in experimental ischemic stroke [34, 35].

2.1.2. Upregulating the Inhibitory Amino Acid Systems.

Inhibitory amino acids could bind to their corresponding receptors and inhibit the postsynaptic excitatory response, and the major inhibitory amino acid in the CNS is gamma-aminobutyric acid (GABA). Cerebral ischemia not only disrupts the balance between glutamate and GABA release but also suppresses the activity of GABA receptors. As a result, the inhibitory effect of GABA is markedly inhibited in ischemic stroke. Hereby, improving the glutamate and GABA balance or upregulating GABA receptors contributes to brain repair. As evidence, the GABA receptor agonist clomethiazole was reported to exert neuroprotection in animal models [36]. Besides, EGCG and ginkgolide B, two natural products that mediated neuroprotection, were found to be achieved partially by improving the balance of excitatory/inhibitory amino acids [37, 38].

2.1.3. Modulating the Activity of NMDA Receptors.

NMDA receptors consist of four subunits: two GluN1 and two GluN2 (glutamate-binding). Early studies regarded the NMDA receptor as a vital regulator for glutamate-mediated neurotoxicity in ischemic stroke. Hence, numerous NMDA receptor antagonists were tested to evaluate their neuroprotective activities. However, researchers found that the toxicities of NMDA receptor antagonists were high, limiting their further application. Recently, studies indicated that the high toxicity of NMDA receptor antagonists might be attributed to the dual function of NMDA receptors in ischemic stroke. It is found that the functions of NMDA receptors depend on their locations and the subunit types. Generally, the GluN2 subunit greatly affects the function of NMDA receptors. GluN2A is mainly expressed at the synapse and promotes cell survival by activating prosurvival pathways such as PI3K (phosphoinositide 3-kinase)/Akt (protein kinase B) and CREB (cyclic AMP response element-binding protein). On the contrary, GluN2B is highly expressed in extrasynaptic sites and activates prodeath pathways such as nNOS (neuronal nitric oxide synthases). During cerebral ischemia, GluN2B is the primary activated NMDA receptor, contributing to cerebral I/R injuries. Hence, selectively inhibiting GluN2B or its downstream prodeath pathways would be a neuroprotective strategy [36, 39]. For example, Tat-NR2B9c, a peptide that inhibited GluN2B-mediated prodeath pathways, was found to protect neurons in MCAO models [40]. In addition, upregulation of GluN2A was reported to contribute to neuronal survival. As evidence, geniposide enhanced the expression of GluN2A and reduced brain damage in tMCAO/R rats [41].

2.1.4. Regulating the Non-Glutamate-Dependent Calcium-Permeable Cation Channels.

The influx of Ca^{2+} is also modulated via non-glutamate-dependent cation channels, including TRP (transient receptor potential) channels and ASICs (acid-sensing ion channels) [42]. TRP channels can be divided into six subgroups, with TRPC6, TRPM7, and TRPV1 being extensively studied in ischemic stroke. The roles of TRPs in ischemic stroke are different. TRPM7 and TRPV1 promote neuronal death by elevating the intracellular Ca^{2+} level. Yet, TRPC6 contributes to neuronal survival via activation of CaMK (calmodulin-dependent protein kinase) and CREB signaling pathways. Notably, cerebral ischemia promotes the expression of TRPM7 and TRPV1 and enhances the degradation of TRPC6. Hereby, upregulation of TRPC6 or downregulation of TRPM7/TRPV1 would decrease cerebral I/R-induced injuries [42–44]. As an example, TRPC6 was activated by resveratrol and calycosin in MCAO models [43, 45], while inhibition of TRPM7 and TRPV1 was observed in carvacrol- and capsaicin-mediated neuroprotection, respectively [46, 47].

ASICs, especially ASIC1a and ASIC2a, are found to mediate cerebral I/R-induced injuries. Among them, ASIC1a promotes Ca^{2+} influx and neuronal injuries after being activated by the increased acidosis during ischemia, while ASIC2a reduces brain damage as observed in a transient global ischemia model [48, 49]. Modulation of ASICs was observed in ginsenoside Rd-mediated neuroprotection, which inhibited ASIC1a and enhanced ASIC2a expression in MCAO/R rats.

2.2. Antioxidation.

Free radicals start to be produced during ischemia, surging in the reperfusion period, in which the free radical production systems such as mitochondrial ETC and enzymatic conversion systems are greatly promoted after oxygen restoration. In mitochondria, excessive Ca^{2+} accumulation during ischemia leads to the dephosphorylation of the oxidative phosphorylation (OxPhos) complexes, hyperactivating the ETC system. After reperfusion, the hyperactive ETC markedly promotes the generation of reactive oxygen species (ROS) with the supply of sufficient oxygen and glucose [50]. The enzymatic systems mainly include xanthine oxidase and NADPH (nicotinamide adenine dinucleotide phosphate) oxidase. Similarly, those enzymes are also hyperactivated during ischemia via accumulation, phosphorylation, or uncoupling, so ROS production in enzymatic systems is markedly enhanced after reperfusion [7].

Oxidative stress plays a critical role in reperfusion injuries. Firstly, oxidative stress directly destroys the cellular membrane system and DNA, leading to necrotic and apoptotic cell death. Secondly, oxidative stress enhances the opening of mPTP (mitochondrial permeability transition pore) in mitochondria, increasing the release of many proapoptotic factors such as cytochrome c and AIF (apoptosis-inducing factor). Thirdly, oxidative stress increases the permeability of the blood-brain barrier (BBB) by activating matrix metalloproteases (MMPs), thus elevating the incidence of cerebral hemorrhage, brain edema, and leukocyte infiltration [51, 52]. Finally, oxidative stress interacts with the cascade of inflammation, further deteriorating reperfusion injuries. Accordingly, antioxidation would be an important strategy to reduce cerebral I/R injuries.

Methods to modulate the oxidative stress in ischemic stroke are relatively uncomplicated, mainly including reducing NADPH oxidase-mediated ROS production and enhancing the antioxidant defense by activating the Nrf2 (nuclear

factor erythroid 2-related factor 2) pathway. Yet, this strategy is found to be modulated by numerous neuroprotective agents including some phytochemicals.

2.2.1. Reducing NADPH Oxidase-Mediated ROS Production.
NADPH oxidase (NOX) is regarded as the primary target to modulate ROS production in ischemic stroke, in which it is relatively hard to pharmacologically inhibit the ETC. NOXs have several homologs, with NOX2 and NOX4 playing critical roles in ischemic stroke. After ischemia, NOX4 expression in neurons is markedly increased, while NOX2 upregulation is mainly found in endothelial cells. Elevated NOX promotes the generation of ROS, so inhibition of NOX would help to reduce cerebral I/R-induced oxidative stress. The effectiveness of NOX inhibition is reported in animal models. To illustrate, NOX inhibitors, such as isoquercetin, ginsenoside Rb1, picroside II, and andrographolide, were all found to protect brain tissues from cerebral I/R damage [53–57].

2.2.2. Enhancing the Antioxidant Defense via the Nrf2 Pathway.
Normally, ROS could be scavenged by the intracellular antioxidant defenses, including enzymatic antioxidants (e.g., SOD and catalase) and nonenzymatic antioxidants (e.g., ascorbic acid) to maintain redox homeostasis [58]. However, cerebral I/R injuries greatly promote ROS production, overburdening the antioxidant defense systems. Hereby, strengthening the antioxidant defense is a critical strategy to reduce oxidative stress in ischemic stroke. Nrf2 is the major transcriptional factor that regulates the intracellular antioxidant defense, especially under stress conditions. Once activated, Nrf2 enhances the expression of various antioxidant enzymes such as GCL (glutamate-cysteine ligase), HO-1 (heme oxygenase-1), and NQO1 (NAD(P)H dehydrogenase [quinone] 1). Overwhelming evidence indicates that Nrf2 reduces cerebral I/R-induced oxidative stress. Nrf2 activators such as sulforaphane, tert-butylhydroquinone, nobiletin, naringenin, astragaloside IV, and neferine were all reported to exert neuroprotection in experimental ischemic stroke [59–63].

2.3. Anti-Inflammation and BBB Protection.
Inflammation is the primary poststroke damage that produces the delayed progression of cell death after ischemic stroke, developing and lasting for several days or weeks after reperfusion. Inflammation is jointly mediated by the infiltrated leukocytes and brain resident immune cells: microglia/macrophages and astrocytes. Under cerebral I/R conditions, microglia are activated rapidly and display two phenotypes: the proinflammatory phenotype (M1) and the anti-inflammatory phenotype (M2). M1 microglia contribute to neuronal cell death via secreting the proinflammatory cytokines, such as IL-1β, IL-6, and TNF-α. Yet, M2 microglia promote the recovery of the injured brain via anti-inflammatory mediators, such as IL-4, IL-10, and neurotrophins [64]. Astrocytes are activated after microglia and release multiple proinflammatory cytokines and inducible NOS (iNOS) after activation [65]. Then, the activated microglia and astrocytes promote the expression of adhesion molecules such as ICAM-1 (intercellular adhesion molecule 1) and induce the leukocyte infiltration into the ischemic brain, triggering a stronger cascade of inflammation. Worse even, the elevated level of proinflammatory factors activates MMPs and increases the BBB permeability. As a result, leukocyte infiltration is further elevated, creating a vicious cycle [66].

The inflammation cascade involves multiple regulators, so many targets could be modulated during this process. Methods to achieve anti-inflammation in experimental ischemic stroke mainly include regulation of microglial/astrocyte activation and leukocyte infiltration, inhibition of arachidonic acid release and metabolism, modulation of the transcriptional factors related to inflammation, and suppression of the TLR signaling pathway.

2.3.1. Regulation of Microglial/Astrocyte Activation and Leukocyte Infiltration.
As discussed above, the activated microglia/astrocytes and infiltrated leukocytes greatly promoted the release of various proinflammatory factors, such as TNF-α, IL-6, IL-1β, MCP-1 (monocyte chemoattractant protein-1), ICAM-1, and iNOS, so inhibition of microglial/astrocyte activation and leukocyte infiltration would contribute to neuroprotection. Accordingly, numerous neuroprotective agents were reported to modulate this strategy in ischemic stroke. To illustrate, scutellarin, epicatechin, fisetin, and calycosin were found to inhibit microglial activation in animal models of ischemic stroke, with epicatechin and fisetin also suppressing leukocyte infiltration [67–70]. Besides, salidroside-, ginkgolide B-, and celastrol-mediated neuroprotection were associated with the promotion of M2 microglial polarization, that is, transferring proinflammatory M1 microglia to anti-inflammatory M2 microglia [71–73]. Furthermore, berberine, harmine, and tanshinone IIA exerted neuroprotection via inhibition of astrocyte activation [35, 74, 75].

2.3.2. Inhibition of Arachidonic Acid Release and Metabolism.
Arachidonic acid (AA), a polyunsaturated fatty acid, is stored in the phospholipid membrane in the form of glycerol under normal conditions. Yet, elevated free radicals during ischemic stroke initiate the hydrolysis of phospholipid via activation of the phospholipases (PL, mainly PLA2 in the case of ischemic stroke). As a result, AA is released to the intracellular space and then degraded to produce several proinflammatory metabolites [76]. The degradation of AA is mediated by three independent enzymes: cyclooxygenases (COX) to form prostaglandins (PG), lipoxygenases (LOX) to form leukotrienes, and cytochrome P$_{450}$ epoxygenases to form epoxyeicosatrienoic acids (EETs), respectively. Among them, COX-2 and 5-LOX are well studied in cerebral I/R-induced inflammation. It is shown that expressions of COX-2 and 5-LOX are increased after cerebral ischemia, and inhibition of COX-2 or 5-LOX by their corresponding inhibitors reduces brain damage in animal models. In addition, 12/15-LOX is also reported to promote cerebral ischemic injuries, as evidenced by few recent studies. Hence, many targets can be modulated in the metabolism of AA including PLA2, COX-2, 5-LOX, and 12/15-LOX [65]. For instance, apigenin-, chrysin-, and picroside II-mediated neuroprotection were

related to the suppression of COX-2 [77–79]. Besides, the 5-LOX inhibitors caffeic acid and boswellic acid and 12/15-LOX inhibitors baicalein and oxymatrine were reported to reduce cerebral damage in MCAO models [80–83].

2.3.3. Modulation of the Transcriptional Factors Related to Inflammation.

A series of transcriptional factors participate in the cascade of inflammation, such as STAT3 (signal transducer and activator of transcription 3), NF-κB (nuclear factor-κB), PPARα (peroxisome proliferator-activated receptor α), and PPARγ. These transcriptional factors target diverse genes and eventually exert different functions in inflammation [84]. NF-κB is a well-known proinflammatory transcriptional factor. After activation, NF-κB promotes the expressions of various proinflammatory factors, such as iNOS, 5-LOX, COX-2, TNF-α, and IL-6. Accordingly, inhibition of the activity of NF-κB is found to reduce the cerebral infarction of MCAO rodents [84]. As an example, the neuroprotective activities of nobiletin and naringenin were mediated by inhibition of NF-κB [60, 85].

JAK2 (Janus kinase 2) is a receptor of proinflammatory cytokines, such as IL-6. Once activated, JAK2 promotes the phosphorylation and nuclear translocation of STAT3, initiating the expression of its target genes. The JAK2/STAT3 pathway is found to play dual roles in ischemic stroke. Some studies reported that the JAK2/STAT3 pathway contributes to brain recovery by promoting neuronal survival and neurogenesis. Yet, JAK2/STAT3 is also found to promote inflammation, especially when activated in the microglia [84]. Hence, several agents, such as atractylenolide III and sinomenine, were reported to suppress inflammation and reduce brain injuries via inhibition of the JAK2/STAT3 pathway in preclinical studies [86, 87].

PPARs are the major regulator of cellular glucose and lipid metabolism. Recent studies found that PPARα/γ agonists exhibit anti-inflammatory activities, indicating that PPARα/γ might also mediate the inflammatory response. PPARα/γ are reported to suppress the inflammation cascade in ischemic stroke [84]. Accordingly, a PPARγ activator, malibatol A, and a PPARα/γ activator, icariin, were found to decrease cerebral damage in tMCAO/R models [88, 89].

2.3.4. Suppression of the TLR Signaling Pathway.

TLR (Toll-like receptor), a transmembrane protein, can initiate inflammation in response to exogenous or endogenous stress. TLRs have several homologs, and TLR2/4 are reported to be involved in the inflammation cascade of ischemic stroke. The activation of TLR2/4 requires endogenous ligands, such as HMGB1 (high mobility group box 1), HSPs (heat shock proteins), hyaluronic acid, and fibronectin. After combination with ligands, the configuration of TLRs is changed, leading to the recruitment of its adaptors such as MyD88 (myeloid differentiation primary response 88) and TRIF (TIR-domain-containing adapter-inducing interferon-β). The recruited adaptors then promote inflammation via activation of NF-κB [90]. Hence, inhibition of the HMGB1/TLR/MyD88/NF-κB pathway could be a potential neuroprotective strategy. Many neuroprotective compounds are reported to modulate this pathway. For

instance, glycyrrhizin and berberine inhibited the HMGB1/TLR4 pathway, and vinpocetine suppressed the TLR4/MyD88/NF-κB signaling [91–93]. Beyond that, baicalin-, luteolin-, and curcumin-mediated neuroprotection were also found to be associated with the inhibition of TLRs [94–96].

2.4. Mitochondrial Protection and Antiapoptosis.

It is known that mitochondria play a vital role in reperfusion-induced injury via the generation of excessive ROS [50]. Elevated intracellular ROS and Ca^{2+} levels lead to the opening of mPTP, a complicated complex existing in the mitochondrial membrane. As a result, the permeability of mitochondria is enhanced and many mitochondrial proapoptotic factors are released such as cytochrome c and AIF [97]. Cytochrome c is a central regulator in caspase-dependent apoptosis. Released cytochrome c promotes the cascade of apoptosis via activation of caspase-9 and caspase-3. AIF is found to mainly mediate caspase-independent apoptosis. After release, AIF is translocated to the nucleus, binds to DNA, and promotes the chromatin condensation and annexin staining, initiating the apoptotic cascade [6].

Since the opening of mPTP is the major initiator for apoptosis, inhibition of the mPTP opening would be an effective neuroprotective strategy. Accordingly, hydroxysafflor yellow A-, gallic acid-, and picroside II-mediated neuroprotection were all found to be related to the inhibition of mPTP [98–100]. In addition, some regulators can modulate the opening of mPTP such as Bcl-2 family proteins and cyclophilin D. Bcl-2 proteins consist of proapoptotic proteins (e.g., Bax, Bad) and antiapoptotic proteins (e.g., Bcl-2, Bcl-xl). It is found that Bax promotes mPTP formation, while Bcl-2 could combine with Bax to inhibit its function. Hence, the ratio of Bcl-2/Bax is regarded as an important indicator of the mPTP opening, and many neuroprotective agents are found to regulate Bcl-2/Bax [97]. As an example, the ratio of Bcl-2/Bax was increased in galangin-treated pMCAO rats [101]. As for the other regulator, cyclophilin D promotes mPTP formation via binding to one of its components, the VDAC (voltage-dependent anion channel). Hereby, inhibition of cyclophilin D was also observed in the neuroprotective activities of some agents such as cyclosporin A and gallic acid [99]. The PI3K/Akt signaling pathway is a critical regulator of apoptosis. It is found that Akt promotes the phosphorylation of Bad, an inhibitor of Bcl-2. After phosphorylation, Bad separates from Bcl-2 and promotes the binding of Bcl-2 with mitochondria, suppressing the mPTP opening and subsequent cytochrome c release [102]. Since the PI3K/Akt signaling pathway is fundamental in cerebral I/R-induced apoptosis, it is modulated by most of the antiapoptotic agents in experimental ischemic stroke. For example, puerarin- and silibinin (silybin)-mediated neuroprotection were associated with the upregulation of the PI3K/Akt signaling pathway [103, 104].

2.5. Autophagy/Mitophagy Regulation.

Autophagy is a complicated process that transports the cytoplasmic proteins or organelles to lysosomes for degradation. The process of

autophagy can be divided into four main steps: initiation, prolongation, fusion, and degradation. Initiation is aimed at forming the phagophore via the ULK1-initiated cascades. Prolongation is extending and closing of the phagophore to form a matured autophagosome that contains the targeted proteins or organelles. This process is mediated by the ATG12 and LC3 ubiquitin-like conjugation systems, in which LC3 II plays central roles. The mature autophagosome is then fused with the lysosome and degraded by lysosomal enzymes [105, 106]. Autophagy is initially regarded as a non-selective process, but now it is widely accepted that autophagy can also be induced by a selective manner, such as through selective degradation of damaged mitochondria (mitophagy). The mitophagy cascade is similar to autophagy, except that it needs to detect the damaged mitochondria first. Generally, mitochondria which possess a decreased mitochondrial membrane potential ($\Delta\psi_m$) are identified and divided into two parts: healthy mitochondria and depolarized mitochondria. The depolarized mitochondria then initiate the mitophagy cascade and eventually are degraded. Notably, it is found that mitophagy is initiated after mitochondrial fission; that is, inhibition of mitochondrial fission will accordingly suppress the mitophagy [107].

Overwhelming evidence shows that autophagy/mitophagy is activated in various ischemic stroke models. Yet, the role of autophagy/mitophagy in cerebral I/R-induced injuries is still controversial at present. Several studies regard autophagy/mitophagy as a type of cell death, playing a detrimental role in ischemic stroke. Those studies indicate that neuronal death or brain damage is reduced after blocking the autophagy/mitophagy cascades via administration of 3-methyladenine (3-MA, an autophagosome formation inhibitor) or after knockdown of Beclin1 and Atg7, two critical regulators in the autophagy cascade in various *in vitro* and *in vivo* models [108]. Accordingly, inhibition of autophagy/mitophagy confers the neuroprotection of several agents, such as baicalein, calycosin, and puerarin [70, 109, 110].

On the contrary, autophagy/mitophagy is also found to play an important role in maintaining cellular homeostasis via degradation of defective or aggregated proteins and organelles [111]. The protective effects of autophagy/mitophagy in ischemic stroke are indicated by many investigations. For instance, Rami reported that inhibition of autophagy/mitophagy by 3-MA (3-methyladenine) or Atg7 knockdown in the reperfusion phase enhanced cytochrome c release and apoptosis both *in vitro* and *in vivo* [112]. In addition, many neuroprotective agents are reported to enhance the autophagy/mitophagy cascade in experimental ischemic stroke. To illustrate, the neuroprotective effects of triptolide, astragaloside IV, and ginsenoside Rb1 were found to be mediated by enhanced autophagy [113–115]. Besides, elevated mitophagy contributed to the neuroprotection of rapamycin, methylene blue, melatonin, and ginsenoside Rg1 in MCAO models [116, 117].

The controversial results are attributed to the differences in drug administration time points, doses, or routes [111]. Although no consensus has been reached at present, autophagy/mitophagy modulation is still considered to be a promising neuroprotective strategy due to its extensive interactions with the other cell death pathways such as necrosis and apoptosis. Yet, more studies are needed to further clarify its role in ischemic stroke.

2.6. Regulation of Neurotrophin Release. Neurotrophins are critical regulators of neuronal survival, development, function, and regeneration. There are many types of neurotrophins in the mammalian CNS, with NGF (nerve growth factor) and BDNF (brain-derived neurotrophic factor) being intensively studied in ischemic stroke. NGF is abundantly expressed in both the hippocampus and the cortex. After release, it binds to the TrkA (tropomyosin-related kinase A) receptor and triggers the activation of the Erk (extracellular signal-regulated kinase)/CREB pathway to improve neuronal recovery. BDNF is the most abundant neurotrophin in the mammalian CNS. BDNF binds to the TrkB receptor, activating several prosurvival pathways including PI3K/Akt signaling and MAPKs (mitogen-activated protein kinases). As one of the self-rescuing mechanisms for neurons, the expression of NGF/TrkA and BDNF/TrkB is upregulated after ischemic stroke [118, 119]. Hence, the promotion of this process would contribute to neuronal survival and recovery. For instance, rutin and astaxanthin were found to upregulate the expression of NGF or BDNF and reduced cerebral infarction and neurological deficits in MCAO models [119, 120]. In addition, some studies also evaluated the effects of exogenous neurotrophins in ischemic stroke. It is found that administration of exogenous neurotrophins exerted neuroprotection in animal models but failed to do the same in the clinical trials due to their low BBB permeability [121].

3. Phytochemicals That Exert Neuroprotection in Experimental Ischemic Stroke

Phytochemicals are the secondary metabolites of plants, such as vegetables, fruits, and herbs. Generally, phytochemicals can be divided into several chemical groups, including phenolics, terpenoids, and alkaloids. Phenolics are a class of compounds that possess at least one aromatic ring, with one or more hydroxyl groups attached. They can be further classified as flavonoids, stilbenes, phenolic acids, phenolic alcohols, and lignans. Terpenoids refer to the compounds that have the isoprene unit as their basic component, while alkaloids possess one or more nitrogen atoms in the heterocyclic ring [122]. Phytochemicals are famous for their antioxidative and anti-inflammatory activities, and some phytochemicals can usually act on more than one target to regulate cellular function. Chen et al. recently proposed a theory that the one-drug-multitarget strategy is more effective for ischemic stroke treatment when considering the complexity of stroke pathophysiology [123]. Hence, phytochemicals may have great potential in ischemic stroke treatment. In this section, we review the recent 10 years of research that reported the neuroprotective effects of phytochemicals in ischemic stroke. Only the phytochemicals that were tested on animal models of ischemic stroke are listed, and the ones that were studied

extensively or possessed great translational potential are further discussed.

3.1. Flavonoids. Flavonoids include six major subgroups: flavones, flavanones, flavanols, flavonols, isoflavones, and anthocyanidins. In addition, flavonoids also largely exist in plants as glucoside derivatives, with the O-glycosidic bonds formed with different carbohydrates such as D-glucose, D-glucuronic acid, and D-galactose [124]. Totally, 46 kinds of neuroprotective flavonoids were found after searching the recent 10 years of studies in PubMed with keywords "Flavonoids, Stroke, Neuroprotection." The neuroprotective flavonoids and their functional mechanisms are listed in Table 1, and the chemical structures of the extensively studied flavonoids are shown in Table 2.

3.1.1. Flavones. Neuroprotective flavones include apigenin [77, 125], apigenin-7-O-β-D-(-6″-p-coumaroyl)-glucopyranoside (APG) [126], vitexin [127], baicalein [82, 109], baicalin [94, 128–131], chrysin [78, 132, 133], diosmin [134], ginkgetin [135], hispidulin [136], luteolin [95, 137, 138], luteoloside [139], orientin [140], nobiletin [60, 141–143], scutellarin [67, 144–147], and tricin 7-glucoside [148].

Scutellaria baicalensis is a traditional Chinese medicine that has long been used to treat ischemic stroke and cerebral edema [128]. Baicalein and baicalin are two principal components extracted from its roots. Baicalein was reported to improve cerebral infarction, brain edema, and neurobehavioral deficits in both the transient and permanent MCAO models [82, 109]. The neuroprotective strategies of baicalein mainly involve anti-inflammation, antiapoptosis, and antiautophagy. Cui et al. found that baicalein inhibited the 12/15-LOX/p38/cPLA2 pathway and thus reduced arachidonic acid release to inhibit inflammation [82]. Besides, baicalein also suppressed the activation of NF-κB, providing another target for its anti-inflammatory activity [109]. Baicalin is also extensively studied in experimental ischemic stroke and found to improve cerebral infarction and poststroke cognitive impairments in different animal models. The most reported neuroprotective mechanism of baicalin was anti-inflammation, which was achieved via inhibition of the TLR2/4/NF-κB pathway [94, 129]. In addition, baicalin-mediated neuroprotection was also related to its antioxidant effect. Xu et al. reported that baicalin possessed a marked ability to scavenge peroxynitrite and reduce peroxynitrite-induced neuronal injuries [128]. Furthermore, baicalin was observed to show neuroprotection in a diabetic MCAO/R rat model via activation of AMPKα- (5′ AMP-activated protein kinase α-) mediated mitochondrial protection [130]. Notably, baicalin had the ability to cross the BBB, reaching its peak concentration of 344 μg/L in cerebrospinal fluid (CSF) after 30 min of administration (24 mg/kg, i.v.) [149]. To conclude, baicalin showed great neuroprotective efficacy and BBB permeability in experimental ischemic stroke, with great potential for clinical application [150].

Nobiletin, a polymethoxylated flavone, is mainly isolated from the peel of *Citrus* fruits. Nobiletin was found to reduce cerebral infarction, improve motor functional deficit, and enhance BBB integrity in MCAO models [60, 141–143].

Two major strategies for nobiletin-mediated neuroprotection were inhibition of the TLR4/NF-κB pathway to reduce inflammation and upregulation of Nrf2/HO-1-mediated antioxidation [60, 141, 142]. In addition, nobiletin was also found to promote neuronal survival by activating cytoprotective pathways such as the BDNF/Akt/CREB pathway and the Akt/mTOR (mammalian target of rapamycin) pathway [141, 143]. Most importantly, nobiletin might be able to cross the BBB during cerebral I/R according to a study performed by Yasuda et al. They reported that nobiletin could be rapidly accumulated in the damaged region of the ischemic brain after being administrated (i.v.) with a dosage of 15 mg/kg after reperfusion onset [142].

Scutellarin (scutellarein-7-O-glucuronide) is one of the major active components of the herb *Erigeron breviscapus*. Its neuroprotection in ischemic stroke has been extensively studied with various animal models. A study found that scutellarin had stronger efficacy than edaravone for reducing the infarct volume and inflammation of pMCAO rats, implying the great potential of scutellarin in clinical application [144]. Recently, the Dengzhanxixin injection (approval number Z53021569), which uses scutellarin as one of the major components, was applied to clinical ischemic stroke treatment in China. The most studied neuroprotective mechanism of scutellarin was the suppression of microglial activation and inflammation [144, 147, 151]. Besides, scutellarin also promoted microglial-mediated astrogliosis and enhanced the expression of neurotrophins in astrocytes, implying an interglial regulation mechanism for scutellarin [67, 146]. Furthermore, scutellarin was found to improve cerebral blood flow in the ischemic brain [147]. To conclude, scutellarin is a key Chinese herbal medicine ingredient that has been primarily applied to clinical treatment, showing great potential in ischemic stroke.

3.1.2. Flavanones. Flavanones including eriodictyol [152], eriodictyol-7-O-glucoside [153], hesperidin [154], naringenin [61, 85, 155], naringin [156], neohesperidin [157], and pinocembrin [29, 158–160] have been reported to be neuroprotective in ischemic stroke in the past 10 years.

Naringenin naturally exists in *Citrus* fruits, such as grapefruit and orange. Naringenin reduced cerebral infarction and poststroke neurological deficits in both the permanent and transient MCAO rats. The neuroprotective strategies of naringenin were found to inhibit NF-κB to lower inflammation, reduce BBB dysfunction, and promote Nrf2-mediated antioxidation [61, 85, 155]. Naringin (naringenin-7-O-rhamnoglucoside), a glucose derivative of naringenin, is also largely present in the *Citrus* species. Naringin is famous for its strong free radical scavenging activity. Feng et al. showed that naringin improved brain damage in tMCAO/R rats by inhibiting $ONOO^-$ (peroxynitrite) and its induced excessive mitophagy [156]. Yet, naringin might not have good BBB permeability. It was found that the concentration of naringin in CSF only reached the peak of 0.95 μg/mL after it was administrated for 15 min (120 mg/kg, i.v.) [156].

Pinocembrin exists in propolis, honey, ginger roots, and wild marjoram. It has drawn much attention in ischemic stroke treatment in the past decade. Pinocembrin exerted

TABLE 1: Neuroprotective flavonoids and their functional mechanisms and targets[a].

Compounds	Mechanisms and targets	Ref.
Flavones (15)		
Apigenin	Anti-inflammation: iNOS↓, COX-2↓, p-p38↓, p-JNK↓; histone deacetylases↓; BDNF/CREB/Syn-1↑	[77, 125]
APG	Antioxidation: p-STAT3↑	[126]
Vitexin	Antiapoptosis: p-Erk↑, p-JNK↓, p-p38↓	[127]
Baicalein	Anti-inflammation: NF-κB↓, p-MAPKs↓, arachidonic acid release↓: 12/15-LOX/p38 MAPK/cPLA2↓; antiapoptosis; antiautophagy: PI3K/Akt/mTOR↑	[82, 109]
Baicalin	Antiapoptosis: p-CaMKII↓; antioxidation: peroxynitrite scavenging↑; anti-inflammation: TLR2/4/NF-κB↓; mitochondrial function↑: Drp-1↓, Mfn2↓, AMPKα1↑	[94, 128–131]
Chrysin	Anti-inflammation: NF-κB↓, COX-2↓, iNOS↓; antioxidation	[78, 132, 133]
Diosmin	Bcl-2/Bax↑; JAK2/STAT3↑	[134]
Ginkgetin	Antioxidation; anti-inflammation: JAK2/STAT3/SIRT1↓	[135]
Hispidulin	NLRP3-mediated pyroptosis↓; AMPK/GSK3β↑	[136]
Luteolin	Anti-inflammation: TLR4/5/p38/NF-κB↓; antioxidation; antiapoptosis	[95, 137, 138]
Luteoloside	Anti-inflammation: PPARγ↑/Nrf2↑/NF-κB↓	[139]
Orientin	Antioxidation; anti-inflammation: TLR4/NF-κB/TNF-α↓; AQP-4↓	[140]
Nobiletin	Anti-inflammation: TLR4/NF-κB↓; antioxidation: Nrf2/HO-1↑; antiapoptosis: Akt/mTOR↑; BDNF-Akt/CREB↑; BBB permeability↓	[60, 141–143]
Scutellarin	Anti-inflammation: ACE/Ang II/AT1R↓, microglial activation↓, microglial-mediated astrogliosis↑, Notch-1/Nestin↑; neurotrophin expression↑: BDNF/NGF/GDNF-Akt/CREB↑; antioxidation	[67, 144–147]
Tricin 7-glucoside	Anti-inflammation: NF-κB activation↓, HMGB1 expression↓	[148]
Flavanones (7)		
Eriodictyol	Anti-inflammation	[152]
Eriodictyol-7-O-glucoside	Antioxidation in astrocytes: Nrf2/ARE↑	[153]
Hesperidin	Antioxidation: NO pathway↓	[154]
Naringenin	BBB protection: NOD2/RIP2/NF-κB/MMP-9↓; antiapoptosis; anti-inflammation: NF-κB↓; antioxidation: Nrf2	[61, 85, 155]
Naringin	ONOO⁻-mediated excessive mitophagy↓	[156]
Neohesperidin	Antiapoptosis; antioxidation: Akt/Nrf2/HO-1↑	[157]
Pinocembrin	Antiapoptosis; autophagy↑; anti-inflammation: sEH/EETs↓; neuronal loss↓; astrocyte proliferation↓	[29, 158–160]
Flavanols (3)		
(−)-Epicatechin (EC)	Anti-inflammation: microglial activation↓; antioxidation: Nrf2/HO-1↑	[68, 163]
(−)-Epigallocatechin-3-Gallate (EGCG)	Calcium modulation and antiexcitotoxicity: TRPC6 degradation↓/MEK/Erk/CREB↑, balance between the excitatory and inhibitory amino acids↑; antiapoptosis: PI3K/Akt/eNOS↑; antioxidation: Nrf2/ARE↑; anti-inflammation: NF-κB↓; BBB protection: MMP-2↓, MMP-9↓; ER stress↓	[37, 164–170]
Procyanidin B2	BBB protection; antioxidation: Nrf2↑	[171]
Flavonols (10)		
Fisetin	Anti-inflammation: macrophage infiltration↓, microglial activation↓, JNK/NF-κB↓	[69]
Galangin	Microenvironment of the neurovascular unit (NVU)↑: Wnt/β-catenin↑, HIF-1α/VEGF↑; mitochondrial protection and antiapoptosis: Bax/Bcl-2↓	[101, 175]
Icariin	HDAC↓/CREB↑; SIRT1/PGC-1α↑; anti-inflammation: PPARα/γ↑, NF-κB↓	[89, 176, 177]
Kaempferol-3-O-rutinoside (KRS)/glucoside (KGS)	Anti-inflammation: STAT3↓, NF-κB↓	[178]
Kaempferide-7-O-(4″-O-acetylrhamnosyl)-3-O-rutinoside	Anti-inflammation; antioxidation; antiapoptosis	[179]

TABLE 1: Continued.

Compounds	Mechanisms and targets	Ref.
Quercetin	Energy metabolism↑; antioxidation; PP2A subunit B↑; antiapoptosis	[180–182]
Rutin	Estrogen receptors↑: BDNF/TrkB/Akt↑ and NGF/TrkA/CREB↑; BBB protection: MMP-9 activity↓	[119, 183]
Isoquercetin	Antiapoptosis; anti-inflammation and antioxidation: Nrf2↑, NOX4/ROS/NF-κB↓, MAPK/TLR4/NF-κB↓	[54, 184]
Isorhamnetin	Nrf2/HO-1↑; iNOS/NO↓	[185]
Myricetin	Anti-inflammation: p38/NF-κB↓; antioxidation; p-Akt↑	[186]
Isoflavones (6)		
Calycosin	Anti-inflammation: microglial activation↓; antiapoptosis; antiautophagy; BDNF/TrkB↑; calcium modulation: TRPC6/CREB	[43, 70, 190, 191]
Calycosin-7-O-β-D-glucoside	BBB protection: NO↓/Cav-1↑/MMPs↓	[192]
Formononetin	Bax/Bcl-2↓; PI3K/Akt↑	[193]
Genistein	Antioxidation: Nrf2↑; antiapoptosis: PI3K/Akt/mTOR↑; Erk activation↑; ROS/NF-κB↓; antiplatelet aggregation; vascular protection	[194–199]
Daidzein	ROS production↓	[200]
Puerarin	Antiautophagy; anti-inflammation: neutrophil activation↓, HIF-1α↓, α7nAchR↑; antiapoptosis: PI3K/Akt1/GSK-3β/MCL-1↑; BDNF secret↑	[70, 109, 110]
Anthocyanidins, chalcones, and flavonolignans (5)		
Cyanidin-3-O-glucoside	Antiapoptosis: oxidative stress-induced AIF release↓	[211]
Hydroxysafflor yellow A (HSYA)	Antioxidation↓; anti-inflammation: TLR4/MAPK/NF-κB↓; antiapoptosis: PI3K/Akt/GSK3β↑, mPTP opening↓; neurotrophin release↑: BDNF↑, GFAP↑, NGF↑; autophagy↑: Akt↑; mitochondrial function and biogenesis↑; phenylalanine synthesis↓	[98, 106, 212–215]
Xanthohumol	Anti-inflammation; antiapoptosis; platelet activation↓	[216]
Silibinin/silybin	Anti-inflammation; antioxidation; antiapoptosis and antiautophagy: PI3K/Akt/mTOR↑	[104, 217]
Silymarin	Antioxidation; antiapoptosis	[218]

[a]Notes: ↑: activation or upregulation; ↓: inhibition or downregulation. Abbreviations do not appear in the text. ACE: angiotensin-converting enzyme; Ang II: angiotensin II; AT1R: angiotensin type 1 receptor; AQP-4: aquaporin-4; Drp-1: dynamin-related protein 1; GFAP: glial fibrillary acidic protein; Mfn2: mitofusin 2; NOD2: nucleotide oligomerization domain 2; RIP2: receptor-interacting protein kinase 2; Syn-1: synaptophysin-1; VEGF: vascular endothelial growth factor.

neuroprotection in experimental ischemic stroke via antiapoptosis, upregulation of autophagy, and anti-inflammation [158]. Besides, it was shown that pinocembrin inhibited the activity of soluble epoxide hydrolase (sEH), an enzyme that degraded EETs (one of the AA metabolites) and lowered its induced neuronal damage [159]. Furthermore, pinocembrin was found to improve cognitive and memory impairments after it was administrated for 14 d in the global ischemia rat model [160]. Most importantly, *in vitro* studies found that pinocembrin could cross the BBB via a P-glycoprotein-conducted passive transport process [161] and extend the therapeutic time window of tPA treatment [29]. Zhao et al. reported that its neuroprotective efficacy was stronger than that of edaravone [158]. Most importantly, pinocembrin possessed high bioavailability and BBB permeability due to its good liposolubility [162]. Recently, pure synthetic pinocembrin has been subjected to a phase II clinical trial (NCT02059785) to evaluate its activity in ischemic stroke. Hereby, pinocembrin is one of the most potential drug candidates for ischemic stroke, showing great potential for clinical application.

3.1.3. Flavanols. Three flavanols are found to exert neuroprotection in ischemic stroke including (−)-epicatechin (EC) [68, 163], (−)-epigallocatechin-3-gallate (EGCG) [37, 164–170], and procyanidin B2 [171].

EGCG is the most abundant catenin in green tea. EGCG has been reported to be effective in improving various CNS disorders including ischemic stroke, Alzheimer's disease, and Huntington's disease in animal models. It has been subjected to clinical trials to evaluate its efficacy in Alzheimer's disease (NCT00951834) and Huntington's disease (NCT01357681). For ischemic stroke, it was found that EGCG reduced cerebral infarction and promoted post-stroke recovery in MCAO models. The neuroprotective strategies of EGCG involved the promotion of Nrf2-mediated antioxidation [166], suppression of inflammation via inhibiting microglial activation and NF-κB [167, 172], antiapoptosis by activating the PI3K/Akt pathway [168], and decrease of ER stress via upregulation of TRPC6 [169]. Besides, EGCG also inhibited the basal lamina degradation of the BBB by lowering the activity of MMP-9 in tMCAO/R mice [170]. Clinical studies further indicated

TABLE 2: Chemical structures of some representative neuroprotective flavonoids.
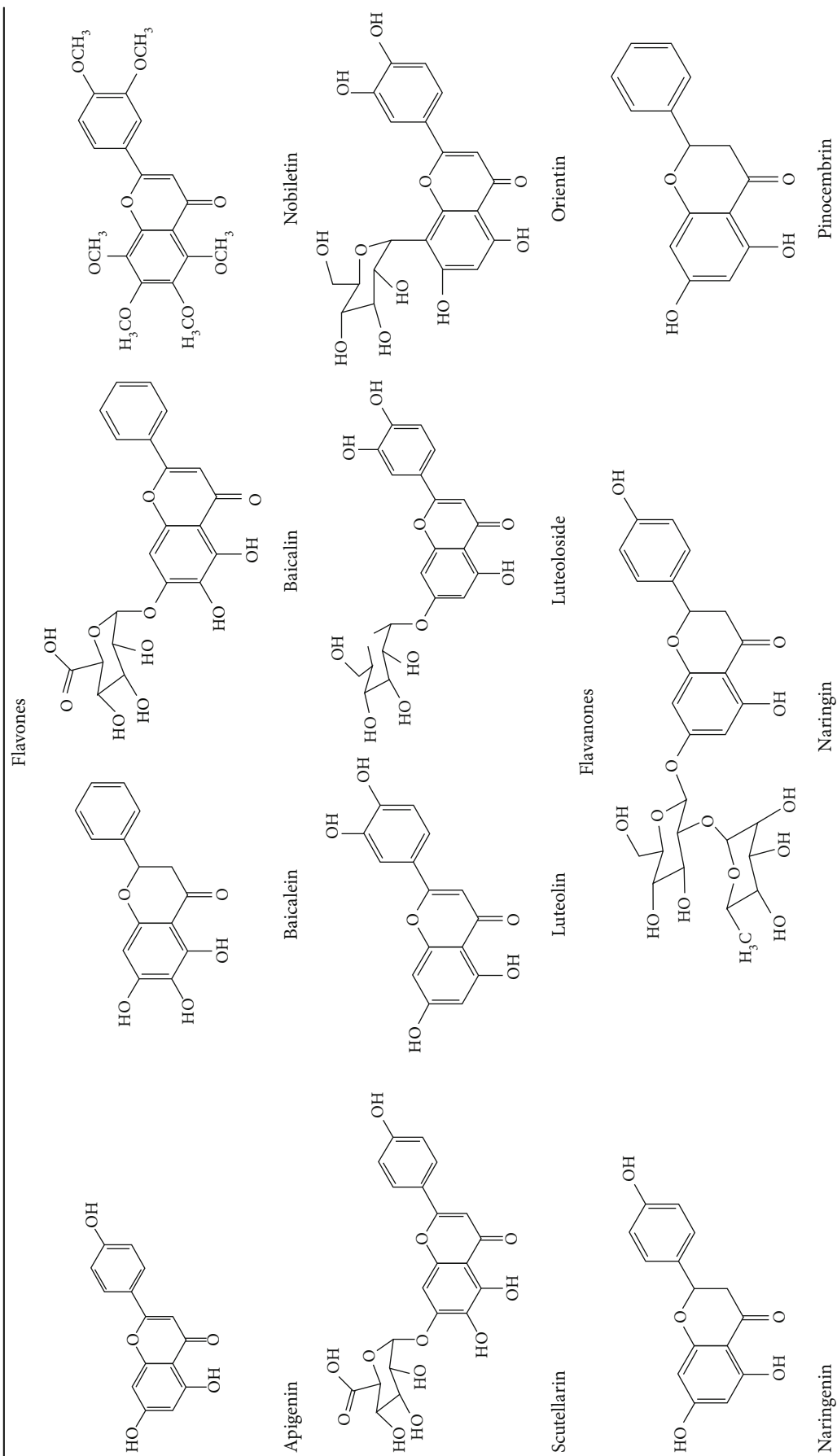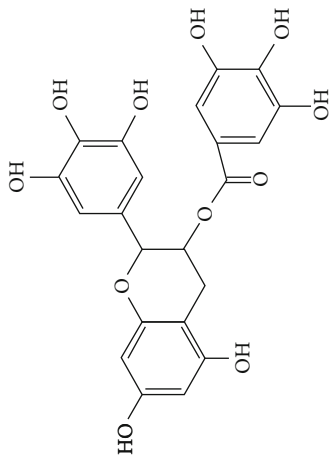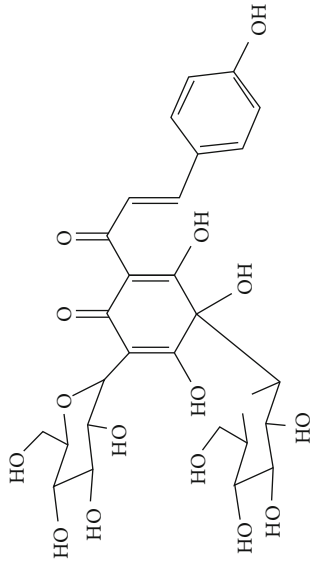
Flavones

Nobiletin

Orientin

Pinocembrin

Baicalin

Luteoloside

Baicalein

Luteolin

Flavanones

Naringin

Apigenin

Scutellarin

Naringenin

TABLE 2: Continued.

Flavanols and chalcones

Hydroxysafflor yellow A (HSYA)

Isoquercetin

Puerarin

Flavonols

Rutin

Daidzein

Quercetin

Isoflavones

Genistein

(−)-Epigallocatechin-3-gallate (EGCG)
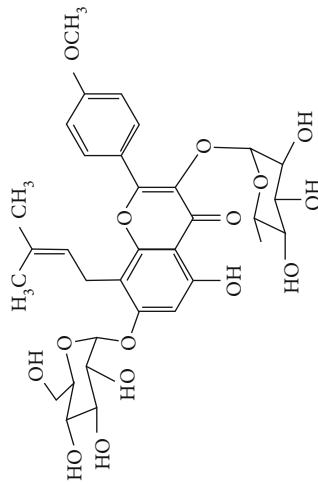
Icariin
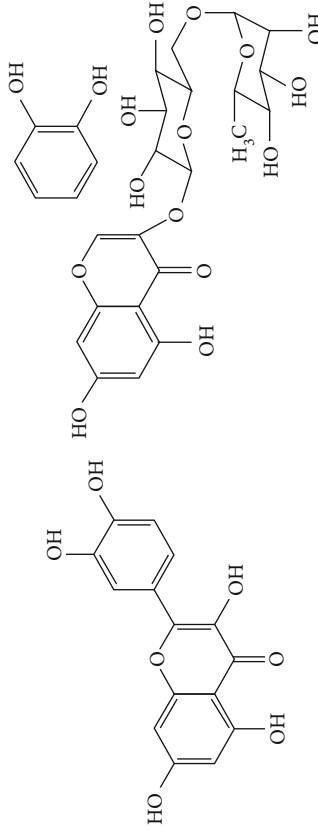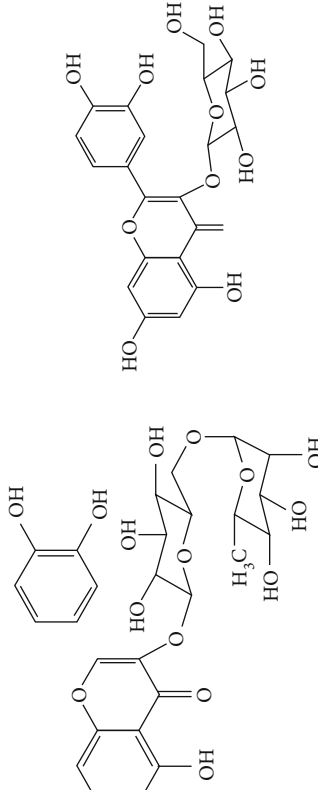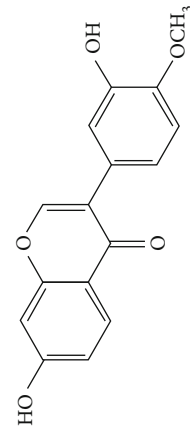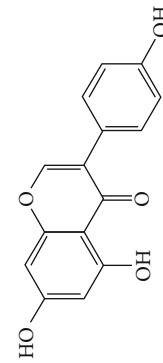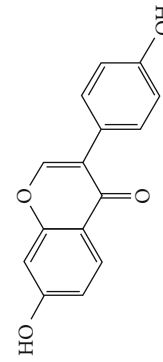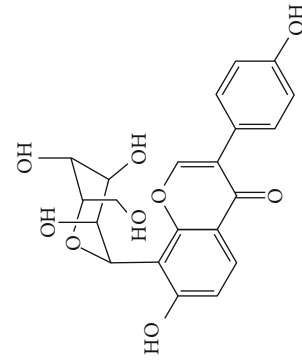
Calycosin

that EGCG decreased the level of MMP-2/9 in the plasma of ischemic stroke patients [164]. Furthermore, EGCG promoted long-term learning and memory recovery by maintaining the balance between the excitatory and inhibitory amino acids [37] and enhancing angiogenesis or neurogenesis [9, 173]. Hereby, EGCG showed neuroprotective activity via regulation of multiple targets in experimental ischemic stroke. Clinically, EGCG was found to extend the therapeutic time window of tPA [165]. Previously, EGCG was considered to possess low bioavailability and BBB permeability, which disqualify it as a drug candidate for ischemic stroke treatment. However, Wei et al. recently reported that BBB permeability was greatly enhanced in aging rats, so EGCG might have great treatment potential in aged patients [174].

3.1.4. Flavonols. Neuroprotective flavonols include fisetin [69], galangin [101, 175], icariin [89, 176, 177], kaempferol-3-O-rutinoside and kaempferol-3-O-glucoside [178], kaempferide-7-O-(4″-O-acetylrhamnosyl)-3-O-rutinoside (A-F-B) [179], quercetin [180–182], rutin [119, 183], isoquercetin [54, 184], isorhamnetin [185], and myricetin [186].

Quercetin is widely distributed in fruits, vegetables, and grains, especially in apples and onions. Quercetin is often used as a dietary supplement due to its good antioxidant and anti-inflammatory activities. In experimental ischemic stroke studies, quercetin was found to reduce the brain injuries of pMCAO rats via multiple mechanisms, including antiapoptosis, promotion of autophagy, regulation of energy metabolism, and upregulation of PP2A (protein phosphatase 2) [180–182, 187]. Recently, quercetin was subjected to a clinical trial to evaluate its effect on improving the cerebral blood flow in the aged population (NCT01376011). However, it was found that quercetin possessed low oral bioavailability (<2%) and weak BBB permeability, limiting its pharmacological application in ischemic stroke [188]. Rutin (quercetin-3-rhamnosyl glucoside), a glycoside of quercetin, abundantly exists in buckwheat, passionflower, and apple. It was found that rutin (10 mg/kg) exerted similar neuroprotective efficacy as quercetin (50 mg/kg) in MCAO/R rats, with much lower effective doses [189]. However, a direct comparison of the efficacy of quercetin and rutin should be carried out. Rutin also inhibited the activity of MMP-9 and exerted BBB protective activity in a photothrombotic ischemic stroke model [183]. Furthermore, Liu et al. reported that rutin was a positive modulator of estrogen receptors. It enhanced the expression of estrogen receptors to upregulate the neurotrophin-mediated prosurvival pathways, such as the NGF/TrkA/CREB pathway and the BDNF/TrkB/Akt pathway in ovariectomized tMCAO/R rats [119]. Isoquercetin (quercetin-3-O-glucoside), another glycoside of quercetin, also possessed neuroprotective activity. The neuroprotective strategies of isoquercetin were found to be antioxidation mediated by Nrf2, inhibition of neuroinflammation via downregulating the TLR4/NF-κB pathway, and antiapoptosis [54, 184].

3.1.5. Isoflavones. In total, 6 isoflavones are found to possess neuroprotective activity in ischemic stroke, that is, calycosin [43, 70, 190, 191], calycosin-7-O-β-D-glucoside [192], formononetin [193], genistein [194–199], daidzein [200], and puerarin [103, 110, 201–203].

Genistein and daidzein, two major isoflavones in soybean and soy products, are described as phytoestrogens due to their structural similarity to human estrogen. Phytoestrogens can bind to the estrogen receptors and mimic the gene transcription of estrogen. However, few studies have reported the direct reaction of genistein or daidzein with estrogen receptors in ischemic stroke [204]. Instead, most of the studies focused on their antioxidant and antiapoptotic activities. It was reported that genistein or daidzein could improve neurological outcomes and reduce cerebral infarction regardless of whether it was administrated before or after MCAO via antioxidation and antiapoptosis [194, 195, 200, 205]. Besides, genistein also inhibited platelet aggregation and kept vascular reactivity in the MCAO rats, which might help to prevent clot formation [196]. Notably, genistein and daidzein played unique roles in treating postmenopausal cerebral ischemia, with several studies reporting the neuroprotective activity of genistein and daidzein in ovariectomized MCAO models. It was found that genistein pretreatment markedly decreased the neurological deficits and infarct volumes of ovariectomized MCAO rodents. The mechanisms involved the promotion of Nrf2-mediated antioxidation and inhibition of apoptosis by activating the PI3K/Akt/mTOR pathway [197–199]. Besides, equol, a metabolite of daidzein, was found to exert neuroprotection in the ovariectomized MCAO/R rats by enhancing the antioxidant defense [206]. Moreover, both genistein and daidzein could cross BBB to some extent. The efficiency of genistein was found to be below 10%, while the penetration index (AUC$_\text{CSF}$/AUC$_\text{plasma}$) of daidzein was about 11.96% in SD rats [207, 208].

Puerarin (daidzein-8-C-glucoside) is the major bioactive component in *Radix Puerariae* (kudzu root). Puerarin showed marked neuroprotection in experimental ischemic stroke. It was reported that puerarin reduced the brain injuries of tMCAO/R rats by suppression of autophagy, apoptosis, and inflammation [110, 201]. The anti-inflammatory activity of puerarin was achieved via upregulation of the cholinergic anti-inflammatory pathway, that is, promotion of α7nAchR (alpha7 nicotinic acetylcholine receptor) to inhibit the JAK2/NF-κB pathway [202]. In addition, puerarin enhanced the BDNF/PI3K/Akt pathway to promote neuronal survival and poststroke recovery [103, 203]. Besides, the AUC$_\text{CSF}$/AUC$_\text{plasma}$ of puerarin in rats was found to be about 9.29%, implying its BBB permeability [208]. Notably, puerarin had shown the primary neuroprotective effect against ischemic stroke in clinical trials. For example, puerarin injection was subjected to a clinical trial, in which ischemic stroke patients were treated with conventional therapies plus an additional puerarin injection (400 mg/d) for one month. Results showed that puerarin injection significantly improved blood viscosity, neurological damage, and language function of ischemic stroke patients [209]. Besides, a meta-analysis of randomized controlled trials concluded that puerarin injection was effective and safe for clinical acute ischemic stroke treatment [210]. Hence, puerarin possessed great potential for clinical ischemic stroke treatment.

TABLE 3: Neuroprotective stilbenoids and their functional mechanisms and targets[b].

Compounds	Mechanisms and targets	Ref.
Stilbenoids (7)		
Resveratrol	Anti-inflammation: T regulatory cells (Treg)↑, intestinal flora-mediated immune cell balance↑; calcium modulation: TRPC6/MEK/CREB↑, TRPC6/CaMKIV/CREB↑, NMDA receptor↓; BDNF↑; modulating energy metabolism and extending the cerebral ischemic tolerance: glycolysis↑, mitochondrial respiration efficiency↑, phosphodiesterase↓, cAMP/AMPK/SIRT1↑, UCP2↓; antioxidation: Nrf2/HO-1; antiapoptosis; synaptic transmission efficiency↑; BBB protection: MMP-9/TIMP-1 balance↑; regulation of hypothalamus-pituitary-adrenal axis function; hedgehog signaling pathway↑; estrogen receptor↑; cellular stress proteins↑	[45, 223–235]
Polydatin	BBB protection; sonic hedgehog pathway↑; anti-inflammation: NF-κB↓; antioxidation; antiapoptosis	[236, 237]
Malibatol A	Mitochondrial dysfunction↓; anti-inflammation: microglial M2 polarization↑, PPARγ↑	[88, 238]
Oxyresveratrol	Antiapoptosis	[239]
Mulberroside A	Anti-inflammation: MAPK/NF-κB↓	[240]
Pterostilbene	Antioxidation; antiapoptosis	[241]
2,3,5,4′-Tetrahydroxystilbene-2-O-β-D-glucoside	Angiogenesis↑	[242]

[b]Notes: ↑: activation or upregulation; ↓: inhibition or downregulation. Abbreviation does not appear in the text. UCP2: uncoupling protein 2.

3.1.6. Anthocyanidins, Chalcones, and Flavonolignans. Cyanidin-3-O-glucoside (anthocyanidin) [211], hydroxysafflor yellow A (chalcone) [98, 106, 212–215], xanthohumol (chalcone) [216], silybin (flavonolignan) [104, 217], and silymarin (flavonolignan) [218] are neuroprotective in experimental ischemic stroke.

Hydroxysafflor yellow A (HSYA), a chalcone, is extracted from *Carthamus tinctorius* (safflower), a Chinese medicine that is widely used in treating cerebrovascular diseases [219]. Safflower yellow for injection (approval number Z20050146) uses HSYA as the major bioactive ingredient and has been approved in China for the treatment of cerebrovascular diseases including ischemic stroke. HSYA was found to improve cerebral infarction and cognitive impairment in animal models. The neuroprotective strategies of HSYA were multiple, including antioxidation, anti-inflammation, antiapoptosis, antiexcitotoxicity, autophagy modulation, and mitochondrial protection [98, 106, 212–215, 220]. Lv et al. reported that HSYA targeted TLR4 to inhibit the NF-κB activation and subsequent cascade of inflammation [212, 214]. Besides, HSYA promoted the activation of the PI3K/Akt pathway to promote cytoprotective autophagy and inhibit apoptosis in MCAO rats [106, 213]. As for mitochondrial protection, HSYA was found to improve mitochondrial function, reduce the mPTP opening, and promote mitochondrial biogenesis by inhibiting the production of phenylalanine [98, 215]. Notably, a single dose of 2 mg/kg (i.v.) HSYA was found to exert neuroprotection in tMCAO/R mice, implying its high bioavailability [212]. In addition, He reported that HSYA was detected in the brain tissue homogenate of the ischemic hemisphere in MCAO rats, with the peak concentration at 90 min after HSYA administration (i.v.), indicating the BBB permeability of HSYA [221]. Hereby, HSYA had marked neuroprotective efficacy and high bioavailability and BBB permeability, so it might be a good drug candidate for ischemic stroke.

3.1.7. Summary of Flavonoids. From the current studies, baicalein and baicalin, scutellarin, pinocembrin, puerarin, and hydroxysafflor yellow A exerted great neuroprotective efficacy and high bioactivity and BBB permeability in experimental ischemic stroke. Besides, plant extracts/concentrates containing scutellarin, puerarin, and hydroxysafflor yellow A have been primarily applied in the clinical treatment of ischemic stroke due to their great neuroprotective effects. However, only pinocembrin as a single pure compound is on a phase II clinical trial at present.

3.2. Stilbenoids. Stilbenoids refer to a class of compounds that have two aromatic rings connected by an ethene bridge. Stilbenoids possess both the *cis* and *trans* forms, and the *trans* form is found to be more bioactive and stable [222]. In total, 7 stilbenoids are reported in the past 10 years for their neuroprotective activity in ischemic stroke, that is, resveratrol [45, 223–235], polydatin (resveratrol-3-β-D-glucoside) [236, 237], malibatol A (a resveratrol oligomer) [88, 238], oxyresveratrol [239], mulberroside A (oxyresveratrol-3,4′-diglycopyranoside) [240], pterostilbene [241], and 2,3,5,4′-tetrahydroxystilbene-2-O-β-D-glucoside [242]. Their neuroprotective mechanisms are explained in Table 3, and the chemical structures of the extensively studied stilbenoids are shown in Table 4.

Resveratrol, the most famous stilbenoid, is widely distributed in plants, such as grapes. The neuroprotective effect of resveratrol in ischemic stroke has been studied extensively, and dozens of related research articles were found. It was found that resveratrol administration, especially preconditioning, improved cerebral infarction, neurological deficits, poststroke depression, and ischemic tolerance in various animal models [223]. The neuroprotective strategies of resveratrol were multiple, including the common mechanisms such as anti-inflammation, promotion of Nrf2-mediated antioxidation, antiapoptosis, and BBB protection [224–227]. In

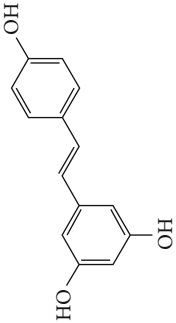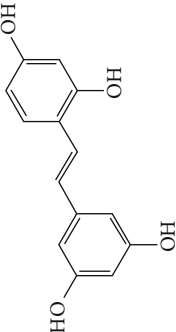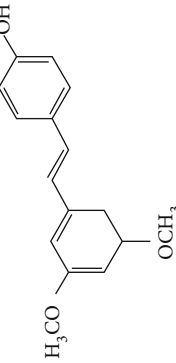TABLE 4: Chemical structures of some representative neuroprotective nonflavonoid phenols.
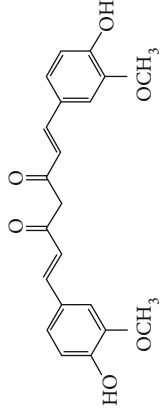

Stilbenoids
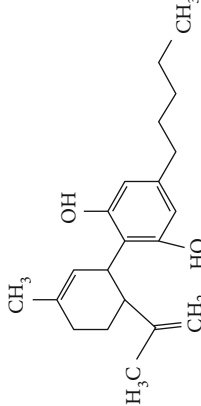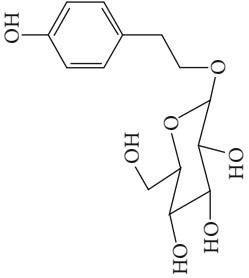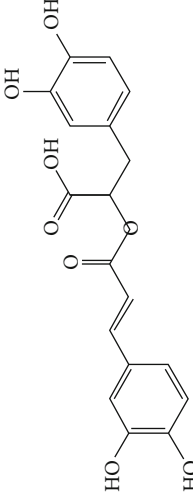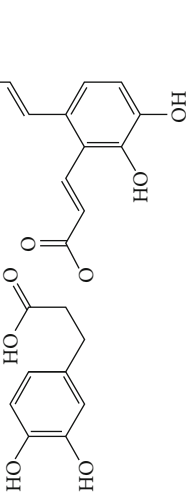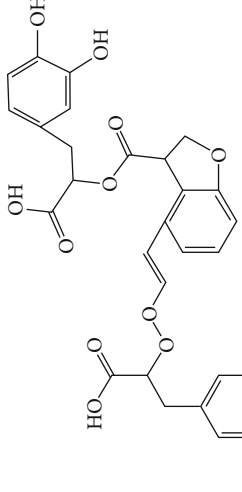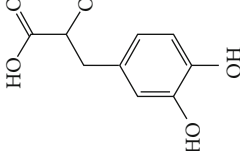
Resveratrol

Pterostilbene

Oxyresveratrol

Other phenols

Caffeic acid

Salidroside

Curcumin (keto form)

Cannabidiol

Salvianolic acid B

Rosmarinic acid

Salvianolic acid A

Table 5: Neuroprotective activity of other phenols and their mechanisms and targets[c].

Compounds	Mechanisms and targets	Ref.
Other phenols (20)		
Creosol	Antiexcitotoxicity; Ca^{2+} influx↓	[243]
Curcumin	Antiautophagy: PI3K/Akt/mTOR↑; anti-inflammation: TLR4/p38/MAPK↓; antiapoptosis; GLUT1 and GLUT3↑; neurogenesis: Notch signaling pathway↑; antioxidation: Akt/Nrf2↑; mitochondrial protection: SIRT1↑; BBB protection	[10, 96, 244–249]
Cannabidiol	BBB protection; anti-inflammation; Na^+/Ca^{2+} exchangers↑; antiapoptosis; antiexcitotoxicity; metabolic derangement↓	[250–252]
Hydroxytyrosol	Anti-inflammation; BDNF↑	[253]
Acteoside	Antioxidation; antiapoptosis	[254]
Hydroquinone	BBB protection: SMI-71↑, GLUT-1↑, ZO-1↓, occludin degradation↓	[255]
Lyciumamide A	Antioxidation: PKCε/Nrf2/HO-1↑; antiapoptosis	[256]
Oleuropein	Antiapoptosis: Bcl-2/Bax↑, Akt↑/GSK3β↓	[257, 258]
Salidroside	Anti-inflammation: microglial M2 polarization↑, PI3K↑/PKB↑/Nrf2↑/NF-κB↓, PI3K/Akt/HIFα↑; antiapoptosis: BDNF/PI3K/Akt↑; complement C3 activation↓; Egrs expression↑	[71, 259–264]
6-Shogaol	Anti-inflammation: CysLT1R↓, MAPK↓	[265]
4-Hydroxybenzyl alcohol	Antioxidation	[266]
4-Methoxy benzyl alcohol	BBB protection: NOS pathway↓, AQP-4↓, tight junction↑	[267]
Cinnamophilin	Gray and white matter damage↓	[268]
Hyperforin	TRPC6/MEK/Erk/CREB↑; TRPC6/CaMKIV/CREB↑	[269]
Punicalagin	Antioxidation; anti-inflammation; antiapoptosis	[270, 271]
Caffeic acid	Antioxidation; anti-inflammation: 5-LOX↓; loss of neuronal cells↓; synaptic density and plasticity↑	[80, 272]
Ferulic acid	Peroxiredoxin-2↑; thioredoxin↑	[273]
Gallic acid	Antiapoptosis and mitochondrial protection: Erk↑/cyclophilin D↓/mPTP↓	[99, 274]
Rosmarinic acid	Anti-inflammation: HMGB1/NF-κB↓; synaptogenic activity↑; BDNF↑; BBB protection	[275, 276]
Salvianolic acid A	Antioxidation; anti-inflammation; metabolic dysfunction↓	[277]

[c]Notes: ↑: activation or upregulation; ↓: inhibition or downregulation. Abbreviations do not appear in the text. CysLT1R: cysteinyl leukotriene receptor 1; ZO-1: zonula occludens 1.

addition, resveratrol was also reported to modulate the energy metabolism of the ischemic brain. It was found that resveratrol enhanced bioenergetic efficiency such as improving glycolysis and mitochondrial respiration efficiency to extend the window of ischemic tolerance, especially in elderly individuals [228–232]. Further studies revealed that this process was achieved by activating AMPK and SIRT1, an NAD^+-dependent deacetylase that can induce adaptive responses under energy depletion conditions [228–232]. Furthermore, resveratrol maintained intracellular calcium homeostasis via the promotion of the TRPC6/CREB pathway and inhibition of the NMDA receptor [45] and activated sonic hedgehog signaling, a pathway that contributes to neurogenesis and neurological recovery [233, 234]. Notably, a novel study that focused on the gut-brain axis indicated that resveratrol inhibited inflammation via modulating the intestinal flora-mediated immune cell balance such as the Th1/Th2 balance and Treg/Th17 balance in the lamina propria of the small intestine, proposing an original hypothesis for resveratrol-mediated neuroprotection [235].

In summary, resveratrol possessed marked neuroprotective activity in experimental ischemic stroke and might have great potential in improving the ischemic tolerance when administrated before cerebral ischemia occurs.

3.3. Other Phenols. Other phenols refer to the phenolic compounds apart from flavonoids and stilbenoids, such as phenolic alcohols, phenolic acids, and lignans. In total, 20 other types of phenols are found to possess neuroprotection in ischemic stroke, including creosol [243], curcumin [10, 96, 244–249], cannabidiol [250–252], hydroxytyrosol [253], acteoside [254], hydroquinone [255], lyciumamide A [256], oleuropein [257, 258], salidroside [71, 259–264], 6-shogaol [265], 4-hydroxybenzyl alcohol [266], 4-methoxy benzyl alcohol [267], cinnamophilin [268], hyperforin [269], punicalagin [270, 271], caffeic acid [80, 272], ferulic acid [273], gallic acid [99, 274], rosmarinic acid [275, 276], and salvianolic acid A [277]. Their neuroprotective mechanisms are clarified in Table 5, and the chemical structures of the extensively studied ones are shown in Table 4.

Curcumin is extracted from the root of *Curcuma longa* (turmeric), a common spice plant in Asian countries [278]. It was found that curcumin reduced cerebral infarction, neurological deficits, and brain edema in tMCAO models regarding preconditioning or postconditioning. Curcumin is a pleiotropic agent for neuroprotection, modulating multiple mechanisms including antiapoptosis, inhibition of inflammation by downregulating TLR4, promotion of Akt/Nrf2-mediated antioxidation, suppression of autophagy by activating the PI3K/Akt/mTOR pathway, protection of mitochondria via upregulating SIRT1, the decrease of ER stress, and BBB protection [96, 244–248, 279]. In addition, curcumin promoted neurogenesis via activation of the Notch signaling pathway that improves poststroke recovery [10]. Xia et al. reported that curcumin also showed neuroprotection in a diabetic stroke model. The mechanism involved antiapoptosis and promotion of glucose uptake by activating GLUT1/3 (glucose transporter 1/3) [249]. Curcumin is one of the most popular phytochemicals in pharmacological research, with numerous clinical trials conducted for various clinical disorders including CNS diseases. As an example, curcumin has been subjected to several clinical trials for Alzheimer's disease (NCT00164749, NCT00099710, and NCT01001637). Yet, those clinical trials failed due to limited bioavailability and the BBB permeability of curcumin, limiting its clinical application in ischemic stroke. Recently, researchers were trying to enhance the bioavailability of curcumin via modulation of its chemical structure or use of the solid lipid particle method. To illustrate, Wicha et al. found that hexahydrocurcumin exerted neuroprotection with lower doses, showing better bioavailability than curcumin [280].

Cannabidiol (CBD), a phytocannabinoid from *Cannabis sativa*, is found to be nonpsychoactive and possesses cytoprotective activities. Cannabidiol has been studied in various therapeutic uses, especially for CNS disorders [281]. For ischemic stroke, cannabidiol was reported to exert neuroprotection with relatively low effective doses (single dose of 5 mg/kg, i.p.) in MCAO models [250–252]. The neuroprotective strategies of cannabidiol included antiapoptosis, antiexcitocitotoxicity, anti-inflammation, BBB protection, Ca^{2+} modulation, and metabolism regulation [250–252]. In addition, a meta-analysis that reviewed 34 publications of cannabidiol-mediated ischemic stroke indicated that cannabidiol markedly reduced cerebral I/R-induced infarction [282]. Most importantly, cannabidiol was highly lipophilic and could easily cross BBB, reaching a relatively high concentration quickly after administration [283]. Notably, more than 100 clinical trials related to the therapeutic application of cannabidiol are being conducted or are completed at present, with several trials for CNS disorders. For example, two phase II clinical trials are being conducted to evaluate the efficacy of cannabidiol on motor and tremor symptom improvement in Parkinson's disease (NCT03582137, NCT02818777).

Salidroside is the main bioactive component of *Rhodiola rosea* L. [284] and showed neuroprotection for ischemic stroke in various MCAO models. The major neuroprotective strategies of salidroside involved anti-inflammation and antiapoptosis. Liu et al. found that salidroside suppressed inflam-

mation by promoting microglial M2 polarization [71]. Other studies showed that salidroside inhibited NF-κB and activated HIFα (hypoxia-inducible factors) via upregulation of the PI3K/Akt pathway, providing another mechanism for its anti-inflammatory activity [261, 263, 264]. In addition, Zhang et al. reported that the antiapoptotic effect of salidroside was achieved via activation of the BDNF/PI3K/Akt pathway in tMCAO/R mice [262]. Furthermore, salidroside upregulated the cytoprotective transcriptional factor Egrs (early growth response genes) to improve neuronal activity and synaptic plasticity [259, 260]. However, the concentration of salidroside in the brain is extremely low after administration (15 mg/kg, i.v.), indicating that salidroside might have difficulty crossing BBB [285].

Salvianolic acids are the bioactive compounds extracted from the roots of *Salvia metrorrhagia* (Danshen), a traditional Chinese medicine for treating cardiovascular disease [286]. Salvianolic acid A was reported to improve brain damage in MCAO/R rats by its antioxidant, anti-inflammatory, and metabolism regulatory activities [277]. Salvianolic acids for injection (SAFI), a commercially available Chinese herb medicine developed by Tianjin Tably Pride Pharmaceutical Company, has been approved for the treatment of ischemic stroke in the recovery phase in China. SAFI is composed of five natural phenolic acids: salvianolic acid B (68.31%), salvianolic acid D (3.7%), salvianolic acid Y (5.1%), alkannic acid (3.86%), and rosmarinic acid (2.68%) [287]. In experimental ischemic stroke, SAFI was found to promote poststroke recovery through two major mechanisms: promotion of neurogenesis via activation of the sonic hedgehog pathway and via upregulation of neurotrophins such as BDNF and NGF [288]. Besides, SAFI also reduced brain damage in the acute phase of ischemic stroke. The mechanisms involved anti-inflammation via inhibition of microglial activation, as well as maintaining mitochondrial permeability in astrocytes through activation of the PI3K/Akt/mtCx43 (mitochondrial connexin 43) pathway [286, 287].

Caffeic acid is widely present in dietary plants such as fruits, vegetables, coffee, and olive oils. It was found that caffeic acid reduced cerebral infarction and improved poststroke learning, memory, and spatial deficits in global ischemia or pMCAO models [80, 272]. The mechanisms involved suppression of oxidative stress, inhibition of 5-LOX-induced inflammation, and reduction of synaptic dysfunction by upregulation of synaptophysin, a biomarker for synaptic density and plasticity [80, 272]. Rosmarinic acid, an ester of caffeic acid, exists in plants of the *Lamiaceae* family such as rosemary and perilla. Rosmarinic acid attenuated brain damage and memory deficits by promoting synaptogenic activity, suppressing inflammation, and upregulating BDNF in pMCAO mice. In addition, rosmarinic acid also exerted neuroprotection in a diabetic ischemic stroke model by promoting BBB function and inhibiting inflammation. As mentioned above, rosmarinic acid is one of the components of SAFI, accounting for 2.68% of the injection.

In summary, salvianolic acids and rosmarinic acid have been primarily applied as key ingredients in a Chinese herbal medicine for clinical ischemic stroke treatment. Yet, there is no clinical data to prove their individual effectiveness at

TABLE 6: Neuroprotective terpenoids and their functional mechanisms and targets[d].

Compounds	Mechanisms and targets	Ref.
Monoterpenoids (14)		
Borneol	Antiapoptosis; anti-inflammation; neurovascular unit function↑	[289, 290]
Carvacrol	Ferroptosis↓; antioxidation; GPx4↑; TRPM7↓; antiapoptosis: Bcl-2/Bax↑, PI3K/Akt↑; anti-inflammation: NF-κB↓	[46, 291–293]
Catalpol	Angiogenesis↑; JAK2/STAT3↑; ATPase activity↑; excitatory amino acid toxicity↓	[294, 295]
Cornin	Mitochondrial protection; antioxidation	[296]
Genipin	Antiapoptosis; UCP2/SIRT3↓	[297]
Geniposide	Antiapoptosis; BBB protection; GluN2A/Akt/Erk↑	[41]
Linalool	Phospholipid homeostasis↑	[298]
β-Myrcene	Antioxidation: free radical scavenging	[299]
Paeoniflorin	Calcium modulation: Ca^{2+}↓/CaMKII↑/CREB↑; anti-inflammation: MAPK/NF-κB↓; antiapoptosis	[300–302]
Perillaldehyde	Anti-inflammation: JNK↓; antiapoptosis: Akt↑	[303]
Perillyl alcohol	Anti-inflammation; antioxidation	[304]
α-Pinene	Antioxidation; anti-inflammation	[305]
Picroside II	Antioxidation: Rac-1/NOX2↓; antiapoptosis: mPTP permeability↓; anti-inflammation: MEK/Erk1/2/COX-2↓; BBB protection: ROCK/MLCK/MMP-2↓/claudin-5↑	[56, 79, 100, 306, 307]
Safranal	Antioxidation	[308]
Sesquiterpenoids (8)		
Alantolactone	Anti-inflammation: MAPK/NF-κB↓	[312]
Atractylenolide III	Anti-inflammation: mitochondrial fission in microglia↓, JAK2/STAT3/Drp-1↓	[86]
Bakkenolide IIIa	Antioxidation; anti-inflammation: Erk↓, Akt/NF-κB↓	[313]
Bilobalide	Mitochondrial protection: complex I function↑; antiexcitotoxicity; anti-inflammation: JNK1/2↓, p38 MAPK↓; antiautophagy; antiapoptosis; angiogenesis↑: Akt/eNOS↑	[314–317]
(−)-α-Bisabolol	Anti-inflammation	[318]
Parthenolide	BBB permeability↓; caspase-1/p38/NF-κB↓	[319]
Patchouli alcohol	Anti-inflammation	[320]
β-Caryophyllene	Anti-inflammation: microglial M2 polarization↑, TLR4↓	[321]
Diterpenoids (11)		
Andrographolide	Anti-inflammation: microglial activation↓, PI3K/Akt-NF-κB/HIF-1α↓, astrocyte activation↓, iNOS; BBB permeability↓; antioxidation: p38/Nrf2/HO-1↑, gp91[phox]/NOX2↓; BDNF/TrkB↑	[57, 325–328]
Erinacine A	Anti-inflammation: iNOS, p38, and CHOP↓	[329]
Ginkgolide B	Anti-inflammation: microglial M2 polarization↑, NF-κB↓; PAF receptor↓; antiapoptosis; antiexcitotoxicity: imbalance of excitatory and inhibitory amino acids↓; BBB permeability↓	[38, 72, 330, 331]
Ginkgolide K	Antioxidation; neurogenesis: JAK2/STAT3↑	[11, 332]
Pseudopterosin A	Antioxidation; anti-inflammation; antiapoptosis: Akt↑	[333]
Salvinorin A	Mitochondrial function↑: AMPK/Mfn2↑, kappa opioid receptor↑	[334]
Tanshinone I	Neuronal death↓; anti-inflammation	[335]
Tanshinone IIA	Antiapoptosis: PI3K/Akt↑; anti-inflammation: HMGB1/NF-κB↓, MIF/NF-κB↓, astrocyte activation, MAPKs↓, PPARγ↑; antioxidation; TORC1↑; BDNF/CREB↑	[75, 336–343]
Totarol	Antioxidation: Akt/HO-1↑	[344]
Triptolide	BBB permeability↓; anti-inflammation: p38/NF-κB↓; autophagy↑; antiapoptosis	[113, 345, 346]
(1S,2E,4R,6R,-7E,11E)-2,7,11-Cembratriene-4,6-diol	Antiapoptosis: PI3K/Akt↑; ICAM-1↓	[347]

TABLE 6: Continued.

Compounds	Mechanisms and targets	Ref.
Triterpenoids (20)		
Arjunolic acid	Antioxidation	[357]
Asiatic acid	Antiapoptosis and mitochondrial protection: cytochrome c and AIF release↓; MMP-9↓	[358, 359]
Acetyl-11-keto-β-boswellic acid	Antioxidation: Nrf2/HO-1↑; anti-inflammation: 5-LOX, NF-κB↓	[81, 360, 361]
11-Keto-β-boswellic acid	Antioxidation: Nrf2/HO-1↑	Ding et al. (2015)
28-O-Caffeoyl betulin	Anti-inflammation; hypothermic effects	[362]
Celastrol	Anti-inflammation: microglial M2 polarization↑, IL-33/ST2↓, JNK/c-Jun/NF-κB↓	[73, 363]
Echinocystic acid	Antiapoptosis; anti-inflammation: JNK↓	[364]
18β-Glycyrrhetinic acid	Antioxidation; antiapoptosis	[365]
Maslinic acid	Synaptogenesis↑: axonal regeneration↑, Akt/GSK-3β↑	[366]
Ursolic acid	Anti-inflammation; antioxidation: Nrf2↑	[367]
Madecassoside	Antioxidation; antiapoptosis; anti-inflammation	[368]
Astragaloside IV	Antiapoptosis: P62-LC3-autophagy↑; antioxidation: Nrf2↑; mitochondrial protection: Akt/hexokinase-II↑; anti-inflammation	[62, 114, 369, 370]
Glycyrrhizin	Anti-inflammation: HMGB1/TLR4/IL-17A↓; antioxidation; antiexcitotoxicity; antiapoptosis	[91, 371–373]
Diammonium glycyrrhizinate	Anti-inflammation	[374]
Ginsenoside Rb1	BBB protection; anti-inflammation; antioxidation: NOX4-derived ROS production↓; abnormal microenvironment↓: glutamate toxicity↓, Ca^{2+} accumulation↓, GLT-1↑, NMDAR↓; autophagy↑; neurogenesis↑; BDNF↑; caspase-3↓	[34, 55, 115, 375, 376]
Ginsenoside Rd	Anti-inflammation: microglial proteasome-mediated NF-κB activation↓, PARP-1↓; antioxidation: free radical scavenging; antiapoptosis; mitochondrial protection; energy restoration; Ca^{2+} modulation: TRPM7↓, ASIC1 a↓, ASIC2 a↑; DNA damage↓: NEIL1/3↑	[49, 377–383]
Ginsenoside Rg1	Anti-inflammation: microglial proteasome-mediated NF-κB activation↓; BDNF↑; excitatory amino acid↓; antioxidation: miR-144↓/Nrf2↑/ARE↑; angiogenesis↑: PI3K/Akt/mTOR↑; BBB permeability↓: aquaporin-4↓, PAR-1↓	[384–389]
20(R)-Ginsenoside Rg3	Antiapoptosis: calpain I↓, caspase-3↓	[390]
Pseudoginsenoside F11	Antiapoptosis; autophagic/lysosomal defects↓; Ca^{2+} overload↓	[391, 392]
Notoginsenoside R1	Antiapoptosis; mitochondrial protection; estrogen receptor-Akt/Nrf2↑	[393]
Tetraterpenoids (3)		
Astaxanthin	Antioxidation; antiapoptosis; neurogenesis↑; neurotrophin expression: BDNF↑, NGF↑	[120, 400, 401]
Fucoxanthin	Antioxidation: Nrf2/HO-1↑	[402]
Lutein	Antiapoptosis; antioxidation; anti-inflammation	[403]

[d]Notes: ↑: activation or upregulation; ↓: inhibition or downregulation. Abbreviations do not appear in the text. CHOP: C/EBP homologous protein; GPx4: glutathione peroxidase 4; MLCK: myosin light chain kinase; PAR-1: protease-activated receptors; ROCK: Rho-associated kinase.

present. Cannabidiol showed good neuroprotective efficacy and high BBB permeability, so it was a good candidate for ischemic stroke drug development. Although curcumin and salidroside showed high neuroprotective efficacy, the poor bioavailability and BBB permeability might limit their further clinical applications.

3.4. Terpenoids. Terpenoids are a class of compounds that have an isoprene unit as their basic component. Depending on the number of isoprene units, terpenoids can be divided into monoterpenoids (two units), sesquiterpenoids (three units), diterpenoids (four units), triterpenoids (six units), and tetraterpenoids (eight units). In total, 56 terpenoids were found to possess neuroprotective activity for ischemic stroke

after searching the recent 10 years of studies in PubMed with keywords "Terpenoids, Stroke, Neuroprotection." The neuroprotective terpenoids and their functional mechanisms are listed in Table 6, and the chemical structures of the extensively studied ones are shown in Table 7.

3.4.1. Monoterpenoids. The neuroprotective monoterpenoids include borneol [289, 290], carvacrol [46, 291–293], catalpol [294, 295], cornin [296], genipin [297], geniposide [41], linalool [298], β-myrcene [299], paeoniflorin [300–302], perillaldehyde [303], perillyl alcohol [304], α-pinene [305], picroside II [56, 79, 100, 306, 307], and safranal [308].

Borneol is present in the plants of *Artemisia* and *Dipterocarpaceae* and has been used in traditional Chinese

TABLE 7: Chemical structures of some representative neuroprotective terpenoids and alkaloids.

Monoterpenoids

Picroside II
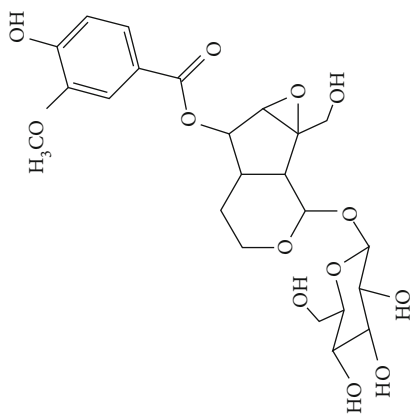
Androgapholide
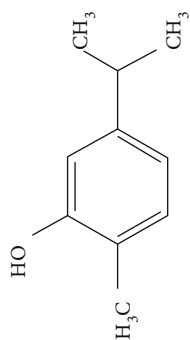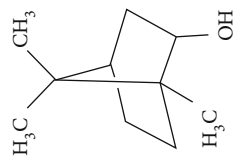
Triptolide

Carvacrol

Sesquiterpenoids and diterpenoids

Ginkgolide K

Ginkgolide B

Tanshinone IIA

(+)-Borneol
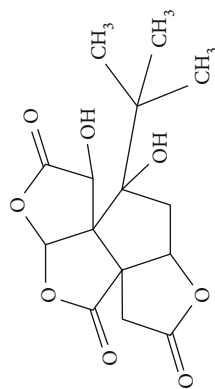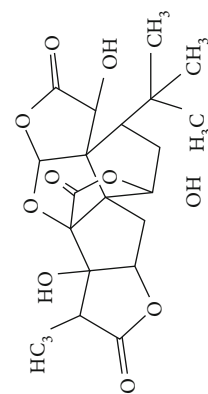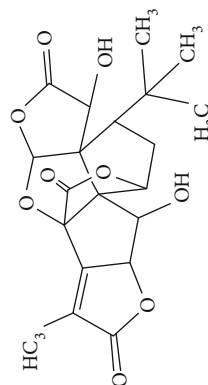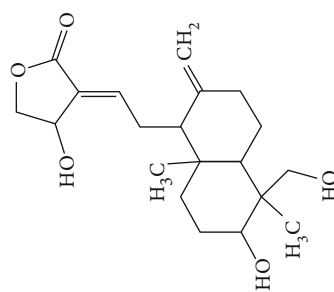
Bilobalide
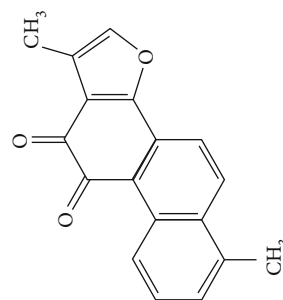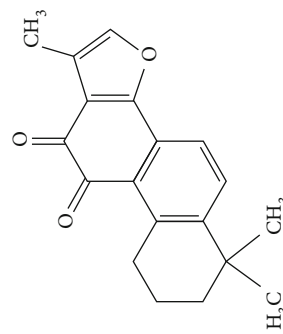
Tanshinone I
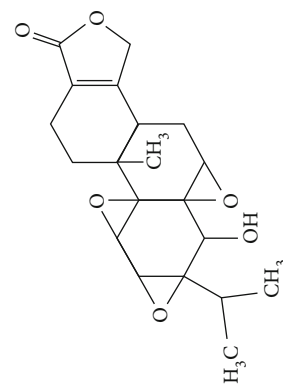
TABLE 7: Continued.

Triterpenoids and tetraterpenoids
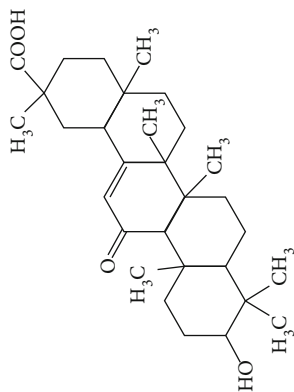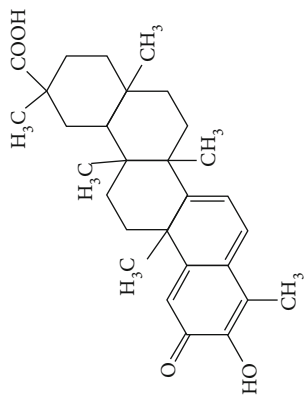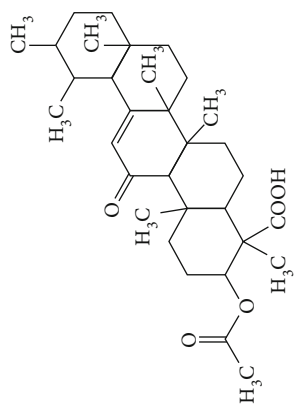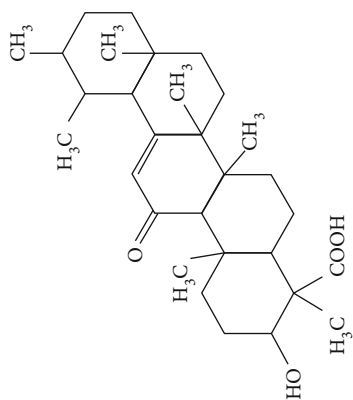
Glycyrrhetinic acid

Celastrol

Acetyl-11-keto-β-boswellic acid (AKBA)

Glycyrrhizin

11-Keto-β-boswellic acid (KBA)
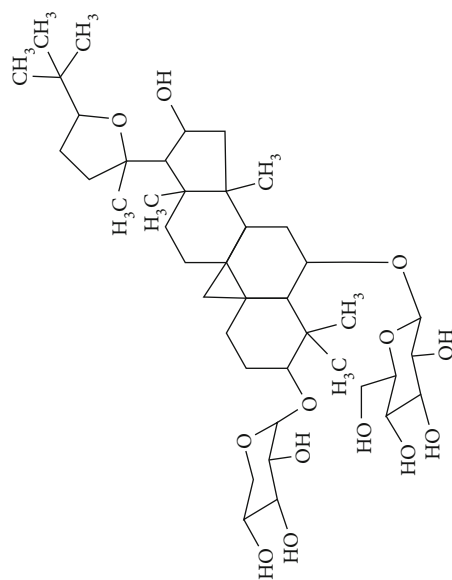
Astragaloside IV
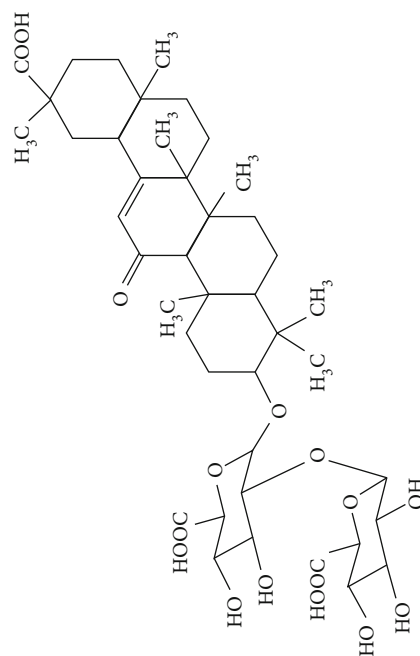
Table 7: Continued.

Ginsenoside Rd
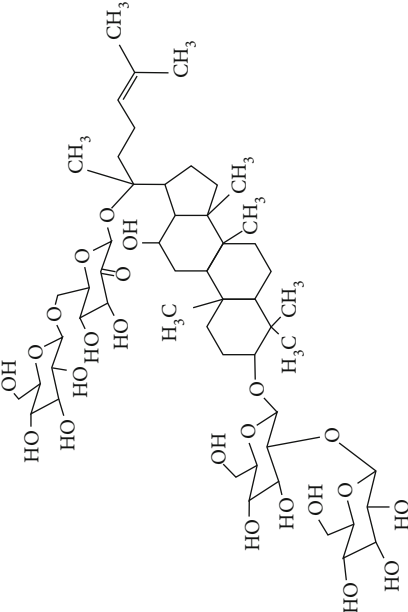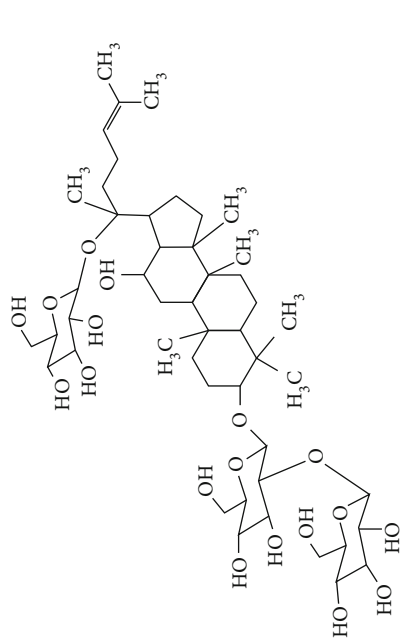
Astaxanthin

Ginsenoside Rb1

Ginsenoside Rg1
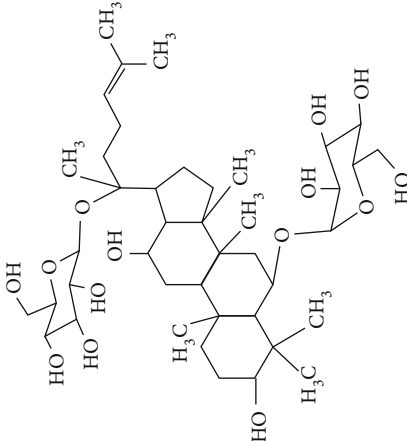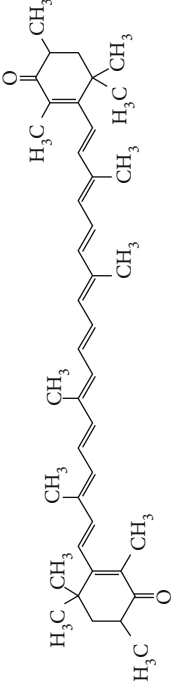
TABLE 7: Continued.

Alkaloids
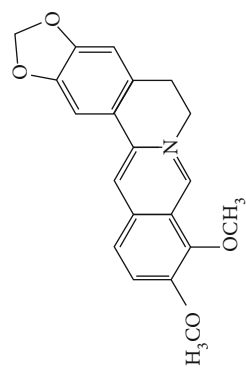
Berberine
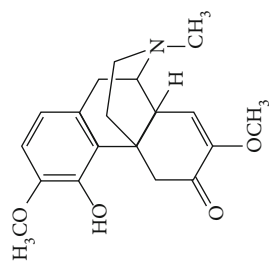
Sinomenine
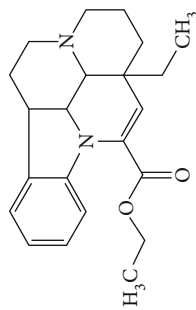
Vinpocetine
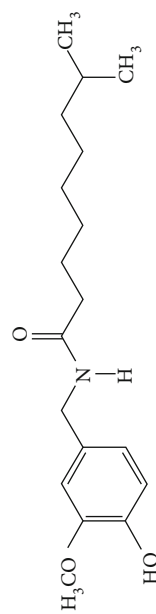
Capsaicin

Dihydrocapsaicin

medicine to restore consciousness after stroke, coma, or other brain injuries for more than 1500 years [309]. There are three types of borneols naturally existing in the herbs: (−)-borneol, (+)-borneol, and isoborneol. Dong et al. compared the neuroprotective effect of these three borneols in pMCAO rats, finding that (−)-borneol possessed the strongest protective efficacy in reducing cerebral infarction, neurological deficits, and brain edema. The mechanism of (−)-borneol included antiapoptosis, anti-inflammation, and protection of the neurovascular units [289]. Notably, the most attractive property of borneol was its strong BBB permeability. Hereby, borneol was usually used as an "assistant" drug in traditional Chinese medicine to deliver neuroprotective medications into the brain, enhancing their therapeutic efficacy [310]. Notably, (+)-borneol possessed synergistic effects with edaravone. It was found that (+)-borneol enhanced the neuroprotective efficacy of edaravone, promoted edaravone-mediated long-term recovery, and extended its therapeutic window in the MCAO model [290]. Accordingly, a sublingual tablet consisting of edaravone and borneol was subjected to a phase I clinical trial to test its safety, tolerability, and pharmacokinetics (NCT03495206). Recently, the edaravone and dexborneol concentrated solution for injection (approval number H20200007), developed by Simcere Pharmacological Company, was approved in China in 2020. Hence, borneol has great potential to be used as an upper ushering drug in ischemic stroke.

Carvacrol is one of the major ingredients in the essential oil of oregano and thyme and is widely used as a food additive. Studies showed that it was lipophilic and able to cross BBB [311]. Carvacrol was found to reduce cerebral infarction and neurological deficits in MCAO models [46, 291–293]. Neuroprotective strategies of carvacrol involved anti-inflammation via inhibition of NF-κB and antiapoptosis via suppression of TRPM7 and promotion of the PI3K/Akt pathway [46, 292]. Besides, carvacrol also improved poststroke learning and memory recovery in the global ischemia gerbil model via antioxidation and inhibition of ferroptosis, a programmed cell death pathway induced by iron ions and ROS [291]. Notably, carvacrol possessed an extended therapeutic window, exerting protective effects even when administrated (i.c.v.) at 6 h after reperfusion [293].

3.4.2. Sesquiterpenoids.
In total, 8 sesquiterpenoids are found to exhibit neuroprotection in ischemic stroke, including alantolactone [312], atractylenolide III [86], bakkenolide IIIa [313], bilobalide [314–317], (−)-α-bisabolol [318], parthenolide [319], patchouli alcohol [320], and β-caryophyllene [321].

The *Ginkgo biloba* leaf extract EGb761, consisting of flavonol glycosides (24%) and terpene lactones (6%), has been reported to exhibit neuroprotection in different CNS disorders such as stroke and Alzheimer's disease [322]. Bilobalide, one of the major bioactive terpenoids in EGb761 (accounting for 3% of EGb761), is widely studied in ischemic stroke. It was found that bilobalide showed neuroprotection in tMCAO/R models regardless of whether it was administrated before or after ischemia [314–317]. The neuroprotective

mechanisms of bilobalide are multiple. It was found that bilobalide restored the energy supply via protection of complex I in mitochondria and reduced the damage induced by energy depletion such as glutamate release, intracellular Ca^{2+} accumulation, and mitochondrial swelling [315, 316]. Besides, bilobalide also possessed antioxidant and anti-inflammatory activities by upregulation of JNK1/2 and p38 [314, 323]. Furthermore, bilobalide promoted angiogenesis and inhibited apoptosis and autophagy via activation of the Akt/eNOS pathway in MCAO/R rats [317]. As for the BBB permeability, it was found that a significant level of bilobalide could be detected in the rat brain after administration of a single dose (8 mg/kg, i.v.), indicating the brain uptake of bilobalide [324].

3.4.3. Diterpenoids.
Neuroprotective diterpenoids include andrographolide [57, 325–328], erinacine A [329], ginkgolide B [38, 72, 330, 331], ginkgolide K [11, 332], pseudopterosin A [333], salvinorin A [334], tanshinone I [335], tanshinone IIA [75, 336–343], totarol [344], triptolide [113, 345, 346], and (1S,2E,4R,6R,-7E,11E)-2,7,11-cembratriene-4,6-diol [347].

Andrographolide is the primary bioactive compound in *Andrographis paniculata*, a traditional Chinese medicine that possesses anti-inflammatory, antiviral, and antibacterial activities [348]. Pharmacodynamic studies have shown that andrographolide could cross the BBB, so it was extensively studied in various CNS disorders such as ischemic stroke, Alzheimer's disease, and multiple sclerosis [349]. Recently, andrographolide was subjected to a phase II clinical trial (NCT02280876) to evaluate its efficacy in multiple sclerosis. For ischemic stroke, andrographolide was reported to reduce cerebral infarction and neurological deficits in both the transient and permanent MCAO models. The neuroprotective strategies of andrographolide mainly involved anti-inflammation via inhibition of NF-κB and HIF-1α, antioxidation via upregulation of Nrf2/HO-1 and suppression of NOX2, and BBB protection [57, 325–327]. Besides, andrographolide also promoted long-term cognitive recovery in a global ischemia model by enhancing the BDNF/TrkB pathway [328]. Notably, andrographolide was able to cross BBB and possessed relatively low toxicity and high bioavailability, as only a single dose of 10 μg/kg (i.v.) was needed to exert neuroprotective activity against tMCAO/R injuries in rats [327]. Hereby, andrographolide might be a great candidate for ischemic stroke treatment.

Ginkgolides, another group of major terpenoids in EGb761, are diterpenoids and have been applied to clinical ischemic stroke treatment in China for a decade. Two intravenous injections that contain ginkgolides as active ingredients are approved as Chinese herbal medicine to treat mild to moderate cerebral infarction in China: ginkgolide injection and ginkgolide meglumine injection. Ginkgolide injection (approval number Z20110035), containing bilobalide, ginkgolide A, ginkgolide B, and ginkgolide C, has been manufactured by Chengdu Baiyu Pharmaceutical Co., Ltd., since 2012. Ginkgolide meglumine injection (GMI, approval number Z20120024), produced by Jiangsu Kanion Pharmaceutical Co., Ltd., excludes bilobalide and only contains ginkgolide A (1.6 mg/mL), ginkgolide B (2.9 mg/mL), and ginkgolide K (0.19 mg/mL) as active

ingredients [350]. Recently, several studies reported the neuroprotective mechanism of GMI in animal models. To illustrate, Geng et al. reported that GMI improved energy metabolism, reduced oxidative stress, and maintained cerebral homeostasis using a metabolomic profiling method [350]. Another study revealed that GMI targeted the PI3K/Akt pathway to activate cytoprotective transcriptional factors such as Nrf2 and CREB [351]. Notably, the neuroprotective efficacy of GMI was found to be as strong as edaravone [351]. Apart from the injections, some pure ginkgolides were also extensively studied in ischemic stroke. For example, ginkgolide B was found to be a natural platelet-activating factor (PAF) receptor antagonist and inhibited the microglial activation via inhibition of the PAF receptor in tMCAO/R mice [72]. Besides, ginkgolide B also possessed multiple neuroprotective strategies including anti-inflammation via suppression of NF-κB, antiapoptosis, antiexcitotoxicity, and BBB protection [38, 330, 331]. In addition, ginkgolide K was also reported to exert neuroprotection in MCAO models. The neuroprotective mechanisms of ginkgolide K involved antioxidation, mitochondrial protection, elevation of autophagy via upregulation of the AMPK/mTOR/ULK1 signaling pathway, and promotion of neurogenesis by activating JAK2/STAT3 [11, 332, 352, 353]. A study compared the neuroprotective efficacy of ginkgolides (A, B, and K) and bilobalide and indicated that ginkgolide B exerted the strongest activities to reduce cerebral infarction and oxidative stress via the promotion of the Akt/Nrf2 pathway [354]. To conclude, ginkgolides and bilobalide have been primarily applied to clinical treatment, showing great potential in ischemic stroke.

Tanshinones are the major components in the root or rhizome of Salvia miltiorrhiza (Danshen), a Chinese medicine that is traditionally used to treat cardiovascular diseases. More than 40 tanshinones were found in the Danshen extract, with tanshinone I and tanshinone IIA being widely studied in the ischemic stroke area [355]. Tanshinone I was found to reduce neuronal death via anti-inflammation in global cerebral ischemic gerbils [335]. Tanshinone IIA was found to improve cerebral infarction and poststroke recovery regardless of administration before or after ischemia. The major mechanisms for tanshinone IIA-mediated neuroprotection were anti-inflammation and antiapoptosis. Anti-inflammatory activity of tanshinone IIA was achieved via suppression of the proinflammatory cytokines HMGB1 and MIF, which then downregulated the MAPKs, upregulated the PPARγ, and inhibited the astrocyte activation [75, 337, 339, 340, 342, 343]. Tanshinone IIA-mediated antiapoptosis was reported to be regulated by activation of the PI3K/Akt pathway [336, 341]. In addition, tanshinone IIA improved neuronal survival and synaptic plasticity by promotion of the BDNF/CREB pathway and elevation of TORC1 (transducers of regulated CREB), a CREB coactivator [338]. Hereby, tanshinone IIA showed marked neuroprotective activity in experimental ischemic stroke. However, tanshinone IIA possessed poor solubility and half-life, limiting its BBB permeability. Accordingly, various methods were developed to enhance its bioavailability. As an example, Liu et al. developed a drug delivery system for tanshinone IIA, called

cationic bovine serum albumin-conjugated tanshinone IIA PEGylated nanoparticles (CBSA-PEG-NPs). They indicated that CBSA-PEG-NPs increased the brain delivery efficiency of tanshinone IIA and thus enhanced its neuroprotective activity in ischemic stroke [339, 340].

Triptolide, a major bioactive diterpenoid in Tripterygium wilfordii, is famous for its anti-inflammatory and immunosuppressive activities. Studies showed that triptolide possessed good neuroprotective efficacy with very low effective doses (single dose of 0.2 mg/kg, i.p.) in tMCAO/R rats [345]. The major neuroprotective strategy of triptolide was anti-inflammation via inhibition of the p38/NF-κB pathway [345, 346]. Besides, triptolide also lowered BBB permeability, suppressed apoptosis, and enhanced autophagy in the MCAO rats [113, 346]. Yet, triptolide exhibited high toxicity on the liver and the heart, limiting its clinical application [356].

3.4.4. Triterpenoids.
Triterpenoids are the most popular group of terpenoids and the major constituents of decoction and the extracts of many medical plants. Triterpenoid saponins, the glycosides of triterpenoids, are an important form of the bioactive triterpenoids. In total, 20 triterpenoids are found to exhibit neuroprotection in ischemic stroke including arjunolic acid [357], asiatic acid [358, 359], boswellic acids [81, 360, 361], 28-O-caffeoyl betulin [362], celastrol [73, 363], echinocystic acid [364], 18β-glycyrrhetinic acid [365], maslinic acid [366], ursolic acid [367], and triterpenoid glycosides: madecassoside [368], astragaloside IV [62, 114, 369, 370], glycyrrhizin [91, 371–373], diammonium glycyrrhizinate [374], ginsenoside Rb1 [34, 55, 115, 375, 376], ginsenoside Rd [49, 377–383], ginsenoside Rg1 [384–389], ginsenoside Rg3 [390], pseudoginsenoside F11 [391, 392], and notoginsenoside R1 [393].

Boswellic acids are present in the gum resin of the herb Boswellia serrata. Several types of boswellic acids are found in B. serrata, and two of them, namely, acetyl-11-keto-β-boswellic acid (AKBA) and 11-keto-β-boswellic acid (KBA), were reported to exert neuroprotection in ischemic stroke [394]. The major neuroprotective strategies of AKBA involved anti-inflammation via inhibition of 5-LOX and promotion of Nrf2/HO-1-mediated antioxidation [81, 360]. Similar to AKBA, the activation of the Nrf2/HO-1 pathway was also observed in KBA-mediated neuroprotection [361]. Yet, boswellic acids were reported to have poor solubility and half-time, largely restricting their pharmacological applications. Efforts were made to develop high-efficiency delivery systems for boswellic acids. For example, Ding et al. reported an AKBA-loaded O-carboxymethyl chitosan nanoparticle system and found that this system enhanced the neuroprotective efficacy of AKBA [81].

Celastrol is another major bioactive terpenoid in the root of Tripterygium wilfordii, in addition to the diterpenoid triptolide. Celastrol exerted neuroprotection in ischemic stroke mainly via its anti-inflammatory activity. It is reported that celastrol promoted the polarization of microglia/macrophages from the proinflammatory M1 phase to the anti-inflammatory M2 phase by decreasing proinflammatory cytokine IL-33 and its corresponding receptor ST2 (growth

stimulation expressed gene 2) in pMCAO rats [73]. Besides, celastrol also inhibited the JNK/NF-κB pathway to suppress the inflammatory cascade in the ischemic brain [363]. The neuroprotective efficacy of celastrol was relatively high, improving cerebral infarction and neurological deficits with low effective doses (1-3 mg/kg, i.p.). Yet, similar to triptolide, celastrol also had high toxicity and poor solubility problems, which limited its pharmacological applications [356].

Astragaloside IV is a saponin abundant in the dry root of *Astragalus membranaceus* (Huangqi), a Chinese herbal medicine that has been used to treat ischemic stroke in China for a long time [395]. Notably, astragaloside IV is usually regarded as a quality control marker of Huangqi. A meta-analysis study revealed that astragaloside IV reduced cerebral infarction, improved neurological impairments, decreased brain edema, and enhanced BBB integrity in experimental ischemic stroke [395]. The neuroprotective mechanisms of astragaloside IV were multiple including antioxidation, antiapoptosis, anti-inflammation, autophagy modulation, and mitochondrial protection [62, 114, 369, 370]. Hexokinase-II (HK-II), an enzyme for glycolysis, inhibited the mPTP opening after binding to mitochondria. Astragaloside IV was found to enhance the activity of HK-II and promote its binding to mitochondria, thus inhibiting mitochondrial dysfunction and mitochondrial apoptosis, as well as improving glycolysis to alleviate energy depletion [369]. Besides, astragaloside IV also activated the Nrf2 pathway to reduce oxidative stress and BBB permeability in an LPS-injured mouse model [62].

Ginseng, the roots of *Panax ginseng*, has been widely used in East Asian countries as a medication for thousands of years. Studies showed that ginsenosides are the major bioactive ingredients that contribute to the numerous therapeutic effects of ginseng. There are more than 180 kinds of ginsenosides extracted from ginseng. Generally, they can be divided into two groups: the protopanaxadiol group, including Rb1, Rb2, Rd, and Rg3, and the protopanaxatriol group, including Rg1, Rf, and Re. Among them, ginsenosides Rb1, Rd, Rg1, and Rg3 were reported to exert neuroprotective activities in ischemic stroke [396].

Ginsenoside Rb1 (GS-Rb1) is the most abundant ginsenoside in ginseng, accounting for about 31% of all ginsenosides in Chinese/Korean ginseng. Wang et al. found that GS-Rb1 improved the abnormal microenvironment of the hippocampus in the photothrombotic cerebral ischemia model, as evidenced by the reduced excitotoxicity, intracellular Ca^{2+} level, and apoptosis, and improved regional cerebral blood flow. The mechanisms for those improvements are reported to be upregulation of GLT-1 and inhibition of NMDA receptors and cytochrome c release [34]. Besides, GS-Rb1 inhibited the NOX4-mediated ROS production and thus reduced BBB permeability due to downregulated MMP-9 activation [55]. Furthermore, GS-Rb1 was found to enhance cytoprotective autophagy, neurogenesis, and BDNF release in MCAO models [115, 376]. Notably, Dong et al. showed that GS-Rb1 also exerted neuroprotective activity in aged mice [375].

Ginsenoside Rd (GS-Rd) has been regarded as one of the important markers for the quality of ginseng. GS-Rd showed marked neuroprotective activity in animal models regardless of preconditioning or postconditioning. Besides, GS-Rd has a relatively wide therapeutic window. Ye et al. found that GS-Rd improved cerebral infarction and neurological outcomes even when administered after 4 h of ischemia in MCAO rats [383]. The neuroprotective mechanisms of GS-Rd were multiple including anti-inflammation, antioxidation, and antimitochondrial apoptosis via inhibition of PARP-1 (poly(ADP-ribose) polymerase 1) [377, 379–382]. Besides, GS-Rd also inhibited DNA damage via upregulation of NEIL1/3 (human endonuclease VIII-like proteins) and reduced intracellular Ca^{2+} accumulation by suppression of TRPM7 and ASIC [49, 378]. Most importantly, GS-Rd could effectively cross the intact BBB and was reported to have much stronger neuroprotective efficacy than edaravone [383]. Hereby, GS-Rd might possess great potential for clinical ischemic stroke treatment. Accordingly, GS-Rd was subjected to clinical trials, including a phase II trial (NCT00591084) and a phase III trial (NCT00815763). In total, 190 ischemic stroke patients in phase II and 390 patients in phase III were recruited. They were intravenously injected with GS-Rd (10, 20 mg) within 72 h after ischemic stroke onset for 14 d [382]. Clinical results showed that GS-Rd improved the NIHSS (National Institutes of Health Stroke Scale) at 15 d, with no significantly elevated mortality or adverse effects [397]. Hence, GS-Rd is one of the most potential drug candidates for ischemic stroke treatment.

Ginsenoside Rg1 (GS-Rg1) accounts for about 23% of all ginseng-derived ginsenosides in Chinese/Korean ginseng. It was indicated that GS-Rg1 possessed equivalent neuroprotective efficacy to GS-Rb1 in tMCAO/R rats [398]. The neuroprotective strategies of GS-Rg1 included anti-inflammation, antiexcitotoxicity, antioxidation via inhibition of miR-144, promotion of angiogenesis via activation of the PI3K/Akt/mTOR pathway, and upregulation of BDNF [384–386, 388]. In addition, GS-Rg1 also protected BBB integrity and reduced brain edema by inhibiting aquaporin-4, a water channel protein highly expressed in the astrocyte foot [387, 389]. Yet, the bioavailability, BBB permeability, and half-time of GS-Rg1 were poor, limiting its clinical application [399].

3.4.5. Tetraterpenoids. In total, 3 tetraterpenoids are reported to be neuroprotective in ischemic stroke, including astaxanthin [120, 400, 401], fucoxanthin [402], and lutein [403]. Notably, they all belong to the xanthophyll type of carotenoids.

Astaxanthin, a well-known antioxidant, exists abundantly in algal species, such as *Haematococcus pluvialis*, and crustaceans. As the only carotenoid that could cross the BBB according to the present studies, astaxanthin has received much attention in ischemic stroke research [404]. It was found that pretreatment with astaxanthin decreased cerebral infarction and neurological deficits in tMCAO/R rats via antioxidation and antiapoptosis [120, 400, 401]. Besides, astaxanthin also promoted neurogenesis and the release of neurotrophins such as BDNF and NGF [120, 401]. Notably, a clinical trial (NCT03945526) was conducted to test the effect of astaxanthin supplementation (2 × 8 mg for

7 d) on plasma MDA levels and neurological deficits of ische-
mic stroke patients.

3.4.6. Summary of Terpenoids. From the present studies, bor-
neol, bilobalide, ginkgolides, and ginsenoside Rd have been
preliminarily applied to clinical ischemic stroke treatment,
and the effectiveness of ginsenoside Rd was further indicated
by the clinical data. Besides, carvacrol, andrographolide, and
astaxanthin were also great candidates for ischemic stroke
treatment due to their high bioavailability and BBB perme-
ability in rodent models. In addition, triptolide and celastrol
showed marked neuroprotective efficacy and high bioavail-
ability in experimental ischemic stroke. Yet, they possessed
high toxicity, limiting their further clinical application. Gen-
erally, terpenoids exhibit strong neuroprotective activity in
experimental ischemic stroke. However, the solubility and
BBB permeability of terpenoids such as tanshinones, boswel-
lic acids, and celastrol are poor. Although several strategies,
such as the development of the nanoparticle delivery systems,
have been tried to solve this limitation, no effective strategies
have been officially approved at present.

3.5. Alkaloids. Alkaloids refer to a class of natural compounds
that have one or more nitrogen atoms in the heterocyclic
ring. Alkaloids can be produced in many species of plants,
especially flowering plants, in the form of organic acids,
esters, or binding with sugars and tannins rather than free
bases. Totally, 19 natural alkaloids were found to exert
neuroprotection after searching the research of the past
10 years, including berberine [74, 92, 405–409], boldine
[410], capsaicin [47, 411], dihydrocapsaicin [44, 412–
414], harmine [35], higenamine [415], neferine [63], nico-
tine [416], levo-tetrahydropalmatine [417], oxymatrine [83,
418], oxysophoridine [419], piperine [420], rhynchophyl-
line [421], sinomenine [87, 422, 423], solasodine [424],
sophoridine [425, 426], tetrandrine [427], trigonelline
[428], and vinpocetine [93, 429]. Their neuroprotective
mechanisms are explained in Table 8, and the chemical
structures of the extensively studied alkaloids are shown
in Table 7.

Berberine is an isoquinoline alkaloid present in the
Chinese medicine *Rhizoma coptidis* (Huanglian). It was
found that berberine could cross the BBB and accumulate
in the brain tissue, so it has been extensively studied in
CNS disorders including ischemic stroke [409]. Berberine
exerted neuroprotection in both the global and transient
cerebral ischemia models via two major mechanisms: anti-
apoptosis and anti-inflammation. The antiapoptosis strat-
egy was mainly achieved by activating the PI3K/Akt
pathway [74, 405, 407]. Yang et al. found that berberine
enhanced the expression of BDNF and its receptor TrkB
to promote the activation of the PI3K/Akt pathway
[407]. Other studies further indicated that berberine could
promote the activity of the PI3K p55γ subunit and
enhance Akt-mediated GSK activation to suppress neuro-
nal apoptosis [405, 408]. As for the anti-inflammatory
strategy, it was found that berberine reduced microglial
and astrocyte activation and enhanced AMPK-dependent
microglial M2 polarization [406, 409]. Besides, the

HMGB1/TLR4 pathway was also involved in inhibiting
the activation of NF-κB and the subsequent inflammatory
cascade [92, 408]. In addition, Zhu et al. also reported the
role of berberine in promoting angiogenesis in tMCAO/R
mice [409]. Hereby, berberine showed marked neuropro-
tection in experimental ischemic stroke and possessed
great potential for clinical application in ischemic stroke.

Capsaicin and dihydrocapsaicin are the main capsaici-
noids that contribute to the pungency of chili peppers.
Capsaicin and dihydrocapsaicin are famous TRPV1 antag-
onists, possessing desensitizing effects on TRPV1 [47].
Hence, capsaicin- and dihydrocapsaicin-mediated neuropro-
tection were mainly attributed to the inhibition of TRPV1.
To illustrate, capsaicin was found to reduce neuronal and
neurovascular damage via inhibition of TRPV1-induced
excitotoxicity [47, 411]. Besides, inhibition of TRPV1 also
led to hypothermia, a state that has been proved to have neu-
roprotective effects in experimental ischemic stroke [413].
Hereby, dihydrocapsaicin has been shown to possess marked
neuroprotection via pharmacological induction of hypother-
mia in MCAO/R models [44, 413]. It was reported that
dihydrocapsaicin-induced hypothermia protected the ische-
mic brain through multiple mechanisms, including anti-
poptosis via activation of the PI3K/Akt pathway and
promotion of Nrf2-mediated antioxidation and anti-
inflammation [412–414]. Yet, it was indicated that the bio-
availability and half-time of capsaicin and dihydrocapsaicin
were low, limiting their clinical application. Hence,
researchers are searching for the proper delivery system for
capsaicin and dihydrocapsaicin.

Sinomenine is the major bioactive ingredient in the herb
Sinomenium acutum. Sinomenine is known for its immuno-
suppressive activity and has been used to treat rheumatoid
arthritis in China [87]. For neuroprotection, sinomenine
was found to reduce cerebral infarction, neurological deficits,
and brain edema in tMCAO/R rodents via its anti-
inflammatory activity [87, 422, 423]. Qiu et al. reported that
sinomenine upregulated AMPK to inhibit the activation of
the NLRP3 (NOD-like receptor pyrin 3) inflammasome,
an activator for the release of proinflammatory cytokines
[422]. Besides, it was shown that sinomenine also pro-
moted the activation of DRD2 (astrocytic dopamine D2
receptor), an anti-inflammatory factor in astrocytes, and
the expression and nuclear translocation of CRYAB (αB-
crystallin), a heat shock protein that is regulated by
DRD2 [87]. Furthermore, sinomenine inhibited cerebral
I/R-induced acidosis and intracellular Ca^{2+} accumulation
in tMCAO/R rats by suppressing ASIC1a and L-type cal-
cium channels [423, 430]. Notably, sinomenine was able
to cross the BBB as indicated by Wu et al. that $0.11\,\mu g/g$
was accumulated in the rat brain after 0.5 h administration
of sinomenine (10 mg/kg, i.p.) [430].

Vinpocetine is naturally present in the periwinkle plant
and has been investigated at length for its effect against
ischemic stroke. The neuroprotective strategy of vinpoce-
tine in ischemic stroke mainly involved anti-inflammation
via inhibition of the TLR4/MyD88 pathway [93, 429].
Notably, vinpocetine also showed a neuroprotective effect
in a phase II clinical trial (NCT02878772), in which 60

TABLE 8: Neuroprotective alkaloids and their functional mechanisms and targets[e].

Compounds	Mechanisms and targets	Ref.
Alkaloids (19)		
Berberine	Antiapoptosis: BDNF-TrkB-PI3K/Akt↑, PI3K p55γ activity↑, Akt/GSK↑; angiogenesis↑; claudin-5↑; anti-inflammation: microglial and astrocyte activation↓, AMPK-dependent microglial M2 polarization↑, HMGB1/TLR4/NF-κB↓	[74, 92, 405–409]
Boldine	Anti-inflammation	[410]
Capsaicin	Antiexcitotoxicity: TRPV1-dependent inhibition of NMDA receptors↑; neurovascular protection	[47, 411]
Dihydrocapsaicin	Hypothermia: TRPV1↓; PI3K/Akt↑; BBB protection; antioxidation; anti-inflammation	[44, 412–414]
Harmine	GLT-1↑; astrocyte activation↓	[35]
Higenamine	HMGB1↓; PI3K/Akt/Nrf2/HO-1↑	[415]
Neferine	Mitochondrial protection: Nrf2 pathway↑	[63]
Nicotine	Anti-inflammation: microglial proliferation↓, α7nAchR↑	[416]
Levo-tetrahydropalmatine	Antiapoptosis: c-Abl↓	[417]
Oxymatrine	Anti-inflammation: arachidonic acid release↓, 12/15-LOX/p38 MAPK/cPLA2↓; Nrf2/HO-1↑	[83, 418]
Oxysophoridine	Antiapoptosis	[419]
Sophoridine	Antiapoptosis; ASIC1↓; TRAF6↓/Erk1/2↑	[425, 426]
Piperine	Anti-inflammation	[420]
Rhynchophylline	PI3K/Akt/mTOR↑	[421]
Sinomenine	Anti-inflammation: NLRP3 inflammasomes↓, DRD2↑/CRYAB↑/STAT3↓; AMPK↑; acidosis↓: ASIC1a↓	[87, 422, 423]
Solasodine	Antioxidation	[424]
Tetrandrine	GRP78 and HYOU1↓; DJ-1↑	[427]
Trigonelline	Glutathione-mediated myeloperoxidase expression↓	[428]
Vinpocetine	Anti-inflammation: TLR4/MyD88/NF-κB↓	[93, 429]

[e]Notes: ↑: activation or upregulation; ↓: inhibition or downregulation. Abbreviations do not appear in the text. c-Abl: nonreceptor Abelson tyrosine kinase; DJ-1: PARK7, Parkinsonism associated deglycase; GRP78: glucose-regulated protein of 78 kDa; HYOU1: hypoxia upregulated protein 1.

ischemic stroke patients were divided into two groups: half of the patients only received standard treatment, while the other half of the patients received 30 mg/d (i.v. for 14 d) vinpocetine treatment plus standard treatment [431]. Results showed that vinpocetine reduced the secondary infarction enlargement and NF-κB-mediated inflammation and improved poststroke neurological functional recovery [431]. More importantly, vinpocetine had high BBB permeability, greatly enhancing its bioavailability in CNS disorders [431]. Accordingly, vinpocetine might be one of the most promising candidates for ischemic stroke treatment.

In summary, vinpocetine and berberine had high BBB permeability and showed great neuroprotective efficacy in experimental ischemic stroke. Besides, vinpocetine also showed neuroprotective activity in the phase II clinical trial. Hence, vinpocetine and berberine might possess great potential in clinical ischemic stroke treatment. As for capsaicin and dihydrocapsaicin, although they showed good neuroprotective efficacy in experimental ischemic stroke, their poor bioavailability and BBB permeability might limit their further clinical applications.

4. Conclusion

Phytochemicals have been well studied in experimental ischemic stroke due to their marked neuroprotective activities. In this review, we listed 148 phytochemicals that were reported to exhibit neuroprotection in various animal models of ischemic stroke, including flavonoids (46), stilbenoids (7), other phenols (20), terpenoids (56), and alkaloids (19). Notably, several phytochemicals have been primarily applied in clinical ischemic stroke treatment or have shown neuroprotective activities in clinical trials. Those phytochemicals include scutellarin, pinocembrin, puerarin, hydroxysafflor yellow A, salvianolic acids, rosmarinic acid, borneol, bilobalide, ginkgolides, ginsenoside Rd, and vinpocetine. However, the clinical application was mainly carried out in China with purified/concentrated plant extracts or a mixture of several compounds. In addition, many phytochemicals, such as baicalein and baicalin, CBD, carvacrol, andrographolide, astaxanthin, and berberine, showed great neuroprotective efficacy and high BBB permeability and bioavailability in experimental ischemic stroke research. Hence, they also possessed great potential for clinical application. However, other

agents such as naringenin, curcumin, EGCG, capsaicin, dihydrocapsaicin, and tanshinone IIA exhibited marked neuroprotective efficacy in experimental ischemic stroke but had poor solubility and BBB permeability. For those phytochemicals, modification of their chemical structures or development of efficient drug delivery systems is needed to enhance their BBB permeability.

Conflicts of Interest

The authors declare no conflicts of interest.

Acknowledgments

References

[1] G. Chauhan and S. Debette, "Genetic risk factors for ischemic and hemorrhagic stroke," *Current Cardiology Reports*, vol. 18, no. 12, p. 124, 2016.

[2] A. Durukan and T. Tatlisumak, "Acute ischemic stroke: overview of major experimental rodent models, pathophysiology, and therapy of focal cerebral ischemia," *Pharmacology Biochemistry and Behavior*, vol. 87, no. 1, pp. 179–197, 2007.

[3] E. S. Donkor, "Stroke in the Century: A Snapshot of the Burden, Epidemiology, and Quality of Life," *Stroke Research and Treatment*, vol. 2018, Article ID 3238165, 10 pages, 2018.

[4] C. Xing, K. Arai, E. H. Lo, and M. Hommel, "Pathophysiologic cascades in ischemic stroke," *International Journal of Stroke*, vol. 7, no. 5, pp. 378–385, 2012.

[5] E. H. Lo, T. Dalkara, and M. A. Moskowitz, "Mechanisms, challenges and opportunities in stroke," *Nature Reviews Neuroscience*, vol. 4, no. 5, pp. 399–414, 2003.

[6] A. Kunz, U. Dirnagl, and P. Mergenthaler, "Acute pathophysiological processes after ischaemic and traumatic brain injury," *Best Practice & Research. Clinical Anaesthesiology*, vol. 24, no. 4, pp. 495–509, 2010.

[7] M. Y. Wu, G. T. Yiang, W. T. Liao et al., "Current mechanistic concepts in ischemia and reperfusion injury," *Cellular Physiology and Biochemistry*, vol. 46, no. 4, pp. 1650–1667, 2018.

[8] J. Minnerup, B. A. Sutherland, A. M. Buchan, and C. Kleinschnitz, "Neuroprotection for stroke: current status and future perspectives," *International Journal of Molecular Sciences*, vol. 13, no. 12, pp. 11753–11772, 2012.

[9] J. C. Zhang, H. Xu, Y. Yuan et al., "Delayed treatment with green tea polyphenol EGCG promotes neurogenesis after ischemic stroke in adult mice," *Molecular Neurobiology*, vol. 54, no. 5, pp. 3652–3664, 2017.

[10] S. Liu, Y. Cao, M. Qu et al., "Curcumin protects against stroke and increases levels of Notch intracellular domain," *Neurological Research*, vol. 38, no. 6, pp. 553–559, 2016.

[11] M. Chen, W. Zou, M. Chen et al., "Ginkgolide K promotes angiogenesis in a middle cerebral artery occlusion mouse model via activating JAK2/STAT3 pathway," *European Journal of Pharmacology*, vol. 833, pp. 221–229, 2018.

[12] L. Catanese, J. Tarsia, and M. Fisher, "Acute ischemic stroke therapy overview," *Circulation Research*, vol. 120, no. 3, pp. 541–558, 2017.

[13] S. Bansal, K. S. Sangha, and P. Khatri, "Drug treatment of acute ischemic stroke," *American Journal of Cardiovascular Drugs*, vol. 13, no. 1, pp. 57–69, 2013.

[14] M. G. Lansberg, M. J. O'Donnell, P. Khatri et al., "Antithrombotic and thrombolytic therapy for ischemic stroke: antithrombotic therapy and prevention of thrombosis, 9th ed: American College of Chest Physicians evidence-based clinical practice guidelines," *Chest*, vol. 141, no. 2, pp. e601S–e636S, 2012.

[15] N. Kapil, Y. H. Datta, N. Alakbarova et al., "Antiplatelet and anticoagulant therapies for prevention of ischemic stroke," *Clinical and Applied Thrombosis/Hemostasis*, vol. 23, no. 4, pp. 301–318, 2017.

[16] A. Moretti, F. Ferrari, and R. F. Villa, "Neuroprotection for ischaemic stroke: current status and challenges," *Pharmacology & Therapeutics*, vol. 146, pp. 23–34, 2015.

[17] O. Y. Bang, "Neuroprotective strategies for acute ischemic stroke: recent progress and future perspectives," *Precision of Future Medicine*, vol. 1, no. 3, pp. 115–121, 2017.

[18] K. Watanabe, M. Tanaka, S. Yuki, M. Hirai, and Y. Yamamoto, "How is edaravone effective against acute ischemic stroke and amyotrophic lateral sclerosis?," *Journal of Clinical Biochemistry and Nutrition*, vol. 62, no. 1, pp. 20–38, 2018.

[19] S. Kobayashi, S. Fukuma, T. Ikenoue, S. Fukuhara, S. Kobayashi, and on behalf of the Japan Stroke Data Bank, "Effect of edaravone on neurological symptoms in real-world patients with acute ischemic stroke," *Stroke*, vol. 50, no. 7, pp. 1805–1811, 2019.

[20] S. Kono, K. Deguchi, N. Morimoto et al., "Intravenous thrombolysis with neuroprotective therapy by edaravone for ischemic stroke patients older than 80 years of age," *Journal of Stroke and Cerebrovascular Diseases*, vol. 22, no. 7, pp. 1175–1183, 2013.

[21] M. Enomoto, A. Endo, H. Yatsushige, K. Fushimi, and Y. Otomo, "Clinical effects of early edaravone use in acute ischemic stroke patients treated by endovascular reperfusion therapy," *Stroke*, vol. 50, no. 3, pp. 652–658, 2019.

[22] Z. Q. Xu, Y. Zhou, B. Z. Shao, J. J. Zhang, and C. Liu, "A systematic review of neuroprotective efficacy and safety of Dl-3-n-butylphthalide in ischemic stroke," *The American Journal of Chinese Medicine*, vol. 47, no. 3, pp. 507–525, 2019.

[23] S. Wang, F. Ma, L. Huang et al., "Dl-3-n-butylphthalide (NBP): a promising therapeutic agent for ischemic stroke," *CNS & Neurological Disorders Drug Targets*, vol. 17, no. 5, pp. 338–347, 2018.

[24] R. G. Robinson, W. J. Shoemaker, M. Schlumpf, T. Valk, and F. E. Bloom, "Effect of experimental cerebral infarction in rat brain on catecholamines and behaviour," *Nature*, vol. 255, no. 5506, pp. 332–334, 1975.

[25] C. J. Sommer, "Ischemic stroke: experimental models and reality," *Acta Neuropathologica*, vol. 133, no. 2, pp. 245–261, 2017.

[26] M. Gennaro, A. Mattiello, and T. Pizzorusso, "Rodent models of developmental ischemic stroke for translational research: strengths and weaknesses," *Neural Plasticity*, vol. 2019, 16 pages, 2019.

[27] M. Mehra, N. Henninger, J. A. Hirsch, J. Chueh, A. K. Wakhloo, and M. J. Gounis, "Preclinical acute ischemic stroke modeling," *Journal of NeuroInterventional Surgery*, vol. 4, no. 4, pp. 307–313, 2012.

[28] C. Kleinschnitz, F. Fluri, and M. Schuhmann, "Animal models of ischemic stroke and their application in clinical research," *Drug Design, Development and Therapy*, vol. 9, pp. 3445–3454, 2015.

[29] Y. Ma, L. Li, L. Kong et al., "Pinocembrin protects blood-brain barrier function and expands the therapeutic time window for tissue-type plasminogen activator treatment in a rat thromboembolic stroke model," *BioMed Research International*, vol. 2018, Article ID 8943210, 13 pages, 2018.

[30] R. J. Traystman, "Animal models of focal and global cerebral ischemia," *ILAR Journal*, vol. 44, no. 2, pp. 85–95, 2003.

[31] K. P. Doyle, R. P. Simon, and M. P. Stenzel-Poore, "Mechanisms of ischemic brain damage," *Neuropharmacology*, vol. 55, no. 3, pp. 310–318, 2008.

[32] U. Dirnagl, C. Iadecola, and M. A. Moskowitz, "Pathobiology of ischaemic stroke: an integrated view," *Trends in Neurosciences*, vol. 22, no. 9, pp. 391–397, 1999.

[33] W. Krzyzanowska, B. Pomierny, M. Filip, and J. Pera, "Glutamate transporters in brain ischemia: to modulate or not?," *Acta Pharmacologica Sinica*, vol. 35, no. 4, pp. 444–462, 2014.

[34] S. Wang, M. Li, Y. Guo et al., "Effects of Panax notoginseng ginsenoside Rb1 on abnormal hippocampal microenvironment in rats," *Journal of Ethnopharmacology*, vol. 202, pp. 138–146, 2017.

[35] P. Sun, S. Zhang, Y. Li, and L. Wang, "Harmine mediated neuroprotection via evaluation of glutamate transporter 1 in a rat model of global cerebral ischemia," *Neuroscience Letters*, vol. 583, pp. 32–36, 2014.

[36] D. Amantea and G. Bagetta, "Excitatory and inhibitory amino acid neurotransmitters in stroke: from neurotoxicity to ischemic tolerance," *Current Opinion in Pharmacology*, vol. 35, pp. 111–119, 2017.

[37] J. Ding, G. Fu, Y. Zhao et al., "EGCG ameliorates the suppression of long-term potentiation induced by ischemia at the Schaffer collateral-CA1 synapse in the rat," *Cellular and Molecular Neurobiology*, vol. 32, no. 2, pp. 267–277, 2012.

[38] Z. Z. Yang, J. Li, S. X. Li, W. Feng, and H. Wang, "Effect of ginkgolide B on striatal extracellular amino acids in middle cerebral artery occluded rats," *Journal of Ethnopharmacology*, vol. 136, no. 1, pp. 117–122, 2011.

[39] Q. J. Wu and M. Tymianski, "Targeting NMDA receptors in stroke: new hope in neuroprotection," *Molecular Brain*, vol. 11, no. 1, p. 15, 2018.

[40] B. Ballarin and M. Tymianski, "Discovery and development of NA-1 for the treatment of acute ischemic stroke," *Acta Pharmacologica Sinica*, vol. 39, no. 5, pp. 661–668, 2018.

[41] B. Huang, P. Chen, L. Huang et al., "Geniposide attenuates post-ischaemic neurovascular damage via GluN2A/AKT/ERK-dependent mechanism," *Cellular Physiology and Biochemistry*, vol. 43, no. 2, pp. 705–716, 2017.

[42] H. S. Sun, "Role of TRPM7 in cerebral ischaemia and hypoxia," *The Journal of Physiology*, vol. 595, no. 10, pp. 3077–3083, 2017.

[43] C. Guo, Y. Ma, S. Ma et al., "The role of TRPC6 in the neuroprotection of calycosin against cerebral ischemic injury," *Scientific Reports*, vol. 7, no. 1, p. 3039, 2017.

[44] Z. Cao, A. Balasubramanian, S. E. Pedersen, J. Romero, R. G. Pautler, and S. P. Marrelli, "TRPV1-mediated pharmacological hypothermia promotes improved functional recovery following ischemic stroke," *Scientific Reports*, vol. 7, no. 1, article 17685, 2017.

[45] Y. Lin, F. Chen, J. Zhang et al., "Neuroprotective effect of resveratrol on ischemia/reperfusion injury in rats through TRPC6/CREB pathways," *Journal of Molecular Neuroscience*, vol. 50, no. 3, pp. 504–513, 2013.

[46] W. Chen, B. Xu, A. Xiao et al., "TRPM7 inhibitor carvacrol protects brain from neonatal hypoxic-ischemic injury," *Molecular Brain*, vol. 8, no. 1, p. 11, 2015.

[47] N. H. Khatibi, V. Jadhav, S. Charles et al., "Capsaicin pretreatment provides neurovascular protection against neonatal hypoxic-ischemic brain injury in rats," *Acta Neurochirurgica. Supplement*, vol. 111, pp. 225–230, 2011.

[48] S. Vullo and S. Kellenberger, "A molecular view of the function and pharmacology of acid-sensing ion channels," *Pharmacological Research*, vol. 154, article 104166, 2020.

[49] Y. Zhang, L. Zhou, X. Zhang, J. Bai, M. Shi, and G. Zhao, "Ginsenoside-Rd attenuates TRPM7 and ASIC1a but promotes ASIC2a expression in rats after focal cerebral ischemia," *Neurological Sciences*, vol. 33, no. 5, pp. 1125–1131, 2012.

[50] T. H. Sanderson, C. A. Reynolds, R. Kumar, K. Przyklenk, and M. Huttemann, "Molecular mechanisms of ischemia-reperfusion injury in brain: pivotal role of the mitochondrial membrane potential in reactive oxygen species generation," *Molecular Neurobiology*, vol. 47, no. 1, pp. 9–23, 2013.

[51] C. L. Allen and U. Bayraktutan, "Oxidative stress and its role in the pathogenesis of ischaemic stroke," *International Journal of Stroke*, vol. 4, no. 6, pp. 461–470, 2009.

[52] S. E. Lakhan, A. Kirchgessner, D. Tepper, and A. Leonard, "Matrix metalloproteinases and blood-brain barrier disruption in acute ischemic stroke," *Frontiers in Neurology*, vol. 4, p. 32, 2013.

[53] T. Kahles and R. P. Brandes, "NADPH oxidases as therapeutic targets in ischemic stroke," *Cellular and Molecular Life Sciences*, vol. 69, no. 14, pp. 2345–2363, 2012.

[54] Y. Dai, H. Zhang, J. Zhang, and M. Yan, "Isoquercetin attenuates oxidative stress and neuronal apoptosis after ischemia/reperfusion injury via Nrf2-mediated inhibition of the NOX4/ROS/NF-κB pathway," *Chemico-Biological Interactions*, vol. 284, pp. 32–40, 2018.

[55] W. Chen, Y. Guo, W. Yang, P. Zheng, J. Zeng, and W. Tong, "Protective effect of ginsenoside Rb1 on integrity of blood-brain barrier following cerebral ischemia," *Experimental Brain Research*, vol. 233, no. 10, pp. 2823–2831, 2015.

[56] L. Zhai, M. Liu, T. Wang, H. Zhang, S. Li, and Y. Guo, "Picroside II protects the blood-brain barrier by inhibiting the oxidative signaling pathway in cerebral ischemia-reperfusion injury," *PLoS One*, vol. 12, no. 4, article e0174414, 2017.

[57] T. L. Yen, R. J. Chen, T. Jayakumar et al., "Andrographolide stimulates p38 mitogen-activated protein kinase-nuclear factor erythroid-2-related factor 2-heme oxygenase 1 signaling in primary cerebral endothelial cells for definite protection against ischemic stroke in rats," *Translational Research*, vol. 170, pp. 57–72, 2016.

[58] E. Birben, U. M. Sahiner, C. Sackesen, S. Erzurum, and O. Kalayci, "Oxidative stress and antioxidant defense," *World Allergy Organization Journal*, vol. 5, no. 1, pp. 9–19, 2012.

[59] L. Liu, L. M. Locascio, and S. Dore, "Critical role of Nrf2 in experimental ischemic stroke," *Frontiers in Pharmacology*, vol. 10, p. 153, 2019.

[60] L. Zhang, X. Zhang, C. Zhang et al., "Nobiletin promotes antioxidant and anti-inflammatory responses and elicits

protection against ischemic stroke in vivo," *Brain Research*, vol. 1636, pp. 130–141, 2016.

[61] K. Wang, Z. Chen, J. Huang et al., "Naringenin prevents ischaemic stroke damage via anti-apoptotic and anti-oxidant effects," *Clinical and Experimental Pharmacology & Physiology*, vol. 44, no. 8, pp. 862–871, 2017.

[62] H. Li, P. Wang, F. Huang et al., "Astragaloside IV protects blood-brain barrier integrity from LPS-induced disruption *via* activating Nrf2 antioxidant signaling pathway in mice," *Toxicology and Applied Pharmacology*, vol. 340, pp. 58–66, 2018.

[63] C. Wu, J. Chen, R. Yang, F. Duan, S. Li, and X. Chen, "Mitochondrial protective effect of neferine through the modulation of nuclear factor erythroid 2-related factor 2 signalling in ischaemic stroke," *British Journal of Pharmacology*, vol. 176, no. 3, pp. 400–415, 2019.

[64] R. Liu, M.-X. Pan, J.-C. Tang et al., "Role of neuroinflammation in ischemic stroke," *Neuroimmunol Neuroinflamm*, vol. 4, no. 8, pp. 158–166, 2017.

[65] M. Ahmad, N. Dar, Z. Bhat et al., "Inflammation in ischemic stroke: mechanisms, consequences and possible drug targets," *CNS & Neurological Disorders Drug Targets*, vol. 13, no. 8, pp. 1378–1396, 2014.

[66] R. L. Jayaraj, S. Azimullah, R. Beiram, F. Y. Jalal, and G. A. Rosenberg, "Neuroinflammation: friend and foe for ischemic stroke," *Journal of Neuroinflammation*, vol. 16, no. 1, p. 142, 2019.

[67] M. Fang, Y. Yuan, P. Rangarajan et al., "Scutellarin regulates microglia-mediated TNC1 astrocytic reaction and astrogliosis in cerebral ischemia in the adult rats," *BMC Neuroscience*, vol. 16, no. 1, p. 84, 2015.

[68] C. C. Leonardo, M. Agrawal, N. Singh, J. R. Moore, S. Biswal, and S. Dore, "Oral administration of the flavanol (-)-epicatechin bolsters endogenous protection against focal ischemia through the Nrf2 cytoprotective pathway," *The European Journal of Neuroscience*, vol. 38, no. 11, pp. 3659–3668, 2013.

[69] M. Gelderblom, F. Leypoldt, J. Lewerenz et al., "The flavonoid fisetin attenuates postischemic immune cell infiltration, activation and infarct size after transient cerebral middle artery occlusion in mice," *Journal of Cerebral Blood Flow and Metabolism*, vol. 32, no. 5, pp. 835–843, 2012.

[70] Y. Wang, Q. Ren, X. Zhang, H. Lu, and J. Chen, "Neuroprotective mechanisms of calycosin against focal cerebral ischemia and reperfusion injury in rats," *Cellular Physiology and Biochemistry*, vol. 45, no. 2, pp. 537–546, 2018.

[71] X. Liu, S. Wen, F. Yan et al., "Salidroside provides neuroprotection by modulating microglial polarization after cerebral ischemia," *Journal of Neuroinflammation*, vol. 15, no. 1, p. 39, 2018.

[72] Z. M. Shu, X. D. Shu, H. Q. Li et al., "Ginkgolide B protects against ischemic stroke via modulating microglia polarization in mice," *CNS Neuroscience & Therapeutics*, vol. 22, no. 9, pp. 729–739, 2016.

[73] M. Jiang, X. Liu, D. Zhang et al., "Celastrol treatment protects against acute ischemic stroke-induced brain injury by promoting an IL-33/ST2 axis-mediated microglia/macrophage M2 polarization," *Journal of Neuroinflammation*, vol. 15, no. 1, p. 78, 2018.

[74] M. Kim, M. S. Shin, J. M. Lee et al., "Inhibitory effects of isoquinoline alkaloid berberine on ischemia-induced apoptosis via activation of phosphoinositide 3-kinase/protein kinase B

[75] L. Zhou, S. C. Bondy, L. Jian et al., "Tanshinone IIA attenuates the cerebral ischemic injury-induced increase in levels of GFAP and of caspases-3 and -8," *Neuroscience*, vol. 288, pp. 105–111, 2015.

[76] C. Rink and S. Khanna, "Significance of brain tissue oxygenation and the arachidonic acid cascade in stroke," *Antioxidants & Redox Signaling*, vol. 14, no. 10, pp. 1889–1903, 2011.

[77] S. K. Ha, P. Lee, J. A. Park et al., "Apigenin inhibits the production of NO and PGE$_2$ in microglia and inhibits neuronal cell death in a middle cerebral artery occlusion-induced focal ischemia mice model," *Neurochemistry International*, vol. 52, no. 4-5, pp. 878–886, 2008.

[78] Y. Yao, L. Chen, J. Xiao et al., "Chrysin protects against focal cerebral ischemia/reperfusion injury in mice through attenuation of oxidative stress and inflammation," *International Journal of Molecular Sciences*, vol. 15, no. 11, pp. 20913–20926, 2014.

[79] T. Wang, L. Zhai, H. Zhang, L. Zhao, and Y. Guo, "Picroside II inhibits the MEK-ERK1/2-COX2 signal pathway to prevent cerebral ischemic injury in rats," *Journal of Molecular Neuroscience*, vol. 57, no. 3, pp. 335–351, 2015.

[80] G. Liang, B. Shi, W. Luo, and J. Yang, "The protective effect of caffeic acid on global cerebral ischemia-reperfusion injury in rats," *Behavioral and Brain Functions*, vol. 11, no. 1, p. 18, 2015.

[81] Y. Ding, Y. Qiao, M. Wang et al., "Enhanced neuroprotection of Acetyl-11-Keto-β-Boswellic acid (AKBA)-loaded O-carboxymethyl chitosan nanoparticles through antioxidant and anti-inflammatory pathways," *Molecular Neurobiology*, vol. 53, no. 6, pp. 3842–3853, 2016.

[82] L. Cui, X. Zhang, R. Yang et al., "Baicalein is neuroprotective in rat MCAO model: role of 12/15-lipoxygenase, mitogen-activated protein kinase and cytosolic phospholipase A2," *Pharmacology, Biochemistry, and Behavior*, vol. 96, no. 4, pp. 469–475, 2010.

[83] L. Cui, X. Zhang, R. Yang et al., "Neuroprotection and underlying mechanisms of oxymatrine in cerebral ischemia of rats," *Neurological Research*, vol. 33, no. 3, pp. 319–324, 2011.

[84] J. Yi, S. Park, R. Kapadia, and R. Vemuganti, "Role of transcription factors in mediating post-ischemic cerebral inflammation and brain damage," *Neurochemistry International*, vol. 50, no. 7-8, pp. 1014–1027, 2007.

[85] X. Bai, X. Zhang, L. Chen et al., "Protective effect of naringenin in experimental ischemic stroke: down-regulated NOD2, RIP2, NF-κB, MMP-9 and up-regulated claudin-5 expression," *Neurochemical Research*, vol. 39, no. 8, pp. 1405–1415, 2014.

[86] K. Zhou, J. Chen, J. Wu et al., "Atractylenolide III ameliorates cerebral ischemic injury and neuroinflammation associated with inhibiting JAK2/STAT3/Drp1-dependent mitochondrial fission in microglia," *Phytomedicine*, vol. 59, p. 152922, 2019.

[87] J. Qiu, Z. Yan, K. Tao et al., "Sinomenine activates astrocytic dopamine D2 receptors and alleviates neuroinflammatory injury via the CRYAB/STAT3 pathway after ischemic stroke in mice," *Journal of Neuroinflammation*, vol. 13, no. 1, p. 263, 2016.

[88] J. Pan, J. L. Jin, H. M. Ge et al., "Malibatol A regulates microglia M1/M2 polarization in experimental stroke in a PPARγ-

dependent manner," *Journal of Neuroinflammation*, vol. 12, no. 1, p. 51, 2015.

[89] D. Xiong, Y. Deng, B. Huang et al., "Icariin attenuates cerebral ischemia-reperfusion injury through inhibition of inflammatory response mediated by NF-κB, PPARα and PPARγ in rats," *International Immunopharmacology*, vol. 30, pp. 157–162, 2016.

[90] Y. Wang, P. Ge, and Y. Zhu, "TLR2 and TLR4 in the brain injury caused by cerebral ischemia and reperfusion," *Mediators of Inflammation*, vol. 2013, Article ID 124614, 8 pages, 2013.

[91] J. Zhang, Y. Wu, Z. Weng, T. Zhou, T. Feng, and Y. Lin, "Glycyrrhizin protects brain against ischemia-reperfusion injury in mice through HMGB1-TLR4-IL-17A signaling pathway," *Brain Research*, vol. 1582, pp. 176–186, 2014.

[92] J. R. Zhu, H. D. Lu, C. Guo et al., "Berberine attenuates ischemia-reperfusion injury through inhibiting HMGB1 release and NF-κB nuclear translocation," *Acta Pharmacologica Sinica*, vol. 39, no. 11, pp. 1706–1715, 2018.

[93] L. R. Wu, L. Liu, X. Y. Xiong et al., "Vinpocetine alleviate cerebral ischemia/reperfusion injury by down-regulating TLR4/MyD88/NF-κB signaling," *Oncotarget*, vol. 8, no. 46, pp. 80315–80324, 2017.

[94] X. K. Tu, W. Z. Yang, S. S. Shi et al., "Baicalin inhibits TLR2/4 signaling pathway in rat brain following permanent cerebral ischemia," *Inflammation*, vol. 34, no. 5, pp. 463–470, 2011.

[95] H. Qiao, X. Zhang, C. Zhu et al., "Luteolin downregulates TLR4, TLR5, NF-κB and p-p38MAPK expression, upregulates the p-ERK expression, and protects rat brains against focal ischemia," *Brain Research*, vol. 1448, pp. 71–81, 2012.

[96] L. Huang, C. Chen, X. Zhang et al., "Neuroprotective effect of curcumin against cerebral ischemia-reperfusion via mediating autophagy and inflammation," *Journal of Molecular Neuroscience*, vol. 64, no. 1, pp. 129–139, 2018.

[97] P. H. Chan, "Mitochondrial dysfunction and oxidative stress as determinants of cell death/survival in stroke," *Annals of the New York Academy of Sciences*, vol. 1042, no. 1, pp. 203–209, 2005.

[98] S. Ramagiri and R. Taliyan, "Neuroprotective effect of hydroxy safflor yellow A against cerebral ischemia-reperfusion injury in rats: putative role of mPTP," *Journal of Basic and Clinical Physiology and Pharmacology*, vol. 27, no. 1, pp. 1–8, 2016.

[99] J. Sun, D. D. Ren, J. Y. Wan et al., "Desensitizing mitochondrial permeability transition by ERK-cyclophilin D axis contributes to the neuroprotective effect of gallic acid against cerebral ischemia/reperfusion injury," *Frontiers in Pharmacology*, vol. 8, p. 184, 2017.

[100] S. Li, T. Wang, L. Zhai et al., "Picroside II exerts a neuroprotective effect by inhibiting mPTP permeability and EndoG release after cerebral ischemia/reperfusion injury in rats," *Journal of Molecular Neuroscience*, vol. 64, no. 1, pp. 144–155, 2018.

[101] S. Li, C. Wu, L. Zhu et al., "By improving regional cortical blood flow, attenuating mitochondrial dysfunction and sequential apoptosis galangin acts as a potential neuroprotective agent after acute ischemic stroke," *Molecules*, vol. 17, no. 11, pp. 13403–13423, 2012.

[102] T. F. Franke, C. P. Hornik, L. Segev, G. A. Shostak, and C. Sugimoto, "PI3K/Akt and apoptosis: size matters," *Oncogene*, vol. 22, no. 56, pp. 8983–8998, 2003.

[103] J. Tao, Y. Cui, Y. Duan, N. Zhang, C. Wang, and F. Zhang, "Puerarin attenuates locomotor and cognitive deficits as well as hippocampal neuronal injury through the PI3K/Akt1/GSK-3β signaling pathway in anin vivomodel of cerebral ischemia," *Oncotarget*, vol. 8, no. 63, pp. 106283–106295, 2017.

[104] C. Wang, Z. Wang, X. Zhang et al., "Protection by silibinin against experimental ischemic stroke: Up-regulated pAkt, pmTOR, HIF-1α and Bcl-2, down-regulated Bax, NF-κB expression, NF-kappaB expression," *Neuroscience Letters. Supplement*, vol. 529, no. 1, pp. 45–50, 2012.

[105] P. Wang, Y. F. Guan, H. du, Q. W. Zhai, D. F. Su, and C. Y. Miao, "Induction of autophagy contributes to the neuroprotection of nicotinamide phosphoribosyltransferase in cerebral ischemia," *Autophagy*, vol. 8, no. 1, pp. 77–87, 2012.

[106] Z. Qi, F. Yan, W. Shi et al., "AKT-related autophagy contributes to the neuroprotective efficacy of hydroxysafflor yellow A against ischemic stroke in rats," *Translational Stroke Research*, vol. 5, no. 4, pp. 501–509, 2014.

[107] S. M. Jin and R. J. Youle, "PINK1- and Parkin-mediated mitophagy at a glance," *Journal of Cell Science*, vol. 125, no. 4, pp. 795–799, 2012.

[108] P. Wang, B. Z. Shao, Z. Deng, S. Chen, Z. Yue, and C. Y. Miao, "Autophagy in ischemic stroke," *Progress in Neurobiology*, vol. 163-164, pp. 98–117, 2018.

[109] S. Yang, H. Wang, Y. Yang et al., "Baicalein administered in the subacute phase ameliorates ischemia-reperfusion-induced brain injury by reducing neuroinflammation and neuronal damage," *Biomedicine & Pharmacotherapy*, vol. 117, article 109102, 2019.

[110] H. Hongyun, G. Tao, Z. Pengyue, Y. Liqiang, and D. Yihao, "Puerarin provides a neuroprotection against transient cerebral ischemia by attenuating autophagy at the ischemic penumbra in neurons but not in astrocytes," *Neuroscience Letters*, vol. 643, pp. 45–51, 2017.

[111] J. Feng, X. Chen, and J. Shen, "Reactive nitrogen species as therapeutic targets for autophagy: implication for ischemic stroke," *Expert Opinion on Therapeutic Targets*, vol. 21, no. 3, pp. 305–317, 2017.

[112] A. Rami, "Review: autophagy in neurodegeneration: firefighter and/or incendiarist?," *Neuropathology and Applied Neurobiology*, vol. 35, no. 5, pp. 449–461, 2009.

[113] Y. Yang, K. Gao, Z. Hu et al., "Autophagy upregulation and apoptosis downregulation in DAHP and triptolide treated cerebral ischemia," *Mediators of Inflammation*, vol. 2015, Article ID 120198, 12 pages, 2015.

[114] Y. Zhang, Y. Zhang, X. F. Jin et al., "The role of astragaloside IV against cerebral ischemia/reperfusion injury: suppression of apoptosis via promotion of P62-LC3-autophagy," *Molecules*, vol. 24, no. 9, p. 1838, 2019.

[115] T. Lu, Y. Jiang, Z. Zhou et al., "Intranasal ginsenoside Rb1 targets the brain and ameliorates cerebral ischemia/reperfusion injury in rats," *Biological & Pharmaceutical Bulletin*, vol. 34, no. 8, pp. 1319–1324, 2011.

[116] S. Cao, S. Shrestha, J. Li et al., "Melatonin-mediated mitophagy protects against early brain injury after subarachnoid hemorrhage through inhibition of NLRP3 inflammasome activation," *Scientific Reports*, vol. 7, no. 1, article 2417, 2017.

[117] N. K. Zenkov, A. V. Chechushkov, P. M. Kozhin, N. V. Kandalintseva, G. G. Martinovich, and E. B. Menshchikova,

"Plant phenols and autophagy," *Biochemistry (Moscow)*, vol. 81, no. 4, pp. 297–314, 2016.

[118] J. Houlton, N. Abumaria, S. F. R. Hinkley, and A. N. Clarkson, "Therapeutic potential of neurotrophins for repair after brain injury: a helping hand from biomaterials," *Frontiers in Neuroscience*, vol. 13, p. 790, 2019.

[119] H. Liu, L. Zhong, Y. Zhang, X. Liu, and J. Li, "Rutin attenuates cerebral ischemia-reperfusion injury in ovariectomized rats via estrogen-receptor-mediated BDNF-TrkB and NGF-TrkA signaling," *Biochemistry and Cell Biology*, vol. 96, no. 5, pp. 672–681, 2018.

[120] L. Pan, Y. Zhou, X. F. Li, Q. J. Wan, and L. H. Yu, "Preventive treatment of astaxanthin provides neuroprotection through suppression of reactive oxygen species and activation of antioxidant defense pathway after stroke in rats," *Brain Research Bulletin*, vol. 130, pp. 211–220, 2017.

[121] D. Wu, "Neuroprotection in experimental stroke with targeted neurotrophins," *NeuroRx*, vol. 2, no. 1, pp. 120–128, 2005.

[122] J. Kim, D. Y. W. Fann, R. C. S. Seet, D. G. Jo, M. P. Mattson, and T. V. Arumugam, "Phytochemicals in ischemic stroke," *Neuromolecular Medicine*, vol. 18, no. 3, pp. 283–305, 2016.

[123] H. S. Chen, S. H. Qi, and J. G. Shen, "One-compound-multi-target: combination prospect of natural compounds with thrombolytic therapy in acute ischemic stroke," *Current Neuropharmacology*, vol. 15, no. 1, pp. 134–156, 2017.

[124] C. Gutierrez-Merino, C. Lopez-Sanchez, R. Lagoa, K. A. Samhan-Arias, C. Bueno, and V. Garcia-Martinez, "Neuroprotective actions of flavonoids," *Current Medicinal Chemistry*, vol. 18, no. 8, pp. 1195–1212, 2011.

[125] F. Tu, Q. Pang, T. Huang, Y. Zhao, M. Liu, and X. Chen, "Apigenin ameliorates post-stroke cognitive deficits in rats through histone acetylation-mediated neurochemical alterations," *Medical Science Monitor*, vol. 23, pp. 4004–4013, 2017.

[126] M. Cai, Y. Ma, W. Zhang et al., "Apigenin-7-O-β-D-(-6″-p-coumaroyl)-Glucopyranoside treatment elicits neuroprotective effect against experimental ischemic stroke," *International Journal of Biological Sciences*, vol. 12, no. 1, pp. 42–52, 2016.

[127] Y. Wang, Y. Zhen, X. Wu et al., "Vitexin protects brain against ischemia/reperfusion injury *via* modulating mitogen-activated protein kinase and apoptosis signaling in mice," *Phytomedicine*, vol. 22, no. 3, pp. 379–384, 2015.

[128] M. Xu, X. Chen, Y. Gu et al., "Baicalin can scavenge peroxynitrite and ameliorate endogenous peroxynitrite- mediated neurotoxicity in cerebral ischemia-reperfusion injury," *Journal of Ethnopharmacology*, vol. 150, no. 1, pp. 116–124, 2013.

[129] X. Xue, X. J. Qu, Y. Yang et al., "Baicalin attenuates focal cerebral ischemic reperfusion injury through inhibition of nuclear factor κB p65 activation," *Biochemical and Biophysical Research Communications*, vol. 403, no. 3-4, pp. 398–404, 2010.

[130] S. Li, X. Sun, L. Xu et al., "Baicalin attenuates in vivo and in vitro hyperglycemia-exacerbated ischemia/reperfusion injury by regulating mitochondrial function in a manner dependent on AMPK," *European Journal of Pharmacology*, vol. 815, pp. 118–126, 2017.

[131] P. Wang, Y. Cao, J. Yu et al., "Baicalin alleviates ischemia-induced memory impairment by inhibiting the phosphoryla-

tion of CaMKII in hippocampus," *Brain Research*, vol. 1642, pp. 95–103, 2016.

[132] A. Sarkaki, Y. Farbood, S. M. T. Mansouri et al., "Chrysin prevents cognitive and hippocampal long-term potentiation deficits and inflammation in rat with cerebral hypoperfusion and reperfusion injury," *Life Sciences*, vol. 226, pp. 202–209, 2019.

[133] M. K. Shooshtari, A. Sarkaki, S. M. T. Mansouri et al., "Protective effects of chrysin against memory impairment, cerebral hyperemia and oxidative stress after cerebral hypoperfusion and reperfusion in rats," *Metabolic Brain Disease*, vol. 35, no. 2, pp. 401–412, 2020.

[134] X. Liu, X. Zhang, J. Zhang et al., "Diosmin protects against cerebral ischemia/reperfusion injury through activating JAK2/STAT3 signal pathway in mice," *Neuroscience*, vol. 268, pp. 318–327, 2014.

[135] B. Xu, X. He, Y. Sui et al., "Ginkgetin aglycone attenuates neuroinflammation and neuronal injury in the rats with ischemic stroke by modulating STAT3/JAK2/SIRT1," *Folia Neuropathologica*, vol. 57, no. 1, pp. 16–23, 2019.

[136] P. An, J. Xie, S. Qiu et al., "Hispidulin exhibits neuroprotective activities against cerebral ischemia reperfusion injury through suppressing NLRP3-mediated pyroptosis," *Life Sciences*, vol. 232, p. 116599, 2019.

[137] H. Qiao, L. Dong, X. Zhang et al., "Protective effect of luteolin in experimental ischemic stroke: upregulated SOD1, CAT, Bcl-2 and claudin-5, down-regulated MDA and Bax expression," *Neurochemical Research*, vol. 37, no. 9, pp. 2014–2024, 2012.

[138] G. Zhao, S. Y. Zang, Z. H. Jiang et al., "Postischemic administration of liposome-encapsulated luteolin prevents against ischemia-reperfusion injury in a rat middle cerebral artery occlusion model," *The Journal of Nutritional Biochemistry*, vol. 22, no. 10, pp. 929–936, 2011.

[139] Q. Li, Z. Tian, M. Wang et al., "Luteoloside attenuates neuroinflammation in focal cerebral ischemia in rats via regulation of the PPARγ/Nrf2/NF-κB signaling pathway," *International Immunopharmacology*, vol. 66, pp. 309–316, 2019.

[140] X. Wang, F. An, S. Wang, Z. An, and S. Wang, "Orientin attenuates cerebral ischemia/reperfusion injury in rat model through the AQP-4 and TLR4/NF-κB/TNF-α signaling pathway," *Journal of Stroke and Cerebrovascular Diseases*, vol. 26, no. 10, pp. 2199–2214, 2017.

[141] Y. Zheng, J. Bu, L. Yu, J. Chen, and H. Liu, "Nobiletin improves propofol-induced neuroprotection via regulating Akt/mTOR and TLR 4/NF-κB signaling in ischemic brain injury in rats," *Biomedicine & Pharmacotherapy*, vol. 91, pp. 494–503, 2017.

[142] N. Yasuda, T. Ishii, D. Oyama et al., "Neuroprotective effect of nobiletin on cerebral ischemia-reperfusion injury in transient middle cerebral artery-occluded rats," *Brain Research*, vol. 1559, pp. 46–54, 2014.

[143] L. Zhang, H. Zhao, X. Zhang et al., "Nobiletin protects against cerebral ischemia via activating the p-Akt, p-CREB, BDNF and Bcl-2 pathway and ameliorating BBB permeability in rat," *Brain Research Bulletin*, vol. 96, pp. 45–53, 2013.

[144] Y. Yuan, H. Zha, P. Rangarajan, E. A. Ling, and C. Wu, "Anti-inflammatory effects of edaravone and scutellarin in activated microglia in experimentally induced ischemia injury in rats and in BV-2 microglia," *BMC Neuroscience*, vol. 15, no. 1, p. 125, 2014.

[145] H. Guo, L. M. Hu, S. X. Wang et al., "Neuroprotective effects of scutellarin against hypoxic-ischemic-induced cerebral injury via augmentation of antioxidant defense capacity," *The Chinese Journal of Physiology*, vol. 54, no. 6, pp. 399–405, 2011.

[146] L. Chai, H. Guo, H. Li et al., "Scutellarin and caffeic acid ester fraction, active components of Dengzhanxixin injection, upregulate neurotrophins synthesis and release in hypoxia/reoxygenation rat astrocytes," *Journal of Ethnopharmacology*, vol. 150, no. 1, pp. 100–107, 2013.

[147] W. Wang, X. Ma, J. Han et al., "Neuroprotective effect of scutellarin on ischemic cerebral injury by down-regulating the expression of angiotensin-converting enzyme and AT1 receptor," *PLoS One*, vol. 11, no. 1, article e0146197, 2016.

[148] W. L. Jiang, Y. Xu, S. P. Zhang, H. B. Zhu, and J. Hou, "Tricin 7-glucoside protects against experimental cerebral ischemia by reduction of NF-κB and HMGB1 expression," *European Journal of Pharmaceutical Sciences*, vol. 45, no. 1-2, pp. 50–57, 2012.

[149] H. Huang, Y. Zhang, R. Yang, and X. Tang, "Determination of baicalin in rat cerebrospinal fluid and blood using microdialysis coupled with ultra-performance liquid chromatography-tandem mass spectrometry," *Journal of Chromatography. B, Analytical Technologies in the Biomedical and Life Sciences*, vol. 874, no. 1-2, pp. 77–83, 2008.

[150] W. Liang, X. Huang, and W. Chen, "The effects of baicalin and baicalein on cerebral ischemia: a review," *Aging and Disease*, vol. 8, no. 6, pp. 850–867, 2017.

[151] S. Wang, H. Wang, H. Guo, L. Kang, X. Gao, and L. Hu, "Neuroprotection of scutellarin is mediated by inhibition of microglial inflammatory activation," *Neuroscience*, vol. 185, pp. 150–160, 2011.

[152] E. . O. Ferreira, M. Y. S. D. Fernandes, N. M. R. . Lima et al., "Neuroinflammatory response to experimental stroke is inhibited by eriodictyol," *Behavioural Brain Research*, vol. 312, pp. 321–332, 2016.

[153] X. Jing, D. Ren, X. Wei et al., "Eriodictyol-7-O-glucoside activates Nrf2 and protects against cerebral ischemic injury," *Toxicology and Applied Pharmacology*, vol. 273, no. 3, pp. 672–679, 2013.

[154] A. Kumar, S. Lalitha, and J. Mishra, "Possible nitric oxide mechanism in the protective effect of hesperidin against pentylenetetrazole (PTZ)-induced kindling and associated cognitive dysfunction in mice," *Epilepsy & Behavior*, vol. 29, no. 1, pp. 103–111, 2013.

[155] S. S. Raza, M. M. Khan, A. Ahmad et al., "Neuroprotective effect of naringenin is mediated through suppression of NF-κB signaling pathway in experimental stroke," *Neuroscience*, vol. 230, pp. 157–171, 2013.

[156] J. Feng, X. Chen, S. Lu et al., "Naringin attenuates cerebral ischemia-reperfusion injury through inhibiting peroxynitrite-mediated mitophagy activation," *Molecular Neurobiology*, vol. 55, no. 12, pp. 9029–9042, 2018.

[157] J. J. Wang and P. Cui, "Neohesperidin attenuates cerebral ischemia-reperfusion injury via inhibiting the apoptotic pathway and activating the Akt/Nrf2/HO-1 pathway," *Journal of Asian Natural Products Research*, vol. 15, no. 9, pp. 1023–1037, 2013.

[158] G. Zhao, W. Zhang, L. Li, S. Wu, and G. Du, "Pinocembrin protects the brain against ischemia-reperfusion injury and reverses the autophagy dysfunction in the penumbra area," *Molecules*, vol. 19, no. 10, pp. 15786–15798, 2014.

[159] S. B. Wang, X. B. Pang, M. Gao, L. H. Fang, and G. H. Du, "Pinocembrin protects rats against cerebral ischemic damage through soluble epoxide hydrolase and epoxyeicosatrienoic acids," *Chinese Journal of Natural Medicines*, vol. 11, no. 3, pp. 207–213, 2013.

[160] F. Meng, Y. Wang, R. Liu, M. Gao, and G. Du, "Pinocembrin alleviates memory impairment in transient global cerebral ischemic rats," *Experimental and Therapeutic Medicine*, vol. 8, no. 4, pp. 1285–1290, 2014.

[161] X. Lan, W. Wang, Q. Li, and J. Wang, "The natural flavonoid pinocembrin: molecular targets and potential therapeutic applications," *Molecular Neurobiology*, vol. 53, no. 3, pp. 1794–1801, 2016.

[162] X. Shen, Y. Liu, X. Luo, and Z. Yang, "Advances in biosynthesis, pharmacology, and pharmacokinetics of pinocembrin, a promising natural small-molecule drug," *Molecules*, vol. 24, no. 12, p. 2323, 2019.

[163] Z. A. Shah, R. C. Li, A. S. Ahmad et al., "The flavanol (-)-epicatechin prevents stroke damage through the Nrf2/HO1 pathway," *Journal of Cerebral Blood Flow & Metabolism*, vol. 30, no. 12, pp. 1951–1961, 2010.

[164] X. Wang and Y. You, "Epigallocatechin gallate extends therapeutic window of recombinant tissue plasminogen activator treatment for brain ischemic stroke: a randomized double-blind and placebo-controlled trial," *Clinical Neuropharmacology*, vol. 40, no. 1, pp. 24–28, 2017.

[165] Y. P. You, "Epigallocatechin gallate extends the therapeutic window of recombinant tissue plasminogen activator treatment in ischemic rats," *Journal of Stroke and Cerebrovascular Diseases*, vol. 25, no. 4, pp. 990–997, 2016.

[166] J. Han, M. Wang, X. Jing, H. Shi, M. Ren, and H. Lou, "(-)-Epigallocatechin gallate protects against cerebral ischemia-induced oxidative stress via Nrf2/ARE signaling," *Neurochemical Research*, vol. 39, no. 7, pp. 1292–1299, 2014.

[167] F. Zhang, N. Li, L. Jiang, L. Chen, and M. Huang, "Neuroprotective effects of (-)-epigallocatechin-3-gallate against focal cerebral ischemia/reperfusion injury in rats through attenuation of inflammation," *Neurochemical Research*, vol. 40, no. 8, pp. 1691–1698, 2015.

[168] W. Nan, X. Zhonghang, C. Keyan, L. Tongtong, G. Wanshu, and X. Zhongxin, "Epigallocatechin-3-gallate reduces neuronal apoptosis in rats after middle cerebral artery occlusion injury via PI3K/Akt/eNOS signaling pathway," *BioMed Research International*, vol. 2018, Article ID 6473580, 9 pages, 2018.

[169] C. Yao, J. Zhang, G. Liu, F. Chen, and Y. Lin, "Neuroprotection by (-)-epigallocatechin-3-gallate in a rat model of stroke is mediated through inhibition of endoplasmic reticulum stress," *Molecular Medicine Reports*, vol. 9, no. 1, pp. 69–72, 2014.

[170] J. W. Park, J. S. Hong, K. S. Lee, H. Y. Kim, J. J. Lee, and S. R. Lee, "Green tea polyphenol (−)-epigallocatechin gallate reduces matrix metalloproteinase-9 activity following transient focal cerebral ischemia," *Journal of Nutritional Biochemistry*, vol. 21, no. 11, pp. 1038–1044, 2010.

[171] S. Wu, Y. Yue, J. Li et al., "Procyanidin B2 attenuates neurological deficits and blood-brain barrier disruption in a rat model of cerebral ischemia," *Molecular Nutrition & Food Research*, vol. 59, no. 10, pp. 1930–1941, 2015.

[172] S. Jin, M. Park, and J. H. Song, "(−)-Epigallocatechin-3-gallate inhibits voltage-gated proton currents in BV2 microglial

cells," *European Journal of Pharmacology*, vol. 698, no. 1-3, pp. 154–160, 2013.

[173] Q. Bai, Z. Lyu, X. Yang, Z. Pan, J. Lou, and T. Dong, "Epigallocatechin-3-gallate promotes angiogenesis via up-regulation of Nfr2 signaling pathway in a mouse model of ischemic stroke," *Behavioural Brain Research*, vol. 321, pp. 79–86, 2017.

[174] B. B. Wei, M. Y. Liu, X. Zhong, W. F. Yao, and M. J. Wei, "Increased BBB permeability contributes to EGCG-caused cognitive function improvement in natural aging rats: pharmacokinetic and distribution analyses," *Acta Pharmacologica Sinica*, vol. 40, no. 11, pp. 1490–1500, 2019.

[175] C. Wu, J. Chen, C. Chen et al., "Wnt/β-catenin coupled with HIF-1α/VEGF signaling pathways involved in galangin neurovascular unit protection from focal cerebral ischemia," *Scientific Reports*, vol. 5, no. 1, article 16151, 2015.

[176] X. Wang, J. Li, L. Qian et al., "Icariin promotes histone acetylation and attenuates post-stroke cognitive impairment in the central cholinergic circuits of mice," *Neuroscience*, vol. 236, pp. 281–288, 2013.

[177] H. R. Zhu, Z. Y. Wang, X. L. Zhu, X. X. Wu, E. G. Li, and Y. Xu, "Icariin protects against brain injury by enhancing SIRT1-dependent PGC-1α Expression in experimental stroke," *Neuropharmacology*, vol. 59, no. 1-2, pp. 70–76, 2010.

[178] L. Yu, C. Chen, L. F. Wang et al., "Neuroprotective effect of kaempferol glycosides against brain injury and neuroinflammation by inhibiting the activation of NF-κB and STAT3 in transient focal stroke," *PLoS One*, vol. 8, no. 2, article e55839, 2013.

[179] S. Wang, H. Xu, Y. Xin et al., "Neuroprotective effects of Kaempferide-7-O-(4″-O-acetylrhamnosyl)-3-O-rutinoside on cerebral ischemia- reperfusion injury in rats," *European Journal of Pharmacology*, vol. 788, pp. 335–342, 2016.

[180] D. J. Park, J. B. Kang, M. A. Shan, and P. O. Koh, "Quercetin alleviates the injury-induced decrease of protein phosphatase 2A subunit B in cerebral ischemic animal model and glutamate-exposed HT22 cells," *Journal of Veterinary Medical Science*, vol. 81, no. 7, pp. 1047–1054, 2019.

[181] D. J. Park, F. A. Shah, and P. O. Koh, "Quercetin attenuates neuronal cells damage in a middle cerebral artery occlusion animal model," *Journal of Veterinary Medical Science*, vol. 80, no. 4, pp. 676–683, 2018.

[182] F. A. Shah, D. J. Park, and P. O. Koh, "Identification of proteins differentially expressed by quercetin treatment in a middle cerebral artery occlusion model: a proteomics approach," *Neurochemical Research*, vol. 43, no. 8, pp. 1608–1623, 2018.

[183] J. W. Jang, J. K. Lee, H. Hur, T. W. Kim, S. P. Joo, and M. S. Piao, "Rutin improves functional outcome via reducing the elevated matrix metalloproteinase-9 level in a photothrombotic focal ischemic model of rats," *Journal of the Neurological Sciences*, vol. 339, no. 1-2, pp. 75–80, 2014.

[184] C. P. Wang, Y. W. Shi, M. Tang et al., "Isoquercetin ameliorates cerebral impairment in focal ischemia through anti-oxidative, anti-inflammatory, and anti-apoptotic effects in primary culture of rat hippocampal neurons and hippocampal CA1 region of rats," *Molecular Neurobiology*, vol. 54, no. 3, pp. 2126–2142, 2017.

[185] J. J. Zhao, J. Q. Song, S. Y. Pan, and K. Wang, "Treatment with isorhamnetin protects the brain against ischemic injury in mice," *Neurochemical Research*, vol. 41, no. 8, pp. 1939–1948, 2016.

[186] L. Sun, P. Xu, T. Fu et al., "Myricetin against ischemic cerebral injury in rat middle cerebral artery occlusion model," *Molecular Medicine Reports*, vol. 17, no. 2, pp. 3274–3280, 2018.

[187] S. Chirumbolo, A. Vella, and G. Bjorklund, "Quercetin might promote autophagy in a middle cerebral artery occlusion-mediated ischemia model: comments on Fawad-Ali Shah et al.," *Neurochemical Research*, vol. 44, no. 2, pp. 297–300, 2019.

[188] R. A. Rifaai, S. A. Mokhemer, E. A. Saber, S. A. A. El-Aleem, and N. F. G. El-Tahawy, "Neuroprotective effect of quercetin nanoparticles: a possible prophylactic and therapeutic role in Alzheimer's disease," *Journal of Chemical Neuroanatomy*, vol. 107, article 101795, 2020.

[189] A. Annapurna, M. A. Ansari, and P. M. Manjunath, "Partial role of multiple pathways in infarct size limiting effect of quercetin and rutin against cerebral ischemia-reperfusion injury in rats," *European Review for Medical and Pharmacological Sciences*, vol. 17, no. 4, pp. 491–500, 2013.

[190] C. C. Hsu, T. W. Kuo, W. P. Liu, C. P. Chang, and H. J. Lin, "Calycosin preserves BDNF/TrkB signaling and reduces post-stroke neurological injury after cerebral ischemia by reducing accumulation of hypertrophic and TNF-α-Containing microglia in rats," *Journal of Neuroimmune Pharmacology*, vol. 15, no. 2, pp. 326–339, 2020.

[191] T. Kuo and C. Chang, "Calycosin may improve outcomes of ischemic stroke in rats by inhibiting activated microglia in brain," *FASEB Journal*, vol. 29, pp. 834–835, 2015.

[192] S. Fu, Y. Gu, J. Q. Jiang et al., "Calycosin-7-O-β-d-glucoside regulates nitric oxide /caveolin-1/matrix metalloproteinases pathway and protects blood-brain barrier integrity in experimental cerebral ischemia-reperfusion injury," *Journal of Ethnopharmacology*, vol. 155, no. 1, pp. 692–701, 2014.

[193] K. Liang, Y. Ye, Y. Wang, J. Zhang, and C. Li, "Formononetin mediates neuroprotection against cerebral ischemia/reperfusion in rats via downregulation of the Bax/Bcl-2 ratio and upregulation PI3K/Akt signaling pathway," *Journal of the Neurological Sciences*, vol. 344, no. 1-2, pp. 100–104, 2014.

[194] A. B. Aras, M. Guven, T. Akman et al., "Genistein exerts neuroprotective effect on focal cerebral ischemia injury in rats," *Inflammation*, vol. 38, no. 3, pp. 1311–1321, 2015.

[195] Y. Qian, T. Guan, M. Huang et al., "Neuroprotection by the soy isoflavone, genistein, via inhibition of mitochondria-dependent apoptosis pathways and reactive oxygen induced-NF-κB activation in a cerebral ischemia mouse model," *Neurochemistry International*, vol. 60, no. 8, pp. 759–767, 2012.

[196] B. Cortina, G. Torregrosa, M. Castello-Ruiz et al., "Improvement of the circulatory function partially accounts for the neuroprotective action of the phytoestrogen genistein in experimental ischemic stroke," *European Journal of Pharmacology*, vol. 708, no. 1-3, pp. 88–94, 2013.

[197] L. Y. Lu, Y. Liu, Y. F. Gong, and X. Y. Zheng, "A preliminary report: genistein attenuates cerebral ischemia injury in ovariectomized rats via regulation of the PI3K-Akt-mTOR pathway," *General Physiology and Biophysics*, vol. 38, no. 5, pp. 389–397, 2019.

[198] Z. Y. Miao, X. Xia, L. Che, and Y. T. Song, "Genistein attenuates brain damage induced by transient cerebral ischemia through up-regulation of Nrf2 expression in ovariectomized rats," *Neurological Research*, vol. 40, no. 8, pp. 689–695, 2018.

[199] S. Wang, H. Wei, M. Cai et al., "Genistein attenuates brain damage induced by transient cerebral ischemia through up-regulation of ERK activity in ovariectomized mice," *International Journal of Biological Sciences*, vol. 10, no. 4, pp. 457–465, 2014.

[200] A. B. Aras, M. Guven, T. Akman et al., "Neuroprotective effects of daidzein on focal cerebral ischemia injury in rats," *Neural Regeneration Research*, vol. 10, no. 1, pp. 146–152, 2015.

[201] Y. Chang, C. Y. Hsieh, Z. A. Peng et al., "Neuroprotective mechanisms of puerarin in middle cerebral artery occlusion-induced brain infarction in rats," *Journal of Biomedical Science*, vol. 16, no. 1, p. 9, 2009.

[202] X. Liu, Z. Mei, J. Qian, Y. Zeng, and M. Wang, "Puerarin partly counteracts the inflammatory response after cerebral ischemia/reperfusion via activating the cholinergic anti-inflammatory pathway," *Neural Regeneration Research*, vol. 8, no. 34, pp. 3203–3215, 2013.

[203] N. Wang, Y. Zhang, L. Wu et al., "Puerarin protected the brain from cerebral ischemia injury via astrocyte apoptosis inhibition," *Neuropharmacology*, vol. 79, pp. 282–289, 2014.

[204] D. A. Schreihofer and A. Oppong-Gyebi, "Genistein: mechanisms of action for a pleiotropic neuroprotective agent in stroke," *Nutritional Neuroscience*, vol. 22, no. 6, pp. 375–391, 2019.

[205] J. M. Stout, A. N. Knapp, W. J. Banz, D. G. Wallace, and J. L. Cheatwood, "Subcutaneous daidzein administration enhances recovery of skilled ladder rung walking performance following stroke in rats," *Behavioural Brain Research*, vol. 256, pp. 428–431, 2013.

[206] Y. Ma, J. C. Sullivan, and D. A. Schreihofer, "Dietary genistein and equol (4′, 7 isoflavandiol) reduce oxidative stress and protect rats against focal cerebral ischemia," *American Journal of Physiology. Regulatory, Integrative and Comparative Physiology*, vol. 299, no. 3, pp. R871–R877, 2010.

[207] A. Kloska, M. Narajczyk, J. Jakóbkiewicz-Banecka et al., "Synthetic genistein derivatives as modulators of glycosaminoglycan storage," *Journal of Translational Medicine*, vol. 10, no. 1, p. 153, 2012.

[208] B. X. Xiao, L. Feng, F. R. Cao et al., "Pharmacokinetic profiles of the five isoflavonoids from Pueraria lobata roots in the CSF and plasma of rats," *Journal of Ethnopharmacology*, vol. 184, pp. 22–29, 2016.

[209] M. Yuan, G. Liu, X. Zheng et al., "Effects of puerarin combined with conventional therapy on ischemic stroke," *Experimental and Therapeutic Medicine*, vol. 14, no. 4, pp. 2943–2946, 2017.

[210] Q. H. Zheng, X. L. Li, Z. G. Mei et al., "Efficacy and safety of puerarin injection in curing acute ischemic stroke: a meta-analysis of randomized controlled trials," *Medicine*, vol. 96, no. 1, article e5803, 2017.

[211] J. Min, S. W. Yu, S. H. Baek et al., "Neuroprotective effect of cyanidin-3-_O_-glucoside anthocyanin in mice with focal cerebral ischemia," *Neuroscience Letters*, vol. 500, no. 3, pp. 157–161, 2011.

[212] Y. Lv, Y. Qian, L. Fu, X. Chen, H. Zhong, and X. Wei, "Hydroxysafflor yellow A exerts neuroprotective effects in cerebral ischemia reperfusion-injured mice by suppressing the innate immune TLR4-inducing pathway," *European Journal of Pharmacology*, vol. 769, pp. 324–332, 2015.

[213] L. Chen, Y. Xiang, L. Kong et al., "Hydroxysafflor yellow A protects against cerebral ischemia–reperfusion injury by anti-apoptotic effect through PI3K/Akt/GSK3β pathway in rat," *Neurochemical Research*, vol. 38, no. 11, pp. 2268–2275, 2013.

[214] L. Deng, H. Wan, H. Zhou, L. Yu, and Y. He, "Protective effect of hydroxysafflor yellow A alone or in combination with acetylglutamine on cerebral ischemia reperfusion injury in rat: A PET study using ^{18}F-fuorodeoxyglucose," *European Journal of Pharmacology*, vol. 825, pp. 119–132, 2018.

[215] S. Chen, M. Sun, X. Zhao et al., "Neuroprotection of hydroxysafflor yellow A in experimental cerebral ischemia/reperfusion injury via metabolic inhibition of phenylalanine and mitochondrial biogenesis," *Molecular Medicine Reports*, vol. 19, no. 4, pp. 3009–3020, 2019.

[216] T. Yen, C. Hsu, W. Lu et al., "Neuroprotective effects of xanthohumol, a prenylated flavonoid from hops (Humulus lupulus), in ischemic stroke of rats," *Journal of Agricultural and Food Chemistry*, vol. 60, no. 8, pp. 1937–1944, 2012.

[217] M. Wang, Y. J. Li, Y. Ding et al., "Silibinin prevents autophagic cell death upon oxidative stress in cortical neurons and cerebral ischemia-reperfusion injury," *Molecular Neurobiology*, vol. 53, no. 2, pp. 932–943, 2016.

[218] S. S. Raza, M. M. Khan, M. Ashafaq et al., "Silymarin protects neurons from oxidative stress associated damages in focal cerebral ischemia: a behavioral, biochemical and immunohistological study in Wistar rats," *Journal of the Neurological Sciences*, vol. 309, no. 1-2, pp. 45–54, 2011.

[219] H. Ao, W. Feng, and C. Peng, "Hydroxysafflor yellow A: a promising therapeutic agent for a broad spectrum of diseases," *Evidence-based Complementary and Alternative Medicine*, vol. 2018, Article ID 8259280, 17 pages, 2018.

[220] X. Wang, Z. Ma, Z. Fu et al., "Hydroxysafflor yellow A protects neurons from excitotoxic death through inhibition of NMDARs," *ASN Neuro*, vol. 8, no. 2, article 175909141664234, 2016.

[221] P. He, "Effect of cerebral ischemia/reperfusion injury on hydroxysafflor yellow A penetrating across the blood-brain barrier," *Scientia Pharmaceutica*, vol. 76, no. 4, pp. 713–723, 2008.

[222] M. Dvorakova and P. Landa, "Anti-inflammatory activity of natural stilbenoids: a review," *Pharmacological Research*, vol. 124, pp. 126–145, 2017.

[223] C. Pang, L. Cao, F. Wu et al., "The effect of _trans_-resveratrol on post-stroke depression via regulation of hypothalamus-pituitary-adrenal axis," *Neuropharmacology*, vol. 97, pp. 447–456, 2015.

[224] H. Yang, A. Zhang, Y. Zhang, S. Ma, and C. Wang, "Resveratrol pretreatment protected against cerebral ischemia/reperfusion injury in rats via expansion of T regulatory cells," *Journal of Stroke and Cerebrovascular Diseases*, vol. 25, no. 8, pp. 1914–1921, 2016.

[225] J. Ren, C. Fan, N. Chen, J. Huang, and Q. Yang, "Resveratrol pretreatment attenuates cerebral ischemic injury by upregulating expression of transcription factor Nrf2 and HO-1 in rats," *Neurochemical Research*, vol. 36, no. 12, pp. 2352–2362, 2011.

[226] Z. Li, L. Pang, F. Fang et al., "Resveratrol attenuates brain damage in a rat model of focal cerebral ischemia via up-regulation of hippocampal Bcl-2," *Brain Research*, vol. 1450, pp. 116–124, 2012.

[227] H. Wei, S. Wang, L. Zhen et al., "Resveratrol attenuates the blood-brain barrier dysfunction by regulation of the MMP-9/TIMP-1 balance after cerebral ischemia reperfusion in rats," *Journal of Molecular Neuroscience*, vol. 55, no. 4, pp. 872–879, 2015.

[228] K. B. Koronowski, N. Khoury, I. Saul et al., "Neuronal SIRT1 (silent information regulator 2 homologue 1) regulates glycolysis and mediates resveratrol-induced ischemic tolerance," *Stroke*, vol. 48, no. 11, pp. 3117–3125, 2017.

[229] D. Wan, Y. Zhou, K. Wang, Y. Hou, R. Hou, and X. Ye, "Resveratrol provides neuroprotection by inhibiting phosphodiesterases and regulating the cAMP/AMPK/SIRT1 pathway after stroke in rats," *Brain Research Bulletin*, vol. 121, pp. 255–262, 2016.

[230] L. M. Wang, Y. J. Wang, M. Cui et al., "A dietary polyphenol resveratrol acts to provide neuroprotection in recurrent stroke models by regulating AMPK and SIRT1 signaling, thereby reducing energy requirements during ischemia," *The European Journal of Neuroscience*, vol. 37, no. 10, pp. 1669–1681, 2013.

[231] K. B. Koronowski, K. R. Dave, I. Saul et al., "Resveratrol preconditioning induces a novel extended window of ischemic tolerance in the mouse brain," *Stroke*, vol. 46, no. 8, pp. 2293–2298, 2015.

[232] N. Khoury, J. Xu, S. D. Stegelmann et al., "Resveratrol preconditioning induces genomic and metabolic adaptations within the long-term window of cerebral ischemic tolerance leading to bioenergetic efficiency," *Molecular Neurobiology*, vol. 56, no. 6, pp. 4549–4565, 2019.

[233] P. Yu, L. Wang, F. Tang et al., "Resveratrol pretreatment decreases ischemic injury and improves neurological function via sonic hedgehog signaling after stroke in rats," *Molecular Neurobiology*, vol. 54, no. 1, pp. 212–226, 2017.

[234] M. C. Saleh, B. J. Connell, and T. M. Saleh, "Resveratrol preconditioning induces cellular stress proteins and is mediated via NMDA and estrogen receptors," *Neuroscience*, vol. 166, no. 2, pp. 445–454, 2010.

[235] Z. Dou, X. Rong, E. Zhao, L. Zhang, and Y. Lv, "Neuroprotection of resveratrol against focal cerebral ischemia/reperfusion injury in mice through a mechanism targeting gut-brain axis," *Cellular and Molecular Neurobiology*, vol. 39, no. 6, pp. 883–898, 2019.

[236] Y. Gao, T. Chen, X. Lei et al., "Neuroprotective effects of polydatin against mitochondrial-dependent apoptosis in the rat cerebral cortex following ischemia/reperfusion injury," *Molecular Medicine Reports*, vol. 14, no. 6, pp. 5481–5488, 2016.

[237] H. Ji, X. Zhang, Y. Du, H. Liu, S. Li, and L. Li, "Polydatin modulates inflammation by decreasing NF-κB activation and oxidative stress by increasing Gli1, Ptch1, SOD1 expression and ameliorates blood-brain barrier permeability for its neuroprotective effect in pMCAO rat brain," *Brain Research Bulletin*, vol. 87, no. 1, pp. 50–59, 2012.

[238] W. Yang, X. Chen, J. Pan et al., "Malibatol A protects against brain injury through reversing mitochondrial dysfunction in experimental stroke," *Neurochemistry International*, vol. 80, pp. 33–40, 2015.

[239] S. A. Andrabi, M. G. Spina, P. Lorenz, U. Ebmeyer, G. Wolf, and T. F. Horn, "Oxyresveratrol (trans-2,3′,4,5′-tetrahydroxystilbene) is neuroprotective and inhibits the apoptotic cell death in transient cerebral ischemia," *Brain Research*, vol. 1017, no. 1-2, pp. 98–107, 2004.

[240] C. P. Wang, L. Z. Zhang, G. C. Li et al., "Mulberroside A protects against ischemic impairment in primary culture of rat cortical neurons after oxygen-glucose deprivation followed by reperfusion," *Journal of Neuroscience Research*, vol. 92, no. 7, pp. 944–954, 2014.

[241] Y. Zhou, X. M. Zhang, A. Ma et al., "Orally administrated pterostilbene attenuates acute cerebral ischemia-reperfusion injury in a dose- and time-dependent manner in mice," *Pharmacology, Biochemistry, and Behavior*, vol. 135, pp. 199–209, 2015.

[242] Y. Mu, Z. Xu, X. Zhou et al., "2,3,5,4'-Tetrahydroxystilbene-2-O-β-D-Glucoside attenuates ischemia/reperfusion-induced brain injury in rats by promoting angiogenesis," *Planta Medica*, vol. 83, no. 8, pp. 676–683, 2017.

[243] N. Nakamichi, R. Fukumori, T. Takarada et al., "Preferential inhibition by antidiarrheic 2-methoxy-4-methylphenol of Ca(2+) influx across acquired N-methyl-D-aspartate receptor channels composed of NR1/NR2B subunit assembly," *Journal of Neuroscience Research*, vol. 88, no. 11, pp. 2483–2493, 2010.

[244] C. J. Xie, A. P. Gu, J. Cai, Y. Wu, and R. C. Chen, "Curcumin protects neural cells against ischemic injury in N2a cells and mouse brain with ischemic stroke," *Brain and Behavior: A Cognitive Neuroscience Perspective*, vol. 8, no. 2, article e00921, 2018.

[245] S. Altinay, M. Cabalar, C. Isler et al., "Is chronic curcumin supplementation neuroprotective against ischemia for antioxidant activity, neurological deficit, or neuronal apoptosis in an experimental stroke model?," *Turkish Neurosurgery*, vol. 27, no. 4, pp. 537–545, 2017.

[246] Y. Miao, S. Zhao, Y. Gao et al., "Curcumin pretreatment attenuates inflammation and mitochondrial dysfunction in experimental stroke: the possible role of Sirt1 signaling," *Brain Research Bulletin*, vol. 121, pp. 9–15, 2016.

[247] W. Li, N. C. Suwanwela, and S. Patumraj, "Curcumin by down-regulating NF-kB and elevating Nrf2, reduces brain edema and neurological dysfunction after cerebral I/R," *Microvascular Research*, vol. 106, pp. 117–127, 2016.

[248] J. Wu, Q. Li, X. Wang et al., "Neuroprotection by curcumin in ischemic brain injury involves the Akt/Nrf2 pathway," *PLoS One*, vol. 8, no. 3, article e59843, 2013.

[249] M. Xia, Z. Ye, Y. Shi, L. Zhou, and Y. Hua, "Curcumin improves diabetes mellitus associated cerebral infarction by increasing the expression of GLUT1 and GLUT3," *Molecular Medicine Reports*, vol. 17, no. 1, pp. 1963–1969, 2018.

[250] M. Ceprian, L. Jimenez-Sanchez, C. Vargas, L. Barata, W. Hind, and J. Martinez-Orgado, "Cannabidiol reduces brain damage and improves functional recovery in a neonatal rat model of arterial ischemic stroke," *Neuropharmacology*, vol. 116, pp. 151–159, 2017.

[251] S. Khaksar and M. R. Bigdeli, "Intra-cerebral cannabidiol infusion-induced neuroprotection is partly associated with the TNF-α/TNFR1/NF-κB pathway in transient focal cerebral ischaemia," *Brain Injury*, vol. 31, no. 13-14, pp. 1932–1943, 2017.

[252] S. Khaksar and M. R. Bigdeli, "Anti-excitotoxic effects of cannabidiol are partly mediated by enhancement of NCX2 and NCX3 expression in animal model of cerebral ischemia," *European Journal of Pharmacology*, vol. 794, pp. 270–279, 2017.

[253] J. Calahorra, J. Shenk, V. H. Wielenga et al., "Hydroxytyrosol, the major phenolic compound of olive oil, as an acute

therapeutic strategy after ischemic stroke," *Nutrients*, vol. 11, no. 10, p. 2430, 2019.

[254] D. Xia, Z. Zhang, and Y. Zhao, "Acteoside attenuates oxidative stress and neuronal apoptosis in rats with focal cerebral ischemia–reperfusion injury," *Biological & Pharmaceutical Bulletin*, vol. 41, no. 11, pp. 1645–1651, 2018.

[255] J. Ha Park, K. Y. Yoo, I. Hye Kim et al., "Hydroquinone strongly alleviates focal ischemic brain injury via blockage of blood-brain barrier disruption in rats," *Toxicological Sciences*, vol. 154, no. 2, pp. 430–441, 2016.

[256] K. Gao, M. Liu, Y. Ding et al., "A phenolic amide (LyA) isolated from the fruits ofLycium barbarumprotects against cerebral ischemia–reperfusion injury via PKCɛ/Nrf2/HO-1 pathway," *Aging*, vol. 11, no. 24, pp. 12361–12374, 2019.

[257] H. Yu, P. Liu, H. Tang et al., "Oleuropein, a natural extract from plants, offers neuroprotection in focal cerebral ischemia/reperfusion injury in mice," *European Journal of Pharmacology*, vol. 775, pp. 113–119, 2016.

[258] W. Zhang, X. Liu, and Q. Li, "Protective effects of oleuropein against cerebral ischemia/reperfusion by inhibiting neuronal apoptosis," *Medical Science Monitor*, vol. 24, pp. 6587–6598, 2018.

[259] W. Lai, X. Xie, X. Zhang et al., "Inhibition of complement drives increase in early growth response proteins and neuroprotection mediated by salidroside after cerebral ischemia," *Inflammation*, vol. 41, no. 2, pp. 449–463, 2018.

[260] W. Lai, Z. Zheng, X. Zhang et al., "Salidroside-mediated neuroprotection is associated with induction of early growth response genes (Egrs) across a wide therapeutic window," *Neurotoxicity Research*, vol. 28, no. 2, pp. 108–121, 2015.

[261] Y. Wei, H. Hong, X. Zhang et al., "Salidroside inhibits inflammation through PI3K/Akt/HIF signaling after focal cerebral ischemia in rats," *Inflammation*, vol. 40, no. 4, pp. 1297–1309, 2017.

[262] X. Zhang, Q. Du, Y. Yang et al., "Salidroside alleviates ischemic brain injury in mice with ischemic stroke through regulating BDNK mediated PI3K/Akt pathway," *Biochemical Pharmacology*, vol. 156, pp. 99–108, 2018.

[263] X. Zhang, W. Lai, X. Ying et al., "Salidroside reduces inflammation and brain injury after permanent middle cerebral artery occlusion in rats by regulating PI3K/PKB/Nrf2/NFκB signaling rather than complement C3 Activity," *Inflammation*, vol. 42, no. 5, pp. 1830–1842, 2019.

[264] W. Zuo, F. Yan, B. Zhang, X. Hu, and D. Mei, "Salidroside improves brain ischemic injury by activating PI3K/Akt pathway and reduces complications induced by delayed tPA treatment," *European Journal of Pharmacology*, vol. 830, pp. 128–138, 2018.

[265] J. Y. Na, K. Song, J. W. Lee, S. Kim, and J. Kwon, "Pretreatment of 6-shogaol attenuates oxidative stress and inflammation in middle cerebral artery occlusion-induced mice," *European Journal of Pharmacology*, vol. 788, pp. 241–247, 2016.

[266] S. S. Yu, J. Zhao, S. P. Lei, X. M. Lin, L. L. Wang, and Y. Zhao, "4-Hydroxybenzyl alcohol ameliorates cerebral injury in rats by antioxidant action," *Neurochemical Research*, vol. 36, no. 2, pp. 339–346, 2011.

[267] F. He, X. Duan, R. Dai, Y. Li, and Q. Lin, "Protective effect of 4-methoxy benzyl alcohol on the blood-brain barrier after cerebral ischemia reperfusion injury," *Journal of Stroke and Cerebrovascular Diseases*, vol. 26, no. 6, pp. 1258–1265, 2017.

[268] T. Y. Chen, S. H. Tai, E. J. Lee et al., "Cinnamophilin offers prolonged neuroprotection against gray and white matter damage and improves functional and electrophysiological outcomes after transient focal cerebral ischemia," *Critical Care Medicine*, vol. 39, no. 5, pp. 1130–1137, 2011.

[269] Y. Lin, J. C. Zhang, J. Fu et al., "Hyperforin attenuates brain damage induced by transient middle cerebral artery occlusion (MCAO) in rats via inhibition of TRPC6 channels degradation," *Journal of Cerebral Blood Flow and Metabolism*, vol. 33, no. 2, pp. 253–262, 2013.

[270] L. Yaidikar, B. Byna, and S. R. Thakur, "Neuroprotective Effect of Punicalagin against Cerebral Ischemia Reperfusion-induced Oxidative Brain Injury in Rats," *Journal of Stroke and Cerebrovascular Diseases*, vol. 23, no. 10, pp. 2869–2878, 2014.

[271] L. Yaidikar and S. Thakur, "Punicalagin attenuated cerebral ischemia-reperfusion insult via inhibition of proinflammatory cytokines, up-regulation of Bcl-2, down-regulation of Bax, and caspase-3," *Molecular and Cellular Biochemistry*, vol. 402, no. 1-2, pp. 141–148, 2015.

[272] F. D. Pinheiro Fernandes, A. P. Fontenele Menezes, J. C. de Sousa Neves et al., "Caffeic acid protects mice from memory deficits induced by focal cerebral ischemia," *Behavioural Pharmacology*, vol. 25, no. 7, pp. 637–647, 2014.

[273] J. H. Sung, S. A. Gim, and P. O. Koh, "Ferulic acid attenuates the cerebral ischemic injury-induced decrease in peroxiredoxin-2 and thioredoxin expression," *Neuroscience Letters*, vol. 566, pp. 88–92, 2014.

[274] J. Sun, Y. Z. Li, Y. H. Ding et al., "Neuroprotective effects of gallic acid against hypoxia/reoxygenation-induced mitochondrial dysfunctions in vitro and cerebral ischemia/reperfusion injury in vivo," *Brain Research*, vol. 1589, pp. 126–139, 2014.

[275] A. A. Fonteles, C. M. de Souza, J. C. de Sousa Neves et al., "Rosmarinic acid prevents against memory deficits in ischemic mice," *Behavioural Brain Research*, vol. 297, pp. 91–103, 2016.

[276] H. Luan, Z. Kan, Y. Xu, C. Lv, and W. Jiang, "Rosmarinic acid protects against experimental diabetes with cerebral ischemia: relation to inflammation response," *Journal of Neuroinflammation*, vol. 10, no. 1, p. 810, 2013.

[277] S. Q. Feng, N. Aa, J. L. Geng et al., "Pharmacokinetic and metabolomic analyses of the neuroprotective effects of salvianolic acid A in a rat ischemic stroke model," *Acta Pharmacologica Sinica*, vol. 38, no. 11, pp. 1435–1444, 2017.

[278] K. Bavarsad, G. E. Barreto, M. A. Hadjzadeh, and A. Sahebkar, "Protective effects of curcumin against ischemia-reperfusion injury in the nervous system," *Molecular Neurobiology*, vol. 56, no. 2, pp. 1391–1404, 2019.

[279] Y. Li, J. Li, S. Li et al., "Curcumin attenuates glutamate neurotoxicity in the hippocampus by suppression of ER stress-associated TXNIP/NLRP3 inflammasome activation in a manner dependent on AMPK," *Toxicology and Applied Pharmacology*, vol. 286, no. 1, pp. 53–63, 2015.

[280] P. Wicha, J. Tocharus, A. Janyou et al., "Hexahydrocurcumin protects against cerebral ischemia/reperfusion injury, attenuates inflammation, and improves antioxidant defenses in a rat stroke model," *PLoS One*, vol. 12, no. 12, article e0189211, 2017.

[281] J. Fernandez-Ruiz, M. A. Moro, and J. Martinez-Orgado, "Cannabinoids in neurodegenerative disorders and

stroke/brain trauma: from preclinical models to clinical applications," *Neurotherapeutics*, vol. 12, no. 4, pp. 793–806, 2015.

[282] T. J. England, W. H. Hind, N. A. Rasid, and S. E. O'Sullivan, "Cannabinoids in experimental stroke: a systematic review and meta-analysis," *Journal of Cerebral Blood Flow and Metabolism*, vol. 35, no. 3, pp. 348–358, 2015.

[283] F. Calapai, L. Cardia, E. E. Sorbara et al., "Cannabinoids, blood-brain barrier, and brain disposition," *Pharmaceutics*, vol. 12, no. 3, p. 265, 2020.

[284] Z. Zhong, J. Han, J. Zhang, Q. Xiao, J. Hu, and L. Chen, "Pharmacological activities, mechanisms of action, and safety of salidroside in the central nervous system," *Drug Design, Development and Therapy*, vol. Volume 12, pp. 1479–1489, 2018.

[285] F. Fan, L. Yang, R. Li et al., "Salidroside as a potential neuroprotective agent for ischemic stroke: a review of sources, pharmacokinetics, mechanism and safety," *Biomedicine & Pharmacotherapy*, vol. 129, article 110458, 2020.

[286] S. Hou, M. M. Zhao, P. P. Shen, X. P. Liu, Y. Sun, and J. C. Feng, "Neuroprotective effect of salvianolic acids against cerebral ischemia/reperfusion injury," *International Journal of Molecular Sciences*, vol. 17, no. 7, p. 1190, 2016.

[287] P. Zhuang, Y. Wan, S. Geng et al., "Salvianolic acids for injection (SAFI) suppresses inflammatory responses in activated microglia to attenuate brain damage in focal cerebral ischemia," *Journal of Ethnopharmacology*, vol. 198, pp. 194–204, 2017.

[288] Y. Zhang, X. Zhang, L. Cui et al., "Salvianolic acids for injection (SAFI) promotes functional recovery and neurogenesis via sonic hedgehog pathway after stroke in mice," *Neurochemistry International*, vol. 110, pp. 38–48, 2017.

[289] T. Dong, N. Chen, X. Ma et al., "The protective roles of _L-_ borneolum, _D-_ borneolum and synthetic borneol in cerebral ischaemia via modulation of the neurovascular unit," *Biomedicine & Pharmacotherapy*, vol. 102, pp. 874–883, 2018.

[290] H. Y. Wu, Y. Tang, L. Y. Gao et al., "The synergetic effect of edaravone and borneol in the rat model of ischemic stroke," *European Journal of Pharmacology*, vol. 740, pp. 522–531, 2014.

[291] X. Guan, X. Li, X. Yang et al., "The neuroprotective effects of carvacrol on ischemia/reperfusion-induced hippocampal neuronal impairment by ferroptosis mitigation," *Life Sciences*, vol. 235, article 116795, 2019.

[292] Z. Li, C. Hua, X. Pan, X. Fu, and W. Wu, "Carvacrol exerts neuroprotective effects via suppression of the inflammatory response in middle cerebral artery occlusion rats," *Inflammation*, vol. 39, no. 4, pp. 1566–1572, 2016.

[293] H. Yu, Z. L. Zhang, J. Chen et al., "Carvacrol, a food-additive, provides neuroprotection on focal cerebral ischemia/reperfusion injury in mice," *PLoS One*, vol. 7, no. 3, article e33584, 2012.

[294] W. Dong, Y. Xian, W. Yuan et al., "Catalpol stimulates VEGF production via the JAK2/STAT3 pathway to improve angiogenesis in rats' stroke model," *Journal of Ethnopharmacology*, vol. 191, pp. 169–179, 2016.

[295] Y. R. Liu, R. Y. Lei, C. E. Wang et al., "Effects of catalpol on ATPase and amino acids in gerbils with cerebral ischemia/reperfusion injury," *Neurological Sciences*, vol. 35, no. 8, pp. 1229–1233, 2014.

[296] W. L. Jiang, S. P. Zhang, H. B. Zhu, Jian-Hou, and J. W. Tian, "Cornin ameliorates cerebral infarction in rats by antioxidant action and stabilization of mitochondrial function," *Phytotherapy Research*, vol. 24, no. 4, pp. 547–552, 2010.

[297] B. Zhao, L. K. Sun, X. Jiang et al., "Genipin protects against cerebral ischemia-reperfusion injury by regulating the UCP2-SIRT3 signaling pathway," *European Journal of Pharmacology*, vol. 845, pp. 56–64, 2019.

[298] A. M. Sabogal-Guaqueta, R. Posada-Duque, N. C. Cortes, J. D. Arias-Londono, and G. P. Cardona-Gomez, "Changes in the hippocampal and peripheral phospholipid profiles are associated with neurodegeneration hallmarks in a long-term global cerebral ischemia model: attenuation by linalool," *Neuropharmacology*, vol. 135, pp. 555–571, 2018.

[299] O. Ciftci, M. N. Oztanir, and A. Cetin, "Neuroprotective effects of β-Myrcene following global cerebral ischemia/reperfusion-mediated oxidative and neuronal damage in a C57BL/J6 mouse," *Neurochemical Research*, vol. 39, no. 9, pp. 1717–1723, 2014.

[300] R. B. Guo, G. F. Wang, A. P. Zhao, J. Gu, X. L. Sun, and G. Hu, "Paeoniflorin protects against ischemia-induced brain damages in rats via inhibiting MAPKs/NF-κB-Mediated inflammatory responses," *PLoS One*, vol. 7, no. 11, article e49701, 2012.

[301] Y. Zhang, H. Li, M. Huang et al., "Paeoniflorin, a monoterpene glycoside, protects the brain from cerebral ischemic injury via inhibition of apoptosis," *The American Journal of Chinese Medicine*, vol. 43, no. 3, pp. 543–557, 2015.

[302] Y. Zhang, L. Qiao, W. Xu et al., "Paeoniflorin attenuates cerebral ischemia-induced injury by regulating Ca2+/CaMKII/-CREB signaling pathway," *Molecules*, vol. 22, no. 3, p. 359, 2017.

[303] L. Xu, Y. Li, Q. Fu, and S. Ma, "Perillaldehyde attenuates cerebral ischemia-reperfusion injury-triggered overexpression of inflammatory cytokines via modulating Akt/JNK pathway in the rat brain cortex," *Biochemical and Biophysical Research Communications*, vol. 454, no. 1, pp. 65–70, 2014.

[304] R. Tabassum, K. Vaibhav, P. Shrivastava et al., "Perillyl alcohol improves functional and histological outcomes against ischemia-reperfusion injury by attenuation of oxidative stress and repression of COX-2, NOS-2 and NF-κB in middle cerebral artery occlusion rats," *European Journal of Pharmacology*, vol. 747, pp. 190–199, 2015.

[305] M. Khoshnazar, M. R. Bigdeli, S. Parvardeh, and R. Pouriran, "Attenuating effect of α-pinene on neurobehavioural deficit, oxidative damage and inflammatory response following focal ischaemic stroke in rat," *The Journal of Pharmacy and Pharmacology*, vol. 71, no. 11, pp. 1725–1733, 2019.

[306] Q. Li, Z. Li, X. Y. Xu, Y. L. Guo, and F. Du, "Neuroprotective properties of picroside II in a rat model of focal cerebral ischemia," *International Journal of Molecular Sciences*, vol. 11, no. 11, pp. 4580–4590, 2010.

[307] H. Zhang, L. Zhai, T. Wang, S. Li, and Y. Guo, "Picroside II exerts a neuroprotective effect by inhibiting the mitochondria cytochrome c signal pathway following ischemia reperfusion injury in rats," *Journal of Molecular Neuroscience*, vol. 61, no. 2, pp. 267–278, 2017.

[308] H. R. Sadeghnia, H. Shaterzadeh, F. Forouzanfar, and H. Hosseinzadeh, "Neuroprotective effect of safranal, an active ingredient of Crocus sativus, in a rat model of transient cerebral ischemia," *Folia Neuropathologica*, vol. 55, no. 3, pp. 206–213, 2017.

[309] Q. L. Zhang, B. M. Fu, and Z. J. Zhang, "Borneol, a novel agent that improves central nervous system drug delivery by enhancing blood-brain barrier permeability," *Drug Delivery*, vol. 24, no. 1, pp. 1037–1044, 2017.

[310] D. D. Luo, X. Y. Chen, Z. B. Zhang et al., "Different effects of (+)borneol and ()borneol on the pharmacokinetics of osthole in rats following oral administration," *Molecular Medicine Reports*, vol. 15, no. 6, pp. 4239–4246, 2017.

[311] F. M. Sisti, N. A. G. Dos Santos, L. do Amaral, and A. C. Dos Santos, "The neurotrophic-like effect of carvacrol: perspective for axonal and synaptic regeneration," *Neurotoxicity Research*, 2021.

[312] L. Tan, J. Li, Y. Wang, and R. Tan, "Anti-neuroinflammatory effect of alantolactone through the suppression of the NF-κB and MAPK signaling pathways," *Cell*, vol. 8, no. 7, p. 739, 2019.

[313] Q. Jiang, R. P. Li, Y. Tang, Y. Q. Wang, C. Liu, and M. L. Guo, "Bakkenolide-IIIa protects against cerebral damage via inhibiting NF-κB activation," *CNS Neuroscience & Therapeutics*, vol. 21, no. 12, pp. 943–952, 2015.

[314] M. Jiang, J. Li, Q. Peng et al., "Neuroprotective effects of bilobalide on cerebral ischemia and reperfusion injury are associated with inhibition of pro-inflammatory mediator production and down-regulation of JNK1/2 and p38 MAPK activation," *Journal of Neuroinflammation*, vol. 11, no. 1, p. 167, 2014.

[315] D. Lang, C. Kiewert, A. Mdzinarishvili et al., "Neuroprotective effects of bilobalide are accompanied by a reduction of ischemia-induced glutamate release _in vivo_," *Brain Research*, vol. 1425, pp. 155–163, 2011.

[316] T. M. Schwarzkopf, S. Hagl, G. P. Eckert, and J. Klein, "Neuroprotection by bilobalide in ischemia: improvement of mitochondrial function," *Die Pharmazie-An International Journal of Pharmaceutical Sciences*, vol. 68, pp. 584–589, 2013.

[317] Y. Zheng, Z. Wu, F. Yi et al., "By activating Akt/eNOS bilobalide B inhibits autophagy and promotes angiogenesis following focal cerebral ischemia reperfusion," *Cellular Physiology and Biochemistry*, vol. 47, no. 2, pp. 604–616, 2018.

[318] M. Y. D. Fernandes, M. Carmo, A. A. Fonteles et al., "(-)-α-Bisabolol prevents neuronal damage and memory deficits through reduction of proinflammatory markers induced by permanent focal cerebral ischemia in mice," *European Journal of Pharmacology*, vol. 842, pp. 270–280, 2019.

[319] L. Dong, H. Qiao, X. Zhang et al., "Parthenolide Is Neuroprotective in Rat Experimental Stroke Model: Downregulating NF- B, Phospho-p38MAPK, and Caspase-1 and Ameliorating BBB Permeability," *Mediators of Inflammation*, vol. 2013, Article ID 370804, 10 pages, 2013.

[320] L. L. Wei, Y. Chen, Q. Y. Yu, Y. Wang, and G. Liu, "Patchouli alcohol protects against ischemia/reperfusion-induced brain injury _via_ inhibiting neuroinflammation in normal and obese mice," *Brain Research*, vol. 1682, pp. 61–70, 2018.

[321] X. Tian, H. Liu, F. Xiang, L. Xu, and Z. Dong, "β-Caryophyllene protects against ischemic stroke by promoting polarization of microglia toward M2 phenotype via the TLR4 pathway," *Life Sciences*, vol. 237, article 116915, 2019.

[322] Z. Feng, Q. Sun, W. Chen, Y. Bai, D. Hu, and X. Xie, "The neuroprotective mechanisms of ginkgolides and bilobalide in cerebral ischemic injury: a literature review," *Molecular Medicine*, vol. 25, no. 1, p. 57, 2019.

[323] J. Xiang, J. Zhang, X. Cai et al., "Bilobalide protects astrocytes from oxygen and glucose deprivation-induced oxidative injury by upregulating manganese superoxide dismutase," *Phytotherapy Research*, vol. 33, no. 9, pp. 2329–2336, 2019.

[324] V. Madgula, B. Avula, Y. Yu et al., "Intestinal and blood-brain barrier permeability of ginkgolides and Bilobalide:In VitroandIn VivoApproaches," *Planta Medica*, vol. 76, no. 6, pp. 599–606, 2010.

[325] S. J. Chan, W. S. Wong, P. T. Wong, and J. S. Bian, "Neuroprotective effects of andrographolide in a rat model of permanent cerebral ischaemia," *British Journal of Pharmacology*, vol. 161, no. 3, pp. 668–679, 2010.

[326] C. M. Chern, K. T. Liou, Y. H. Wang, J. F. Liao, J. C. Yen, and Y. C. Shen, "Andrographolide inhibits PI3K/AKT-dependent NOX2 and iNOS expression protecting mice against hypoxia/ischemia-induced oxidative brain injury," *Planta Medica*, vol. 77, no. 15, pp. 1669–1679, 2011.

[327] Y. C. Hou, Y. H. Wang, K. T. Liou, and Y. C. Shen, "Neuroprotective effect of andrographolide against ischemic stroke in rats through reducing iNOS and gp91phox/NOX2 expression," *Journal of Chinese Medicine*, vol. 21, pp. 85–98, 2010.

[328] D. P. Wang, H. Yin, Q. Lin et al., "Andrographolide enhances hippocampal BDNF signaling and suppresses neuronal apoptosis, astroglial activation, neuroinflammation, and spatial memory deficits in a rat model of chronic cerebral hypoperfusion," *Naunyn-Schmiedeberg's Archives of Pharmacology*, vol. 392, no. 10, pp. 1277–1284, 2019.

[329] K. F. Lee, J. H. Chen, C. C. Teng et al., "Protective effects of Hericium erinaceus mycelium and its isolated erinacine A against ischemia-injury-induced neuronal cell death via the inhibition of iNOS/p38 MAPK and nitrotyrosine," *International Journal of Molecular Sciences*, vol. 15, no. 9, pp. 15073–15089, 2014.

[330] J. H. Gu, J. B. Ge, M. Li, F. Wu, W. Zhang, and Z. H. Qin, "Inhibition of NF-κB activation is associated with anti-inflammatory and anti- apoptotic effects of Ginkgolide B in a mouse model of cerebral ischemia/reperfusion injury," *European Journal of Pharmaceutical Sciences*, vol. 47, no. 4, pp. 652–660, 2012.

[331] P. Lv, W. Fang, X. Geng, Q. Yang, Y. Li, and L. Sha, "Therapeutic neuroprotective effects of ginkgolide B on cortex and basal ganglia in a rat model of transient focal ischemia," *European Journal of Pharmaceutical Sciences*, vol. 44, no. 3, pp. 235–240, 2011.

[332] S. Ma, H. Yin, L. Chen, H. Liu, M. Zhao, and X. Zhang, "Neuroprotective effect of ginkgolide K against acute ischemic stroke on middle cerebral ischemia occlusion in rats," *Journal of Natural Medicines*, vol. 66, no. 1, pp. 25–31, 2012.

[333] X. Niu, C. Yu, G. Jiang et al., "Pseudopterosin A ameliorates ischaemia-induced brain injury by acting on Akt signalling pathway," *Folia Neuropathologica*, vol. 56, no. 2, pp. 104–111, 2018.

[334] H. Dong, W. Zhou, J. Xin et al., "Salvinorin A moderates postischemic brain injury by preserving endothelial mitochondrial function _via_ AMPK/Mfn2 activation," *Experimental Neurology*, vol. 322, article 113045, 2019.

[335] J. H. Park, O. Park, J. H. Cho et al., "Anti-inflammatory effect of tanshinone I in neuroprotection against cerebral ischemia-reperfusion injury in the gerbil hippocampus," *Neurochemical Research*, vol. 39, no. 7, pp. 1300–1312, 2014.

[336] Y. Chen, X. Wu, S. Yu et al., "Neuroprotective capabilities of tanshinone IIA against cerebral ischemia/reperfusion injury

via anti-apoptotic pathway in rats," *Biological & Pharmaceutical Bulletin*, vol. 35, no. 2, pp. 164–170, 2012.

[337] Y. Chen, X. Wu, S. Yu et al., "Neuroprotection of tanshinone IIA against cerebral ischemia/reperfusion injury through inhibition of macrophage migration inhibitory factor in rats," *PLoS One*, vol. 7, no. 6, article e40165, 2012.

[338] L. Liu, X. Zhang, L. Wang et al., "The neuroprotective effects of tanshinone IIA are associated with induced nuclear translocation of TORC1 and upregulated expression of TORC1, pCREB and BDNF in the acute stage of ischemic stroke," *Brain Research Bulletin*, vol. 82, no. 3-4, pp. 228–233, 2010.

[339] X. Liu, C. An, P. Jin, X. Liu, and L. Wang, "Protective effects of cationic bovine serum albumin-conjugated PEGylated tanshinone IIA nanoparticles on cerebral ischemia," *Biomaterials*, vol. 34, no. 3, pp. 817–830, 2013.

[340] X. Liu, M. Ye, C. An, L. Pan, and L. Ji, "The effect of cationic albumin-conjugated PEGylated tanshinone IIA nanoparticles on neuronal signal pathways and neuroprotection in cerebral ischemia," *Biomaterials*, vol. 34, no. 28, pp. 6893–6905, 2013.

[341] Q. Tang, R. Han, H. Xiao, J. Shen, Q. Luo, and J. Li, "Neuroprotective effects of tanshinone IIA and/or tetramethylpyrazine in cerebral ischemic injury in vivo and in vitro," *Brain Research*, vol. 1488, pp. 81–91, 2012.

[342] J. G. Wang, S. C. Bondy, L. Zhou et al., "Protective effect of tanshinone IIA against infarct size and increased HMGB1, NFκB, GFAP and apoptosis consequent to transient middle cerebral artery occlusion," *Neurochemical Research*, vol. 39, no. 2, pp. 295–304, 2014.

[343] L. Zhou, J. Zhang, C. Wang, and Q. Sun, "Tanshinone inhibits neuronal cell apoptosis and inflammatory response in cerebral infarction rat model," *International Journal of Immunopathology and Pharmacology*, vol. 30, no. 2, pp. 123–129, 2017.

[344] Y. Gao, X. Xu, S. Chang et al., "Totarol prevents neuronal injury in vitro and ameliorates brain ischemic stroke: potential roles of Akt activation and HO-1 induction," *Toxicology and Applied Pharmacology*, vol. 289, no. 2, pp. 142–154, 2015.

[345] S. Bai, Z. Hu, Y. Yang et al., "Anti-inflammatory and neuroprotective effects of triptolide via the NF-κB signaling pathway in a rat MCAO model," *The Anatomical Record*, vol. 299, no. 2, pp. 256–266, 2016.

[346] M. Hao, X. Li, J. Feng, and N. Pan, "Triptolide protects against ischemic stroke in rats," *Inflammation*, vol. 38, no. 4, pp. 1617–1623, 2015.

[347] A. H. Martins, J. Hu, Z. Xu et al., "Neuroprotective activity of (1 _S_ ,2 _E_ ,4 _R_ ,6 _R_ ,-7 _E_ ,11 _E_)-2,7,11-cembratriene-4,6-diol (4R) _in vitro_ and _in vivo_ in rodent models of brain ischemia," *Neuroscience*, vol. 291, pp. 250–259, 2015.

[348] T. Jayakumar, C. Y. Hsieh, J. J. Lee, and J. R. Sheu, "Experimental and clinical pharmacology of Andrographis paniculata and its major bioactive phytoconstituent andrographolide," *Evidence-based Complementary and Alternative Medicine*, vol. 2013, Article ID 846740, 16 pages, 2013.

[349] J. Lu, Y. Ma, J. Wu et al., "A review for the neuroprotective effects of andrographolide in the central nervous system," *Biomedicine & Pharmacotherapy*, vol. 117, article 109078, 2019.

[350] J. L. Geng, J. Y. Aa, S. Q. Feng et al., "Exploring the neuroprotective effects of ginkgolides injection in a rodent model of cerebral ischemia-reperfusion injury by GC-MS based metabolomic profiling," *Journal of Pharmaceutical and Biomedical Analysis*, vol. 142, pp. 190–200, 2017.

[351] W. Zhang, J. K. Song, R. Yan et al., "Diterpene ginkgolides protect against cerebral ischemia/reperfusion damage in rats by activating Nrf2 and CREB through PI3K/Akt signaling," *Acta Pharmacologica Sinica*, vol. 39, no. 8, pp. 1259–1272, 2018.

[352] X. Zhou, H. Y. Wang, B. Wu et al., "Ginkgolide K attenuates neuronal injury after ischemic stroke by inhibiting mitochondrial fission and GSK-3β-dependent increases in mitochondrial membrane permeability," *Oncotarget*, vol. 8, no. 27, pp. 44682–44693, 2017.

[353] Y. Zhang and J. M. Miao, "Ginkgolide K promotes astrocyte proliferation and migration after oxygen- glucose deprivation via inducing protective autophagy through the AMPK/mTOR/ULK1 signaling pathway," *European Journal of Pharmacology*, vol. 832, pp. 96–103, 2018.

[354] Q. Liu, Z. Jin, Z. Xu et al., "Antioxidant effects of ginkgolides and bilobalide against cerebral ischemia injury by activating the Akt/Nrf2 pathway in vitro and in vivo," *Cell Stress & Chaperones*, vol. 24, no. 2, pp. 441–452, 2019.

[355] Z. Jiang, W. Gao, and L. Huang, "Tanshinones, critical pharmacological components in Salvia miltiorrhiza," *Frontiers in Pharmacology*, vol. 10, p. 202, 2019.

[356] S. R. Chen, Y. Dai, J. Zhao, L. Lin, Y. Wang, and Y. Wang, "A mechanistic overview of triptolide and celastrol, natural products from *Tripterygium wilfordii* Hook F," *Frontiers in Pharmacology*, vol. 9, p. 104, 2018.

[357] L. Yaidikar and S. Thakur, "Arjunolic acid, a pentacyclic triterpenoidal saponin of _Terminalia arjuna_ bark protects neurons from oxidative stress associated damage in focal cerebral ischemia and reperfusion," *Pharmacological Reports*, vol. 67, no. 5, pp. 890–895, 2015.

[358] K. Y. Lee, O. N. Bae, K. Serfozo et al., "Asiatic acid attenuates infarct volume, mitochondrial dysfunction, and matrix metalloproteinase-9 induction after focal cerebral ischemia," *Stroke*, vol. 43, no. 6, pp. 1632–1638, 2012.

[359] K. Y. Lee, O. N. Bae, S. Weinstock, M. Kassab, and A. Majid, "Neuroprotective effect of asiatic acid in rat model of focal embolic stroke," *Biological & Pharmaceutical Bulletin*, vol. 37, no. 8, pp. 1397–1401, 2014.

[360] Y. Ding, M. Chen, M. Wang et al., "Neuroprotection by Acetyl-11-Keto-β-Boswellic Acid, in Ischemic Brain Injury Involves the Nrf2/HO-1 defense Pathway," *Scientific Reports*, vol. 4, 2015.

[361] Y. Ding, M. Chen, M. Wang, Y. Li, and A. Wen, "Posttreatment with 11-Keto-β-Boswellic acid ameliorates cerebral ischemia-reperfusion injury: Nrf2/HO-1 pathway as a potential mechanism," *Molecular Neurobiology*, vol. 52, no. 3, pp. 1430–1439, 2015.

[362] Z. Ruan, H. M. Wang, X. T. Huang et al., "A novel caffeoyl triterpene attenuates cerebral ischemic injury with potent anti-inflammatory and hypothermic effects," *Journal of Neurochemistry*, vol. 133, no. 1, pp. 93–103, 2015.

[363] Y. Li, D. He, X. Zhang et al., "Protective effect of celastrol in rat cerebral ischemia model: Down-regulating p-JNK, p-c-Jun and NF-κB," *Brain Research*, vol. 1464, pp. 8–13, 2012.

[364] H. Yu, W. Li, X. Cao et al., "Echinocystic acid, a natural plant extract, alleviates cerebral ischemia/reperfusion injury via inhibiting the JNK signaling pathway," *European Journal of Pharmacology*, vol. 861, article 172610, 2019.

[365] M. N. Oztanir, O. Ciftci, A. Cetin, M. A. Durak, N. Basak, and Y. Akyuva, "The beneficial effects of 18β-glycyrrhetinic acid following oxidative and neuronal damage in brain tissue caused by global cerebral ischemia/reperfusion in a C57BL/J6 mouse model," *Neurological Sciences*, vol. 35, no. 8, pp. 1221–1228, 2014.

[366] Y. Qian, M. Huang, T. Guan et al., "Maslinic acid promotes synaptogenesis and axon growth via Akt/GSK-3β activation in cerebral ischemia model," *European Journal of Pharmacology*, vol. 764, pp. 298–305, 2015.

[367] L. Li, X. Zhang, L. Cui et al., "Ursolic acid promotes the neuroprotection by activating Nrf2 pathway after cerebral ischemia in mice," *Brain Research*, vol. 1497, pp. 32–39, 2013.

[368] Y. Luo, Y. P. Yang, J. Liu et al., "Neuroprotective effects of madecassoside against focal cerebral ischemia reperfusion injury in rats," *Brain Research*, vol. 1565, pp. 37–47, 2014.

[369] Y. Li, Y. Yang, Y. Zhao et al., "Astragaloside IV reduces neuronal apoptosis and parthanatos in ischemic injury by preserving mitochondrial hexokinase-II," *Free Radical Biology & Medicine*, vol. 131, pp. 251–263, 2019.

[370] J. Yang, J. Li, J. Lu, Y. Zhang, Z. Zhu, and H. Wan, "Synergistic protective effect of _astragaloside IV_ - _tetramethylpyrazine_ against cerebral ischemic-reperfusion injury induced by transient focal ischemia," *Journal of Ethnopharmacology*, vol. 140, no. 1, pp. 64–72, 2012.

[371] W. Barakat, N. Safwet, N. N. el-Maraghy, and M. N. Zakaria, "Candesartan and glycyrrhizin ameliorate ischemic brain damage through downregulation of the TLR signaling cascade," *European Journal of Pharmacology*, vol. 724, pp. 43–50, 2014.

[372] G. Gong, L. Xiang, L. Yuan et al., "Protective effect of glycyrrhizin, a direct HMGB1 inhibitor, on focal cerebral ischemia/reperfusion-induced inflammation, oxidative stress, and apoptosis in rats," *PLoS One*, vol. 9, no. 3, article e89450, 2014.

[373] S. W. Kim, Y. Jin, J. H. Shin et al., "Glycyrrhizic acid affords robust neuroprotection in the postischemic brain via anti-inflammatory effect by inhibiting HMGB1 phosphorylation and secretion," *Neurobiology of Disease*, vol. 46, no. 1, pp. 147–156, 2012.

[374] S. Z. Hou, Y. Li, X. L. Zhu, Z. Y. Wang, X. Wang, and Y. Xu, "Ameliorative effects of diammonium glycyrrhizinate on inflammation in focal cerebral ischemic-reperfusion injury," *Brain Research*, vol. 1447, pp. 20–27, 2012.

[375] X. Dong, L. Zheng, S. Lu, and Y. Yang, "Neuroprotective effects of pretreatment of ginsenoside Rb1 on severe cerebral ischemia-induced injuries in aged mice: involvement of antioxidant signaling," *Geriatrics & Gerontology International*, vol. 17, no. 2, pp. 338–345, 2017.

[376] X. Q. Gao, C. X. Yang, G. J. Chen et al., "Ginsenoside Rb1 regulates the expressions of brain-derived neurotrophic factor and caspase-3 and induces neurogenesis in rats with experimental cerebral ischemia," *Journal of Ethnopharmacology*, vol. 132, no. 2, pp. 393–399, 2010.

[377] G. Hu, Z. Wu, F. Yang et al., "Ginsenoside Rd blocks AIF mitochondrio-nuclear translocation and NF-κB nuclear accumulation by inhibiting poly(ADP-ribose) polymerase-1 after focal cerebral ischemia in rats," *Neurological Sciences*, vol. 34, no. 12, pp. 2101–2106, 2013.

[378] L. X. Yang, X. Zhang, and G. Zhao, "Ginsenoside Rd attenuates DNA damage by increasing expression of DNA glycosylase endonuclease VIII-like proteins after focal cerebral ischemia," *Chinese Medical Journal*, vol. 129, no. 16, pp. 1955–1962, 2016.

[379] R. Ye, X. Kong, Q. Yang, Y. Zhang, J. Han, and G. Zhao, "Ginsenoside Rd attenuates redox imbalance and improves stroke outcome after focal cerebral ischemia in aged mice," *Neuropharmacology*, vol. 61, no. 4, pp. 815–824, 2011.

[380] R. Ye, Q. Yang, X. Kong et al., "Ginsenoside Rd attenuates early oxidative damage and sequential inflammatory response after transient focal ischemia in rats," *Neurochemistry International*, vol. 58, no. 3, pp. 391–398, 2011.

[381] R. Ye, X. Zhang, X. Kong et al., "Ginsenoside Rd attenuates mitochondrial dysfunction and sequential apoptosis after transient focal ischemia," *Neuroscience*, vol. 178, pp. 169–180, 2011.

[382] G. Zhang, F. Xia, Y. Zhang et al., "Ginsenoside Rd is efficacious against acute ischemic stroke by suppressing microglial proteasome-mediated inflammation," *Molecular Neurobiology*, vol. 53, no. 4, pp. 2529–2540, 2016.

[383] R. Ye, X. Kong, Q. Yang et al., "Ginsenoside Rd in experimental stroke: superior neuroprotective efficacy with a wide therapeutic window," *Neurotherapeutics*, vol. 8, no. 3, pp. 515–525, 2011.

[384] J. Chen, X. Zhang, X. Liu et al., "Ginsenoside Rg1 promotes cerebral angiogenesis via the PI3K/Akt/mTOR signaling pathway in ischemic mice," *European Journal of Pharmacology*, vol. 856, article 172418, 2019.

[385] S. F. Chu, Z. Zhang, X. Zhou et al., "Ginsenoside Rg1 protects against ischemic/reperfusion-induced neuronal injury through miR-144/Nrf2/ARE pathway," *Acta Pharmacologica Sinica*, vol. 40, no. 1, pp. 13–25, 2019.

[386] L. Wang, H. Zhao, Z. Z. Zhai, and L. X. Qu, "Protective effect and mechanism of ginsenoside Rg1 in cerebral ischaemia-reperfusion injury in mice," *Biomedicine & Pharmacotherapy*, vol. 99, pp. 876–882, 2018.

[387] C. L. Xie, J. H. Li, W. W. Wang, G. Q. Zheng, and L. X. Wang, "Neuroprotective effect of ginsenoside-Rg1 on cerebral ischemia/reperfusion injury in rats by downregulating protease-activated receptor-1 expression," *Life Sciences*, vol. 121, pp. 145–151, 2015.

[388] T. Zheng, H. Jiang, R. Jin et al., "Ginsenoside Rg1 attenuates protein aggregation and inflammatory response following cerebral ischemia and reperfusion injury," *European Journal of Pharmacology*, vol. 853, pp. 65–73, 2019.

[389] Y. Zhou, H. Q. Li, L. Lu et al., "Ginsenoside Rg1 provides neuroprotection against blood brain barrier disruption and neurological injury in a rat model of cerebral ischemia/reperfusion through downregulation of aquaporin 4 expression," *Phytomedicine*, vol. 21, no. 7, pp. 998–1003, 2014.

[390] B. He, P. Chen, J. Yang et al., "Neuroprotective effect of 20(R)-ginsenoside Rg$_3$ against transient focal cerebral ischemia in rats," *Neuroscience Letters*, vol. 526, no. 2, pp. 106–111, 2012.

[391] Y. Y. Liu, T. Y. Zhang, X. Xue et al., "Pseudoginsenoside-F11 attenuates cerebral ischemic injury by alleviating autophagic/lysosomal defects," *CNS Neuroscience & Therapeutics*, vol. 23, no. 7, pp. 567–579, 2017.

[392] T. Zhang, C. Wu, X. Yang et al., "Pseudoginsenoside-F11 protects against transient cerebral ischemia injury in rats involving repressing calcium overload," *Neuroscience*, vol. 411, pp. 86–104, 2019.

[393] X. Meng, M. Wang, X. Wang et al., "Suppression of NADPH oxidase-and mitochondrion-derived superoxide by notoginsenoside R1 protects against cerebral ischemia–reperfusion injury through estrogen receptor-dependent activation of Akt/Nrf2 pathways," *Free Radical Research*, vol. 48, no. 7, pp. 823–838, 2014.

[394] N. K. Roy, D. Parama, K. Banik et al., "An update on pharmacological potential of boswellic acids against chronic diseases," *International Journal of Molecular Sciences*, vol. 20, no. 17, article 4101, 2019.

[395] H. L. Wang, Q. H. Zhou, M. B. Xu, X. L. Zhou, and G. Q. Zheng, "Astragaloside IV for experimental focal cerebral ischemia: preclinical evidence and possible mechanisms," *Oxidative Medicine and Cellular Longevity*, vol. 2017, Article ID 8424326, 13 pages, 2017.

[396] X. Huang, N. Li, Y. Pu, T. Zhang, and B. Wang, "Neuroprotective effects of ginseng phytochemicals: recent perspectives," *Molecules*, vol. 24, no. 16, p. 2939, 2019.

[397] X. Liu, L. Wang, A. Wen et al., "Ginsenoside-Rd improves outcome of acute ischaemic stroke - a randomized, double-blind, placebo-controlled, multicenter trial," *European Journal of Neurology*, vol. 19, no. 6, pp. 855–863, 2012.

[398] X. S. Zeng, X. S. Zhou, F. C. Luo et al., "Comparative analysis of the neuroprotective effects of ginsenosides Rg1 and Rb1 extracted from Panax notoginseng against cerebral ischemia," *Canadian Journal of Physiology and Pharmacology*, vol. 92, no. 2, pp. 102–108, 2014.

[399] J. Shen, Z. Zhao, W. Shang et al., "Ginsenoside Rg1 nanoparticle penetrating the blood-brain barrier to improve the cerebral function of diabetic rats complicated with cerebral infarction," *International Journal of Nanomedicine*, vol. 12, pp. 6477–6486, 2017.

[400] Y. P. Lu, S. Y. Liu, H. Sun, X. M. Wu, J. J. Li, and L. Zhu, "Neuroprotective effect of astaxanthin on H_2O_2-induced neurotoxicity in vitro and on focal cerebral ischemia in vivo," *Brain Research*, vol. 1360, pp. 40–48, 2010.

[401] Y. Nai, H. Liu, X. Bi, H. Gao, and C. Ren, "Protective effect of astaxanthin on acute cerebral infarction in rats," *Human & Experimental Toxicology*, vol. 37, no. 9, pp. 929–936, 2018.

[402] L. Hu, W. Chen, F. Tian, C. Yuan, H. Wang, and H. Yue, "Neuroprotective role of fucoxanthin against cerebral ischemic/reperfusion injury through activation of Nrf2/HO-1 signaling," *Biomedicine & Pharmacotherapy*, vol. 106, pp. 1484–1489, 2018.

[403] S. Y. Li, D. Yang, Z. J. Fu, T. Woo, D. Wong, and A. C. Lo, "Lutein enhances survival and reduces neuronal damage in a mouse model of ischemic stroke," *Neurobiology of Disease*, vol. 45, no. 1, pp. 624–632, 2012.

[404] C. Galasso, I. Orefice, P. Pellone et al., "On the neuroprotective role of Astaxanthin: new perspectives?," *Marine Drugs*, vol. 16, no. 8, p. 247, 2018.

[405] J. Hu, Y. Chai, Y. Wang et al., "PI3K p55γ promoter activity enhancement is involved in the anti-apoptotic effect of berberine against cerebral ischemia-reperfusion," *European Journal of Pharmacology*, vol. 674, no. 2-3, pp. 132–142, 2012.

[406] S. N. Maleki, N. Aboutaleb, and F. Souri, "Berberine confers neuroprotection in coping with focal cerebral ischemia by targeting inflammatory cytokines," *Journal of Chemical Neuroanatomy*, vol. 87, pp. 54–59, 2018.

[407] J. Yang, H. Yan, S. Li, and M. Zhang, "Berberine ameliorates MCAO induced cerebral ischemia/reperfusion injury via activation of the BDNF-TrkB-PI3K/Akt signaling pathway," *Neurochemical Research*, vol. 43, no. 3, pp. 702–710, 2018.

[408] X. Zhang, X. Zhang, C. Wang et al., "Neuroprotection of early and short-time applying berberine in the acute phase of cerebral ischemia: Up-regulated pAkt, pGSK and pCREB, down-regulated NF-κB expression, ameliorated BBB permeability," *Brain Research*, vol. 1459, pp. 61–70, 2012.

[409] J. Zhu, D. Cao, C. Guo et al., "Berberine facilitates angiogenesis against ischemic stroke through modulating microglial polarization via AMPK signaling," *Cellular and Molecular Neurobiology*, vol. 39, no. 6, pp. 751–768, 2019.

[410] N. M. de Lima, E. O. Ferreira, M. Y. Fernandes et al., "Neuroinflammatory response to experimental stroke is inhibited by boldine," *Behavioural Pharmacology*, vol. 28, no. 2 and 3, pp. 223–237, 2017.

[411] M. Huang, G. Cheng, H. Tan et al., "Capsaicin protects cortical neurons against ischemia/reperfusion injury via down-regulating NMDA receptors," *Experimental Neurology*, vol. 295, pp. 66–76, 2017.

[412] A. Janyou, P. Wicha, J. Jittiwat, A. Suksamrarn, C. Tocharus, and J. Tocharus, "Dihydrocapsaicin attenuates blood brain barrier and cerebral damage in focal cerebral ischemia/reperfusion via oxidative stress and inflammatory," *Scientific Reports*, vol. 7, no. 1, article 10556, 2017.

[413] D. Wu, J. Shi, O. Elmadhoun et al., "Dihydrocapsaicin (DHC) enhances the hypothermia-induced neuroprotection following ischemic stroke via PI3K/Akt regulation in rat," *Brain Research*, vol. 1671, pp. 18–25, 2017.

[414] Z. Cao, A. Balasubramanian, and S. Marrelli, "Pharmacologically induced hypothermia via TRPV1 channel agonism provides neuroprotection following ischemic stroke when initiated 90 min after reperfusion," *American Journal of Physiology. Regulatory, Integrative and Comparative Physiology*, vol. 306, no. 2, pp. R149–R156, 2014.

[415] Y. M. Ha, M. Y. Kim, M. K. Park et al., "Higenamine reduces HMGB1 during hypoxia-induced brain injury by induction of heme oxygenase-1 through PI3K/Akt/Nrf-2 signal pathways," *Apoptosis*, vol. 17, no. 5, pp. 463–474, 2012.

[416] Y. Z. Guan, X. D. Jin, L. X. Guan et al., "Nicotine inhibits microglial proliferation and is neuroprotective in global ischemia rats," *Molecular Neurobiology*, vol. 51, no. 3, pp. 1480–1488, 2015.

[417] R. Sun, Y. Song, S. Li et al., "Levo-tetrahydropalmatine attenuates neuron apoptosis induced by cerebral ischemia–reperfusion injury: involvement of c-Abl activation," *Journal of Molecular Neuroscience*, vol. 65, no. 3, pp. 391–399, 2018.

[418] M. Li, X. Zhang, L. Cui et al., "The neuroprotection of oxymatrine in cerebral ischemia/reperfusion is related to nuclear factor erythroid 2-related factor 2 (nrf2)-mediated antioxidant response: role of nrf2 and hemeoxygenase-1 expression," *Biological & Pharmaceutical Bulletin*, vol. 34, no. 5, pp. 595–601, 2011.

[419] C. Rui, L. Yuxiang, J. Ning et al., "Anti-apoptotic and neuroprotective effects of oxysophoridine on cerebral ischemia both in vivo and in vitro," *Planta Medica*, vol. 79, no. 11, pp. 916–923, 2013.

[420] K. Vaibhav, P. Shrivastava, H. Javed et al., "Piperine suppresses cerebral ischemia-reperfusion-induced inflammation through the repression of COX-2, NOS-2, and NF-κB in middle cerebral artery occlusion rat model," *Molecular and Cellular Biochemistry*, vol. 367, no. 1-2, pp. 73–84, 2012.

[421] H. Huang, R. Zhong, Z. Xia, J. Song, and L. Feng, "Neuroprotective effects of rhynchophylline against ischemic brain injury via regulation of the Akt/mTOR and TLRs signaling pathways," *Molecules*, vol. 19, no. 8, pp. 11196–11210, 2014.

[422] J. Qiu, M. Wang, J. Zhang et al., "The neuroprotection of sinomenine against ischemic stroke in mice by suppressing NLRP3 inflammasome via AMPK signaling," *International Immunopharmacology*, vol. 40, pp. 492–500, 2016.

[423] S. Yang, F. Ning, J. Li et al., "Therapeutic effect analysis of sinomenine on rat cerebral ischemia-reperfusion injury," *Journal of Stroke and Cerebrovascular Diseases*, vol. 25, no. 5, pp. 1263–1269, 2016.

[424] T. Sharma, V. Airao, N. Panara et al., "Solasodine protects rat brain against ischemia/reperfusion injury through its antioxidant activity," *European Journal of Pharmacology*, vol. 725, pp. 40–46, 2014.

[425] Z. Liu, D. He, X. Zhang et al., "Neuroprotective effect of early and short-time applying sophoridine in pMCAO rat brain: down-regulated TRAF6 and up-regulated p-ERK1/2 expression, ameliorated brain infaction and edema," *Brain Research Bulletin*, vol. 88, no. 4, pp. 379–384, 2012.

[426] Y. Miao, B. Wu, W. Zhang, Y. Qiu, B. Li, and X. Lu, "Neuroprotective effect of sophocarpine against transient focal cerebral ischemia via down-regulation of the acid-sensing ion channel 1 in rats," *Brain Research*, vol. 1382, pp. 245–251, 2011.

[427] L. Ruan, H. S. Huang, W. X. Jin, H. M. Chen, X. J. Li, and Q. J. Gong, "Tetrandrine attenuated cerebral ischemia/reperfusion injury and induced differential proteomic changes in a MCAO mice model using 2-D DIGE," *Neurochemical Research*, vol. 38, no. 9, pp. 1871–1879, 2013.

[428] K. Pravalika, D. Sarmah, H. Kaur et al., "Trigonelline therapy confers neuroprotection by reduced glutathione mediated myeloperoxidase expression in animal model of ischemic stroke," *Life Sciences*, vol. 216, pp. 49–58, 2019.

[429] H. Wang, K. Zhang, L. Zhao, J. Tang, L. Gao, and Z. Wei, "Anti-inflammatory effects of vinpocetine on the functional expression of nuclear factor-kappa B and tumor necrosis factor-alpha in a rat model of cerebral ischemia-reperfusion injury," *Neuroscience Letters*, vol. 566, pp. 247–251, 2014.

[430] W. N. Wu, P. F. Wu, X. L. Chen et al., "Sinomenine protects against ischaemic brain injury: involvement of co-inhibition of acid-sensing ion channel 1a and L-type calcium channels," *British Journal of Pharmacology*, vol. 164, no. 5, pp. 1445–1459, 2011.

[431] F. Zhang, C. Yan, C. Wei et al., "Vinpocetine inhibits NF-κB-Dependent inflammation in acute ischemic stroke patients," *Translational Stroke Research*, vol. 9, no. 2, pp. 174–184, 2018.